IMWA2023
CASNEWYDD ▸ NEWPORT

Y DYFODOL | THE FUTURE



Peter Stanley, Christian Wolkersdorfer, Karoline Wolkersdorfer




IMWA 2023
Y DYFODOL | THE FUTURE





Proceedings of the International Mine Water Association Conference

July 17 – 21, 2023

Newport, Wales

Editors

Peter Stanley

Christian Wolkersdorfer

Karoline Wolkersdorfer

International Mine Water Association 2023 Conference
Y DYFODOL | THE FUTURE
2023, Newport, Wales

ISBN 978-3-9825293-1-8

© International Mine Water Association 2023

Editors
Peter Stanley, Christian Wolkersdorfer, Karoline Wolkersdorfer

Proceedings Production Assistant
Elke Mugova

Cover Design
Christian Wolkersdorfer

Layout and Typesetting
Jigsaw Graphic Design & Christian Wolkersdorfer

Cover Photographs
Nick Cozier on Unsplash (sheep), Natural Resources Wales (Parys Mountain, Cwmystwyth), Peter Stanley (Welsh Dragon)

All abstracts were reviewed by 2 – 3 experts of the International Scientific Committee.

All full papers were reviewed by 1 – 2 experts of the International Scientific Committee.

www.IMWA.info

Organizers

Cardiff University

CARDIFF UNIVERSITY

PRIFYSGOL CAERDYDD

The Coal Authority

The Coal Authority

Resolving the impacts of mining

Welsh Government

Noddir gan
Lywodraeth Cymru

Sponsored by
Welsh Government

International Mine Water Association

Natural Resources Wales

Cyfoeth Naturiol Cymru
Natural Resources Wales

IMWA 2023

Y DYFODOL | THE FUTURE

International Scientific Committee (ISC)

Bert Allard, Sweden
Tim Aubel, Germany
Jeff Bain, Canada
Selina Mary Bamforth, United Kingdom
Maria Dolores Basallote, Spain
Melanie Lise Blanchette, Australia
Andrey Bogomolov, Russia
Camilo Raul de los Hoyos, Argentina
Gareth Digges La Touche, United Kingdom
Lee Evans, Australia
Elvis Fosso-Kankeu, South Africa
Jabulani Gumbo, South Africa
Ryan Thomas Jakubowski, United States
Raymond H. Johnson, United States
Lucinda Johnson, United States
David Richard Jones, Australia
Lisa Bithell Kirk, United States
Robert Lawrence Kleinmann, United States
Konstantinos Kollias, Greece
Natalie A Kruse Daniels, United States
Jorge Loredo, Spain
Simon Antony Lorentz, South Africa
Paul Joel Lourens, South Africa
Rudzani Lusunzi, South Africa
Dmitriy Makarov, Russia
Cherie McCullough, Australia
Matthew P. McGann, Peru
Michael Arthur Milczarek, United States
Kevin Myers, United States
Carmen Mihaela Neculita, Canada
Darrell Kirk Nordstrom, United States
James Pope, New Zealand
Pierre Rousseau, Australia
Carlos Ruiz Cánovas, Spain
Liudmila Rybnikova, Russia
David Anthony Salmon, Australia
Christopher James Satterley, United Kingdom
Ralph Schöpke, Germany
Robert R Seal, United States
Viktor Sjöberg, Sweden
Peter Clive Stanley, United Kingdom
Wanghua Sui, China
Jacek Szczepiński, Poland
Esther Takaluoma, Finland
Gilles Tremblay, Canada
Teresa Maria Valente, Portugal
Denys Villa Gomez, Australia
Roderick David Williams, United States
Christian Wolkersdorfer, South Africa
Peter Woods, Australia
Jorge Zafra, Peru

Local Organizing Committee (LOC)

Peter Stanley
Trystan James
Karoline Wolkersdorfer
James Parsons
Devin Sapsford
Fei Jin
Chris Satterley
Abby Moorhouse-Parry
Eifiona Williams
James Dowling
Aaron Todd
Tobias Roetting
Rob Bowell
Rhys Savage



IMWA 2023
Sponsors & Partners

Gold Sponsor

srk

Bronze Sponsor

MEM MINE ENVIRONMENT MANAGEMENT

CONCRETE CANVAS®

Gala Dinner and Workshop Sponsor

ERM

WATER GENICS

Trip 1 and Lanyard Sponsor

Geochemic Ltd
www.geochemic.co.uk

Opening Ceremony Drinks Sponsor

KLM Consulting Services
Ground Water Consultants
www.klmcs.co.za

Opening Ceremony Entertainment Sponsor

wsp

IMWA 2023
Y DYFODOL | THE FUTURE



Contents

Abfertiawan, Muhammad Sonny; Hasan, Faiz; Handajani, Marisa; Syafila, Mindriany; Gunawan, Firman; Djali, Febriwiadi
High Total Suspended Solid (TSS) Removal for Coal Mining Water Using Electrocoagulation 1

Alvarez, Ignacio; Brown, Martin
Uncertainty Analysis In Groundwater Flow Models As A Tool To Support Decision Making: Assessing The Influence Of Infiltrations From A TSF Over An Open Pit 6

Annandale, John George; Tanner, Phillip Dale; Heuer, Sarah Nicole; van der Walt, Gideon; Deane, Karabo; du Plessis, Heinrich Meiring
Facilitating Sustainable Mine Water Irrigation 13

Apeiranthitis, Nikolaos; Finlay, Alexander; Greenwell, H. Chris; Merrick, Eddie
Passive Leached Water Mine (P.L.W.M.) - A sustainable approach to mine water remediation and metals extraction 19

Bäckström, Mattias; Sartz, Lotta
Mesocosm Experiments Performed in 1975, 1993 and 2017 to Determine Changes in Release Rates of Zinc from Sediments Affected by an Old Mining Operation 25

Bamforth, Selina Mary; Cox, Nick; Potter, Hugh
Innovative Passive Treatment Technologies for UK Metal Mine Waters: Results from field scale trials 31

Banks, Vanessa J; Bruce, Edward; Dashwood, Benjamin; Gandy, Catherine; Kirkham, Matthew R; Nedumpallile-Vasu, Nikhil; Longstaff, Tim; Moorhouse-Parry, Abby; Palumbo-Roe, Barbara; Potter, Hugh
Geotechnical Characterisation of Mine Waste for Modelling Potential Climate Change Impacts. on Mine Waste Mobility 38

Basallote, M Dolores; Gerardo, Amaya; Maira, Castellanos; Cánovas, Carlos R; Nieto, José Miguel; Rafael, Pérez-López
Sustainable Removal of Metal/loids from As-Rich Mine Waters Using Mine and Industry Waste Materials 45

Battaglia-Brunet, Fabienne; Jacob, Jérôme; Dure, Frederic; Huron, Justine; Gatellier, Gaelle
Passive Treatment Of Mine Seepage With High Arsenic Concentrations 51

Bellin, James; Declercq, Julien; Stewart, Michael; Pearson, Callum
Integrated Catchment-scale Mine Water Impact Assessment: A Case Study 57

Genc, Mihriban; Boddaert, Florent; Beale, Geoff; Samuel, Toddy; Ruthman, Rahardian
Characterization and Groundwater Modelling of a New Block-Caving Project 63

Morton, Kym Lesley; Bovim, Alastair
Advanced monitoring of Tailings Storage Facilities and dams to prevent failure. Illustrated with case studies from UK, Africa and South America 69

Bowell, Rob; Bamforth, Selina; Walton, J; Brabham, P
An assessment of the current operation of the Coal Authority Six Bells Mine Water Treatment Scheme, South Wales 77

Breckenridge, Larry; Harvey, Todd
Modeling Heap Leach Solutions to Optimize Safety and Revenue 83

Burton, Rob; Hudson, Emily
Flow Monitoring at Mine Water Discharges and Treatment Schemes in Wales – Challenges and Lessons Learnt 89

Clode, Karen; Gurieff, Nicholas Bagger; Freeman, Neil; Storey, Michael
Innovative Approach To The Development of a Mine Water Remediation R&D Portfolio 96

Cochrane, James; Williams, Tom; Knott, Richard; Williams, Heilyn; Craxford, Stuart; Stanley, Peter Clive
Sediment Harvesting Using A Nautilus Pond™ Within Surface Water Management At Esgair Mwyn 102

Cooke, Dave; Mason, David; Williams, Heilyn; Jones, Liz; Byfield, Rebecca; Mansell, Lindsey; Carline, Richard; Stanley, Peter Clive
Working With Designation Constraints At Cwmystwyth 108

Cooke, Dave; Hudson, Emily; Jones, Liz; Mason, David; Wylie, Richard; Stanley, Peter Clive
Surface Water Management To Reduce Pollution At Dylife, Mid Wales 116

Cox, Melanie; Tait, David; Bowell, Robert; Griffiths, Ruth
An Overview of Challenges Associated with Defining and Applying Water Quality Standards in the Absence of Applicable Regulatory Limits 122

Dent, Julia; Pearce, Steven; Savage, Rhys; Marsden, James; Schultz, Ryan; Williams, Tom; Stanley, Peter; Roberts, Mark; Barnes, Andrew; Gersten, Ben
Optimising Circum-Neutral Mine Drainage Treatment By Implementing High Shear Degassing Into A Sustainable Active Treatment System 129

Dent, Julia; Pearce, Steven; Malam, Claudia; Barnes, Andrew; Roberts, Mark; Mueller, Seth
Review Of Laboratory Methodologies To Determine The Sorption And Release Of Metals Related To The Interaction Of Mine Drainage Water With Natural Media (Peat, Till And Bedrock). A Case Study From A Base Metal Mine In Arctic Finland 135

Dorman, Dayton M; Nairn, Robert W
Effect of Time and Mineralogy on Sorption Capacity of Mine Drainage Passive Treatment Residuals: Is Sustainable Reuse Possible? 142

Dzimbanhete, Vimbainashe L; Hegg, Frej; Alakangas, Lena; Karlsson, Torbjörn; Peinerud, Elsa; Paulsson, Oscar; Aiglsperger, Thomas
Uranium Sources And Mobility At An Iron Ore Mine Site In Northern Sweden 148

Ebel, Tom; Oppelt, Lukas; Wunderlich, Timm; Grab, Thomas; Fieback, Tobias
Development of an Improved Model to Investigate Heating Potentials in Abandoned Mines Utilising Mine Water 154

Farahnaz, Ibtisani; Abfertiawan, Muhammad Sonny; Syafila, Mindriany; Handajani, Marisa; Gunawan, Firman; Djali, Febriwiadi
Metals Distribution in River Sediment from Open-Pit Coal Mine Activity 159

Golian, Saeed; El-Idrysy, Houcyne; Stambuk, Desana
How Climate Would Likely Change in Future: Case Study of a Mine Site in Kazakhstan 166

Gomes, Patricia; Valente, Teresa Maria; Sousa, Mafalda
Study Of The Toxicity Of Mine Waters: Implications Of Suspended Matter On The Performance Of Tolerant Plants 172

Gutierrez, Manuel; Brown, Martin
Use of Groundwater Numerical Model to Support Decision Making at Large Open Pit 178

Hällström, Lina
Secondary Gypsum And HFO Affected The Mobility Of Critical Metals (Be & W) In Historical Skarn Tailings, Yxsjöberg, Sweden 185

Heaney, Paul Clive
Sustainable Mine Water Management Strategies 191

Kotte Hewa, Dileesha Jayahansani; Durce, Delphine; Salah, Sonia; Smolders, Erik
Rare Earth Elements Association with Predominant Elements in Solids Precipitated during Alkalinization of Acid Mine Water 196

Holopainen, Joonas; Tolvanen, Hanna; Tiihonen, Tommi; Lehto, Vesa-Pekka; Riikonen, Joakim; Nissinen, Tuomo Juhani
Analytical Validation of 3AWater MWAS, a Fast On-site Analysis Tool of Dissolved Metals in Waters 203

Hubbard, Paul; Palmer, Michael
A Review of Downhole Field Methodologies Applied for the Hydrogeological Exploration of Lithium Enriched Groundwater 208

Hudson, Ashlene; Murnane, John G; Courtney, Ronan
Constructed Wetlands For Treatment Of Bauxite Residue Leachate: 7.5 Years Of Monitoring 215

Hughes, Andrew; Blanchard, Ryan; Kofoed, Val O.; Jessop, Mike
Using Innovative Geophysical Techniques to Characterize Abandoned Mine Workings and Mine Water 220

El idrysy, Houcyne; Kirillov, Nikolai; Harding, William; Hurban, Gary
Use Of Evaporation Ponds In The Mining Industry. How Necessary And Effective Is This In Various Parts Of The World 227

Im, Dae gyu; Kim, Duk-Min; Kwon, Hye-Lim; Lee, Joon-Hak; Park, Mi-Sun; Yun, Seong-Taek
Assessing Removal Efficiencies of Mn and Ni in Mine Drainage Using Bench- and Pilot-Scale Slag Reactor and Design of Treatment System 233

Imrie, Sheila; Bennett, Adam; Bellin, James; Ebeling, Patrick
Hydrogeological Numerical Modelling to Assess Active Dewatering Options at a Sand Quarry Site – A Case Study and Associated Methodology 237

Jackson, Scott; Momeyer, Steve; Stockwell, Justin; Francoeur, Nicolas
A Flexible Approach To Modelling Seepage From Coal Mine Waste Rock 243

Jacob, Jerome; Moreau, Ulysse; Dure, Frederic; Engevin, Jeremy; Huron, Justine; Lassin, Arnault; Guerin, Valerie
AMD Passive Treatment Using DAS At An Old Tin Mine In France 250

Jarvis, Adam Paul; Banks, Vanessa; Crewdson, Emma; Lofts, Stephen; Palumbo-Roe, Barbara; Pullen, Jasmine; Gandy, Catherine Jane
Sources Of Diffuse Zinc And Lead Contamination In An Abandoned Mine Watershed 257

Jasnowski-Peters, Henning; Melchers, Christian
Natural Tracers For Mine Water Fingerprinting III – an Approach to Identify Mine Waters from Distinct Mine Water Provinces during Mine Water Rebound in the Ruhr District Area 263

Juholin, Piia; Haanpää, Kirsi-Marja; Laurila, Tea; Anttila, Eeva-Leena; Picken, Päivi
Minimizing Xanthate Impacts on Watercourses in Cold Climate – Review on Available and Potential Approaches 270

Karlsson, Teemu Eemeli; Paalumäki, Ville-Pekka; Kauppila, Tommi; Hietaharju, Eila
Effect of a Till Cover in Harmful Element Reduction in Waste Rock Drainage 276

Kim, Duk-Min; Im, Dae-Gyu; Lee, Joon-Hak; Park, Mi-Sun
Flow and Baffle Configurations of Reactor and Settling Pond for Treatment of Mine Drainage 281

Kunze, Katja; Blumenstein, O
Field Trial on the Use of Iron Hydroxide Sludge for Revegetation Measures and to Improve the Productivity of Structurally Weak Soils 287

Kusuma, Ginting Jalu; Badhurahman, Abie; Gautama, Rudy Sayoga; Dwiki, Sendy; Salmawati, Salmawati
Acid Mine Drainage from Epithermal Gold Deposits: Characterization and Classifying for Various Rock Types 294

Kwon, Hye-Lim; Kim, Duk-Min; Im, Dae-Gyu; Kang, Bu-Sung; Park, Mi-Sun
Assessment of Feasibility and Scale Generation of Hydrothermal Energy in Abandoned Mine Area 299

Lafont, Charlotte; D. van Hullebusch, Eric; Battaglia-Brunet, Fabienne; Vaxelaire, Stéphane
Elucidation of The Factors Controlling The Oxidation Kinetics Of Manganese In Passive Treatment Systems : Monitoring Of Aerobic Wetland Removal Technologies 303

Liu, WeiTao; Yang, ChunHui; Du, YanHui
Numerical Simulation Of Small-Size Aggregate Accumulation Structure Under Dynamic Water Conditions 309

Lorentz, Simon; Imrie, Sheila; Bennett, Adam; Clulow, Alistair
Evaporation from Platinum Tailings in a Semi-Arid Environment 315

Lund, Mark; Blanchette, Melanie; Bernasconi, Rachele
Water Column Profiles And Instrument Chains Provide Complementary Understanding Of Stratification In Pit Lakes 320

Lynch, Sarah F. L.; Cox, Michael; Warnes, Louis; Satterley, Christopher J.
Experience and outcomes of a mine water pumping test including temporary High Density Sludge treatment at Thorpe Hesley, Yorkshire, UK 326

Maest, Ann; Cojoianu, Theodor
Pollution Registries for Mines: Current State and Future Needs 333

Martin, Alan J.; Salvador, Silvano
Pit Lake Water Quality Prediction: Insights into the Modelling of Non-Conservative Processes 338

Masaki, Yusei; Washio, Tsubasa; Hagihara, Kana; Hamai, Takaya; Horiuchi, Kengo; Semoto, Yuki; Kamiya, Taro; Takamoto, Kosuke; Sato, Naoki
A Biological Sulfate-Reducing Process for Zinc-Containing AMD in Japan: Comparison of Annual Treatment Performances Among Nutrient Conditions of Ethanol, Rice Bran and Their Hybrid for Sulfate-Reducing Bacteria 344

Moorhouse-Parry, Arabella Mary Louise; Satterley, Christopher J.
Assessment of Manganese Removal in Passive Systems Based on Operational Data and Experience of Treating Net-alkaline Coal Mine Waters in the UK 351

Moorhouse-Parry, Arabella Mary Louise; Smithson, Stephen; Satterley, Christopher J.
Holistic Approach to Reed Bed Management on UK Coal Mine Water Treatment Schemes 358

Morton, Kym Lesley; Millsteed, Barry D; van Heerden, Wayne L; Carow, Albert; Msitsini, Moses
Structural Logging And Modelling For Use In Simulation Of Inflows In Underground Hard Rock Mines 365

Mugova, Elke; Wolkersdorfer, Christian
Mine Water Research with Analogue Modelling – The Agricola Model Mine 371

Naidu, Tamlyn Sasha; Moyo, Nkosilomusa; Hardwick, Ed; Falconer, Jenny; Smith, Janet; Sheridan, Craig; van Dyk, Lizelle
Exploring the Potential for Rare Earth Element Recovery from Coal Mine Acid Mine Drainage using Ion Exchange Technology 376

Naidu, Jivesh; Franzsen, Sebastian; Espach, Johan
Methodology For The Performance Monitoring Of An Unconventional Acidic RO 383

Nairn, Robert W.; Shepherd, Nicholas L.; Dorman, Dayton M.; McCann, Justine I.; Knox, Robert C.
Stream Recovery through Managed Biogeochemical Redox Coupling in Ecologically Engineered Passive Treatment Systems: A Natural Infrastructure Approach 390

Nurmesniemi, Emma-Tuulia; Juholin, Piia; Picken, Päivi; Haanpää, Kirsi-Marja; Vaarasuo, Anne; Vähänen, Kaisa
How to Determine Financial Guarantees of Water Treatment for Mine Closure: A Summary of Affecting Factors 397

Palumbo-Roe, Barbara; Crewdson, Emma; Jarvis, Adam; Gandy, Catherine; Banks, Vanessa; Mulcahy, Alex; Zarate, Manny; Arrowsmith, Carol; Loft, Stephen; Pullen, Jasmine; Moorhouse-Parry, Arabella; Potter, Hugh
Insights Into Catchment Connectivity Using Water Stable Isotopes To Address Diffuse Mine Pollution In Streams 402

Paramananda, I K Dwika; Badhurahman, Abie; Kusuma, Ginting Jalu; Gautama, Rudy Sayoga; Dwiki, Sendy; Salmawati, Salmawati
Modelling of Coal Pit Lake Quantity and Quality for Mine Closure (Case Study ON2 Area, Lati Mine Operation, Berau Coal) 409

Park, Seong-Sook; Choi, Kung-Won; Kang, Chan-Ung; Lee, Joon-Hak; Park, Mi-Sun; Kim, Sun-Joon; Lee, Ga-Hyeon
Column Adsorption Experiments for the Removal of Arsenic and Fluoride Ions in Mine Drainage using Adsorbents 415

Riley, Alex L; Onnis, Patrizia; Gandy, Catherine J; Kanu, Chimaobim V; Umeobika, Chinedu V; Cameron, James; Burke, Ian T; Hudson-Edwards, Karen A; Jarvis, Adam P; Mayes, William M
The Contribution Of Major Historical Orefields To Coastal Trace Metal(loid) Fluxes In North-East England 421

Roetting, Tobias Stefan; Hall, Iain; Digges La Touche, Gareth; Siddorn, Louise; Stanley, Peter
Field Trials of Dispersed Alkaline Substrate to Passively Treat Highly Polluted Acid Mine Drainage at two Emblematic Abandoned Mines in Wales 428

Romero-Matos, Jonatan; R. Cánovas, Carlos; Macías, Francisco; León, Rafael; Millán-Becerro, Ricardo; Nieto, José Miguel
Wildfire Effects On A Watercourse Affected By Acid Mine Drainage (Odiel River, SW Spain) 434

Satterley, Christopher James; Moorhouse-Parry, Arabella Mary Louise
Beyond Piramid: The Coal Authority's Approach to Design of Passive and Semi-Passive Treatment Schemes for Ferruginous Mine Waters in the UK 439

Schmidt, Roxane
Life-Cycle Water Balance Modelling as a Tool for Water Management Risk Assessment to Minimise Legacy Effects 445

Schramm, Andrea; Meyer, Jürgen; Metschies, Thomas; Jenk, Ulf
Challenges of Water Management at the Uranium Mining Site Schlema-Alberoda of Wismut (Germany) 450

Schreuder, Heinrich; Lourens, Paul Joel Havemann; Vermeulen, Petrus Daniel; Lubbe, Rolene
Cost Effective Method to Depressurise Perched Aquifers to Prevent Slope Failures in Open-Pit Mines, South Africa 456

Semoto, Yuki; Horiuchi, Kengo; Hamai, Takaya; Ikegami, Naoki; Masaki, Yusei; Takamoto, Kosuke; Takaya, Yutaro; Tokoro, Chiharu
Multi-Step Passive Treatment Using Limestone and Concrete Waste Material for Zn and Cd Removal 464

Shiimi, Rosalia Tuwilika; Savage, Rhys John; Pearce, Steven; Barnes, Andrew; Roberts, Mark; Schoen, Daniel; Sapsford, Devin
The Development Of A Multi Parameter Respirometric Laboratory Testing Method To Estimate Site-Specific Net Carbon Dioxide Flux From Metalliferous Mine Waste 471

Shubin, Ivan; Imrie, Sheila; Rex, Tony
Assessment of Hydrogeological Hazards in Operational Mines using Objective-Focussed Modelling and Hazard Mapping Tools 477

Smith, Janet; Hardwick, Ed; Falconer, Jenny; Sheridan, Craig; Naidu, Tamlyn Sasha; Holm, Peter Engelund; van Dyk, Lizelle
The Development of a Sample Preparation Technique for the Analysis of Trace Elements in Mine Impacted Waters containing High Levels of Iron 484

Terry, Peter; Leyland, John; Mason, David; Williams, Heilyn; Jones, Liz; Carline, Richard; Stanley, Peter Clive
Preventative Methods To Avoid Blow-out At Cwm Rheidol Adit 9, Ystumtuen Mine Sett 491

Theron, Charne; Lorentz, Simon Anthony
Rainfall Induced Transient Pressure Wave Mechanisms in Tailings 497

Thobejane, Kgaugelo; Ochieng', Levi; Mokoena, Kopano
Pre-mining Waste Rock Sampling – A Case Study in Sample Selection 504

Vaezihir, Abdorreza; Jowdat, Younes; Mazaheri, Nader; Aghili, Somayeh
Evaluation of Leakage Potential from Tailing Dam of Sungun Copper Mine Using Hydrogeological Findings and Numerical Modelling 510

Vaxelaire, Stéphane; Battaglia-Brunet, Fabienne
Treatment Of A Mine Water Containing Arsenic And Thiocyanates: Four Years Results On A Pilot Plant Scale 517

Weber, Anne; Bruns, Stefan; Wolf, Petra
Pit Lake Runstedt as "Reactor" for Remediation – On the Way to Better Energy Efficiency 523

Welman Purchase, Megan Dayl; Hansen, Robert
Modelling The Behaviour Of Ferric and Ferrous Iron In A Goldmine Tailings Environment, Free State – South Africa 529

Westermann, Sebastian; Rudakov, Dmytro; Melchers, Christian
Sensitivity Analysis of Flooding-influencing Factors by Design of Experiment (DoE) Applied at Three Underground Hard-coal Mines 534

Wolkersdorfer, Christian; Worsa-Kozak, Magdalena; Chudy, Krzysztof
The Colourful Lakes in Wieściszowice, Sudetes Mountains, Poland – An example of Chemical Variation in Abandoned open pit Pyrite Mine Mine Water 540

Wunderlich, Timm; Oppelt, Lukas; Ebel, Tom; Grab, Thomas; Fieback, Tobias
Abandoned Mines As A Source Of Heat And Cold For Quarter Solutions 545

Wyatt, Lee M; Leyland, John; Watson, Ian A
Long-Term Mine Water Management Of Abandoned Coal Mines In The United Kingdom: Almost 30 Years Of Process, Experience, and Lessons Learned 552

Wyatt, Lee M; Leyland, John; Watson, Ian A
Pumping Borehole For Saline Mine Water in Whitburn, North East England: Problems and Novel Resolution 558

Yungwirth, Grace; Coleman, Trevor; Norwood, William Jay; Dama-Fakir, Piyal; Bruton, Mark; Ali, Niyaz; Singh, Givarn
ESG & Mine Water: A Procedural Approach to Support Setting Water Savings Targets in the Mining Sector 564



High Total Suspended Solid (TSS) Removal for Coal Mining Water Using Electrocoagulation

Muhammad Sonny Abfertiawan[1], Faiz Hasan[2], Marisa Handajani[1], Mindriany Syafila[1], Firman Gunawan[3], Febriwiadi Djali[3]

[1]*Water and Wastewater Research Group, Faculty of Civil and Environmental Engineering, Bandung Institute of Technology, Jl Ganesha No 10, Bandung, West Java 40132, Indonesia*

[2]*Environmental Engineering Program Study, Faculty of Civil and Environmental Engineering, Bandung Institute of Technology, Jl Ganesha No 10, Bandung, West Java 40132, Indonesia*

[3]*Environmental Department, PT. Berau Coal, Indonesia*

Abstract

Coal mine water contains high concentrations of suspended solids due to clay minerals carried away by surface run-off. Removing it becomes problematic since it requires chemicals, especially in large catchment areas in mining sites. Due to this, Total Suspended Solid (TSS) concentration in coal mining water can reach up to 5,400 mg/L. In Indonesia, it mainly occurs in Kalimantan, which still adopts an open-pit mining system. This research aims to implement the electrocoagulation technique as a potential alternative active treatment to solve high TSS concentration in wastewater of an actual mining site.

Keywords: Total suspended solid, electrocoagulation, mine water, run-off.

Introduction

Open pit mining is done by stripping the topsoil of the mining material. This method results in tiers and basins downward, allowing accumulated rainwater to enter the mining front, erode the mine walls (soil), and form sludge. Sludge entering the mining site's front area can inhibit the mining process and cause equipment damage. Therefore, sludge formed is usually pumped from the front mining area into a settling pond. The goal of 6th Sustainable Development Goals (SDG's) is to improve water quality by reducing pollution, eliminating disposal, minimizing the release of hazardous materials and chemicals, halving the proportion of untreated wastewater, and significantly increasing recycling and reuse of recycled goods that are globally safe are to be concerned. Active treatments such as chemical neutralization and deposition, membranes, and filters have been used at many mine sites to minimize the environmental impact of mining-affected waters (Oncel *et al*. 2013). One of the active treatment technologies developed in mining water treatment is electrocoagulation.

Electrocoagulation is the process of agglomeration or coagulation using electricity. Electric power flowing through the electrodes resulted in an electrolysis process. Electrocoagulation can reduce the concentration of ferrous metal ions from 743.5 mg/L to 0.001 mg/L at 40 minutes of operating conditions and a current density of 500 A/m^2 (Oncel *et al*. 2013). The electrocoagulation process can be done even in remote areas where electricity is unavailable. In this case, energy for the electrocoagulation process can be obtained from solar panels. Solar Powered Electrocoagulation (SPEC) can remove turbidity up to 87% (Sharma *et al*. 2011). Based on these conditions, this study aims to examine coal mining water treatment using the electrocoagulation process of aluminum electrode pairs to meet the quality standards of wastewater from coal mining activities, especially for the High Total Suspended Solid (TSS) parameter.

Methods

This study used actual mining water waste from one of the settling ponds of coal mines

in Kalimantan (Initial TSS of 5,400 mg/L). An electrocoagulation reactor with a batch operating system is used. The reactor was made of acrylic (5 mm) with a capacity of three liters and length, width, and height of 14; 10.5; and 20 cm, respectively. The working volume used was 1000 mL. The electrodes were installed monopolar with 8 electrodes (i.e., 4 anodes and 4 cathodes) with a thickness of 0.2 cm. The dimensions of the electrode plate were 16 by 8 cm. The electrode plate was immersed in the solution for 7.5 cm, producing a total anode wet surface area of 0.024 m^2. The electrodes were installed using a frame with a distance between plates of 1.5 cm and connected to a DC electric current source (MDB 0–60 V and 0–20 A).

Electrocoagulation was done by using a pair of aluminum electrodes (99.9%,) at the Water Quality Laboratory, ITB. The electric current variations used in this study were 0.5, 1, and 2 A, with 15, 30, and 45 minutes of detention time. The treated mining water was analyzed on the supernatant taken at the same depth of 3 cm from the surface of the water samples. Electrical current and voltage measurements were carried out using a multimeter MASDA DT830B. Measurement was done twice (duplo) within the same time of treatment (i.e., same configuration) after 60 minutes of settling time. The process of floc formation and changes in the electrodes were observed. The parameters measured were pH, temperature, Total Dissolved Solid (TDS), and Total Suspended Solid (TSS) using a pH meter, thermometer, TDS meter, and TSS meter with the standard curve of the gravimetric method as follows

Results and Discussion

The steps in electrocoagulation are the formation of coagulants from anode oxidation, destabilizing contaminant particles, and followed by particle aggregation to form flocs (Mollah *et al.* 2004).

The process of floc aggregation into a larger size, which allows the particles to settle, occured in the electrocoagulation process (Figure 3). Furthermore, large-sized floc settled through the sedimentation process (Figure 3c). Floc deposition can also occur during electrocoagulation (Figure 3b) because the production of Al3+ ions from the electrodes is sufficient to form a floc. Therefore, larger flocs can settle before the sedimentation process starts. The following major reaction take place in the electrocoagulation process:

$$2H_2O + 2e^- \rightarrow H_2 + 2OH^- \quad (1)$$

$$Al_{(s)} \rightarrow Al^{3+}_{(aq)} + 3e^-_{(aq)} \quad (2)$$

$$Al^{3+}_{(aq)} + 3OH^-_{(aq)} \rightarrow Al(OH)_{3(s)} \quad (3)$$

According to Faraday's First Law, the amount of aluminum that dissolves from the electrode is proportional to the current and detention time applied to the system. A greater current and longer detention time will release more Al^{3+} ions (coagulant agent) from the anode and bind strongly to OH-. The particles destabilize and form flocs quickly in large numbers.

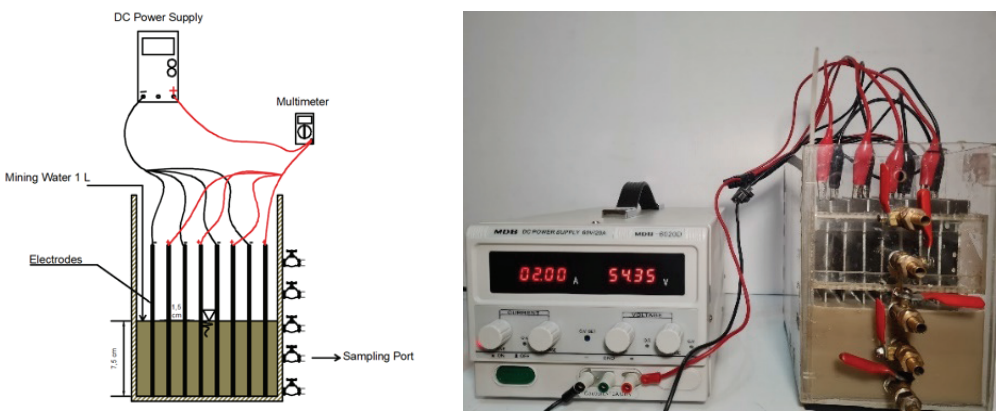


Figure 1 *Electrocoagulation reactor scheme (batch)*

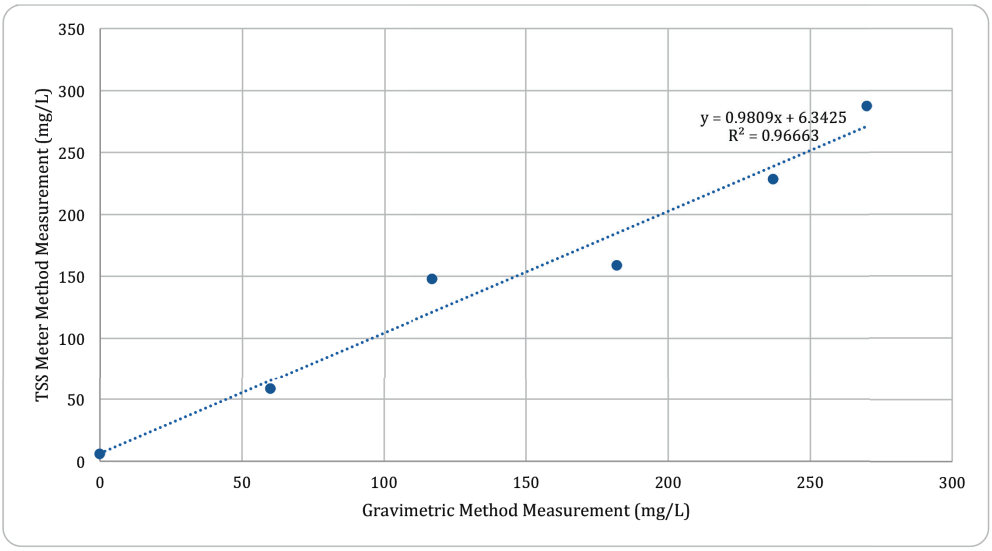


Figure 2 *Standard curve of gravimetric method*
(y=TSS Meter measurement,x=Gravimetric method measurement)

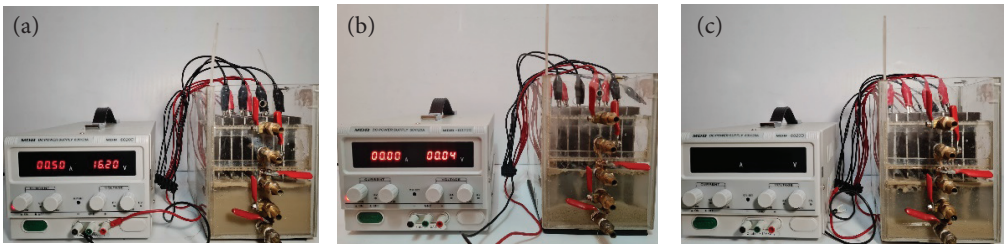


Figure 3 *(a) Electrocoagulation* ***on 15th minute with 0.5 A current (b) electrocoagulation on 45th minute with 2 A current, dan (c) after settling for 60 minutes (tec = 15 minutes, I = 0.5 A)***

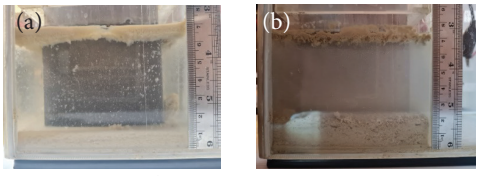


Figure 4 *Treated mining* ***water sample after settling for 60 minutes (a) tec = 30 minutes, I = 0.5 A (b) tec = 45 minutes, I = 2 A***

Electrocoagulation with a detention time of 30 minutes and a current of 0.5 A resulted in a 1 cm floc forming at the reactor's bottom (Figure 4a). Increasing detention time (45 minutes) and current (2 A) resulted in a higher floc height (2.5 cm) (Figure 4b). The number of coagulant agents formed affects the amount of floc that settles at the bottom of the reactor. Larger currents and longer detention times tend to result in higher floc generation at the bottom of the reactor.

The floc formed in the electrocoagulation process was not only settled to the bottom of the reactor. Bubbles were formed during the electrolysis process, bringing the floc particles to the surface (flotation). The bubbles occurred due to the production of H2 gas that appears at the cathode. The greater the current applied to the system, the faster the production of hydrogen bubbles occurs (Attour *et al.* 2014). The bubbles are very small and vary from 15 to 80 micrometers and help move pollutant particles to the

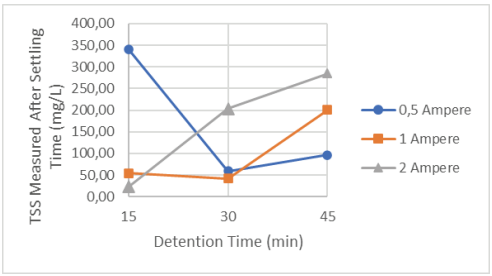


***Figure 5** Measured TSS (mg/L) after settling time*

surface of the liquid (Murugananthan *et al.* 2004). Electrolyte bubbles caused a mixing in solution through an upward momentum flux. Therefore, bubbles can increase the effectiveness of contact between coagulant particles and pollutants (Holt *et al.* 2002).

TSS reflects the amount of organic or inorganic compounds suspended in water. The TSS value in the electrocoagulation process carried out is presented in the graph above.

Only the lowest variation treatment (0.5 A and detention time of 15 minutes) did not meet the Regional Regulation of East Kalimantan Province Number 2 of 2011 concerning Water Quality Management and Water Pollution Control quality standard (300 mg/L). The coagulant produced from the electrodes was possibly insufficient to remove contaminant particles in the wastewater. Variation of 2 Ampere and detention time of 15 minutes resulted in the highest percentage of TSS removal of 99.58% from the initial concentration of 5,400 mg/L to 22.84 mg/L. Longer detention time in the current of 2 Ampere causes the TSS level to increase to 203.9 mg/L (30 minutes) and 285,10 mg/L (45 minutes). TSS levels increased due to the excess coagulant dose produced from the electrode plate.

The highest variation (I = 2A, t_d = 45 minutes) yields white supernatant, while the lowest variation (I = 0.5 A, td = 15 minutes) yields brown color (Figure 6). In the lowest variation, the coagulant formed cannot remove solids from the mine water due to the lack of the required coagulant dose. The highest variation yields white supernatant, indicating the formation of Al(OH)4-compounds. The pH value increased during the electrocoagulation process. The final value of the measured pH was influenced by the current and detention time given to the system. At the highest variation (I = 2A, t_d = 45 minutes), the final measured pH value reached 10.9, indicating a hydrolysis reaction of Al^{3+} into $Al(OH)^{4-}$.

The solubility of metal hydroxide precipitates determines the efficiency of the coagulant. The solubility of alum coagulants was determined by pH. At lower pH (below 4), the solubility of metal hydroxide precipitates produced a positive charge and Al3+ ions, while at higher pH (above 10) negative charge was formed along with Al(OH)4-. The result aligns with a study by Hudori *et al.* (2009) that showed the best pollutant removal in the electrocoagulation process occurs in the pH range of 4-10. PH values below 4 formed Al3+ ions, and at pH above 10 formed Al(OH)4-, which were less effective in coagulation.

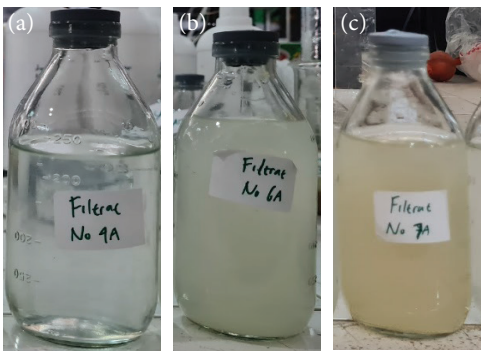


***Figure 6** Electrocoagulation supernatant on (a) I = 2 A, t_d = 15 minutes, (b) I = 2 A, t_d = 45 minutes, and (c) I = 0,5 A, t_d = 15 minutes*

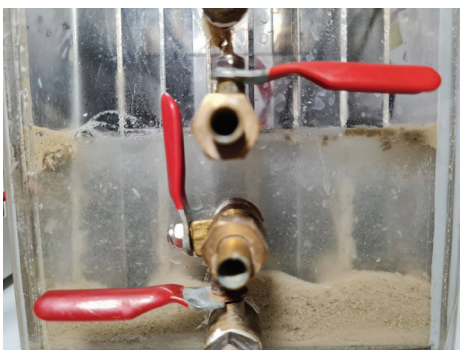


***Figure 7** Electrocoagulation reaction in 2 A at 45 minutes detention time*

Apart from the pH solubility, the increase in TSS was possibly due to the bubble produced from the cathode. The bubbles in the electrolyte solution stir the solution through an upward momentum flux. A proper amount of bubbles formed can increase the contact between coagulant and pollutant particles. However, floc cannot develop when bubbles are too much, and particles cannot agglomerate. Only a few floating flocs were found on the surface due to the rapid bubble production (Figure 7). Operation at low currents produces relatively low bubbles, causes gentle agitation, and allows flocculation to occur properly. According to Holt *et al.* (2002), when the current density increases, the bubble production increases, and the upward momentum movement accelerates. This condition will change the mixing, where the shear force from mixing in the solution can damage and break the floc, reducing pollutant removal effectiveness.

Conclusions

There is a relationship between detention time and current on measured TSS results. At currents of 0.5 A and 1 A, the optimum detention time was 30 minutes (TSS 59.04 mg/L and 42.21 mg/L); for a current of 2 A, the optimum detention time was 15 minutes (TSS 22.46 mg/L). The magnitude of electric current and detention time determines the amount of coagulant produced in the solution. An optimum combination is required to achieve the highest TSS removal. The current and detention time lower than the optimum conditions cannot eliminate TSS due to the lack of coagulant produced. In comparison, increasing current and detention time above the optimum condition increased the production of hydrogen bubbles which damage and break up the floc, thereby reducing pollutant removal effectiveness. The optimum variation based on the highest TSS removal was 2 Ampere with a detention time of 15 minutes, reaching TSS removal of 99.58% from the initial concentration of 5,400 mg/L to 22.84 mg/L.

Acknowledgments

This study was supported by the Bandung Institute of Technology through the Water and Wastewater Engineering Research Group (KK-RALC), Faculty of Civil and Environmental Engineering Research Grant as part of the "Program Penelitian dan Pengabdian kepada Masyarakat (P2MI) ITB 2022," and the Environment Department of Berau Coal.

References

Attour, A., Touati, M., Tlili, M., Ben Amor, M., Lapicque, F., & Leclerc, J. P. (2014). Influence of operating parameters on phosphate removal from water by electrocoagulation using aluminum electrodes. Separation and Purification Technology, 123, 124–129. https://doi.org/10.1016/j.seppur.2013.12.030

Holt, P. K., Barton, G. W., Wark, M., & Mitchell, C. A. (2002). A quantitative comparison between chemical dosing and electrocoagulation. Colloids and Surfaces A: Physicochemical and Engineering Aspects, 211(2), 233–248. https://doi.org/https://doi.org/10.1016/S0927-7757(02)00285-6

Hudori, H., & Soewondo, P. (2009). Pengolahan Deterjen Menggunakan Teknologi Elektrokoagulasi dengan Elektroda Aluminium. Jurnal Sains &Teknologi Lingkungan, 1(2), 117–125. https://doi.org/10.20885/jstl.vol1.iss2.art3

Mollah, M. Y. A., Morkovsky, P., Gomes, J. A. G., Kesmez, M., Parga, J., & Cocke, D. L. (2004). Fundamentals, present and future perspectives of electrocoagulation. Journal of Hazardous Materials, 114(1–3), 199–210. https://doi.org/10.1016/j.jhazmat.2004.08.009

Murugananthan, M., Bhaskar Raju, G., & Prabhakar, S. (2004). Removal of sulfide, sulfate and sulfite ions by electro coagulation. Journal of Hazardous Materials, 109(1–3), 37–44. https://doi.org/10.1016/j.jhazmat.2003.12.009

Oncel, M. S., Muhcu, A., Demirbas, E., & Kobya, M. (2013). A comparative study of chemical precipitation and electrocoagulation for treatment of coal acid drainage wastewater. Journal of Environmental Chemical Engineering, 1(4), 989–995. https://doi.org/10.1016/j.jece.2013.08.008

Sharma, G., Choi, J., Shon, H. K., & Phuntsho, S. (2011). Solar-powered electrocoagulation system for water and wastewater treatment. Desalination and Water Treatment, 32(1–3), 381–388. https://doi.org/10.5004/dwt.2011.2756

Uncertainty analysis in groundwater flow models as a tool to support decision making: Assessing the influence of infiltrations from a TSF over an open pit

Ignacio Álvarez[1], Martin Brown[2]

[1]*Itasca Chile, Providencia, Santiago, Chile, ignacio.alvarez@itasca.cl*

[2]*Itasca Australia, Scarborough, WA 6019, Australia, mbrown@itasca.com.au*

Abstract

A large Open Pit excavated in a very low permeability rock mass shows a limited presence of water on its slopes. Infiltrations from the nearby tailing storage facility (TSF) have produced a groundwater mound that extends towards the pit. To understand the potential effect that this flow could generate over the pit slopes and support the decision-making process, an uncertainty analysis was performed on a MINEDW 3D hydrogeological numerical model. Results indicate that while there could be an increase in pit seepage, there is a high probability that increases will be low compared to the seepage currently observed.

Keywords: Uncertainty analysis, numerical modelling, pit seepage, tailings infiltrations

Introduction

It is well documented that the presence of water has a detrimental effect on mining operations (Read & Stacey 2011; Read & Beale 2013). Water pressure acting on the pores, fractures or other discontinuities of the materials that make up a pit slope reduces its stability (Devy & Hutahayan 2021). This can lead to an increase in the risk of the mining operation, having to reduce slope angles and/or implement a drainage and depressurization program, in addition to drilling, blasting, exploitation and haulage problems (Morton & Van Niekerk 1993).

To control and overcome the negative effects generated by the presence of water, it is essential to have a correct understanding of the hydrogeological system (Read & Beale 2013). This is only possible through field characterization campaigns that include obtaining the hydraulic properties of the rock mass, data on anthropogenic and/or natural water inflows and outflows and monitoring of the hydrogeological system (Evan *et al* . 2015). This information is fundamental for the elaboration of a good conceptual model, as well as to support a subsequent numerical modelling work that can be used for the design of depressurization and drainage program (Read & Beale 2013; Evan *et al*. 2015).

Commonly, due to limited resources, the large dimensions of mining projects and the heterogeneity of fractured rock masses, it is not possible to fully characterize the hydrogeological domain of the models, which generates uncertainties related to the lack of information and, reduces the reliability of groundwater model predictions (Read & Beale 2013; Nilsson *et al*. 2006). Hence, decisions should not be made from the results of a single predictive model, but rather from modelling results that include estimates of uncertainty (Middlemis *et al*. 2019).

Situated in an area with low rainfall, high evaporation rates and low natural recharge, the deposit is within a low-permeability fractured rock mass classified as a rock aquiclude. These characteristics explain that to date, observed seepage flows have been low, allowing the mining operation to develop without the need for a drainage and depressurization program. However, since 2015, infiltration from the tailings storage facility (TSF) located 2 km from the pit have been observed in different monitoring boreholes, which have produced a groundwater mound that currently extends 700 m towards the pit. Eventually, the mound could generate a hydraulic connection with the pit, triggering problems

for the mine operation due to an increase on in pit seepage and pore pressures on the slopes.

To support the decision-making process associated with the drainage and slope stability of the open pit, an uncertainty analysis was carried out over the 3D numerical hydrogeological model built in MINEDW™ (Azrag *et al.* 1998; Itasca Denver 2019). Results allowed estimating the probability of occurrence and the magnitude of the potential increase in seepage and pore pressures because of infiltration from the tailings.

Conceptual groundwater flow model

Located in the Atacama Desert in the north of Chile, the open pit and TSF are subject to scarce rainfall with an average of 1 mm/year and high evaporation rates with magnitudes close to 2,800 mm/year. The only natural recharge comes from higher elevations located to the east and that moves through the study area following the hydraulic gradient to the west, north and south.

At this site, the geological setting consists of a layer of unsaturated unconsolidated alluvial and colluvial deposits, which overly a rock mass with different fracture degrees and alteration, composed of volcanic and intrusive rocks. The volcanic rocks form the host rock for porphyries in the mine area, therefore they are highly fractured, altered and mineralized in the pit sector because of hydrothermal processes during emplacement of intrusive rocks.

Due to alluvial deposits that are naturally unsaturated, the fractured rock constitutes the most relevant hydrogeological unit in the area. However, hydraulic tests have shown that rock mass permeability is low and has the characteristics of an aquiclude. This means that the flow and hydraulic properties of the rock mass depend on its fracture degree and the interconnectivity of the fractured zones, as well as on the presence of large structures which act as low permeability flow barriers or as high permeable flow conduits (Read & Beale 2013). Due to this condition, a high spatial heterogeneity and compartmentalization occurs, which is associated with a high uncertainty about the distribution, orientation, dimensions, and hydraulic properties of the fractures at different scale (Nilsson et al. 2006).

Two regional systems of low permeability faults are the most important structures, which divide the study area into three compartmentalized subdomains, which have independent hydraulic behaviors (fig. 1a). Monitoring boreholes located downstream of the TSF, in the western subdomain, and upstream of the pit, in eastern subdomain, record water levels which remain constant, showing that the regional water table in these areas is not influenced by mining activity. Unlike the central subdomain that is affected by the excavation of the pit and the infiltration at the TSF.

Conceptual model defined three main hydrogeological units based on the available groundwater level data, hydraulic tests, geological model and RQD measurements. In the pit area, the rock basement has been subdivided into three subunits due to the presence of rocks with genetic and mineralogical differences. Additionally, three hydrogeological units were conceptualized to represent the regional faults zones (RFZ) outside the pit and the in-pit faults systems, one that groups conductive faults (CF) and another, grouping barrier faults (BF) (fig. 1a).

Because of the low permeability of the fractured medium, natural groundwater flow through the study area has been estimated to be from 0.5 to 2.5 L/s. Besides the low natural recharges, anthropic recharges from the eastern sector of the TSF have been estimated to be from 1 to 10 L/s. On the other hand, in pit seepage has been estimated between 5 to 6 L/s.

MINEDW numerical groundwater flow model

Modelled area has an irregular geometry with an E-W width and N-S length of 14.5 and 10 km, respectively, and a depth of 2,390 m. The thickness of the model is large enough to model the projected final pit in 2040 (fig. 1a; 1b). Model has a total of 4,415,820 nodes and 8,551,955 elements.

TSF is in the center and the open pit in the east of the model domain. Constant hydraulic head boundary conditions were established at five edges of the model, considering pre-mining and current water

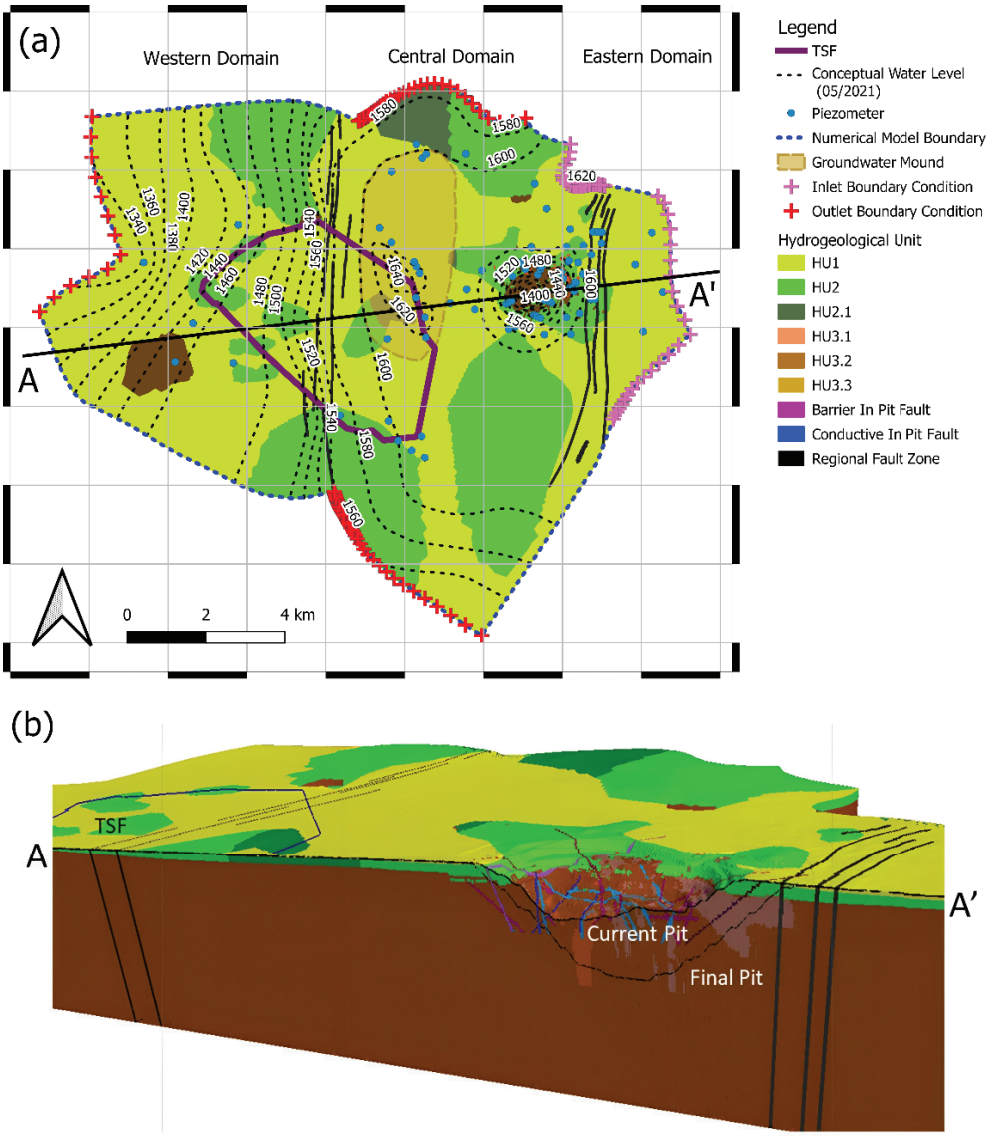


Figure 1 *Conceptual and numerical groundwater model. (a) Plan view; (b) Numerical model isometric view*

levels (fig. 1a), while a no flow boundary condition was assumed for the rest. The anthropic recharge zone was added according to conceptual model in the northeast of the TSF, while the recharge rate from TSF was calibrated through time using SEEP/W 2D and Hydrus 1D flow models according to tailings deposition records and the groundwater mound evolution.

Hydrogeological units were added as conceptualized. Based on higher permeability observed in hydraulic tests, an anisotropy zone was incorporated in HU2 in the north-eastern sector of the TSF, which allowed modeling the N-S direction of the groundwater mound.

Monthly observed groundwater level data from December 2012 to May 2021 of 67 monitoring boreholes were used for the calibration of the model. Most of the monitoring boreholes are located east of the TSF and in the pit zone (fig. 1a).

A pre-mine topography (2011) and 90 monthly historical topographies that record

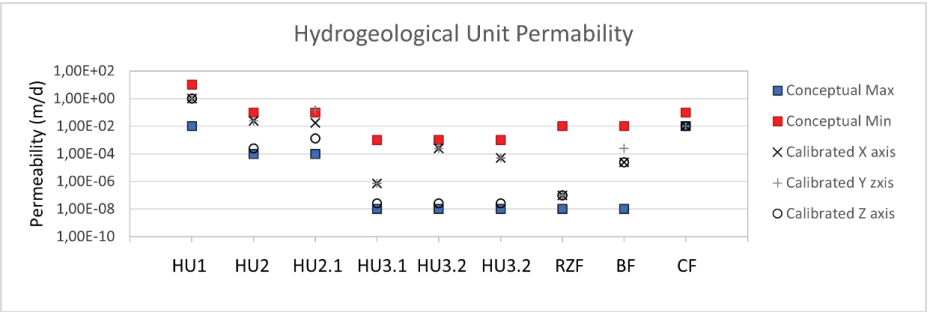


Figure 2 *Conceptual and calibrated permeability for hydrogeological units*

the excavation of the pit from February 2012 to July 2021, were used in the calibration process. Twelve predictive topographies, until year 2040, corresponding to the mining plan were added for the predictive analysis.

Calibration

Steady state calibrated water table levels were used as the pre-mining hydrogeological condition in the transient calibration, which reproduced the evolution of the water table during the mining activity to the final date of calibration. Both calibration stages considered the conceptualized permeabilities (fig. 2) as well as the estimated flow rates in the water balance, among other factors.

Emphasis was placed on calibrating monitoring boreholes with higher changing hydraulic gradients, located in the recharge zones near the TSF and those affected by depressurization in the vicinity of the pit. The best calibrated model reproduced conceptualized recharge and discharge flows, with inflows and outflows from the edges of 2.2 L/s, pit seepage of 6.7 L/s and recharges from the TSF of 6.2 L/s. Standards recommended by the guidelines (SEA 2012; Barnett *et al.* 2012) were also met, with a mean absolute error (MAE) in water level of 11.7 m (recommended: <45 m), normalized mean absolute error (nMAE) of 3.6% (recommended <5.0%) and a standardized root mean square residual (SRMS) of 5.1% (recommended: <10%). In addition, the extent of the groundwater mound was reproduced.

Predictive simulation

With the calibrated model, a predictive simulation was done until 2040, considering the excavation sequence of the mining plan and the evolution of the TSF recharge obtained from the 2D simulations of the tailing's deposition plan (Base Case). To assess if a hydraulic connection could be generated between TSF and the pit, a hypothetical simulation in which no recharge from the TSF ever occurred (No Recharge Case) was done and used as comparison.

Base Case simulation results show an advance of the mound that extends mainly to the north reaching a maximum advance of 800 m by 2026. The mound remains in this position until 2030 and then begins to gradually recede due to the end of tailings deposition according to the current plan. Advance towards the pit is less noticeable, possibly because it overlaps with the depressurization effect caused by the pit.

Base case predictive simulation shows that the mound will intersect the pit at the beginning of 2023. This connection would increase the seepage by 2.5 L/s at the most compared with the No Recharge Case in 2034.

Uncertainty Analysis

Since the predictive simulation shows a potential hydraulic connection between the TSF and the pit, which could generate an increase in pore pressure and seepage on its slopes, potentially triggering instabilities and causing operational problems (Read & Beale, 2013), an uncertainty analysis was performed

over predicted simulations to better support the related decision-making process. The wide range of permeabilities measured in the field suggests a high level of uncertainty related to the heterogeneity of the rock medium (fig. 2), so the uncertainty analysis was focused on the variability of the parameters, using the deterministic modelling approach with linear probability quantification method (Refsgaard *et al.* 2006; Nilsson *et al.* 2006; Middlemis *et al.* 2019).

With the objective of quantifying the risk of the groundwater mound expansion in time, one hundred numerical models were run to perform the uncertainty analysis, considering random different permeabilities for HU2 and HU2.1, that has the higher hydraulic transmissivity between both facilities. To account for a more extreme range of results, the permeability of these units was varied expanding the conceptual upper limit by one order of magnitude (for example 1,0E-04 to 1,0E-01 m/d for HU2).

Results

All the uncertainty models obtained met the standards recommended by the modeling guidelines from water table approach (i.e., SRMS and MAE), therefore, all models could have been considered acceptable (i.e., calibrated) for analysis. However, 23 models were excluded from the probabilistic analyzes

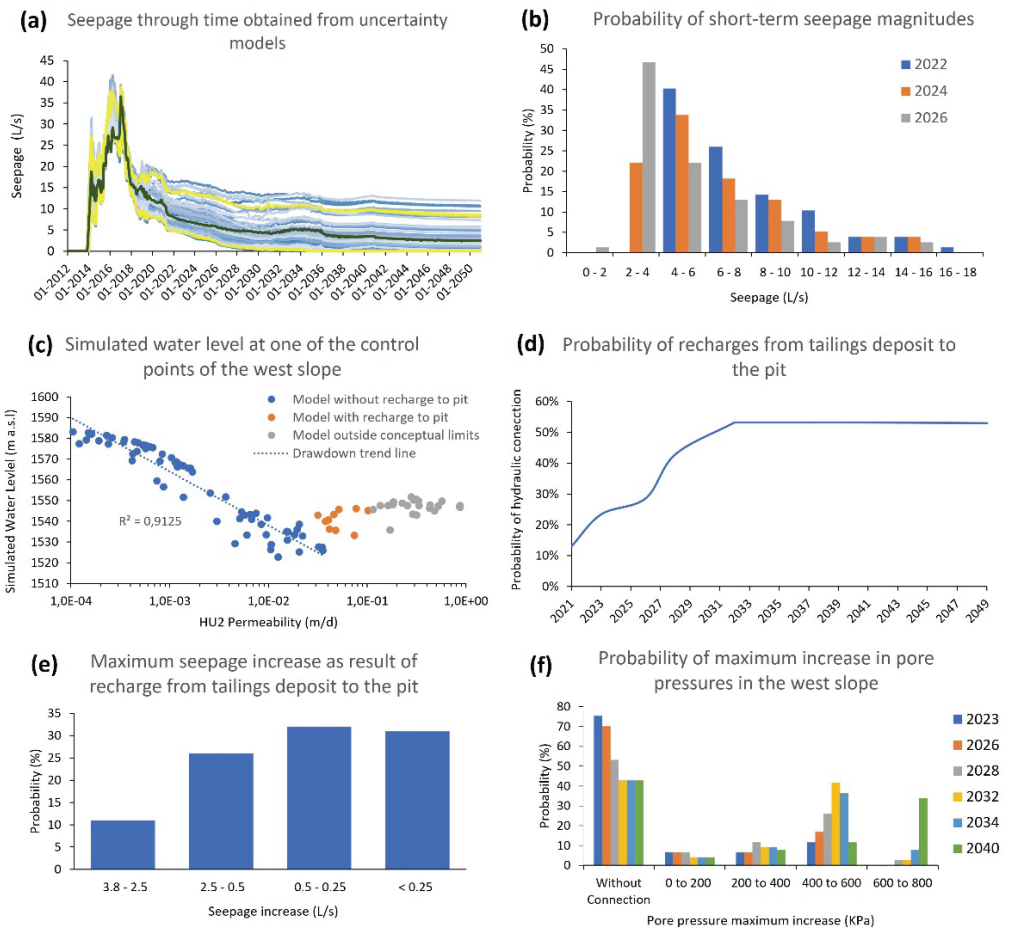


Figure 3 *Results of uncertainty analysis. (a) Seepage over time; (b) Pit seepage magnitudes for short-term; (c) Correlation between drawdown in west slope water level and HU2 permeability; (d) Probability of recharges to reach the pit; (e) Magnitude of the maximum seepage increase; (f) Increase of pore pressure through time*

because they exceeded the conceptualized seepage flow for the current condition by more than two times. These models, which were considered improbable from a mass balance standpoint, correspond to the models that have a permeability outside the conceptual ranges in the HU2.

Accepted models showed seepage flows between 4.9 and 16.4 L/s for the calibration date, all decreasing over time in the predictive simulations (fig. 3a). This is consistent with a pit being excavated into less permeable rock and with an aquiclude that has been drained through time. Since all the models are considered equiprobable, the results can be used to define the probability of the magnitude of the seepage flows for the following years (fig. 3b).

Pit seepage shows a good correlation (R^2 = 0.94) with the HU2 permeability in the models, which is reasonable because this unit has the highest control in the transmissivity of groundwater flow. It should be noted that this correlation doesn't mean that there is necessarily a direct hydraulic connection between the TSF and the pit, since the increase of the HU2 permeability generates an increase in the inflow to the pit from all directions.

Hence, the hydraulic connection between the TSF and the pit seepage was evaluated by analyzing the water level on the west slope of the pit, comparing the effect of depressurization between the models. Since it is expected that for a certain point and same date models with higher HU2 permeabilities will show a greater drawdown due pit depressurization, a correlation should be observed between these two variables. In this way, water table in models deflected from this correlation, would indicate the influence of the mound coming from the TSF (fig. 3c).

Thus, the analysis (fig. 3d) shows that there is a 13% probability that TSF infiltration is already producing recharge in the pit, influencing seepage zones and pore pressures. Over the years, the probability of the hydraulic connection between both operational facilities increases to 23% in 2023, 29% in 2026, 43% in 2028 and 53% in 2032. After 2032, the probability remains constant due to the end of the expansion of the mine to the west and the decrease in infiltrations from the tailings.

Increase in seepage was quantified through predictive simulations without infiltrations from the TSF using six models with different ranges of HU2 permeability. The results show that in the most unfavorable scenario the maximum increase in the inflow to the pit could be of 3.8 L/s during the forecast period, although it is very likely that the increase in flow would be low, with a probability of 63% that would be less than 0.5 L/s (fig. 3e).

Likewise, this recharge to the pit would generate greater pressures on the west slope, which in some cases would generate an increase in groundwater levels over time instead of the expected decrease due to depressurization. In the most unfavorable case analysed, this increase could raise groundwater levels up to 25 m compared to the current condition by the year 2032 and generate levels 75 m higher than the cases without hydraulic connection during the year 2028. Additionally, the analysis shows that there is a probability of 42% of having pore pressure increases between 400 and 600 KPa on the west slope during the year 2032 and 34% that it would increase between 600 and 800 KPa by 2040 (fig. 3f).

Discussion and Conclusions

Uncertainty analysis results indicate there is a probability of 53% that TSF infiltrations will result in seepage to the pit in the coming years due to a hydraulic connection between the TSF and the pit. However, there is a probability of 63% that the increase in seepage will be low, and less than 0.5 L/s compared to the models without recharge from the TSF. Even though there is a probability of 11% that the increase could be greater than 2.5 l/s, all analyzed simulations show that the seepage will decrease over time to values under those currently conceptualized and observed.

Recharges to the pit would also increase pore pressures in the west slope of the pit, with a probability of 45% that they would increase more than 400 KPa from 2032 onwards. The implication of these increases is uncertain and should be further studied with adequate pit slope stability analysis.

This analysis has shown that the effects associated with infiltration from the TSF correlate and depend on the permeability of HU2, which reinforces the need to keep the hydrogeological characterization of this unit. It has also allowed estimation of the possible impacts that infiltrations from the TSF would have on the pit and their probabilities of occurrence. This provides useful information to support decision-making in terms of risks assessments for the operation, and the generation of prevention plans.

Acknowledgments

The authors acknowledge Dr. Steve Meyerhoff and Mr. Cliff Tonsberg for their comments and review of this paper.

References

Azrag E, Ugorets V, Atkinson L (1998) Use of a finite element code to model complex mine water problems. Proceedings of Symp on Mine Water Environ Impacts, International Mine Water Association, Johannesburg.

Barnet B, Townley LR, Post V, Evans RE, Hunt RJ, Peeters L, Richardson S, Werner AD, Knapton A, Boronkay A (2012) Australian Groundwater Modelling Guidelines – June 2012. National Water Commission Australia, Waterlines Report Series No. 82, ISBN:978-1-921853-91-3.

Beale G, Read J (2013) Guidelines for evaluating water in pit slope stability. CSIRO Publishing, Collingwood.

Devy S, Hutahayan P (2021) Groundwater Effect on Slope Stability in Open Pit Mining: A Case of West Kutai Regency, East Kalimantan, Indonesia. Jour. of Geosc., Eng., Env., and Tech., 6(4): 192-205.

Evan, G, Henriquez, F, Ugorets V (2015) Pit Slope Optimization Based on Hydrogeologic Inputs. IMCET – Int'l Mining Congress and Exhibition of Turkey.

Itasca Denver Inc (2020) MINEDW – 3D Groundwater Flow Code for mining applications in 3D. Denver.

Middlemis H, Walker G, Peeters L, Richardson S, Hayes P, Moore C (2019) Groundwater Modelling Uncertainty – Implications for decision-making. Summary report of the national groundwater modelling uncertainty workshop, 10 July 2017. Flinders Univ, National Centre for Groundwater Research and Training, Australia.

Morton K, Van Niekerk F (1993) A phased approach to mine dewatering. Mine Water Environ. 12: 27-33.

Nilsson B, Højberg A, Refsgaard J, Troldborg L (2006) Uncertainty in geological and hydrogeological data. Hydrology and Earth System Sciences Discussions, European Geosciences Union 3(4):2675-2706.

Read J, Stacey P (2009) Guidelines for Open Pit Slope Design. CSIRO Publishing, Collingwood.

Refsgaard J, Van der Sluijs J, Brown J, Van der Keur P (2006) A framework for dealing with uncertainty due to model structure error, Adv. Water Resour., 29:1586–1597, doi: 10.1016/j.advwatres.2005.11.013

Servicio de Evaluación Ambiental (SEA) (2012) Guide for the use of groundwater models in the SEIA [in spanish]. Santiago, Chile.

Facilitating Sustainable Mine Water Irrigation

John George Annandale[1], Phillip Dale Tanner[1], Sarah Nicole Heuer[1], Gideon van der Walt[1], Karabo Deane[1], Heinrich Meiring du Plessis[1]

[1]*Department of Plant and Soil Sciences, University of Pretoria, South Africa*

Abstract

Responsible mine water irrigation can reduce water treatment costs and create sustainable livelihoods upon closure. However, guidance is required to assess mine water fitness-for-irrigation, and the steps to take to set up a successful mine water irrigation scheme need to be clearly set out. As proof of concept and to facilitate informed decision making around establishment and regulation of mine water irrigation schemes, a carefully monitored commercial scale Demonstration Site has been successfully irrigated for five cropping seasons with untreated circum-neutral mine water. Technical Guidelines for Mine Water Irrigation were developed to assist potential irrigators and regulators.

Keywords: Mine water irrigation, irrigation water quality guidelines, irrigation site selection, monitoring, adaptive management

Introduction

Modelling and past experience has shown that irrigation with especially gypsiferous mine waters, can be successfully and sustainably undertaken (Annandale *et al.* 2002). However, regulators and practitioners are understandably concerned about the productivity and environmental impacts of a large-scale roll out of mine water irrigation. To overcome their concerns, and to facilitate informed decision making around the establishment and regulation of mine water irrigation schemes, support is needed. To this end, a commercial scale Mine Water Irrigation Site was established to demonstrate the feasibility of mine water irrigation, and Technical Guidelines for Mine Water Irrigation were developed to assist potential irrigators and regulators.

Commercial Scale Mine Water Irrigation Demonstration

Location and Water Quality

A 19 ha irrigation centre pivot was established on previously un-mined land in Middelburg, Mpumalanga Province, South Africa. This field has been irrigated with untreated circum-neutral mine water since September 2017, and has been carefully monitored to ascertain if crops are economically produced, if produce is safe to consume, and if any environmental impact is within acceptable limits. A Google Earth image of the Demonstration Site is presented in Figure 1, with the location of ground and surface water monitoring points indicated.

The irrigation water quality is gypsiferous, with pH ranging over the last five cropping seasons from 7.5 to 8.1, electrical conductivity (EC) was between 140 and 240 mS/m, with sulfate levels as low as 640 and as high as 1070 mg/L. Cumulative irrigation of this site is in excess of 1400 mm, with 23.6 t/ha sulfate, 4.7 t/ha Ca, 2.3 t/ha Mg, 1.8 t/ha Na, 0.65 t/ha K and 0.5 t/ha Cl applied to this field.

Cropping System and Food Safety

The field is farmed commercially by a local farmer who specialises in maize (*Zea mays*) production. Except for a three-month period in which stooling rye, a small grain planted for grazing, was produced on request of the research team, this field has been under mono-culture maize production. It is important to know whether crops produced are safe for human and animal consumption, as it is pointless to produce high yields of a food or fodder crop that cannot be utilised. In such cases, non-edible industrial crops could be considered.



Figure 1 *Location of the Demonstration Pivot and surface and ground water monitoring points*

It is therefore important to analyse grain and whole plant samples and compare their elemental concentrations to current guidelines for food and fodder safety. Since maize is produced for local and international markets, it is important to ensure that it falls within both local and international guidelines for food and fodder safety.

The guidelines provide accepted thresholds for elements of concern such as arsenic, lead and other trace elements. Table 1 presents concentrations of the five elements of potential concern found in the local and international food and fodder guidelines for maize grain. It can be seen that grain elemental concentrations were an order or two of magnitude below the accepted local and international thresholds, thus indicating that they are extremely safe for human and animal consumption.

Table 1 *Comparison of grain element concentrations with accepted food and fodder safety thresholds for the 2021-2022 season*

Element	Average concentrations in white maize grain	China	EU/USA	Ireland	SA Feed safety
			ppm or mg/kg		
As	-	0.5	-	-	2
Cd	0.01	0.1	0.1	0.1	1
Zn	0.2	-	-	-	150
Pb	0.01	0.2	0.2	0.1	10
Hg	<0.001	0.02	-	-	0.1

Table 2 *Yields and profitability of dryland and irrigated maize (current exchange rate ~ R18/USD)*

Season	Yield (t/ha)		Cost per ha		Maize price	Earnings per ha		Profit/Loss per ha	
	Irrigated	Dryland	Irrigated	Dryland	per ton	Irrigated	Dryland	Irrigated	Dryland
2017/18	13.5	4.5	R18000	R16000	R2103	R28390	R9460	R10390	R6540
2018/19	11.6	5.5	R18770	R16800	R2910	R33760	R16010	R14990	R790
2019/20	14.3	4.9	R19700	R17700	R2450	R35040	R12010	R15340	R5690
2020/21	12.2	8.4	R20600	R18580	R3508	R42800	R29470	R22200	R10890
2021/22	14.2	8.7	R2200	R19509	R4079	R57920	R35490	R35920	R15980

Environmental Impact

No discernible changes in soil quality have been observed since the commencement of irrigation. Surface water quality is monitored at the downstream Beestepan Dam (Figure 1). This water body's quality is closely monitored, and it was initially decided that if a 20% increase in sulfate concentration was observed from the average pre-irrigation SO4 concentrations between 2014 and 2017, then irrigation would need to stop immediately. This trigger value, however, was later deemed flawed, as the monitoring point is also downstream of a discard dump (Figure 1). As a result, any increases in sulfate or any other elements could not automatically be deemed to be as a direct consequence of irrigation alone, and accordingly the "stop" instruction has been modified so that irrigation will only cease if any increase in pollution of the Beestepan Dam can be directly attributed to flows from the Unmined Pivot. Despite this concern, the threshold for sulphate concentration (642 mg/L) is yet to be reached (see Table 3).

Groundwater is monitored at a shallow (10 m) and deeper (30 m) depth, in boreholes sited both up and downstream of the irrigated field. Figure 2 presents SO4 concentrations since the commencement of irrigation in 2017. It is clear that the discard dump downstream of the irrigated field influenced groundwater quality before mine water irrigation started. The sharp increase in SO4 concentration in the wet summer months of 2020 is suspected to reflect the effect of runoff water from the stockpile, and it seems that no deterioration in groundwater quality can be ascribed to irrigation at this stage.

Technical Guidelines for Mine Water Irrigation

A Technical Guideline has been developed to support water users considering irrigation with mine waters, and those who will be required to regulate such irrigation schemes (Heuer *et al*. 2021). A separate set of guidelines, aimed at providing guidance for obtaining regulatory approval of irrigation with mine waters has also been published (Pocock and Coetzee, 2021).

The *Technical Guideline for Irrigation with Mine-Affected Waters*, follow a logical decision tree structure, with a source-pathway-receptor approach to determining monitoring requirements and thresholds for action. They provide a standardised framework for the establishment and stewardship of irrigation with specific mine-affected waters in South Africa. They advise on the use of the Irrigation Water Quality Decision Support System (DSS) published by du Plessis *et al*. (2017), to provide site-specific, risk-based assessments of the fitness for use of mine

Table 3 *Average water quality for Beestepan Dam*

Parameters	Oct '14 to May '17	Sept '17 to May '18	Sept '18 to May '19	Sept '18 to May '20	Sept '20 to Aug '21	Sept '21 to Aug '22
pH	7.1	8.1	7.93	7.7	7.72	7.52
EC(mS/m)	115	70	102	105	122	111
SO_4 mg/L	535	282	406	402	485	401
Na	52	30	45	45	48	48

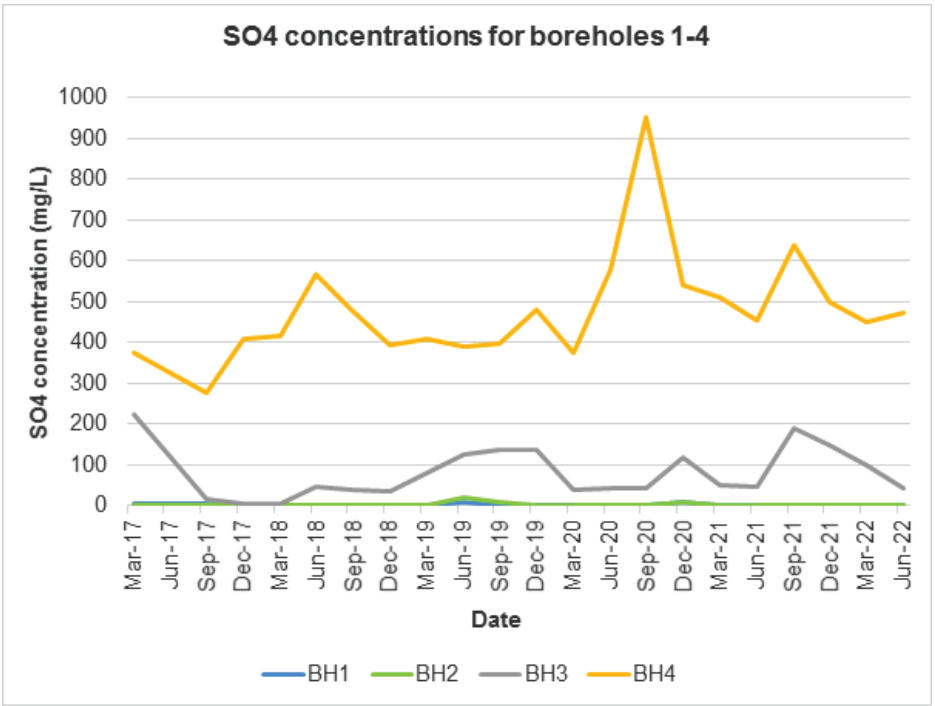


Figure 2 *Borehole sulfate concentrations since the commencement of irrigation. BH1 – deep upstream, BH2 – shallow upstream, BH3 – deep downstream, BH4 – shallow downstream*

waters for irrigation. In addition, appropriate site irrigability characterisation procedures are provided in order to identify an irrigation landscape capable of sustainably supporting a mine water irrigated cropping system. A risk assessment framework to identify potential key unwanted events that may occur as a result of irrigation with mine water is proposed, with guidance on a methodology to identify constituents of potential concern and to determine thresholds for action. An integrated monitoring regime is proposed to ensure that qualities of soils, waters and crops fall within acceptable environmental thresholds, and in the event that monitoring identifies constituents of concern exceeding acceptable levels, adaptive management strategies to remedy the situation are recommended.

The recommendations of the guideline should be of value regardless of geographical region, the resource mined, and the nature of the mine water considered for irrigation. The consideration of site-specific factors is emphasized as key to project success. Key aspects of the guideline are briefly highlighted:

Water Resource

It is essential that estimates are made as reliably as possible, of mine water volumes and quantities expected over time, as these are the key drivers of any mine water irrigation scheme. In addition, it is important to estimate the seasonality of water supply and to ascertain if water storage is available for times when irrigation is not possible, like in wet weather or during crop maturation drying off or fallow periods. If the site does not have a long-term positive water balance, then irrigation should not be considered.

Fitness-for-Use (FFU) Assessment

Having determined that surplus water of an estimated or known quality will need to be managed, the next step is to ascertain if there are conditions under which it can be used for irrigation. Such assessments are site specific, as climate, cropping system, and irrigation method and management, all affect the usability of a specific water source. The

Irrigation Water Quality DSS of du Plessis *et al*. (2017) can be used to make site-specific and risk-based FFU assessments. The DSS considers the effect of irrigation with a specific water quality on soil resources, crop yield and quality, and possible effects like corrosion and scaling of irrigation infrastructure. These simulations also estimate crop water use of different cropping systems, thereby enabling estimates of irrigated area required to utilise the available water. Crop water use predictions also assist with estimates of storage capacity, if required. If the mine water can be responsibly used for irrigation, and a cropping system and irrigation management strategy has been selected, then Water Quality Requirements (WQR) can be assessed with the DSS to provide benchmark water qualities required for this specific use. These are useful, because if water quality deteriorates, decisions need to be taken around partial water treatment, or perhaps an alternative cropping system with more tolerant crops needs to be considered. Obviously if the mine water source is not suitable for irrigation, other water management options need to be investigated.

Siting the Irrigation Scheme

It will clearly be most economical, from an irrigation infrastructure point of view, to site irrigated fields as close to the water source as possible. However, it is essential that free draining fields of gentle slope be selected, as excessive levels of soluble salts building up in the soil profile will result in the scheme failing over time. Ecologically sensitive and wetland areas are to be avoided.

Gypsiferous mine waters are particularly suitable for mine water irrigation (Annandale *et al*. 2006), as root water uptake concentrates the soil solution and gypsum precipitation results. This lowers root zone salinity, which is beneficial for crop production, and reduces salt mobilisation to ground and surface water bodies, thereby reducing environmental impact. The position of irrigated fields in the hydrological landscape is also important, as it is essential to ensure that the increase in recharge rate brought about by irrigation, will not result in water logging and salinization of the irrigated fields.

Environmental Monitoring and Adaptive Management

It is important to identify potentially negative impacts of irrigation with mine waters. Effects on soil, water and crop resources should be considered. The DSS highlights potential constituents of concern, and a monitoring programme needs to be put in place, with clearly defined thresholds for action. Adaptive management is suggested should thresholds be exceeded, but if environmental impact appears to be unacceptable, then irrigation should cease and alternative water management plans need to be implemented.

Competent, independent experts' recommendations and oversight are essential to the success and sustainable use of mine water for irrigation.

Conclusions

A successful commercial scale mine water irrigation demonstration site has been established, that has proved useful as a proof of concept for regulators and mining houses considering irrigation as a water management option. Technical Guidelines set out propose processes to follow to establish mine water irrigation schemes, that include assessing volumes, seasonality and quality of water available, as well as storage requirements, the selection of appropriate cropping systems, site selection to ensure that soils are irrigable and well positioned in the hydrological landscape, and the development of monitoring programmes, thresholds for action, and adaptive management strategies.

Acknowledgements

The authors thank the Water Research Commission of South Africa, Mafube Colliery and the Mine Water Co-ordinating Body for financial support for this research.

References

Annandale JG, Jovanovic NZ, Tanner PD, Benadé N, du Plessis HM (2002). The sustainability of irrigation with gypsiferous mine water and implications for the mining industry in South Africa. Mine Water and the Environment, 21: 81-90

Annandale JG, Jovanovic NZ, Hodgson FDI, Usher B, Aken ME, van der Westhuizen AM, Bristow KL, Steyn JM (2006) Prediction of the environmental impact and sustainability of large-scale irrigation with gypsiferous mine-water on groundwater resources. Water SA, 32 (1): 21-28

Du Plessis M, Annandale J, Benade N, Van Der Laan M, Jooste S, Du Preez C, Barnard J, Rodda N, Dabrowski J, Nell P (2017) Risk based, site-specific, irrigation water quality guidelines: Volume 2: Technical Support. WRC Technical Report. No TT 728/17. Water Research Commission, Pretoria, South Africa

Heuer S, Annandale JG, Tanner PD, du Plessis HM (2021) Technical Guidelines for Irrigation with Mine-Affected Waters. WRC Technical Report. No TT 855/2/21. Water Research Commission, Pretoria, South Africa

Pocock G, Coetzee L (2021) Guidance for Attaining Regulator Approval of Irrigation as a Large Scale, Sustainable Use of Mine Water. Water Research Commission Technical Report No TT 837/21, Water Research Commission, Pretoria, South Africa

Passive Leached Water Mine (P.L.W.M.) – A sustainable approach to mine water remediation and metals extraction

Nikolaos Apeiranthitis[1], Karl Kraavi[1], Alexander Finlay[1], H. Chris Greenwell[2], Eddie Merrick[1]

[1]*X-ray Mineral Services Ltd, 1 Claughton Road, Colwyn Bay, LL29 7EF, UK*

[2]*Durham University, Science Site, DH1 3LE, Durham, UK*

Abstract

Although there is little active mining in Wales, legacy mine sites still cause large scale environmental disruption; limiting grazing time in fields affected by metals leaching from spoil heaps, and over 200 km of rivers are impacted by historic metal mines. Furthermore, the transition to "green" technologies is necessitating an increase in mining, and the realisation of supply security, of both traditional and "critical" metals such as Rare Earth Elements (REE), Cobalt and Lithium. Passive Leached Water Mine (PLWM) remediation is a new technology developed by X-ray Minerals Service Ltd (XMS) and Durham University which seeks to address both of these issues.

Introduction

PLWM technology is both passive (relying on gravity to enable waters to pass through the filter media with no pumping required) and is highly effective at remediating mine waste water contaminated with (potentially critical) metals. Furthermore, there is also the potential to recover these extracted metals as a valuable by-product of the process. In this paper, the results of the latest trial (part funded by the Welsh Government SMARTCymru scheme) at Pugh's Adit, Cwmystwyth (Figure 1) will be presented and discussed. The first field test demonstrated the technical and commercial feasibility of the process. A 200 L filter unit with a retention time of 20 min, treating 85,000 L of water over 10 days in December 2019 recovered 80% of Pb, 75% Zn, 70% Ni,70% of Co and 92% of REE. Following this in May 2021, a larger industrial research phase of work enabled a 1000 L filter to be run at the same rate over 58 days, treating up to 500,000 litres of water. This longer test extracted 1kg of both Pb and Zn from Pugh's Adit.

XMS is currently further developing the technology, through an 18-month part funded Innovate UK SMART award, enabling a 1 year, 4000 L filter test to be undertaken. We are envisaging that by the end of this project, the full remediation capacity of this filter technology will be determined, in terms of water initial and variable concentrations, pH, seasonal changes, filter media reusability as well as operations costs and positive environmental impact.

Alginate material fundamentals

Alginate forms the basis of our filter material. It is well studied and descripted (Draget and Taylor 2011, Mohammed *et al*. 2022) and its robust nature, forming egg-box gel structure after a (divalent) cation is introduced, makes it versatile to be used across applications, (Hu *et al*. 2021) . In the case of the alginate (and PLWM), metal adsorption series has been established (Equation 1), through experimental work (Haug 1961) and corroborated by (Wang 2016). It can be seen that Pb has higher affinity than Ca which in turn has higher affinity than Zn, Ni and Co.

$Pb^{2+} > Cu^{2+} > Cd^{2+} > Ba^{2+} > Sr^{2+} > Ca^{2+} > Co^{2+}$, Zn^{2+}, $Ni^{2+} > Mg^{2+}$ (Equation 1)

The binding mode also is different for these elements, with Ca inducing the known egg-box configuration while Zn inducing a weak and less homogenous structure, (Hu *et al*. 2021) This different configuration and binding modes should play a role on the performance of the initial Ca-alginate egg-box structure, on any multi-metal adsorption process, along with pH, initial

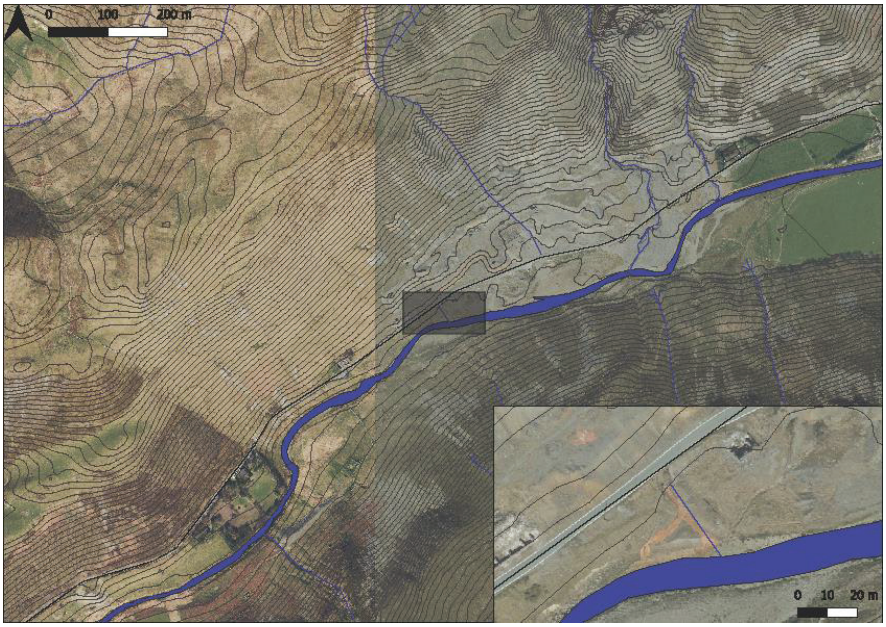


Figure 1 *Aerial imagery and elevation contour map of the old mine area of Cwmystwyth Lead mine. River Ystwyth and streams are in blue, while Pugh's Adit is shown at the bottom right on a different observation scale.*

metal concentration, temperature, and contact time (Montazer-Rahmati *et al*. 2011)

Materials and field trial set-up

Alginate beads

Starting with alginate raw material, beads were made in the lab, using tap water and onsite by mixing with water at Cwmystwyth, by dripping into a non-toxic gelling agent to form 5mm semi spherical filter beads.

Filter unit

For this field trial, 2 X 2 filter units were used in parallel, Filters A & B and Filters X & Y, all with same volume capacity of 225 L. In Filters A & B, the lab-made alginate beads were used, while in Filters X & Y, the on-site alginate beads were used.

End-to-end system water flow description

Water flow from Pugh's Adit is controlled by a metal box, connected by pipe to our filter system, (Figure 2). It has been established from the previous internal research projects that 20 min retention time through the two filter units, translated to 3 L/min water flow through the filter media, is a cost-effective rate for high metal remediation. An entry water flow of 7-8 L/min was regulated for achieving a complete passive flowing system.

Water analysis

Water samples were collected over the period of the trial, at the inlet of the filter units, after filter A, and filter X, and after filter B and filter Y, which constitutes the treated water

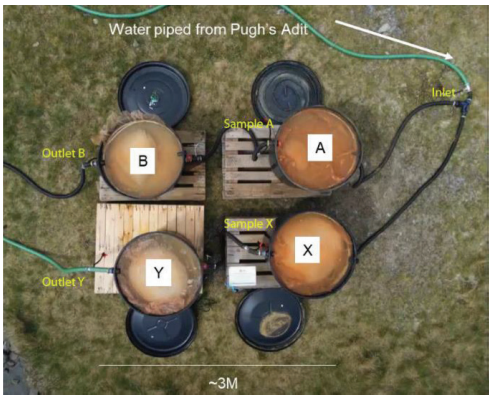


Figure 2 *Aerial imagery of filter A-B and filter X–Y, as laid out during the field trial. Water pipe from Pugh's Adit, filter units, A, B & X, Y as well as sampling points Inlet, Sample A, Outlet B, Sample X and Outlet Y are annotated. System's footprint is 3 m × 3 m.*

concentrations. Water samples were kept in a cool box and sent for analysis the next day. All analysis was done with ICP-OES/MS at Greenwich University, with NIST 1640a being the used standard.

Results

The following results correspond to a field trail during May-July 2021, for assessing how filter media would respond in temperature fluctuation in our testing area of Cwmystwyth mine. This 2-months test was part of a set of field trials assessing filter media performance to higher or lower temperature and rainfall, spanned from November 2020 to August 2021.

The key findings of the series of trials study demonstrated that:

- General changes in temperature and rainfall did not affect filter performance.
- The filters were not affected by freezing (although pipe work did freeze leading to a blockage of water to the filter which will be rectified by insulating pipework in the future)
- The filters did not dry out when water levels fell to the extent that the filter system lost the necessary head to have waste-water flow through it. They stayed damp in the filter and continued to work when flow recommenced.

Focusing more on the analytical findings of the May-July test, the first samples (inlet and filter outlets) were taken on 26/05/2021, with overall sampling placed every 1–4 days until 23/07/2021. The main elements of interest monitored were Pb and Zn, followed by Ni, Co and Total_REE elements (In + Lanthanides). The inlet concentrations of these elements along with the Environmental Quality Standard (EQS) for Pb at 1.2 ug/L and Zn at 15 ug/L, are given in Figure 3. For both elements, the concentrations found over the course of the trial were above those environmental guidelines as established in the Water Framework Directive. For the EQS of Zn, the ambient background concentration of the area is taken into account, as well.

Interestingly, it can be clearly seen how different elements are related to each other. As Pb (Figure 3, top left) and Zn (Figure 3, top right) are the main elements of interest, in the second row the total REE concentration and Ni, Co concentrations are plotted, respectively. The concentration response of REEs is following that of Pb, while Ni and Co is following that of Zn, demonstrating elemental relevance of the expected metalliferous mineralogy of galena (PbS) and sphalerite (ZnS).

Assessing the performance of filter A–B and filter X–Y, on adsorbing Pb, Zn measured

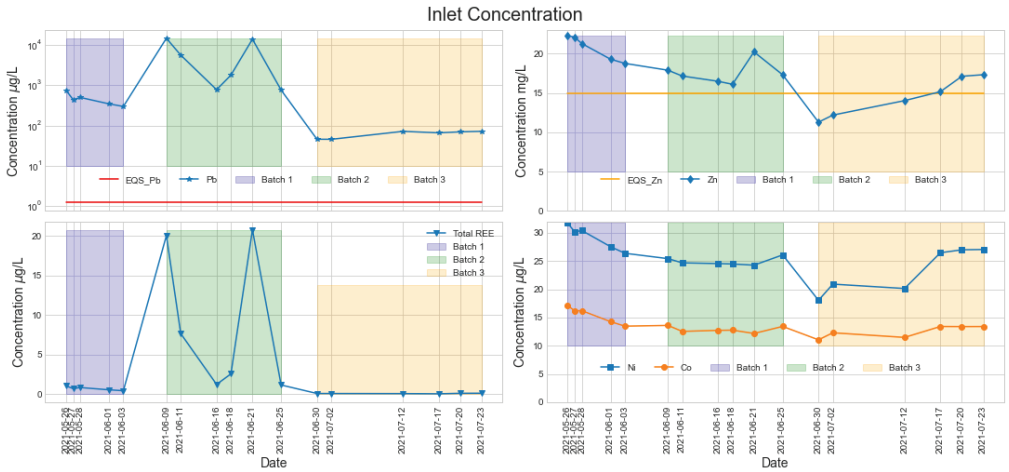


Figure 3 Inlet concentration time series of Pugh's Adit, as collected at the inlet of the filter system and analysed, between 26/05/2021 and 23/07/2021. Different batches of collected samples, Batch 1, Batch 2 and Batch3 dates are shaded accordingly.

at the outlet of each linear set-up, Figure 4, it can be said that, both exhibited very high adsorption capability removing Pb from the water, despite the fact that filter X–Y alginate beads were made with river water.

Zinc was problematic. To start with, the filters were highly effective, however this, combined with the order of magnitude higher level of zinc in the waste water compared to other elements, meant that the filter media was quickly overwhelmed. Therefore, for the majority of the filter test, Zn adsorption was not as good as for Pb. If the Batch 1 pattern of Zn is carefully observed (Figure 4, top right), the effluent concentrations for the first three incidents, is between 25–50 % of the inlet, while after that the filter system seems saturated in Zn. Similarly, for filter X–Y (Figure 4, bottom right), the first concentration incidents show a good Zn adsorption while for the rest of the trial, the filter is also saturated with Zn.

Total adsorption % was calculated and presented in Figure 5 for filter A & B and filter X & Y. It can be seen that the difference in adsorption capacity based on the initial water used for constructing filter media, tap water vs river water, has a small effect. It should be noted that for Pb (in both filter system) and for Batch 1, the adsorption % drops, while for Batch 2 reaches 99% Pb recovery, before it drops below 60% for Batch3. That can be described as an anomalous recovery pattern, while on the other hand Zn, starts with a 40% total recovery in both filter systems, fluctuating downwards to 0% or negative % (meaning filter desorbs Zn into the water). One explanation for Pb adsorption pattern is the destructive behaviour of Zn towards the Ca-alginate structure as discussed previously, for Batch 1, which is minimised for Batch 2 & Batch3, allowing higher adsorption % for Pb, consistent for both filter systems.

On average, for Batch1, Batch 2 and Batch 3, different metal recovery % was achieved, as shown in Table 1. No standard deviations of concentrations are given, as the scope of that trial was to assess, at a high level only, adsorption efficiency of filter material. Furthermore, the adsorption patterns of Pb and for the REE show some irregularity through the three batches, which is a point for further research during the 1-year trial imminently commencing. All standard

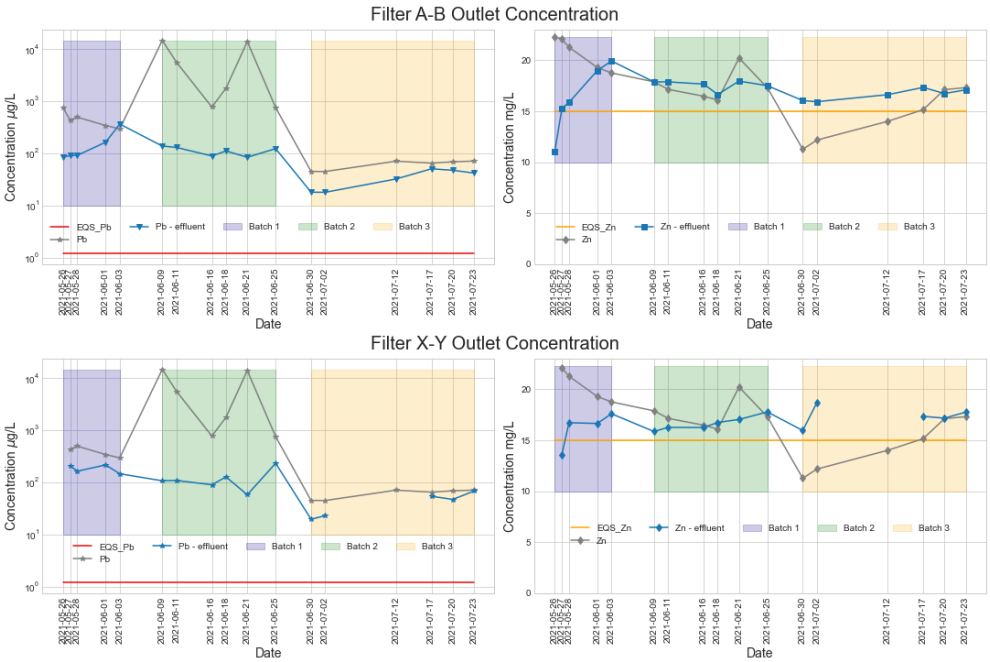


Figure 4 *Effluent concentrations of Pb and Zn for both filter systems, A-B (top row) & X-Y (bottom row). Blue lines are the effluent concentrations while grey lines are the inlet concentrations plotted for comparison.*

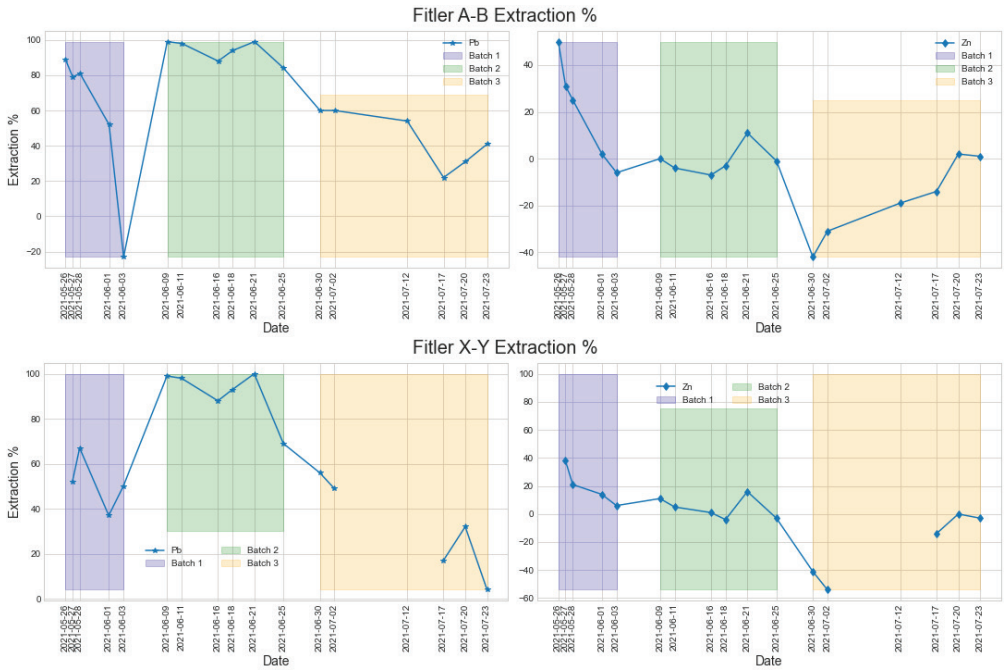


Figure 5 Extraction % of Pb and Zn for filter A-B (top row) and filter X-Y (bottom row).

practise, for water analysis, and element concentration reporting, is to be followed during this extended trial.

Social and economic value

- After this series of trials, and despite of the small relative scale of treated water, we deem the results as having a positive environmental impact for the old mine area and the river system in overall. It demonstrates the ability of a simple and adaptable technology as a solution for treating mine waste water. Additionally, the local community has also being interested of this technology implementation seeing the positive outcomes for improved river water quality, affecting livestock and other local activities. We envisage that the 1-year long trial will further establish the technology for the described benefits
- Despite this test being on a small, industrial research scale, over 500,000 litres of water were treated, leading to the removal of ~1kg of Zinc and Lead (and 10s of grams of Rare Earth Elements and Lithium). Furthermore, lab-based research has demonstrated the feasibility of extracting these metals in a form amenable to commercial extraction. As described above, the main control on removal efficiency appears to be the overloading of the filter media by Zinc. The addition of a new dosing system will be implemented in the imminent new large-scale test of the filter system, tackling the Zinc oversaturation media

Table 1 Average metal recovery % of key elements for Batch 1, Batch 2, Batch 3

Filter A–B	Pb	Zn	REE	Ni	Co
B1	56%	20%	35%	19%	14%
B2	94%	-1%	90%	-3%	-3%
B3					
Filter X–Y					
B1	52%	20%	33%	20%	15%
B2	78%	4%	86%	2%	1%
B3	32%	-22%	-20%	-23%	-13%

effects. If successful, it is expected that metal removal will increase, highlighting the real potential to "remine" metals during the water remediation process. We look forward to presenting the results of this test in a future IMWA conference.

Conclusion

In this work it was demonstrated a new passive technology for mine water treatment. The system was employed at a highly Pb and Zn contaminated abandoned mine stream, showcasing a strong potential water mine clean up, with highest metal adsorption of over 90% across the course of a 2-months trial. Due to high adsorption of other valuable elements such as REE, Ni, Co and potentially Cu, this technology can have a positive impact on partially covering operational costs of system deployments. Batch experiments of spent filter media re-charging, with concomitant metal recovery, show strong results of using the same bead media volume for several adsorption/ desorption cycles, further reducing the operational costs.

As it was apparent from results shown above, Zn has saturating / destructive effects on the system. For more efficient adsorption, several established precipatation solutions are being considered, prior to water entering the main filter system.

In attempt to make beads on-site, river water was used successfully, having minor effect on final adsorption capacity and life of filter system, thereby massively reducing the need to transport raw materials to a remediation site, making it highly suitable for remote rural sites, and lowering the cost of transport and making the technology more practical.

Acknowledgements

We wish to acknowledge the support provided to this project through the SmartCymru funding scheme.

Authors would like to thank Chris Hughes, a retired X-Ray Mineral Services, Technical Development Manager, for leading this work the past years. His commitment to the project was beyond valuable.

Also, thanks should be extended to the many Durham University and the Greenwell Group students, who worked in the lab and the field trials, completing significant part of the research, with their work being the basis of our technical understanding of the filter media.

References

Draget KI, Taylor C (2011) Chemical, physical and biological properties of alginates and their biomedical implications. Food Hydrocoll 25:251–256. https://doi.org/10.1016/j.foodhyd.2009.10.007

Haug A (1961) The affinity of some divalent metals to different types of alginate. Acta Chem Scand 8:1794–1795

Hu C, Lu W, Mata A, *et al* (2021) Ions-induced gelation of alginate: Mechanisms and applications. Int J Biol Macromol 177:578–588

Mohammed C, Lalgee L, Kistow M, *et al* (2022) On the binding affinity and thermodynamics of sodium alginate-heavy metal ion interactions for efficient adsorption. Carbohydrate Polymer Technologies and Applications 3:. https://doi.org/10.1016/j.carpta.2022.100203

Montazer-Rahmati MM, Rabbani P, Abdolali A, Keshtkar AR (2011) Kinetics and equilibrium studies on biosorption of cadmium, lead, and nickel ions from aqueous solutions by intact and chemically modified brown algae. J Hazard Mater 185:401–407. https://doi.org/10.1016/j.jhazmat.2010.09.047

Mesocosm experiments performed in 1975, 1993 and 2017 to determine changes in release rates of zinc from sediments affected by an old mining operation

Mattias Bäckström[1], Lotta Sartz[2]

[1]*Man-Technology-Environment Research Centre, Örebro University, 701 82 Örebro, Sweden, mattias.backstrom@oru.se*

[2]*Bergskraft Bergslagen AB, Södra Kungsvägen 49, 692 30 Kumla, Sweden, lotta.sartz@bergskraft.se*

Abstract

Processing of zinc/lead/silver ore started in Åmmeberg, Sweden, in 1860 and ceased in 1977. Water from the operation was discharged into a northern part of Lake Vättern called Kärrafjärden.

Mesocosm experiments were performed on sediment cores sampled at the same five locations in 1976, 1993 and 2017 close to the mining operation. Experiments were performed in the same way as the original experiment in 1976 to determine the release rates of zinc as a function of time.

In 2017 the release rates were in the range 0.18–1.5 for zinc, 0.00021–0.0015 for cadmium and 0.00098–0.016 mg/day*m^2 for lead with the highest rates closest to the historical mining site.

Most of the reduction in release rates occurred between 1976 and 1993, while the difference between 1993 and 2017 was lower. This indicates that the release of zinc from the historical site is continuing, albeit at a significantly lower rate compared to 1976. It can also be concluded that this type of experiments can assist in understanding the mass transfer of trace elements from sediments to surface waters.

Keywords: Mining, leaching, sediments, trace elements, release, mass transfer

Introduction

Sediments impacted by historical mining operations can be an important secondary source for trace elements through different redistribution mechanisms (Ciszewski *et al*. 2012). It is important to understand what happens with trace elements in sediments when mining operations cease as this will increase the understanding about the possible future environmental impact.

Processing of zinc/lead/silver ore started in Åmmeberg, Sweden, in 1860 and operation ceased in 1977. During that period several different methods were used to process and enrich the ore; from mechanical treatment to more modern flotation. Water from the operation was discharged into a northern part of Lake Vättern called Kärrafjärden.

Sediments downstream Åmmeberg are contaminated with trace elements (primarily lead, zinc and cadmium) to a varying degree. Different external factors can affect the chemistry in the sediments and thus increase the mobility of the trace elements. Several different leaching schemes for laboratory studies have been suggested to determine leachability of trace elements from sediments (Guo *et al*. 1997; Ciszewski *et al*. 2012; Cai *et al*. 2021). They are all, more or less, suffering from the drawback that the obtained results are difficult to translate into real world leachability. The purpose of the present investigation is to estimate the amount of trace elements (primarily zinc, lead and cadmium) that are being released from the sediments by determining the current release rates. Identical investigations were performed at the same sampling sites in 1976 (Borg *et al*. 1977) and 1993 (Göthberg *et al*. 1993), making it possible to

study changes in the release rates since the operation closed in 1977.

Methods

During the spring 2017 sediment cores were retrieved from 5 stations in the northern part of Lake Vättern (the second largest lake in Sweden) (fig. 1). Two replicates were retrieved from all stations and all 10 sediment cores were transported undisturbed to the laboratory and stored in a cold room. Dilution water for the mesocosm leaching experiments was collected in the northern part of the lake approximately 10 km from the sampling stations. This water has the same basic water chemistry as the water above the sediment cores, but with lower trace elements concentrations.

Mesocosm experiments were performed on sediment cores sampled in 2017 at the same five locations as in 1976 and 1993 close to the mining operation. Experiments were performed in the same way as the original experiment in 1976 to determine the release rates of cadmium, lead, sulfate and zinc as a function of time.

Mesocosm experiments were initiated by removing the original water from the sediment cores and gently adding 1 L dilution water instead. Mesocosm release rate experiments were performed in duplicates at +8°C. Lake water (dilution water) above the sediment surface was aerated slowly and samples were withdrawn after 1, 4, 11, 18, 33, 47, 62, 77 and 110 days and analysed for pH, sulfate and elements. At every sampling

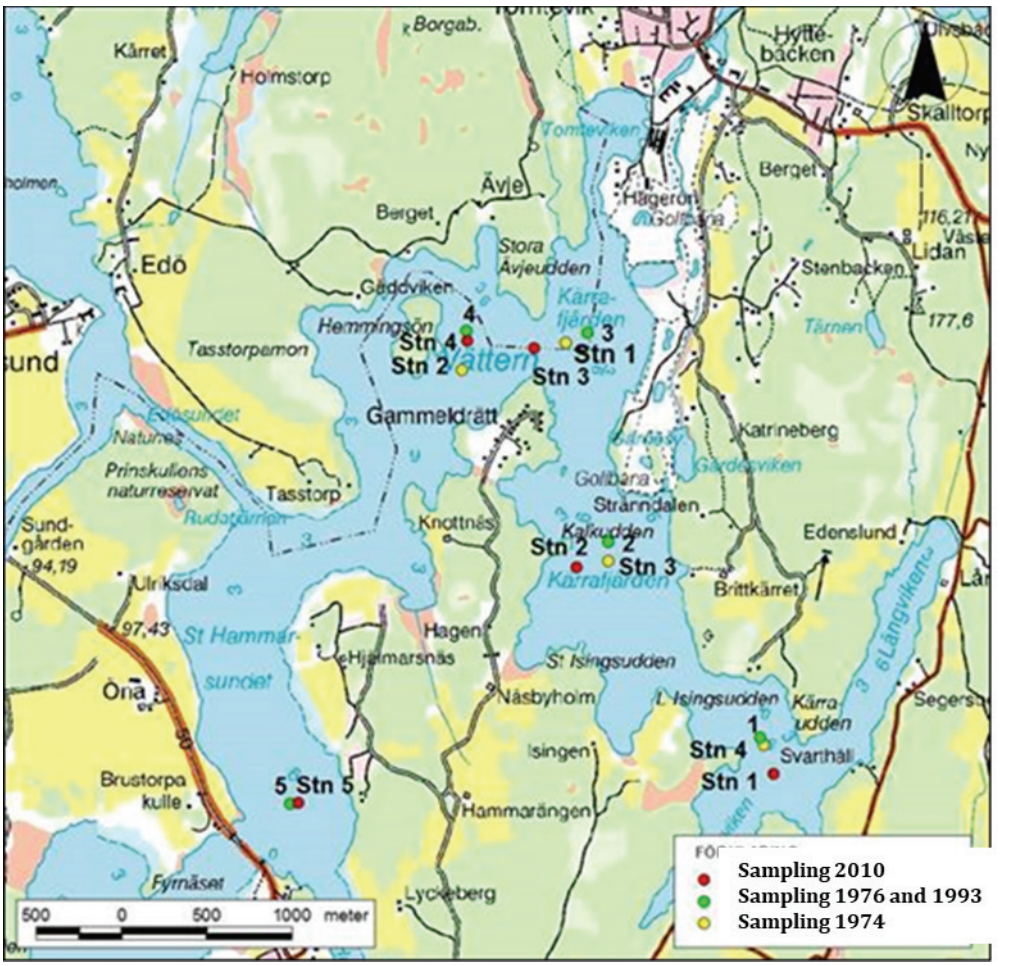


Figure 1 *Illustration showing the sampling stations in 1976, 1993 and 2017 (green dots) in the northern part of Lake Vättern, Sweden. Discharge from the operation is just north of station 3 (green dot).*

Table 1 Parameters analyzed. Sulfate and PTE are in mg/L; RF = filtered water; RNF = unfiltered water. N.d.= not determined.

	Pb mg/kg dw	Cd mg/kg dw	Zn mg/kg dw	Sulfur %	Carbon %
1a	5 070	19.0	7 690	0.34	6.38
1b	4 930	18.7	7 300	0.28	6.00
2a	4 710	24.4	12 000	0.64	5.91
2b	4 710	25.0	12 000	0.57	5.88
3a	5 230	24.1	14 300	0.78	6.72
3b	5 420	24.0	14 300	0.93	6.58
4a	6 800	20.1	14 700	0.19	5.22
4b	6 970	20.7	14 800	0.26	5.32
5a	820	11.6	2 890	0.15	4.14
5b	810	11.6	2 800	0.15	3.89

occasion 200 mL water was retrieved and replaced with fresh dilution water.

After the initial leaching period (110 days) the top organic sediment layer (ca 0.5-1 cm) was removed from all sediment cores. The water was also replaced with fresh dilution water and the leaching experiments carried on for an additional 59 days. Samples were retrieved from the water (200 mL) after 4, 11, 18, 31 and 59 days in the same way as during the initial period. The purpose with the second leaching period is to study the release rates from the sediments without the presence of the surficial organic top layer.

The removed top layer of the sediment cores was analysed for total trace element concentrations as well as for carbon and sulfur.

In 1976 only a few elements were analysed and only zinc concentrations are thus reported here.

Results and discussion

When it comes to the total concentrations in the top layer of the sediment cores (0–1 cm) it

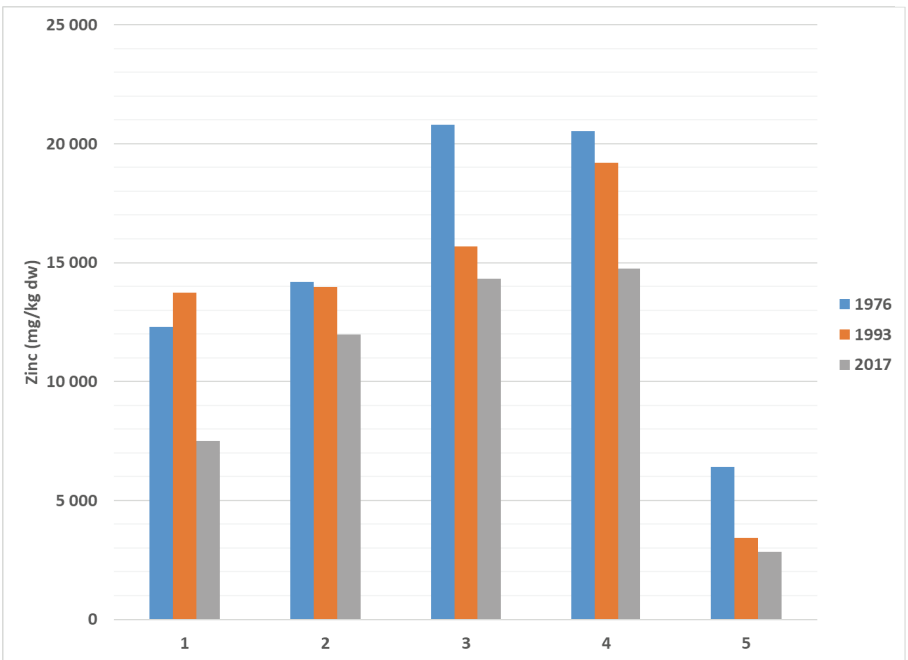


Figure 2 Total concentrations (n 2) of zinc (mg/kg dw) in the top layer (0-1 cm) of the sediments in 1976, 1993 and 2017.

is clear that the concentrations have decreased since 1976 and 1993 (tab. 1 and fig. 2).

It is also clear that the decrease in concentrations since 1993 is relatively modest at some stations considering the high initial concentrations. This indicates that either there is a source for trace elements to the sediments or that there are significant redistribution processes going on in the sediments. Total concentrations for cadmium, lead and sulfur can be found in tab. 1.

In fig. 3 the zinc concentrations (µg/L) measured in the water above the sediment cores during the mesocosm experiments can be found. From the measurements the release rates in mg/m^{2}*d have been calculated.

In 2017 the release rates were in the range 0.18-1.5 for zinc, 0.00021-0.0015 for cadmium and 0.00098-0.016 mg/day*m2 for lead with the highest rates closest to the historical mining site.

Calculated release rates (mg/d*m2) for the initial 110 days are presented in tab. 2 below. The release rate is highest for zinc followed by lead. If you compare the release rates with the total concentrations all trace elements have roughly the same release rates, except for lead where the average release rate is approximately 75 times lower compared to zinc.

It is also clear that the highest release rates for zinc are still found closest to the old mining operation (2, 3 and 4). The highest release rates for sulfate are found at stations 1–3, with somewhat lower release rates at stations 3 and 4. Even though the total concentrations have not decreased dramatically since 1976 the release rates have decreased (fig. 4).

When the surficial organic sediments were removed after 110 days the release rates changes for some of the trace elements (tab. 3).

For the most interesting trace elements the release rates increase when the surficial sediments are removed (tab. 3). For lead, cadmium and zinc the average increase in release rates are +176%, +148% and +113%, respectively.

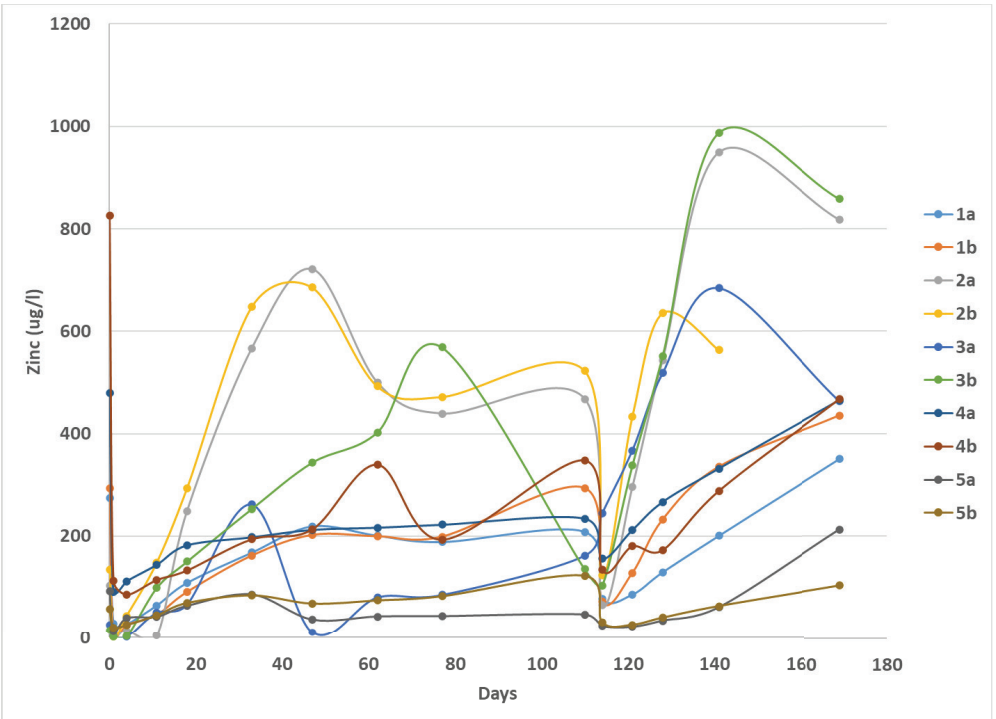


Figure 3 *Concentrations of zinc (µg/L) in all 10 systems. Day 0 is the original water. Note that at day 110 the surficial sediments were removed. Average zinc concentration in the dilution water was 2.4 µg/L (n 13).*

*Table 2 Release rates (mg/d*m²) for lead, cadmium, zinc and sulfate during the first 110 days in 2017. a and b are replicates from the same sampling station.*

	Pb mg/d*m²	Cd mg/d*m²	Zn mg/d*m²	Sulfate mg/d*m²
1a	0.0068	0.00086	0.73	597
1b	0.0082	0.0013	0.63	
2a	0.016	0.0011	1.36	350
2b	0.0074	0.0012	1.51	
3a	0.0031	0.00015	0.41	331
3b	0.0040	0.00038	1.19	
4a	0.0021	0.00093	0.69	256
4b	0.0077	0.0015	1.26	
5a	0.00098	0.00021	0.18	209
5b	0.0019	0.00022	0.30	

*Table 3 Release rates (mg/d*m²) for lead, cadmium, zinc and sulfate after removal of the surficial sediments (day 110–169). a and b are replicates from the same sampling station.*

	Pb mg/d*m²	Cd mg/d*m²	Zn mg/d*m²	Sulfate mg/d*m²
1a	0.016	0.0013	1.09	444
1b	0.022	0.0028	1.41	
2a	0.042	0.0026	2.84	400
2b	0.012	0.0012	3.65	
3a	0.024	0.0010	1.98	407
3b	0.015	0.0013	3.00	
4a	0.0097	0.0024	1.57	251
4b	0.0084	0.0019	1.49	
5a	0.0015	0.00091	0.58	201
5b	0.0031	0.00027	0.32	

For sulfate the release decreases at station 1, while it increases at stations 2 and 3 and is roughly the same for stations 4 and 5. This indicate that there are oxidizable sulfides in the upper parts of the sediment cores.

The different sampling stations are assumed to represent different parts of the lake with different areas. By multiplying the area for each sampling station with the corresponding release rate a yearly amount released can be calculated. Considering the area of the different parts of the lake close to the historical mining site it was found that the release of zinc had decreased from 7.3 ton/year in 1976 to 1.8 ton/year in 2017 (75% reduction). In significantly larger areas further away from the site the release of zinc hade decreased from 6.6 ton/year in 1976 to 0.69 ton/year in 2017 (90% reduction). Redistribution of zinc from the sediments thus partly explain missing pieces of the larger zinc mass balance budget for the entire area.

Conclusions

From the mesocosm experiments it is clear that both the total concentrations and the release rates have decreased since the operations ceased, indicating that released trace elements get buried in the sediments with time. Most of the reduction in release rates occurred between 1976 and 1993, while the difference between 1993 and 2017 is lower. In some cases, close to the site of the mining operation, the release rates had even increased somewhat. This indicates that the release of zinc from the historical site is continuing, albeit at a significantly lower rate compared to 1976. It can also be concluded that this type of experiments can assist in understanding the mass transfer of trace elements from sediments to surface waters.

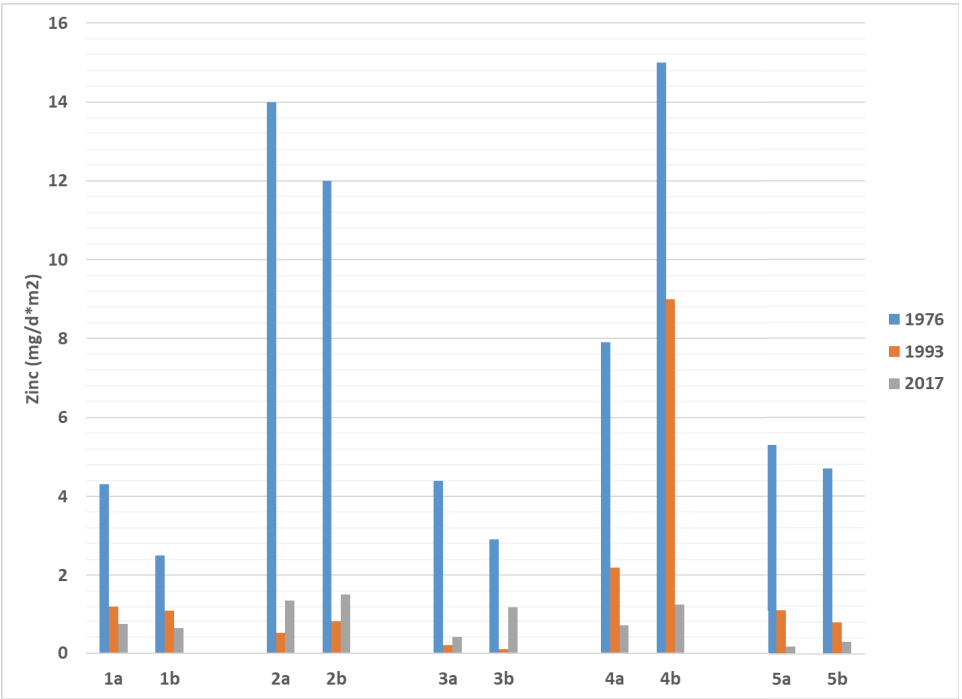


Figure 4 *Release rates (mg/d*m²) for zinc during the years 1976, 1993 and 2017*

Acknowledgements

Zinkgruvan Mining AB and SWECO AB are acknowledged for providing funding for this study.

References

Borg H, Lithner G, Unger M (1977) Metallavgång från förorenat Vätternsediment – Resultat av laboratorieförsök. SNV PM 821, Statens Naturvårdsverk (in Swedish)

Cai Y, Xu N, Meng F, Li F, Xie Y, Zhang H (2021) Speciation and release kinetics simulation of Zn and Cd from river sediments contaminated by gold mining. Water Air Soil Pollut 232: 21

Ciszewski D, Kubsik U, Aleksander-Kwaterczak U (2012) Long-term dispersal of heavy metals in a catchment affected by historic lead and zinc mining. J Soils Sediments 12: 1445-1462

Guo T, DeLaune RD, Patrick Jr WH (1997) The influence of sediment redox chemistry on chemically active forms of arsenic, cadmium and zinc in estuarine sediment. Environ Int 23(3): 305-316

Göthberg A, Lithner G, Fröberg E, Johansson A-M, Korhonen M (1993) Minskad utlösningspotential för zink och kadmium i Kärrafjärdens sediment och möjliga orsaker. ITM rapport 30, Stockholms universitet (in Swedish)

Innovative Passive Treatment Technologies for UK Metal Mine Waters: Results from Field Scale Trials

Selina Mary Bamforth[1], Nick Cox[1], Hugh Potter[2]

[1]*The Coal Authority, 200 Lichfield Lane Mansfield NG18 4RG, selinabamforth@coal.gov.uk, nick.cox@coal.gov.uk*

[2]*The Environment Agency, Tyneside House, Newcastle, NE4 7AR, hugh.potter@environment-agency.gov.uk,*

Abstract

The UK Government's Water and Abandoned Metal Mines (WAMM) Programme was created to clean up the 1,500km of rivers polluted by metal mines in England. Existing mine water treatment technologies typically have high operating costs (active chemical schemes) or take up large areas of land (biochemical reactors relying on bacterial sulphate reduction).

This paper outlines several pilot-scale field trials designed to decrease whole life cycle (financial and carbon) costs of removing zinc from mine waters whilst minimising the land take required. This work has relevance for the design of passive metal mine water treatment schemes across the world.

Keywords: Metal Mine Waters, Treatment, Innovation, Pilot Trials

Introduction

Drainage from abandoned metal mines accounts for approximately 50% of the total load of zinc, lead and cadmium to the freshwaters of England and Wales (Mayes et al, 2013) and is the largest source of metals to the marine environment (Environment Agency, 2023). These mine water discharges can cause significant ecological damage to freshwater ecosystems and without treatment, will continue to pollute rivers for hundreds more years. Most abandoned metal mines in Britain are in remote rural locations with very limited land available to build large passive treatment schemes and where active industrial treatment plants would not be acceptable to planning authorities.

Contaminated groundwater draining from abandoned metal mines is difficult to treat without adding chemicals and energy since treatment has to result in very low concentrations of metals being discharged to receiving waters. Most British mine water discharges have relatively low concentrations of ecotoxic metals and circumneutral pH although there are examples of lower pH and higher metal concentrations (Mayes et al, 2010).

The Water and Abandoned Metal Mines (WAMM) Programme is a partnership between the Environment Agency, the Coal Authority and the Department for Environment, Food and Rural Affairs (Defra) which was created to clean up the 1,500km of rivers polluted by these mines in England. Because the mines closed before 2000, the law says that former mine operators do not have to deal with the water pollution they created. The responsibility for cleaning up this legacy of Britain's industrial revolution therefore falls to the taxpayer. WAMM therefore has a strong emphasis on innovation and R&D with a particular focus on decreasing the footprint and whole life cycle costs of metal mine water treatment systems.

Considerable research has been conducted on treatment technologies based on microbially mediated sulphate reduction to remove metals from mine water as sulphides (Byrne et al, 2012). Since 2014, the WAMM programme has been operating the passive Force Crag compost-based bioreactor system, developed by Newcastle University following lab and pilot-scale research (Gandy et al, 2016), which continues to demonstrate the efficacy

of sulphate reduction, removing >90% of Zn and Cd with a hydraulic residence time in the reactive media of about 15 hours. At these residence times, large footprint treatment ponds are required for which land can be difficult to find, and they can be expensive to construct. Removal rates vary, are sensitive to seasonal variations and the availability of reactive organic matter, and in some locations, potential emissions of hydrogen sulphide need to be controlled to avoid nuisance odours. Therefore, identifying and testing technologies that will provide **low-cost**, **low maintenance**, **low hydraulic residence time** (and therefore **small footprint**) passive removal of metals from mine water, is a key driver for applied research.

The majority of mine water treatment studies are carried out at a laboratory scale which allows close control of parameters such as flow rate and temperature. However, testing under field conditions using 'fresh' mine water is essential to avoid changes to the microbiology and geochemistry of the waters during transport, and to understand the influence of seasonal and temperature effects. There are disadvantages to field trials since it is often necessary to have very low flows, often using small tubing, to test representative residence times. Most UK mine sites do not have mains power supply and remote locations means problems such as blockages or variation in flow rates can go unnoticed for days.

The WAMM programme has carried out pilot-scale field trials to assess the performance of various passive treatment substrates which remove metals by a range of processes, many of which are microbially mediated although influenced by the reactive media. This paper presents initial findings of the assessment of our 'long-list' of technologies and/or substrates that have the potential to be deployed at a larger scale for metal mine water treatment along with results to date from various field trials.

Methodology

Pilot scale field treatment trials have been undertaken at different scales, using two mine water discharges with different concentrations of polluting metals and pH. Field scale reactors ($1m^3$) were constructed in IBC style units by Aquaenviro to evaluate several treatment technologies which are described in Table 1. At sites testing multiple substrates, a $2.4m^3$ 'header tank' was used as a water balancing tank; this contained high matrix media (HMM) as an iron pre-treatment step to minimise clogging of the main reactors. HMM is the term used by the Coal Authority for plastic filter pack discs with a high surface area (~$200m^2/m^3$, see Table 1). The header tank had two water distribution manifolds with fitted globe valves that allowed water to be directed to the IBCs at a determined flow rate. The IBCs were configured with a 2" slotted delivery or drainage pipe network at the base, which was bedded in an inert quartzite gravel drainage layer. In all cases, the reactive media was placed above the quartzite gravel drainage layer, at a predetermined depth. See Plates 1A to 1D for some images of the trials and sites.

Reactors were monitored on a weekly frequency (minimum), when flow rates were checked and amended where required, lines were flushed, levels checked and samples taken. On site water quality parameters were measured with an Aquatroll 500, specifically pH, dissolved oxygen (DO), conductivity (EC, $\mu s/cm^3$) and temperature. Water samples were taken by Enitial Services and analysed by Socotec UK, a UKAS accredited laboratory. This data is not discussed in this paper but will be used for future modelling and understanding of the different waters.

Bridford (Devon):

A low-flow (<10 l/s) net acidic water, with average concentrations of iron (~56 mg/L), zinc (~11 mg/L) and other metals, which pollutes about 14km of the River Teign. A series of naturally formed 'iron terraces' are encouraging oxidation and precipitation of iron whilst decreasing the pH (see Plate 1D). Trials have been conducted on both the raw mine water, and water discharging from the end of the terraces.

Phase 1 trials put water collected after the iron terraces into a header tank containing HMM before passing through IBCs with either Coir (coconut shell outer fibre), Limestone Bioreactor (LST-BR) or Vertical

Flow reactor (VFR) (down-flow). An up-flow fish bone apatite trial was quickly stopped due to concerns over the high BOD of the media. Phase 2 and 3 investigated an alkaline pre-treatment step using Blast Furnace Slag (BFS), Basic Oxygen Steel Slag (BOSS) and limestone (LST) before a granitic VFR reactor.

Cambokeels (County Durham):

A low flow (<10 l/s) net alkaline circumneutral water with elevated zinc (~2 mg/L) and cadmium which pollutes up to 16km of the River Wear. Phase 1 put mine water into a header tank containing HMM, followed by IBCs with coir, LST-BR, BOSS or VFR (down-flow). Phases 2 and 3 involved larger scale (6 m^3) reactors which are not presented here.

Results

Operation of trials

The IBC trials were operated for approximately 18 months at Cambokeels and nearly 2 years at Bridford. All trials ran passively, using gravity, siphons and valves to convey the water to the IBCs. Operationally, the systems worked well for 6 to 8 weeks,

Table 1 *Summary of substrates trialled*

Reactor name	Media/Substrate/information	(Bridford –B, Cambokeels –C)	Material source(s)
Vertical Flow Reactor (VFR)	Fine grained (6mm granite over a 20mm granite gravel drainage layer) developed by D.Sapsford, Cardiff University	B and C	Cloburn Quarry Company, Lanarkshire
Limestone (LST)	20mm single sized calcareous limestone aggregate	C	Heights Quarry, Bardon Aggregate, Westgate, Bishop Auckland
		B	Hanson Aggregates, Batts Combe Quarry, Cheddar, Somerset
Limestone Bioreactor (LST-BR)	Organic rich mix of limestone, barley straw and bark, developed by Newcastle University 2:1:1 mix of 20mm limestone gravel (calcareous), barley straw, 25-45mm pine bark nuggets	B and C	Limestone as per LST Barley straw: Local Pet centre Bark: 'Maritime Pine', CPA Horticulture
Coir	Coconut fibres, various lengths. From untreated lignin-rich coconut husk fibres, a by product of the coconut farming industry	B and C	Fertile Fibre UK
Basic Oxygen Steel Slag (BOSS)	Granulated by product from steel production (8 to 14mm). By-product of the steel industry	B and C	Tarmac, Scunthorpe
Blast Furnace Slag (BFS)	Granulated by product from iron smelting (20 to 32mm). By-product of the iron industry	B	Tarmac, Scunthorpe
High Matrix Media (HMM)	Cascade YTH1170 Filterpak Media (200m2/m3). High surface area plastic filter pack discs	B and C	Veolia
Apatite	Fish bone derived apatite (1-2mm ground/granulated). By-product of the cod liver oil industry	B	Pelagia, Grimsby

after which the systems became less stable. Pipework in both sets of trials became choked with iron oxide which meant flow rates often dropped between sampling events. Pipes were regularly cleaned using a pipeline pig and valves exercised following every sampling event. This led to variation in retention times within the substrates.

We undertook a number of modifications to the system to minimise the water delivery issues, such as running a bleed line to speed up flow through the main delivery pipework, with short spurs from the bleed pipe to the reactor, and also designing a valve less flow control header tank, that has been successfully deployed in the Phase 3 trials.

Metal removal results

Key results from the Bridford and Cambokeels trials are summarised in Tables 2A and 2B along with percent zinc removal at Cambokeels in Figures 1A and 1B. At both sites, the limestone bioreactor (LST-BR) and steel slag (BOSS) proved to be most effective in removing metals. At Bridford, alkalinity pre-treatment followed by a VFR showed promise. The LST-BR reactor harnesses microbial sulphate reduction to remove the metals as sulphides although sorption and precipitation will also play a role. Removal by BOSS system is assumed to be a surface chemistry catalysed mechanism although microbial mediated metal removal cannot be

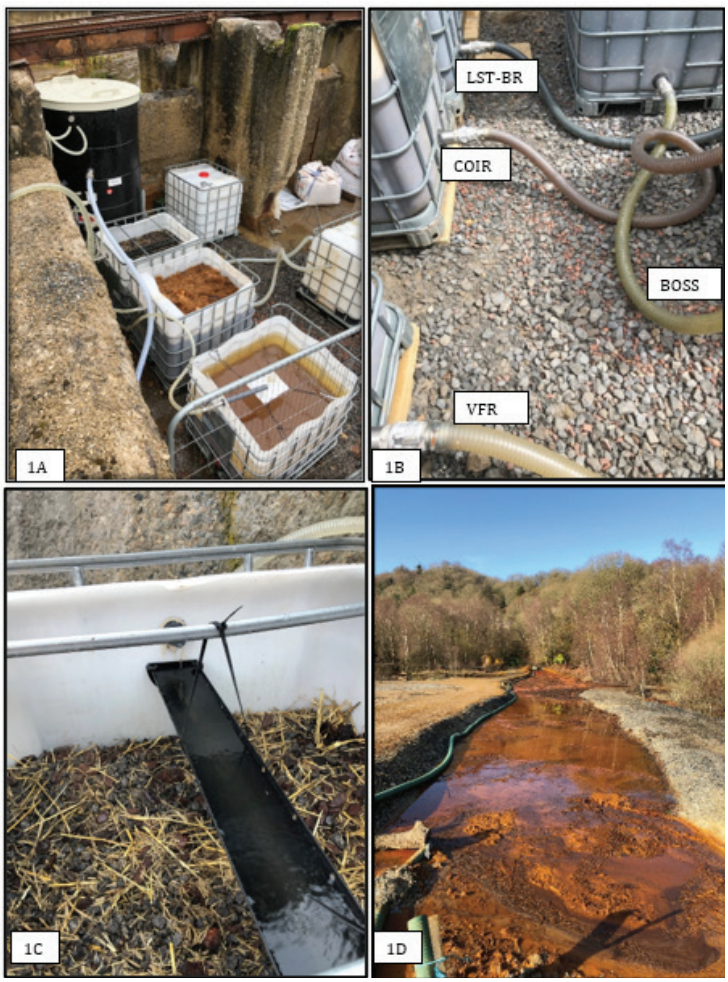


Plate 1. ***1A****: Cambokeels IBC trial.* ***1B****: Cambokeels IBC effluent pipework.* ***1C****: LST-BR substrate with gutter to distribute water.* ***1D****: Bridford 'Iron Terraces'. (Images: Selina Bamforth).*

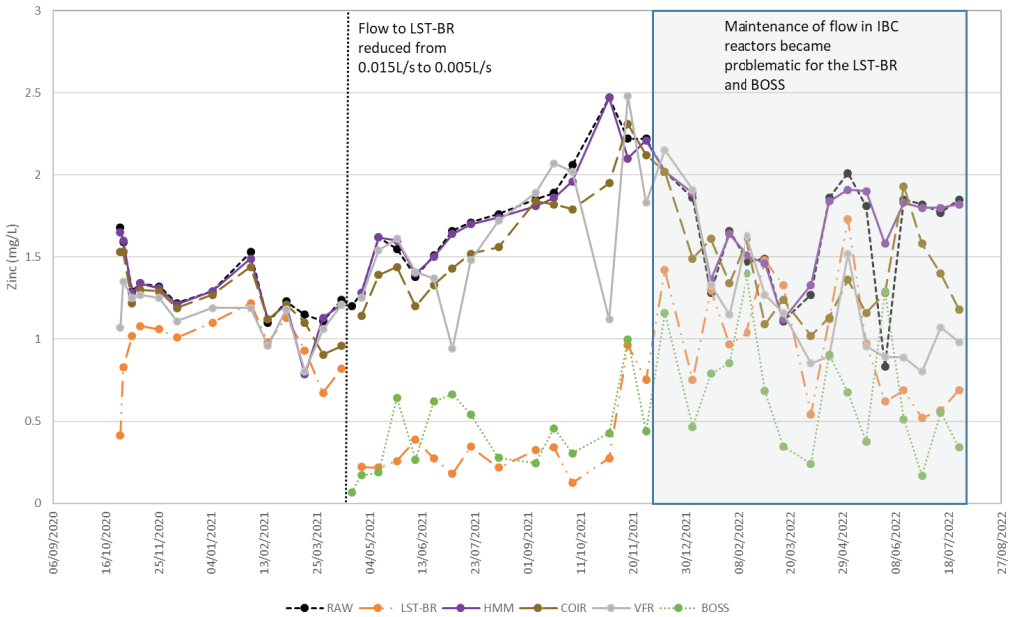


Figure 1A *Cambokeels: zinc influent and effluents (see Table 1 for substrate descriptions).*

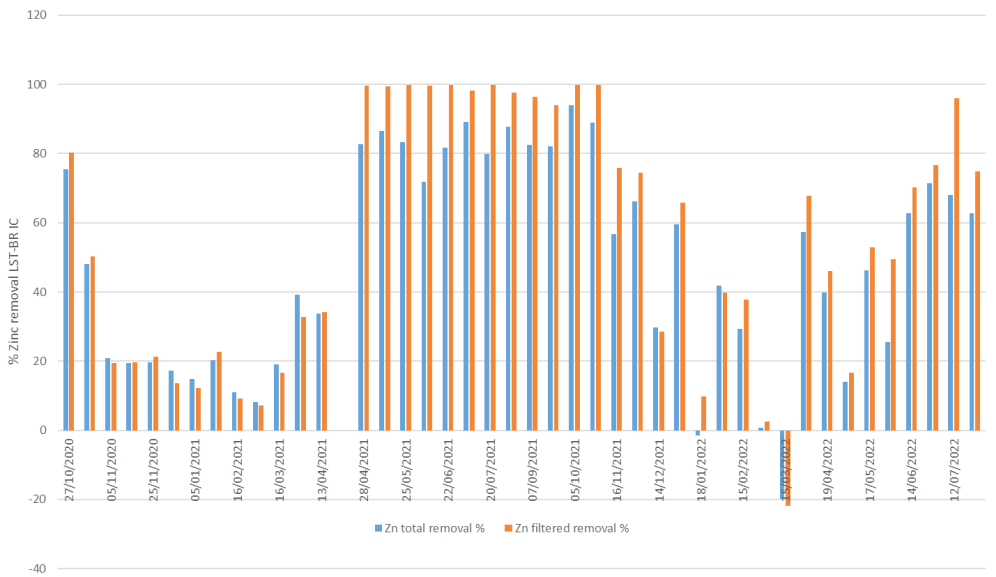


Figure 1B *Cambokeels: zinc percentage removal in the LST-BR IBC (total and filtered (<0.45µm)).*

ruled out; this system may add resilience if used in combination with the LST-BR.

Next steps

Based on the positive results from the 'long-list', longer term and larger scale trials of the LST-BR, BOSS and VFR are currently underway. Key research questions relate to whether hydrogen sulphide emissions need to be managed, seasonal variability in metal removal, effects of residence times and substrate life.

Table 2A Summary of results from trials at Bridford January 2020 - November 2021

Phase	Date range	Trial type	Flow rate (L/s)	Results summary
1	January –June 2020	VFR	0.05	Good Fe removal for first 3 months, limited removal of other heavy metals
		Coir	0.2	Limited iron and other heavy metal removal
		LST BR	0.05	Good Pb and Al removal for first 3 months, limited Zn removal, tracer test conducted highlighting significant short circuiting
	January 2020	Fish bone apatite	0.015	Excellent metals removal for first week (nearly 100%), becoming less effective in week 2, with high BOD and ammonia, therefore terminated early
2	September-December 2020	pre-treat LST - VFR	0.005	Initial zinc removal in LST VFR. Problems with lines blocking, unable to continue.
		BFS pre-treat - VFR	0.005	Limited Zn removal in BFS VFR. Problems with lines blocking, unable to continue.
	September 2020-November 2021	LST BR	0.005	Good Pb and Cd removal but high variability. Some Zn removal – could; be seasonal patterns (better summer time removal)
3	March – November 2021 -	LST pre-treat – VFR 1	0.005	Good lead removal, variable Cd, Zn, Pb, As removal. Metals removed in VFR stage more than the pre treat stage but high variability, likely due to flow rate variation
		LST pre-treat – VFR 2	0.005	Good lead removal, variable Cd, Zn, Pb, As removal. Metals removed in VFR stage more than the pre treat stage Up to 100% Fe removal from circa 50mg/L in the VFR element
		BOSS pre-treat - VFR	0.005	The BOSS media removed the majority of the heavy metals without the VFR element, good Pb, Cd As, removal variable Zn removal. Up to 100% Fe removal from circa 50mg/L in the VFR element

Table 2B Summary of results from trials at Cambokeels October 2020 - April 2023

Phase	Date range	Trial type	Flow rate (L/s)	Results summary
1	October 2020 – June 2022	VFR	0.015	Good Fe, Al, Mn removal, limited Zn, Cd removal
		Coir	0.015-0.2	Limited removal of metals
		LST BR	0.005-0.015	Good Zn, Cd, Al removal for first 6 months
	April 2021 – June 2022	BOSS	0.015	Variable but promising Zn removal, possible variation due to poor flow control
2	June 2021-February 2023	LST BR	0.7	Good Zn removal through summer months, higher particulate Zn during winter months
3	August 2022-present	LST BR	0.6	Ongoing

Conclusions

The WAMM programme is committed to developing and trialling innovative treatment technologies which require minimal input of chemicals and energy. Initial results presented here indicate that the LST-BR is very effective at removing metals in a higher permeability media than used at the Force Crag scheme. BOSS merits further investigation at larger scale since the small diameter pipework clogged in all trials. For net-acidic mine waters, alkalinity pre-treatment followed by VFR appears to be effective.

Several larger pilot scale trials (6 to >200m^3) are underway, being commissioned or are planned including a large VFR trial for the Coombe mine water (www.gov.uk) in Cornwall. The programme is also investigating mitigation options for odour management and different reactive media.

Acknowledgements

This work was funded by the UK Government Department for Environment, Food and Rural Affairs (Defra) and a Welsh Government's SMARTExpertise grant. The views expressed are those of the authors and not necessarily the Environment Agency, or any other organisation mentioned herein.

References

Byrne, P., Wood, P. J., & Reid, I. 2012. The Impairment of River Systems by Metal Mine Contamination: A Review Including Remediation Options. Critical Reviews in Environmental Science and Technology, 42(19), 2017-2077.

Environment Agency, 2023. State of the environment: the coastal and marine environment. Available from State of the environment: the coastal and marine environment (www.gov.uk), last accessed 18 April 2023.

Gandy CJ, Davis JE, Orme PHA, Potter HAB, Jarvis AP. 2016. Metal removal mechanisms in a short hydraulic residence time subsurface flow compost wetland for mine drainage treatment. Ecological Engineering, 97, 179-185.

Mayes, WM, Potter, HAB, Jarvis, AP, 2010. Inventory of aquatic contaminant flux arising from historical metal mining in England and Wales. Science of the Total Environment, 408, 3576-3583.

Mayes, WM, Potter, HAB, Jarvis, AP, 2013. Riverine flux of metals from historically mined orefields in England and Wales. Water Air & Soil Pollution, 224, 1-14.

Geotechnical characterisation of mine waste for modelling potential climate change impacts on mine waste mobility.

Vanessa J Banks,[1] Edward Bruce,[1] Ben Dashwood,[1] Catherine Gandy[2]
Matthew R. Kirkham,[1] Nikhil Nedumpallile-Vasu,[1] Tim Longstaff,[3]
Abby Moorhouse-Parry,[4] Barbara Palumbo-Roe [1] and Hugh Potter[5]

[1]*British Geological Survey, Nicker Hill, Keyworth NG12 5GZ, vbanks@bgs.ac.uk;*

[2]*School of Engineering, 3rd Floor Devonshire Building, Newcastle University Newcastle upon Tyne NE1 7RU;*

[3]*orkshire Dales Rivers Trust, 8 Kings Ct, Pateley Bridge, Harrogate HG3 5JW;*

[4]*Coal Authority 200 Lichfield Lane, Mansfield NG18 4RG;*

[5]*Environment Agency, Horizon House, Bristol BS1 5AH*

Abstract

Driving spoil, mine waste and tailings are common in stream valleys that have been subject to lead-zinc mining, where they comprise potential diffuse contaminant sources. Climate change is predicted to increase rainfall intensity and peak stream flows in some periods but also lead to decreased rainfall and lower stream flows in other periods, both of which may affect their environmental impacts from abandoned metal mines. Here we report on the challenges of investigating geotechnical processes and material characterisation at abandoned metal mines as part of the DIFFUSE (Newcastle University, Centre for Ecology and Hydrogeology and British Geological Survey) project.

Introduction

Water, as a source of power, was fundamental to the siting and layout of many of the now abandoned, lead-zinc metal mines in the UK. Many were engineered to optimise the use of gravity in processing. Consequently, driving spoil, mine waste and tailings are common in stream valleys that have been subject to mining, where they comprise diffuse contaminant sources. There is an associated potential for the diffuse contamination to manifest by rainfall infiltration, groundwater leaching, or by sediment mobilisation. Although apparently largely stable, mine waste instability in the context of future climate change has implications for long-term river quality. Here we report on techniques and the challenges for geotechnical characterisation as a component of the DIFFUSE project (CA18/2/1/4) undertaken at Great Eggleshope in the North Pennines, UK, in the context of the broader project aims to assess the impacts of diffuse mine waste on surface water quality using rapid and transferable technologies. The DIFFUSE project is funded by the Water and Abandoned Metal Mines (WAMM) Programme, a partnership between the Environment Agency, Coal Authority and Defra (the UK Dept for Environment, Food and Rural Affairs).

Mine waste in the Great Eggleshope valley originates from a number of mines, including the Wiregill (California) Mines (operated intermittently from the mid-1700s to 1930s; spoil heaps reworked in the 1970 (Fairburn 2009)) and East and West Hush, first recorded in the mid-1500s with East Hush on the valley side and West Hush in the valley floor with abandoned valley side leats that suppled the water for hushing. The host (Mississippian to Pennsylvanian) geology comprises fine-to very coarse- grained feldspathic sandstones, siltstones, mudstones with marine shaley mudstones, claystone, coal and seatearths of the Stainmore Formation, overlying the limestones, sandstones, mudstones, with rare coals of the Alston Formation, which crops out in the valley floor. Vein hosted mineralisation is classified as a fluoritic sub-type of the Mississippi-Valley type. The veins strike on various bearings and there is a

mapped fault that crosses Great Eggleshope Valley ENE to WSW, with a downthrow to the south.

Although variable in their grading and geotechnical properties mine wastes can be subdivided into zones that reflect the source of the mine waste in the context of the historic site operation. Research at Great Eggleshope focused on (i) a "bund" adjacent to the west side of the Great Eggleshope Beck, comprising mine waste that ranged from boulder to silt grade, interpreted as driving spoil and (ii) an historic dressing floor (shown on historic maps) that comprised slightly gravelly, sandy silt and sand with some clay (Figure 1a). Mine waste from the dressing floor was identified as a contaminant source with respect to concentrations of lead, zinc and cadmium, which exceed environmental standards (Higgins and Lovett 2017) and was confirmed in analyses undertaken within the Tees-Swale naturally connected project) and field leaching tests undertaken by Newcastle University.

Great Eggleshope Beck, an upland stream with a catchment area of 11.68 km2, is classified as an alluvial stream (Carling 1988). The stream is flashy with a relatively low base-flow index (0.33). Data from comparative studies by Carling and Reader (1982) indicate that 75% of the suspended sediment load of the beck is derived from mine waste delivered via a tributary stream. This is reflected in the finer bedload component being more uniformly graded than other upland streams. Fine sediment can be stored temporarily as lenses of fine material in zones of flow separation; alternatively, it may be transported through the system as bedload. The contribution of bedload from strata rendered unstable by stream undercutting is evident (Carling and Reader, 1982). Additionally, we have noted that mine waste sediment is also mobilised by suffosion processes within the driving spoil heap and evidenced by substantial depressions in the upper surface of the bund, as well as by surface erosion and channelling of the materials on the dressing floor.

Geotechnical (pertaining to the geological, geophysical and hydrological) characterisation of the mine waste is fundamental for generating model input parameters as required for assessment of firstly the mine waste slope stability assessment and secondly the fines or tailings erodibility. Typical of abandoned mine sites, Great Eggleshope is remote with difficult access for sampling and in-situ testing demanding portable and rapid techniques. A further challenge is that mine waste properties stretch conventional geotechnical testing techniques. Firstly, because of the extreme range in grain size, particularly the distribution of cobble and boulder grade material, which undermines the value of in-situ probing techniques. Secondly the volume and heterogeneity of the waste, from which it can be difficult to obtain truly representative samples. Mine waste differs to naturally occurring soils (engineering definition) in that it is commonly angular and platy, which affects the geotechnical properties, requiring consideration in laboratory-scale testing. We



Figure 1 *a Left: areas of investigation, looking north with drainage crossing the dressing floor in foreground and vegetation free driving spoil bund mid-distance. b Right: field sampling of the stream side of the driving spoil bund. Note range in grain size and seepage.*

Table 1 *Hydrological data: Great Eggleshope Beck (Carling 1988; Carling and Reader 1982).*

Mean Annual discharge	Mean Annual Flood	Bank full discharge	Bank full return period	Storm event suspended sediment	Suspended sediment transport	Bedload transport
$m3s^{-1}$	m^3s^{-1}	m^3/s^{-1}	Years	mg/L	$t\ km^{-2}\ year^{-1}$	$t\ km^{-2}\ year^{-1}$
0.1923	6.38	5.60	0.9	30	12.07	0.55

phased geophysical techniques (to explore representation) with targeted sampling of the driving spoil (hand excavated pits) and testing (cohesive strength meter) of the finer sediments associated with the dressing floor. The investigation approach and methods were guided by BSI (2020). Monitoring techniques were established with baseline ground-based LiDAR and unmanned aerial vehicles (Centre for Ecology and hydrology drone surveys). These techniques were combined to optimise 3D monitoring of mine waste erosion. Here we present an overview of the field and laboratory techniques, the generated data its application, and the remnant knowledge gaps.

Methods

Conceptual understanding with respect to the historic operation of the abandoned mine site, in conjunction with reconnaissance visits, which benefitted from the sparsely vegetated nature of the mine waste, provided the context of the broad classification of mine waste and selection of investigatory techniques (Figure 1b and Table 2). Subsequent stages of investigation were designed to address uncertainty in geotechnical representation of the mine wastes. Two areas were targeted for reconnaissance investigation with geophysics: the former dressing floor (fine-grained, high metal concentration) and driving wastes (coarser, lower metal concentration). In the area of the former dressing floor there was uncertainty regarding sediment thickness, sediment stratigraphy and distribution of stream channels evident from channels in the dressing floor. For the driving spoil, the investigation aimed to address uniformity of the bund and groundwater conditions with two key questions posed: *what are the in-situ geotechnical properties of the mine waste? and were there any changes in material type or placement techniques during the "construction" of the bund?*

Sampling for geotechnical characterisation (Figure 1b, Table 2) was scheduled to achieve the parameters required for slope stability analyses (driving spoil bund) and erodibility analysis (dressing floor). A reliable digital terrain model was a pre-requisite for the slope stability modelling, and this was achieved using ground-based LiDAR scanning techniques.

Electro-magnetic (EM) conductivity was carried out using a *CMD Explorer* (GF Instruments, sro) instrument. Deployed in walking, continuous measurement, mode with an integrated GPS sensor for positioning, the three transmitter-receiver dipoles at differing separations undertake simultaneous determinations of electrical

Table 2 *Great Eggleshope Beck geotechnical mine waste characterisation.*

Test Area	Analysis	Analytical technique requirements	Sampling method	Laboratory methods	Standards
Driving spoil bund	Slope stability	Slope angles, density, shear strength, water content	3 No. hand excavated pits and surface sampling	Grading, water content, small shear box [parallel graded]	BS 5930 BS 1377 (BSI 2020 and 1990)
Dressing floor	Erodibility	Grading	Surface and density ring samples	Grading	BS 1377

conductivity and magnetic susceptibility at depths of approximately 2.2m, 4.2m and 6.7m. The EM conductivity readings were inverted to represent material resistivity.

Ground penetrating radar (GPR) imaging was deployed on the western side of the dressing floor to assess the potential of the technique for mapping the thickness of tailing deposits. A *Sensors & Software Noggin Smart Cart* system was used, incorporating a 250 MHz GPR antenna, an odometer wheel, battery and a digital video logger providing the operator with an instant display of the GPR signal. This instrument transmits high frequency electromagnetic waves downwards and measures the reflected EM radiation resulting from contrasts in the electrical properties of the subsurface materials that influence reflection, dispersion, and attenuation of the transmitted pulse as it propagates through the sub-surface.

A Riegl VZ-1000 LiDAR (Light Detection and Ranging) scanner was used to generate a high-resolution baseline survey (accuracy of ± 8 mm). It was deployed in conjunction with GPS to facilitate subsequent nesting of UAV monitoring and to fix the repeat LiDAR scanning to monitor the stability of the driving spoil bund beside the beck. Repeat scanning was carried out with a Pegasus backpack LiDAR set-up, facilitating more rapid slightly lower resolution data collection.

Field testing of the erodibility of the mine waste on the dressing floor was conducted with a cohesive strength meter, which uses a vertical water jet fired at the sediment surface in short pulses (0.5s) of increasing force with data logged every 0.1 s for 3 s. Testing was carried out in accordance with a standardised procedure (Sediment Services 2004 Operating Manual). The jetting programme is adjusted (in a series of pre-set routines) to reflect the anticipated grading of the soil. Changes in the volume of sediment suspended in response to jetting are determined from the reduction of (infra-red) light transmission across the test chamber and logged to an onboard computer. Small, disturbed samples were taken from each of the test locations for moisture content and grading analyses.

Although the majority of the field and laboratory testing procedures were guided by British Standard approaches, some mine-waste specific adjustments were required. The mine waste in the driving spoil bund necessitated modification to the material preparation procedure for the shear box testing, as discussed below. The direct shear box technique, using a 100 mm shear box (imposing an upper grain size of 3.3 mm), was used to determine the shear strength parameters along a shear surface within representative samples of the granular material from the driving bund. Drained testing was carried out with normal stresses of 6, 12 and 24 kPa (calibrated 504.8 N/mm proving ring). Each stage of the test commenced with consolidation of the sample. The rate of shear was 0.15 mm/min.

Method evaluation, results and application

Internal erosion or subrosion (suffosion) processes, as suspected in the driving spoil bund, can occur where particle size, density and packing conditions allow particle movement through the matrix. One of the simplest index parameters for assessing suffosion potential is the uniformity coefficient, defined from the particle size distribution curves as U= D60/D10 where D60 is the grain size below which 60% of the sample falls and D10 the grain size below which 10% of the sample falls. U values for both the driving spoil and the dressing floor were variable but high (6.44 to 343 in 20 dressing floor samples and even higher in the driving spoil) confirming the potential susceptibility of these materials to suffosion. The grading analyses were also used to provide a preliminary assessment of the hydraulic conductivity of the dressing floor waste (0.81 to 1 x 10-4 cm/sec) and of the driving spoil (0.3969 to 1 x 10-4 cm/sec).

There were no obvious consistent changes in the conductivity properties of the driving spoil bund, as interpreted from the EM survey, supporting the hypothesis that geotechnical properties determined from hand-excavated pits in the near-surface of the bund could be assumed to be representative of

the bund mass. Magnetic susceptibility data indicated a small, but consistent, increase in magnetic susceptibility with depth, perhaps due to the presence of more mineral-rich fine material towards the base of the bund. U values described above show that this could be a secondary suffosion feature. The EM survey of the dressing floor identified a continuous, low resistivity feature, running along the south-east length of the site (Figure 2), which joins the Great Eggleshope Beck. This may be a manifestation of the former course of the Great Eggleshope Beck (as suspected from a comparison of satellite images of the area) and potentially indicating a fluid/ contaminant pathway through the mine tailings to the Beck. Results from the GPR indicated a material change at 2 to 3 m. Further interpretation is required.

The erosion meter, designed to measure the critical erosion shear stress of fine sediments, returned the results as a transmission percentage against eroding pressure for each 0.1s period of the incrementally increased (0.5 Psi) jetting pressure increments. These were converted from Psi to kPa for analysis. The equivalent horizontal stress was approximated from the vertical pressure using the conversion curve established by Tolhurst et al. (1999). This is valuable in modelling the depth and velocity of flowing water that might lead to sediment mobilisation in the event of flooding. The results indicate that there is spatial variability in the erodibility of the dressing floor tailings with a critical shear stress of 5–10 N m^2.

Overcoming the material challenges in the laboratory context required consideration of scaling issues. Near surface disturbed, bulk samples of the driving spoil were taken for direct shear box testing, but in the absence of access to a very large shear box to accommodate the coarse grain size of the driving spoil, techniques for assessing the representation of the mass by the finer-grained material were required. Optical analysis of the shape and material composition of the finer grained component of the samples formed a gateway for the application of parallel grading techniques (Lowe 1964). Further, the low percentage of fines, necessitated combining the bund samples to achieve the required volume. Resulting shear strength parameters comprised a friction angle of 68 degrees and a residual cohesion of 1.54 kPa. Using these data, slope stability modelling was undertaken using firstly a limit equilibrium based USGS code Scoops3D, implementing the 3D Simplified Bishops method which calculates a factor of safety (FoS) across the bund as the factor by which the shear strength could be reduced to bring it in equilibrium with the shear stress. Secondly, a 2D finite element-based shear strength reduction slope

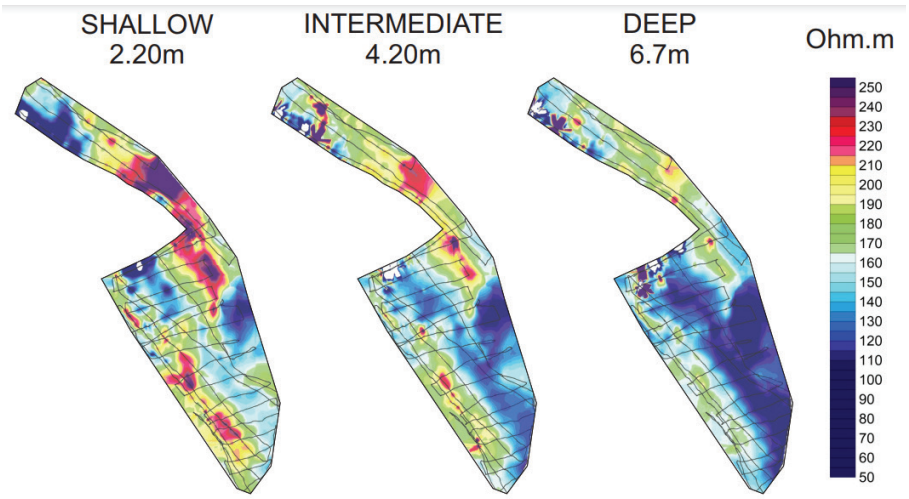


Figure 2 *EM returns as electrical resistivity of the dressing floor at Great Eggleshope; low resistivity areas link to stream to east with increasing depth. Looking north to the top of the page.*

stability with RS2 software (Rocscience) was run. Using this code, the impact of stream undercutting on bund stability calculated as a strength reduction factor (assessed using an elastoplastic Mohr-Coulomb model with input parameters taken from the shear box test results with literature-based estimates of Young's modulus and Poisson's ratio under drained and saturated conditions along a cross section of the bund) was examined.

Conclusions and future research directions

Data from a 6-year hydrological monitoring project reported by Carling and Reader (1982) and Carling (1988) provided evidence of ongoing mine waste erosion. The results of the geotechnical testing undertaken on samples from Great Eggleshope have been used to characterise the mine, for example in terms of its propensity to suffosion and to provide input parameters for slope stability and erodibility modelling. The geophysical surveys, together with more traditional geotechnical testing provide the basis for assessing the potential impacts of diffuse sediment on the Great Eggleshope Beck and farther downstream.

A distinct advantage of the continuous measurement mode of the EM and GPR geophysics is the profile-based returns that facilitates greater volumetric coverage of the ground than is the case with conventional intrusive investigation techniques (Figure 2). This provided reassurance with respect to representation of the surface materials for the full thickness of the driving spoil bund. Another advantage, which is also an interpretative challenge necessitating calibration and validation, is that the geophysical returns directly reflect the physical condition of the ground (composition, density and water content). Electrical techniques are particularly responsive to changes in soil moisture, which is likely the reason for the low conductivity zone in the EM returns in the area of the dressing floor from which the channel is suspected (from satellite images) to have migrated.

This investigation has highlighted the additional challenge associated with calibrating the geophysics with coarser mine waste density. The deployment of in-situ techniques requires an appropriate scale and capacity for application with the risk of measurements being representative of individual boulders rather than the mass. This situation is exacerbated where the mine waste has been placed or regraded at steep angles that require engineered access for investigation. Therefore, a key knowledge gap remains with respect to the in-situ density of the dressing spoil, necessitating parameter estimation for slope stability modelling. Pragmatic approaches such as this introduce modelling uncertainty that requires accommodation in the design factors of safety.

Repeat LiDAR scanning did not identify any significant change in the bund profile between between November 2021 and November 2022, a period of relatively benign meteorological conditions. Baseline data are available for comparison with any future surveys. The slope stability and erodibility modelling approaches can be parameterised to further explore the impact of anticipated extremes.

More leaching analyses of the driving spoil and other mine heaps, as well as of the stream bedload, together with statistical analyses of the data, would be required to quantify the potential load from these sources. Whilst hydrological parameters such as permeability can be estimated from grading curves, given the different shape and packing properties of the mine waste when compared with natural soils from which these empirical methods have been derived, it is considered that in-situ hydraulic testing would be beneficial for refining the permeability data and any estimates of groundwater flow in the mine waste.

Acknowledgements

The work reported here was funded by a variety of organisations, including the UK Government Department for Food and Rural Affairs (Defra), via the Water and Abandoned Metal Mines Programme and the National Lottery Heritage Fund (via the Tees-Swale: naturally connected project). The views expressed are those of the

authors and not necessarily the Environment Agency, or any other organisation mentioned herein. BGS authors publish with the permission of the Director of the British Geological Survey (UKRI).

References

Anon. 1990. BS 1377: British Standard Methods of test for Soils for civil engineering purposes. British Standards Institution, London

BSI 2020. BS 5930:2015+A1:2020. Code of practice for ground investigations.

Carling, P. 1988. The concept of dominant discharge applied to two gravel-bed streams in relation to channel stability thresholds. Earth Surface Processes and Landforms, 13, 355-367.

Carling, P. and Reader, N.A. 1982. Structure, composition and bulk properties of upland stream gravels. Earth Surface Processes and Landforms 7, 349-365.

Fairbairn, R.A. 2009. The mines of Upper Teesdale. 2nd Edition. 152 pp.

Higgins, D. and Lovett, L. 2017. Tees and Wear Diffuse Metals Project Hudeshope and Egglestone catchments. Tees Rivers Trust. 98 pp.

Lowe, J. 1964. Shear strength of coarse embankment dam materials. In Proc., 8th Int. Congress on Large Dams, 3, 745 – 761. Paris: International Commission on Large Dams, 1964.

Tolhurst, T.J., Black, K.S., Shayler, S.A., Mather, S., Black, I., Baker, K. and Paterson, D.M. 1999. Measuring the in situ Erosion Shear Stress of Intertidal Sediments with the Cohesive Strength Meter (CSM). Estuarine, Coastal and Shelf Science 49, 281-294.

Sustainable Removal of Metal/loids from As-Rich Mine Waters Using Mine and Industry Waste Materials

Marí a Dolores Basallote[1]*, Gerardo Amaya[2], Maira Castellanos[2], Carlos Ruiz Ca novas[2], Jose, Miguel Nieto[2], Rafael Pe rez-Lo pez[2]

[1]*Department of Ecology and Coastal Management, Institute of Marine Sciences of Andalusia (ICMAN), Spanish National Research Council (CSIC), 11510 Puerto Real, Cádiz Spain*

[2]*Department of Earth Sciences & Research Center on Natural Resources, Health and the Environment. University of Huelva, Campus "El Carmen", 21071, Huelva, Spain.*

Abstract

Removal efficiency of metal/loids from a highly acidic (pH 2.0) and metal/loid rich waters (6111 mg/L of Fe, 906 mg/L of Al, 748 mg/L of Zn or 13 mg/L of As) from the Iberian Pyrite Belt has been evaluated using industrial and mining waste materials (i.e., biomass ashes (BA) and schwertmannite-rich wastes (SRW)) by column and batch experiments. The batch experiments evidenced a high removal efficiency for As, with values ranging from 86 to 96% using BA and from 20 to 88% using SRW, with the maximum values reached at the end of the experiment. High removal rates for Fe (72%), Cu (88%), Pb (99%) and U (98%) were also achieved using a S:L ratio 1:10 of BA. In the case of the batch experiment using SRW, up to 90% of Pb, 77% of As 22% of Cr and 14% of Fe was removed from solution. In the case of the column experiment (25 days), the removal efficiency of As ranged from 87 to 98% in the BA-column during the whole period, while in the case of the SRW, the efficiency ranged from 63 to 96%, with the maximum values observed at the beginning and end of the experiment.

Keywords: Metal/loid removal; column experiments; batch experiments; waste recycling

Introduction

Acid mine drainage (AMD) is one of the main causes of water pollution worldwide. The oxidation of sulfides can lead to the occurrence of high concentrations of a variety of contaminants in water bodies. One representative example of AMD processes is the Iberian Pyrite Belt, one of the largest polymetallic sulfide deposits in the world, with many examples of extreme pollution by AMD (Nieto *et al*., 2013). To mitigate environmental impacts on water bodies, mining operators and environmental authorities put into practices costly measures to neutralize the acidity and reduce metal concentration in AMD generated in mining sites, generally applying alkaline raw materials (Basha *et al*., 2008), which extraction has a negative environmental footprint. Therefore, more environmentally friendly and costly measures need to be applied, especially in orphan mines, where local or regional authorities often assume the environmental liabilities.

Alternative options for costly alkaline raw materials are low-cost sorbents from agricultural and industrial wastes (Mohan and Pittman, 2007). Among them, biomass ash (BA) is a promising option due to their elevated alkalinity and high concentration in Ca and Mg. This material has been successfully used for the treatment of highly acid effluents from the fertilizer industry, with removal rates of 87-100% for Fe, U, F and Cr, and around 50% for Al, Zn, Cu and As (Milla n Becerro *et al*., 2020). These ashes are generated at high volumes during biomass burning to generate electricity. Considering the current global biomass power generation market, with more than 4,500 biomass power plants by 2022 and signs that they are quickly catching up when comparing with coal power plants, the amount of ashes generated is expected to grow up in the following years.

Although the main fate of these wastes is landfilling, its application to treat acid mine waters could be a promising route of waste valorization if biomass generation is close to mine areas (Bogush *et al*., 2020). On the other hand, Fe oxides and oxyhydroxides are materials with a high sorption capacity (Gutierrez *et al*., 2010). Among these minerals, schwertmannite ($Fe_8O_8(OH)_{5.5}(SO_4)_{1.25}$), jarosite ($KFe_3(SO_4)_2(OH)_6$) and goethite (FeOOH), usually control trace metal/loid mobility in AMD systems (AMD) (Asta *et al*., 2009). In the case of schwertmannite, this mineral precipitates naturally in the vicinity of AMD sources, the riverbanks of AMD-affected water courses and within the components of passive treatment systems. In this latter case, a decrease of 40% of initial As concentration was observed in a lagoon placed before the passive treatment plant of Mina Esperanza (SW Spain). This plant is based on the Disperse Alkaline System technology, which is basically composed of an initial lagoon, and successive tanks filled with alkaline materials such as limestone and magnesia, and settling ponds to ease the removal of metals. Thus, the Fe(II) and As rich waters are oxidized before entering to the plant, and the precipitation of schwertmannite scavenged large quantities of As by sorption processes (Orden *et al*., 2021). Passive treatment plants like those based on DAS technology require minor maintenance, being one of them the removal of Fe precipitates accumulated along the lagoons, channels, settling ponds and tanks. This material may be removed periodically and landfilled, which obviously have economic and environmental costs. However, the use of these wastes as sorptive material to remove metal/loids from AMD-affected waters could help to solve the problems related to its management. Therefore, the main goal of this work is to assess the suitability of waste materials such as biomass ash and schwertmannite-rich wastes (SRW) as sorptive agent to treat metal/loid rich AMD waters.

Methods

Biomass ash samples (5 kg) were collected from the biomass electricity complex of ENCE at Huelva (50 MW), which generates around 56000 tonne/yr of ash, close to the main AMD sources of the IPB. Schwertmannite-rich wastes (5 kg) were collected from Mina Esperanza passive treatment plant. It worth noting that this material already accumulate high concentration of metal/loids, compared to schwertmannite precipitating from less polluted waters. In addition, 25 L of extremely metal/loid rich and acidic waters were collected from Tharsis mines. These starting materials were chemically (through ICP-MS and ICP-OES) and mineralogically characterized (through XRD and SEM-EDS) before starting the experiments. In this sense, two different experiments were performed to study the suitability of BA and SRW to be used as remediation agent of AMD waters.

Batch experiments were performed by duplicate using 4 different solid: liquid ratios (1:2, 1:5, 1:10 and 1:20). Kinetic aspects were also evaluated considering different reaction times for each experiment (15 min, 1 h, 3 h, 6 h, 12 h, 24 h, 48 h and 96 h). Samples were agitated during the experiment, and samples corresponding to each reaction time were removed, centrifuged and the supernatant was filtered through 0.45 μm cellulose nitrate filters and acidified with ultrapure HNO3 before analysis. Physico-chemical variables (pH, ORP, electrical conductivity (EC) and temperature) were measured in each sample using a HACH multiparameter probe, previously calibrated.

Column experiments were also performed, consisting on an initial tank (5L) to store AMD waters, connected to a column with a peristaltic pump at a constant rate of 0.3 mL/min. The columns (40 cm length, 6 cm of diameter) were made of HDPE and filled with either SRW or BA mixed with wood shaving (80%:20%) to provide porosity. The column bottom was filled with 3 cm of silicic sands to enhance drainage. The column was connected to a settling pond (445 mL) to store the treated waters. Column experiments lasted 25 days, where samples were collected at a variable frequency (daily the first week and each 2-3 days the remaining time), following the same procedure as for batch experiments (measure of physico-chemical parameters, filtration and acidulation before analysis). The analysis (ICP-OES and ICP-MS) were

performed at the Central Research Services of the University of Huelva (Spain).

Results and discussion

Characterization of starting materials

The chemical composition of starting materials used in the experiments are shown in Table 1. As can be seen, SRW showed a high concentration in Fe and S, with values around 48% and 6%, which apparently coincides with the stoichiometric ratio in schwertmannite ($Fe_8O_8(OH)_{5.5}(SO_4)_{1.25}$). This material also showed high concentration of As (870 mg/kg), Al (867 mg/kg), P (377 mg/kg) or V (274 mg/kg). The presence of gypsum cannot be ruled out due to the high concentration of Ca found (541 mg/kg). The XRD patterns indicated that SRW are of amorphous nature, although the main peaks of schwertmannite were identified. In the case of the BA, this is mainly composed of Al, Ca, Fe and K oxides (Table 1), with high concentrations of other elements such as Na (2405 mg/kg), P (1315 mg/kg), Ti (1114 mg/kg) or Mn (840 mg/kg). The alkalinity of BA is evidenced by the high pH value (9.2), reached after a pH paste procedure. This material showed a low crystallinity, and only quartz was detected in XRD patterns. AMD samples exhibited a very low pH value (2.0) and high EC (14 mS/cm), with high concentrations of sulfate (20814 mg/L), and metal/loids (e.g., 6664 mg/L of Fe, 910 mg/L of Al, 794 mg/L of Zn, 196 mg/L of Cu and 14 mg/L of As).

Batch experiments

The contact of AMD with BA caused a sharp increase of pH values, especially at lower rates (1:10 and 1:20), from 2.0 to 3.3 within the first hour of the experiment (Fig. 1), due to the high alkalinity of BA. The pH values exhibited an increasing tendency towards the end of the experiment (4.7 and 3.7 for rates 1:10 and 1:20 at 96h). At higher rates (1:100 and 1:200), the increase was moderate (3.4 and 2.0, respectively). In the case of the SRW, a slight increase in pH was observed (from 2.0 to 2.2) probably associated to Fe(II) oxidation.

Regarding the elimination of metal/loids, the removal of As with BA at lower ratios (1:10 and 1:20) was very high, with values of 86% (1:10) and 96% (1:20) after only 5 min of contact, reaching values close to 100% at the end of the experiment. In the case of higher ratios (1:100 and 1:200) the removal reaction was slower. However, high removal rates were also achieved at the end of the experiment (100% and 95%, respectively). In the treatment with SRW, a progressive increase

Table 1 *Chemical composition of biomass ash (BA), schwertmannite-rich wastes (SRW) (in mg/kg) and AMD (in mg/L) used in the experiments*

	Schwertmannite	Biomass ash	AMD
Al	867	30593	910
Ca	541	53663	210
Fe	476379	17141	6664
K	174	16813	48
Mg	439	6028	391
Mn	11	840	78
Na	74	2405	28
P	377	1315	<5
S	55201	230	6938
As	870	2,6	14
Cr	8,8	29	0,6
Cu	112	77	196
Co	<1	5,5	1,1
Pb	31	8	0,5
Sr	<1	5,5	1,1
Ti	25	1114	0,04
V	274	127	0,7
Zn	80	50	794

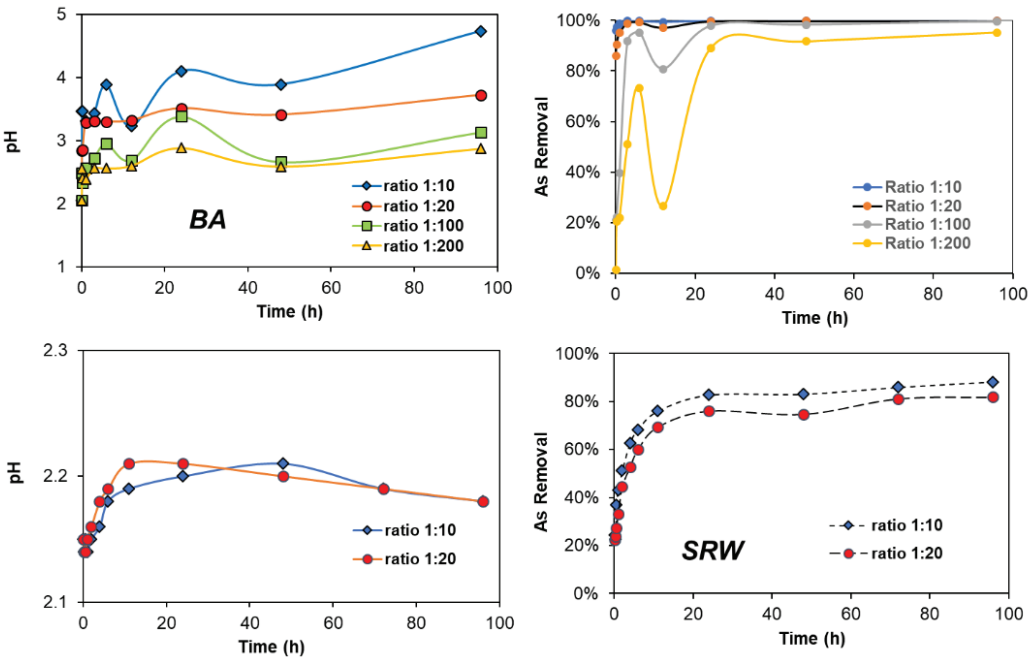


Figure 1 Evolution of pH and As removal during the batch experiments with biomass ash (BA, top) and schwertmannite rich wastes (SRW, bottom).

in As removal was observed, with final values of 88% (1:10) and 82% (1:20). During the experiments with BA, the removal of other contaminants was observed; up to 72% of Fe, 85% of Cu or 98% of U was removed at a ratio 1:10, with moderate removal rates for the rest of ratios ((< 40% and 20%). In the case of V and Pb, the removal ranged from 88% to 98% and from 56% to 100% respectively. Lower values were observed for sulfate and Zn with removal rates of 24-48%, and 13-26%. Higher removal rates were also observed during the batch experiments with SRW, with values of up to 90% of removal for Pb, 69-77% for Cs or 22% for Cr. However, due to the contact of the acidic waters with BA and SRW some elements were released to the solution. On the one hand, the dissolution of BA increased the concentration of Ca, Mg, K or Mn. Conversely, the competitive sorption processes with As, caused the released back to solution of some elements such as V or U.

Column experiments

The alkalinity contained in BA caused a sharp increase of pH values (a maximum of 4.8), although temporarily until the depletion of the reagent, recovering the initial values at the end of the experiments (Fig. 2). In the case of the SRW column, the pH values increased slightly until a value of 2.2, remaining afterwards as the initial values. Regarding the removal of contaminants, the elimination of As in both columns was successful with removal rates of 60-100%, although with a different evolution in both columns (Fig. 2). The removal rate was above 98% in the BA column most of the experiment, decreasing progressively until a final value of 87%, while in the SRW column higher rates were observed at the beginning and the end of the experiment (>90%), with lower rated during the intermediate period (60–80%).

As in the batch experiments, a remarkable removal of other pollutants was observed. For example, 60-73% of Fe, 58-100% of Al, 58-64% of sulfate, or 49-60% of Mn (Fig. 2) was removed from the initial solution, decreasing progressively until the end of the experiment. These concentrations were even higher than initials for Al, Mn and Si in the case of BA due to the dissolution of oxides contained in this material, and for Fe and sulfate in the case of SRW, due probably to re-dissolution processes of Fe oxyhydroxisulfates. The columns were also efficient to remove Pb and U. In the case

of SRW column, the removal of Pb was very high (75–93%) and constant through the time, while for BA column higher values were observed at the beginning and the end of the experiment (76–96%). For U, a high removal was initially observed (66–99%), decreasing progressively through the experiment, and reaching values even higher than initials.

A high retention of V and Cr was also observed during the first days of the experiment, with values ranging from 53–99% and 70–99%, respectively. However, a progressive decrease is observed afterwards, reaching in the SRW column V concentrations higher than initials, probably due to competence with other oxyanions for sorption sites of schwertmannite. A similar behavior was observed for Cu and Zn, initially removed from solution at high rates (58–99% and 60–64%), and a progressive decrease afterwards. As in the case of the batch experiments, a remarkable increase in concentration of elements such as Ca and Si was observed, associated to the dissolution of oxides in the BA column. In this sense, it is remarkable the solubility differences between Ca and Si oxides, evidenced by a high initial increase of Ca and a latter increase of Si.

Conclusions

This work evaluates the removal efficiency of metal/loids from a highly acidic (pH 2.0) and metal/loid rich (6111 mg/L of Fe, 906 mg/L of Al, 748 mg/L of Zn or 13 mg/L of As) waters using industrial and mining waste materials. Column and batch experiments were performed. The batch experiments evidenced a high removal efficiency for As, with values ranging from 86 to 96% using BA and from 20 to 88% using SRW, with the maximum values reached at the end of the experiment. In the case of the batch experiment using SRW, up to 90% of Pb, 77% of As 22% of Cr and 14% of Fe was removed from solution. In the case of the 25-days-column experiment, the removal efficiency of As ranged from 87 to 98% in the BA-column during the whole period, while in the case of the SRW, the efficiency ranged from 63 to 96%, with the maximum values observed at the beginning and end of the experiment. Both in batch and column experiments, high removal rates were also observed for other pollutants such as Fe, Cu, Pb, Al, Mn, sulfate, or U, evidencing the suitability of these materials to treat AMD waters. Increased concentrations of some elements (e.g., Ca, Al, K for BA and sulfate, Fe, or V for SRW) were observed during the experiments due to dissolution of oxides contained in BA or desorption processes and re-dissolution of Fe minerals in SRW. Deeper research is needed to evaluate the reactivity of the solids after the treatments, especially the potential release back of pollutants, and about the binding mechanisms behind the metal/loid removal in these materials.

This investigation emerges as a collaboration with the company ATLANTIC COPPER. In this context, the shown results are essential for the development of appropriate, environmentally friendly and economically rational waste management. Our results have also shown potential for being scaled up and used as the base of modeling studies with other industrial by-products.

Acknowledgements

The authors thank all co-organisers for hosting the IMWA2023 Conference. This work has been funded by the supported by the Spanish Ministry of Economic and Competitiveness through the project TRAMPA (PID2020–119196RB-C21) and the ATLANTIC COPPER Cátedra through the ARCHENICAL project.

References

Asta MP, Cama J, Martí nez M, Gime nez J (2009) Arsenic removal by goethite and jarosite in acidic conditions and its environmental implications. J Hazard Materials 171, 965-972, doi.org/10.1016/j.jhazmat.2009.06.097

Basha CA, Selvi SJ, Ramasamy E, Chellammal S (2008) Removal of arsenic and sulphate from the copper smelting industrial effluent. J. Chem. Eng 141, 89– 98, doi.org/10.1016/j.cej.2007.10.027

Bogush AA, Dabu C, Tikhova VD, Kim JK, Campos L (2020. Biomass Ashes for Acid Mine Drainage Remediation. Waste Biomass Valor 11, 4977–4989, doi.org/10.1007/s12649-019-00804-9

Gutierrez C, Hansen HK, Nuñez P, Jensen PE, Ottosen LM (2010) Electro-chemical peroxidation as a tool to remove arsenic and copper from smelter wastewater. J. Appl.

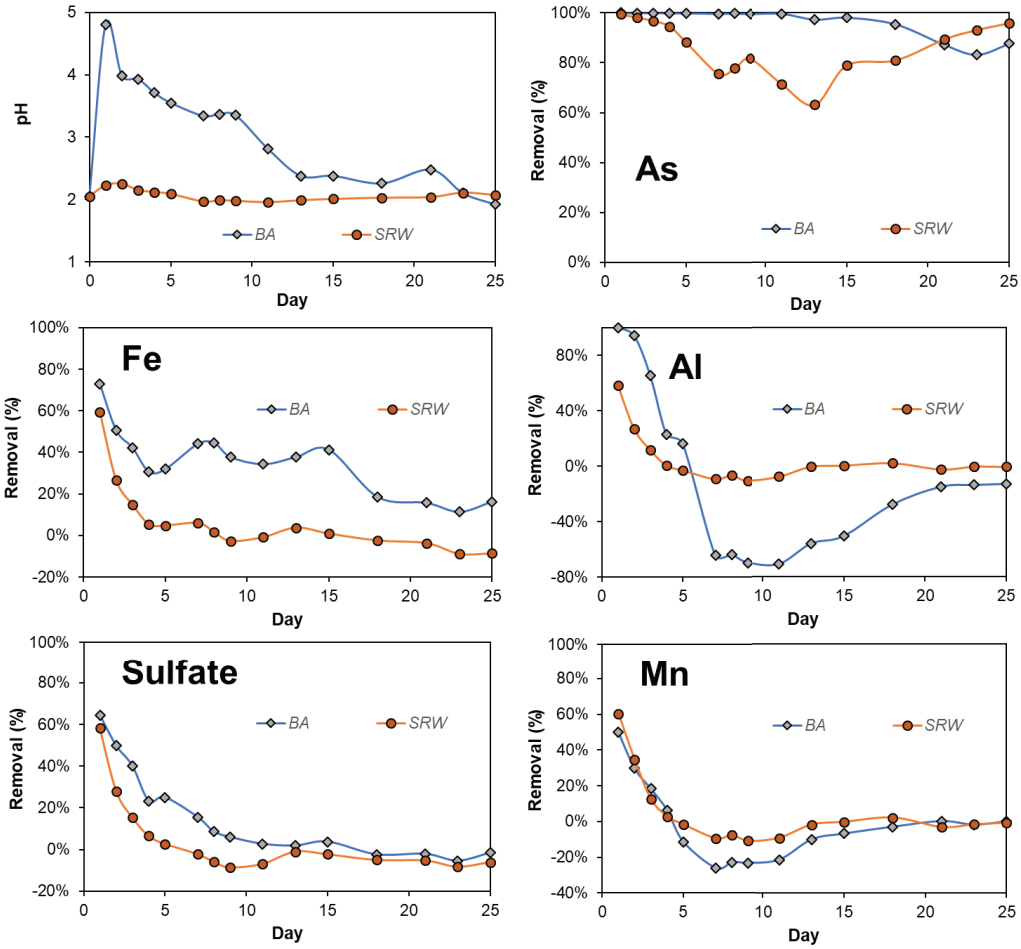


Figure 2 Evolution of the pH and removal rates for different contaminants during the column experiments with biomass ash (BA) and schwertmannite rich wastes (SRW).

Electrochem. 40, 1031-1038, doi.org/10.1007/s10800-009-0045-6

Milla n-Becerro R, Pe rez-Lo pez R, Mací as F, Ca novas CR (2020) Design and optimization of sustainable passive treatment systems for phosphogypsum leachates in an orphan disposal site. J. Environ. Manage. 275, 111251, doi.org/10.1016/j.jenvman.2020.111251

Nieto JM, Sarmiento AM, Canovas CR, Olias M, Ayora C (2013) Acid mine drainage in the Iberian Pyrite Belt: 1. Hydrochemical characteristics and pollutant load of the Tinto and Odiel rivers. Environ. Sci. Pollut. Res. 20 (11), 7509–7519, doi.org/10.1007/s11356-013-1634-9

Orden S, Mací as F, Ca novas CR, Nieto JM, Pe rez-Lo pez R, Ayora C (2021) Eco-sustainable passive treatment for mine waters: full-scale and long-term demonstration. J. Environ. Manag. 111699, doi.org/10.1016/j.jenvman.2020.111699

Passive treatment of mine seepage with high arsenic concentrations

F. Battaglia-Brunet[1], J. Jacob[1], F. Duré[1], J. Huron[1], G. Gatellier[1]

BRGM, 3 av. Claude Guillemin, 45060 Orléans, France. J.jacob@brgm.fr, f.battaglia@brgm.fr, g.gatellier@brgm.fr

Abstract

In the tailings dump of the closed gold mine "Le Châtelet" (France), a containment cell created to store highly contaminated As wastes is slowly filling up due to water infiltration. Two passive solutions were investigated to treat this acidic water containing 2 to 4 g/L As, i.e. evaporation and adsorption. The evaporation rate studied in the laboratory and on site was in the range 415-523 L/m²/4 months (treatment only in summer). Adsorption tests carried out with iron waste (shavings) or iron-based commercial material ASP® (Ovive) showed that these two materials used in series allowed both an efficient As removal and acid consumption without releasing dissolved Fe.

Keywords: Seepage, arsenic, evaporation, adsorption

Introduction

In the tailings dump of the closed gold mine "Le Châtelet" (north of Massif Central, France), a containment cell was created for the storage of 12,000 m³ of arsenic (As) contaminated wastes. This cell is slowly (42 m³/y) filling with a seepage which then becomes acidic (pH 3.0) and must be emptied every 5 to 6 years to maintain its structural integrity. Due to the high As concentration (2 to 4 g/L), the pumped water is currently disposed of within an incinerator. Two passive alternative solutions were investigated: evaporation and adsorption.

Adsorption of As on iron (Fe) oxides is one of the most common processes used to remove As from water (Mohan and Pittman, 2007). Arsenate As(V) is more efficiently adsorbed than As (III) on goethite and ferrihydrite type-oxides under moderately acidic conditions (Dixit and Hering, 2003). It should thus be possible to use an inexpensive material rich in metallic Fe as the adsorbent, after iron oxidation induces the formation of Fe(III) oxides which adsorb As. As zerovalent Fe powder can be quite expensive, in this study it is proposed to replace it with industrial Fe waste. Neumann *et al.* (2013) used industrial granular waste rinsed with water then treated with acetic or citric acid to form Fe (III) on the surface. Their system consists of tanks in series, with multilayer filling (sand, Fe, layer of activated carbon). Bretzel *et al.* (2020) also used tanks filled with nails, sand and gravel to remove As from drinking water in Burkina Faso; in this case the initial As concentration was around 1 mg/L. Sekula *et al.* (2018) used industrial Fe scrap to treat As in neutral mine drainage containing on average 0.5 mg/L of As. The residence time in this reactor was 2.2 h. The reactor operated for 2 years, treating 360 L/h. It contained 150 kg of Fe, and made it possible to eliminate approximately 3.15 kg of As in total, which represents 21 mg of As eliminated per g of Fe, a value close to that mentioned by Leupin *et al.* (2005). However, in both cases, the treated water was much less contaminated than this seepage water. In more comparable conditions, Makris *et al.* (2006) used Fe-based wastes from water treatment plant to adsorb As. The As concentrations tested ranged from 300 to 3000 mg/L (therefore the order of magnitude of the seepage water from Le Châtelet). Their experiments were carried out at pH 6 with As (III) or As (V). Adsorption kinetics was a little higher with As (V) but efficient adsorption was also observed with As (III). About 50% of the As (with an initial concentration of 3 g/L) was adsorbed in 1 hour, with adsorption increasing to as much as 80-90% after 50 hours.

Evaporation is not a traditional technique for treating mine drainage, probably

because large areas in an arid climate are necessary for the treatment of AMD and these areas generate naturally low flow rate AMD. However, work by Hanahan 2000, Mapanda *et al.* 2007 and Ravengai *et al.* 2004 demonstrate its potential to reduce the volume of water requiring treatment. This is especially true where water flow is low. Le Châtelet site makes it possible to consider this solution. The objective of the present study was to compare adsorption and evaporation in small scale systems to treat acidic seepage containing a high concentration of As.

Methods

The seepage water presents the following range in chemistry : pH 2.7-4.5, total As 500 – 4 000 mg/L, SO_4 2500 mg/L, Cl 400 mg/L, Fe 100–250 mg/L, Si 60 mg/L, PO_4 8–140 mg/L, Mn 10 mg/L, Ni 0.7 mg/L, Zn 0.5 mg/L, Al 0.5 mg/L, Sb 0.4 mg/L.

Evaporation tests at laboratory scale (5.4 L in 257 cm^2) were carried out for 37 days in an environmental chamber at a temperature of 16.7°C and a relative humidity of 70%, representative of the average conditions during the 4 summer months over the past 20 years on the site. Wind speed was uncontrolled and not measured. Evaporation was monitored via mass measurement. At pilot scale, tests were carried out for 122 days from May 7 to September 19 2022, on site, in a 64 L container (1660 cm^2) located under a 2.3 m roof cover to prevent rain from refilling the pilot. Evaporation was monitored via water level measurement. Temperature and relative humidity were monitored nearby at Montluçon aerodrome (19 km from the mine) by the French national meteorological service. Evaporation rates were compared to a simulation based on Penman equation (1948) and taking into account the effect of salinity with the formula proposed by Bonython (1966): Salinity Factor = 1-salinity (‰) x 0.00086 and assuming no precipitation. The mineral precipitation produced during evaporation was analyzed by x-ray diffraction (XRD) (BRUKER™ D8 ADVANCE).

Adsorption tests were carried out in two 300 mL glass columns (32 X 3.5 cm), equipped with sampling ports, spaced 6 cm apart, used to take samples (syringes and needles) for profiles. One column was filled with 145 g Fe waste (IW), (5 mm long shavings) and a second column was filled with 381 g Fe-based commercial adsorption material ASP® (2-4 mm, Ovive). Both columns were continuously fed with the seepage water (SW) for 60 days. The residence time measured by weighting the filling water and controlling the flow rate, was 80 h in the ASP column and 189 h in the IW column. After 30 days, the IW column was aerated by air bubbling to increase Fe oxidation and adsorption potential. Dissolved As was analysed by inductively coupled plasma mass spectrometry (ICP-MS), and total dissolved Fe was quantified by colorimetric method (phenanthroline complex), after reducing dissolved Fe (III) to Fe (II) using hydroquinone (Duke and Parchen, 1955).

Results

Evaporation

The evaporation rate measured in the laboratory was 0.11 L/d (Fig. 1) which corresponds to 523 L/m^2 evaporation over 4 months, a value that is 19% greater than the theoretical value calculated with Penman's formula. This is probably due to the unknown "wind" speed in the environmental chamber. Due to a technical issue, the experiment was interrupted before complete evaporation was achieved. Therefore, the effect of salinity on evaporation rate, which should be significant at higher salinity was not properly assessed. However, this does not undermine the conclusions, as during the evaporation of at least 85% of the water, the effect of salinity is negligible. Furthermore, dewatering should not be carried excessively for safety reasons (flying dust) and for practical reasons (sludge pumping).

During summer 2022, average onsite temperature and humidity was 20.7°C and 65.5% rH respectively. The evaporation rate was 0.56 L/d (Fig. 2), which is 415 L/m^2 for four months or 22% less than the theoretical value, shown in orange. This could be due to the unknown wind speed on site or because of the effect of the roof (limitation of air renewal above the evaporator). Based on these results and considering the average temperature and relative humidity during the four summer months over the past 20

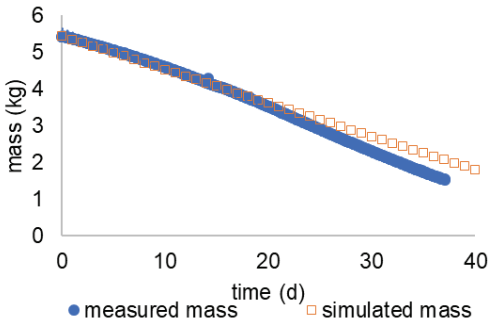


Figure 1 Measured and simulated water mass evolution during lab scale test in the environmental chamber

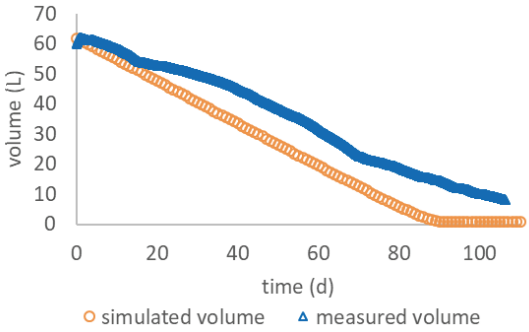


Figure 2 Measured and simulated water volume evolution during pilot scale test on site

years on the site, the surface area required to treat one year's accumulation of seepage was estimated at 122 m². In September, the decrease in temperatures and the increase in humidity caused a slowdown of evaporation and the experiment was therefore stopped. Once again, this experiment cannot inform the effect of salinity. However, the sample was fully evaporate in the laboratory oven, which produced 1.3 kg of sludge (at 50% humidity). Complete evaporation induces a decrease of waste volume by at least 98%.

The partial chemical composition of the solid produced during the on-site evaporation test is: SO4 24.7%, Fe as Fe_2O_3 3.1% and As 27.1%. Iron was analysed by XRF, sulfate by gravimetric determination and arsenic by ICP-MS after tri-acid digestion. The XRD results (Fig. 3) shows that the main As bearing mineral is Juansilvaite ($Na_5Al_3[AsO_3(OH)]_4[AsO_2(OH)_2]2(SO_4)_2$), and that it co-precipitated with gypsum and other phases listed in Figure 3.

Adsorption

During the first experimental step, the two adsorption columns worked independently, with each directly fed with the seepage water. The ASP column effectively removed dissolved As, with As concentration decreasing from 1800 mg/L in the inlet to less than 100 µg/L in the outlet. The IW column did not remove As prior to aeration, but following aeration, the dissolved As concentration was decreased from 1800 mg/L in the feed to values close to 10 mg/L in the effluent.

Phase	%
Gypsum	39.2
Juansilvaite	23.7
Jarosite	9.1
Smectite	5.9
Arsenolite	5.5
Tilasite	5.1
Claudetite	5.1
Spangolite	2.0
Stromeyerite	1.6
Litharge	1.2
Halite	1.1
Sulfur	0.4

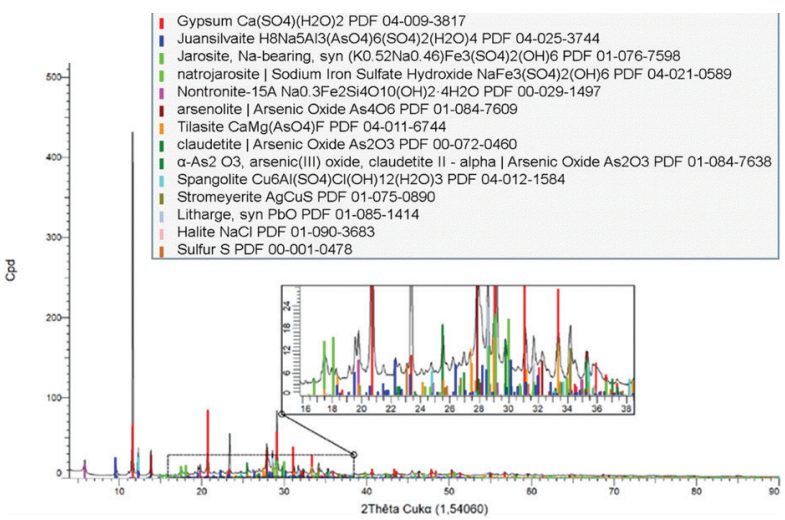


Figure 3 Results of XRD analysis of the final waste resulting from evaporation

The profile of dissolved As, dissolved Fe and pH were was measured on day 50 as shown in Figure 4. The dissolved As concentration decreased along the ASP profile down to 22 µg/L, but remained higher than 1 mg/L in the IW column (Fig. 4A). The ASP column did not release dissolved Fe, whereas Fe was dissolved in the IW column (Fig. 4B). Dissolved Fe peaked at 500 mg/L in the IW column, probably due to Fe corrosion (Bretzel *et al*., 2020, Srin *et al*., 2004). Soluble Fe was probably oxidized and precipitated downstream of L4 with final dissolved Fe concentration remaining elevated (100 mg/L) in the effluent. An increase in pH was initially observed in both columns (Fig. 4C), neutral pH was observed in the ASP column effluent whereas the IW maintained a pH of 5, reflecting equilibrium with iron until it dropped due to acid production following iron oxidation. These results are likely explained by the presence of carbonate minerals in the ASP adsorbant, and by the corrosion of Fe by H+ in the IW column. Corrosion of Fe in the IW column was followed by oxidation of dissolved Fe (II) and precipitation of Fe (III) hydroxides, this last reaction producing H+ ions.

The amount of As adsorbed during this experimental phase was calculated for the ASP material from the total volume of seepage water treated during this experimental phase. This calculation indicated that ASP had adsorbed 18.25 mg As/ g Fe and retained capacity for further sorption. Leupin *et al.* (2005) found an adsorption capacity of 18 mg As / g Fe using granular elemental Fe mixed with sand to treat a groundwater containing 500 µg/L As. Here, we showed that the adsorption capacity of ASP material was at least as efficicent as other Fe-based adsorbants, in spite of the high concentration of As and other dissolved minerals present in the seepage. Columns with ASP and IW materials had different capacity for As sorption from the seepage water. The commercial ASP adsorbant was more efficient for As removal and acid consumption, but it is more expensive than IW which was able to reduce the initial As concentration by 99%. These results suggest that a combination of these materials in a two-step adsorption process could optimize both treatment efficiency and cost. To this end, we tested the two columns in series, where the IW column was fed with seepage and the ASP column was fed with effluent from the IW column.

Samples were collected after 3 weeks of continuous experimentation under these operating conditions. Dissolved As concentrations decreased from 2044 mg/L (seepage feed) to an effluent concentration of 350 µg/L (Fig. 5A). Dissolved Fe concentration peaked at 58 mg/L in the IW column, then decreased to less than 50 µg/L in the outlet (Fig. 5B). The pH in the IW column increased from 2.36 (seepage feed) to 6.67 in the outlet (Fig. 5C). These results confirmed the efficiency of combining the two materials

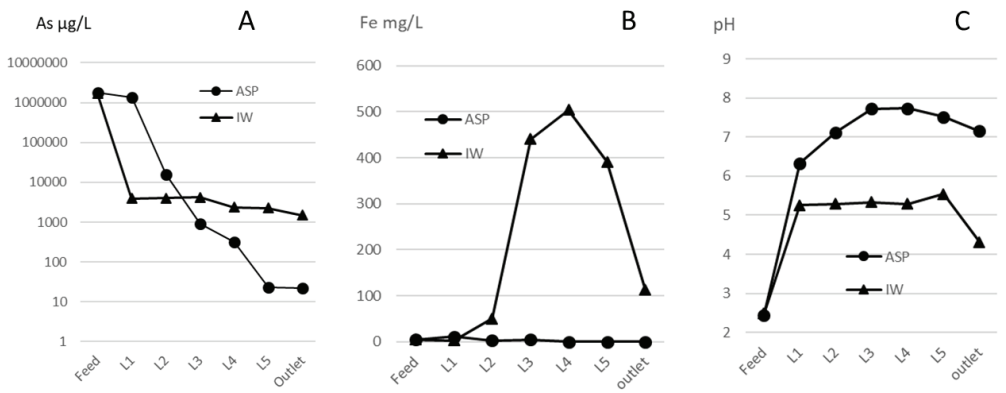


Figure 4 *Profiles of dissolved As (A), dissolved Fe (B) and pH (C) in the two adsorption columns independently fed with the seepage water on day 50. Ovive ASP commercial adsorbent (ASP), iron waste (IW). L1 to L5: sampling levels in the columns spaced 6 cm apart.*

to remove As from the seepage water and increase pH without increasing the dissolved Fe concentration in the treated water.

Conclusions

The results of laboratory and on-site pilot evaporation tests showed that the theoretical and measured rates of evaporation were close. The overall measured rate of evaporation during the pilot test was only slightly lower than the theoretical value. Accounting for this difference and based on the average temperatures and humidity of the past 20 years, the required surface area was calculated (122 m^2) and is compatible with the space available on site. The objective is to pump the water annually to an evaporation pond located at the top of the site, protected from rain by a roof, to enhance removal of As via mineral precipitation due to evaporation during the four summer months.

Passive filters filled with the tested Fe-based materials could be considered as a treatment step to remove As and consume acidity from the seepage water. The high concentration of potential competing chemical species (PO_4, SO_4, Cl…) present in the seepage did not limit the As-adsorption efficiency of the tested materials compared with data from other similar applications (Makris *et al.*, 2006; Bretzel *et al.*, 2020). Complementary experiments including adsorption isotherms to determine the sorbents maximum capacity and complementary analysis are needed to up-scale the process and evaluate its capacity to remove other chemical species from the seepage, such as Ni, Zn, Sb, and PO_4, which could also be adsorbed on Fe oxides. However, this process will probably not remove other solutes from the seepage water, such as Cl, Mn, and SO_4. Other treatment steps might be needed to reduce the concentrations of these chemical species if their impact on the receiving water is estimated to be significant.

Acknowledgements

The authors thank I. Girardeau for the project conceptualisation and resources, and H. Tris and C. Becquet for experimental work. Financial support for these studies was provided by DPSM within the framework of its mission as delegated post-mining operator on behalf of the French state.

References

Bonython, C. W. (1966). Factors Determining the Rate of Solar Evaporation in the Production of Salt. Reprinted from Second Symposium on Salt The Northern Ohio Geographical Society Inc.

Bretzel A, Nikiema J, Lalanne F, Hoffmann L, Biswakarma J, Siebenaller L, Demange D, Schirmer M, Hug SJ (2020) Arsenic removal with zero-valent iron filters in Burkina Faso: Field and laboratory insights. Sci Tot Environ 737:139466, https://doi.org/10.1016/j.scitotenv.2020.139466

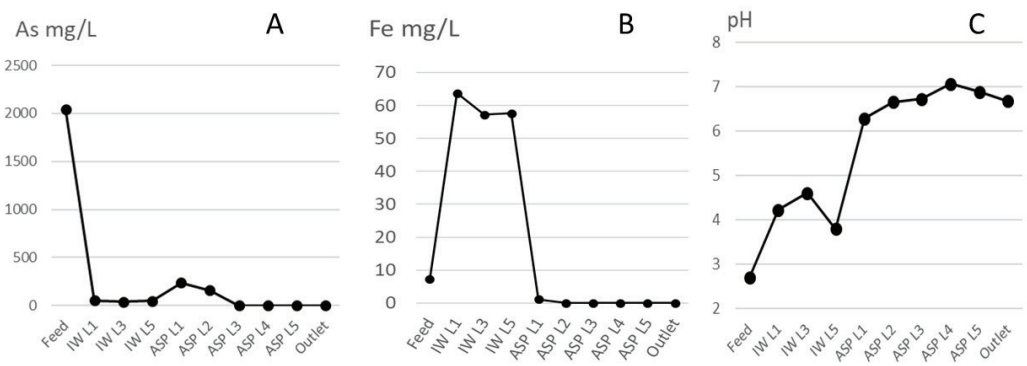


Figure 5 *Profiles of dissolved As (A), dissolved Fe (B) and pH (C) in the adsorption system composed of the columns working in series. IW column was fed with the seepage water. Ovive ASP commercial adsorbent (ASP), iron waste (IW). L1 to L5: sampling levels in the columns spaced 6 cm apart.*

Dixit S, Hering JG (2003) Comparison of Arsenic(V) and Arsenic(III) sorption onto iron oxide minerals: implications for arsenic mobility. Environ Sci Technol 37:82-4189, https://doi.org/10.1021/es030309t

Duke FR, Parchen FR (1955) Kinetics of the Reduction of Ferric Ion by Hydroquinone in the Presence of 1, 10-Phenanthroline1. J American Chem Soc 77:3198-3199

Hanahan C (2000) An alternative to evaporation for the management of acid mine drainage at coal mines in the Bowen Basin, Qld. Australian coal science conference, Brisbane, Qld. (Australia), 26-29 Nov 2000, https://www.osti.gov/etdeweb/biblio/20322793

Leupin OX, Hug SJ, Badruzzaman ABM (2005) Arsenic Removal from Bangladesh Tube Well Water with Filter Columns containing Zerovalent Iron. Environ Sci Technol 39:8032-8037, https://doi.org/10.1021/es050205d

Makris KC, Sarkar D, Datta R (2006) Evaluating a drinking-water waste by-product as a novel sorbent for arsenic. Chemosphere, 64:730-741, https://doi.org/10.1016/j.chemosphere.2005.11.054

Mapanda F, Nyamadzawo G, Nyamangara J, Wuta M (2007) Effects of discharging acid-mine drainage into evaporation ponds lined with clay on chemical quality of the surrounding soil and water. Phys Chem Earth, Parts A/B/C, 32(15-18):1366-1375, https://doi.org/10.1016/j.pce.2007.07.041

Mohan D, Pittman Jr. CU (2007) Arsenic removal from water/wastewater using adsorbents – A critical review. J Haz Mat 142:1-53, https://doi.org/10.1016/j.jhazmat.2007.01.006

Neumann A, Kaegi H, Voegelin A, Hussam A, Munir AKM, Hug SJ (2013) Arsenic Removal with Composite Iron Matrix Filters in Bangladesh: A Field and Laboratory Study. Environ Sci Technol 47:4544–4554, https://doi.org/10.1021/es305176x

Penman HL (1948). Natural evaporation from open water, bare soil and grass. Proceedings of the Royal Society of London. Series A. Mathematical and Physical Sciences, 193(1032), 120-145.

Sarin P, Snoeyink VL, Lytle DA, Kriven WM (2004) Iron Corrosion Scales: Model for Scale Growth, Iron Release, and Colored Water Formation. J Env Eng 130: 364. https://doi.org/10.1061/(ASCE)0733-9372

Sekula P, Hiller E, Šottník P, Jurkovič L, Klimko T, Vozár J (2018) Removal of antimony and arsenic from circum-neutral mine drainage in Poproč, Slovakia: a field treatment system using low-cost iron-based material. Environ Earth Sci 77:518, https://doi.org/10.1007/s12665-018-7700-3

Integrated Catchment-scale Mine Water Impact Assessment: A Case Study

James Bellin[1], Julien DeClerq[1], Michael Stewart[2], Callum Pearson[2]

[1]*SRK Consulting UK Ltd, Churchill House, 17 Churchill Way, Cardiff, CF11 9QA, Wales, jbellin@srk.co.uk*

[2]*Kaya Consulting Ltd, Stanhope House, 12 Stanhope Place, Edinburgh, EH12 5HH, Scotland*

Abstract

This paper seeks to demonstrate the value of using GoldSim as the glue to combine and integrate various hydrological, hydrogeological and geochemical models such that they provide a holistic evaluation of potential catchment-scale water impacts. We share a template for water impact assessment modelling and also demonstrate how findings from this modelling and evaluated risk controls can be fed back into the project design to reduce water risk and take advantage of opportunities.

Keywords: Water stewardship, catchment-scale, GoldSim, water risk

Introduction

Water stewardship, namely equitable, environmentally sustainable and economically beneficial water use, demands that we look beyond hydrologically arbitrary site boundaries and consider interactions at a catchment level (AWS, 2019). This often requires a multidisciplinary approach to modelling potential impacts that is not limited to a single software package or model type.

The objective of this paper is to provide a real-world case study of integrating surface water, groundwater and water chemistry models into a catchment scale GoldSim model for prediction of water impacts from mining. The study focuses on a predevelopment, brownfield iron-copper-gold project in Finnish Lapland, approximately 100 km north of the Arctic Circle (Figure 1). Precipitation falls as snow from around October to around May when the spring snow melt begins. River flows are often lowest during the winter when hydrological processes are locked up in ice and snow. The project site is located around 15 km to the north-east, and draining to, the Muonio River. The Muonio drains to the Tornionjoki River which is a key transboundary river and subject to a Transboundary River Agreement between Sweden and Finland as part of the Water Framework Directive.

The project area is highly sensitive with very good baseline water quality. All rivers and lakes in the catchment are important aquatic habitats with protected Natura 2000 status and there are several "classified" groundwater zones in the area. The larger catchment watershed constitutes an international water management area and water resources in the area are highly valued by local communities with high stakeholder interest. The key water risks therefore relate to potential river flow and water quality impacts on water dependent ecosystems as well as stakeholder perception.

The purpose of this study was to produce a catchment scale water impact assessment of the proposed mining project both during operational conditions and post-closure. The study also aimed to validate some specific design proposals such as waste rock dump liner and cover configurations as well as proposed post-closure water management strategies. Water impact modelling requires collation of various discipline-specific models into a coherent and integrated catchment scale assessment. The study represented an update of a previous study which used a series of independent hydrological and geochemical models, with the results brought together in a spreadsheet. However, this approach was difficult to follow, not well-suited to representing a dynamic system and cannot handle uncertainty.



Figure 1 *Aerial photo of the current site (image: Hannukainen Mining Oy).*

The key risks to surrounding water features that were identified prior to the modelling exercise and which were to be investigated by the model included:

- Potential impacts on base flow to rivers, especially during pit late recovery.
- Release of poor-quality water from waste dumps and/or pick lakes to either groundwater or surface water systems.
- Potential changes in run-off from the site compared to baseline conditions affecting surface water flows downstream.

Methods

In the case of this study, the GoldSim software was selected to integrate various stand-alone models into a single consolidated water impact assessment tool, on a non-coupled basis but in other cases, such as with the pit lake geochemistry, on a fully coupled basis.

GoldSim is a Monte Carlo simulation software for modelling complex systems which can be used as the "glue" to link various models and calculations in a very logical and visual way. Models can accept a range of inputs and are able to quantitatively represent uncertainty to support decision-making and risk analysis. Results are easily communicated using graphs and schematics.

GoldSim can be directly coupled to a virtually unlimited variety of other modelling software using "DLL" files which allow GoldSim to interact with various other packages on an iterative basis. This allows a relatively unrestricted choice of modelling tool for any given process. DLL files have been created some well-known water and geochemical modelling packages, such as to allow the integration of GoldSim with PHREEQC as described in Eary (2007) as well as with FEFLOW as described by Martin and Gabora (2018).

Once constructed, GoldSim models can be quick to update and adapt, allowing efficient evaluation of potential mitigation options and/or other design opportunities. Furthermore, models can be run stochastically to produce a probabilistic result and evaluate uncertainty. Finally, the ability to produce "player" files with dashboards that allow non-GoldSim users to run and interrogate model scenarios and results without running the full GoldSim model or requiring paid software is extremely useful.

Figure 2 outlines the models and calculations which were integrated into the

GoldSim model, effectively using GoldSim as the "glue" to integrate results together as well as to couple models, where required.

Key processes that were represented using stand-alone modelling tools and then integrated into the GoldSim model included:

Waste rock and pit wall run-off source-term modelling.

Release rates were derived from laboratory tests on samples of key lithologies and scaled up to field conditions. PHREEQC 1D (Parkhurst and Appelo, 2013) geochemical modelling was used to represent mixing of the source terms with rainwater running off the pit walls and infiltrating into waste rock dumps as well as subsequent geochemical mixing processes, when combined with flow modelling, to provide an estimate of the chemical load entering the environment.

Cover infiltration modelling.

Unsaturated zone modelling was undertaken in HYDRUS-1D (Šimůnek , 2013) to represent infiltration of precipitation into the waste rock dumps through an engineered cover proposed to be emplaced at closure. This modelling was used to interrogate various proposed cover designs as well as to define waste rock dump seepage and infiltration.

Groundwater flow and contaminant transport modelling.

A MODFLOW USG (Panday *et al*, 2013) three-dimensional numerical groundwater flow model was constructed to evaluate impacts on baseflow to rivers and water levels. This model was then combined with MT3D three-dimensional contaminant transport modelling to evaluate potential for seepage and transport of potential contaminants.

Hydrological modelling.

Modelling of rainfall-runoff and river flow using HBV (Bergström, 1995) to evaluate surface water flows across the site and into site infrastructure, as well as flow in the receiving rivers.

Physical pit lake modelling.

CEQUAL-W2 (Cole and Wells, 2013) was used to define potential stratification of the post-closure pit lake that is expected to form. This could then be used to define into vertical zones that might be represented in the overall pit lake geochemistry model.

Pit lake water quality modelling.

A dynamic pit lake water quality model that reflects a range of geochemical processes that may occur in the post-closure pit lake was produced using PHREEQC. GoldSim and PHREEQC were coupled using the previously mentioned DLL to compute geochemical calculations for each timestep, producing a dynamic water model. After physical mixing in relative proportions, a PHREEQC model is run for each timestep to simulate the following geochemical processes in the pit lake:

- Equilibration with air (pH)
- Precipitation and dissolution of key minerals
- Kinetic biodegradation of N and P

Results from PHREEQC are then fed back into the next timestep. The results were calibrated to water sampling results from two existing pit lakes at the site.

Results

The GoldSim model was successfully able to integrate model outputs at varying scales and to represent physical mixing of flows and contaminants in site water ponds in the surrounding site surface watercourses in order to produce a predicted average water chemistry for key receptors.

Although exact concentrations cannot be shared due to confidentiality, some example post-closure results at four key surface water receptors are shown in Figure 3.

Model results were used both for early identification and management of water risks as well as opportunities to add value to the project design. For example, in terms of risk mitigation the results informed key focus areas for definition of trigger and threshold values based on bioavailability and toxicity. Furthermore, they were used to define the scope and duration of post-closure active water treatment that might be required and to validate proposed changes to the waste rock dump and process pond liner designs and post-closure water management strategies. In terms of value addition, opportunities for modifications to the post-closure waste rock

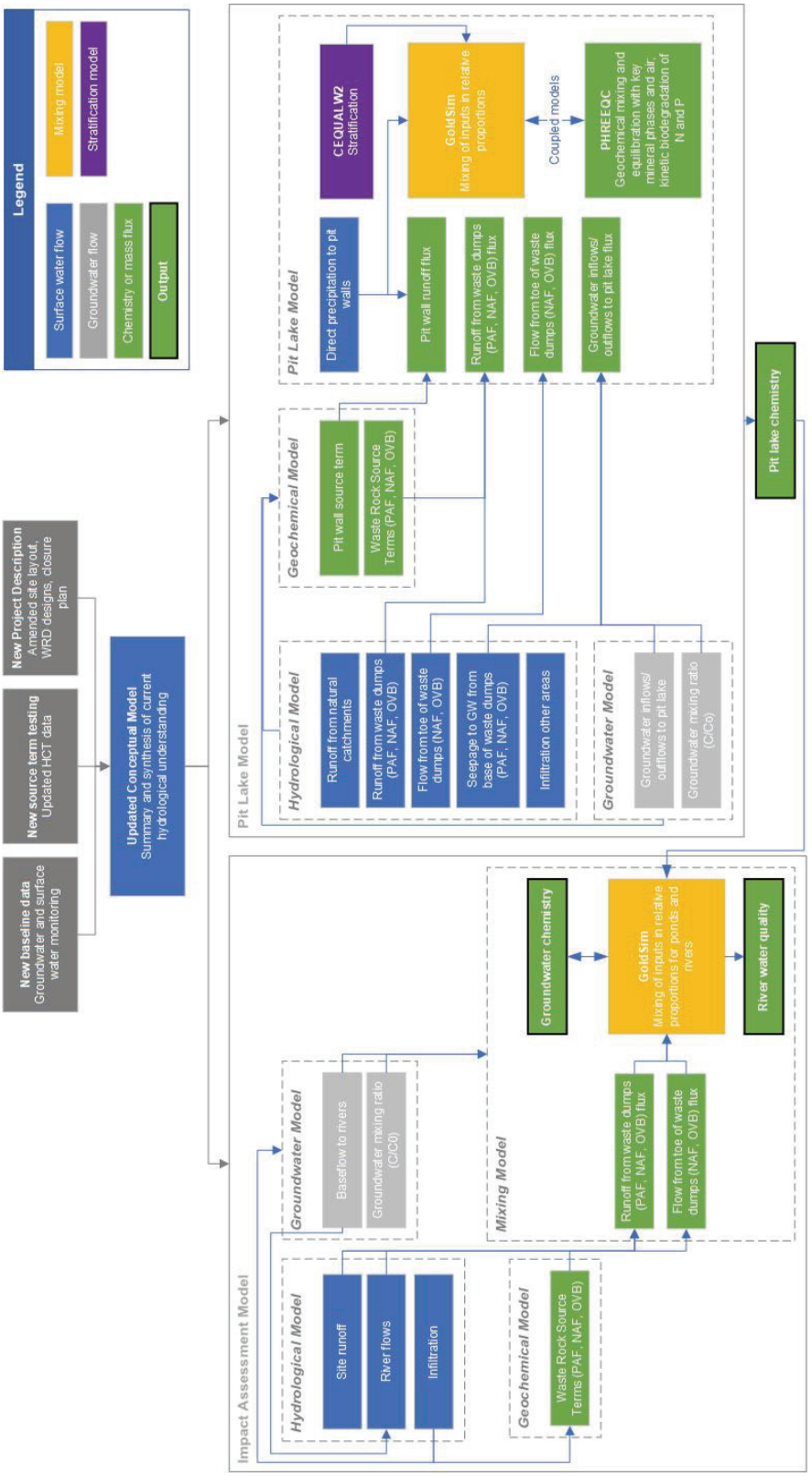


***Figure 2** Schematic summary of the GoldSim model make up showing interactions between models and calculations feeding into the GoldSim model as well as elements of the GoldSim model which were fully coupled with other models such as PHREEQC*

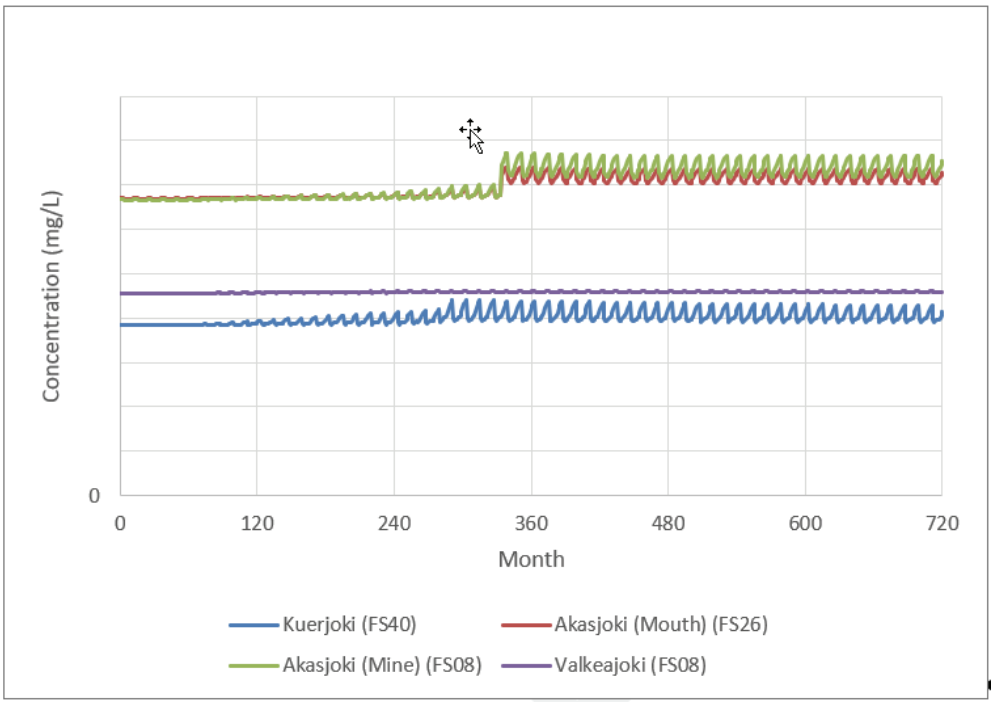


Figure 3 *Post-closure results for an example parameter at four key surface water receptors. The results show seasonal variation with flushing of source terms during the snowmelt season as well as the point at which the pit lake fills and overflows into surrounding surface watercourses.*

dump cover design were identified which had the potential to significantly reduce closure costs. Furthermore, it was demonstrated that active measures for post management of pit lake acidity were unlikely to be required.

Conclusions and Limitations

In this case study, GoldSim has been used to combine various independent models of catchment processes into a single holistic and integrated water impact assessment model. Such an approach provides a central point from which to link models and calculations, either directly or indirectly, in a logical and visual way as well as a tool to communicate results using graphs, schematics and "player" files. Bringing the models together in this way can also help to ensure that individual models do not adopt conflicting assumptions. Once constructed, the model has proven to be quick to update and adapt to assess design changes and new mitigation options. This type of integrated water impact modelling therefore has many advantages with regards to identifying and managing water risks at a catchment scale over other, more traditional approaches.

Although inputs can be represented stochastically in GoldSim enabling uncertainty analysis, few model outputs were available on a probabilistic basis including those which drove the largest changes in results. For example, water quality at the receptor as modelled by the GoldSim model is most sensitive to source term concentration which was difficult to quantify probabilistically in this case. Probabilistic modelling, and therefore quantification of uncertainty in the model results, would require further work to determine reliable stochastic outputs from all of the key model components in order to produce a useful quantification of uncertainty in this case.

Acknowledgements

We appreciate the use of site data and the ability to develop the project methodology as part of a study undertaken for Hannukainen Mining Oy.

References

Alliance for Water Stewardship (2019) International Water Stewardship Standard Version 2.0. Alliance for Water Stewardship (SCIO), North Berwick, Scotland.

Bergström S (1995) The HBV model. In: Singh, V.P. (Ed.) Computer Models of Watershed Hydrology. Water Resources Publications, Highlands Ranch, CO., pp. 443-476.

Cole TM and Wells SA (2013) CE-QUAL-W2: A two-dimensional, laterally averaged, hydrodynamic and water quality model, Version 3.71. Department of Civil and Environmental Engineering, Portland State University.

Eary T (2007) Linking GoldSim with the PHREEQC Geochemical Model with a Dynamic Link Library. 2007 GoldSim User's Conference, San Francisco, CA.

GTG (2017) Dynamic Monte Carlo Simulation Software. GoldSim Technology Group, LLC (www.goldsim.com)

Martin N and Gabora M (2018) Modelling Complex Mine Water Closure Challenges using a Coupled FEFLOW-GoldSim Model. In: 11th ICARD | IMWA | WISA MWD 2018 Conference – Risk to Opportunity, Pretoria, South Africa, January 2018.

Panday S, Langevin CD, Niswonger RG, Ibaraki M and Hughes JD (2013) MODFLOW-USG version 1: An unstructured grid version of MODFLOW for simulating groundwater flow and tightly coupled processes using a control volume finite-difference formulation. In: U.S. Geological Survey Techniques and Methods, book 6, chap. A45, pp 66.

Parkhurst DL, Appelo CAJ (2013) Description of Input and Examples for PHREEQC Version 3 – A Computer Program for Speciation, Batch-Reaction, One-Dimensional Transport, and Inverse Geochemical Calculations. US Geological Survey Techniques and Methods 6:1-497.

Šimůnek J, Šejna M, Saito H, Sakai M, and van Genuchten M (2013) The Hydrus-1D Software Package for Simulating the Movement of Water, Heat, and Multiple Solutes in Variably Saturated Media, Version 4.17, HYDRUS Software Series 3, Department of Environmental Sciences, University of California Riverside, Riverside, California, USA, pp. 342.

Characterization and Groundwater Modelling of a New Block-Caving Project

Boddaert F[1], Genc M[1], Beale G[1], Samuel T[2], Rahardian R[2]

[1]*Piteau Associates, Canon Court, West Abbey Lawn, Shrewsbury, SY2 5DE, United Kingdom, fboddaert@piteau.com, mgenc@piteau.com, gbeale@piteau.com*

[2]*PT Merdeka Copper, 92GQ+497, Perhutani, Sumberagung, Kec. Pesanggaran, Kabupaten Banyuwangi, Jawa Timur 68488, Indonesia, toddy.samuel@merdekacoppergold.com, rahardian.ruthman@merdekacoppergold.com*

Abstract

The Tujuh Bukit Project is operated by PT Merdeka Copper and is located in East Java, Indonesia. A block cave operation is planned beneath the existing open pits. An extensive campaign of deep exploration drilling is being carried out from the surface and underground. Consequently, hydrogeological conditions and future water management requirements are well understood and dewatering of the first underground production level has already been achieved.

A 3D FEFLOW groundwater numerical model has been constructed to help evaluate groundwater level variations above and around the proposed block cave, with the objective to assess the interaction between the planned underground workings and the surrounding environment. The numerical model is flexible enough to evaluate different mine plans.

Keywords: Block-cave, underground, groundwater, mine dewatering, numerical model

Introduction

The mining area is located on the slopes of Mount Tumpang, about 55 km southwest of Banyuwangi in southeast Java. The climate of southeast Java is tropical. Mean annual rainfall on the higher ground at the site is about 2 m, with about 80% of the rainfall typically occurring in a 7-month wet season.

Recent volcanic rocks dominate the site geology, predominantly dacite, and volcanic breccias. The project area is centered in and around a nested tonalite porphyry complex, with a structurally controlled advanced argillic alteration. Several primary and secondary geological structures offset the lithological units and create hydraulic boundaries in the non-weathered bedrock. There is a distinct upper weathered zone around 100 to 150 m in thickness, although weathering may extend deeper adjacent to fault zones.

The existing surface mining operation commenced in 2016 with three main pits (Pits A, B, and C), a heap leach operation (HLO), waste rock areas, and support facilities. The current plan is for a 6-year sub-level caving (SLC) operation mining downward from about 300 m depth, with concurrent development of a 20-year block caving (BC) operation starting at about 800 m depth (Figure 1). Planned access from the surface is by multiple declines.

Surface water drainage is radially outward from the high ground towards the west and south flank, and towards the Katak Creek drainage to the northeast and north. There are no major watercourses within the project area.

Groundwater levels are mostly near the ground surface and exhibit a natural seasonal fluctuation of a few meters. Under natural conditions, most active groundwater flow occurs within the weathered zone. The only source of groundwater is infiltration and recharge in the wet season. All groundwater movement is localized. There is no regional-scale groundwater flow in the project area. Although there are zones of interconnected fracture permeability that may extend several hundreds of meters laterally, the groundwater

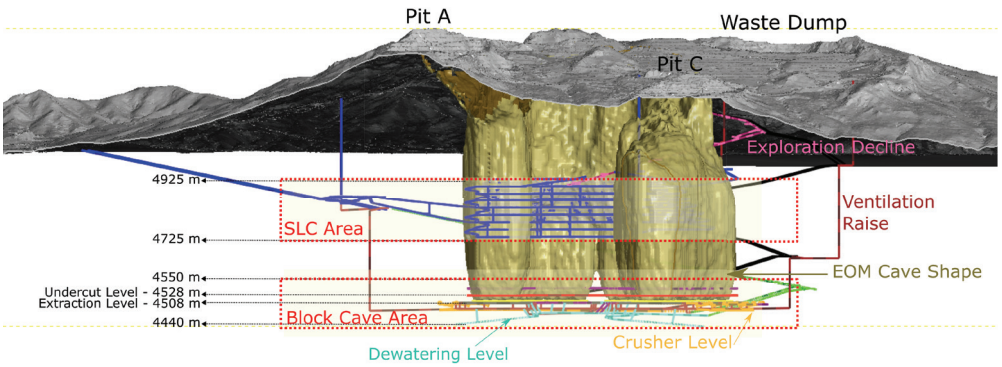


Figure 1 Sub-level cave and block cave details (looking Northwest)

system in the non-weathered (fresh) bedrock is compartmentalized by the lithological contacts and geological structures. As a result, widespread groundwater movement does not occur.

Dewatering is being achieved by allowing selected underground exploration drill holes to permanently flow (Figure 2). In the dewatered area, groundwater levels in the non-weathered (fresh) bedrock have become decoupled from the overlying weathered zone groundwater levels with two distinct phreatic surfaces. Multi-level piezometers typically show a strong dewatering response in the fresh bedrock but little to no drawdown in the overlying weathered zone.

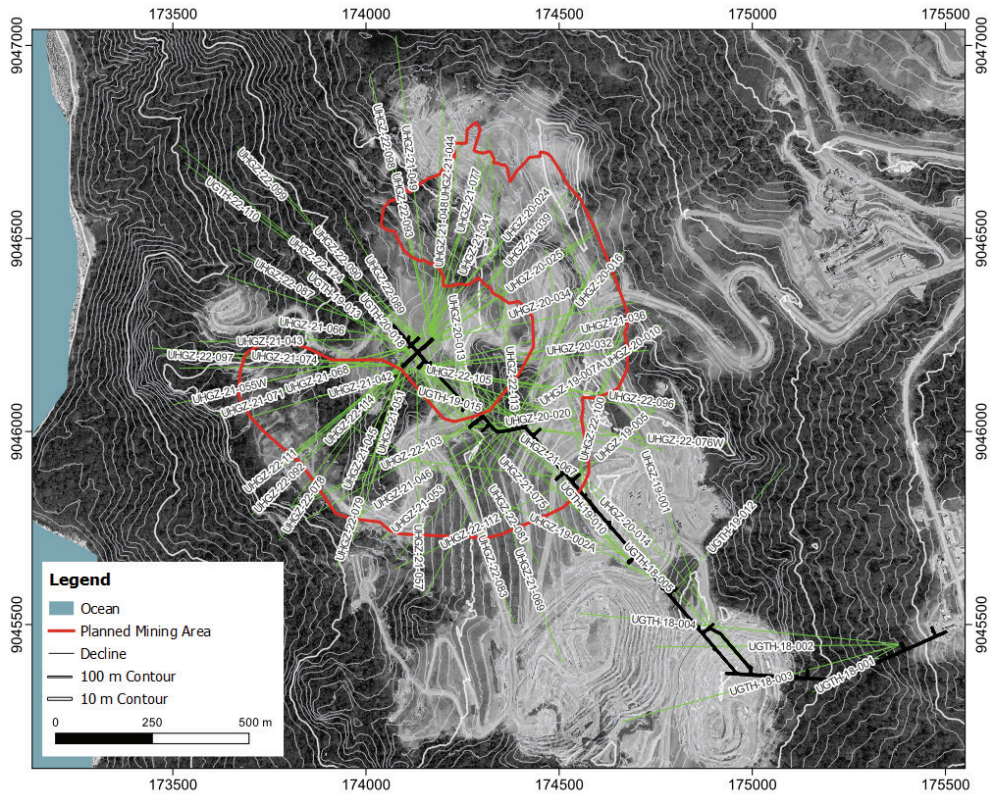


Figure 2 Underground drill holes used for dewatering the decline

The extensive collection of hydrogeological data from the surface and underground resource drilling represents global best practices. Consequently, hydrogeological conditions and future water management requirements are well understood. The decline has been successfully dewatered since 2019. Over 250 m of drawdown has already been achieved at a dewatering rate of between 30 and 35 L/s. Water management infrastructure for the current underground and surface mining is already in place.

Numerical Model

The numerical model is built to evaluate potential impacts on the local water resources and is designed to evaluate different designs of the underground mine. At this stage, model predictions are focused on the construction of underground infrastructure, extraction activities and development of a cave zone from the sub-level caving and block-caving operations. Model predictions are supported by a strong conceptual model which is underpinned by a large amount of field observations and testing. The currently available dataset guarantees that the main concepts characterizing the local groundwater system are included in a numerical model that reasonably simulates the site-specific conditions.

1. Model domain and construction

The domain, or area of coverage, of the numerical groundwater model is populated within FEFLOW by a finite element mesh which defines all stratigraphic and structural features plus existing mine voids which are likely to exert control on groundwater flow. The spatial limits of the model were determined primarily on a natural catchment boundary basis. The overall area of coverage of the model domain is 22 km². This encompasses all major mine facilities in the centre of the model area. The model is distributed vertically in 14 layers, with the upper layer defined with a maximum thickness of 5 m.

Development of the FEFLOW model was undertaken using discrete time-steps, within which either the physical conditions prevailing within the model domain or the 'operational rules' applicable to variables such as underground mine dewatering, were considered likely to remain reasonably constant.

2. Model calibration

Calibration of the FEFLOW model was performed by running simulations for the current period and comparing the results of simulated groundwater head elevations against recorded groundwater levels across the model domain. Iterative adjustments were successively made to recharge and model hydraulic parameters until optimum replication of measured water level distributions was obtained.

A total of 73 points within Tujuh Bukit's empirical database were considered to provide

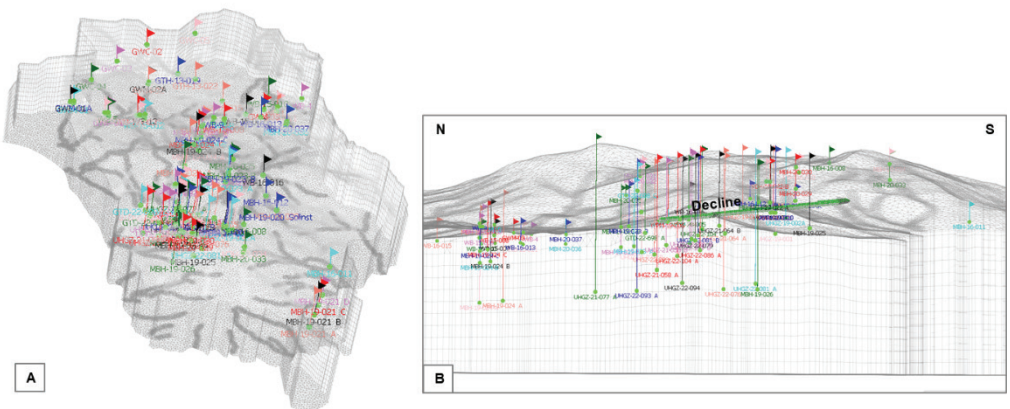


Figure 3 *Monitoring network currently included in the FEFLOW model. A) spatial distribution of monitoring points in the model domain. B) Cross-section view with the decline and VWP sensors*

reliable groundwater level measurements for use in calibration. Different types of monitoring points have been included in the numerical model (Figure 3).

The long-term simulated inflow into the decline (which currently includes the discharge from 72 underground exploration (UHGZ) holes) is equivalent to 25 L/s. The numerical model simulates a groundwater inflow of 20 L/s to the exploration decline. The simulated inflow into the decline is slightly below current groundwater extraction measured from the decline, but the model scenario is considering a steady-state simulation representative of a long-term equilibrium for the groundwater system with a total depletion of water available in storage. It, therefore, appears that the flow simulated in the drain holes is of the same order of magnitude.

UHGZ holes drilled as part of the drilling program have the potential to dewater the area of the cave zone if they are left open. The numerical model indicates that the depletion on the near-surface phreatic level in the Weathered Zone over the cave footprint is limited, but the UHGZ holes effectively depressurize the fresh, unweathered bedrock to the level of the exploration tunnel (Figure 4).

3. *Model prediction*

Once the numerical model was calibrated, a series of predictive simulations were executed from the calibrated model to predict the potential effects of the project development.

The predictive simulations are based on assumed dates adopted for the purpose of modelling and which may change as the mine plan is refined. The total duration of the predictive scenario is 28 years including all the major developments provided in the mine plan. It is divided into monthly and yearly stress periods to follow the current (January 2023) mine plan.

Underground infrastructures: The extraction level is represented with a series of seepage nodes at an elevation comprised of between 400 and 1,000 mbgl. The use of modulation functions enables the progressive activation of seepage nodes representing the underground infrastructure and mine expansion. The project will start with the construction of SLC infrastructures enabling the first ore to be extracted in 2025. By 2031 BC infrastructure will be fully developed below the SLC. Similar to the existing decline, seepage nodes are used to represent the drainage caused by the linear underground infrastructure (Figure 5). The exact location

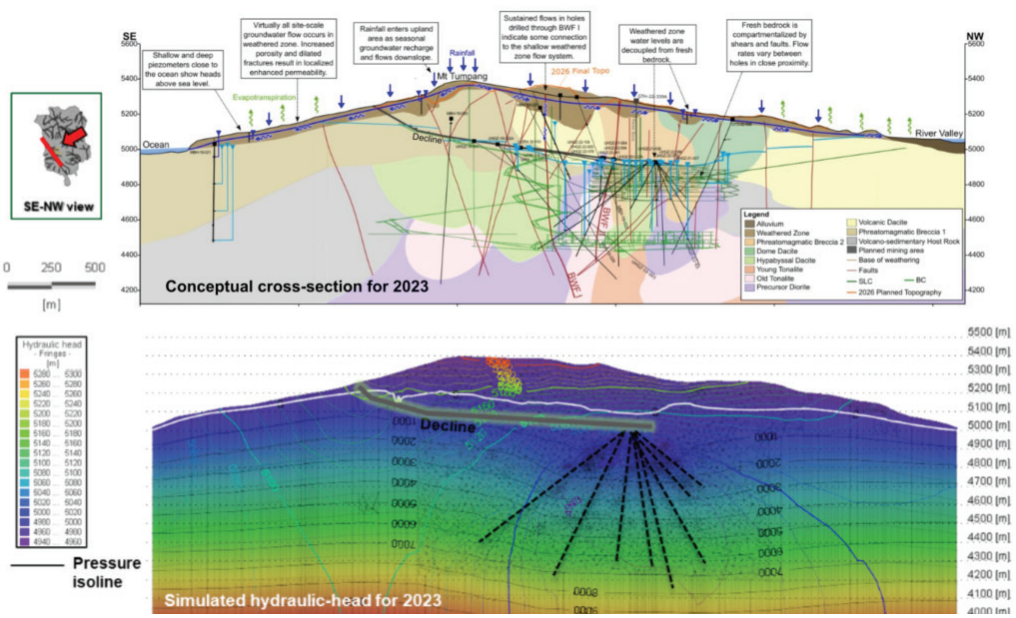


Figure 4 Effects of the UHGZ drilling program on pressure and hydraulic head distribution

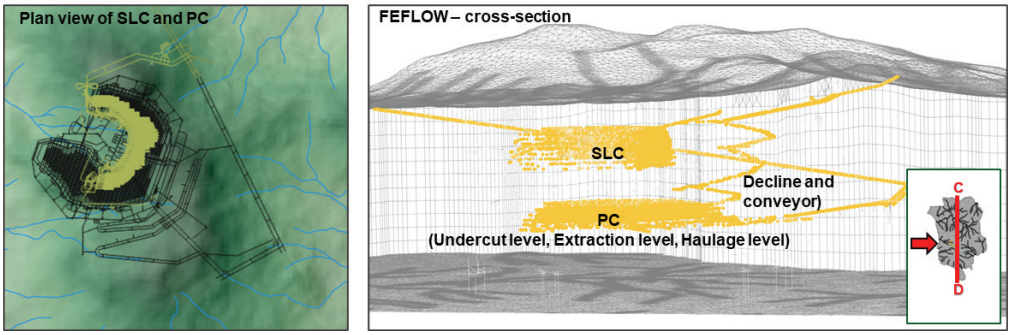


Figure 5 Implementation of underground infrastructures in the numerical model

of underground infrastructures is obtained by a local remeshing using the TetGen mesh generator. This powerful tool enables to evaluate alternative mine plans proposed during the development of the study.

Cave propagation: The model includes the transition of fractured bedrock caused by the release of confining stress which forms a halo around the cave zone (Figure 6). This is included in the FEFLOW model with a time-variant hydraulic conductivity that is linearly interpolated between the different cave shapes derived from a geomechanics model. Increased fracturing facilitates the drainage of groundwater towards the cave zone. The influence of the cave zone on the groundwater level distribution is simulated to occur mostly in the fresh and unweathered bedrock. Given the low hydraulic conductivity associated with the deep bedrock, the halo of fractured bedrock could easily move the groundwater further away from the cave zone in its deeper part, but probably with a minimal effect on the total groundwater inflow.

4. *Model results*

The higher hydraulic conductivity associated with the fractured and caved material generates an area of drawdown around the cave zone. Groundwater levels in the fresh, unweathered bedrock around the cave zone become decoupled from weathered zone groundwater levels. Groundwater level trends in the weathered zone are more subdued than in the deeper rock.

The model results show that drawdown is mostly limited to the local area of the cave zone because of the low conductivity and compartmentalized nature of the bedrock. Drawdown at the end of mining is developed around the cave, but the lateral extension is limited to less than 1 km.

Community wells located in the floodplain to the north of the project area are unlikely to be affected by any groundwater level variation because simulated drawdown in the fresh bedrock is centered over the cave zone and propagates essentially below Mount Tumpang.

Inside the zone of influence of the cave zone, the groundwater flow direction is modified towards the extraction level under the cave zone. Outside the zone of influence of the block cave, the groundwater flow continues to discharge towards the natural drainage system.

The BC's western limit of underground infrastructure is about 440 m laterally offset from the western hydraulic boundary (at 600 m depth) (Figure 7). Development of the overlying fracture zone and cave zone includes groundwater level variations in the fresh unweathered rock below the level of 5000 m.

The numerical model indicates that the hydraulic gradient, which is initially towards the west of the block cave, decreases and is almost neutralized by 2050. Simulated groundwater discharge towards the section located to the west of the project area decreases from 26 L/s in current conditions to 2.5 L/s at the end of the life of the mine. The current model has no simulated flow from the sea towards the block cave.

The model provides results based on the assumption that the drawdown remains local to the active block cave area. The development

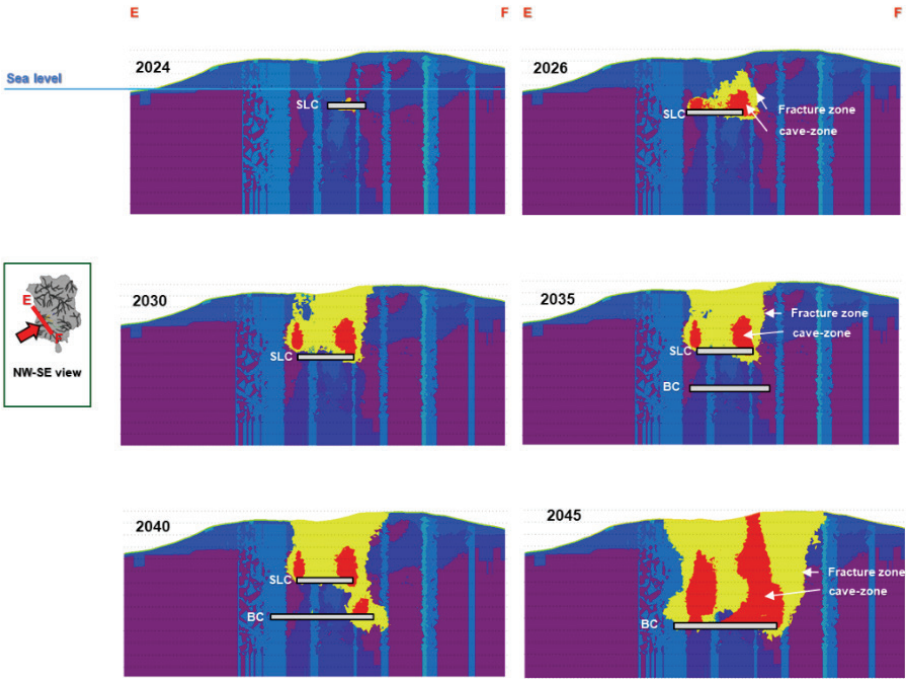


Figure 6 Implementation of underground infrastructures in the numerical model

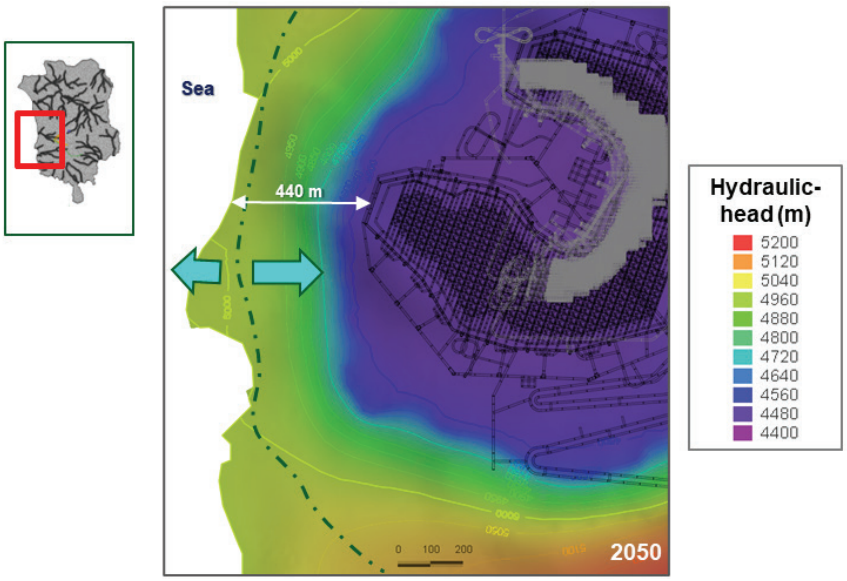


Figure 7 Current limit of simulated drawdown

of a fracture zone in direct contact between the underground workings and the other hydraulic boundary conditions would clearly create the potential for higher magnitude inflows. There are uncertainties associated with expected future stress release from structures in the vicinity of the fracture zone. This stress release could be transformed into preferential pathways, as such a monitoring program will need to be implemented to identify potential displacement and increases in fracture permeability. Modeling results can be used for developing an effective dewatering program for both the sub-level cave and the block cave.

Advanced Monitoring of Tailings Storage Facilities and Dams to Prevent Failure. Illustrated with Case Studies from UK, Africa and South America

Alastair B Bovim[1], Kym L Morton[2]

[1]*Insight Terra UK Limited, 112 Jermyn Street, St James, London,*

[2]*KLM Consulting Services Pty Ltd, 22 Central Road, Sunrella AH, South, PO Box, 119, Lanseria, 1748, South Africa, kmorton@klmcs.co.za, ORCID 0000-0002-5865-1979*

Abstract

Following the publication of the Global International Standard for Tailings Management (GISTM) many different types of monitoring network have been launched for use in the de-risking of Tailings Storage Facilities (TSF). Management of risk depends on using accurate data that is translated into information, then knowledge. Very fast data transmission coupled to real-time bespoke dashboards have become a significant tool for risk reduction. This paper summarises the monitoring networks available and ranks them for effectiveness in preventing failures.

The main finding is that the best monitoring systems include measurement of the factors behind causes of failure, such as measurement of hydraulic pressures and their speed of change both beneath and around TSF's and dam walls. Groundwater monitoring is an important component for risk management. Linkage to cost effectiveness encourages the systems to be installed and contribute to TSF management. Automation reduces human error. Recalculation of Safety Factors is possible and can be frequently updated.

The essential components of TSF risk reduction are discussed and a blueprint for accurate risk management with practical outcomes is presented. Techniques such as real time geo-resistivity profiling are illustrated.

Case studies from Europe (Keilder Water), Africa and South America (El Soldado) are given and the future of TSF monitoring is discussed.

This work will be very useful to TSF managers and all those involved in promoting the safety of TSF's in all types of climates and terrain. Transparency in information sharing and the international dissemination of TSF health to shareholders, stakeholders, communities and insurers can become routine.

Keywords: Tailings storage facilities (TSF), global international standard for tailings management (GISTM), monitoring, risk, pressures, failure

Introduction

Following the tragic failure of the Tailings Storage Facility (TSF) at Vale's Corrego de Feijao mine in Brumadinho in Brazil in 2019 the combined initiatives of the International Council on Mining and Metals (ICMM), the United Nations Environment Programme (UNEP) and the Principles for Responsible Investment (PRI) – collectively the Global Tailings Review – resulted in the publication in August 2020 of the Global Industry Standard on Tailings Management (GISTM), designed to improve TSF management[1] – see Figure 1 on the next page.

The standard lists six topic areas, 15 principles and 77 auditable requirements. The standard provides a framework for safe tailings facility management while affording operators flexibility as to how to best achieve this goal.

Principle 7 concentrates on the need for monitoring. It includes the design, implementation, and operation of monitoring systems to manage risk at all phases of the facility lifecycle including closure.

[1] https://globaltailingsreview.org/wp-content/uploads/2020/08/global-industry-standard_EN.pdf



Figure 1 *GISTM (https://globaltailingsreview.org/wp-content/uploads/2020/08/GISTM-Summary.png)*

Five specific requirements are listed under Principle 7:

1. Design, implement and operate a comprehensive and integrated performance monitoring programme for the tailings facility and its appurtenant structures as part of the Tailings Management Strategy (TMS) and for those aspects of the Environmental and Social Management Systems (ESMS) related to the tailings facility in accordance with the principles of Adaptive Management.
2. Design, implement and operate a comprehensive and integrated engineering monitoring system that is appropriate for verifying design assumptions and for monitoring potential failure modes. Full implementation of the Observational Method shall be adopted for non-brittle failure modes. Brittle failure modes are addressed by conservative design criteria.
3. Establish specific and measurable performance objectives, indicators, criteria, and performance parameters and include them in the design of the monitoring programmes that measure performance throughout the tailings facility lifecycle. Record and evaluate the data at appropriate frequencies. Based on the data obtained, update the monitoring programmes throughout the tailings facility lifecycle to confirm that they remain effective to manage risk.
4. Analyse technical monitoring data at the frequency recommended by the Engineer of record (EOR), and assess the performance of the tailings facility, clearly identifying and presenting evidence on any deviations from the expected performance and any deterioration of the performance over time. Promptly submit evidence to the EOR for review and update the risk assessment and design, if required. Performance outside the expected ranges shall be addressed promptly through Trigger Action Response Plans (TARPs) or critical controls.
5. Report the results of each of the monitoring programmes at the frequency required to meet company and regulatory requirements and, at

Table 1 GISTM Principle 7 monitoring implementation for mine water.

Requirement	Implementation		
	Surface water	Groundwater	Climate and hydrology
1 Performance monitoring programme	TSF pond, river and catchment design. Relate to dam breach analysis	Instrument pore water pressure monitoring	Precipitation capture and use of predictive climate models
2 Engineering monitoring	Pumps, pipelines and water balance	Drains, pumps and groundwater balance	Weather stations
3 Establish performance objectives	Limits for flood lines and freeboard	Determine Safety factors and integrate with slope geotechnical design	Determine resilience to extremes and determine risk values
4 Assess performance and link to TARPs	Install TARPs for breaches of dam levels	Design TARPs to intercept and reduce excess pore pressures	Early warning system to predict and manage impact of extreme events
5 Reporting	Dashboard and reviews	Dashboard and numerical modelling	Dashboards and simulations

a minimum, on an annual basis. The Responsible Tailings Facility Engineer (RTFE) and the Engineer of Record (EOR) shall review and approve the technical monitoring reports.

These five requirements emphasise the improvement of monitoring by focussing not only on monitoring critical parameters but also monitoring the effectiveness of the monitoring parameters and equipment used.

Historically, monitoring has emphasised measuring the movement of a TSF but this does not enable management of risk. Measurement of movement is often too late to prevent failure. It is more important to measure the causes behind movement (Morton *et al* 2008 and Morton 2020). Failure in a slope, known as volume deformation, will present (under various pressures and stresses) as three possible scenaria:

1. Compression of water in the pores of the material;
2. Compression of individual particles (sediments, etc.);
3. Re-arrangement of particles, usually to a more compact configuration.

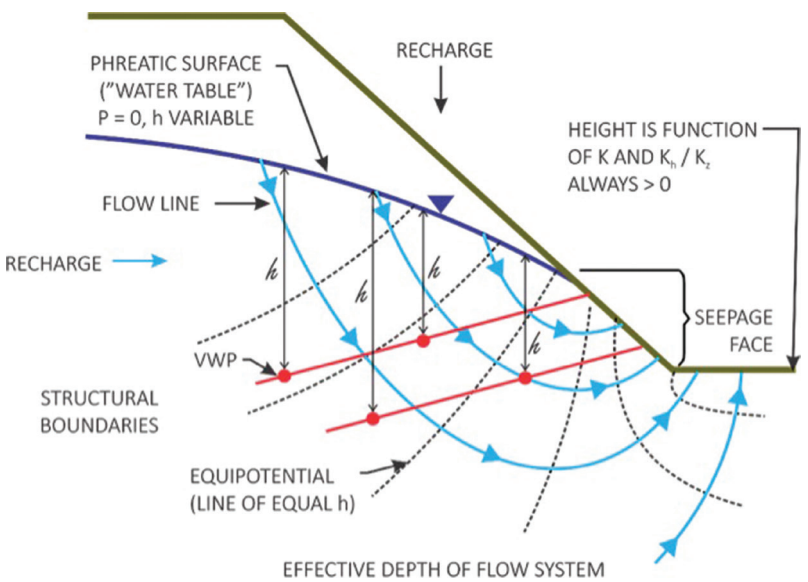


Figure 2 Anatomy of a slope

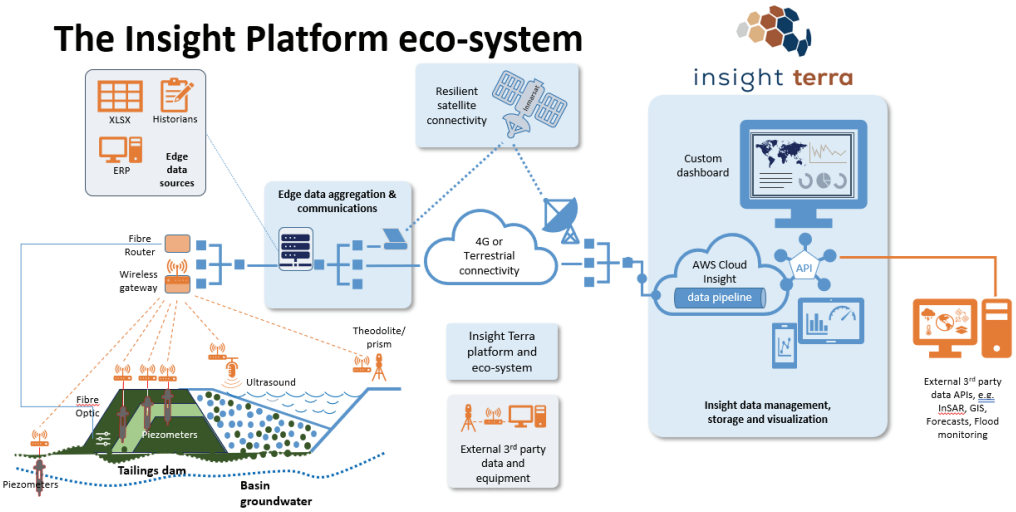


Figure 3 A monitoring system eco-system

Once a slope is established the only factor that can be changed to improve the stability of a slope is reducing the weight on, or pressure within, that slope. Figure 2 illustrates the hydraulic anatomy of a slope and the type of installation used to measure the hydraulic pressure gradient.

By draining or pumping the water within the slope the pressures are decreased and the stability of the slope improved. Monitoring systems that not only measure movement of a slope but also measure the causes of failure enable the engineer to better manage the risk and reduce the probability of failure. Figure 3 shows the ideal eco-system for a monitoring network around and on a TSF.

It is also possible to measure the saturation of a slope using geophysical techniques such as geo-resistivity arrays. A permanently installed system called G.Re.T.A. is illustrated

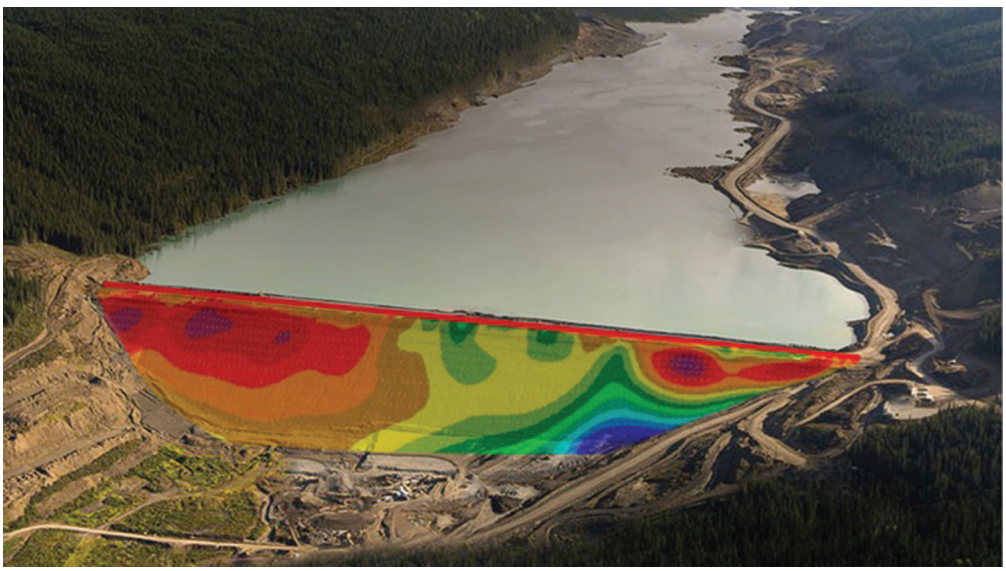


Figure 4 Permanent resistivity array installation to reveal weak zones in a dam wall (https://www.lsi-lastem.com/products/G.Re.T.A./)

Table 2 Methods for TSF Monitoring

Method	Instrumentation Examples	Advantages and considerations
In-situ – ground based and environmental monitoring	Vibrating wire piezometers, geo-resistivity, inclinometers / shape arrays, load sensors, freeboard, slurry density, weather station – rainfall, evaporation, temperature – downstream boreholes, air quality	Various real-time data from instruments can provide insights into safety states and when integrated with alerts and notifications can provide an early warning of potential failure.
Satellite and aerial monitoring	InSAR satellite, drone imagery, drone – LIDAR, drone surveys, bathymetric surveys	Monitor wide area, however lower frequency of data and post-processing required
Geotechnical modelling	Finite Element Modelling (FEM), seeping modelling, slope stability modelling, Fluid modelling	Identification of potential stability issues before they occur, helps to identify critical risks and preventative measures.

in Figure 4. The red areas are areas of low resistance and therefore highlight weak seepage zones within the TSF of dam wall.

There are many different systems for monitoring the stability of a TSF. Table 2 lists the types and their advantages.

Typically, a combination of the above mentioned methods will be utilised during the phases of the TSF lifecycle. Each of the methods has its advantages depending on the specific requirements of TSF being monitored.

Three case studies are presented:

HDS Case Study

Customer need: to evaluate the effectiveness of its new approach to mine tailings treatment.

Hydraulic Dewatered Stacking (HDS) is part of Anglo American's FutureSmart Mining programme and real-time monitoring of the trial is an essential aspect of this demonstration facility in Chile. The project has multiple objectives:

- To continuously monitor, report on and visualize the facility's health and structural integrity;
- To deliver real time monitoring of the evolving moisture content in the novel dewatered stack approach (HDS); and
- To develop a comprehensive data management platform for the HDS demonstration facility, effectively serving as a proof-of-concept for a broader tailings monitoring solution.

The system comprises a resilient and secure edge- and cloud-based data management and monitoring platform. The edge-based computer node integrates with all nine different sensor types, totalling 108 separate



***Figure 5** El Soldado HDS demonstration facility*



Figure 6 *All weather communications container*



Figure 7 *Keilder Water Dam Wall*

instruments monitoring 500 data monitoring points in, under, around and on the tailings storage facility. All this raw monitoring data is transformed, validated, processed, stored and displayed in the cloud based application, supporting analytics and decision making.

To address the need for reliable communications at the remote location, a satellite communications service – Inmarsat Broadband Global Area Network Machine-2-Machine – is utilised.

An all-weather container houses all the equipment, and is supported by PV solar arrays for totally independent remote operation.

Kielder Water & Dam Monitoring

Customer need: to ensure the continued integrity of the Keilder Water dam wall

Keilder Water is the largest freshwater reservoir in Europe and feeds a catchment area of 23,000 people and 120 businesses. The continued integrity of the dam wall is of utmost importance to these communities and the environment around the reservoir.

The project implemented an IoT-based monitoring system to monitor the stability of the dam wall and the volume of water entering the reservoir from its tributaries. Types of instrumentation included existing standpipe piezometers, biaxial tiltmeters on the dam wall and water level sensors placed in tributaries feeding the reservoir.

An additional challenge was that the whole area around the reservoir has reduced or no cell phone network coverage, and therefore the communications solution supporting the monitoring network needed to consume low power and have long durability, low maintenance and support a very reliable and secure data transfer from sensors to users. Reliable transmission of all the data from the reservoir was made possible by a resilient, all-weather telecoms kiosk that operated 24/7 fully independently off-grid.

Platinum Mine Tailings Facility – South Africa

Customer need: To move from entirely observational monitoring to automated and integrated performance monitoring.

A customer in Africa has implemented a programme of improvement to ensure that its mine tailings facilities all comply with the requirements of the GISTM, published in August 2020. A comprehensive monitoring solution is being rolled out to all its platinum mines in Africa.

The high level solution architecture includes the use of data loggers connected to various sensor types that communicate wirelessly to a central wireless gateway, which then aggregates and transmits the raw data into an AWS cloud-based platform for conversion into engineering data and metrics in a time-series database. The data is processed by the cloud platform in real-time, validated and transformed into insightful metrics and visualisation, ensuring



Figure 8 Location of tiltmeters on dam wall



Figure 9 Tributary sensor locations



Figure 10 Water level device

higher levels of confidence and trust in the interpretation of the data.

Instrumentation was automated in a phased approach, starting with phreatic surface monitoring and additional monitoring uses cases were implemented by priority in an iterative approach over an 18 month period.

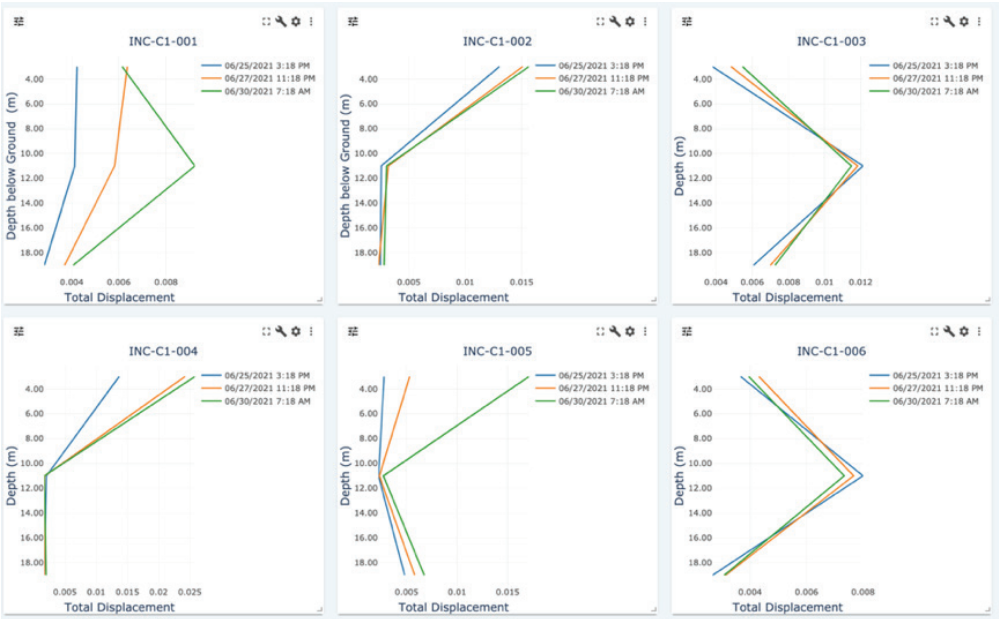


Figure 11 Inclinometer displacement data visualisation

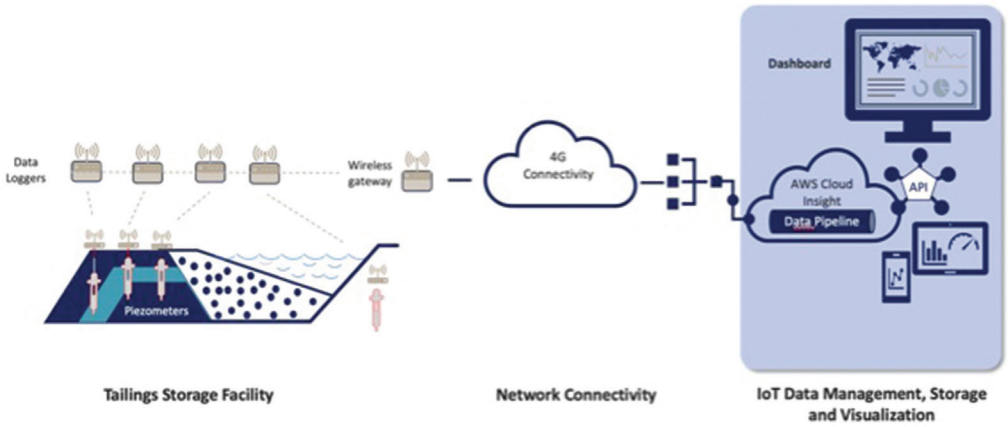


Figure 12 High level monitoring solution architecture

Acknowledgements

The authors acknowledge the contribution by Philip Newton of Anglo American plc UK

References

GISTM https://globaltailingsreview.org/wp-content/uploads/2020/08/global-industry-standard-on-tailings-management.pdf

Morton, K. L; Muresan, M.C and Ramsden, F., 2008. Importance of pore pressure monitoring. The Journal of The Southern African Institute of Mining and Metallurgy, Volume 108, pp. 662–667.

Morton, K. L., 2020. Tailing dam risk reduction using accurate pore pressure monitoring. IMWA, pp. 1–9.

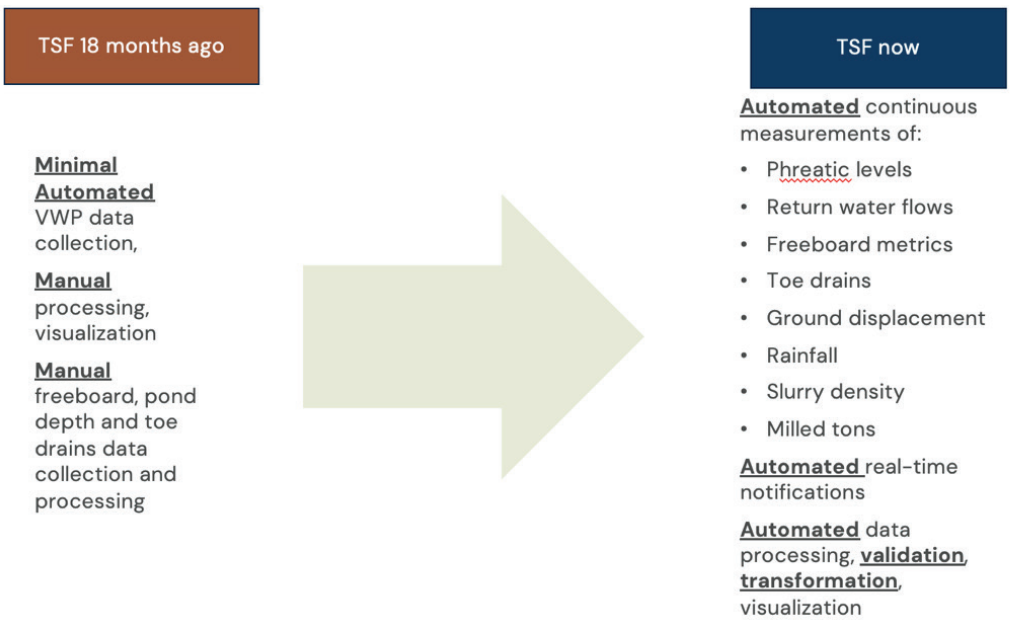


Figure 13 High level monitoring solution architecture

An assessment of the current operation of the Coal Authority Six Bells Mine Water Treatment Scheme, South Wales

R.J.Bowell[1,2], S.Bamforth[3], J.Walton[2], P. Brabham[2]

[1]*SRK Consulting, Churchill House, Churchill Place, Cardiff CF102HH*

[2]*School of Earth and Environmental Sciences, Cardiff university, Park Place, Cardiff, CF10 3AT*

[3]*The Coal Authority, 200 Lichfield Ln, Mansfield NG18 4RG*

Abstract

The Six Bells Mine Water Treatment Scheme is a semi-passive Coal Authority scheme within the South Wales Coalfield, near Abertillery. Hydrogen peroxide is used to promote iron and sulphide oxidation in the mine water.

This paper investigates the performance of the scheme over the last two decades whether the chemistry of the discharge has changed over time, and if hydrogen peroxide dosing is still required to effectively remove iron. Both iron and manganese in the mine water have decreased over time, with results suggesting that peroxide may no longer be required to fully treat the mine water.

Introduction

Over the last forty years coal mining has been phased out in the United Kingdom due to economic, environmental, and cultural reasons. This has resulted in environmental impacts in the years following closure, particularly in South Wales. Recovering groundwater in the old mines has flushed the products of pyrite oxidation and dissolution of siderite into the discharge water generating acidic to neutral high iron chemistry discharge waters.

The principles of mine drainage generation are well understood, with extensive research in the last 50 years due to the serious impact it can have on wildlife and ecology of river systems. Mine drainage imposes a significant threat across the South Wales Valleys, where such a concentrated band of vast, profitable coal mines existed. Coal mining has scarred the landscape and left behind an unmistakable legacy of orange, odorous contaminated water. Waters affected by mining can be acidic, circumneutral, basic, dilute, mineralised and saline (Nordstrom *et al*, 2015). The array of different chemical properties mine waters can exhibit often requires intricate water sampling investigations when planning what remediation strategies to impose. Remediation schemes aim to return water from its contaminated state by oxidising the water, promoting the oxidation and settling of dissolved metals, and eventually returning the pH to a circum neutral state by reducing acidity (Bowell *et al* 1999).

This paper presents an evaluation of one such scheme at the former Six Bells Colliery. This joint project between SRK Consulting, The Coal Authority and Cardiff University aims to assess the current operational effectiveness of the Six Bells Mine Water Treatment Scheme. The main focus is on the performance of the scheme, and whether the chemistry of the water has changed sufficiently over time (with respect to the iron loading) so as to no longer require hydrogen peroxide as an oxidising agent, and if the same productive treatment can be done without the expense of dosing.

Background

The Six Bells Colliery was in operation from 1895, located just to the south of Abertillery in the Ebbw Fach Valley. Closure occurred in 1986 following the miners' strike of the previous two years (Lawrence, 2009). After the cessation of pumping, groundwater began to fill the void space of the deep workings. Mine waters began discharging into the Ebbw Fach River by 1998, exhibiting the typical orange ochre staining associated with historic coal mining areas. As of 2001, this site was

regarded as one of the most contaminated and significant mine drainage discharges in the UK (Jarvis *et al*, 2003), inflicting severe ecological and biological impacts within the Ebbw Fach River.

In 2000, The Coal Authority added the Six Bells mine drainage discharge to its list for treatment, with the preliminary treatment feasibility study of the discharge recommending a combination of passive and active remediation techniques. The scheme consists of two parallel settlement ponds, followed by an aerobic wetland, before the treated water is discharged into the Ebbw Fach River. Hydrogen peroxide (H_2O_2) dosing was implemented at the scheme, in lieu of an aeration cascade, due to restrictions, with topography and space, the high iron loading, and the potential for hydrogen sulphide odour. Hydrogen peroxide dosing accelerates the oxidation of ferrous iron (Fe^{2+}) to ferric iron (Fe^{3+}), which promotes the settling of iron solids and removes the hydrogen sulphide by oxidation of the sulphide to sulphate.

An aeration cascade was constructed in 2013, and the mine water quality has steadily improved over the last two decades (reduced iron loading), so this study was conducted to assess the ongoing requirement of hydrogen peroxide dosing. Six Bells MWTS has been in operation for nearly 20 years, and, as with all mine water treatment schemes, regular assessment of the scheme performance is required, as treatment may need to be refined as the mine water chemistry matures.

Methodology

Six Bells MWTS is located near the old village of Six Bells, now part of Abertillery, South Wales. The aim of this study is to evaluate the role of hydrogen peroxide dosing as an oxidising agent, and if the dosing can be reduced or stopped, allowing a discounted operational cost. The peroxide dosing was turned off for 2 days over a 4 day period (August 3rd to 6th 2021) to assess the difference in the scheme operation with and without dosing.

Field sampling occurred over four consecutive days. A total of eight sampling points were established at sequential points through the scheme, the first being raw mine water pumped from the shaft, and last being the reed bed outflow, just before its confluence with the Ebbw Fach River.

Analysis was completed at Cardiff University using Inductively Coupled Plasma Mass Spectrometry (ICP-MS) instrument. Samples were filtered into 25 ml plastic bottles using a 0.45 µm filter and 10 ml plastic syringe. This removed suspended iron from the solution. Samples were transferred to 15ml centrifugal tubes and were diluted by a factor of 5 (2 ml of sample and 8 ml of Milli-Q reference water) and subsequently acidified with 1 ml nitric acid (HNO_3). A correction was later made for the dilution to give native values.

Results

Review of Overall Water Chemistry

The main parameters that will be discussed are field parameters of pH, dissolved oxygen (DO), total suspended solids (TSS) and laboratory analysis of, alkalinity, iron (Fe), manganese (Mn), aluminium (Al) and sulfate (SO_4). These will indicate the efficiency of the scheme and also what processes are occurring in different parts of the system before the mine water is discharged.

Long-term trends of key parameters are presented in Figure 1. The pH is highly variable over the period of monitoring showing gradual increase over time. All values for pH lie within the permitted range for discharge.

Total and filtered iron concentrations and the ratio of filtered iron to total iron have been monitored. Total iron encompasses all the iron in the sample, while filtered iron only accounts for iron in the <0.45 µm fraction. Raw influent concentrations of total iron have generally shown a decrease, whilst outflowing concentrations have remained relatively constant (Figure 2). A large spike in total iron is observed at the end of 2011, rising to 43 mg/L before falling again, which is likely an artefact of the sampling methodology, or the sloughing of particulate iron from pipework. Concentrations in the outflow from settlement ponds 1 and 2 have also remained constant, at ~2 mg/L.

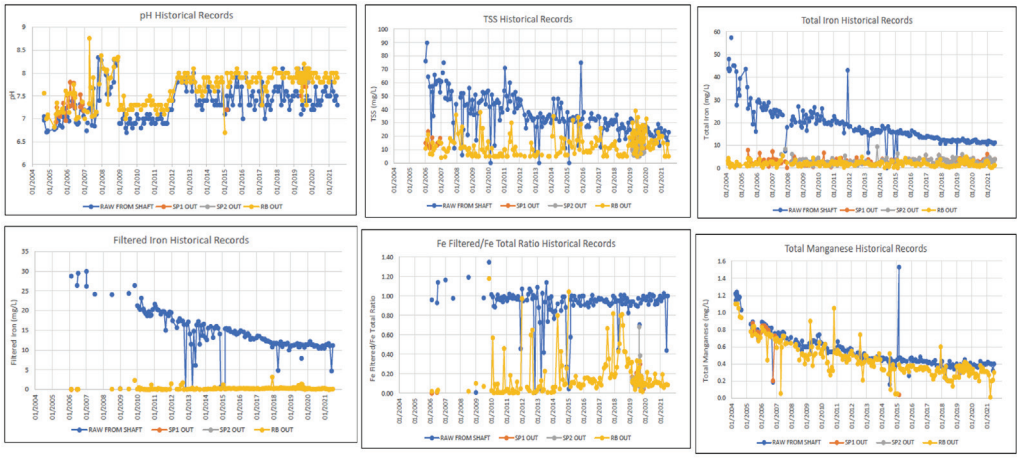


Figure 1 *Monitoring data from shaft mine water (raw from shaft), outflow from settlement ponds (SP1/2 OUT) and final discharge post reed beds (RB OUT). Monitoring data for the period 2004 to 2021. Source: The Coal Authority*

Outflowing loads are consistent, between 6 and 9 kg/day. Total iron removal rates have decreased from an average of 93% in 2004-2006 to 85% in 2019-present (Figure 3). Overall, similar iron levels at the outflow but reducing influent levels and that will lead to slight reductions in removal performance over time (Fig. 3).

Long-term ratios of filtered iron to total iron show a contrast between inflowing ratios and outflowing. Inflowing ratios remain constant at a near 1:1, whilst outflowing ratios fluctuate heavily, averaging a 0.1:1 ratio until 2017, where it increases to an average of 0.3:1, before falling back to its original ratio.

Total manganese concentrations have decreased over time, from an approximate 1.2mg/L in 2004, to most recently 0.4mg/L.

Hydrogen Peroxide Assessment

Hydrogen peroxide dosing was introduced to tackle sulfide odour and to oxidise ferrous iron in the mine water. Assessment of the benefit of peroxide addition shows slightly lower pH in the settlement ponds, presumably reflecting hydrogen ion liberation

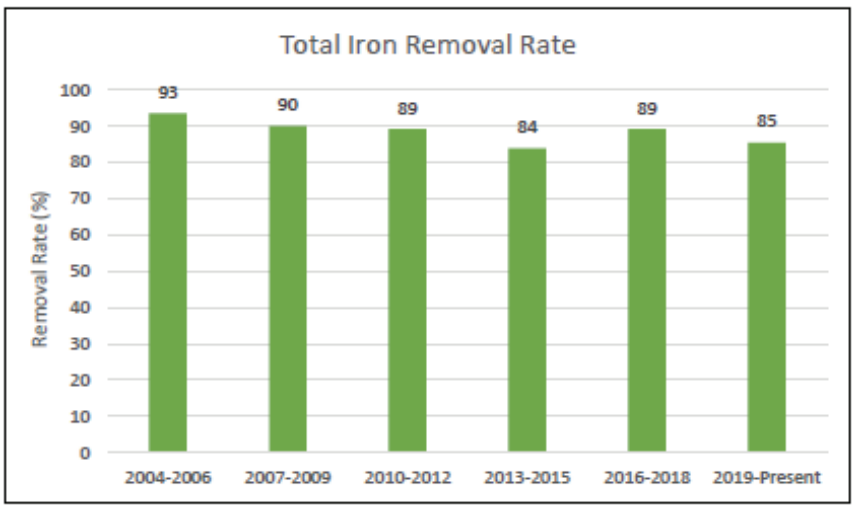


Figure 2 *Long-term total iron removal rates at Six Bells broken down into 3 year periods from 2004 to the present day.*

on oxidation of ferrous iron at different stages of the treatment system (Figure 4). Incoming total iron concentrations exhibit a very similar trend for peroxide dosed (peroxide on) and natural waters (peroxide off). A clear drop in concentrations can be seen for both waters through settlement pond, with dosed water concentrations slightly lower at 3.96 mg/L compared to 4.12 mg/L. Iron loads inflowing to the system are also very similar, at 45.36 kg/day and 46.66 kg/day, respectively. Outflowing loads were measured at 3.2 kg/day and 3.97 kg/day. Removal rates are 93% for dosed waters compared to 91% for natural waters. Filtered iron concentrations show a stark contrast when compared to one another (Figure 3). Natural water concentrations greatly reduce through the settlement pond, from 10.2 mg/L to 0.07 mg/L, whilst dosed waters remain constant. Inflowing loads are significantly higher for natural waters, at 47.95 kg/day, compared to only 0.82 kg/day for dosed waters. Output loads are much closer, measured at 0.09 kg/day (natural) and 0.13 kg/day (dosed). Removal rates show waters without hydrogen peroxide have 100% efficiency against only 84% for hydrogen peroxide dosed waters.

The ratio of filtered iron to total iron begins much higher for natural waters at 1.03:1, compared to 0.02:1 for peroxide dosed waters. The raw ratio then drops significantly to 0.02:1 at the end of the settlement pond, identical to the ratio of the dosed waters at this point in the scheme (0.02:1). The raw waters remain at 0.02:1 until they are output, however the dosed waters rise slightly to 0.04:1.

Concentrations of total manganese remain relatively stable until the reed bed, where dosed waters decrease from 0.36 mg/L to 0.29 mg/L, and natural waters from 0.38 mg/L to 0.26 mg/L (Figure 4). Inflowing loads are identical regardless of hydrogen peroxide dosing, at 1.68 kg/day. Output is slightly higher for the dosed waters at 1.25 kg/day compared to 1.12 kg/day for natural waters. Removal rates for peroxide dosed waters were measured at 26% and natural waters at 33%.

Discussion

Since its inception in 2004, the Six Bells discharge pH has varied between 7 and 8 pH, and increasing pH is not a main priority when operating the site. However, a period of decreased pH can be observed between

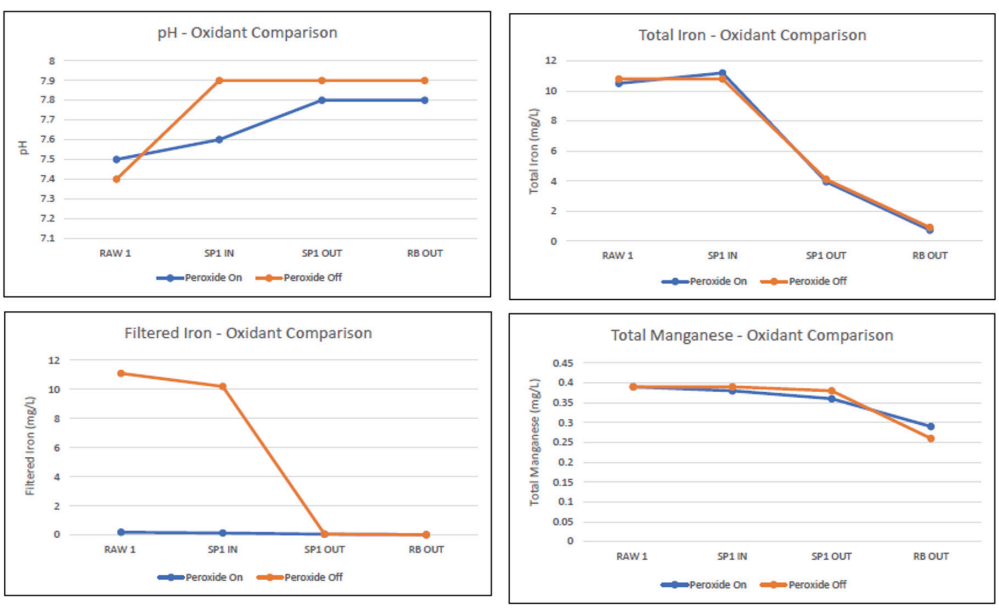


Figure 3 *Influence of hydrogen peroxide dosing on chemistry of pH, total and filtered iron and manganese, Six Bells MWTS.*

the end of 2009 and the beginning of 2012. This cannot be the result of changes at the site on an operational level, as the only major change, the aeration cascade, was constructed the following year. A likely explanation for the decreased period is that of insufficient groundwater recharge.

Six Bells has maintained a consistent removal rate for both total and filtered iron of above 85% since 2004. Total iron removal rates have shown some sign of decrease, dropping from 93% in 2004-2006 to 85% from 2019 onwards. Analysis of the field samples shows a removal rate of 93%, which suggests this decline may have been temporary, or the field sample is not indicative of the longer-term trend. Relatively high removal rates imply oxidation and subsequent hydrolysis reactions are occurring. The majority of iron is removed through the settlement ponds, indicating they are performing as intended, with the iron being successfully oxidised in the scheme.

Removal rates of manganese have generally increased, from 10% in 2004-2006 to 24% within the last 3 years. Manganese precipitation is difficult to predict and analyse due to its many oxidation states. Abiotic oxidation and complete removal will usually occur above pH 9 (Jacobs *et al*., 2014). Six Bells mine water has a pH of between 7-8, which is not high enough for purely abiotic oxidation. However, as the iron content is over four times greater than the manganese concentration, co-precipitation can occur (Jacobs *et al*., 2014). As iron forms iron hydroxide (Fe(OH)3) and precipitates, small amounts of manganese can co precipitate with the ochre flocs within the settlement ponds.

Iron is oxidised preferentially over manganese and will only begin to undergo oxidation when iron has been reduced significantly. The main portion of manganese removal occurs biotically in the reed bed once the majority of iron has been removed. This explains the low rate of manganese removal at Six Bells, which sits at 26% currently. A jump in manganese removal rate occurred after 2013 due to the construction of the aeration cascade, rising from 15% in 2010-2012, to above 20% from then on. The aeration cascade increased dissolved oxygen within the settlement ponds, likely accelerating the oxidation rate of iron, in turn having a direct effect on oxidation of manganese.

Seasonal variability of metal concentrations within mine water can play a huge part in the effectiveness of the scheme throughout the year. Manganese and iron concentrations are most susceptible to this (August *et al*., 2002). Flow rate would only partially vary at Six Bells as the mine water is pumped at a continuous 40 L/s, however, manganese and iron concentrations may drop in summer compared to winter months.

Despite the short duration of the testwork, the addition of hydrogen peroxide (H_2O_2) appears to now have little effect on the pH at Six Bells. Waters without dosing show a quicker pH increase through the scheme, starting at 7.4 and increasing to 7.9. These conditions are still more than enough for the oxidation of iron. Total iron removal rates are almost identical regardless of hydrogen peroxide addition, with waters at Six Bells experiencing a 2% decrease when dosing is turned off. Removal rates remain over 90%, suggesting that the aeration cascade supplies enough dissolved oxygen (DO) to the settlement ponds to sufficiently promote iron oxidation and counteract the loss of H_2O_2.

Filtered iron concentrations experienced the biggest variation. After dosing, raw filtered iron concentrations were measured at 0.19 mg/L, whilst when dosing was turned off, they rose to 11.1 mg/L. The results indicate that iron oxidation is almost complete and this would infer that the peroxide is causing rapid oxidation of dissolved iron by the time it reaches the top of the cascade.

Manganese removal rates increase when peroxide dosing is turned off, at 33% compared to 26%. Concentrations decrease quicker in the settlement ponds when dosed, likely as the iron is oxidised faster, which would remove manganese via sorption within iron hydroxides (Stumm and Morgan, 1981). Waters without dosing remove a significant amount of manganese through the reed bed. This is most likely explained by formation of insoluble Mn2+ oxides at low oxygen fugacity and mobilization of Mn in higher oxidation systems.

Conclusions

Total iron concentrations output from Six Bells have averaged 2 mg/L. Removal rates have decreased 8% since its inception, despite a lower incoming load. Filtered iron removal rates remain exceptionally high, which will be promoted by the addition of hydrogen peroxide. The majority of iron is removed through the settlement ponds rather than the reed bed, suggesting the ponds are working as expected. Manganese concentrations at Six Bells are relatively low, with removal rates of around 26%. Manganese removal is mainly conducted through the reed bed once iron has been preferentially oxidised. An increase in residence time may bolster removal rates, shown by the significant jump in 2013, presumed to be a result of additional aeration by the aeration cascade. From the short-term assessment conducted, hydrogen peroxide dosing at Six Bells had limited benefit over an entirely passive treatment process. The aeration cascade, implemented in 2013, now provides sufficient dissolved oxygen levels for the reduced concentrations of contaminants it receives, and an additional longer term and closely monitored trial (3-6 months) is now required to assess scheme performance without peroxide dosing.

References

Bowell, R.J., Connelly, R.J. Dodds, J.E., Sadler, P.J.K. and Williams, K.P. 1999 Chemical containment of mining waste. In: Chemical Containment of Waste in the Geosphere (ed: R. Metcalfe& C.Rochelle) Geological Society of London Special Publication, 157, 213-240.

Hedin, R.S., Nairn, R.W. and Kleinmann, R.L.P., 1994. Passive Treatment of Coal Mine Drainage. US Bureau of Mines Information Circular, (9389).

Jarvis, A., England, A. and Mee, S., 2003. Mine water treatment at Six Bells colliery, South Wales: problems and solutions, from conception to completion. Land Contamination & Reclamation, 11(2), pp.153-160.

Nordstrom, D., Blowes, D. and Ptacek, C., 2015. Hydrogeochemistry and microbiology of mine drainage: An update. Applied Geochemistry, 57, pp.3-16.

Rose, A.W. and Cravotta III, C.A., 1998. Geochemistry of coal mine drainage. Coal mine drainage prediction and pollution prevention in Pennsylvania, 1, pp.1-22.

Wood, S., Younger, P. and Robins, N., 1999. Long-term changes in the quality of polluted minewater discharges from abandoned underground coal workings in Scotland. Quarterly Journal of Engineering Geology and Hydrogeology, 32(1), pp.69-79.

Walton J. 2022 Performance assessment of the Six Bells Mine Water Treatment Scheme, Abertillery, South Wales. MSC thesis, Cardiff University. 157p.

Younger, P., 2000. The adoption and adaptation of passive treatment technologies for mine waters in the United Kingdom. Mine Water and the Environment, 19(2), pp.84-97.

Modeling Heap Leach Solutions to Optimize Safety and Revenue

Larry Breckenridge[1], Todd Harvey[1]

[1]*Global Resource Engineering, 600 Grant St. Suite 975, Denver, Colorado. www.global-resoruce-eng.com*

Abstract

For many mining projects, the most important water is not the effluent from a treatment plant or the fresh water supply, but the solution working its way through the Heap Leach Pad (HLP). Heap leaching of both gold and copper minerals produce their revenue from the interactions between water and ore. Unsaturated-zone groundwater modeling platforms allow for the accurate and effective prediction of the flow-through behavior of leach solutions within HLPs. GRE has applied this methodology on a gold heap leach pad using agglomerated ore. The simulation was used to optimize the leaching process and to aid in geotechnical and environmental safety analysis.

Keywords: Heap leaching, gold, unsaturated flow, agglomeration, groundwater flow simulation.

Introduction

Heap leaching is often the most cost-effective way to extract value from gold or copper ores. Heap leaching involves placing ore-grade material on an impermeable liner foundation with a solution collection system of drainpipes and irrigating the surface with either cyanide solution (for gold) or acid (for copper). Within the heap, chemical reactions occur which liberate the payable metal from the rock. The resultant solution, called pregnant leach solution (PLS), reaches the liner and the collection pipes, and then reports to a storage facility (pond) for processing where the metal is removed, the solution conditioned, and re-applied to the HLP as barren leach solution (BLS).

Flow modeling is an especially useful tool in HLPs with low conductivity ore. Low conductivity can occur for a number of reasons, but at this HLP, there are high proportions of fine or swelling clay minerals. Agglomeration is a process employed prior to leaching to improve solution conductivity. Agglomeration involves adding a binder, along with water or fresh lixiviant, to the crushed ore in a tumbling cylinder to bind fine-grained particles into gravel-sized material. The formation of agglomerates helps to improve the solution flow through the HLP.

Objectives

GRE has utilized modern unsaturated flow modeling platforms to better-understand the dynamics of heap leach flow in order to resolve several issues within an HLP. Specifically, simulations were performed to determine:

- If under-leached zones exist from poor solution distribution;
- If the pad had saturated zones which may impact geotechnical stability;
- If excess head was accumulating on the liner, augmenting the risk of a PLS leak through a pinhole-sized failure in the liner;
- If agglomeration process was adequate to ensure good leaching solution flow; and,
- If special conditions may detrimentally impact the operation or safety of the HLP.

Understanding the issues above is essential to the safe and profitable operation of an HLP.

Background

The flow in an HLP is dominated by unsaturated flow (Sheikhzadeh, 2005). Unsaturated flow is different from saturated flow because hydraulic conductivity is a non-linear function of the material moisture constant (Equation 1), rather than a constant. As a result, the practitioner must define the function of the conductivity of the material

over a range of possible moisture contents of the materials. This is done through the application of the Van Genutchen equation and the Genutchen-Mualem model (Gurdal & Benson, 2003):

$$\theta = \theta_r + (\theta_s - \theta_r)\left[\frac{1}{1+(\alpha\psi)^n}\right]^2 \quad (Eq.\,1)$$

$$K_\psi = K_s \frac{\{1-(\alpha\psi)^{n-1}[1+(\alpha\psi)^n]^{-m}\}^2}{[1+(\alpha\psi)^n]^{\frac{l}{2}}} \quad (Eq.\,2)$$

Where:
θ_r = residual water content (≈ 0)
θ_s = saturated water content (equals porosity),
K_ψ = unsaturated hydraulic conductivity (as a function of soil matric suction)
K_s = saturated hydraulic conductivity
α, n = parameters fitted to Soil Water Characteristic Curve data (m= 1-n-1) (see below).
l = pore interaction term (0.5 for coarse grained soils)
These parameters can be derived from soil testing.

Methods

The process of unsaturated flow modeling is similar to other groundwater modeling projects that include: data collection, data analysis, model creation, model calibration, and predictive simulations. The system under investigation is a gold ore with significant argilized clay minerals that are crushed to a P80 of 12.5mm and agglomerated with cement, lime, and barren leach solution.

The agglomerates are conveyor stacked on the HLP and allowed to cure for 24 hours before solution application.

Data collection involved the collection of geotechnical and hydrogeologic data on the heap material. GRE collected a sample of the agglomerated ore and submitted it for the following laboratory test work:

- Gradation (ASTM D4318-17e1, 2018; D6913-04, 2017)
- Atterberg (ASTM D4318-17e1, 2018)
- Saturated Hydraulic Conductivity (Ks) (D5084-16a, 2019)
- Soil water Characteristic curve (SWCC) (ASTM D6836-16, 2016)

Of these variables, the K_s and SWCC are the most important for flow modeling. The SWCC is a curve which shows how the heap material retains moisture at various matric suction levels and it is an essential input to unsaturated flow modeling. The laboratory-derived SWCC was fitted to the Van Genutchen equations using a least squares minimization technique derived by (Gurdal & Benson, 2003).
Figure 1 is interpreted as follows:

- The saturated moisture content is ~30%.
- The material has a wide range of soil pore sizes. This can be seen because the overall slope angle of the SWCC is generally low. Conversely, homogenous materials typically have a very steep SWCC at a particular suction, meaning that all the water is held in a homogenous-sized pore space.

Table 1 *Gradation of the Agglomerated Ore on the Heap*

Size (mm)	% Passing	Description	Percentage
37.5	100	Coarse	
Gravel	7.83		
25.0	98.6		
19.0	92.2		
9.5	61.6	Fine Gravel	51.75
4.75	40.4		
2.0	25.3	Coarse Sand	15.17
0.85	13.0	Medium Sand	17.55
0.425	7.7		
0.25	5.5	Fine Sand	4.65
0.15	4.2		
0.075	3.1		
<0.075		Silt or Clay	3.06

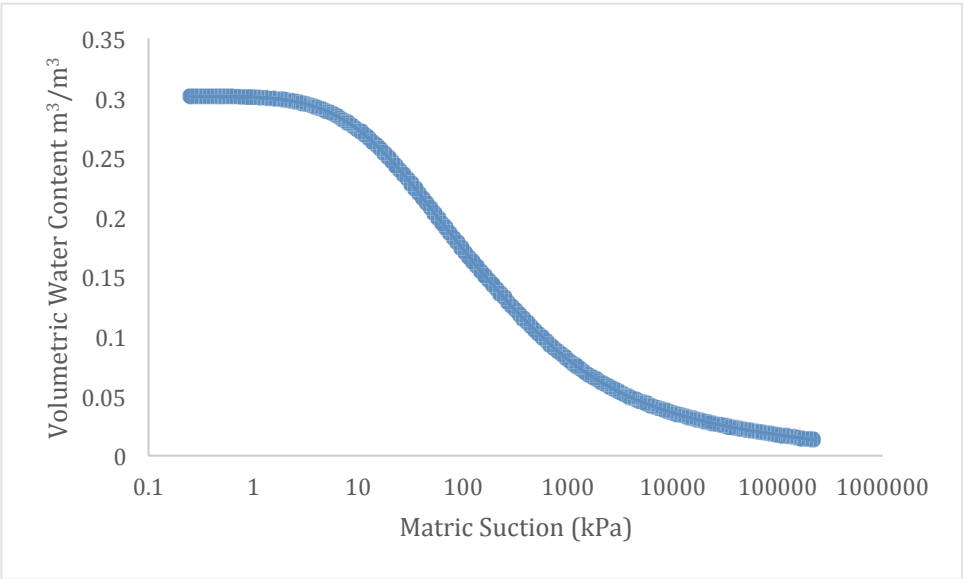


Figure 1 *Soil Water Characteristic Curve for Agglomerated Gold Ore*

- The material is largely fined-grained. This can be seen from the gentle slope of the upper right side of the SWCC curve.
- Residual moisture is 5%. This moisture appears to be held in clays, and cannot be removed without very high suction, if at all.

For the simulation, GRE utilized the GeoStudio SEEP/W modeling platform. This software is a finite-element groundwater modeling platform, which is fully compatible with slope stability analysis. Within this platform are tools to enter the SWCC as well as tools to derive the *K-θ* curve. As mentioned above, in unsaturated flow, hydraulic conductivity is a function of moisture content (see Eq. 2). This is a non-linear relationship called the K-theta (*K-θ*) curve; where theta is the moisture content of the soil, and where K is the conductivity (in m/s). SEEP/W will derive a *K-θ* curve for the agglomerated ore based on the Van Genutchen parameters. The heap material *K-θ* curve is shown in Figure 2.

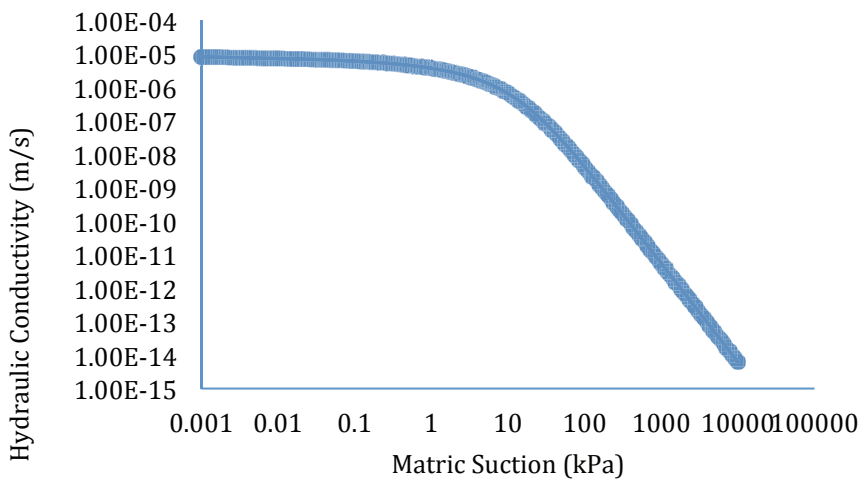


Figure 2 *Moisture vs. Hydraulic Conductivity* K-θ *Curve for Agglomerated Ore*

The *K-θ* curve is used by the groundwater modeling program to determine the conductivity at each model node based on the moisture content. The saturated hydraulic conductivity testing of the heap material had results from 8.1×10^{-4} cm/s to 1.7×10^{-4} cm/s, and Figure 2 shows how that conductivity decreases as a function of matric suction. The moisture-dependent conductivity value is then substituted into the flow simulation for each step and each node in the model.

GRE simulated a two-dimensional (2D) cross-section through the heap for unsaturated flow analysis; this section corresponds to the "critical slope" for slope stability analysis. The simulation included definitions for the ore heap, the liner, collection pipes, and the proper surface application rate of leach solution. A particle tracking program (CTRAN/W, also from GeoStudio) was used to track the time it took for a particle within the leach solution to flow to the collection pipes at the bottom of the pad. Only transient (time-variant) models are useful for this application.

Results

The model simulated the solution flow through the HLP and predicted areas that are both fully-saturated and under-saturated. Figure 3 shows an example of the results for the base case conditions with $K = 8.0 \times 10^{-4}$ cm/s and the drainage system performing as designed. The irrigation application rate employed was 9.78 L/hr/m^2.

In Figure 3, the image is focused on the most-interesting part of the simulated domain. The "warmer colors" show the higher moisture content, and the dashed blue line shows the developing water table. The results of the base case show the following:

- There is a flooded zone at the top of the HLP (as indicated by the blue shading above the ground surface) This is not best-practice and indicates an area where the leach application rate should be decreased.
- There is a phreatic surface accumulating on the liner in the upper part of the slope. This may impact the stability of the HLP by reducing the strength of the material. As mentioned above, it may also increase the risk of PLS leakage through the liner.
- One can see migrating moisture fronts within the HLP. These are the natural processes of wetting the material, increasing the conductivity, and establishing flow.
- There are no obvious under-leached areas in this heap. Most of the ore is fully wetted and near saturation.
- For the average HLP height of 50 or 60 meters, it takes 35–40 days for the solution to flow to the liner and piping system.

The results will be further discussed on the next page.

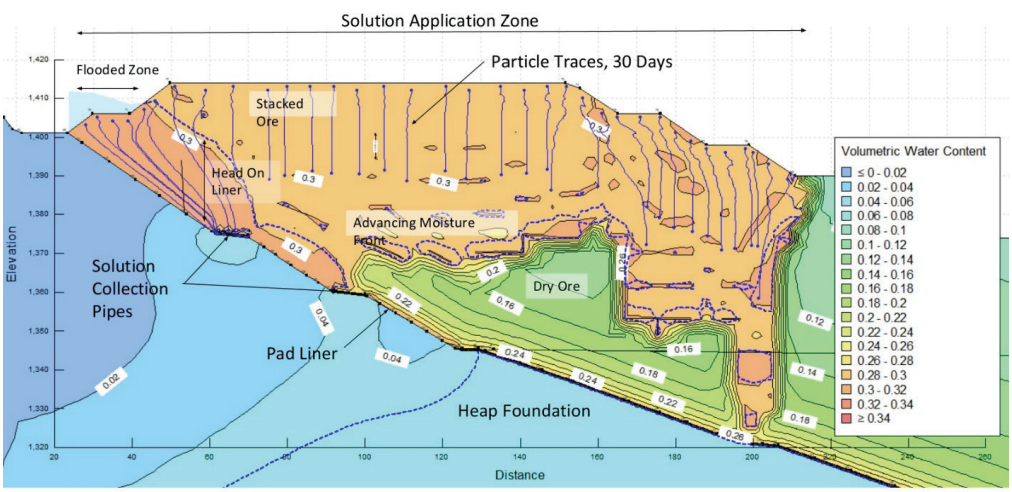


Figure 3 *Seepage Model Results: Moisture Content and Particle Tracks*

Discussion

The role of HLP modeling is to increase the stability and safety of the HLP, and to increase revenue by optimizing leaching. As a result, the base-case may not be the most-important simulation. The model allows the user to look at the impact of less-than optimal conditions on the dynamics of HLP flow. As a result, the model was used to simulate the following design permutations:

- Broken/collapsed collection pipes
- Lower conductivity (resulting from more argilized clay in the ore or poor agglomeration performance)
- Extreme precipitation atop the heap during leaching
- Observation of under-leaching

As discussed above, the base case model (Figure 3) already showed excess head on the liner which does not match best practice. With broken pipes, the head on the liner increased. As a result, GRE recommended a more robust pipe and underdrain design in the upper part of this HLP cross section.

Simulations at the lower conductivity range of the permeability testing ($1.7\ 10^{-4}$ cm/s) resulted in a flooded model. Ponding on the surface is a problem with many heaps containing argilized ore (Lewandowski and Kawatra, 2009). GRE believes that this HLP's application rate requires a saturated conductivity at the high end of the agglomerated ore tested in the lab, at approximately 8×10^{-4} cm/s. As a result, GRE would recommend a reduced maximum irrigation rate and/or a strict design criterion establishing a minimum conductivity value for the agglomerated ore on the HLP.

For the extreme precipitation case, GRE was able to simulate a 100 year, 24-hour storm event falling atop the HLP. Results showed that, when compared to the leach application rate, extreme precipitation events did not appear to greatly change the leach solution moisture content nor the collection rate at the bottom of the HLP. The high water storage capacity of the agglomerated ore can easily accommodate the extra water without substantially changing the flow dynamics. As a result, the site does not need to modify solution collection piping or the emergency pond size to safely contain the 100-year storm event.

This project had a 45-day leaching cycle. An additional 45 days after the leaching cycle has ended, the HLP is largely drained down to its static moisture level of 22%. However, particle tracking analysis with CTRAN/W shows that the solution at the top of the HLP does not make it to the collection pipes before it gets "stranded" by matric suction (see particle traces, Figure 3).

This behavior indicates that stranded solution in the HLP could hold metal that would not be recovered. Depending on the grade of the solution it could be a significant revenue delay. A longer leach period may yield higher recovery by displacing this locked solution with lower grade barren solution, and maintaining the conductive high-moisture conditions for a longer period of time. The flow dynamics of a PLS particle is further complicated by secondary leaching, where solution from fresh upper lifts flows downward into lower ore zones where additional leaching occurs. As a result, using flow modeling with other process models like MetSim® can allow for a more in-depth understanding of the flow regime and the potential recovery impacts (Marsden, and Botz).

Because HLPs are often difficult to build and permit, miners have a strong incentive to stack as much ore on an HLP as is possible, yet HLP geotechnical stability is an essential element of operational and environmental safety. In this case, the moisture distribution and phreatic surface outputs from the seepage model were utilized to calculate heap stability. In this case, the high phreatic surface on the uphill liner (from meter marker 0–100 in Figure 3) did not have a significant impact on HLP stability.

Conclusions

The use of unsaturated flow modeling can be a powerful tool in understanding HLP operations. The proceeding example shows that simulations can aid in the geotechnical stability evaluations, the environmental safety, and the profitability of HLP operations. GRE also believes it is useful to expand the focus of mine water studies from the traditional

environmental or water supply fields to a study of the type of mine water that mining operations care about the most – the leach solution that provides the metal.

References

Albright, William. Cover Design Concepts: Selection, Validation, Basic Soil Physics. Alternative Cover Assessment Program Workshop. Slide Deck No. 1. U.S. EPA Alternative Cover Assessment Workshop, Denver Colorado, 2003.

ASTM D4318-17e1. (2018). Standard Test Methods for Liquid Limit, Plastic Limit, and Plasticity Index of Soils. American Society of Testing and Materials.

ASTM D6836-16. (2016). Standard Test Methods for Determination of the Soil Water Characteristic Curve for Desorption Using Hanging Column, Pressure Extractor, Chilled Mirror Hygrometer, or Centrifuge. West Conshohocken, PA, USA: ASTM International.

ASTM D5084-16a, A. (2019). Standard Test Methods for Measurement of Hydraulic Conductivity of Saturated Porous Materials Using a Flexible Wall Permeameter. American Society of Testing And Materials.

ASTM D6913-04, A. (2017). Standard Test Methods for Particle-Size Distribution (Gradation) of Soils Using Sieve Analysis. American Society of Testing and Materials.

Geostudio 2021. Seep/W and CTran/W models. Geostudio 2021.4 version 4.

Gurdal, T., & Benson, C. (2003). Hydrologic Properties of Final Cover Soils From the Alternative Cover Assessment Program. Geo Engineering Report No. 03-02: University of Wisconsin-Madison

Lewandowski, K.A., Kawatra, S.K. Binders for heap leaching agglomeration. Mining, Metallurgy & Exploration 26, 1–24 (2009). https://doi.org/10.1007/BF03403413

Marsden, J.O., Botz, M.M. Heap leach modeling — A review of approaches to metal production forecasting. Mining, Metallurgy & Exploration 34, 53–64 (2017). https://doi.org/10.19150/mmp.7505

Sheikhzadeh, G. et. al. (2005). Computational modelling of unsaturated flow of liquid in heap leaching—using the results of column tests to calibrate the model. International Journal of Heat and Mass Transfer, Volume 48, Issue 2, pages 279-292.

Flow Monitoring at Mine Water Discharges and Treatment Schemes in Wales – Challenges and Lessons Learnt

Rob Burton, Emily Hudson

Coal Authority, 200 Lichfield Lane, Mansfield, Nottinghamshire, NG18 4RG, United Kingdom, RobBurton@coal.gov.uk, EmilyHudson@coal.gov.uk

Abstract

A key metric used in both the operational management of mine water treatment schemes, and the design of new schemes or other interventions, is flow. This paper considers the challenges of measuring mine water flows accurately, and the effect that these have on the uncertainty in the data. Through the Coal Authority's ongoing flow monitoring improvement programme, flow data uncertainty has been reduced by measures such as the installation of baffle plates, gauge boards, non-contact, low power, digital water level sensors and improved maintenance. New flow monitoring sites on the metal mine programme have also benefited from the revised 'best practice' approach.

Keywords: Mining, Uncertainty, Flow Data, Operations, Design

Introduction

The Coal Authority operate over 75 coal mine water treatment schemes (MWTS) managing water from historical coal mines across the UK, 15 of which are located in Wales. The Coal Authority is a partner in the Natural Resources Wales (NRW) joint Metal (Non-Coal) Mine Programme (MMP) investigating sources of pollution from metal mining activity and formulating solutions to mitigate these.

Flow is a key metric used in both the design of new schemes or other interventions, and effective management of existing treatment schemes. Operationally, the Coal Authority uses flow data for performance monitoring, including maintenance scheduling, dosing control and capacity assessment, as well as for permit and licence compliance monitoring. It is therefore clear that accurate flow data is essential to the efficient management of MWTS. In the first instance, flow data collected for the NRW MMP is used in the assessment of environmental impact from mine water discharges by calculating solute loads. Subsequently, the data will inform requirements for treatment solutions. As the MMP is in its relative infancy, this data will feed into longer term prioritisation of pollution mitigation measures.

Flow Monitoring Structures

The majority of flow data collected by the Coal Authority is via primary flow monitoring structures, which provide a volumetric flow rate. These predominantly consist of thin-plate weirs and flumes, though a variety of other methods are also used (broad-crested weirs, compound weirs, in-pipe sensors). Electromagnetic pipe flow meters also provide continuous flow data of the inflow to pumped MWTS. Thin-plate V-notch weirs have a triangular notch with an opening angle ranging from α=20-100°, installed perpendicular to the flow of water in a stream or channel (Achour & Amara 2021; Pospíšilík & Zachoval 2023). Water should spring clear of the weir plate through the notch, creating a fully aerated nappe. Rectangular thin plate weirs work in much the same way, but with a rectangular opening in the weir plate of a given size as opposed to a triangular one. By measuring the depth of water, or head h, upstream of these notches, and through knowledge of the approach channel and weir plate dimensions, flow rate can be accurately determined (Shen 1981). The requirement to have an aerated nappe, and the specific weir crest dimensions required, mean that thin-plate weirs are not best suited to measuring raw mine water, where iron levels will likely

be high and the weir crest and approach channel will be subject to ochre accretion.

Flumes work to similar principles, with the discharge equations based upon boundary layer and hydraulic theory. They create a constriction in the channel via a narrowed throat section, with the upstream depth of water and flume geometry used to determine the rate of flow through the structure. They have the advantage that they do not cause a barrier to the flow, since the flume throat is usually set at the same level as the approach channel, and thus are better suited to measuring raw mine water as solids do not tend to accrete to the flume sides or in the approach channel. The Coal Authority has employed both rectangular and trapezoidal flumes, but a variety of flume geometries are available (Ribeiro et al. 2021).

A variety of hydrometric ISO standards detail how flow should be measured by primary structures (ISO 1438:2017; ISO 4359:2022; ISO 3846:2008; ISO 4377:2012). Since these standards are largely based on laboratory test conditions, the regulatory organisations in England and Wales have developed the Monitoring CERTification Scheme (MCERTS) which makes some concessions to the ISO standards, in order to allow the installation and maintenance of flow monitoring structures in often less than perfect real-world scenarios. MCERTS requires measurement at mean flow to an uncertainty of ±8%. The standard only legally applies in England and Wales, but the Coal Authority have adopted the principles to flow monitoring installations across the UK.

Flow Data Uncertainties

All measurements of a physical quantity are subject to uncertainties. The result of a measurement is only an estimate of the true value of the measured quantity, and therefore is only complete when accompanied by a statement of its uncertainty. In order to know the reliability of a flow record, it is necessary to identify the areas that give rise to errors in the process of estimating flow.

Flow data uncertainty is a measure of a number of parameters, all playing a part in determining the accuracy of flow data collected. In terms of V-notch (Q_t) and rectangular (Q_r) thin-plate weirs, the uncertainty calculation (u_c) comprises uncertainty in the discharge coefficient (C_d), uncertainty in the weir dimensions (b_e,α), and uncertainty in the head measurement (h_e) (Eq. 1).

Further errors may also be included, such as data treatment/ telemetry error, head to flow conversion error and others associated with non-conformance to ISO and MCERTS standards. Since the uncertainty in the discharge coefficient (C_d) and uncertainty in the weir dimensions (b_e,α) are typically small, it is clear from ***Equation 1*** that the uncertainty in head measurement has the greatest impact on data uncertainty, as this parameter has a 1.5 and 2.5 multiplier for rectangular and V-notch weirs respectively.

Equation 2 describes the uncertainty calculation for a flume (Q_f). Again, total uncertainty is a combination of uncertainty in head measurement (h), uncertainty in the flume dimensions (b, D, m), and uncertainty

$$u_c \times (Q)_r = \sqrt{u \times (C_d)^2 + u \times (b_e)^2 + [1{,}5u \times (h_e)]^2}$$

$$u_c \times (Q)_t = \sqrt{u \times (C_d)^2 + u \times \left[tan\left(\frac{\alpha}{2}\right)\right]^2 + [2{,}5u \times (h_e)]^2}$$

Equation 1 *Uncertainty equations for thin-plate weirs*

$$u \times (Q)_{flume} = \sqrt{u \times (C)^2 + \gamma^2 \cdot u \times (b)^2 + \varphi^2 \cdot u \times (h)^2 + \Psi^2 \cdot u \times (m)^2}$$

Equation 2 *Uncertainty equation for flumes*

in the discharge coefficients (C_D, C_S, C_V). As with thin plate weirs, a multiplier is applied to the head uncertainty in the range 1.5 (rectangular flumes) to 2.5 (trapezoidal flumes). It can therefore be concluded that whilst there are other uncertainties involved, when combining all of the uncertainties the uncertainty in water level measurement has the largest effect (Burton & Willis 2005).

Challenges

The uncertainty in water level measurement itself comprises a number of factors, such as the zero head error, accuracy of manual readings, the implications of a clinging nappe, sensor selection and error. Each of these factors are discussed in turn below.

Zero head error is the accuracy with which the gauge board is zeroed to the crest or cease to flow level of the structure (e.g. the throat of a flume). Gauge boards must be installed using surveying equipment such as a dumpy or laser level to achieve tolerances of ±1 mm.

Accuracy of manual readings of the water level at a weir or flume are impacted by factors such as turbulence and reading location. Turbulent approach conditions can reduce the resolution at which manual readings can be taken, often from ±1 mm when laminar flow conditions persist to ±10-15 mm in turbulence. If a manual water level reading is taken within the notch of a thin-plate weir, or in the throat of a flume, then the drawdown effect will lead to an under-estimate of the water level (**Figure 1**). As the flow passes over a notch or into a flume, the water surface is pulled downwards (or 'drawn down'). On the other hand, if the water level measurement is taken further upstream away from any drawdown effects, it will not be under-estimated. Also, a lack of safe and easy access to sites may limit vital maintenance activities, meaning ochre and debris can build up on the weir crests and gauge boards, making manual readings difficult and imprecise. Ochre build up on the weir crest will cause an overestimation of the water level and thus flow.

A **clinging nappe** is where the flow is unable to freely spring clear of a weir plate. It can be caused by a lack of regular cleaning, the weir crest being too thick or the water level being below the minimum recommended in the standard. The effect of this is also to artificially drawdown the upstream head measurement, leading to an underestimation of the flow (Kay 1998).

Finally, the **choice of water level sensor** is important to ensure accurate flow data, at sites where continuous data collection via a data logger is required. At many Coal Authority sites there is no mains power, and thus battery powered solutions are required. Until recent years, this limited the choice of sensors to pressure transducers which have to be installed below the water surface, and therefore can be compromised by ochre

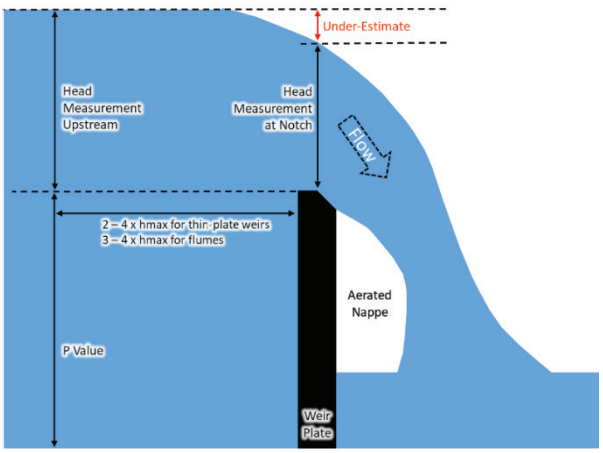


Figure 1 Drawdown effect over a thin-plate weir

accretion. However, low powered non-contact radar sensors, which can be mounted above the water surface, are now available. These are therefore preferred, except at sites where there is surface turbulence or the treatment process results in foam on the water surface. Digital, rather than analogue sensors are also preferred.

Given the numerous potential sources of error in water level measurement, and the fact that many of them cause compounding errors, it is worth considering the sensitivity to a ±10 mm water level measurement error in the estimation of flow (**Table 1**), bearing in mind the MCERTS requirement of uncertainty at mean flow of better than +/- 8%.

Solutions

The Coal Authority has been working to reduce uncertainty in our flow data, both from operational MWTS and the NRW MMP. Through this work, the Coal Authority has developed a new 'best practice' approach when upgrading existing flow monitoring structures, as well as when designing and installing new structures.

To lower manual reading error, the Coal Authority has retrofitted baffle plates at various sites, reducing turbulence in the approach channel to weirs (**Figure 2a**). Furthermore, improved weir maintenance training to site operators has been initiated to ensure weir plates, approach, downstream channels and gauge boards are regularly cleaned and cleared. This minimises the build-up of debris and ochre on and around primary monitoring structures (**Figure 2b**).

Non-contact battery operated MCERTS approved digital radar sensors have been deployed at a number of sites, where conditions are appropriate and no mains power is available (**Figure 2c**). The non-contact sensors have also been fitted with vandal resistant covers, to reduce the risk of damage where sites are publicly accessible (**Figure 2c**). Weir plates that were damaged, corroded or non compliant with MCERTS standards have also been replaced (**Figure 2d**). Not only has this returned many sites to compliance, but the use of carrier plates has also improved the durability and flexibility of these sites. Damaged, corroded or incorrectly sized weir plates can be easily replaced in isolation in the future, without the need to replace the entire structure (**Figure 2e**). The example in **Figure 2e** shows a compound weir structure, which has a small low level notch with a wider high level notch. Such structures are useful when the anticipated flow range is great, but there is a low base flow, as they can accommodate both low and high flows.

Implementation of additional access and health and safety measures at sites improves worker safety allowing easier maintenance, and more accurate manual readings (**Figure 2f**). The Coal Authority has routinely installed fixed gauge boards where possible, so that accurate manual readings can be taken to a resolution of ±1 mm, and the effects of the drawdown zone do not influence data. The Coal Authority is also now trialling aluminium gauge boards, intended to withstand more frequent and vigorous cleaning activities required at our schemes. Upgrading sites so that data may be transferred via telemetry has also progressed, allowing for better remote monitoring and interpretation of flow data, in turn improving ability to pro-actively manage sites.

Table 1 *Percentage difference in flow estimate caused by a ±10 mm error in the Head reading*

	Head (*h*) Flowing Over Weir		
	200 mm	100 mm	Minimum Head*
V-Notch	± 13%	± 26%	± 45%
Rectangular Notch	± 7.5%	± 15%	± 52%

Note: *60 mm for a V-notch weir, 30 mm for a rectangular weir.



Figure 2 Improvements to primary flow monitoring structures



Figure 3 Glyncorrwg MWTS flow monitoring upgrades

Case Study: Glyncorrwg

Glyncorrwg MWTS is located in the Afan Valley, South Wales, 13 km northeast of Port Talbot. The scheme provides passive treatment to mine water discharging from both the East and West bank of the Afon Corrwg, comprising 11 reed beds in series. Flow monitoring at the scheme is undertaken at three locations via primary flow monitoring structures (**Figure 3**):

a. Thin plate V-notch weir at Reed Bed 4 (East Bank) Discharge
b. Thin plate rectangular weir Final Consented Discharge
c. Thin plate rectangular flume West Bank Discharge

These structures suffered from a variety of issues, including incorrect sizing, weir crests being too thick and not chamfered, turbulent approach conditions, no gauge boards upstream and ochre build-up. In 2023, the Coal Authority undertook a weir improvement project at the site, with the three locations upgraded as a result (**Figure 3**).



Figure 4 Parc Mine flow monitoring structures

The flow structures were re-designed to accommodate a greater flow range with, increased peak capacity. The thick, coated plywood weir plates were replaced with stainless steel plates chamfered to 1-2 mm thickness. Non-contact battery powered water level sensors were installed at each location, to mitigate ochre-build up. Solar panels were also installed to provide battery recharging for each logger and sensor, thus reducing the need for frequent battery replacements. Aluminium gauge boards were installed at an appropriate distance upstream of each structure, providing a durable and maintainable water level measurement point. The West Bank discharge was re-configured as a flume rather than a thin-plate weir, due to the limited upstream head. This location was also prone to ochre accumulation which would have quickly built up behind a replacement weir plate.

Case Study: Parc Mine

Parc Mine is located approximately 1.6 km south-west of the town of Llanrwst, North Wales. The Coal Authority, in conjunction with NRW, have an ongoing project to monitor the discharge of mine water from Parc Mine, with a view to potential remediation measures in the future. As part of this project, flow monitoring data is required to understand the magnitude and composition of mine water discharging at surface. To meet this requirement, the Coal Authority commissioned the design of seven flow monitoring sites for the Parc Mine in 2021. Construction and installation began in 2022 and was completed in April 2023 (**Figure 4**).

The prefabricated Glass Reinforced Plastic (GRP) weir tank used at Cutting Level is a good example of where preformed units can provide accurate measurement of smaller flows, with baffle plates, carrier plate, weir plate, gauge board and instrumentation all contained within a covered unit. A level base and an appropriately levelled inlet and outlet channel are required, but no further civils work is needed. Pre-fabricated twin trapezoidal GRP flumes were deployed elsewhere on the site. These require more civils work to adequately secure in place. Non-contact sensors were used to measure flows of highly ochreous water discharging from historical tailings.

Conclusions

As shown above, the factor with the greatest impact of flow measurement uncertainty at weirs and flumes is the water level measurement, and there are numerous sources of error which can compound to create large uncertainties in the data. The approach taken by the Coal Authority to tackle

these challenges and reduce measurement uncertainty includes the installation of gauge boards and baffle plates, the use of non-contact digital water level sensors with battery power connected to solar, training provision, replacement weir plate and flume upgrades and the use of carrier plates.

The flow monitoring challenges experienced by the Coal Authority are not unique to mine water or to specific locations in Wales or the UK. The learnings and approach described here could therefore be applied elsewhere to improve monitoring of existing or future mine water and reduce uncertainty in flow data around the world.

Acknowledgements

The authors thank Severn Trent Services for operating Coal Authority MWTS, as well as Hydrometry Framework Partners Hydro-Logic Services (HLS) and their civils contractor Edwards Diving Services (EDS).

References

Achour B, Amara L (2021) Discharge coefficient for a triangular notch weir theory and experimental analysis. Larhyss Journal, 1112-3680(46):7-19

Burton R, Willis A (2005) MCERTS: Meeting the requirements (a practitioners perspective), Proceedings of the 3rd CIWEM National Conference, 389 – 404

Edwards GM (2010) Parc Lead Mine. Coflein. https://coflein.gov.uk/en/site/411616/. Accessed 28 March 2023

Kay M (1998) Practical Hydraulics, 1st edn. CRC Press, London, 192

Pospíšilík Š, Zachoval, Z (2023) Discharge coefficient, effective head and limit head in the Kindsvater-Shen formula for small discharges measured by thin-plate weirs with a triangular notch. Journal of Hydrology and Hydromechanics, 71(1):35-48

Ribeiro AS et al. (2021) Parshall flumes flow rate uncertainty including contributions of the model parameters and correlation effects. Measurement: Sensors 18: 100108

Shen J (1981) Discharge characteristics of triangular-notch thin-plate weirs, No. 1617, United States Department of the Interior, Geological Survey

Innovative approach to the development of a mine water remediation R&D portfolio

Karen Clode[1], Nicholas B. Gurieff[2], Neil Freeman[3], Michael V. Storey[1]

[1]*Isle Utilities, Sydney, NSW, Australia, karen.clode@isleutilities.com*

[2]*Rio Tinto – Closure R&D, Brisbane, QLD, Australia*

[3]*Rio Tinto – Office of the Chief Scientist, Perth, WA, Australia*

Abstract

Rio Tinto recognises that its impact and responsibilities do not end with the cessation of its mining operations, but instead it should leave a positive legacy that delivers value to its shareholders, the environment and the community at large. To achieve this goal Rio Tinto built a mining-influenced water (MIW) remediation and valorization roadmap to guide the development of a diversified portfolio of research and development (R&D) initiatives now and into the future. To accelerate the identification of MIW R&D opportunities a novel crowdsourcing campaign was launched, which was successful in identifying 14 R&D initiatives with 27 research institutions across the globe.

Keywords: Crowdsourcing innovation, mining-influenced water, circular economy, research and development

Introduction

Mine closure is a growing concern for the global mining industry. Around the world, Rio Tinto has 97 active closed and legacy assets, with a further 20 sites planning to transition to closure in the next 10-15 years. Each of these sites represents a unique challenge with regards to the approach and technologies required to deliver the best possible outcome for the business and the receiving environment. Through the adoption of a circular economy mindset, many of these sites also present an opportunity for valorizing valuable metals and other materials from resources that are otherwise considered waste. In recognition of this challenge and by applying this mindset, Rio Tinto established a closure-focused R&D group with the aim of discovering and supporting the development of cutting-edge technologies that can significantly reduce the long-term impacts of mine asset closure, by not only treating wastes, but simultaneously valorizing these waste resources.

When considering the broad range of challenge themes related to mine closure – mineral and non-mineral wastes, earthmoving and landforming, mining-influenced water (MIW), restoring and repurposing, demolition, post-closure monitoring – innovative technologies may have a limited impact on improving outcomes for some of these challenge themes. Rio Tinto Closure R&D reviewed the needs, opportunities and the potential to deliver impactful technology development for each challenge theme. Sustainable MIW treatment was determined to be particularly suitable as an R&D focus theme. The reasons for this were:

- MIW treatment can play a significant role in minimising environmental impacts as well as potentially contributing to the circular economy by recovering resources, such as metals and water for reuse
- Water treatment processes are technology-based which fits with Rio Tinto Closure R&D's focus
- Experience from other industries (municipal and industrial wastewater treatment) have shown that significant step-changes in treatment capability and capacity can be achieved through innovative technology development and application

Based on the outcomes of this review, a decision was made to invest in a long-term, diversified R&D program focused on changing the dynamics of MIW treatment. In 2021, Rio Tinto commissioned the Sustainable Minerals Institute at The University of Queensland to undertake a foresight study for MIW treatment technology (Sustainable Minerals Institute, 2021). One of the key outcomes from this study was that the sheer number and diversity of technologies that could be applied to meet the challenge of MIW treatment was a limiting factor in the ability to assess and select the best available technologies (BAT) for Rio Tinto's needs. A novel approach to sourcing R&D projects was therefore required.

Roadmap development

To guide the development of mine closure focused R&D opportunities into the future, an MIW remediation and valorization R&D roadmap was established by Isle Utilities (Isle) in collaboration with Rio Tinto. The purpose of the roadmap was to provide inspiration and act as a platform to engage internal and external stakeholders and ultimately catalyse the development of new projects to achieve Rio Tinto Closure's goals. At the same time, the roadmap would be a structural element to guide discussions and for collating and organising the inputs received.

The roadmap included input from sites operated by Rio Tinto Closure regarding their current needs and expectations for future requirements. The roadmap defined the key areas of interest together with the goals and challenges expected over three horizons of time (NOW 1-3 years, NEW 3-5 years and NEXT 5-10 years), along with the drivers behind each area of interest. These areas of interest (AOIs) are listed in Figure 1.

The roadmap also identified existing technologies that have the potential to be transformational if deployed specifically for MIW treatment. These technologies were generally sourced from non-mining related applications and would require some development to meet the demands of MIW treatment or were technologies that were still at a very early technology readiness level (TRL) and had not been tested outside of the lab or even on real MIW.

Solution Identification

Following the development of the MIW R&D roadmap, Isle undertook a survey of the current global technology market capabilities for treatment and valorization of

SELECTIVE	Solutions that can target and **effectively remove targeted constituents for enhanced water recovery**, reduce residual wastes, and resource valorization (in a high-quality form) to generate new revenue streams and offset closure costs
SUSTAINABLE	Solutions with **low and/or renewable chemical and energy** use for increased supply chain resilience and minimal carbon footprint
VERSATILE	**Modular and scalable** solutions are those are innovatively designed and fabricated for reduced cost and manufacturing lead time, increased reusability and rapid scale-up, down or out
RESILIANT	Solutions that are **adaptable regardless of changing environmental regulations**, climate uncertainty and variable mine water quality and quantity enabling reliable treatment systems
AUTONOMOUS	**Passive water remediation solutions that can operate independently**, with minimal component replacement to improve treatment resilience, longevity, and staff safety at remote sites

Figure 1 *Five R&D opportunity areas, or areas of interest were developed as part of the technology roadmap.*

MIW. Several solutions were identified across the TRL spectrum, from concept through to pre-commercialisation. However, despite the number and diversity of solutions identified, few options were suitable for Rio Tinto's specific needs as identified in the roadmap.

This survey made it clear that there is a wide range of technology development underway across the globe related to MIW treatment. Given the constraints on internal R&D team resources and the imperative for a sustainable R&D pipeline, traditional pathways of sourcing R&D projects were considered unfeasible and likely unable to deliver a strong pipeline of projects within 12 months. Therefore, a crowdsourcing campaign was designed to accelerate the identification of MIW R&D opportunities, improve Rio Tinto's innovation network within the field, while at the same time supporting a competitive comparative assessment of solutions to meet the requirements laid out in the MIW R&D roadmap.

Crowdsourcing Campaign

Rio Tinto has a strong tradition over the past 150 years of innovation in the mining industry. To support the sourcing of innovative solutions, Rio Tinto has an online innovation platform called the "Pioneer Portal" which many innovators around the globe were already familiar with. Therefore, as it became clear that an innovation crowdsourcing campaign was the preferred pathway to identify solutions for the MIW treatment R&D portfolio, Rio Tinto in collaboration with Isle decided to re-purpose the Pioneer Portal for the campaign. By changing the dynamics of technology identification through a direct crowdsourcing approach, the objectives were:

- To increase the number of technologies that Rio Tinto would have a direct relationship with
- Support a competitive, comparative assessment of the technologies to meet the requirements identified in the roadmap and translated into the crowdsource campaign

An important requirement posed in the challenge were the water quality and treatment objectives the technologies would need to address at Rio Tinto sites. A summary of the four MIW examples provided in the challenge is presented in Table 1.

The crowdsourcing campaign was launched in April 2022 and received 98 submissions after six weeks. This vastly exceeded the expectations and connected Rio Tinto with organisations that they would not otherwise have unearthed via traditional means of identifying and sourcing innovation. A two-phase assessment program was developed with the aim of ensuring that not only was the solution concept robust and there was a diverse range of technology types, but also that the MIW type and constituent recovery was relevant to Rio Tinto's sites. A summary of this selection process is outlined in Figure 2. As illustrated, the final 14 projects selected represent a range of technology readiness levels, target contaminants/metals in MIW and are based at sites around the globe that reflect the presence of Rio Tinto as a company.

The process for selecting the final 14 projects to be part of the MIW treatment R&D pipeline was rigorous. From the start of the process, a detailed set of assessment

Table 1 *Summary of MIW examples from Rio Tinto sites provided as part of the crowdsourcing campaign. More detailed water chemistry was provided through the Pioneer Portal*

Specification	Source	Contaminants of interest for recovery	Rio Tinto treatment objectives
AMD – high flow	Metalliferous mining site	Cu, Co, Zn, REEs, Ni, S	Recovery of target metals
AMD – low flow	Metalliferous mining site	Cu, Co, Zn, REEs, Ni, S	Recovery of target metals
Neutral MIW	Groundwater at mining site	As, B	Removal to meet environmental regulations. Valorization of B and potentially As
Alkaline leachate	Bauxite residue storage facility	V, Ga, REEs	Adjustment of pH and recovery of target metals

criteria were applied in the assessment of each project. The process relied on internal and external subject matter experts (SMEs) to provide diverse input based on experience in the mining and water treatment industries. An online collaborative software package (Sideways 6) was applied to allow a global team of SMEs to collaborate around this project. Throughout the process, feedback was provided to each shortlisted project with the responses provided forming part of the material being assessed by the SMEs. During the review period, the assessment team was able to connect several technology-adjacent projects with each other to create stronger collaborative projects.

When considering the outcomes from the challenge, analysing the TRL level of the projects selected provides an insight into how Rio Tinto has approached the development of this specific R&D pipeline. Fifty percent of the projects are TRL 4-6, the area between laboratory proof of concept (POC) and piloting/scaling. This is not surprising as weighting in the assessment gave credit to technologies that had a proof of concept in place but still fit the definition of an R&D project. Forty percent of the projects are early stage and represent high reward/high risk type projects that Rio Tinto felt could deliver game changing advances in selective treatment of MIW. The high TRL projects (7-8) represent technologies that are already commercially viable in other sectors, but where the adaptation of the technologies for MIW treatment requires investment in fundamental R&D to understand how they can be adapted to deliver the outcomes required by Rio Tinto.

In recognition that the objective of this challenge is to create and populate a sustainable and productive R&D pipeline, a key requirement is to understand the technical risks in each project and how this portfolio wide risk can be managed effectively. The approach taken was to map out the technology "family" of each project. As illustrated in Figure 3, there is a wide spread of technologies being addressed as part of the MIW R&D pipeline, with no one technology family dominating. This approach should ensure a balanced outcome from the R&D pipeline, with a toolbox of options being developed and made available to Rio Tinto, rather than a single technology. Technology taxonomies and other R&D management approaches were applied to ensure that each component of interest in the example MIWs was being addressed and a broad range of technologies were part of the pipeline.

Discussion and Conclusion

The entire process from the launch of the Sustainable MIW Treatment Crowdsource



Figure 2 *Summary of the MIW crowdsourcing campaign process*

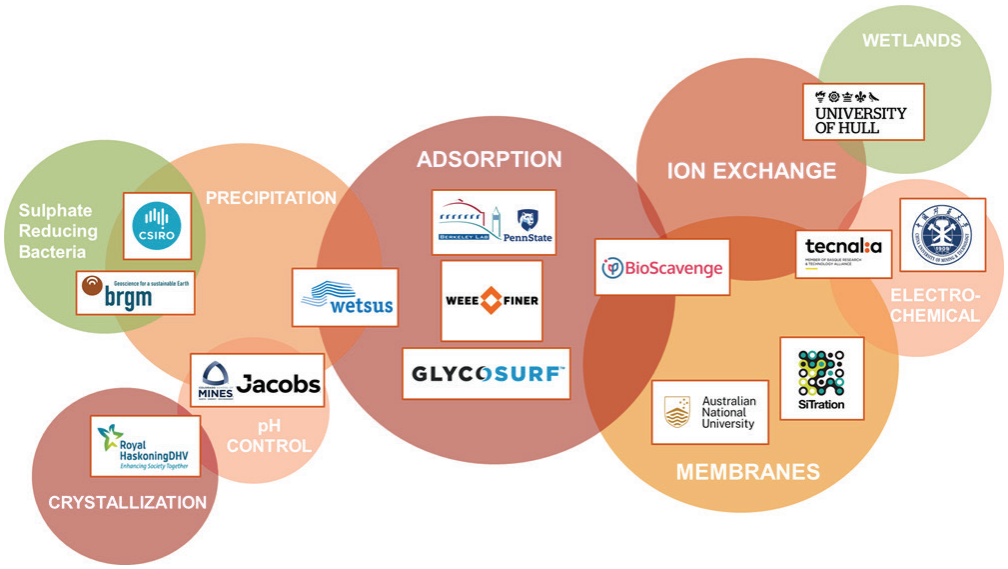


Figure 3 *Technology map of the 14 selected technology providers and the approach being taken in the projects submitted to the crowdsourcing campaign.*

Challenge to the selection of 14 projects to enter project agreement negotiations lasted seven months. Compared to traditional approaches of sourcing R&D in Rio Tinto, this represents a significant reduction in time and increase in number and quality of projects entering the R&D pipeline. Another benefit of the crowdsourcing approach has been that several promising technologies that did not meet the requirements for the MIW treatment challenge have been connected with other business units within Rio Tinto – for example technologies related to battery mineral recovery. These outcomes have demonstrated that despite taking an untried, broad and high-risk approach to sourcing innovation for a focused specialised topic area such as selective MIW treatment, the outcome has been very successful with Rio Tinto attaining its objective of populating a sustainable R&D pipeline for innovative MIW treatment technologies in a cost and time efficient way. The success of this challenge has inspired other functions and product groups within Rio Tinto to pursue a similar approach.

A key learning from this novel process is that having a clear objective, detailed preparation (in the roadmap development), strong stakeholder engagement and a clear set of criteria for assessing the projects that are submitted will provide strong outcomes that meet the expectations of the sponsoring R&D group. Marketing is also key in order to reach the broadest possible audience. In respect to this, professional social media channels such as LinkedIn provided an opportunity to reach a global yet relevant audience for the crowdsourcing campaign.

An unexpected positive outcome from the process has been the development of a connectivity map between many of the submitted projects, allowing synergistic partnerships to deliver stronger outcomes and further the scope of progress during the project delivery phase. This process has resulted in 14 projects being selected with 27 participating entities from across the globe. This unique approach is expected to deliver positive outcomes for the MIW R&D pipeline at Rio Tinto over the next 2-5 years and the methodology has already been replicated in another program to

develop next-generation in-situ and remote sensing technology solutions. Rio Tinto's goal to have a toolbox of technically strong and commercially viable technologies to meet the long-term challenges related to selective MIW treatment now has a greater chance of success after the positive outcomes of this novel R&D crowdsource campaign.

This example clearly demonstrates the value that a well-designed and executed R&D crowdsourcing campaign can be adapted to fit the needs of the end-user (in this case, Rio Tinto) and has significant potential to be applied across the mining industry to meet fundamental technology challenges and deliver significant value to the end-users.

Acknowledgements

The authors thank every technology provider that made a submission to the Rio Tinto Sustainable MIW Treatment Challenge 2022 as it is recognised that each submission required a significant investment in time and effort to produce.

References

Sustainable Minerals Institute, 2021. "Foresight Study for Treatment of Mine-Influenced Water". The University of Queensland. Internal Report for Rio Tinto

Sediment Harvesting using a Nautilus Pond™ within Surface Water Management at Esgair Mwyn.

James Cochrane[1], Tom Williams[2], Richard Knott[1], Heilyn Williams[2], Stuart Craxford[2], Peter Stanley[2]

[1]*Aecom, 5 Callaghan Square, Cardiff, CF10 5BT, UK, james.cochrane@aecom.com and richard.knott@aecom.com*

[2]*Natural Resources Wales, Tŷ Cambria, 29 Newport Rd., Cardiff, CF24 0TP, UK, geowyddor@cyfoethnaturiolcymru.gov.uk*

Abstract

The abandoned Esgair Mwyn lead mine is situated astride a ridge in Mid Wales. Surface water run-off drains to the north in braided streams into the Nant y Garw, then Marchnant and Afon Meurig. Run-off to the south drains into the Meurig before entering the Afon Teifi. It presents the largest source of Pb to the Teifi, contributing to it failing Water Framework Directive (WFD) standards. A large steep conical tip contains ≈2% Pb, and planned surface water management includes a Nautilus Pond™ below the tip to harvest sediment, plus leat restoration with capping, conveying clean water away from spoil.

Keywords: Nautilus Pond™, surface water management, remediation, intervention.

History

The Esgair Mwyn lead mine is located 21 km southeast of Aberystwyth. There has been mining in the district since Romano-British times. Lewis Morris claimed the Ancient Britons dug an open cast or trench along the vein after their manner for 100 yards, 20 yards wide and 18 yards depth (Lewis 1967). Hall (2012) considered the quarry subsidence from a roof collapse with the old or main lode 9 m wide carrying ore at the foot and hanging walls. The resource had apparently lain abandoned for centuries when rediscovered by poor miners and reported to Morris for the Crown in 1751 (Lewis 1967), making this mine socially and historically important. It is possible that portions of the main lode were the richest ever worked in Mid Wales (Hall 2012). Morris exported 1,767 tons prior to dismissal in 1756 with c.70 tons removed from site (Lewis 1967).

A new operator discovered appreciable quantities including a vein of sphalerite in 1765. Drainage into the old, flooded workings was secured in 1766, which enabled working down to the adit level, yielding 2,379 tons between 1767 and 1772. Another 970 tons were recorded by century-end, the miners extending the old workings to 50 fathoms below adit level, a remarkable achievement for the time (Hall 2012). Probably due to the roof collapse into the wide worked lode, the mine yielded only 250 tons between 1802-18 and then lay idle. Production recommenced in 1851, which through to 1917 yielded 10,430 tons (Lewis 1967) and between 1917 to 1927 2,304 to 2,784 tons (Hall 2012). The minimum recorded production is therefore 18,170 tons of galena or lead ore between 1751 and 1927.

The Engine Shaft (Penmynydd) at 410 mAOD was 64 m deep from surface around 1850, reaching 137 m under adit in 1857. Crushing rolls and the dressing floor operated close by. In 1878 Penmor or Western Shaft was sunk to ore at 55 m near adit entrance with a tramway laid, before closing in the 1890s. The mine plant was acquired in 1897 for dismantling, but the operator was persuaded by local miners to exploit the Penmor ore body which continued over 183 m vertically, where the solid galena was almost 1 m wide. Workings extended to 165 fathoms (302 m) below adit level of 330 to 340 mAOD, the deepest from surface in Ceredigion. Many thousands of tons were recovered until closure

in 1927 (Bick 1974), employing about 60 men. Renewed activity occurred in 1947 with plant installed to treat the large waste dumps, and an unsuccessful attempt to clear the adit to reach sphalerite reserves. Captain Nancarrow, the general manager at Glogfawr Mine, and who erected the mill at Gwaith Goch, had sampled the tips in the 1920s and estimated 60,000 tons with an average grade of 2% Pb (Hall, 2012). In 1973 Elenith Mining Company redesigned plant and produced some Pb that was subsequently stolen from site.

Site Setting & Geology

Surface water run-off drains to the north in braided streams into the Nant y Garw, then Marchnant. Run-off to the south drains into the Afon Meurig, which is joined by the Marchnant before entering the Afon Teifi and Cardigan Bay. The site comprises areas of mine spoil, former rod mill, ball mill, tailings deposits, disused shafts, derelict structures and open works / surface pits along the mineral lode outcrop. A small tailings dam sits beneath the conical tip, its capacity extending to 2,273 m3 when the embankment crest was twice increased. Seepages along the original crest to the toe of the structure remain evident and caused a small translational failure. There is reference to three leats used to convey water originating at Llyn Fyrddon 4 km to the east. The lowest leat to the northeast of the conical tip was constructed around 1907 to pass used water via a turbine on to Glogfach Mine, which had reopened (Hall 2012). Sections of this leat have subsequently failed, allowing water to flow over fine mine waste, presumably periodically cleaned out of the leat when operating, and enter drainage channels 1.1, 1.2 and 1.3 (fig. 1).

Located in the Central Wales Orefield, the bedrock is the Devil's Bridge Formation of Llandovery Age in the Silurian. The lode strikes ENE, dip 64° NNW with outcrop sub-parallel to an east-west ridge line. The lode is defined as the Main lode in ENE, Hospital vein and Western ore shoot.

Site characterisation, run-off modelling and options assessment

Mining and mineral processing operations have resulted in elevated Zn, Pb and Cd concentrations above Environmental Quality Standards (EQS) in the Nant y Garw and Afon Meurig in Cwm Gwyddyl (Scorey 2012). This results in the Afon Meurig waterbody failing to achieve Water Framework Directive (WFD) 'Good' status and contributes to the 'Moderate' status of the receiving Afon Teifi waterbody.

An initial remedial options appraisal was undertaken, including a review of existing data and additional site characterisation (AECOM 2016). A single round of water quality and salt dilution flow monitoring was undertaken, and mine spoil was characterised using pXRF at 49 locations, supplemented by wet chemistry at seven locations. These seven samples were also subject to XRD analysis, identifying frequent cerussite (5), occasional anglesite (2) together with sphalerite (4) and galena (2) indicating some oxidation to more soluble carbonates and sulphates.

To the south the dissolved metal loadings from the adit into Afon Meurig were estimated at 68 kg/yr Zn and 1 kg/yr Pb. It was considered that mine water represents 20-25% of the normal flow in the river.

The primary sources of contamination to the Nant y Garw were identified as the former leat, where tailings have been deposited, the main conical tailings tip, the former dressing floor and sediment in drainage channels and the tailings dam. Two first-step intervention measures were recommended to reduce pollution and the amount of contaminated water requiring future treatment: surface water diversion/rationalisation and sediment arrest to reduce the off-site migration of contaminated sediments into the downstream catchment.

The data review also identified evidence gaps, in particular the availability of reliable flow data in the northern drainage network feeding the Nant y Garw. Between 2015 and 2022 NRW pursued a programme of concurrent water quality and flow monitoring, utilising salt dilution gauging where possible, in the Nant y Garw catchment. The data have been periodically analysed and reported to inform the optioneering and design of remediation measures (Hudson 2015; Francis 2018; Hudson *et al.* 2018). A summary of the full dataset is presented in Table 1.

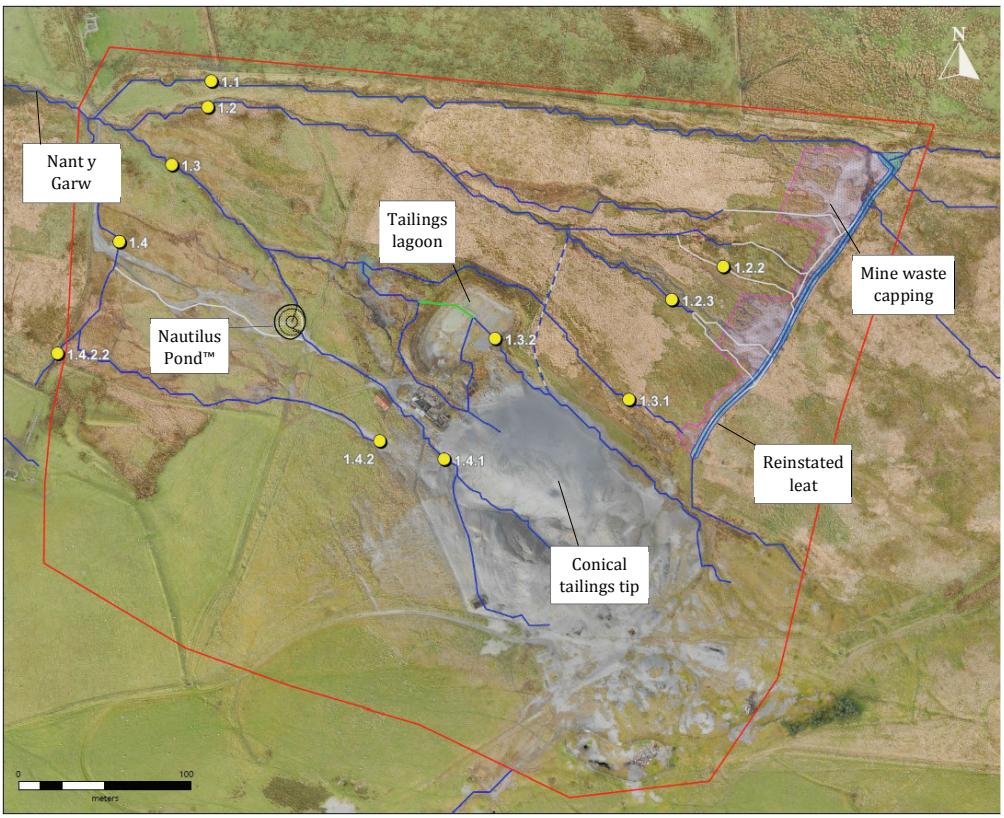


Figure 1 *Aerial image of northern site area identifying key features, braided network of drainage channels (numbered nodes) and proposed remedial measures.*

Metal loadings to the Nant y Garw from Esgair Mwyn are estimated as 1,897 kg/yr Pb, 766 kg/yr Zn and 3.2 kg/yr Cd. The primary source of Pb is ephemeral drainage channel 1.4 which originates from the main tailings tip (fig. 1). The second largest source of Pb is channel 1.2 which includes run-off from the historical leat and associated areas of tailings. This suggests that entrained sediments from tailings sources are the main driver of Pb contamination. The primary source of Zn and Cd is channel 1.3 which includes discharge from the tailings dam. It should be noted that the sum of loadings in channels 1.1, 1.2, 1.3 and 1.4 only accounts for 69% of the Zn and Cd loading and 37% of the Pb loading measured in the Nant y Garw. This could be due to measurement error, groundwater sources not captured by the monitoring locations and/or in-stream sediments between input channels and the Nant y Garw monitoring location.

Table 1 *Flow and metal loadings to Nant y Garw from NRW monitoring data 2015-2022.*

Channel	Flow (L/s)	Metal loading (kg/yr)		
		Zn	Pb	Cd
1 (Nant y Garw)	20.4	766	1,897	3.2
1.1	9.0	11	97	0.1
1.2	6.3	38	130	0.2
1.3	2.0	294	83	1.4
1.4	1.1	184	383	0.6

NB: Loadings based on unfiltered water quality samples to provide dissolved and suspended metal load in the water column; not including particulate transport associated with stream bed sediments

To enable remedial options shortlisting, modelling of the site's existing drainage network was undertaken (AECOM 2018a). A topographic survey of the site was completed using an Unmanned Aerial Vehicle (UAV) to an accuracy of 30-50 mm, with a more detailed ground survey within the drainage channels to an accuracy of 20-30 mm. A TUFLOW rainfall run-off model was created and run, comprising synthetic rainfall over a Digital Terrain model (DTM) produced from the topographic survey. This identified the Nant y Garw as the receiving watercourse, with the four principal run-off channels 1.1, 1.2, 1.3 and 1.4 feeding it, with additional nodes on each channel (fig. 1). The TUFLOW model derived that in a 1% Annual Exceedance Probability (AEP) event (1 in 100 year) contribution to total site run-off (Nant y Garw) was 32% from 1.1, 45% from 1.2, 14% from 1.3 and 6% from 1.4. This demonstrated that most of the flow from the site is not conveyed through the existing tailings lagoon. It was therefore recommended that remedial options should focus on re-routing the flow paths associated with channels 1.2, 1.3 and 1.4.1 to a sediment arrest feature around 1.3 as this would require the least length of channel diversion.

Spoil erosion and sediment yield analysis was completed using the Soil Loss by Water Erosion in Europe Revised Universal Soil Loss Equation model (RULSE2015) and application of a Sediment Delivery Ratio (SDR), providing a modelled sediment yield for the site of 20-40 tonnes per year. This theoretical figure includes areas of visibly eroding mine spoil but requires confirmation through monitoring of sediment accumulation in the proposed sediment arrest structure.

Based on observation of on-site stream discharge rates and erosion / slumping of the main spoil tip, a large proportion of the mine spoil erosion and transport to the off-site surface water receptors is expected to be linked to high rainfall events. Flow monitoring indicates that the typical flow range in the Nant y Garw at the downstream site boundary is in the range 2-12 L/s, with flows up to 215 L/s recorded during storm events. TUFLOW modelling gives a 20% AEP peak flow of approximately 400 L/s – equivalent to a 1 in 5 year event.

Portable XRF and wet chemistry analysis of mine spoil samples confirm lead concentrations in the range 822–185,433 mg/kg (i.e. 0.8-18%), mean 27,683 mg/kg with the highest concentrations within the leat sediments. At the lower range of erosion rates and mean mine spoil concentration (20 t/yr, 27,683 mg/kg) the potential sediment based lead loading to the Nant y Garw is estimated as 550 kg/yr. The erosion and transport of high lead concentration mine spoil represents a major lead input to the surface water network and also represents a major secondary source of lead once incorporated into the downstream river bed sediments. Reducing transport of contaminated sediments from Esgair Mwyn is a priority for remediation.

Three potential locations were initially proposed for a sediment arrest pond (AECOM 2019a). At an optioneering workshop, reinstatement of the historical mining leat was suggested as an option to separate cleaner upslope flows from those routed through the existing leat alignment and associated areas of tailings. A subsequent leat modelling exercise confirmed that reinstatement of the existing leat alignment would reduce flows to channels 1.2 and 1.3 by 46%-48% (AECOM, 2018b). It was recognised that rainfall on the exposed tailings along the leat would continue to mobilise contaminated sediment into the leat and channels 1.1 and 1.2. The proposed solution was to cap the exposed tailings with a low permeability barrier, such as Geosynthetic Clay Liner (GCL).

The leat modelling informed a sediment analysis exercise which demonstrated that at least 20 tonnes of particulate sediment could be mobilised from the entire site each year, highlighting that previous options underestimated the size of the required sediment arrest pond, which may need to be up to 70 m diameter. With the reinstated leat reducing flows in channels 1.2 and 1.3, and the lower metals content of sediments in 1.3 (Francis, 2018), a smaller pond was proposed to solely capture sediments generated from channel 1.4, downstream of the main tailings tip. The preferred option taken forward to outline design (AECOM, 2019b) was

reinstatement of the historical leat with associated capping of tailings deposits and construction of a sediment arrest pond on channel 1.4, which would discharge into channel 1.3. The potential sediment retention on channel 1.4, following leat reinstatement and channel rationalisation, is expected to be considerably lower than the modelled 20-40 t/yr site total. Scaled by 25% of site catchment area would give an estimated 5-10 t/yr.

Habitat, Heritage & Landscape Constraints & Opportunities

Selection of the proposed remedial interventions has included assessment and consideration of environmental constraints and opportunities. An Environmental Constraints and Opportunities Record and associated Environmental Constraints and Opportunities Plan have been prepared to document the constraints, plus develop opportunities for maintaining and improving environmental conditions at the site. Public amenity assets include a national walking route and public footpath, both Public Rights of Way (PRoW) to be retained.

Ecological and habitat conditions have been assessed through a Preliminary Ecological Appraisal (PEA) and supporting surveys, including a Lower Plant Species Survey, National Vegetation Classification Survey, Habitats Regulations Assessment (Test of Likely Significant Effect, and Appropriate Assessment) and a Raptor / Breeding Birds Survey. The PEA recorded a common lizard observed in 2018 with potentially suitable reptile habitat provided for slow worm and adder. A Reptile Mitigation Plan requires that winter working during brumation is to be avoided and an environmental watching brief will be required during construction activity.

The Historic Environment Record and National Monument Record identify 31 heritage assets on the site, with an additional nine identified through on-site inspection, all relating to the industrial heritage of the mining site / activities. An archaeological watching brief is anticipated for leat reinstatement works, an area classified as having high archaeological potential. Esgair Mwyn is within the registered historic landscape of Upland Ceredigion and the Banc Esgair Mwyn and Rhos Tanchwarel character areas.

The proposed remedial works have been designed to fit within these constraints without adverse impact and will be managed with an Environmental Action Plan and provide a number of opportunities for improvement. The works will avoid key areas of heritage interest around the lagoon and former process structures, plus lower plant species both here and on areas of bare spoil to the east of the conical tip. The principal opportunity for improvement is the reduction in contamination of surface waters, with the Afon Teifi being an important salmon and sea trout fishery. Additional opportunities for improvement include reinstatement of the PRoW along the leat, which is currently in very poor condition and difficult to traverse. Improving access and provision of interpretation boards will enhance the public amenity value of the site.

Nautilus Pond™ & Leat Reinstatement

Sediment arrest was recognised as a primary requirement to reduce metal loading to downstream watercourses and the Nautilus Pond™ was identified as a potential solution. The pond uses an outer circular chamber with spiralling flows that minimises velocity across the whole area, enabling settlement of particulate matter. Cleaner water enters a central chamber that effects drainage. The diameter is anticipated at 15 m with normal water levels at 2 m, and bypass at 3 m depth. The outer chamber requires periodic removal of harvested sediment.

Reinstatement of an historical leat was determined an effective means of capturing cleaner upslope water and conveying it away from tailings deposits into channel 1.1 (fig. 1), as well as having heritage benefits. In-keeping with historical construction methods, puddle clay was initially considered for lining the leat. In view of the periodic flows encountered and the risk of desiccation, it was decided to use the more robust concrete canvas. The reinstatement will also incorporate capping of the downslope tailings deposits with GCL

and a 300 mm confining layer with 100 mm soil cover prior to hydroseeding with specialist seed mix, biochar and tackifier.

Detailed design of the leat reinstatement and capping is complete. The Nautilus Pond™ design is being finalised with support from the parent company Source2Source prior to construction.

When applied to legacy metal mine environments, the harvested sediment if determined as waste, as it currently would be, will be classed as hazardous, which doesn't readily comply with Natural Resources Wales's Natural Resources Policy or Sustainable Management of Natural Resources (SMNR). Being categorised hazardous waste, the harvested sediment must be transported to a suitable disposal facility, currently in England. This will incur expensive carbon and monetary costs for ongoing operation and maintenance unless policy or guidance is changed enabling valorisation, stabilisation or direct use in the upper catchment of origin, thus achieving SMNR.

Conclusions

The Esgair Mwyn mine site is the largest single source of Pb contamination within the Teifi catchment. Monitoring data indicates that lead and zinc loadings to the Nant y Garw / Marchnant are approximately 1,900 kg/yr Pb and 800 kg/yr Zn. Sediment modelling and mine spoil analysis suggests that particulate contaminant loads to the Nant y Garw / Marchnant are likely to be considerably higher. Conservative modelled erosion rates and mean spoil lead concentrations predict 550 mg/kg Pb load to the Nant y Garw. The distinctive grey coloured mine spoil and tailings sediments can be visually identified in the Nant y Garw immediately downstream of Esgair Mwyn and represent an ongoing secondary metals source within the stream bed sediments.

Remedial intervention to reduce the transport of Pb-rich sediments to the Nant y Garw, Marchnant and Teifi represents the first and highest priority step to reduce the impact of the site on the downstream water body.

Reinstatement of a former mine leat and capping of mine spoil / tailings along the leat, will reduce surface water contact with contaminated sediments, with a modelled 45–50% reduction in flow within three currently contaminated surface water drainage channels. A corresponding increase in clean water flows will be routed around the site.

Installation of a Nautilus Pond™ to provide sediment arrest / harvesting on the principal outflow channel from the main conical spoil tip will reduce off-site transportation of contaminated sediments within the streams.

Acknowledgements

This study is funded by the joint Metal (Non-Coal) Mine Programme of NRW and the Coal Authority sponsored by Welsh Government. We extend our thanks to Dr Nina Menichino, Team Leader, Evidence Portfolio, Programmes and Processes at NRW for supporting this paper.

References

AECOM (2018a) Existing Site Drainage Report

AECOM (2018b) Leat Options Modelling

AECOM (2019a) Site Drainage Options Shortlist

AECOM (2019b) Outline Design Technical Note

Bick DE (1974) The Old Metal Mines of Mid-Wales. Part 1. Cardiganshire – South of Devil's Bridge.

Francis M (2018) Assessment of heavy metal contamination in sediment and water sources at an abandoned metal mine in mid-Wales, UK. MSc thesis. Swansea University.

Hall GW (2012) Esgairmwyn: Some History, and a Personal Story. Towards a Better Understanding. New Research on Old Mines. Proceedings of the Welsh Mines Society Conference 2010. Welsh Mines and Mining No. 2 p1-11

Hudson E (2015) Assessing Surface and Sub-surface Hydrological Contamination at an Abandoned Metal Mine in Mid-Wales, UK. MSc thesis. Swansea University.

Hudson E, Kulessa B, Edwards P, Williams T, and Walsh R (2018) Integrated Hydrological and Geophysical Characterisation of Surface and Subsurface Water Contamination at Abandoned Mines.

Lewis WJ (1967) Lead Mining in Wales. University of Wales Press.

Scorey AJ (2012) Assessment of metal (Cd, Cu, Ni, Pb and Zn) contamination from an abandoned metal mine in Mid-Wales, UK, to inform detailed remediation design. MSc thesis. Swansea University.

Working with Designation Constraints at Cwmystwyth

Dave Cooke[1], David Mason[1], Heilyn Williams[2], Liz Jones[2], Rebecca Byfield[3], Lindsey Mansell[1], Richard Carline[1], Peter Stanley[2]

[1]*The Coal Authority, 200 Lichfield Lane, Mansfield, NG18 4RG, UK, davecooke@coal.gov.uk, davidmason@coal.gov.uk. lindseymansell@coal.gov.uk, richardcarline@coal.gov.uk*

[2]*Natural Resources Wales, Tŷ Cambria, Newport Rd., Cardiff, CF24 0TP, UK, geowyddor@cyfoethnaturiolcymru.gov.uk*

[3]*Byfield Environment and Ecology Ltd., 81 Melton Road, West Bridgford, Nottinghamshire, NG2 6EN, UK rebecca.byfield@b-ee.co.uk*

Abstract

The Cwmystwyth mine remediation project aims to significantly reduce metal loading inputs into the Afon Ystwyth by addressing point source and diffuse pollution using interventions including active treatment and surface water management measures to prevent leaching and erosion of mine spoil. The Cwmystwyth mines have considerable ecological, heritage and landscape value, recognised by numerous statutory designations. Undertaking recent ground investigation works to inform the initial remediation project design required extensive environmental surveying, assessment and consenting to proceed under ecological and archaeological watching briefs. Further detailed environmental assessment work is ongoing to navigate the site's complex constraints moving towards project delivery.

Keywords: Heritage, calaminarian habitat, landscape, environmental assessment, intervention

The Cwmystwyth Metal Mine Remediation Project

This project is being delivered within the joint Metal (Non-Coal) Mine Programme between Natural Resources Wales (NRW) and the Coal Authority (CA). The programme supports the Western Wales River Basin Management Plan 2021–2027 that has a statutory function relating to the Water Framework Directive (WFD) required under The Water Environment (Water Framework Directive) (England and Wales) Regulations 2017.

Project motivation is WFD failure of the Afon Ystwyth downstream of the Cwmystwyth mines, which fails to meet the WFD chemical criteria for good water quality. The Afon Ystwyth is derogated by numerous metal mines for most of its length. The river headwaters typically contain little to no metal contamination, but metal concentrations subsequently increase to levels above recognised Environmental Quality Standards (EQS) due to diffuse pollution and point source inputs from the Cwmystwyth mines that adds major metal loading causing Zn, Cd, Pb and Cu EQS failures. There are further downstream contaminated inputs from Frongoch, Grogwynion, Gwaith Goch, Wemyss and Graiggoch mines, Frongoch Adit via Nant Magwr and the Level Fawr adit serving Logaulas, Glogfach and Glogfawr mines, which all result in EQS failure.

Some 24 tonnes of metals per year are discharged from Cwmystwyth into the Afon Ystwyth, eight tonnes from the permanent Pugh's Adit discharge in the far west. Two other adits contribute additional metal loadings, but are both blocked, buried and discharges are not directly visible. The post mineralisation Ystwyth fault cuts across all the adits and is considered an additional pollutant conduit. Visual observation of ochreous staining, sedimentation, efflorescence on stream cobbles and thermal imagery support the conceptual model of active pollutant linkages. In addition to these point source discharges, four tributary streams (Nant y Gwaith, Nant y Graig, Nant y Watcyn and Nant yr Onnen) cascade down the mountain to the north of the Afon Ystwyth, cutting through extensive

mine spoil and floodplain deposits, eroding sediments and leaching diffuse metals under typically highly variable flow conditions, all of which are additional contamination sources.

Design at Cwmystwyth aims to reduce the concentrations of dissolved Pb and Zn in the Afon Ystwyth by up to 50% in downstream sections, along with a major reduction in the amount of fine grained, metal rich sediment entering the river through erosion of exposed spoil and in-channel deposits. The proposed remediation works are located in an area of considerable ecological, heritage and landscape value, recognised by numerous statutory designations. This paper discusses the complexities posed by these statutory designations and describes the necessary consenting and environmental assessment requirements that forms an integral part of the project design and delivery.

Introduction to the Cwmystwyth Mine Site

The Cwmystwyth mines are situated 23km east south east of Aberystwyth, Ceredigion, in the steep sided valley of the upper Afon Ystwyth. Mining at Cwmystwyth began in the Bronze Age and continued during construction of the Cistercian Abbey at Strata Florida before 1200AD. Cwmystwyth is believed to be the source of lead for the abbey church roof. Mining ceased and the site was abandoned without any restoration or remediation in 1932. The site is owned by a dedicated mine preservation group, the Cambrian Mines Trust.

The land at the Cwmystwyth mines is predominantly a mosaic of grassland, exposed spoil and rock with some areas of gorse scrub. The central parts of the mine site on the northern side of the Afon Ystwyth contain extensive ruins of a complex of mine buildings, associated working areas and spoil tips. The ruins and associated spoil heaps make a notable contribution to the landscape character of the valley.

Cwmystwyth Feasibility Study and Proposed Remediation Interventions

NRW and CA completed a feasibility study at Cwmystwyth in 2021 which identified potential intervention options to achieve remediation at the site as follows: The

- capture and transfer of pollution point sources (adits) into an active mine water treatment scheme.
- diversion of selected diffuse pollution sources emanating from spoil run-off and seepages into the active treatment scheme via interceptor drains.
- removal or relocation of slime heaps from the functional Afon Ystwyth floodplain preventing erosion.
- provision of interception drainage to prevent clean surface water infiltrating mine spoil.
- implementation of various engineering works on the four tributaries to reduce diffuse pollution and prevent clean surface water infiltrating mine spoil; including reinstatement of their former channels, protection of stream banks and lining of the stream channels across spoil and floodplain sediments.

Cwmystwyth Site Designations and Legislative Requirements

The long abandoned ancient mines and surrounding areas have developed features of considerable ecological value which are recognised by several ecological designations; the site also has designations for its heritage and landscape importance, which are summarised below along with their legislative context.

Elenydd SAC (Special Area of Conservation) and Elenydd SSSI (Site of Special Scientific Interest).

Covering an area of 8,600 hectares, Elenydd is one of the most important areas of Welsh hill land and is of outstanding nature conservation interest for its vegetation. The Elenydd SAC and SSSI are designated for several upland vegetation communities, including blanket bog and heathland habitats. Calaminarian grasslands of Violetalia calaminariae are also a primary reason for selection of the Elenydd SAC and are considered one of the UK's best examples of this habitat type. Calaminarian grasslands include a range of semi-natural and anthropogenic sparsely vegetated habitats on substrates characterised

by high metal toxicity and are associated with natural outcrops of serpentine rocks, river gravels rich in metals, as well as metal mine workings and spoil heaps. The calaminarian grassland comprises only 26 hectares of the entire Elenydd SAC habitats with the Cwmystwyth site containing the majority of the SACs calaminarian grassland resource. Areas of rock outcrop, scree, spoil-heaps, abandoned shafts, adits and buildings are colonised by specialist metal-tolerant lichens and bryophytes (metallophytes) including several scarce species, which are of individual conservation value.

Mapping of the calaminarian grassland at Cwmystwyth (Forster Brown 2017) has shown the site comprises a mix of calaminarian communities (Simkin 2014); the site is clearly of importance for the patchy but widespread extent of its calaminarian habitats. The mapping highlighted that calaminarian communities at Cwmystwyth vary in their distribution depending on the degree of contamination. The most contaminated areas are devoid of vegetation even after cessation of mining decades ago. Factors influencing bryophyte and metallophyte distribution include, substrate moisture, slope aspect, the spoil geochemical composition, the degree of spoil compaction and slope stability. Many spoil areas are very species-poor and lack the presence of metallophytes; other spoil tips are much more species-rich and these are often isolated from other spoil tips that support a similarly rich assemblage of metallophyte species.

Elenydd-Mallaen SPA (Special Protection Area).

Elenydd is also one of the most important areas of hill land in Wales for its outstanding range of breeding birds. The Elenydd-Mallaen SPA is notified for the breeding raptors Red Kite Milvus Milvus, Merlin Falco Columbaris and Peregrine Falcon Falco Peregrinus.

Mwyngloddfa Cwmystwyth SSSI.

Mwyngloddfa Cwmystwyth SSSI is of special interest for its calaminarian plant communities and metallophyte lichens, including several rare species. The SSSI is also of special interest for its primary and significant secondary mineralisation associated with the spoil tips and the underground workings adjacent to the road and on the lower slopes of Graig-Fawr and Copper Hill (Bryn Copa). Complex sets of hushes and leats cross the heavily mined landscape (Bevins *et al*. 2010). The underground mine workings are also important for hibernating bats, and the site is the best known location in Ceredigion for hibernating bats. Long-term monitoring has shown that Myotis species and Brown long-eared bats Plecotus auritus are regularly present during the winter.

Grogwynion SAC

Grogwynion SAC covers 42 hectares located in the Ystwyth floodplain 9 km downstream of the Cwmystwyth mines. It is designated for its' shingle heath which comprises of calaminarian grassland and heathland habitats, which both contain a rich metallophyte lichen species assemblage. These habitats cover four hectares within the overall SAC. Cwmystwyth is hydrologically connected to the Grogwynion SAC via the Afon Ystwyth. The shingle heath feature and its notable metallophytes depend on the presence of metalliferous coarse and fine-grained substrates for colonisation and the fluvial processes and river realignment that expose or deposit new areas of fresh shingle and silts. Metalliferous substrate is present at Grogwynion due to historical metal mining in the catchment, and the input of metalliferous material at the site is likely dominated by the localised contribution from the former Grogwynion and Gwaith Goch Pb mines. Metal mining wastes have intermingled with natural river gravels to create the foundations of an extensive area of shingle heath on the Afon Ystwyth floodplain. The dynamic river processes at Grogwynion regularly rework gravels creating a series of river shoals, with fresh material being deposited when the river overflows. Additionally, a range of seral successional stages of bare shingle substrate, calaminarian grassland, heathland and scrub communities are found. Metallophyte lichens are locally dominant in the calaminarian grassland and heath, with a number of rare species present.

In flood events the supply of contaminated material at Grogwynion is refreshed by deposition of metal-rich silts that have been eroded from upstream metal mine sites such as Cwmystwyth, although the current inputs are significantly less compared to when the mines were active. A further source of metalliferous material to the Grogwynion SAC are sediments already stored in the Afon Ystwyth's bed and banks, which are subsequently eroded and transported downstream by fluvial processes. These sediments derive from a combination of the historical mining sediments within the river and new metalliferous sediment eroded from mine spoil via surface runoff. The Afon Ystwyth hydrologically connects the Cwmystwyth mines to the Grogwynion SAC and it is considered that the proposed remedial intervention measures may represent a potential impact pathway to the Grogwynion SAC by reducing downstream sediments.

Biodiversity Legislation and Policy in Wales Relating to the Sites.

The Conservation of Habitats and Species Regulations 2017 provides the legislative framework for the designation and protection of SACs and SPAs. This requires that statutory bodies such as NRW and Local Planning Authorities, referred to as Competent Authorities, must follow the strict Habitats Regulations Assessment (HRA) process set out in legislation to test if a proposal could significantly harm any designated features of a SAC/SPA. The HRA process has three sequential steps in considering any project's effects. Firstly, a project screening for any "likely significant effects" is undertaken, which checks for pathways of effect between the project and the protected site. If there are no connections the project is then screened out and no further assessment is required, otherwise the project proceeds to the next step. Secondly, a project must be assessed in detail, via Appropriate Assessment, to determine its effects on the protected ecological features for which the site is designated and identify ways to avoid or minimise any effects. If any effects can be avoided or mitigated these are then implemented and the process is complete, otherwise the process proceeds to the final step. Finally, if it is considered a proposal that would have an adverse effect on a SAC/SPA, then the process requires an examination of whether the project would qualify for various derogations. In order to qualify, the project must meet three criteria; there must be no alternative to the project, it must have Imperative Reasons of Overriding Public Interest (IROPI), and lastly that compensatory measures can be put in place to ensure no negative effects occur on the national network of SAC and SPA sites as a whole.

The Wildlife and Countryside Act 1981 (as amended) (WCA) is the primary legislation which protects animals, plants and habitats in the UK. The WCA covers the protection and designation of protected areas including SSSIs. When carrying out works that may affect a SSSI it is a requirement to notify NRW and obtain SSSI assent under section 28H of the WCA.

The ecological value of metal mine lichen assemblages across Wales are recognised by their inclusion on the Section 7 list of species and habitats of principal importance for conservation of biological diversity in Wales under the Environment (Wales) Act (2016). There is also a Section 6 duty under this legislation for public bodies to maintain and enhance Section 7 habitats and species.

Heritage Designations

Extensive parts of the Cwmystwyth mine site and the buildings are designated for their heritage interest as the Copa Hill/ Cwmystwyth Lead, Copper and Zinc Mines Scheduled Monument. The Scheduled Monument comprises the remains of the lead mining complex, which also produced Cu and Zn. Work at the Cwmystwyth mines has been dated back as far as the Early Bronze Age with radio carbon dating of deer antler implements and charcoal (Timberlake 1988). Mining continued intermittently over many centuries until all activity finally ceased in the 1930s. The visible features within the scheduled area include numerous shaft and adit entrances, areas of opencast working, water-management and transport systems, extraction and dressing processes with their power systems, as well as remains of office and residential buildings, garden plots and even an early 20th-century tennis court for

the mine captain's daughter. The monument is of national importance for its potential to enhance and illustrate the knowledge and understanding of mining technologies from a variety of periods.

Any works within a Scheduled Monument (SM) requires SM consent (SMC) under the Ancient Monuments and Archaeological Areas Act 1979 as amended by The Historic Environment (Wales) Act 2016. An application is considered in accordance with Conservation Principles for the Sustainable Management of the Historic Environment in Wales (Welsh Government 2011) and Annex A of Technical Advice Note 24: The Historic Environment (Welsh Government 2017). The main purpose of scheduling is to ensure the preservation of ancient monuments and, when considering an application for SMC, there is a presumption against proposals which would involve significant alteration or cause damage or which would have a significant impact on the setting of remains. Projects are expected to demonstrate that no practicable alternative location that would avoid the scheduled area exists and that the need to undertake works outweighs the presumption in favour of the protection of the SM.

Landscape Designations

The Cwmystwyth mines are located wholly within the Northern Uplands Special Landscape Area (SLA). SLAs are noted in Ceredigion County Council's Local Development Plan which states: 'Proposals for development within SLAs will be assessed in relation to scale and nature of development and their ability to be accommodated without significant damage to, and where possible the enhancement of, the valued visual, historic, geological, ecological and cultural characteristics of the SLA.' The Cwmystwyth mines are also located within the Upper Ceredigion registered historic landscape. Landscapes of outstanding or special historic interest are non-statutory designations compiled by Cadw (Welsh Government's historic environment service), NRW and the International Council on Monuments and Sites. Landscapes are registered to recognise their historic landscape value and raise awareness of their importance.

Practical Delivery of Recent Ground Investigation Works

A ground investigation (GI) to inform the design of pollution alleviation measures was completed in early 2023 comprising geotechnical and geo-environmental investigations using a combination of machine and hand dug trial pits. The aim was to provide information on ground conditions to help design proposed channels and drainage interventions, outline spoil heap composition to inform future relocation or stabilisation options and to accurately establish the blocked adit locations for future water capture structures.

The GI works were subject to HRA and required SSSI assent in relation to the SAC, SPA and SSSI designations. HRA screening ruled out any significant effects to Grogwynion SAC as a result of the GI. Significant impacts on the Mwyngloddfa Cwmystwyth SSSI spoil tip mineralisation processes was also ruled out as all disturbed spoil was reinstated post works. Impacts on the Elenydd-Mallaen SPA raptor features were avoided by being undertaken in early 2023 outside the breeding season. The GI works were assessed for any effects on the calaminarian grassland SAC and SSSI communities within the Cwmystwyth mines site through the HRA, and the Mwyngloddfa Cwmystwyth SSSI hibernating bat features were addressed via the SSSI assenting process.

Initially, the GI was designed to avoid mapped areas of high value lower plant habitats. This approach was however, unable to completely remove the conflict as several trial holes were required within high value zones to gather information for further design stages. This was therefore followed by a detailed risk assessment to assess the calaminarian grassland and metallophyte lichen interest at the GI locations and access routes. Subsequently, a method statement to minimise effects to lower plants resulting from the works was implemented to secure mitigation to allow works to proceed. All works were progressed under an ecological watching brief by a lower plant specialist; micro-siting of GI locations was undertaken to avoid disturbance of high conservation value lower plants where possible. Translocation of rocks and spoil crusts that

supported nationally rare species that could not be avoided was undertaken; these were placed separately on tarpaulin in a safe location away from the working area and then reinstated carefully following completion of the excavations. A low impact tracked vehicle was used for the works to avoid or reduce disturbance. With the adoption of these mitigation measures the HRA appropriate assessment concluded that the Elenydd SACs site integrity would not be adversely affected by the works, furthermore SSSI assent was granted for the GI with conditions securing the mitigation measures.

A bat survey was completed to inform the project proposals and assess hibernating bat potential. Four features with bat hibernation potential were noted within the Mwyngloddfa Cwmystwyth SSSI. The survey recorded a single pipistrelle summer day roost. The timing of works in early 2023 avoided disturbance to the summer roost. The work period coincided with the bat hibernation period; however, it was concluded that the GI works would not significantly disturb the hibernating bat SSSI feature associated with underground workings, as these were not directly affected by the works. Further mitigating factors included, the short duration of GI at each location and also that the GI locations closest to bat features were to be hand dug and required no machinery access. In addition buffer zones were implemented between underground structures and GI locations ensuring minimal disturbance. Ecological Clerk of Works (ECoW) supervision was put in place to ensure there was no access into the buffer zones by personnel and equipment and no light spill occurred. The ECoW was also present to ensure if accidental access into an adit occurred this could be immediately assessed for bat risk. SSSI assent was granted as the mitigation measures would protect the SSSI bat interest.

SMC was secured for the GI and noted that some locations would specifically target historic features, whereas unknown archaeology may also be uncovered elsewhere. The SMC noted that the GI may potentially damage nationally important archaeological remains that would be contrary to the scheduling, which is to preserve features in situ. The SMC considered that the GI was justified in order to fully understand the site conditions and to allow the development of the remediation works. The SMC concluded that any localised damage because of the GI would be outweighed by obtaining an improved understanding of the SM and also by the project aims to address water pollution.

An archaeological watching brief undertaken by a suitably qualified archaeologist during the GI ensured that archaeological features were identified and recorded. The SMC required that if significant features were identified works must stop to enable Cadw to undertake an assessment and request trial pit relocation. The watching brief information, gathered improved knowledge and understanding of the SM and informed future remedial design. The watching brief recorded a subsurface buddle, which will now be avoided during design. The ground disturbance caused a temporary negative impact to the SM's aesthetic value, which ceased following reinstatement. The SMC included conditions ensuring Cadw officers access for the works duration; compliance with the consent documentation which included an Environmental Action Plan (EAP), Reinstatement Method Statement, the Archaeology Written Scheme of Investigation (WSI) and provision of post work reports to Cadw.

Ongoing Habitats Regulations Assessment (HRA) Process

One of the operational project aims is to significantly reduce the amount of metalliferous sediment entering the Afon Ystwyth from the Cwmystwyth mines. Due to the Grogwynion SAC shingle heath feature depending upon the supply of metalliferous substrate and its hydrological connection to the Cwmystwyth site, it was screened in at the first step of the project HRA. During the second step, the Appropriate Assessment, it has been challenging to predict the potential changes expected at Grogwynion that will result from the project. It is difficult to differentiate the sources of metalliferous fluvial sediment reserves present within the Afon Ystwyth, to determine which originate from other historical mining activities and from the Cwmystwyth mines. Due to these

complexities, it has not been possible during the appropriate assessment phase to rule out that the project will not adversely affect the Grogwynion SAC. The legislation requires that a precautionary approach must be adopted. It has therefore been concluded that there may be possible degradation of the physical, chemical or biological processes that support the Grogwynion SAC shingle heath feature. Any such degradation of these processes may result in potential changes to the extent or the vegetation composition of the shingle heath. It has therefore not been possible to determine beyond reasonable scientific doubt the scale to which the SAC feature would be affected by remedial interventions at Cwmystwyth, therefore, an adverse effect on site integrity during the operational phase cannot be ruled out.

Further detailed HRA is required for the Elenydd SAC and the Elenydd-Mallaen SPA designations to demonstrate compliance with the Conservation of Habitats and Species Regulations 2017 (as amended). This will be completed following further scaling and refinement of ongoing remedial designs. Bespoke environmental mitigation and compensation will need to be integrated into the project. Whilst alternatives have been considered, there are no feasible ones that will allow metal sediment loadings from Cwmystwyth to continue feeding the shingle heath habitat at Grogwynion SAC via the Afon Ystwyth, given that it is contradictory to the project objectives and WFD. It is therefore necessary to demonstrate IROPI, devising suitable compensation measures to fulfil legislative requirements. The case for the intervention measures is due to environmental benefit and WFD; the project therefore meets the criteria of being imperative and in the public interest.

Further Considerations for the Future Project

A Cultural Heritage and Archaeology Appraisal was undertaken in 2019 to provide preliminary information on the sites cultural heritage and archaeology, to identify potential archaeological issues and heritage constraints, along with wider landscape constraints that must be considered during project design and planning. Given that the Cwmystwyth mines and all the features and structures within the site are high value heritage assets, the protection and preservation of surface and sub-surface remains must be a principal consideration in our remediation design proposals to avoid adverse effects. As the site is positioned entirely within a SM, remediation design proposals will be accompanied by a SMC application, to include detailed plans and full desk-based assessment following consultation with Cadw. The full desk-based assessment will form part of the required statutory Environmental Impact Assessment (EIA) once the remediation design is finalised. As part of this study, an Assessment of Significance of Impact of Development on Historic Landscape (ASIDOHL2) may be needed to assess the potential impact on the Uplands Ceredigion registered historic landscape.

A preliminary landscape appraisal following the Guidelines for Landscape and Visual Assessment (LVIA), (Landscape Institute 2013) has been compiled to inform the project; this comprised a desktop review and site visit. The report compiled baseline landscape information for the site and identified design considerations, opportunities and constraints, such as visual screening, maintenance of the sites open character, using sensitive materials and colour palettes, stabilising and preserving the existing ruined mining buildings and structures, and promoting walking and cycle routes. Given the project will be located in an SLA, a full LVIA with reference to the aforementioned guidelines will be produced, along with a landscape mitigation plan as part of the EIA.

The treatment of mine waters at Cwmystwyth may be considered to be continuing the mining landscape narrative. An approach which seeks concealment of treatment works may represent a missed opportunity in allowing the public to appreciate the ongoing mining story within the landscape. Nonetheless, given the landscape character and the landscape designations that apply to the Cwmystwyth site, a design approach which is sympathetic to the local landscape character, visual

amenity, heritage and ecology is required. The extremely rich history and prehistoric origins of the Cwmystwyth mines provide a substantial opportunity as part of the remedial interventions to promote regional and local distinctiveness, and a sense of place by utilising the mines remains as an educational, economic and social asset in conjunction with relevant stakeholders.

Conclusions

The Cwmystwyth mines have a rich tapestry of statutory ecology, heritage and landscape designations and various environmental assessment and consenting procedures have been undertaken or are required to navigate the sites complex constraints and move the pollution remediation project towards delivery.

Acknowledgements

This study is funded by the joint Metal (Non-Coal) Mine Programme of NRW and CA sponsored by Welsh Government. We extend our thanks to Dr Nina Menichino, Team Leader, Evidence Portfolio, Programmes and Processes at NRW for supporting this paper. The authors also extend thanks to Cambrian Mines Trust who help us deliver this project. This paper is dedicated to the memory of two exceptional lower plant ecologists Chris Forster Brown and Alan Orange.

References

Forster Brown C, Chambers SP (2017) Mapping the extent of calaminarian grassland at Mwyngloddfa Cwmystwyth SSSI. NRW Evidence Report No: 203, 29pp, NRW, Bangor

The Landscape Institute and Institute of Environmental Management and Assessment. (2013). Guidelines for Landscape and Visual Impact Assessment, Third Edition

Simkin J (2014) Defining and mapping Calaminarian grassland in mid-Wales. Natural Resources Wales Evidence Report: 024.

Bevins RE, Young B, Mason JS, Manning DAC and Symes RE (2010) Mineralization of England and Wales, Geological Conservation Review Series, No. 36, Joint Nature Conservation Committee, Peterborough, 598pp

Timberlake S (1988) Bronze Age Mining at Cwmystwyth: the radio carbon dates. Archaeology in Wales, 28, 50

Welsh Government (2011) Conservation principles for the sustainable management of the historic environment in Wales

Welsh Government (2017) Technical Advice Note 24: The Historic Environment

Surface Water Management to Reduce Pollution at Dylife, Mid Wales

Dave Cooke[1], Emily Hudson[1], Liz Jones[2], David Mason[1], Richard Wylie[1], Peter Stanley[2]

[1]*The Coal Authority, 200 Lichfield Lane, Mansfield, NG18 4RG, UK, davecooke@coal.gov.uk, emilyhudson@coal.gov.uk, davidmason@coal.gov.uk and richardwylie@coal.gov.uk*

[2]*Natural Resources Wales, Tŷ Cambria, Newport Rd., Cardiff, CF24 0TP, UK, geowyddor@cyfoethnaturiolcymru.gov.uk*

Abstract

The abandoned Dylife metal mine presents many legacy issues and environmental constraints requiring consideration when developing remedial solutions. Extensive monitoring and conceptualisation of pollution pathways has allowed the development of a phased approach dealing with identified pollution sources. The ambition is to manage surface water to reduce the need of installing a mine water treatment system, which is subject to post-intervention monitoring and validation. Surface water management is presented as an effective tool at many legacy metal mines with lodes typically worked to surface and intimately connected with watercourses that continue to be polluted many years after mining has ceased.

Keywords: Surface water management, erosion, run-off, intervention, drainage

Introduction

The former Dylife Pb and Cu mine is situated 16 km northwest of Llanidloes, Powys within the upper Afon Twymyn catchment, a tributary of the Afon Dyfi which flows into Cardigan Bay at Aberdyfi. Pb mining began in Romano-British times and the Roman fortlet Pen y Crocbren sits atop the mountain to the south of the now abandoned underground mine site. Mineral exploitation is recorded from 1640 with almost 37,000, 1,500, and 400 tonnes of Pb, Cu and Zn ores respectively produced between 1845 and 1901 (Bick 1985). A later attempt to recover metal by reprocessing old spoil tips in the 1920s resulted in extensive riverside spoil deposits to the north, separated from the rest of the site by a modern road embankment that crosses much of the former mill and mineral processing area. The layout and extent of the mine is shown on Ordnance Survey maps from the late 19th Century (fig. 1).

No remediation or restoration was undertaken upon abandonment and the site continues to pollute the entire length of the Twymyn contributing significant metal loading to Dyfi, which is also polluted by other abandoned mines to a lesser degree. The mine pollution is confirmed as a principal reason for the Twymyn waterbody not achieving Good status and the site has been identified as a target for improvement under the joint Metal (Non-Coal) Mine Programme (MMP), a partnership between Natural Resources Wales (NRW) and the Coal Authority.

The mine sits immediately above the impressive Ffrwd Fawr Waterfall and the northerly draining Twymyn Gorge, all within the Dyfi Biosphere area. The large deposits of riverside spoil known as the Great Tip and Hirnant Tip are designated as a geological Site of Special Scientific Interest (Dylife Mine SSSI). The mine site to the south and west of the road embankment is not formally designated but contains further spoil deposits and other important mine heritage features including parts of the former dressing floor, the 19.2 m diameter Red Wheel pit and in-situ pumping rods in the Llechwedd Ddu Engine Shaft. Ecological surveys of the site have confirmed the presence of large established Calaminarian Grassland species and habitat (Simkin 2014) including the nationally rare Lead-moss Ditrichum plumbicola (Pryce 2020).

The assessments (PB 2005, URS 2012, AECOM 2016) and feasibility study (Coal Authority 2020) have confirmed a number of active pollutant linkages and identified potential intervention targets for each linkage. Local infiltration and surface water / groundwater interaction is controlled by historical mining activity (surface and underground). The local bedrock comprises the turbidite sequences of the Silurian Rhayader Mudstones Formation that would have very limited natural groundwater flows, restricted to post-lithification fractures and mineralisation zones. Due to the complexity of underground workings, surface spoil deposits and surface water run-off a staged approach to design and implementation of surface water management measures is recommended. This will enable the effectiveness of each stage to be assessed before starting the next. Measures to control infiltration, reduce erosion and minimise contaminated surface run-off. Once these measures are in place, the need for treatment of remaining mine water discharges can be reassessed /confirmed.

Limiting Surface Water Inflows

The site sits at the confluence of Nant Dropyns and the Afon Twymyn, although the original confluence location is now buried beneath a newer road embankment, road junction and informal car park. Upstream of the confluence, both watercourses are ephemeral, losing their flow entirely in some reaches during drier conditions. Mine workings on the southwest – northeast trending Esgairgaled Lode are recorded beneath both watercourses, with numerous connections with the surface suspected but not visible due to the channel bed infill. The Llechwedd Ddu Lode trends almost along the Twymyn channel and was accessed via the Llechwedd Ddu Engine Shaft, that remains open and visible on the slope above the right-hand bank of the river. There is a junction between the two lodes upstream and the Esgairgaled workings are connected to the Llechwedd Ddu workings via a crosscut adit, referred to as Level Goch (Bick 1985). Further connection to the Esgairgaled workings was made by driving another cross-cut north 73 m, although this was then abandoned due to

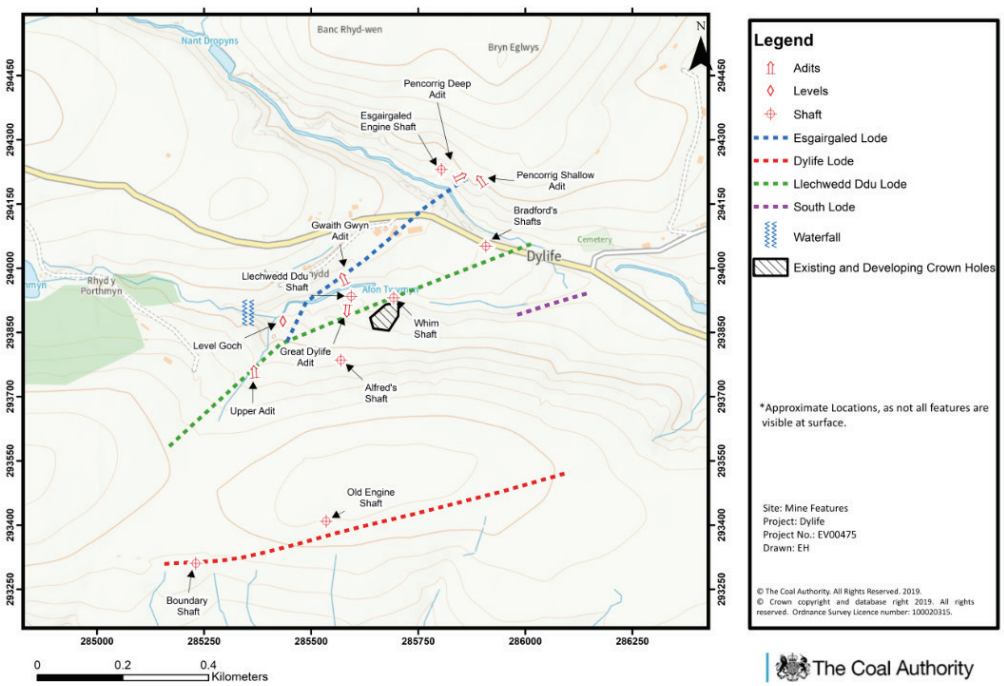


Figure 1 *Schematic plan identifying the lodes and mine entries at Dylife and Dyfngwm mines.*

excessive water ingress. Improved pumping capacity was required to permit expansion and exploitation of the rich Pb ore to the north of the river (James 2014).

The Llechwedd Ddu workings drain via an adit from the Whim Shaft (fig. 1) further east and downstream, i.e. at an elevation lower than the losing channel reach. This Llechwedd Ddu adit portal is now buried and discharges are suspected to be constricted, especially under high flow conditions with the Whim Shaft pool observed overtopping on occasion.

Water is also observed to re-emerge from the left-hand bank of the Twymyn immediately downstream of the rock tunnel under the modern road embankment, suspected to be the result of underground flow along the original Nant Dropyns channel to the former confluence location (Margary 1992). The latest conceptual site model infers substantial infiltration of river and stream flows into underground workings, with the constricted outflow leading to mine water levels rising and falling on a continual basis with the release of metal contaminated water to the downstream Afon Twymyn (fig. 2). Contamination is also introduced through the underground flows along the original Dropyns channel alignment now backfilled with spoil and overlain by an unsurfaced car park area, which represents the majority of Nant Dropyns flow in most normal weather conditions. In all cases, it is assumed that infiltration and flow through unmined bedrock is negligible. These water pollution pathways are exacerbated by the flashy nature of the small upland catchments that enhances the flushing effects of rising and falling water levels in mine workings and metalliferous made ground deposits. Surface water flow gauging and monitoring continues to further define losses to workings and help inform the design of proposed engineering interventions.

Installation of impermeable lining to the channel bed and banks has been identified as the most feasible option for preventing inflows of uncontaminated surface water into underground workings and metalliferous made ground deposits. Flows also need to be conveyed through and under the modern road

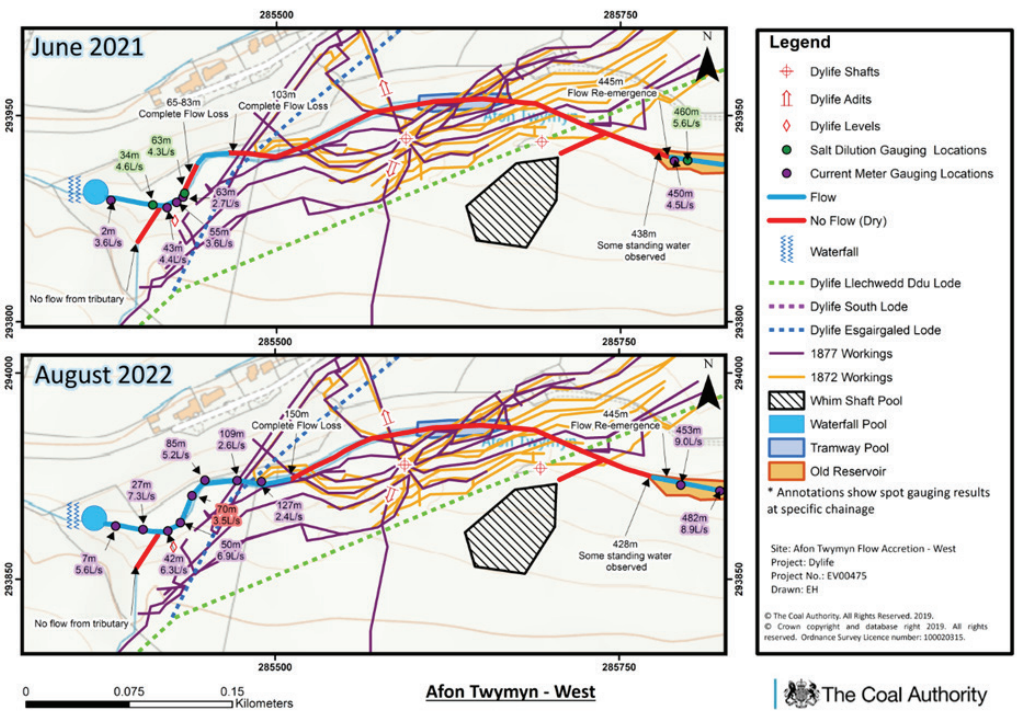


Figure 2 *Afon Twymyn flow gauging results revealing the scale and location of flow losses.*

embankment / car park area, as alternatives to crossing the remaining exposed dressing floor area thus entering the Afon Twymyn upstream of a constraining rock cut tunnel. Ongoing flow monitoring is critical to sizing the new culvert and lined channel sections. It is intended that on completion, the mine water levels in the flooded workings beneath the site will permanently revert to the base level of the buried discharge at the Llechwedd Ddu adit and be much reduced in volume. This will need to be confirmed and validated by post installation monitoring.

Preventing Erosion and Contaminated Run-off

Extensive monitoring, including source apportionment using salt dilution gauging and synoptic sampling has identified the remaining exposed dressing floor area and riverside spoil tips as major contributing sources of downstream metal pollution. The Twymyn channel is observed to directly erode spoil deposits and receive run-off from steep, gullied largely unvegetated slopes as the river traverses the main mine site and particularly as it runs directly along the toe of the Hirnant Tip within the eastern part of the designated Dylife Mine SSSI area (plates 1–3).

The Nant Dropyns has previously been diverted under the road from north to south and across the exposed former dressing floor. Although the channel is dry in low flow conditions, storm events can quickly result in very high flows through the channel, with severe erosion of fine grained ore processing spoil deposits. Much of the channel now is on bedrock downstream of the road culvert concrete / rip rap channel. Diversion of the Dropyns into the Twymyn upstream of an original rock cut mining tunnel results in backing up of the combined flows during severe storm / sustained heavy precipitation events. The frequency of these events has not been determined, but is likely increasing due to climate change, leading to further erosion of the bankside spoil deposits. The absence of defined drainage from the road embankment and adjacent land also leads to increased surface run-off, gullying the remaining dressing floor deposits and loss of mine heritage artefacts buried within it.

Due to the visible severity of the erosion and damage to vulnerable mine heritage features such as the bored wooden drainage pipes strapped with metal, early intervention measures were introduced. These used pre-filled 'rock roll' plastic mesh protection placed in front of the current eroded channel banks across the dressing floor and along the left-hand bank of the Twymyn that is subject to inundation and erosion during flooding (plates 4–5).

Additional erosion protection and drainage will be required to protect the main Hirnant Tip toe and other exposed spoil slopes directly adjacent to the Afon Twymyn. The upstream channel lining work is anticipated to also mitigate the erosion and run-off impacts in those sections. The erosion protection for the Hirnant Tip toe will need to be combined with interception drainage, to prevent hillside run-off infiltrating into the up-gradient spoil deposit and with surface drainage to prevent gullying of the exposed fine grained reprocessed spoil. This will involve reprofiling of the tip to provide separation from the bedrock river channel that can't be moved and to produce a long term stable landform with minimal ongoing maintenance or protection requirements. Alternative options included extensive



Figure 3, *4 & 5 Afon Twymyn looking downstream eroding Hirnant Tip toe.*

capping or off-site disposal of spoil were discounted at feasibility stage, although it is noted from a review of the Dylife Mine SSSI citation that the mineralogical interest of the site lies exclusively in the Great Tip deposit, which does not require extensive treatment at this stage.

The feasibility study (Coal Authority 2020) noted that if the proposed engineering interventions were insufficiently effective due to ongoing leachate seepages from the Dylife Mine SSSI deposits, there is an option to install passive treatment media within the toe drainage channels, to be designed based on future monitoring results. It is acknowledged that this would in turn require substantial ongoing maintenance to clear clogging and refresh absorbent media. Additionally, further engineering would be required to prevent river or clean surface runoff ingress into the toe drains as opposed to using simple French drains presently proposed.

Working with Environmental and Heritage Constraints

Abandoned metal mine sites are typically in remote, otherwise undeveloped areas and often allow the development of sensitive and unusual Calaminarian habitats that host a diverse mosaic of sometimes rare flora and fauna. This, along with associated formal designation of the habitat, geology or mine heritage features, usually prevents wholesale removal or encapsulation of identified pollution sources. The original Dylife mine has been obscured and degraded by subsequent mineral exploitation, such as the spoil reprocessing by Hirnant Minerals plus the lead works by the modern road embankment and car park. The remaining exposed mining features and diverse habitat merit ongoing preservation and protection.

The creation of sterile artificial channels and long culverts are counter to current 'green engineering' good practice and mitigation. They are however essential parts of pollution prevention interventions and can be designed more sympathetically and innovatively from the outset. They can incorporate sinuosity or thalwegs and steps to retain gravel substrate over the impermeable lining. New culvert sections can be provided with a mammal transit shelf to allow for unrestricted movement of animals along the riverbank under most flow conditions.

Surface water run-off from the site and surrounding areas needs improved management to attenuate surface flows and encourage conveyance around or through contaminated areas thereby restricting direct infiltration. Provision of effective drainage and landforms to more extensive areas of exposed spoil such as Hirnant Tips will also help reduce direct infiltration.

Spoil deposits sufficiently remote from active watercourses and not representing



***Figure 6** & 7 Erosion Protection Intervention in the Nant Dropyns Channel across the Former Dressing Floor, working in extreme wet conditions.*

notable pollution sources with direct run-off connection will remain in-situ undisturbed by future engineering works. Accordingly, sensitive and valuable habitats created by mining operations can be preserved without substantial reduction of essential pollution prevention interventions.

Conclusions

Dylife is a typical example of how historical metal mining activities continue to cause surface water pollution across the Western Wales River Basin District, despite having no visible discharge of mine water into the main river. Long standing problems centre on the absence of effective surface water management on and around this extensive site bisected by two watercourses and now with road infrastructure crossing the site. Surface water courses and run-off flowing into the underground workings and through surface spoil deposits lead to metal leaching and direct erosion of metal rich materials, resulting in substantial dissolved and solid phase pollution of the downstream Afon Twymyn and Dyfi waterbodies.

The superimposition of multiple pollution pathways within short river reaches means that quantification of individual pollution source contributions is very difficult. A phased approach to intervention is therefore necessary, so that the effectiveness of each phase can be evaluated and taken into consideration before the next is suitably refined and implemented.

Pollution prevention through the managed conveyance of clean water, reducing infiltration to mine workings and metal rich spoil deposits is central to the management of most abandoned mine sites. It is also important that long term stable landforms created as part of remedial interventions are sympathetic to the rich heritage and diverse habitats typically present on metal mine sites such as Dylife.

Acknowledgements

This study is funded by the joint Metal (Non-Coal) Mine Programme of NRW and The Coal Authority sponsored by Welsh Government. We extend our thanks to Dr Nina Menichino, Team Leader, Evidence Portfolio, Programmes and Processes at NRW for supporting this paper.

References

Bick D (1985) Dylife A Famous Welsh Lead Mine. Revised Edition.

Simkin (2015) A Survey of Calaminarian Grassland in Mid Wales. Evidence Report No. 061.

Pryce Consultant Ecologists (2020) Dylife and Esgair Galed Metal Mines, Preliminary Ecological Appraisal

Parsons Brinckerhoff Limited (2005) Remedial Design of Former Metal Mines in Wales: Dylife Feasibility Report

URS Infrastructure & Environment UK Ltd (2012) Dylife Underground Workings Conceptual Model Development

AECOM Infrastructure & Environment UK Limited (2018) Dylife 2016 - 2017 Monitoring Rounds Interpretative Report

Coal Authority (2020) Dylife Metal Mine Remediation Feasibility Report

James DMD (2014) Metal Mining in Mid Wales 1822 – 1921. G.W.Hall. Welsh Mines and Mining No. 3. pp13

Margary H (1992) The Old Series Ordnance Survey Maps of England and Wales. Volume VI Wales

An Overview of Challenges Associated with Defining and Applying Water Quality Standards in the Absence of Applicable Regulatory Limits

Melanie Cox, David Tait, Robert Bowell, Ruth Griffiths

SRK Consulting (UK) Ltd, Cardiff, United Kingdom

Abstract

Water quality protection is a key guiding principle for responsible mining companies. This paper reviews challenges with identifying appropriate water quality standards for mining projects in various jurisdictions that lack comprehensive standards.

Baseline conditions and criteria for 'compliance' need to be defined before a risk assessment can be completed. However, the development of site-specific criteria can require extensive effort. Various internationally recognised standards are available, but these vary with respect to parameters and values. Stakeholder engagement is essential to develop a shared understanding with regulators and communities of the water quality objectives (what receptors need protecting and what are the risks) and how to achieve that compliance.

Keywords: Water Quality, Regulations, Environmental Protection, Mining

Introduction

Mining activities have the potential to impact water quality through modification of receiving water physciochemical conditions as well as concentrations of metal(loid)s (Nordstrom, 2011). Water quality impacts are a potential risk wherever geochemically reactive minerals are disturbed and subject to oxidation and leaching processes. Such impacts could cause harm to human health and/or environmental ecosystems and can occur at any stage during a mining project life cycle from exploration through to post-closure.

Mining companies are typically striving towards responsible mining and usually have a significant focus on environmental and social governance (ESG) and water stewardship. Water quality protection is therefore a key priority for many mining companies and is an important part of the social license to operate. As such, there is a drive to understand risks associated with the potential deterioration of water quality so that effective water management measures can be implemented to prevent, minimise or mitigate those risks.

This paper highlights some of the risks and challenges associated with establishing and applying water quality standards to mine site data. When a mine is located within a greenfield site, establishing and applying water quality standards can be particularly challenging if there is limited or no regional baseline monitoring, and if there are no pre-existing mines within the surrounding area and in regions where there is not a history of modern industrial scale mining.

Challenges and Considerations for Existing Water Quality Standards

There are a number of steps that should be considered when undertaking risk assessments for mine sites, and these often focus on the characterisation of the rock materials and the associated potential oxidation and weathering behaviour. However, it is key to identify early on whether there are applicable environmental standards, and if not, to develop a defensible approach to assigning water quality standards for the protection of the environment and all relevant stakeholders. These steps are outlined as follows.

Do water quality standards exist?

There are significant differences between the level of information available for the protection of surface waters and groundwaters across

different jurisdictions. In some cases, well-established thresholds and clear guidance exist. Conversely, there are a significant number of countries often with rich resources yet to be developed, where water quality standards have not been developed. Where standards are available, those standards may not be suitably protective of key receptors or may not meet the levels of protection that the mining company are required to meet by their own corporate standards. There are several considerations which should be made even where localised or national standards exist. These are discussed further below.

Who, what and where are the potential receptors?

Water quality standards typically include thresholds for industrial effluent discharges, thresholds for the protection of aquatic organisms within freshwaters or marine waters, drinking water standards for the protection of human health and agricultural limits for irrigation and livestock purposes. When reviewing any existing water quality standards in the context of a particular site, it is important to consider whether the standards are relevant to all potential receptors. It is possible that the standards are tailored towards a particular receptor, for example, there may be drinking water standards but no environmental quality standards for the protection of sensitive ecosystems, or generic industrial effluent discharge standards may not be relevant or adequately stringent to be protective of the receiving watercourses for domestic consumption or in remote pristine environments.

Identifying potential receptors is a critical task but may not be straightforward. It will likely require consultation with specialists responsible for undertaking baseline studies such as biodiversity or social baselines to obtain a clear understanding of who or what may be impacted by potential changes to water quality in the vicinity of the proposed mining project.

Are the existing standards suitable for use?

When existing standards are available it is important to interrogate the available information to ensure that the standards offer a suitable level of protection. The parameter suite should be reviewed to ensure that there are no missing key parameters which could pose a risk of impact to the receptors identified, particularly for parameters that may be affected by the planned activities. The threshold limits should be reviewed to ensure that they offer an appropriate level of protection to potential receptors. When reviewing threshold limits it is also necessary to consider if these are reasonable based upon existing water quality baseline data and what is realistically achievable by a suitable laboratory. Care should be given as to whether the guideline relates to total or dissolved concentrations. Comparison of in-country standards with common internationally recognised standards (such as WHO drinking water guideline values (WHO, 2022), Australian and New Zealand Guidelines for Fresh and Marine Water Quality (ANZECC, 2000), US EPA Aquatic Life Criteria (US EPA, 2022), or similar) can provide a useful comparison, although it should also be recognised that the values assigned within the various standards can vary over orders of magnitude for some parameters (discussed in Section 3).

Having an adequate water quality baseline is essential to assess any potential future impacts which might arise from mine development, operations or closure. Baseline monitoring data should ideally be representative of pre-mining conditions to accurately allow assessment of impacts from mining. Baseline solute concentrations may be naturally elevated in arid, highly mineralised areas and lower where precipitation is high, or bedrock has a high neutralising capacity for example. It may be necessary to distinguish the natural baseline from water quality data impacted by anthropogenic activities when deciding which standards to apply. For example, at Questa Project, New Mexico, US, it was proven that pre-mining baseline conditions were already elevated relative to standards which enabled site-specific standards to be negotiated with regulators (Nordstrom, 2008).

Surface water and groundwater quality baseline data should be spatially and temporally representative of the mining

project area. Sampling frequency should be sufficient to assess seasonal trends (ideally a minimum of monthly sampling for greater than one year).

Baseline sampling should include field measurements, laboratory analyses and appropriate quality assurance quality control (QA/QC) such as blanks, standards and duplicates. Laboratory detection limits must be sufficiently low to enable assessment against potential water quality standards. QAQC review should incorporate checks on trends that might indicate a bias or systematic analytical error to identify errors or anomalies. In addition to the QAQC review, the data should be suitably interrogated as part of the data interpretation to identify any trends or correlations which could assist in the application of water quality standards.

Consideration should be given to any localised physio-chemical changes, which might affect specific parameters such as changes to pH or water hardness and in turn may have implications for constituent toxicity. Baseline water quality data are also important for understanding whether certain parameters are naturally elevated in a particular area prior to mining, for example because of natural weathering of mineralised rock.

Where and how should compliance be assessed?

If suitable water quality standards exist, the next stage should be identifying where and how compliance should be assessed. The actual point of compliance should be specified and agreed upon with regulators. Will the standards be at the point of discharge ('end-of-pipe'), or should the evaluation be based upon maintaining or achieving a certain quality level within the receiving water? If the latter, dilution within the receiving water needs to be understood and factored in. For example where assessment is 'in-river', the compliance point is usually set at a location downstream of the discharge point to allow for mixing.

The frequency of monitoring should comply with regulatory requirements and consideration should be given to a risk-based monitoring approach where the frequency is adapted to site specific requirements. For example, more frequent monitoring could be undertaken at specific locations such as close to waste rock dumps or tailings storage facilities. It may also be necessary to alter the sampling frequency to accommodate localised weather conditions to account for important seasonal variations, such as first-flush events as dry seasons turn to wet seasons, following storm events or as snowmelt occurs and stream flows increase.

When assessing compliance with standards it is important to understand what represents a trigger where further immediate action should be undertaken. A good understanding of any applicable local regulations and a strong water management plan should inform decisions. It is possible that compliance is based upon an absolute limit but more often, compliance is percentile based. ANZECC (2000) specify that no action is required where 95% of data at a particular compliance point fall below guideline values.

Options in the Absence of Suitable Water Quality Standards

In the absence of existing water quality standards, the mine operator will need to decide how to address this issue and set appropriate standards that are protective of the environment and water users. There are two broad options to achieve this:

1. Using existing internationally recognised standards; or
2. Establishing new site-specific standards

Either option may be applied entirely where there are no existing standards or may be used selectively to target specific parameters that are not included for the in-country standards.

In some instances, even where mining projects decide to apply internationally recognised standards, it may also be necessary to develop site-specific standards where baseline conditions are elevated above the water quality standards.

Applying Internationally Recognised Standards

In the absence of a suitable dataset from which to derive site-specific standards, the most straight-forward option is to apply internationally recognised standards. There

are a wide range of internationally recognised standards to select, including International Finance Corporation Effluent Guidelines (IFC, 2007), WHO Drinking Water Guidelines (WHO, 2022), US EPA National Recommended Water Quality Criteria (US EPA, 2022), Canadian Council of Ministers of the Environment, Environmental Quality Standards (CCME, 2023), DWAF Water Quality Guidelines (DWAF 1996a,b), ANZECC Guidelines for Fresh and Marine Water Quality (ANZECC, 2000), EU Directive 2013/39/EU and the Initiative for Responsible Mining Water Quality Criteria (IRMA, 2018).

The standards all vary in the parameters included and the values applied, and where or how they are applied. Some standards are ecologically-based, some are human-health based, some apply as end-of-pipe, some are applicable within the receiving water after mixing has occurred. Figure 1 presents water quality standards for several parameters from multiple international guidelines and jurisdictions. This figure highlights the variability of the standards and emphasises that the challenge for a mining project becomes selecting which is the most appropriate standard to use.

It may not be sufficient to apply standards based upon similar geographical locations alone, particularly if receptors vary. Selecting the lowest internationally recognised standard may be the most conservative approach but could be inappropriate if baseline water quality is already at levels above these thresholds. Selecting the lowest criterion may also be overly conservative and lead to unnecessary requirements to manage, mitigate or treat water. Conversely, selecting the highest, most lenient thresholds may not offer a suitable level of protection.

IRMA (2018) is of particular note, as they have acknowledged the difficulty of the wide range of potential water quality standards that may be used and have aimed to address this by presenting a set of water quality criteria as a standardised approach for international mining. The standards set out in IRMA were compiled from internationally recognised sources, based on scientific evidence or from international agreement across a number of jurisdictions.

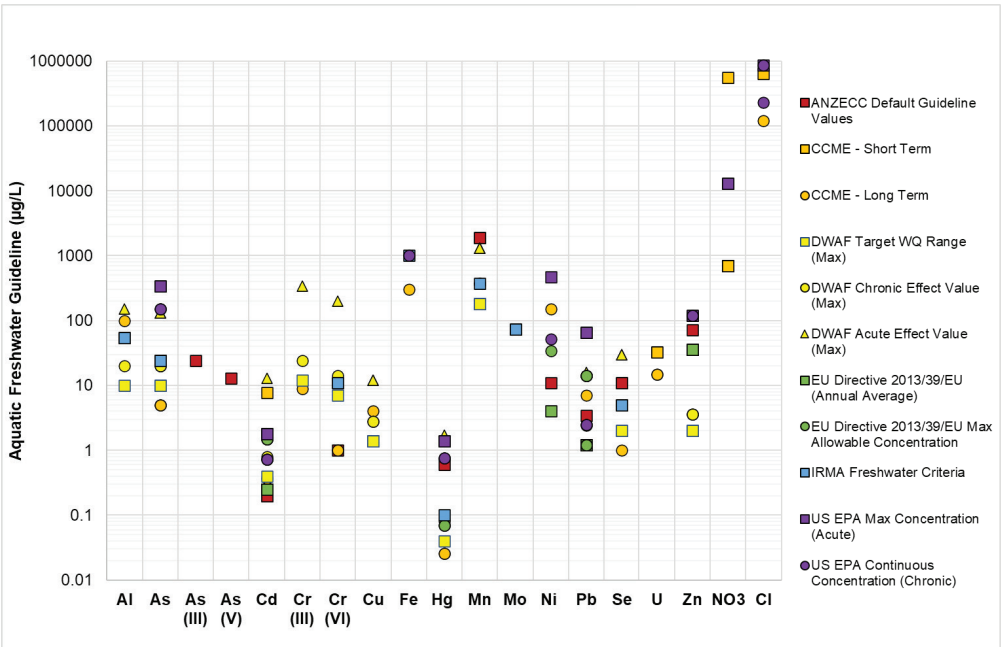


Figure 1 *Summary of Internationally Recognised Standards for Key Parameters (Freshwater Aquatic Ecosystems)*[1]

Water quality standards are also updated as new information becomes available. For example, WHO (2017) reported an aesthetic drinking water standard for manganese of 0.1 mg/L and a health-based standard of 0.4 mg/L. However, because the health-based standard was greater than the aesthetic standard, the health-based guideline was not presented. In WHO (2022) the health-based standard was subsequently reduced to 0.08 mg/L.

Existing water quality standards applied to a mining project should be periodically reviewed to ensure they are current and up to date. As the above example shows, it is possible that water quality standards could decrease through the course of a mining project life cycle which has the potential to affect compliance. In this instance, regulator liaison would be essential to establish a resolution.

Developing or Adapting Site-Specific Water Quality Standards

The second option available is to develop site-specific standards. These can be developed where appropriate standards are absent, or at sites where the standards may not be appropriate (for example due to an elevated baseline). In some jurisdictions, developing site-specific thresholds is encouraged. ANZECC (2000) recommends using default guideline values (DGVs) as a generic starting point for assessing water quality only in the absence of more relevant local jurisdiction standards or site-specific standards. The US EPA (2022) has established national water quality standards, but localised standards also exist for several states, for example Idaho, Alaska, Nevada, New Mexico, North and South Carolina. On the other hand, throughout Europe, all EU Member States are required to adopt the Water Framework Directive (WFD) Environmental Quality Standards (EQS) which cover a wide range of parameters, although the WFD also allows member states to set their own standards for some parameters where this can be justified.

Setting and agreeing to site-specific water quality standards is a challenging and highly variable process. As detailed above, existing internationally recognised standards sometimes show significant differences. For example van Dam et al., (2019) states that a lack of clear guidance for developing site-specific standards often leads to under-estimating or over-estimating limits which can result in unintentional environmental impacts or unnecessary costly management measures. Establishing new site-specific standards is also an extremely long and data intensive process which often takes a significant investment of time and money, so isn't necessarily the most practical option – hence another benefit to the use of internationally recognised standards is that they are immediately available. When generating site-specific standards engaging with regulators and relevant stakeholders at the earliest opportunity is key. It is important to ensure that the process followed is transparent and defensible. Any guideline levels established should offer an appropriate level of protection whilst remaining realistic in terms of natural baseline levels and achievable detection limits. ANZECC (2000) provides guidance for developing guideline values using a pressure-stressor-ecosystem receptor (PSER) causal pathway. The ANZECC recommended approach uses local baseline data to determine thresholds around the 80th percentile, or lower if there is a need to apply a more precautionary approach. According to ANZECC (2000) site-specific thresholds should be based on at least two years of monthly monitoring data from suitably representative unimpacted water bodies. Seasonal variations should be included, and it may be appropriate to set limits specifically for wet or dry seasons or high and low flows.

The Department of Water Affairs and Forestry (DWAF), South Africa, also provides options to modify water quality standards in accordance with very specific criteria. DWAF require adequate site-specific data for at least one annual hydrological cycle and site-specific studies including toxicity tests for at least three locally significant species confirming that any modifications offer the same level of protection to aquatic organisms.

Engaging in Discussions with Regulators and Stakeholders

Early engagement with regulators and stakeholders is crucial to the successful implementation of any water management

plan. Identification of receptors is key, and this process should involve stakeholders and regulators from the outset. The process of agreeing and establishing water quality standards should include ongoing discussions and workshops with regulators and stakeholders to ensure that there is a defensible and transparent approach. Regulator and stakeholder engagement is particularly important in the event of needing to amend existing water quality standards or generate entirely new site-specific standards. DWAF (1996b) states that modifications to standards should only be considered under expert advice.

It is possible that regulators and/or stakeholders may not have much familiarity or experience with potential impacts associated with mining activities. In this instance, it is even more important to engage with regulators early in the process to identify key competencies and strengths. An open dialogue will ensure that all parties are confident and comfortable with the proposed approach.

Conclusions

Mining has the potential to create changes in baseline water quality and where there is a risk of acidity generation or solute leaching this can lead to an increase in constituent concentrations. Understanding potential risks is a key priority for operators as part of their ESG policy. Early identification of appropriate water quality standards is crucial to understanding and mitigating risks posed to key receptors, but the approach of establishing water quality standards can be complex where suitable standards are not available. Even if standards exist for the jurisdiction where the mine will be located, there can still be challenges which need to be considered, such as whether the standards offer sufficient protection to receptors, how standards compare to existing baseline data and how standards should be implemented, where compliance should be measured and what triggers a failure. The absence of relevant water quality standards presents a bigger challenge. Operators are faced with a decision to implement internationally recognised standards or go through the often long and expensive process of establishing site-specific standards. The large variances seen between international standards highlights the difficulties faced when deciding what to apply.

Regulators and stakeholder inputs will ultimately determine if and when mining permits are approved. Early engagement is therefore crucial especially when the proposed approach involves any deviation from existing water quality standards. A transparent approach of regular ongoing discussions can help ensure the success of the implementation process.

References

ANZECC (2000), Australian and New Zealand Guidelines for Fresh and Marine Water Quality, Australian and New Zealand Environment and Conservation Council and Agriculture and Resource Management Council of Australia and New Zealand, Canberra.

CCME (2023), Canadian Council of Ministers of the Environment (CCME) Environmental Quality Guidelines.

DWAF (1996a) Department of Water Affairs and Forestry, 1996. South African Water Quality Guidelines (second edition). Volume 1: Domestic Use.

DWAF (1996b) Department of Water Affairs and Forestry, 1996. South African Water Quality Guidelines. Volume 7: Aquatic Ecosystems.

EU Directive 2013/39/EU. Directive 2013/39/EU of the European Parliament and of the Council of 12 August 2013 amending Directives 2000/60/EC and 2008/105/EC as regards priority substances in the field of water policy.

IFC (2007) International Finance Corporation Environmental, Health and Safety Guidelines, Mining, Effluent Standards, December 10, 2007.

IRMA (2018). The Initiative for Responsible Mining Assurance, Water Quality Criteria by End-Use Tables, IRMA Standard v1.0, June 2018.

Nordstrom, DK (2008). What was the groundwater quality before mining in a mineralized region?

Lessons from the Questa Project. Geosciences Journal, Vol 12, No. 2, p 139-149, June 2008.

Nordstrom, D.K., (2011), Hydrogeochemical processes governing the origin, transport, and fate of major and trace elements from mine wastes and mineralized rock to surface waters. Applied Geochemistry, v. 26, p. 1777-1791.

US EPA (2022), National Recommended Water Quality Criteria – Aquatic Life Criteria Table, US Environmental Protection Agency. Last Updated September 15, 2022. Available at: National Recommended Water Quality Criteria - Aquatic Life Criteria Table | US EPA (Accessed 26 April 2023).

van Dam RA, Hogan AC, Humphrey CL & Harford AJ (2019), How specific is site-specific? A review and guidance for selecting and evaluating approaches for deriving local water quality benchmarks, Integrated Environmental Assessment and Management 15: 683–702.

WHO (2017), World Health Organisation, Guidelines for Drinking Water Quality, Fourth edition incorporating the first addendum.

WHO (2022), World Health Organisation, Guidelines for Drinking Water Quality, Fourth Edition incorporating the first and second addendum.

Optimising Circum-Neutral Mine Drainage Treatment By Implementing High Shear Degassing Into A Sustainable Active Treatment System

Julia Dent[1], Steven Pearce[1], Rhys Savage[1], James Marsden[1], Ryan Schultz[1], Tom Williams2, Peter Stanley[2], Mark Roberts[3], Andrew Barnes[3], Ben Gersten[3]

[1]*Cambrian Environmental Technologies Ltd, Wales, United Kingdom, jdent@memconsultants.co.uk,*

[2]*Natural Resources Wales, Wales, United Kingdom, geowyddor@cyfoethnaturiolcymru.gov.uk*

[3]*Geochemic Ltd, Wales, UK, abarnes@geochemic.co.uk*

Abstract

An alternative approach to treat circum-neutral metal mine drainage is being trialled using a degassing step within a sustainable active treatment (SAT) system. Typical discharges from Welsh metal mines have high dissolved CO_2 content and elevated alkalinity due to unique REDOX conditions. Although mine water has elevated alkalinity the pH is typically <7 upon discharge, keeping metals like Zn in solution. Degassing CO_2 raises the pH to >8.2, enabling metal removal by precipitating hydroxides or by sorbing to iron oxides. Degassing CO_2 is considered a potentially more sustainable, lower carbon and chemical-free method of removing metals from solution.

Keywords: Water treatment, CO_2 degassing, lead, zinc, mine drainage

Introduction

The removal and potential recovery of metals from circum-neutral mine drainage is a challenge, particularly in locations such as Wales where many historical mine discharges exist in remote areas. Metals such as Zn and Pb typically require a high pH (>8) to immobilise the soluble phase by precipitation/sorption, which is beyond the range achievable in many passive systems. Even if passive systems can be installed metal recovery can be difficult, and long-term performance is subject to uncertainty. Active treatment such as high-density sludge (HDS) is considered the only viable solution in many cases.

The approach taken within this study was to utilise well-established scientific principles used in passive water treatment, such as aeration and sorption, and integrate them into SAT to create an effective water treatment process for metal-contaminated circum-neutral mine water. This approach allows for cost-effective treatment of difficult to treat waters (circum-neutral with high Zn and Pb concentrations) and provides an opportunity to recover and reuse or resell metals from the treated water to potentially offset legacy site management.

Aeration is recognised as an opportunity in mine water treatment due to the effect of oxidation state on metal mobility. Dissolved gases such as CO2 also affect the carbonate system and ultimately solution pH, which in turn can be used for metal mobility manipulation (Marsden *et al*. 2021). Underground mine drainage waters are typically reducing and low in oxygen, and may be supersaturated with carbon dioxide due to reactions with host rocks such as limestone or by the oxidation of available organic carbon (Geroni *et al*. 2012). In Wales many circum-neutral mine waters are located in carbonate-rich host rock (Warrender and Pearce 2007), and thus circum-neutral mine waters may be affected by increased dissolved carbon dioxide. Previous studies on the aeration of mine drainage within treatment systems have shown that the chemistry of the mine water can be altered. The pH can rise by increasing the dissolved oxygen (DO) concentration as well as degassing of dissolved carbon dioxide (Kirby *et al*. 2009).

The use of the Maelgwyn Mineral Services (MMS) Aachen High Shear Reactor technology (fig. 1), more commonly used to enhance gold and silver leach kinetics through

supersaturation of oxygen into slurry and mass transfer, has allowed for efficient aeration and degassing in a smaller physical area which is used to alter the pH of circum-neutral mine water. The theory of degassing circum-neutral mine water has been tested on a circum-neutral discharge from the abandoned Nant y Mwyn Pb-Zn mine in Mid Wales.

The degassing methodology at beaker trial level was also repeated on four additional samples of circum-neutral mine drainage waters from four separate Pb/Zn mines in Wales.

Site Background

Nant y Mwyn Mine is located in the village of Rhandirmwyn, 10 km north of Llandovery, Carmarthenshire. Underground workings and extensive spoil heaps are major sources of metals pollution to downstream watercourses, causing the River Tywi to fail Water Framework Directive (WFD) standards for Zn for approximately 25 km. A river system review (Coal Authority 2020) identified that clean-up at Nant y Mwyn would singularly benefit the failing waterbodies downstream, with no other major sources of metals pollution in the catchment.

The mine is geographically split into two sites, the Upper Boat Level (Nant y Bai tributary) and the Lower Boat Level (Nant y Mwyn tributary). The portal of the Lower Boat Level drainage adit is blocked and water discharges from the crown hole of an air shaft in-bye of the blockage. This mine water enters Church Terrace Tributary before joining the Nant y Mwyn and subsequently the River Tywi.



Figure 1 *Aachen reactor cartridge that introduces gas under pressure to generate fine gas bubbles*

Initial degassing tests

In 2021 water samples were collected from the Lower Boat Level discharge for beaker trials and a laboratory scale trial of the Aachen High Shear Reactor to assess the feasibility of degassing mine water to adjust pH as part of a larger treatment system. Field measurements taken at the site at a later sampling date (autumn 2022) (Table 1) show the effect of natural degassing from the shaft discharge, down the stream to the flow gauging station weir, and further downstream in the Church Terrace Tributary. The overall elevation change is approximately 6 metres. Small increases in DO and pH are seen from natural degassing downstream.

The mine water samples were taken to Geochemic Ltd (Geochemic) laboratory for the treatability study. Active aeration, by sparging the raw mine water sample with air, was completed at beaker scale and the pH of the solution recorded during this process. The test gives an indication of the expected pH change following loss of volatiles that are not in equilibrium with the atmosphere (such as the degassing of CO2 and SO2 gasses). The resultant pH increase during the initial degassing beaker trial is shown in Fig. 2, which overall showed a pH increase of 1.3 units.

In summer 2021 a larger sample (c.500 L) of Nant y Mwyn mine water was collected using submersible pumps directly from the shaft discharge. This was transported to Geochemic Ltd laboratory for use in a trial of the Aachen High Shear Reactor for degassing of the raw mine water. The tank capacity of the Aachen was 100 L, the liquid flow 1,540 L/hr and the air flow rate set as 20 Ln/min. Time was recorded and this was combined with the water and airflow rates were used to calculate the number of passes through the Aachen, where a pass indicates a full circulation of the Aachen system. Data is typically presented as a pass through the system rather than by time. The pH results from the initial trial of the Aachen system on Nant y Mwyn raw mine water are shown in Fig. 3. The pH was successfully increased from an initial pH 6.7 to pH 8.3, which is the targeted pH for Zn removal.

Table 1 Field measurements at Nant y Mwyn indicating variation due to distance from adit and potential degassing.

Parameter	Unit	Nant y Mwyn – LB1 at shaft pool	Nant y Mwyn at weir	Nant y Mwyn in stream edge of the property	Nant y Mwyn – water pumped through pipe during collection
Date-time	-	14/09/22 – 11:30	14/09/22 – 11:33	14/09/22 – 11:35	14/09/22 – 13:30
Temperature	°C	10.2	10.3	10.3	13.5
Dissolved oxygen	%	34	38	50	40
Specific conductivity	µS/cm	301	300	300	301
pH	s.u.	6.6	6.4	6.6	6.8
ORP	mV	230	211	186	172

Extended beaker trials

Following the success of degassing the water from Nant y Mwyn a further set of samples were gathered from potentially suitable abandoned mine site discharges in Mid Wales. These included Nant y Mwyn (lower boat level), Level Fawr, Pugh's Adit (Cwmystwyth), Frongoch and Van Mine (fig. 4). The samples were collected in autumn 2022 after a relatively dry summer, with most of England and Wales being under drought conditions. As such, it can be expected that the flow rates were at the lower end of the range experienced at the sites.

The raw mine water was used to complete aeration and adsorption beaker trials by Geochemic's laboratory to test the potential treatability of each mine water by the degassing process. The pH of the mine water samples was continuously monitored whilst the sample was degassed using air sparging. The aim of this aeration step is to allow CO_2 dissolved in the water to be released as gas, raising the pH. The change in pH of the degassing stage are shown in Fig. 5. The pH of all mine water samples increased, but the range of increase varied. Pugh's Adit and the Van Mine duplicate pH increased the least, at around 0.3 pH

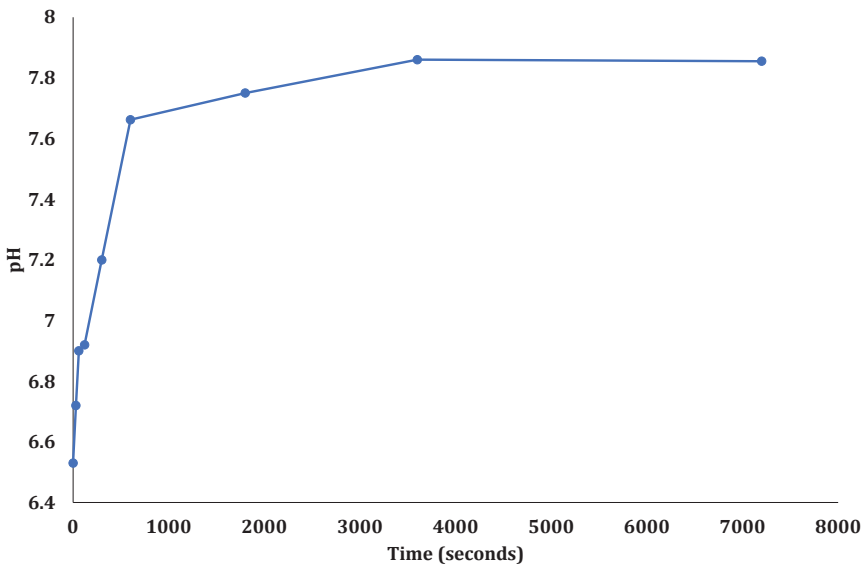


Figure 2 Initial pH change following the beaker degassing test on Nant y Mwyn mine water.

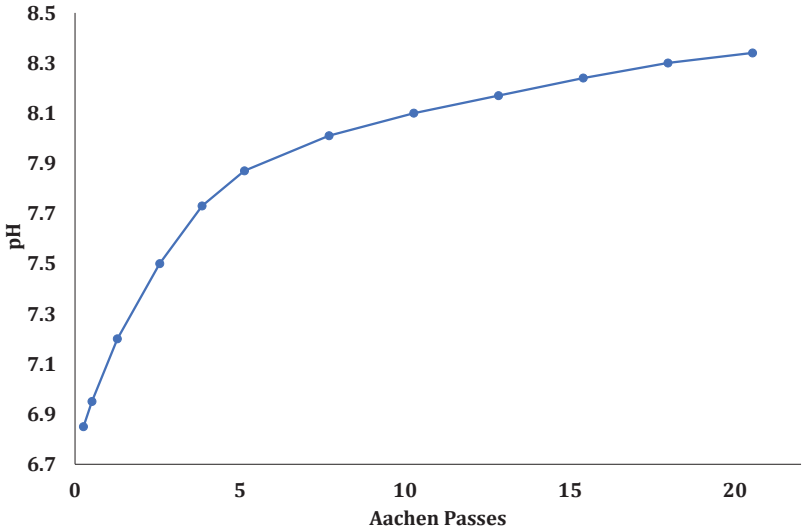


Figure 3 *Initial laboratory trial of degassing Nant y Mwyn mine water using the Aachen High Shear Reactor*

units, however the second Van Mine sample increased by 0.6 pH units. The pH increase at Frongoch and Level Fawr was much greater at 1.3 and 1.5 pH units respectively. This is equivalent to the 1.3 pH units achieved in the original Nant y Mwyn degassing beaker trial. Frongoch, Level Fawr and Nant y Mwyn only showed an increase in pH following commencement of degassing, however, Van Mine and Pugh's Adit both showed a dip in the pH before it then began to increase. It is believed that this dip could be related to latent acidity due to oxidation of reduced iron and/or sulfur species in the mine water.

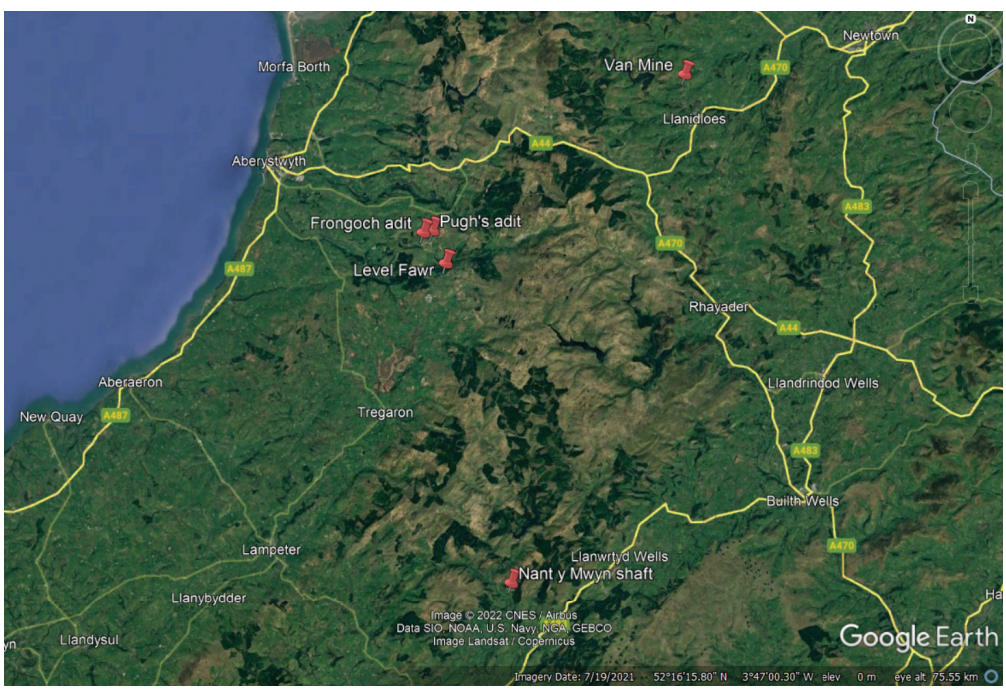


Figure 4 *Location of mine discharges where water was collected for the beaker trials (Google Earth)*

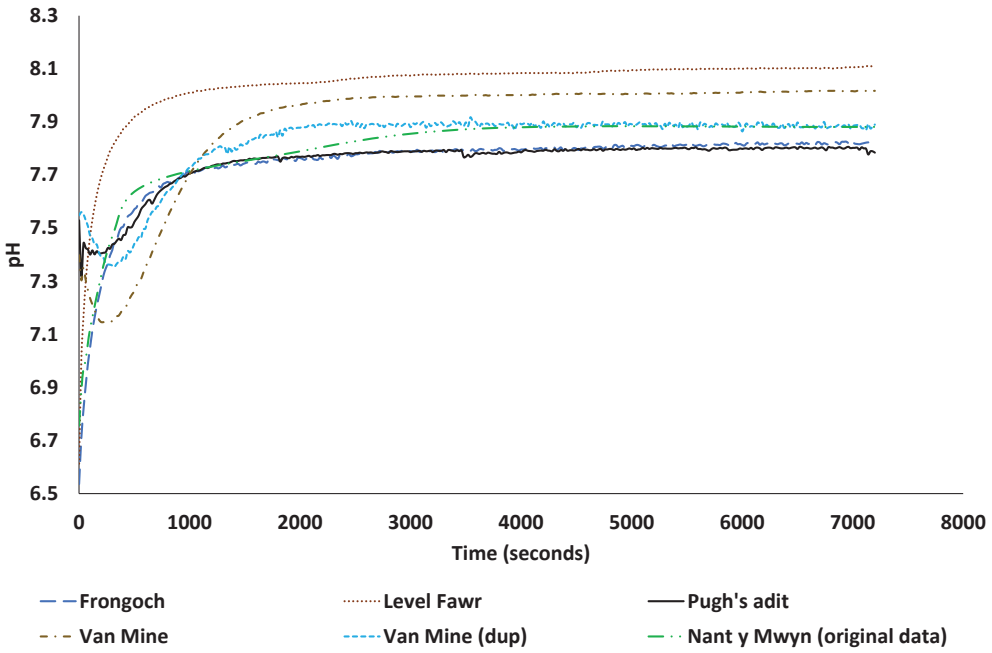


Figure 5 *pH increase in different mine waters following degassing.*

The second part of the beaker trials was to test the effect of adding FeOx as an adsorbent at 10 g/L to the degassed mine water. The metal removal rates are shown in Fig. 6. Following the adsorption step 100% of Pb was removed from all sites other than Van, where 72% of Pb was removed. Level Fawr showed the highest removal rate of Zn at 98% (the final concentration was 40 µg/L), followed by 85% in the Van mine water (the final concentration was 415 µg/L). Nant y Mwyn Zn removal was at around 60%, which is similar to the initial beaker trial results (remaining concentration 6,072 µg/L). Frongoch and Pugh's Adit showed lower Zn removal rates, only 45% and 38% respectively, relating to concentrations of 9,800 and 16,670 µg/L respectively. Cd was removed by over 50% in all the mine waters, and up to 90% in Level Fawr. Cu was also successfully removed in all mine waters where it was present. Co was removed in some mine waters (Level Fawr and Nant y Mwyn) but concentrations remained similar in the others. Mn was removed from Frongoch, Pugh's Adit and Van Mine waters, but not from Nant y Mwyn.

The metal removal rate for Zn, the target metal, was very high where the initial concentrations are lower (Level Fawr and Van Mine). As such, the removal rate from Frongoch, Pugh's Adit and Nant y Mwyn is likely limited by the amount of FeOx added during the beaker trials. A higher amount would be expected to increase removal rates, increasing the efficiency of Zn removal. Overall, there is metal removal recorded at all sites (fig. 6), suggesting this system could be adapted to work at all sites tested during this assessment.

Conclusions

The results presented outline the potential efficacy of incorporating active aeration steps into a SAT system for manipulating pH in circum-neutral mine water to better allow precipitation or sorption of targeted metal species removal, such as Zn, Pb and Cd. A similar pH increase was successfully achieved in all four mine waters tested, confirming the approach may have wider applications and is not restricted to the original study site.

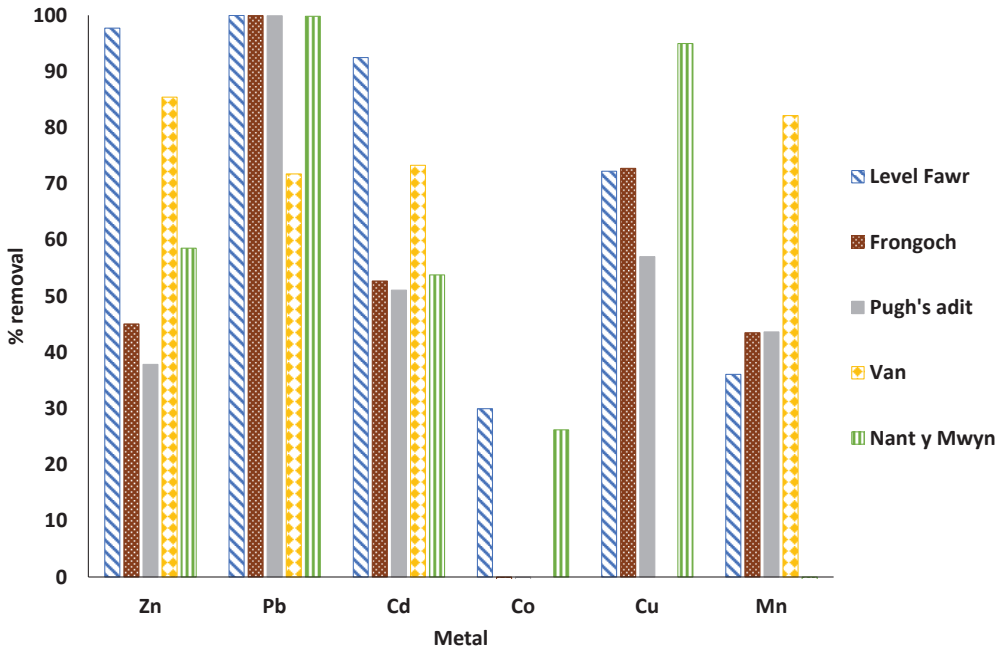


Figure 6 Metal removal in mine water discharges following degassing and FeOx treatment.

The environmental and economic value of incorporating a degassing step into a SAT system provides a more sustainable, lower carbon and chemical-free alternative to HDS systems.

Acknowledgements

This study is funded by the joint Metal (Non-Coal) Mine Programme of NRW and the Coal Authority sponsored by Welsh Government. We extend our thanks to Dr Nina Menichino, Team Leader, Evidence Portfolio, Programmes and Processes at NRW for supporting this paper.

References

Coal Authority (2020) Metal Mine Failing Waterbodies Assessment. – Overview Report OP16-154/F13/0.

Geroni JN, Cravotta III CA, Sapsford DJ (2012) Evolution of the chemistry of Fe bearing waters during CO_2 degassing. Applied Geochemistry 27 (2012) 2335-2347.

Kirby CS, Dennis A, Kahler A (2009) Aeration to degas CO_2 increase pH, and increase iron oxidation rates for efficient treatment of net alkaline mine drainage. Applied Geochemistry 24 (2009) 1175-1184.

Marsden J, Pearce S, Sambrook T, Dent J, Barnes A (2021) Site specific optimisation assessment of cirucm-neutral water treatment using a cost-treatability curve assessment. IMWA 2021 Proceedings: Mine Water Management for Future Generations (2021) 334–339.

Warrander R, Pearce NJG (2007) Remediation of circum-neutral, low-iron waters by permeable reactive media. IMWA Symposium 2007: Water in Mining Environments, 27–31 May, 2007, Cagliari, Italy.

Review Of Laboratory Methodologies To Determine The Sorption And Release Of Metals Related To The Interaction Of Mine Drainage Water With Natural Media (Peat, Till And Bedrock). A Case Study From A Base Metal Mine In Arctic Finland.

Julia Dent[1], Steven Pearce[1], Seth Mueller[2], Andrew Barnes[3], Mark Roberts[3], Claudia Malam[1]

[1]*Mine Environment Management, Wales, UK, jdent@memconsultants.co.uk,*

[2]*Boliden, Sweden, seth.mueller@boliden.com*

[3]*Geochemic Ltd, Wales, UK, mroberts@geochemic.co.uk,*

Abstract

Mine waste storage facility seepage may be a groundwater contamination source. Contamination transport in the sub-surface is influenced by adsorption and/or exchange of metals from soil and rock surfaces. The quantitative determination of metal adsorption and exchange using laboratory testing is complex and site-specific. This study considered methods including partition coefficients (K_d), upflow columns and batch tests to assess the long-term sorption/exchange behaviour in peat, till and bedrock at an Arctic Finnish base metal mine. Upflow columns provided empirical data to calculate sorption/release factors for input to contaminant transport models, potentially more representative information than Kd or batch tests methodology.

Keywords: Sorption, Contaminant transport, Mine waste, Ion exchange, K_d

Introduction

Seepage draining to ground from mine waste and tailings facilities may lead to metal rich mine drainage entering ground and surface waters. Prediction of this seepage quality, and the ultimate water chemistry following mixing with ground and surface waters is common, but the effect of adsorption or exchange on soil and rock surfaces along the flowpath on the downstream water quality may be missing or assumed to be nil for a conservative estimate. Deriving appropriate sorption or exchange characteristics can be difficult unless site specific data is available as numerous surfaces affect sorption or exchange reactions such as clays, metal oxides and hydroxides (particularly iron species), metal carbonates, phosphates and organic colloidal matter (Bradl 2004). Key variables controlling sorption and exchange include soil type, metal speciation, element concentrations, soil and water pH, liquid: solid mass (L:S) ratios and contact times.

This study looked at analytical options for deriving site-specific sorption or exchange data for a base metal mine in Arctic Finland. Ni and Co are the key metals of interest at this site, as high concentrations of Ni are seen in seepage water from mine waste and tailings, but elevated Co seen in potential downgradient water bodies. Underlying the mine waste and tailings facilities are a mixture of peat soils, till/moraine and weathered bedrock, each with noticeably different potential sorption and exchange capacities. Partition coefficient (Kd) tests were completed on a range of sub-surface samples from the site. These tests are completed on relatively small sample sizes and are short duration. Additional batch and column tests were also completed on samples to better understand the mechanism and sorption capacity. All sub-surface samples were collected using drilling and trial pitting methods at the site and maintained in as close to in-situ conditions as possible prior to analysis, completed at Geochemic Ltd, Pontypool.

K_d tests

The partition coefficient (K_d) is a descriptor of the distribution of a species between a solid and aqueous phase after equilibrium. In groundwater assessments it represents the overall sorption of a specific species in liquid to the contact geological material. K_d is a critical parameter for modelling the potential retardation of specific solutes in geological materials.

The British Geological Survey (BGS) (BGS 2000) and Environment Agency of England and Wales (EA) (EA 2005) established an industry method for Kd testing. This method uses a known mass of geological material in a vessel with synthetic groundwater. The groundwater-geological material mix is left to equilibrate for 72 hours. A leachate containing the contaminant of interest is added to the mixture and equilibrated for 48 hours. The mass of contaminant added and the remaining contaminant in solution is used to calculate Kd using the following (where I = initial concentration (mg/L), F = final concentration (mg/L), V = liquid volume (l) and M = solid mass (kg):

$$K_d = \left(\frac{I - F}{F}\right) \times \left(\frac{V}{M}\right)$$

The studies main parameters of interest were Ni and Co, and the typical ranges found in the tailings storage facility (TSF) and waste rock storage facility (WRSF) seepage were used as the basis for the initial concentration. The concentration range for Ni was 1 mg/L – 10 mg/L, and for Co 0.1 mg/L – 1 mg/L. The synthetic groundwater was also based on site baseline measurements. The material used in the Kd testing included:

- Peat from the WSRF area and TSF area
- Weathered bedrock (as weathered bedrock coatings, likely metal oxides/ hydroxides) from the WRSF
- Glacial till from the TSF area

A number of rounds of testing were completed aiming to provide validated results based on the standard method. The initial L:S ratio used for the peat samples was 25:1 and for the weathered bedrock coatings 5:1. For accurate Kd results the percentage of the contaminant absorbed within a test should be between 25–75% but the initial results for both the weathered bedrock and peat showed very high adsorption (> 95%). The sorption capacity was not reached so the results of the first round do not provide accurate assessment of the K_d value, limiting the results. In subsequent testing rounds on the same materials, and also the TSF till and WRSF peat, higher L:S ratios were used aiming to reach sorption capacity. The concentration of the simulated seepage was also increased to aid in reaching sorption capacity. Overall, 33 K_d tests were completed and only five were considered valid based on the standard methodology (Table 1).

The results for K_d are high, suggesting that Ni and Co are strongly adsorbed onto the material, and mobility of these elements from the material will be lower. These high values likely reflect the high organic carbon content of the peat and the high iron hydroxide content of the weathered bedrock coatings.

The WRSF peat material has a K_d for Ni ranging between 2992–611 L/kg, the TSF peat material 504–0817 L/kg, the TSF till 351–1052 L/kg and the WRSF weathered bedrock coatings 135–1430 L/kg. As the weathered bedrock coatings would need to be normalised to account for the bulk weathered bedrock mass and surface area, the peat appears to have a much higher and the till somewhat higher K_d and Ni will be adsorbed to the peat at a stronger level than the weathered bedrock. The WRSF peat material Co Kd ranges between 2582–4355 L/kg, for the TSF peat 103–26340 L/kg, for the TSF till 1195–4078 L/kg, and for the weathered bedrock coatings 452–6582 L/kg. The variation between the K_d is less distinct in rounds 1 between peat, till and the weathered bedrock coatings for Co, but the Co appears to be more mobile than Ni. However, in rounds 2, 3 and 4 the K_d is much higher and also higher than the Ni range, which contradicts the results from round 1 as it suggests that Co has a stronger affinity for the peat than Ni. However, it should be noted that no results from the peat material gave results within the method validity range (based on percentage adsorption). The variation could be linked to the variable L:S ratios and the difference between the spiked concentration of contaminant used and the final K_d calculated. The methodology

also assumes material can be easily milled or pulped, which was not possible on peat samples and thus the inherent heterogeneity of the peat is likely to be exacerbated by the low masses required. As a reference the Kd range for Pb on a Cornish siltstone sample was calculated between 37–318 L/kg on spiked Pb concentrations between 10–100 mg/L (EA 2005).

The overall K_d ranges are relatively similar between the two parameters, however the K_d does appear to be limited by the initial concentration, as K_d increases as the initial concentration increases. This is also the case for L:S ratios as they increase the K_d increases. The value of K_d is sensitive to small changes in solute concentration if the ratio of the final/initial concentrations is small, which occurs when the Kd for a material type is high and to derive a result a higher L:S ratio is needed. As the L:S ratio increases this typically increases the error within the Kd measurement (BGS 2000).

Peat material typically has much higher K_d values than weathered bedrock coatings or till, which can be expected by the nature of the material as peat has high organic carbon content compared with the other material.

Table 1 *K_d test results – rounds 1 to 4.*

Round of Testing	Sample	L:S Ratio	Contaminant (mg/L)	I (mg/L)	F (mg/L)	V (L)	M (kg	Kd (L/kg)	% Adsorbed
Round 1	WRSF peat	25:1	Ni 10	10.03	0.033	0.025	0.001	7611	100
			Ni 1	0.72	0.006	0.025	0.001	2992	99
			Co 1	1.21	0.007	0.025	0.001	4355	99
			Co 0.1	0.12	0.001	0.025	0.001	2582	99
	TSF peat	25:1	Ni 10	10.5	0.132	0.025	0.001	1959	99
			Ni 1	0.75	0.035	0.025	0.001	504	95
			Co 1	1.25	0.032	0.025	0.001	948	97
			Co 0.1	0.12	0.023	0.025	0.001	103	81
	WRSF Bedrock	5:1	Ni 10	12.21	0.058	0.025	0.005	1044	100
			Ni 1	0.67	0.024	0.025	0.005	135	96
			Co 1	1.14	0.003	0.025	0.005	1818	100
			Co 0.1	0.14	0.002	0.025	0.005	452	99
Round 2	WRSF Bedrock	50:1	Ni 10	5	0.181	0.025	0.0005	1430	97
			Co 1	1	0.016	0.025	0.0005	3052	98
		100:1	Ni 10	5	0.407	0.025	0.00025	1217	92
			Co 1	1	0.015	0.025	0.00025	6582	99
	TSF Peat	125:1	Ni 10	5	0.081	0.025	0.0002	8113	98
			Co 1	1	0.012	0.025	0.0002	9961	99
		250:1	Ni 10	5	0.121	0.025	0.0001	10817	98
			Co 1	1	0.019	0.025	0.0001	12443	98
	TSF Till	25:1	Ni 10	5	0.188	0.025	0.001	687	96
			Co 1	1	0.02	0.025	0.001	1195	98
		100:1	Ni 10	5	0.465	0.025	0.00025	1052	91
			Co 1	1	0.046	0.025	0.00025	2012	95
Round 3	WRSF bedrock	500:1	Ni 20 *	22	10.65	0.25	0.0005	510	50
			Co 2 *	2	0.863	0.25	0.0005	716	59
	TSF peat	1000:1	Ni 20 *	22	8.86	0.25	0.00025	1429	59
			Co 2	2	0.219	0.25	0.00025	8580	90
	TSF Till	250:1	Ni 20 *	22	8.94	0.25	0.001	351	58
			Co 2	2	0.339	0.25	0.001	1299	84
Round 4 (Average Repeats)	TSF peat	2000:1	Ni 20 *	20	8.63	0.25	0.00025	1358	58
			Co 2	2	0.168	0.5	0.00025	26340	93
	TSF Till	500:1	Co 2	2	0.26	0.25	0.0005	4078	89

* Denotes result valid according to methodology.

The till tends to show lower affinity for the Ni and Co, however, if the weathered bedrock is normalized for original sample surface area and mass then this is not the case when Ni is the contaminant.

Alternative methods: batch tests

An alternative method for assessing sorption and exchange mechanisms was assessed using batch leaching tests with spikes of key species (such as Cl, SO_4 and Na). The tests were completed on one sample of peat from the TSF area to determine sorption mechanisms and key controls and the effect on the key metals Co and Ni. The spiked desorption tests used the following desorbents: $CaCl_2$, KCl, $MgCl_2$, Na_2HPO_4 and Na_2SO_4. The desorbents were leached at 2 different concentrations, one high (1M) and one low (0.1M). The aim of the batch leach tests was to leach a sample of the peat at a liquid to solid ratio of 20:1. An equivalent dry mass of the peat sample (10 g) was used and 167 ml of each desorbent solution added, which made a total volume of 200 ml with the original pore water. The original volume and chemistry of pore water and the lixiviant was estimated to allow the calculation of net mass release or adsorption in the final leachate produced. The mixture was allowed to equilibrate, before the liquid and solid were separated and the resulting leached solution analysed for cations and metals. A blank deionized water was also analysed as a QA/QC measure.

Ca is net adsorbed and the pre-lixiviant concentration is higher than the post-leachate (net release is negative). Mg shows a similar trend to Ca, for most desorbents types there is net release of Mg. However, when Mg is the desorbent there is net absorption. For K and Na, the cations are typically net released when the desorbent does not contain the cation being measured, but the net release rates are much lower than for Mg

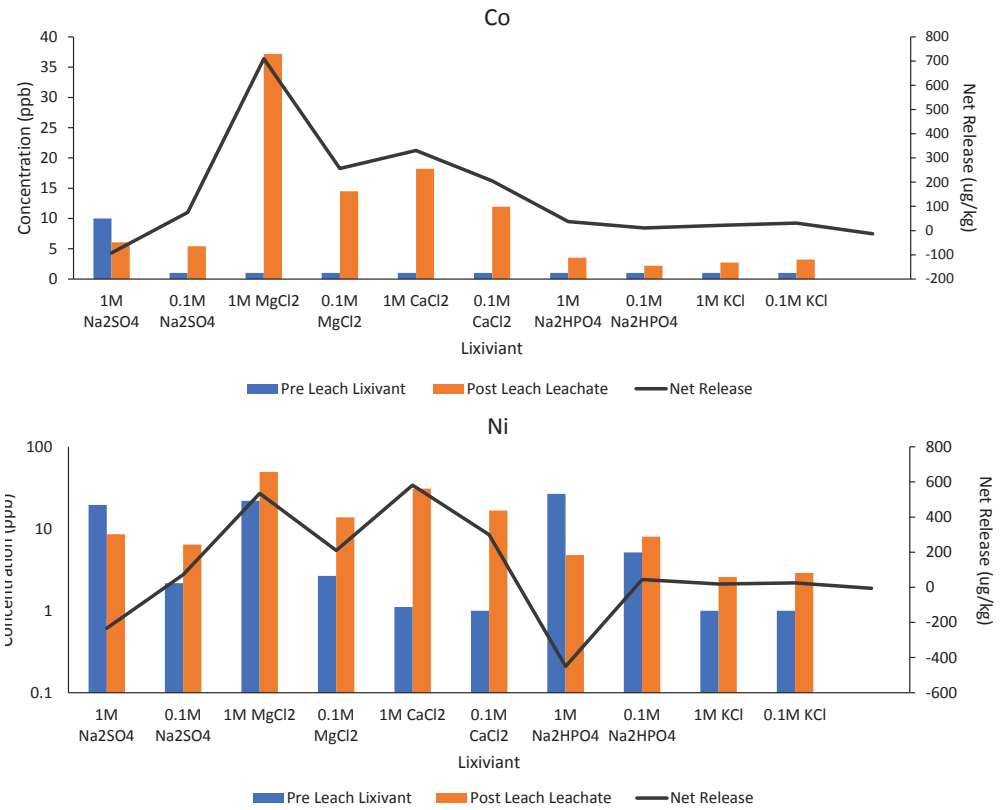


Figure 1 *Co and Ni results in pre-leach lixiviant and post-leach leachate in the batch tests.*

and Ca. When the desorbent contains either K or Na the net release rate tends to be highly negative. The behaviour of sodium in relation to sorption and desorption of other elements is important due to the high concentration of Na in tailings leachate. The sorption preference for these cations appears to be Na > K > Mg > Ca.

The results for Co and Ni are shown in Fig. 1. Co concentrations tend to be higher in post-leach leachate than pre-leach lixiviant. Net release tends to be positive for all desorbents, but particular for those containing Mg and Ca, so Co is readily released from the peat particularly by bivalent cations. Ni concentrations are also released at a relatively high net release (> 500 µg/kg) by bivalent desorbents like Mg and Ca. However, in contrast sodium leachates, particularly at higher 1M concentrations, tend to show a higher Ni concentration in pre-leach lixiviant and the net release is negative suggesting adsorption of Ni rather than release.

Alternative methods: column tests

A second alternative method for assessing sorption/exchange included in this study was kinetic upflow columns. A range of materials from the site were tested but only the peat samples are discussed here. The columns were loaded with <22 mm size fraction peat (TSF peat (238 g) and WRSF peat (240 g)) and were not open to the atmosphere (fig. 2). Testing was completed in a cold room (8 and 10 °C) and irrigated at ~24 ml per day using either tailings or waste rock leachate as influent feed. Following a break in testing a second version of influent feed was introduced, which was typically lower in metals than the initial feed. Outflow effluent volumes were measured weekly and collected in-situ analyses and bimonthly metals and major ion analysis.



Figure 2 *Peat column experiment set-up (Geochemic Ltd).*

Ni (fig. 3) has a high influent concentration (a maximum of ~ 2110 µg/L for waste rock and 1320 µg/L for tailings), but post-hiatus the concentration of tailings influent lower than previously measured, with a notable drop from ~1320 to ~50 µg/L. Even though the influent concentration is very low, it's higher than effluent concentrations suggesting that Ni is being actively sorbed by the peat. Ni in the waste rock influent peat column is also being sorbed effectively to the peat, as effluent values only reach a maximum of ~ 50 µg/L. Post-hiatus the effluent influent concentration remain high whilst the effluent concentration remain low, suggesting a continuation of Ni sorption in the peat. The cumulative loading also suggest sorption as the influent rises continually, but the effluent's increase is far slower, although this is more pronounced pre-hiatus.

The tailings and waste rock peat columns show different Co concentration trends. Effluent Co concentrations from the tailings peat column is typically higher than the influent. Post-hiatus the influent reduces to the detection limit and the effluent concentration decreases to between 3 µg/L and the detection limit. The waste rock influent Co concentration is always higher than that of the effluent released from the column. The influent reduces gradually from ~140 to ~6 µg/L between the start and week 34 post-hiatus. The effluent is consistently lower than the influent throughout the testing from around 40 µg/L at the start to ~ 2 µg/L post-hiatus. The cumulative mass loads clearly

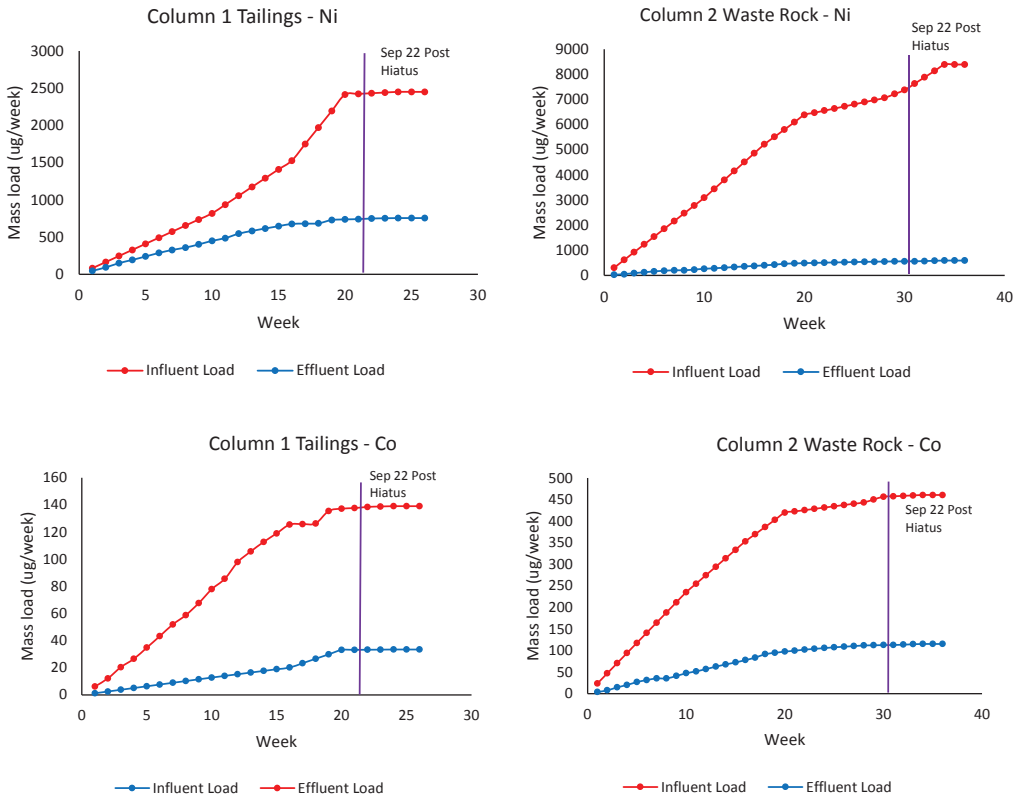


Figure 3 Upflow peat column Co and Ni

show a difference in the behaviour of Co between the two columns. In the waste rock peat column Co is net adsorbed by the peat, whereas in the tailings column, particularly pre-hiatus and to a lesser extent in post-hiatus, Co is net released from the peat.

A key advantage of upflow columns is they are carried out at L:S ratios representative of site conditions within a test environment and are run over a progressive and wide range of L:S ratios (0.1 to >20).

Conclusions

K_d testing is potentially a less valuable method for understanding the sorption capacity and material variation. There is potential for higher error at high concentrations and L:S ratios required to verify results, whereas the upflow columns appear to give more consistent results. Based on the valid results the peat has a higher K_d value than either the bedrock coatings or the till. The weathered bedrock coatings, once normalised for bulk sample surface area and mass, have the lowest calculated K_d.

The batch testing aided understanding of sorption and exchange mechanisms. Monovalent cations (Na or K) and bivalent cations (Ca or Mg) showed differences in mechanism and behaviour, which is important for the mine site as tailings leachate has high process salt concentrations (Na and K). In the column tests, the Ni tends to be adsorbed in the peat material, whereas Co is released. The cumulative increase in L:S ratios with column progression allows assessment of metal sorption/exchange rates over differing conditions, and often shows similarities in overall results regardless of L:S ratio variation.

Although individual analytical methods with short timeframes and sample sizes can provide information on certain aspects of sorption and exchange (such as mechanisms

in the batch tests), to derive data which is realistic to the site-specific conditions, larger sample sizes and longer timescales used in the column tests are beneficial. As L:S ratio varies through the column tests the mechanism and action of sorption and exchange often maintains it's rate, rather than the variation seen in the K_d tests, potentially making column tests a more useful analytical tool for deriving site-specific sorption and exchange data.

References

Bradl (2004) Adsorption of heavy metal ions on soils and soils constituents. J of Coolid and Interface Science 277 (1):1—18, doi:/10.1016/j.jcis.2004.04.005

BGS (2000) CEC & Kd Determination in Landfill Performance Evaluation, R&D Technical Report P340 Research conducted for the Environment Agency of England and Wales, British Geological Survey.

EA (2005) Development of the partition coefficient (K_d) test method for use in environmental risk assessments, Science Report SC020039/4 , Environment Agency

Effect of Time and Mineralogy on Sorption Capacity of Mine Drainage Passive Treatment Residuals: Is Sustainable Reuse Possible?

Dayton M Dorman and Robert W. Nairn

Center for Restoration of Ecosystems and Watersheds, School of Civil Engineering and Environmental Science, 202 West Boyd St, Room 334, University of Oklahoma, Norman, OK 73019, USA

Abstract

Sustainable reclamation design must consider the economic and environmental impact of the management of mine drainage treatment residuals. Iron-rich solids have substantial surface area and considerable sorption capacity for phosphorus. In this study, iron oxide solids were collected and analyzed from net-alkaline hard-rock mine drainage passive treatment systems (PTS), net-acidic coal mine drainage discharges and net-alkaline coal mine drainage PTS in Oklahoma, USA. These solids have a large sorption capacity for phosphorus (90 mg/g) and demonstrated minimal desorption of metals showing the sustainable reuse of these solids as a sorbent is possible.

Keywords: Iron Oxides, Mineralogy, Phosphorus, Sorption, Sustainable

Introduction

Sustainable reclamation design must consider the full life cycle impacts and costs of any selected remedy, including the ultimate disposition, disposal, or reuse of accumulated residual solids resulting from treatment of mine water containing elevated concentrations of metals. Solids disposal represents approximately 10% of global water treatment cost depending on the solids content of the sludge and the distance of delivery (Zinck and Griffith 2013). At many active mines, disposition of solids generated through active chemical treatment of mine waters is addressed on site through disposal to pond, pit lake, or mine workings, co-disposal with refuse or other wastes, or as backfill (Zinck 2006). In addition, mining companies, federal and state agencies, and non-profit organizations have designed and constructed hundreds of passive treatment systems throughout mining impacted regions (e.g., Skousen *et al.* 2017). In these cases, although funds for design and construction may be adequate, additional dollars for monitoring or maintenance are typically wholly lacking. Although these systems are often designed with operational lifetimes of two to three decades, they do require maintenance and principal among the needed tasks is management of accumulated water treatment solids. These solids are most often iron oxides. The chemical composition of the solids is based on the untreated mine water and the specific treatment mechanisms resulting in solids retention. The resulting chemical composition, along with environmental conditions and time, drives the mineralogy of these solids. It is well-established that iron oxides have substantial surface area per unit mass and considerable sorption capacity (Acero *et al.* 2006, Cornell and Schwertmann 2003; Dempsey and Jeon 2001; Fenton *et al.* 2009; Figueiredo and Silva 2011; Gagliano *et al.* 2004; Hedin 2012; Rakotonimaro *et al.* 2017; Sibrell *et al.* 2015; Sibrell and Tucker 2012; Tang and Nairn 2021; Zeng *et al.* 2004).

Initial forms of iron oxide typically produced in mine drainage systems are schwertmannite and ferrihydrite and more amorphous forms of goethite (Acero *et al.* 2006; Cornell and Schwertmann 2003; Gagliano *et al.* 2004; Murad and Rojík 2005). The small crystal structures of these minerals give these solids a large specific surface area facilitating them to act as sinks for trace metals and anions (Acero *et al.* 2006; Gagliano *et al.* 2004; Murad and Rojík 2005). However, these amorphous forms of iron oxide are metastable and will

transform into more thermodynamically stable and crystalline forms of iron oxide such as goethite, hematite and jarosite. This transformation can occur on a timescale of weeks to years depending on pH, redox conditions and other physicochemical properties of the water (Acero *et al.* 2006; Gagliano *et al.* 2004; Murad and Rojík 2005). Although larger crystals allow goethite to be more easily identified, they also decrease the surface area of goethite which can potentially decrease the sorption capacity for metals and other ions to the mineral phase.

Due to their high surface area and surface charge, iron oxides have been used as sorbents in a variety of water treatment applications (Cornell and Schwertmann 2003). Schwertmannite and ferrihydrite are preferred due to their low crystallinity and high surface area, yet all known iron oxide minerals exhibit relatively strong sorption capacities (Acero *et al.* 2006; Cornell and Schwertmann 2003; Gagliano *et al.* 2004). One of these water treatment applications is phosphorus sorption. The release of phosphorus, most commonly found in the form of phosphate, to surface waters is an environmental concern. Phosphorus is often a limiting nutrient for growth of organisms and thus is an important wastewater contaminant due to its role in eutrophication which leads to oxygen depletion and aquatic toxicity in receiving surface water bodies (Rakotonimaro *et al.* 2017; Sibrell and Tucker 2012; Zeng *et al.* 2004). Iron and aluminum oxides have a strong affinity for phosphorus and thus it is standard in wastewater treatment to remove phosphorus with iron and aluminum salts (Sibrell and Tucker 2012). Due to the high reagent costs associated with manufactured iron and aluminum salts, research into the more cost-effective use of iron and aluminum waste products has been explored (Fenton *et al.* 2009; Sibrell and Tucker 2012; Sibrell *et al.* 2015; Zeng *et al.* 2004). Given the variety of iron oxide minerals found in natural systems, a thorough understanding of the factors affecting their sorption capacity is necessary to sustainably use residual iron oxides as sorbents.

Methods

This research examines iron oxide solids from six locations throughout Oklahoma, USA that represent different mine drainage chemistries (Figure 1). Two of the locations are the Mayer Ranch Passive Treatment System (MRPTS) and the Southeast Commerce Passive Treatment System (SECPTS) oxidation ponds treating naturally net-alkaline hard rock mine drainage in the north-eastern Oklahoma portion of the Tri-State Mining District. The other four locations are in the Arkoma Basin in south-eastern Oklahoma where Desmoinesian coal deposits were mined. Iron oxide solids were collected from the Leboskey (LEB) and Rock Island #7 (RI7) passive treatment systems where net-acidic coal mine drainage has been rendered alkaline by utilizing an anoxic limestone drain before the water reaches the surface. Similarly, iron oxide samples were collected from two untreated net-acidic mine drainage discharges (GOWEN and HOWE).

Water quality data were collected routinely to characterize the host mine drainage chemistry in which the iron oxides were produced. Water quality data include physicochemical parameters (pH, DO, temperature, specific conductance, ORP, alkalinity, turbidity), sulfate, chloride, and a suite of total and dissolved metals and base cations (Al, As, Ba, Ca, Cd, Co, Cr, Cu, Fe, K, Li, Mg, Mn, Na, Ni, Pb, Si, Zn). Data for pH, alkalinity, and Fe, because they typically affect iron oxide mineralogy and Cd, Pb and Zn because desorption of ecotoxic metals is a concern regarding using these solids in the environment, will be explored in this paper.

Grab samples of iron oxide precipitates were collected at each location using a stainless-steel shovel. Samples were collected near the surface where the solids are typically fresher and have experienced less crystallization and are relatively free of organic debris. These samples were promptly frozen and freeze dried at a vacuum of 10 μm mercury and a vessel temperature of -40°C with a Labconco benchtop freeze drying system. Freeze drying was utilized to avoid any phase transformations that could occur (especially with ferrihydrite) during conventional air or oven drying

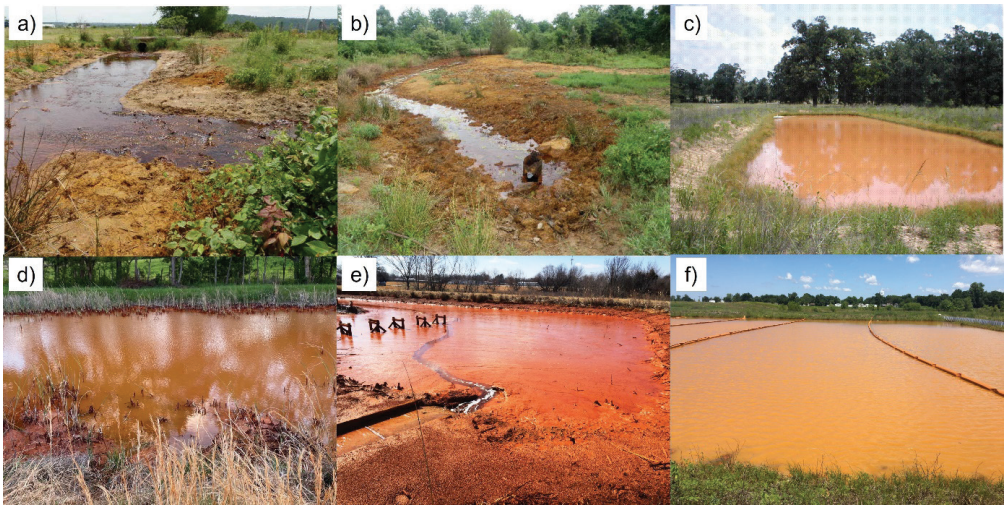


Figure 1 *Iron oxide deposits at untreated coal mine discharges a) Gowen and b) Howe; coal mine drainage passive treatment system oxidation ponds c) Leboskey and d) Hartshorne; and hard-rock mine passive treatment system oxidation ponds e) Mayer Ranch (during managed drawdown) and f) Southeast Commerce.*

Table 1 *Selected water quality data for the iron oxides collected at mine drainage discharges (GOWEN and HOWE) and PTS oxidation ponds (LEB, RI7, MRPTS and SECPTS)*

Site	pH	Net-Acidity (mg/L $CaCO_3$)	Fe (mg/L)	Cd (µg/L)	Pb (µg/L)	Zn (µg/L)
GOWEN (n=10)	4.47 ± 0.35	309 ± 138	120 ± 52	14 ± 6.4	189 ± 94	443 ± 223
HOWE (n=10)	4.46 ± 0.34	85 ± 37	37 ± 17	4.4 ± 2.3	64 ± 33	277 ± 126
LEB (n=8)	6.63 ± 0.32	-125 ± 25	31 ± 3.9	3.6 ± 1.1	54 ± 20	11 ± 4.6
RI7 (n=8)	6.41 ± 0.26	9.5 ± 157	173 ± 116	22 ± 14	299 ± 200	25 ± 15
MRPTS (n=79)	5.97 ± 1.16	-84 ± 52	168 ± 39	15 ± 6.6	101 ± 69	7297 ±1469
SECPTS (n=53)	6.16 ± 0.14	-114 ± 43	127 ± 35	15± 5.0	177 ± 80	6387 ± 1129

processes (Schwertmann and Cornell 2003). The solids were then analyzed for their physical, chemical, and mineralogical characteristics including moisture content, organic matter content, total metals concentrations, percent crystallinity, and mineralogical make up. Center for Restoration of Ecosystems and Watersheds (CREW) standard operating procedures follow US Environmental Protection Agency (USEPA) methods for all analyses.

After the solids were characterized, phosphorus sorption capacity tests were performed. In each case, 0.5 g of freeze-dried sample and 100 mL of various phosphorus concentrations (0, 1, 5, 10, 50, 100, 250, 500, 1000, 2000, 3000 and 4000 mg/L) were added into sealed 250-mL glass Erlenmeyer flasks. All the flasks were placed on an orbital shaker at 100 rpm for 24 h. After mixing, the samples were analyzed for pH and then filtered through 0.45 µm syringe filters into clean sample bottles and analyzed for soluble reactive phosphorus and dissolved metals concentrations.

Results

A summary of the host water quality in which the iron oxide solids are produced is shown in Table 1. All the sites have elevated Fe concentrations and the sites receiving hard-rock mine drainage have higher concentrations of Cd, Pb and Zn. The resulting

Table 2 Selected characteristics of the iron oxide samples collected at each site (n=3)

Site	% (α-FeOOH)	Cd (mg/kg)	Pb (mg/kg)	Zn (mg/kg)	% Crystallinity	Phosphorus Sorption Capacity (mg/kg)
GOWEN	65 ± 0.40	52 ± 0.5	8.17 ± 0.54	83 ± 2.9	64 ± 5.2	94785 ± 31684
HOWE	53 ± 1.5	43 ± 0.74	7.23 ± 0.10	49 ±2.2	69 ± 4.1	35828 ± 9080
LEB	61 ± 2.4	50 ± 0.53	40 ± 0.47	77 ± 4.4	52 ± 3.9	77561 ± 10710
RI7	83 ± 6.6	69 ± 1.1	9.8 ± 1.4	84 ± 6.7	55 ± 8.4	48977 ± 18161
MRPTS	78 ± 3.3	64 ± 1.3	10 ± 0.74	6448 ±91	56 ± 0.4	82568 ± 32426
SECPTS	65 ± 3.2	70 ± 0.07	80 ± 4.7	7256 ±315	56 ± 12	116231 ± 32693

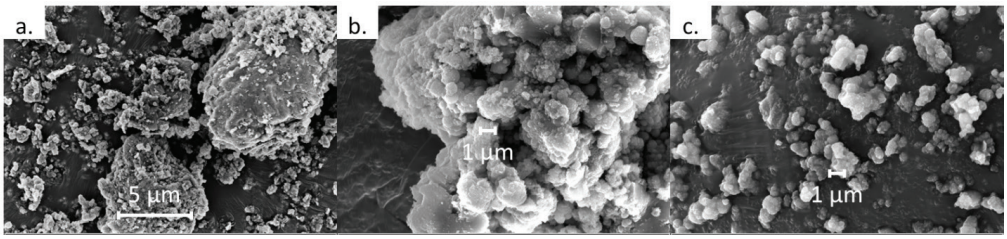


Figure 2 *SEM photos at a magnification of 5000 of the surface morphology of iron oxides collected from a) the LEB site, b) the RI7 site and c) the MRPTS site*

produced solids are mostly mineral (<20% organic) with a high moisture content (>60% moisture). These solids were also found to be mostly iron oxide with concentrations of metals including Cd, Pb and Zn associated with them (Table 2).

Initial characterization of these solids shows that the dominant mineral phase at all locations was goethite with more poorly-ordered goethite and amorphous ferrihydrite present. Although it was hypothesized that the net-acidic discharges would produce the less crystalline iron oxides, that was not the case. This result is perhaps due to the fact that these solids are produced in a shallow channel receiving mine drainage in which the increased oxic conditions and lower pH increased the transformation rate of ferrihydrite to goethite (Cornell and Schwertmann 2003). Despite the higher percent crystallinity of the solids, the phosphorus sorption capacity of the iron oxide solids recovered from mine drainage systems ranged from 35 mg/g from net-acidic coal mine drainage discharges to 116 mg/g from net-alkaline hard-rock mine drainage PTS (Table 2). The difference in sorption capacity is perhaps due to the difference in mineral morphology and surface area of the solids as demonstrated by images captured from scanning electron microscopy (SEM) at a magnification of 5000X (Figure 2). The solids from LEB are larger (≈5 µm) and have a more globular morphology, perhaps exacerbated by the aggregation of smaller iron oxide particles onto larger iron oxide particles and clay particles. These samples were observed to have a higher clay content associated with them due to the shallow pond depth, presence of natural clay and low iron content. The solids from the RI7 and MRPTS systems also have a globular morphology but are smaller in size (1-2 µm) and show a smaller (<1 µm) spiky morphology on the surface indicating the aggregation of less amorphous ferrihydrite on their surface providing an even higher surface area for phosphorus sorption mechanisms.

Despite the elevated metals concentrations associated with these solids, minimal desorption of metals was observed during the 24-h batch static sorption studies. Most aqueous metals concentrations were

below the detection limits and increased in concentration as the concentration of the phosphorus solution increased. This may be due to the decrease in solution pH with increasing phosphorus concentrations which caused the surface charge of the iron oxides to become more positive and thus less attractive to metal cations. These elevated phosphorus concentrations are not commonly seen in the environment but were necessary to develop sorption isotherms and determine the ultimate sorption capacity of these solids. Therefore, they do not represent a real-world scenario in which these iron oxides would be used.

Conclusions

This research has shown that iron oxides recovered from mine drainage systems, especially PTS, are an effective and sustainable sorbent for phosphorus. All iron oxides studied had a high (>35 mg/g) sorption capacity for phosphorus and experienced minimal desorption of metals in the 24-h study. The primary factor affecting the sorption capacity of these solids is surface morphology and their subsequent surface area. More investigation is needed to explore how environmental conditions such as pH and cation/anion concentrations affect the formation of iron oxide precipitates and their sorption capacities. Ongoing research is also looking at how these solids age over time in a phosphorus solution and how the subsequent changes in mineralogy and morphology affect their sorption capacity for phosphorus and metals to help determine the long-term feasibility of reusing these iron oxides as sorbents in the environment.

Overall, this research has shown that iron oxides can be beneficially reused as a phosphorus sorbent which is economically and environmentally more sustainable than traditional management and disposal of these solids. Similarly, these iron oxides are less expensive than iron and aluminum salts typically used in water treatment processes to remove contaminants and excess nutrients.

Acknowledgements

This work was supported by the Oklahoma Department of Environmental Quality (Agreement PO2929019163), the Office of Surface Mining Reclamation and Enforcement (Agreement S21AC10011-00), and the U.S. Environmental Protection Agency (Agreement X7-97682001-0). Several private landowners provided access. The authors also wish to thank the Oklahoma Conservation Commission Abandoned Mine Lands Program for assistance.

References

Acero P, Ayora C, Torrentó C, Nieto JM (2006) The behavior of trace elements during schwertmannite precipitation and subsequent transformation into goethite and jarosite. Geochim Cosmochim Acta 70 (16): 4130-4139. doi: 10.1016/j.gca.2006.06.1367

Cornell RM, and Schwertmann U (2003) The Iron Oxides – Structure, Properties, Reactions, Occurrences, and Uses. 2nd edition. Wiley-VCH Verlag GmbH and Co. KGaA, Weinheim.

Dempsey BA, Jeon B-H (2001) Characteristics of sludge produced from passive treatment of mine drainage. Geochem-Explor Env A 1(1):89–94. doi: 10.1144/geochem.1.1.89

Fenton O, Healy MG, Rodgers M (2009) Use of ochre from an abandoned metal mine in the south east of ireland for phosphorus sequestration from dairy dirty water. J Environ Qual 38:1120–1125. doi: 10.2134/jeq2008.0227

Figueiredo MO, Silva TP (2011) The positive environmental contribution of jarosite by retaining lead in acid mine drainage areas. Int J Environ Res Public Health 8: 1575-1582. doi: 10.3390/ijerph8051575

Gagliano WB, Brill MR, Bigham JM, Jones SF, Traina SJ (2004) Chemistry and mineralogy of ochreous sediments in a constructed mine drainage wetland. Geochim Cosmochim Acta 68 (9): 2119-2128. doi: 10.1016/j.gca.2003.10.038

Hedin RS (2012) Advances in the production of marketable products from mine water treatment systems. In: Proc. of the 9th ICARD, May 20–26, Ottawa, ON, Canada, 8p

Murad E, Rojík P (2005) Iron mineralogy of mine-drainage precipitates as environmental indicators: review of current concepts and a case study from the Sokolov Basin, Czech Republic. Clay Miner 40: 427-440. doi: 10.1180/0009855054040181

Rakotonimaro VT, Neculita CM, Bussière B, Benzaazoua M, Zagury GJ (2017) Recovery and reuse of sludge from active and passive

treatment of mine drainage-impacted waters: a review. Environ Sci Pollut Res 24:73-91. doi: 10.1007/s11356-016-7733-7

Sibrell PL, Tucker TW (2012) Fixed bed sorption of phosphorus from wastewater using iron oxide-based media derived from acid mine drainage. Water Air Soil Pollut. 223:5105-5117. doi: 10.1007/s11270-012-1262-x

Sibrell PL, Penn CJ, Hedin RS (2015) Reducing soluble phosphorus in dairy effluents through application of mine drainage residuals. Commun Soil Sci Plant Anal. 46: 545–563. doi: 10.1080/00103624.2014.998339

Skousen J, Zipper CE, Rose A, Ziemkiewicz PF, Nairn RW, McDonald LM, Kleinmann RL (2017) Review of passive treatment systems for acid mine drainage treatment. Mine Water Environ 36: 133-153. doi: 10.1007/s10230-016-0417-1

Tang Z, Nairn RW (2021) Recovered mine drainage passive treatment residuals address legacy sediment pollution: A field mesocosm study at Grand Lake o' the Cherokees, Oklahoma. Ecol Eng 170: 106358. doi: 10.1016/j.ecoleng.2021.106358

Zeng L, Li XM, Liu JD (2004) Adsorptive removal of phosphate from aqueous solutions using iron oxide tailings. Water Res 38:1318-1326. doi: 10.1016/j.watres.2003.12.009

Zinck J (2006) Disposal, reprocessing and reuse options for acidic drainage treatment sludge. Proceedings from the 7th International Conference on Acid Rock Drainage (ICARD), St. Louis, MO.

Zinck J, Griffith W (2013) Review of acidic drainage treatment and sludge management operations, MEND Report3.43.1.CANMETMMSL,101p.

Uranium Sources and Mobility at an Iron Ore Mine Site in Northern Sweden

Vimbainashe L Dzimbanhete[1], Frej Hegg[1], Lena Alakangas[1], Torbjörn Karlsson[2], Elsa Peinerud[2], Oscar Paulsson[1], Thomas Aiglsperger[1]

[1]*Division of Geosciences, Luleå University of Technology, S-97 187 Luleå, Sweden, vimbainashe.dzimbanhete@ltu.se*

[2]*Luossavaara-Kiirunavaara AB, SE-981 85 Kiruna, Sweden*

Abstract

Discharge of process water containing uranium from an iron ore mine site in northern Sweden can be of environmental concern due to uranium's chemical toxicity and radioactivity. Water and solid samples were collected from the recipient and upstream along the mine value chain to identify potential sources of uranium and gain an understanding of the mobility of uranium. Mine water pumped from the open pit to the processing plant was identified to be the main source of uranium. $Ca_2UO_2(CO_3)_3$ and $CaUO_2(CO_3)_3^{-2}$ dominated uranium speciation in the process water and promote uranium mobility from the mine site to the recipient.

Keywords: Uranium, Mine Water, Mobility, Sources, Recipient

Introduction

Potential contamination of recipients (natural lakes and rivers) by uranium (U) from mining is a global concern because dissolved U is linked to numerous health effects due to U's radioactivity and chemical toxicity. To prevent U contamination from mining operations, sources of U must be identified, and the mobility of U must be tracked along the whole mine value from mining, through processing and refining to the recipient where U is potentially causing harm. However, potential U sources can be difficult to identify at mine sites due to the multitude of water-rock interactions that occur between solid and liquid phases for example in the mine (underground or open pit), mineral processing plant, tailings dam, waste rock piles, thickening, and water treatment plants. In each of these steps, the chemical composition of the process water changes and determines the possible U aqueous species at the mine site.

Studies of U contamination in mining have been primarily conducted on specific steps of the mine value chain at U mine and mill sites, for example, on tailing dams, waste rock piles, and exposed mine workings. This makes it difficult to get a holistic view of the mobility of U at the mine site in order to implement efficient prevention measures. Studies on the potential sources and release of U from iron ore mine sites where U can occur as a trace element but in concentrations exceeding the average crustal abundance are limited. Furthermore, U contamination studies that consider the critical factors that can affect U mobility along the whole value chain at a mine site are scarce. In this study, water and solid samples were collected at an iron ore mining site in northern Sweden to identify potential U sources and gain an understanding of the geochemical behavior and mobility of U.

Mine Site Description

The mine site is located in northern Sweden in the Kiruna Municipality. The ore deposit is an apatite-bearing iron ore deposit where magnetite is the main ore mineral and the main gangue minerals are apatite, calcite, actinolite, and quartz (Bergman *et al.*, 2001). The mine site consists of two open pits referred to as open pits A and B. Open pit A is currently mined at a rate of over 4 million tonnes per year whereas mining has ceased from open pit B. A mixture of infiltrating groundwater and precipitation

(referred to as mine water) is pumped from both open pits to be used in the processing plant where magnetite in the iron ore is concentrated. Grinding and wet magnetic separation are conducted alternately in several steps to produce a final magnetite concentrate, which is sent to pelletization. Slurry waste that consists of gangue minerals and magnetite that could not be recovered by wet magnetic separation in the processing plant is pumped to thickener 1 for water recovery. Water is recovered in an overflow product. The thickener 1 overflow is pumped to a return water tank, which is used to recycle process water back to the processing plant. A thickened slurry is recovered in the underflow of thickener 1 and pumped to thickener 2 where additional water is recovered in the overflow product and pumped to the storage dam. The underflow product is pumped to the tailings dam. The storage dam also receives water from the open pit B and acts as both a reservoir and a clarification dam where particles are allowed to settle before the process water is pumped back into the processing plant or discharged to the recipient.

Methods

Water samples (points 1 to 7) and solid samples (a to c) were collected in March 2021 to be able to identify potential U sources (Figure 1) (Hegg, 2021). The samples were analyzed for their element concentrations by Inductively coupled plasma mass spectrometry (ICP-MS) and inductively coupled plasma atomic emission spectroscopy ICP-AES) at ALS Scandinavia AB in Luleå. Element concentrations in the solid samples were analyzed after lithium metaborate and HNO_3/HF/HCl digestion. The pH, temperature, electrical conductivity (EC), anions (F^-, Cl^-, SO_4^{2-}, NO_3^-), cation (NH_4^+), and alkalinity (determined as HCO_3^-) were also measured in the water samples to determine the chemical conditions prevailing at the different water sample points. The element concentrations and chemical parameters at each water sample point were then used to calculate U speciation in PHREEQC Interactive 3.7.3.15968 (Parkhurst & Appelo). 2013 with the Thermochimie thermodynamic database (Giffaut *et al.*, 2014).

The solid samples (samples a to c) were mineralogically characterized with Scanning electron microscopy with energy dispersive spectroscopy (SEM-EDS) to identify U-bearing minerals. Sequential extraction tests focusing on the water-soluble (Milli-Q water), exchangeable (1M ammonium acetate, pH 7.0), and acid-soluble (1M sodium acetate, pH 5.0) fractions were conducted on the solid samples to distinguish mobile U, which can

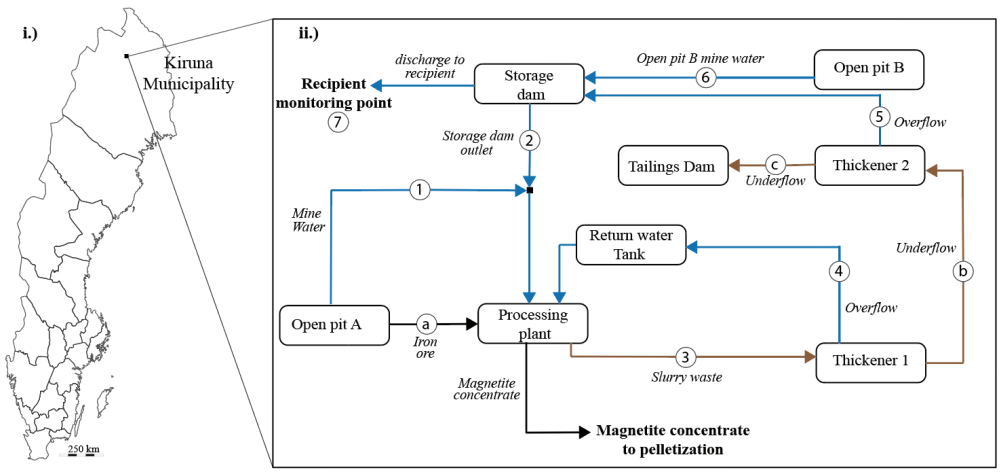


Figure 1 *a) Location of the mine site in northern Sweden. b.) block flow diagram showing water (blue arrows), slurry (brown arrows), and solid (black arrows) exchange between the different components at the mine site. Water sample locations are numbered from 1 to 6 whereas solid sample locations are labeled from a to c.*

be potentially released to the process water from stable U that requires weathering for U release to occur.

Results and Discussion

Chemical conditions and element concentrations

Water at the recipient monitoring point is characterized by close to neutral pH (7.4), low electrical conductivity (EC) (38.9 mS/m), and low element concentrations (Table 1). In contrast, process water at sample points 2 to 5 is characterized by alkaline pH of around 8.0, high EC, and high element concentrations. Temperature is highest at point 3 due to heat generation during grinding in the processing plant. The EC is higher at sample points 2 to 5, which are part of the process water recirculation system at the mine site compared to samples 1 (open pit A mine water), 6 (open pit B mine water), and 7 (monitoring point in the recipient), which are independent of the recirculation system. The higher EC at sample points 2 to 5 is due to the dissolution of soluble minerals such as gypsum, halite, and sylvite and explosives containing $NaNO_3$ that are liberated during grinding and dissolve when they come into contact with process water in the processing plant (Karlsson *et al*., 2017; Lundkvist, 1998). Process water recirculation at the mine site through the return water tank and storage dam also causes elements such as Ca, K, Mg, Na, Cl^-, SO_4^{2-}, NO_3^- Sr, Ba, and Mo to accumulate in the process water over time and be higher in magnitude at sample points 2 to 5 compared to sample points 1, 6 and 7. Alkalinity was found to be the highest at point 1 compared to the other sample points. The U concentration is highest in the mine water from Open Pit A (59.9 µg/L) compared to the other sample points. Process water that is discharged from the storage dam has a U concentration above the maximum allowable limit of 8.6 µg/L set by the Swedish Agency for Marine and Water Management in regulation HVMFS 2019:25. However, the U concentration at the monitoring point in the recipient (sample point 7) was 1.4 µg/L due to dilution in the recipient.

Table 1 *Chemical composition of the water sample points: 1) open pit A mine water, 2) storage dam outlet, 3) slurry waste from the processing plant, 4) overflow water from thickener 1, 5) overflow water from thickener 2, 6) open pit B mine water, 7) monitoring point in the recipient*

Sample points	1	2	3	4	5	6	7
pH	8.2	7.9	8.3	8.2	8.1	8.1	7.4
Temperature (°C)	0.9	3.6	29.4	27.7	8	0	0
Conductivity (mS/m)	56.3	249	378	359	268	38.64	38.9
SO_4^{2-} (mg/L)	110	1100	1700	1600	1100	86	107.6
Cl^- (mg/L)	28	170	310	280	190	20	18.2
HCO_3^- (mg/L)	153	85	50	60	85	79	43
NO_3^- (mg/L)	0.58	9	16	14	9.7	0.17	0.86
Ca (mg/L)	78.9	428.0	639.0	607.0	461.0	52.9	49.8
K (mg/L)	7.1	55.9	88.70	103.0	62.7	4.4	6.1
Mg (mg/L)	12.8	36	55.1	54.3	39.4	6.8	5.4
Na (mg/L)	18.8	113	160	198	129	12.3	12.5
Sr (µg/L)	133	1170	1890	1920	1290	85.9	133.5
Ba (µg/L)	15.0	78.5	84.2	135.0	84.8	15.4	18.4
Mo (µg/L)	6.9	22.2	23.8	30.9	22.5	6.1	1.5
U (µg/L)	59.9	18	11.5	12.3	19.6	12.4	1.4

U speciation in the process water

U behavior is influenced by pH, Eh, U oxidation state (U^{4+}, U^{6+}), and the presence of common complexing ligands such as CO_3^{2-}, PO_3^{4-}, and SO_4^{2-} (Cumberland *et al*., 2016). Through the weathering and oxidation of U(IV) minerals, U forms the more mobile and soluble U(VI) oxidation state, which occurs as the uranyl ion (UO_2^{2+}). Above pH 5 under oxidizing conditions, UO_2^{2+} forms carbonate complexes (CO_3^{2-}) of the form $UO_2(CO_3)_n^{2-2n}$, where n =1 – 3 (Cumberland *et al*., 2016). Depending on the availability of calcium (Ca), UO_2^{2+} can form the calcium uranyl carbonate complexes Ca $(UO^2)(CO_3)_3^{2-}$ and $Ca_2UO_2(CO_3)_3^0$ above pH 7 (Bernhard *et al*., 2001; Dong & Brooks, 2006. Geochemical modeling in PHREEQC suggested that the calcium uranyl carbonate complexes $Ca_2UO_2(CO_3)_3$ and $CaUO_2(CO_3)_3^{2-}$ dominate U speciation at all the sample points (1 to 7) (Table 2). The presence of calcium (Ca), and HCO_3^- in the process water and alkaline pH conditions prevalent at the mine site and the recipient are conducive to the formation of calcium uranyl carbonate complexes. Calcium uranyl carbonate complexes have been shown to enhance U mobility by reducing U's adsorption efficiency on mineral surfaces (Fox *et al*., 2006).

U mineralogy and sequential extraction

U can occur as a trace element but in concentrations exceeding the average crustal abundance in iron ore. In the iron ore, U can occur in minerals of its own such as uraninite [UO_2], coffinite [$U(SiO_4)_{1-X}(OH)_{4X}$)], or pitchblende (UO_2), or in accessory minerals such as apatite [$Ca_5(PO_4)_3(OH,F,Cl)$], thorite [$(Th,U)SiO_4$], monazite [(Ce, La, Nd, Th) PO_4], or zircon [$ZrSiO_4$] (Misra, 2000). The U content in the iron ore (1.0 ppm) was lower than the average U content in the earth's crust (2.7 ppm) (Kalin *et al*., 2005) (Table 3). Further downstream, the U content increased to 2.9 ppm and 3.2 ppm in thickener 1 (sample b) and thickener 2 (sample c) underflow solids, respectively. Further downstream, gangue minerals potentially containing U are concentrated as magnetite is recovered to the magnetite concentrate as indicated by the increasing Ca, Mg, Si, K, P, and Th concentrations compared to decreasing Fe contents in Table 3.

Sequential extraction was used to investigate the potential mobility of U and showed that more than 98 % of the U in the iron ore was associated with the residual fraction (Figure 2i). Further downstream at sample points b and c, more than 90 % of the U was associated with the residual fraction.

Table 2 *Uranium speciation at water sample points 1 to 7*

Sample location	1	2	3	4	5	6	7
$Ca_2UO_2(CO_3)_3$ (%)	89.83	97.06	97.56	97.78	97.56	86.83	80.62
$CaUO_2(CO_3)_3^{2-}$ (%)	9.64	2.86	2.38	2.12	2.38	12.59	15.74
$MgUO_2(CO_3)_3^{2-}$ (%)	0.50	0.08	0.06	0.05	0.06	0.51	0.56
$UO_2(CO_3)_3^{4-}$ (%)	0.03	0.00	0.00	0.00	0.00	0.06	0.19
$UO_2(CO_3)_2^{2-}$ (%)	0.00	0.00	0.00	0.00	0.00	0.01	1.14

Table 3 *Element concentrations in solid samples; a) iron ore, b) thickener 1 underflow, c) thickener 2 underflow*

Sample points	Fe (wt.%)	Ca (wt.%)	Mg (wt.%)	Si (wt.%)	K (wt.%)	P (wt.%)	Th (ppm)	U (ppm)
a	60.3	1.7	0.9	3.4	0.3	0.5	9.0	1.0
b	10.7	8.6	4.2	18.3	1.2	2.3	28.9	2.9
c	14.4	7.2	3.9	13.6	1.3	2.0	36.4	3.2

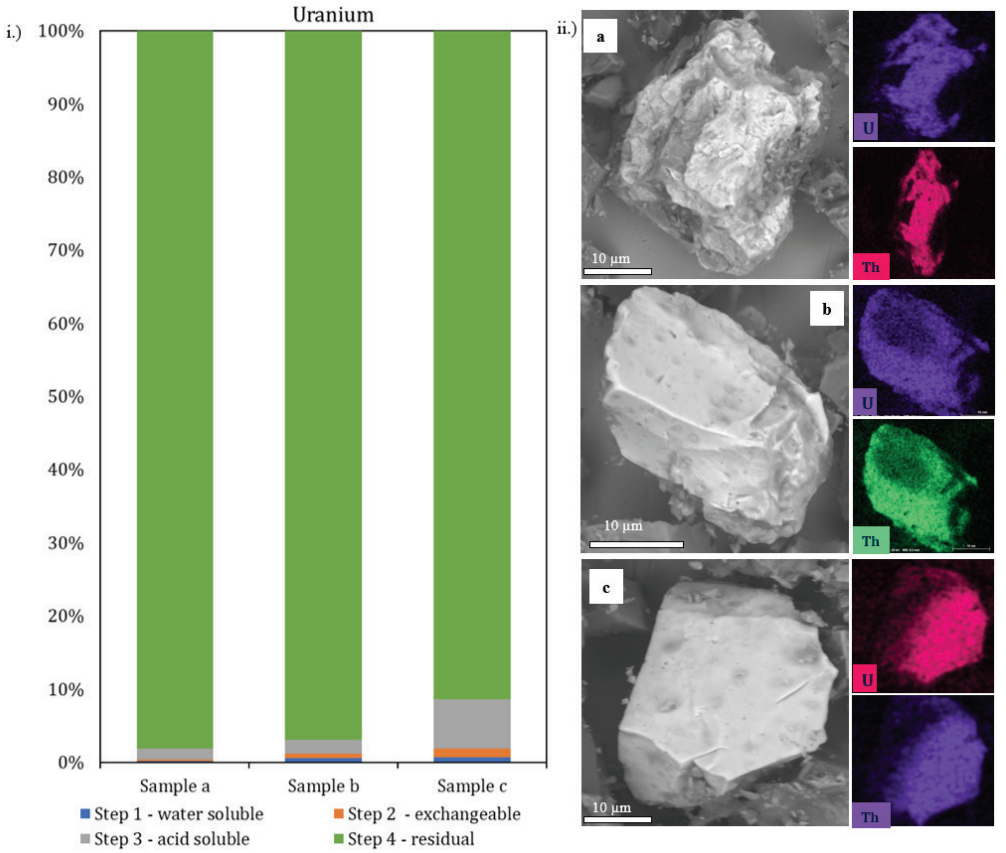


Figure 2 i.) Percent distribution of U in the iron ore (sample a), thickener 1 underflow (sample b), and thickener 2 underflow (sample c) solid samples. ii.) SEM images with U and Th distribution maps in samples a, b, and c.

In the residual fraction, U is strongly bound within mineral lattices and is not expected to be released to the process water. Mineralogical characterization by SEM-EDS revealed thorite containing 1 to 2 wt. % to be the main U-bearing mineral in the solid samples a to c Figure 2ii. Thorite is known for its low solubility and has been shown to dissolve mainly in aqua regia and hydrofluoric acid in thorium speciation studies (Guo *et al.*, 2007; Okeme *et al.*, 2022). Thorite insolubility at the different steps of the mine value chain is also supported by the fact that thorite grains identified downstream at sample points b and c looked unweathered and similar to grains identified in the iron ore (Figure 2ii). Therefore, the iron ore, which has a low U content where U predominantly occurs in the insoluble mineral thorite is not an important source of U to the process water. Instead, the mine water that is pumped from the open pit to be used in the processing plant is a more important source of U.

Conclusions

- Mine water from Open pit A, which is a mixture of infiltrating groundwater and precipitation that is used in the processing plant is the main source of U to the process water. Further studies focusing on the open pit are required to identify U sources and gain an understanding of U-weathering processes that might be taking place in the open pit.
- The calcium uranyl carbonate complexes, $Ca_2UO_2(CO_3)_3$ and $CaUO_2(CO_3)_3^{-2}$ were found to dominate U speciation at all the sample points. The presence of calcium (Ca), alkalinity (HCO_3^-) and alkaline pH

prevalent at the mine site are conducive to the formation of these complexes. The complexes enhance U mobility in the process water by stabilizing U in the process water and decreasing U's adsorption efficiency on mineral surfaces.

- Iron ore is not an important U source to the process water. The iron ore has a low U content (1.0 ppm). 98 % of U in the iron ore was found to be associated with the residual fraction which contains minerals where U is strongly bound in mineral lattices and is not expected to be released at the chemical conditions prevailing in the processing plant and thickeners.
- Thorite was identified as the main U-bearing mineral in the iron ore and thickener underflow solids. The thorite remains unweathered downstream in the thickener 1 and thickener 2 underflow solids indicating that it is stable along the mine value chain.
- The results highlight the importance of tracing contaminants upstream from the recipient along the mine value chain to identify potential contaminant sources.

References

Bergman, S., Kübler, L., & Martinsson, O. (2001). Description of regional geological and geophysical maps of northern Norrbotten County (east of the Caledonian orogen) (Vol. 56).

Bernhard, G., Geipel, G., Reich, T., Brendler, V., Amayri, S., Nitsche, H., & Nitsche, H. (2001). Uranyl(VI) carbonate complex formation: Validation of the Ca2UO2(CO3)3(aq.) species. Radiochimica Acta, 89(37104), 511. https://doi.org/10.1524/ract.2001.89.8.511

Cumberland, S. A., Douglas, G., Grice, K., & Moreau, J. W. (2016). Uranium mobility in organic matter-rich sediments: A review of geological and geochemical processes. In Earth-Science Reviews (Vol. 159, pp. 160–185). Elsevier B.V. https://doi.org/10.1016/j.earscirev.2016.05.010

Dong, W., & Brooks, S. C. (2006). Determination of the formation constants of ternary complexes of uranyl and carbonate with alkaline earth metals (Mg2+, Ca2+, Sr 2+, and Ba2+) using anion exchange method. Environmental Science and Technology, 40(15), 4689–4695. https://doi.org/10.1021/ES0606327

Fox, P. M., Davis, J. A., & Zachara, J. M. (2006). The effect of calcium on aqueous uranium(VI) speciation and adsorption to ferrihydrite and quartz. Geochimica et Cosmochimica Acta, 70(6), 1379–1387. https://doi.org/10.1016/j.gca.2005.11.027

Giffaut, E., Grivé, M., Blanc, P., Vieillard, P., Colàs, E., Gailhanou, H., Gaboreau, S., Marty, N., Madé, B., & Duro, L. (2014). Andra thermodynamic database for performance assessment: ThermoChimie. Applied Geochemistry, 49, 225–236. https://doi.org/10.1016/j.apgeochem.2014.05.007

Guo, P., Duan, T., Song, X., & Chen, H. (2007). Evaluation of a sequential extraction for the speciation of thorium in soils from Baotou area, Inner Mongolia. Talanta, 71(2), 778–783. https://doi.org/10.1016/j.talanta.2006.05.038

Hegg, F. (2021). Uranium in LKAB's process water in Svappavaara - a geochemical study on fixation and release. [Master's thesis, Luleå University of Technology]. diva2:1608916

Kalin, M., Wheeler, W. N., & Meinrath, G. (2005). The removal of uranium from mining wastewater using algal/microbial biomass. Journal of Environmental Radioactivity, 78(2), 151–177. https://doi.org/10.1016/j.jenvrad.2004.05.002

Karlsson, T., Siergieiev, D., Andersen, T. J., & Modin, H. (2017). Waste management plant for LKAB's operations in Svappavaara.

Lundkvist, A. (1998). The Process Water Geochemistry of the Kiirunavaara Magnetite Ore. http://urn.kb.se/resolve?urn=urn%3Anbn%3Ase%3Altu%3Adiva-26157

Misra, K. C. (2000). Understanding Mineral Deposits. In Understanding Mineral Deposits (pp. 613–659). Springer Netherlands. https://doi.org/10.1007/978-94-011-3925-0

Okeme, I. C., Crane, R. A., Nash, W. M., Ojonimi, T. I., & Scott, T. B. (2022). Characterization of rare earth elements and toxic heavy metals in coal and coal fly ash. RSC Advances, 12(30), 19284–19296. https://doi.org/10.1039/D2RA02788G

Parkhurst, D., & Appelo, C. (2013). Description of Input and Examples for PHREEQC Version 3-A Computer Program for Speciation, Batch-Reaction, One-Dimensional Transport, and Inverse Geochemical Calculations. In U.S Geological Survey Techniques and Methods, book 6, chap.A3 (pp. 1–497). https://pubs.usgs.gov/tm/06/a43/.

Development of an Improved Model to Investigate Heating Potentials in Abandoned Mines Utilising Mine Water

Tom Ebel, Lukas Oppelt, Timm Wunderlich, Thomas Grab, Tobias Fieback

Professor for Technical Thermodynamics, Institute of Thermal Engineering,
TU Bergakademie Freiberg, Chair for Technical Thermodynamics, Gustav-Zeuner-Straße 7,
09599 Freiberg, Germany

Abstract

Compared to the ambient, mine water has a natural constant temperature throughout the year. The heat energy stored in the water can contribute towards a more sustainable energy infrastructure in the mining regions. Although mines can have potentials of up to hundreds or thousands of megawatts, the methods of estimation are limited to either detailed numerical simulations or simplified analytical solutions. For small stakeholders, analytical solutions are often used as a basis for estimation. This paper will investigate the results of an analytical approach and ways to implement additional calculations, which are crucial for a realistic energy estimation.

Introduction

Although mine rehabilitation results in challenges, it can also hold unique opportunities. One of these opportunities is conditioned by the large body of mine water created by the flooding of the mining cavities. By contacting the surrounding ground, it naturally takes on its temperature in form of heat energy. With mine water geothermal systems having comparatively high contact areas, they consequently possess higher heat potentials particularly since conventional geothermal systems may be limited by the amount of ground they can effectively cover. The energy can be utilised by using heat pumps to supply space heating or hot water production. By providing an environmentally friendly, safe and stable heat supply, this alternative energy source could be a crucial component in enhancing a mining region's perceived attractiveness.

Before evaluating energy potentials, it has to be taken into account, how the energy from the mine -water can be utilised. At some locations it has to be pumped continuously to keep the level at a safe depth and prevent environmental damage. On the other hand, not every mining region needs to provide active water management. Drainage galleries may provide a safe and adequate method of dewatering, where the water could be used energetically analogous to the usage of the actively pumped water. In both cases, it is possible to estimate the energy potentials when the water flow rate and the temperatures are known. Although this accessible energy should be utilised as far as available, it is only a fraction of possible heat potentials of the mine, since not all mine workings are contacted by the flow of the water equally. To exploit the heat source more fully, dipole open-loop mine water geothermal systems can be deployed (Banks 2019). In such systems, mine water is extracted from one part of the mine, its heat is harnessed and subsequently, it is reinjected into another part of the mine. The resulting flow of the cooler water between the geothermal wells extracts heat energy from the rock which is contacted on its flow path. In comparison to heat extraction from active water management and gallery drainage, it brings the important advantage of being locational more flexible. This makes this method an attractive possibility to supply quarters with heat and cold.

Despite the mentioned advantages, higher costs are usually involved in making dipole open-loop mine water geothermal systems operational (Hoffmann 2014, Loredo 2011). Thus, special attention must be given to designing mine water systems appropriately. This prevents premature energy exhaustion of the mine water and the contacted rock over the lifetime of the system. Since calculating

the amount of sustainable heat extraction with detailed numerical models is not feasible for many stakeholders concerned with mine rehabilitation, user-friendly approaches must be developed or expanded. Several analytical models are discussed in the literature, which can calculate the amount of sustainable heat extraction with comparatively simple input parameters (tunnel length, temperature level, etc.). However, the calculations often only focus on one heat regeneration mechanism at a time, i.e., the heat conduction in the rock or the geothermal heat flux. Additionally, there is no method of evaluating energy from water that might infiltrate the mine workings or gets transported indirectly to the geothermal wells of the dipole open-loop system. By bringing in energy from locations not directly influenced by the primary this mine water pumping cycle, can have a positive effect on the heat extraction potentials.

In this paper, a state-of-the-art analytical approach, together with its drawbacks and possible solutions is discussed. The foundation of the calculation was laid out by (Rodriguez 2009) and expanded by (Loredo 2017) in the project "Low-Carbon After Life" (Banks 2019) by implementing correlations for the Nusselt number and flow-coupling the heat transfer.

Model Analysis and Improvements

The analytical model uses a recurring calculation algorithm to estimate the outlet temperature of a mine water flow through a gallery. When entering the gallery, the mine water has a different temperature than the surrounding rock. Therefore, depending on the temperature, it takes up or transmits heat to the rock. The quantity of heat transmission between fluid and solid is dependent on their thermophysical properties as well as on the specified flow characteristics. An example case is given in Figure 1. Further calculations will be done referring to this example case with the specified major parameters.

Besides enabling fast calculations with few comparatively easy-to-estimate parameters, the algorithm has some drawbacks. First, the thermal influence radius, which is crucial in estimating the energy transmission through the rock mass, is calculated by implementing simplifications, which cannot be explained satisfactorily. Second, a constant mine water inlet temperature has to be specified, whereas, in a practical system, the reinjection temperature is dependent on the abstraction temperature and the heat extracted from the mine water. This leads to a varying amount of heat output, visualized in the given example in Figure 2. This effect is more pronounced in the early stages of system operation. Third, it considers only heat conduction through the rock as a heat regeneration mechanism for the mine water, while in reality, additional

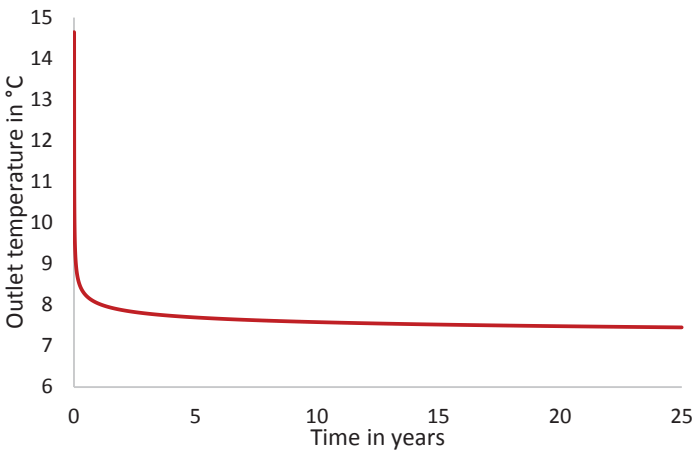


Figure 1 *Outlet temperature and thermal influence radius evolution for an example case and 25 years (gallery length = 1000 m, water reinjection temperature = 6 °C, rock temperature = 15 °C, volumetric flow rate = 5 L/s).*

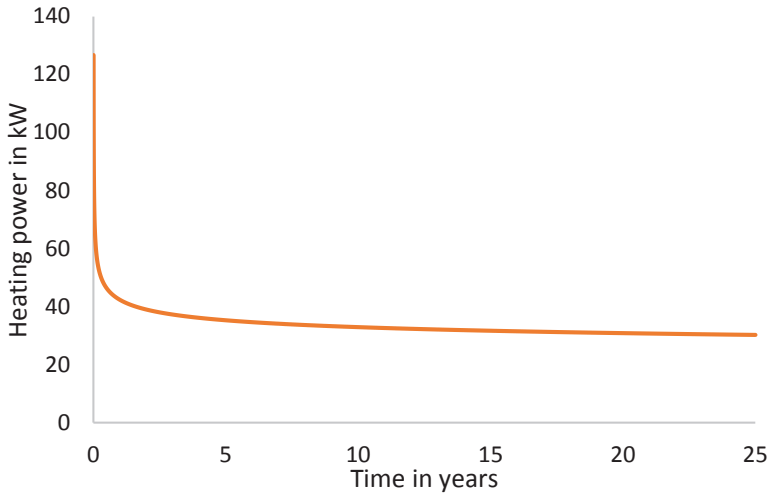


Figure 2 Heating power evolution, calculated for the example case.

water inflows are likely to occur, which yield increases in heating potentials. In addition, it's not possible to specify the geothermal heat flow and to consider the energy of the mine water.

While the structure of the solution made it possible to use it in accessible spreadsheets, ensuring a wide variety of potential users, an implementation in a numerical code can help to add another layer of calculation flexibility and implement improvements. At the same time the quick estimates with few input parameters are still possible so as to keep user accessibility.

To implement the system of formulae into a numerical code, the general programming language Python (V3.10) was used. Using the formulae as a foundation, several improvements can be worked into the syntax.

First, an improved version of thermal radius calculation was implemented. As suggested by (Loredo 2017) the logarithmic (Cooper 1946) approximation can be used to achieve a better foundation for this calculation. Thereby the thermal radius is obtained by specifying an incremental temperature change and calculating at which radius this displacement occurs. This temperature increment was set

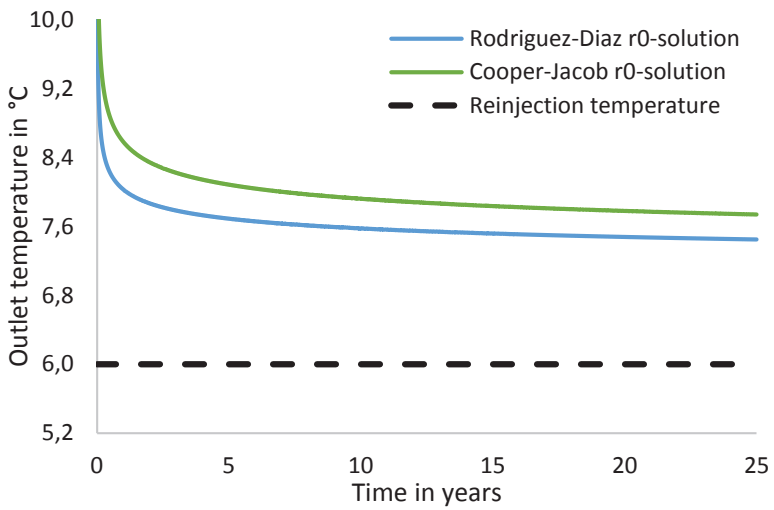


Figure 3 Outlet temperature evolution for different calculation approaches of the thermal radius for 25 years for the example case.

at a constant value of 0.01 K for the following calculations. A comparison between the two calculation approaches is shown in Figure 3.

The outlet temperatures display, that in total, more heat can be extracted from the gallery system. Since the thermophysical approach is more justifiable in the Cooper-Jacob approximation, it will be used for the continued calculations.

Since the heat output is a crucial parameter in designing a geothermal system, in the second step the code gets modified in order to allow specification of the heat power. This is done by coupling the entrance temperature into the mine gallery (mine water reinjection temperature) to a specified heating power and the outlet temperature (mine water abstraction temperature). If heat is constantly extracted, the temperature of the mine water will fall over time. To prevent chilling below a certain point, a critical reinjection temperature of 6 °C was defined, which is usually used as the lower limit for energetical utilisation of groundwater in Europe (LANUV 2018). Furthermore, chilling the water lower than that potentially causes technical problems in system operation. As soon as the calculated reinjection temperatures fall below this threshold, the calculation is terminated. For the specified case a constant heating power of 60 kW was used for the example calculation. The results are displayed in Figure 4.

Lastly, the influence of additional water inflow will be investigated. The value of the effect of water inflow is highly individual and dependent on the respective mine and the detailed location of water abstraction. Since the hydrodynamic information for closed mines may be very limited, the assumptions must be chosen with adequate caution. An investigation of the effect of inflowing water may be nonetheless reasonable if heat transport from the gallery wall alone is economically not sufficient for a mine water geothermal plant at a given location. In particular, if practical operation shows that a certain degree of additional water inflows is to be expected in most system locations (Oppelt 2021). The effect of this influence on the maximal possible heating power is displayed in Figure 5.

This maximum value is determined by observing at which heating power the critical reinjection temperature is undercut after 25 years. From the results, the conclusion can be made that even small mixing rates with inflowing water can lead to notable changes in the available heat potential. While being dependent on the volumetric flow rate of the system, even small mixing rations can lead up to severalfold increases in energetical potential. Since the potentials are most sensitive to this parameter, additional ways to characterize the amount of expectable inflow rates for future systems need to be discussed. The current model gives a foundation in which the results of further research could be implemented.

Conclusion and Outlook

While numerical methods of estimation of geothermal energy potentials in

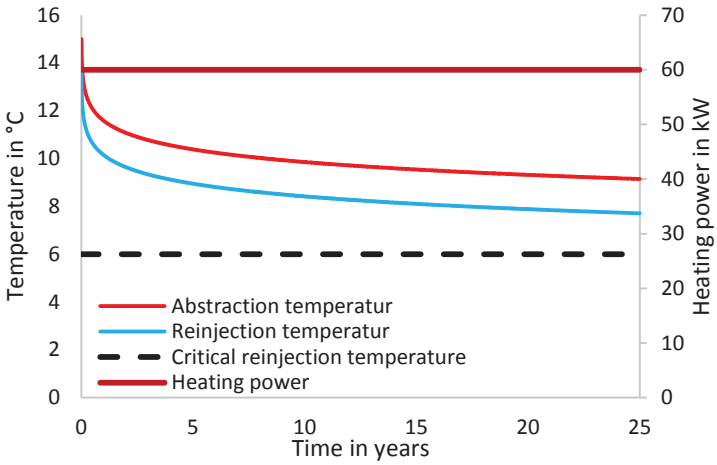


Figure 4 Temperature evolution with constant heating power of 60 kW and 25 years for the example case.

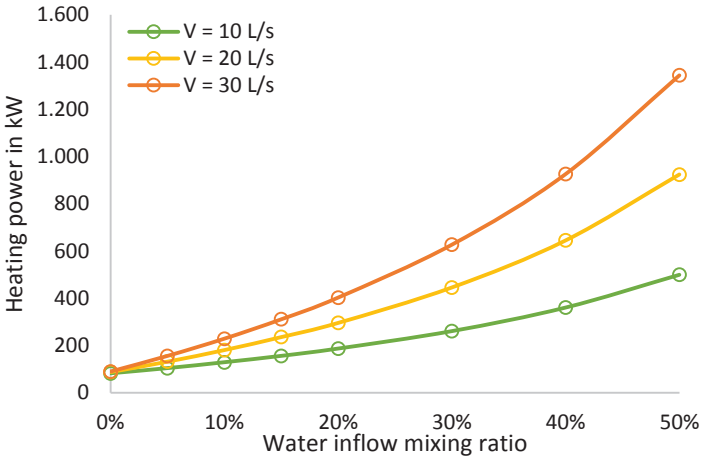


Figure 5 *Maximal heating power for three different volume flow rates at different water inflows and 25 years for the example case.*

mines provide detailed solutions to an increasing field of interest, the threshold of user accessibility often hinders more implementations on a larger scale. As a first step, this paper showed an approach to utilise a state-of-the-art analytical approach and how to compensate for the weak points by implementing the solution in an algorithm, where improvements can be built in more easily. The resulting calculation framework will work as a foundation where data from existing geothermal mine water plants can be implemented, in order to achieve more realistic estimations of the energetic potentials of mine water geothermal plants. Additionally, further research with a finite-difference-code will be conducted in order to compare the created analytical method to a numerical approach. Once the functionality of the potential calculation is validated, further research should focus also on the above ground distribution of the heat. Cold district heating networks might be suited optimally for transporting heat with minimal losses over long distances to consumers.

References

Banks D, Loredo C (2019) Low-Carbon After-Life: sustainable use of flooded coal mine voids as a thermal energy source – a baseline activity for minimising post-closure environmental risks (LoCAL). European Comission

Hoffmann M, Epperlein G (2014) EnEff:Wärme: Energieeffiziente Fernwärmeversorgung unter Nutzung der Wärme aus Grubenwässern und anderen natürlichen Wärmequellen. AGFW, Frankfurt am Main, Germany

Loredo J, Ordóñez A, Jardón S, Álvarez R (2011) Mine water as geothermal resource in Asturian coal mining basins (NW Spain), IMWA 2011, Mine Water – Managing the Challenges, Aachen, Germany

Rodriguez R, Diaz M (2009) Analysis of the utilization of mine galleries as geothermal heat exchangers by means a semi-empirical prediction method. J Renewable Energy 34:1716–1725, doi. org/10.1016/j.renene.2008.12.036

Loredo C, Banks D, Roqueñí N (2017) Evaluation of analytical models for heat transfer in mine tunnels. J Geothermics 69:153–164, doi. org/10.1016/j.geothermics.2017.06.001

Cooper, H.H., Jacob, C.E., (1946) A generalised graphical method for evaluating formation constants and summarizing well field history. Trans. Am. Geophys. Union 27:526–534, doi. org/10.1029/TR027i004p00526

LANUV – Landesamt für Natur, Umwelt und Verbraucherschutz Nordrhein-Westfalen (2018) Potenzialstudie Warmes Grubenwasser. LANUV-Fachbericht 90, Recklinghausen, Germany

Oppelt L, Grab T, Pose S, Storch T, Fieback T (2021) Mine water geothermal energy as a regenerative energy source – status quo and results from five years of monitoring. Oil Gas European Magazine:14-19

Distribution of Metals in River Sediment from Open-Pit Coal Mine Activity

Ibtisani Farahnaz[1], M. Sonny Abfertiawan[1], Mindriany Syafila[1], Marisa Handajani[1], Firman Gunawan[2] and Febriwiadi Djali[2]

[1]*Water and Wastewater Engineering Group Expertise, Faculty of Civil and Environment, B andung Institute of Technology, Jl. Ganesha No. 10, Bandung, West Java 40132*

[2]*Environmental Departement, PT. Berau Coal, Indonesiat*

Abstract

As a country rich in coal reserves and resources, Indonesia faces a potential problem of metal compounds polluting its river. Unfortunately, the quality standards for metals in Indonesia are only available in water, not sediment. This study aims to determine the distribution of metal contamination (Fe, Mn, Pb, Cr, Ni) in Lati River sediments, East Kalimantan Province, as drainage effluent from the mine wastewater treatment systems using ICP-MS. The highest to the lowest metal concentration is Fe>Mn>Cr>Pb>Ni and the highest accumulation of metals was found in streams that become drainage from the active mine wastewater treatment system.

Keywords: Metals, Acid Mine Drainage, Sediment

Introduction

Indonesia is a tropical country known for its rich resources, such as coal. Indonesian coal reserves reach 38.84 billion tons, with an annual average coal production of 600 million tons. Kalimantan island of Indonesia has the most significant potential, storing 62.1% of the country's total coal reserves and resources. The high potential of coal reserves supports demand, market forces, and politics that increases coal mining activities (ESDM 2021). Coal mining activities can cause acid mine drainage (AMD) due to the oxidation of sulfide minerals in open land, characterized by a pH lower than 3 and various concentrations of metals (Younger *et al*. 2012; Abfertiawan *et al*. 2013). Mine wastewater can cause metal pollution in aquatic ecosystems when not appropriately treated. The contamination of river sediments can also cause metal pollution in the waters. Sediment plays a vital role in the movement and accumulation of metals that can potentially cause toxicity to biota. The quality standards of metals in Indonesia are only available in water, define and monitored by government regulation No. 22/2021. Whereas, sediments have not been determined in Indonesia, even though metal compounds accumulate more in sediments than in water (Nasir *et al*. 2021).

One of the largest coal site mining in Kalimantan has the potential to form acid mine drainage (AMD) (Gunawan *et al*. 2014). AMD stored in the pit is channeled to the treatment and management system mine water treatment plant (MWTP). A previous study (Abfertiawan *et al*. 2016) showed that the Lati River, used as drainage from mining wastewater treatment effluents, is impacted by AMD and showed increased metal levels and acidic water.

This study aims to determine the distribution of metal contamination (Fe, Mn, Pb, Cr, Ni) in Lati River sediments, East Kalimantan Province, as drainage effluent from the mine wastewater treatment systems. The results of this study can hopefully provide historical information on the concentration of metal in Lati River sediments, and therefore better management scenarios can be formulated to fulfill the environmental standards.

Methods

Study Area

The study area is Lati River, Berau Regency, East Kalimantan Province, which is the effluent drainage from the mining wastewater treatment system. The sampling area is divided into 15 sampling points along 15.4 km. Sediment sampling locations are based on the 10 effluent of mine water treatment plant (MWTP) location as a mine wastewater treatment system. The study area map and illustration of the sampling point shows in Figure 1. Sediment samples were collected from the river in 5-10 cm depth using Ekman grab sampler with capacity around 250 gr (composite from left, middle, and right sides of the river) for each sampling point. All samples were stored in a cooler box at 4° during transportation from the field to the laboratory. The wet sediment samples were dried using oven until the weight was constant. The dry samples were pulverized and sieved using number 250 mesh. The measurement of metal concentration was carried out using ICP-MS under the near-total acid digestion method.

Data Analysis

Metal contamination was evaluated by comparing the concentration of metals with existing quality standards. Currently, there are no quality standards for sediment available in Indonesia. Therefore, a sediment quality guideline approach refers to the *Ontario Ministry of Environment and Energy* on *Sediment Quality Guidelines* (SQGs) (Hayton, 1993). The spatial distribution pattern of metal concentration in Lati river sediments was described by the Inverse Distance Weighted (IDW) spatial analysis tool in ArcGIS. The geo-accumulation index, Contamination Factor (CF), and Pollution Load Index (PLI) are applied to evaluate metal contamination in sediment. The background value (BKG) of metal concentration in this

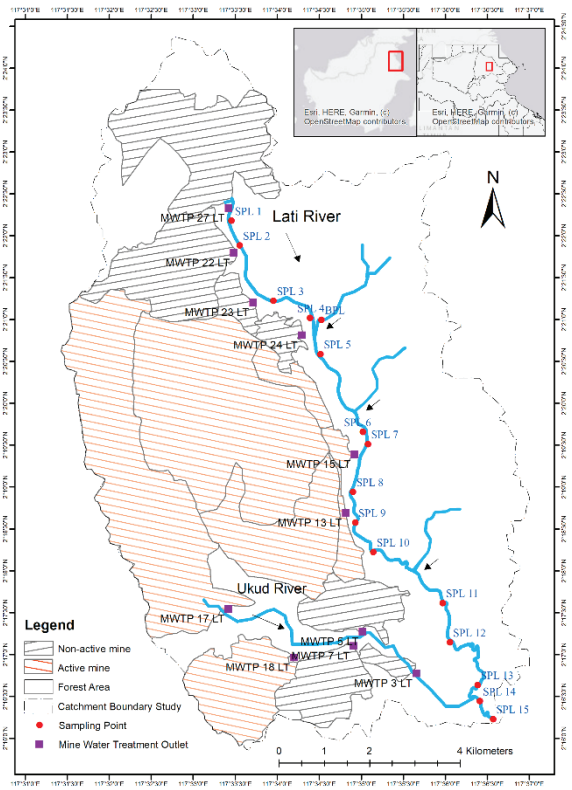


Figure 1 Map of the study area

study was based on areas with geological similarities, which the composition of heavy metals on freshwater sediments referring to Hákanson (1979).

Result and Discussion

Metal concentration

Five primary metals with the highest concentrations approaching or exceeding the limit background value in the sediment (Hákanson *et al.* 1979) in this study include Fe, Mn, Pb, Cr, and Ni. Concentrations of metals are summarized and compared with the *Sediment Quality Guidelines* (SQGs) based on the long-term toxic effects of contaminant on aquatic organism (Table 1).

The order of the highest metal concentrations in Lati River sediments was Fe > Mn > Cr > Ni > Pb. The result is in line with a study by Dlamini *et al.* (2013), where the order of metals with the highest concentration in acid mine drainage was Fe > Mn > Cr > Ni > Pb > Co > Cd > Cu > Zn.

Spatial distribution of metals in sediments

Concentrations of metals that exceed their background value can potentially act as a contaminating factor in river sediments. The distribution pattern of metal accumulation in river sediments at each sampling point is shown in Figure 2.

Based on the metal distribution in sediments of the Lati River data (Figure 2), SPL 10 (i.e., the effluent from the active mine wastewater treatment system) has the highest metal concentration, especially Mn, Cr, and Ni. An operational coal mine in the middle of the segment has the largest catchment area (1,900 hectares) of other mining sites. The larger mining area with a high Potential Acid Forming (PAF) layer will have more potential to form AMD containing various metals (Maharani *et al.* 2018). Based on the data gathered, the volume of PAF in active mining areas reached 69.76% of the total overburden layer. This partially explains the highest accumulation of metals found in the sediment of the middle river since it serves as the drainage of the mining waste treatment system with a high potential for forming AMD.

Accumulation of sediment bounded by metals can be affected by the transport and deposition of sediment on the riverbed, as well as physicochemical parameters in river water. The decrease in sediment rate can affect sediment deposition capacity in a river flow (Raposa *et al.* 2016; Asadi *et al.* 2021). In SPL 10, the sediment rate decreased (41.57 tons/day), indicating a decrease in suspended particles carried by river flows, as the potential for suspended particles to settle on the sediment surface increased (Sitorus and Susanto 2019).

Table 1 *Metal concentration in Lati River sediment*

	Metal concentration (mg/kg)				
	Fe	Mn	Pb	Cr	Ni
Mean	33,856	1,615	17.11	162.80	56.60
SD	11,466	2,664	2.11	32.63	41.38
Median	32,400	705.50	17.00	161.50	48,.0
Max	65,800	10,000	21,2	241	173.70
Min	21,700	81.5	13.75	114.50	17.05
LEL[1]	20,000	460	31	26	16
SEL[2]	40,000	1100	250	110	75
BKG[3]	40,000	860	20	49	50

[1]LEL = *Lowest Effect Level*

[2]SEL = *Severe Effect Level*

[3]BKG = *Background Value*

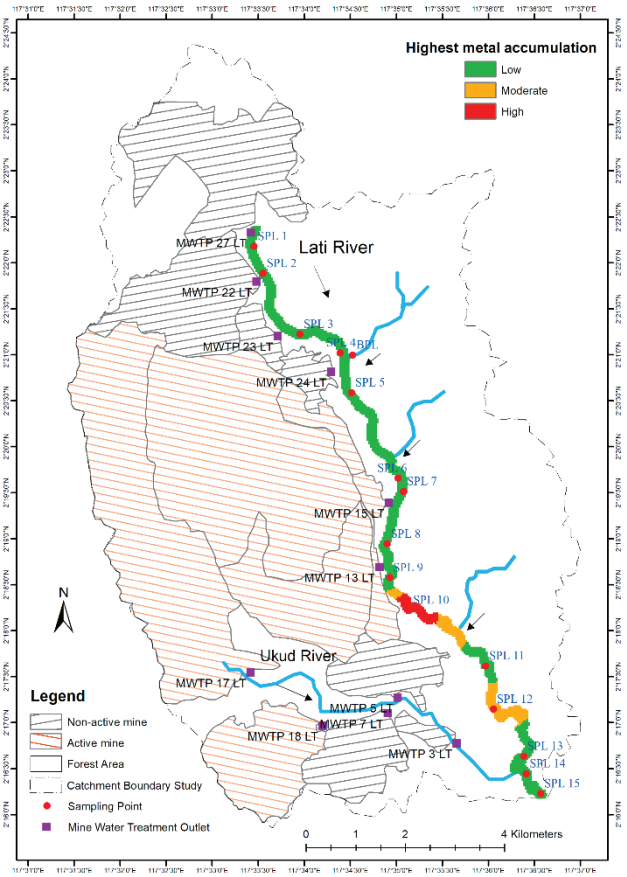


Figure 2 *Accumulation of metal contamination in the sediment of Lati River*

High velocity can cause more sediment particles carried by river flow (Erwanto and Sugata 2019). Sediment deposition is greater in areas with low gradient slopes or elevations (Wang *et al.* 2016). The velocity in SPL 10 has decreased to 0.4 m/s, with a downward slope gradient of <0.01%. This result is related to the highest accumulation of metals found in sediment at this site, where the sediment rate decreases, and the slope gradient is low so that the sediment carried in the flow decreases and has the potential to settle on the sediment surface. Physico-chemical parameters can also influence metal concentration in sediments of river water. High concentrations of the Total Dissolved Solid (TDS) in river water and a pH below 6 can indicate metal contaminants, e.g., iron, manganese, sulphate, bromide, and arsenic in river water (Alanazi *et al.* 2021).

On the other hand, the upstream segment between SPL 1 to SPL 3, which is the drainage of non-active mine wastewater treatment, showed the highest iron (Fe) concentration of 65,800 mg/kg. According to SQGs, the concentration of metal Fe at SPL 1 to 3 has exceeded the *Severe Effect Level* (SEL). The results of monitoring the outlet of the non-active mine wastewater treatment system show that the Fe concentration of 5.17 mg/L or below the quality standard. However, Fe concentration in the ex-mining pond was still high (11.58 mg/L). The runoff from the catchment area can act as a source of diffuse pollution to the river ecosystem (Debska *et al.* 2022). The catchment area from the

non-active mine wastewater treatment in the upstream river was the second largest area (1,153 ha). This condition shows that, although the metal concentration from the mine wastewater treatment outlet (as point sources) is still below quality standard, the high concentration of Fe in the ex-mining pond and runoff water from the non-active mine catchment area can be a diffuse source of Fe in river sediment. The flow rate can affect the high concentration of Fe in the sediment. A decrease in the flow rate indicates that suspended particles carried by the river flow decrease, so the particles settle on the sediment surface (Raposa *et al.* 2016; Asadi *et al.* 2021). SPL 1 to SPL 3 has a low flow rate compared to other sampling points, which ranges from 0.1 to 0.4 m^3/second.

The geoaccumulation index value (Figure 3) shows that the sediment is not contaminated (class 0) by Pb metals. Moderate contamination in sediment (class 1) was demonstrated by several metals, i.e., Fe (SPL 1), Ni (SPL 10 and 12), also Mn and Cr (several sampling points). Several sampling points tend to be highly contaminated (class 3) by Mn metals (SPL 10 and SPL 12). Another study (Wang *et al.* 2021) also showed high sediment contamination by the metal Mn, mainly from industrial waste.

The Contamination Factor (CF) load (Figure 4) differs between metals, i.e., relatively moderate at some sampling points for Fe, Mn, Cr, and Ni; high for Cr and Mn; and low for Pb. These features indicate that the Lati River sediment is high to moderately polluted with Mn and Cr metals.

Mn easily moves and dissolves in water under acidic conditions (low pH values). On the contrary, the movement of this metal in water decreases with increasing pH; thus, the metal's potential to precipitate on the sediment surface is higher. This is consistent with the results of water pH measurements in the upstream river segment, which tend to be low (ranging from 3-4), with high concentrations of Mn (1.5–2.7 mg/L) in river water and low in river sediments. Meanwhile, in the middle

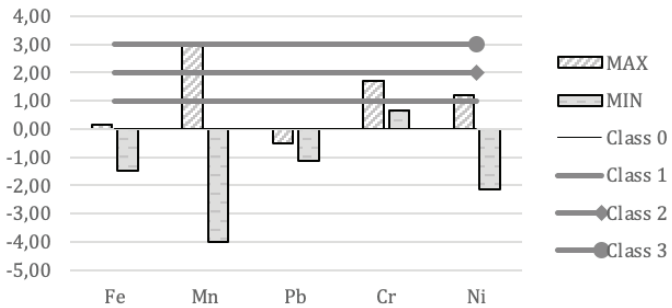


Figure 3 *Geoaccumulation index in Lati River sediment*

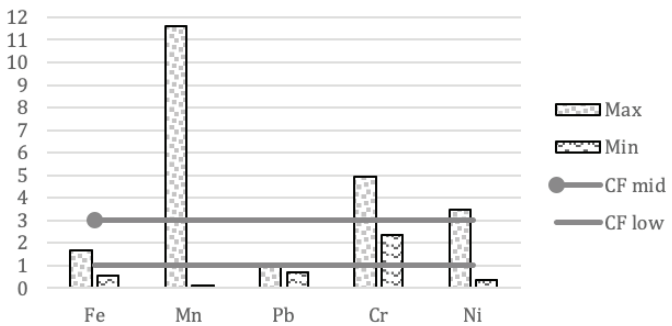


Figure 4 *Contamination factor in Lati River sediment*

part of the river, the pH of the water tends to be high (6.75), with the concentration of Mn in the river water decreasing, reaching 0.01–0.2 mg/L (HEM 2009; Aigberua 2020).

Pollution *Load Index* (PLI) was used to estimate the level of metal pollution load at the research site. PLI values at 15 sampling points showed a value of PLI < 1 (0.72 ± 1.79), indicating a basic pollutant level in the Lati River sediment. Therefore, the metal contamination did not cause a progressive decline in sediment quality. Nevertheless, regular monitoring must be done to assess the accuracy of the metal pollution load index in Lati River sediments.

Conclusions

Open-pit coal mine activity produces AMD, which has the potential to cause metal sedimentation along river sediment. Metal concentration from open-pit coal mining activities in Lati River sediment is Fe > Mn > Cr > Ni > Pb from the highest to the lowest. Based on I-geo, CF, and PLI, the river sediment surface is moderately contaminated by Fe and Ni metals; highly contaminated by Mn and Cr metals. Cr and Mn metals are high contamination factors in sediments. Overall, metal contamination in Lati River sediment has not caused a progressive decline in sediment quality. Fe, Mn, Cr, and Ni are potential metals contaminating the Lati River sediment. The highest accumulation of metals in Lati River sediments is found in streams that become drainage from the active mine wastewater treatment system.

Acknowledgments

This study was supported by the Bandung Institute of Technology through the Water and Wastewater Engineering Research Group (KK-RALC), Faculty of Civil and Environmental Engineering and the Environmental Departement of PT. Berau Coal. Additional finance and technical assistance was provided by Ganeca Environemental Services.

References

Abfertiawan MS, Gautama RS, Kusuma GJ, Wiedhartono A, Gunawan F (2013) The Challenges in Acid Mine Drainage Management in Lati Coal Mine Operation, East Kalimantan. Mine Planning and Equipment Selection Conference. Dresden, Germany

Abfertiawan MS, Gautama RS, Kusuma SB, Notosiswoyo S (2016) Hidrology simulation of Ukud River in Lati Coal Mine. Journal of Novel Carbon Resources & Green Asia Strategy. Vol 3 (1): 21-31

Aigberua AO. (2018) Effects of spatial, temporal, and pH changes on fractionated heavy metals in sediments of the Middleton River, Bayelsa State, Nigeria. MOJ Toxical. Vol 4 (6): 424-430

Alanazi YJ, Al-Masoud FI, dan Ababneh ZQ (2021) Assessment of the level of heavy metals in tap water networks system of Riyadh, Saudi Arabia. Journal of Environmental Science and Public Health 5. Pp: 137-154

Asadi H, Dastorani MT, Sidle RC, and Shahedi K (2021) Improving flow discharge-suspended sediment relations: intelligent algorithms versus data separation. Water, 13, 3650

Debska K, Rutkowska B, dan Szulc W (2022) Influence of the catchment area use in the water quality in the Utrata River. Environmental Monitoring and Assessment. 194;65

Dlamini CL, Fadiran AO, and Thwala JM (2013) A study of environmental assessment of acid mine drainage in Ngwenya, Swaziland. Journal of Environmental Protection. Vol 4 (11B): DOI:10.4236/jep.2013.411B003

ESDM (2021) Kementerian Energi dan Sumber Daya Mineral Republik Indonesia. Siaran Pers. Nomor: 246.Pers/04/SJI/2021

Gammons CH, Mulholland TP, Frandsen AK (2000) A comparison of filtered vs. unfiltered metal concentrations in treatment wetlands. Mine Water Environ 19(2):111—123, doi:10.1007/ BF02687259

Gunawan F, Gautama RS, Abfertiawan MS, Kusuma GJ (2014) Penelitian dan pengembangan sistem pengelolaan air asam tambang di Lati Mine Operation. Seminar Air Asam Tambang ke-5 dan pascatambang di Indonesia

Hákanson L (1979) An ecological risk index for aquatic pollution control – A sedimentological approach. The National Swedish Environment Protection Board. Water Quality Laboratory. Vol 14: 975-1001

Hayton A (1993) Guidelines for The Protection and Management of Aquatic Sediment Quality in Ontario. Environmental Monitoring and Reporting Branch.

Hossain Z, Hossain QH, Sultan-Ul-Islam (2015) Spatial distribution of metals in surface sediments from the Ganges River basin, Bangladesh. Arabian Journal of Geoscience. 12: 676 (209)

Maharani S, Purwanto P, Hidayat JW, and Triraharjo J (2018) Potential formation of acid mine drainage in Putra Perkasa Abadi Coal Mining Company-Girimulya site (BIB), Tanah Bumbu Regency, South Kalimantan. ICENIS

Nasir M, Muchlisin ZA, Saiful S, Suhendrayatna S, Munira, M, Iqhrammullah M (2021) Metals in the Water, Sediment, dan Fish Harvested from the Krueng Sabee River Aceh Province, Indonesia. Journal of Ecological Engineering. 22(9): 224-231

Raposa KB, Wasson K, Smith E, Crooks JA, Delgado P, Fernald SH, Ferner MC, Helms A, Hice L, Mora JW, Pucket B, Sanger D, Shull S, Spurrier L, Stevens R, Lerberg S (2016) Assessing tidal marsh resilience to sea-level rise at broad geographic scales with multi-metric indicates. Biological Concervation. Elsevier.

Sitorus A, and Susanto E (2019) A sediment rating-curve method to determine sediment discharge for rainy season inmicro-scale watershed. Indonesian Journal of Agricultural Research. Vol 2 (1): 21-27

Wang H, Resing JA, Yang Q, Buck NJ, Michael SM, Zhou H (2021) The characteristics of Fe speciation and Fe-binding ligands in the Mariana back-arc hydrothermal plumes. Geochimica et Cosmochimica Acta. Vol 292: 24-36

Younger PL, Potter HAB (2012) Hazard management and steps towards remediation of the UKs most polluted acidic mine discharge. In: 9th International Conference on Acid Rock Drainage. Canada. Parys in springtime

How Climate would likely change in future: Case study of a mine site in Kazakhstan

Saeed Golian[1], Houcyne El-Idrysy[2], Desana Stambuk[3]

[1]*SRK Consulting (Kazakhstan) Ltd, 77 Kunayev St., Park View Office Tower, 14th Floor, Almaty, Kazakhstan, sgolian@srk.kz, ORCID 0000-0001-5451-3977*

[2]*SRK Consulting (Kazakhstan) Ltd, Head Office, 5th Floor, Churchill House, 17 Churchill Way, Cardiff, CF10 2HH, Wales, hidrysy@srk.co.uk*

[3]*SRK Consulting (UK) Ltd, Head Office, 5th Floor, Churchill House, 17 Churchill Way, Cardiff, CF10 2HH, Wales, dstambuk@srk.co.uk*

Abstract

Global warming and climate change can be a threat to mining and other industries, especially those involving water supply and management, since such change could induce/amplify some climatic parameters, e.g. change in precipitation regime and temperature extremes. This study quantifies the level of climate change that may affect the development of a mine site in the northeast part of Kazakhstan, using the latest NASA NEX-GDDP-CMIP6 datasets. For this purpose, daily precipitation as well as maximum and minimum temperature for 18 global circulation models (GCMs) were analysed over three future time periods, namely 2040s, 2060s and 2080s under two shared socioeconomic pathway scenarios, i.e. SSP245 and SSP585. The period 1981-2014 was considered as the baseline period to and future climate condition compared to this period. The analysis results revealed that: (1) Both maximum and minimum temperature will increase under both SSPs in those time periods with the rate of change for minimum temperature being higher than maximum temperature. (2) The mean annual precipitation will increase by an average rate of 7% in 2040s for both SSPs and 14% and 17% for SSP245 and SSP585 in 2080s, respectively. It is also observed that summer months will experience drier condition whilst all other months will have increase in precipitation. (3) The values of 24-hr precipitation with 10-year return period will also increase under both SSP and future time period combination for most of the 18 GCMs. These predicted changes should be considered as design criteria adjustment for project water supply and water management structures.

Keywords: Climate Change, SSPs scenarios, Water Management, Mining, Kazakhstan

Introduction

With growing threat of climate change in the past few decades and exacerbation of the worst scenarios in the areas of energy, water and desertification, the pressures on natural resource management as a result of poverty has also been intensified (Deere-Birkbeck, 2009). It is believed that the risk associated to climate change is one of the most prominent threats to human societies (Hui-Min *et al*., 2021), manifested by increasing intensity, frequency and impacts of extreme weather events such as hurricanes, floods, droughts and heatwaves. Also Global Industry Standard on Tailings Management (GISTM) suggested to strengthen protections required as a result of evolving climate change impacts (ICMM, 2020).

It is widely recognised that available mining deposits are increasingly deeper and of declining ore grade. This will lead to growing demands for water as well as greater mine waste (Ruttinger and Sharma, 2016) while it is expected that climate change would increase pressure on the mining industry since more frequent droughts and floods are expected in future leading to alteration in water supply and disruption of mining operations. Climate change studies for mining projects should be adopted as a consistent

approach to help mining companies identify the risks and opportunities related to the management of water resources in all stages of the mine development and closure phase (Krogerus and Pasanen, 2016).

It is essential for mining companies to consider the climate change and its impact on sustainability and cost of water and energy supplies and use decision making tools that help them optimise use of available water resources. Climate change analysis coupled with stochastic project water balance models can provide good predictions of water surplus or deficit over mine life (and closure) and so solutions/measures are prepared and costed for at early stage of project development. To address climate change, Coupled Model Intercomparison Project (CMIP) models provides the required feasible tool to predict future climate condition under the changing conditions (Farjad *et al*., 2019). CMIP6 is the latest version of the CMIPs based on IPCC's sixth assessment report (AR6).

Due to climate models' structural uncertainties, complexity in earth-atmosphere systems and finally coarse resolution of the GCMs, the application of their outputs is limited to some extent (Chen *et al*., 2021). NASA implemented a project named NASA Earth Exchange Global Daily Downscaled Projections 6 (NEX-GDDP-CMIP6) to provide downscaled historical and future projections for the period 1950 to 2100 based on CMIP6 models (Thrasher *et al*., 2022).

While the outputs of global models provide an appropriate tool for understanding future climate conditions, however very few research has been reported on using the latest NASA NEX-GDDP-CMIP6 product in Central Asia countries. The purpose of this study is to evaluate the future climate condition at a mine site located in northeast part of Kazakhstan using the NEX-GDDP-CMIP6. The change in projected average and extreme precipitation and temperature conditions in future was evaluated to provide a more in-depth information on potential future climate conditions in the region.

Data and Methods

As mentioned above, the case study site selected for assessing the future climate condition based on different emission scenarios, is located in the northeast part of Kazakhstan (Figure 1). Based on historical data, the air temperature variability in the region is high, ranging from −14.9°C in winter (December-January-February) and +22.3 °C in the summer (June-July-August). The average annual air temperature is 4.1 °C with a mean annual precipitation of about 270mm/year.

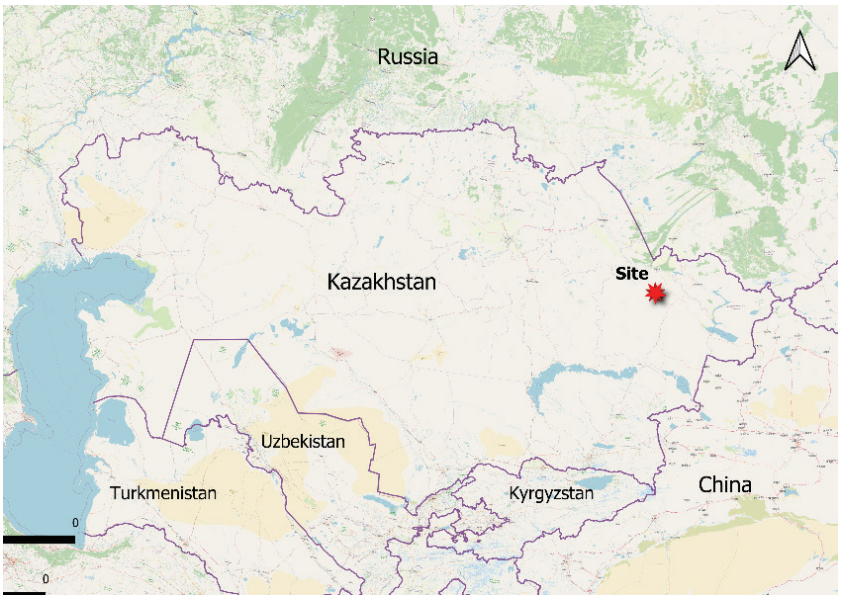


Figure 1 *Site location*

In this study, climate change for the site is assessed based on global circulation models (GCM) from NASA's NEX-GDDP dataset. Such data set is compatible with Phase 6 of the Coupled Model Intercomparison Project (CMIP6). The statistical downscaling algorithm used is a daily Bias-Correction–Spatial Disaggregation (BCSD) method (Thrasher, 2022). The NEX-GDDP-CMIP6 dataset spans the entire globe with a 0.25° (≈25 km) spatial resolution for the periods from 1950 through 2014 (historical) and from 2015 to 2100 (climate projections). Under the latest IPCC Assessment Report, AR6, two scenarios following the Shared Socioeconomic Pathway (SSP) framework where defined (SSP2-4.5 and SSP5-8.5) and are included in the analysis. Scenarios SSP245 and SSP585 shows an additional radiative forcing of 4.5 and 8.5 W/m2 representing the intermediate and high limits of the climate change projections, respectively. To reduce uncertainty in climate projections, an ensemble of GCMs' outputs is used to obtain a spectrum of possible future outcomes. The climate change studies usually take the following steps: (1): Historical data review to have a more transparent picture of the climate condition at the study site. (2) Downloading downscaled outputs of available GCMs at the site location from NEX-GDDP-CMIP6 datasets and comparing the outputs of GCMs with observed values for the baseline period. If required, bias-correction of the GCM outputs should be carried out. (3) Analysing time series of variables for interested time horizons in future under different climate change scenarios and assessing the rate of change compared to the baseline period.

To have a better projection of future climate condition, the observed data at the mine site were used to bias-correct the outputs of GCMs using quantile delta mapping (QDM) method. Finally, the effect of climate change on (1) Mean annual precipitation (MAP) as well as monthly precipitation, (2) maximum and minimum temperature at monthly time scale and (3) 24-hr precipitation with 10-year return period have been evaluated.

Results and Discussion

The change in minimum and maximum temperature at monthly scale has been calculated and the results are presented in Figure 2. This Figure is based on median temperature from all 18 models used in this study.

The results suggest that whilst both maximum and minimum temperatures will increase over the future periods the rate of increase is higher based on the pessimistic SSP585 scenario compared to the moderate scenario of SSP245. Also, the increase in temperature is higher in the far future period, i.e. 2080s compared to middle (2060s) and near (2040s) periods. The number of freezing days (days with average temperature bellow zero) will also decrease especially in March and then April and November which means less freezing condition is expected to happen during these months at the mine site (results not shown). Significant change in freezing periods and air temperature can have defining consequences on the development of projects that would rely on water sources such as glaciers or groundwater baseflow that feeds streams/rivers/lakes.

For precipitation, almost all climate models for both SSP scenarios and all future time periods predict an increase in annual precipitation (Figure 3). The only exceptions are MPI-ESM1-2-HR (all cases) and ACCESS-ESM1 over 2040s for SSP245 and 2040s and 2060s for SSP585 scenarios which show less precipitation in future compared to the baseline period. The median increase in MAP in 2040s will be approximately 5.9% and 7.9% based on RCP245 and RCP585, respectively. On the other hand, and at monthly time scale, the results suggest that July and August will experience decrease in precipitation over all time periods and SSPs whilst SSP585 shows June will also experience less precipitation over 2080s (Figure 4). All other months will experience increase in precipitation with the SSP585 causing more increase compared to SSP245 in those months.

Finally, the change in precipitations with 24-hr duration and with 10% annual exceedance probability (10-year return period) was also assessed, as illustrated in Table 2. Again, it can be seen that except a few GCMs, SSP and time horizons (e.g. CMCC-CM2-SR5 in most combination of SSPs and time horizons and FGOALS-g3 for both SSP245 and SSP585 in 2080s), in most of the cases the 24-hr precipitation

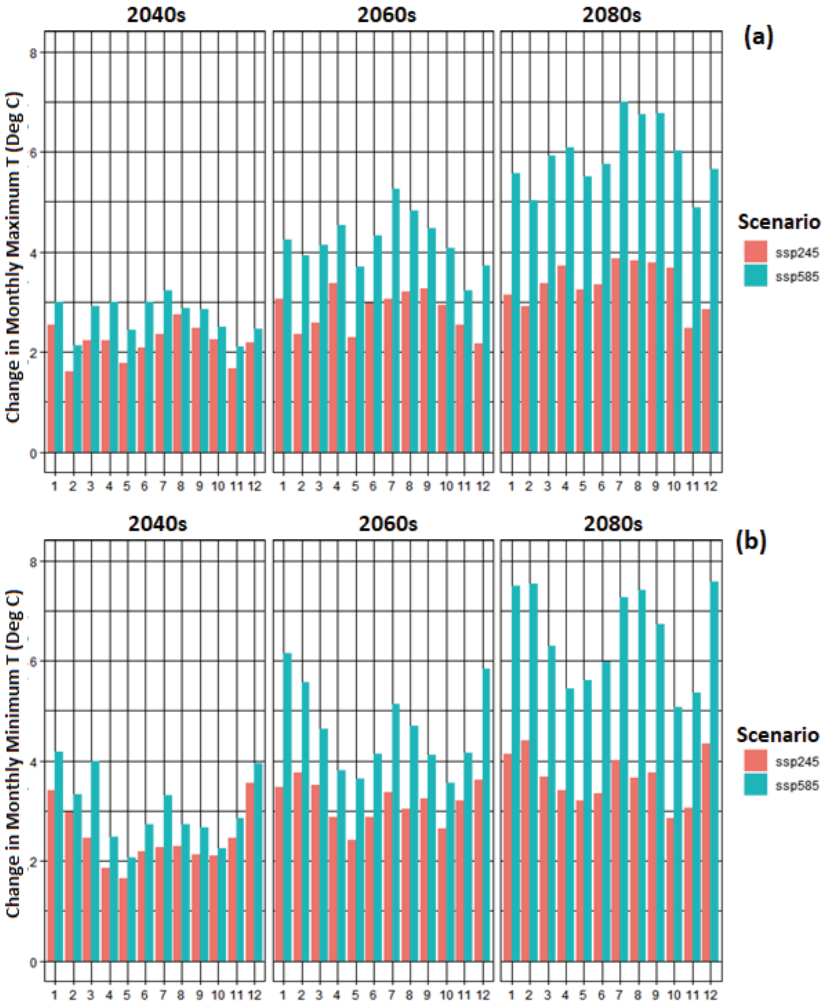


Figure 2 Change in monthly maximum (a) and minimum temperature (in Day) over future periods

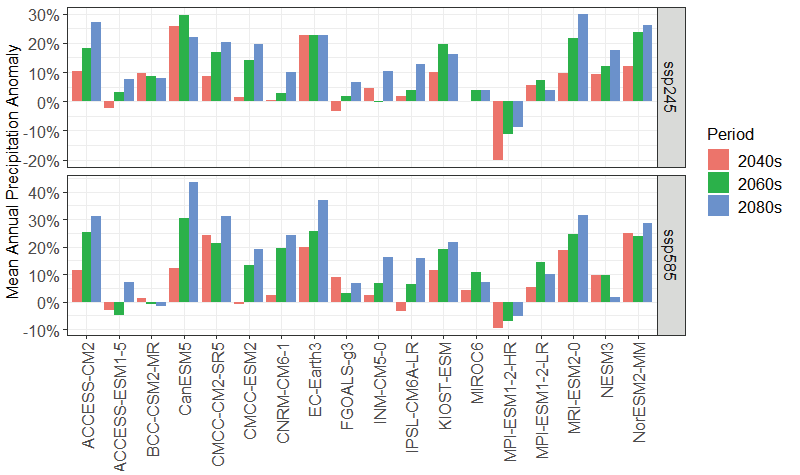


Figure 3 Rate of change (%) in MAP over future time periods and two climate change scenarios

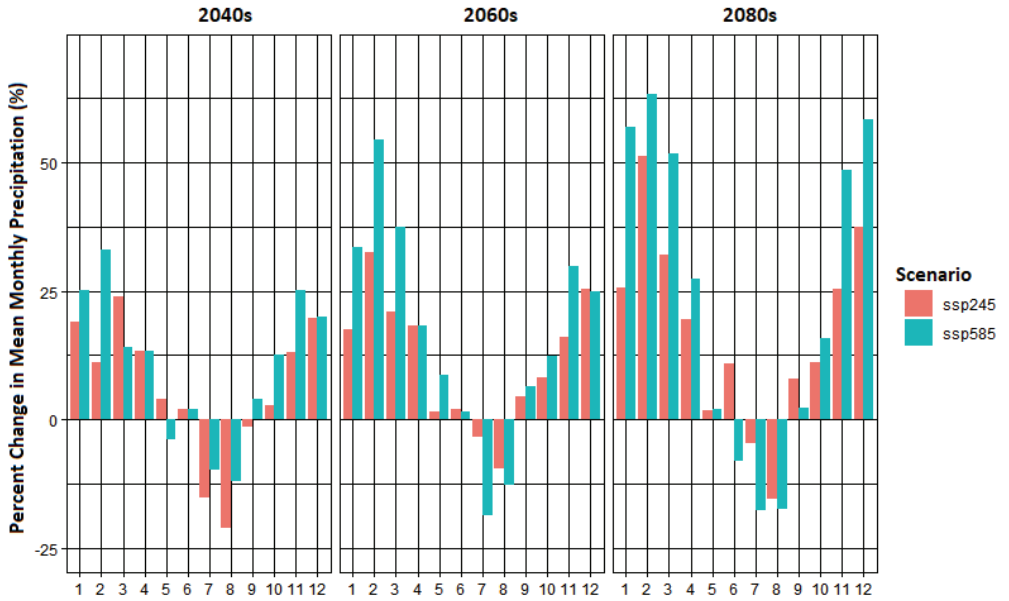


Figure 4 Rate of change in monthly precipitation over future time periods and different SSPs based on median of all GCMs used in this study

with 10-year return period is predicted to increase at the site.

Conclusion

Kazakhstan is ranked sixth in the world in terms of estimated mineral resources, and mining and metallurgy are key industries that make considerable contribution to Kazakhstan GDP. On the other hand, most of Kazakhstan is in arid and semi-arid climate with limited water resources, and the origin of the rivers used for water supply being in neighboring countries. Despite the risk of water supply shortage in near future, from

*Table 1 Percent change in 24-hr precipitation with 10-yr return period based on different GCMs**

period	2040s		2060s		2080s	
RCP	SSP245	SSP585	SSP245	SSP585	SSP245	SSP585
ACCESS-CM2	16.6	13.2	17.9	16.5	13.7	20.6
ACCESS-ESM1-5	13.5	10.8	23.2	10.7	20.9	19.2
BCC-CSM2-MR	19.2	11.6	17.9	9.6	13.7	4.5
CanESM5	4.8	3.9	7.5	11.4	8.5	19.8
CMCC-CM2-SR5	0.9	1.4	1.5	-2.6	6.9	15
CMCC-ESM2	-3.6	-9.1	-4.2	-5.4	-2.4	4.1
CNRM-CM6-1	-3.3	-3.9	8.4	6.3	17.7	5.7
EC-Earth3	17.9	20.3	18.2	17.3	24.7	13.2
FGOALS-g3	6.6	-4.1	6.4	-8.7	-8.7	-8.3
INM-CM5-0	-1.2	1.9	0	7.1	9.6	9.5
IPSL-CM6A-LR	9.8	-0.3	0.7	5.8	13.9	22.7
KIOST-ESM	15.9	4.6	20.4	5.7	8.7	10.7
MIROC6	-3.2	-1.6	-6.4	1.8	2.1	-0.8
MPI-ESM1-2-HR	8.5	9.1	14.8	11.1	6.2	9.9
MPI-ESM1-2-LR	6.5	6.8	3.1	6	6.5	10.6
MRI-ESM2-0	11.4	7.3	8.9	14.5	12.8	24.8
NESM3	-1.5	1.9	-0.4	2.6	-0.5	-5.2
NorESM2-MM	2.6	14.5	5.2	3.4	5.6	8.8

SRK's experience only a few projects have conducted studies to evaluate the future climate condition as a result of global warming and climate change.

In this research, the climate change effects on precipitation and temperature at a mine site in the northeast part of Kazakhstan were evaluated using the latest IPCC Assessment Report, AR6 Socioeconomic Pathway-Representative Concentration scenarios, namely SSP245 and SSP585.

The downscaled outputs of 18 global circulation models (GCMs) were bias corrected using observed historical values, then used to evaluate how maximum and minimum temperature as well as precipitation would likely change in three future periods, namely 2040s, 2060s, and 2080s.

The results showed that the maximum and minimum temperature is very likely to increase in future periods based on all climate models and both SSP245 and SSP585 scenarios. More increase in temperature is expected based on SSP585 in all future time periods and more increase in the far future period, i.e. 2080s compared to other two periods under both SSP scenarios. For minimum temperature, the increase will be more in winter months, i.e. in January, February and December which means less freezing hours/days are expected in the light of climate change. such predicted change is significant considering the fact that aquifer recharge and highest river flows in Kazakhstan is mainly due to snowmelt. Also this warmer climate means freeze-thaw cycles (FTCs) will increase leading to more freeze-thaw induced landslides which are one of the major geohazards especially on grasslands (Yang *et al*., 2022).

For precipitation, the average annual increase will be around 7% under both SSP245 and SSP585 in 2040s whilst under SSP245 and SSP585 in 2080s an increase of up to 14% and 17% is to be expected, respectively. At seasonal time scale, winter, spring and autumn months show increase in precipitation under most SSP and future time period combinations, whereas it is expected to have drier summer months, i.e. July and August. This could have significant consequences as under current condition the summer is the wettest season in this region with high temperature. Therefore, the analysis results suggest that climate change will alter the precipitation regime in the area, and this should be considered in the mine design and cost implication, especially in relation to water supply and management.

Finally, the results of the analysis of 24-hr precipitation with 10-year return period suggest an average increase in precipitation ranging from 4% to 10% for SSP585/2040s and SSP585/2080s scenario/future period combination. This predicted increase in precipitation and resulting runoff should be considered in the design of infrastructures, e.g. tailing facilities and diversion channels.

References

Chen, S. and Yuan, X. (2021) CMIP6 projects less frequent seasonal soil moisture droughts over China in response to different warming levels. Environmental Research Letters, 16(4), p.044053.

Deere-Birkbeck, C. (2009) Global governance in the context of climate change: the challenges of increasingly complex risk parameters. International Affairs, 85(6), pp.1173-1194.

Dike, V.N., Lin, Z., Fei, K., Langendijk, G.S. and Nath, D. (2022) Evaluation and multimodel projection of seasonal precipitation extremes over central Asia based on CMIP6 simulations. International Journal of Climatology, 42(14), pp.7228-7251.

Farjad, B., Gupta, A., Sartipizadeh, H. and Cannon, A.J. (2019) A novel approach for selecting extreme climate change scenarios for climate change impact studies. Science of the Total Environment, 678, pp.476-485.

Hui-Min, L.I., Xue-Chun, W.A.N.G., Xiao-Fan, Z.H.A.O. and Ye, Q.I. (2021) Understanding systemic risk induced by climate change. Advances in Climate Change Research, 12(3), pp.384-394.

ICMM, U. (2020) Global industry standard on tailings management.

Krogerus, K. and Pasanen, A. (2016) Management of water balance in mining areas–WaterSmart.

Rüttinger, L. and Sharma, V. (2016) Climate change and mining: a foreign policy perspective.

Thrasher, B., Wang, W., Michaelis, A., Melton, F., Lee, T. and Nemani, R. (2022) NASA global daily downscaled projections, CMIP6. Scientific Data, 9(1), p.262.

Yang, J., Wu, G., Jiao, J., Dyck, M. and He, H., 2022. Freeze-thaw induced landslides on grasslands in cold regions. Catena, 219, p.106650.

Study Of The Toxicity Of Mine Waters: Implications Of Suspended Matter On The Performance Of Tolerant Plants

Patrícia Gomes[1], Teresa Valente[1], Mafalda Sousa[1]

[1]*ICT, Institute of Earth Sciences, Pole of the University of Minho, Earth Sciences Department, Campus de Gualtar, 4710 Braga, Portugal, patriciagomes@dct.pt*

Abstract

Systems affected by acid mine drainage are extremely reactive, mainly due to the presence of nanometric particle size. The study investigates the role of suspended matter in mobilizing pollutants and increasing AMD toxicity in plants.

So, tests conducted by tolerant plants and natural acidic solutions rich in sulfate, iron, and aluminum were used in unfiltered and filtered water samples. Physical-chemical monitoring revealed improvements in the sampled effluent. The species showed a favorable vegetative evolution and no signs of senescence.

The research is intended to contribute to optimizing the biological stages of passive systems, demonstrated by the ability of Phragmites sp. for AMD remediation.

Keywords: AMD, toxicity, colloids, Phragmites sp., passive treatment

Introduction

Acid mine drainage (AMD) represents an extreme type of pollution associated with mining wastes. These highly reactive acidic solutions (pH < 3), mainly due to the presence of small particles often of nanometric sizes, present high content of sulfate and potentially toxic elements (PTE), such as iron, aluminum, and zinc (Chen *et al*., 2021). They are responsible for environmental degradation at pernicious levels of different environmental compartments (Gomes *et al*., 2014). Aquatic ecosystems are susceptible to anthropogenic activities, especially vulnerable to multistressor effects (Vári *et al*., 2022). So, the surrounding rivers and reservoirs are characterized, from an ecological point of view, by low biodiversity (Gomes *et al*., 2021). In this way, urgent mitigation and remediation measures are necessary to improve and preserve natural resources, in line with the United Nations Sustainability Development Goals (SDG-UN, Agenda, 2030).

Although there is an extensive bibliography on AMD, the toxicity of colloids and other small particles still needs to be better known. Thus, this study intends to understand what impact the content of suspended matter (typical of AMD environments), including nanometric-sized colloids, could have on phytoremediation treatment. The investigation includes using natural solutions collected in an abandoned sulfide mine, in the North of Portugal. In this sense, pilot tests were performed with the plant Phragmites sp to evaluate the remediation potential of the sampled water in two different scenarios. So, filtered water samples with 0.22 μm membranes were used to remove suspended material and unfiltered samples.

Results are intended to contribute to optimizing the biological stages of passive systems from an environmental sustainability perspective.

Methods

Valdarcas mine, exploited for W (NW Portugal), is an abandoned mine closed without environmental rehabilitation (e.g., Valente *et al*. 2007). Constituting a skarn deposit with massive sulfides, mainly pyrrhotite, and pyrite, can neutralize minerals, such as calcite and Ca-silicates. The rejected materials were deposited in waste dumps, responsible for effluent with AMD characteristics.

This mine was classified as having a high degree of danger (Santos Oliveira *et al*., 2002)

as it has one of Portugal's most reactive waste dumps. The environmental recovery project occurred between 2005 and 2007 with competent authorities (EDM).

The region has a maritime temperate climate, with an average temperature of 20.5°C, with July and August as the hottest. With 9.5°C, appear January as the coldest month. According to Gomes *et al.* (2014), it represents one of the rainiest regions of Portugal, with annual precipitation of 1470 mm.

Here, a point was chosen (V4w), where approximately 80 L of the natural solution was collected (December 2021) for pilot tests. Measurements of physical-chemical parameters were also carried out. Furthermore, 500 mL of surface water was collected in a sterilized polyethylene container for laboratory analyses. The other 50 mL was filtered with 0.22 µm membrane and acidified with HNO3. Thermo Scientific Orion was used in situ to temperature (°C), pH, electrical conductivity (EC µS/cm, at 25°C), potential redox (Eh), and total dissolved solids (TDS).

The study carried out involved the development of pilot tests that used phytoremediation as an environmental remediation technique using the species Phragmites australis. At the laboratory, 40 L of water was filtered (0.22 µm) to carry out two pilot tests: one with filtered water and another with colloids in suspension (unfiltered water).

A multiparameter HQd Field Case (Hach) was used to monitor daily procedures. This includes evaluating in situ physical-chemical parameters (pH, EC, TDS, dissolved oxygen (DO), and Eh). The follow-up of plants evolution, such as chlorophyll content (measured by spectrophotometry), number of new leaves, and color, are also contemplated. To analyze the growth of the plants during the monitoring, the Adobe Photoshop 2020 program was used to obtain measurements of a random plant from each replicate from the 1st and 11th day of monitoring. For each image, it was necessary to carry out a scale of its own. In the program, the width of the box used to carry out the tests was measured in pixels, and later the size was associated with the size in cm.

A complete hydrochemical characterization (sulfate, metals, and arsenic) took place on the 7th and the 11th day of the experiment period, by turbidimetric method (Standard Methods 4500 E) and inductively coupled plasma-mass spectrometry (ICP/MS), respectively. All the reagents were of analytical grade or Suprapur quality (Merck, Darmstadt, Germany). The standard solutions were Merck AA Certificate. Milli-Q water was used in all the experiments. Metals and arsenic analyses were performed at Activation Laboratory, Lda (Actlabs, Canada), including analysis of duplicate samples and blanks to check.

Results and discussion

Physical-chemical properties

Table 1 represents the summary of parameters evolution during the monitoring time. The results reveal that both tests showed similar behavior for replicates, presenting improved pH characteristics.

Concerning TDS and EC, it shows an immediate reduction on the first day. However, the tests revealed an increase around the 7th day, ending up with very similar EC (2520 and 2476 µS/cm in Filtered and Unfiltered replicates, respectively). The sum of the PTE analyzed showed the same behavior. The evolution of the effluent, namely the dissolution of hydroxysulfates present in the water (filtered and unfiltered), together with the interaction reactions between the effluent, the plants, and the soil, can explain the increase observed.

Regarding DO, the Filtered (RF) and Unfiltered water (RNF) replicates initially show quite different values. The NF sample shows much lower concentrations (3.08 mg/L) when compared to the Filtered sample (7.80 mg/L) right on the 1st day. There is a positive evolution of the increased concentration of this parameter up to the 7th day. However, after this period, the oxygen value tended to decrease, eventually coming close in both experiments (6.91 and 6.44 mg/L, unfiltered and filtered, respectively).

The Eh is used to characterize the reducing or oxidizing system capacity. Its evolution shows that this parameter decreased for the two pilot tests. Despite the final values

Table 1 *Parameters analyzed. Sulfate and PTE are in mg/L; RF = filtered water; RNF = unfiltered water. N.d.= not determined.*

Parameters	V4w	RF			RNF		
		1st day	7th day	11th day	1st day	7th day	11th day
pH	3,19	3,06	3,063	5,003	3,013	3,013	5,28
EC (µS/cm)	2020	1 803	1803	2520	1828	1828	2477
TDS (mg/L)	990	866	866	1517	857	857	1488
DO (mg/L)	6,35	7,80	7,80	6,91	3,07	3,68	6,44
T (°C)	8,0	28,6	33,2	33,1	25,7	34,5	32,0
Sulfate	25209	-	35196	42721	-	35905	42276
Eh (mV)	410	445	455	312	462	462	318
∑(As, Pb, Cu, Zn, Cd, Al, Fe, Mg)	2055224	n.d	113406	175821	n.d.	108022	171338

showing improvements, according to Reddy & DeLaune (2008), they continue to reflect the oxidizing environment in which they are found since they present values between 700 mV and 300 mV.

Vegetative evolution

Phragmites australis is a species used worldwide in treating contaminated water due to its resistance to PTE, presenting characteristics that promote efficient phytoremediation (Rezania *et al*., 2019). In order to understand the evolution of the plant itself in the face of stressful situations, a count was carried out to analyze the development capacity by increasing or not the number of shoots. Table 2 presents these results, showing the number of shoots and compared to the starting number.

The results indicate that both tests showed an increase in the number of shoots at the end of the experiments. These had identical behavior in both pilot tests for Filtered Water and Non-Filtered Water; however, the Filtered Water test had a higher number (average of 35). The number of shoots in the Filtered Water test may be related to decreased suspended colloids. This increase appeared more evidently next to the stems of the larger Phragmites australis.

It is possible to observe, through Figure 1, a replica of the tests, which contains Filtered Water, on the 1st and 11th day of monitoring. The plants, in general, showed good growth and development.

In general, the species used remained healthy, from a visual point of view, and showed no signs of loss of vitality. The leaves, with a yellowish color observed, are the same as at the beginning of the monitoring, with no signs of senescence.

The results (tab. 3) reveal that the Pilot Test of Filtered Water presents a greater growth than the Pilot Test of Unfiltered Water. Shoots measurements were also done using the same program (Adobe Photoshop 2020).

For each replica, a shoot was selected, and through a scale specific to each photograph, the measurements of the 1st day of the test and the 11th day were taken so that it was possible to make a difference and achieve growth, which is recorded in Table 4.

Table 2 *New shoots that emerged during monitoring.*

Quantification of shoots – Phragmites australis				
Replica	Number of shoots		Difference	Mean
	Start	End		
R1F	8	50	42	35
R2F	12	35	23	
R3F	13	53	40	28
R1NF	10	39	29	
R2NF	16	43	27	
R3NF	11	39	28	

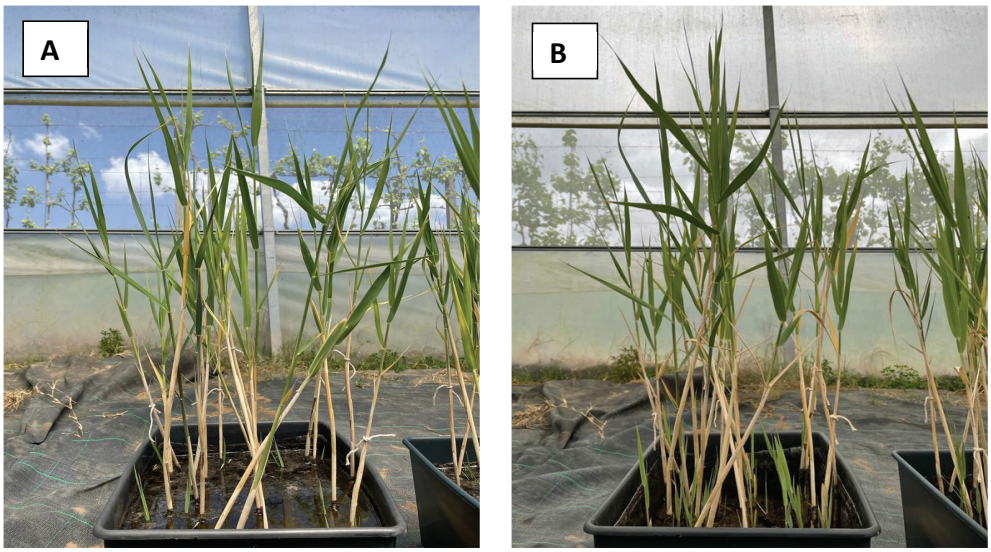


Figure 1 *Replica of the Filtered Water Pilot Test. "A" corresponds to the 1st monitoring day, and "B" corresponds to the last day.*

Table 3 *Phragmites australis growth (in cm), performed using Adobe Photoshop 2020 measurements.*

Measurement	R1F	R2F	R3F	R1NF	R2NF	R3NF
1st Day	17.06	24.56	23.99	22.74	20.87	22.86
11th Day	20.90	28.24	24.63	23.51	26.11	23.48
Difference	3.84	3.68	0.64	0.77	5.24	0.62
Mean	2.72			2.21		

Table 4 *Phragmites australis shots growth (in cm), performed using Adobe Photoshop 2020 measurements*

Measurement	R1F	R2F	R3F	R1NF	R2NF	R3NF
1st Day	4.92	6.27	4	3.50	7.17	8.36
11th Day	11.59	11.48	9.22	10.37	12.13	10.96
Difference	6.67	5.21	5.22	6.87	4.96	2.60
Mean			5.7			4.81

Generally, the Phragmites australis plants from the Filtered Water Pilot Test show better results; however, the difference compared to the Non-Filtered Water Pilot Test is irrelevant. Both tests gave their plants a healthy appearance and increased the number of shoots. Exposure to the effluent had no visible consequences on the *Phragmites australis* used. The high values of EC, sulfate, TDS, and the presence of PTE seem not to have created restrictions for their development, as can be seen by the formation of new shoots. The plants thus demonstrated, in all replicates, a good adaptation and development in the face of the subject conditions.

Photosynthetic pigments: chlorophyll a and b

Figure 2 shows chlorophyll a and b, evaluated at the end of the tests, for both replicates: filtered and unfiltered, as it also considers the control group, plants not subject to AMD. The results indicated that the RNF pilot trial has higher Chl a and Chl b values than the control group and the RF trial. However, the difference between the latter was not

relevant. The characteristic elements of this type of water have boosted the plant's development and its chlorophyll levels. The results indicate that the plants used to treat the mining effluent present regular activity even when exposed to several pollutants and a low pH. According to Khaleghi *et al.* (2012), water stress can potentiate a decrease in chlorophyll concentration due to the sensitivity that this pigment has to environmental pressures. However, this fact was not verified. Despite being subjected to high evaporation conditions, the plant used in the phytoremediation tests maintained and increased its concentrations of chlorophyll a and b, showing no signs of senescence. The same results would have already been reported by Gomes *et al.* (2020) in studies related to acidophilic algae, where the authors reported obtaining higher concentrations of chlorophyll in the dry season when evidence of AMD was more intense.

It is believed that Phragmites australis, through the phytoremediation technique, may be resistant to PTE contained in its effluents. As observed by other authors (e.g., Romaní and Sabater, 2000), despite extreme conditions, photosystem II (PSII) is not damaged, most likely due to adaptation mechanisms. Therefore, it is thought that the plants used have stable vital functions, with the amount of chlorophyll not being affected.

Conclusions

The pilot tests demonstrated that, in general, there was a reduction in the contaminating potential of AMD. The plants included in the tests (Phragmites australis) seemed to support high amounts of contaminants, efficiently reducing elements with disruptive characteristics for the environment. Trial monitoring revealed that they maintained their growth rates and healthy development, including forming new shoots. Chlorophyll a and b concentrations were even higher than the control group, showing no signs of senescence. Particles of nanometric dimensions do not influence the toxicity of the evaluated plants. The interaction of these with the substrate may be the key to dynamic phytoremediation processes, and its more in-depth study is critical.

Acknowledgments

The authors thank the company PhytoClean (www.phytoclean.pt), which provided the plants

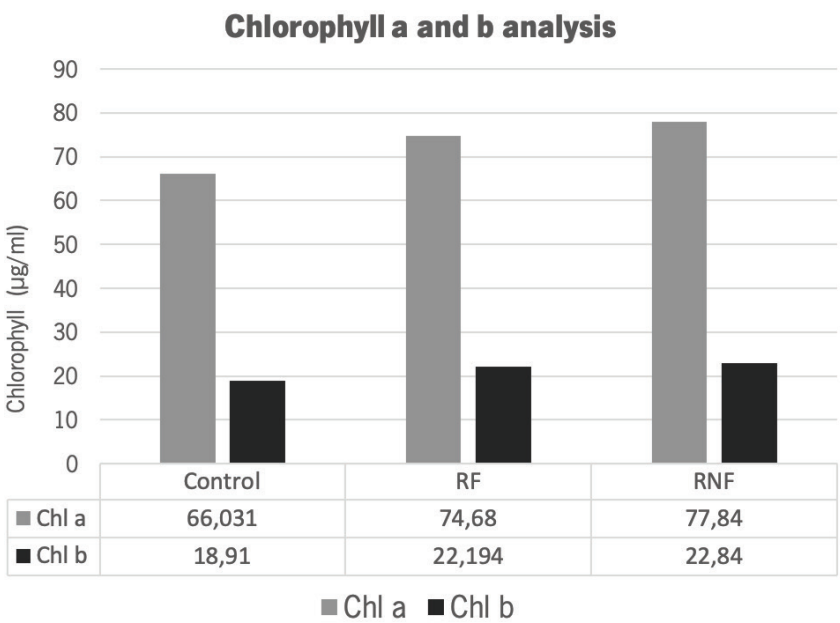


Figure 2 *Concentration of Chl a and Chl b in the tests carried out: RF, RNF, and control.*

and allowed the performance of the pilot tests. This work was co-funded by FCT through projects UIDB/04683/2020, UIDP/04683/2020, and Nano-MINENV 029259 (PTDC/CTAAMB/.29259/2017).

References

Gomes P, Valente T, Pamplona J, Sequeira Braga MA, Pissarra J, Grande Gil J A, de la Torre ML (2014) Metal Uptake by Native Plants and Revegetation Potential of Mining Sulfide-Rich WasteDumps. International Int. J. Phytoremediation, 16(11), 1087–1103. doi:/10.1080/15226514.2013.810586

Gomes P, Valente T, Geraldo D, Ribeiro C (2020). Photosynthetic pigments in acid mine drainage: Seasonal patterns and associations with stressful abiotic characteristics. Chemosphere, 239, 124774, doi: /10.1016/J.CHEMOSPHERE.2019.124774

Gomes, P (2021) Impact of acid mine drainage on the environmental quality and potential accumulation of strategic metals in water dams located in the Iberian Pyrite Belt. University of Minho

Khaleghi E, Arzani K, Moallemi N, Barzegar M (2012) Evaluation of Chlorophyll Content and Chlorophyll Fluorescence Parameters and Relationships between Chlorophyll a , b and Chlorophyll Content Index under Water Stress in Olea europaea cv . Dezful. International Scholarly and Scientific Research & Innovation, 6(8), 2108–2111.

Portuguese Environment Agency (2021) Criteria for the Water Masses Classification. 160. https://apambiente.pt/sites/default/files/_Agua/DRH/ParticipacaoPublica/PGRH/2022- 2027/3_Fase/PGRH_3_SistemasClassificacao.pdf

Reddy KR, DeLaune RD (2008) Biogeochemistry of Wetlands: Science and Applications. CRC Press, doi:/10.1201/9780203491454

Rezania S, Park J, Rupani PF, Darajeh N, Xu X, Shahrokhishahraki R (2019) Phytoremediation potential and control of Phragmites australis as a green phytomass: an overview. Environ. Sci. Pollut. Res. 2019 26:8, 26(8), 7428–7441. doi:/10.1007/S11356-019-04300-4

Romaní A, Sabater S (2000) Influence of Algal Biomass on Extracellular Enzyme Activity in River Biofilms. Microb Ecol 40, 16–24. doi: 10.1007/s002480000041

Santos Oliveira JM, Farinha Ramos J, Matos JX, Ávila P, Rosa C, Canto Machado MJ, Danie, FS, Martins L, Machado Leite MR (2002) Diagnóstico Ambiental das Principais Áreas Mineiras Abandonadas do País. Boletim de Minas, 39(January), 67–85.

Valente T, Gomes C (2007) The role of two acidophilic algae as ecological indicators of acid mine drainage sites. J. Iber. Geol., 33

Vári Á, Podschun SA, Erős T, Hein T, Pataki B, Iojă IC, Adamescu CM, Gerhardt A, Gruber T, Dedić A, Ćirić M, Gavrilović B, Báldi A (2022) Freshwater systems and ecosystem services: Challenges and chances for cross-fertilization of disciplines. Ambio, 51(1), 135–151, doi:/10.1007/s13280-021-01556-4

Use of Groundwater Numerical Model to Support Decision Making At Large Open Pit

Manuel Gutierrez[1], Martin Brown[2]

[1]*Itasca Chile, Providencia, Santiago, Chile, manuel.gutierrez@itasca.cl*

[2]*Itasca Australia, Scarborough, WA 6019, Australia, mbrown@itasca.com.au*

Abstract

Predictive simulations of a Large Open Pit groundwater numerical model were used to support investment decisions on dewatering and depressurization infrastructure. As the obtained results are deterministic, an uncertainty analysis was developed applying the linear Monte Carlo methodology.

A series of numerical models were run using 100 random combinations of hydraulic conductivities ranging within conceptual values. Results were validated in the calibration period to assess their compliance with the conceptual understanding and calibration standards used as reference. Model outputs were interpreted as a probability of occurrence and enabled providing confidence limits to the predictive flow rates to be managed.

Keywords: Dewatering, depressurization, oredictive simulations, uncertainty analysis.

Introduction

Presence of water in mining operations has an adverse effect (Read & Stacey 2009; Beale & Read 2013). Pore pressure in the rock mass reduces pit slope stability (Hoek & Bray 1981; Sullivan 2007), while seepage in pit slopes generates surface water flow, that lead to losses in efficiency, unsafe working conditions, and higher costs of operation.

Groundwater numerical models are commonly used as a tool in the decision-making process related with slope designs and, dewatering and depressurization infrastructure planning. They are based on conceptual models that are developed from geological and hydrogeological interpretation and hydraulic tests field data, which are subject to different levels of uncertainty. These models are typically calibrated against measured water levels, pore pressures and seepage zones. Even when they comply with state-of-the-art calibration standards and may accurately reflect field data, the models will always have a level of uncertainty that needs to be assessed. Uncertainty analysis of predictive simulations is recommended before using them as support tools.

Life of Mine (LoM) of the open pit under study extends for at least 40 years, and will become one of the deepest worldwide, facing big depressurization challenges to maintain slope stability and dewatering requirements to support mining operations.

As some decisions rely on the accuracy of hydrogeological characterization and numerical models built with it, it is crucial to lower the risk related to the uncertainties of available information and predictive simulations. Besides increasing the number of boreholes and hydraulic tests to improve conceptual understanding and numerical representation, which involves time and considerable costs, a way to face this uncertainty is by identifying the main parameters that affect predictive simulation results and developing an uncertainty analysis. This methodology allows going from a deterministic to a probabilistic approach where results are interpreted as the probability of occurrence that helps to account for the risk of the decisions made.

Background Information and Conceptual Model

Situated in the highlands of the Atacama Desert, the main recharge to the open pit comes from precipitation occurring from

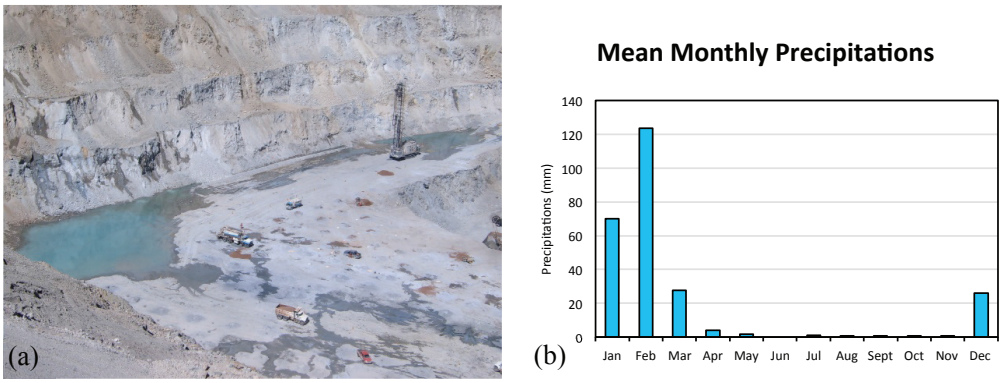


Figure 1 *(a) Pit floor flooding due to seepage. (b) Mean monthly precipitations in the vicinity of the pit.*

December to March (fig 1b). Groundwater flows through low to very low permeability rocks and is mainly controlled by faults that generate anisotropy and high heterogeneity. Outflows take place through creeks, evapotranspiration, seepage in the pit (fig 1a) and active dewatering and depressurization infrastructure.

Geology consists of pyroclastic and volcanics deposits with plutonic intrusives, covered by alluvial, colluvial and glacial sediments. Hydrogeological units (HU) (fig 2a) are separated by the main structures that have been identified either as hydraulic barriers (LP3, LP4 and LP5) to groundwater flow or as conduit faults (LP1 & LP2) that favour it. This criterion also matches with different lithologies, grouping HUs with similar characteristics, like the predominance of sedimentary rocks over volcanic ones. Subsequently, these groups have been subdivided considering their hydraulic response to the pit drainage, accounting for areas of similar hydraulic conductivity.

A large amount of data has been collected since the operation started in the mid-1990s with the pre stripping of the open pit. More than 100 Vibrating Wire Piezometers (VWP) with 2 to 5 sensors at different depths have been installed and more than 80 dewatering wells are active in the vicinity of the pit. Most of these infrastructures are connected to wireless networks, enabling real time data to be gathered by the operation from areas with difficult access which lowers the risk of errors from manual data collection. Collected data are regularly analysed and compared with the existing conceptual model to verify and adjust conceptual understanding.

New hydraulic test data were used to assess the definition of hydrogeological units and the hydraulic conductivity ranges that were assigned to them, suggesting no changes or reinterpretation was needed from what had been determined in previous conceptual models. A general trend of lower permeability with depth is observed from hydraulic tests (fig 2b), following what has been noted in crystalline rocks due to greater total stress acting on the rock at larger depths (Beale & Read 2013).

Geological mapping of fault zones focussed on estimating their potential permeability by describing the clay content observed in core logs from drilled boreholes. This information was used to confirm the hydraulic characterization of the main faults zones that control flow direction in the study area.

Numerical Model

A 3D groundwater model was developed using MINEDW™ (Azrag *et al.* 1998: Itasca Denver, 2019), which uses a finite-element approach to simulate groundwater flow in both saturated and unsaturated domains. MINEDW simulates the excavation of a pit by allowing the elevation of nodes to vary through time, adjusting the zone of relaxation (ZOR) based on the mining schedule and predicting pore pressures that can be used in geomechanical modelling.

The model grid consists of triangular prism elements with variable horizontal and vertical sizes depending on their location in

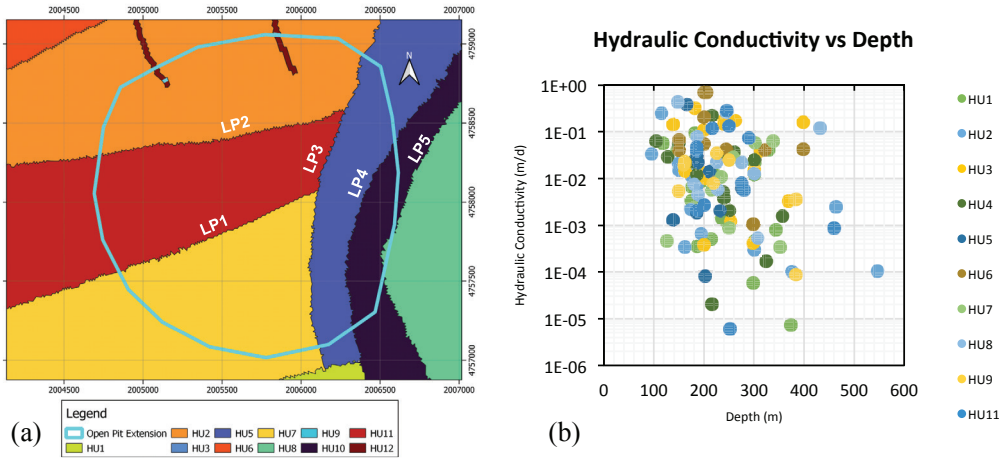


Figure 2 *(a) Plan view of Hydrogeological Units and Principal Faults in the open pit. (b) Relation between Hydraulic Conductivity and depth of hydraulic tests.*

the model domain. Elements within the open pit and fault zones areas are 15 to 16 m, and gradually increase their size to the boundaries of the model, reaching 500 m horizontally and 750 m vertically. This model has a total of 7,268,487 nodes and 14,197,601 elements. The vertical extension is from the topography of the area 4,600 m.a.s.l. to 2,000 m.a.s.l.

HUs and structural model were explicitly incorporated independently into the model from the 3D geometries, which enables making individual changes to assigned hydraulic parameters to perform sensitivity or uncertainty analysis. Twenty-five years of excavation sequence of the open pit was incorporated implicitly from real monthly topographies, to match the monthly time-step temporal discretization. Annual topographies were included for predictive simulations considering mining development for the next 40 years.

Zone of Relaxation (ZOR) is explained by the decompression of the different materials that compose the rock mass due to continuous

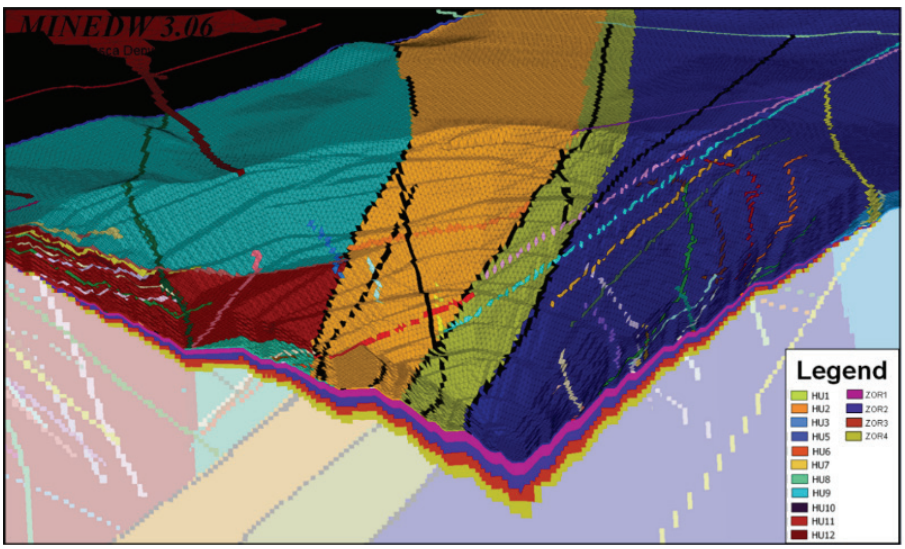


Figure 3 *Hydrogeological Units and Zone of Relaxation of the open pit. Visualization in MINEDW software.*

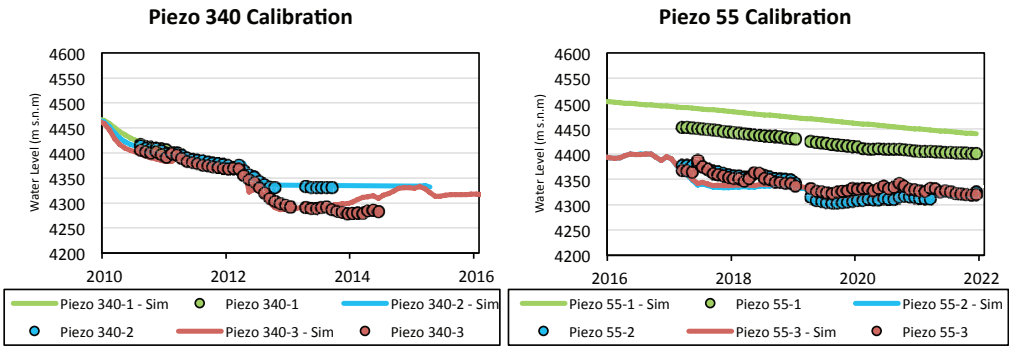


Figure 4 *Calibration examples for different piezometers. Dots represent field data and lines simulations.*

lithostatic unloading and blast operations, which result in increased permeability in the pit slopes, and is directly related to the "damage factor D" defined in slope stability models (Itasca 2014). Following geomechanical modelling previously done, ZOR has been considered in the groundwater model with a total thickness of ¼ of the depth of the pit for each time step, divided into 4 uniform layers that account for its total thickness (fig 3). Different ZOR configurations were sensitized, showing that this criterion fits the best for the calibration period.

Calibration and Simulations

Calibration of the numerical model considers water levels and its trends due to depressurization or pressurization, and vertical hydraulic gradients that have been measured in VWP sensors at different depths (fig 4). Results indicate that while the calibration meets the recommended standards (Barnett et at 2012; SEA 2012), with a standard root mean square error (SRMS) of 6.2% (recommended <10%), mean absolute error (MAE) of 35.7 m and normalized MAE (nMAE) of 4.6% (recommended <5.0%), it also reproduces mapped seepage faces and flow rates defined in the conceptual model.

After calibration, the numerical model is used to make predictive simulations for different time horizons. Short-term predictions are used to understand location of seepage faces and groundwater presence within a bench depth, to plan for depressurizations and dewatering needs as the mine progresses.

Medium-term predictions are used to assess pore pressure distribution for slope stability analysis, and to plan for future dewatering and depressurization infrastructure. This simulation is also used to estimate potential dewatering flow rates to plan for water management infrastructure.

As the Life of Mine extends for 40 years, the pit is expected to reach dimensions that require careful stability analysis of slope designs. Hence, the main output from Long-term predictions is pore pressure distribution for specific long-term topographies that are key for the operation. As the pit expands to areas with less amount of field data, it is expected that uncertainty of long-term predictive simulations increases.

Uncertainty Analysis

Uncertainty is caused by different factors and depends on the complexity of the hydrogeological system (fig 5), with four main sources affecting numerical models at different levels (Middlemis *et al.* 2019); structural and conceptual, parameterization, measurement error, and scenario uncertainties, including climate change variations. Considering these sources, it is important to define an objective for the uncertainty analysis outcome, making sure it answers the management questions.

In this study, medium-term predictive simulations were used to plan for dewatering and depressurization wells and, other related water management infrastructure, based on the expected location of groundwater within the pit, seepage faces and the flow rates that need to be managed.

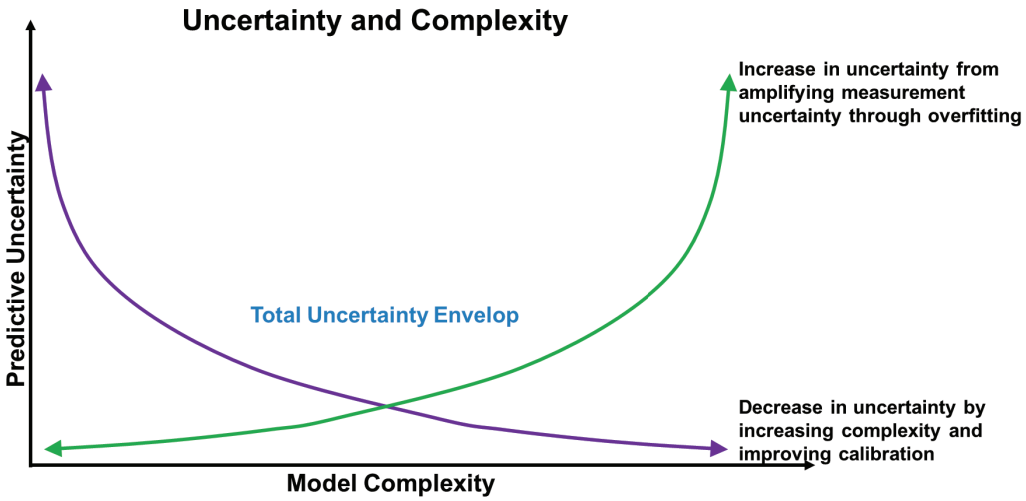


Figure 5 Relation of the Total Uncertainty and Model Complexity (Adapted from Barnett et al. *2012).*

As the calibrated model provides deterministic results based on the calibration of hydraulic parameters, which don't necessarily account for their specific distribution within the different hydrogeological units, nor if these are linked, a "Deterministic modelling with linear probability quantification" uncertainty analysis was developed (Middlemis H & Peeters LJM 2018). This methodology is less complex than a Bayesian analysis, but it provides an understanding regarding uncertainty, and is not subjective as an analysis of subjective probability (Barnett *et al* 2012).

Therefore, the uncertainty analysis was carried out by running the numerical model with 100 random combinations of hydraulic conductivities, varying their values within those defined by the conceptual model. Results of each model were validated in the calibration period to determine if they reproduced the assumptions indicated in the conceptual model and the calibration standards used as reference, and these validated results were used to understand the probability of seepage flow rates and pumping rates from dewatering and depressurization wells.

Results and Discussion

Outputs from the uncertainty analysis were interpreted as a probability due to its normal distribution, enabling the definition of confidence limits. Total expected seepage flow rate for 2015 is expected to be between 3,400 to 7,900 m^3/d with 90% of

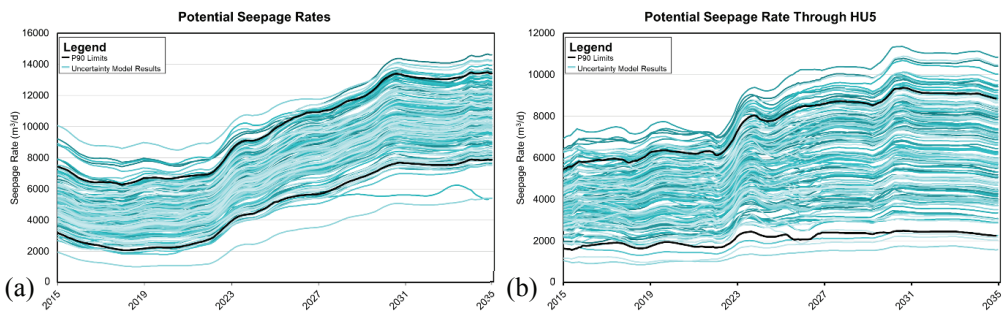


Figure 6 (a) Total Seepage flow to the pit; (b) Seepage flow through HU5 unit.

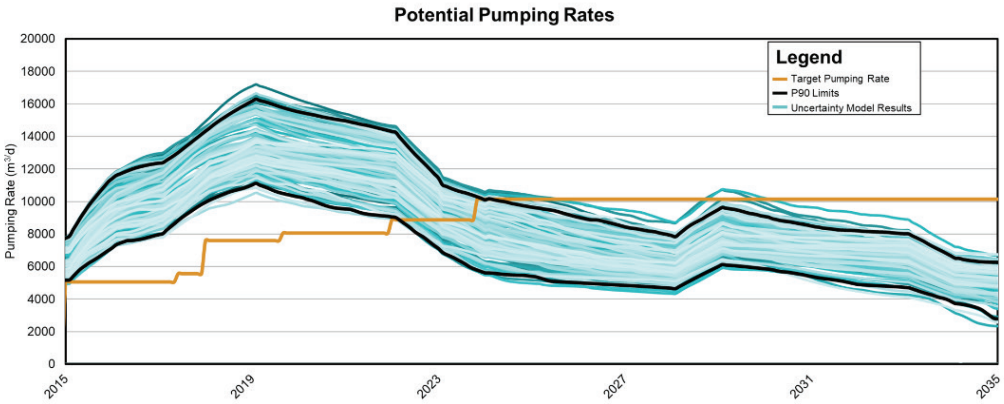


Figure 7 *Pumping wells flow rates.*

confidence (fig 6a), with most of it seeping through HU5 (1,800 to 5,200 m3/d) (fig 6b). The higher groundwater contribution and variability of predictions throughout the simulation period, suggests that HU5 represent the most uncertain unit and that further hydrogeological characterization is of high priority.

This operation must ensure a certain flow rate from dewatering and depressurization wells, so the uncertainty analysis was also focused in understanding pumping flow rates from the current wells plan with 90% confidence (fig 7). Results show that since year 2024 there is a risk that the target flow rates won't be met, suggesting the need of revisiting the current plan, via replacing lower flow rate pumping wells or adding new ones. It also indicates that further field studies should be developed to lower the conceptual uncertainty of future years, especially in areas with less amount of information.

Conclusions

Based on the current conceptual understanding, the hydrogeological numerical model developed in MINEDW reasonably simulates past and current hydrogeological conditions of the open pit and, was used to conduct predictive simulations to help with the decision making of the mine operation in different scopes. To provide additional input, an uncertainty analysis was developed over the conceptual hydraulic parameters used in the calibration, with the aim of identifying confidence limits of predictive seepage and pumping rate flow rates.

Predictive flow rates from HU5 present high variability and are found to be the highest contributor to overall seepage flows in the open pit, being above the conceptual understanding. This suggests that further characterization is needed to better understand ongoing and future hydrogeological processes as the mining progresses to improve its numerical representation. Based on the current dewatering and depressurization plan that was studied using the numerical model, predictive pumping flow rates since 2024 would not be enough to meet environmental commitments, suggesting the need of revisiting the current plan.

Investment strategical decisions regarding the definition of dewatering and depressurization infrastructure were made considering the results from the uncertainty analysis developed. It also provided input on zones within the current open pit and projected mine designs, with higher conceptual uncertainty that need to be addressed via additional hydrogeological characterization (field works) and data reinterpretation. With the new data gathered the conceptual model needs to be updated to improve the numerical tool used in the dewatering and depressurization decision-making process.

Acknowledgments

The authors acknowledge Dr. Steve Meyerhoff and Mr. Cliff Tonsberg for their comments and review of this paper.

References

Azrag, E, Ugorets, VI & Atkinson, LC. (1998). Use of a finite element code to model complex mine water problems, Proceedings of Symposium on Mine Water and Environmental Impacts, IMWA, Johannesburg.

Barnett *et al.* (2012). Australian groundwater modelling guidelines, Waterlines report, National Water Commission, Canberra.

Beale, G., Read, J. (2013) Guidelines for evaluating water in pit slope stability. CSIRO Publishing, Collingwood.

Hoek E., Bray J.W. (1981). Rock Slope Engineering, London: Institution of Mining and Metallurgy, 527.

Itasca Denver (2019). MINEDW Ver. 3.06. Denver: Itasca.

Middlemis H and Peeters LJM (2018) Uncertainty analysis – Guidance for groundwater modelling within a risk management framework. A report prepared for the Independent Expert Scientific Committee on Coal Seam Gas and Large Coal Mining Development through the Department of the Environment and Energy, Commonwealth of Australia 2018.

Middlemis H, Walker G, Peeters L, Richardson S, Hayes P, Moore C. (2019). Groundwater modelling uncertainty – implications for decision making. Summary report of the national groundwater modelling uncertainty workshop, 10 July 2017, Sydney, Australia. Flinders University, National Centre for Groundwater Research and Training, Australia.

Read, J., Stacey, P. (2009). Guidelines for Open Pit Slope Design. CSIRO Publishing, Collingwood.

Servicio de Evaluación Ambiental, SEA. (2012) Guide for the Use of Groundwater Models in the SEIA [in Spanish]. Santiago.

Sullivan, T. (2007). Hydromechanical Coupling and Pit Slope Movements, in Y Potvin (ed.), Slope Stability 2007: Proceedings of the 2007 International Symposium on Rock Slope Stability in Open Pit Mining and Civil Engineering, Australian Centre for Geomechanics, Perth, pp. 3-43.

Walker G. (2017). Predictive uncertainty in groundwater modelling: how is it best used? Discussion paper no.1 in Middlemis *et al.* 2019. Groundwater modelling uncertainty – implications for decision making. National Centre for Groundwater Research and Training, Australia.

Secondary gypsum and HFO affected the mobility of critical metals (Be & W) in historical skarn tailings, Yxsjöberg, Sweden

*Lina P.B. Hällström, Emma Flodin

*Applied Geochemistry, Lulea University of Technology; *Lina.Hallstrom@ltu.se;*
ORCID iD: 0000-0003-3438-4818

Abstract

Beryllium (Be) and tungsten (W) are both classified as Critical Raw Materials (CRM), but their geochemistry in near-surface environments is not well understood. The mobility is largely dependent on the stability of hosting minerals. Uptake of Be and W in secondary gypsum and hydrous ferric oxides (HFO) on the shore of Smaltjärnen skarn tailings, Sweden, was studied with sequential extraction, low-vacuum SEM-EDS and DXRD (Differential X-ray Diffraction). The results showed that W was hosted to HFO, while Be adsorbed/co-precipitated temporarily with secondary gypsum. Gypsum was dissolved upon rainfall and Be was released to the surface water while W settled to the sediments a few hundred meters from the mine site.th America (El Soldado) are provided and the future of TSF monitoring is discussed.

Introduction

The EU is striving for a higher domestic production of CRM, e.g., Be and W, to secure that the European Green Deal is reached by 2050 (European Commission, 2023a). On March 16th, 2023, The European Commission published an updated list of CRM together with the Critical Raw Materials ACT, stressing the importance to implement domestic production of CRM in Europe (European Commission, 2030a, b). The CRM Act also states the need to increase efforts to mitigate any adverse impact regarding environmental protection related to CRM mining. To achieve sustainable mining, environmental standards must be high, minimizing adverse effects on ecosystems and human health. Inadequate mine waste storage and closure can result in negative consequences on water quality downstream of the mine site and generate expensive remediation costs. However, the geochemical knowledge regarding Be and W is too limited to determine which precautions that should be taken. Without this knowledge, mine waste and water management containing Be and W might be insufficient, and reclamation to "pre-mining conditions" after mine closure may be unachievable. Even though mineral processing aims for a high recovery, metal extraction is unlikely to reach 100%, generating concentrations of CRM in the tailings. The poor knowledge of Be and W geochemistry can adversely impact groundwater due to element leaching. Beryllium has been identified as the most toxic element in the periodic table if inhaled by dust, and other exposure pathways are not sufficielty studied to be excluded as toxic (Taylor *et al*., 2003). Tungsten is classified as an emerging contaminant of concern (US EPA 2014).

The risk of having groundwater polluted with Be and W highly depends on the stability of hosting minerals and the surrounding geochemical environment. The mobilities of Be and W in mine tailings are affected by co-precipitation with secondary minerals and their stabilities. Gypsum and hydrous ferric oxides (HFO) are common secondary minerals in mine waste, either formed naturally in skarn tailings (Hällström *et al*., 2018) or produced by liming in sulfidic tailings. Researchers have mainly focused on adsorption/co-precipitation of metals with HFO, while studies regarding uptake in gypsum are lacking. Studies regarding co-precipitation of Be and W to secondary minerals in field are limited, but some have been completed in the laboratory (Gustafsson, 2003).

Both Be and W have previsouly been considered as immobile elements (Koutsospyros *et al.* 2006; Taylor *et al.* 2003), but Hällström (2021) found that both elements were released from their primary minerals in W-skarn tailings in Yxsjöberg and transported to the groundwater in high concentrations. The groundwater drains at the shore of the tailings, where secondary minerals have precipiated. In this study, the adsorption/co-precipitation of Be and W to secondary gypsum and HFO was studied.

Study site

At the Smaltjärnen repository, 2.8 million tons of tailings from a W-skarn deposit in Yxsjöberg, Sweden (1918-1989) have been stored open to the atmosphere for more than 50 years (fig. 1b). In 1993, a cover of sludge was placed on the tailings to supress dust. The height difference between the industrial area and downstream lake Smaltjärnen is 15 – 20 m with a relatively uniform slope, except at the shore where it flattens out (fig. 1c). The average Be and W concentrations in the tailings were 284 and 960ppm, respectively. The tailings contained 88 wt% of silicates, and lower quantities of fluorite (CaF_2), calcite ($CaCO_3$), pyrrhotite ($Fe_{(1-x)}S$), pyrite (FeS_2), scheelite ($CaWO_4$), danalite [$Be_3(Fe_{4.4}Mn_{0.95}Zn_{0.4})(SiO_4)_{3.2}S_{1.4}$) (Hällström *et al.*, 2018). Hällström *et al.* (2019) found that several geochemical zones have developed with depth in the tailings due to sulfide oxidation and calcite neutralization (fig. 5).

Method

The tailings at the shore of Smaltjärnen Repository were identified covered by HFO and secondary gypsum in several areas on the shore (fig. 1c). A combination of sequential extraction, low vacuum SEM-EDS and DXRD was used to study the adsorption of Be and W to the secondary minerals.

Five step sequential extraction

The sequential extraction combined the methodologies by Dold (2003) and Hall *et al.*

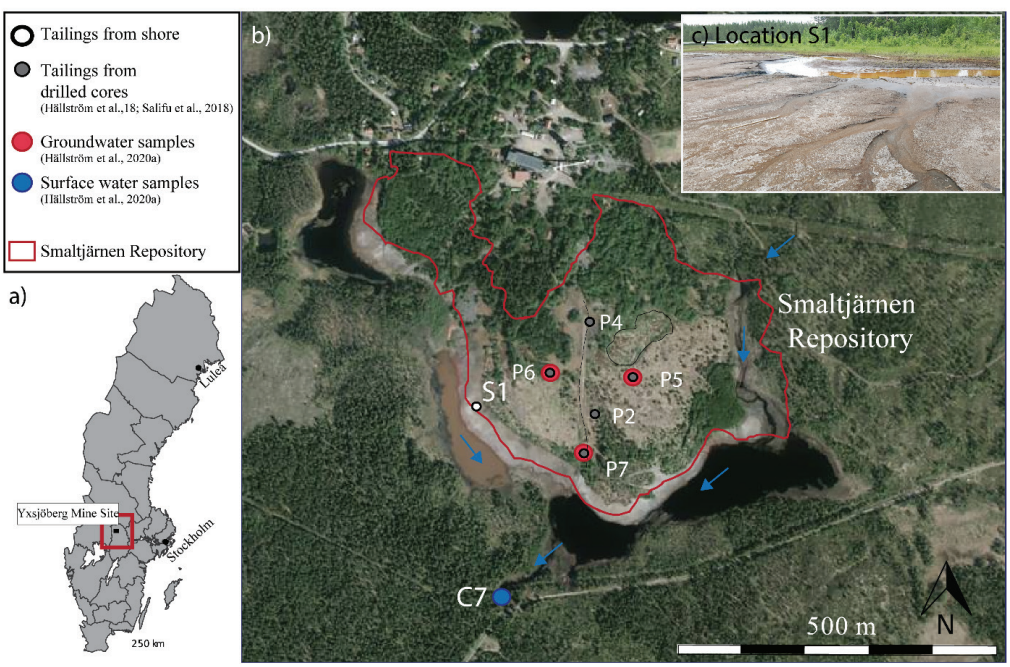


Figure 1 *The Smaltjärnen tailings are located in Yxsjöberg/ Sweden (a), and the tailings have been deposited inside the red line from 1912–1963 (b). Intact core samples (P2, P4, P5, P6 and P7), groundwater (P5, P6, P7) and surface water samples (C7) have been sampled previously (Hällström* et al.*, 2020a). In this study secondary gypsum and HFO from the tailings shore (c) were sampled at S1 (b). The map was collected from www.eniro.se at 2022-12-05.*

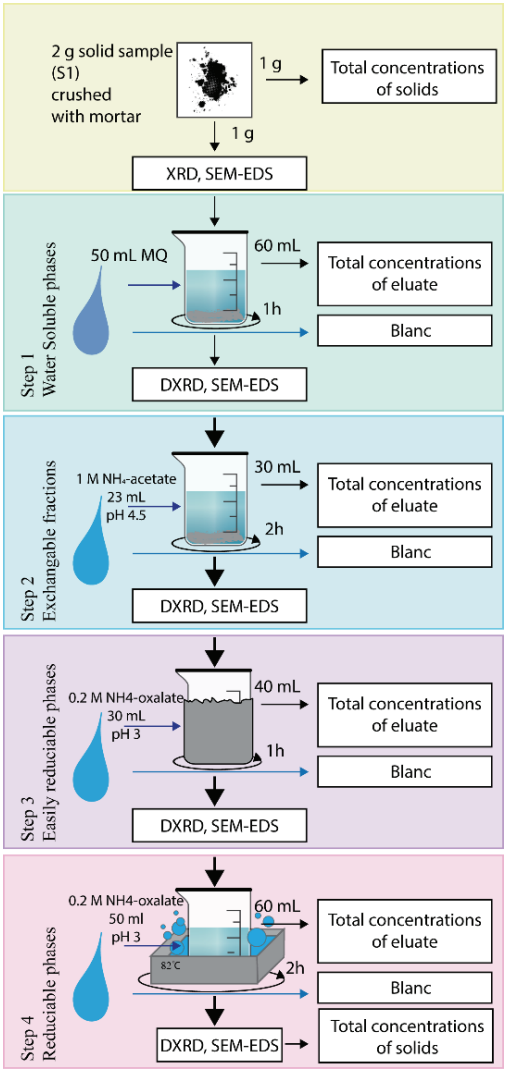


Figure 2 *Step sequential extraction scheme together with analysis of total concentrations, blancs, SEM-EDS and DXRD.*

(1996). The first four steps of sequence B as in Dold (2003) were conducted and the final step included total digestion of the solid residue after the extraction. The tailing sample (S1) was crushed and homogenized with a mortar. One gram of the sample was used as starting material for the sequential extraction and 1 g was sent to ALS Scandinavia for analysis of total concentrations. The laboratory procedures and analysis performed are summarized in figure 2. In Step 1 (water soluble phases), milliQ water was added in a L/S ratio of 1:50. The sample was shaken for one hour and centrifuged 10 minutes with 2800 rpm, and afterwards decanted and filtered with a syringe through 0.45 µm cellulose filter. The material was rinsed two times with 5 mL of milliQ, centrifuged for 10 minutes and decanted as described above. A total of 60 mL eluate was collected from the sample.

In Step 2 (Exchangeable phases), 23 ml of 1 M NH4-acetate was added to the solid residue from step 1. The sample was shaken for two hours, and then the same procedure was done as described for step 1 for removing the eluate and rinsing the sample. A total of approximately 30 mL eluate was collected from the sample.

Step 3 (Easily reducible phases) was performed in the dark by wrapping aluminum foil around the sample container. 30 ml of 0.2 M NH4 oxalate, with pH 3, was added to the sample. The sample was shaken for one hour, then the same procedure for removing water and rinsing as described for the two previous steps were performed. A total of approximately 40 mL was collected for analysis.

In Step 4, the same reagent as for step 3 was used, and 50 mL was added to the residue. The sample was placed in an 82 OC water bath for two hours and was shaken every 30 minutes. Then it was centrifuged, decantated, and rinsed twice. Approximately 60 mL fluid was collected for analysis.

Mineralogy

Between each step of the sequential extraction, the residues of S1 were studied with SEM-EDS mapping and DXRD. The SEM-EDS measurements were carried out with a high-resolution Zeiss Merlin FEG-SEM at Luleå University of Technology. The samples were uncoated and investigated in low vacuum, with a WD (working distance) = 8.5 mm, EHT = 20 kV.

XRD measurements were performed on the grinded, homogenized sample residues with a PANalytical Empyrean X-ray diffraction diffractometer, utilizing Cu-Kα radiation. For the first analysis on the dry, powdered, sample (before the sequential extraction), the analysis was performed with 45 kV, using a 10 mm mask, ¼ anti-

scatter, 1/ programmable, and anti-scatter RM5.7 (detector side). For the recording of the semi-dry residual samples from the leaching a 5 mm mask was used while the rest of the parameters were the same. The mineral identification was performed with the HighScore Plus Version 3 software package, utilizing XRD reference patterns from ICSD-2016.

Results

The results showed enriched concentration of Be in Step 1 and 2, together with high release of Ca and S. Modelling with PhreeqC indicated a saturation of gypsum in the eluate after Step 1, explaining the high content of Ca and S after Step 2 of the sequential extraction. Tungsten was released in step 3 and 4 together with high concentrations of Fe.

Low vacuum SEM-EDS measurements of the samples showed that Ca and S occurred together in the starting material, and that they were present all over the sample (fig. 3). Iron was also present in high content. After Step 1 (water soluble fractions), much Ca and S had disappeared while Fe still was present in high amounts. However, Ca and S were still found together in the tailings. After Step 2 (Exchangeable fractions), Ca and S were no longer found together in the sample and Fe remained intact. After Step 3 (easily reducible fractions) small areas of Ca were present in the sample and S was only found in low quantities showing similar patterns as Fe. After step 4 (reducible fractions) the content of Fe decreased.

The XRD measurement identified monoclinic gypsum ($CaSO_4$ * $2H_2O$; Gp), ferrohornblende (Fe2-hbl) and hedenbergite (Hd) in the starting material (fig. 4). Ferrohornblende and hedenbergite are primary minerals from the ore (Hällström *et al*., 2019). The main peak of gypsum reached 1500 counts. Rietveld refinement estimated gypsum to account for 94% of the minerals in the sample. After Step 1 in the sequential extraction, peaks of gypsum, calcite, hedenbergite and ferrohornblende were present. Gypsum was still the dominating mineral (82%) even though it is supposed to dissolve by water.

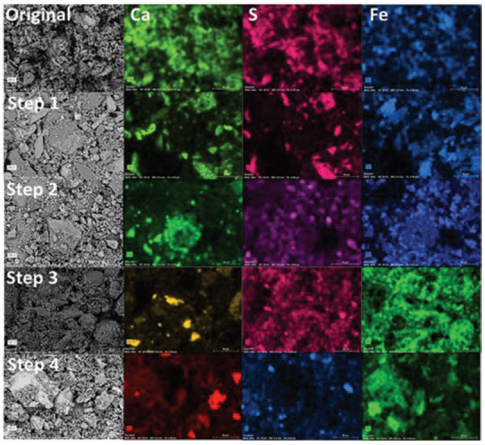


Figure 3 *Low vacuum SEM-EDS mapping between each step of the sequential extraction shows a decrease in Ca and S after step 2, and Fe after step 3.*

After Steps 2,3,4 of the sequential extraction, gypsum was completely dissolved, and ferrohornblende and hedenbergite were the dominating minerals. Hydrous ferric oxides could not be identified with the XRD measurements in any of the steps of the sequential extraction.

Discussion

The shore at Smaltjärnen repository acts as a chemical barrier, scavenging Be temporarily and W more permanently by adsorption/ co-precipitation with gypsum and HFO,

Table 1 *Major and trace elements released from Step 1, 2, 3, 4 and in the residue in the sequential extraction.*

	Major elements mg/kg					Trace elements mg/kg	
	Al	**Ca**	**Fe**	**Mn**	**S**	**Be**	**W**
Step 1	360	36600	32,4	66	30000	13	0.002
Step 2	360	36000	93	69	29400	13	0,01
Step 3	680	68	4800	200	960	1.8	100
Step 4	660	72	31200	174	2100	3	114
Residue	27000	92000	150000	6000	8400	200	2600

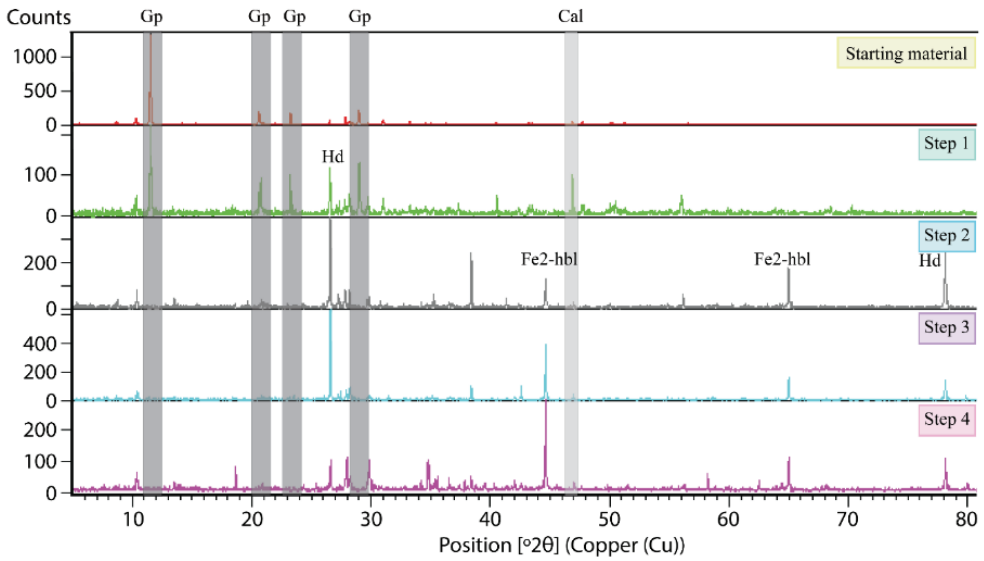


Figure 4 *DXRD analysis between each step of the sequential extraction showed decreased peaks of gypsum after step 2, hydrous ferric oxides could not be identified with XRD. Gp = gypsum, Cal = calcite, Fe_2-hbl = Ferrohornblende, Hd = Hedenbergite.*

respectively (fig. 5). The groundwater of the tailings contained high concentrations of Ca, Fe, and S (615, 50, 590 mg/L, respectively), primarily released from pyrrhotite oxidation (Fe, S) and calcite neutralization (Ca) in the upper parts of the tailings (Hällström *et al.* 2021). The groundwater in the tailings flows out at the shore and makes the tailings saturated. On the shore, secondary gypsum has tentatively formed due to evaporation and HFO has formed due to oxidation of Fe2+ where the groundwater meets the atmosphere.

Sequential extraction combined with XRD and SEM showed that Be preferentially adsorbs/co-precipitates with secondary gypsum. Thus, elevated concentrations of Be, Ca and S released during the first step in sequential extraction were correlated with removal of gypsum peaks in the XRD spectra and decreasing appearance of Ca and S during SEM-EDS mapping. This is interesting since Be previously has been considered to have high affinity for HFO (Taylor *et al.* 2003). Correlated concentrations of Be, Ca and S in surface water downstream of the tailings

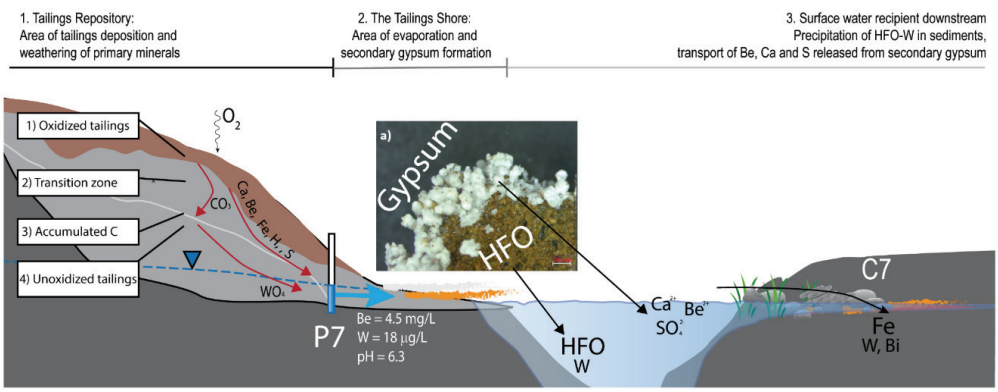


Figure 5 *A schematic figure illustrating 1. Be and W mobility from different zones in the tailings to groundwater, 2. Uptake by secondary gypsum and HFO at the shore of the tailings, and 3. Be released to surface water downstream and settling of W with HFO.*

suggest that secondary gypsum has been dissolved due to snowmelt or rainfall and released Be in high concentrations. Tungsten released from weathering of scheelite in the tailings was mainly associated to HFO according to the sequential extraction. Both Fe and W were found as suspended matter in the surface water, and erosion from the shore has probably transported the particles there. Tungsten settled into the sediment close to the mine site, while Be was transported in concentrations above guideline values from aquatic organism for more than 5 km from the site. This shows that the stability of the secondary minerals formed at the shore plays an important role regarding the impact on surface water quality.

Conclusions

This study shows that Be preferentially adsorbes/co-precipitates with secondary gypsum, while W has high affinity for HFO. Tungsten settled to the sediments a few hundred meters from the repository together with HFO and does not pose a threat to ecosystems. A strong correlation between dissolved Be, Ca and S in high concentrations in surface water downstream the mine site showed that gypsum only acted as a temporary sink for Be. Gypsum dissolved upon rainfall and decreased the surface water quality. Co-precipitation of Be with gypsum has not been seen in the field before and is interesting since Be is assumed to have high affinity for HFO. This needs to be taken into consideration when evaluating methods for remediation of mine waste containing Be and W.

Acknowledgements

We thank our colleagues within Swedish School of Mines at Luleå University of Technology. This work was supported by SGU (DNR 36-2802/2021), and J. Gust. Richert stiftelse (DNR 2018-00420), and co-funded by the Centre of Advanced Mining and Metallurgy (CAMM2) at LTU.

References

Dold B (2003) Speciation of the most soluble phases in a sequential extraction procedure adapted for383

geochemical studies of copper sulfide mine waste. J. Geochem. Explor. 80: 55-68

European Commission (2023a) Critical Raw materials: ensuring secure and sustainable supply chains for EU's green and digital future. https://ec.europa.eu/commission/presscorner/detail/en/ip_23_1661. Date: 2023-03-27

European Commission (2023b) Study of the Critical Raw Materials for the EU 2023 – Final Report. https://single-market-economy.ec.europa.eu/publications/study-critical-raw-materials-eu-2023-final-report_en. Date: 2023-03-27

Gustafsson JP (2003) Modelling molybdate and tungstate adsorption to ferrihydrite. Chem. Geol. 200: 105-115

Hall GEM, Vaive JE, Beer R & Hoashi M (1996) Selective leaches revisited, with emphasis on the amorphous Fe oxyhydroxide phase extraction. J. Geochem. Explor. 56: 59-78. Doi: https://doi.org/10.1016/0375-6742(95)00050-X

Hällström LPB, Alakangas L, Martinsson O (2018) Geochemical characterization of W, Cu and F

skarn tailings at Yxsjöberg, Sweden. J. Geochem. Explor. 194: 266-279

Hällström LPB, Alakangas L, Martinsson O (2019) Scheelite weathering and tungsten (W) mobility

in historical oxidic-sulfidic skarn tailings at Yxsjöberg, Sweden. Environ. Sci. Pollut. Res. 27: 6180-6192

Hällström LPB (2021) Source, Mobility and Fate of Critical Be, Bi, F and W in Historical Sulfidic-Oxidic Skarn Tailings. [Doctoral thesis, Luleå University of Technology]. Luleå University of Technology Graphic Production. ISBN: 987-91-7790-731-2 (electronic).

Koutsospyros A, Braida W, Christodoulatos C, Dermatas D, Strigul N (2006) A review of tungsten: from environmental obscurity to scrutiny. J. Hazard. Mater. 136: 1-19

Taylor TP, Ding M, Ehler DS, Foreman TM, Kaszuba JP, Sauer NN (2003) Beryllium in

the environment: A review. J. Environ. Sci. Health A Tox. Hazard. Subst. Environ. 38: 439-469

U.S Environmental Protection Agency (2014) Technical Fact Sheet – Tungsten, EPA 505-F-14-004.

Sustainable Mine Water Management Strategies

Paul Heaney

ERM, The Greenway, 112 – 114 St Stephen's Green, Dublin 2, D02 TD28, Ireland. paul.heaney@erm.com

Abstract

Mine water management is critical to most mines across the globe. Effective and sustainable water management is imperative to facilitate the successful permitting of new mines, to achieve community acceptance, to maintain regulatory compliance during operation, and to avoid long term legacy issues following mine closure. Mine water supply, mine dewatering and site water discharge are critical aspects for successful mining operations. Building in water resilience to mining operations with regards to climate risk, ESG, geopolitics and sustainability is imperative in the mining industry today. Holistic water management approaches and integrated mine design are critical to building the mines that we all want to see. Climate change, ESG and sustainability are all key drivers in society today and water is central factor in all these globally important topics.

Keywords: Water, resilience, ESG, climate change, sustainability

Introduction

There are numerous different water management challenges facing mines today, these challenges vary throughout the mine life cycle and vary with differing climate, environment and geopolitical circumstances. Climate change will play a key role in shaping effective mine water management practices and designs. Mine water management can include many different aspects including groundwater aspects (mine water supply, mine inflows, mine dewatering), surface water aspects (mine water supply, managing catchment runoff, managing existing surface water features, flood risk/protection, spring snow melt release and site water discharges), the interaction between both groundwater and surface water and the associated impacts. It is important to not only consider the mine site itself but also to consider the wider catchment and all other water users or water features which the locality. Understanding the site wide water balance is critical to effective and sustainable water management and provides critical insight to broader mine design decision making.

The Role of Water in Mining

Water plays an important part in most mines around the world, with most mines having to consider the following aspects:

- Water supply
- Mine dewatering/depressurisation
- Surface water management
- Site discharges
- Seepage from tailings dams and waste rock dumps
- Interaction with the environment and local communities

The importance of these aspects varies depending on where the project is in the mine life cycle and varies as it progresses through the mine life cycle. Projects at early exploration stage, while primarily focussed on expanding the mineral resource, must also consider aspects such as securing a water supply for the drill rigs and in many jurisdictions require permits associated with discharge to groundwater/surface water and often lead to disputes that the exploration drilling activities are impacting other domestic or commercial wells within the immediate area. Exploration stage is also an ideal time to initiate baseline water data collection, where valuable insight on the water environment can be gathered with little additional cost and there is the opportunity to start the baseline water data collection clock.

As mining projects progress into scoping and feasibility phases the focus on water increases, with a requirement to identify

a sustainable water supply to m*eet al*l the mines various life of mine water demands, to develop practical and effective mine dewatering strategies, to provide preliminary mine water management designs and estimate water related capital/operational costs. Appropriately addressing these aspects requires a more in depth understanding of the water environment, such that an appropriate level of confidence can be derived with respect to the proposed water related designs, strategies and costs.

Prior to mine construction and operation Environmental Impact Assessments (EIA) and various water related permits (which may include abstraction, discharge and/or impoundment) are likely to be required. This further raises the level of water environment understanding required (usually including the requirement for an appropriate duration baseline dataset) to accurately assess the potential water related impacts and the expected interaction of the proposed mine on the environment and the community. A key focus being to ensure that appropriate measures are in put in place to monitor, manage and mitigate any potential impacts.

Once a mine moves into the operational phase the water focus often shifts to confirming and validating the predictions from the earlier mine planning stages. There is a focus on gathering operational data, ensuring compliance with permit conditions, regulatory reporting and often looking to ensure optimal and sustainable mine water management. Throughout the operational phase integrated water management across the mine operation is a key aspect, with water playing a key role in many of the different mining departments including mining, mineral processing, waste management, tailings management, infrastructure, environment and community liaison.

Finally, as the mine moves towards closure phase the water related focus generally moves to ensuring no long-term negative water related impacts and minimising active mine water management strategies. The water related aspects of mine closure, in most cases, will have been considered during the earlier planning stages, prior to the mine even being constructed but these early mine closure plans will have been reviewed and updated throughout the operational life of the mine, and it is at this stage that many of the closure strategies and designs will be finalised.

So water plays an integral role in mining throughout its progression through the mine life cycle, although the key elements themselves and the level of detail/certainty required vary throughout the journey. The exact nature of the role will also vary depending on the climate, location, geology, regulatory environment and many other factors but water plays a critical role in most mines across the globe.

Water Related Risks to Mining Operations

The important role that water plays through the mine life cycle is detailed in the section above. Consequently, appropriate management of water related risks is critical to ensure successful mining operations.

Water can be a constraint on mining projects as a result:

- Insufficient water of suitable quality, where there is an imbalance between available water and mine water demand.
- Discharge limitations, where the operation is not able to discharge water from site at rates or from locations required and this negatively impacts operation.
- Water related licence/permit conditions impacting optimal water management practices.

Water can also cause disruptions and/or unplanned downtime to mining operations. Commonly the cause can be related to mine dewatering (underground or open pit) or to the ineffective management of extreme rainfall events, leading to in some cases flooding of mine access roads causing restricted access (Figure 1) or pit inundation (Figure 2).

Mine water risks have the potential to impede mining or curtail processing which can have substantial financial impacts on the mine. In addition, they have the potential to lead to legal ramifications, company reputation damage, breakdown of trust and good stakeholder relationships, environmental damage and in extreme instances loss of life.



Figure 1 *Surface Flooding in Pilbara Region of Western Australia*



Figure 2 *Flooded Gold Mine Cote d'Ivoire*

Mining in a Changing World

Mining is undertaken in highly variable environments across the globe ranging from arid deserts to tropical rainforests, high mountains to coastal plains, arctic circle to searing heat. These environments all pose their own specific challenges but on top of these we are living in a changing world.

We live in a world with changing weather patterns, which include more frequent and longer droughts, increased number of extreme weather events and higher temperatures (more hot days and more heatwaves). The impact of climate change is very closely related to water, as clearly portrayed in the below two quotes:

- "*If climate is the Shark, water is its teeth*" – Alexis Morgan, Global Water Stewardship Lead for Global Conservation Group, WWF (Morgan 2022).
- "*Climate change is primarily a water crisis.*" – United Nations, Water & Climate Change Website (UN 2023).

The consequence of increased extreme weather events is predicted to lead to increased flood risk across the globe as illustrated across the American continent in Figure 3 taken from the WWF Water Risk Filter website (WWF 2023).

Environmental Social Governance (ESG) is a key focus of both mining

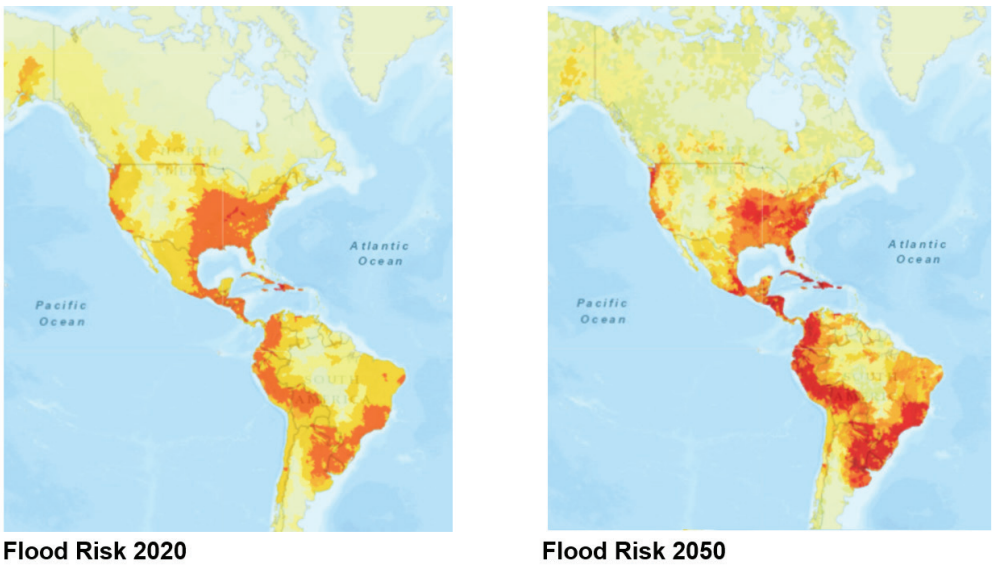


Figure 3 *Flood Risk Predictions 2020 vs 2050 (WWF Water Risk Filter-Maps)*

companies and society, with strong ESG being a critical element for any successful mine. Some of the main ESG focusses being sustainability, transparency, accountability, stricter regulation, low carbon emission (net zero), nature positive, social responsibility and multi-stakeholder consideration. All these aspects have strong links with water and again focus operations on effective and acceptable mine water management practices.

Geopolitical influences also play a key role when considering mine water management aspects. Some of the geopolitical factors being conflict, transboundary agreements/ water rights, rising energy/materials prices and changing demographics (including urbanisation and population growth).

This changing world of climate, ESG and geopolitics not only presents new water related risks to the mining industry but also provides opportunities. Effective mine water management practices, particularly where it includes a strong focus on the environment and community engagement across the wider catchment, provides opportunities related to economic growth, social improvement, the protection and enhancement of the natural environment, reduced operational costs and improved operational performance.

Navigating the challenges, managing the risks and realising the opportunities leads to successful mining operations. Getting the water balance right needs to be the focus and few mines across the globe have mastered the perfect water balance. Mines with the ability to balance the water deficits and the water surpluses, effectively manage the impacts, be adaptive and flexible throughout the mine life cycle, manage seasonality and effectively control the influences of our changing world are building resilience into their operations and will be the mines of the future.

Water Resilience

Resilience is a measure of the ability to recover quickly after a stress has occurred, to return to a previous state after being impacted, to transform and adapt to new circumstances, and to adapt in line with future stresses. A key consideration is water stewardship and the fact that water is a shared resource within the catchment. Incorporating water resilience into mining projects can be achieved by following an approach which has the following characteristics:

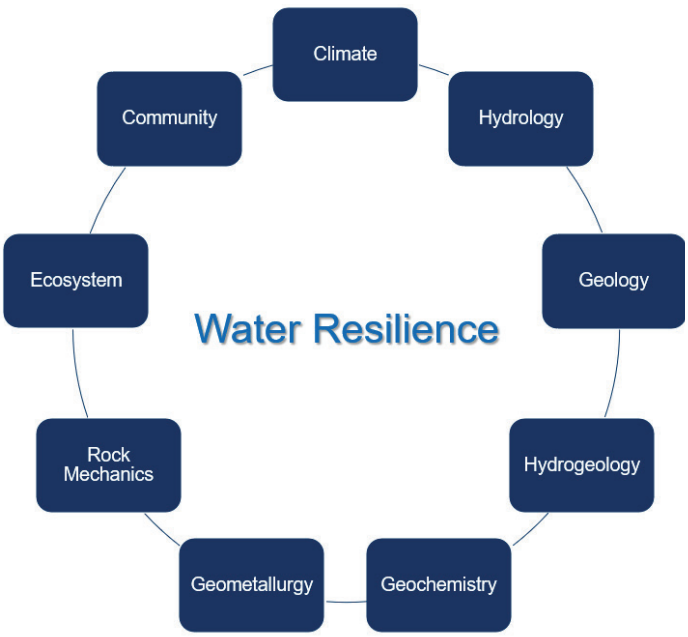


Figure 4 *Water Resilience - Integrated Approach*

1. Starts early
2. Holistic
3. Integrated
4. Clearly defines goals and targets
5. Practical roadmaps
6. Water stewardship
7. Dynamic

Imbedding water resilience into mining projects necessitates consideration of all the various relevant aspects. The relevant aspects are likely to vary for different mines, in different locations at different stages of their development, an example is illustrated in Figure 4.

A fundamental pre-requisite to building water resilience into a mining project is developing a comprehensive understanding of the following aspects:

- the entire water system and all water users within the catchment,
- the baseline water environment,
- the water resources within the catchment,
- the mine water demand throughout the life of mine,
- the mine water discharge requirements throughout the life of mine,
- the impact that the mine is predicted to have on the water environment,
- the impact that the water environment is predicted to have on the mine,
- the regulatory environment,
- stakeholder expectations/requirements and
- ultimately what the water related aspects of mine closure will look like.

Understanding the water system and the role that the mine plays within the catchment is vital and is achieved by instigating a phased approach (often lopping back through earlier phases) of appropriately detailed data collection, data management, data analysis and interpretation, modelling and subsequent planning/permitting. This provides the framework for developing appropriate and effective water management designs, and the implementation of sustainable water management strategies.

The water management strategy developed needs to incorporate appropriate mine water management designs and procedures, which are based on an appropriate understanding of the integrated water system and due consideration of the influences of changing climate, ESG, sustainability and geopolitical factors. The mine water management strategy needs to be a live document (regularly updated), integrated, practical, efficient, effective, and sustainable. Achieving a sustainable water management strategy is not only an obligation in the world we live in today, but also ensures maintenance of asset value for the company, helps maintain a

Conclusion – The Mine We All Want To See

Developing robust strong sustainable mine water management strategies facilitates:

- Water resilience
- Optimal mine operation (not constrained)
- Reduced carbon foot print
- Regulatory compliance
- Good company reputation
- Community collaboration

Sustainable mine water management strategies are a key element of "The Mine We All Want to See". This is a mine that the mining company are proud of, that the staff who work in the mine are proud of, that customers are happy to buy from, that regulators consider fulfils all their requirements, that communities are proud of, that minimises environmental impact and that generates value for all stakeholders even following mine closure.

References

Morgan (2022) Digging for climate change "If climate is the shark, water is its teeth" interview with Mining Journal 7th July 2022.

United Nations (2023) Water & Climate Change UN-Water website (https://www.unwater.org/water-facts/water-and-climate-change)

World Wildlife Fund (2023) WWF Water Risk Filter website (https://riskfilter.org/water).

Rare Earth Elements Association with Predominant Elements in Solids Precipitated during Alkalinization of Acid Mine Water

Dileesha Jayahansani Kotte-Hewa[1,2], Delphine Durce[1], Sonia Salah[1], Erik Smolders[2]

[1]*Belgian Nuclear Research Centre (SCK•CEN), Expert Group Waste & Disposal, Boeretang, 2400, Mol, Belgium, dileesha.kotte.hewa@sckcen.be, ORCID 0000-0001-7757-1571*

[2]*KU Leuven, Department of Soil and Water Management, Kasteelpark Arenberg 20, 3001 Heverlee, Belgium, erik.smolders@kuleuven, ORCID 0000-0003-3054-2444*

Abstract

Rare Earth Elements (REE) scavenging during remediation of acid mine water using Passive Treatment Systems (PTS) resulted in PTS to be considered as a potential source of REE. This has sparked interest in the possible retrieval of REE from the solids precipitated along PTS. The development of an efficient retrieval method requires first to assess the REE scavenging mechanisms and to identify any possible association/correlation of REE with predominant elements (i.e. Fe, Al, Mn, Ca, S) present in the precipitated solids. These first steps were here tackled using Laser Ablation (LA) Inductively Coupled Plasm-Mass Spectrometry (ICP-MS) in combination to Scanning Electron Microscope/Energy Dispersive X-ray spectroscopy (SEM/EDX). PTS was simulated by batch alkalinization experiments, which were performed to sequentially increase the pH of an acid mine water sample through $CaCO_3$ addition. The solids precipitated up to pH≈4 and between pH 4–6 were collected separately for characterization. Results revealed a medium positive correlation ($R^2 > 0.5$) between Ca and S in the solids collected up to pH≈4 indicating gypsum precipitation which was also confirmed by SEM/EDX. In addition, a strong positive correlation ($R^2 > 0.7$) between Ca, S and light REEs (LREEs) was observed pointing also to an association of LREEs with gypsum. In the solid collected between pH 4–6, LREEs and Gd showed strong positive correlations with Fe and medium positive correlations with Al. The observed correlations indicate that during the alkalinization of acid mine water by CaCO3, gypsum acts as a host mineral for LREEs at low pH (up to pH≈4) while at higher pH (between pH 4–6), Fe and Al oxyhydroxides appear to be the preferential host minerals for LREEs, Gd and Er. This implies that for the possible recovery of REE from PTS, gypsum can be targeted mostly in the first layers of the PTS and especially for LREEs whereas Fe- and Al- oxyhydroxides can be targeted for all REE further on in the PTS, i.e. where higher pH are obtained.

Keywords: AMD remediation, passive treatment systems (PTS), alkalinization, REE scavenging mechanisms, laser ablation ICP-MS

Introduction

REE are crucial for the production of modern high technological devices due to their unique optical, magnetic and paramagnetic properties and thus they are considered as technology critical elements (Bau *et al*. 2018; Costis *et al*. 2021; Soyol-Erdene *et al*. 2018). Passive treatment systems (PTS) installed for the remediation of acid mine water have recently gained much attention due to their ability to scavenge Rare Earth Elements (REE) and as such PTS are considered as a potential source of REE (Ayora *et al*. 2016; Hedin *et al*. 2019). REE include 15 Lanthanides (from La to Lu) plus Y. REE are further classified as light REE (LREE), i.e. from La to Sm, middle REE (MREE), i.e. from Eu to Dy and heavy REE (HREE), i.e. from Ho to Lu although this classification is not always consistent in the literature (Bau *et al*. 2018; Costis *et al*. 2021; Soyol-Erdene *et al*. 2018). Acid mine water remediation using PTS mostly involves use

of alkaline materials, e.g. calcite to neutralize the pH thereby leading to the precipitation of metals (Orden *et al*. 2021). Upon contact, calcite dissolution begins and is associated to the consumption of protons present in the acid mine water and thus pH gradually goes up. Along this alkalinization process, at specific/characteristic pH ranges, the major constituents of the acid mine water, i.e. Fe and Al start to precipitate as secondary mineral phases. As reported in literature, Fe-bearing phases generally start to precipitate first, e.g. as iron oxyhydroxysulfates (i.e. schwertmannite) at pH between 3–4.5 and Al-comprising phases rather precipitate later at pH between 4.5–6 as e.g. Al oxyhydroxysulfates (i.e. basaluminite) (Lozano *et al*. 2019a, 2020; Sánchez-España *et al*. 2011). Related to the calcite dissolution during alkalinization is the precipitation of gypsum which has been reported to occur in the acid (pH = 3) to alkaline (pH = 9) range (Lozano *et al*. 2019a, 2020; Lozano *et al*. 2019b; Sánchez-España *et al*. 2011). If present, Mn can also be precipitated (i.e. as Mn oxyhydroxysulfates, Mn oxides and Mn carbonates) at pH above 8 (Hedin *et al*. 2019). REE are also scavenged inside these PTS and are attributed mainly to being associated with Al containing mineral phases (i.e. basaluminite) (Ayora *et al*. 2016; Orden *et al*. 2021). REE scavenging along the PTS with those mineral phases has sparked interest in their possible retrieval from these solids. To develop an efficient retrieval method it is necessary to first assess the REE scavenging mechanisms and to identify any possible association/correlation of REE with predominant elements (i.e. Fe, Al, Mn, Ca, S) present in the precipitated solids. However, the presence of REE at trace level (i.e. µmol) limits the identification of such associations/correlations using conventional solid characterization techniques such as Scanning Electron Microscope/Energy Dispersive X-ray spectroscopy (SEM/EDX) or X-Ray Fluorescence Spectroscopy (XRF). Laser-Ablation (LA) Inductively Coupled Plasm-Mass Spectrometry (ICP-MS) represents a powerful tool in this regards as it simultaneously enables multi-element analysis including REE at µmol or below (Danyushevsky *et al*. 2011; Merten *et al*. 2005). LA ICP-MS was therefore used in this study with the objective of identifying REE associations with the aforementioned predominant elements present in the solids precipitated at characteristic pH ranges.

Methods

A sample of acid mine water was collected from the Tharsis mining area in the Iberian Pyrite Belt (IPB) in southwest Spain. The pH of the water was measured to 2 and its cationic composition (major and trace elements including REE) measured by ICP-MS was as follows. Fe = 70 mmol/L, Al = 40 mmol/L, Ca = 10 mmol/L, Mn = 4 mmol/L, Zn = 7 mmol/L, Cu = 1 mmol/L, La = 2 µmol/L, Ce=6 µmol/L, Pr = 0.8 µmol/L, Nd = 4 µmol/L, Sm = 1 µmol/L, Eu = 0.3 µmol/L, Gd = 2 µmol/L, Tb = 0.2 µmol/L, Dy = 1 µmol/L, Ho = 0.2 µmol/L, Er = 0.7 µmol/L, Tm = 0.09 µmol/L, Yb = 0.5 µmol/L and Lu = 0.07 µmol/L. Sulfate concentration measured by IC was 400 mmol/L.

Batch alkalinization experiments were performed to sequentially increase the pH of the acid mine water and to obtain solid precipitates up to pH≈4, as the representative pH for Fe-oxyhydroxysulfate precipitation, and solid precipitates between pH 4–6, as the representative pH for Al-oxyhydroxysulfate precipitation. Alkalinization was achieved through addition of CaCO3 to aliquots of the acid mine water sample. The required solid ($CaCO_3$) to liquid (acid mine water) ratio to increase pH up to pH≈4 was 11 g/L, and to sequentially increase the pH from 4 to 6, an additive 4 g/L was needed. The precipitated solids were separated from the supernatant by centrifugation (Sigma 6-16KS) at 7000 × g for 10 min after a reaction time of two weeks in an orbital shaker (Ohaus Orbital Shaker) at constant speed. The solid phases were then freeze-dried and subsequently sieved with a 50 µm sieve for characterization using LA-ICP-MS and SEM/EDX. Each solid was pressed into 1.3 cm sized pellets before characterization by LA ICP-MS and by SEM/EDX. An Analyte Excite Excimer LA coupled with 8900 Triple Quadrupole ICP-MS was used to determine the correlation of selected LREE, i.e., La, Ce, Pr and Nd, the MREE, i.e. Gd and the HREE, i.e. Er with the

predominant major elements, such as Fe, Al, Mn, Ca and S. A summary of operational parameters used in the LA ICP-MS analysis is given in Table 1.

Calibration was performed using two National Institute of Standards and Technology (NIST) Standard Reference Materials (SRM), NIST SRM 610 and NIST SRM 612. To maximize the sensitivity, the LA ICP-MS operational parameters were optimized using NIST SRM 612, 1) for low laser-induced elemental fractionation based on $_{238}U/_{232}Th$ ratio (≈1) and 2) for low oxide formation based on $_{248}ThO/_{232}Th$ ratio (< 2%). 25 spots per each solid (pellet) were analyzed for Fe, Al, Mn, Ca, S, La, Ce, Pr, Nd, Gd and Er. Each spot was ablated and measured at every 0.65 s for 30 s time period (thus ≈46/spot). Before and after the analysis of each sample, the NIST 610 and NIST 612 were also ablated each at four different locations and were measured. The average counts of each elements per spot were calculated after correcting for background signal and the correlation of REE with the other elements were determined based on correlation coefficient (R2).

SEM/EDX (Phenom Desktop equipped with EDX) was used to observe the morphology and to identify the elemental composition of the solid phases. The pellets were mounted on aluminum stubs and coated with an ultrathin layer (5 nm) of gold to make their surfaces conductive before analysis by SEM/EDX. Imaging was done at a voltage of 10 kV, while EDX spot analyses targeting major phases were performed at an elevated voltage of 15 kV.

Results and Discussion

SEM images of formed solids up to pH≈4 and between pH 4–6 are shown in Figure 1. It is

Table 1 *Summary of operational parameters used in the LA ICP-MS analysis*

Parameter	Value
Spot size (μm)	40
Laser mode	Burst
Fluence (J/cm^2)	2.5
Repetition rate (Hz)	10
Shot count	300
Pre-ablation time (s) (for measuring background signal)	30
Ablation time (s)	0.65
Post-ablation time (s) (as cleaning step)	30
Waiting time between each spot analysis (s)	30

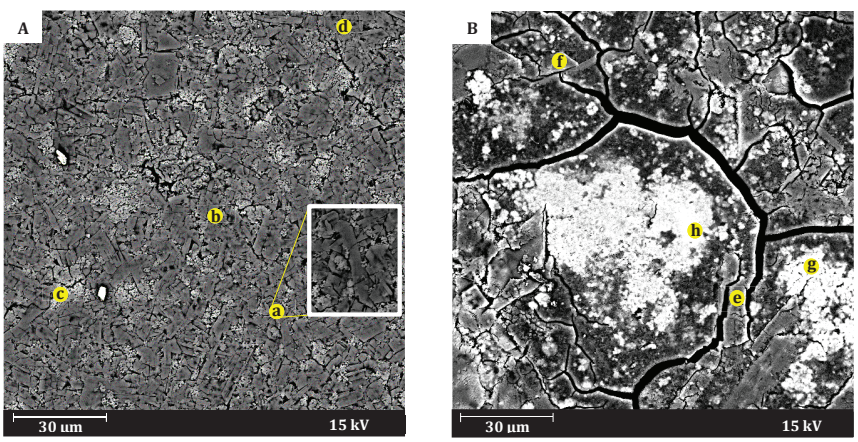


Figure 1 *SEM images of formed solid samples up to pH≈4: A and between pH 4–6: B. A zoomed-in view of spot a is shown inside the white framed area.*

noteworthy that at low pH (up to pH≈4), the surface is mainly covered by Ca, S and O rich phases (as revealed by EDX) corresponding to gypsum minerals with characteristic elongated shape having a length of < 30 µm and a width of < 10 µm (denoted by the spots of a and b). In addition, Fe, O and S rich phases (denoted by the spots of c and d) with rather amorphous morphology are also present at low pH (up to pH≈4). The latter comprise also minor amounts of Al, revealing that part of Al has been co-precipitated with the Fe mineral phases although Al mineral phase precipitation is rather favored at slightly higher pH (> 4.5).

At higher pH (between pH 4–6), comparatively wider forms of gypsum minerals (Ca, S and O rich phases) having a width of > 10 µm could be observed (denoted by the spots of e and f) together with Al, S and O rich mineral phases (denoted by the spots of g and h). The latter are clearly amorphous which is in agreement with literature (Lozano *et al.* 2019a, 2020; Sánchez-España *et al.* 2011). Furthermore, considerable amounts of Zn and Cu are also present revealing favorable co-precipitation of those metals along with Al mineral phases. However, neither Mn nor selected REEs were detectable with SEM/EDX.

The calculated La, Ce, Pr, Nd, Gd and Er correlations (R^2) each with Fe, Al, Mn, Ca and S b up to pH≈4 and between pH 4–6 obtained using LA ICP-MS data analysis are shown in Figure 2. Further Fe, Al, Mn and Ca correlations (R^2) each with S up to pH≈4 and between pH 4–6 obtained using LA ICP-MS data analysis are shown in Figure 3. Results revealed, regardless of the pH range, medium positive correlations ($0.4 \leq R^2 < 0.7$) between Ca and S confirming the presence of gypsum minerals in each precipitate (Figure 3) in agreement with observations made by SEM/EDX.

At low pH (up to pH≈4), LREE showed strong positive correlations ($R^2 \geq 0.7$) with Ca and S (Figure 2), indicating association of LREE with gypsum. In addition, Gd showed a medium positive correlation ($R^2 \approx 0.6$) with Ca and S, while those elements are not correlated with Er ($R^2 \approx 0$) (Figure 2). The association of LREE and gypsum can be attributed to similarities between their ionic radii and Ca^{2+} in the gypsum structure (8-fold coordination) (Ma *et al.* 2020). Results further revealed that all the selected REE are not correlated with Fe and Al at low pH (up to pH≈4) (Figure 2). Moreover, Fe and Al are also not correlated with S at this low pH (up to pH≈4) (Figure 3) showing that S concentration is mostly controlled by the gypsum precipitation even though some Fe oxyhydroxysulfate phases are expected to

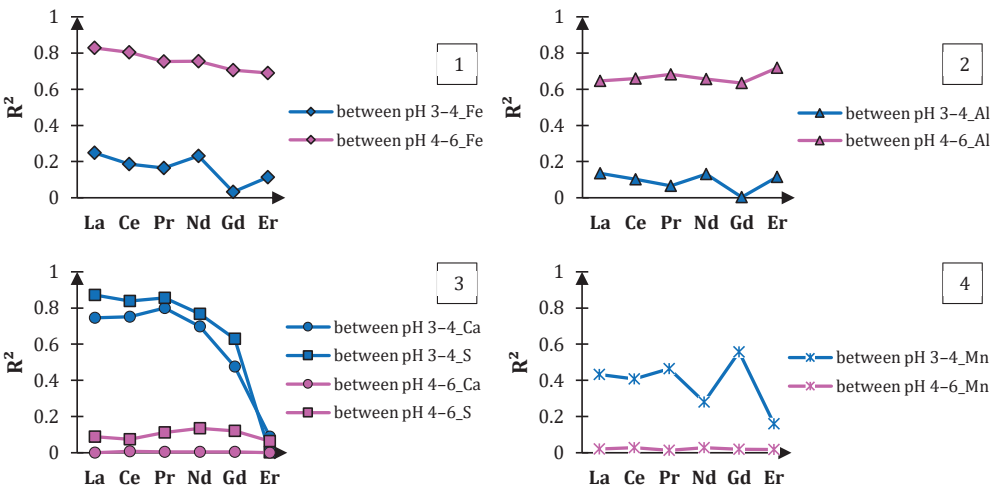


Figure 2 *La, Ce, Pr, Nd, Gd and Er correlations (R^2) with 1: Fe, 2: Al, 3: Ca and S and 4: Mn up to pH≈4 (denoted by blue lines) and between pH 4–6 (denoted by pink lines) obtained using LA ICP-MS data analysis.*

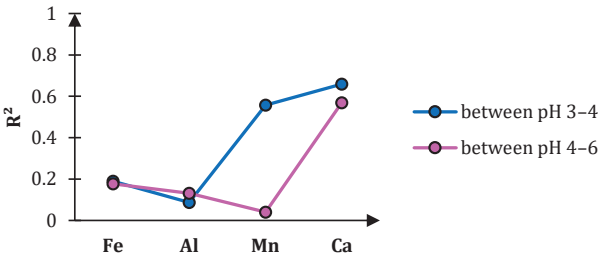


Figure 3 *Fe, Al, Mn and Ca correlations (R^2) each with S up to pH ≈ 4: A (denoted by blue lines) and between pH 4–6 (denoted by pink lines) obtained using LA ICP-MS data analysis.*

precipitate. Conversely, Mn shows a medium positive correlation with S ($R^2 \approx 0.6$) (Figure 3) most likely due to co-precipitation as Mn phases precipitation is not favored at this pH. Further, La, Ce, Pr and Gd show a medium positive correlation with Mn ($0.4 \leq R^2 < 0.7$) while Nd and Er are poorly correlated with Mn ($R^2 < 0.4$).

On the contrary, at higher pH (between pH 4–6) the correlations are mostly reversed. All the selected REE show positive correlations with Fe ($R^2 \geq 0.7$) yet, it decreases from LREE to Er. With Al however, LREE and Gd reveal medium positive correlations ($0.4 \leq R^2 < 0.7$) whereas Er shows a higher positive correlation ($R^2 \approx 0.7$). However, Fe and Al correlations with S have not changed even in the higher pH range (between pH 4–6) and stay as not correlated. No correlations exist between selected REE and Ca ($R^2 \approx 0$) and also between those of and Mn ($R^2 \approx 0$). Correlation between Mn and S has changed to none.

Based on the correlations described above, it is clear that gypsum immediately gets precipitated during alkalinization of acid mine water through addition of $CaCO_3$. Therefore, when gypsum precipitation predominates (i.e. at low pH up to pH≈4), LREE are co-precipitated due to the ionic radii similarity mentioned above. This implies for the possible recovery of REE from PTS, gypsum can be targeted especially for LREEs. Even beyond pH 4, the concentration of Ca^{2+} and sulfur appear to be controlled by gypsum precipitation. During the stepwise increase of pH from pH 4–6, association of REE was observed to shift from gypsum to Fe- and Al-phases. The positive correlations of REE with Fe and Al at higher pH might be explained either by co-precipitations or sorption to respective mineral phases, but needs still to be confirmed. The fact, that no correlation was identified between Al, Fe and S (see above), suggests that instead of Fe-/Al-oxyhydroxysulfates (i.e. schwertmannite, basaluminite), rather Fe and Al oxyhydroxides could be the host minerals for REE or that the precipitation of gypsum still controls the S concentration at higher pH and screen the correlation of S with Fe/Al.

Conclusions

This study sought at investigating the association/correlation of selected LREEs, i.e. La, Ce, Pr and Nd, MREE, i.e. Gd and HREE, i.e. Er with the predominant major elements, such as Fe, Al, Mn, Ca and S present in the formed solids in AMD during the sequential increase of pH (i.e. up to pH≈4 and between pH 4–6) through the addition of CaCO3. This was achieved by using LA ICP-MS complementary to SEM/EDX. It was thereby intended to identify possible scavenging mechanisms of the selected REEs in the mentioned pH ranges.

Correlations (R^2) obtained using LA ICP-MS data analysis revealed medium positive correlations ($0.5 < R^2 < 0.7$) between Ca and S up to pH≈4 and between pH 4–6 indicating gypsum precipitation, which was also confirmed by SEM/EDX. In addition, a strong positive correlation ($R^2 > 0.7$) between Ca, S and the LREEs was observed revealing association of LREEs with gypsum between pH 4–6, LREEs and Gd showed strong positive correlations with Fe ($R^2 > 0.7$) and medium positive correlations with Al ($0.5 < R^2 < 0.7$). No correlation was however

observed of the latter elements with sulfur. This suggests that at higher pH either Fe and Al oxyhydroxides to be host minerals for REE or due to S concentration being still controlled by the gypsum precipitation might have screened the correlation of S with Fe/Al. This implies that for the possible recovery of REE from PTS, gypsum can be targeted mostly in the first layers of the PTS and especially for LREEs whereas Fe- and Al- oxyhydroxides can be targeted for all REE further on in the PTS, i.e. where higher pH are obtained.

Acknowledgements

The authors want to acknowledge that this study is part of the ITN PANORAMA – This project has received funding from European Union's Horizon 2020 research and innovation program under the Marie Sklodowska-Curie Grant Agreement N°857989. The authors gratefully acknowledge the valuable assistance of the following people as well: Dr. Carlos Ruiz Cánovas and Dr. Raul Moreno Gonzalez from the Department of Earth Sciences, University of Huelva in Spain for assistance in collecting acid mine water samples; Dr. Alicia Van Ham-Meert, Dr. Charlotte Vermeiren and Mr. Jesse Dekeyrel, Division of Soil and Water management, KU Leuven for their immense assistance in measuring samples for LA ICP-MS; All the technicians, Waste and Disposal Group, SCK.CEN for their assistance in various ways.

References

Ayora C, Macias F, Torres E, Lozano A, Carrero S, Nieto JM, Perez-Lopez R, Fernandez-Martinez A, Castillo-Michel H (2016) Recovery of Rare Earth Elements and Yttrium from Passive-Remediation Systems of Acid Mine Drainage. Environ Sci Technol 50(15):8255-62. https://doi.org/10.1021/acs.est.6b02084

Bau M, Schmidt K, Pack A, Bendel V, Kraemer D (2018) The European Shale: An improved data set for normalisation of rare earth element and yttrium concentrations in environmental and biological samples from Europe. Applied Geochemistry 90:142-149. https://doi.org/10.1016/j.apgeochem.2018.01.008

Costis S, Mueller KK, Coudert L, Neculita CM, Reynier N, Blais J-F (2021) Recovery potential of rare earth elements from mining and industrial residues: A review and cases studies. Journal of Geochemical Exploration 221. https://doi.org/10.1016/j.gexplo.2020.106699

Danyushevsky L, Robinson P, Gilbert S, Norman M, Large R, McGoldrick P, Shelley M (2011) Routine quantitative multi-element analysis of sulphide minerals by laser ablation ICP-MS: Standard development and consideration of matrix effects. Geochemistry: Exploration, Environment, Analysis 11(1):51-60. https://doi.org/10.1144/1467-7873/09-244

Hedin BC, Capo RC, Stewart BW, Hedin RS, Lopano CL, Stuckman MY (2019) The evaluation of critical rare earth element (REE) enriched treatment solids from coal mine drainage passive treatment systems. International Journal of Coal Geology 208:54-64. https://doi.org/10.1016/j.coal.2019.04.007

Lozano A, Ayora C, Fernández-Martínez A (2019a) Sorption of rare earth elements onto basaluminite: The role of sulfate and pH. Geochimica et Cosmochimica Acta 258:50-62. https://doi.org/10.1016/j.gca.2019.05.016

Lozano A, Ayora C, Fernández-Martínez A (2020) Sorption of rare earth elements on schwertmannite and their mobility in acid mine drainage treatments. Applied Geochemistry 113. https://doi.org/10.1016/j.apgeochem.2019.104499

Lozano A, Fernandez-Martinez A, Ayora C, Di Tommaso D, Poulain A, Rovezzi M, Marini C (2019b) Solid and Aqueous Speciation of Yttrium in Passive Remediation Systems of Acid Mine Drainage. Environ Sci Technol 53(19):11153-11161. https://doi.org/10.1021/acs.est.9b01795

Ma X, Gomez MA, Yuan Z, Bi R, Zhang J, Wang S, Yao S, Kersten M, Jia Y (2020) Incorporation of trace metals Cu, Zn, and Cd into gypsum: Implication on their mobility and fate in natural and anthropogenic environments. Chemical Geology 541. https://doi.org/10.1016/j.chemgeo.2020.119574

Merten D, Geletneky J, Bergmann H, Haferburg G, Kothe E, Büchel G (2005) Rare earth element patterns: A tool for understanding processes in remediation of acid mine drainage. Geochemistry 65:97-114. https://doi.org/10.1016/j.chemer.2005.06.002

Orden S, Macias F, Canovas CR, Nieto JM, Perez-Lopez R, Ayora C (2021) Eco-sustainable passive treatment for mine waters: Full-scale

and long-term demonstration. J Environ Manage 280:111699. https://doi.org/10.1016/j.jenvman.2020.111699

Sánchez-España J, Yusta I, Diez-Ercilla M (2011) Schwertmannite and hydrobasaluminite: A re-evaluation of their solubility and control on the iron and aluminium concentration in acidic pit lakes. Applied Geochemistry 26(9-10):1752-1774. https://doi.org/10.1016/j.apgeochem.2011.06.020

Soyol-Erdene TO, Valente T, Grande JA, de la Torre ML (2018) Mineralogical controls on mobility of rare earth elements in acid mine drainage environments. Chemosphere 205:317-327. https://doi.org/10.1016/j.chemosphere.2018.04.095

Analytical Validation of 3AWater MWAS, a Fast On-site Analysis Tool of Dissolved Metals in Water

Joonas Holopainen[1], Hanna Tolvanen[1], Tommi Tiihonen[2], Vesa-Pekka Lehto[2], Joakim Riikonen[2,3], Tuomo Nissinen[3]

[1]*Ramboll Finland Oy, Puutarhakatu 9, 70300 Kuopio, Finland*

[2]*University of Eastern Finland, Kuopion kampus Yliopistonranta 1, 70210 Kuopio, Finland*

[3]*3AWater Oy, Microkatu 1M, 70210 Kuopio, Finland*

Abstract

3AWater has commercialised a Multimetal Water Analysis System (MWAS) that analyses six dissolved metals (Mn, Ni, Cu, Zn, Pb and U) in the field conditions in less than ten minutes. The performance and usability of the system was validated for actual mine and environmental waters. The results of MWAS analysis were compared to laboratory results and system was found reliable and easy to use by environmental professionals. The real-time water quality results provide and enable fast decision making on-site that can make managing metal containing mine waters more effective and safer than the current standard of laboratory analysis.

Keywords: Water analysis, dissolved metals, on-site analysis methods

Introduction

Currently, the standard way of analysing dissolved metals from water is to send a sample to a laboratory for analysis with AAS, ICP-MS or ICP-OES techniques. The delay between sampling and obtaining the results can be considerably long because of logistics of delivering the sample to the laboratory. An onsite laboratory typically produces results within 4 to 24 hours while results from an external laboratory can take a few days or even several weeks. Therefore, the real-time information on dissolved metals in waters is not available.

Real time data on dissolved metals is essential to rapid decision making in mine water management such as optimising water treatment processes, determining leakages, and assessing environmental impacts. Ability to obtain such data quickly is also essential when fast reaction to water quality issues is needed e.g. after such incidents as storms, power outtakes, or dam failures.

3AWater has developed a measurement technology for analysis of low levels of dissolved metals in water. The Multimetal Water Analysis System (MWAS, Figure 1) is a portable system that gives almost real-time results on-site. The core of the technology is a metal collector made of a proprietary nanomaterial. A water sample is pumped through the metal collector, which gathers the metal ions from the solution. The metals are concentrated up to 200 times in the collector compared to the original water sample. Concentrating the metals into the collector, enables the metals to be analysed with a small and relatively affordable handheld X-ray fluorescence spectrometer (hXRF), which is too insensitive for measuring the water samples as such. The original metal concentrations in the analysed water samples are calculated and shown on screen of hXRF. Everything needed for the analysis are packed in an accessory kit backpack. The principle and an early prototype of the system were previously published by Tiihonen *et al*. (2022).

Method

In this study, the MWAS was used with a Hitachi X-MET8000 Expert hXRF. The analysis procedure for the study involved taking a water sample and measuring pH and conductivity on-site. 10 ml of sample was filtrated subsequently through 0.45 µm syringe filter and 3AWater metal collector with syringe pump (2 ml/min). The metal collector was flushed with 20 ml of air to

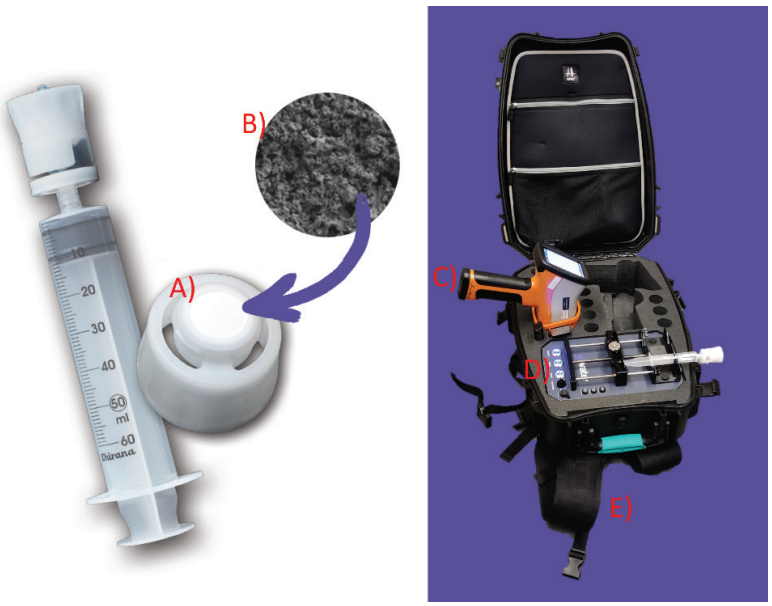


Figure 1 *3AWater Multimetal Water Analysis System: A) metal collector made of a B) proprietary nanomaterial, C) handheld X-ray fluorescence (hXRF), D) Syringe pump and E) Accessory Kit backpack containing the everything needed for the analysis.*

remove excess water. The metal collector was opened, and the metal concentrations were measured with help of sample adapter in the radiation shield. The analysis was performed with hXRF for two minutes.

The default calibrations made by 3Awater were used to analyse eighteen mine and environmental water samples. Each sample was analysed ten times with MWAS and reference samples were analysed by ICP-MS in two independent commercial laboratories. Five samples were spiked with some extra metals to create more variable set of samples. The calibration used for the analysis was selected from the default calibrations integrated in hXRF, depending on sample pH and electric conductivity (EC) listed in Table 1. The default calibration limits the conditions of the sample: pH needed to be 3.5–7.7 and EC <1000 µS/cm. All the experiments related to validation were done by personnel of a consultancy, Ramboll Finland, with assistance of 3AWater.

When the specifications of the pH range or conductivity were deseeded or exceeded, matrix specific calibrations can be created. This was demonstrated with two water samples, A and B, which were obtained from different locations of an active mining site. The samples had EC slightly over 2500 µS/cm and pH from 7.3 and 7.6. The calibration samples were created with sample A by spiking the water with 0-1.1 mg/L of Ni, Cu, Zn, Pb and U. Linear calibration equations were created based on the MWAS and ICP-MS analyses from the calibration samples. To test the performance of the matrix specific calibrations, the sample B as such and spiked with 1.1 mg/L of Ni, Cu, Zn, Pb and U were measured with MWAS in the field and with ICP-MS in the laboratory.

The effect of pH and EC on the MWAS results determined with the matrix specific calibrations were studied in a water matrix that was a 1:1 mixture of the samples A and

Table 1 *MWAS default calibration selection according to pH and electric conductivity.*

Electric conductivity (µS/cm)	pH	
	3.5 – 5	5 – 7.5
0 – 299	A1	B1
300 – 549	A2	B2
550 – 799	A3	B3
800 – 1000	A4	B4

B. The water was first spiked with 1 mg/L of Ni, 0.65 mg/L of Cu, Zn and Pb, and 0.5 mg/L of U. The pH was adjusted back to the original 7.7 after spiking. The spiked water sample was then split into three aliquots. The first one was measured as such. The second aliquot was used to test the effect of EC change. Its EC was increased from 3300 to 3800 µS/cm by adding a solution with 360 mg/L of Ca and 1140 mg/L of Mg. The sample was then measured with MWAS. The pH of the third aliquot was decreased from 7.7 to 7.2 by adding HCl before measurement with MWAS. All experiments done with matrix specific calibration were done by 3AWater and University of Eastern Finland.

Results and discussion

The on-site results obtained with default calibrations were compared to the standard dissolved metal analysis results obtained from the commercial laboratories (Figure 2). The limits of detection for the default calibrations are presented in Appendix and the results below these values are not reported. The results of MWAS analysis were mostly within ±30% limits compared to the laboratory results and all the results were within ±50% limits. This can be considered as a good result for a fast field analysis from an environmental expert's perspective. The MWAS system was found to be easy to use in the field. Less than an hour of training was needed for the trainee at Ramboll to perform the measurements reliably.

Matrix specific calibration was studied by determining the limits of detection for each metal (Ni, Cu, Zn, Pb and U) according to the equation $LOD = I + S(1.645\sigma_{blank} + 1.645\sigma_{sample})$. The limits of detection of the matrix specific calibrations varied greatly between the metals (Table 2). For Cu, Pb and

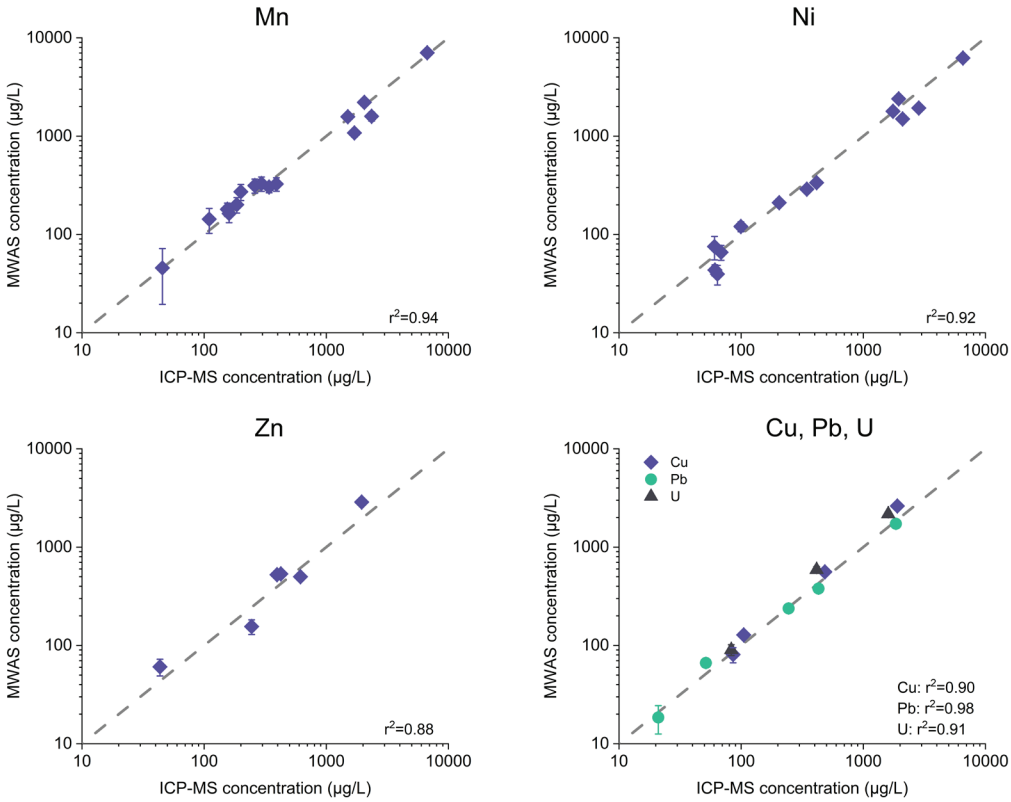


Figure 2 3AWater on-site MWAS analysis (N=10 with std) was compared to average of two commercial laboratories.

Table 2 Limits of detection (LoD) in the matrix specific calibrations.

Element	Ni	Cu	Zn	Pb	U
LoD (µg/L)	110	20	110	10	20

U the detection limits were between 10 and 20 µg/L whereas for Ni and Zn the detection limits were 110 µg/L. The detection limits for Ni and Zn increased, whereas Cu, Pb and U decreased compared to the limits of detection for default calibration in Appendix. This can be due to industrial water being more complex matrix, when the pH and conductivity are different from default calibration.

The sample B was measured as such and spiked with Ni, Cu, Zn, Pb, and U using the matrix specific calibrations. The results are shown in Figure 3. All the MWAS results were within ±26% of the ICP-MS results, when considering the results of metal concentrations above the LoDs.

The effect of changes in pH and EC on the accuracy of the matrix specific calibrations was studied by either decreasing the pH or increasing the conductivity and observing how the results of the MWAS change. The increase in conductivity of 500 µS/cm did not have significant effect on determined U concentrations but caused a decrease in the concentrations of Ni, Cu, Zn and Pb of between 22-34%. The decrease in pH of half a unit did not cause a statistically significant changes in the results ($p>0.05$). As conclusion, the matrix specific calibrations had good accuracy, detection limits were relatively close to default calibrations and not very sensitive to slight changes in pH or conductivity.

Conclusions

The default calibrations were accurate against the commercial laboratory. According to environmental professionals, the system was found easy to use and learn. The water matrix specific calibrations were also found accurate and reliable to demonstrate the applicability of MWAS for more complex mining waters. The study highlights the usability of the MWAS in the different water conditions.

The main advantage of MWAS comes from the easy and fast analysis. The system requires minimal maintenance and no calibrations by the end- user within default

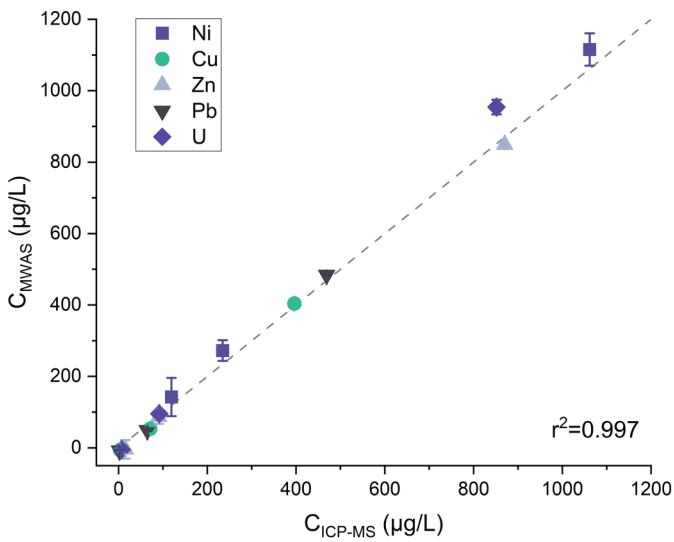


Figure 3 Metal concentrations of sample B measured with MWAS using the matrix specific calibrations plotted against metal concentrations measured with ICP-MS. The dashed line represents the perfect correlation between MWAS and ICP-MS results.

calibration conditions or after matrix specific calibrations are done. The almost real-time water quality data gives multiple advantages in the mining related water management operations. First optimisation of water treatment processes (such as metal removal) ensuring the compliance with regulation and savings in chemical and energy costs. Second, pinpointing leakages and other water quality issues and preventing further damage to the processes or the environment. Third, adaptive sampling i.e. pre-screening the water quality with the MWAS in order to select only relevant samples for further laboratory studies.

Acknowledgements

The authors thank Savonia University of Applied Sciences from collaboration and Centre for Economic Development, Transport and the Environment of Finland for financial support for this study.

References

Tiihonen TE, Nissinen TJ, Turhanen PA, Vepsäläinen JJ, Riikonen J, and Lehto V-P (2022) Real-Time On-Site Multielement Analysis of Environmental Waters with a Portable X-ray Fluorescence (pXRF) System. Anal. Chem. 94:34:11739–11744 https://doi.org/10.1021/acs.analchem.2c01490

Appendix

Limit of detection in mg/L for the default calibrations for MWAS

			pH	
			3.5 - 5	5 - 7.5
Mn	EC [µS/cm]	0 - 299	0.150	0.050
		300 - 549	0.150	0.100
		550 - 799	0.300	0.200
		800 - 1000	2.000	0.300
Ni	EC [µS/cm]	0 - 299	0.060	0.060
		300 - 549	0.100	0.060
		550 - 799	0.100	0.100
		800 - 1000	0.200	0.100
Cu	EC [µS/cm]	0 - 299	0.025	0.025
		300 - 549	0.025	0.025
		550 - 799	0.025	0.025
		800 - 1000	0.025	0.025
Zn	EC [µS/cm]	0 - 299	0.040	0.040
		300 - 549	0.060	0.040
		550 - 799	0.060	0.040
		800 - 1000	0.060	0.040
Pb	EC [µS/cm]	0 - 299	0.025	0.025
		300 - 549	0.025	0.025
		550 - 799	0.025	0.025
		800 - 1000	0.025	0.025
U	EC [µS/cm]	0 - 299	0.050	0.080
		300 - 549	0.050	0.080
		550 - 799	0.050	0.080
		800 - 1000	0.050	0.080

A Review of Downhole Field Methodologies Applied for the Hydrogeological Exploration of Lithium Enriched Groundwater

Paul Hubbard and Michael Palmer

SRK UK, 5th Floor Churchill House, Churchill Way, Cardiff, CF10 2HH, Wales,
phubbard@srk.co.uk, mpalmer@srk.co.uk

Abstract

This paper focusses on the type of hydrogeological testing and sampling methods applied at two UK geothermal lithium exploration sites, to define their extent and extraction potential. The results highlight the value of combining different hydrogeological, geophysical, and geochemical techniques to further the interpretation of geothermal structures. Hydraulic testing and samples from packer isolated intervals provided higher precision and higher confidence data that form the basis needed for exploration. Combing geophysical methods such as pumped impellor, Electrical Conductivity (EC), temperature, and Acoustic Televiewer (ATV) logging, provided higher resolution data, which has proved useful for the identification of controlling structures and refinement of conceptual models.

Keywords: Geothermal Lithium, Packer Testing, Geophysics

Introduction

This paper reviews the application of downhole exploration and hydrogeological testing methods for the exploration geothermal lithium brine resources for extraction, with reference to two UK case studies. In both case studies locations for exploration had already been determined based on historical records and other methods of non-intrusive exploration. The exploration boreholes in this review were part of early intrusive investigations to define this resource and plan further exploration.

Mining hydrogeologists are familiar with a number of methods to characterise the variability of hydraulic properties and flowing fractures vertically in deep rock strata. This paper explores a selection of such methods applied to geothermal lithium investigation, and how those methods provided both the requisite sampling and in combination, provided useful insights for understanding subsurface structures and flows.

The Emergence of Geothermal Lithium Resources

Increasing domestic production of lithium, amongst other minerals, is a key aim in UK's Critical Minerals Strategy for meeting future demand for battery supply. With demand exceeding supply internationally and uncertainty in complex supply chains for minerals that are generally produced outside the UK, sometimes in regions of geopolitical instability, the UK aims to strengthen its supply of critical minerals (Gov. UK 2023)

Currently the main international sources of lithium are typically brines from shallow salt lake deposits (salars) and hard rock mining. The grade of lithium found in geothermal brines is typically orders of magnitude less than such sources, yet internationally it has recently gained interest, due to the lower costs of exploration, development, and potentially, extraction. Advancements in Direct Lithium Extraction (DLE) methods, together with concerns over the environmental sustainability of existing methods has also facilitated increased interest in geothermal supplies.

The genesis and chemistry of each geothermal source is likely to be unique, and as such exploration requirements tailored as this understanding develops. Geothermal brines have the potential to be enriched in other valuable minerals such as borates, magnesium, and potassium, that could also be extracted, but they can also contain minerals

that hinder the extraction process and reduce its economic value (Vera *et al*. 2023). The temperature of the fluid may be sufficient that geothermal energy can be produced and opportunity to extract the lithium is a by product to an existing process.

Practically a geothermal lithium operation can be expected to comprise of a deep abstraction well or wells, a processing plant and similar number of injection wells for the re-injection of brine once the lithium is removed. As the re-injected fluid remains saline it needs to be injected back into a suitable environment, often at similar depths as the fluid that was extracted for processing.

Hydrothermal Lithium in the UK

Through involvement with UK lithium geothermal projects in Cornwall (Cornish Lithium Plc) and County Durham (Northern Lithium Ltd), SRK has had the opportunity to apply experience in deep hydrogeological testing and sampling methods used in mine projects to geothermal lithium exploration. Hydrothermally enriched lithium groundwater in the UK is related to low-enthalpy systems developed in areas with slightly elevated geothermal gradients or where structures provide a pathway for fluid upwelling from deep within the earths crust. In the case of the North Pennines and Cornwall, the elevation in lithium is associated with the granite rock which underlies these areas.

In the North Pennines, interest in the Weardale Granite began in the early 1980s when saline water was found in Cambokeels Mine (Manning *et al*, 2007). Chemical analysis suggested these waters had originated from deep within the Weardale Granite through ascent via the main mineral vein fracture system. Subsequent investigations occurred for the purposes of geothermal exploration of targeted mineral veins, such as the Slitt Vein, and these supported the geothermal potential within the granite (Younger and Manning, 2010). The lithium analysis collected from these investigations became of interest to Northern Lithium Ltd, who commenced intrusive exploration in 2022.

Similarly, lithium was first discovered in the 'hot springs' in deep Cornish mines in the late 19th-centuary derived from deep, permeable structures. Cornish Lithium is evaluating the economic viability of extracting lithium from these waters through regional exploration and targeted drilling campaigns.

Hydrogeological Characterisation Requirements

Tapping concentrated geothermal features inevitably involves deep investigation, to intercept higher grade fluids prior to dilution in shallower groundwaters. The projects in Cornwall and the Pennines were able to use historical mining or geothermal projects to initially target exploration. However, deep saline aquifer systems have limited prior characterisation with which to define possible resource extents and behaviours.

Key requirements at the exploration phase are the determination of economic lithium grades in the fluid, the sufficiency of flows from the generating structures, and the sustainability of this supply. A viable project only exists if all these elements are present. First round exploration boreholes aim to provide the information for the first of those two elements directly and supporting information for long-term supply sustainability. Supply sustainability highly depends on the connection to the underlying geothermal system that is generating the enriched fluid, thus measurements which characterise the wider geological and hydrogeological conceptual model are important, combined with sound understanding of the regional geological and structural systems.

To be an economically feasible project, it is likely that the processed or spent brine will require disposal by re-injection at the site or nearby. Approach to injection site selection is highly site specific, however practical considerations may limit the distances injection wells can be sited from abstractions. As such, detailed hydrogeological conceptual understanding of the geothermal reservoir and structural controls can be critical to minimise grade dilution at abstraction wells.

Aims of Downhole Hydrogeological Testing

Primary testing requirements for downhole exploration are those that directly determine the grade and flow of the resource in that exploration borehole. These are:

- Obtaining representative brine water quality samples, for a given depth or depth interval.
- Obtaining permeability /flow for the same interval.

Together these can be used to infer the overall solute volumes per day that can be obtained.

Several additional aims help build the conceptual model of the hydrothermal system. These include:

- Detection of key or controlling features. Both in terms of boundary and supply.
- Extent of geothermal alteration.
- Measurement of temperature and salinity profiles in-situ.
- Measurement of hydraulic gradients, both vertical and horizontal.
- Measurement of rock or fracture properties such geothermal alteration, aperture, fills and orientations and linkage of properties to target host features.
- Recording of variations of fluid in the test interval overtime.

Downhole Field Investigation Approach

The test methodology utilised is outlined in Table 1 with reference to the methodology applied at the Pennines investigation area. Similar methods have been applied in Cornwall.

In the early exploration stages orientated core drilling is recommended over rotary drilling methods due to the additional geological data that can be obtained. Fracture surfaces can be examined for traces of flow, hydrothermal precipitates and alteration as the core arises to target testing intervals. The resultant smoothness of the borehole wall formed from diamond core drilling lends itself high resolution acoustic televiewer (ATV). Diamond drilling works well with wireline packer systems to isolate intervals for hydraulic testing and water sampling, however, fluid introduction through the core drilling process needs to be taken account of.

A hydraulic through the bit packer system was selected (IPI – SWiPS®) so that the drill string would not have to be removed during testing. This enables more rapid packer deployment than conventional gas inflated or other wireline packers. The improved speed means that completing numerous single packer tests concurrent with drilling is economically viable, and therefore this was selected as the primary mode for this investigation. Straddle packer testing has also been conducted for follow-up measurements on targeted sections.

Packer isolated test intervals were sampled using a submersible pump, with inline flow through cell and logging multi-parameter water quality to obtain real-time transient readings. This process acted as a constant rate abstraction test (CRT), as well as enabling purging for sampling. The combination of packer isolation and purging equipment was selected over grab-sample methods to obtain stabilisation of the real-time monitored water quality parameters to verify sample data. This was used to confirm interference from drilling or injected fluids had been removed. Prior to the CRT phase, shut in pressure tests were also undertaken to obtain in-situ pressure of packer isolated zones and short constant pressure/head injection tests (CHT) were performed for confirmation of transmissive zones and verification readings for hydraulic conductivity (K).

Wireline geophysical methods were conducted following borehole completion. Methodologies used included ATV, impellor, electrical conductivity (EC), temperature, nuclear magnetic resonance, and resistivity logging. ATV is beneficial in conjunction with extracted core as it allows in-situ definition of structures, reducing misinterpretation of fractures in the core caused by the core handling. It also allows for interpretation of fracture aperture and orientation.

The main aim of other geophysical methods was to provide high resolution data to attempt to identify permeable structures or geothermal inflows (via EC or temperature signatures). Impellor, EC and temperature logging under pumped conditions is a procedure that aims to generate sufficient drawdown in the borehole

such that flow is induced from all key fractures the borehole intersects (described further in Moltz *et al*. 1994).

Review of Performance of Testing Methods

In both test sites core drilling provided a wealth of information in terms of confining structures, hydrothermally altered rock, hydrothermal precipitates, evidence of water movement on fracture planes (via freshness/ staining / infill) and discontinuity of fracture surfaces. Visible hydrothermal alteration was often coincident with increases in salinity and lithium content, however this was not always the case, indicating that the enriched fluid had permeated through adjacent fracture systems.

Data obtained from packer isolated sections provided the principal data for confirmation of both chemistry and hydraulic conductivity variation vertically in the boreholes due to reliability and capability to undertake QA/QC measurements (Figure 1).

Single packer isolated interval carried out concurrent with drilling, enabling full testing coverage of the borehole proved to be key. This allowed for rapid repeat tests to refine intervals. Whilst a preconception of target depth or structures can be useful, testing the entire borehole is critical for a data led, non-biased conceptual model. Characterising extents of any non-productive zones is equally important for well design and contemplating potential reinjection depths.

Shorter term injection CHT tests generally proved more useful for both comparative measurements between packer intervals at a field level, as in most cases the same test pressures can be reapplied. The packer CRTs were taken over longer periods, with greater influence of vertical drainage into test section observed and potential boundary effects sometimes encountered. Therefore, the analysis of hydraulic properties was more involved and more subjective. This ambiguity makes the pumped CRTs less useful for relative comparisons. It also highlights how the simple extrapolation of total well yield from the summation packer isolated intervals could lead to overestimates in productivity if vertical flow influences are not appropriately account for in the analysis.

High head gradients can exist in geothermal zones; therefore, it is not uncommon to find strong interflows between structures in an open borehole under ambient conditions. Figure 2 shows this situation in a highly productive zone of one of the exploration boreholes. The discrete depth of a set of hydraulically active structures is well correlated between pumped and ambient EC, temperature, and impellor logs (shown by numbered horizontal red lines in Figure 2). The ambient impellor logging also shows a strong upward flow, generally from the set of structures at positions 3 and 4 to those at 1 and 2, higher in the borehole. Head pressures obtained during single packer shut-in phases illustrate the pressures in the intervals relative to ground level. These show progressively increasing groundwater pressure at depth and are consistent with the upward flows observed in the ambient impellor to the structures located at positions 1 and 2. Full

Table 1 *Field methods utilised in lithium exploration boreholes*

Field methodology	Main data targeted
Pumped samples via inflatable packer isolation	Depth dependant water samples for laboratory testing
Constant head injection (CHT) and constant rate abstraction tests (CRT) in packer isolated sections	Hydraulic conductivity (K) measurements (at same intervals)
Ambient and pumped impellor, electrical conductivity (EC) and temperature logging	Detection of location of discrete structures via flow, salinity or heat changes
Acoustic televiewer logging	Determination of in-situ fracture properties
Core sample logging	Immediate indication of rock properties (for test targeting). Lithology and confining layers. Determination of hydrothermal alteration. Fracture surface properties
Nuclear Magnetic Resonance (NMR) and Resistivity logging	Used to evaluate if useful high resolution information for hydraulic active fractures could be obtained

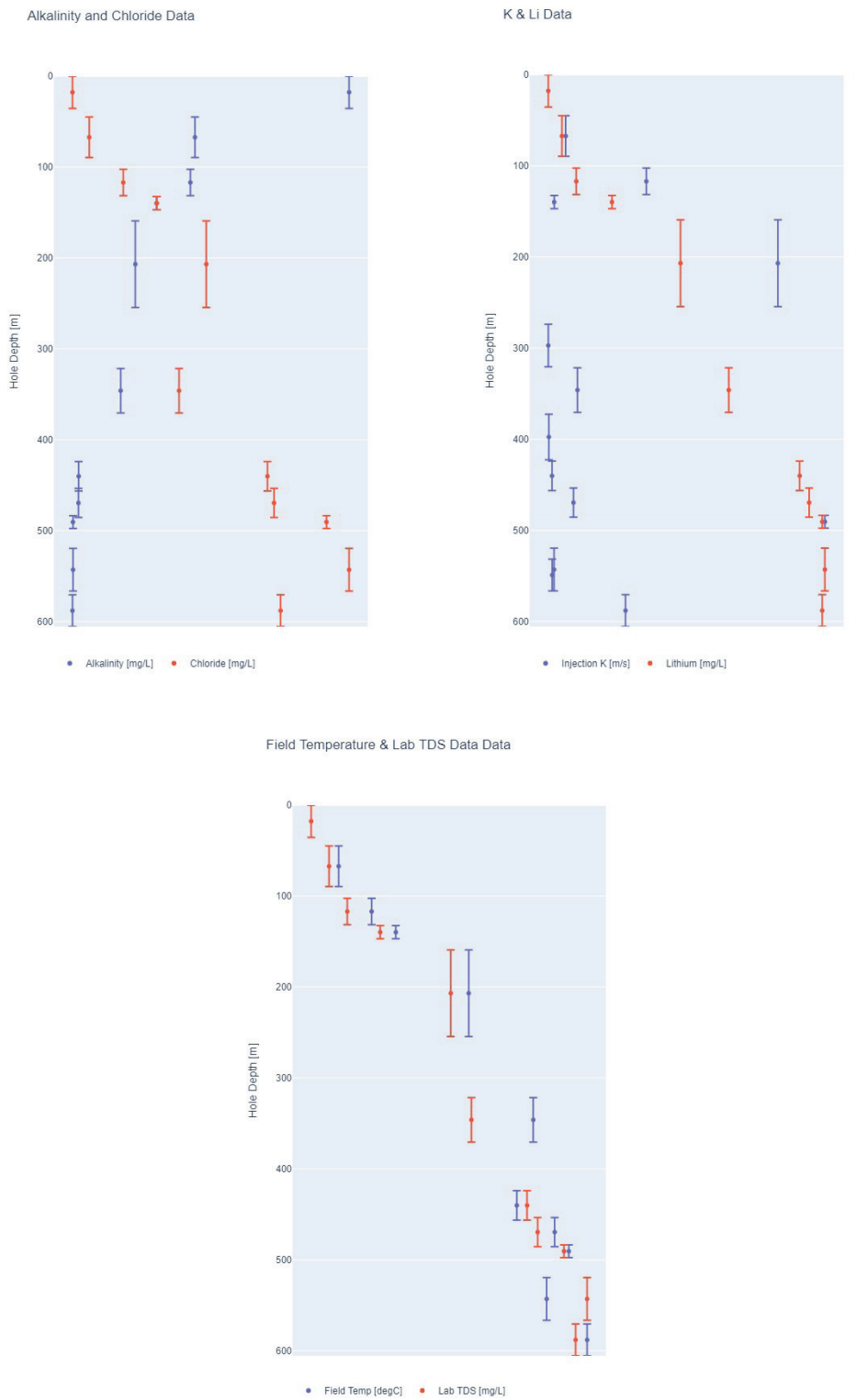


Figure 1 *Example of depth dependant hydrogeological data derived from packer testing combined with water quality sampling*

account of such ambient flows within the borehole is needed to prevent error when resolving flow proportions for structures solely using pumped impellor observations.

As can be seen in Figure 2, a reduced correlation was observed between the vertical position of hydraulic conductivity reported in NMR logs and responses in the temperature, EC and impellor logs. In this borehole the magnitude of hydraulic conductivity reported in NMR logging showed limited correlation with results from packer CHT and CRT tests, however, increases in NMR hydraulic conductivity were overall consistent with the sections of the boreholes that showed the most flow.

The utilisation of packers enabled the collection of discrete purged water quality samples. Purging methods comprised removal of the monitored drilling water losses together with field water quality parameter stabilisation checks. Whilst obtaining purged samples had clear advantages over grab methods in a situation where fluids are introduced in the drilling process, this also meant storage and disposal of large volumes of pumped brine and as well as obtaining appropriate saline resistant pumping equipment.

Conclusions

Several downhole hydrogeological characterisation methods have been successfully applied to geothermal lithium exploration. The results highlight the value of combining different hydrogeological and geophysical techniques to further the interpretation of geothermal structures. Different methods have different strengths, in either data resolution, rapidity, precision, and repeatability, and need careful consideration for an integrated cost-effective approach. For example, the repeatability and high and low transmissivity range of constant head packer tests proved invaluable for determining the relative inflows over the borehole length. The high resolution of pumped impellor, EC and temperature logging helped ascertain discrete inflow positions for review against ATV and extruded core to characterise structures of interest. Observed ambient flows in the borehole were better understood when comparing to section pressures obtained in packer shut in tests. This exploration data continues to provide the basis for the development of early conceptual models, sufficient for the planning of further investigation boreholes and design of optimised test wells.

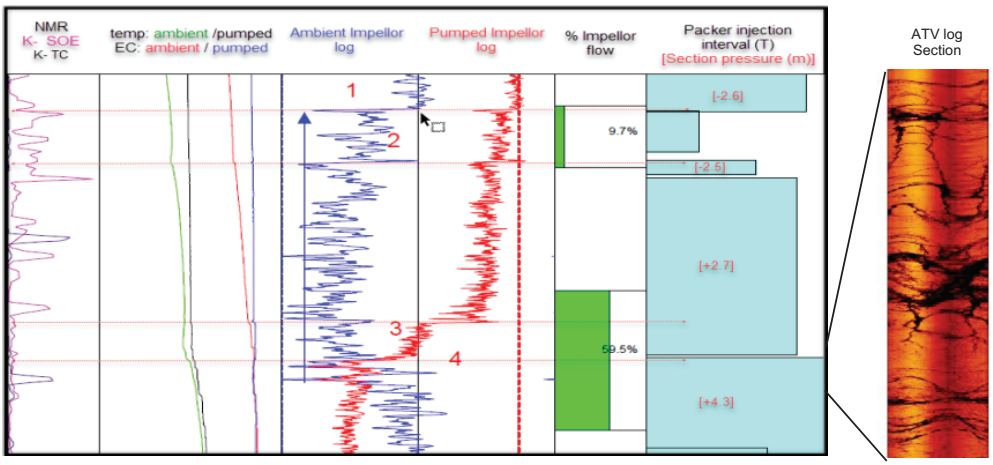


Figure 2 *Example of downhole data comparison, showing from the left: interpretated hydraulic conductivity from NMR, pumped and ambient temperature, electrical conductivity (EC), and impellor logs together with packer isolated CHT transmissivity and section pressure results (in red brackets). A shorter portion of the ATV log is also shown indicating significant fracturing at a depth consistent with changes in the readings position 4*

References

Gov. UK 2023 Critical Minerals Refresh: Delivering Resilience in a Changing Global Environment (published 13 March 2023)

Manning D.A.C. *et al*. A deep geothermal exploration well at Eastgate, Weardale, UK: a novel exploration concept for low-enthalpy resources. Journal of the Geological Society, London, Vol. 164, 2007, pp. 371–382

Vera, M.L., Torres, W.R., Galli, C.I. *et al*. Environmental impact of direct lithium extraction from brines. Nat Rev Earth Environ 4, 149–165 (2023). https://doi.org/10.1038/s43017-022-00387-5

F.J. Molz a, G.K. Boman a, S.C. Young b, W.R. Waldrop b. 1994. Borehole flowmeters: field application and data analysis. Journal of Hydrology 163 (1994) 347-371

Younger, P. L and Manning D. A .C. (2010). Hyper-permeable granite: lessons from test-pumping in the Eastgate Geothermal Borehole, Weardale UK. Quarterly Journal of Engineering Geology and Hydrogeology, 43, 5–10. DOI 10.1144/1470-9236/08-085

Constructed Wetlands For Treatment Of Bauxite Residue Leachate: 7.5 Years Of Monitoring

Ashlene Hudson[1], John Murnane[2], Ronan Courtney[1]

[1]*Department of Biological Sciences and Bernal Institute, University of Limerick. Ireland. ashlene.hudson@ul.ie; ronan.courtney@ul.ie*

[2]*School of Engineering, University of Limerick. Ireland. john.murnane@ul.ie*

Abstract

Constructed wetlands (CWs) have been proven as an effective, nature-based alternative for effective treatment of predominantly acidic waters. Alkaline wastes and leachates, including bauxite residue, have received far less focus, with long term studies limited to around 5 years.

The work presented demonstrates that a CW can effectively treat bauxite residue (BR) leachate from a pH ca. 11.2 to pH <9 over a period of 7.5 years, providing evidence CWs may be a viable treatment method for BR leachate.

Keywords: Bauxite residue leachate, constructed wetlands, longevity, alkaline leachates.

Introduction

The extraction and refining of metals has led to the accumulation of tailings and waste deposits globally, amounting to over 100 billion tonnes, with drainages and leachates from such stockpiles potentially of environmental concern if not managed appropriately (Mishra *et al*. 2022). Of this global stockpile, the alumina industry is estimated to have produced and stored over 4 billion tonnes of bauxite residue (BR), increasing by 150 MT annually (International Aluminium Institute 2022). BR leachates are inherently alkaline owing to the Bayer process utilising NaOH, with leachate pH between 9 and 13.2, as well as elevated Al, As, V, and Na (Burke *et al*. 2013; Higgins *et al*. 2017)

As BR leachates and other drainages can have the potential to form for decades post-closure, long term management can pose a challenge to operators and environmental regulators (Higgins *et al*. 2017; Riley and Mayes 2015; Roadcap *et al*. 2005). Both active and passive technologies can be employed, but each site and its individual chemical, geographical and climatic parameters may determine the appropriate technique to be applied. Globally, increasing attention to water quality and a shift to passive, nature-based technologies has resulted in the increased application of constructed wetlands (CWs) for leachate and drainage treatment as performance has been found comparable to active chemical treatment, whilst also being cost effective (Chen *et al*. 2021; Hedin 2020).

While CWs have been extensively utilised for the treatment of acidic and neutral mine drainage (Acharya and Kharel 2020; Ighalo *et al*. 2022), their use for the remediation of alkaline drainages has received far less research focus (Gomes *et al*. 2019; Hudson *et al*. 2021). Although efficacy has been assessed in acidic and neutral mine drainages for up to 20 years (Hedin 2020), published longevity studies for CWs mostly cover operational periods of 1-5 years, with a limited number covering over 10 years. Monitoring of CWs used for treatment of alkaline leachates is particularly lacking (Gomes *et al*. 2019; O'Connor and Courtney 2020). This study presents results of an ongoing pilot scale CW treating BR leachate for over 7.5 years.

Methods

Site Description.

A 4 m × 11 m pilot scale constructed wetland (CW) was constructed at a bauxite residue disposal area (BRDA) at Aughinish Alumina, Ireland. Local soil was transplanted for use as the substrate with the following characteristics: pH = 6.7, EC = 188µS cm^{-1}, CEC 38 cmol kg^{-1}, and 2.8% organic C content. The system was

planted with Phragmites australis, Typha latifolia and Sparganium erectum supplied locally (FH Wetland Systems Ltd) and acclimatised with fresh water for 6 months.

A PLC mixing system was installed to feed the CW at a pre-determined pH and flow rate as per modelling of a closed BRDA (Residue Solutions 2007). The system consists of three 1000 L tanks. Alkaline leachate and water were pumped to a mixing tank until a target pH ca. 11 was reached. The mixed influent was then conveyed to a dosing tank and discharged to the CW at 45-55 L hr^{-1} (summer loading) and 10-30 L hr^{-1} (winter loading). Seasonal variation in loadings were due to increased winter precipitation. Initially, the system was operated using tap water to dilute the leachate, but due to the formation of calcite deposits within the mixing and dosing system that compromised efficiency, system was converted to utilise deionised (DI) water for leachate dilution (Higgins *et al*. 2018; Higgins *et al*. 2017). Additionally, the conversion to DI water allowed the investigation into the use of CW for a system which would have a low to negligible Ca content. The system has been receiving the deionised water leachate since May 2015.

Monitoring and Sampling Campaigns.

Inflow and outflow pH was measured daily using a field probe, with monthly averages reported over the 7.5-year study period. Wetland inflow and outflow samples were also taken for elemental analysis, filtered to 0.45 µm and determined by inductively coupled plasma mass spectrometry (ICP-MS).

Additional sampling campaigns were conducted to determine pH, EC and trace metal concentrations (Al, As, Ca, Mg, Na & V) within the wetland cell in the 4th and 5th years of operation in both the supernatant and sediments (air-dried and sieved <2 mm). Microbial analyses were also conducted in the 5th year. Detailed analyses from the 4th and 5th year are available separately (Hudson *et al*. 2023; O'Connor and Courtney 2020).

Results

Monthly average pH (Figure 1) was reduced from an influent pH ca. 11.5 to 7.1 over the 7.5-year study period. Within the additional sampling campaigns, it was shown that the reduction to pH < 9 threshold was obtained between 3.5 m and 5 m into the cell in the 5th year of sampling (Figure 2). The primary objective of the CW is to obtain a pH < 9, which the system has been successfully maintaining throughout its operation.

In addition to pH, EC and trace elements have also shown reductions from inlet to outlet. Reductions in average Al were 98% and 84% in year 4 and 5 respectively, with corresponding average V reductions of 90% and 57% respectively (Hudson *et al*. 2023; O'Connor and Courtney 2020). The dominant cation in the effluent across the 7.5 years was Na. Reductions in effluent Na have decreased over time, with a 31% removal reported over the first year by Higgins *et al*. (2017), versus 13% reported in year 5 (Hudson *et al*. 2023).

Sediment analysis indicated elevated trace element content in addition to microbial biomass in the first 5 m of the wetland. Trace elements Al, As and V were found to be mostly recalcitrant (>94% of total content), with Na content found to be mostly present in the water-soluble fraction (48–62% of the total). Microbial respiration rate utilising endemic Phragmites australis matter also showed an elevated rate in the first 5 m of the CW.

Discussion

Interest in CWs and implementation of nature-based treatment solutions has been increasing, with their potential to provide a cost effective and passive treatment solution appealing to operators. Most available studies are focused on acidic drainage sites and for short operating periods (<5 years) (Pat-Espadas *et al*. 2018).

The primary treatment objective for this CW was to reduce leachate pH to below a threshold of pH 9. The sustained decreases in pH over 7.5 years demonstrates that this CW has been successful in providing an effective treatment for alkaline BR leachate. Further investigations within the cell in the 5th year showed pH reduction to below threshold was achieved by 5 m (less than halfway) into the CW, implying sufficient capacity for another 7.5 years approximately. Obtaining pH < 9 threshold is required in several alkaline

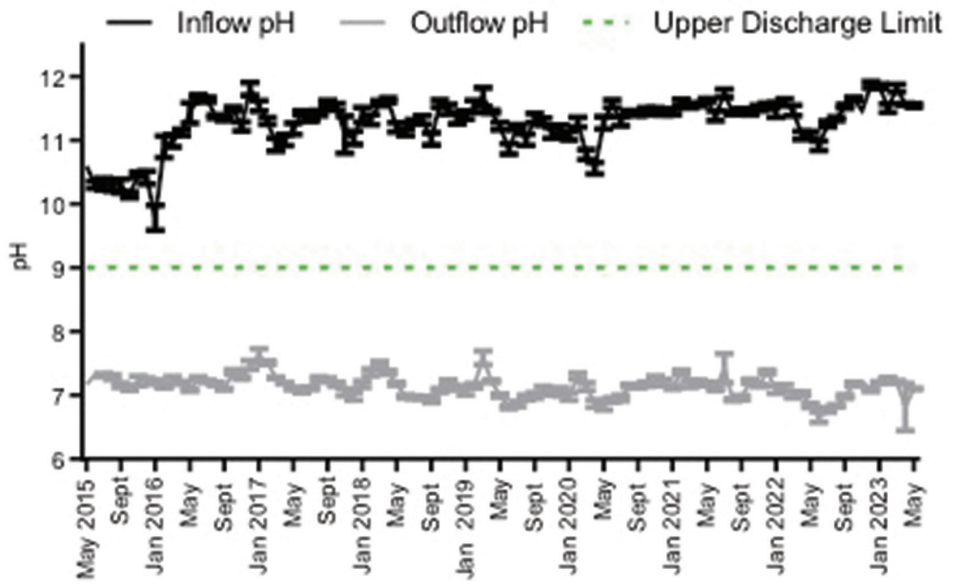


Figure 1 *Average monthly inflow and outflow pH of a constructed wetland treating bauxite residue leachate, measured from May 2015 to January 2023.*

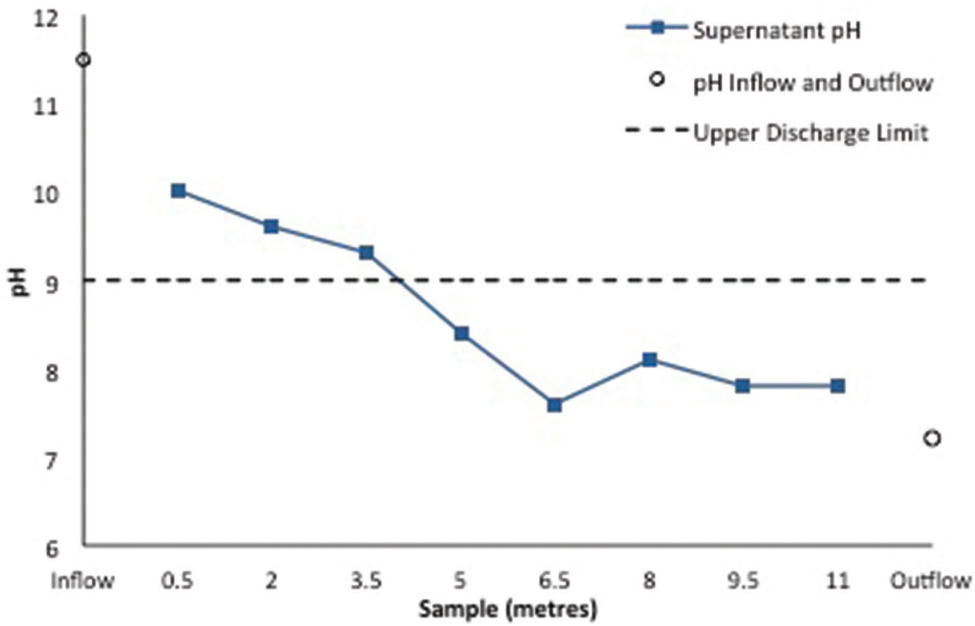


Figure 2 *Supernatant pH within the wetland cell sampled after 5.5 years of operation, adapted from Hudson* et al. *(2023).*

waste streams including steel slag leachates. Although CWs treating steel slag leachate have also achieved pH reductions of 2.5 units, from 12.8 to 10.3, they still exceeded the pH 9 threshold (Gomes *et al.* 2019). Mechanisms suggested to be responsible for pH reduction include microbial respiration, carbonation and the production of organic acids (Mayes *et al.* 2009b; Mayes *et al.* 2009a; O'Connor and Courtney 2020), and is supported by the elevated microbial respiration and biomass found in the first 5 m of the BRDA CW cell (Hudson *et al.* 2023).

Reduction in trace elements from the leachate demonstrates that CWs can also reduce contaminant load in BR leachate. Al and As removal of over 90% and 86% respectively is comparable with or exceeds that reported in CWs treating municipal wastewater (Kröpfelová *et al.* 2009; Vymazal and Krása 2003). V removal in this cell (57%) was also greater than that reported for steel slag leachate (Gomes *et al.* 2019).

Water quality has been the focus of most monitoring projects; however, CW sediment must also be investigated when considering the trace element removal. In this study, sediment Na has increased with time, particularly in the first 5 m of the wetland, following a front-loading pattern. Water-soluble Na increased from 9% in the baseline soils to >48% at all sampling points within the cell in the 5th year of operation. The reduction in Na removal from 31% to 13% could be attributed to the sediment base becoming saturated or the release of water-soluble Na due to displacement from the cation exchange surface. Although Na is elevated, effluent total Na remains below the 200 mg L-1 limit set by the EU Drinking Water Regulations (Environmental Protection Agency 2014). Further monitoring of the Na concentration in the cell sediment is needed to determine why Na removal rate has reduced, and to monitor its influence on nutrient uptake in vegetation (Ruyters *et al.* 2011).

Conclusions

This monitoring campaign provides evidence that a CW can successfully maintain pH<9 (from pH ca 11.5) in BR leachate for over 7.5 years. In addition, trace elements Al, As and V in the leachate were reduced, with sediment concentrations of these elements mostly in residual forms. To date, this study provides one of the longest datasets for CW treatment of alkaline leachates. Further monitoring is needed to assess performance as the system ages and to determine additional design optimisations that may improve its longevity.

References

This research was supported by funding from Aughinish Alumina.

Acharya BS, Kharel G (2020) Acid mine drainage from coal mining in the United States – An overview. Journal of Hydrology 588:125061. https://doi.org/https://doi.org/10.1016/j.jhydrol.2020.125061

Burke IT, Peacock CL, Lockwood CL, Stewart DI, Mortimer RJ, Ward MB, Renforth P, Gruiz K, Mayes WM (2013) Behavior of aluminum, arsenic, and vanadium during the neutralization of red mud leachate by HCl, gypsum, or seawater. Environ Sci Technol 47(12):6527-35. https://doi.org/10.1021/es4010834

Chen G, Ye Y, Yao N, Hu N, Zhang J, Huang Y (2021) A critical review of prevention, treatment, reuse, and resource recovery from acid mine drainage. Journal of Cleaner Production 329:129666. https://doi.org/https://doi.org/10.1016/j.jclepro.2021.129666

Environmental Protection Agency (2014) Drinking Water Parameters. Microbiological, Chemical and Indicator Parameters in the 2014 Drinking Water Regulations 2014. An overview of parameters and their importance. Environmental Protection Agency., Wexford

Gomes HI, Mayes WM, Whitby P, Rogerson M (2019) Constructed wetlands for steel slag leachate management: Partitioning of arsenic, chromium, and vanadium in waters, sediments, and plants. Journal of Environmental Management 243:30-38. https://doi.org/https://doi.org/10.1016/j.jenvman.2019.04.127

Hedin RS (2020) Long-term Performance and Costs for the Anna S Mine Passive Treatment Systems. Mine Water and the Environment 39(2):345-355. https://doi.org/10.1007/s10230-020-00676-9

Higgins D, Curtin T, Burke I, Courtney R (2018) The potential for constructed wetland mechanisms to treat alkaline bauxite residue

leachate: carbonation and precipitate characterisation. Environmental Science and Pollution Research 25(29):29451-29458

Higgins D, Curtin T, Courtney R (2017) Effectiveness of a constructed wetland for treating alkaline bauxite residue leachate: a 1-year field study. Environmental Science and Pollution Research 24(9):8516-8524. https://doi.org/10.1007/s11356-017-8544-1

Hudson A, Murnane J, Courtney R (2021) Use of Constructed Wetlands for Treating Mine Waste Leachates: Assessment of Longevity and Management Implications., Report № 978-1-84095-022-4. Environemtnal Protection Agency42 p

Hudson A, Murnane JG, O'Dwyer T, Pawlett M, Courtney R (2023) Influence of sediment quality and microbial community on the functioning capacity of a constructed wetland treating alkaline leachate after 5.5 years in operation. Science of The Total Environment 867:161259. https://doi.org/https://doi.org/10.1016/j.scitotenv.2022.161259

Ighalo JO, Kurniawan SB, Iwuozor KO, Aniagor CO, Ajala OJ, Oba SN, Iwuchukwu FU, Ahmadi S, Igwegbe CA (2022) A review of treatment technologies for the mitigation of the toxic environmental effects of acid mine drainage (AMD). Process Safety and Environmental Protection 157:37-58. https://doi.org/https://doi.org/10.1016/j.psep.2021.11.008

International Aluminium Institute (2022) SUSTAINABLE BAUXITE RESIDUE MANAGEMENT GUIDANCE. In: Healy S (ed). p 92

Kröpfelová L, Vymazal J, Švehla J, Štíchová J (2009) Removal of trace elements in three horizontal sub-surface flow constructed wetlands in the Czech Republic. Environmental Pollution 157(4):1186-1194

Mayes WM, Aumonier J, Jarvis AP (2009b) Preliminary evaluation of a constructed wetland for treating extremely alkaline (pH 12) steel slag drainage. Water Science and Technology 59(11):2253-2263

Mayes WM, Batty LC, Younger PL, Jarvis AP, Kõiv M, Vohla C, Mander U (2009a) Wetland treatment at extremes of pH: A review. Science of The Total Environment 407(13):3944-3957. https://doi.org/10.1016/j.scitotenv.2008.06.045

Mishra UC, Sarsaiya S, Gupta A (2022) A systematic review on the impact of cement industries on the natural environment. Environmental Science and Pollution Research 29(13):18440-18451. https://doi.org/10.1007/s11356-022-18672-7

O'Connor G, Courtney R (2020) Constructed wetlands for the treatment of bauxite residue leachate: Long term field evidence and implications for management. Ecological Engineering 158:106076. https://doi.org/10.1016/j.ecoleng.2020.106076

Pat-Espadas AM, Loredo Portales R, Amabilis-Sosa LE, Gómez G, Vidal G (2018) Review of constructed wetlands for acid mine drainage treatment. Water 10(11):1685

Residue Solutions (2007) Residue Management Sustainability Review Aughinish Alumina Limited, Report №, Brisbane, Queensland,

Riley AL, Mayes WM (2015) Long-term evolution of highly alkaline steel slag drainage waters. Environmental Monitoring and Assessment 187(7). https://doi.org/10.1007/s10661-015-4693-1

Roadcap GS, Kelly WR, Bethke CM (2005) Geochemistry of extremely alkaline (pH> 12) ground water in slag-fill aquifers. Groundwater 43(6):806-816

Ruyters S, Mertens J, Vassilieva E, Dehandschutter B, Poffijn A, Smolders E (2011) The Red Mud Accident in Ajka (Hungary): Plant Toxicity and Trace Metal Bioavailability in Red Mud Contaminated Soil. Environmental Science & Technology 45(4):1616-1622

Vymazal J, Krása P (2003) Distribution of Mn, Al, Cu and Zn in a constructed wetland receiving municipal sewage. Water Science and Technology 48(5):299-305. https://doi.org/10.2166/wst.2003.0336

Using Innovative Geophysical Techniques to Characterize Abandoned Mine Workings and Mine Water

Andrew Hughes[1], Ryan Blanchard[2], Val Kofoed[2], Mike Jessop[2]

[1]*Dams and Reservoirs, Ltd., Hall Farm, Church Lane, North Clifton Newark on Trent, Notts NG23 7 AP, UK, andy.hughes@damsandreservoirs.co.uk*

[2]*Willowstick Technologies, P.O. Box 754, Spanish Fork, Utah 84660, USA, rblanchard@willowstick.com*

Abstract

Mine operators and consultants play a crucial role in the management of abandoned mine water and drainage systems, which can have significant impacts on waterbodies and the surrounding environment. These systems are often complex and difficult to characterize due to subsurface hydrogeologic complexity and a lack of historical data. Traditional approaches to water treatment, such as mine water treatment schemes, can be costly and may not address the root cause of contamination. As a result, there is a need for more accurate and comprehensive methods for assessing and understanding abandoned mine water and drainage systems. This paper describes two innovative geophysical techniques by case studies and how they enabled characterization of abandoned mine workings and mine water.

Keywords: Geophysics, seismic, groundwater, 3D modeling

Introduction

In recent years, innovative geophysical techniques have been developed to provide a more detailed understanding of mine water flow and identify potential sources of pollution. One such technique is Micro Seismic Resonance (MSR), which can identify locations of geologic, lithologic, and structural anomalies as well as stratigraphic units; assisting in the holistic understanding of an abandoned mining complex. MSR works by detecting structural weakness in rocks by measuring the resonance intensity and thus can also locate weak or fractured zones of high permeability. Another technique, Willowstick magneto-metric resistivity, is able to map and model groundwater flow paths and patterns through abandoned mine workings in three dimensions.

In our work, we have employed these innovative techniques in two case studies to assess groundwater conditions in abandoned adits and interconnected mine workings. The results of these studies have provided valuable insights into how and where water preferentially infiltrates the underground mine workings. By combining the results of the MSR and Willowstick techniques, Willowstick is able to help clients identify locations of potential contamination and develop a comprehensive model of groundwater flow through the mine workings. Holistic modeling and interpretation allow for the implementation of targeted remediation measures and the rehabilitation of the site, reducing the potential for ongoing water pollution.

The use of innovative geophysical techniques has significant implications for the management of abandoned mine water and drainage systems. By providing a more accurate and comprehensive understanding of these systems, mine operators and consultants can take targeted remediation efforts to reduce the long-term costs of traditional water treatment approaches and protect waterbodies and the surrounding environment from potential pollution pathways. Our work is an example of the potential of these techniques to improve the management of abandoned mine water and drainage systems and reduce their impact on the environment.

Non-Intrusive Investigative Geophysical Techniques

This paper describes two geophysical techniques. The MSR method is a passive seismic technique which detects structural

weaknesses in soil and rock and is apt at locating zones of higher permeability. The constant cycle of tidal motion that affects the oceans, resulting in high and low tides twice a day, is common knowledge. It is a well-established fact that the moon and sun drive these ocean-tidal events. A lesser-known fact is that there are tidal movements in the earth's crust as a result of these same gravitation forces. Earth tides fluctuate between 15 cm (6 inches) and 45 cm (18 inches) a day depending on the location on the earth's surface and the position of the sun, moon and earth in relation to one another. As a result, it is now an established fact the ground below our feet is constantly in motion—rising and falling on a continuous 12-hour cycle. Although we cannot feel the earth's movement (other than during relatively large seismic events—i.e., earthquakes and tremors), it is only detectable with sophisticated and sensitive equipment. Movement of 15 to 45 cm (6 to 18 inches) a day may seem minor in comparison to the earth's diameter; nevertheless, when considering there are hundreds of meters (thousands of feet) of rock and soil beneath our feet in constant motion, we can start to appreciate the magnitude of this geologic fact.

Over time, stresses build in the earth's crust from the repeated rising and falling of the earth's crust until stress release points or zones are established along faults and fractures in rock formations and along zones of secondary permeability in soil formations. As the earth moves, frictional grinding takes place. This grinding creates a resonance signal. The movement and grinding of the earth's crust in conjunction with groundwater naturally collecting in these areas produce resonance signals that can be measured and modeled to identify zones of higher permeability in the rock and soil matrix. MSR measurements, which identify active resonance signals with high resonance frequencies within the resonance frequency domain, indicate that the stress relief point is near the surface. Lower resonance frequencies (within the resonance frequency domain) indicate a deeper anomalous zone. Thus, the zones of highest structural weaknesses within the alluvium and rock matrix can be identified beneath the earth/s surface.

This technique is compact and easily deployable, and 2D acoustic profiles showing strengths or weaknesses of the underlying stratigraphy can be produced rapidly in the field (see Figure 1). 3D modeling is also provided to show pertinent site features in relation to subsurface features and anomalous zones, 3D site models of the subsurface are created to serve as helpful tools in the interpretation and presentation of the results.

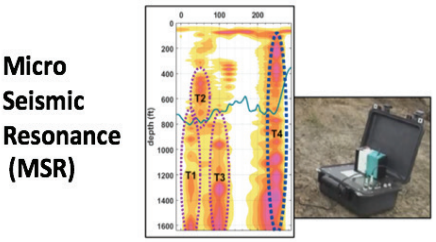


Figure 1 *MSR Equipment & Stratigraphy Profile*

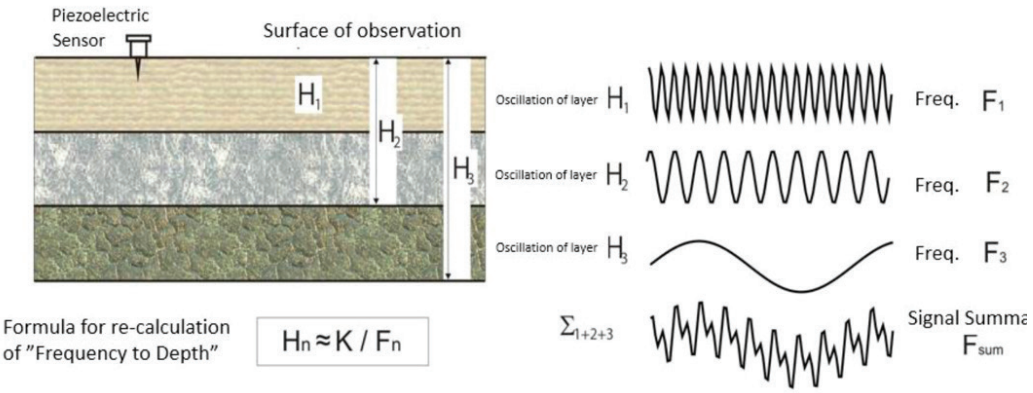
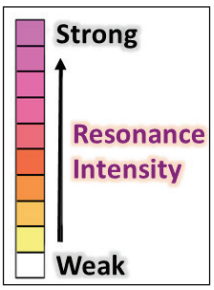


Figure 2 MSR Measurement and Data Collection Illustration

Full analysis and detailed 3D models can be produced within days of collecting the data.

The MSR measurements are conducted by utilizing two types of sensors: a spike geophone piezoelectric sensor for soils or a flat sensor for hard surface or rock. MSR surveys do not require bulk source excitation (sledgehammer) or vibration machines, explosives, etc. The method is easily deployed and non-destructive, falling under the sub-category of passive seismics with the exception of a tap on the ground next to the sensor to trigger the data collection (see Figure 2).



In the MSR profiles, we provide a Resonance Intensity Indicator. The white to yellow colors indicate a relatively competent soil or rock formation (i.e., void of any anomalous features that would indicate a weakness—stress relief point or permeable zone within the alluvium/rock matrix). The orange to pink colors, going up the scale, represent higher degrees of signal strength—strong pink zones representing the strongest signal or more permeable zones.

The Resonance Intensity Indicator does not provide any measurement of the geo-mechanical properties of the soil or rock matrix (i.e., strength, consolidation, shrinkage, swell, permeability, particle analysis, etc.). The Resonance Intensity Indicator simply reflects a relative comparison of where resonance signals are stronger or weaker. Based on our experience, resonance rich measurements (producing strong resonance signals) have proven to be helpful in identifying weak and permeable zones in the soil and rock matrix (i.e., faulting and fractures in rock formations and increased secondary permeability in alluvium formations).

The Willowstick magneto-metric resistivity technique uses a low voltage, low amperage, alternating electrical current to energize subsurface water by electrodes placed strategically upgradient and downgradient of the study area and an electrical circuit is established between the two electrodes (Figure 1).

The application of the technique to mine water is based on the principle that water increases the conductivity of earthen materials through which it flows. As the signature electric current travels between electrodes strategically placed upstream and downstream of the mine water, it concentrates in the more conductive zones, or highest transport porosity areas. Measuring the resultant magnetic field at the surface reveals the electric current flow and distribution. Data is processed and compared to a predicted magnetic field from a theoretical homogenous earth model to highlight deviations from the

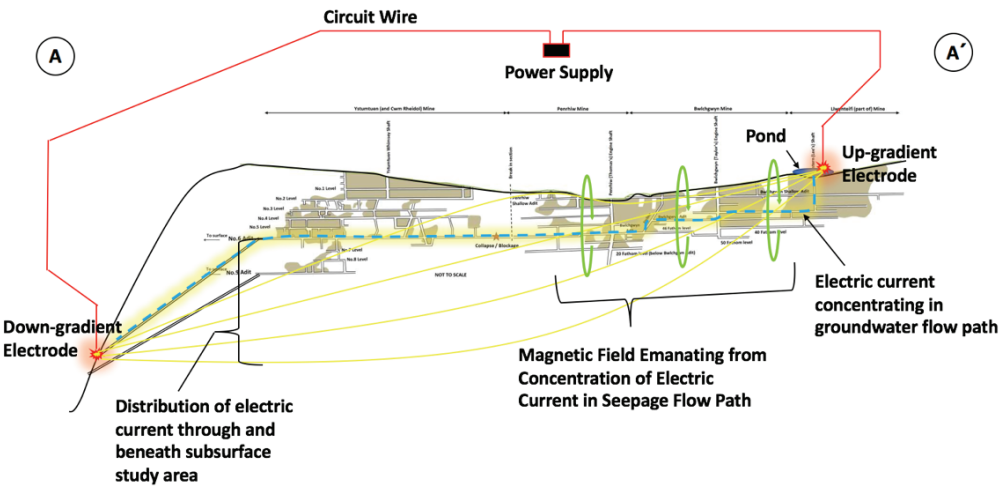


Figure 3 Cross-sectional Schematic of Willowstick Technique at Abandoned Mine

"uniform" model. 3D models are generated and combined with known sub-surface data to enhance preferential seepage path definitions. The technique maps and models preferential groundwater flow paths like an angiogram that lets doctors to "see" blood vessels in a human body.

This paper, through three tailings dam studies, illustrates the procedures, findings and benefits of this technology. Results range from confirmation of design decisions to identifying new seepage paths. In the latter case, the designs are now being updated based on the new information to provide a more safe and stable tailings dam and reduce the risk of failure.

Mine Water Case Study

A close-up aerial photograph of an earthen dam with a grout curtain is shown in Figure 5. The dam was currently under construction at the time of the investigation. The dam consisted of a bedrock grout curtain (see red vertical line), a cement-bentonite (CB) slurry wall with vibro-compacted gravel zones on both sides of the grout curtain on top of native gravels. It should be mentioned that the CB slurry wall failed to reach bedrock in some locations due to very dense gravelly material, leaving a gap between the red and green lines.

A longitudinal profile drawing of the dam's grout curtain is shown in Figure 6. The drawing represents the completion of the grout curtain prior to the investigation. The brown line identifies the top of bedrock. The blue line identifies the top of native gravels.

While constructing the grout curtain, unexpected grout takes occurred—more specifically in the center area of the grout curtain. Before completing grout work (which was nearing completion), the owner wanted to identify any potential weaknesses where seepage could possibly escape the impoundment through, beneath or around the grout curtain. Therefore, the purpose of the investigation was to identify, map and model preferential electric current flow paths and patterns that indicate high-probability pathways for seepage to follow as electric current was biased to flow through, beneath and around the grout curtain (i.e., the Willowstick Method). The investigation also included a MSR survey to detect structural weaknesses in the soil/rock matrix to identify any potential weaknesses or fractured zones of high permeability through the fill and foundation materials. Therefore, the overall intent of the investigation was to identify areas that warrant additional grouting while the grouting contractor was still on site.

The Willowstick Method identified two preferential electric current flow paths through the dam's existing grout curtain (see Figure 7).

In Figure 7, the green shading represents areas where the signature electric current density is more concentrated than expected. On the other end of the scale, the dark-purple shading identifies areas where electric current

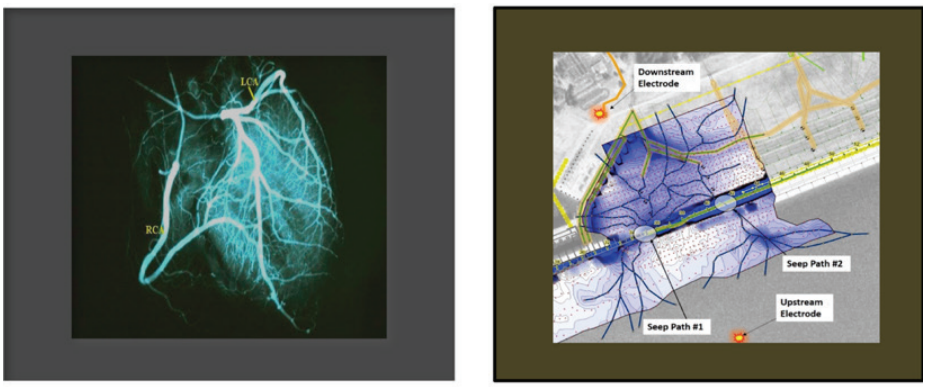


Figure 4 Angiogram / Willowstick Comparison

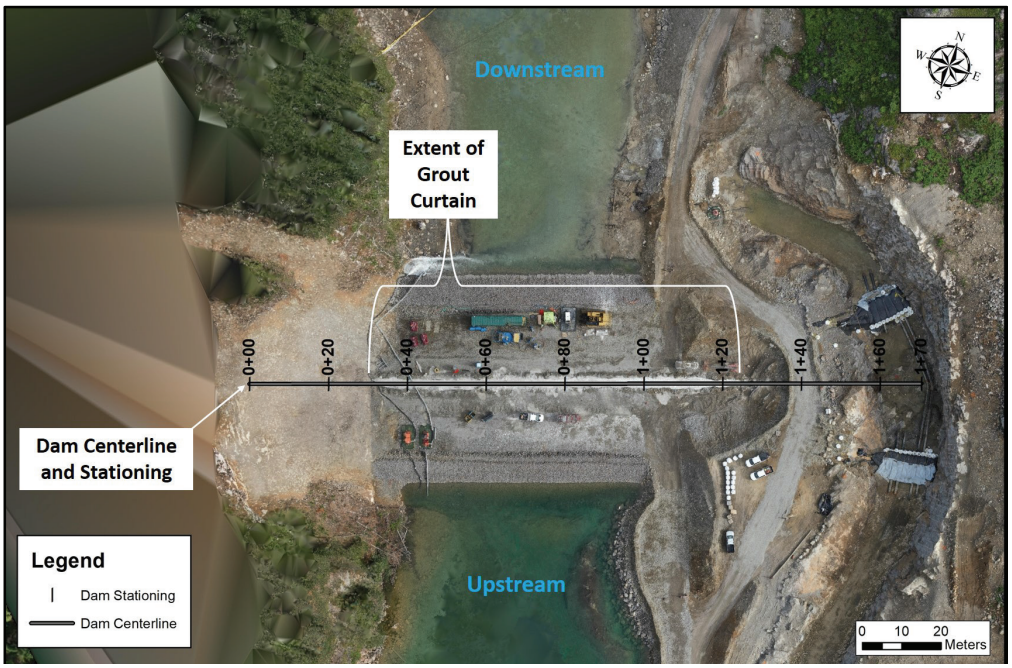


Figure 5 Site Map of Dam w/ Mine Water

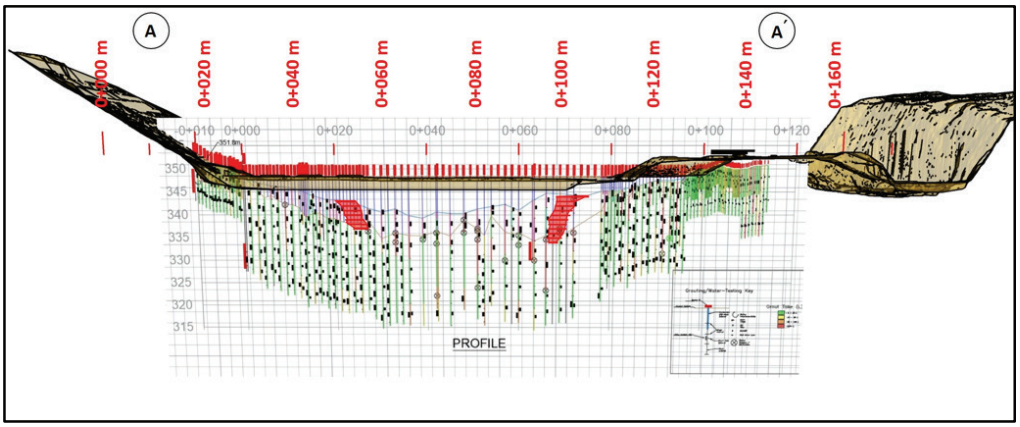


Figure 6 Longitudinal Profile As-built Drawing of Grout Curtain

is less concentrated. The yellow arrows highlight the more intense locations where the signature electric current preferentially concentrates as it escapes the impoundment – interpreted as following along preferential seepage flow paths.

To describe the depths of the seepage flow paths, Figure 8 (Section A–A´) presents a longitudinal profile slice of the electric current distribution model taken directly beneath the center axis of the dam—looking downstream through the embankment and grout curtain.

To further describe the location of the electrically conductive flow paths, Figure 6 presents Section A–A´ (i.e., the same view as shown in Figure 8, but with the ECD model slice turned "off"). The red hatched horizontal lines remain to show the position of the preferential flow of electric current in

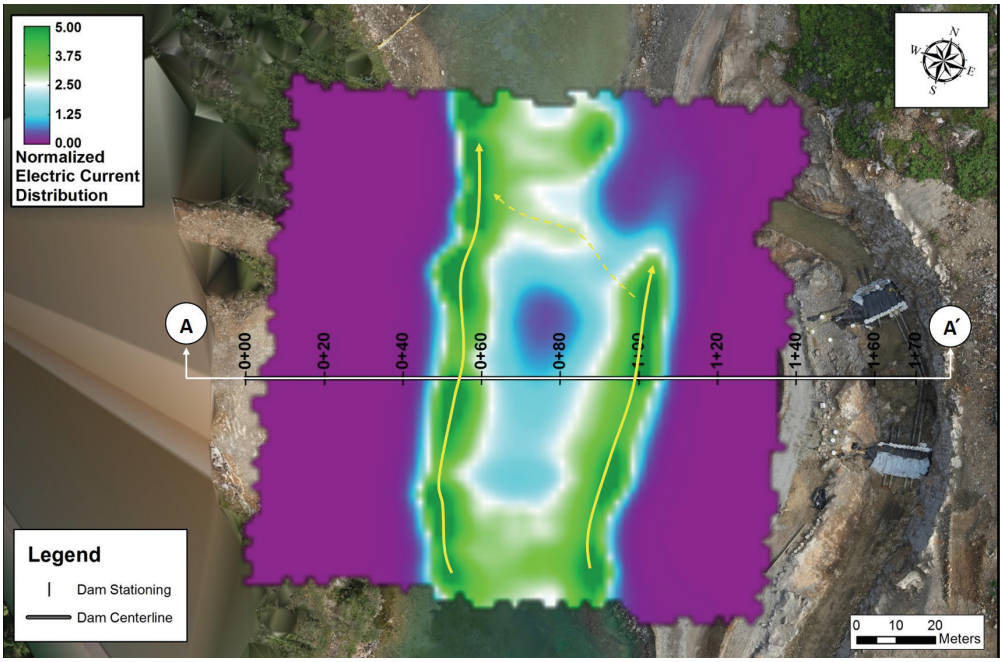


Figure 7 Willowstick Method Results (Plan View)

relation to the grout curtain, bedrock surface, native gravels and earthen embankment fill interface. The brown line identifies the top of the bedrock. The blue line identifies the top of native gravels. The preferential flow of electric current (red hatched area) is located above the bedrock surface in native gravels and below the embankment fill.

The MSR results revealed several weak areas at or just below the bedrock surface with a few deeper anomalous features noted (i.e., representing possible fracture or faulted zones – see Figure 9). Please know that the MSR line shown in Figure 9 is taken upstream of Section A–A´ (center axis of dam roughly 4 m).

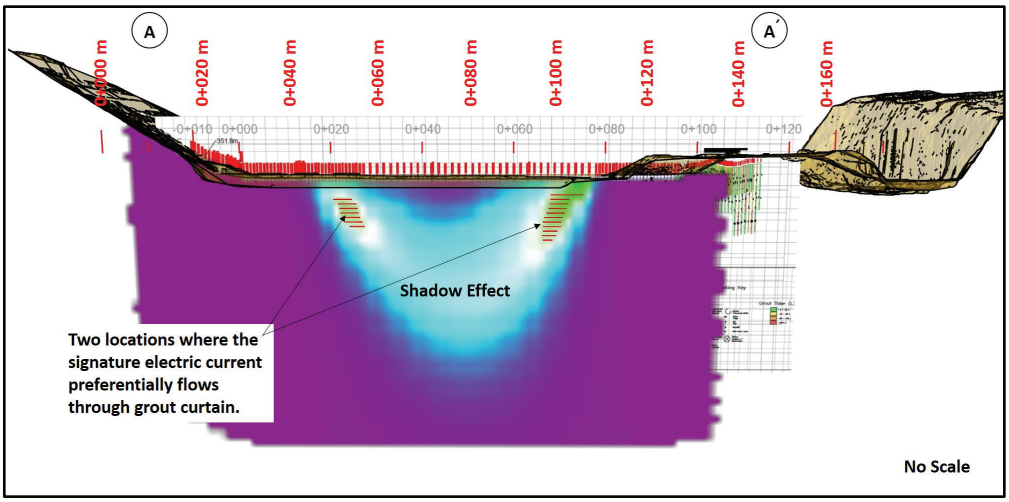


Figure 8 ECD Model Slice Section A–A´

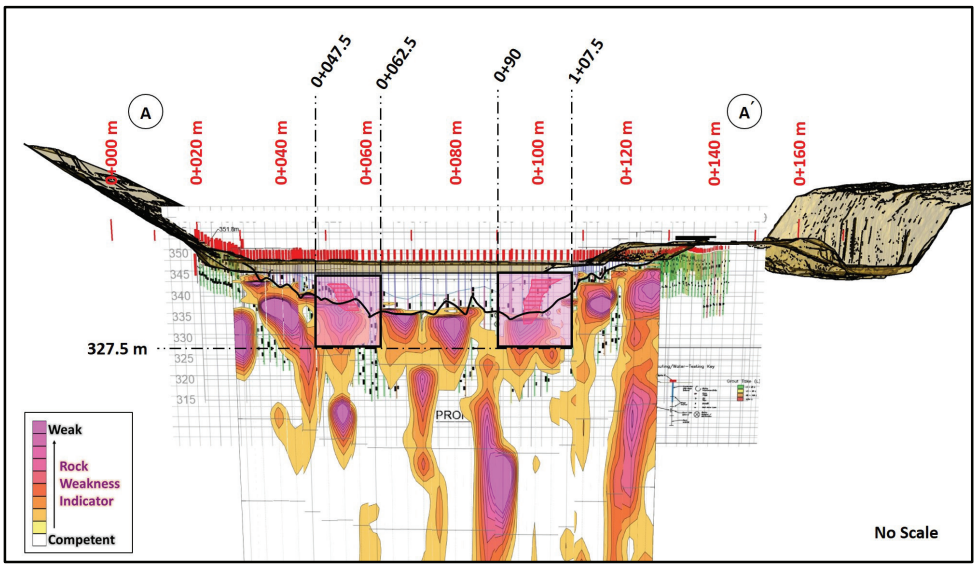


Figure 9 *Willowstick Method Results (Plan View)*

In Figure 9, the transparency (white shaded areas) on the MSR profile indicates competent soil and rock. The yellow to orange to pink shading, going up the scale, represents higher degrees of soil/rock weakness—strong pink shading representing the weakest, highly fractured or weathered and permeable zones. The anomalous vertical features identify what is interpreted as deeper fractures. The bedrock grout curtain appears to extend down through the weathered zone.

During a conference call with the owner and grout contractor, wherein the preliminary results of the investigation were presented, the grouting contractor revealed that unexpected grout takes occurred in the center of the grout curtain. Based on the results of the Willowstick and MSR techniques in conjunction with known grout takes, weaknesses were found in the native gravel layer on either side of the center area of the grout curtain. Target locations were recommended for additional grout work to reduce potential seepage out of the impoundment. These locations are represented by the pink rectangular windows shown in Figure 9.

The investigation confirmed that the grout has filled voids in the weathered bedrock and porous zones in the native gravel layer; however, on either side of this area, it appears more grout was needed to minimize seepage. The fact that both techniques identified common anomalous features and patterns (which use entirely different scientific principles) provides a great deal of confidence in the results of the investigation.

Conclusions

The case study shows how non-intrusive techniques can be used to supplement known geological, geotechnical, hydrological and groundwater information to enhance the knowledge of existing mine water and mine workings conditions. This knowledge can then be used to cost-effectively support the remediation efforts and to provide long-term safety and stability for abandoned mine water and drainage systems.

Acknowledgements

The authors thank all co-organisers for hosting the IMWA2023 Conference. The authors also gratefully acknowledge the support of our Mining Client and consultants in the preparation of this paper.

Use of evaporation ponds in the mining industry. How necessary and effective is this in various parts of the world

Houcyne El Idrysy[1], Nikolai Kirillov[2], William Harding[3], Gary Hurban[4]

[1]SRK Consulting (Kazakhstan) Ltd, Head Office, 5ih Floor, Churchill House, 17 Churchill Way, Cardiff, CF10 2HH, Wales, hidrysy@srk.co.uk

[2]SRK Consulting (Kazakhstan) Ltd, 77 Kunayev St., Park View Office Tower, 14th Floor, Almaty, Kazakhstan, nkirillov@srk.kz

[3]SRK Consulting (UK) Ltd, 5th Floor, Churchill House, 17 Churchill Way, Cardiff, CF10 2HH, Wales, wharding@srk.co.uk,

4SRK Consulting (US), Inc, Suite 300, 5250 Neil Rd., Reno, Nevada, ghurban@srk.com

Abstract

Water resources and their sustainability are increasingly under threat in several parts of the world due to scarcity and to the added complication of climate change. The preservation and optimal use of water should therefore be made a priority across all domestic, industrial, and commercial sectors and countries to avoid shortages and potential future conflicts. In this context, funding for development and/or closure of mining projects, which often have an impact on water resources, are increasingly dependent on Environmental Social and Governance (ESG) principles to encourage companies to act responsibly.

The rapid growth of ESG investment funds in recent years is revolutionising current water use and environmental regulations worldwide, and mining companies may encounter constraints on mine water management practices that are perceived as counter to the principle of preservation of water resources. In this context, to pre-empt further changes in water use regulation, a question arises regarding the use of evaporation ponds as a water management tool at mine sites - Are evaporation ponds an appropriate strategy for managing excess water at mine sites, or do evaporation ponds waste water and should alternative strategies or technologies be considered?

This paper examines the use of evaporation ponds in mining projects from the following perspectives:

- The various contexts in which evaporation ponds are utilized.
- Current regulations and permitting of evaporation ponds in various parts of the world.
- Potential environmental and social effects of evaporation ponds and related studies.
- Potential alternatives to evaporation ponds considering their effects, technical feasibility, and cost.

Keywords: Water resources, climate change, ESG, evaporation pond, Mine Water Management

Contexts in which evaporation ponds are utilized in mining

Evaporation ponds in the mining industry are employed at mine sites around the world for disposing of excess or unusable water, i.e., water not needed nor suitable for other activities at the mine site. This water cannot be easily separated from the dissolved constituents and can range from salt water to a solution containing metals, minerals, organic and/or inorganic compounds, and micro-organisms. Evaporation ponds are primarily used at mine sites for two purposes:

1. Mineral extraction/processing, and
2. Management of mine water.

A common characteristic of both applications is that the influent (source water) is of insufficient quality to be used by people, animals, or plants.

Other uses of evaporation ponds include disposal of poor-quality surface water runoff, storage of excess water used by the mine facilities or processes, or management of low-flow draindown solutions in closure.

Mineral extraction/ processing

Most evaporation ponds in the mining industry are used to evapo-concentrate mineral rich brines as a key step in the processing and recovery of minerals or metals. Lithium, Potash (Potassium Chloride) and sea salt are products mined in this manner. An example operation would be the Sociedad Química y Minera (SQM) site on the Salar de Atacama in Chile. In this process, mineral enriched groundwater is pumped from the halite crust on the salar and placed in a succession of lined evaporation ponds to concentrate the brine through passive evaporation. Salts from the brine are left to precipitate on the bottom of the pond where they are harvested using excavators. The first product is sodium chloride with the supernatant transferred to a sylvinite pond, then carnalite pond and finally a pond designed to maximise the concentration of lithium chloride.

Management of mine water

Mine water at a mining operation can be generated from several sources including 1) excess water from mine dewatering, 2) acid mine drainage from underground workings, tailings piles, or low pH native soils from disturbed areas, 3) residual effluent from the mine process circuit, and 4) sewage treatment plant effluent. Natural evaporation of mine water containing metals, minerals, etc. can reduce cost while safely storing contaminants in lined facilities. Use of evaporation ponds to dispose of mine dewatering water may have the most potential for alternatives to be considered due to the typically high volumes of water and large areas of land required for this use.

In-situ mining

In-situ mining is another sector of mining industry that utilizes evaporation ponds. Salt, Potash, Uranium and Copper are commodities extracted by In-situ mining. In this process, a wellfield is established within the orebody and water with reagents (lixiviant) is circulated through the orebody to leach metals or dissolve minerals. For Salt and Potash mining the ponds are used for mineral extraction; for Uranium and Copper mining the ponds are used to concentrate the spent liquid effluent from the plant or to concentrate effluent from groundwater restoration activities.

Other uses

Runoff from mine impacted soils can be diverted and collected in evaporation ponds as a source control measure to minimize effluent of contaminated surface water off site.

In mine closure, draindown of process solutions in heap leach pads and tailings impoundments will decrease exponentially until a stable flow is achieved. These low-flows can be managed in an Evaporation Cell (E-Cell). An E-Cell utilizes a matrix of soil, rock or engineered material that can store low volumes of drain down with evaporation from the soil surface.

Considerations & Limitations

Some considerations and limitations on use of evaporation ponds include the following.

- They require an arid to semi-arid climate where annual evaporation considerably exceeds annual precipitation. Their application in some parts of the world is therefore limited.
- They can require a large land footprint for adequate water disposal and are not suited for mine sites with limited land positions. As influent flow rates increase, more land is required to increase the surface area of the ponds to increase evaporation volumes.
- For passive management of excess water in mine closure, evaporation ponds or E-Cells are limited to low flow systems.
- In mine water reduction applications, precipitates and/or sediment need to be regularly removed from the pond to maintain design capacity.
- Due to the slow rate of the evaporation process, they are not suited for situations in which a rapid inventory reduction is required.
- If the mine process does not optimize the recycling and reuse of process

water, evaporation ponds could result in a permanent loss of water that might otherwise be re-used in the mine circuit.

Current regulations and permitting of evaporation ponds

The regulations and permitting that govern evaporation ponds as part of mining operations extend over multiple areas (environmental, water, land use, industrial safety) in most jurisdictions. Use of these facilities as part of mining operations or on its own can have effects and present risks to receptors such as land, water, air, wildlife, and the socioeconomics, health and safety of the nearby communities as described in the next section. Thus, most of the regulations and permitting requirements are aimed to avoid the negative effects and risks of evaporation ponds to the named receptors. A brief overview of the Australian, Chilean, Kazakh, and the United States' regulations and permitting related to evaporation ponds in mining is provided below.

Australia

In Australia, environmental regulations are primarily governed by state and territory laws, while the federal government also oversees matters related to the environment and climate change. The Environment Protection and Biodiversity Conservation Act 1999 (Cth) manages developments that may significantly impact "matters of national environmental significance" through an additional approval process. For instance, a proposed project that could severely affect a nationally listed threatened species or ecological community necessitates approval from the federal government, as well as state or territory-level approvals.

Significant developments, such as mining projects, must undergo an environmental impact assessment to ascertain whether they will have a "major" impact on the environment and, if so, under what conditions they may proceed. Potential effects on the social environment, including communities and First Peoples, are relevant considerations, in addition to the effects on landscape, flora, and fauna. The legislation promotes in order of priority application of the following water management strategies for mines, with only strategies 6 to 8 applicable to the evaporation ponds:

1. Avoidance,
2. Reduction,
3. Reuse,
4. Recycling,
5. Recovery of energy,
6. Treatment,
7. Containment,
8. Disposal

Environmental laws take precedence over all mining rights. Mining projects are required to undergo environmental assessment and obtain necessary environmental approvals before proceeding. In recent times, both state and federal governments have increasingly introduced intricate legislation, policies, and mechanisms, along with heightened penalties, to regulate industries and activities with the potential to negatively impact the environment. This may affect the favourableness of the use of evaporation ponds as the legislation evolves. Currently, evaporation ponds are a suitable means of managing excess water if no alternative method is available or cost-effective.

Chile

In Chile, the principal authorization required to operate an evaporation pond as part of a mine is the environmental permit, also known as the Environmental Qualification Resolution (EQR). The EQR follows an environmental assessment (EA) process, the environmental authority grants this permit. The EA process involves the participation of all public entities with environmental competence in a centralized manner, and if applicable, citizen participation processes and indigenous consultations are conducted. The National Environmental Assessment Service (NEAS) oversees this process.

The Chilean government is soon to announce a policy aimed at development of new mineral deposits. As part of this policy, lithium projects specifically, will be required to use a more targeted or precise process that will lead to significantly lower evaporation levels. Major Chilean lithium producers are exploring these methods, which have not been widely tested in commercial settings. The Chilean government supports the direct lithium extraction (DLE) process, where the

brine is reinjected back after the extraction of lithium. This would result in lesser environmental effects on the groundwater system and a reduction of land disturbance for evaporation ponds.

Thus, traditional passive evaporation is considered less favourable than other more selective or direct processing techniques. If the new policy in Chile is approved, it is unlikely that NEAS will grant an EQR to use evaporation ponds to extract lithium, possibly prohibiting use of traditional evaporation ponds in the future.

Kazakhstan

The main legal act in Kazakhstan that governs the design and permitting of evaporation ponds is the Environmental Code. It requires that the selection and substantiation of water treatment technologies prior to the commissioning of an evaporation pond must be part of the environmental impact assessment process.

The majority of the evaporation ponds in Kazakhstan are used to manage excess water from the dewatering of mine workings. While some of the pumped water is non-contact "clean" water, in many cases the chemical composition of the pumped groundwater (including mineralization) does not allow for direct discharge into the environment without prior treatment which is expensive due to the required methods and volumes. Notably, while the use of evaporation ponds is legally possible, the Environmental Code treats them as a "last resort" in the hierarchy of water management techniques and is permitted when no other option is possible. The use of this "last resort" option must be justified during the environmental impact assessment process.

United States

In the U.S., the Clean Water Act (CWA) as amended in 1972, establishes the basic structure for regulating discharges of pollutants into waters of the United States. The Environmental Protection Agency (EPA) administers the requirements of the CWA through the National Pollutant Discharge Elimination System (NPDES), making it unlawful to discharge any pollutant from a point source to waters of the U.S. Specific regulations governing mining operations are promulgated by each state based on the requirements of the NPDES program and other federal or state statutes.

Mining projects must go through an Environmental Impact Statement (EIS) process that documents baseline studies, proposed effects of mining, mitigation measures and alternatives. Public comments regarding the use of evaporation ponds may require additional studies or documentation to demonstrate the use of evaporation pond is an appropriate strategy.

Potential environmental and social effects of evaporation ponds

Potential Risks on Water Resources

There are two mechanisms that could lead to negative effects of evaporation ponds on water resources, as follows:

- Breach of the evaporation pond embankment, which could occur due to (1) physical instability of the embankment, 2) internal erosion through the embankment, and 3) overtopping from within the pond.
- Seepage and infiltration of contaminated water through the embankment and/or within the pond footprint.

The first mechanism results in failure of the dam and downstream consequences to the environment and potential loss of life. For the second mechanism, which consists of seepage of contaminated water through the pond embankment and/or footprint, impact on water resources can occur if a contaminant source-pathway-receptor system is present, as illustrated in Figure 1.

The Source is the evaporation pond, the Pathway is a (lateral or vertical) preferential flow path via porous medium or fracture network that connects the source to an underlying aquifer or surface water body. The presence of each of the three elements should therefore be demonstrated as part of risk assessment, before potential effects on water resources or users can be envisaged.

Potential Environmental and Social Risks

Depending on site setting, common social and environmental effects that may occur

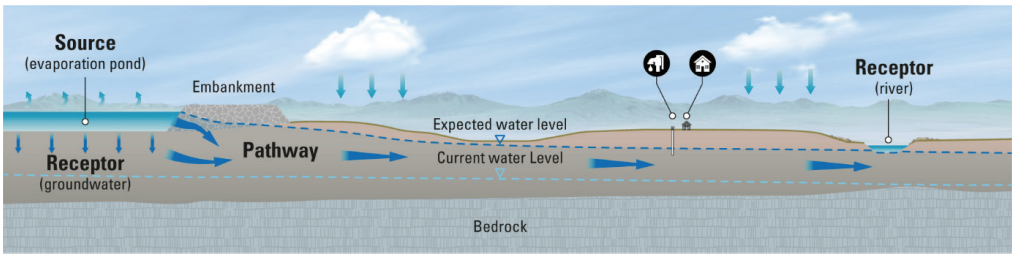


Figure 1 Illustration of contaminant source-pathway-receptor concept

because of discharge of excess water into an evaporation pond can be summarised as follows:

- Impact and possibly destruction of protected or sensitive flora and fauna species
- Social impact (water users and stakeholders) due to Contamination of water sources

Potential Geotechnical and Stability Risks

Key common geotechnical risks of evaporations ponds could be summarised as follows:

- The risk of overtopping the facility exists if strict operational limits are not specified and maintained during the operational life of the facility. If foundation materials are collapsible, seepage underneath the embankment may lead to excessive settlement
- Weak foundation material may lead to global embankment instability leading to total or partial collapse of the embankment and potential release of ponded water
- Excessive seepage through the foundation and embankment, due to high exit hydraulic gradient for example, may lead to piping failure in the foundation materials.

Potential alternatives to evaporation ponds

Passive evaporation has the obvious advantage of needing little or no energy beyond that produced by the sun to facilitate water removal from enriched brines or mine water. Per the limitations discussed earlier in this paper, operators in non-arid climates for example, must resort to using alternative methods for the treatment and removal of excess water from the mine. These alternative methods are technologically more sophisticated than evaporation ponds.

Mechanical evaporation using various technologies is an increasingly common approach deployed on mine sites. This includes spraying and atomising water in the atmosphere (using mist canons) to increase the evaporative surface area thereby greatly accelerating the evaporation process. The utility of mechanical evaporation depends on local climatic conditions but has the advantage of being modular and portable and provides flexibility for use at mine sites. Limitations of this technology include potential drift of atomised water droplets containing salts or metal compounds being deposited outside of lined containment.

The other form of actively promoted evaporation technology is the thermal brine concentrator and crystallisation plant. Unlike mechanical evaporation, this technology is a substantial and fixed piece of infrastructure that is frequently an extension of the mine process circuit. It is also a more costly method, both in terms of initial capital outlay and operational costs. However, it achieves a high clean water recovery rate and is uniquely suited for removing high salt levels (TDS > 50g/L) with a solid waste product that is easy to package and remove from site.

At lower TDS, operations tend to use Reverse Osmosis (RO) or exotic variants of it such as High Efficiency RO and Osmotically Assisted RO to remove excess water. These also produce clean water, but the liquid brine discard (waste) still needs to be disposed of, which means there are additional costs implications.

Another alternative to the evaporation pond is the injection well, which has been used by some mining operations to dispose of highly saline water into ground. The viability of the approach is very dependent on there being favourable hydrogeological conditions near to the mine site, i.e., a deep disposal location with high permeability and storage, isolated from the surface by a naturally impermeable capping layer. This method has a lower capital and operating cost than the other alternatives and needs no water treatment. However, it does require a high degree of maintenance, is logistically complex and faces challenges as far as environmental compliance is concerned. These and the absence of favourable ground conditions means that removal of surplus water using injection wells is not a common practice in the mining sector.

Furthermore, in some cases, depending on the level of contamination, the hydrogeological setting and local regulation, use (creation) of wetlands to discharge mine water, especially from dewatering, can be envisaged.

Conclusions

Use of evaporation ponds in the mining industry is a low-cost, effective method for concentrating mineral rich brines and/or to reduce mine water volumes in dry- to semi-dry climates. Regulations governing use of evaporation ponds are increasingly focused on prudent use of water resources, which parallels the growth of ESG investment funds and interest in adhering to ESG principles. In this sense, water loss in mining projects due to engineered evaporation may not be considered an ideal outcome in a water scarce environment if that water could have been reused. This paper has highlighted some alternative technologies such as thermal brine concentrators and RO that do conserve water, but which by comparison, are costly processes that may not be economically viable for some marginal operations. Due to the high relative impacts of evaporation ponds as a strategy to dispose of mine dewatering water, they may face tighter scrutiny in this application by regulators looking to preserve water resources.

To answer the question posited in this paper whether evaporation ponds are an appropriate strategy for managing excess water at mine sites, the answer is – they are where climatic conditions are favourable, land is plentiful, and the reuse and recycling of the impacted water is optimized as part of processing and infrastructure engineering. If it cannot be shown that reuse and recycling have been optimized, in line with responsible water stewardship practices, and that there is an over-reliance on fresh surface and groundwater sources to make up the shortfall, then it becomes increasingly difficult to make the case for evaporation as a sustainable strategy.

References

Brown MC, Wigley TC, Ford, DC (1969) Water budget studies in karst aquifers. J Hydrology 9:113—116, doi:10.1016/0022-1694(69)90018-3

Caruccio FT, Geidel G (1984) Induced alkaline recharge zones to mitigate acidic seeps. In: Groves DH, DeVere RW (Eds), 1984 Symp of Surface Mining, Hydrology, Sedimentology and Reclamation, Univ of Kentucky, p 27—36

Day TJ (1977) Field Procedures and Evaluation of a Slug Dilution Gauging Method in Mountain Streams. J Hydrol New Zealand 16(2):113-133

Gammons CH, Mulholland TP, Frandsen AK (2000) A comparison of filtered vs. unfiltered metal concentrations in treatment wetlands. Mine Water Environ 19(2):111—123, doi:10.1007/ BF02687259

Edwards RW, Stoner JH (1990) Acid Waters in Wales. Monographiae Biologicae, vol 66. Kluwer, Dordrecht

U.S. Nuclear Regulatory Commission (NRC). Chapter 2 - In-Situ Uranium Recovery and Alternatives.

Assessing Removal Efficiencies of Mn and Ni in Mine Drainage Using Bench- and Pilot-scale Slag Reactors and Design of Treatment System

Dae-gyu Im[1], Duk-min Kim[2], Hye-Lim Kwon[3], Joon-Hak Lee[4], Mi-Sun Park[5], Seong-Taek Yun[6]

[1]*Department of Earth and Environmental Sciences, Korea University, Anam-ro 145, Seongbuk-gu, Seoul, 02841, Republic of Korea, daegull1995@korea.ac.kr, ORCID 0000-0002-7499-8403*

[2]*Department of New Energy and Mining Engineering, Sangji University, Sangjidae-gil 83, Wonju, Gangwon-do, 26339, Republic of Korea, kdukmin8@sangji.ac.kr, ORCID 0000-0002-1537-6866*

[3]*Department of New Energy and Mining Engineering, Sangji University, Sangjidae-gil 83, Wonju, Gangwon-do, 26339, Republic of Korea, ossgpfla@naver.com*

[4]*Korea Mine Rehabilitation and Mineral Resources Corporation, Hyeoksin-ro 199, Wonju, Gangwon-do, 26464, Republic of Korea, jun292@komir.or.kr*

[5]*Korea Mine Rehabilitation and Mineral Resources Corporation, Hyeoksin-ro 199, Wonju, Gangwon-do, 26464, Republic of Korea, mspark@komir.or.kr*

[6]*Department of Earth and Environmental Sciences, Korea University, Anam-ro 145, Seongbuk-gu, Seoul, 02841, Republic of Korea, styun@korea.ac.kr*

Abstract

This study aimed to treat mine drainage containing Mn and Ni using a passive slag reactor. Bench-scale and pilot-scale experiments were conducted to optimize the residence time for the reactor and assess its effectiveness in removing pollutants. The generated precipitates from the reactor showed effective adsorptive removal of Ni. Pilot-scale experiments showed decreased Mn concentration over time, attributed to autocatalytic oxidation by MnO_2. The study suggests that a slag reactor with accumulating Mn oxides can be a promising technology for removing Mn and Ni. Furthermore, adding a precipitation tank can improve its long-term operation.

Keywords: Slag Reactor, Mn Oxide, Autocatalytic Oxidation, Passive Treatment of Mine Water

Introduction

Manganese and nickel are the water pollutants in mining areas and are the most challenging metals to remove. Typically, they are removed by large amounts of alkaline agents such as $Ca(OH)_2$ and Na(OH) in (semi-) active facilities to increase the pH < 9. In the United States, SLB (Slag leach bed) has been applied to mine drainage, but it is difficult to constantly meet environmental standards for the final effluent of Mn concentration and pH due to variations in stream flow rate, as non-contamination stream water reacts with steelmaking slag and produces alkaline water, which then reacts with mine drainage to remove Mn. But this study treated Mn and Ni, which are difficult to remove by passive treatment, using a slag reactor. The primary reaction material used in this study, steelmaking slag, can replace $Ca(OH)_2$, the most commonly used neutralizing agent for mine drainage, as an alkaline agent. It also has the advantage of reducing CO_2 emissions from $Ca(OH)_2$ manufacturing processes and recycling waste generated from steel mills.

Materials and methods

Steelmaking slag and limestone

The steelmaking slag used in the experiment had a 2–5mm particle diameter and was composed of Fe oxides, CaO, SiO_2, MnO, MgO, P_2O_5, and TiO_2. Based on previous research, the limestone with a 3–5cm particle diameter was mixed with the slag at a

volumetric ratio of 4:6. Both materials were washed with distilled water before use.

Bench-scale slag reactor

The bench-scale slag reactor, with a volume of 491 mL and a 4:6 volume ratio of steelmaking slag and limestone, was used to treat Mn and Ni reagents dissolved in mine drainage from Taewoo coal mine in Cheong Ju, South Korea, for 456 days. The reactor used a downflow from the upper inlet with a pore volume of 173 mL and a porosity of 38%. And manganese, nickel, and iron sulfate reagents modified the mine drainage composition.

Pilot-scale slag reactor

The study assessed three types of slag reactors for their efficiency in removing manganese from Cheongsan coal mine water in Boeun, South Korea. The characteristics of mine drainage quality in the Cheongsan coal mines were that iron was oxidized and existed as suspended solids before reaching the surface, which could cause clogging in the reactors. Therefore, an upper baffle-type precipitation tank was assessed as a pretreatment process to minimize this phenomenon. This study also estimated the hydraulic conductivity in the slag reactor using Darcy's law to derive process and design factors for a full-scale passive treatment facility.

Results and discussion

Results of bench-scale slag reactor

In the initial stabilization stage, the pH rose to 9 due to active elution of CaO, resulting in Mn of 0.3-0.57 mg/L, Ni 0.07-0.37 mg/L, and Fe concentration was 0.0-0.41 mg/L if simulating the case when untreated Fe was inflowed to before the slag reactor. Fe was inflowed only in the initial stabilizing stage. As a result, manganese was mostly saturated with manganite and hausmannite. In the Acidic (1st) stage, when acidic influent with Mn 2.9-6.9 mg/L inflows, Mn is removed to 2 mg/L at a residence time of more than 12 hours. In the Acidic (2nd) stage, the removal efficiency of Ni increases as the residence time required for treatment increases, and a pH of 7.4 or higher is required. The residence time to remove Ni at 2.7-4.5 mg/L is more than 20 hours when the influent pH is acidic. Manganese removal efficiency improved with longer residence time for neutral influent with a pH of 6.96-8.16, except for some samples taken at short residence times. Manganese concentrations were 0-1.1 mg/L at around 2 hours of residence time. In the Neutral (2nd-1) phase, a relatively short residence time of 0.5-2.0 hours, they have achieved Mn concentrations ranging from 0.1-0.5 mg/L. Manganese was mostly saturated with manganite in this case. A neutral influent with

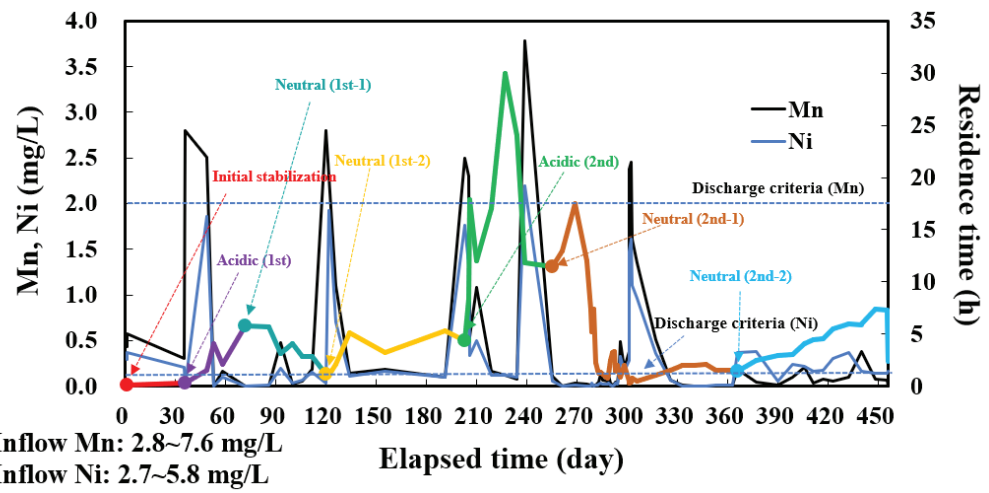


Figure 1 Results of bench-scale slag reactor with 7 phases

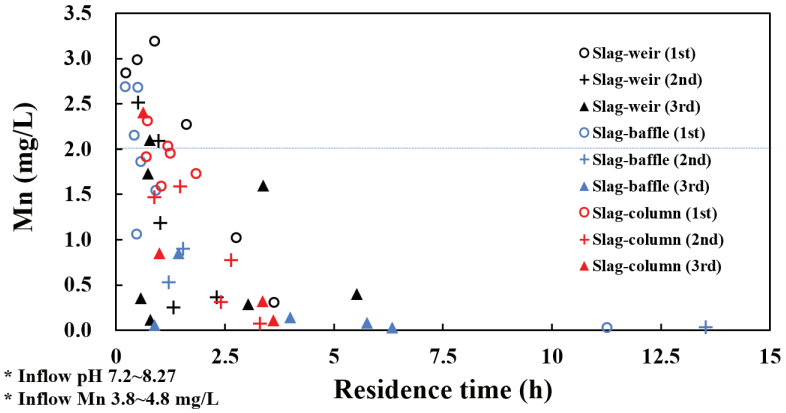


Figure 2 *Results according to an operating period of three types of pilot-scale slag reactors*

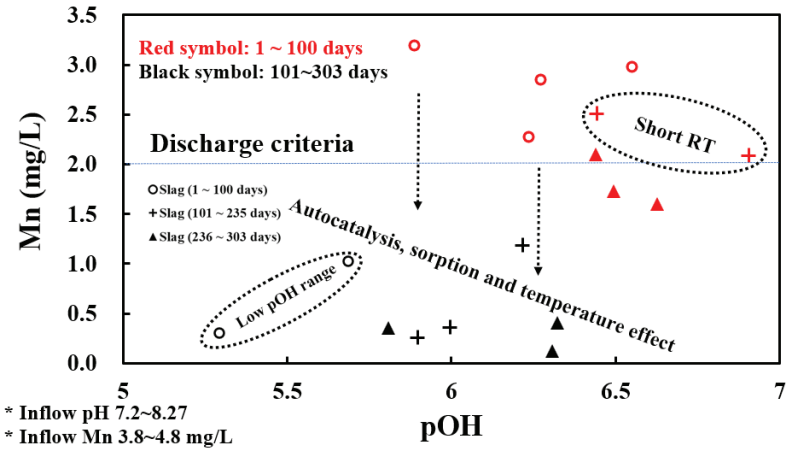


Figure 3 *Mn concentration according to the pOH of the weir-type slag reactor*

Ni concentrations of 2.76-5.46 mg/L and pH 7.03-7.89 was inflowed. Ni removal efficiency improved with longer residence time due to residual hydrogen ions from the acidic inflow. Ni removal efficiency was similar to Mn removal efficiency and was affected by acidic influent washing and deionized water effect. In the Neutral (2nd-1) phase, Ni was mostly removed at concentrations of 0.002-0.020 mg/L over a residence time of 1.0-3.5 hours. The results of the PHREEQC geochemical model showed that Ni was generally undersaturated with $Ni(OH)_2$ and $NiCO_3$. SEM-EDS analysis of the black precipitate inside the column showed flower-like crystal structures similar to birnessite.

Results of pilot-scale slag reactor

The efficiency of Mn removal was assessed for three types of reactors (weir, baffle, column) installed in the Cheongsan coal mine in Boeun, South Korea. The Baffle-type slag reactor had the highest removal efficiency, followed by the Column and Weir-type slag reactors. The Column-type slag reactor showed higher Mn removal efficiency as the residence time increased. The Weir-type slag reactor showed a similar trend to the Baffle and Column types for a residence time of 1.5–3.5 hours. The pilot experiment results showed saturation with calcite, manganite, and rhodochrosite, attributed to the influent's high Ca concentration and alkalinity and

the release of CaO and $CaCO_3$ from the slag reactor.

Mn removal efficiency increased as the slag reactor's operation period progressed, and the residence time became longer. It is estimated that the high Mn removal efficiency was due to Mn autocatalytic oxidation and adsorption by accumulated manganese precipitates in the slag reactor. MnO_2, the final oxidized form of Mn, is known to be effectively removed by autocatalytic oxidation of Mn. The Mn removal efficiency increased in a similar pOH range over time, and it increased due to the seasonal effect of increasing water temperature (Fig 3). These results were observed in the other types of slag reactors.

Conclusion

This study investigated the removal of manganese (Mn) and nickel (Ni) from mine drainage using slag reactors under different pH conditions and residence times. The results showed that the removal efficiency of Mn and Ni was influenced by the residence time and pH level. The pilot experiments showed that the baffle-type slag reactor had the highest removal efficiency. This study also derived process design factors for the passive treatment facilities of the Cheongsan and Taewoo coal mines in South Korea, which included using slag reactors with a mechanism for precipitating manganese hydro (oxide)s series and other carbonates form. This study suggests that the autocatalytic oxidation and adsorption effect of the accumulated manganese precipitate could positively affect Mn and Ni removal efficiency.

Acknowledgements

This study was partly supported by the R&D projects of the Korea Mine Rehabilitation and Mineral Resources Corporation (KOMIR), South Korea (2020–2021; 2022–2024).

Hydrogeological Numerical Modelling to Assess Active Dewatering Options at a Sand Quarry Site – A Case Study and Associated Methodology

S Imrie[1a], A Bennett[1b], J Bellin[1c], P Ebeling[2]

[1]*SRK Consulting (UK) Limited, 5th Floor, Churchill House, 17 Churchill Way, Cardiff, CF10 2HH, Wales, UK.* [1a]*simrie@srk.co.uk,* [1b]*abennett@srk.co.uk ,* [1c]*jbellin@srk.co.uk*

[2]*Holcim Technology Ltd, Im Schachen, 5113 Holderbank, Switzerland, patrick.ebeling@holcim.com*

Abstract

In this paper, we describe an innovative numerical modelling approach used to rapidly assess the potential effectiveness of various dewatering options in reducing moisture content at the Holly Hill limestone quarry and cement manufacturing plant in South Carolina, United States. The numerous predictive scenarios output estimated moisture content of the quarried sands under varying assumptions of active dewatering options. The results were used to input into a wider cost-benefit assessment which is currently underway. However, the project additionally resulted in the development of a useful modelling and coding approach that can be applied to operational planning and scheduling decisions in the future.

Keywords: Carbon emission reduction, quarry, numerical modelling, dewatering, moisture content

Introduction

Reducing the in-situ moisture content of carbonatic sand used for cement production can significantly reduce the energy consumption associated with furnace-drying, as often used in the cement manufacturing process, which in turn can be of financial benefit as well as reducing carbon emissions. In this paper, we describe an innovative numerical modelling approach used to rapidly assess the potential effectiveness of various dewatering options in reducing moisture content at the Holly Hill limestone quarry and cement manufacturing plant in South Carolina, United States. We also discuss how this approach might be applied to future operational decisions.

Design Considerations and Conceptual Site Model

A highly flexible model with fast (< 10 minute) runtimes was required by the site as an operational tool not only to assess options for reducing in-situ moisture content but also to support operational planning decisions in the future. The model was therefore designed with simplicity and efficiency as essential. Importance was placed on capturing the main hydrogeological processes identified in the conceptual modelling. These key processes (see Figure 1) are:

- Large upgradient catchment area (extending c.18 km upgradient) and relatively constant hydraulic gradient (and groundwater flux) towards the site, even when taking into account seasonal variations. Thus, by calculating the minimum upgradient boundary that is outside the potential drawdown zone of the quarry, a 'constant head' (or 'constant flux') upgradient boundary condition could be placed well within the catchment area thereby reducing the area to be modelled.
- The overburden contains a shallow 3 – 6 m thick clay and sand layer which partially isolates the underlying carbonitic sand from vertical recharge from above i.e., greater than 90% of the precipitation at the site either runs-off or flows horizontally as shallow interflow. However, during overburden stripping,

which is undertaken between 6 months and a few years before quarrying, this clay layer is removed allowing direct recharge of a much higher percentage of precipitation to the 'target' carbonatic sand (Unit 1). This is confirmed by observed groundwater level response to rainfall once vegetation has been removed. Thus, the stripping schedule is considered a critical element in the model simulation.

- Downgradient, at the quarry boundary, there is a large swamp which flows perennially and can thus be considered a 'constant head' source/sink. However, groundwater-surface water interaction between the swamp and Unit 1 is minimised by the low permeability clay overburden.
- There is a diversion channel around the site which has exposed Unit 1 and which has been found to permit direct recharge to Unit 1. The diversion channel previously existed around both the northern and eastern property boundaries, however the eastern part has now been mined out.
- Previous trials were undertaken where c.1-2 m wide by c.16 m deep trenches were dug to intersect groundwater flow from the north, thus having the aim of reducing in-situ moisture content in the quarry. These were partially successful. However, the reductions in moisture content were very localised and the development and maintenance of the trench very costly and difficult. Groundwater level, trench discharge and in-situ moisture content data collected during this period is limited.
- Within Unit 1 (c.16 m thick), there is a low permeability hardpan layer that separates the upper half from the lower half.
- Below Unit 1 there is a hard and compact layer, with low fracture density, which thus creates a hydraulic separation between Unit 1 and an underlying aquifer which is under artesian pressures. For the purposes of modelling, it is assumed that there is no interaction with Unit 2 and thus the base of Unit 1 is a no flow boundary (bottom of the model). However, management considerations with regard to Unit 2 and ensuring it not be penetrated were included in the project recommendations.

Model Setup and Coding

The *Feflow* model represents both partially and fully saturated conditions. The vertical discretisation (layering) needed to be kept thin (2 m) within Unit 1 to sufficiently represent the variation in moisture content expected across the unsaturated zone. Local modelled and calibrated flow processes include:

- Representation of deep, high-sided historic trenches using seepage nodes along the edges of each layer at the base of the trench.
- Representation of the stripping of the overburden, by transiently de-activating the relevant elements using a callout to the *Python IFM FeflowDoc Class*, embedded to run with the Feflow model at the start of each time period. The progression of the stripping is calculated using mathematical

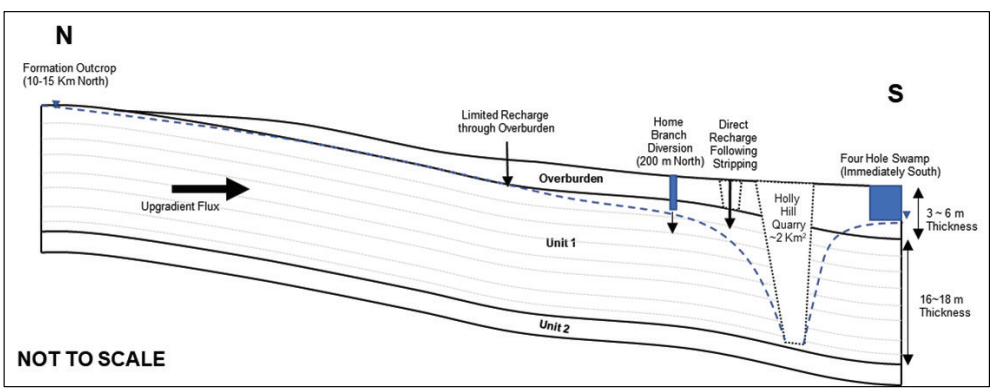


Figure 1 *Conceptual Site Model*

equations representing sequential spread across areas of 'block' format, and later change to a circular progression layout, as per the quarry stripping schedules. Once the upper overburden layer is deactivated, there is a significant natural increase in recharge to the next active layer (top of Unit 1) below.

- Mining of the sands is undertaken using a Bucket Wheel Excavator (BWE). There are two benches, each of c.8-10 m depth (see Figure 2). Sands are removed over the upper bench first, represented in the model using seepage nodes and inactive cells within Unit 1, and then the same area is later restarted as new depths as the bottom bench is mined out.

  In both cases, and as for the stripping, the progress of the benches is calculated using mathematical equations of sequencing over the mining area (see Figure 3) to represent a relatively well established and constant BWE quarrying pattern. Furthermore, the model representation using inactive elements and seepage nodes is coded using the *Python IFM FeflowDoc Class*, embedded to run with the *Feflow* model at the start of each time period.

  The advantages of using *Feflow Python Coding* of the mining activity include both the speed at which the mine plan can be implemented into the model, as well as the flexibility for change if there is an alteration to the mine schedule or area in the future.

- Additional boundary conditions used in the model include those representing interaction with local streams and stream diversions, as well as the swamp (see Figure 4).
- The hydrogeological units (representing variations in hydraulic conductivity, specific yield and unsaturated zone parameters) are varied vertically and include the Overburden, Upper Unit 1 (Marl), Middle Unit 1 (Hardpan) and Lower Unit 1 (Marl).
- The model was transiently calibrated to available water level measurements, with particular focus on response to high rainfall events, the implementation of historic trenches, and historical constant rate testing (Shafer *et al.*, 2006).
- Sensitivity analysis scenarios were implemented to identify which parameters had the greatest influence on model results. These were found to be hydraulic conductivity in the Overburden (influencing seepage rates and the interaction with surface water), followed by the hydraulic conductivity of Unit 1 (influencing the drawdown zone).

Predictive Scenarios and Interpretation of Results

Predictive scenarios simulate future mine plans, as well as options for the stripping schedule and active dewatering solutions (including boreholes, wellpoints, horizontal drains and trenches). As previously described, these transient features are coded to automatically



Figure 2 *Quarry showing Benches and Bucket Wheel Excavator (Holcim US Inc ,2008)*

Mining Plan

Example of mining timing calculations

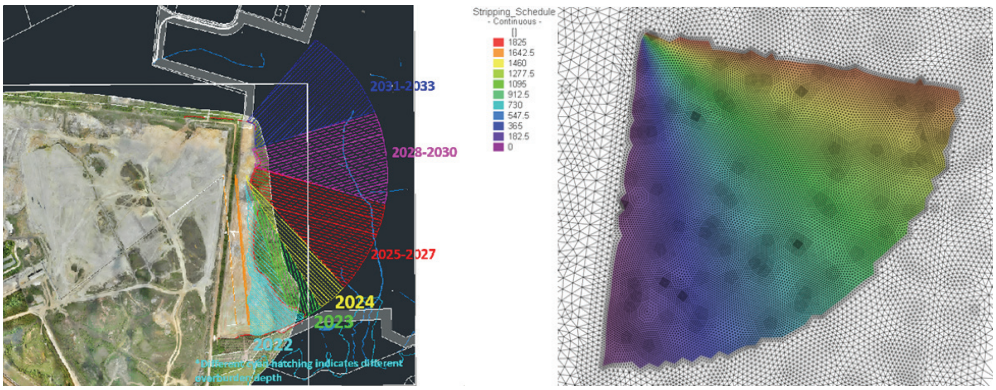


Figure 3 *Example of Mine Sequencing in Feflow using User Defined Equations to form Nodal Distributions*

update the associated boundary conditions and parameters using interactive Python scripts that read the data and assumptions from user-defined nodal distributions.

In addition, interactive Python scripts were used to extract and report the bulk moisture content within the wall of the 'next section to be mined' during the transient simulation, thus providing the model predictive outputs in a format relevant for immediate use in the cost-benefit analysis (Figure 5).

Various dewatering approaches were evaluated using the model, including horizontal drains, trenches and wellpoints (Figure 6).

Figure 7 shows the average modelled moisture content for nodes that will be mined out in next 30 days. The trench design shows diminishing reduction in moisture content with time from day 500. Wellpoints show more impact than drains at the same 100 m spacings. Implementing separate layers of drains in both the upper and lower

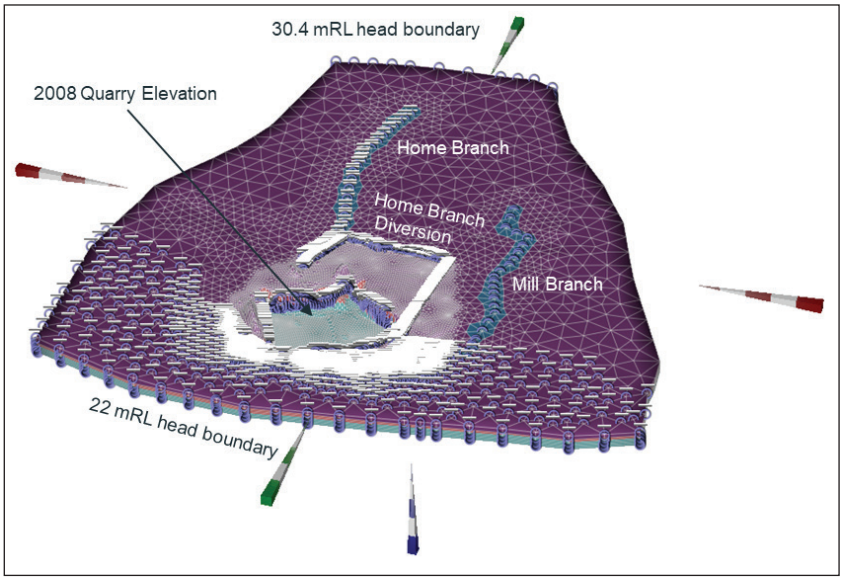


Figure 4 *3D Numerical Model and Boundary Conditions*

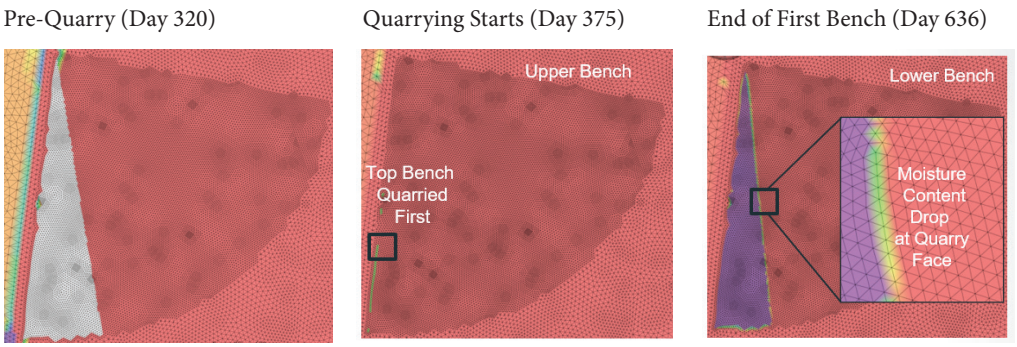


Figure 5 *Simulation Results Showing Moisture Content in Walls*

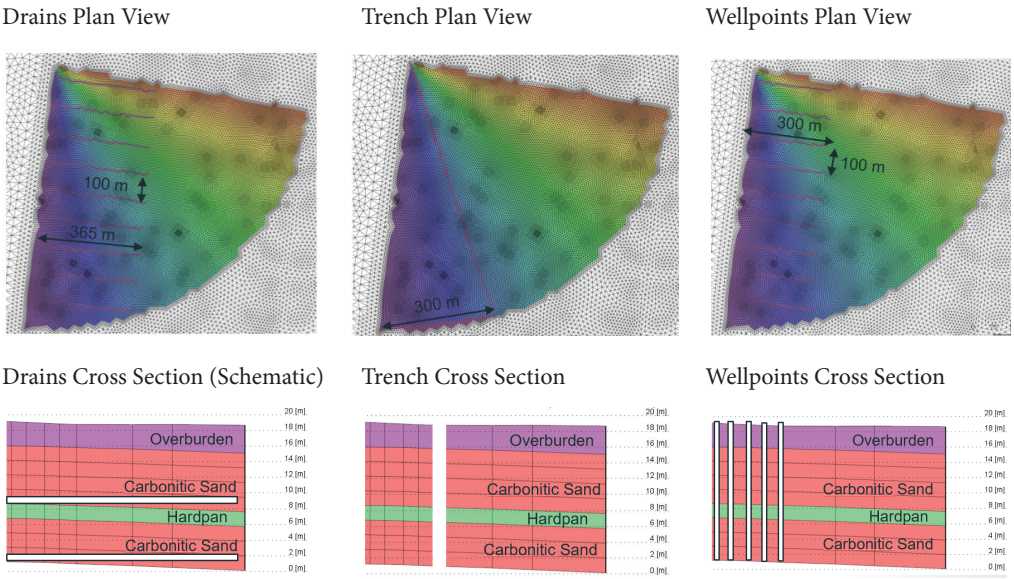


Figure 6 *Model Representation of some of the Dewatering Approaches*

benches appears to have little overall impact on moisture content reduction, suggesting that the low-K hardpans play a limited role in controlling drainage. The moisture content appears to drop semi-linearly with reduced drain spacing.

Next Steps

At the time of writing this paper, the following next steps are under discussion:

- Prototyping of the use of horizontal under-drainage.
- Regular monitoring, including flows from drains and moisture content at various agreed locations on site including in-situ in the walls (both benches and multiple heights and distances from the drains), as well as along the conveyor which takes the material form the quarry face and at the process plant.
- Cost-benefit analysis to decide on the future of a more permanent implementation of this solution or to test other potential options.
- Development of an interactive methodology and/or tool to regularly update and keep track of progress in decreasing moisture contents, and for ease of comparison between observed, predicted and 'updated predictive' results,

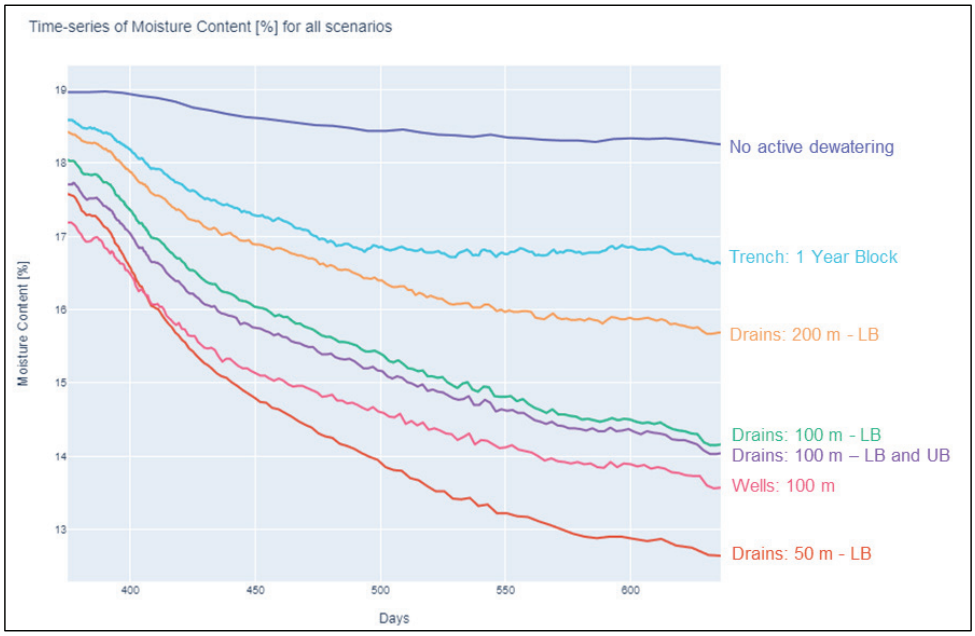


Figure 7 *Modelled Time-series of Moisture Content (%)*

thus forming an important tool for future management decision making.

Conclusions

This modelling approach has successfully simulated various dewatering options in terms of estimated bulk in-situ moisture content of quarried sands. The outputs provide a comparative assessment to input into a wider trade-off and cost-benefit assessment of various options (which is currently underway). The resulting simple and flexible model will be applicable to future operational planning and scheduling decisions. Additionally, the continued monitoring during implementation will assist in stream-lining the approach further.

Reducing the in-situ moisture content at the Holly Hill limestone quarry should result in financial benefit by significantly reducing the cost of processing and will additionally reduce the carbon emissions of the site. It is hoped it will also form an innovative prototype for use in the wider industry.

References

Holcim (US) Inc (2008). Holly Hill Dewatering and New Mine Plan PowerPoint Presentation, South Carolina, US.

Shafer, J.M., Brantley, D.T. and Waddell, M.G. (2016). Feasibility of Reducing Moisture Content Induced by Shallow Groundwater at the Holcim, Inc. Quarry, Holly Hill, South Carolina. University of South Carolina.

A Flexible Approach To Modelling Seepage From Coal Mine Waste Rock

Scott Jackson[1], Steve Momeyer[1], Justin Stockwell[1], Nicolas Francoeur[2]

50-60%

Abstract

A flexible model was assembled to represent the two dominant flow types within a large unsaturated end-dumped coal mine spoil. The proportion of total spoil basal discharge comprised of preferential flow through large macropores, and pressure waves driven by large infiltration events was proportional to spoil thickness, while the matrix flow component dominates the basal seepage hydrograph for large spoils. The proportion of total spoil discharge comprised of these flow regimes changed as spoiling progresses. Spoil wet-up is well represented by the modelling approach, as is seasonal variability in constituent concentrations, and the nitrate decay signature following spoil wet up.

Keywords: Waste rock water balance, water quality modelling, coal, nitrate

Introduction

The West Line Creek (WLC) catchment (10 km2; median elevation is 2,076 masl) is located within the Line Creek Operations mine site, operated by Teck Resources Ltd. in the Elk Valley coal block in eastern British Columbia, Canada. Spoiling of mine waste rock within the WLC catchment began in 1981 and ceased in 2014, with a total of 214 Mm3 of waste rock deposited via end-dumping methods. Total spoil area is approximately 27% of total catchment area, with an average thickness of 85 m. Mean annual precipitation (MAP) is 630 mm, with 50%-60% of this falling as snow. Potential evapotranspiration (PET) is approximately 300 mm/year, with the actual evapotranspiration (AET) from the spoil surface approximately half of PET. This results in a natural catchment yield of 300 mm/yr (48% MAP), and a spoil yield of 495 mm/year – approximately 79% of MAP. Shallow groundwater bypass of the LC_WLC gauge is a factor, accounting for approximately 33% of the spoil basal seepage, and 54% of the natural catchment flow. Key constituents of interest (CIs) are SO4, Se and $N\text{-}NO_3$. At the LC_WLC monitoring station, Peak concentrations for SO_4 are relatively stable at ~1,400 mg/L, while Se peaked approximately 35 years after spoiling began at 650 µg/L and have dropped slightly to 600 µg/L. $N^{-}NO_3$ concentrations peaked at 50 mg/L 25 years after spoiling began and have been decreasing since approximately 2006 (36 years after spoiling began), to 20 mg/L currently (fig. 1).

Coal mine waste rock (spoil) facilities like that in WLC present unique modelling challenges due to their heterogenous and poorly sorted grain size distributions, high precipitation inputs, and large size. In addition, managing constituent loadings presents challenges with respect to receiving environment water quality, and requires a flexible, accurate and rapid modelling approach to evaluate the need for, and effectiveness of, mitigation measures from initial spoiling, through operations and into closure.

A regional survey of drainages containing large coal spoils indicated that most displayed slopes near zero on log-log plots of concentration vs. discharge, indicating that CI export from spoils is limited by transport capacity (discharge) rather than availability (Wellen *et al.* 2018). These relationships imply that as the proportion of waste rock coverage in a catchment increases, the export of weathered solutes is less limited by material availability and more limited by transport capacity. This relationship was not found to be correlated with waste rock position within

the watershed (i.e., headwater or outlet). Instead, the available evidence indicates that most solute loads are mobilized via vertical percolation of meteoric water through the spoil, with the transit of non-contact run-on through the base of the spoil picking up minimal additional loads.

Log:log plots of concentration and discharge for SO_4, $N{\cdot}NO_3$, and Se at LC_WLC indicate that the WLC spoil behaves chemostatically, in that CI load release is proportional (positively correlated) to flow (fig. 2). This supports the conceptual model that solutes are readily mobilized from the spoil at rates that are proportional to spoil size (thickness, footprint, and volume) and flow through the spoil. Note that this finding diverges from the common assumptions used in water quality models that either the loading rate per mass waste rock is constant, and therefore concentrations decrease as flows increase, or that concentrations are fixed at constant values per month, allowing loads to increase with increasing discharge according to an average hydrograph, but not allowing replication of outlier high-magnitude discharge events (e.g., autumn rain on snow events) that can drive significant loading to the receiving environment.

Methods

To accurately represent the flow driven chemistry signatures in the WLC drainage, a simple and flexible model was set up in the GoldSim environment. The modelling approach described herein strikes a balance between more complex physically based unsaturated zone flow models, and simple runoff coefficient-based flow models which are typically used in mine site water balance and water quality models. To achieve this, a two-reservoir water balance model was conceptualized as: 1) 'fast' flow representing flow via large interconnected macropores within the waste rock, and pressure wave flows resulting from large infiltration events (e.g.,

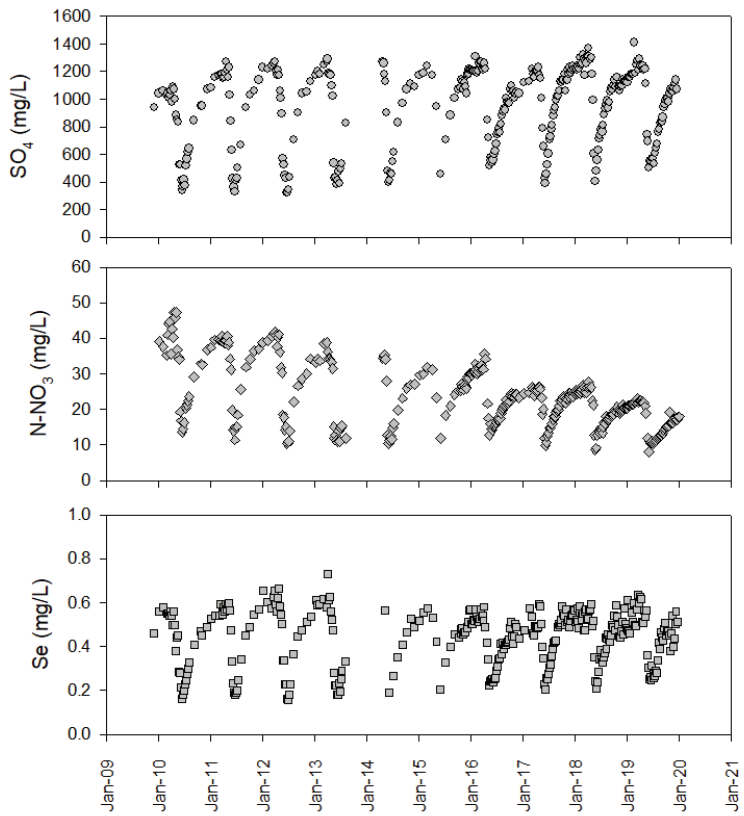


Figure 1 *Time-series of sulfate, nitrate, and selenium concentrations at the LC_WLC monitoring station.*

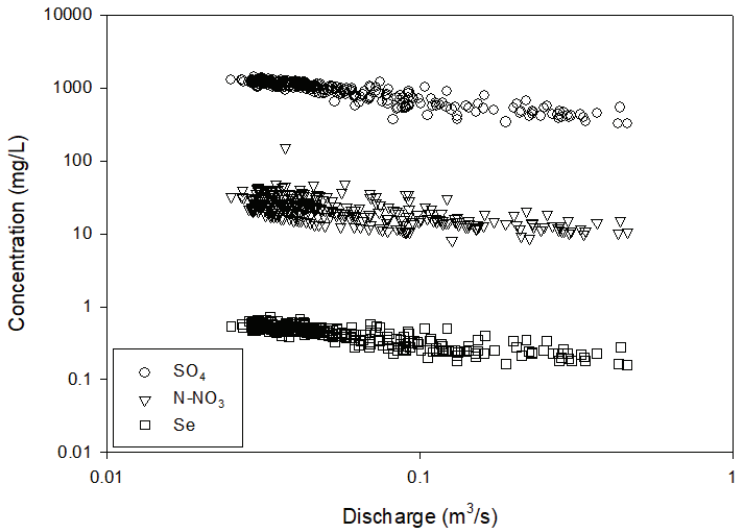


Figure 2 *Log:log plot of discharge vs. concentration for LC_WLC (2009-2019).*

Nichol *et al.* 2005; Neuner *et al.* 2013); and 2) 'slow' flow representing matrix flow through the smaller pore spaces, which typically lags large infiltration events (Blackmore *et al.* 2015; Barbour *et al.* 2016; Appels *et al.* 2018). Fast flow responses may result in large episodic loadings to downstream receiving environments, while slow flow responses comprise the majority of total annual loadings reporting from the spoil. These two processes act in tandem, and while some degree of hydraulic connection is expected to exist between the 'quick' and 'slow' flow pathways, for the purposes of this model they are assumed to be separate (fig. 3). This modeling approach is intended to provide greater flexibility in larger GoldSim mine site models, and direct integration (as opposed to standalone 1D or 2D unsaturated zone hydraulic models) allows for faster model turnarounds (in response to upset conditions, or to allow for multiple rapid sensitivities to be run to inform mine planning). Importantly, the use of a two-reservoir model allows the transition from new spoils dominated by preferential flow to mature spoils dominated by matrix flow to be accurately represented, without relying on hardcoded assumptions related to the timing of this transition (i.e., lag time between spoil placement, wet-up and resulting basal seepage response). Rather, transitions in basal seepage chemistry are a function of local climate, spoiling rate, spoil area, volume and thickness, and spoil moisture content.

The non-contact portion of WLC is located upgradient of the spoil and is characterized as high relief sub-alpine and alpine terrain, with extensive colluvial deposits. This area contributes substantial runoff that transits the base of the spoil rapidly through the coarse waste rock fractions that function as underdrains. Available evidence indicates

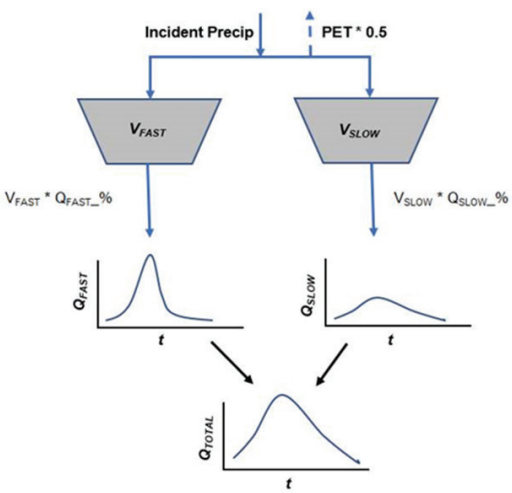


Figure 3 *Conceptual model of LCO-Dry Creek spoil hydrology.*

that these non-contact flows do not pick up substantial additional CI loads due to their limited transit times, and therefore low water:rock contact ratios. Runoff from the undisturbed areas in the WLC catchment was estimated using the GR4J model (Perrin et. al. 2003), and shallow groundwater bypass of the WLC hydrometric station was estimated to be 170 mm/yr on average (54% of total undisturbed catchment runoff, and 34% of total spoil seepage).

The R2 model incorporates the following assumptions:

- Spoil infiltration is allocated to the V_{FAST} (1%) and V_{SLOW} (99%) reservoirs according to a set fraction of the total amount and these proportions are held constant over the full model run. Note that for younger (i.e., thinner) spoils, as much as 20% of total infiltration is directed to the V_{FAST} reservoir.
- CI loads are partitioned between the two reservoirs equivalent to the infiltration proportions.
- Each reservoir has an upper volume limit set equal to the field capacity of the spoil, or the point above which water would drain freely from the spoil pore spaces. The difference between the field capacity and initial moisture content was assumed to represent the effective water retention capacity of the spoil and was relied on as a guideline which the modeled spoil water volumes could not exceed. This threshold also defines the equilibrium point between infiltration and basal seepage.
- Preferential flow pathways or pressure waves (V_{FAST} reservoir) are only expected to activate during high-magnitude infiltration events. The R2 model replicates this process by routing all infiltration to the V_{SLOW} reservoir if the infiltration amount is less than 10 mm/d.
- Seepage is released from the reservoirs by applying a negative exponential decay function to each reservoir volume, and the draindown rate (Q_{SLOW} = 0.0003) from the V_{SLOW} reservoir is two orders of magnitude lower than the draindown rate (Q_{FAST} = 0.06) from the VFAST reservoir. This parameterization was determined through model calibration to flows, concentrations and loads.
- As the spoil water content increases immediately following a large input of meteoric water (i.e., freshet), the total spoil water content approaches, but does not reach field capacity. Gravity drainage predominates, seepage rates are at annual maximums and are proportional to both the size of the spoil reservoir, and the magnitude of meteoric inputs. As spoil drainage progresses over the summer months and into the autumn, the seepage rate continues to drop, as a greater proportion of the water available for discharge is held by suction forces within the spoil matrix. This physical phenomenon is typical of unsaturated flow conditions and is represented in the spoil water balance model by allowing a set percentage of the available water to drain each timestep.
- As the seepage rates from the V_{FAST} reservoir are greater than the meteoric inputs in many months, the volume of available water within this reservoir decreases each month, and thus the seepage rate decreases in turn. Annually the water in the V_{FAST} reservoir drains completely.
- Because the seepage rate is much lower for the V_{SLOW} reservoir, the draindown rates are not sufficient to completely drain this reservoir on an annual basis, and thus the total reservoir volume increases over time as the spoil increases in size, until it reaches the equilibrium condition.
- The total basal seepage volumes and loads for each time-step are the sum of seepage from both the V_{FAST} and V_{SLOW} reservoirs.

Initially the V_{FAST} reservoir discharges the highest volumes on daily time-step (reflective of the flushing and pressure wave response), but as the spoil grows and wets up over time the discharge volumes from the V_{SLOW} reservoir dominate on an annual basis, consistent with other investigator's findings that matrix flow dominates the discharge signature of mature spoils.

Geochemical source terms for the WLC spoil were derived from WLC water quality data for SO4 and Se as a function of average spoil thickness, which is a surrogate for flow path length, and therefore water:rock

contact ratios (tab. 1). The nitrate source term is applied for two distinct time periods; initial nitrate concentrations increase following a similar trend as selenium, and peak in 2006, about 7 years after a period of no spoiling (fig. 1). When the spoil appears to have wet up and reached equilibrium, nitrate concentrations decline, as seen in the monitoring data (fig. 1). This is a result of the finite source associated with blasting residue and rock type. The empirical relationship defining the nitrate source term in spoil discharge during wet-up is presented in tab. 1. While the spoil is wetting up, and nitrate concentrations in the spoil discharge are increasing, the finite nitrate source is modelled by accumulating a nitrate load in the spoil (matrix) reservoir with waste rock placement as:

Bulk Density * $N\text{-}NO_3$ Loading Rate
* Spoiling Rate

Where, the bulk density is assumed as 1,500 kg/m^3 and the nitrate loading rate was set as 5 mg $N\text{-}NO_3$ / kg of rock. The spoiling rate is in m3/day. The declining spoil nitrate concentrations are represented after spoil wet-up, by flushing the accumulated nitrate load from the spoil per the R2 model water balance. Spoil wet-up is defined by when the volumetric moisture content reaches long term average.

Results

The combined R2 and GR4J flow models were calibrated to measured flows at the LC_WLC hydrometric station over the 2012-2016 period and validated to the 2017–2020 period (fig. 5). Over the 2012–2020 period, measured average annual runoff was 184 mm, with modeled runoff slightly lower at 176 mm (not including groundwater bypass). The log-Nash-Sutcliffe Efficiency Index (which is more useful for assessing model predictive skill for the low-flow regime) was 0.93 and 0.90, and the RMSE values were 0.061 m^3/s and 0.016 m^3/s for the calibration and validation periods, respectively. Finally, calibration period R2 was 0.83, and 0.91 for the validation period. These values are indicative of a very well calibrated model, well exceeding the 'satisfactory' threshold suggested by Moriasi *et al*. 2015. Similarly, the progression of CI concentrations over the model run period, including the inter- and intra-annual variability, as well as the increases in all CIs up to the mid-2000's are accurately replicated by the model. Notably, the decay in nitrate concentrations is also well represented, following the peak in approximately 2006 (fig. 5).

Spoil yield is not stationary and net percolation to the spoil is greater than discharge from the spoil while the spoil is wetting up (fig. 6). Model results suggest approximately 36 years passed after spoiling began in 1980 before net percolation and spoil yield converged in 2007 (fig. 6). Note that the spoil dimensions have remained relatively stationary since about 2001. Nitrate concentrations reflect this transition from the spoil water balance 'wetting up,' to reaching equilibrium (net percolation = spoil discharge). The switch from an accumulating nitrate load to a declining one is governed by this transition in the water balance, after which the accumulated nitrate load in the spoil reservoir is released and allowed to flush from the spoil reservoir. The spoil is considered to reach this equilibrium once the moisture content reaches 11%.

Table 1 *West Line Creek spoil source terms.*

Parameter	Unit	Source Term	Notes
SO_4	mg/L	20.5 mg/L/m*T_{spoil}	
$D\text{-}Se$	mg/L	0.0004*[SO_4] + 0.082	
$NO^{3-}N$	mg/kg	1,500*5*R_{spoil}	Applied during spoil wet-up

Notes:

1. [SO_4] is sulphate concentration (mg/L); [Se] is selenium concentration (mg/L)
2. T_{spoil} is average spoil thickness per unit area (m)
3. R_{spoil} is the spoiling rate in m^3/day

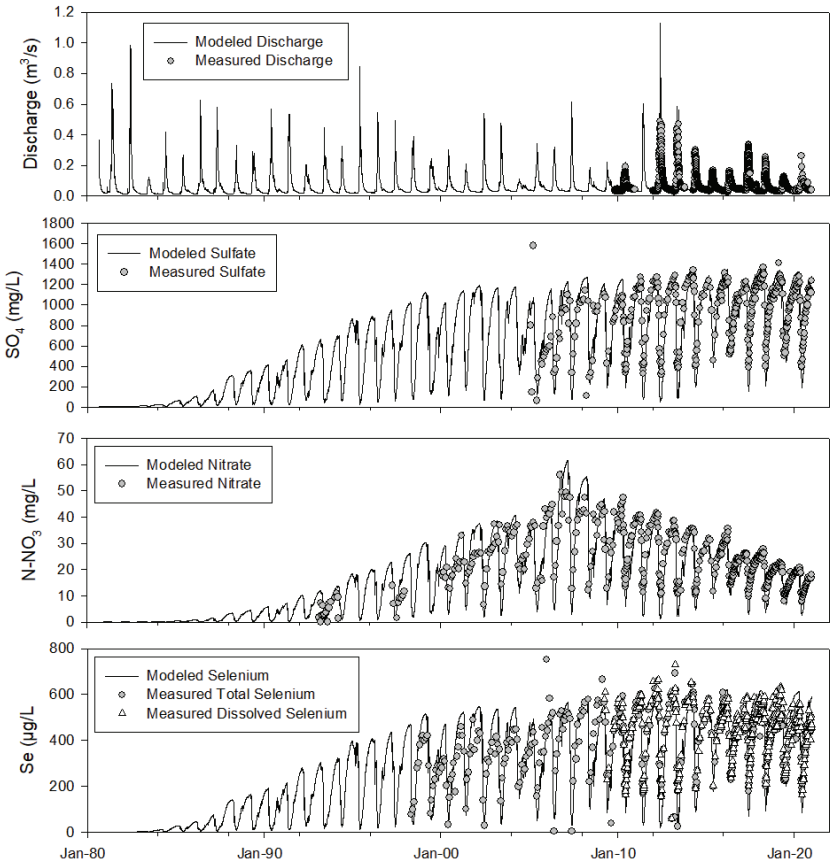


Figure 4 *Modelled (top to bottom) LC_WLC discharge, sulphate, nitrate, and selenium between 1980 and 2020 generated by spoil thickness-based approach.*

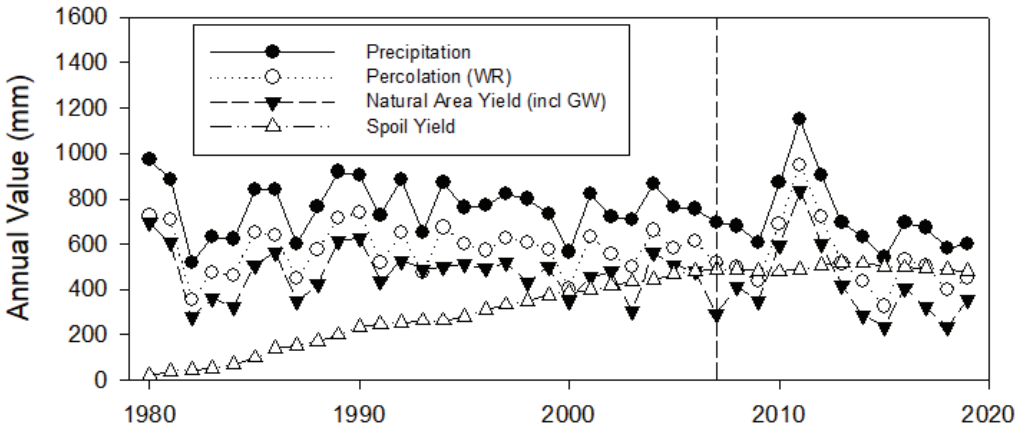


Figure 5 *Time series of annual water balance terms from integrated GR4J and R2 model for LC_WLC. Dashed line indicates 2007, when model indicates spoil was 'wetted up'.*

The empirically derived nitrate source term represents the observed nitrate decay by simple mass balance and flushing of the spoil reservoir. Flushing of the accumulated nitrate load from the spoil matrix produces modelled concentrations that are very well aligned with measured data and portray the long-term declining trend and seasonal range (fig. 5).

Conclusions

The model was applied to a mature waste rock facility and calibrated to observed streamflow and constituent concentrations and loadings in the receiving environment. Model results indicate that the proportion of total spoil seepage generated by the 'fast' flow pathway is proportional to spoil size/thickness, with basal discharge for large spoils comprised almost entirely of 'slow' matrix flow. Flows, CI concentrations and loadings are accurately replicated by the model, including the unique nitrate decay signature evident in the monitoring data, which is interpreted to be a function of a finite reservoir being flushed out according to the spoil water balance.

The modeling approach described here is intended to be incorporated into a large mine site water balance and water quality model. The relatively simple representation of the key processes governing the seepage and loading signatures of large coal spoils is computationally efficient, and digestible by a wide range of stakeholders. This modelling approach was applied successfully to several large coal mine spoils, with one representative example presented.

References

Appels WM, Ireson AM, Barbour SL (2018). Impact of bimodal textural heterogeneity and connectivity on flow and transport through unsaturated mine waste rock. Advances in Water Resources. 112: 254-265.

Barbour SL, Hendry JM, Carey SK (2016). High-resolution profiling of the stable isotopes of water in unsaturated coal waste rock. Journal of Hydrology. 534: 616-629.

Blackmore S, Smith L, Mayer KU, Beckie RD (2014). Comparison of unsaturated flow and solute transport through waste rock at two experimental scales using temporal moments and numerical modeling. J. Contam. Hydrol. 171: 49–65. http://dx.doi.org/10.1016/j.jconhyd.2014.10.009.

Moriasi DM, Gitau MW, Pai N, Daggupati P (2015). Hydrologic and Water Quality Models: Performance Measures and Evaluation Criteria. Trans. ASABE. 58(6): 1763-1785. DOI 10.13031/trans.58.10715

Neuner ML, Smith DW, Blowes DC, Sego LJD, Smith L, Fretz N, Gupton M (2013). The Diavik waste rock project: Water flow through mine waste rock in a permafrost terrain. Applied Geochemistry. 36: 222-233.

Nichol C, Smith, L, Beckie R (2005). Field-scale experiments of unsaturated flow and solute transport in a heterogeneous porous medium. Water Resources Research, 41: doi:10.1029/2004WR003035.

Perrin C, Michel C, Andréassian V (2003) Improvement of a parsimonious model for streamflow simulation. J. Hydrol. 279: 275-289

Wellen CC, Shatilla NJ, Carey SK (2018). The influence of mining on hydrology and solute transport in the Elk Valley, British Columbia, Canada. Environmental Research Letters, 13: https://doi.org/10.1088/1748-9326/aaca9d.

AMD Passive Treatment using DAS at an Old Tin Mine in France

J. Jacob, U. Moreau, F. Duré, J. Engevin, J. Huron, A. Lassin, V. Guérin

BRGM, 3 avenue Claude-Guillemin 45060 ORLÉANS, France, j.jacob@brgm.fr

Abstract

Tailings from a closed Sn mine in Abbaretz (France) produce an AMD containing high concentrations of Fe and Al, but also a few mg/L of Mn, Zn, Ni and Co. A passive water treatment based on a DAS with a high ratio of limestone sand to wood chips (37%$_{v/v}$) was tested on site at pilot scale during 5 months. Over the study period, removal rates were 88% for net acidity, 100% for Al, 82% for Fe, 71% for Zn, 23% for Co, 24% for Ni and 0% for Mn. After 122 days, the pilot was stopped due to excessive clogging.

Keywords: AMD, DAS, Clogging, Passive Treatment

Introduction

The treatment of acid mine drainage (AMD) is a complex and challenging issue, especially when the water is very acidic or the flow rate is too high for classical passive treatment methods (Trumm 2010). Anoxic limestone drain is a common treatment method used for moderately acidic mine drainages, but it may not be effective in treating partially oxidized or aluminium-containing AMD (Watzlaf *et al.* 2000). With technological advancements in the field of mine drainage treatment, efforts have been made to push the limits of the applicability of passive treatment methods. Moreover, the traditional binary division between passive and active treatments is increasingly being replaced by a more nuanced continuum of treatments, ranging from fully passive to semi-passive (Kleinmann *et al.* 2023). DAS technology is clearly part of the progress made in this area in recent years (Ayora *et al.* 2013).

In this study, we focus on the treatment of AMD from a closed Sn open-pit mine using a dispersed alkaline substrate reactor (DAS). The lifespan of a DAS is limited by two phenomena: limestone depletion and clogging. Increasing the proportion of limestone in the packing material can delay its depletion, but accelerates pressure drop by reducing the porosity of the mixture, increasing the specific surface area, and increasing the amount of metals that can precipitate in the packing material. The aim of this study is to determine the optimal design of a full scale treatment plant for Abbaretz AMD with the longest possible service life and to predict its service life before failure, regardless of the cause.

Methods

Site

The tin deposit in the Abbaretz region near Nantes (west of France) has been mined industrially from 1952 to 1957 after producing 3750 tonnes of cassiterite (SnO_2). It is located onto a carboniferous quartz vein of the Armorican massif. The mineralisation is in the form of cassiterite associated with other minerals: mispickel (FeAsS), beryl ($Be_3Al_2Si_6O_{18}$), molybdenite (MoS_2) and chalcopyrite ($CuFeS_2$). The mineral is associated with inter-layered quartz in micaschists that form the bedrock of the area. The tailings produce an AMD (pH 2.9) containing high concentrations of Fe (300 mg/L at 85% Fe^{2+}), Al (24 mg/L), Mn (4.3 mg/L), Zn (4.5 mg/L), Ni (2.1 mg/L), Co (1.8 mg/L), As (190 µg/L) and sulfate (1270 mg/L) at a mean flow rate of 5 m^3/h.

Water treatment system

The components of the pilot scale treatment system are: a DAS reactor, followed by an aeration stage, then a settling stage (fig. 1). The DAS is a downflow PMMA square column (0.3 m x 0.3m x 1.5 m) filled with a 64 L of mixture (porosity 55%) of 63%$_{v/v}$ wood chips (grain size 0-30 mm) and 37%$_{v/v}$ limestone sand (grain size 0-4 mm). The reactor was

equipped with 2 sampling ports (at 8 cm and 38 cm) and 2 transparent graduated tubes for measurement of pressure drop at 8 cm and 38 cm (total thickness 73 cm). The outlet pipe was adjusted to maintain 15 cm of supernatant and 30 cm of freeboard to handle the build-up of pressure drop. The aeration step was composed of one, then 2 pseudo-cylindrical PVC reactors (working volume respectively 5.5 L and 3.2 L) supplied with 3 L/min of air each. The settling step consisted of 3 rectangular PP containers in series of 77 L each. A peristaltic pump (Watson-Marlow QDOS120) fed the treatment system at 1.3 L/h. The only modification of operating condition was the addition of a 2nd aeration reactor after day 60, increasing residence time in the oxidation step from 2.4 h to 6.5 h. Residence time was 36h in the DAS and 7.4 days in the settling stage. The pilot scale treatment system operated for 122 days from October 2022 to March 2023 and was shut down due to excessive clogging.

Sampling and analytical techniques

Sampling and measurements were made every weeks at the inlet and at the outlet of the DAS reactor, in the aeration reactors and at the outlet of the 3rd settling tank. In total, 19 measurement and sampling campaigns were carried out. Redox, pH and temperature, conductivity and dissolved oxygen were measured using a WTW Multi 3620 with Sen Tix 950, Sen Tix ORP-T900, TetraCon 925 and FDO925 probes respectively. Samples were immediately filtered using 0.45 µm filters and acidified at pH 2 with nitric acid (HNO_3) 67%. Ferrous iron was analysed on site with Merck® Spectroquant kits. Dissolved Iron, Ca, Al, Mn, Ni, Co, Zn and Mn were quantified by Agilent 4210 MP-AES (microwave plasma atomic emission spectroscopy). Flow rates were checked using a graduated container and a stopwatch.

Results and discussion

The physico-chemical characteristics of the AMD before and during treatment in the pilot plant, as well as the removal percentage of metals and net acidity, are summarized in Table 1. These are averages over the entire study period. An important increase in pH is observed between the inlet and outlet of the DAS, followed by a more moderate increase in

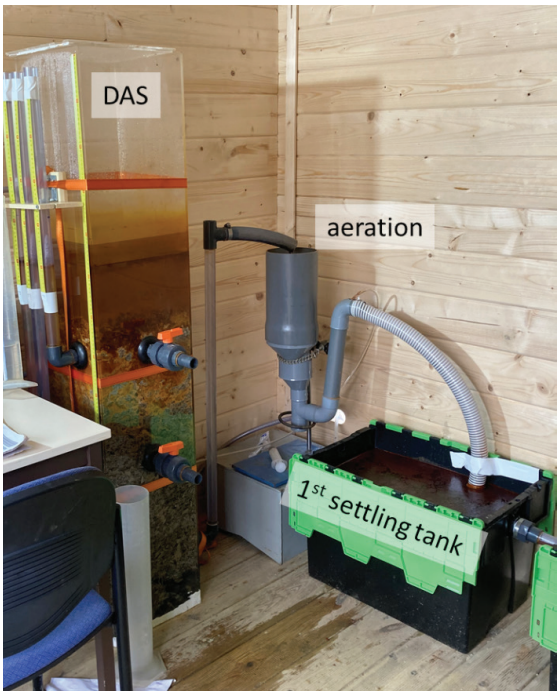


Figure 1 *AMD pilot plant on site*

the aeration step likely due to CO_2 degassing, and finally a decrease in pH in the settling step, probably due to residual Fe hydroxide precipitation.

Regarding the metals, in the treatment system, there is: a total removal of Al ; only a partial removal of iron (82%), caused by insufficient oxidation of Fe II to Fe III in the aeration step; and various removal for other metals, Zn (71%), Co (23%), and Ni (24%). After the DAS, the soluble Fe is almost exclusively composed of Fe II, as Fe III is insoluble at these pH levels. There is no removal of Mn, probably due to the presence of residual Fe II which is known to prevent Mn precipitation. Metals removal is mainly concentrated in the DAS, except for iron, for which 42% of the removal occurs in the aeration and settling steps.

The temporal evolution of Fe and Al in the treatment system is presented in Figure 2. There were relatively minor variations in

Table 1 *AMD characteristics and treatment performances in the pilot plant*

Parameter	Measured values				Removal rate	
	Inlet	DAS	Aeration	Settling	DAS	DAS+Settling
pH	3.0	6.5	6.8	5.9		
Conductivity (µS/cm)	1766	1739	1612	1621		
Dissolved O_2 (mg/L)	8.9	0.8	11.2	7.1		
Temperature (°C)	8.8	9.1	8.5	8.1		
Eh SHE (mV)	627	166	190	347		
Net acidity (mg/L eq. $CaCO_3$)	726	256		90	65%	88%
Fe (mg/L)	279	146		49	48%	82%
Fe II (mg/L)	235	153	87	51	35%	78%
Al (mg/L)	24	<0.25		<0.25	>99%	>99%
Zn (mg/L)	3.19	1.31		0.91	59%	71%
Co (mg/L)	1.25	1.04		0.97	17%	23%
Ni (mg/L)	1.42	1.12		1.08	21%	24%
Mn (mg/L)	3.68	3.93		4.07	-7%	-11%
Ca (mg/L)	20	254		263		

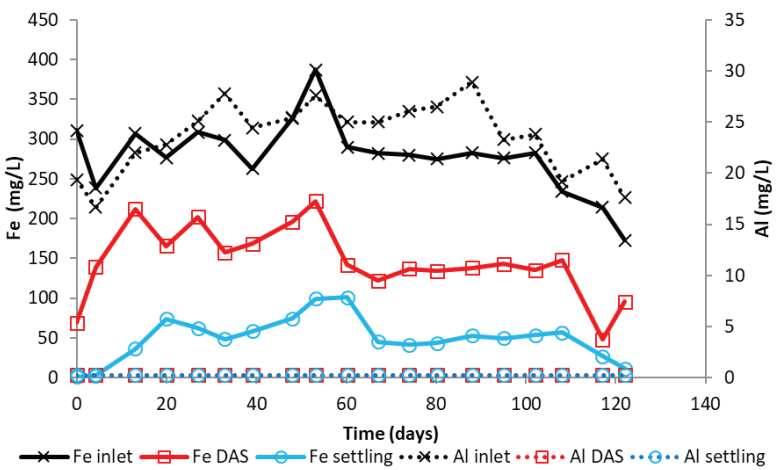


Figure 2 *Dissolved Fe and Al in the pilot plant*

Fe and Al concentrations during the study period. However, it is worth noting that the addition of a 2nd aeration reactor on day 60 led to an average decrease in Fe concentration at the pilot outlet from 74 mg/L to 49 mg/L. Additionally, during the last two measurement campaigns, Fe concentrations throughout the system were lower, likely due to a reduction in the treatment load resulting from dilution of the AMD by heavy rainfall.

Figure 3 shows the evolution of net acidity in the pilot as well as the amount of $CaCO_3$ that has dissolved in the DAS, calculated based on Ca concentration difference between the outlet and the inlet. This calculation assumes no gypsum precipitation, as sulfate concentrations do not decrease between the inlet and outlet of the DAS (data not shown). It is observed that the alkalinity produced in the DAS by calcite dissolution is almost always lower than the net acidity of the AMD, and there is a regular decrease in the amount of dissolved calcite. The net acidity removed averages 473 mg/L (65%) in the DAS and 638 mg/L (88%) in the entire system. The amount of dissolved limestone in the DAS shown in Figure 3 corresponds to an increase in Ca concentration from 20 to 250 mg/L. In the literature, limestone dissolution can be greater, for example, Ca concentration in DAS increases from 200 to 700 mg/L in the study of Rotting *et al.* (2008a) and in the paper of Carabello *et al.* (2011b), while also experiencing gypsum precipitation. These studies also show much greater reduction in net acidity (from 900 to 1600 mg/L), indicating greater metal removal and hence more clogging. The generation of proton during metal precipitation in the DAS is a factor that promotes the dissolution of limestone, the kinetics of which depend on pH.

Figure 4 shows the temporal evolution of Ca dissolution along DAS depth as percent of total Ca dissolution. At the beginning of the experiment, the majority of the calcite was dissolved within the first 8 cm of the DAS. However, this zone became less effective over time and starting from day 102, it no longer contributed much to the dissolution of calcite. The middle zone (8-38 cm) became predominant starting from day 74 and remained so until the end of the pilot. The deepest zone of the pilot started to produce an important amount of alkalinity from day 102 onwards, but at the end of the pilot, it remained a minor contributor. The reasons for this shift in activity could be limestone passivation, depletion of the fine fraction of the calcite, and/or partial clogging that reduces water residence time. Limestone depletion can be ruled out since at the end of the pilot study, only 30% of the limestone initially present in the 1st layer (0 – 8 cm) was consumed.

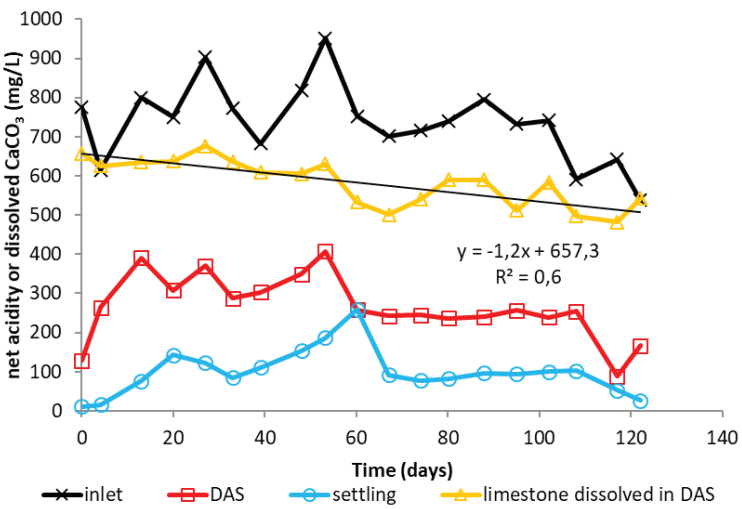


Figure 3 *Net acidity and dissolved $CaCO_3$ in the DAS reactor*

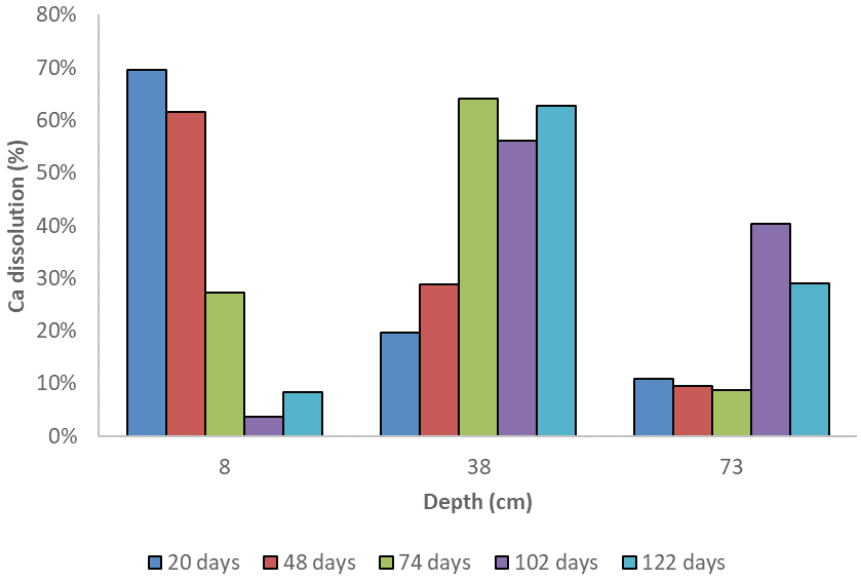


Figure 4 Evolution of Ca dissolution in the DAS

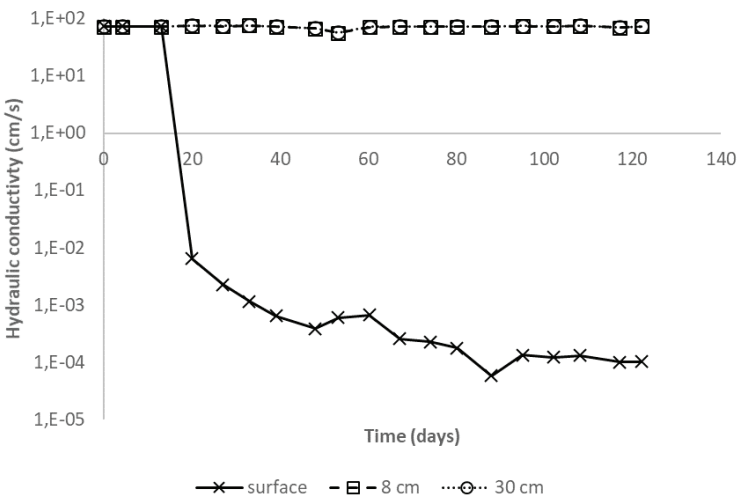


Figure 5 Evolution of hydraulic conductivity

Although the decrease in the amount of alkalinity produced is perfectly measured, it is difficult to estimate the lifetime of the DAS in this configuration as this amount has been insufficient (lower than AMD net acidity) since the beginning of the study, despite a high limestone fraction.

Hydraulic conductivity in the upper part of the pilot started to decrease 20 days after the beginning, and continued to decrease steadily during the study period (fig. 5). By the end of the experiment, head loss had reached 300 mm H_2O. Surprisingly, hydraulic conductivity remained constant in the middle and lower parts of the DAS.

As Fe is the contaminant present in the highest concentration, its precipitation is a major driver of head loss. Initially iron precipitation is concentrated almost exclusively in the first 8 cm of the DAS, then

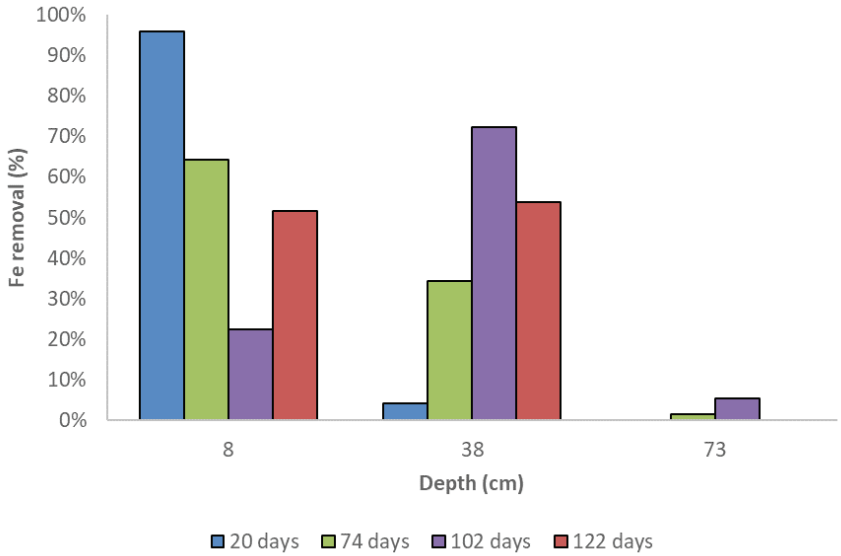


Figure 6 *Evolution Fe precipitation in the DAS*

precipitation also takes place in the middle part of the reactor while remaining largely located in the upper part (Fig. 6). At the end of the experiment, there is still no Fe precipitation in the lower part. This explains why the pressure drop is concentrated in the 1st layer of the DAS and the absence of pressure drop in the 8-38 cm zone indicating that the iron precipitation might be more spread out there.

Conclusions

This DAS configuration has achieved promising acidity and metals removal, but it can still be improved, both in terms of performance and lifespan. The first parameter to modify is obviously the proportion of limestone sand in the filling material. It must be reduced because using such a high limestone fraction not only causes rapid clogging, but also does not help to delay limestone depletion. Indeed, it was found that, after 100 days, there is no more limestone dissolution in the first layer of the DAS (0 to 8 cm) while only 30% of the initially present limestone has been consumed, meaning 70% of the limestone in it unused. A new DAS with much less limestone has recently been started: $18\%_{v/v}$ instead of $37\%_{v/v}$ and packing were added in the aeration reactors to improve Fe II oxidation. To improve the system performance, several other measures could be taken, including increasing the residence time, oxidizing a small portion of Fe before the DAS and adding a 2nd DAS after the sedimentation step. A geochemical modelling is currently underway to validate the operating hypotheses and limitations of the pilot.

Acknowledgements

Financial support for this study was provided by DPSM within the framework of its mission as delegated post-mining operator on behalf of the French state.

References

Ayora, C., Caraballo, M. A., Macias, F., Rötting, T. S., Carrera, J., & Nieto, J. M. (2013). Acid mine drainage in the Iberian Pyrite Belt: 2. Lessons learned from recent passive remediation experiences. Environmental Science and Pollution Research, 20, 7837-7853.

Caraballo, M. A., Macías, F., Rötting, T. S., Nieto, J. M., & Ayora, C. (2011). Long term remediation of highly polluted acid mine drainage: A sustainable approach to restore the environmental quality of the Odiel river basin. Environmental Pollution, 159(12), 3613-3619.

Kleinmann, R., Sobolewski, A., & Skousen, J. (2023). The Evolving Nature of Semi-passive Mine Water Treatment. Mine Water and the Environment, 1-8.

Rötting, T. S., Thomas, R. C., Ayora, C., & Carrera, J. (2008). Passive treatment of acid mine drainage with high metal concentrations using dispersed alkaline substrate. Journal of Environmental Quality, 37(5), 1741-1751.

Trumm, D. (2010). Selection of active and passive treatment systems for AMD—flow charts for New Zealand conditions. New Zealand journal of geology and geophysics, 53(2-3), 195-210.

Watzlaf, G. R., Schroeder, K. T., & Kairies, C. L. (2000). Long-term performance of anoxic limestone drains. Mine Water and the Environment, 19(2), 98-110.

Sources of diffuse zinc and lead contamination in an abandoned mine watershed

Adam P. Jarvis[1], Vanessa Banks[2], Emma Crewdson[2], Stephen Lofts[3], Barbara Palumbo-Roe[2], Jasmine Pullen[3], Catherine J. Gandy[1]

[1]*School of Engineering, Newcastle University, Newcastle upon Tyne, UK, NE1 7RU*

[2]*British Geological Survey, Nicker Hill, Keyworth, Nottingham, UK, NG12 5GG*

[3]*UK Centre for Ecology & Hydrology, Lancaster Environment Centre, Library Avenue, Bailrigg, Lancaster, UK, LA1 4AP, UK*

Abstract

Synoptic monitoring of a mined watershed in north-west England aimed to quantify point and diffuse sources of zinc and lead. The main point source of pollution has Zn and Pb fluxes of 3.0 kg/d and 16 g/d, respectively, but stream Zn and Pb flux measured below the mine site were up to 6.1 kg/d and 300 g/d. Groundwater in riparian zones has very high metal concentrations, and appears to be a key source of diffuse metal flux to the receiving watercourse. The results have implications for point source remediation benefits, and for overall management of metal burden in mining-impacted watersheds.

Keywords: Synoptic monitoring, diffuse, abandoned mine, zinc, lead

Introduction

Synoptic mass balance monitoring is a critical technique to quantify diffuse inputs and their spatial distribution. It has previously been applied to many mining-impacted river catchments to quantify the spatial variation in metal loads (e.g. Jarvis et al. 2019; Onnis et al. 2023; Runkel et al., 2023). The approach entails synchronous water quality and flow monitoring of all point sources in a catchment, together with instream locations upstream and downstream of point sources. Pollutant loads in mining-impacted catchments have been shown to fluctuate considerably with varying hydrological conditions. Whilst the contribution of point sources to the overall instream metal load typically remains relatively constant across all hydrological conditions, the importance of diffuse sources has been shown to increase considerably at higher flows. It is therefore imperative that synoptic mass balance monitoring is undertaken across the full range of hydrological conditions so that the overall importance of diffuse sources of pollution can be determined and the variability of diffuse sources across hydrological conditions quantified.

Such data are crucial to inform remedial interventions at mine sites, but also to evaluate benefits of any such remedial efforts (Jarvis et al., 2019). However, to plan remedial interventions in more detail it is necessary to know the exact provenance of diffuse sources, and the pathway by which they reach sensitive receptors. At the abandoned Force Crag mine, north-west England, monitoring infrastructure has been installed to facilitate this more detailed evaluation of diffuse sources. The infrastructure available includes hydrometric monitoring installations (sharp-crested and flat-V weirs), a suite of piezometers on riparian ground that lies between the main mine site and the receiving watercourse (the Coledale Beck), and a surface water collection system to intercept runoff from waste rock.

Here we report on the findings of an investigation of diffuse pollution issues at the Force Crag mine site, and specifically the relationship between the results of synoptic monitoring in the watershed and water quality in shallow subsurface groundwaters of riparian areas between the mine site and the receiving watercourse. Whilst a previous investigation examined diffuse pollution across the whole of the Coledale Beck catchment (Jarvis et al., 2019), here we present results of more intensive, reach-scale

monitoring of diffuse pollution, to enable a more refined understanding of the nature and location of diffuse sources of metals.

Methods

Study site

Force Crag mine lies towards the head of a steep valley (Figure 1) in the Lake District National Park of north-west England (54.5835°N 3.2397°W). The mine worked a mineralised vein in a steeply dipping fault, hosted in slates of the Ordovician Skiddaw Group (Young and Cooper, 1988). Glacial deposits of yellow boulder clay, overlain by peat, predominate in the valley floor, but there are also areas of waste rock, and an area adjacent to the mine that was the site of a tailings pond (now occupied by a passive mine water treatment system; see below).

The vein was accessed via eight levels (adits) at different elevations, the lowest of which was Level 0 (at an elevation of 267 m a.s.l.). Galena, and subsequently barite and sphalerite, were the primary minerals of interest through the 19th and early 20th Centuries, but mining was abandoned entirely in 1991 (Oswald and Pearson, 1999). The abandoned mine site is now owned by the National Trust, given the site's archaeological and geological value as the last working metal mine in this part of England.

The main point source of contaminated mine drainage at the site arises from Level 1, at an elevation some 20 m above Level 0 (which is largely blocked due to a collapse within the workings). The primary metal contaminants of concern are Zn, Cd and Pb. A detailed examination of the water quality and hydrology of the Level 1 discharge, and its variability, is provided by Jarvis et al. (2023). To alleviate pollution in the Coledale Beck, in 2014 a passive mine water treatment system was installed at the site by the UK Coal Authority (as part of the Water & Abandoned Metal Mines Programme, a partnership with the Environment Agency and the UK Department for Environment, Food and Rural Affairs). It treats a portion (up to 6 L/s) of the drainage from Level 1. Other point sources of mine drainage also exist at the site. Apart from Level 0 they emerge not from mine portals but as groundwater upwellings in areas immediately below the main mine site (and their exact provenance remains unclear). In addition, a previous investigation (Jarvis et al, 2019) concluded that diffuse

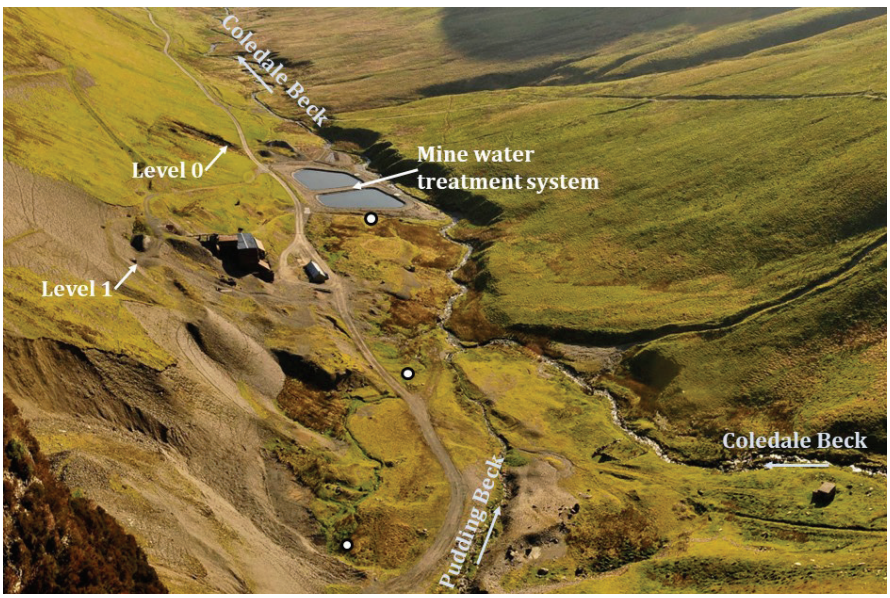


Figure 1 *Force Crag mine and Coledale Beck, showing locations of abandoned mine buildings, mine adits (levels), groundwater upwellings of metal-contaminated water (white circles), and mine water treatment system (Photo reproduced with permission of John Malley)*

pollution contributed to the metal flux of the Coledale Beck, and in fact that diffuse sources of pollution are the majority contributor to metal flux in the stream at high flows.

In late 2020 a suite of piezometers were installed at the Force Crag site, in areas of mine waste and riparian zones adjacent to the mine site (with one, BH16, located the opposite side of the Coledale Beck, as a control; Figure 2). During 2021 and 2022 this enabled synchronous synoptic monitoring of the Coledale Beck and point sources, alongside water level and water quality monitoring of groundwaters across the site.

Sampling and analysis

At each sampling location, field measurements of temperature, pH, oxidation-reduction potential (ORP) and electrical conductivity were taken using a pre-calibrated Myron L 6P Ultrameter. Total alkalinity was determined using a Hach test kit with 0.16 N sulfuric acid and bromcresol green-methyl red indicator powder to a pH 4.5 end-point. Three water samples were collected, for total and filtered (<0.45 μm) cations and filtered anions (<0.45 μm). Samples for cation analysis were acidified with 2% v/v concentrated nitric acid and 1% v/v concentrated hydrochloric acid. All samples were then stored at 4 °C prior to analysis using Inductively Coupled Plasma-Optical Emission Spectrometry (ICP-OES; Agilent Technologies 5800 Series) and Inductively Coupled Plasma-Mass Spectrometry (ICP-MS; Agilent Technologies 7700 Series). Anion concentrations were determined using a Thermo Scientific Dionex Integrion HPIC Ion Chromatograph (IC). QA/QC protocols were followed, including periodic collection and analysis of triplicate samples, use of blanks and standards throughout analysis, and calculation of charge balances to ensure they were within ±10%.

Flow-rate of point sources of mine water drainage were determined using sharp-crested V-notch weirs in all cases. For the Coledale Beck and tributaries, a flat-V weir enabled direct flow measurement at one key location (FC3) on the Coledale Beck. At all other locations salt gulp dilution gauging was used for flow measurement, since in this turbulent upland stream velocity-area measurement is inappropriate. Full details of the salt gauging method used are provided in Jarvis et al. (2019).

Results and Discussion

Figure 2 illustrates the results of intensive synoptic monitoring along a 500 m reach of the Coledale Beck, with the most upstream location above the mine site (FC16 on Figure 2), and the most downstream locations (FC3 and CB0; Figure 2) below the mine site. In addition to in-stream measurement of flow and water quality, all point sources were monitored. On each monitoring campaign all locations were measured on the same day, and during stable hydrological conditions, but campaigns on different days were intentionally under different hydrological conditions. Monitoring took place between April 2021 and February 2022, on eight occasions for surface waters and point sources (and six occasions for groundwaters; see below).

Diffuse metal input within an individual stream reach, between two instream monitoring locations, is defined as the difference between (1) the sum of the upstream metal load plus any point source metal loads within the stream reach and (2) the instream metal load at the downstream monitoring location. The cumulative diffuse metal input to a catchment is the sum of the individual reach-scale diffuse inputs.

Figure 2 illustrates that diffuse inputs of Zn to the Coledale Beck increase with absolute flow-rate over the 500 m study reach. At the lowest flows there is evidence of attenuation of zinc due to in-channel processes (e.g. adsorption; Jarvis et al., 2019), but at higher flows diffuse inputs contribute up to 41% of the Zn load in the Coledale Beck below the mine site. To put this in context, the total diffuse input along the 500 m study reach is up to 2.50 kg/d at the highest Coledale Beck flow reported here (250 L/s), which is approximately the same as the mean Zn load contributed to the Beck by the main point source of pollution in the catchment (2.59 kg/d), the Level 1 discharge (Figure 1). The flow of the Coledale Beck at FC3 can be substantially higher than conditions monitored during this work. Jarvis et al. (2019), for example, monitored at flows of up to 670 L/s at FC3. Under such flow conditions, the diffuse Zn load was

concomitantly higher – in excess of 5 kg/d – and therefore under such hydrological conditions diffuse inputs of Zn are higher than point source inputs. Although not discussed in detail here, Pb dynamics in the Coledale Beck watershed were somewhat different. The data collected during this study indicated no diffuse contribution to filtered Pb load at the downstream Coledale Beck location (FC3), other than at the highest flow recorded (250 L/s at FC3). This is in contrast to the conclusions of Jarvis et al. (2019), who did observe an increasing trend of diffuse Pb input to the Beck, and therefore further work is required to clarify Pb dynamics.

Nevertheless, the reach-scale monitoring reported here enables more accurate identification of sources of diffuse metals inputs to the Coledale Beck. Figure 2 illustrates that the upper segment of the reach monitored, from FC16 (above the mine site) to approximately 100 m downstream, receives up to 0.84 kg/d of diffuse Zn. At higher flows there are also substantial diffuse inputs of Zn between 159 m and 257 m downstream of FC16 (Figure 2). Higher resolution identification of zones of diffuse pollution are an important first step in consideration of possible interventions to remediate diffuse pollution in abandoned mine watersheds.

To begin to ascertain the possible role of groundwater inputs as sources of diffuse pollution, samples collected from 15 piezometers across the mine site (Figure 2) were also analysed for Zn and Pb concentration. Filtered Zn and Pb concentrations in these groundwaters are shown in Figure 3(A) and (B), alongside equivalent data for the point sources of mine drainage across the site (Figure 3(C) and (D)). It is apparent that Zn and Pb concentrations are highly variable (over more than two

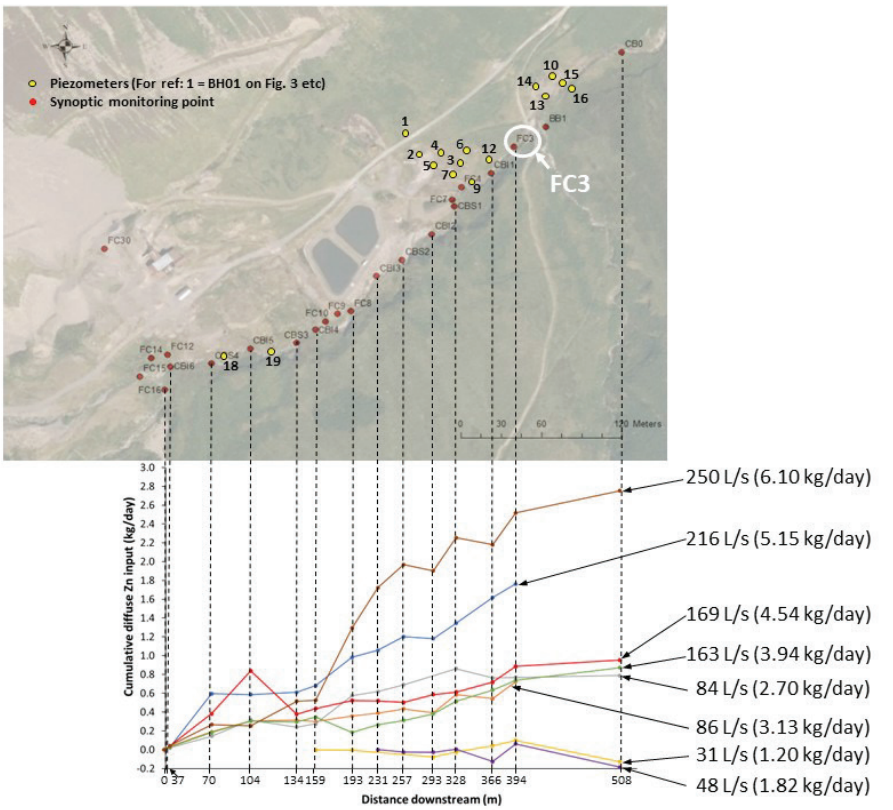


Figure 2 *Cumulative diffuse filtered zinc input to the Coledale Beck during reach-scale synoptic mass balance monitoring. Flows are shown for monitoring point FC3 with zinc load at FC3 in brackets (High resolution (25cm) vertical aerial imagery, EDINA Aerial Digimap Service, https://digimap.edina.ac.uk)*

orders of magnitude) in the groundwaters, even between piezometers located close to one another. It is also clear that Zn and Pb are substantially higher in many of the groundwaters than in the point source mine water discharges; up to 67 800 µg/L Zn and 3 020 µg/L Pb in groundwaters compared to concentrations of up to 3 700 µg/L Zn and 93 µg/L Pb in point source discharges.

The much higher concentrations of Zn and Pb in the groundwaters may reflect long residence times of water in close interaction with fine grained mine wastes in the subsurface, in contrast to the comparatively short residence time of water draining through the underground mine workings and emerging from mine adits. The variability of Zn and Pb concentrations in the groundwaters, even between piezometers in close proximity to each other (those to the north-east of the treatment system; Figure 2), suggests the presence of discrete bodies of groundwater and / or marked heterogeneity in subsurface lithology and mineralogy. A key issue is the extent to which these contaminated groundwaters are in hydraulic connection with the Coledale Beck, and therefore whether they are responsible for the diffuse source contribution to Zn and Pb loads in the Beck. Water levels in the piezometers respond to rainfall, and there is a correlation between piezometer water level and Coledale Beck flow (unpublished data). In some riparian areas of the Coledale Beck the ground is perennially waterlogged, indicating groundwater levels at surface, and visual observations confirm that water from these areas flows into the Beck in a dispersed manner (i.e. as seepages and trickles). Finally, Jarvis et al. (2019) showed that there was additional flow in the Coledale Beck that could not be accounted for by the sum of all upstream flows i.e. there are additional inflows to the Beck via diffuse pathways. These lines of evidence all suggest that groundwater inputs to the Coledale Beck are contributing to the diffuse metal load in the stream. However, the quantitative role of such groundwater inputs to metal load in the Coledale Beck has yet to be determined.

Conclusions

Synoptic monitoring of a stream impacted by an abandoned Ba-Pb-Zn mine, in an upland location in north-west England, illustrates the importance of diffuse sources of pollution

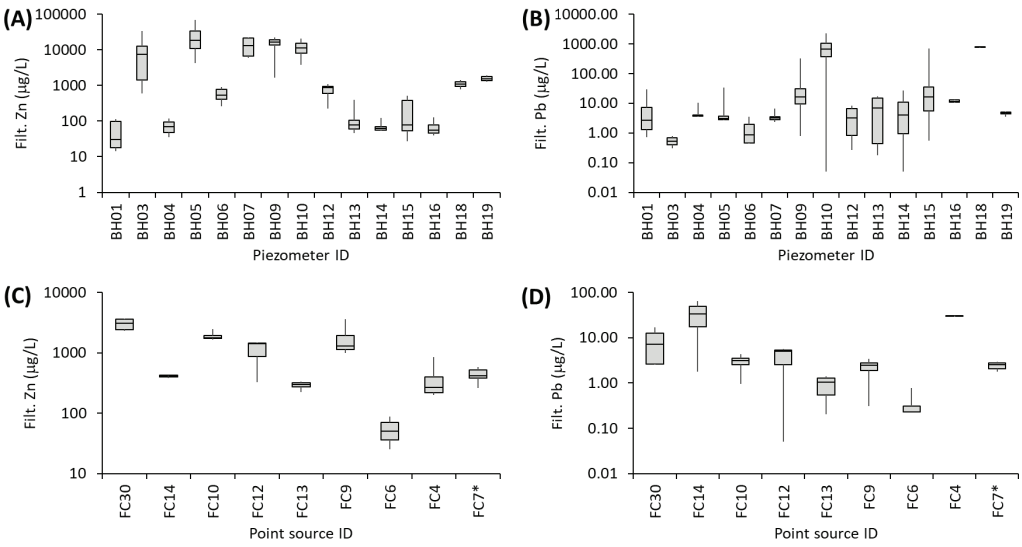


Figure 3 *Box plots of filtered (Filt.) Zn and Pb concentrations at various locations in the Force Crag mine catchment, showing (A) Zn concentrations in groundwaters, (B) Pb concentrations in groundwaters, (C) Zn concentrations of point sources and (D) Pb concentrations of point sources (See Figure 2 for locations; note: BH02 dry on all occasions).*

to absolute metal load in the receiving watercourse, which in turn influences aqueous metal concentrations. Intensive synchronous monitoring of stream flow-rate and metals concentrations (16 stream water locations and nine point sources over a 500 m stream length), across hydrological conditions, reveals specific reaches along which diffuse inputs occur. Groundwaters in riparian areas between the main mine site and the receiving watercourse, the Coledale Beck, collected in parallel to synoptic monitoring of the Beck, have very high concentrations of Zn and Pb (up to 67 800 µg/L Zn and 3 020 µg/L Pb) compared to concentrations up to 3 700 µg/L Zn and 93 µg/L Pb in point source discharges to surface. Although yet to be quantified, these contaminated groundwaters appear to contribute to the diffuse metal burden of the Coledale Beck.

A passive treatment system at the Force Crag mine site successfully removes metals from a portion of the main point source of mine water (the Level 1 discharge). Further improvements in downstream water quality could be achieved by treatment of other point sources of pollution at the site (land availability permitting), but diffuse source mining pollution would remain, and become the limiting factor to any subsequent improvements. Diffuse source pollution is evident at many other abandoned mine catchments across the UK (Jarvis et al., 2019; Onnis et al., 2023).

Design of engineering interventions to remediate such diffuse sources of mining pollution requires detailed information on the location and nature of such sources, in addition to a clear understanding of the likely benefits accruing from treatment (to ensure cost-effectiveness). At Force Crag, the locations of diffuse inputs are more clearly understood, but the quantitative impact of groundwaters to metal loading in the Coledale Beck still needs confirming, as does the exact role of other possible diffuse sources and pathways (e.g. surface runoff from mine waste). The Force Crag site is well equipped with infrastructure (piezometers and hydrometric facilities, in particular) to quantify diffuse sources, and to test new approaches (e.g. geophysics, remote sensing) to identifying and quantifying diffuse mining pollution.

Acknowledgements

The research was funded by the UK Coal Authority, via contract No. CA18/2/1/4 (DIFFUSE project), under the umbrella of the Water and Abandoned Metal Mines Programme (WAMM). The WAMM programme is a partnership between the Environment Agency, the Coal Authority and the UK Department for Environment, Food and Rural Affairs (Defra). We express our gratitude to Clair Roper and Henriette Christensen (Newcastle University) for their invaluable assistance with field work and lab analysis. We are grateful to Dr Hugh Potter (Environment Agency) for many insightful discussions about UK mine water pollution, including at Force Crag, and to the DIFFUSE project management team at the Coal Authority. We are also indebted to the National Trust, in particular Mr. John Malley, for site access and background information. Disclaimer: the views expressed in this article are those of the authors only, and do not necessarily represent those of any other organisations mentioned herein.

References

Jarvis AP, Davis JA, Orme PHA, Potter HAB, Gandy CJ (2019) Predicting the Benefits of Mine Water Treatment under Varying Hydrological Conditions using a Synoptic Mass Balance Approach, Environmental Science & Technology, 53(2): 702-709, doi.org/10.1021/acs.est.8b06047.

Jarvis AP, Gandy CJ, Webb JA (2023) Controls on the Generation and Geochemistry of Neutral Mine Drainage: Evidence from Force Crag Mine, Cumbria, UK, Minerals, 13: 592. doi.org/10.3390/min13050592.

Onnis P, Byrne P, Hudson-Edwards KA, Frau I, Stott T, Williams T, Edwards E, Hunt CO (2023) Source apportionment of mine contamination across streamflows. Applied Geochemistry, 151: 105623, doi.org/10.1016/j.apgeochem.2023.105623.

Oswald A, Pearson T (1999) Force Crag mine, Cumbria. English Heritage Archaeological Investigation Report Series AI/1/1999, 109 pp.

Runkel RL, Verplanck PL, Walton-Day K, Blaine McCleskey R, Byrne P (2023) The truth is in the stream: Use of tracer techniques and synoptic sampling to evaluate metal loading and remedial options in a hydrologically complex setting, Science of the Total Environment 876:162458, doi.org/10.1016/j.scitotenv.2023.162458.

Young B, Cooper AH (1988) The geology and mineralisation of Force Crag Mine, Cumbria, Proceedings of the Cumberland Geological Society, 5: 5-11.

Natural Tracers For Mine Water Fingerprinting III – an Approach to Identify Mine Waters from Distinct Mine Water Provinces during Mine Water Rebound in the Ruhr District Area

Henning Jasnowski-Peters, Christian Melchers

Research Center of Post Mining, Technische Hochschule Georg Agricola University, Herner Str. 45, 44787 Bochum, Germany, henning.peters@thga.de

Abstract

This long-term hydrogeochemical research initiative associated with the mine water rebound in the former hard coal mining area of the Ruhr District, Germany, aims to characterize specific water bodies in the mine water provinces as a major prerequisite for a sustainable and controlled rebound process. A combined natural tracer approach has been applied and comprises classical major cation/anion species analyses, inorganic tracer compounds (Cl^-/Br^-, Li^+,) as well as stable and radiogenic isotope geochemistry measurements (δD, $\delta^{18}O$, $^{87}Sr/^{86}Sr$). Here, we focus on detailed test cases for the bromide tracer. In order to assess the bromide (Cl^-/Br^-) tracer's precision and limitations as the most prolific and ubiquitous tracer in this multi-tracer approach, it has been evaluated for single colliery mine workings and adjacent mine water compartments to identify separate mine water bodies. Examples comprise the mine workings of the colliery Prosper Haniel and adjacent mine workings in the northern part and a dataset in the eastern part of the former mining area. The latter has been partly infiltrated by aquifers and formation waters of the Upper Cretaceous overburden section. Shaft profiles with a multi-parameter probe were able to identify separate water bodies at depth in the eastern province. The bromide tracer exhibits very narrow ranges within the water provinces in the Ruhr District mining area and hence, was able to identify water bodies from distinct mine workings and water provinces. In the eastern part, where in isolated water provinces the mine water rebound is very mature, an already infiltrated mixture of mine water with the overburden formation waters was identified. This data based on "geochemical-independent" natural tracers aims to build a foundation for a robust integrated risk management approach accompanying the rebound process in the Ruhr District.

Keywords: Mine water, hard coal, Ruhr district, tracer, risk management

Introduction

After mine closure, mine water management associated with mine water rebound becomes increasingly difficult due to limited access to the underground mine workings. Apart from major dewatering stations and backup stations as well as a vertical pipe network acting as piezometers and methane degassing facilities implemented into shafts, there remains no direct accessibility to the underground mine workings anymore. This limited access is a major issue to study mine water hydrogeochemistry and hydrodynamics. For risk management purposes and hence, to ensure a sustainable and controlled mine water rebound process, a profound monitoring system including a detailed hydrochemical assessment of mine waters and surrounding aquifers is therefore essential. It leads to thorough understanding of the mine water and regional hydrology and builds a foundation for benchmarking and modelling. Therefore, it helps to mitigate or even overcome this accessibility obstacle during the rebound process.

This research is a continuation of a first and second assessment on mine water hydrogeochemistry and regional hydrogeology (Jasnowski-Peters & Melchers 2021 & 2022) as well as former shaft depth

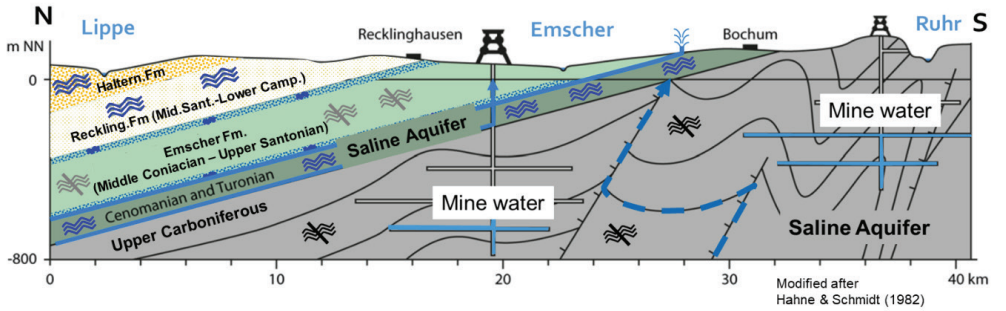


Figure 1 *Generalized cross section of Rhenish Massif to south western Muensterland Basin; Upper Carboniferous strata with coal measures gently dipping towards the North, unconformably overlain by Upper Cretaceous marls and carbonates; the regional saline aquifer is situated within Cenomanian to Turonian fractured carbonates which is overlain by marly to clayish strata of up to 1500m called Emscher Formation. Drinking water reservoirs consists of fine calcareous sandstones of Haltern Fm. pinching out close to the river Lippe (modified after Hahne & Schmidt 1982)*

profiling using a multi probe setup (Henkel & Melchers 2017). Major aim was to identify useful natural tracers within the mine water hydrochemistry, which identifies mine waters and its mixtures from adjacent aquifers in the overburden section during rebound. Bromide (Br^-) has been found so far to be able to act as a profound tracer as it is ubiquitous present in measurable amounts and is very conservative in its geochemical behaviour. Mixtures of mine water with regional aquifers cannot be excluded when mine water level rises up reaching the overburden rocks, which consists of Upper Cretaceous marls and carbonates (Fig.1). Here, we closely evaluated the bromide tracer normalized to chloride concentrations (Cl^-/Br^-) within mine waters and adjacent aquifers to test its suitability for identifying single distinct water bodies within the extensive mine workings network in order to track them during rebound.

Is there a geochemical fingerprint based on the chloride to bromide tracer, which is related to a gradient within the host formation of Upper Carboniferous strata or a regional hydrogeological fingerprint related to overburden thickness and various formation waters and aquifers influencing the Upper Carboniferous mine waters in the past?

The dimensions of the entire mine workings network in the Ruhr district is about 5000 km2. In the past, Permian (Zechstein) sourced waters and Upper Cretaceous saline waters from the regional Cenomanian-Turonian aquifer situated near the base of the overburden rocks already infiltrated Upper Carboniferous strata and mixed with hosted mine waters. In the eastern part, an influence of formation waters of the Emscher Formation, which can mimic mine waters as it hosts a lot of framboidal pyrite, is apparent. Such candidates of already mixed waters with fingerprints of the various water bodies in the overburden section need to be identified. In the eastern part of the Ruhr District tectonically isolated mine water provinces exists adjacent to central ones taking part of the rebound. In the isolated mine water provinces, mine water rebound has already been accomplished with mine waters rising close to the surface. Such showcases might act as a natural laboratory for the future major rebound.

A case study of water samples from shafts and surrounding mine workings of adjacent collieries will be presented here in order to have a closer look, if the bromide (Br^-) tracer is still valuable for identifying such mixing with different formation waters of the overburden (Fig.2).

Methods

Hydrogeochemical analyses of major cations and anions were conducted by certified lab analyses according to DIN ISO 11885 and DIN 10304- 1 protocols. Trace elements included barium, boron, bromide, fluoride, lithium, strontium and various transition metals. Bromide concentrations were measured using ion chromatography combined with UV

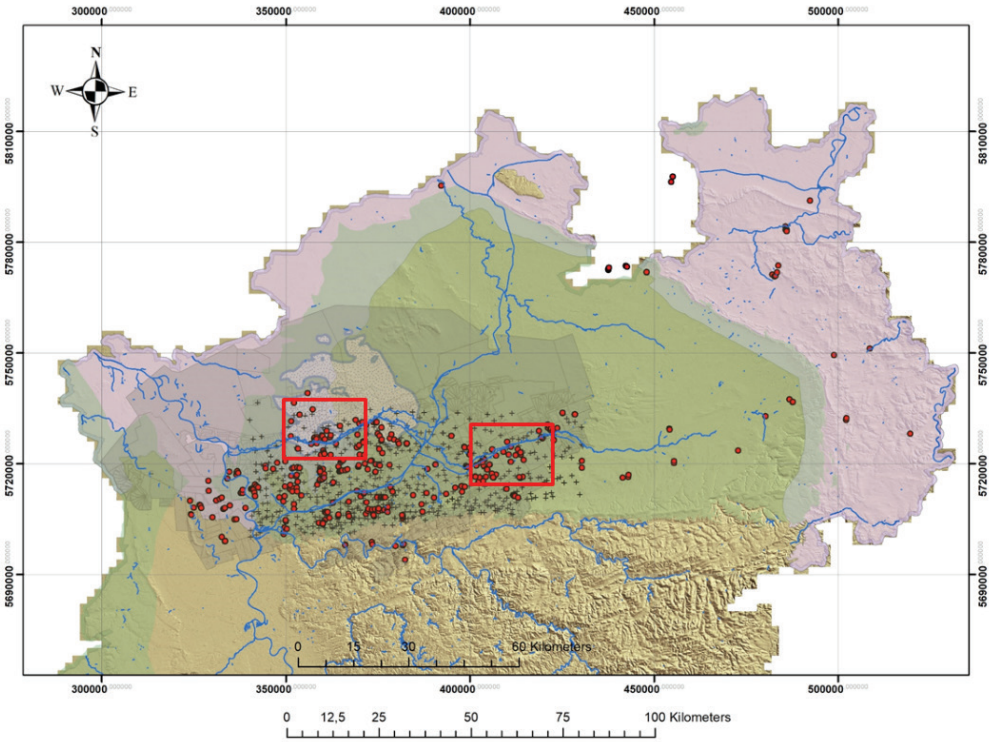


Figure 2 *Overview of mine area concessions (shaded bright green) of the Ruhr District on a bedrock geological map; the extent of Upper Cretaceous sediments (green) and of saline formations (magenta), i.e. Permian Zechstein and Upper Bunter Roet Fm. Are highlighted; red dots are mine water sample locations; crosshairs mark shaft locations; red rectangles mark the two areas of case studies in the northern and eastern part of the Ruhr District hard coal mining area*

detection in order to be not influenced by high chloride concentrations.

Results

A more accurate test for chloride to bromide ratio as tracer has been conducted using water samples taken during depth profiling of flooded vertical shafts in isolated mine water compartments of the eastern part of the mine area together with historical water samples from adjacent collieries. Former degassing and monitoring (plumbing) pipes in direct exchange with shaft related mine waters have been used for discrete depth water sampling. The shaft profiles have been formerly investigated using a multi-diver-probe setup measuring continuously electrical conductivity, temperature, ORP and pH in order to identify potential density stratifications and convection cells (Henkel & Melchers, 2017). Cl^-/Br^- ratios of discrete depth water samples from shafts with known lithostratigraphic correlation have been plotted together with historical water samples taken during mine operations at adjacent mine workings in a log-log plot based on mass concentrations (Fig.3). In Fig. 3, mine waters hosted in Upper Carboniferous strata vs. Upper Cretaceous formation water samples were subdivided in order to highlight the sharp boundary between the two major water body signatures. Chloride to bromide ratios in the range of 300 to 1000 have been recorded in the data. There is a good spread of data of higher bromide containing and less saline water samples from Upper Cretaceous sources with high saline less bromide-rich mine water samples. Cl^-/Br^- ratios of <600 can be related to formation water signatures of the Emscher Formation which makes up most of the overburden, whereas mine water influenced waters range up to Cl^-/Br^- ratios

of 1000. Formerly, the boundary has been set more conservative to be Cl^-/Br ratio <450. The sharp boundary of the two compartments can be related to former density stratifications.

In Fig. 4 a closer look at the dataset from Fig. 3 is presented in adding detailed mine locations of the data points. It is remarkable that single shafts like Waltrop and Koenigsborn (incl. KB LT and KB EG) or single boreholes like Waltrop 2 as well as groundwater monitoring wells like Landwehr/Ost, Stuckenbusch exhibit distinct chloride to bromide ratios. The shaft profile at Koenigsborn sets the boundary for chloride to bromide ratios. It distinguishes between the water bodies more influenced by overburden lithology of the Emscher Formation and the Upper Carboniferous hosted mine waters in the former mine workings (green dots). Potential outliers (blue dots in the lower left corner of the graph) with higher Cl^-/Br^- ratio of >850 might be influenced by the Cenomanian-Turonian saline aquifer contributions leading to much lower bromide concentrations. The dataset from Haus Aden identifies two locations, which have been already infiltrated by waters from the overburden rocks of the Emscher Formation indicated by higher chloride to bromide concentrations due to higher bromide contents affiliated with bromide contributions from organic material.

The second test case focuses on a dataset from the northern part of the Ruhr District in which mine waters exclusively hosted in former mine workings of the colliery Prosper Haniel were assessed. In Fig. 5, mine waters from the colliery Prosper Haniel comprise various mine water samples from the last 30 years including own data acquired in 2019. The data exhibit a very narrow range of chloride to bromide ratios, which level off at very high chloride concentrations. Own acquired data (grey dots) which range from 40.000 to 100.000 mg/L chloride concentrations indicate a similar trend. Explanation for such a trend range from analytical errors using no UV detection for bromide, that bromide reaches a saturation at chloride levels of 100.000 mg/L or more or, if the trend is real, then it can be related to incremental amounts of halite dissolution waters from Zechstein strata mixed with mine waters. Zechstein strata crop out closely to the extent of mine workings from Prosper Haniel and have been clearly identified in relation to large fault lines with offsets of up to 200 meters.

In Fig. 6, the original concentrations of bromide to chloride in the mine water samples are plotted. Two trends can be

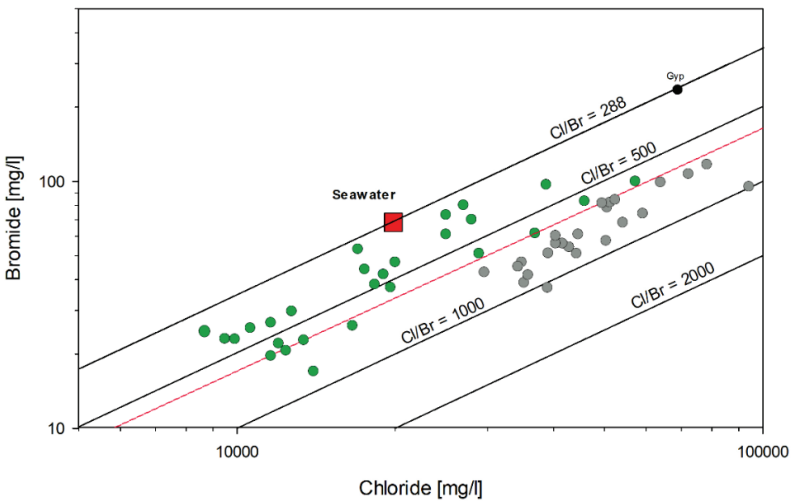


Figure 3 *Chloride to bromide mass concentrations plotted in a log-log plot; water samples from shafts and samples from adjacent collieries are compared with overburden samples. The data consists of Upper Cretaceous lithostratigraphic horizons (green dots) and Upper Carboniferous hosted mine waters (grey dots); red rectangle marks the chloride to bromide content of seawater.*

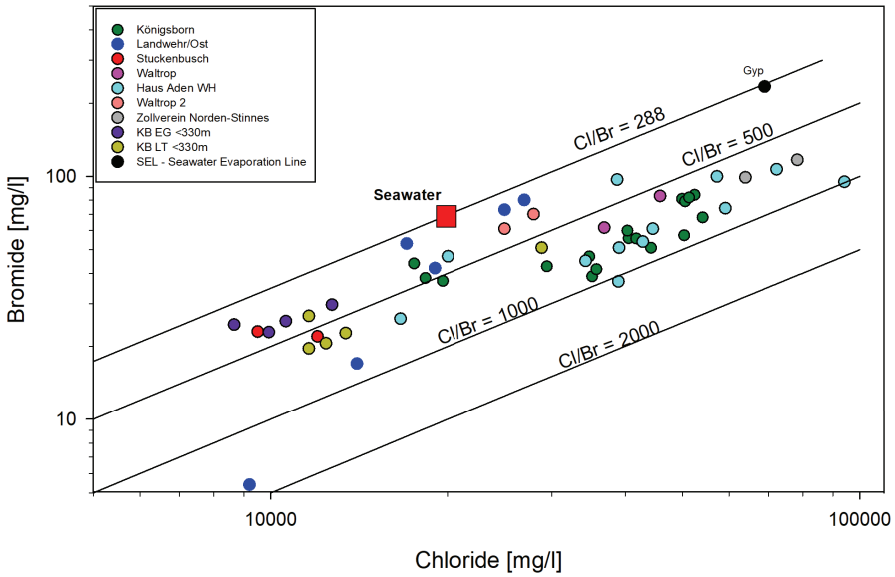


Figure 4 *Detailed origin of water samples including mine and formation waters of Fig. 3.*

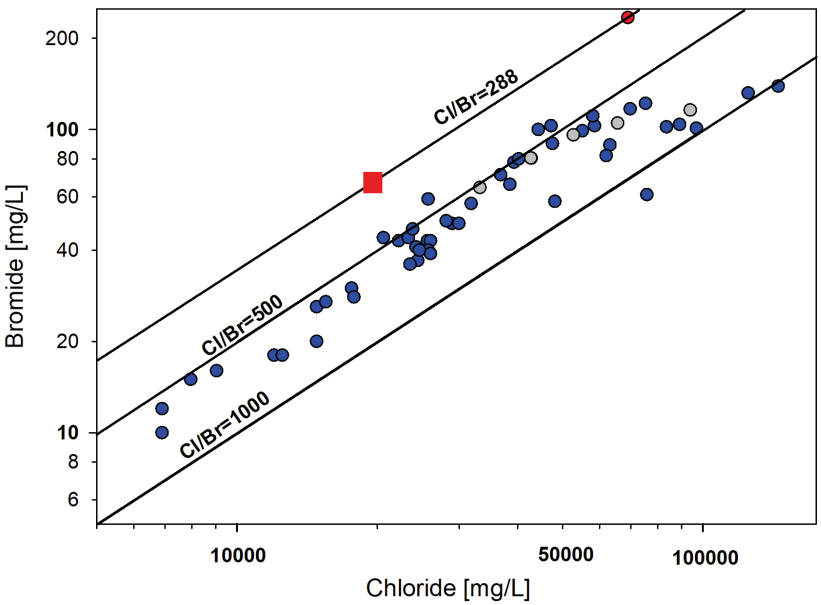


Figure 5 *Mine water samples from the mine workings associated with the colliery Prosper Haniel located in the northern part of the Ruhr District; own data (grey samples) were taken in 2019 at depths from 800 to 1400 meters; historical data (blue dots) were gathered during the last 30 years; red square and red dot marks seawater composition and evaporation path.*

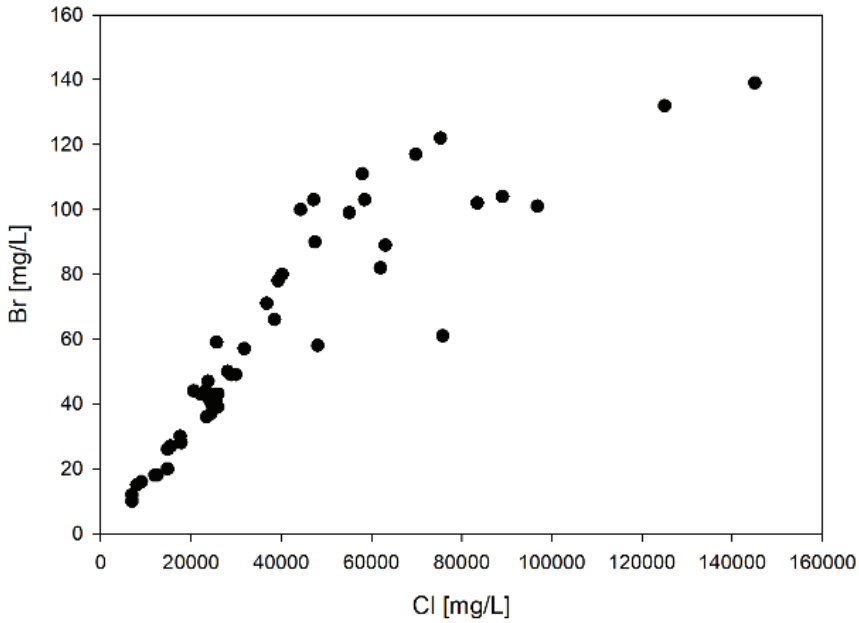


Figure 6 *Original, non-normalized bromide and chloride concentrations in [mg/L] of the mine water samples plotted in Fig. 5.*

identified at chloride concentrations > 60.000 mg/L. A linear trend of Late Carboniferous hosted mine waters and a trend of higher chloride concentration, which add very little bromide concentration and could resemble additions of halite dissolution originated waters like Zechstein waters.

Conclusions

The already tested chloride to bromide ratio as a useful tracer to distinguish mine water brines from saline aquifers has been further evaluated on two distinct water provinces in the Ruhr Valley. The two water provinces are: (1) Prosper Haniel, the last colliery decommissioned at the end of 2018, and (2) the isolated water province of Koenigsborn, for which the mine water rebound has already taken place adjacent to the active one at Haus Aden, which just started its mine water rebound with a mine water level at 1000 meters depth. The ratio that marks the boundary between Upper Cretaceous sourced waters from Emscher Fm. vs. mine waters had a better precision with Cl-/Br- ratios of <600 compared to previous data in the subset. The chloride to bromide ratio was successfully tested to distinguish formation waters from the Emscher Formation compared to pristine mine waters and the mixture of both. Similar sulphide oxidation processes for mine waters were recognized in the formation waters of the Emscher Formation due to ubiquitous framboidal pyrite in the strata. This leads to a sulphate rich formation water, which could very much resemble original mine waters of the Upper Carboniferous mine workings and result in false positive alarms associated with the monitoring scheme. Bromide tracer might elucidate such cases and mitigate false positive alarms. For the subset of mine water samples at the colliery Prosper Haniel, the bromide tracer exhibited a narrow range of chloride to bromide concentrations up to very high chloride concentrations. The bromide content indicated a higher spread of values at >80 mg/L bromide content for which the addition of formation waters from Permian Zechstein strata is a plausible scenario. The bromide/chloride tracer is a suitable candidate to be included in risk management and monitoring strategies for the future rebound management of the operator RAG AG and the control measures of the District Council of North Rhine Westphalia. The evaluation will continue to apply sophisticated statistical tools in order to better quantify the various groundwater origins in the future.

Acknowledgements

The authors thank the foundation "Forum Bergbau und Wasser" for financial support. RAG AG is thanked for data access and site support. Laura Cebula is very much thanked for valuable discussions, extensive support during fieldwork and data pre-work of this study.

References

Hahne, C, Schmidt, R (1982): Die Geologie des Niederrheinisch-Westfälischen Steinkohlengebietes – Einführung in das Steinkohlengebirge uns seine Montangeologie. Verlag Glückauf, Essen, pp. 106.

Henkel, L.; Melchers, C. (2017): Hydrochemical and isotopegeochemical evaluation of density stratification in mine water bodies of the Ruhr coalfield. In: Wolkersdorfer, C.; Sartz, L.; Sillanpää, M.; Häkkinen, A. (Eds.): Proceedings 13th International Mine Water Association Congress – Mine water & circular economy. Lappeenranta, 430-436

Jasnowski-Peters, H. & Melchers, Chr. (2021): Natural Tracers For Mine Water Fingerprinting – A First Step To A Hydrogeochemical Monitoring Plan For Risk Assessment During Mine Water Rebound In The Ruhr District Area, Germany. – In: Stanley, P.; Wolkersdorfer, Ch.; Wolkersdorfer, K.: Mine Water Management for Future Generations. – p. 212 – 217; Cardiff, Wales, United Kingdom (Natural Resources Wales, The Coal Authority, Welsh Government, Cardiff University).

Jasnowski-Peters, H. & Melchers, Chr. (2022): Natural Tracers For Mine Water Fingerprinting II – a multi tracer approach to unravel underground fluid movements during Mine Water Rebound in the Ruhr District Area. – In: Pope, J.; Wolkersdorfer, C.; Rait, R.; Trumm, D.; Christenson, H.; Wolkersdorfer, K.: IMWA 2022 – Reconnect. – p. 167 – 173; Christchurch, New Zealand (International Mine Water Association).

Minimizing Xanthate Impacts on Watercourses in Cold Climate – Review on Available and Potential Approaches

Piia Juholin[1], Kirsi-Marja Haanpää[1], Tea Laurila[2], Eeva-Leena Anttila[1], Päivi Picken[3]

[1]*AFRY, Elektroniikkatie 13, FI-90590 Oulu, Finland, piia.juholin@afry.com, kirsi-marja.haanpaa@afry.com, eeva-leena.anttila@afry.com*

[2]*AFRY, Jaakonkatu 3, FI-01620 Vantaa, Finland, tea.laurila@afry.com*

[3]*AFRY, Koskikatu 27B, FI-96100 Rovaniemi, Finland, paivi.picken@afry.com*

Abstract

Xanthates are essential process chemicals used as collectors in sulfide ore flotation, but they may be toxic to aquatic organisms even at low concentrations. The primary ways of controlling xanthate impacts are species type selection, dozing optimization, and prolonging the delay times. These means may be adequate to decrease the concentrations to acceptable levels. However, in some cases, separate xanthate removal may be needed. Particularly this concerns mines at cold climates and mines with neutral and/or alkaline discharge waters because spontaneous xanthate degradation rates are slower. This paper summarizes the current knowledge about xanthate management and removal.

Keywords: Xanthate, cold climate, water treatment, water management

Introduction

Xanthates are used as collectors in the flotation process in sulfide mineral concentration. Xanthates are organic sulfur compounds that have a polar and a non-polar charged end. Metal-sulfides attach to the polar end, and the hydrophobic non-polar end rises to the water surface with air bubbles forming a froth that can be skimmed. The concentrate will have most of the xanthates, but residual xanthates will follow the tailings or effluent. (Lam 1999; Bach *et al*. 2016) Approximately 2 billion tonnes of ore are processed in flotation with xanthates per year, dosage generally ranging from 30 to 300 g t-1 ore (Pearse 2005). Thus, xanthates constitute a considerable usage of chemicals.

Xanthates have been found to be harmful to aquatic organisms and they increase toxicity of metals. The degradation of xanthates produces highly toxic carbon disulfide (CS2), which is rapidly volatilised from solution into air. (Lam 1999; Bach *et al*. 2016)

Xanthates degrade in warm and acidic water, especially at high xanthate concentrations. (Hawley 1977) Also, the presence of metal salts, such as copper, iron, zinc, or lead, catalyzes degradation. (Bach *et al*. 2016) At mines in cold climates having low water temperatures and ice cover on tailings management facility (TMF) or recycle water facility, xanthates' slow degradation kinetics combined to site wide positive water balance may lead to noteworthy concentrations of xanthate residues in the discharge water. (Muzinda and Schreithofer 2018) The challenge may be emphasized at alkalic conditions due to lower xanthate degradation rates in neutral or alkaline water. (Walterson 1984; Fischer and Jarsjö 2023)

The risk of xanthate residues causing environmental impacts cannot be ignored at mine sites in cold climates as xanthate residues have been detected in the discharge water (Walterson 1984; Fischer and Jarsjö 2023), meaning that degradation has been inadequate in the mine water cycle. Additionally, the importance of controlling xanthate residues seems to be increasing as the Swedish regulator has recently set the first discharge limit for residual xanthate concentration in discharge water. (Umeå Tingsrätt 2022) In Finland, the Finnish Environment Institute has suggested monitoring of xanthate concentrations in discharges and in recipient waterbodies of selected mines and industrial plants. When

more data is available from monitoring, the need for national legislation will be evaluated. (Mehtonen *et al*. 2022)

Methods to manage the environmental risks related to residual xanthates are: 1) using environmentally least harmful xanthate species, 2) avoiding overdosing, 3) increasing water recycle rate between the concentrator and tailings management facility. Additionally, active water treatment processes can be applied to remove residual xanthates. For example, 1) oxidation and especially Fenton processes, 2) sorption, and 3) coagulation processes can be applied for xanthate removal.

Most of the studies related to xanthates discuss wet tailings deposition. However, dry tailing deposition methods are gaining popularity also in cold climate environments. In dry stacking, even more than 75% of process water can be reclaimed and circulated back to process prior to final deposition. This decreases the residence time of xanthates in the water cycle, which decreases spontaneous degradation, but also offers a more efficient method of managing xanthate containing water streams. Same methods of xanthate management and residual xanthate removal may be applied to wet and dry tailings deposition. In all cases, the precise execution of xanthate management needs to be planned site-specifically considering the individual characteristics of each mine, the prevailing weather, and the local environment.

Controlling Xanthate Concentrations

The most important means of decreasing environmental risks related to xanthates should be avoidance of overdosing. Correct dosage does not only decrease the risk of residual xanthate concentrations in discharge water, but also improves metal recovery and process selectivity (Rao and Finch 1989; Muzinda and Schreithofer 2018). As an example, Cu-Pb-Zn ore flotation selectivity decrease has been observed due to degradation of copper collector Z-200 (Ozkan and Acar 2004).

Xanthate degrades spontaneously with time. Xanthate concentrations decrease due to degradation and dilution during their residence time in TMFs and mine site water storage facilities. The residence time may be sufficient to reduce xanthate concentrations to environmentally harmless levels. Seasonal variation influences the process water composition in cold climate. In wintertime, low temperatures, lack of xanthate destructing UV-light (especially under ice covered ponds), and a low amount of dilution may increase the concentration of xanthate in process water until spring flood. (Muzinda and Schreithofer 2018) In Sweden, highest xanthate concentrations in mine discharge water were observed during springtime, whereas the highest concentrations in water streams inside the mining facilities were observed during winter (Walterson 1984; Fischer and Jarsjö 2023)

The harmfulness of residual xanthates may be reduced by choosing chemicals with lower environmental risk compared to other alternatives. The harmfulness of xanthates is assessed in the environmental risk assessment with predicted no-effect concentration (PNEC), which varies between xanthate chemicals. If several applicable flotation chemicals are identified, the least harmful should be chosen.

PNEC is derived by dividing the lowest toxicity concentration by assessment factor (AF) (Okonski *et al.* 2021). Assessment factor reflects the uncertainty related to the experimental work behind the concentration value. In this comparison, SIBX and PAX have the highest PNEC values in freshwater, whereas SEX and PIAX have considerably lower values for intermittent release.

Table 1 *PNECs of Xanthate Compounds (ECHA 2023).*

Xanthate compound	CAS No.	AF	PNEC aqua, freshwater	PNEC aqua, freshwater (intermittent releases)
Sodium ethyl xanthate SEX	140-90-9	100	0.47 µg L^{-1}	0.0001 mg L^{-1}
Potassium ethyl xanthate PAX	2720-73-2	10	0.36 mg L^{-1}	0.18 mg L^{-1}
Sodium isopropyl xanthate SIPX	140-93-2	10	0.01 mg L^{-1}	0.021 mg L^{-1}
Sodium isobutyl xanthate SIBX	25306-75-6	10	1.4 mg L^{-1}	0.7 mg L^{-1}
Potassium isoamyl xanthate PIAX	928-70-1	1000	3.67 µg L^{-1}	0.037 mg L^{-1}

Substitution of xanthates with other flotation chemicals, such as ether diamines or phosphoric acid esters, have been studied with some promising results. However, the introduction of new chemicals with inadequately known properties and without any long-term observational data, whereas xanthates have been used for decades without major environmental impacts, introduces a host of new risks that are hard to evaluate. (Fischer and Jarsjö 2023)

Xanthates end up from concentration plant to TMF with tailings and, from there, recycle back to the process as reclaim water or migrate to other parts of the mine site water cycle. On site water cycle, xanthate containing water mixes with other water streams diluting xanthate concentrations. The loading of xanthate per ton of tailings transported to tailings pond is higher in slurry deposition than in thickened or filtered tailings deposition. In the case of thickened and filtered tailings, xanthate containing process water can be more efficiently circulated between concentration process and tailings thickener or filtration unit promoting lower xanthate concentrations. Recirculation rate should be kept as high as possible to reduce water discharge from the TMF and, thus, to contribute to reduced xanthate emissions to the environment.

Technologies for Residual Xanthate Removal

If the above-mentioned methods cannot be applied or they are inadequate to decrease the xanthate concentrations to environmentally acceptable concentrations, active xanthate removal may need to be applied. Xanthate removal is most efficient from concentrated solutions, e.g., in association with the concentration plant or before the point where TMF excess water is mixed with other mine site water streams. This will also help to minimise the amount of water to be treated. Concentrations are lower in the mine discharge water due to dilution and degradation of the chemical, but treatment of them can also be a good option, especially if xanthates can be removed together with other pollutants at the effluent water treatment facility. Some applicable methods for xanthate removal are presented below.

Oxidation

In oxidation processes, chemicals such as ozone or hydrogen peroxide are used for xanthate degradation. Alternatively, xanthate may also be oxidised by UV light. Oxidation processes aim at degrading the xanthates fully into harmless bicarbonate, sulfate, and water. The challenge with all oxidation methods is production of intermediate products that may be even more harmful than the parent substance, like highly toxic carbon disulfide (CS_2).

In laboratory experiments, potassium ethyl xanthate (PEX) has been degraded in 20 min with removal efficiency of 96.5 % using a $UV_{185 + 254\ nm}$ lamp and 74.8 % using a $UV_{254\ nm}$ lamp. The removal efficiency increases with time. In 75 min, the removal efficiencies were 99.9 % with $UV_{185 + 254}$ nm lamp and 97.9 % with UV254 nm lamp. In these experiments, the PEX concentration was 100 mg L^{-1} and pH 10. (Fu *et al.* 2019) The advantage of UV light is the simplicity of the process and lack of chemical usage. UV treatment is commonly used in applications such as disinfection of domestic water. Successful UV treatment requires that there is no turbidity in the water, which would impede the transmission of light.

Hydrogen peroxide (H_2O_2) has been shown to degrade ethyl xanthate (EX) up to 90% in 30 min. However, EX does not degrade to harmless substances by hydrogen peroxide alone. Reaction may be catalyzed by Fe^{2+} ions, which remove TOC. Use of Fe^{2+} alone has led to TOC removal up to 41% and accompanied by UV light up to 48% (García-Leiva *et al.* 2019). Chen *et al.* (2015)observed that H_2O_2 concentration influences the degradation, but pH does not.

Ozone (O_3) has been used to decompose sodium n-butylxanthate (SBX) to low concentrations in just 5 min. Ozonation alone increased the total degradation rate to 16.2-23.3%. With a combination of ozonation and visible UV light (VUV), the total degradation rate increased to 30.4-41.6% (Fu *et al.* 2016).

Sorption

Sorption is a general term for various molecule level processes that remove xanthates from dissolution using surface active particles, such as bentonite or activated carbon. In

comparison to oxidation processes, a major benefit is that none or considerably less intermediate products are formed.

Ethyl xanthate (EX) has been removed from solution in laboratory experiments using activated carbon (AC). Activated carbon removed up to 99 % of ethyl xanthate at concentrations below 268 mg L^{-1}. At higher concentrations, the removal efficiency was reduced. Also, high pH slightly reduced the efficiency of the material. (Salarirad *et al.* 2021)

Oliveira and Rubio (2009) tested zeolite for isopropylxanthate removal. They found that zeolite needed to be modified for efficient removal. With modified zeolite, 98% removal of xanthate was obtained. The adsorbent was collected from the water by flotation and required a low recycling rate of 20% (Oliveira and Rubio 2009). Also, applicability of bentonite as sorption material has been assessed in some studies. (Rezaei *et al.* 2018; Amrollahi *et al.* 2019)

Coagulation – Flocculation

Coagulation-flocculation is used for the removal of organic substances from solutions and has also been found to remove xanthate. Xanthate anions can form sparingly soluble compounds and precipitate, e.g., with iron, aluminum, and copper ions which can then be separated (Yuan *et al.* 2023).

A combination of ferric chloride and polymerised aluminum chloride has been shown to work effectively with polyacrylamide in removing xanthate from alkaline and turbid flotation waters. Also, use of ferric sulfate, polymerized ferric sulfate, and polyacrylamide have been effective (over 99% removal) in xanthate removal under neutral conditions. (Yuan *et al.* 2023)

Electrocoagulation

Çırak (2022) has investigated electrocoagulation for xanthate removal with aluminum, iron, and copper electrodes. 100 % removal was gained using a copper electrode at pH 9 and with electric current 0.6 A. Treatment produced Cu(I) ethyl xanthate or Cu(II) ethyl xanthate precipitates. Similarly, the iron electrode removed 82.3 % of the xanthate at pH 6.5 and with electric current 0.6 A (Çırak 2022).

Biological Water Treatment

Using biological methods Chen *et al.* (2011) were able to remove 81.8 % of n-butyl xanthates in 8 days (Chen *et al.* 2011). High xanthate concentrations can inhibit microbial activity and the method appears to be more viable in treatment of dilute xanthate concentrations. It is deduced that the challenge of biological xanthate degradation is its retention time and low efficiency (Yuan *et al.* 2023) which may be emphasized in cold climate.

Conclusions

Xanthate concentration in mine discharge water can be controlled with several methods. Most applied methods are: 1) avoiding overdosage of the chemical, 2) promoting long residence times in water ponds and in TMF to enhance spontaneous degradation, and 3) promoting closed water circulation between concentration plant and TMF. Furthermore, the environmental impact may be decreased by selecting the least harmful xanthate type. If these methods are inadequate to decrease the discharge water xanthate concentrations to environmentally safe concentrations, active water treatment techniques can be applied to assist xanthate removal.

Degradation of xanthate by oxidation is currently one of the most favored techniques. Its challenge is the tendency to produce intermediates having even higher toxicity than xanthate itself. Hydroxyl radical producing advanced oxidation processes were often seen as a better alternative because they degrade the compound further. Also, a variety of adsorbents have been developed for xanthate removal. The advantage of sorption is that it does not form intermediates. Also, coagulation-flocculation and biological processes have been developed for xanthate removal.

Treatment process for xanthate removal can be applied to concentration plant process water, TMF discharge water, or mine site discharge water. Water treatment efficiency may be limited in treatment of dilute water streams.

References

Amrollahi A, Massinaei M, Zeraatkar Moghaddam A (2019) Removal of the residual xanthate from flotation plant tailings using bentonite modified by magnetic nano-particles. Miner Eng 134:142-155. https://doi.org/10.1016/j.mineng.2019.01.031

Bach L, Dyrmose Nørregaard R, Hansen V, Gustavson K (2016) Review on Environmental Risk Assessment of Mining Chemicals Used for Mineral Separation in the Mineral Resources Industry and Recommendations for Greenland. Scientific Report from DCE - Danish Centre for Environment and Energy no. 203. ISSN 2245-0203.

Chen S, Gong W, Mei G, *et al* (2011) Primary biodegradation of sulfide mineral flotation collectors. Miner Eng 24:953–955. https://doi.org/10.1016/J.MINENG.2011.01.003

Chen X Hua, Hu Y Hua, Peng H, Cao X Feng (2015) Degradation of ethyl xanthate in flotation residues by hydrogen peroxide. J Cent South Univ 22:495–501. https://doi.org/10.1007/s11771-015-2548-0

Çırak M (2022) Performance evaluation of electrocoagulation using aluminum, iron and copper electrodes for removal of xanthate. Chemical Papers 76:3661–3677. https://doi.org/10.1007/s11696-022-02120-4

ECHA (2023) REACH - Registration, Evaluation, Authorisation and Restriction of Chemicals Regulation. In: https://echa.europa.eu/fi/information-on-chemicals/registered-substances

Fischer S, Jarsjö J (2023) Flotation chemicals at Swedish mines Review of their potential environmental impact Flotationskemikalier vid svenska gruvor Sammanställning över deras potentiella miljöpåverkan. Stockholm University Department of Physical Geography.

Fu P, Feng J, Yang H, Yang T (2016) Degradation of sodium n-butyl xanthate by vacuum UV-ozone (VUV/O3) in comparison with ozone and VUV photolysis. Process Safety and Environmental Protection 102:64–70. https://doi.org/10.1016/J.PSEP.2016.02.010

Fu P, Li G, Wu X, *et al* (2019) UV185þ254 nm photolysis of typical thiol collectors: Decomposition efficiency, mineralization and formation of sulfur byproducts. R Soc Open Sci 6. https://doi.org/10.1098/rsos.190123

García-Leiva B, Teixeira LAC, Torem ML (2019) Degradation of xanthate in waters by hydrogen peroxide, fenton and simulated solar photo-fenton processes. Journal of Materials Research and Technology 8:5698–5706. https://doi.org/10.1016/j.jmrt.2019.09.037

Hawley JR (1977) The use, characteristics, and toxicity of mine-mill reagents in the province of Ontario. Ontario Ministry of the Environment

Lam K-S (1999) Biodegradation of xanthate by microbes isolated from a tailings lagoon and a potential role for biofilm and plant/microbe associations. University of Western Sydney, Nepean

Mehtonen J, Siimes K, Leppänen M, Junttila V, Äystö L, Vähä E (2022) Vesiympäristölle vaarallisten ja haitallisten aineiden asetuksen (VNa 1022/2006) 12 §:n mukainen suunnitelma [in Finnish]. Draft 15.11.2022

Muzinda I, Schreithofer N (2018) Water quality effects on flotation: Impacts and control of residual xanthates. Miner Eng 125:34–41. https://doi.org/10.1016/j.mineng.2018.03.032

Okonski AI, MacDonald DB, Potter K, Bonnell M (2021) Deriving predicted no-effect concentrations (PNECs) using a novel assessment factor method. Human and Ecological Risk Assessment: An International Journal 27:1613–1635. https://doi.org/10.1080/10807039.2020.1865788

Oliveira CR, Rubio J (2009) Isopropylxanthate ions uptake by modified natural zeolite and removal by dissolved air flotation. Int J Miner Process 90:21–26. https://doi.org/10.1016/j.minpro.2008.09.006

Ozkan SG, Acar A (2004) Investigation of impact of water type on borate ore flotation. Water Res 38:1773–1778. https://doi.org/10.1016/J.WATRES.2003.12.036

Pearse MJ (2005) An overview of the use of chemical reagents in mineral processing. Miner Eng 18:139–149. https://doi.org/10.1016/J.MINENG.2004.09.015

Rao SR, Finch JA (1989) A review of water re-use in flotation. Miner Eng 2:65–85. https://doi.org/10.1016/0892-6875(89)90066-6

Rezaei R, Massinaei M, Zeraatkar Moghaddam A (2018) Removal of the residual xanthate from flotation plant tailings using modified bentonite. Miner Eng 119:1-10. https://doi.org/10.1016/j.mineng.2018.01.012

Salarirad MM, Behnamfard A, Veglio F (2021) Removal of xanthate from aqueous solutions by adsorption onto untreated and acid/base treated activated carbons. Desalination Water Treat 212:220–233. https://doi.org/10.5004/dwt.2021.26683

Umeå Tingsrätt (2022) Tillstånd enligt miljöbalken till fortsatt och utökad gruvverksamhet vid Tapuli, Palotieva och Sahavaara gruvor med tillhörande verksamhet vid Kaunisvaara anrikningsverk, Pajala kommun. 2022-12-01. Mål M 2090-19. [in Swedish]

Walterson E (1984) Effects from xanthates at Swedish mineral enrichment plants (Swedish title: Effekter av anrikningsreagenser -Fördelning och spridning av xantater och xantatderivat vid anrikningsverk) Institutet för vatten- och luftvårdsforskning No. 748

Yuan J, Li S, Ding Z, *et al* (2023) Treatment Technology and Research Progress of Residual Xanthate in Mineral Processing Wastewater. Minerals 13:435. https://doi.org/10.3390/min13030435

Effect of a Till Cover in Harmful Element Reduction in Waste Rock Drainage

Teemu Karlsson[1], Ville-Pekka Paalumäki[2], Tommi Kauppila[1], Eila Hietaharju[2]

[1]Circular Economy Solutions, Geological Survey of Finland, Viestikatu 7, 70211 Kuopio, Finland, email: teemu.karlsson@gtk.fi; 2Department of Geography and Geology, University of Turku, Akatemiankatu 1, 20500 Turku, Finland

Abstract

This study investigates the effectiveness of a thin (0.3 m) till cover layer in reducing harmful element mobilization in waste rock drainage at the closed Särkiniemi Ni-Cu mine site in Finland. In the study, lysimeters (diameter 1.0 m, height 0.3 m) were filled with crushed waste rock, buried in the upper parts of the waste rock pile, and drainages were monitored through 2020-2021. Results demonstrate that the till cover reduced the mobility of elements like Cu, Co, Ni, SO4, and Zn, primarily by decreasing the amount of infiltrating water. However, more efficient cover layers may be necessary depending on closure objectives.

Keywords: Acid mine drainage, mine closure, cover structure, lysimeter, Särkiniemi

Introduction

The environmental impacts of mining activities, particularly related to acid mine drainage (AMD) originating from mine waste facilities, are one of the main concerns of the mining industry. AMD, generated by the exposure of sulfide minerals to atmospheric water and oxygen, poses significant risks to ecosystems, water resources, and human health (Lottermoser 2010). Effective strategies for mitigating AMD and managing mine waste facilities are crucial to minimize these risks.

Various cover systems are commonly used in mine waste management (INAP 2017). Till covers, which act as a physical barrier to reduce water and oxygen infiltration, are a widely adopted closure technique for mine waste facilities in Nordic countries (Kauppila 2023). Typical layer thicknesses of the single-layer till/soil covers range from 0.3 to 1.5 m (Garbarino *et al*. 2018). However, comprehensive studies assessing the effectiveness of the covers with lower-end thicknesses in reducing harmful element mobilization in waste rock drainage remain limited, and the optimal thickness and long-term performance of till covers warrant further research.

This study investigates the impact of a relatively thin, 0.3 m, cover layer made of local till on waste rock drainage at the closed Särkiniemi Ni-Cu mine in Finland. Through the analysis of lysimeter monitoring data, we will assess the extent to which the till cover reduces the mobility of harmful elements, such as Cu, Co, Ni, SO_4, and Zn from weathered waste rock material. The insights gained from this study can be utilized in modelling and designing mine waste cover structures and helping to minimize the environmental impacts of mining.

Materials and methods

The study was conducted at the closed Särkiniemi Ni-Cu mine site, located in Northern Savo, Finland (Fig. 1). The mine was active in 2007-2008, during which approximately 165000 tons of waste rock was excavated. The waste rock material consists mainly of mica gneiss, gabbro, and amphibole rock (Karlsson *et al*. 2018).

Due to inadequate closure, piles of uncovered waste rock material can still be found at the site, including material crushed for aggregates. The actual waste rock pile was unevenly covered with till and some waste rock boulders can still be seen. Currently, the surrounding environment is affected by waste

rocks-originated AMD, characterized by a low pH (around 3-4) and elevated amounts of Ni, Co, Cu, Zn and SO4 (Karlsson *et al*. 2021).

A lysimeter study was carried out to evaluate the effect of a 0.3 m cover layer made of local till on waste rock drainage water quality. In 2019, three lysimeters (diameter 1.0 m, height 0.3 m) were buried in the upper parts of the waste rock pile and filled with weathered waste rock material obtained from the aggregate piles. One of the lysimeters was left uncovered as a control lysimeter (LY1) and two were covered with 0.3 m of till (LY2 and LY3).

The mineralogy of the crushed waste rock material was characterised at GTK Research laboratory with a FE-SEM-EDS. The geochemical properties, including aqua regia extractable element concentrations and total S were investigated in an accredited commercial laboratory, as well as the geotechnical properties of the till material, including water conductivity and grain size distribution.

The lysimeter drainages were monitored throughout the study period of May 2020 – December 2021. Water samples were collected at approximately monthly intervals of around once per month and analysed for harmful elements, including Cu, Co, Ni, SO4, and Zn. Precipitation data was also recorded by installing a weather station (Campbell Scientific WXPro) at the site, and the amount of water infiltrating the lysimeters was compared between the covered and uncovered setups.

Oxygen (O_2) concentrations below the till cover were measured using O-sensors (Campbell Scientific SO-110), providing data on the availability of oxygen within the covered lysimeter setups. These measurements were compared to the atmospheric O_2 concentrations, which were determined by an O-sensor installed above the cover layers (open air, atmospheric conditions), to determine the influence of till cover on oxygen availability. The mV data was transformed to O_2 % by first calculating a conversion factor, which was obtained by dividing the median mV value of the O-sensor installed in open air by the standard atmospheric O_2 % of 20.9. Then, the mV values were multiplied by this factor to yield the corresponding O_2 % measurements.

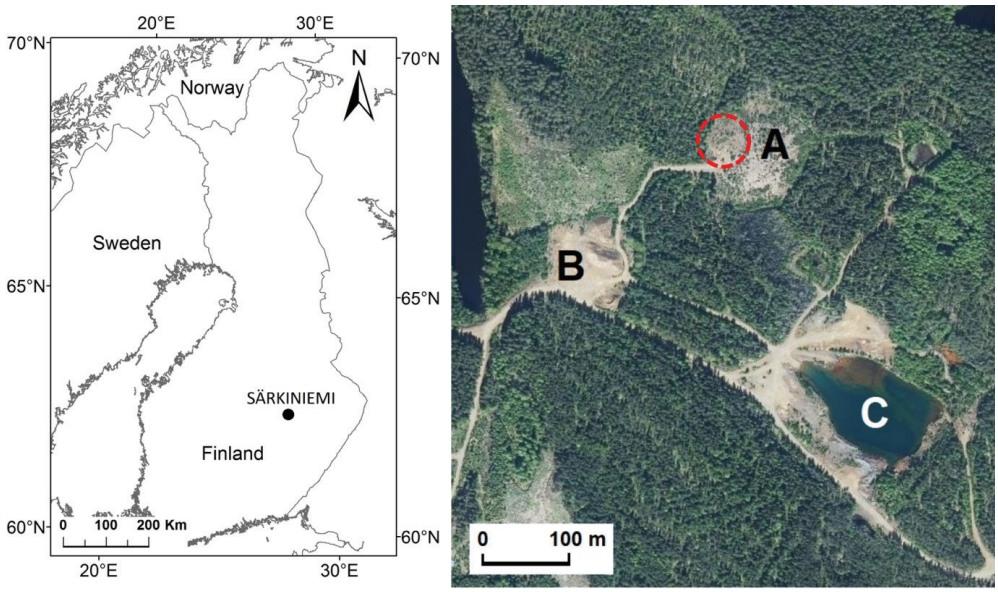


Figure 1 *The location of the Särkiniemi mine in Finland and an aerial image of the mine site. A = waste rock area, B = piles of crushed waste rock, C = open pit filled with water. The area where the lysimeter test was conducted is presented by red circle. Basemap and aerial image © National Land Survey of Finland and HALTIK 2013.*

The monitoring data collected from the lysimeter study was analysed to quantify the reduction in harmful element mobility due to the 0.3 m till cover. Reduction percentages were calculated for each element by comparing the concentrations in the covered lysimeters to those in the uncovered control lysimeter.

Results and discussion

The crushed waste rock material used in the lysimeter tests contained elevated aqua regia extractable amounts of Co (67 mg/kg), Cu (522 mg/kg), Ni (560 mg/kg) and Zn (92 mg/kg). The total S concentration was 1.6 %. Based on the FE-SEM-EDS results, the main minerals (wt% > 5) included quartz (20.3 wt%), biotite (18.1 wt%), non-albitic plagioclase (15.3 wt%), a mixture of chlorite (smectite), jarosite and sulfides (14.9 wt%), and hornblende (6.6 wt%). The detected sulfide minerals included pyrrhotite (0.8 wt%), pyrite (0.2 wt%), chalcopyrite (traces) and pentlandite (traces), while no carbonates were detected. As the orange colour of the crushed waste rock aggregate piles already indicated, the material was weathered and contained detectable amounts of secondary mineral jarosite.

The till material used to construct the cover can be classified as sandy till, comprising approximately 50 % cobble and gravel (>2 mm), 40 % sand (0.06 – 2 mm) and 10 % fine-grained material (<0.06 mm). The hydraulic conductivity of the till was measured to be $4.5*10^{-7}$ m/s, indicating its classification as permeable material (Garbarino *et al.* 2018).

The till cover demonstrated a notable impact on the amount of water infiltrating the waste rock material. During the summer seasons 2020-2021, approximately half of the precipitated water was recorded as drainage from the uncovered lysimeter, while the corresponding amount for the till-covered lysimeters was around one-tenth. Previous studies conducted by Wilson *et al.* (1995) have demonstrated that increasing the thickness of the till cover, such as the 0.8 m thickness they investigated, can further enhance the reduction of rainwater infiltration to as low as 1-5 % of the total precipitation.

According to the lysimeter monitoring results, the amounts of mobilized harmful elements were substantially reduced by the till cover (Table 1). On average during the monitoring period, the Cu mobility was reduced the most, around 86-93 %. Reduction for Co was 60-71 %, for Ni 48-61 %, for SO4 52-64 % and for Zn 17-40 % (Fig. 2). In general, the element concentrations were lower in the LY1 drainage compared with the LY2 and LY3, but the amount of drainage water was significantly higher. The till cover had only a minor effect on the drainage pH; the average pH of the uncovered LY1 was 3.6, while the average pH's of the LY2 and LY3 drainages were only slightly higher, 3.8 and 3.7, respectively (Table 1).

According to the O-sensor data, the O_2 concentrations below the till cover were not substantially lower than the atmospheric O_2 concentration of 20.9 % (Fig. 3). On top of LY1, in atmospheric conditions, the median O-sensor value was 51.8 mV (assuming 20.9 O_2 %, which implies a conversion factor of 2.48 mV per O_2 %), while under the till cover, the median values were 44.0 mV (17.7 O_2 %) in LY2 and 46.6 mV (18.8 O_2 %) in LY3. This suggests that oxygen is diffusing through the till cover. While the exact impact of these oxygen levels on sulfide oxidation is difficult to determine without further investigation, it is likely that the main factor affecting the reduced harmful element mobility in the

Table 1 *The masses (grams) of Co, Cu, Ni, Zn and SO4 leached out from the lysimeters LY1-3 and the average drainage pH during the monitoring period 2020-2021. The masses have been calculated based on drainage concentrations and amounts of drainage water.*

Lysimeter	Average pH	Co	Cu	Ni	Zn	SO_4
		g	g	g	g	g
LY1	3.6	2.55	2.61	10.45	0.84	453.76
LY2	3.8	0.73	0.19	4.04	0.51	164.48
LY3	3.7	1.02	0.38	5.44	0.70	217.08

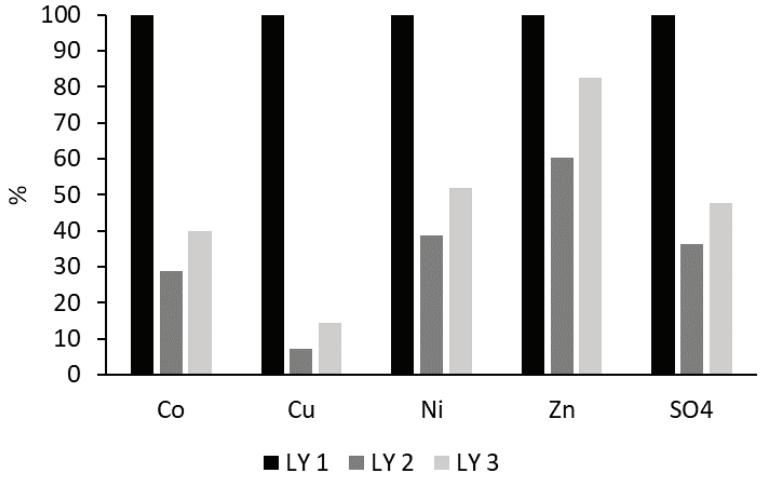


Figure 2 *The mobilities of the harmful elements Co, Cu, Ni, Zn and SO4 from the till covered lysimeters LY2 and LY3 compared with the uncovered LY1.*

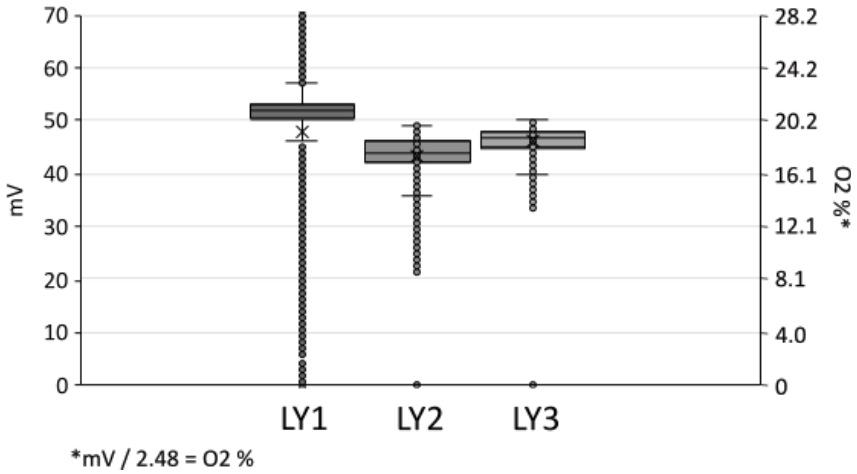


Figure 3 *O-sensor data from LY1-LY3. In LY1, the sensor was positioned above the lysimeter in atmospheric conditions, while in LY2 and LY3, the sensors were placed below the till cover. The O_2 %Is calculated assuming that the median LY1 sensor value of 51.8 mV represents the average atmospheric O_2 concentration of 20.9 %, which implies 2.48 mV per O_2 %.*

covered lysimeters is the lower amount of infiltrated water, rather than the decreased oxygen availability. Furthermore, in the case of the weathered waste rock material of the Särkiniemi mine, the previously accumulated secondary minerals and adsorbed metal(loid) concentrations most likely participate in sustaining acidic pH and elevated harmful element concentrations in the drainage (Kaasalainen *et al.* 2019), which decreases the significance of O2 reduction by the cover.

This study demonstrates that even a relatively thin (0.3 m) till layer can substantially reduce the mobility of harmful elements, primarily by decreasing the amount of infiltrating water. However, the efficiency of the till cover in reducing harmful element mobility varied depending on the specific element. Depending on closure objectives and impacts on the surrounding environment, the achieved reduction may not be sufficient, and more efficient cover layers

or additional mitigation measures might be needed. Indeed, such thin single-layer cover systems are not recommended for acid generating mine waste material (Garbarino *et al*. 2018, INAP 2017).

The findings of this study provide valuable insights into the effectiveness of till covers as a mitigation strategy for AMD, contributing to a broader understanding of sustainable mining practices and the development of more effective mine closure techniques. Since large quantities of natural till may be difficult to obtain for larger mine waste areas, future research should explore the potential of utilizing secondary materials and examine their long-term performance as alternative cover materials.

Conclusions

The results of this study indicate that even a relatively thin till layer (0.3 m) can substantially reduce the mobility of harmful elements. During the monitoring period from 2020 to 2021, the average reduction in element mobility was as follows: Cu mobility decreased by 86–93%, Co mobility by 60–71%, Ni mobility by 48–61%, SO4 mobility by 52–64%, and Zn mobility by 17–40%. The oxygen concentrations below the till cover were not substantially lower than atmospheric levels, suggesting that the primary factor in reducing harmful element mobility was the decreased water infiltration rather than the reduced oxygen availability.

While the results of this study contribute to our understanding of till covers as a mitigation strategy for AMD, it is essential to recognize that the achieved reduction in harmful element mobilities may not be sufficient for all closure objectives and environmental contexts. More efficient cover layers or additional mitigation measures may be required in some cases. Moreover, as obtaining large quantities of natural till for mine waste cover applications may be challenging, future research should explore the use of secondary materials and assess their long-term performance as alternative cover materials. Overall, this study offers valuable insights for the development of sustainable mining practices and the improvement of mine closure techniques.

References

Garbarino E, Orveillon G, Saveyn H, Barthe P, Eder P (2018) Best Available Techniques (BAT) Reference Document for the Management of Waste from Extractive Industriesin accordance with Directive 2006/21/EC, EUR 28963 EN, Publications Office of the European Union, Luxembourg, 2018, ISBN 978-92-79-77178-1, doi:10.2760/35297, JRC109657.

INAP (2017) Global Cover System Design – Technical Guidance Document. The International Network for Acid Prevention (INAP), November 2017.

Kaasalainen H, Lundberg P, Aiglsperger T, Alakangas L (2019) Impact of declining oxygen conditions on metal(loid) release from partially oxidized waste rock. Environmental Science and Pollution Research 26, 20712–20730, doi:10.1007/s11356-019-05115-z

Karlsson T, Räisänen ML, Lehtonen M, Alakangas L (2018) Comparison of static and mineralogical ARD prediction methods in the Nordic environment. Environmental Monitoring and Assessment 190:719, 11-25, doi:10.1007/s10661-018-7096-2

Karlsson T, Alakangas L, Kauppila PM, Räisänen ML (2021) A Test of Two Methods for Waste Rock Drainage Quality Prediction: Aqua Regia Extraction and Single-addition Net-acid Generation Test Leachate Analysis. Mine Water and the Environment, published online 21 May 2021, doi: 10.1007/s10230-021-00784-0

Kauppila PM (2023) Single soil layer, Mineclosure website, Geological Survey of Finland, accessed 5 April 2023, https://mineclosure.gtk.fi/single-soil-layer/

Lottermoser, BG (2010) Mine wastes: Characterization, treatment and environmental impacts (3rd ed.). Berlin, Springer-Verlag, 400 p.

Wilson GW, Barbour SL, Swanson D, O'Kane M (1995) Instrumentation and modelling for saturated/unsaturated performance of soil covers for acid generating waste rock. Hydrogéologie 4, pp. 99-108.

Flow and Baffle Configurations of Reactor and Settling Pond for Treatment of Mine Drainage

Duk-Min Kim[1], Dae-Gyu Im[2], Joon-Hak Lee[3], Mi-Sun Park[4]

[1]*Department of New Energy and Mining Engineering, Sangji University, Sangjidae-gil 83, Wonju, Gangwon-do, 26339, Republic of Korea, kdukmin8@sangji.ac.kr, ORCID 0000-0002-1537-6866*

[2]*Department of Earth and Environmental Sciences, Korea University, Anam-ro 145, Seongbuk-gu, Seoul, 02841, Republic of Korea, daegull1995@korea.ac.kr*

[3]*Korea Mine Rehabilitation and Mineral Resources Corporation, Hyeoksin-ro 199, Wonju, Gangwon-do, 26464, Republic of Korea, jun292@komir.or.kr*

[4]*Korea Mine Rehabilitation and Mineral Resources Corporation, Hyeoksin-ro 199, Wonju, Gangwon-do, 26464, Republic of Korea, mspark@komir.or.kr*

Abstract

This study assessed various flow configurations with baffles and weirs in substrate reactors and settling ponds on a bench- and pilot-scale. Also, required hydraulic heads for several types of substrate reactor were assessed to give the range of maximum allowable flow rate for several types of the reactor. If the hydraulic head difference is sufficiently high by pumping or the flow rate is sufficiently low, application of zigzag baffles in the longitudinal direction is highly encouraged in substrate reactors. Moreover, the installation of hanging baffles rather than zigzag baffles is recommended in settling ponds.

Keywords: Flow configuration, baffle, substrate reactor, settling pond, mine water treatment

Introduction

Efforts for the passive treatment of mine drainage have developed various reactors such as adsorption reactors, successive alkalinity producing system (SAPS), bioreactors, slag leach beds, and slag reactors (Ziemkiewicz 1998; Younger *et al*. 2002; Hamilton *et al*. 2007; Skousen *et al*. 2017; Kim *et al*. 2022a, b). The flow configuration of reactors is generally vertical, including column reactors and vertical flow ponds. Improvements in the shape and flow configuration can increase the actual residence time and decrease the dead zone in the reactor and settling pond, which can reduce the required area and construction cost for the facilities.

The objectives of this study are to 1) improve the shape and flow configurations of a reactor to treat low-flow contaminated water which includes longitudinal and latitudinal directions of baffles and 2) suggest a more efficient baffle configuration for settling ponds between zigzag and hanging baffles. To achieve these objectives, this study assessed various flow configurations with baffles and weirs in substrate reactors and settling ponds on a bench- and pilot-scale using results of treatment efficiencies. Also, required hydraulic heads for several types of substrate reactor were assessed to give the range of maximum allowable flow rate for each type of the reactor.

Methods

Characteristics of substrate

The slag reactors used in this study contained 40% steelmaking slag and 60% limestone in a volumetric percentage. The slag and limestone used in this study had sizes of 2–5 mm and 2–3 cm, respectively. The slag was generated in a basic oxygen furnace and contained 36.5% CaO and 40.9% Fe_2O_3, as demonstrated by x-ray fluorescence spectrometry.

Pilot-scale experiments

Three types of pilot-scale slag reactors were installed and operated at the same time to treat adit drainage from the abandoned Cheongsan coal mine in South Korea. The slag reactor can increase the pH and decrease

the Mn concentration in mine drainage owing to the generation of OH- and precipitation of Mn carbonates and/or (oxyhydr)oxides (Kim *et al.* 2022a, b). The reactor types were baffle, weir, and column. All reactors had a length-to-width ratio of 3:1. In the baffle-type slag reactor, five zigzag baffles were installed in the longitudinal direction, and auxiliary hanging baffles were installed (Fig. 1). Zigzag-shaped weirs were installed at the inflow of the weir-type slag reactor to distribute the flow lines laterally, and the outflow part was cone shaped to evenly collect the flow lines. The flow direction of the column-type slag reactor was downward, and the inflow part had a perforated circular plate to distribute the flow lines laterally.

A pilot-scale rectangular settling pond was installed to reduce the suspended solids (SS) in the adit drainage. It had two types of baffle configurations that could be attached and detached: zigzag baffles and hanging baffles (Fig. 2). There were four zigzag baffles, and the baffle direction was longitudinal. The depth of the hanging baffles was 40% (0.28 m) of the water depth (0.7 m), and they were located at 1/3 and 2/3 of the length of the pond because these conditions were reported to be efficient (Yoon *et al.* 1999; MIRECO 2011). To laterally distribute flow lines in the settling pond with hanging baffles, weirs were installed at the inflow and outflow.

Results and discussion

Treatment efficiencies of various flow configurations at pilot-scale slag reactors

Mn treatment efficiencies of weir-type, baffle-type, and column-type slag reactors were assessed on a pilot scale to decrease Mn from 3.8–4.6 mg L^{-1}. The residence time required to decrease the Mn concentrations in the reactor with baffles was evidently lower than that in the reactor with a weir (Fig. 3; Kim *et al.* 2022c). For example, the maximum residence times to fulfill the effluent standard of Mn (2 mg L^{-1}) were inferred by each regression line of four samples at the boundary of maximum residence times for the weir-type and baffle-type reactors. The estimated maximum

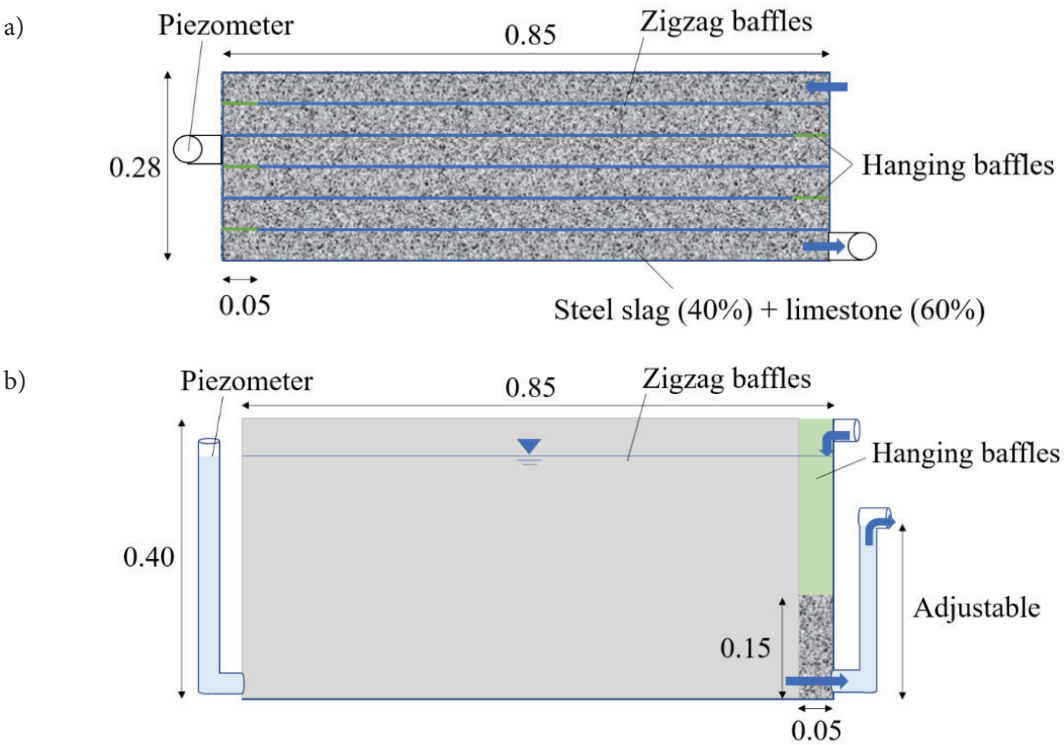


Figure 1 *(a) Plan view and (b) cross-section of baffle-type slag reactor. The unit of dimension is m.*

residence times with respect to 2 mg L^{-1} of Mn were ~40 min and ~100 min in the baffle-type and weir-type reactors, respectively, which resulted in an approximate ratio of 2.5. This difference indicates that the baffle-type reactor can increase the actual residence time by ~2.5 times from the weir-type reactor. Moreover, the column-type reactor exhibited Mn removal efficiencies comparable to those of the weir-type reactor.

Consideration of hydraulic head and suggestion of flow configuration

The required hydraulic heads to determine the allowed maximum flow rates were assessed in weir-type, baffle-type, and column-type reactors. For each type of reactor, the maximum allowable flow rates according to the difference in hydraulic head and hydraulic conductivity are shown in Fig. 4 (Kim *et al.* 2022c). The number of zigzag baffles was assumed to be two. In Fig. 4a, the hydraulic conductivity was assumed to be 0.03 cm s-1, which was measured in the slag reactors after ~1 yr of operation. The differences in the hydraulic head were assumed to be the height of the substrate (1.5 m for weir-type and baffle-type reactors and 2.5 m for the column-type reactor) in Fig. 4b, and they were assumed to be 10 m for the case of pumping for all types in Fig. 4c.

Pilot-scale experimental results and suggestions of baffle configurations in the settling pond

The settling pond was operated with zigzag baffles and hanging baffles. The treatment efficiencies of the SS for each baffle configuration were compared. To decrease SS to 21–22 mg L^{-1} with removal efficiencies of 57%–61%, the zigzag baffle configuration required residence times of 72–81 h, whereas the hanging baffle configuration required a residence time of 41–50 h (51–69%) to

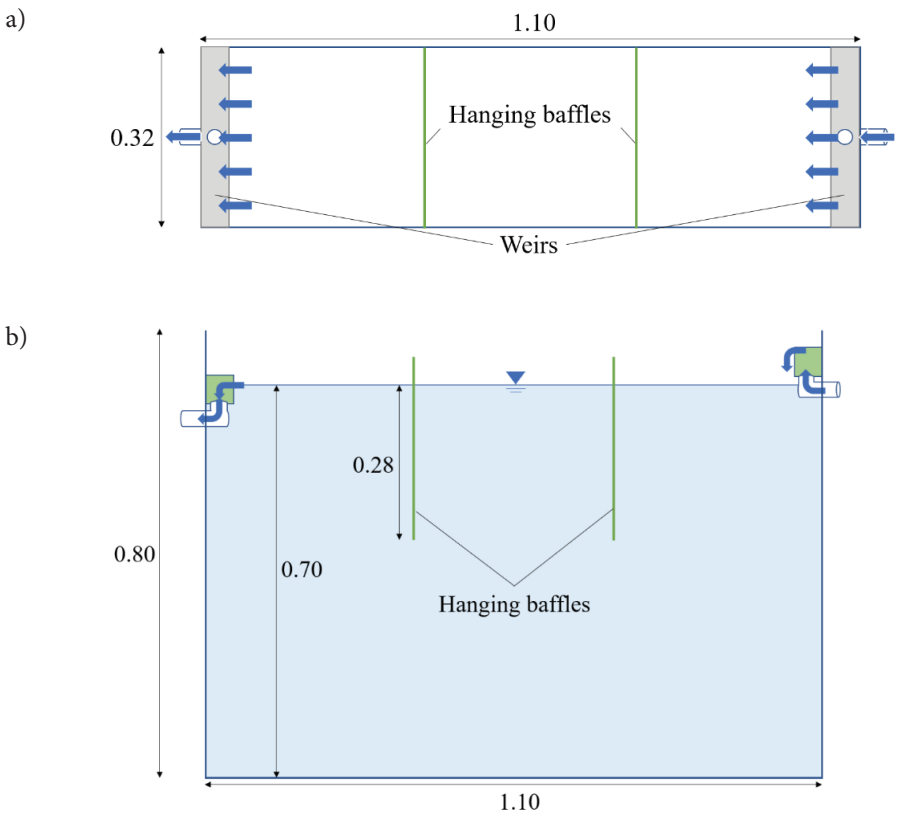


Figure 2 *(a) Plan view and (b) cross-section of the pilot-scale settling pond with hanging baffles. The unit of dimension is m.*

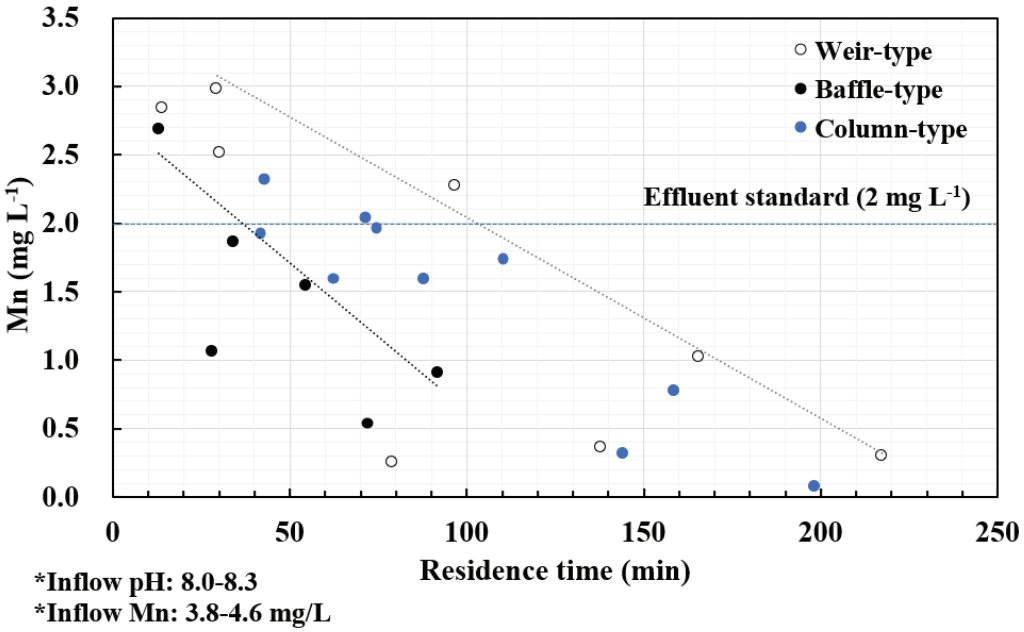


Figure 3 Relationship between Mn concentrations and residence time for weir-type, baffle-type, and column-type slag reactors in pilot scale. Each regression line was derived from four samples at the boundary of maximum residence times for the weir-type and baffle-type reactors (Kim et al. 2022c)

decrease SS to 18–21 mg L^{-1} with removal efficiencies of 64%–69% (Table 1; Kim *et al.* 2022c). Thus, the application of hanging baffles exhibited higher SS treatment efficiencies than those of zigzag baffles.

Although the zigzag baffles could efficiently utilize the horizontal area of the pond, they could not help to utilize the lower part of the settling pond. In contrast, the hanging baffles could induce the flow utilizing the lower part. Moreover, the weir could be installed at the inflow and outflow when the hanging baffles were applied, which could distribute the flow to facilitate efficient utilization of the horizontal area of the pond, as in the case of the weir-type slag reactor. Notably, for the treatment of adit drainage, because the surface flow is likely to occur in winter because the adit drainage at the inflow of the pond is generally warmer and lighter than the stagnant water in the settling pond, hanging baffles to reduce the surface flow are necessary. Therefore, the application of hanging baffles is suggested over that of zigzag baffles in settling ponds.

Conclusions

Efficient flow and baffle configurations of reactors and settling ponds for the treatment of low-flow water were studied. The pilot-scale baffle-type reactor with zigzag baffles in the longitudinal direction exhibited the highest treatment efficiencies among the baffle-type, weir-type, and column-type reactors. Nevertheless, the required hydraulic head is a critical constraint for the application of various types of reactors. If the hydraulic head difference is sufficiently high by pumping or the flow rate is sufficiently low, application of zigzag baffles in the longitudinal direction is highly encouraged in substrate reactors. Furthermore, the pilot-scale experiments with a settling pond with zigzag baffles and hanging baffles indicated that the prevention of surface flow using the hanging baffles reduced the required residence times to 51%–69% of those at the pond with the zigzag baffles. This difference suggests that the installation of hanging baffles rather than zigzag baffles is recommended in settling ponds in passive and semi-active

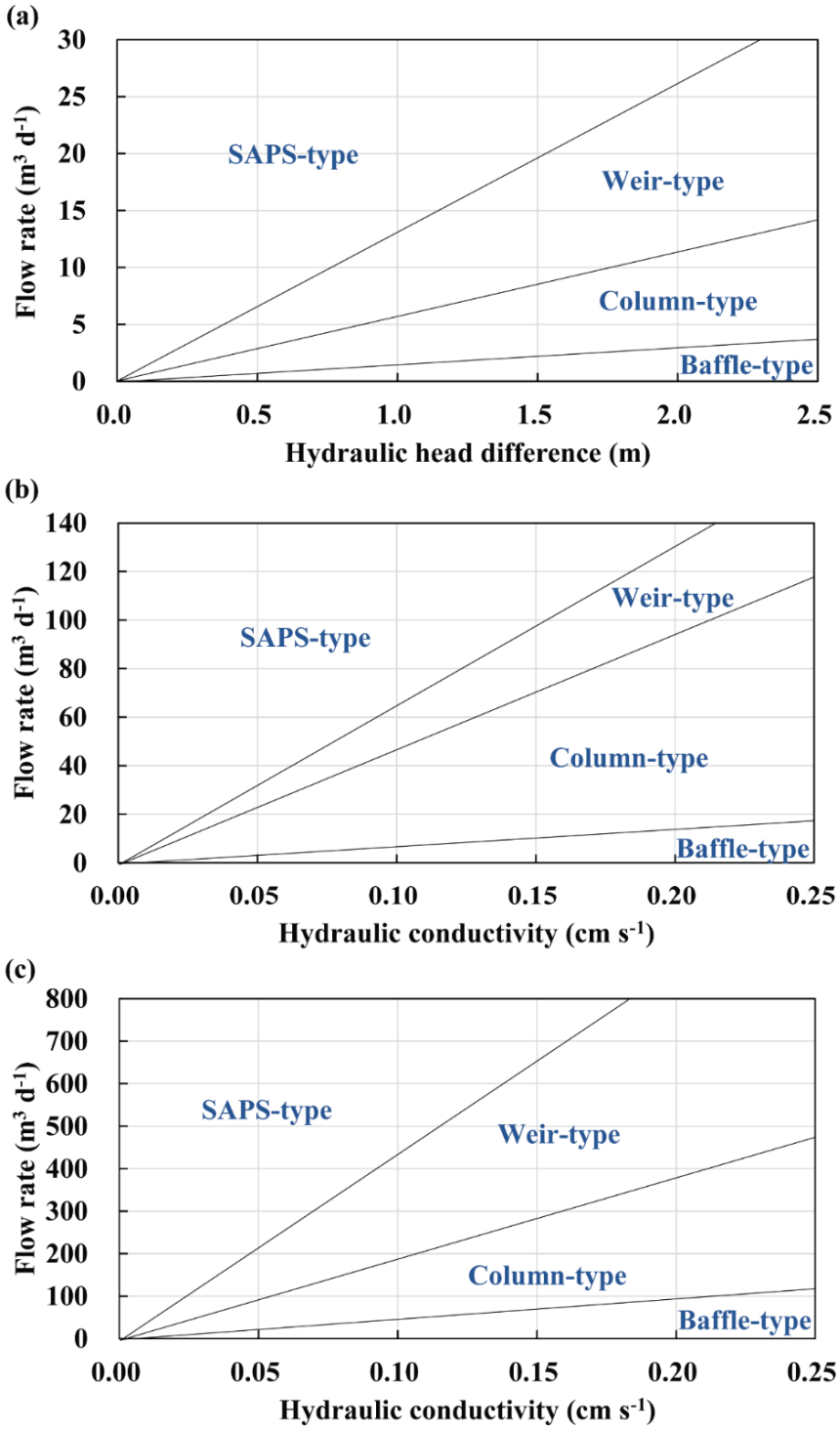


Figure 4 *Applicable types of reactors according to flow rate and (a) difference in hydraulic head and (b, c) hydraulic conductivity (Kim et al. 2022c). The hydraulic conductivity in (a) was assumed to be 0.03 cm s^{-1}. Differences in the hydraulic head were assumed to be 1.5 m for the weir-type and baffle-type reactors and 2.5 m for the column-type reactor in (b) and were assumed to be 10 m in (c).*

Table 1 Treatment efficiencies of SS for application of zigzag baffles and hanging baffles in pilot-scale settling pond (Kim et al. 2022c).

Baffle configuration	Residence time (d)	SS Inflow (mg L^{-1})	Outflow	Treatment efficiency
Hanging baffle	41	67	21	69%
	50	50	18	64%
Zigzag baffle	81	53	21	61%
	72	51	22	57%

treatment facilities. The increased efficiency of the suggested reactors and settling ponds will decrease the required area and cost of construction.

Acknowledgements

This study was partly supported by the R&D projects of the Korea Mine Rehabilitation and Mineral Resources Corporation (KOMIR), South Korea (2020–2021; 2022–2023), and the completion of this work was partly supported by Korea Environmental Industry and Technology Institute (KEITI) through the project (Integrated environmental forensic approaches to trace source and pathways of subsurface contaminants) funded by Korea Ministry of Environment (MOE) (2021002440003). The authors gratefully acknowledge the contributions of Mr. Woong-Lim Lim and Ms. Hye-Lim Kwon at Sangji University for conducting the experiments.

References

Hamilton J, Gue J, Socotch, C (2007) The use of steel slag in passive treatment design for AMD discharge in the Huff Run watershed restoration, in: Proceedings of the 24th ASMR. 272–282.

Kim DM, Park HS, Hong JH, Lee, JH, (2022a) Assessing pilot-scale treatment facilities with steel slag-limestone reactors to remove Mn from mine drainage. Mine Water Environ. 41(2): 402–414

Kim DM, Oh YS, Park HS, Kim DK, Lee JH (2022b) Steel slag-limestone reactor for Mn removal with tolerance to Fe: experiments and mechanisms. J. Environ. Chem. Eng. 10(3): 107468. https://doi.org/10.1016/j.jece.2022.107468

Kim DM, Im DG, Lee JH (2022c) Flow and baffle configurations of settling pond and low-flow reactor for water treatment. J. Water Process Eng. 49: 103173. https://doi.org/10.1016/j.jwpe.2022.103173

MIRECO (2011) Technology Development for Semi-active Treatment of Mine Drainage, Technology Report 2011-129, Korea Mine Reclamation Corporation (MIRECO), Seoul, Republic of Korea (in Korean).

Skousen J, Zipper CE, Rose A, Ziemkiewicz PF, Nairn R, McDonald LM, Kleinmann RL, 2017. Review of passive systems for acid mine drainage treatment. Mine Water Environ. 36: 133–153. https://doi.org/10.1007/s10230-016-0417-1

Yoon TH, Lee SO (2000) Hydraulic behavior and removal efficiency of settling tanks. KSCE J. Civ. Eng. 4: 53–57. https://doi.org/10.1007/BF02829174

Younger PL, Banwart SA, Hedin RS (2002) Mine Water: Hydrology, Pollution, Remediation, Kluwer Academic Publishers, Dordrecht, Netherlands. https://doi.org/10.1007/978-94-010-0610-1

Ziemkiewicz PF (1998) Steel slag: applications for AMD control, in: Proceedings of the 1998 Conference on Hazardous Waste Research, 44–62

Field Trial of Iron Hydroxide Sludge for Revegetation and Improved Productivity of Structurally Weak Soils

K. Kunze[1], O. Blumenstein[2]

[1]*Lausitzer und Mitteldeutsche Bergbau-Verwaltungsgesellschaft (LMBV), Knappenstr. 1, 01968 Senftenberg, Germany, Katja.Kunze@LMBV.de*

[2]*InterEnviroCon GmbH, Spitzweggasse 2, 14482 Potsdam, Germany, oblustei@InterEnviroCon.de*

Abstract

In Eastern Germany the majority of the open-cast mines in the former GDR that could not be privatized were taken over by the federal government and the lignite states (LMBV) with the aim of rehabilitating them. In this area iron hydroxide sludge (IHS) is produced as a result of diffuse groundwater inflow into watercourses. This sludge is removed regularly from the riverbeds as a part of remedial action. In addition to iron , the sludge contains high concentrations of organic compounds.

The suitability of this IHS for improving the productivity of overburden soils was tested in a three-year field trial. To date, IHS appears to be suitable for soil improvement, both physically by facilitating storage of rainwater and biochemically through availability of minerals and nutrients for vegetation. There is a clear improvement in the growth conditions of the cultures tested.

Field trial results presented here demonstrate, that soil supplements from IHS can improve the fertility of structurally weak overburden soils if environmental regulations can be met. Using the sludge as a soil amendment reduces waste and supports sustainable, circular economy.

Keywords: Iron Hydroxide Sludge, Soil Productivity, Sustainability

Introduction

The Lusatian and Central German Mining Administration Company (LMBV) is responsible for remediation of former lignite mining legacy sites in Lusatia / Eastern Germany (Bund 2022). This requires water management, especially the replenishment of ground water deficits, creation of safe pit lakes, their connection to the public water system, and the improvement of water quality. Large amounts of iron hydroxide sludges (IHS) are produced, both in water treatment plants and through diffuse groundwater inflow into watercourses, where reduced iron is oxidized and precipitates as oxyhydroxide minerals. In addition to high iron content, IHS from riverbeds contains high concentrations of organic compounds. LMBV is working to recycle these sludges as much as possible.

When the post-mining landscapes in Lusatia are rehabilitated, large dump areas made of sandy overburden material remain, without fertile soil horizon. Revegetation in preparation for subsequent agricultural and forestry use requires the addition of fertilizer and lime. Here, we report the results of a pilot project which examined whether sludge collected during clearing of watercourses would be suitable for improvement of structurally weak overburden soils.

Suitability of iron hydroxide sludge

The occurrence of iron compounds in soils is natural. Iron oxide compounds directly influence the fertility of soil. Plants meet their metabolic iron requirements using ferrous and ferric iron organic acid complexes, (fulvic and humic acids) and using organic substances in the root area. Beyond being a nutrient, iron contributes to soil improvement forming amorphous iron minerals with a large specific surface area that can store large amounts of nutrients (UPT 2016). Further, iron precipitated from pore water within the soil acts as a mineral cement (concretion), and therefore reduces erosion.

Legal regulations

The Circular Economy Act (Bund 2012) must be observed when dealing with IHS. This requires that materials should be avoided if possible, before recycling, subaqueous disposal in post-mining lakes, and placement in a surface dump can be considered. The aim is to conserve natural resources and manage waste in an environmentally friendly manner. When using IHS to improve the productivity of soil, the applicable statutory provisions of the Federal Soil Protection Act (Bund 1998) and waste legislation must be observed.

Before further use, dredged material from the clearing of riverbeds must be characterized with respect to pollutant and physical properties. This step is also essential due to the strong spatial heterogeneity of the IHS and the seasonal material dynamics of many state variables, for example TOC. This ensures that its application to the soil does not negatively affect the soil quality. Prior to this field test, characterization analyses and ecotoxicological tests were carried out on IHS from various origins. Risks were assessed based on these data to chose suitable IHS.

Not all IHS occurring in the area regulated by the LMBV can be used for soil improvement. In particular, IHS with increased arsenic concentrations (i.e. > 20 mg/kg) were excluded from this study. The ecotoxicological tests on the living conditions of the soil organisms showed a) no negative effects with an admixture of 12.5% IHS, and b) no lasting negative effects with an admixture of 20% IHS. Only IHS met soil protection law and ecotoxicology requirements was used for the test.

Conceptual design of field test

The effect of IHS was tested both on trees and on a grass-herb mixture. An organic component (K3) was used in the test for comparison purposes. Admixture proportions of 12.5 or 20% IHS and 5% organic component (K3) in various combinations were compared to an untreated test area as described in figure 1.

A typical regional herb-grass mixture was chosen that is commonly used in re-cultivation work in Lusatia. This consists of perennial rye, perennial lupine (alfalfa), brown mustard, radish and four clover variations. In tree trials, the typical trees birch, oak and pine were used.

The field tests were conducted at the former Spreetal opencast mine (Saxony, Germany) within a 30,000 m² test area filled with quaternary silica sand. The amended area was compacted and levelled prior to planting.

Methods

Prior to the addition of IHS, the test areas were delineated and the existing substrate was analysed physically and chemically.

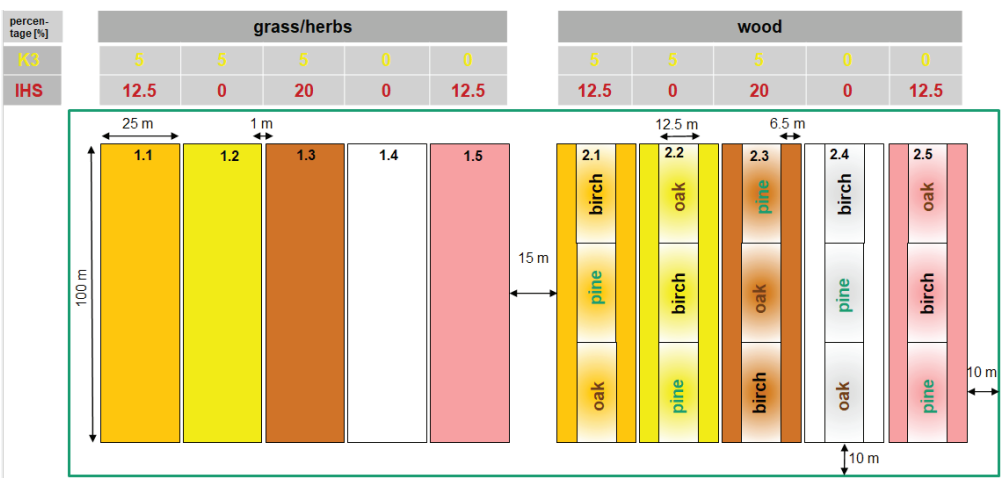


Figure 1 Field trial experimental design showing geometry, amendment percentages and type of planted vegetation

The supplied IHS was screened before it was incorporated into the soil to remove macroscopically visible foreign matter (e.g., wood debris, coarse rock, etc.) The existing substrate was loosened and soil supplements were applied in the areas to a depth of 0.3 m for the grass-herb mixtureand to a depth of 0.75 m in the areas planting with trees.

As shown in Figure 1, specific areas of the test field were planted with different species: 900 Silver Birch trees (*Betula pendula*) were planted. These pioneer trees are fast-growing and can establish on nutrient-poor, acidic soils. The Common Oak (*Quercus robur*) was established with 1,200 specimens. Widespread in Central Europe, it shows good growth performance on nutrient-poor sandy soils, especially when young. 2,500 Scots Pines (*Pinus sylvestris*) were planted as conifers. This species is also relatively undemanding and therefore also suitable for nutrient-poor sandy soils.

Seeding and planting took place in May 2020. As the spring of 2020 was very dry and there was no water in the ground from the snowmelt, all test areas were watered (approximately 3 mm) before seeding and planting. Further irrigation and fertilization of the test field was deliberately avoided in order to collect data under the prevailing natural conditions.

Separation foils were placed between the individual test areas to reduce erosive displacement of substrate between the individual testareas as well as the unwanted migration of plants from the grass-herb mixture during the field trial. A protective fence was erected to prevent browsing damage with accessibility ensured via a wide gate. An observation well was installed in the outflow of the test area and regularly monitored to prove that the seepage water discharged to groundwater is harmless.

Monitoring

In the three years between 2020 and 2022, the growth of the trees, grasses and herbs was monitored several times a year, especially at the beginning and end of the vegetative growth period. The growth height and the degree of coverage were examined on site on the test areas with grass-herb mixture. The above-ground phytomass and dry matter were determined in a laboratory by weighing and drying and weighing (fig. 2).

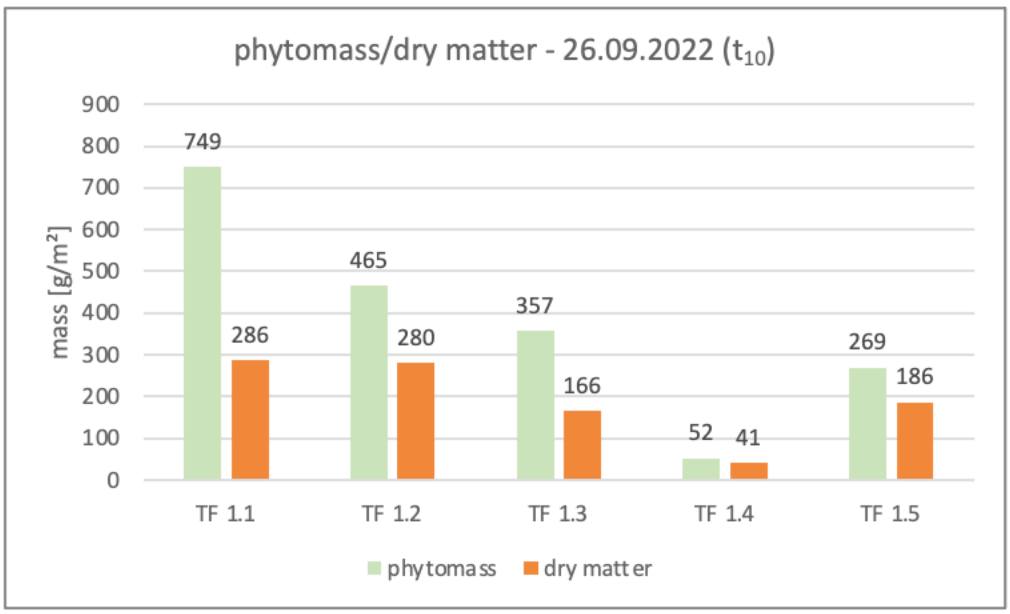


Figure 2 *Grass and herb above-ground phytomass 09/2022 (IEC 2022)*



Figure 3 *Birch growth height and trunk diameter 09/2022 (IEC 2022)*

Twenty-four randomly selected trees were monitored per planting unit. The growth height and trunk diameter were measured (fig. 3), and vitality was determined using a tree growth method. Samples of solids and water were analyzed from all test areas in order to record possible changes in the soil chemistry. In addition, meteorological conditions were recorded.

Results and discussion

Amendment with IHS added iron, manganese, and calcium to the soil. The arsenic content in the IHS selected for the experiment was significantly lower than the geogenic concentrations in the dump sands, which were generally less than 5 mg/kg. The IHS amendment therefore did not increase arsenic soil concentration. In addition, no increase of metals such as cadmium, chromium, nickel, mercury, and lead was determined through the application of IHS, shown by chemical analyses. Except for the untreated sub-areas (TF1.4 and 2.4), the measured pH values in the soil fluctuated around 6.0, ensuring a good nutrient supply under slightly acidic conditions.

To date, the pilot test shows that IHS is suitable for soil improvement, both physically through better storage of rainwater and biochemically through storage and improved availability of nutrients for vegetation.

The improvement of the soil structure and the fertility of the soil was proven with monitoring: Both the grass-herb mixture and the tree plantings grew significantly better with IHS input compared to the untreated subfields. These results were achieved despite additional stress of above-average temperatures and below-average precipitation during the three growing seasons.

The value of the IHS as a water-storing substrate is particularly evident from the degree of coverage (fig. 4 to 7). No negative change in water quality of the groundwater is evident in the data. The groundwater quality has been the same. Optimum growth conditions were achieved for grasses and herbs with an admixture of 5% by volume of the organic component (K3), with the addition of either 20% or 12.5% by volume IHS. The best growth results were achieved for the woody plants with 12.5% by volume IHS amendment and 5% by volume of organic component (K3). After three years, the dry matter of the grass-herb mixture on the treated test areas (TF 1.1 – 1.3 and 1.5) is at least 4 times higher than on the untreated reference area (TF

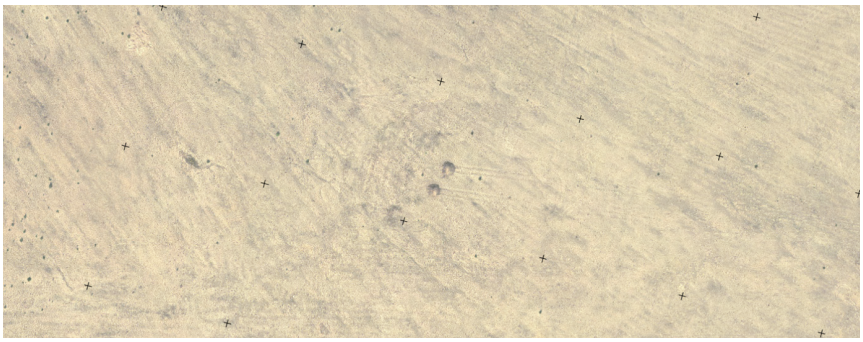


Figure 4 *Aerial photo – test field (300 x 100m) before the start of the test (10/2019)*



Figure 5 *Aerial photo – test field (300 x 100m) after the start of the test (06/2020)*

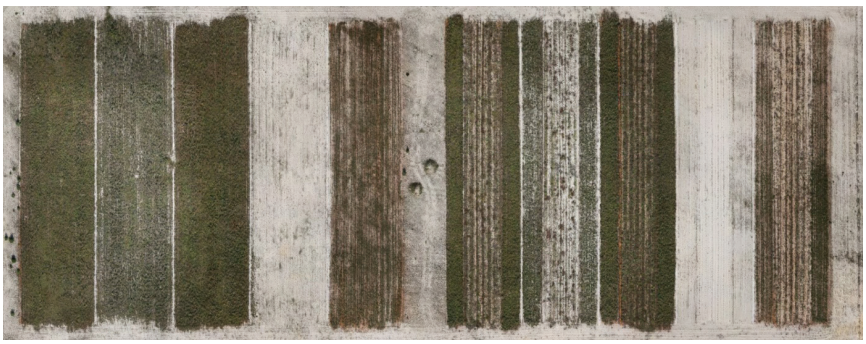


Figure 6 *Aerial photo – test field (300 x 100m) after two growing season (09/2021)*



Figure 7 *Aerial photo – test field (300 x 100m) after three growing seasons (10/2022)*



Figure 8 *Oak on untreated test area 2.4 (left) and test area 2.5 (right) treated with IHS (08/2022)*

1.4) (fig. 2). After three vegetation periods, the trunk diameter and growth height of the birches on the treated test area (TF 2.1 – 2.3 and 2.5) are at least twice as high as those on the untreated test area.

Long-term predictions for the development of woody plants are still hypothetical, because equilibrium between development, degradation and conversion processes of material and energetic resources between vegetation and soil can only occur at climax stage of the stands. However, it is expected that the future development of the trees will be comparatively better on the areas treated with IHS, as water and the nutrient cycling conditions have improved equally. Monitoring will be continued on the test area for long-term observations. This approach offers both economic and ecological value in terms of sustainability. As a next step, the LMBV is planning a large-scale test to improve the productivity of dump soils on an area of around 500,000 m^2 in Lusatia, with subsequent use for agriculture and forestry.

Conclusion

A three year field trial has demonstrated that the fertility-determining parameters of quaternary overburden sands improved following the addition of IHS and organic amendment K3. In addition to an improved storage and availability of nutrients for vegetation, physical properties were enhanced through better storage of rainwater. As such, IHS, commonly considered as waste material, can be utilized in the sense of circular economy and sustainability.

References

Bundesrepublik Deutschland, Land Brandenburg, Freistaat Sachsen, Land Sachsen-Anhalt, Freistaat Thüringen (09/2022) Sechstes ergänzendes Verwaltungsabkommen zum Verwaltungsabkommen über die Regelung der Finanzierung der ökologischen Altlasten (VA Altlastenfinanzierung) in der Fassung vom 10. Januar 1995 über die Finanzierung der Braunkohlesanierung in den Jahren 2023 bis 2027 (VA VII Braunkohlesanierung)

Bundesrepublik Deutschland (02/2012) Gesetz zur Förderung der Kreislaufwirtschaft und Sicherung der umweltverträglichen Bewirtschaftung von Abfällen (Kreislaufwirtschaftsgesetz KrWG)

Bundesrepubilk Deutschland (03/1998) Gesetz zum Schutz vor schädlichen Bodenveränderungen und zur Sanierung von Altlasten (BBodSchG)

UP Transfer GmbH an der Universität Potsdam (12/2016) Argumentationspapier - Genehmigungsfähigkeit der Nutzung von Eisenhydroxidschlämmen zur Bodenverbesserung auf landwirtschaftlich genutzten Kippenböden

InterEnviroCon GmbH (12/2021) Planung, Durchführung und Auswertung des Feldversuches zur Verwertung von Eisenhydroxidschlämmen zur Nutzung für Begrünungsmaßnahmen und die Verbesserung der Ertragsfähigkeit strukturschwacher Böden - Abschlussbericht nach 2 Vegetationsperioden

InterEnviroCon GmbH (12/2022) Planung, Durchführung und Auswertung des Feldversuches zur Verwertung von Eisenhydroxidschlämmen zur Nutzung für Begrünungsmaßnahmen und die Verbesserung der Ertragsfähigkeit strukturschwacher Böden – Weiterführender Bericht nach 3 Vegetationsperioden

Acid Mine Drainage from Epithermal Gold Deposits: Characterization and Classifying for Various Rock Types

Ginting Jalu Kusuma, Abie Badhurahman, Rudy Sayoga Gautama, Sendy Dwiki, Salmawati

Department of Mining Engineering, Faculty of Mining and Petroleum Engineering, Bandung Institute of Technology, Indonesia

Abstract

Epithermal gold deposits, both low-sulfidation and high-sulfidation, are the main gold deposits in Indonesia. For mining and metallurgical purposes, rocks from epithermal gold deposits are classified based on alteration, and lithology or rock types/lithotypes. This study aims to ascertain the possibility of acid mine drainage classification using rock types applied in mining companies. Classification of acid mine drainage attributed to the existing individual rock types will be beneficial for acid mine drainage and waste management. Characterization of waste rock in epithermal deposits which are based on rock types (alteration, metallurgical extractability and lithology) is associated with the geochemical classification of acid mine drainage. Alunite as a product of alteration processes gives a false indication of acid mine drainage classification, thus alunite-rich waste rock needs to be classified separately.

Keywords: Epithermal Deposits, Alteration, Classification, Acid Mine Drainage, Alunite

Introduction

Epithermal gold deposits, both low-sulfidation and high-sulfidation, are the main gold deposits in Indonesia. In Indonesia, epithermal deposits are related to major Cenozoic magmatic arcs, which are related to tectonic activities of plate movements. There are five major magmatic arcs related to this type of deposit, i.e., Sunda-Banda Arc, Kalimantan Arc, Sulawesi Arc, Halmahera Arc and Papua Arc, as shown in the following figure.

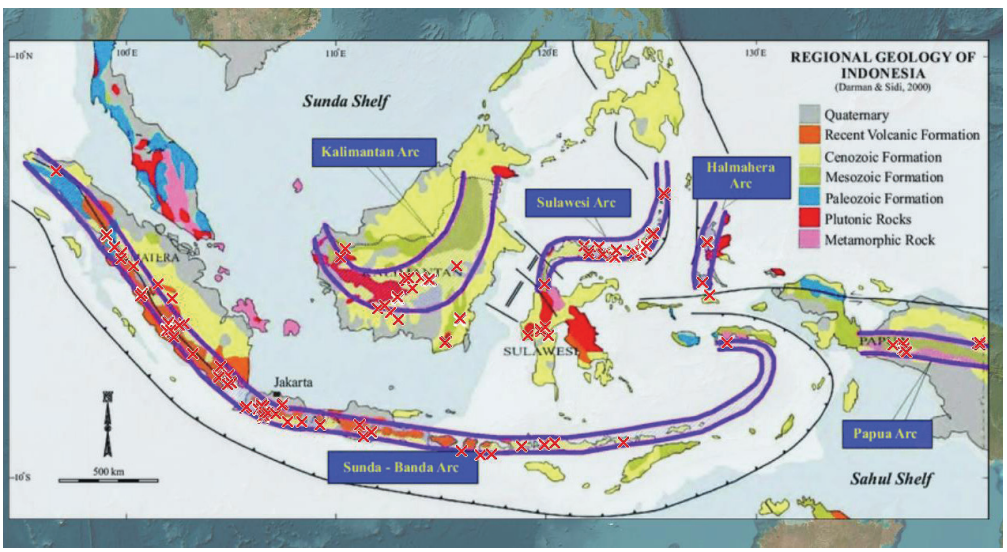


Figure 1 Geology of Indonesia, including Major Cenozoic Magmatic Arc and Primary Gold Deposits (denotes by red × marks). Modified from Darman & Sidi, 2000

Epithermal gold deposits are formed as a result of interaction between hydrothermal liquids with surrounding rocks producing different minerals called mineral alteration and assemblages. Various minerals can be deposited in the epithermal system, mainly regulated by the pH of the hydrothermal solution and temperature, as explained in the following figure.

Alteration or mineralogical and textural changes in host rock are the results of reactions between host rock and hydrothermal solutions deposited by various minerals such as phyllosilicates including clay minerals, alunite and the most important mineral in acid mine drainage formation i.e., pyrite. Jarosite and alunite as sulfate minerals are at a lower temperature in a high-sulphidation epithermal system. These minerals are also observed as secondary precipitates or minerals from acid mine drainage generation in a broader temperature condition. On the other hand, pyrite occurs at all temperatures and in acidic to neutral epithermal deposition (epithermal high sulphidation – epithermal low sulphidation). Calcite as a neutralizing mineral is also found in alkaline depositional environments at all temperatures. Mineral deposition processes are associated with mine drainage formation and their geochemical characterization. Management of acid mine drainage is complex and problematic not only because the occurrences of pyrite vary in different rock types, but also other minerals related to acid mine drainage are deposited differently.

For mining and metallurgical purposes, rocks from epithermal gold deposits are classified based on alteration, and lithology. Oxidation states related to metallurgical extractability, the higher oxidation types (completely oxidized), the easier the leaching process of the material, since most sulphides are already 'oxidized'. Alteration related to the changes of aluminosilicates into other forms of aluminosilicates, i.e., micas and clay minerals. Lithology is related to major mineral constituents and the texture of these minerals.

This study aims to ascertain the possibility of acid mine drainage classification using rock types applied in mining companies. Classification of acid mine drainage attributed to the existing individual rock types will be beneficial for remediation of acid mine drainage and for waste management. Samples of waste rocks from different epithermal deposits and various rock types in

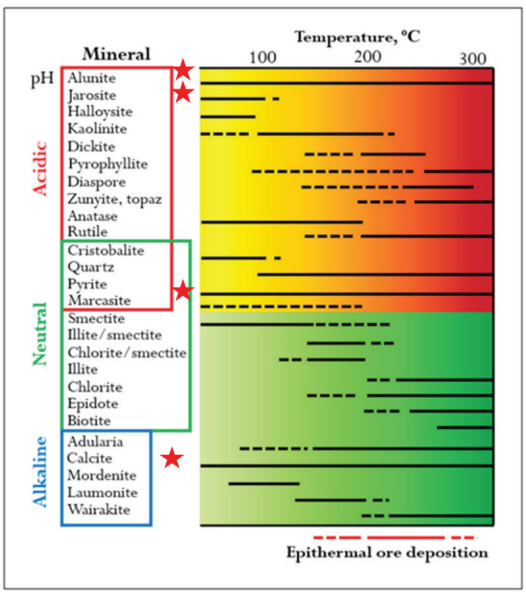


Figure 2 *Mineral Stability at various conditions of temperature and pH at epithermal deposition. Minerals related to acid mine drainage are marked by red stars. (Hedenquist et.al., 1996)*

Table 1 Sample Description

Sample ID	Lithology	Alteration	Oxidation	Notes
Sample 1	Brecciated Diatreme	SM (Silica Massive)	Moderately Oxidized	High Alunite
Sample 2	Brecciated Diatreme	AA (Advance Argillic)	Moderately Oxidized	High Alunite
Sample 3	Vulcanic-Dacitic	SM (Silica Massive)	Completely Oxidized	High Alunite
Sample 4	Vulcanic-Dacitic	AR (Argillic)	Completely Oxidized	-
Sample 5	Vulcanic-Dacitic	AR(Argillic)	Fresh/Unoxidized	-
Sample 6	Vulcanic-Dacitic	AA (Advance Argillic)	Completely Oxidized	-
Sample 7	Diatreme	AA (Advance Argillic)	Fresh/Unoxidized	-

Indonesia are characterized using static tests, mineralogical and elemental tests and kinetic tests using the free draining column leach test (FDCLT) method in the laboratory

Methods

Samples

Selected samples are taken from different epithermal gold deposits of various magmatic arcs, mostly from mines located in the Sunda-Banda Arc and Sulawesi Arc, which are tested in the Mining Environmental Laboratory, Institut Teknologi Bandung in the period of the year 2014 – 2021.

Rock types as previously described are lithology (2 classes: diatreme/brecciated diatreme and volcanic-dacitic rocks), alteration (3 classes: silica massive, advanced argillic and argillic) and oxidation states (fresh, moderately oxidized, completely oxidized). Samples 1 – 3 are identified as high-alunite samples since alunite is detected for a fraction of more than 2% in those samples based on UV-VIS-NIR Spectroscopy, XRD and XRF test results. Alunite is usually found in samples from silicic (silica massive mostly) and advanced argillic alteration.

Testing Methods

Static tests based on AMIRA 2002 (adopted in SNI Indonesian National Standards No. 7742:2021) and kinetic tests using the free draining column leach test (FDCLT) method were performed for all samples. Kinetic test runs for 100 days with different wet-dry cycles (initiated by daily spraying then 3 days spraying and weekly spraying). Water used for the kinetic test was deionized water (pH ~7.00 and TDS < 1mg/L).

Result and discussion

Static Test results

The static test results for all 7 samples are shown in the table below:

Table 2 Static Test Results

Sample ID	pH paste	NAG Test			Acid-Base Accounting					Geochemical Class.
		NAG pH	NAG pH= 4.50	NAG pH= 7.-00	TS	MPA	ANC	NAPP	NPR	
			kg H_2SO_4/ton		%		kg H_2SO_4/ton			
Sample 1	6.76	4.89	<0.5	2.7	4.95	151.59	<0.5	151.59	0	UC
Sample 2	7.13	4.50	<0.5	3.6	3.9	119.44	<0.5	119.44	0	UC
Sample 3	6.5	4.77	<0.5	10.5	3.75	114.84	<0.5	114.84	0	UC
Sample 4	5.04	5.19	<0.5	12.7	0.11	3.37	<0.5	3.37	0	UC
Sample 5	4.78	2.88	10.3	15.4	4.05	124.03	<0.5	124.03	0	**PAF**
Sample 6	5.77	5.30	<0.5	13.7	0.28	8.58	<0.5	8.58	0	UC
Sample 7	4.04	2.23	79.9	91	4.32	132.3	<0.5	132.3	0	**PAF**

Note: NAG=net acid generating, TS=total sulphur; MPA=Maximum Potency Acidity; ANC=Acid Neutralizing Capacity; NAPP=Net Acid Producing Potency, NPR=Neutralizing Potency Potential; UC=uncertain; PAF=potentially acid-forming.

From static test results, all samples from the alunite group are characterized as uncertain and the MPA value exceeds 110 kg H_2SO_4/ton. Sample 4 and Sample 6 are characterized as uncertain, yet MPA values are less than 5 kg H_2SO_4/ton and NAG pH value > 5.00. Sample 5 and Sample 7 are categorized as potentially acid-forming with NAG value < 3.00 and MPA > 120 kg H_2SO_4/ton

Kinetic Test Results

Kinetic test results, i.e., leachates pH values for test running of 100 days are shown in the following figures (figure 3 for Samples 1 – Samples 4 and Figure 4 for Samples 5 – Samples 6).

Samples 1, 2 and 3 which are grouped as alunite group samples produced slightly acid leachates during the kinetic test runs (pH leachates > 4.00). On the other hand, sample 4 and sample 6 which are characterized as uncertain (UC) are producing circumneutral pH (>6). Sample 5 and sample 7 are producing acidic leachates (pH <4.00) and are also characterized as PAF materials by static test results.

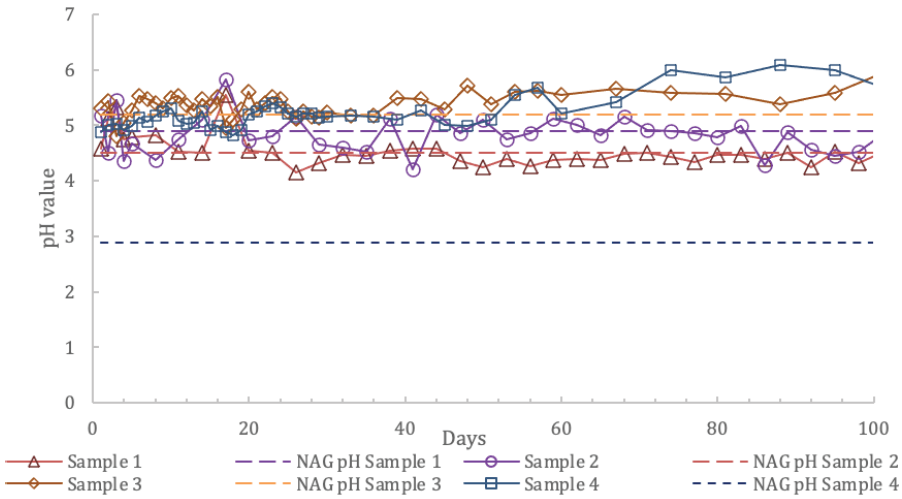


Figure 3 *Kinetic Test Results (pH Value) for Sample 1 – Sample 4*

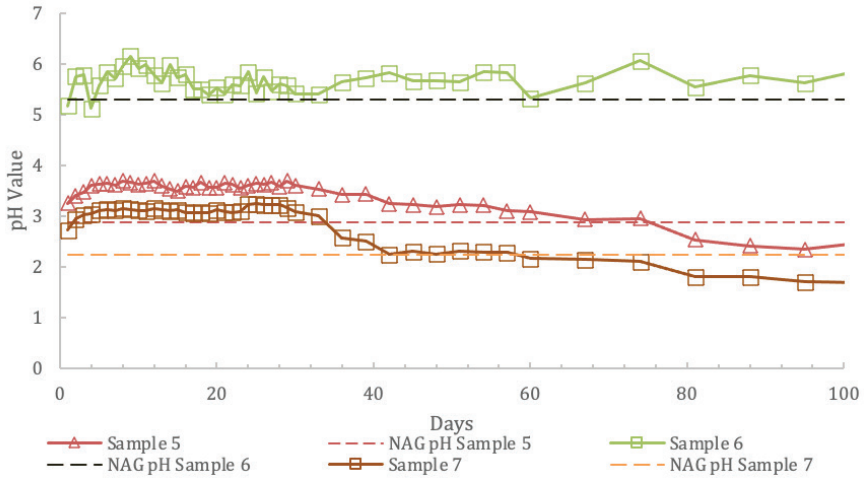


Figure 4 *Kinetic Test Results (pH Value) for Sample 5 – Sample 7*

Geochemical Classification based rock types

Based on static test and kinetic test results and further categorization based on various lithotypes, geochemical classification is related to oxidation states, which is understandable since the higher the oxidation states (fully oxidized), the more oxidized mineral is found. These samples are categorized as non-acid forming. On the other hand, fresh or moderately oxidized samples are categorized as potentially acid-forming since sulphide minerals are more abundant, including pyrite as acid producing mineral. Other lithotypes such as alteration and lithological rock types are less related to the geochemical classification of acid mine drainage since the alteration is only indicating the evolution of aluminosilicates minerals in the samples. Various lithological rock types are also related to major minerals in the rock samples (quartz and alumino-silicates) and are related least to the geochemical classification of acid mine drainage

Alunite Group Geochemical Classification

Alunite group geochemical classification is separated from previous geochemical characterization. Alunite reaction with acidity yields sulphate, potassium, aluminium and water, as described as follows:

$$K\,Al_3\,(SO_4)_2(OH)_6 + 3H_2O \leftrightarrow 3Al(\mathrm{OH})_3 + \mathrm{K^+} + 2\mathrm{SO_4^{-2}} + 3\mathrm{H^+}$$

Alunite production of acidity is lesser in extent than oxidation of sulphide or dissolution of soluble iron sulfate minerals since alunite is less soluble (Lapakko, 2002; Nordstrom, 1982). High-alunite samples are overestimated in producing acidity, as showed by very high MPA values, yet producing NAG pH value of more than 4.00) since MPA is calculated from total sulphur and assumed all sulphur is in form of sulphide minerals (i.e. pyrite). Nevertheless, alunite group samples are classified by their NAG pH and kinetic test pH value. And the final classification is barren or non-acid forming.

Conclusions

Characterization of waste rock in epithermal deposits based on rock types (alteration, metallurgical extractability and lithology) is compatible with the geochemical classification of acid mine drainage. The classification of rock based on oxidation type and metallurgical extractability is closely related to the geochemical classification of acid mine drainage. Alunite as a product of alteration processes gives a false indication of acid mine drainage classification, thus alunite-rich waste rock needs to be classified separately due to high sulphur content but produces less-acid leachates in laboratory kinetic tests.

Acknowledgements

The authors would like to thank all supported parties for their kind assistance and help during data acquisition, data processing, laboratory testing and manuscript preparation.

References

AMIRA (2002) ARD Test Handbook. Project P387A. Prediction and Kinetic Control of Acid Mine Drainage, AMIRA International Limited, Melbourne, Australia.

Darman H. Sidi F. H. & Ikatan Ahli Geologi Indonesia. (2000). An outline of the geology of Indonesia. Indonesian Association of Geologists.

Hedenquist, J & Arribas, A & Gonzalez-Urien, E. (2000). Exploration for Epithermal Gold Deposits. Reviews in Economic Geology. 13. 245-277.

Lapakko, K. (2002) Metal Mine Rock and Waste Characterization Tools: An Overview. Mining, Minerals and Sustainable Development, No. 67.

Nordstrom, D. K. (1982). The effect of sulfate on aluminum concentrations in natural waters: some stability relations in the system Al2O3-SO3-H2O at 298 K. Geochimica et Cosmochimica Acta, 46(4), 681–692. doi:10.1016/0016-7037(82)90168-5

Assessment of Feasibility and Scale Generation of Hydrothermal Energy in Abandoned Mine Area

Hye-Lim Kwon[1], Duk-Min Kim[2], Dae-Gyu Im[3], Bu-Sung Kang[4], Mi-Sun Park[5]

[1]*Department of New Energy and Mining Engineering, Sangji University, Wonju 26339, South Korea, ossgpfla@naver.com*

[2]*Department of New Energy and Mining Engineering, Sangji University, Wonju 26339, South Korea, kdukmin8@sangji.ac.kr, ORCID 0000-0002-1537-6866*

[3]*Department of Earth and Environmental Sciences, Korea University, Seoul 02841, South Korea, daegull1995@korea.ac.kr*

[4]*Korea Mine Rehabilitation and Mineral Resources Corporation (KOMIR), Wonju 26464, South Korea, civilebs@komir.or.kr*

[5]*Korea Mine Rehabilitation and Mineral Resources Corporation (KOMIR), Wonju 26464, South Korea, mspark@komir.or.kr*

Abstract

The feasibility of applying hydrothermal energy in abandoned mine areas was assessed, and experiments on scale generation and removal were conducted. In the effluent of active treatment facilities that applied a cylindrical settling tank, the annual water temperature variation was particularly low. However, in semi-active treatment facilities that used long rectangular sedimentation tanks, the retention time was excessive and showed temperature fluctuations similar to those of surrounding stream water. In a bench scale heat exchanger, iron concentration decreased at effluent, which indicated deposition of Fe oxides as scale. The accumulated iron was discharged by washing using a weak acid.

Keywords: Hydrothermal energy, mine water, socio-economic, heat exchanger

Introduction

Hydrothermal energy supplies cooling and heating to buildings by utilizing the high specific heat of water (Jeong *et al*., 2017). It has recently been in the spotlight as a new renewable energy for heating and cooling that reduces use of fossil fuel. To be used as a water source for hydrothermal energy, water temperature should not change much with time, which can be found in inclined or vertical shafts. Temperature of mine water in adits and shafts in South Korea is generally around 15°C throughout the year. Meanwhile, in the case that scales composed of Fe/Al/Mn (hydr)oxides and/or calcium carbonate are accumulated in the heat exchanger, heat conductivity is decreased, water passing cross-sectional area is decreased, and pressure loss is increased (Shin *et al*., 2001; Korea Energy Agency, 2003; Jiwon Tech, 2011; EcoScale, 2014). The disadvantage of using mine water is the high scaling potential. Some coal and limestone mining areas have mine water saturated with calcium carbonate, which usually contains dissolved iron, manganese, aluminum, or suspended solids (SS) of several to tens of mg/L or more. In this study, the annual water temperature variations of the influent and effluent of mine water treatment facilities, divided into active and semi-active treatment facilities, were assessed. Experiments on the deposition and washing of scale generated from mine water were also conducted.

Material and Methods

Continuous flow experiment method for bench-scale heat exchangers

A heat exchanger (CB14–4H, V: 120 mL, BHE Manufacturing, Ronneby, Sweden) was used on-site to pass the mine water. The residence time in the heat exchanger was one minute, referring to the heat exchangers at the High1 Resort that use the mine water

as a hydrothermal energy source, as well as other experimental cases. After 20–25 minutes of continuous flow experiment, field measurements of the inflow and outflow of the heat exchanger were conducted at the studied mine, and samples were collected for the analysis of cations and anions. After the experiment was completed, the inside of the heat exchanger was washed with 1 L of 0.06 N HCl to dissolve any accumulated scale, and a sample for cation analysis was collected.

Analytical methods

The collected water samples during the experiments were filtered through 0.45 μm membrane filters and transferred into conical tubes. The samples for the cation analysis were preserved by adding a few drops of concentrated HNO_3 to keep the pH < 2. The cations were analyzed using inductively coupled plasma atomic emission spectroscopy (ICP-AES; ICP-730ES, VARIAN, Australia) at the National Instrumentation Center for Environmental Management (NICEM), Seoul National University, South Korea. The anions were analyzed by ion chromatography (Dionex ICS-3000, ThermoFisher Scientific, USA) at the National Instrumentation Center for Environmental Management (NICEM), Seoul National University, South Korea. For both analyses, the relative standard deviations (RSD) were less than 5% of the measured value.

Result and discussion

Assessment of annual water temperature variation for active and semi-active facilities

The water temperature variations in influent and effluent of the water treatment facilities for mine drainage at Hanbo mine were investigated in 2020. Although the air temperature varied between −15 to +32°C in 2020, the water temperature of the mine water and the effluent from the treatment facilities ranged from 11.9 to 19.4 °C and 10.3 to 20.5 °C, respectively, showing a similar range of variation with each other (Fig 1). This indicates that there is not a substantial change in water temperature depending on the air temperature while staying in the cylindrical settling tank, especially with a short residence time, in the water treatment facilities owing to the high specific heat of water. This indicates the feasibility of utilizing the effluent with low potential for scale formation, such as low concentration of suspended solids.

The water temperature variations in influent and effluent of the water treatment facilities for mine drainage at Yeongdong coal mine were assessed in 2020 (Fig 2). Although the air temperature varied between −8 to +28°C in 2020, the water temperature of the mine water ranged from 10.9 to 19.2°C. In contrast, the water temperature of the effluent ranged from 6.9 to 22.0°C, showing a large water temperature variation similar to that

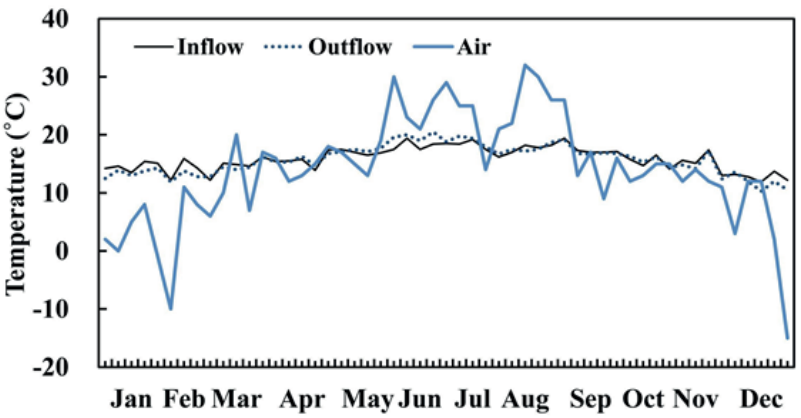


Figure 1 *Variation in air and water temperature of influent and effluent from Hanbo active treatment facilities in 2020*

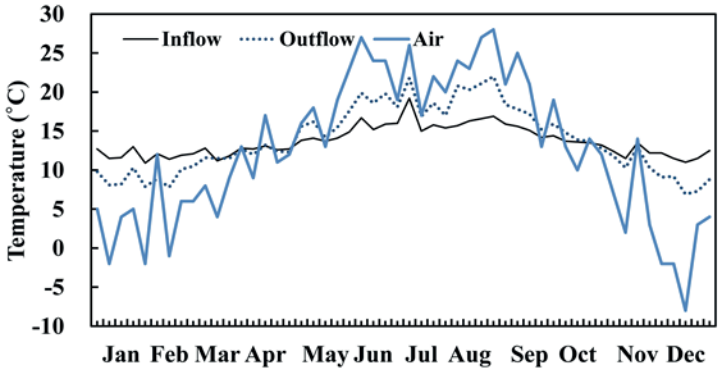


Figure 2 *Variation in air and water temperature of influent and effluent from Yeongdong semi-active treatment facilities in 2020*

of the stream water. The rectangular settling tank of the Yeongdong coal mine water treatment facilities had a long residence time of 48 h, which induced sufficient time for heat exchange with ambient air.

The scale deposition and washing experiments in mine water

The Fe concentration decreased from 13.88 mg/L in the influent to 12.61 mg/L in the effluent of the heat exchanger (Fig 3). This is possibly due to oxidation, precipitation or adsorption inside the heat exchanger. The composition of the effluent after washing the heat exchanger with 1 L of 0.06 N HCl exhibited an iron concentration of 10.61 mg/L. Additionally, copper, lead, zinc, and nickel concentrations were not low, which is thought to be due to the stainless steel and copper included in the heat exchanger material, and additional assessment of the effluent from washing, such as using a weak acid with higher pH, is needed in the future.

Conclusions

The assessment of annual water temperature variations in active and semi-active treatment facilities showed that the effluent from semi-active treatment facilities can exhibit temperature variations similar to those of surrounding stream water and active treatment systems or mine water were highly applicable to hydrothermal energy. The scale deposition and washing experiments conducted on mine water showed that the Fe concentration in the outflow of heat exchanger decreased, and the composition of the effluent after washing the heat exchanger with 1 L of 0.06 N HCl confirmed that iron was accumulated then washed. Hydrothermal energy from the effluent of treatment facilities and mine water can be used as energy needed in local communities surrounding abandoned mine area, which needs socio-economic revitalization due to the decrease of



Figure 3 *Results of continuous flow experiments and washing assessment of heat exchangers using mine water at Dongwon coal mine*

economic power. Additionally, carbon dioxide generated indirectly in the heating and cooling process using fossil fuels can be reduced by alternatively using hydrothermal energy. In the future, it will be necessary to conduct verification experiments on scale deposition and washing, assess the variations in the influent water temperature and the circulating water temperature of the heat exchanger-heat pump system, and assess the efficiency variations due to scale deposition.

Acknowledgements

This work was supported by R&D Project of the Korea Mine Rehabilitation and Mineral Resources Corporation in 2021 and 2022-2023.

References

Shin, S., Kim, K., & Mo, J. (2001). Performance assessment of scale prevention devices for heat exchangers. Journal of the Korean Society of Mechanical Engineers, B, 25.9 (2001): 1149-1156.

Econonscale, 2014. "An Overview of Pipe Scale", November 7, 2014, http://blog.naver.com/econonscale/220174301051

Jeong, J.W., Nam, J.S., and Kim, H.S., 2017. "Utilization cases of thermal energy from domestic sewage and stream water in Korea." Journal of Korea Water Resources Association (Water and Future) 50.10: 50-58.

Jiwon Tech, 2011. "Optimization of heat exchangers for energy savings", September 22, 2011, http://www.jiwontech.com/index.html

Elucidation of the factors controlling the oxidation kinetics of manganese in passive treatment systems : monitoring of aerobic wetland removal technologies

Charlotte Lafont[1,2], Éric D. van Hullebusch[1], Fabienne Battaglia-Brunet[2], Stéphane Vaxelaire[2]

[1]*Université Paris Cité, Institut de Physique du Globe de Paris, CNRS, 75005, Paris, France, lafont@ipgp.fr*

[2]*Bureau de Recherches Géologiques et Minières, 45060 Orléans, France*

Abstract

The determination of parameters controlling the oxidation kinetics of manganese (Mn) during passive treatment is essential to improve the management of mine drainage water treatment. Mn removal processes are mainly driven by microorganisms, but the conditions controlling Mn removal efficiency have not been elucidated yet. To distinguish the factors associated with Mn removal efficiency, the surface water of a passive treatment plant composed of Phragmite-wetlands was monitored for one year. It has been observed that the Mn removal efficiency vary with the concentration of suspended iron particles and the water temperature.

Keywords: Manganese, iron, removal efficiency, neutral coal mine drainage water, wetland

Introduction

France, like many other countries, faces environmental and long-term management challenges caused by mine drainage waters as a result of historical coal mining activities. Thus, passive water treatment plants have been designed to remove manganese (Mn) from mine drainage water before discharge into natural water bodies (Neculita and Rosa 2019). A treatment plant composed of constructed aerobic wetlands systems, located in Alès (South-East France), aims to remove Mn and iron (Fe) from a neutral coal mine drainage water. In these systems, dissolved Mn is oxidised and precipitates as Mn(III/IV) minerals. During passive treatment of neutral mine drainage water, it is now well established that the processes governing Mn oxidation are mainly controlled by biological processes and autocatalytic mechanisms (Skousen *et al.* 2017). Previous studies have highlighted the difficulties to remove Mn during passive treatment (Watzlaf *et al.* 2004). Indeed, Mn removal efficiency is highly variable, depending on mine drainage water chemistry and passive treatment configuration (Hallberg and Johnson 2005; Batty *et al.* 2005; Bamforth *et al.* 2006; Tan *et al.* 2010; Le Bourre *et al.* 2020; Jacob *et al.* 2022). In this context, the present study aims to specify the factors influencing Mn oxidation kinetics by a one-year monitoring programme of the temporal evolution of geochemical and physical-chemical parameters at a coal-mine water treatment plant.

Methods

The studied passive water treatment plant is located in Alès (South-East France). It is composed of aerobics wetlands for Mn and Fe removal. It includes a six-step oxygenation cascade, a settling pond of 2400 m^2 with a depth of 6 m and three *Phragmite*-planted wetlands of 1540 m^2, 1480 m^2 and 1750 m^2, respectively (Fig. 1). Mine drainage water is pumped from the old coal mining galleries and injected at the inlet of the water treatment plant at an average flow rate of 105.9 ± 3.3 $m^3.h^{-1}$. The mine drainage water is mainly composed of sulphate, carbonate and of Fe and Mn which are the targets contaminants.

From march 2022 to February 2023, surface waters of the passive treatment plant were sampled and analysed for their chemical composition every two months. In order to determine the Mn and Fe removal efficiency of process unit, water samples were collected at different points through the treatment plant (Fig. 1). Sampling was carried out from the less contaminated point to the most

contaminated point (i.e. from the station outlet to the station inlet). Filtered (0.45 µm, cellulose acetate filters, Sartorius) and unfiltered fraction of the surface water was sampled for each point. Vacuum-filtration was done onsite with a Nalgene filtration unit. For dissolved and total major ions analysis, aliquots of filtered and non-filtered water were acidified with nitric acid (HNO3 0.1 M). For Fe(II) measurement, an aliquot of filter water was acidified with concentrated hydrochloric acid (HCl) (Kirby *et al.* 1999). Unfiltered water was kept for the titration of alkalinity. Filtration blanks were done onsite with MilliQ water for each measured parameter. Samples were stored at 4°C until analysis. The physicochemical parameters (temperature (T), pH, redox potential (ORP), dissolved O_2 (DO) and electrical conductivity (EC)) of all sampled waters were measured onsite with field WTW® 3430.

Bulk concentrations of dissolved and total major elements (Ca, Mg, Na, K, Mn, Fe, Al, P and Zn) of sampled surface water were determined by ICP-OES (SPECTROGREEN, SPECTRO Analytical Instruments). Quality control solution containing multi-element were used to assess accuracy and reproducibility of the analytical method. Dissolved Fe(II) concentrations were measured by 1,10-phenanthroline method described by Kirby *et al.* (1999). Alkalinity measurements were performed using HCl 0.1 M titration according to the standard Gran method (Gran 1952). Removal efficiency calculation was done using Eq. 1. Total Mn concentration at the inlet and at the outlet of the passive treatment plant was consider to calculate the total removal efficiency of the treatment plant.

$$Mn\ removal\ efficiency\ (\%) = \frac{([Mn]_{inlet} - [Mn]_{outlet})}{[Mn]_{inlet}} \times 10$$

(Eq. 1)

A principal component analysis (PCA) was performed to highlight the factors involved in Mn removal efficiency. Data from all the sampling campaigns were used. Physicochemical parameters and water composition (i.e. T, pH, ORP, DO, EC, dissolved Mn, dissolved Fe, total Fe concentrations and alkalinity) were selected to carried out PCA. Total major ions results from some sampling points (Wetland 1 in June 2022 and Wetland 2 in April and June 2022) have been excluded due to an overestimation of the concentration caused by resuspension of sediment during sampling. This analysis was performed by R software using the FactoMineR package.

Results

Physicochemical parameters (T, pH, ORP, DO and EC) were measured at each sampling point and at every sampling campaign. At the pumping sample point (inlet, Fig. 1), the water showed a stable pH around 6.5, dissolved O_2 at 0 mg.L^{-1}, redox potential values between -35.4 mV and -67.8 mV and temperature values between 22.2 °C to 24.6

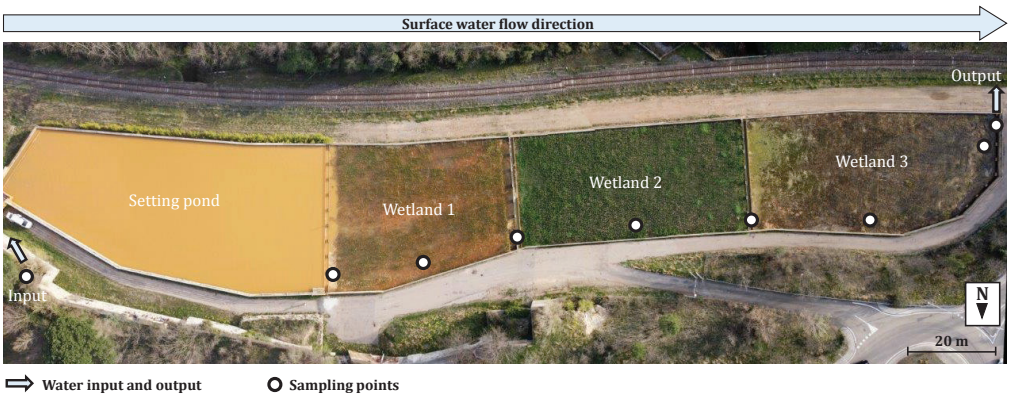


Figure 1 *Sampling locations in the studied passive treatment plant, Wetlands 1, 2 and 3 are composed of Phragmite plants (image: F. Duré, BRGM).*

°C. Along the passive treatment plant, these parameters increased up to a pH around 8 and positives values of O_2 and ORP were found. In the wetlands, the water temperature was found to vary with the seasons. The highest temperatures were recorded in June and August, with an average value of 25 °C. The lowest temperatures were recorded in December, with a value of 15 °C. It should be taken into account that the measured surface water temperatures depend on the sampling time, which is not representative of the temperature evolution during the day.

Mn and Fe concentrations decrease in surface water during the treatment process (Fig. 2, D). These concentrations have been shown to vary with sampling campaigns season time. Significant decreases in Mn concentration across all wetlands are observed in April, June and February. In August, October and December, Mn only shows a significant decrease of its concentration in the last wetland (Wetland 3 and End Wetland 3, see Fig. 2, D). Mn removal efficiency was calculated considering Mn inlet and outlet concentrations (Eq. 1). As shown in Figure 2, the highest Mn removal efficiency was around 92% in June and at its lowest value (43%) in December. Fe was characterized by its dissolved and total content. At all sampling campaigns, dissolved Fe concentrations are significantly low after passing through the settling pond, generally found under 0.2 $mg.L^{-1}$ (Fig. 2, A and B). In contrast, total Fe concentrations are gradually decreasing through the wetlands (Fig. 2, C). It decreases with average concentrations going to 9.43 ± 3.37 $mg.L^{-1}$ to 0.57 ± 0.62 $mg.L^{-1}$. In wetlands, because dissolved Fe concentrations are significatively low, total Fe can be consider as Fe particles larger than 0.45 µm. For this parameter, missing data occurs due to concentration overestimation caused by sediment remobilisation during sampling.

PCA results, presented in Fig. 3, show 74.67% of the total inertia of the dataset, allowing to observe most of the variability of it (i.e. 60.66% for dimension 1 and 14.01% for dimension 2). The graph of variables can be divided in four mains clusters (Fig. 3, A). Cluster 1 is composed of DO, pH and ORP. The second includes Fe and total Fe concentrations. The third one is associated to alkalinity and Mn concentration. Cluster 4 is represented by EC and temperature. Figure 3 allows to observe correlated and anticorrelated parameters during passive treatment of mine drainage water. The first

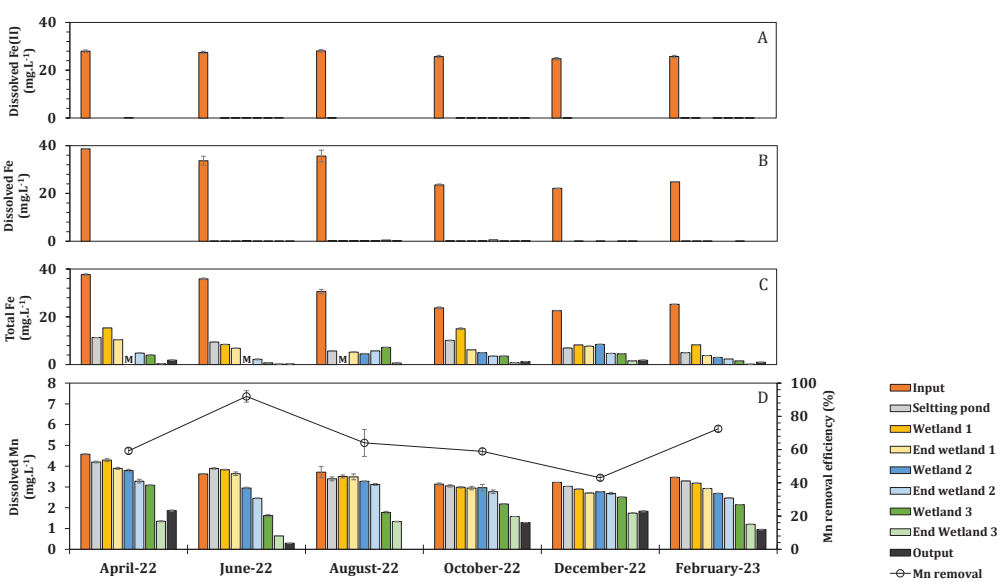


Figure 2 *Evolution of (A) dissolved Fe(II), (B) dissolved Fe, (C) total Fe and (D) dissolved Mn concentrations in surface mine water through the studied passive treatment plant (M refers to missing data).*

interesting observation is the anticorrelation of Fe, Total Fe, alkalinity, Mn, Temperature and EC parameters compared to the pH, DO (25°C) and ORP parameters according to dimension 1. It represents the differences comparing physicochemical characteristics of inlet water and the outlet treated water, which is illustrated by sampling points qualitative variables (Fig. 3, B). The sampling dates, added as a qualitative supplementary variable (Fig. 3, B), expose the seasonal effects on water physiochemistry. It shows similarities in water chemistry when comparing sampling time. Two main groups are distinguished, on one hand, the sampling campaigns of April 2022, June 2022 and August 2022 and on the other hand the sampling campaigns of October 2022, December 2022 and February 2023.

Discussion

The design of aerobic wetland for passive water treatment is largely dependent on the mine drainage pH and on the concentration of contaminants which is affected by the geology of the mine site. It is especially valid for Mn removal which is particularly dependent on Fe water content (Calugaru *et al.* 2021). Furthermore, the poor understanding of the mechanisms and factors controlling manganese removal is an obstacle to define design criteria for treatment plants (Neculita and Rosa 2019). Therefore, Mn removal effectiveness can be highly variable comparing treatment plants (Hallberg and Johnson 2005; Lesley *et al.* 2008; Tan *et al.* 2010; Jacob *et al.* 2022). The discussion below relates some parameters impacting the elimination of Mn in a passive water treatment plant to better understand variations in Mn removal efficiency.

The water DO, pH and ORP increase all along the plant, creating optimal conditions for Fe oxidation. For Mn abiotic oxidation optimal parameters are not reached during passive treatment process. In this kind of systems, biotic oxidation processes most likely control Mn oxidation. But in these environments, the optimal conditions for biotic Mn removal remain unknown. Our results show that manganese removal efficiency decreases with temperature, from high temperature conditions in June to lower temperature conditions in December (Fig. 2). The biological oxidising activity of Mn is probably controlled by temperature seasonal variations. Previous studies have shown that some microorganisms were able to oxidise Mn at temperatures similar to those recorded in June (Neculita and Rosa 2019). Recent studies, carried out in laboratories, have observed Mn oxidation processes by microorganisms at different temperatures. Yu and Leadbetter (2020) observed an optimal Mn oxidation at temperatures ranging between 34 °C and 40 °C. This result was in line with those reported by Boogerd and de Vrind (1987), who have studied especially manganese oxidation by *Leptothrix discophora*. But as described by Neculita and Rosa (2019), several laboratories experiments have observed microbial communities that can efficiently contribute to Mn oxidation at temperature as low as 4°C. Studies of real

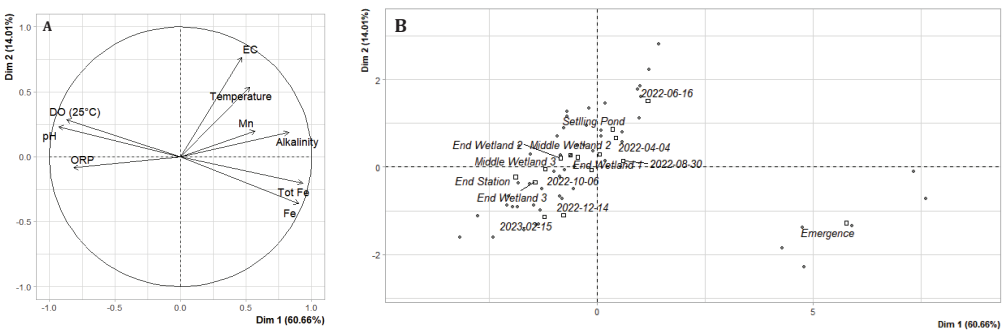


Figure 3 *Principal Component Analyses (PCA) based on water physicochemical variables (pH, T, EC, ORP and DO corrected at 25 °C, dissolved Mn (Mn), dissolved Fe (Fe), total Fe (Tot Fe) concentrations and alkalinity), (A) Graphic of variables and (B) Graphic of individuals.*

constructed wetland for coal mine drainage water treatment have also brought diverse conclusions on temperature effect but have also consider other factors to explain removal variation such as pH, DO, alkalinity, nutrient availability (Ye *et al.* 2001). Temperature appears to be a key parameter affecting Mn removal efficiency by biotic process, indeed the activity and development of certain Mn-oxidising microbial communities seems temperature dependant.

The simultaneous presence of Fe and Mn in mine drainage water has already been reported as a limiting parameter for Mn removal during passive water treatment (Lesley *et al.* 2008). Indeed, it is well known that ferrous iron can reduce Mn oxidised forms (Liu *et al.* 2022). Our results shows that dissolved Fe and dissolved Fe(II) concentrations are close or under the limit of analytical detection at wetlands sampling points (Fig. 2). In contrast, total Fe considering as Fe particles larger than 0.45 µm, is found at different concentrations through the wetlands. Due to water pH, ORP and dissolved organic carbon concentrations (i.e. < 1 $mg.L^{-1}$), we hypothesize that total Fe can be defined as Fe oxide(hydroxides) aggregate in water suspensions. Figure 4 was plot to study the impact of total Fe concentration on Mn removal. This graph shows the evolution of the Mn concentration as a function of the total Fe concentration along the station and for different sampling campaigns. Our results shows that Mn concentrations significantly decrease when total Fe concentration is below 5 $mg.L^{-1}$ in surface water. Watzlaf *et al.* (2004), who have studied a real passive treatment plant, reported that most of Mn removal takes place in "iron-free zone" corresponding to surface water containing low suspended Fe particles. Our results are consistent with Watzlaf *et al.* (2004) observations, significant Mn removal were found in wetland 3 which contained the lowest total iron concentration. However, these observations require further investigation to understand the interdependence of Fe and Mn biogeochemical cycling in this environment.

Conclusions

This study presents data from a one-year monitoring programme of a coal-mine water treatment plant in order to highlights which factors affect the Mn removal efficiency. According to the results, Mn concentrations are dependent to water temperature and suspended Fe particles concentrations. Indeed, the higher Mn removal efficiency was observed during summer season when total Fe removal efficiency was the highest. We hypothesised that the microbial communities that oxidise Mn in this environment are temperature dependent. Also, it appears that Fe particles larger than 0.45 µm have an impact on Mn oxidation, but this needs to be understand by further investigations. It would be interesting to determine whether if the presence of suspended Fe in mine water has an impact on Mn biotic oxidation to predict long-term Mn immobilization in passive water treatment plants.

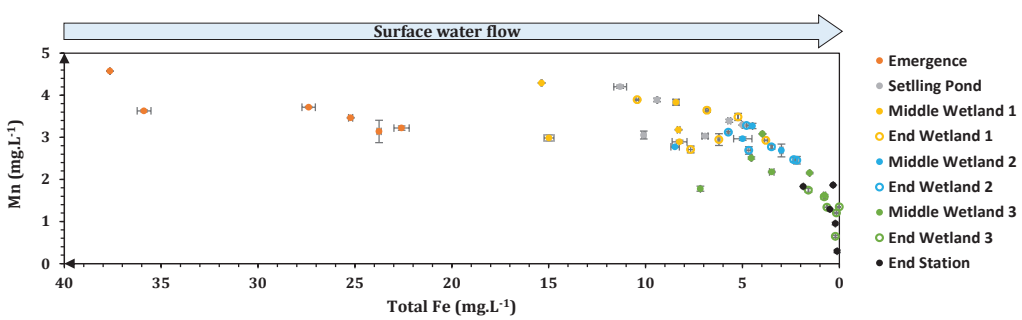


Figure 4 *Dissolved manganese and total iron (fraction > 0.45 µm) in surface waters sampled through the passive treatment plant. Sampling locations are illustrated Fig.1.*

Acknowledgements

This study is supported by a PhD project funded by BRGM (post-mining division DPSM) and IPGP.

References

Bamforth SM, Manning DAC, Singleton I, *et al.* (2006) Manganese removal from mine waters – investigating the occurrence and importance of manganese carbonates. Applied Geochemistry 21:1274–1287. https://doi.org/10.1016/j.apgeochem.2006.06.004

Batty LC, Atkin L, Manning DAC (2005) Assessment of the ecological potential of mine-water treatment wetlands using a baseline survey of macroinvertebrate communities. Environmental Pollution 138:412–419. https://doi.org/10.1016/j.envpol.2005.04.022

Boogerd FC, de Vrind JP (1987) Manganese oxidation by Leptothrix discophora. J Bacteriol 169:489–494. https://doi.org/10.1128/jb.169.2.489-494.1987

Calugaru IL, Genty T, Neculita CM (2021) Treatment of manganese, in the presence or absence of iron, in acid and neutral mine drainage using raw vs half-calcined dolomite. Minerals Engineering 160:. https://doi.org/10.1016/j.mineng.2020.106666

Gran G (1952) Determination of the equivalence point in potentiometric titrations. Part II. Analyst 77:661–671

Hallberg KB, Johnson DB (2005) Biological manganese removal from acid mine drainage in constructed wetlands and prototype bioreactors. Science of The Total Environment 338:115–124. https://doi.org/10.1016/j.scitotenv.2004.09.011

Jacob J, Joulian C, Battaglia-Brunet F (2022) Start-Up and Performance of a Full Scale Passive System In-Cluding Biofilters for the Treatment of Fe, as and Mn in a Neutral Mine Drainage. Water 14:1963. https://doi.org/10.3390/w14121963

Kirby CS, Thomas HM, Southam G, Donald R (1999) Relative contributions of abiotic and biological factors in Fe (II) oxidation in mine drainage. Applied geochemistry 14:511–530

Le Bourre B, Neculita CM, Coudert L, Rosa E (2020) Manganese removal processes and geochemical behavior in residues from passive treatment of mine drainage. Chemosphere 259:127424. https://doi.org/10.1016/j.chemosphere.2020.127424

Lesley B, Daniel H, Paul Y (2008) Iron and manganese removal in wetland treatment systems: rates, processes and implications for management. Science of the total environment 394:1–8

Liu J, Chen Q, Yang Y, *et al.* (2022) Coupled redox cycling of Fe and Mn in the environment: The complex interplay of solution species with Fe- and Mn-(oxyhydr)oxide crystallization and transformation. Earth-Science Reviews 232:104105. https://doi.org/10.1016/j.earscirev.2022.104105

Neculita CM, Rosa E (2019) A review of the implications and challenges of manganese removal from mine drainage. Chemosphere 214:491–510. https://doi.org/10.1016/j.chemosphere.2018.09.106

Skousen J, Zipper CE, Rose A, *et al.* (2017) Review of Passive Systems for Acid Mine Drainage Treatment. Mine Water Environ 36:133–153. https://doi.org/10.1007/s10230-016-0417-1

Tan H, Zhang G, Heaney PJ, *et al.* (2010) Characterization of manganese oxide precipitates from Appalachian coal mine drainage treatment systems. Applied Geochemistry 25:389–399. https://doi.org/10.1016/j.apgeochem.2009.12.006

Watzlaf GR, Schroeder KT, Kleinmann RL, *et al.* (2004) The passive treatment of coal mine drainage. United States Department of Energy National Energy Technology Laboratory Internal Publication 1–72

Ye ZH, Whiting SN, Lin Z-Q, *et al.* (2001) Removal and Distribution of Iron, Manganese, Cobalt, and Nickel within a Pennsylvania Constructed Wetland Treating Coal Combustion By-Product Leachate. J Environ Qual 30:1464–1473. https://doi.org/10.2134/jeq2001.3041464x

Yu H, Leadbetter JR (2020) Bacterial chemolithoautotrophy via manganese oxidation. Nature 583:453–458. https://doi.org/10.1038/s41586-020-2468-5

Numerical Simulation Of Small-Size Aggregate Accumulation Structure Under Dynamic Water Conditions

Weitao Liu[1,2], Chunhui Yang[1,2], Yanhui Du[2,3]

[1]*College of Energy and Mining Engineering, Shandong University of Science and Technology, Qingdao, Shandong 266590, China, skych521@163.com*

[2]*Shandong University of Science and Technology State Key Laboratory of Mine Disaster Prevention and Control, Qingdao, Shandong 266590, China*

[3]*College of Safety and Environmental Engineering, Shandong University of Science and Technology, Qingdao, Shandong 266590, China*

Abstract

The flow velocity is the key factor to determine the effect of dynamic water grouting. The accumulation body accumulated in the water passing roadway can effectively reduce the flow velocity. In this paper, non-spherical particles are used to simulate the accumulation of aggregates in roadways. The accumulation effect and force chain distribution of 5-10 mm small-sized aggregates in pipeline flow are calculated by the CFD-DEM method. Combined with IMAGE-J software, the anisotropic porosity and average porosity are obtained. The effect of dynamic water on the accumulation effect of small-sized aggregates and its influence on the accumulation porosity are analyzed.

Keywords: Dynamic water grouting, CFD-DEM, aggregate accumulation, numerical simulation, pore structure

Introduction

The movement of aggregate in dynamic water can be regarded as a kind of sediment movement under specific boundary conditions. When the aggregate is thrown into the water from the top of the dynamic water. The particles produce resistance to the fluid, and the fluid also produces drag force on the aggregate particles. The drag force is the force of the fluid on the relatively moving object, including pressure and shear force (viscous force). The size of the drag force is determined by a variety of physical quantities, which is the most important factor in the migration of aggregate particles and the basis for studying the influence of dynamic water on the morphology of aggregate deposits. In 1879, French scientists proposed the concept of drag force and the theory of bed load motion (Du Boys 1879). At the beginning of the century, Gilbert studied the movement of sediment through flume experiments (Gilbert 1914). Then Meyer-Peter used the empirical analysis method of isolated factors to establish the bed load transport rate formula based on the flume test data (Meyer-Peter *et al*. 1934). Sha summarized and put forward the basic law hypothesis of the critical velocity of sediment movement, and proved that the effective velocity of the open channel is the main factor to determine the amount of sand carried by flowing water (Sha 1996). Zhang and Dou adopted the principle of resistance superposition to derive a unified settling velocity formula for single-particle sediment in the stagnation zone, transition zone, and turbulent zone (Zhang 1998; Dou 1999).

Compared with irregular aggregate particles, the pore characteristics and permeability characteristics of regular shape particles such as circular particles are now more clear (Furnas 1928; Matuttis *et al*. 2000; Horsfield 1934; Stovall *et al*.1986; Isaia *et al*. 2003). As a kind of irregular granular material, the structure's internal pore structure composed of aggregate particles is relatively complex. The shape, gradation, and compactness of aggregate particles will affect the pore structure of the deposit, and then affect the permeability characteristics of the deposit (Peng *et al*.2020). It is difficult

to quantify the entire pore network. Studies have shown that pore characteristics at the particle scale are closely related to the stress characteristics and conductivity between particle materials. The emergence of discrete element numerical simulation technology provides a new technical means for people to study the system composed of a large number of granular particles. This method can accurately describe the velocity, position, force, and other parameters of a single particle in a particle group. The pore law of aggregate deposits can be obtained directly or indirectly through the above parameters. The CFD-DEM coupling calculation method calculates the interaction force between fluid and particles through momentum exchange, forming a mesoscopic simulation method for studying the coupling of particles and fluid. This paper uses the CFD-DEM coupling calculation method to study the structure of aggregate particle accumulation under dynamic water impact.

Numerical simulation parameter setting

Determination of roadway parameters

Mine roadway has strict design standards, most of the roadways arranged in the working face of coal mines are rectangular section roadways. When a water rush occurs in the working face, these roadways arranged in the working face often become the channel of water spreading to other working areas. This kind of roadway that plays a connected role in the water rush is called an "over-current roadway". For the CFD-DEM simulation method, before the numerical simulation, it is necessary to adjust the prototype roadway and study the similarity criteria. The roadway with a length and width of 4m and a rectangular section is selected as the prototype of simulation calculation.

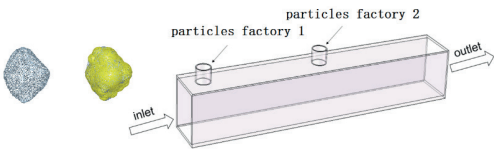


***Figure 1** Particle model and flow field model*

The Length similarity, Area similarity, and Volume similarity are

$$\frac{L'}{L} = \frac{l'}{l} = C_l \quad (1)$$

$$C_A = \frac{A'}{A} = \frac{l^2}{l^2} = C_l^2 \quad (2)$$

$$C_V = \frac{V'}{V} = \frac{l^3}{l^3} = C_l^3 \quad (3)$$

Where L is the characteristic length of the roadway, A is the section area, V is the section volume, the set length ratio Cl = 20, and the length and width of the model roadway are 20cm. Based on the geometric similarity, the kinematic similarity can be determined, such as speed similarity, time similarity, acceleration similarity, and flow similarity.

EDEM pellet property setting

In the engineering practice of dynamic water grouting and water interception, the particle size of aggregate is mostly between 5 and 50mm, and the large size aggregate is used as the "skeleton" of the structure and plays the role of water resistance. Particles with relatively small particle sizes are used to fill the gaps in the "skeleton" and act as an interception. 5-10mm small-size particles were selected as the research object for CFD-DEM coupling calculation.

To make the simulation calculation more realistic, the particle shape is fitted using the EDEM software MultiSphere option, as shown in Figure. 1. The aggregate particle calculation parameters are set up in Table 1.

Fluent flow field setting

The movement of water inrush flow in the roadway can be approximately regarded as pipeline flow, and the length, width, and height of the flow field model are set to 150cm, 20cm, and 20cm respectively. The initial flow velocity at the entrance is 0.3m/s. The distance between the two particles factory and the water inlet is 10cm and 75cm respectively. The overall flow field model is shown in Figure 1.

For practical engineering, in the process of aggregate transportation, part of the gravitational potential energy will be transformed into the kinetic energy of the aggregate particles. When the aggregate enters the water tunnel, there will be a certain

Table 1 Solution parameter setting for aggregate particles

Young modulus	Poisson ratio	Coefficient of restitution	Coefficient of sliding friction	Coefficient of rolling friction	Particle density
E(N/m^2)	v	a	f_1	f_2	ρ (kg/m^3)
5×10^6	0.3	0.4	0.4	0.1	2450

initial velocity. Because there are many factors affecting the initial velocity, it is difficult to be characterized by calculation. Therefore, an initial velocity of 0.4 m/s is given directly.

Numerical simulation results and analysis

Determination of accumulation angle and porosity of accumulation body in the pipeline under anhydrous condition

To determine the influence of dynamic water on aggregate accumulation, the accumulation angle and porosity of the particles are determined by EDEM software before the coupling calculation, and the accumulation pattern is shown in Figure. 2.

Slice analysis is performed on EDEM using its Slices function, slicing along the x-axis, and y-axis directions of the accumulation to obtain the cross-sectional structure of the accumulation at that location, as shown in Figure. 3. Use IMAGE J to binarize the section and measure it using a measuring tool, as shown in Figure. 3. Divide the area of the white area within the designated area by the total area of the area, and the result obtained can be approximately considered as the porosity of the accumulation in that section.

The data as shown in Table 2 are obtained after the area calculation of each section.

From it, we can see that the natural accumulation state of aggregate, the various section porosity is not much change, porosity fluctuates around 39.7%, the overall pore, particle distribution is relatively uniform, accumulation body y-axis section close to the isosceles triangle, accumulation Angle is 32, on both sides of the wall on the influence of aggregate accumulation is not obvious.

Changes of aggregate morphology and flow field during the aggregate accumulation

The ratio of surface area to mass of the same shape particles will be different. At the same density, the large size particles will sink faster in the water than the small size particles, and the impact of fast water velocity will make this situation more obvious. As shown in Figure. 4. A.

Set the water flow velocity at the inlet to 0.3m/s, The movement morphology of the particle group has undergone significant changes compared to Figure. 4. A. As shown in Figure. 4. B.

When the aggregate particles are initially accumulated, by the friction between the particles and the friction between the particles and the tube wall, the low-speed water flow is



Figure 2 *Particle accumulation morphology in the pipeline*

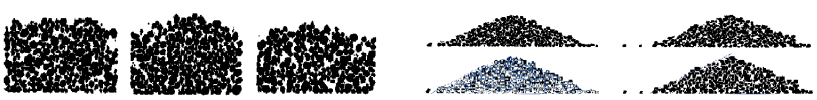


Figure 3 *Chart of the accumulation of body*

Table 2 Porosity of each section of the accumulation body

Number	x-axis 1	x-axis 2	x-axis 3	x-axis 4	x-axis 5	x-axis 1	x-axis 2
Porosity	39.62%	39.75%	39.65%	39.62%	40.12%	39.79%	39.86%

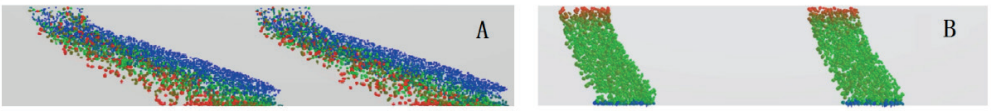


Figure 4 The movement morphology of the particle group

insufficient to cause the accumulated stable particles to move again, as shown in Figure. 5.

According to the setting, the generation speed and grading of the particle factories are the same. As the aggregates continue to accumulate, there is a significant difference in the accumulation shape of the adjacent two accumulation bodies. As shown in Figure. 5.

In the later period of aggregate accumulation, it is difficult for aggregate particles of 5-10mm particle size to raise the height of the whole accumulation body as shown in Figure. 5. Because the decrease of the Water cross-section makes the water flow velocity above the accumulation body increase, it is difficult to retain the small particle size particles on the top of the accumulation body. At this time, the velocity cloud atlas of the flow field is shown in the figure, and the flow velocity at the outlet is about 0.2 m/s, as shown in the Figure. 6, the water flow rate decreases significantly from the simulation.

From the above simulation results, it can be seen that the accumulation form of aggregates is not only related to the size, shape, and grading of aggregate particles but also to factors such as water flow velocity. Accurately predicting the shape of aggregate accumulation is difficult, but we can use numerical simulation calculations to determine whether particles of specific size, grading, and quantity can form an effective stacking structure at a specific speed.

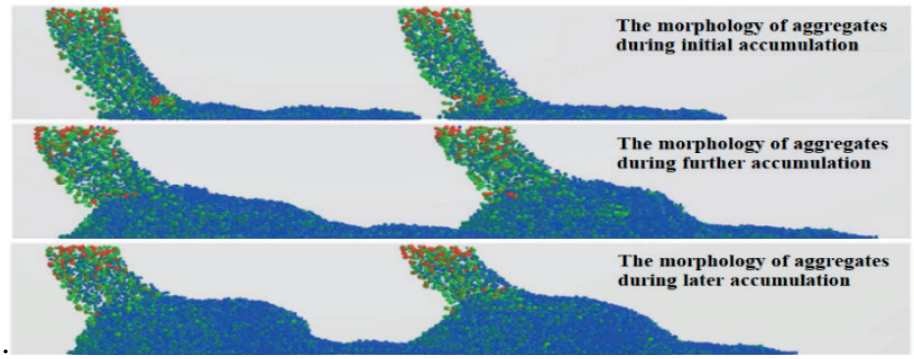


Figure 5 The morphology of aggregates accumulation

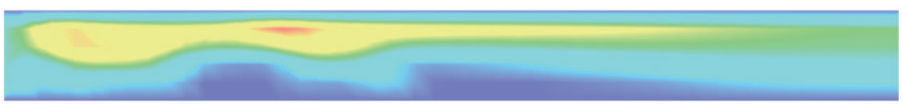


Figure 6 The velocity cloud atlas of the flow field in the later stage of aggregate accumulation

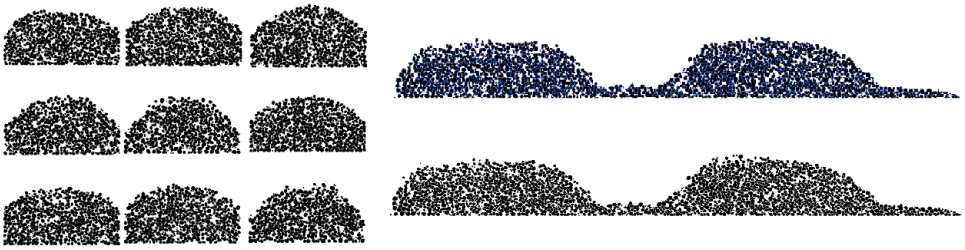


Figure 7 Accumulacking section under dynamic water impact

Treatment and analysis of the internal structure of accumulation body under dynamic water impact

The accumulated aggregate accumulation body was sectioned, binarized, measured, and counted by IMAGE J, as shown in Figure. 7.

The statistical results are shown in Table 3. From the statistical results we can conclude, the porosity of the upstream face section is relatively high, with the lowest porosity in the middle of the accumulation body away from the inflow direction; from the direction of water to the direction of water, the pores of the aggregate accumulation body decrease first and then rise. The bottom of the accumulation body is close to the center, and the porosity is the lowest. The dynamic water impact makes the aggregate accumulation porosity anisotropic, and the accumulation porosity along the y-axis is significantly higher than along the x-axis.

The simulation results were post-processed using Python to obtain a force chain distribution diagram of the accumulation body, as shown in Figure. 8. According to the calculated contact force, the force chain is divided into three levels for coloring. The contact force of red, green, and blue colors decreases sequentially, and the contact force can confirm the reliability of the structure from the side. The greater the contact force, the closer the bonding between particles. On the contrary, the smaller the contact force, the looser the particle bonding and the lower the strength. It is obvious that under this condition, the contact force distribution of the whole accumulation body is layered, and the blue force chain is the region where the accumulation body is the most vulnerable and most prone to structural instability.

Conclusion

Firstly, injecting aggregates into the water roadway can effectively reduce the flow

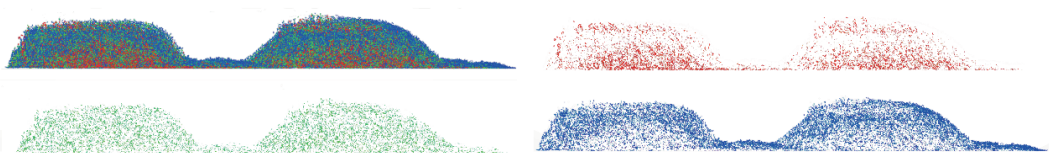


Figure 8 Force chain distribution diagram of accumulation body

Table 3 The porosity of each section of the accumulation body under dynamic water impact

Number	x-axis 1	x-axis 2	x-axis 3	x-axis 4	x-axis 5	x-axis 6
Porosity	37.50%	37.07%	36.50%	36.80%	37.68%	38.12%
Number	x-axis 7	x-axis 8	x-axis 9	x-axis 10	The y-axis section	
Porosity	37.90%	36.45%	36.48%	37.22%	38.78%	

velocity of the dynamic water. Under this simulated condition, the presence of an accumulation body reduces the flow velocity from 0.3m/s to 0.2m/s.

Secondly, the aggregate accumulation pattern of 5-10mm particle size is greatly affected by the dynamic water. When the accumulation body reaches a certain height, it is difficult to retain the smaller aggregate particles above the accumulation body. In the dynamic water state, the porosity of the accumulated aggregate will appear anisotropy, and the porosity distribution is not uniform and has certain regularity.

Finally, Due to the impact of dynamic water and the aggregate's gravity, the force chain distribution of the accumulation body is not uniform, and the particle structure near the surface layer of the accumulation body is loose, which is prone to structural instability so that the overall structure of the accumulation body is destroyed.

References

Du Boys P. Le (1879) Rhone et les rivieres a lit affouillable. [J] Annales des Ponts et Chaussees, Series 5,1879,18:141-195.

Gilbert G. K (1914) Transportation of debris by running water [J] Professional Paper U.S. Geological Survey,1914(86).

Meyer-Peter E, Muller R (1948) Formulas for bed-load Transport [C] Paper No.2, Proceedings of Second Meeting International Association for Hydraulic Research,1948:39-64.

Sha YQ. (1996) Introduction to Sediment Dynamics [M]. Beijing; China Industrial Press, 1996.

Zhang RJ. (1998) Dynamics of fluvial sedimentation [M]. Beijing; China Water Conservancy and Hydropower Press, 1998.

Dou GR. (1999) On the starting flow rate of sediment [J]. Sediment Research, 1999, (6): 1-9.

C. C. Furnas (1928) Bureau of Mines Reports of Investigation, No, 2894, 1928.

Matuttis HG, Luding S, Herrmann HJ. (2000) Discrete element simulations of dense packings and heaps made of spherical and non-spherical particles. Powder Technology, 109:278-292.

Horsfield HT. The strength of asphalt mixtures[J]. Journal of the Society for Chemical Industry, 1934, 53(2): 107–115.

Stovall T, De Larrard F, Buil M. (1986) Linear packing density model of grain mixtures [J]. Powder Technology, 1986, 48(1): 1–12.

Isaia GC, Gastaldini ALG, Moraes R. (2003) Physical and pozzolanic action of mineral additions on the mechanical strength of high-performance concrete[J]. Cement and Concrete Composites, 2003, 25(1): 69–76.

Peng JY, Zhang JF, Shen ZZ, *et al* (2020) Effect of grain shape on pore characteristics and permeability of coarse-grained soil [J]. Rock and Soil Mechanics, 2020, 41(02);592-600. DOI:10.16285/j.rsm.2019.0066.

Surface Boundary Conditions for Finite Element Simulation of Platinum Tailings in a Semi-Arid Environment

S. Lorentz[1,2] S. Imrie[1] A. Bennett[1] and A. Clulow[2]

[1]*SRK Consulting (South Africa)*

[2]*University of KwaZulu-Natal (South Africa)*

Abstract

The evaporation fluxes from a platinum tailings beach were measured before, during and after a period of slurry deposition. The time series measurements were made using a surface renewal system, set up above the tailings beach. Results of the measured evaporation were compared with atmospheric potential evaporation. The comparisons demonstrated that actual evaporation was lower than potential prior to deposition, equal to potential during, as well as following deposition, and finally lower than potential some days after cessation of deposition. These phenomena were assumed to result from the simultaneous evaporation drying and consolidation processes in the deposited layer, and implication for appropriate beach surface boundary conditions for finite element modelling of the tailings, were developed and tested. The final outcome will contribute to realistic simulation of the ingress and fate of slurry water and rain in tailings impoundments.

Keywords: Tailings water evaporation, infiltration, surface renewal, tailings water modelling

Introduction

In the semi-arid areas of southern Africa, Annual Potential Evapotranspiration (PET), the atmospheric demand for water uptake, can exceed annual rainfall by more than threefold. Nevertheless, the intensity and volumes of daily rainfall result in water ingress into platinum tailings porous media and result in periodic recharge to a phreatic surface. In this semi-arid environment, evaporation losses from bare surfaces are primarily dependent on the hydraulics of the porous medium, which controls the fluxes of water and vapour to the surface, rather than the atmospheric demand. However, the fate of deposited water and rainfall is difficult to assess, particularly at high rates of rise, due to the partition of fluxes, comprising surface runoff to the pool, infiltration during rain and slurry deposition, percolation from the deposited layer post deposition, entrainment of interstitial water and evaporation from wetted and drying surfaces. Practitioners have often resorted to empirical approaches to estimate evaporation losses and infiltration rates. This can result in significant error to the overall water budget, poor estimates of recharge to the phreatic surface and confounding conditions for water management.

In this paper, a series of simultaneous observations of atmospheric driving forces, material characteristics and water dynamics were conducted in situ. The observations included full meteorological monitoring and characterisation of the tailings hydraulic properties. In-situ observations included automatic recording lysimeters in the tailings beach to measure evaporation rates and tailings pore water sensors in selected profiles on the beach to measure infiltration and percolation flux states. Finally, a Surface Renewal station was erected on the tailings beach to observe actual evaporation fluxes prior to, during and post deposition. The Surface Renewal observations, presented in this paper, were compared with estimates of PET, using meteorological observations, and the possible mechanisms controlling the evaporation from the beach were deduced. The results are used to inform finite element modelling simulations of the saturated and unsaturated pore water processes.

Methodology

Evaporation from surfaces can be determined directly from the Latent Energy Flux (λE) above the surface. The Latent Energy Flux is one of the terms making up the total energy balance of evaporating water, given by:

$$Rn = G + H + \lambda E \quad (1)$$

where:
Rn = Nett Irradiance (Watts/m^2);
G = Soil Heat Flux (Watts/m^2) and
H = Sensible Heat Flux (Watts/m^2).

Equation 1 can be solved for the Latent Energy Flux as:

$$\lambda E = Rn - G - H \quad (2)$$

The evaporation rate, E, can be calculated from the Latent Energy Flux (λE), since the Specific Latent Heat of Vaporisation (λ) is known. The nett irradianc, Rn, can be measured with a Nett Radiance sensor and G can be measured using Soil Heat Flux Plates. This leaves the Sensible Heat Flux, H, which is measured using Surface Renewal (SR) principles (Mengistu and Savage, 2010; Savage, 2017; Hu *et al*., 2019).

The SR method is based on the premise that a parcel of air connected to the surface (a in Figure 1), after it has been enriched or depleted (b in Figure 1), is renewed by an air parcel from above (g ang h in Figure 1). The SR technique for estimating Sensible Heat Flux from surfaces therefore involves high-frequency temperature measurements (10 Hz, in this case), using unshielded and naturally-ventilated fine wire thermocouples at a specific height above the surface, (Mengistu and Savage, 2010). The high-frequency temperature measurements are analysed to describe the temperature "ramping" (renewal) process (e-h in Figure 1). These functions are saved and solved for the amplitude "a" (see g in Figure 1) and period "τ" (see g in Figure 1). The Sensible Heat Flux is calculated as a function of a/τ.

The instrumentation established on the platinum tailings impoundment beach is illustrated in Figure 2.

The instrumentation was raised on stands to allow for the deposition of a tailings slurry layer (Figure 3). The observation period lasted for 68 days comprising 25 days prior to deposition, 16 days of deposition and 27 days post deposition. At the cessation of deposition, the tailings reached the lower of the two fine-wire temperature sensors (Figure 4), but consolidated some 0.3 m post deposition. During the data processing, allowance was made of the changing distance between the tailings surface and the fine-wire temperature sensors.

Results

The results of the actual evaporation derived from the Surface Renewal data are compared to the potential evaporation in the form of A-Pan estimates, made from applying the Penman-Monteith equation to the meteorological data observed during the test period (Figure 5).

The actual evaporation falls well below the potential at the start of the observation over dry tailings. Even after the slurry deposition

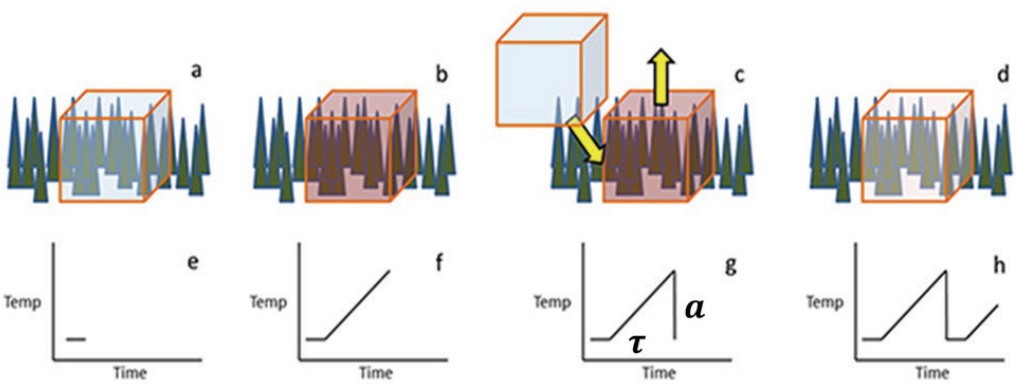


Figure 1 *Illustration of the Surface Renewal process and temperature trace*

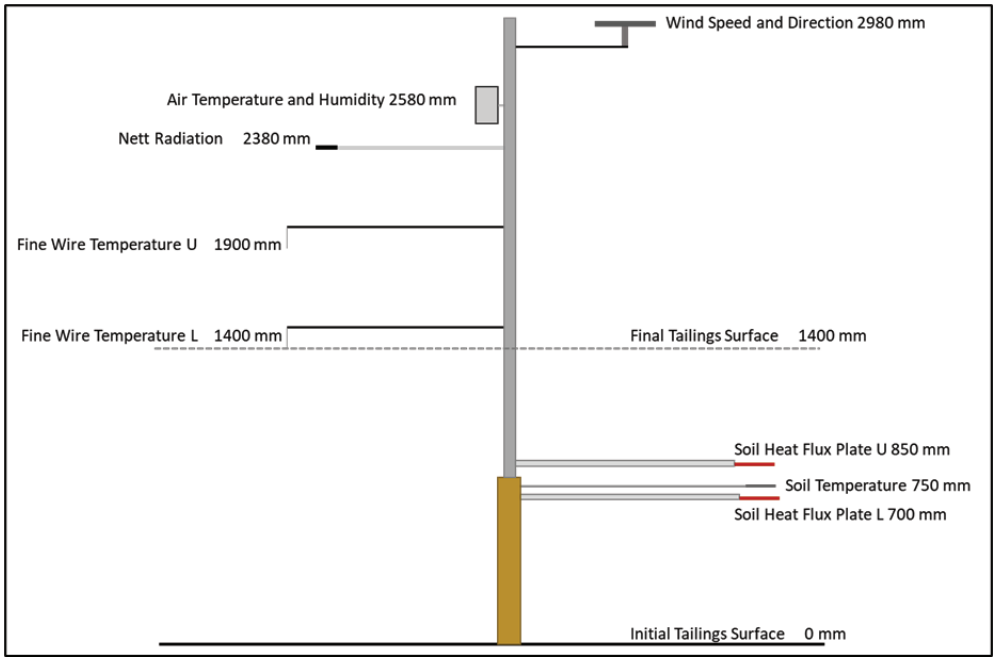


Figure 2** Instrumentation positions **for the Surface Renewal station



Figure 3** Surface Renewal **station at the start of the observations



Figure 4** Surface Renewal **station at cessation of deposition

has reached the Surface Renewal station, the actual evaporation continues to lie below the potential. This is most likely due to the albedo of the slurry limiting evaporation at potential rates. As the tailings particles settle, the water phase at the surface evaporates at the potential rate and continues to do so, even after cessation of deposition. This is assumed to occur due to the consolidating tailings resulting in a diminishing pore space, and thus continuing to provide free water (fully saturated water) to evaporate at the potential rate. As the drying and draining processes progress, however, evaporation becomes lower that potential, as the hydraulic properties of the tailings result in increasing pore water tension. Where the atmospheric demand drops significantly, though, the actual evaporation matches the potential, even though unsaturated conditions prevail.

The assumed progress of the actual/potential evaporation ratio is illustrated in Figure 6. The observed evaporation ratio is shown in blue line with red markers. The

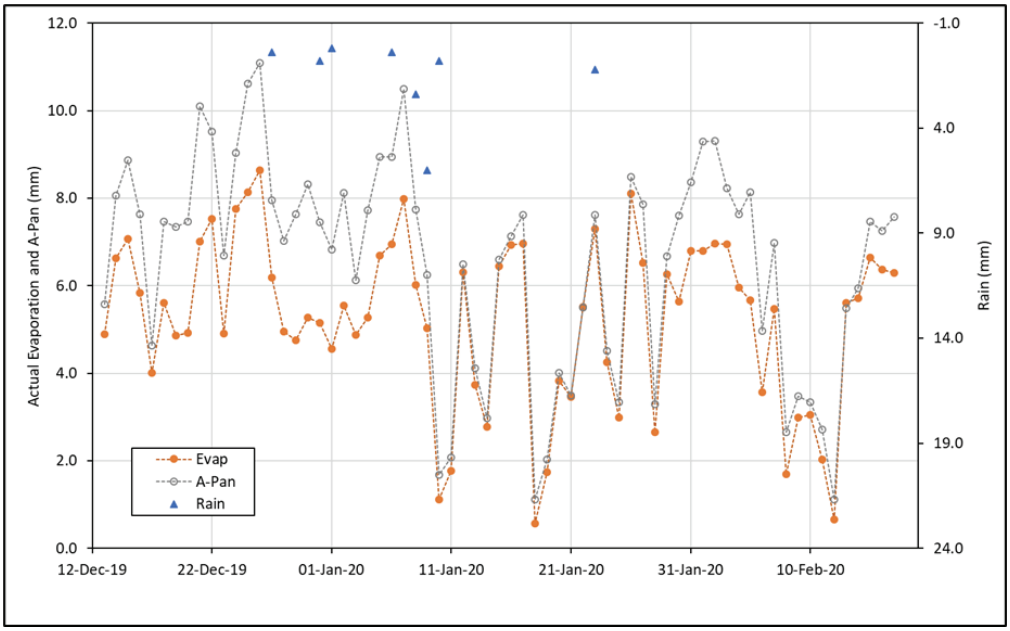


Figure 5 *Results of the actual evaporation, (Evap) and potential evaporation (A-Pan).*

actual evaporation is shown the continue at the potential rate after cessation of deposition and over the initial consolidation and drying phase. In a rigid soil or porous media, the evaporation rate would start diminishing as soon as water application or rain ceases, as illustrated by the orange line in Figure 6.

In many instances of estimating evaporation losses from a tailings surface, during water balance calculations, a general rule-of-thumb is used, in which a ratio of 0.8 is assumed for a wetting beach and 0,2 for a drying beach, as illustrated by the grey dashed line in Figure 6. It is clear that this could lead to erroneous estimations. Moreover, the parameterisation of numerical models in 2- and 3-Dimensions, to evaluate the ingress and seepage of rain and slurry water into variably saturated tailings porous media, could be significantly improved through taking into account the imbibition and evaporation fluxes derived in this study.

Indeed, recently, with the backing of the rigorous field experience described in this study, and a robust conceptual model, we have successfully implemented multiple transient iterations within multiple HYDRUS-1D models, that:

- Simulate the deposition of tailings over time, with alteration in column height, and importing of heads, saturation and mass water balance (including runoff to the pond) from previous iterations;
- Multiple model designs to represent various key locations within the tailings, depending on paddocks, under-drainage, and including beach and pond variations. Each of these can later be
- numerically upscaled to the full areal coverage for calculation of total flux and input to other models; and
- Sensitivity testing of model results using different conditions regarding climatic inputs, depositional time-series and material properties.

This multifaceted HYDRUS-1D implementation was undertaken using the PHydrus Python package (Collenteur *et al.*, 2019). An advantage of using PHydrus includes the ability to run HYDRUS-1D without interacting with the user interface manually, thus it enabled us to customise various algorithms to modify the model setup, run simulations and extract results. These algorithms additionally utilise other Python

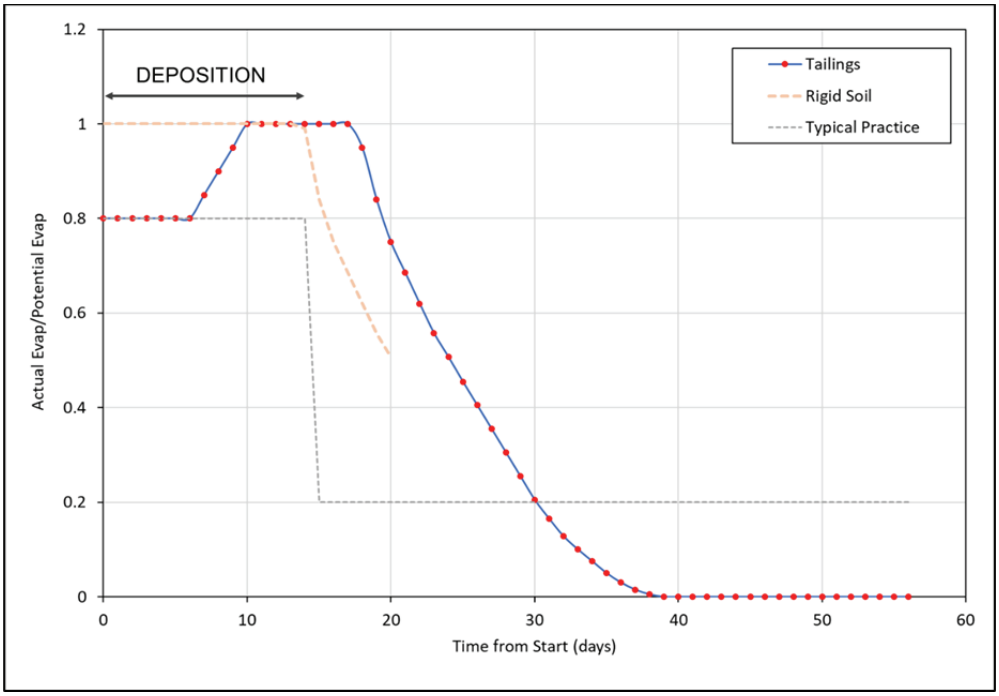


Figure 6 *Evaluation of the Actual/Potential Evaporation ratio*

libraries for data visualisation (including Plotly: Inc, 2015) to present model outputs.

Conclusions

The actual evaporation has been measured over a 60-day period pre-, during and post-deposition of platinum tailings on the impoundment beach. Guidelines have been developed to be used in water balance calculations and in detailed numerical modelling.

These techniques and findings can be applied to:

- tailings water management,
- prediction of phreatic surfaces for stability analyses and
- estimation of solute migration through and out of tailings impoundments.

Thus satisfying many of the requirements of the Global Industry Standard on Tailings Management (GISTM).

References

Collenteur, R.A., Brunetti, G., and M. Vremec (2019). Phydrus: Python implementation of the HYDRUS-1D unsaturated zone model. [Available Online: https://github.com/phydrus/phydrus]

Hu,Y., Buttar, NA., Tanny, J., Snyder, RL., Savage, MJ. and Lakhiar, IA. (2019). Surface Renewal Application for Estimating Evapotranspiration: A Review. Advances in Meteorology V2018. Article 1690714, pp11.

Inc., P.T., (2015). Collaborative data science. Available at: https://plot.ly.

Mengistu, MG. and Savage, MJ. (2010). Surface Renewal Method for Estimating Sensible Heat Flux. Water SA 36(1):9-17.

Savage MJ, (2017). Estimation of grass reference evaporation and sensible heat flux using surface renewal and Monin-Obukhov similarity theory: A simple implementation of an iterative method. Journal of Hydrology 547: 742-754

Šimůnek, J., Šejna, M., Saito, H., Sakai, M. and van Genuchten, M. Th. (2013) The HYDRUS-1D Software Package for Simulating the One-Dimensional Movement of Water, Heat, and Multiple Solutes in Variably-Saturated Media. Dept. of Environmental Sciences, University Of California Riverside, Riverside, California.

Water Column Profiles And Instrument Chains Provide Complementary Understanding Of Stratification In Pit Lakes

Mark Lund[1], Melanie Blanchette[1] and Rachele Bernasconi[1]

[1]*Mine Water and Environment Research Centre, Edith Cowan University, 270 Joondalup Drive, Joondalup 6027, Western Australia, m.lund@ecu.edu.au*

Abstract

In pit lakes, stratification is normally investigated using 'spot' water column profiles, whereas continuous monitoring of stratification using instrument chains (ICs) is uncommon. This research evaluated the benefits of using ICs in conjunction with spot profiles.

We collected temperature and conductivity profiles through spot measurements and ICs from 3 pit lakes in 2019-2021 from the major Australian coalfields in New South Wales and Queensland.

ICs revealed temporary mixing and rain-driven turnover in the lakes that were missed with spot profiles. However, ICs required regular maintenance, instrument failures limited the data, and sensor fouling was problematic. Combining water column profiles and IC data improved insights into the limnology of these lakes.

Keywords: Limnology, rain events, mixing, thermal stratification

Introduction

Thermal stratification results in pit lakes being divided into layers with minimal interaction between those layers, allowing different chemistries to develop (Boehrer and Schultze 2008). Salinity stratification has been of particular interest to pit lake scientists as the monimolimnion potentially will never mix with the rest of the lake and so is a stable place to store waste materials (Schultze et al. 2011). From a biological perspective, one aspect of stratification is that the hypolimnion or monimolimnion can become hypoxic to anoxic due to either chemical or biological oxygen demand. These low-oxygen environments are 'out-of-bounds' to most freshwater organisms, other than bacteria, limiting total habitat availability and therefore populations.

Stratification is typically measured using a multi-parameter instrument lowered vertically through the profile (e.g.Balistrieri et al. 2006; Kennedy and Johnstone 2018). The use of multiparameter probes can also highlight other important physico-chemical changes with depth such as in pH, ORP, dissolved oxygen and chlorophyll a. Deep chlorophyll a maxima occur in pit lakes (Tittel et al. 2003) and are missed with simple surface sampling but with a suitable probe can be detected in spot profiles (Lund and Blanchette 2018). Spot measurements can be collected at multiple sites across the lake and may record internal waves and seiches (Boehrer and Stevens 2005). In Lake Kepwari (Collie, Western Australia) we found that spot profiles revealed likely discharges of groundwater at particular depths through slight declines (100-200 µS cm-1) in electrical conductivity (hereafter called conductivity) (Lund and Blanchette 2018).

Monitoring water quality in pit lakes is rarely a priority unless they are discharging, and due to the work health and safety challenges of boating, monitoring is often restricted to one site at the lake's edge (but see Castendyk et al. 2020). Water quality models are widely used in closure planning and need to be calibrated against real data for the lake (Imberger 2004), and the absence of profiles or bottom samples limits that ability. Therefore, using a variety of sampling techniques that cover the area of the lake over time are likely to yield a more complete picture of the lake's water quality. Imberger (2004) proposed the use of an instrument chain designed specifically to provide data for modelling of stratification, that captured specific weather

and water column parameters and supplied these in real time. Designing environmental sampling to improve water quality modelling is covered in detail by Oldham (2014). Despite advances in technology, the cost of instrumentation for water quality remains high and is still relatively complex to maintain and install. In active lease areas where pit lakes are many years from closure, it is hard to justify installation of complex real-time monitoring stations for measuring stratification, therefore the opportunity is lost for companies to build up data that could ultimately inform their closure planning, and capture events that would otherwise be missed.

We have approached the challenge of monitoring pit lakes by developing instrument chains that are relatively inexpensive (≈AUD$10,000 each) and relatively low maintenance (Lund and Blanchette 2018). Our chains focus on in-lake parameters and contain sensors for temperature, light, conductivity, dissolved oxygen, and depth that are off-the-shelf, and self-contained with logging capability. Removing real-time reporting and use of independent battery powered loggers simplifies the chain design. The use of independent loggers allows as many sensors to be used as needed and allows sensors to be easily relocated along the chain if the lake depth changes substantially or to target specific depths. Our chains can be typically serviced at 3–6 monthly intervals and are recommended to be accompanied by at least one spot profile near the chain for calibration purposes. Limited regular calibration of the sensors is required. These independent loggers are typically lower in precision and accuracy compared to the system designed by Imberger (2004) but is sufficient to still provide valuable insights across more sites for lower cost.

In this paper, we show how data collected from both spot profiles and low-cost instrument chains provides complementary and valuable insights into pit lake limnology.

Methods

Study area

Three Australian coal mine pit lakes were selected for this study, one (HL1) from the Hunter Basin (21, 500 km2) in New South Wales, and two (BL1, BL2) from the Bowen Basin (60, 000 km2) in Queensland (see Blanchette and Lund 2021, for more details). The Hunter Basin is in Köppen climate type Cfa (humid subtropical, mild with no true dry season and hot summers), with rains typically occurring during summer (Peel et al. 2007). The Bowen Basin is within Köppen climate type BSa (arid steppe, with hot summer) with predominantly summer rainfall (Peel et al. 2007).

None of these lakes had been rehabilitated at the time of sampling 2019-2021. HL1 was actively used for water storage and the other lakes used occasionally for water management. HL1 was approximately 20 years old at the time of sampling, BL1 was still filling, and BL2 was 10 years old. Aspects of the data for this paper were originally published in Blanchette and Lund (2021) and are re-written with an emphasis on practical application.

Sampling

An instrument chain was installed in each of the three lakes in early 2019 to investigate stratification (chains described in Blanchette and Lund (2021)). Each chain collected data on surface and bottom electrical conductivity, and temperature at a variety of depths. The instrument chain was serviced and downloaded during sampling trips (see below).

The lakes were sampled quarterly (February, May, August and December) in 2019, at three sites approximately equidistant across each lake which included the deepest location. On each occasion, an in situ spot physico-chemical profile was collected through the entire water column using a Hydrolab Datasonde DS5 multiparameter instrument (Hach, Austin, USA). Water column profile data were: temperature, pH, dissolved oxygen (mg L-1 and % saturation; luminescent), conductivity standardized at 25 ˚C and oxidation-reduction potential (ORP, platinum electrode).

Results and Discussion

Spot profiles

All three lakes were thermally stratified yet not salinity stratified during summer with winter mixing (Figure 1). Only HL1 developed anoxia in the hypolimnion, with

the other lakes showing no substantive decrease in hypolimnetic dissolved oxygen concentrations. pH varied by <1 in all lakes down the profile. All profiles showed positive ORP values across all lakes and times. In HL1, the high ORP might be linked to the presence of NOx (mean 65 µ g L^{-1}) in the bottom waters. Hypolimnetic anoxia in HL1 resulted in a moderate increase in conductivity, whereas in the other lakes high evaporation rates resulted in small (100-200 µS cm-1) increases in surface waters that had insufficient impact on water density to overcome the thermal gradient (Figure 1).

Instrument Chains

Heat maps showing the stratification in all the lakes can be seen in Blanchette and Lund (2021). In summary from Blanchette and Lund (2021) HL1 was thermally stratified between February and early March 2019, was 'mixed' from April-September, and re-stratified in early October to November. BL1 was thermally stratified over the spring/summer (late September to March), completely mixed from late March-June, and then weakly thermally stratified (19–21°C) in July and August. The hypolimnion started at 17m. BL2 was thermally stratified for most of the study except between late April and late May when the lake mixed. The hypolimnion formed at about 4 m. During winter, thermal stratification was weak with only 1–2°C difference between top and bottom.

Temperatures during both stratification events in HL1 ranged from a high of 27°C at the surface to a low of 12°C at the bottom, with bottom waters increasing briefly to a

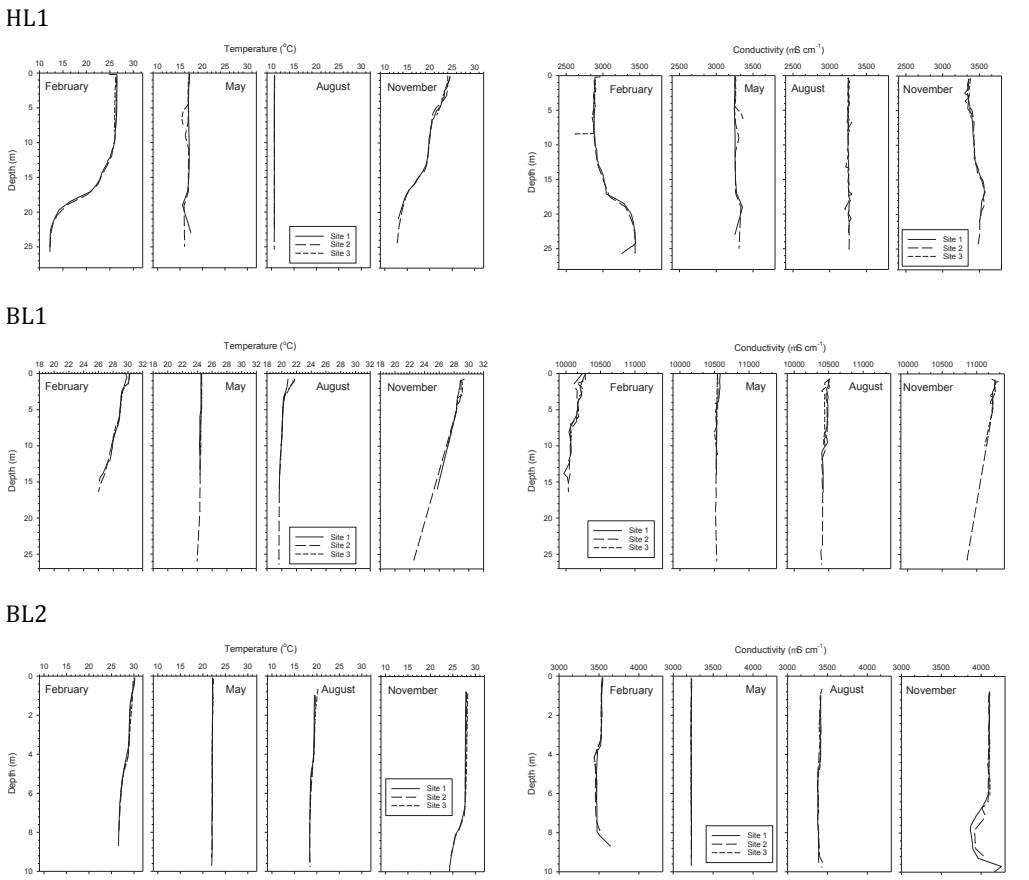


Figure 1 *Water profiles for temperature (left) and conductivity (right) for HL1, BL1 and BL2 lakes measured at three sites (1 to 3) in 2019 (n.b., in November, equipment issues meant that profiles in BL1 were measured at approximately 0.5 m intervals to 5 m and then a single bottom sample was collected using the Kemmerer bottle which may mask trends between 5 m and the bottom).*

high of 18°C due to mixing. To investigate the phenomenon of warm surface water moving to the bottom of the lake prior to complete mixing, first we compared rainfall events to lake temperatures from February to April (Figure 2). Sporadic small rainfall events followed by one large rain event in March (40mm on 30/3/2019, Ulan Water, Australian Bureau of Meteorology (BOM) 2020) coincided with a rise in temperature in water at the bottom of the lake. However, surface water temperature declined at the same time bottom water temperature was rising (Figure 2) and therefore rainfall did not appear responsible for the observed increase in bottom water temperatures. Secondly, comparing minimum air temperature between March and April 2019 was difficult due to missing data in April, although April did have a few substantially cooler days than March. As air temperature cooled, the top 1 m layer of the lake cooled, but did not reach the same temperature as the bottom water which would have triggered full mixing. During stratification, bottom conductivities were ~500 µS cm-1 higher than surface waters indicating that weak salinity and strong thermal stratification occurred simultaneously (Figure 2). The rainfall in late March resulted in a temporary increase in conductivity of surface waters, presumably from surface runoff (Figure 2). Although the rainfall did not directly result in any obvious mixing, variability in both bottom temperatures and conductivity increased indicating small amounts of mixing. This mixing was probably caused by overnight cooling of surface waters plunging through the water column, pulling lower conductivity and warmer waters down with them. This small scale mixing increased bottom temperatures and reduced conductivity over time allowing the lake to mix completely by start of May. The salinity stratification was not sufficient to prevent mixing.

Instrument chain surface conductivity loggers generally reflected the spot profile observations (Figures 1 & 2). However, after the May 2019 sampling, there were substantial increases in conductivity at 33 m in BL1 to approx. 15,000 µS cm^{-1} that returned to baseline (approx. 10,500 µS cm^{-1}) in the August sampling before increasing again to approx. 15,000 µS cm^{-1} (Figure 3). A similar pattern in conductivity was observed in surface conductivity in HL1 which appeared to reflect instrument drift correction from using spot profile data. High drift appeared to be due to observed biofouling on the sensors, which in HL1 was due to algae and in BL1 was a deposition of a hard precipitate (believed to be a carbonate, as it dissolves readily in acid with odourless gas evolution potentially CO_2). Biofouling in some lakes limited reliable data collection times.

The effect of a 100-mm rain event in March 2019 at lakes BL1 and BL2 likely influenced surface and bottom water temperatures and conductivity (Figure 3). In BL1, the rain event resulted in a ~2,000 µS cm^{-1} drop in

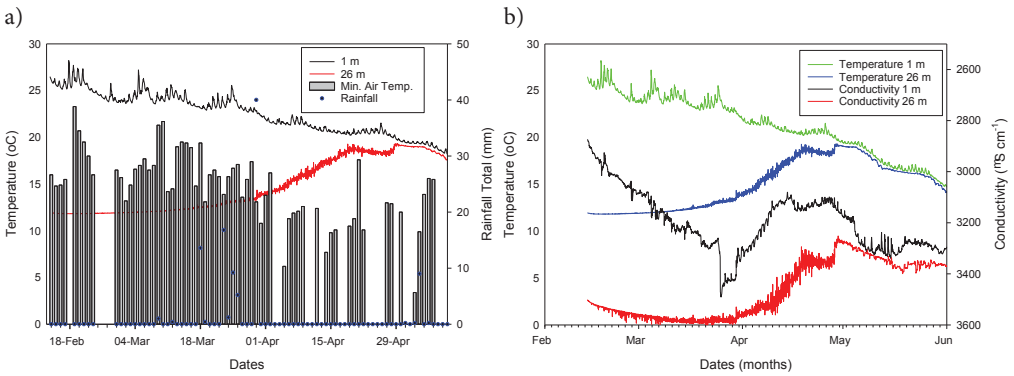


Figure 2 *In 2019 for HL1, a) water temperatures at surface (1 m) and bottom (26 m), with minimum daily air temperatures (Gulgong Post Office, BOM 2020) and daily rainfall (Ulan Water, BOM 2020) between February and May and b) water temperature (1 and 26 m) and conductivity (surface and bottom; inverted axis – to reflect increasing water density) for the winter mixing event*

a) BL1

b) BL2

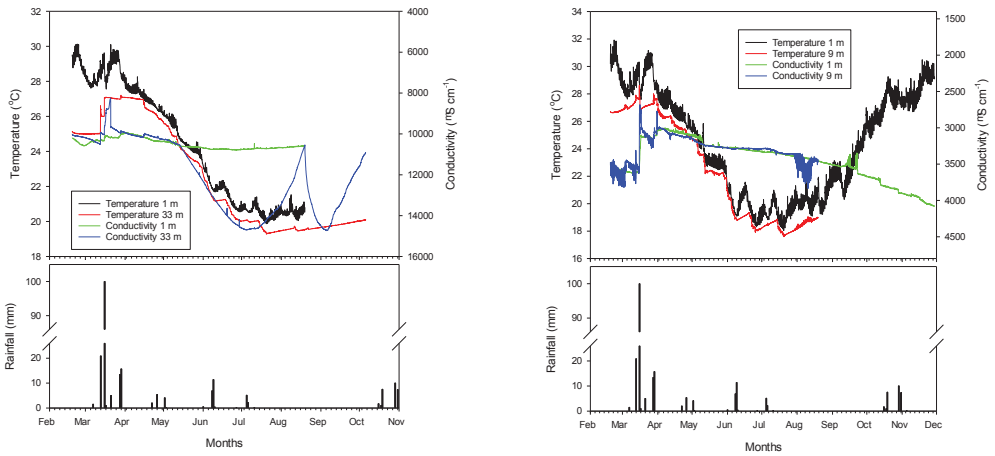


Figure 3 *Daily rainfall, and surface (1 m) and bottom (33 m, 9 m respectively) conductivity and temperature in a) BL1 and b) BL2 in 2019 (Note the inverse conductivity scale to reflect density).*

conductivity at 33 m. The lowest conductivity reading at 33 m (approx. 8,000 µS cm 1) was reached 5 days after the rainfall event, although this pattern was not replicated in the surface waters. By day 6 conductivity rose by ~1,000 µS cm^{-1} and then slowly reached surface conductivity levels 11 days after the rain event (Figure 3). Examining individual sensor data in Figure 4, temperatures increased in the hypolimnion (23 and 33 m) but declined in the metalimnion and epilimnion (12, 9, 6 and 3 m). Rain and lake water interaction likely occurred when 1) rainwater (about 27°C) cooled the surface waters and 2) water washing down the steep highwalls plunged to the lake bottom, diluting the hypolimnion, reducing conductivity, and increasing temperature causing mixing. Essentially, warm rainwater pushed the bottom water upwards (thermal contour map – Figure 4). Although the high air temperature subsequently does re-establish a slight thermal gradient, it is short-lived. Lake BL2 was shallower, and the temperature gradient was re-established more quickly than at BL1, partially as bottom waters only briefly increased in temperature before dropping to temperatures lower than before the event. The steep walls and larger catchment of BL1 probably resulted in a larger inflow of rainwater than in BL2 which might explain the longer-term effects of the rain event at BL1 than BL2.

Conclusions

Spot profiles of physico-chemical properties provide reference values for calibration of instrument chain sensors and can include a broader range of sensors at lower cost (e.g. ORP, Chlorophyll a) than instrument chains. We found that instrument chains need to be serviced at 3–6 monthly intervals due to biofouling of both conductivity and oxygen sensors, although temperature sensors appeared unaffected and could survive up to 1 year depending on the battery. For relatively low cost and minimal intervention, instrument chains provide insights into mixing processes that would otherwise be missed with spot profiles alone. For example, instrument chains revealed he importance of intense rainfall events to mixing, how weak stratification was maintained most of the year in BL1 and BL2, and how bottom temperatures can rise prior to mixing. Therefore, the use of both spot profiles and instrument chains complements our understanding of basic limnological processes in pit lakes with benefits for improved models and closure outcomes.

Acknowledgements

This research was funded by the Australian Coal Association Research Program and supported by several mining companies and Edith Cowan University. Blanchette and Lund (2021) previously

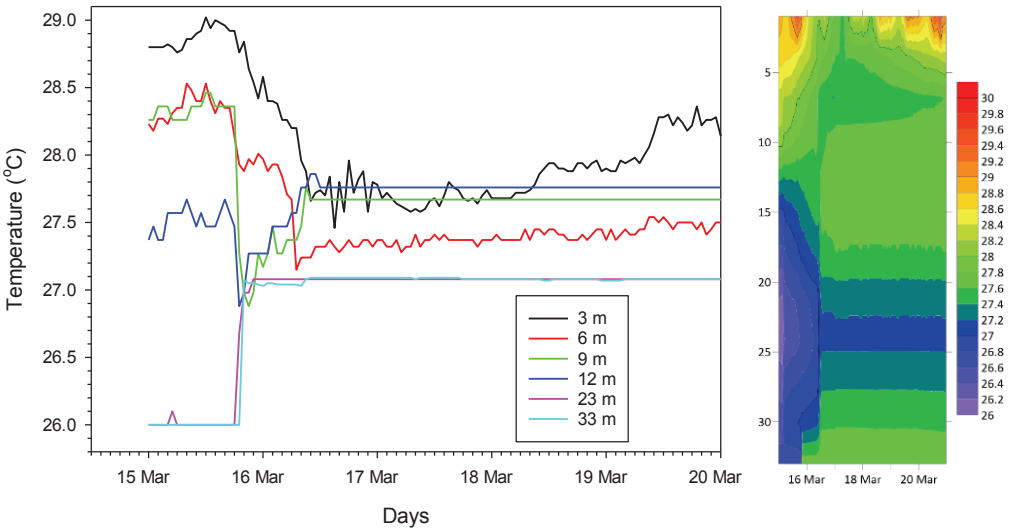


Figure 4 *Water temperatures with depth at BL1 before and after the 100 mm rain event (on 15 March 2019).*

examined the microbial dynamics of the study lakes and water quality as cited in text.

References

Balistrieri LS, Tempel RN, Stillings LL, Shevenell LA (2006) Modeling spatial and temporal variations in temperature and salinity during stratification and overturn in Dexter Pit Lake, Tuscarora, Nevada, USA. Applied Geochemistry 21(7):1184-1203. https://doi.org/https://doi.org/10.1016/j.apgeochem.2006.03.013

Blanchette ML, Lund MA (2021) Aquatic Ecosystems of the Anthropocene: Limnology and Microbial Ecology of Mine Pit Lakes. Microorganisms 9(6):1207

Boehrer B, Schultze M (2008) Stratification of lakes. Reviews of Geophysics 46(2). https://doi.org/10.1029/2006rg000210

Boehrer B, Stevens C (2005) Ray waves in a pit lake. Geophysical Research Letters 32(24). https://doi.org/10.1029/2005gl024678

Castendyk D, Voorhis J, Kucera B (2020) A Validated Method for Pit Lake Water Sampling Using Aerial Drones and Sampling Devices. Mine Water and the Environment 39(3):440-454. https://doi.org/10.1007/s10230-020-00673-y

Imberger J (2004) A Lake Diagnostic System for Managing Lakes and Reservoirs. Water Resources IMPACT 6(1):7-11

Kennedy L, Johnstone A An investigation of the water quality of four coal mine pit lakes in South Africa. In: Wolkersdorfer C, Sartz L, Weber A, Burgess J, Tremblay G (eds) 11th ICARD & IMWA Annual Conference Mine Water – Risk to Opportunity, Pretoria, South Africa, 2018. Proceedings, vol 1. Tshwane Univeristy of Technology, 647-653 p

Lund MA, Blanchette ML (2018) C23025 Coal pit lake closure by river flow through: risks and opportunities, Report № 2018-3. Edith Cowan University, Perth,

Oldham C (2014) Environmental Sampling and Modelling for the Prediction of Long-term Water Quality of Mine Pit Lakes. UWA Publishing, Perth, Western Australia

Peel MC, Finlayson BL, McMahon TA (2007) Updated world map of the Köppen-Geiger climate classification. Hydrology and earth system sciences discussions 4(2):439-473

Schultze M, Boehrer B, Friese K, Koschorreck M, Stasik S, Wendt-Potthoff K (2011) Disposal of waste materials at the bottom of pit lakes. Paper presented at the Proceedings of the Sixth International Conference on Mine Closure, Alberta:555-564. https://doi.org/10.36487/ACG_rep/1152_58_Schultze

Tittel J, Bissinger V, Zippel B, Gaedke U, Bell E, Lorke A, Kamjunke N (2003) Mixotrophs Combine Resource Use to Outcompete Specialists: Implications for Aquatic Food Webs. Proceedings of the National Academy of Sciences of the United States of America 100(22):12776-12781

Experience and outcomes of a mine water pumping test including temporary High Density Sludge treatment at Thorpe Hesley, Yorkshire, UK

Sarah F. L. Lynch, Michael Cox, Louis Warnes and Christopher J. Satterley

The Coal Authority, 200 Lichfield Lane, Mansfield, Nottinghamshire, NG18 4RG

Abstract

Modular, high density sludge (HDS) treatment was chosen to meet permitted discharge limits during a six month pumping test at Thorpe Hesley, Yorkshire. Modular HDS treatment was favourable because it was temporary, with a relatively small footprint and the resilience to treat significant changes in iron content. Pumping successfully controlled water levels within a 3.5 km radius and provided chemical data to allow the design of a passive treatment scheme. Innovative solutions to challenges were required for this novel approach to treatment. Lessons learned will benefit future pumping tests where treatment of total iron is required under similar constraints.

Keywords: Pumping test, temporary treatment system, high density sludge, mine water treatment

Introduction

Thorpe Hesley, South Yorkshire, was the site of Smithywood Colliery (active 1886–1974), situated to the east of Chapeltown, South Barnsley, (Figure 1). Mining undertaken at Smithywood colliery was relatively shallow and abandoned earlier than deeper collieries to the east. Most of the water reaching the deeper mines of the South Yorkshire coalfield was from recharge waters in the shallow area to the west of Thorpe Hesley. Thorpe Hesley was retained by the National Coal Board as a pumping station to intercept the water flowing eastwards towards the deeper mines such as Kilnhurst (Figure 1). Pumping from shallower depths at Thorpe Hesley, rather than from the deeper mines, was justified because of the lower capital and operational costs and better water quality having shorter residence time in the workings. Pumping ceased at Thorpe Hesley in 1988.

Since cessation of pumping, the mine water levels have been monitored. Mine water in the shallower mining area surrounding the village of Thorpe Hesley is considered to have completely recovered, there are no known risks within this area. Instead the risks associated with mine water rise are related to the contribution to the recharge of the deeper mine waters to the east.

Coal Authority hydrogeological investigations concluded that complete recovery of water levels in the deeper mining area to the east would result in a major surface discharge via the Kilnhurst pumping shaft located in a low lying position within the Don Valley that would subsequently reach the River Don via the Kilnhurst Cut of the Sheffield and South Yorkshire Navigation (canal). Also, if levels rise sufficiently, saline mine water would intrude into a Principal Aquifer within Cadeby Formation bedrock that overlies the coal measures and is currently exploited as a major source of drinking water. Based on the rising mine water trend at Kilnhurst there is a need to have gained control of mine water levels by 2030.

To mitigate the identified risks of mine water recovery in the deeper mining area to the east of Thorpe Hesley a pumping test was proposed. Thorpe Hesley was an ideal location and chosen because the pumping station was historically effective at controlling mine water levels and therefore it was expected to have good connectivity into wider mine workings; it is located to the east of recharge waters and therefore pumping would intercept mine water travelling eastwards towards the deeper mine waters. The site is owned by the Coal Authority and a pumping test could therefore

commence relatively quickly without the need for lengthy land purchase negotiations.

Pumping commenced in November 2021 and the test ran for six months. Key objectives were to:

- Confirm the connectivity of the wider workings and determine the effectiveness of pumping at the site in controlling mine water levels;
- Record the flow rates required to control mine water rise;
- Monitor and record mine water chemistry over the pumping test to feed into a permanent treatment design.

Mine water sampling undertaken from No.2 shaft at Thorpe Hesley in May 2018, provided the parameters used to predict mine water chemistry (Table 1). Treatment choice was based on the results of this sampling. However, uncertainty surrounded potential changes to mine water quality during the pumping test and there was a possibility that iron concentrations could double (at least).

Iron concentration recorded in the shaft was too high (≈ 15 mg/L) to release to a small brook that had been designated as the discharge location due to a sensitive receptor, Morley Ponds, (a series of commercial angling ponds), ≈ 800 m downstream of discharge. Therefore treatment prior to discharge was necessary to meet the Environment Agency Permit limit of 5 mg/L total iron and 50 mg/L total suspended solids (TSS) in the effluent.

Hydrogeological modelling, undertaken prior to the pumping test, indicated that maintaining a flow rate of 50 L/s during the pumping test at Thorpe Hesley would be sufficient to control mine water levels in the area. This was the maximum rate of discharge permitted by the Environment Agency.

Predicted mine water chemistry, and flows required to control water levels

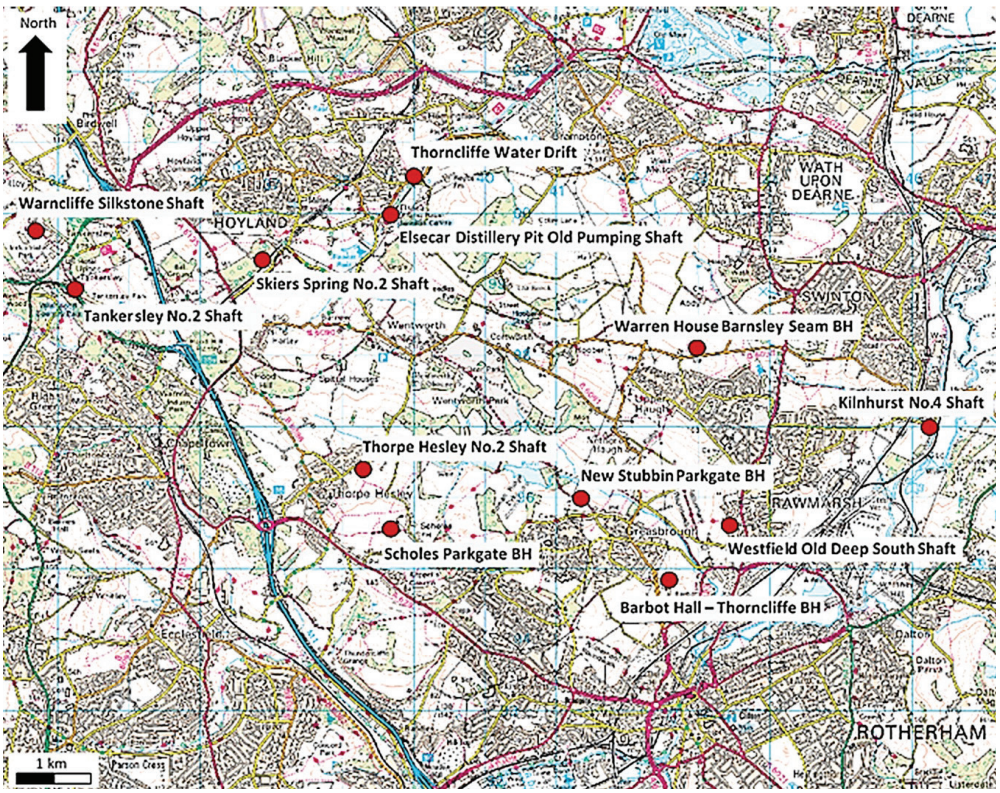


Figure 2 *Water level monitoring sites including Thorpe Hesley No.2 shaft (base map reproduced by permission of Ordnance Survey Licence Number 100020315).*

indicated that a passive treatment scheme was feasible and this is the preferred option long term. However a temporary modular HDS treatment scheme was favoured for the short duration pumping test due to:

- Land availability – procuring sufficient land for a passive treatment scheme would have required lengthy negotiations with the current owners and delayed the programme targets. Whereas the temporary active treatment plant could be built within the footprint of Coal Authority land-holding.
- Planning – some adjacent land areas are green belt land and added significantly to the programme risk of developing a passive treatment scheme at Thorpe Hesley. Whereas, deployment of a temporary active treatment system on existing Coal Authority land was deemed as permitted development.
- Outcome uncertainty – there was uncertainty regarding how effective pumping at Thorpe Hesley would be in controlling water levels within the wider area. Using a temporary active treatment system meant should the pumping test not be fully successful system could be relocated.
- Mine water quality variation – there was the potential for significant mine water quality variation during the pumping test. Active treatment processes are more resilient to significant changes in iron content in the mine water than passive treatment processes.

Temporary modular high density sludge (HDS) treatment system design

JN Bentley Ltd, the principal contractor assigned by the Coal Authority, sub-contracted Siltbuster Ltd to design and build a temporary HDS treatment system. The process plant and equipment, supplied by Siltbuster, was housed in shipping containers. The treatment plant occupied an area of ~700m^2.

Mine water was pumped from No.2 shaft via a borehole pump mounted 75 mBGL. Flow rate varied between 10–15 L/s at the start of the pumping test, to allow a period of treatment adjustment and calibration, and increased up to a maximum of 50 L/s. A two stream treatment system was used each stream treating up to 25 L/s flow (Figure 3). This approach to operating meant the plant could run at minimum required capacity potentially saving on the operational costs of running large mixers in low load conditions and enabled continuity of treatment if one stream encountered operational issues.

Treatment was designed to oxidise up to 100 mg/L dissolved iron, and precipitate it as iron oxyhydroxide, resulting in an effluent water containing < 3 mg/L total iron. Each treatment stream had a MT100 mix tank

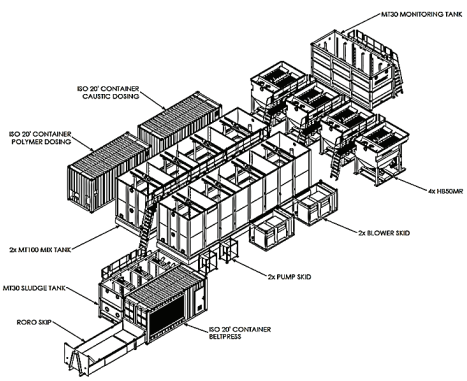


Figure 2 *HDS Plant Layout Design Note. Install. included a plate and frame press, not a belt press.*



Figure 3 *Containerised Temporary Plant Setup (stream A right, stream B left of photo)*

Table 1 Shaft mine water chemistry (180 mBGL) (prior to pumping test) and Pumped mine water chemistry (raw and treated)

	Pre-pumping	Pumped mine water (Raw)						Pumped mine water (Treated)				
Analyte	Shaft sample	Mean	Max	Min	Std. Dev.	90th Percentile	Count	Mean	Max	Min	Std. Dev.	90th Percentile	Count
Iron, Total (mg/L)	14.8	11.39	16	7.77	1.60	12.86	50	1.13	3.49	0.01	0.82	2.25	50
Iron, Dissolved (mg/L)	13.9	10.44	14.1	6.28	1.42	11.4	48	0.08	0.68	0.01	0.14	0.17	50
Chloride (mg/L)	110	84	102	71	6.04	90	50	90	116	72	7.24	95	50
Sulfate (mg/L)	991	1,017	1,160	904	59.98	1,090	51	1019	1150	907	59.86	1091	50
Manganese, Total (mg/L)		1.24	1.52	0.84	0.11	1.38	51	1.21	1.51	0.98	0.11	1.34	50
*Manganese, Dissolved (mg/L)		1.25	1.57	0.83	0.12	1.43	51	1.21	1.53	0.98	0.11	1.31	50
Alkalinity, as Calcium Carbonate (mg/L)	573	569	655	467	38.69	602	51	668	819	523	67.25	744	51
pH	7.0	6.48	6.97	6.00	0.21	6.19	157	7.02	8.1	6.25	0.37	6.75	157
Conductivity µS/cm	3070	2,910	3,165	2,679	81.25	3,004	157	3010	3285	1674	163.04	3172	147
Temperature °C	14.6	13.0	17.3	10.2	1.1	14.1	156	12.58	16.55	9.25	1.31	13.99	156

*Dissolved manganese is higher than total, but within analytical error of the instrument.

that combined the mixing and pH adjustment stages. In the first section mine water mixed with the re-circulated ochre sludge. The resulting mixture flowed into the second section where 20% w/w sodium hydroxide was added to raise the pH together with aerial oxidation via a blower system.

Hydraulic retention time (HRT) of water in the MT100 mix tank was ≈ 80 minutes whilst running at 25 L/s. An anionic polymer was added to encourage flocculation as the water passed through to two lamella tanks (HB50MR Settlement Units) for settlement of the solids.

Settled sludge was expected to have a dry solids content of ≈ 12% w/w. Sludge was then either re-circulated to the first section of the MT100 mix tank at a mass ratio of 50:1 total iron oxyhydroxide concentration in the mine water, or pumped to a plate and frame press capable of producing a dry solids content of up to 45% w/w.

Following clarification the treated effluent from both streams was directed to a baffled monitoring tank with a Programmable Logic Controller system set to recirculate treated mine water back to shaft if TSS exceeded 25 mg/L (50 mg/L at the start of the pumping test) and/or pH went out of permitted range (pH 6 to pH 9).

Hydrogeological and geochemical findings – summary

Pumping at an abstraction rate of 50 L/s resulted in a maximum drawdown of 5.55 m within Thorpe Hesley No. 2 shaft. Over a wider 3.5 km radius from Thorpe Hesley (Figure 1), pumping was found to control the water level at two sites, New Stubbin, located ≈ 3 km east, and Skiers Spring just under 3.5 km north west, of Thorpe Hesley No.

2 shaft. Water levels were not controlled at Scholes Parkgate despite it being the closest monitoring site to Thorpe Hesley. This is likely due to poor hydraulic connectivity within the workings. Overall influence of pumping at Thorpe Hesley on water levels over a radius wider than 3.5 km was uncertain and longer term pumping (over years) would be required to confirm control.

Hydrogeological drawdown, through pumping at Thorpe Hesley, was found to align with previous predictions for Thorpe Hesley, by intercepting mine water before it migrates to the deeper mine workings to the east. Therefore it was recommended that long term mine water treatment options were explored to enable continued pumping at the site.

Water monitoring was undertaken at four locations, from the inlet pipe prior to treatment (raw mine water), the monitoring tank (treated mine water), 20 m downstream from discharge and at Morley Ponds (a downstream sensitive receptor).

Results from the raw mine water monitoring indicated there was no major variation in mine water chemistry in response to flow rate change (Figure 4). Average total iron was 11.4 mg/L of which ≈ 90 % was in dissolved form (Table 1). A maximum of 16 mg/L total iron was recorded on three occasions while pumping at 50 L/s. Total suspended solids were generally quite low (15.9 mg/L average). Throughout the trial raw water pH remained ≈ pH 6.5. Mine water was net alkaline and sulfate and chloride showed no variation in response to pumping rate. The high percentage of dissolved iron and sulfate concentration in the mine water are reflective of partial pyrite weathering within a limited oxygen environment (Younger *et al*. 2002). The net alkaline waters served to buffer acidity and maintain a circum neutral pH. The raw mine water chemistry results indicated that treatment through a passive scheme was feasible.

HDS treatment successfully oxidised the mine water and raised the pH (Table 1). Average total iron and TSS concentration in the effluent water was 1.13 mg/L and 10 mg/L respectively. Treated mine water remained below the Environment Agency permitted discharge limit of 5 mg/L total iron

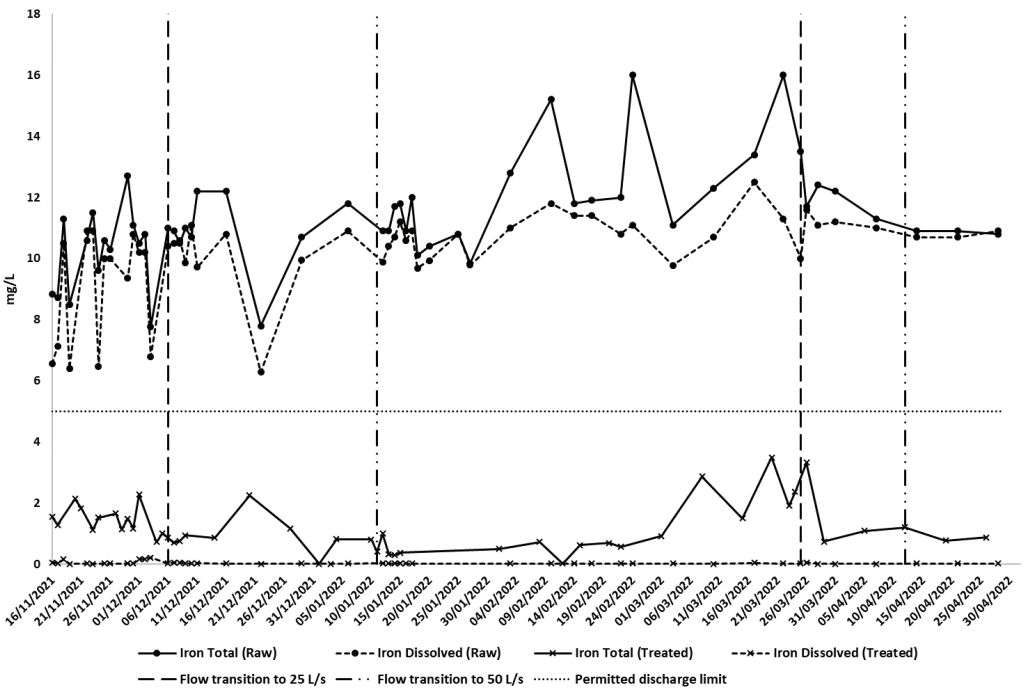


Figure 4 *Total and dissolved iron concentration in the raw and treated mine water in response to flow transitions.*

and 50 mg/L TSS throughout the pumping test. Results of water sampling undertaken at Morley Ponds indicated the treated mine water discharge did not impact water quality at that location.

Discussion (challenges and learnings)

Whilst the pumping test was successful in meeting the key objectives of the project, there were a number of challenges during the operation of the plant. The Coal Authority have experience of operating permanent or long term temporary HDS installations. However this was the first time it had used a containerised temporary HDS plant to support a pumping test.

Site specific adjustments were required to improve treatment performance when the plant was commissioned. Initially the fines in the lamella tank were not settling sufficiently for the ochre sludge to reach the optimum 12% w/w dry solids content. This hindered the re-circulation of ochre sludge to encourage further iron oxyhydroxide precipitation. Whilst the total iron content of the mine water was too high to discharge without treatment, it was too low for treatment using a high density sludge system. Ferric chloride solution was added to the MT100 mix tank to 'seed' the mine water and encourage iron hydroxide formation. Dry solids content of the ochre sludge increased and performance improved.

During commissioning the TSS alarm was triggered in the monitoring tank and water was discharged back down to shaft. Jar tests demonstrated that the sludge going to the clarifier contained two phases; an iron high density sludge that settled quickly and a 'haze' containing fine calcium carbonate crystals and 2–3 mg/L total iron. The latter was an issue because it exceeded the agreed internal site specification of 3 mg/L total iron in the discharge, but not the Environment Agency permitted limit of 5 mg/L. Prior to this the plant operated at > pH 8.4 to precipitate as much iron oxyhydroxide as possible and the sludge density was 1035 kg/m3. The operating pH was changed to pH 8, the sludge density decreased to 1020 kg/m3. Further tests showed that the treated water contained calcium ions which contributed to the observed calcium carbonate haze. At > pH 8.4 the calcium carbonate precipitated as much larger crystals that collected in the sludge. To rectify the situation the plant was run at ≈ pH 8.7, with the aim of precipitating calcium carbonate and flocculating it to form larger crystals that settled. The plant was run for 48 hours in this mode and when total iron and TSS concentrations were below internal discharge limits the treated water was discharged to stream. With sufficient high density sludge recirculated to collect the calcium carbonate the plant remained at pH < 8 for the duration of the pumping trial.

For the first three months the site was powered by a 415 V generator due to delays connecting to the electricity grid. At the time the COVID-19 pandemic was on going and it was during a period of fuel shortages. So measures needed to be taken to ensure sufficient supply of diesel particularly during sensitive periods. A second generator was installed to mitigate power loss and subsequent plant shut down especially over the Christmas holiday period.

In order to assess water level recovery rates, instantaneous changes in flow were needed. Increasing or reducing the flow rate required a period of calibration and dosing adjustment to optimise treatment. Therefore it was not possible to instantaneously modify chemical treatment. This meant that the water team, chemistry team and on site contractor needed to work in close association to accommodate all needs. At times compromises were made.

Conclusions

Novel, temporary, modular high density sludge (HDS) treatment carried out during a six month pumping test at Thorpe Hesley, Yorkshire was found to successfully control water levels within a 3.5 km radius and provided chemical data to allow for the design of a passive treatment scheme at the site.

HDS design included two streams each treating up to 25 L/s raw mine water and up to a maximum of 100 mg/L iron (although

total iron concentration did not exceed 16 mg/L). Water chemistry was not found to vary in response to flow rate. Treatment was successful and discharge waters remained within permitted consent limits of 5 mg/L total iron and 50 mg/L total suspended solids and the sensitive receptor Morley Ponds was not affected. Innovative solutions to challenges were required, particularly during commissioning and due to the ongoing COVID-19 pandemic. Lessons learned will benefit future pumping tests where treatment of total iron is required under similar constraints.

References

Younger PL, Banwart SA, and Hedin RS (2002) Mine Water Hydrology, Pollution, Remediation, Kluwer Academic Publishers.

PIRAMID Consortium (2003) Engineering guidelines for the passive remediation of acidic and/or metalliferous mine drainage and similar wastewaters. European Commission 5th Framework TRD Project no. EVK1-CT-1999-000021 "Passive in-situ remediation of acidic mine/ industrial drainage" (PIRAMID). University of Newcastle Upon Tyne, Newcastle Upon Tyne, UK

Pollution registries for mines: Current state and future needs

Ann Maest[1] and Theodor Cojoianu[2]

[1]*Buka Environmental, Vice President, Telluride, Colorado, USA aamaest@gmail.com*

[2]*University of Edinburg Business School, Associate Professor in Sustainable Finance, Edinburgh, Scotland & Member of EU Platform on Sustainable Finance and HM GTAG theodor.cojoianu@ed.ac.uk*

Abstract

A worldwide assessment of pollution releases from mines has never been conducted. This paper compares disclosure requirements and results from mine pollution registries in Europe and the United States. The available data only account for total mass releases to the environment. Although most mines collect large amounts of site-specific water quality data, the generally low availability of the data and lack of interpretation present challenges for regulators and the public. Without increased transparency of water quality data in water bodies affected by mining, the extent and effects of mine-related pollution cannot be fully understood, prevented, or mitigated.

Keywords: Mine releases, pollution registry, mine certification, U.K. screening criteria, data transparency

Introduction

The European Union (EU) is in the process of designing technical screening criteria for pollution prevention and control related to the mining and quarrying sectors. Mining has several unique characteristics when it comes to its pollution profile that distinguish it from other industrial activities and must be considered when developing pollution prevention and control criteria that will minimize pollution from mining sources and prevent or reduce mining-related pollution in water bodies. Such characteristics include unique priority and geogenic pollutants, naturally occurring mine-related contaminants, and the importance of nonpoint/diffuse pollution. Although end-of-pipe data are available across the EU, the availability of water quality data in water bodies potentially affected by mining activities is scant, and the data are not organized at the Member State or EU level.

A worldwide assessment of releases from mine sites has never been conducted, and such an assessment presents many challenges. In general, the transparency and availability of mine pollution data are low. Several sources of end-of-pipe discharge data available worldwide were reviewed. The EU maintains a pollution transparency register that includes 8000 mines in Europe and an industrial emissions directory. The portal merged data from 2017 with data from the past. The data are presented in kilograms rather than concentrations in water bodies, accounting only for total mass releases. The same applies to the US, Australia, and other jurisdictions. For example, the US Environmental Protection Agency requires mines to submit their discharges to air, land, and water to the Toxics Release Inventory (TRI). The largest dischargers to land are mining sites, but the tons of mining waste discharged does not necessarily correlate with pollutant concentrations in water bodies.

Mines around the world are collecting site-specific water quality data, but the quality and quantity of data from modern mines are beyond the capacity of regulators to evaluate. How can access to data be accomplished and be made meaningful? Site-specific water quality data are needed for responsible mining certification programs aimed at improving practices and reducing environmental effects of the sector. Without site-specific data in water bodies affected by mining, the extent and effects of mine-related pollution cannot be fully understood, prevented, or mitigated.

Table 1 Comparison of pollution registry reporting requirements in Europe and the U.S.

Reporting Requirement	European Pollutant Release and Transfer Register (E-PRTR)	U.S. Toxics Release Inventory
Required criteria for reporting	underground mines must report; opencast mining and quarrying must report if area under extractive operation ≥25 hectares.	1) in TRI-listed industry sector (includes metal mines) or federally owned/ operated, 2) ≥10 full-time employee equivalents, 3) processes >25,000 lbs or uses >10,000 lbs of TRI-listed chemical annually
Mines reporting	Mineral industry installations (including coal and metal mining)	Coal, metal, non-metallic mines
# Mines/activities reporting in 2021	141	87 (metal mines)
Releases to land	Yes	Yes
Releases to water	Yes	Yes
Releases to air	Yes	Yes
Reporting units[1]	kg/year	pounds/year
# Chemicals/ chemical categories	91	787/33
Basis for reporting	Yearly aggregations; measured, calculated, or estimated	Continuous monitoring data, periodic or random monitoring data, or mass balance calculations

Disclosure Reporting Requirements for Pollution Registries

The reporting requirements for pollution registries in Europe and the U.S. are listed in Table 1.

European registry

The primary pollution registry for mines in Europe is the European Pollutant Release and Transfer Register (E-PRTR; European Commission 2023). The E-PRTR is deeply connected to the Industrial Emissions Directive, having similar reporting obligations for the emission and transfer of pollutants that adhere to the permit conditions outlined in the directive. The functions of the E-PRTR include: 1) providing dependable and uniform data on emissions of pollutants by the industry in the EU and 2) enhancing transparency and public involvement in environmental policy making. In addition to the requirements set for individual economic activities to disclose, 91 pollutants across air, land, and water have specific disclosure requirements if the quantity released surpasses certain thresholds as per Regulation (EC) No 166/2006. Guidance for data reporting can be found in European Environmental Agency (2021). The E-PRTR, while granular on the reporting of pollutants, does not identify the type of mine that reports, and users of the registry cannot differentiate across commodities.

U.S. registry

The only national-level, mandatory pollution registry for industries in the United States is the Toxics Release Inventory (TRI) of the U.S. Environmental Protection Agency (US EPA). The metal mining sectors reporting to the TRI are covered under North American Industry Classification System (NAICS) code 2122 and include facilities mining gold, silver, lead, zinc, copper, and nickel ores; NAISC code 212299 includes many other less common metal mines that must report (e.g., Sb, Cr, Co, Mn, Pt, Pd, rare earth elements (REEs)) but does not include iron ore or uranium mines. According to the reporting guidance document for metal mines (US EPA 1999), the total amount of waste rock and tailings and an estimated amount of metal in these wastes (using estimated percentages in the wastes) must be reported to TRI on their Form R, but reporting the amount is optional. For heap and dump leaching activities, reporting is not required until the leaching activity is completed, assuming the amount exceeds threshold values (US EPA 1999). The US EPA provides reporting software with built-in data quality alerts and makes calls to facilities to evaluate reporting accuracy if certain conditions are triggered, including those with the largest changes in reporting amounts from the previous year, the largest releases to air or water, and those reporting to

Table 2 Reporting incompleteness across air and water pollutants by metal mines in the EU Member States in 2021.

Release Medium	Pollutant	Reporting Completeness %
Water	Zinc and compounds (as Zn)	22%
Air	Arsenic and compounds (as As)	18%
Air	Nickel and compounds (as Ni)	18%
Air	Copper and compounds (as Cu)	14%
Water	Lead and compounds (as Pb)	13%
Water	Total nitrogen (as N)	11%
Water	Cadmium and compounds (as Cd)	9%
Water	Chromium and compounds (as Cr)	9%
Air	Mercury and compounds (as Hg)	8%
Water	Cyanide (as total CN)	5%

other EPA or non-EPA programs but not to TRI (US EPA 2023a).

Results and Discussion

European registry

In 2021, across the 141 mining-related economic activities in Europe we find sparse reporting by most mines and countries for 27 pollutants. In 2021, data reporting for Czechia, Liechtenstein, Lithuania, Malta, Serbia, Slovakia, and Switzerland was incomplete. In addition, emissions to land have generally been very scarcely reported, and the data that are reported are incomplete (European Environmental Agency 2023). The reporting completeness[2] varies between 22% for zinc and compounds to water and 5% for cyanide to water (Table 2).

The selective reporting for metal mine pollutants by individual Member States makes comparisons across Member States difficult. The lack of access to the permit details and concentration data in water bodies related to these releases results in the poor ability of stakeholder to scrutinise the pollution record of most mining facilities in Europe. Table 3 further illustrates that across Europe, under the current disclosure regime, one could conclude that mines in Germany and Poland are the biggest polluters; however, this would likely be an unreliable conclusion given the lack of reporting completeness.

U.S. Toxics Release Inventory

The TRI does allow identification of different types of mines (e.g., coal vs metal). The results in this section refer to metal mines. The metal mining sector had the largest TRI releases of any industrial sector and accounted for 68% of land disposal and 44% of all TRI releases to land, water, and air. The largest releases by far for metal mines are to land. The metals of potential environmental interest that are required to be reported to TRI include:

- Al (fume or dust)
- Sb, Sb compounds
- As, As compounds
- Ba, Ba compounds
- Be, Be compounds
- Cd, Cd compounds
- Cr, Cr compounds
- Co, Co compounds
- Cu, Cu compounds
- Pb, Pb compounds
- Mn, Mn compounds
- Hg, Hg compounds
- Molybdenum trioxide
- Ni, Ni compounds
- Se, Se compounds
- Ag, Ag compounds
- Tl, Tl compounds
- V, V compounds
- Zn, Zn compounds

For the metals and metalloids that include "compounds," the compound itself is not required to be reported. For example, if the copper compound is CuFeS2, or chalcopyrite, approximately 35% of the compound is copper by weight. Therefore, for metal compounds, the amount of metal (e.g., copper) is less than the reported amount of the metal compound, and the actual amount of metal is not known.

[2] The percent of mines reporting a specific pollutant in their releases to land, air, or water.

Table 3 Total quantities, kg, of air and water pollutants released by mines across EU Member States (2021).

Member State	Air	Water	Air and Water	% Contribution to total pollutant discharge to air and water
Austria	789	0	789	0.01%
Belgium	217	0	217	0.00%
Bulgaria	0	4,607	4,607	0.05%
Estonia	27	0	27	0.00%
Finland	364	99	463	0.00%
France	592	4	596	0.01%
Germany	1,012,319	1,398,893	2,411,212	25.16%
Greece	113	0	113	0.00%
Hungary	125	0	125	0.00%
Ireland	16	1	17	0.00%
Italy	518,975	0	518,975	5.41%
Poland	5,208,153	1,431,485	6,639,638	69.27%
Portugal	105	0	105	0.00%
Romania	2,376	10	2,386	0.02%
Slovenia	3,501	0	3,501	0.04%
Spain	1,692	0	1,692	0.02%
Sweden	297	63	360	0.00
Total (kg released in 2021)	6,749,660	2,835,161	9,584,821	100.00%

Using all the metals listed above, in 2021 the metal mining sector released 643,952 tonnes (metric tons) to land, 27.7 tonnes to water, and 147 tonnes to air (49.5% by fugitive air emissions and 50.5% by stack emissions). Total TRI releases for the metal mining sector in 2021 for the 17 metals listed above were 1,421,728,215 lbs. The top ten metal mines in terms of releasing the 17 TRI metals to land, air, and water in 2021 are shown in Table 4.

Other chemicals used on site that do not derive from constituents in the ore or waste include nitrate and ammonia (from blasting using ammonium nitrate-fuel oil, or ANFO) and cyanide and hydrogen cyanide (used to extract gold and other precious metals from the ore). Releases of these chemicals from the metal mining sector reporting to the TRI are included in Table 5. With the exception of hydrogen cyanide, which is a poisonous liquid or gas, releases to land were higher than to air or water. The majority of the releases in Table 5 were from gold ore mining facilities, and the majority of the reporting metal mine facilities are gold mines in Nevada.

Conclusions and Recommendations for Improvement

Given that much of the emerging EU Sustainable Finance legislation includes pollution prevention as one of its key environmental objectives, having access to a usable and complete pollution registry is paramount. In this respect, we urge policymakers to enable sustainable investment decisions by mandating a better coverage of pollutant disclosures across entities, in particular the concentrations of the different discharges across air, land and water. Reporting of pollutant emissions to land is scarce in the E-PRTR but is especially important for the mining sector, as shown by the dominance of land releases from metal mines in the U.S. TRI.

Knowing the composition of metal compounds would improve TRI reporting. Additional constituents of interest for metal mines that could be added to the TRI list include radioactive elements (uranium, thorium, radon), and chemicals of interest for renewable energy, including lithium, tellurium, gallium, and certain REEs. Although uranium, iron ore, and lithium mines are not currently included in the sectors that must report their releases to the TRI,3 ores and wastes from these and other metal mines can include these constituents, and knowing the amounts in waste releases would help with environmental protection (for the radioactive constituents) and could

Table 4 *Top 10 U.S. metal mines with total TRI releases to land, air, and water in 2021.*

Facility Name	State	Metal Mining Category	Total TRI Releases (lbs)
Red Dog Operations	Alaska	All Other Metal Ore Mining	601,564,301
Nevada Gold Mines LLC – Goldstrike Mines Inc	Nevada	Gold Ore Mining	272,060,230
Kennecott Utah Copper Mine Concentrators & Power Plant	Utah	Copper, Nickel, Lead, and Zinc Mining	149,354,786
Hecla Greens Creek Mining Co	Alaska	Gold Ore Mining	70,879,234
Nevada Gold Mines LLC – Carlin South Area	Nevada	Gold Ore Mining	48,552,839
Montana Resources LLP	Montana	Copper, Nickel, Lead, and Zinc Mining	41,575,557
Nevada Gold Mines LLC-Cortez District	Nevada	Gold Ore Mining	35,958,324
Robinson Nevada Mining Co	Nevada	Copper, Nickel, Lead, and Zinc Mining	19,032,085
Nevada Gold Mines LLC – Phoenix Mine	Nevada	Gold Ore Mining	15,906,928
Nevada Gold Mines LLC – Turquoise Ridge	Nevada	Gold Ore Mining	15,311,057

Metals include (metals + metals and compounds): Sb, As, Ba, Be, Cd, Cr, Co, Cu, Pb, Mn, Hg, Ni, Se, Ag, Tl, V, and Zn. Source: US EPA, 2023b

Table 5 *Releases of nitrogen and cyanide compounds from the metal mining sector, TRI data for 2021 (US EPA 2023b).*

Chemical	Total releases lbs	Land releases lbs	Air releases lbs	Water releases lbs	Releasing metal ore mining sector
Nitrate	13,281,024	12,430,185	–	848,932	Gold (98%)
Ammonia	1,775,632	1,470,588	274,424	30,599	Gold (41.5%); Cu, Ni, Pb, Zn (1.7%); All other (56.7%)
Cyanide	1,911,473	1,887,641	23,376	–	Gold (~100%)
Hydrogen cyanide	61,996	–	61,996	–	Gold (100%)

be a first step for examining the remining potential of the wastes for renewable energy (World Bank 2020; IEA 2022).

References

European Commission (2023) The European Pollutant Release and Transfer Register (E-PRTR). https://environment.ec.europa.eu/topics/industrial-emissions-and-safety/european-pollutant-release-and-transfer-register-e-prtr_en

European Environmental Agency (2023) European Industrial Emissions Portal. About the Industrial Emissions Portal. https://industry.eea.europa.eu/about

European Environmental Agency (2021) E-PRTR and LCP Integrated data reporting Manual for reporters, Version 1.3 – 05/05/2021. https://cdr.eionet.europa.eu/help/eprtr_lcp/Documents/E-PRTR-LCP_Manual_for_reporters_v1.3.pdf

IEA (International Energy Agency) (2022) The role of critical minerals in clean energy transitions. 287 pgs. https://www.iea.org/reports/the-role-of-critical-minerals-in-clean-energy-transitions

US EPA (2023a) Toxics Release Inventory (TRI) Program. TRI Data Quality. https://www.epa.gov/toxics-release-inventory-tri-program/tri-data-quality#q2

US EPA (2023b) TRINA Dashboard. Selected Industry code 2122 (metal mines), 17 chemicals, 2021, releases to all media. https://awsedap.epa.gov/public/extensions/TRINA_dashboard_2021/TRINA_dashboard_2021.html

US EPA (2022) Factors to Consider When Using Toxics Release Inventory Data. Revised 2022. 5 pgs. https://www.epa.gov/system/files/documents/2022-02/factorstoconsider_approved-by-opa_1.25.22-copy.pdf

US EPA (1999) EPCRA Section 313 Industry Guidance. Metal Mining Facilities. Office of Pollution Prevention and Toxics. Washington, DC. January EPA 745-B-99-001. https://www.epa.gov/sites/default/files/documents/1999metal.pdf

World Bank (2020) Minerals for Climate Action: The Mineral Intensity of the Clean Energy Transition. World Bank. https://pubdocs.worldbank.org/en/961711588875536384/Minerals-for-Climate-Action-The-Mineral-Intensity-of-the-Clean-Energy-Transition.pdf

Pit Lake Water Quality Prediction: Insights into the Modelling of Non-Conservative Processes

Alan J. Martin[1] and Silvano Salvador

[1]*Lorax Environmental Services Ltd., 2289 Burrard St., Vancouver, BC, Canada, V6J 3H9*

alan.martin@lorax.ca Abstract

Abstract

The ability to accurately model pit lake water quality is a prerequisite to the development of defensible closure management strategies. In this paper, non-conservative processes that have the potential to influence the evolution of pit lake water quality are reviewed. Key topics examined include oxygen consumption, biogeochemical (redox) processes that may occur in the suboxic strata of stratified pit lakes, mineral precipitation, and lake primary production (algal growth) in relation to the scavenging of trace metals and their export to bottom waters via particle settling. A modelling platform (PitMod) that may be used to quantify non-conservative mechanisms is described. Bioremediation measures that may be employed to take advantage of naturally-occurring passive removal mechanisms are also discussed.

Keywords: Meromixis, bioremediation, redox, PitMod

Introduction

Pit lakes represent common features of the post-closure landscape at mining operations, often serving as focal points for water and waste management at the end of mine life. Pit lake systems are also complex, with the evolution of water quality governed by various physical (mixing), geochemical and biological mechanisms. Pit lake models must therefore be able to account for such processes to allow for the development of scientifically-defensible and cost-effective closure management strategies.

Numerous non-conservative processes have the potential to influence the evolution of pit lake water quality over time, including:

- Lake primary production (algal growth), binding of trace elements to biogenic particles, and particle settling,
- Oxygen consumption leading to development of suboxic bottom waters in stratified pit lakes,
- Suboxic redox processes that may occur in the suboxic strata of stratified pit lakes, and
- Mineral precipitation

In this paper, non-conservative processes that have the potential to influence the evolution of pit lake water quality are reviewed. The pit lake modelling software PitMod (Martin *et al.*, 2015; Dunbar, 2013) is used to illustrate how the effects of non-conservative mechanisms can be modelled. Bioremediation measures that may be employed to take advantage of naturally-occurring passive removal mechanisms are also discussed.

Description of PitMod Modelling Software

PitMod is a proprietary, one-dimensional numerical hydrodynamic model developed by Lorax Environmental Services Ltd. (Vancouver, Canada). PitMod is used for predicting the spatial and temporal distribution of temperature, density, dissolved oxygen, and water quality parameters in lakes, and incorporates physical processes similar to those found in other lake models such as DYRESM (Imerito 2007) and CE-QUAL-W2 (Wells, 2022). In addition to physical processes, PitMod is coupled to geochemical equilibrium model PHREEQC (Parkhurst and Appelo *et al*. 1999) for determinations of metal speciation, mineral precipitation, gas equilibria, and pH. Specifically, at each time step of the model, PitMod integrates the effect of all inputs governing the physical

properties of the pit lake by solving a set of governing hydrodynamic equations followed by calls to PHREEQC to calculate equilibrium concentrations of all chemical species within each model layer. The output from PHREEQC includes the equilibrium concentration and speciation of all aqueous components, as well as the equilibrium concentrations of all relevant minerals. This PHREEQC output then serves as the input for the next time step in the model. PitMod can also simulate the removal of trace elements from the surface mixed layer in association with biogenic scavenging and particle settling.

Oxygen Consumption

The development of suboxia in pit lakes has important implications from the perspective of aquatic habitat as well as predicting the effects of redox processes on pit lake chemistry. Dissolved oxygen is introduced to surface waters through interaction with the atmosphere and is distributed through the water column by mixing and diffusion. Dissolved oxygen is consumed via the bacterially-mediated oxidation of organic matter (OM) (Fenchel and Blackburn, 1979). OM produced in the surface water photic zone (including phytoplankton and zooplankton) is exported to depth via the settling of organic detritus. In the absence of deep water mixing and associated replenishment of oxygen (as in stratified lakes), oxygen-consuming reactions can result in the development of anoxic bottom waters.

In PitMod, oxygen consumption is allowed to occur on both horizontal surfaces (e.g., for sediments that accumulate on pit benches) as well as within the water column. Given that pit lakes tend to exhibit low levels of algal growth, the benthic oxygen flux (units of mg/m2/d) and volumetric oxygen consumption rate (units of mg/m3/d) in PitMod are typically assumed to be representative of empirically-derived rates measured for deep oligotrophic lakes (Charlton, 1980).

Biogeochemical Processes in Suboxic Waters

Pit lakes have a tendency to develop permanently stratified water columns (meromixis), which can have profound influences on the chemical and biological processes that occur in both the water column and sediments. In particular, the restricted exchange of constituents across the pycnocline can result in the depletion of dissolved oxygen in lake bottom waters. Under conditions of suboxia, redox-related mechanisms can greatly influence the behaviour of trace elements and other parameters. Biogeochemical processes relevant to suboxic lake strata include:

- Nitrate reduction
- Ammonia generation
- Reductive dissolution of Fe+Mn oxyhydroxides, and liberation of sorbed trace elements.
- Sulfate reduction
- Metal sulfide precipitation
- Alkalinity generation

To account for such processes, PitMod includes an algorithm that allows for redox reactions to proceed from oxygen reduction to sulfate reduction, based on the aqueous concentrations of the various electron acceptors and their respective energy yields (fig. 1). For Fe(III) and Mn(IV) reduction, the inventory of Fe and Mn oxide concentration can be specified in PHREEQC. In this regard, the availability of Fe and Mn oxide particles can represent a large uncertainty in redox predictions, given that the inventory of these constituents in the water column is governed by complex processes such as pit wall weathering and pit wall erosion rates.

Other key biogeochemical processes simulated by PitMod include alkalinity generation in response to suboxic redox reactions (Sigg *et al.* 1991) and metal sulfide precipitation. Alkalinity generation has relevance to the neutralization of acidity that may be introduced to the pit lake via pit wall runoff or input of acidic source waters from waste management facilities. Of additional importance for bioremediation is the reduction of sulfate, which liberates dissolved hydrogen sulfide (H2S) (fig. 1). Many trace elements (e.g., Fe, Co, Ni, Zn, Cd, and Pb) react rapidly with dissolved sulfide to precipitate as insoluble sulfide minerals (Balistrieri *et al.* 1994). Consequently, the precipitation of metal sulfides, and their subsequent settling to the lake bottom, can provide an effective, and largely permanent,

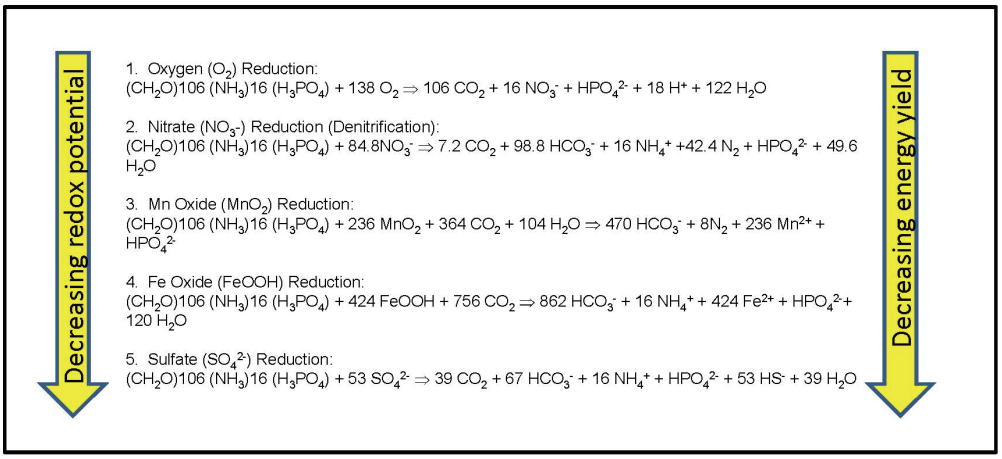


Figure 1 *Redox reactions associated with the re-mineralization (oxidation) of organic matter, represented as* $(CH_2O)_{106}(NH_3)_{16}(H_3PO_4)$*, showing the relationship to redox potential and energy yield.*

removal mechanism of trace elements from the water column (Green *et al.* 1989; Achterberg *et al.* 1997).

Mineral Precipitation

Within PitMod, coupling to PHREEQC allows for mineral precipitation. At each time step in the model, equilibrium concentrations and speciation of all aqueous components, as well as saturation indices (SI) for relevant minerals, are calculated. In this step, mineral precipitation is allowed to occur to maintain SI = 0. In the progressive neutralization of acidic drainage, for example, PitMod can account for pH buffering afforded by minerals such as K-jarosite $[KFe_3(SO_4)_2(OH)_6]$, schwertmanite $[Fe_8O_8(OH)_6(SO_4)\cdot nH_2O]$, bausaluminite $[AL_4(OH)_{10}SO_4]$ gypsum ($CaSO_4\ 2H_2O$), gibbsite $[Al(OH)_3]$, ferrihydrite $[Fe(OH)_3]$ and calcite ($CaCO_3$). For pit lakes, the inclusion of mineral precipitation has particular relevance for systems where acidic inflows (e.g., acidic pit wall runoff) are neutralized by alkaline water sources within the pit lake (e.g., groundwater inflows, surface runoff).

Metal Scavenging by Biogenic Particles

In lake environments, the dominant vertical transport mechanism for trace elements is particle settling. Settling particles, especially organic aggregates (e.g., algal particles), play a dominant role in the binding and transfer

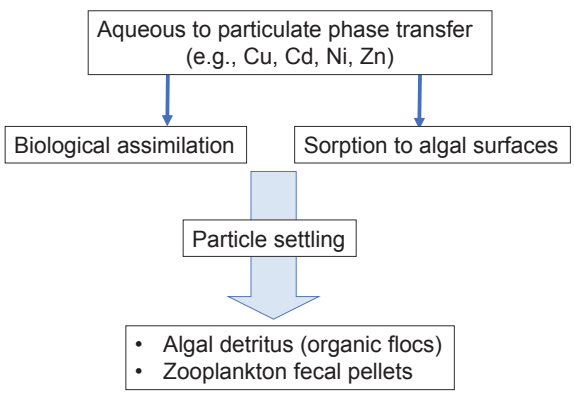


Figure 2 *Schematic illustrating uptake/assimilation of trace elements by biogenic particles followed by particle settling.*

of trace elements to lake bottom waters, thereby regulating the concentrations of dissolved species in surface waters (Sigg, 1985). This scavenging mechanism can be viewed as a two-stage process: 1) phase transfer from dissolved to particulate phase (via assimilation by algae or adsorption to cell surfaces); and 2) particle settling, which may include the sinking of organic aggregates or zooplankton faecal pellets (fig. 2). In general, pit lakes tend to be oligotrophic, exhibiting low rates of in situ primary production (algal growth). However, algal production and associated metal scavenging can be enhanced through fertilizer addition (discussed below).

PitMod includes functionality to allow for metal removal from the surface layer in response to the processes highlighted in fig. 2. Removal fluxes have been specifically developed for Cu, Ni, Zn, Co and Cd given the tendency to these elements to associate with biogenic particles as well as the availability of information for these elements in the primary literature. Removal rates (expressed as $mg/m^2/d$) were developed based on empirical data for lakes of varying levels of metal contamination (e.g., Nriagu *et al.* 1981; Kubota *et al.* 1974). Upper rates for metal removal were additionally informed by data for in pit bioremediation studies designed to foster eutrophic conditions in response to fertilizer addition (e.g., Dessouki *et al.* 2005).

In PitMod, metal export terms are applied to the uppermost 10 m of the water column, since metal scavenging will be primarily associated with biogenic processes in the photic zone (zone of active algal production). For colder climates that exhibit seasonal ice formation, the export terms are only applied during the ice-free period (June through October), as algal growth will greatly diminish during ice-covered periods.

Opportunities for In Pit Bioremediation

The *in-situ* bioremediation of pit lakes involves the addition of nutrients and/or organic matter to create conditions conducive to the removal of target parameters (Martin *et al.* 2003). The addition of organic matter as liquid or solid amendments provides a direct source of organic matter to the pit lake. In contrast, lake fertilization (e.g., addition of phosphorus fertilizer) adds organic carbon indirectly by stimulating photosynthetic production. Pit lakes tend to be oligotrophic in nature, whereby algal production is typically limited by available phosphorus. In this regard, algal productivity can be effectively stimulated through phosphorus addition. For every mole of phosphorus added, algae fix ~106 moles of carbon via photosynthesis (Redfield 1958). The efficiency in this process translates to the ability to treat large volumes of water at relatively low cost.

Key processes relevant to metal removal in response to lake fertilization are illustrated in fig. 3, which illustrates the links between nutrient addition, algal growth, particle concentration, particle flux and export of metals to the lake bottom via particle settling. In this regard, in-pit bioremediation can be viewed as a means to enhance naturally occurring lake processes as illustrated in fig. 2.

Bioremediation as modelled by PitMod demonstrates that with lake fertilization and the achievement of meso-eutrophic conditions, concentrations of dissolved Cd, Cu, Ni and Zn can be reduced to near-background levels (Martin 2023). These results highlight the potential merits of in pit bioremediation in reducing the concentrations of trace metals prior to the onset of pit lake

Table 1 *Metal removal rates applied in PitMod for pit lakes of varying trophic status.*

Parameter	Oligotrophic $mg/m^2/d$	Mesotrophic $mg/m^2/d$	Eutrophic/ Bioremediation Scenario $mg/m^2/$
Zn	0.03	2.4	12
Ni	0.003	2.0	10
Cu	0.013	1.6	8.0
Co	0.003	0.5	2.7
Cd	0.0007	0.1	0.32

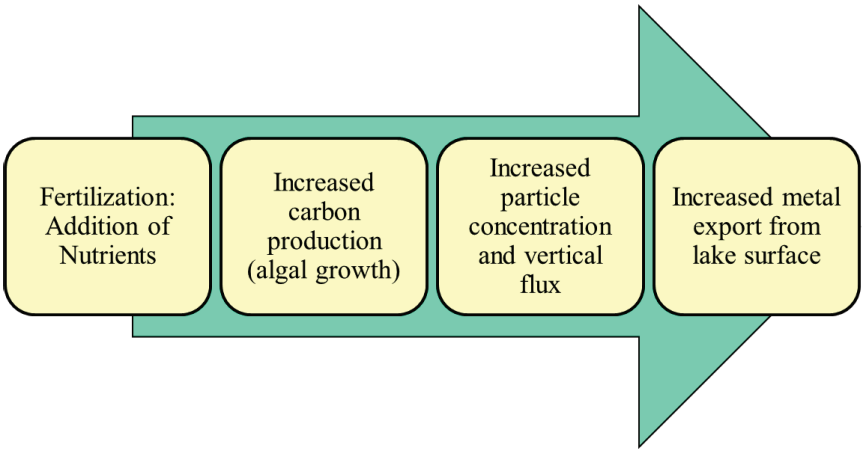


Figure 3 *Schematic illustrating linkages between lake fertilization, algal growth and export of metals from lake surface layer via particle settling.*

discharge to the environment. Further, since many pit lakes tend to develop meromictic density structures, any metals removed from the surface layer and sequestered to the pit bottom can be assumed to remain at depth. In other words, the flux can be assumed to be uni-directional (permanent metal removal from the surface layer).

Conclusions

Non-conservative processes, such as oxygen consumption, suboxic redox processes, mineral precipitation, and metal scavenging by biogenic particles, have the potential to greatly influence the behaviour and concentration of mine-related constituents in pit lake systems. While such processes are complex, modelling platforms (e.g., PitMod) are available to describe such mechanisms in meaningful ways. In turn, being able to model non-conservative processes offers mine managers opportunities more effective ways to optimize closure water management, minimize post-closure treatment requirements, and enhance environmental protection of downstream systems.

References

Achterberg EP, van den Berg CMG, Boussemart M, Davison W (1997) Speciation and cycling of trace metals in Esthwaite Water: A productive English lake with seasonal deep-water anoxia. Geochim. Cosmochim. Acta, 61(24): 5233-5253.

Balistrieri LS, Murray JW, Paul B (1994) The geochemical cycling of trace elements in a biogenic meromictic lake. Geochim. Cosmochim. Acta, 58(19): 3993-4008.

Charlton MN (1980) Hypolimnion oxygen consumption in lakes: discussion of productivity and morphometry effects. Can. J. Fish. Aquat. Sci. 37: 1531-1539.

Dessouki T, Hudson J, Neal B., Bogard M (2005) The effects of phosphorus additions on the sedimentation of contaminants in a uranium mine pit-lake. Wat. Res. 39: 3055-3061.

Dunbar, D (2013) Modelling of Pit Lakes. In: Geller W, Schultze M, Kleinmann R, Wolkersdorfer C (Eds), Acidic Pit Lakes - The Legacy of Coal and Metal Surface Mines, p 186-224, Springer-Verlag Berlin Heidelberg.

Fenchel T, Blackburn TH (1979) Bacteria and Mineral Cycling. Academic Press, London. 225 pp.

Green, WJ, Ferdmelman TG, Canfield DE (1989) Metal dynamics in Lake Vanda (Wright Valley, Antarctica). Chem. Geol. 76: 85-94.

Imerito A (2007) Dynamic Reservoir Simulation Model DYRESM v4. v4.0 Science Manual.

Kubota J, Mills EL, Oglesby RT (1974) Pb, Cd, Zn, Cu and Co in streams and lake waters of Cayuga Lake Basin, New York. Environ. Sci. Technol. 8: 243-248.

Martin AJ, Crusius J, McNee JJ, Whittle P, Pieters R, Pedersen TF, Dunbar D (2003) Field-Scale Assessment of Bioremediation Strategies for two Pit Lakes using Limnocorrals. International Conference on Acid Rock Drainage, Cairns, Australia, July 2003.

Martin AJ, Salvador S, Fraser C (2022) Strategies for pit lake water management and in-pit bioremediation. 12th International Conference on Acid Rock Drainage (ICARD) 2022. VIRTUAL, Australia. September 18-24, 2022

Martin AJ, Fraser C, Dunbar D, Mueller S (2015) Modelling of pit lake filling scenarios using a coupled physical and biogeochemical model. Tailings and Mine Waste 2015. October 26-28, 2015, Vancouver, B.C.

Nriagu JO, Wong HKT, Coker RD (1981) Particulate and dissolved trace metals in Lake Ontario. Water Res. 15: 91-96.

Parkhurst DL, CAJ Appelo (1999) User's guide to PHREEQC (version 2) - a computer program for speciation, reaction-path, 1D-transport, and inverse geochemical calculations. Rep. 99-4259, United States Geological Survey.

Redfield, AC (1958) The Biological Control of Chemical Factors in the Environment. American Scientist. 46 (3): 205–221

Sigg L (1985) Metal transfer mechanisms in lakes; the role of settling particles. In: Stumm, W. (Ed.), Chemical Processes in Lakes. Wiley-Interscience.

Sigg, L, Johnson CA, Kuhn A (1991) Redox conditions and alkalinity generation in a seasonally anoxic lake (Lake Greifen), Marine Chemistry, 36 (1-4): 9-26.

Wells, SA (2022) CE-QUAL-W2: A Two-Dimensional, Laterally Averaged, Hydrodynamic Water Quality Model (Version 4.5). www.ce.pdx.edu/w2.

A Biological Sulfate-Reducing Process for Zinc-Containing AMD in Japan: Comparison of Annual Treatment Performances Among Nutrient Conditions of Ethanol, Rice Bran and Their Hybrid for Sulfate-Reducing Bacteria

Yusei Masaki[1], Tsubasa Washio[1], Kana Hagihara[1], Takaya Hamai[2], Kengo Horiuchi[2], Yuki Semoto[2], Taro Kamiya[1], Kosuke Takamoto[2], Naoki Sato[2]

[1]*Metals Technology Center, Japan Organization for Metals and Energy Security, Furudate 9-3, Kosaka-kouzan, Kosaka, Akita, Japan, masaki-yusei@jogmec.go.jp*

[2]*Metals Environment Management Department, Japan Organization for Metals and Energy Security, Toranomon 2-10-1, Minato-ku, Tokyo, Japan*

Abstract

The performance of anaerobic sulfate-reducing processes was compared in a large-scale test with water flow rate of 100 L/min in winter period under different nutrient conditions: ethanol addition, rice bran addition, and their hybrid. Soluble Zn concentrations were efficiently decreased to < 0.06 mg/L on average under all conditions even in winter, whereas differences were found in sulfate reduction capacity and total Zn removal efficiency among the conditions. Total Zn removal was affected by ethanol feed concentration, the timing of rice bran feeding rather than rice bran feed weight, and the microbial community structure in the media.

Keywords: Passive Treatment, Sulfate-Reducing Bacteria, Zinc, Ethanol, Rice Bran

Introduction

A large amount of money is spent for continuous mine water treatment to meet domestic discharge standards at approximately 100 abandoned metal mines in Japan (Ministry of Economy, Trade and Industry, Japan 2023). JOGMEC (Japan Organization for Metals and Energy Security) has been conducting research on passive mine water treatment processes in order to reduce treatment costs. Since a limited area is available for mine water treatment at domestic mine sites, passive systems with relatively short hydraulic retention time were developed; approximately 2 h for Fe oxidation and precipitation and 25 h for anaerobic sulfate reduction (Hayashi *et al.* 2021). A multi-step passive mine water treatment test was started with a water flow rate of 100 L/min in 2020 (Figure 1). After the Fe oxidation using Fe-oxidizing bacteria and its removal, the AMD was introduced into the anaerobic process in a vertical down-flow biochemical reactor (BCR) containing a mixture of rice husk (an agricultural waste) and limestone. Ethanol and rice bran were used as direct and indirect nutrients for the sulfate-reducing bacteria, respectively. The treatment capability of the passive process should be lower in winter due to lower microbial activity at relatively low water temperatures. The aim of this study was to investigate treatment performance in winter among three different nutrient conditions, ethanol, rice bran and their hybrid.

Methods

Test Site and Mine Water Chemistry

The passive treatment test was carried out at an abandoned metal (gold, silver, copper, lead and zinc) mine located in northeast Japan. Annual temperatures at the site changed from -10 to +40 °C. A portion of the AMD (Table 1) flow was distributed to the passive treatment system using a pipe without exposure to air. The AMD was first introduced into vertical down-flow BCRs filled with rice husk media to a depth of 0.5 m, in order to remove much of the Fe. In these aerobic BCRs, the Fe^{2+} were oxidized by Fe-oxidizing bacteria; thereafter, the Fe^{3+} precipitated mainly as

schwertmannite (Masaki *et al.* 2021). The aerobic BCRs effluent water was introduced into the anaerobic BCRs (Table 1).

Anaerobic BCR Structures

In 2020, two vertical downflow BCRs (Width 5 m × Length 16 m × Depth 3.5 m) were constructed in parallel with concrete walls and floor below the prevailing ground surface to maintain the water temperature above approximately 4 °C. The surface of the anaerobic BCRs was open to facilitate maintenance. At the bottom, perforated pipes and limestone (20 to 40 mm) bed were placed to collect the effluent water. A mixture of rice husk and limestone (20 to 40 mm) was placed in the anaerobic BCRs with different weight ratios in the lower and upper layers: The weight ratios of rice husk/limestone in the lower (1 m thick) and upper (0.5 m thick) layers were 1/4 and 1/8, respectively, anticipating higher limestone consumption rates in the upper layer than in the lower. The total media volume was 120 m^3 in each reactor. Effluent water from the aerobic BCRs (100 L/min) was evenly distributed (50 L/min each) into the two anaerobic BCRs by adjusting the heights of the BCR's water introduction pipe ends. The hydraulic retention time in the media was calculated to 22.5 h. Note that limestone was added to the upper media layers in both anaerobic BCRs in 2022, resulting in a 1/16 weight ratio of rice husk/limestone in the upper layer.

Organic Nutrient Conditions

Three different organic nutrient conditions were tested in the two parallel anaerobic BCRs from 2020 to 2023 (Figure 2). One was an ethanol condition where industrial

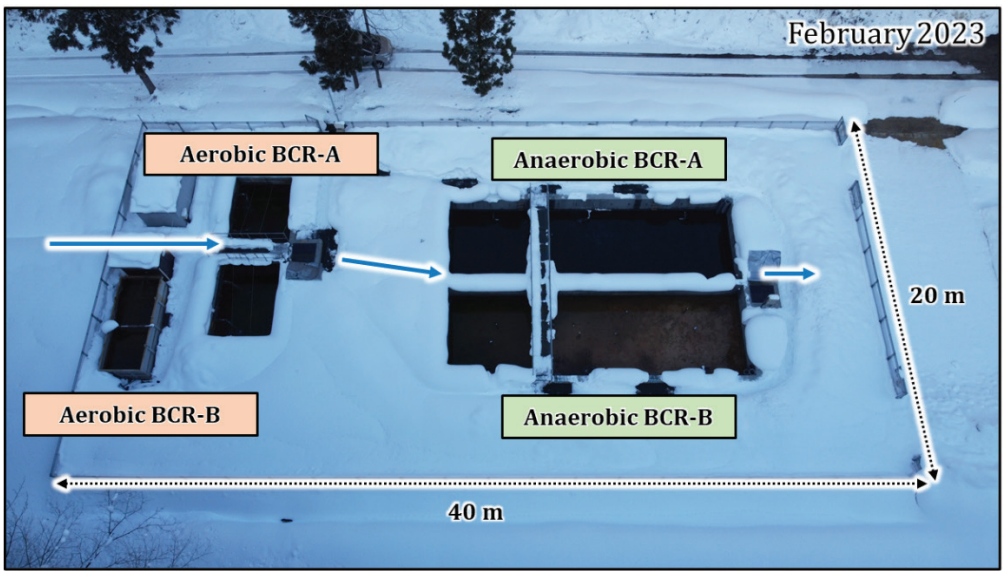


Figure 1 *multi-step passive mine water treatment test in the large-scale (image: Yusei Masaki)*

Table 1 *Water chemistry of the AMD and the influent of the anaerobic BCRs after Fe removal*

	Temp. °C	pH	Total Fe mg/L	Total Zn mg/L	Total Cu mg/L	Sulfate mg/L	DO mg/L
AMD	10-18	3.2-4.0	32-47	13-20	1-10	256-339	0.1
Influent of the anaerobic BCRs	9-16	2.8-3.3	4-14	15-20	2-11	257-328	1-3

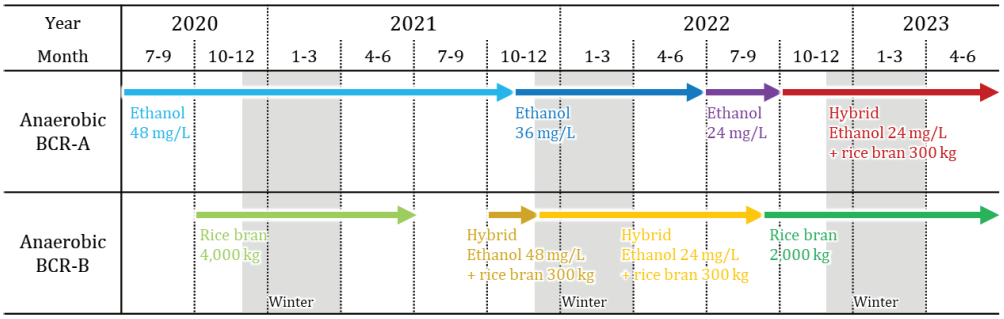


Figure 2 *Changes in the nutrient conditions in the anaerobic BCRs*

ethanol stock solution (50% alcohol) was continuously added using a metering pump into the anaerobic BCRs to set final feed ethanol concentrations of 48 mg/L (July 2020 to November 2021) and 36 mg/L (November 2021 to July 2022). The second condition was an initial addition of rice bran (2,000 or 4,000 kg) on the media of rice husk and limestone, to be indirectly used by the sulfate-reducing bacteria after aerobic bacteria decomposed the high molecular weight organic compounds (extracted from rice bran) to low molecular weight organic compounds. The third was a hybrid condition where ethanol was continuously supplied at a final concentration of 24 mg/L, and 300 kg of rice bran was initially added as a supplemental nutrient to support biodiversity in the rice husk media.

Monitored Parameters and Analytical Methods

Monitored parameters on the site were temperature, pH, oxidation-reduction potential (ORP, vs. Ag/AgCl) and dissolved oxygen (DO). Un-filtered and filtered (0.45 μm) water samples were regularly collected to determine the concentrations of Zn and Cu (ICP-OES; Agilent 5110 ICP-OES, Agilent Technologies Inc.). The detection limits were 0.08 μg/L for Zn and 0.18 μg/L for Cu. Sulfate concentrations and total organic carbon (TOC) in the filtrates were determined by ion chromatography (IC, Dionex ICS-6000, Thermo Fisher Scientific Inc.) and TOC analyzer (TOC-L, Shimadzu Corp.), respectively. Concentrations of organic acids and ethanol in the filtrates were quantified by UPLC using an IC-Pak ion exclusion column (7 μm, 7.8 mm × 300 mm; Waters), with photodiode array detection (λ = 210 nm) and refractive index detection, respectively.

Results and Discussion

Treatment Performances of the anaerobic BCRs in Non-Winter Periods

Our previous studies revealed that this biological sulfate-reducing process showed stable and effective treatment performances in non-winter periods (from April to November) in 2020 to 2022, regardless of organic nutrient conditions. Table 2 shows a water quality of the effluents in the anaerobic BCRs under

Table 2 *Water quality of the effluents in the anaerobic BCRs in non-winter periods (April - November)*

	Temp.	pH	Soluble Fe (filtered)	Soluble Zn (filtered)	Total Zn	Total Cu	Sulfate reduced
	°C		mg/L	mg/L	mg/L	mg/L	mg/L
Average	15	7.0	0.8	0.01	0.2	0.01	80
Min-Max	8-24	6.5-7.3	nd-8.0	nd-0.23	nd-2.6	nd-0.22	20-192

"nd" indicates that metal concentrations were less than detection limits of ICP-OES.

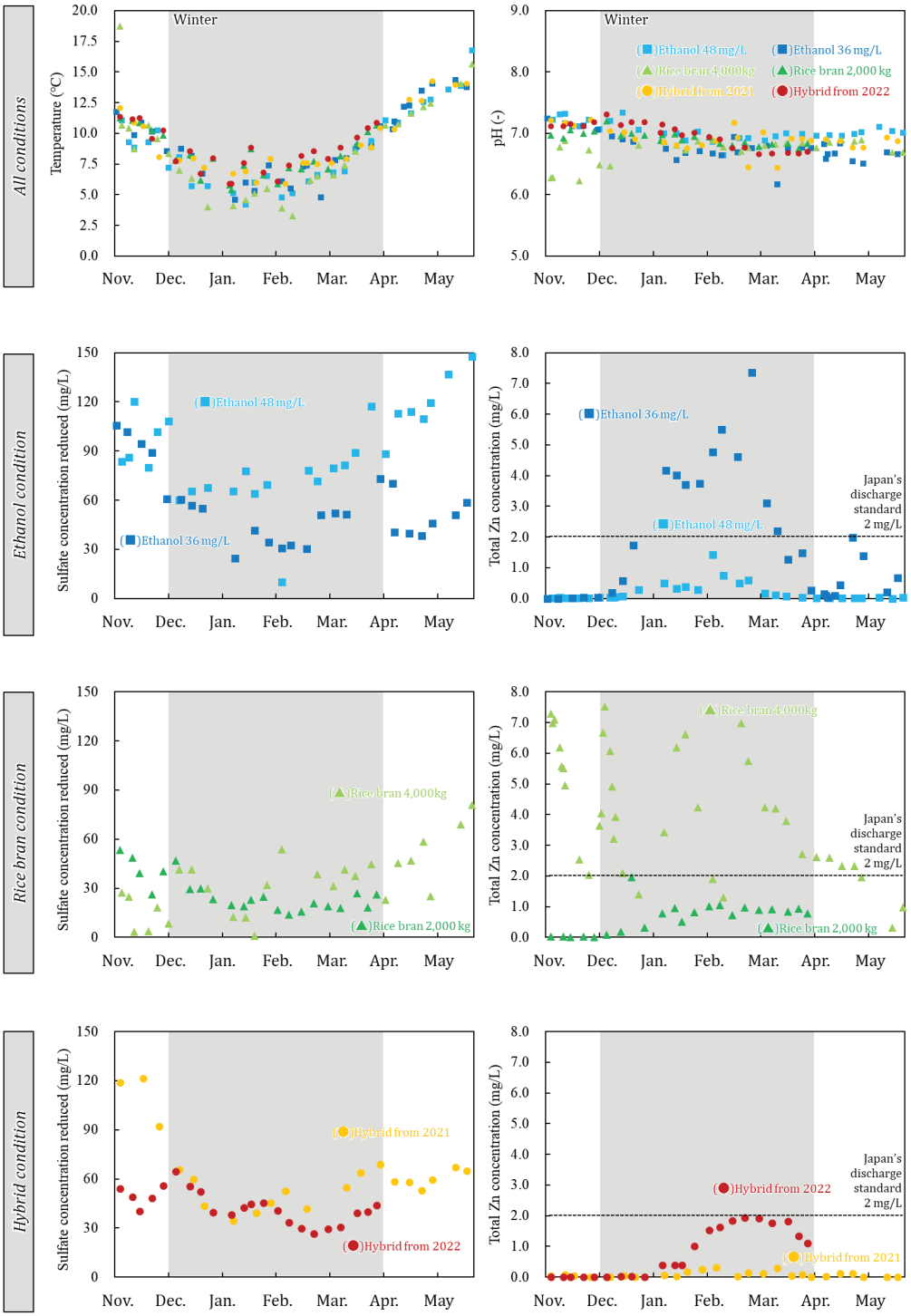


Figure 2 *Changes in temperature, pH, concentrations of sulfate reduced and total Zn under the condition of 48 mg/L ethanol (■ in light blue color), 36 mg/L ethanol (■ in blue color), 4,000 kg rice bran (▲ in light green color), 2,000 kg rice bran (▲ in green color), hybrid began from 2021 (● in yellow color), and hybrid began from 2022 (● in red color), from November to May in years when tested.*

three different nutrient conditions in non-winter periods. Effluent pH was 7.0 on average, and the total Zn concentration on average was 0.2 mg/L, which is much less than Japan's discharge standard. Note that domestic discharge standards are 5.8-8.6 for pH, 10 mg/L for soluble Fe, 2 mg/L for total Zn, and 3 mg/L for total Cu.

Water Temperature and pH in Winter Periods

The temperatures of the influent water into the anaerobic BCRs changed from 8.2 to 11.9 °C from December to March in 2020 to 2023, corresponding to changes in ambient temperatures. Dissolution of limestone mixed with rice husk media and microbial sulfate reduction reaction contributed to an increase in pH in the effluents, compared to the influents (approximately pH 3). The pH value in the effluents was found to be approximately 7.0, even during the winter periods, regardless of the organic nutrients conditions.

Treatment Performance Under the Ethanol Condition in Winter Periods

Water temperatures in the effluent from the anaerobic BCRs changed between 3.3 to 10.9 °C during the winter periods (from December to March) in 2020 to 2023, corresponding to changes in ambient temperatures. Dissolution of limestone mixed with rice husk media and microbial sulfate reduction contributed to an increased pH in the effluents (approximately pH 7). Under the ethanol conditions, ethanol concentrations of 48 and 36 mg/L were tested during 2020-2021 and 2021-2022, respectively. The average effluent pH in winter was found to be 7.0 at 48 mg/L of ethanol and 6.8 at 36 mg/L of ethanol, which implies that higher microbial sulfate reduction capacity corresponded to higher ethanol concentration, which contributed to the higher pH in the effluent. The lowest sulfate reduction capacity was found in February at both ethanol concentrations, which indicates that microbial SRB sulfate reduction was well-influenced by water temperatures. A stoichiometric requirement of sulfate reduction for contaminated metals removal from the influent water was calculated as approximately 30 mg/L. Sulfate reduction capacities in winter were 10-117 and 24-73 mg/L at ethanol concentrations of 48 and 36 mg/L, resulting in redox potential (SHE) of +115 to -106 and +32 to -131 mV, respectively. The results indicate that microbial sulfate reduction capacity was highly influenced by ethanol concentration added into the anaerobic BCRs. As for the Zn concentration in the effluent, Zn ions (filtered water samples) were removed below 0.1 mg/L in winter regardless of the ethanol concentrations, whereas total Zn (un-filtered water samples) were detected up to 1.4 and 7.4 at the ethanol concentrations of 48 and 36 mg/L, respectively. In the anaerobic BCRs, it is suspected that metal precipitates were trapped on the rice husk surface, which is in a reductive layer where sulfate is actively being reduced by SRB. Therefore, the reductive zone likely became relatively thinner due to a weaker SRB microbial activity in winter, also resulting in a thinner metal trapping zone in the following rice husk layer. This might have caused detection of suspended Zn precipitates, but not Zn ions, in the effluent in winter. The total Zn concentrations in the effluent gradually decreased from February to April or May (depending on the ethanol concentration) toward the same concentration level as the rest of the year.

Treatment Performance Under the Rice Bran Condition in Winter Periods

The changes in pH and water temperature in the effluent with the rice bran addition was similar to those with the ethanol condition. Rice bran was externally provided with weights of 4,000 kg in October 2020 and 2,000 kg in September 2022. Those rice bran weights were for a year of operation; therefore, the residues were removed from the BCRs after a year passed from the addition. When 4,000 kg of rice bran was used, the decrease in sulfate concentration was readily observed in the effluent, followed by Zn ion concentrations (filtered water) below 0.2 mg/L after 2 weeks passed from the rice bran addition. However, total Zn removal efficiency was limited and unstable until May 2021; the total Zn concentrations in the effluent changed between 0.7-7.6

mg/L from October 2020 to May 2021, and then decreased to less than 2 mg/L after May 2021. This implies that sufficient microbial community structure in the media layer might have not been established before the winter period in 2020. Therefore, earlier rice bran addition before October would lead to higher total Zn removal performance. When 2,000 kg of rice bran was used, sulfate reduction capacity was 14-47 mg/L and redox potential (SHE) was +44 to -60 mV. The concentrations of Zn ion (filtered water) were found to be stably below 0.02 mg/L. Total Zn concentration was observed to be below 1.0 mg/L from December 2022 to March 2023, meeting the domestic discharge standard for total Zn (2 mg/L).

Anaerobic BCRs Treatment Performance Under the Hybrid Condition in Winter Periods

The hybrid condition was tested twice using 300 kg of rice bran and ethanol addition at 24 mg/L. In 2021, rice bran was added to the anaerobic BCR, and ethanol addition began at series concentrations of 48 mg/L in October, 48-24 mg/L with a gradual decrease in November, and 24 mg/L after December until August 2022. The other anaerobic BCR that had been operated under the ethanol condition was used to test the hybrid condition: In October 2022, rice bran was added in the BCR, and ethanol solvent began to be added at a concentration of 24 mg/L. Sulfate reduction capacity in winter was relatively stable, ranging between 27-69 mg/L in both tests, corresponded to redox potential (SHE) of +48 to -87 mV. Furthermore, Zn ion concentrations (filtered water) were also efficient (below 0.02 mg/L). However, total Zn removal behaviours in both cases were different even though the nutrient condition was the same in winter: The total Zn concentration in the effluent was observed to average 0.08 mg/L in winter in the test that began in 2021, whereas the total Zn concentrations gradually increased from January 2022 and reached 1.9 mg/L in late February 2023 in the latter test. This difference might be due to different structures of microbial community in the media since residual ethanol concentrations in the effluents were found to be 0.3 (1.3% in the feed) and 5.4 mg/L (22.5% in the feed) on average in winter in the test that began from 2021 and 2022, respectively.

Conclusions

The winter treatment performance of anaerobic BCRs was monitored with three different nutrient conditions: ethanol, rice bran and their hybrid. The effluent pH and Zn ion concentrations were similar, while the sulfate reduction capacity and total Zn concentration varied. Under all conditions, the effluent water pH and Zn ion concentrations were found to be 7.0 and 0.06 mg/L on average, respectively, in winter. The test with an ethanol concentration of 48 mg/L had approximately twice the sulfate reduction capacity of that with an ethanol concentration of 36 mg/L. The corresponding effluent total Zn concentrations were 1.4 and 7.4 mg/L, respectively. Under the rice bran condition, the timing of rice bran addition was implied to be more critical than rice bran weight to establish an appropriate microbial community structure in the media, leading to efficient treatment performance. When tested with an addition of 2,000 kg of rice bran from September 2022, sulfate reduction capacity was 14-47 mg/L and total Zn concentration was found to be below 1.0 mg/L in winter. The hybrid conditions where 300 kg rice bran was fed, and 24 mg/L ethanol was continuously added, was tested through the year twice (began from 2021 and 2022), resulted in effluent total Zn concentrations of 0.08 and 0.8 mg/L on average in winter, respectively. In this study, all three conditions were found to show the capability for total Zn removal below its domestic discharge standard of 2 mg/L throughout the year, indicating that an appropriate condition could be chosen depending on AMD chemistry and site situations on mine sites. Other nutrient conditions will be tested in the future in this large-scale BCRs.

References

"Mine polution control", Ministry of Economy, Trade and Industry, Central Mine Safety Committee in Japan, https://www.meti.go.jp/policy/safety_security/industrial_safety/sangyo/mine/2017_newpage/kogaiboshi.html, 22 July 2023

Hayashi K, Washio T, Masaki Y, Hamai T, Sakata T, and Sato N (2021) Full-scale compact passive treatment system for a Japanese AMD by aerobic bioreactor for Fe removal and sulfate reducing bacteria bioreactor for Zn removal. Proceedings, 14th International Mine Water Association, Cardiff, Wales, UK. 12-15 July 2021 (Online)

Masaki Y, Hayashi K, Hamai T, Washio T, Sakata T, Kanayama A, Horiuchi K, Sakoda M, Masuda N, and Sato N (2021) A full-scale test of iron removal from acid mine drainage using iron-oxidizing bacteria. Proceedings of The Mining and Materials Processing Institute of Japan. Minato-ku, Tokyo, Japan. 8-10 March 2021 (Online)

Assessment of Manganese Removal in Passive Systems Based on Operational Data and Experience of Treating Net-alkaline Coal Mine Waters in the UK

Arabella M. L. Moorhouse-Parry and Christopher J. Satterley

The Coal Authority, 200 Lichfield Lane, Mansfield, Nottinghamshire, UK, NG18 4RG

Abstract

Passive treatment of net-alkaline coal mine waters in the UK is well established, with over seventy schemes currently operated by the Coal Authority. Some of these mine waters contain appreciable amounts of manganese, which is coming under increasing scrutiny from environmental regulators following the introduction of a bioavailable environmental quality standard in 2015. To date, the Coal Authority's mine water treatment schemes have been designed remove iron. However, there is now a possibility that some future schemes may also need to treat manganese. This paper reviews operational data from sixteen sites across the UK to improve understanding in designing future passive systems to remove manganese.

Keywords: net-alkaline, manganese, passive treatment, operational data

Introduction

Information for the passive removal of manganese from mine waters is much more limited when compared to the existing knowledge base on the passive removal of iron, and its application to the design of mine water treatment schemes in the UK is still in its infancy. This is despite passive manganese removal being discussed by Hedin *et al.* (1994) and in the Piramid Guidelines (2003). In order to improve understanding in designing future conventional passive systems for manganese treatment, or to facilitate the retro-fitting of existing schemes to reliably achieve a target concentration, a review of sixteen operational mine water treatment schemes (MWTS) located across the UK (ten in England, three in Scotland and three in Wales) has been conducted. These sites have been chosen as they provide a range of raw manganese concentrations (0.7 – 3.4 mg/L) and have sufficient operational flow and reed bed chemistry data available for review.

All sixteen sites included in this review treat net-alkaline mine waters and have iron concentrations that range between ≈3 and ≈130 mg/L. This review focuses exclusively on sites where chemical dosing is not used, in order to provide information on fully passive treatment for manganese. Table 1 provides a summary of the schemes included in this review, in addition to an overview of the typical flow rates, mean raw total iron and manganese concentrations and the total area of reed beds present at each site.

Data sourcing and limitations

This paper solely focuses on reporting operational observations recorded at selected sites, with the aim to improve future scheme design for manganese removal. Further investigations are required to better understand the control mechanisms of manganese removal and any relationships that may exist with other parameters. Operational data, going back to 2015 for some sites, and ending in December 2022 have been used in this review. Any data collected during reed bed refurbishments or maintenance activities when reed beds were either offline, or treatment performance was impacted, are excluded from the dataset. Previous work undertaken by the Coal Authority has shown that manganese removal predominantly takes place in reed beds rather than settlement ponds (Bamforth and Satterley, 2022). This paper therefore focuses on manganese removal in reed beds. Where multiple reed beds are present at site, they are considered together as a whole, rather than

Table 1 Summary of mine water treatment scheme locations included in this review with raw total iron and manganese concentrations (mg/L), flow rate (to the nearest 5 L/s) and reed bed area (to the nearest 100 m²)

Mine Water Treatment Scheme	Location	Start of Dataset	Mean Raw Concentration		Flow Rate	Reed Bed Area
			Iron	Manganese		
A Winning+	England, Derbyshire	2018	10.5	0.67	50	7000
				0.75	75	
				0.9	95	
Aspull Sough	England, Lancashire	2015	37.6	2.76	20	3200
Bates	England, Northumberland	2015	15.0	3.20	210	8400
Blenkinsopp (RB2)	England, Northumberland	2015	77.2	1.64	25	2200
Blindwells	Scotland, East Lothian	2015	4.63	2.24	280	17000
Chell Heath	England, Stoke-on-Trent	2016	20.3	3.28	10	2900
Craig-yr-Aber	Wales, Bridgend	2018	18.4	2.77	20	3300
Downbrook	England, Lancashire	2018	8.52	1.62	15	1300
Glyncastle	Wales, Neath Port Talbot	2016	18.9	1.58	15	3200
Hockery Brook	England, Lancashire	2017	14.8	2.09	20	2600
Mountain Gate	Wales, Carmarthenshire	2015	4.13	1.18	10	2400
Mousewater	Scotland, S. Lanarkshire	2016	16.0	1.73	45	8900
Pitfirrane	Scotland, Fife	2016	2.39	1.95	225	17900
Saltburn*	England, Cleveland	2016	128	2.64	30	4500
Stony Heap	England, County Durham	2016	15.0	1.91	20	1500
Summersales	England, Lancashire	2019	29.0	2.76	20	3200

+ Seasonal pumping takes place at A Winning, resulting in seasonal variation in chemistry. * Ironstone mine

individually, to maximise the available data. For treatment schemes that are comprised solely of reed beds, the raw mine water manganese concentrations have been used in this review for the influent concentration, in conjunction with the consented discharge point as the final effluent. For schemes where settlement ponds are present however, data from partially treated water between the final ponds and primary reed beds have been used where available.

Datasets based on routine operational sampling and monitoring have their limitations. Intermediate sample points often solely focus on iron, as this is the metal for which permit conditions are set, and is therefore the main focus for operational sampling budgets. Where no manganese data are available from settlement pond outlets, the raw manganese concentrations have therefore been used as a proxy. A more intensive sampling programme was established between 2019 and 2021 (Bamforth and Satterley, 2022), therefore some settlement pond outlet data are available for most sites during this specific timeframe. These data have therefore been used to ascertain what, if any, manganese removal occurs in the ponds, to enable a correction to be applied to the raw mine water concentrations in the remaining data set if applicable. This adjustment has been applied in order to model manganese concentrations entering the reed bed across the entire available data range. Such an approach introduces some conservatism to the dataset, reducing the risk of calculated removal rates being over estimated.

Manganese Removal

All the schemes listed in Table 1 were designed to remove iron, with any manganese removal considered an added benefit. Despite the range of mine water flow rates (≈10 – ≈300 L/s) examined in this review, the data from the schemes assessed to date suggest that iron concentrations entering the reed beds need to be low before manganese removal occurs. Blenkinsopp MWTS, which comprises two settlement ponds operating in parallel, followed by two reed beds operating in series, provides a good example. Figure 1 shows that the majority of the manganese removal at Blenkinsopp takes place in the second reed bed, where inlet total iron concentrations are lower (mean concentration ≈10 mg/L), compared to those entering the first reed bed (mean concentration ≈20 mg/L) see (fig. 2). Data from other sites suggest that iron

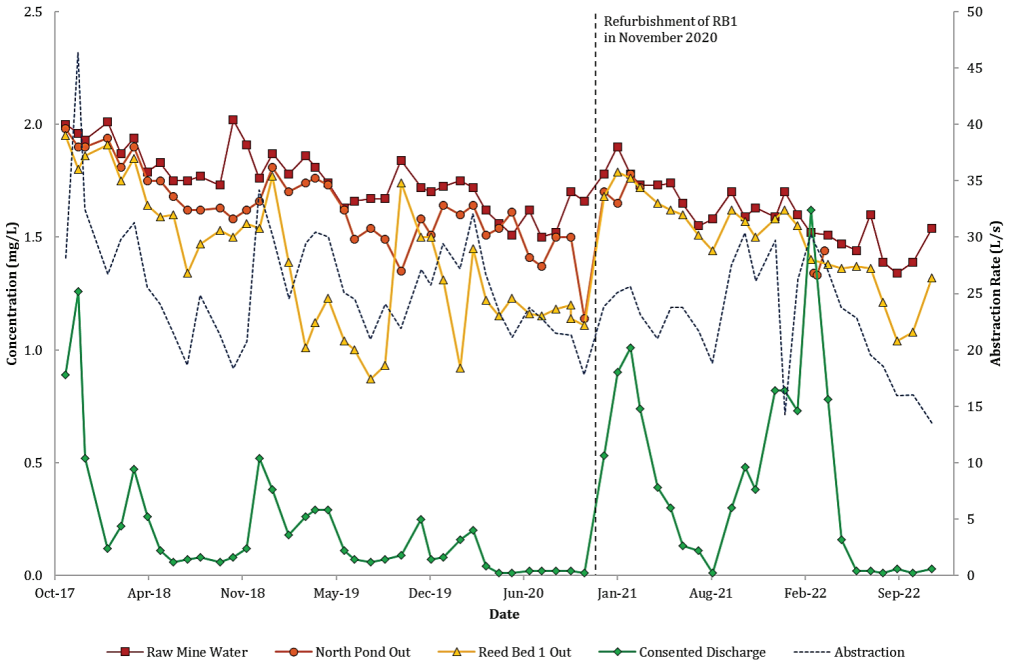


Figure 1 *Manganese removal at Blenkinsopp mine water treatment scheme vs. abstraction rates*

concentrations ideally need to be lower than those measured at Blenkinsopp however. At schemes where iron concentrations are sufficiently high to warrant settlement ponds, iron concentrations entering the reed beds are generally lower (≈5 mg/L) than those reported at Blenkinsopp (see tab. 2). This corroborates a review undertaken by Batty *et al.* (2008), who found that iron concentrations at Whittle MWTS needed to be reduced to ≈5 mg/L before manganese removal commenced. Raw manganese concentrations at Whittle today are ≈0.4 mg/L (vs. ≈1.5 mg/L during 2004 - 2005), therefore this site has not been included in this review.

For the purpose of any treatment design intending to include manganese removal, it is therefore recommended that iron concentrations are reduced to ≈5 mg/L, either by settlement ponds or primary reed beds, depending on raw iron concentrations. Additional secondary reed beds can then be incorporated into the design, where manganese removal is more certain to occur.

In November 2020, Reed Bed 1 at Blenkinsopp was refurbished, albeit unsuccessfully as the replacement reeds failed to establish (hence why this reed bed has been excluded from this review). This resulted in manganese removal being restricted to Reed Bed 2 (see fig.1), with very limited removal taking place in Reed Bed 1. Following the refurbishment, the removal of manganese at this site became more varied, with a strong seasonal pattern developing. This seasonal pattern in manganese removal is repeated at other MWTS across the UK (see fig. 3).

Figure 3 shows that manganese removal rates are generally at their highest during the months when ambient temperatures in the reed beds are at their warmest (May – October), compared to the cooler months (November – April) when temperatures fall. It is postulated that microbial activity is a primary control mechanism of manganese removal (Batty *et al.*, 2008), which increases when temperatures in the reed beds rise as the summer progresses, with latent heat sustaining activity into the autumn; in the colder winter / spring months, the autocatalytic effect of manganese oxide for manganese oxidation is most likely the predominant control mechanism for manganese removal. This seasonal trend appears to differ nationally however, with the start of the manganese removal season

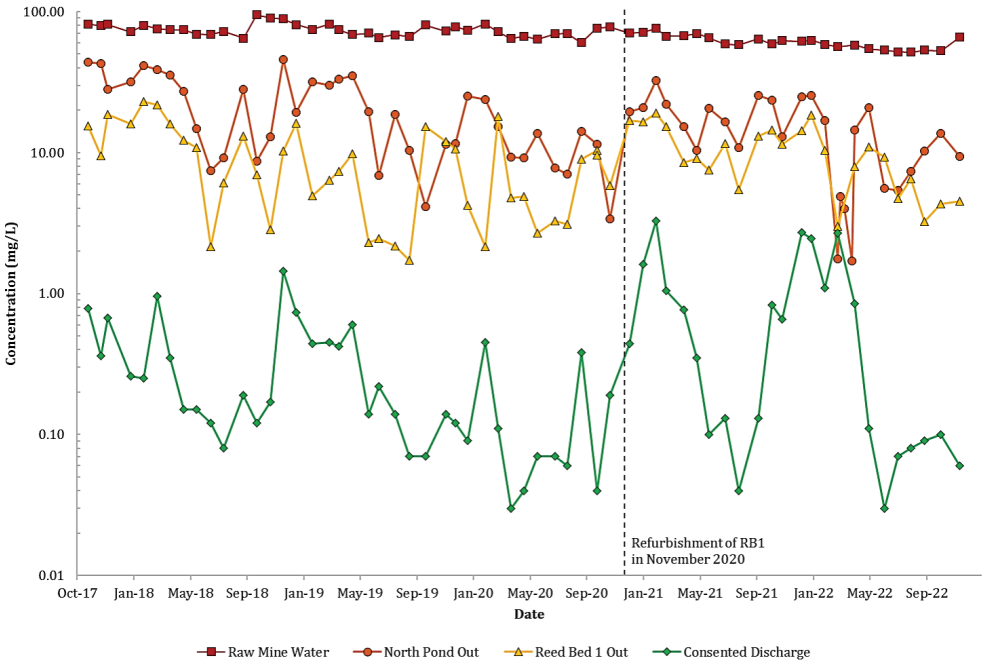


Figure 2 *Iron removal at Blenkinsopp mine water treatment scheme*

Table 2 *Summary of mean iron concentrations entering reed beds at treatment schemes where primary iron removal takes place in settlement ponds (all data quoted in mg/L)*

Treatment Scheme	Treatment Unit	Mean Iron Concentration	Treatment Scheme	Treatment Unit	Mean Iron Concentration
A Winning	Pond 1	5.08	Downbrook	Pond 1	3.4
	Pond 2	4.97		Pond 2	3.39
Aspull Sough	Pond 3	4.97	Glyncastle	Pond 1	7.68
				Pond 2	4.97
Bates	Pond 3	6.51	Hockery Brook	Pond 3	3.79
	Pond 4	5.95	Mousewater	Pond 1&2	9.53
Blenkinsopp	North Pond	22.2	Saltburn	Pond 4	2.06
	Reed Bed 1	10.4	Stony Heap	Pond 1	5.56
Craig-yr-Aber	Pond 1	5.64		Pond 2	5.78
	Pond 2	5.17	Summersales	Pond 2	4.31

generally commencing later further north, where spring arrives slightly later in the UK. This could have an implication for manganese removal at schemes in Scotland or at sites with a higher elevation, where the manganese removal season may be relatively shorter compared to sites located either further south, or at a lower elevation.

Manganese Removal Rates

Reed bed areal removal rates (g/m^2/day) for manganese have been calculated for each scheme included in this review (see tab. 3). Data collected during initial reed bed establishment, or periods when reed beds were offline for maintenance work have been excluded in this review in order to provide realistic removal rates that are achievable during normal operating conditions. A review of the operational data included in this review suggests that areal removal rates between 0.2 – 3.4 g/m^2/day are possible. This compares to a range of 0.17 – 1.07 g/m^2/day quoted by Hedin *et al.* (1994) and a nominal

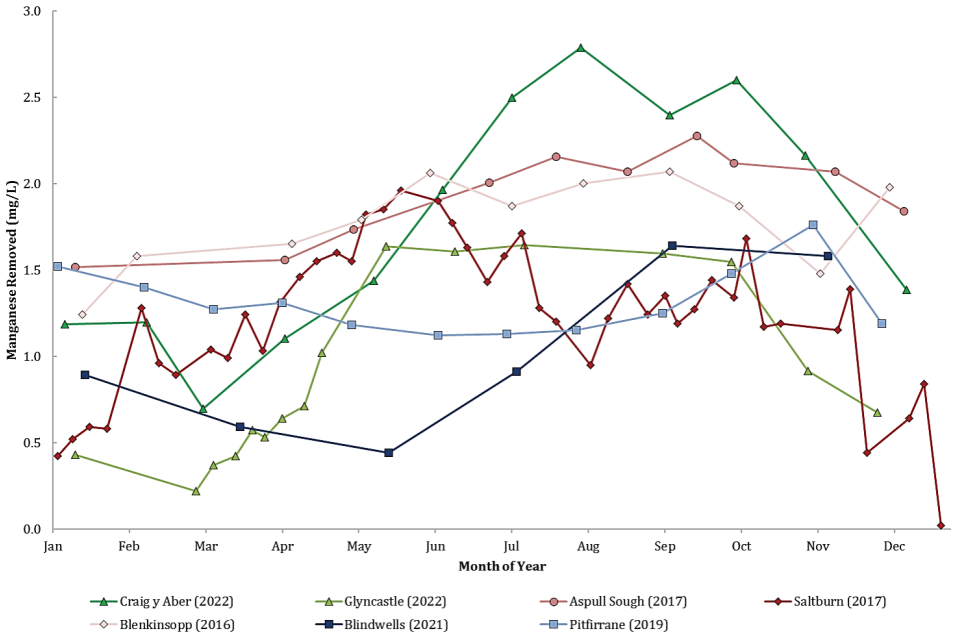


Figure 3 *Seasonal manganese removal patterns at seven sites across the UK from the south (Craig-yr-Aber) moving northwards (Pitfirrane). The years data are taken from are shown in brackets*

removal rate of 0.5 g/m^2/day quoted in the Piramid Guidelines (2003). Table 3 indicates that most sites included in this review (11 out of the 16) have areal removal rates that fall between 0.6 and 1.5 g/m^2/day. If the sites with the highest (Bates) and lowest (Mousewater) removal rates are discounted, the mean areal removal rates for manganese in the UK is estimated at 0.75 g/m^2/day. This value is based on an annualised mean in order to offset the seasonal variation seen in manganese removal.

Reasons behind the high removal rate at Bates are currently unknown, although it may in part be driven by the higher raw manganese concentrations compared to the other schemes considered here. It is worth noting however, that the five sites in North America reviewed by Hedin *et al.* (1994) had raw manganese concentrations >9 mg/L, which is twice the amount typically seen in the UK. The relatively poor performance of the reed bed at Mousewater is down to the poor recovery of the reeds after maintenance works.

Table 3 *Summary of mean areal removal rates (g/m2/day) for manganese at each site included in this review in additional to the amount of manganese removed in the reed beds (mg/L)*

Site	Mean Areal Removal Rate	Manganese Removed			Site	Mean Areal Removal Rate	Manganese Removed		
		Min	Mean	Max			Min	Mean	Max
A Winning (50L/s)	0.38	0.02	0.58	1.01	Downbrook	0.68	0.01	0.69	1.62
A Winning (85L/s)	0.62	0.31	0.61	0.88	Glyncastle	0.39	0.03	1.12	1.89
A Winning (100L/s)	0.65	0.49	0.57	0.74	Hockery Brook	0.80	0.03	1.23	1.96
Aspull Sough	0.74	0.10	1.63	2.63	Mountain Gate	0.35	0.26	0.96	1.29
Bates	3.39	0.90	2.10	3.89	Mousewater	0.22	0.04	0.50	1.36
Blenkinsopp RB2	1.17	0.54	1.27	1.91	Pitfirrane	1.30	0.70	1.20	1.86
Blindwells	1.49	0.34	1.02	1.90	Saltburn	0.78	0.02	1.51	2.51
Chell Heath	0.49	0.40	2.06	3.48	Stony Heap	0.38	0.22	1.32	1.80
Craig yr Aber	0.86	0.57	1.84	3.04	Summersales	0.84	0.47	1.23	1.59

Reed Bed Maintenance

Figure 1 clearly demonstrates the potential negative impact of maintenance activities on the performance of reed beds to remove manganese, as effluent concentrations at Blenkinsopp prior to the works taking place were ≤0.5 mg/L, whereas afterwards, at times they increased to >1 mg/L, particularly in the colder months. Similarly, Figure 4 shows that after Reed Bed 1 at Mousewater was replanted in 2017, manganese removal also decreased, primarily due to the poor regrowth of *Phragmites sp.* reeds despite the newly planted *Typha sp.* reeds re-establishing well.

Calculated areal removal rates at both sites decreased from a mean value of 0.21 g/m^2/day to 0.10 g/m^2/day in Reed Bed 1 at Blenkinsopp (noting that manganese removal in Reed Bed 1 at Blenkinsopp is low due to the elevated iron concentrations), and decreased from 0.68 g/m^2/day to 0.22 g/m^2/day at Mousewater. Figure 4 also illustrates that it took six months before the reed bed at Mousewater began to remove manganese after the scheme was commissioned. This suggests manganese removal will only commence once the reed beds have established.

Conclusions

Although the number of schemes looked at in this review is relatively small, two key design principals have been identified that build on the Hedin *et al.* (1994) work, which can be taken forward for further investigation. Firstly, iron concentrations must be low (ideally ≤5 mg/L) before manganese removal will take place in reed beds and secondly, an areal removal rate of 0.75 g/m^2/day is proposed for designing reed beds for future schemes where manganese concentrations exceed 0.7 mg/L. Furthermore, this review has also highlighted two key considerations that apply to manganese removal that contrast to iron removal. Firstly, manganese removal tends to be seasonal with greater concentrations typically removed in the warmer months and secondly, manganese removal will likely only commence once reed beds have established. Finally, this work has highlighted that reed beds can also be

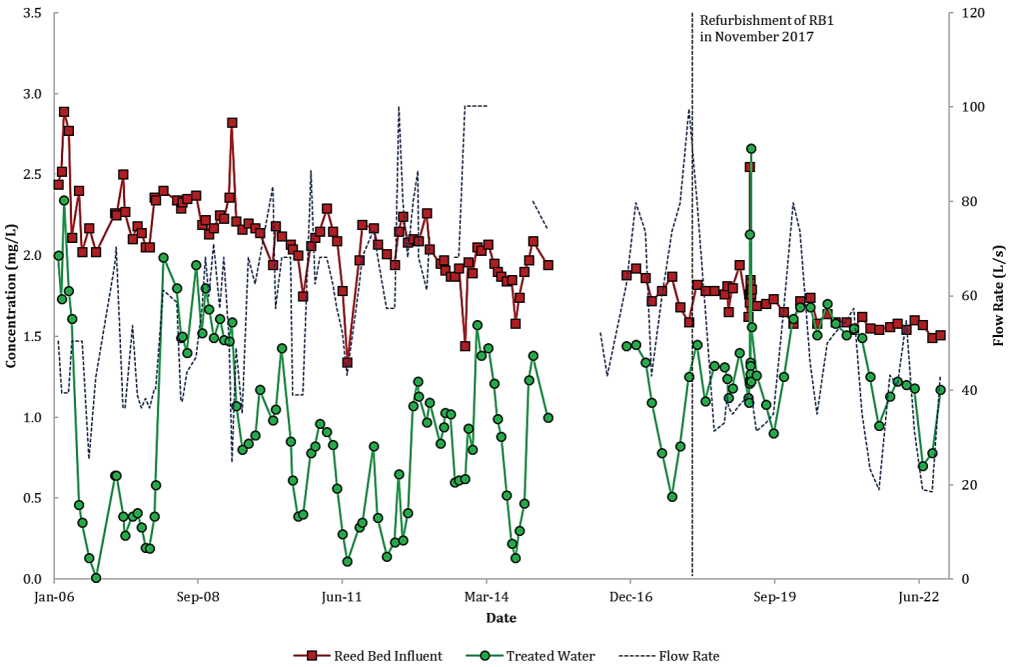


Figure 4 *Manganese removal in the reed beds at Mousewater mine water treatment scheme vs. flow rate (no data are available between June 2015 and May 2016)*

negatively impacted by refurbishment works for several years if the freshly replanted reeds fail to establish correctly.

Acknowledgements

The authors thank all co-organisers for hosting the IMWA 2023 Conference. Thanks are also extended to the people at Severn Trent Services who operate and look after our mine water treatment schemes.

References

Bamforth, S.M. and Satterley, C.J (2022): Evaluating Manganese in Mine Water in UK Coal Authority Mine Water Schemes. – In: Pope, J.; Wolkersdorfer, C.; Rait, R.; Trumm, D.; Christenson, H.; Wolkersdorfer, K.: IMWA 2022 – Reconnect. – p. 7 – 13; Christchurch, New Zealand (International Mine Water Association).

Batty, L., Hooley, D. and Younger, P. (2008) Iron and manganese removal in wetland treatment systems: Rates, processes and implications for management. Science of the Total Environment, 394, 1 - 8

Hedin. R.S., Nairn, R.W. and Kleinmann, R.L.P. (1994) Passive treatment of coal mine drainage. USBM IC 9389, US Dept. of the Interior, Washington DC, 35 pp

PIRAMID Consortium, Engineering guidelines for the passive remediation of acidic and/or metalliferous mine drainage and similar wastewaters. (2003)

Holistic Approach to Reed Bed Management on UK Coal Mine Water Treatment Schemes

Arabella M. L. Moorhouse-Parry, Stephen A. Smithson and Christopher J. Satterley

The Coal Authority, 200 Lichfield Lane, Mansfield, Nottinghamshire, UK, NG18 4RG

Abstract

As part of its UK mine water treatment portfolio, the Coal Authority operates sixty treatment schemes with surface flow wetlands for the treatment of ferruginous mine waters. Typically, these reed beds are planted with either a monoculture of Phragmites australis (common reed) or mixed planting with *Phragmites sp.* and *Typha latifolia* (Bulrush). Initially, many of these reed beds were operated as self-managing systems receiving minimal maintenance, however, this led to a range of operational issues, which reduced treatment efficiency. Over time, the Coal Authority has developed a holistic approach to the management of these reed beds that recognises their need to be actively managed in order to perform effectively, alongside protecting the biodiversity value of these systems and identifying sustainable methods of reed bed waste disposal.

Keywords: Mine water; passive treatment; reed beds; operational experience

Introduction

Aerobic wetlands have been used for passive mine water treatment for over thirty years, having been first proposed in the late 1980's and early 1990's e.g. Girts *et al.* (1987) and Wieder (1989). Key papers such as Hedin *et al.* (1994) and Tarutis *et al.* (1999), which focus on wetland treatment systems, are often cited in the literature, along with the slightly later Piramid Design Guidelines (2003). Today, aerobic wetlands are a mainstay of the passive mine water treatment toolbox, with countless examples used across the globe. In the UK, the Coal Authority alone currently operates sixty schemes, which include surface flow reed beds for the treatment of ferruginous mine waters. Some of these schemes have been in operation since the mid 1990's, whereas others are more recent, having been constructed in the past five years. The current scheme portfolio manages approximately 37 hectares (370,000 m2) of reed bed, operating at various altitudes (400 m to sea level) and with a range of mine water qualities (fresh to saline). Typically, these reed beds are planted with either a monoculture of *Phragmites australis* (common reed) or mixed planting with *Phragmites sp.* and *Typha latifolia* (Bulrush) (fig. 1); *Iris pseudacorus* (yellow flag iris) has also been planted at some sites. Reed beds are not only very effective treatment systems if maintained appropriately, they also have the added benefit of providing priority wetland habitat for a range of small mammals, invertebrates and birds when managed well.

A common misconception in the early days of reed bed management was that these natural systems could be operated with a "minimum amount of attention and money" if they were "properly designed and constructed" (Hedin *et al.*, 1994). This statement has been taken somewhat literally at many sites in the past, with often little, to sometimes even no maintenance taking place. Operational experience in the UK has shown that this lack of intervention inevitably results in a reduction in treatment efficiency of a reed bed. Ochre and organic debris accumulation increases over time, reducing the freeboard of water. This can result in water over topping the reed bed bunds, which can cause localised flooding with part treated mine water if not promptly rectified. Furthermore, the accumulation of detritus in the reed bed combined with a reduction in water depth, allows natural plant succession to take place, with invasive trees (e.g. alder and birch) and shrubs (e.g. gorse and hawthorn) often colonising reed beds and, over time, out competing the reeds (fig.



Figure 1 *Overgrown reed bed with trees and scrub at Whitworth A&B, South Wales (left), vs. mixed plant (Typha sp. and Phragmites sp.) maintained reed bed at Allerdean Mill, Northumberland (right)*

1). These larger terrestrial plants not only have the potential to damage the infrastructure of the reed bed itself if left unchecked, with the roots breaching liners (clay or plastic), but also cause preferential flow pathways to develop, reducing treatment performance further.

If left unattended for ten years or more, the reed beds eventually become redundant as they become so congested with ochre and organic detritus that mine water can no longer effectively flow through them. Insufficient maintenance of reed bed treatment systems therefore not only results in inefficient treatment systems, which increases the risk of breaching environmental permit conditions and causing an environmental incident, but ultimately, also cost much more to rectify. Over the past seven years, the Coal Authority has moved away from the minimal intervention model, to one where the aim is for routine maintenance to take place every 2 – 3 years in each individual reed bed unit. A number of key operational learning points have been identified over this transitional period that are discussed in more detail in this paper.

Controlling Water Levels

Controlling water levels, and having the ability to increase water levels in a reed bed during maintenance works, is one the most important factors when maintaining reed beds. The majority of material that builds up in a reed bed over time originates from the plants themselves due to the annual cycle of reed growth and die-back. To reduce the build-up of this organic debris, it is important to cut the reeds back regularly. The principal equipment used for reed cutting by the Coal Authority is an amphibious vehicle called a 'Truxor'™. This machine floats out into the reed bed, minimising any damage occurring to the rhizomes. In order for a Truxor to be deployed however, water levels in the reed bed need to be increased so that there is sufficient distance between the cut reed height, the rhizomes, and the normal operating water level; this is not always achievable if the reed bed is full of detritus.

When the Truxor was first deployed at Coal Authority sites, the blades were set at the lowest level, water levels were increased, where possible, so that the machine would float, and the reeds were cut at the water level. This procedure had the disadvantage that when the reed beds were full of detritus, the rhizomes were at risk of being pulled out of the substrate. Furthermore, any surviving reed stems were often drowned as the water level was too high. Both of these outcomes resulted in the reeds failing to recover, with either a few plants surviving around the edges of the reed bed, or the reed beds becoming devoid of plants altogether, examples include the reed beds at Sheephouse Wood and Old Meadows, Lancashire (fig. 2).

Following a number of failed attempts at a variety of sites, a different strategy is now deployed. Where reed beds have become so full of detritus that it is no longer possible to increase water levels, a full reed bed refurbishment is now planned, as the wetland has gone beyond the point of recovery. Where



Figure 2 *Old Meadows, Lancashire, where the reeds failed to recover following a reed cut (left), and Chell Heath, Stoke-on-Trent, where grasses and thistles have out competed the reeds (right)*

water levels are being successfully controlled however, they are increased to allow the Truxor to float freely (600 mm minimum water depth is required), and the reeds are cut 300 mm above the water level. This activity is repeated on a 2 – 3 year cycle depending on how vigorous the reed growth is at site, with the organic reed waste currently composted. It is worth noting that new trials commenced in 2023 to investigate the suitability of this material to be turned into a biochar product for use in land reclamation.

In addition to controlling water levels during routine maintenance activity, another key consideration for managing water levels is to minimise invasive plant species (e.g. grasses) from colonising reed beds. If water levels are kept too shallow, common grasses can get a foothold in a reed bed and in some circumstances, out compete the reeds e.g. Chell Heath, Staffordshire (fig. 2). Freshly planted reed beds are most at risk of this, however, if reed cuts are too brutal, the plants can be weakened, allowing other plant species to establish. Water depths in Coal Authority reed beds are generally maintained at a minimum depth of 300 mm to help mitigate this risk.

Reed Selection for Planting

When planting a new or refurbished reed bed, the choice of plants is the second most important consideration. As discussed above, reeds beds operated by the Coal Authority are typically planted with Phragmites sp. reeds, with some sites also including mixed planting with *Typha sp*. When the reed bed refurbishment programme commenced around seven years ago, small young plants, ≈100 mm in height were purchased due to the lower expenditure. However, these plants took longer to establish and were more prone to failure. In the last three years, older plants (1 – 2 years old) have been purchased, that are allowed to mature in the nursery and reach a height of 300 – 450 mm. Despite the higher initial outlay, these more mature plants settle into their new positions more quickly, and establish faster than the younger plants, thereby allowing the reed beds to be recommissioned sooner. In addition, wherever possible, local nurseries are also used to supply the reeds; this helps to reduce the reed mortality rate, as the plants are acclimatised to the local conditions.

At some sites, where sufficient reeds are present and it is possible to extract them from the existing substrate without damaging the rhizomes, it has proved feasible to use the existing reeds that are already acclimatised to a particular site. Preventing damage to the rhizomes is key to the success of this activity, as if the rhizomes are damaged, the

reeds will fail to recover leaving areas of open water (e.g. Acomb, Northumberland). This procedure has been important at sites where conditions are more challenging due to either the climate (i.e. wind exposure) or elevation of the location (e.g. Deerplay, Lancashire), or at sites where the mine water is more saline (e.g. Horden, North East Coast). This technique has the added advantage that the reeds are mature and therefore more tolerant of being moved, thereby allowing the reed bed to re-establish more quickly. This process is done in a phased approach, starting at one end of the reed bed and gradually working forwards. The reeds are extracted in 'sods' at least 200 mm deep (or deeper depending on the depth of the rhizomes in the substrate) so they can be temporarily stored on site between being extracted and re-planted, minimising the time they are out of water. Any excess or damaged reeds are disposed of at the end of the works, although the numbers are generally small. This more sustainable practice has the added advantage of minimising waste, which is either spread to land (in England and Scotland) or used in anaerobic digesters.

Reeds used to be planted individually and evenly spaced (3–4 plants per m^2) across the reed bed (fig. 3), however, this offered limited protection to plants from the prevailing weather conditions, and exposed them to greater risk of predation from birds (as happened at Summersales, Lancashire and Kimblesworth, County Durham). This methodology has been replaced by planting reeds together in rows (fig. 3), with the tops of the plants kept above the minimum water outlet level of the reed bed. Planting the reeds close together affords the plants greater protection from the weather, and reduces the risk of the tender plants being eaten by geese in the winter months, before they become fully established. Where predation from birds is a known risk, young reeds are planted into hessian mats and grown to ≈50 cm in height before being taken to site. This minimises the risk of the rhizomes being pulled directly from the growing media by the grazing birds.

Growing Media

In order for reeds to flourish, whether they be new or transplanted plants, it is essential to ensure that the correct growing media is placed in the reed bed. At sites where young reeds are planted, fresh growing substrate (BS3882:2015 British Standard Multi-Purpose Grade Top Soil) is imported to site. It is important to import fresh growing media when fully refurbishing a reed bed, as testing has indicated that the existing substrate is generally depleted in nutrients, and no longer



Figure 3 *Individual planting of young plants at Pool Farm, Scotland (left), which failed to establish vs. acclimatised reeds replanted in rows at Deerplay, Lancashire (right)*

fit for purpose (e.g. Deerplay, Lancashire). Generally a clay-rich loam is preferred, which has been found to have the correct nutrient balance for reeds. Where reeds are being transplanted however, the original substrate is typically used to minimise disturbance to the reeds, with fresh soil only added if required.

In areas where reeds are to be planted (at least 2 m wide open water zones are left at both the inlet and outlet ends of the reed bed in order to prevent the reeds choking the inlet and outlet channels over time), a layer of growing media (thickness ≈200 mm) is evenly placed across the reed bed; 200 mm provides sufficient depth of growing media for the rhizomes to take root. Once in place, it is important that the soil is wetted (generally with treated mine water), to stabilise it ready for the reeds to be planted; this prevents the soil from being blown away and helps maintain an even depth across the reed bed. This activity has to be done with care however, as if too much water is introduced, the growing media becomes too wet, and no longer holds its form, resulting in the reeds failing to establish properly (e.g. Silverdale, Staffordshire).

Where transplanted reeds are being re-planted, it is important to ensure that the growing media is evenly spread between the rows so that the reeds can colonise the full reed bed. When the Coal Authority first attempted transplanting reeds, insufficient growing media was placed between the rows, primarily due to logistical issues at site. It was assumed that over time, the build-up of ochre and some organic detritus material would provide sufficient substrate for subsequent new plants to spread out across the gaps between the rows (e.g. Deerplay, Lancashire and Silverdale Staffordshire). However, this has not proved to be the case, and no further reed colonisation has taken place. Where substrate has been spread across the reed bed however, be that for young (e.g. Gwenffrwd, South Wales) or transplanted reeds (e.g. Caphouse, Yorkshire), the reeds have successfully recolonised the entire reed bed quickly.

Reed Bed Establishment and After Care

Once reed beds have been refurbished, it is important that the plants are given time to fully establish prior to the reed bed being brought back online. If reed beds are recommissioned too quickly, the reeds often die back, resulting in sparse reed coverage at best, or at worst, the complete loss of a reed bed (e.g. Blenkinsopp, Northumberland). Initially, mine water was used to keep the freshly planted reed bed wet, however, this led to undesirable ochre deposition, which limited reed uptake and stunted their growth, particularly at sites where the mine water is more brackish. In preference to mine water, rainwater is now allowed to accumulate in the reeds beds to a depth of at least ≈50 mm, which has resulted in a much higher success rate; in periods of dry weather, freshwater is either obtained from the local receiving waterbody, subject to the necessary consents and approvals, or transported to site from an appropriate source. Water levels need to be kept at a minimum of 50 mm, in order to prevent other plant species (e.g. grasses), from colonising the reed bed and out competing the reeds. Once at least one third of new reed growth is above the water level, mine water is gradually re-introduced to the reed bed, with the level increased incrementally until the water depth is ≈300 mm deep. Generally, a minimum of at least six months is required before a reed bed is brought back online.

Maintenance Activity Window

Although generally small in area compared to natural wetlands, mine water treatment reed beds still provide key nesting habitat for a variety of bird species, including some red and amber listed species in the UK (Jaques *et al.*, 2021), often in areas where wetland habitats are rare. Consequently, any operational activity at these sites has to be restricted to prevent any accidental damage to nesting birds. Reed bed cuts and reed bed refurbishment works in the UK therefore only take place between the months of September and early March. Ideally reed bed cuts are undertaken earlier

in the maintenance window, as reed beds can be brought online relatively quickly (three weeks) after the works have been completed. Reed bed refurbishments are however far more invasive. These works are best done later in the operational season, nearer to spring, to minimise the time new plants remain dormant in the colder winter months. By planting early in the calendar year, the young or transplanted plants establish more quickly and are at less risk of predation from winter migratory birds, thereby having a higher success rate.

Prioritisation Model

Currently, the Coal Authority manage ≈160 individual reed beds, many of which are now in need of refurbishment, or for those that have been refurbished, require a reed cut every 2–3 years. In order to prioritise the programme of works, a new model has been established that assess the condition of the reed bed (i.e. reed height (used as a proxy for health); reed coverage; infestation of other plants; flow distribution; and available freeboard) and how well the reed bed is performing in terms of iron removal and permitted limits. Each item has a weighted score and is divided into five different scoring categories ranging from 1 (excellent) to 5 (bad). A reed bed that is performing well and is in good condition would gain a priority score of 20 (Grade 1), whereas a reed bed in poor condition would have a priority score of 100 (Grade 5). Data for each reed bed are collected at the end of each financial year by the Coal Authority's operational contractor, and the data are then uploaded into the model. Although it will vary from year to year due to budget constraints, the top ten reed beds are generally taken forward to the reed bed refurbishment programme for the following financial year (in the UK the financial year starts every April). With thirty-three reed beds successfully refurbished to date, it will take approximately fifteen years before all the reed beds in the current portfolio are brought back into good working order.

Conclusions

Based on nearly thirty years of operational experience, it has become clear that the original assumption that well designed reed beds required minimal maintenance was incorrect. When reed beds are left unattended, they eventually cease to work as intended and not only cost significant sums to refurbish (the average spend in 2022 for refurbishing a reed bed in the UK was £236,000), there is also a risk to permit compliance and associated reputational damage. In order to keep reed beds working effectively for longer, they need to be cut regularly (every 2–3 years), with a suitable avenue found for the waste material (currently composting). It is imperative that water levels are controlled to not only maintain even flow distribution but also facilitate regular reed cuts. When reed beds do need refurbishing, it is important to use reeds of an appropriate size when replanting (or transplant the existing reeds if possible), plant the reeds in rows in suitable substrate, and gradually introduce mine water after allowing the reeds to establish for at least six months. By following the approach described herein, the risk of the reed bed failing, and requiring replacement within two years is minimised. With such a large number of reed beds to manage, a prioritisation model has been created to help identify the reed beds most in need of refurbishment, which can then be moved across to the rolling reed bed cut programme once the works are successfully completed. It is however estimated that it will take around fifteen years and cost ≈£53 million, to rectify the damage caused by the low maintenance operational model.

Acknowledgements

The authors would like to thank the organisers and hosts of the IMWA 2023 and all the operatives at Severn Trent Services who help us deliver the reed bed refurbishment programme and manage our mine water treatment schemes. This paper is dedicated to the memory of Adam D.

References

Girts, M. A., Kleinmann, R. L. P. and Erickson, P. E. (1987), Performance Data on Typha and Sphagnum Wetlands Constructed to Treat Coal Mine Drainage. In Proceedings of the 8th Annual Surface Mine Drainage Task Force Symposium, Morgantown, West Virginia

Hedin R. S., Nairn R. W. and Kleinmann, R. L. P. (1994) Passive Treatment of Polluted Coal Mine Drainage. Bureau of Mines Information Circular 9389. United States Department of Interior, Washington D.C. 35 pp.

Jaques, R. O., Moorhouse-Parry, A. M. L., Carline, R., Mayes, W. M. and Hull, S. L. (2021) Biodiversity Benefits of Coal Mine Water Remediation Schemes for Bird Life. In Proceedings of IMWA 2021 "Mine Water Management for Future Generations", 206 - 211

PIRAMID Consortium (2003) Engineering Guidelines for the Passive Remediation of Acidic and/or Metalliferous Mine Drainage and Similar Wastewaters. European Commission 5th Framework RTD Project no. EVK1-CT-1999-000021 "Passive in-situ remediation of acidic mine / industrial drainage (PIRAMID). University of Newcastle Upon Tyne, UK, pp 166.

Tarutis, W. J., Stark, L. R. and Williams, F. M. (1999) Sizing and performance estimation of coal mine drainage wetlands. Ecological Engineering 12, 315-372

Wieder, R. K. (1989) A survey of constructed wetlands for acid coal mine drainage treatment in the Eastern United States, Wetlands 9, 299 - 315.

Structural logging and modelling for use in simulation of inflows in underground hard rock mines

Kym L Morton[1], Barry D Millsteed[2], Wayne van Heerden[1], Moses Msitsini[1]

[1]*KLM Consulting Services Pty, kmorton@klmcs.co.za, www.klmcs.co.za*

[2]*Barry Millsteed Geological Services Pty, barry.millsteed@millsteedgeological.com*

Abstract

African mines are predominately located in hard rock. Inflows to the underground or surface workings are typically along geological structures. Often the matrix permeability of the country rock is very low, individual water bearing structures provide some 80% of the inflows. It is therefore very important to map geological structures and plot the sources of water flowing into the mine.

Fractured rock aquifers have very distinct anisotropy and in Southern Africa, North – South striking structures are usually tensional, carrying most of the water into a mine. East-West structures tend to be compressional because of the plate tectonic regime and can be barriers to groundwater flow.

Permeability is proportional to aperture cubed, therefore, the width, vertical and lateral extent of the apertures in the water bearing geological structures are important to know for use in inflow calculations.

Accurate logging of core and underground or in-pit structural mapping is essential to understand the direction and risks of inflows to mine workings in both the short term and for life of mine. This paper describes the occurrence of fracture-controlled flow in mines, methods of mapping, logging and use in mine inflow simulations.

Keywords: Structural mapping, inflows, dewatering, faults, boundaries, compartments

Introduction

African mines are predominately located in hard (well lithified) rock where inflows to the underground or surface workings are typically along geological structures. Often the matrix permeability of the country rock is very low. Individual water bearing structures can provide some 80% of the inflows to the mine. To intercept the water, it is very important to map the structures carrying or diverting the water and plot with the sources of water to understand the risks to the mine.

Fractured rock aquifers often have very distinct anisotropy and in Southern Africa North – South structures are typically tensional and carry most of the water into a mine. In contrast, East – West structures tend to be compressional because of plate tectonic regimes, and therefore can be barriers to groundwater flow.

Permeability is proportional to aperture cubed therefore knowledge of the width and lateral extent of the apertures in the water bearing structures is important for use in calculations of inflow for life of mine and for specific sectors.

Individual structures such as faults can be both open and closed along strike and down dip. Accurate logging of core and underground structural mapping is essential to understand the direction and risks of inflows to mine workings in both the short term, for each mine sector and for life of mine.

Experience

The authors work on African mines. The rock successions comprising the African continent are predominantly composed of well lithified and often metamorphically altered successions that comprise the cationic cores of the continent, of the intervening, heavily deformed mobile belt successions. It is the combination of the thermal and tectonic history of these sequences that underpins the existence of most the continent's economic mineral deposits. Even coal bearing cover

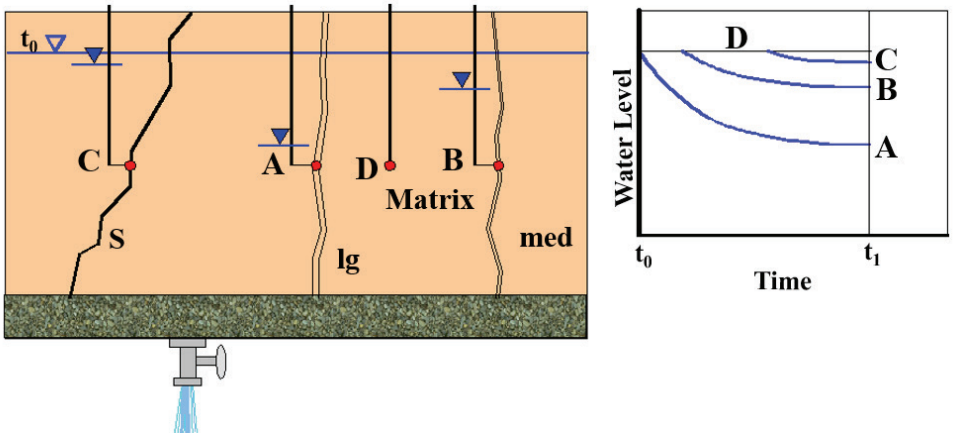


Figure 2 Speed of drainage from different types of water bearing structures (Morton et al *2008 after Atkinson 2007).*

sequences such as the Karoo Supergroup strata that are relatively undeformed and unmetamorphosed are well lithified. Because of the antiquity of the rocks as well as their complex thermal and tectonic history Africa tends to have some of hardest and least permeable rock types encountered.

Aquifers are mostly hard, fractured rock aquifers with inflows to mines occurring along open and often vertical structures that connect sources of water to both open pit or underground workings. Figure 1 illustrates the types of structures carrying water in hard rock mines.

Understanding the types and location of structures for use in a dewatering design is essential because each type of structure drains at different speeds into the mine workings. Figure 2 illustrates the speed of drainage.

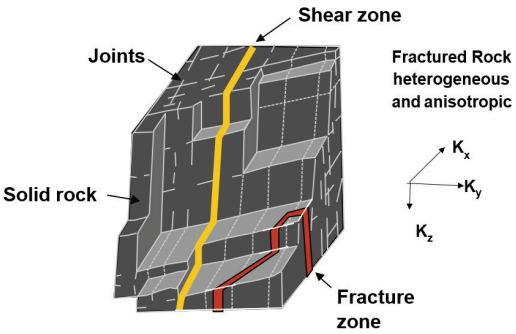


Figure 1 Types of structures carrying water in hard rock mines. (Atkinson 2007

Types of geological structures that carry water into mines

Geological structures affecting the rock mass of a mine can be tectonically derived, sedimentary or man-made.

Pre-mining geological structures.

There are numerous tectonically derived geological structures that may be potentially identified within a rock sequence. However, not all are equally capable of transmitting water. Some like axial pane cleavage are closed when unexposed to weathering and/or decompression at surface, as they are in fact simply planes of weakness within the rock fabric, not discontinuities.

Similarly gneissic foliation and many bedding planes represent a change of rock type of mineral composition and are not originally open voids in the rock. Other structures (e.g., jointing) have, by definition very small aperture dimensions of up to several millimetres and tend to be closed or transmit small (i.e., nuisance) amounts of water within mines.

Faults are major water carrying structures. This can be true of either the central fault core zone (i.e., the zone of slippage), or the enclosing, fractured fault damage zone (Figure 3).

Faults may be "open" to water transport along their strike in extensional tectonic regimes, "closed" in compressional regimes, or be a combination of both depending on

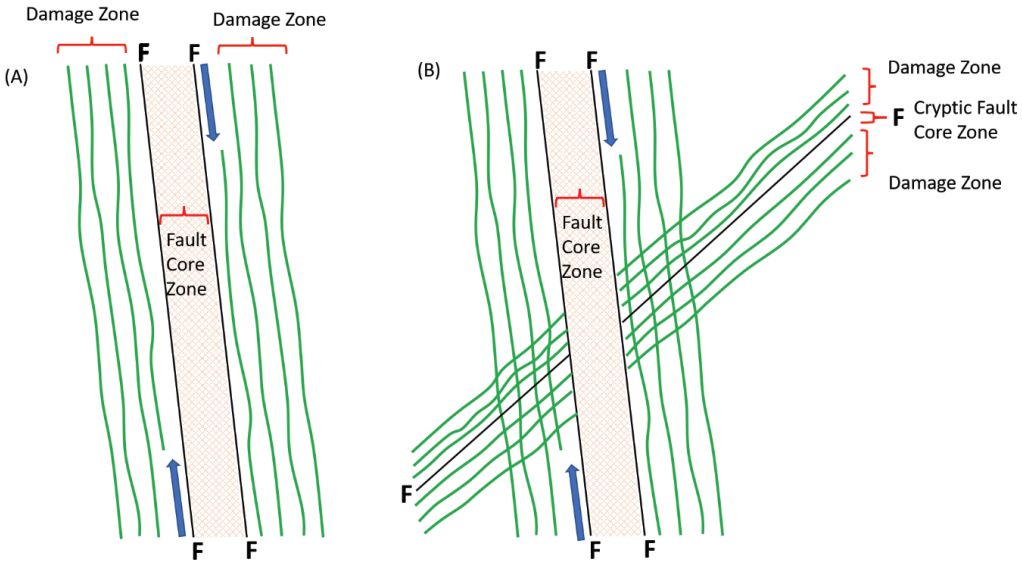


Figure 3 *Schematic cross-section diagrams of faults and associated increased permeability. and may cause older closed structures to become open (see Figure 4).*

the orientation of a fault segment relative to the extant tectonic regime in curved faults (Figure 4).

Fault core zones may be open or closed depending upon the presence or absence of fault gouge or mylonite that can act as a sealant. These sealants may also be inconsistently present along a fault. In terms of lateral transport of water across fault planes they can also act as aquicludes or aquitards in more porous rock materials. The emplacement of younger, cross cutting structures can also affect the water bearing abilities of that part of an older structure that is crosscut by a younger structure (Figure 5).

The intrusion processes of Kimberlite bodies results in them having circular, unbonded contacts around the pipe that connect upper and lower aquifers in the country rock allowing rapid movement of water into workings (Morton 2008).

Geological structures that may have originally been "open" can become closed due to post formation infilling with minerals such as quartz or calcite. While structures that may have originally been "closed" may become "open", due to changes in the extant compressional regime, rock movements due to mining activities, the development of younger cross cutting geological structures (e.g., faults) etc or a combination of multiple factors.

For the implementation of appropriate mine dewatering strategies to be put in place the anisotropy in the rock mass that acts as the structural aquifers must be characterised in terms of its capacity to connect areas of recharge to the mine, to act as aquifers and to determine where that water is transported to. Geological and Geotechnical logging assist with plotting the anisotropy.

Manmade structures

On surface a zone of relaxation (ZOR) occurs around and within a pit. Figure 6 and Figure 7 show the ZOR in plan and section. This rapidly transmits surface and ground water into the workings.

Similarly, the entire network of voids in an underground mine creates a 3D interconnected zone of preferential groundwater flow. This 3D network of interconnected voids and fractures both store and transmit water throughout the mine. When the open pit overlies the underground workings the ZOR can be connected to structures associated with the ore body and the crown pillar.

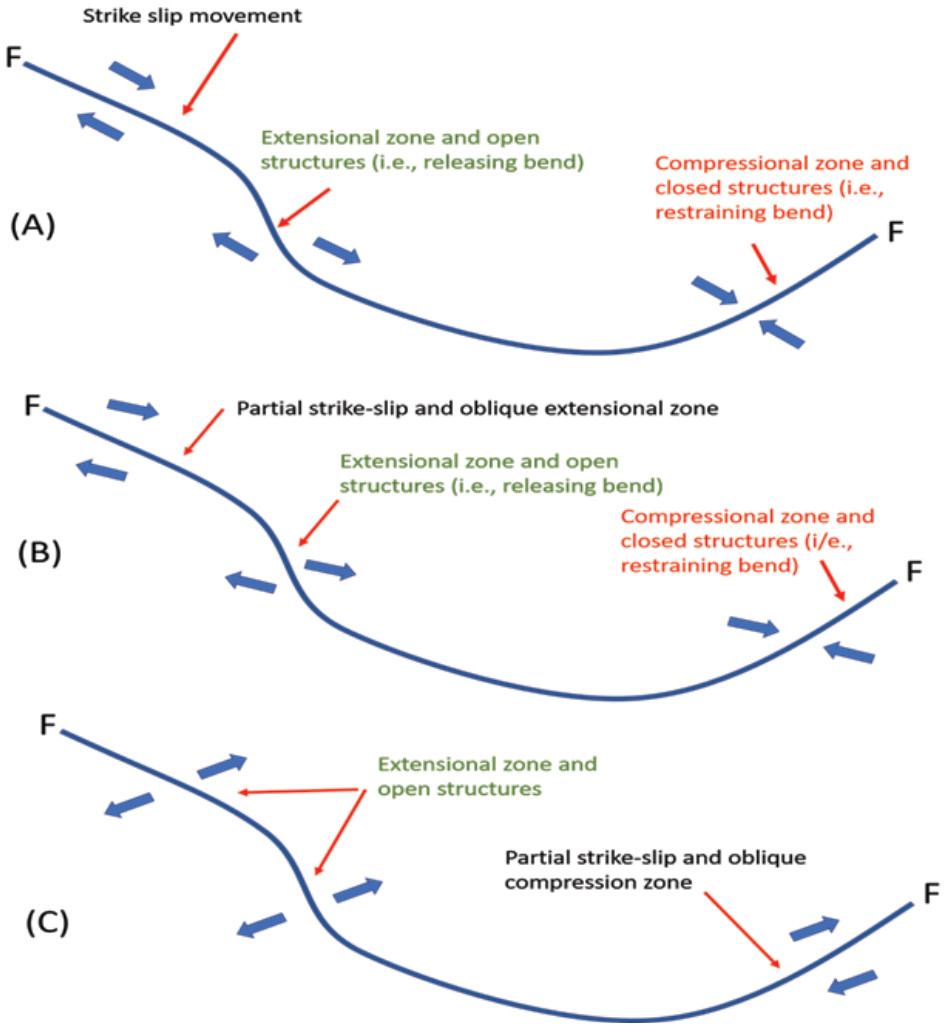


Figure 4 Schematic plan views diagram of the same curved strike slip fault showing the sense of movement of the rocks either side of the fault in three different compressional/extensional regime orientations.

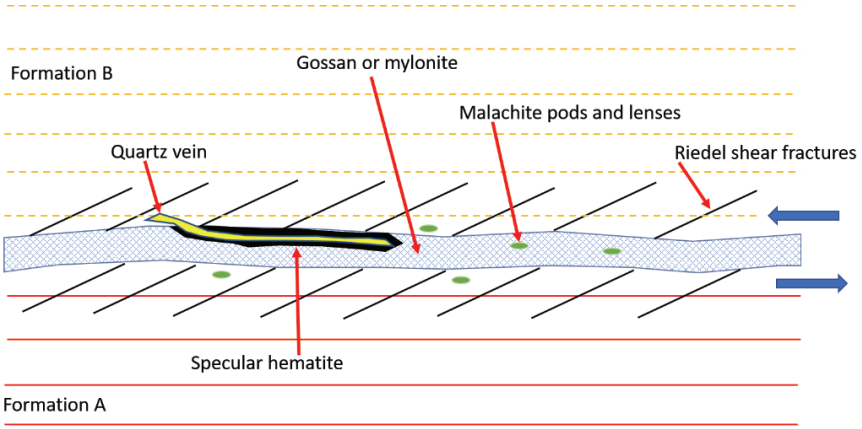


Figure 5 Schematic cross-section diagram through a bedding parallel thrust fault (blue cross hatching)

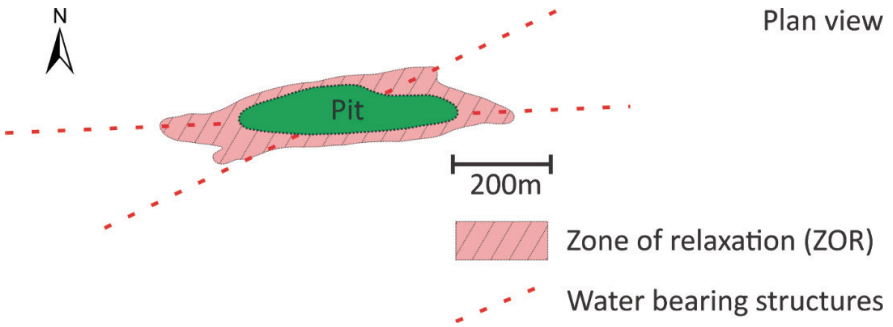


Figure 6 Plan view of structural influence on the zone of relaxation (ZOR)

Risk map

Once all the main water bearing structures and underground voids have been mapped, they can be combined with measurements of groundwater gradient, sources of water (both on surface and underground) then used to produce a risk map. The map can be used in combination with a mine planning tool such as Deswik® to inform production crews of water risk and enable planning for nimble dewatering systems. Figure 8 shows an example of a risk matrix for an underground mine.

Use in numerical modelling

Important structures can be incorporated into finite element numerical models such as FEFLOW to simulate inflows to specific mine sectors and provide more realistic inflow estimates. Using measurements of groundwater gradients, targets for reducing water pressures in and around a mine can be set and achieved by draining the main water bearing structures in advance of mining.

Conclusions

It is essential for hard rock mines to plot and understand the major structures that carry water into the mine. The anisotropy needs to be understood to be able to give numerical models better predictive capabilities. Structures can be used in a risk map to guide dewatering in advance of mining.

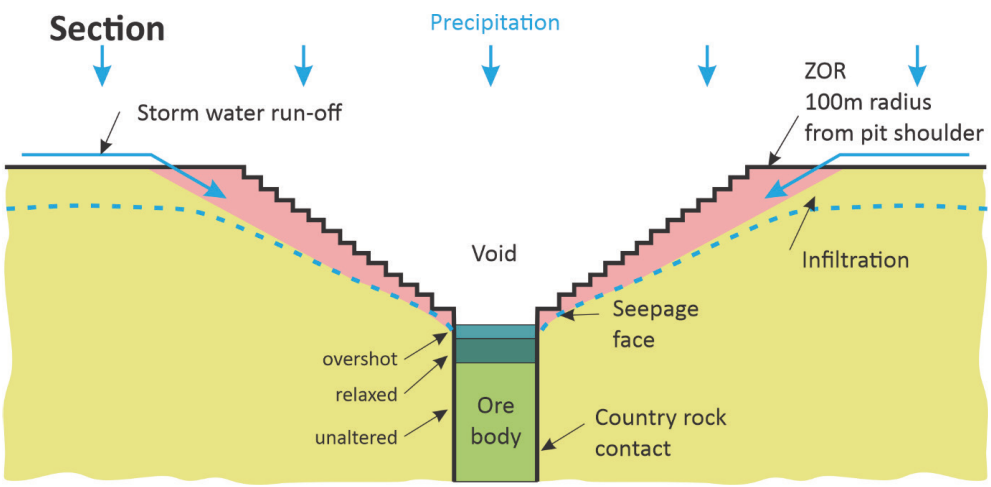


Figure 7 Section view of the ZOR

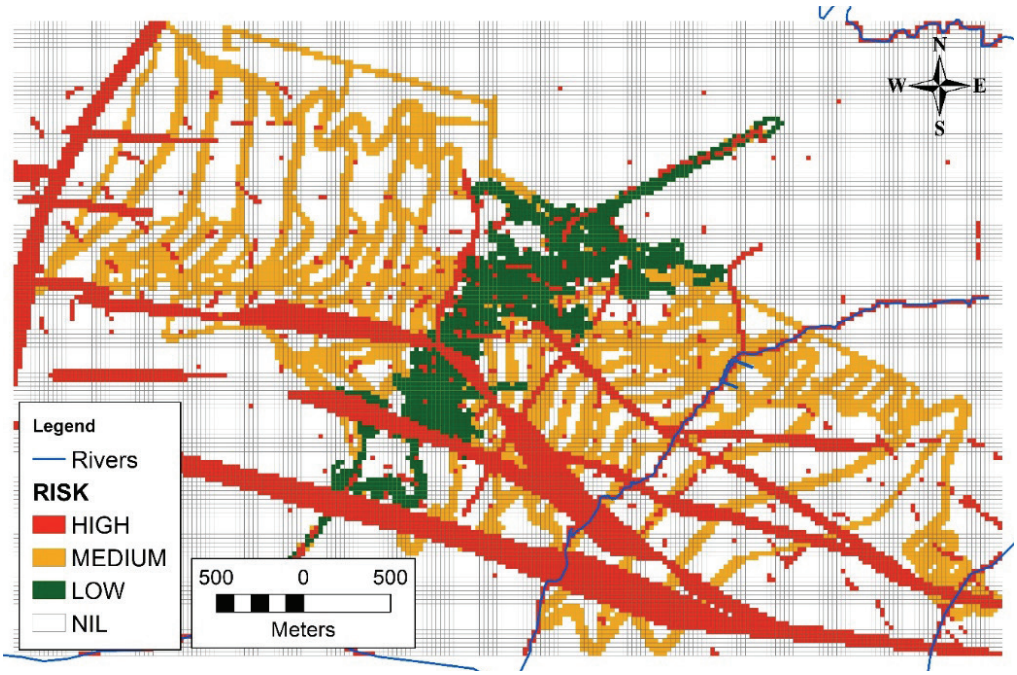


Figure 8 *Risk matrix for an underground mine*

References

Atkinson LC (2007) Debswana mining hydrology short course notes – Gaborone 2007 (unpublished)

Morton KL and Muller S (2003) Hydrogeology of Venetia diamond mine, South Africa, South African Journal of Geology 106(2-3):193-204 , doi: 10.2113/106.2-3.193

Morton KL (2008) The hydrogeology of kimberlite mines with specific reference to Finsch mine. Unpublished PhD thesis Imperial College London

Morton KL, Muresan MC, Ramsden F (2008) Importance of pore pressure monitoring in high walls. Journal- South African Institute of Mining and Metallurgy 108(11):661-667 License CC BY 4.0

Mine Water Research with Analogue Modelling – The Agricola Model Mine

Elke Mugova[1], Christian Wolkersdorfer[2]

[1]*Technische Universität Bergakademie Freiberg (TUBAF), Department of Hydrogeology and Hydrochemistry, Otto-Meißer-Bau, Gustav-Zeuner-Str. 12, 09599 Freiberg, Germany, elke.mugova@grubenwasser.org, ORCID: 0000-0001-6019-9945*

[2]*South African Research Chair for Acid Mine Drainage Treatment, Tshwane University of Technology (TUT), Private Bag X680, Pretoria 0001, South Africa, christian@wolkersdorfer.info, ORCID: 0000-0003-2035-1863*

Abstract

Investigations in flooded underground mines can be difficult to perform, expensive and, above all, time-consuming. An alternative to field work is the use of an analogue model such as the Agricola Model Mine (AMM). This is the world's unique 4 × 6 m analogue model of a flooded underground mine with four shafts, which are connected to each other on four levels. Based on three different experiments about density stratification, the first flush using fluorescent dye tracers, it could be shown that it is possible with the AMM to replicate different scenarios in a flooded mine.

Keywords: Analogue model, stratification, first flush, tracer test

Introduction

To investigate hydrodynamic processes in flooded mines, field experiments in the flooded mine itself are usually carried out. These may include depth profile measurements to investigate density stratification, or artificial tracer tests to investigate flow paths and velocities. In addition, water samples may be taken within the mine water pool or at the discharge point. If this is done over a longer period, the development of water quality can be evaluated. Analogue modelling can be used to gain further insight into the processes in the flooded mine if investigations in the real mine are not possible. Investigations can also be conducted using an analogue mine model. An analogue model allows different conditions and experiments in the flooded mine to be represented and evaluated. At the Tshwane University of Technology in Pretoria, South Africa, this is done using the *Agricola Model Mine* (AMM). The possibilities of analogue modelling will be demonstrated by means of various experiments, to indicate that analogue modelling of different scenarios in flooded mines helps to understand mine water related issues.

Methods

The AMM is a 4 × 6 m analogue model of a mine that can be flooded completely or only in certain sections. It consists of 4 shafts connected by 4 horizontal levels made of insulated PVC pipes. Different parts of the mine can be separated by valves and 36 sampling ports allow for water sampling and tracer injection. Electrical conductivity and temperature loggers are installed in various sections of the AMM. To simulate thermal gradient, heating foils are placed around the sumps. Flooding takes place via inlet hoses at each shaft, with continuous flow possible using peristaltic pumps (Figure 1).

To investigate different applications of the AMM such as density stratification or the first flush different fluorescent dye tracers were used. Therefore, in experiment 1, shafts #3 and #4 were separated and only shafts #1 and #2 were flooded. In shaft #2, a density stratification was created below level 145 by placing NaCl bags in this area. After flooding, a continuous flow from shaft #2 to shaft #1 in the upper part of the mine was achieved by using a peristaltic pump at the inflow (shaft

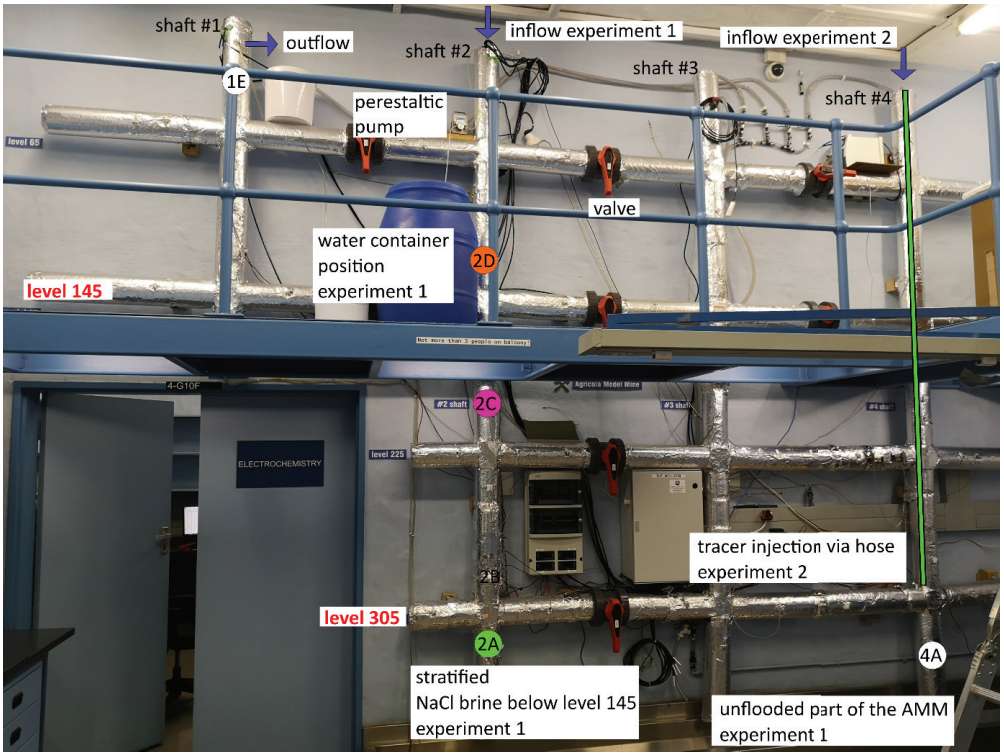


Figure 1 *Agricola mine model (AMM) with water container and peristaltic pump position for experiment 1; in round circles selected injection and sampling ports; 2D (orange) injection EoY, 2C (pink) injection SRB, 2A (green) injection EoY; green hose in shaft #4 injection EoY above level 305*

#2). After 69 days, the heating foil in the sump of shaft #2 was turned on to determine whether the geothermal gradient affected the stratification (heating the water to 20–21 °C). Fluorescent tracers were injected into shaft #2 at three different depths (eosinY, EoY, at section 2D, sodium rhodamine B, SRB, at section 2C and sodium fluorescein, NaFl, at section at 2A) to investigate the stability of the stratification and the first flush effect. To examine the stability of the stratification, a depth profile of the electrical conductivity was recorded in shaft #2 towards the end of experiment 1.

In the second experiment, the possibility of injecting the tracer into the mine water pool by using a hose and the behaviour of the tracer after the injection were investigated. For this purpose, the entire AMM was flooded and a low continuous inflow (20 mL/min) was established using a peristaltic pump at the inflow of shaft #4. As in experiment 1, the outlet was at the top of shaft #1. A hose was then lowered down in shaft #4 and tracer was pumped into the shaft via the hose. Just above level 305 the NaFl was injected into the flooded shaft.

In both experiments 1 and 2, samples were taken at regular intervals from the sampling ports along the flow paths and analysed using a spectrofluorometer (Cary Eclipse Fluorescence Spectrophotometer; Agilent) to observe the concentrations at the various sections and the development of the concentrations over time. In experiment 2, a continuous flow fluorimeter (P.-A. Schnegg, Neuchâtel) was installed behind the point of discharge to continuously measure the tracer concentration at a 1-min-interval (10 min towards the end of the experiment).

Results and Discussion

In both experiments 1 and 2, hydrodynamic processes were modelled in the AMM. In experiment 1, stratification remained stable over the entire experimental period (133 days), even after the heating foils in shaft #2 were switched on. Stability and barrier function

of the stratification could be confirmed by the depth profile (Figure 2) as well as by the tracer concentrations. Almost no SRB and NaFl could be detected above level 145, both tracers remained in the lower water body. Some of the EoY injected in the upper part of shaft #2 sank into the sump due to its higher density compared to tap water. However, some remained around the injection port and was flushed out of the upper part of the AMM (above level 145). Based on the tracer concentrations at section 1E, a typical first flush curve of EoY could be identified (Figure 3). After about 10 days, the outflow as section 1 E showed very low EoY concentrations. A periodicity in the tracer concentrations was observed in shaft #2, below level 145 (Figure 3). This indicates the formation of convection cells (Kories *et al.* 2004; Taylor 1988). As experiment 1 was conducted analogue to the conditions and observations in the Finnish Metsämonttu mine, the observations of the analogue modelling can be used to interpret the real word scenario (Wolkersdorfer 2017). Stable stratification could be studied in the Finnish flooded mine as well as in the AMM. In addition, convection cells suspected in the real mine can be directly observed in the AMM.

Experiment 2a aimed in investigating dye tracer injection into a flooded underground mine and the flow through the AMM. One of the reasons for this test was to identify processes that caused the very low tracer recovery rates at the Georgi Unterbau

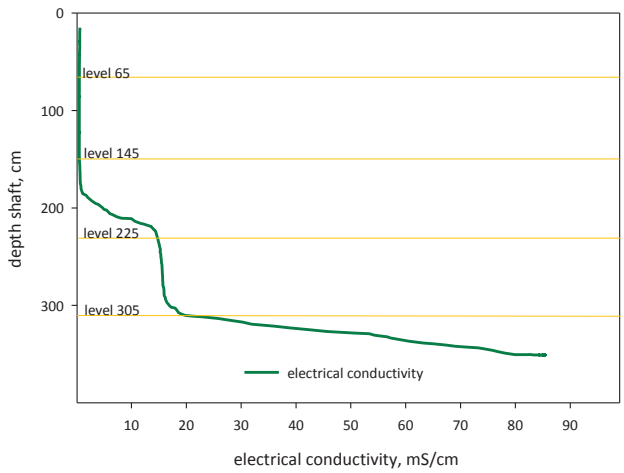


Figure 2 *Depth profile of electrical conductivity in shaft #2 (experiment 1)*

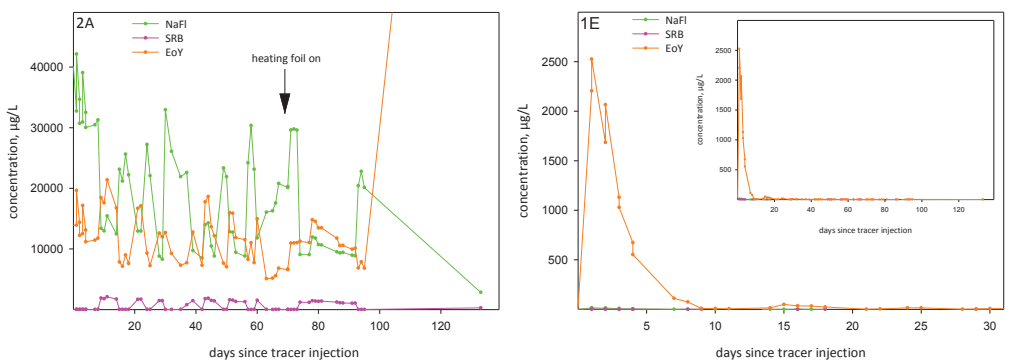


Figure 3 *left: NaFl, SRB and EoY concentrations at sampling port 2A (last measured values after a long sampling gap, presumably contamination during sampling); right: NaFl, SRB and EoY concentrations at sampling port 1E, before discharge (experiment 1)*

dye tracer test and the increase in tracer concentrations after the first breakthrough (Wolkersdorfer *et al*. 2002). In the first trial, the hose through which the tracer was injected was placed just below level 305. As a result, almost all the tracer sank down into the sump, and only a small amount of NaFl flowed through the AMM because the tracer accumulated in the sump. Due to the higher density most of the tracer was therefore "stuck" in the sump. Positioning a hose or pipe for tracer injection at the correct location is an important finding for tracer tests in real mines. From the analogue model it could be identified that an accurate knowledge of the injection depth is essential for a successful tracer test. For experiment 2b, the hose was positioned just above level 305. Through a window in the AMM insulation, the exact position and injection process could be visually observed. It was evident that a large amount of the tracer sank into the shaft sump, while some of this tracer was flowing with the overall flow into the connected level 305. Visual records from section 4A clearly show that a large fraction of the tracer accumulates in the sump (Figure 4). Samples along the flow path and fluorometer records indicate that the tracer passed through the AMM and reached the outflow after about 1 day. Several peaks can be seen at sampling section 1E (below the outlet) as well as at the other sections sampled along the flow path, indicating that tracer was released from the sump at shaft #4 at regular intervals. This very likely was caused by convection cells in the sump but will require further investigation.

Conclusion and Outlook

With the different experiments and scenarios described here, it has been shown that the real conditions in a flooded underground mine can be simulated with an analogue model mine (AMM) and that the AMM is an important tool for the investigation of flooded mines. In real mines, stable stratification was observed over months, years and decades. This stable stratification could also be confirmed in the AMM, with a shortened experimental period. Furthermore, the first flush can be simulated in the analogue model and thus examined

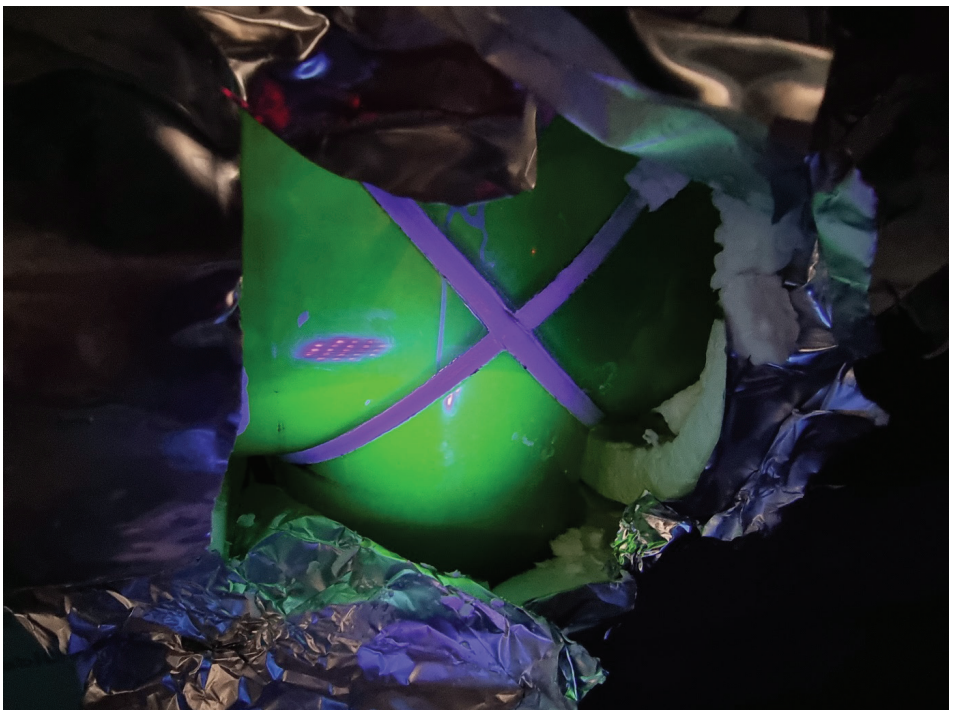


Figure 4 *Tracer injection via a hose into shaft #4, accumulation of tracer in the shaft sump (experiment 2*

both at the discharge and in the mine pool itself. It is beneficial that the boundary conditions of the AMM are well defined and known, there are fewer unknown influences. In the laboratory, changes in the mine water can be measured or sampled at various points in the analogue mine. In a real mine, this is difficult or impossible. Experiments in the AMM can be repeated under slightly different conditions, which is not feasible in most field experiments. This makes it possible to find an ideal setup for field experiments, especially for tracer tests. In the AMM experiment, for example, it was shown that there are sources of error, such as the wrong injection level for tracers, which strongly influence the results of the experiment and may lead to incorrect assumptions. A further advantage of the AMM is that the much shorter duration of experiments in the AMM saves resources. AMM experiments are cheaper than field experiments. Despite these advantages, it is important to note that the AMM is only a simplified version of a flooded mine. For example, it is currently not possible to simulate the interaction between the shaft and the surrounding rock. Combining analogue and numerical modelling bridges this gap. CFD software such as COMSOL Multiphysics® can be used to numerically model the experiments in the AMM, allowing comparison of the analogue and numerical results, as well as more advanced approaches that are not viable with the AMM. Analogue models in mine water research can explain observations in real mines that could not previously be demonstrated with sufficient data.

Acknowledgements

The authors thank their respective research institutions for providing support in conducting this research. The German foundation "Forum Bergbau und Wasser" made travel funds available. The NRF SARChI chair for Mine Water Management, Department of Environmental, Water and Earth Sciences, Tshwane University of Technology under Grant № 86948 supported this research. Many thanks to our colleagues for their assistance in the lab.

References

Kories H, Rüterkamp P, Sippel M Field and numerical studies of water stratification in flooded shafts. In: Jarvis AP, Dudgeon BA, Younger PL (eds) International Mine Water Association Symposium 2004, Newcastle upon Tyne, 2004. vol 1. University of Newcastle, 149-159 p

Taylor OJ (1988) Predicted effects of underground mine flooding at Tract C-b in Piceance Basin, northwestern Colorado. Water Resour Investig Rep WRI 87-4189:1-16.

Wolkersdorfer C (2017) Mine Water Hydrodynamics, Stratification and Geochemistry for Mine Closure – The Metsämonttu Zn-Cu-Pb-Au-Ag-Mine, Finland. In: Wolkersdorfer C, Sartz L, Sillanpää M, Häkkinen A (eds) IMWA 2017 – Mine Water & Circular Economy. vol I. Lappeenranta University of Technology, Lappeenranta, p 132-139

Wolkersdorfer C, Hasche A, Unger K, Wackwitz T (2002) Tracer Techniken im Bergbau – Georgi-Unterbau bei Brixlegg/Tirol. Wiss Mitt Inst Geol 19:37-43.

Exploring the Potential for Rare Earth Element Recovery from Coal Mine Acid Mine Drainage using Ion Exchange Technology

Tamlyn S. Naidu[12], Nkosilomusa Moyo[3], Ed Hardwick [3,4], Jenny Falconer[4], Janet Smith[2,3,5], Craig Sheridan[1,2], Lizelle van Dyk[2,3]

[1]*School of Geography, Archaeology and Environmental Studies, University of the Witwatersrand, Bernard Price Building, 1 Jan Smuts Ave, Johannesburg, 2000, South Africa*

[2]*Centre in Water Research and Development, University of the Witwatersrand, Johannesburg, Private Bag 3, Wits, 2050, South Africa*

[3]*School of Chemical and Metallurgical Engineering, University of the Witwatersrand, Richard Ward Building, 1 Jan Smuts Ave, Johannesburg, 2000, South Africa*

[4]*CwengaTechnologies (Pty) Ltd, 28 Boeing Road East, Dunvegan, 1609, South Africa*

[5]*Crundwell Management Solutions Metallurgical Consultancy and Laboratory (Pty) Ltd, Pinelands Office Park, Unit T5, 1 Ardeer Road, Modderfontein, 1609, South Africa*

Abstract

Rare earth elements (REEs) are crucial in multiple industrial applications, but their limited distribution in the Earth's crust has led to worldwide supply shortages. A sustainable alternative is recycling REEs from waste streams, such as mine-impacted water. This study examined the REE concentration in coal mine acid mine drainage (AMD) and used ion exchange (IX) technology to extract them. Results showed that the collected AMD contains Ce La, Nd, Gd, Pr, Dy and Y which amount to approximately €1 /m3 in value, and that cationic resin effectively extracts more REEs from AMD than chelating resin. Iron in AMD lowers the adsorption capacity of resins and may need to be removed before REE extraction. This study provides a proof of concept for REE extraction using IX technology, potentially allowing for reduced costs of AMD treatment, generation of profits, and promotion of a circular economy in the mining industry.

Keywords: Rare earth elements (REEs); acid mine drainage (AMD); ion exchange technology; circular economy.

Introduction

Treatment costs for mine impacted waters are amongst the highest in the industrial wastewater treatment sector, with limited sustainable options available to date (Brewster *et al*., 2020). Interestingly, many acid mine drainage (AMD) sources contain significant amounts of lanthanides and actinides (commonly referred to as rare earth elements (REEs) (Vaziri Hassas *et al*., 2023)) which remain a valuable resource because of their critical use in many high-tech industrial and commercial products. The recovery of REEs from AMD is an important development in AMD processing as it has the potential to offset the traditionally high treatment costs associated with remediation. Global REEs supply challenges as well as their abundance in many AMD streams, may even allow for revenue generation from AMD sources and thus deserves consideration in the mining wastewater sphere.

There are several techniques that have been used to recover metal ions from AMD including staged chemical precipitation, solvent extraction, cloud point extraction, ion flotation, ion-exchange (IX), adsorption, molecular recognition technology, magnetic separation and membrane filtration (Mwewa *et al*., 2022). Of these techniques, IX using resins is considered an environmentally sustainable option, as none of the toxic organic solvents employed in other types of metal recovery are used (Felipe *et al*., 2021). Moreover, in some AMD streams REEs are found in small amounts, and IX technology is particularly efficient for treating large volumes

of acidic water containing metals in trace concentrations (Simate & Ndlovu, 2014).

IX is the formation of ion pairs on functional groups attached to a crosslinked polymer matrix. Ions in solution can exchange with ions attached to the functional groups, via electrostatic attraction. Higher charged ions and ions with a small, hydrated radius are most strongly held (Dahman *et al.*, 2017). REEs form mainly trivalent cations and therefore the chemistry of adjacent REEs are very similar and difficult to separate. As the atomic weight of the REE increases, the f-orbitals are filled, reducing the atomic (and ionic radii) of the elements (known as "Lanthanide Contraction") (Hubicki *et al.*, 1968). In water solutions, cations are hydrated which results in a stronger attraction, and a subsequent increase in hydrated ionic radius with atomic weight. Strong Acid Cation (SAC) resins will have selectivity sequence from the light to the heavy lanthanides: $>Ce^{3+}>Eu^{3+}>Lu^{3+}>Y^{3+}>Fe^{3+}$. The differences are small, and so it is difficult to separate adjacent Lanthanides. Chelating resins have interactions with the F-orbitals and so the selectivity effect is amplified and the selectivity sequence is reversed: $Fe^{3+}>Y^{3+}>Lu^{3+}>Eu^{3+}>Ce^{3+}$(Hubicki *et al.*, 1968).

Although IX has been used for AMD treatment in the past (Chen *et al.*, 2022; Vecino *et al.*, 2021), the use of cationic resins in the enrichment of a variety of REEs has not been studied in depth. The kinetics of these systems are of importance to large scale implementation or practical applications, and thus research which delves into the mechanisms of REE extraction from AMD is much needed in the water treatment and the REE sphere.

The aim of this research was to explore this concept by studying the use of IX in REE recovery from coal mine AMD waste, and to investigate the behaviour of this extraction and recovery. The behavioural parameters which were identified as important in this study, were (i) isotherm parameters, (ii) batch kinetics, (iii) breakthrough capacities and (iv) desorption behaviour. In addition, (v) determining the concentration of REEs in an AMD dam as well as coal samples taken from the area surrounding the AMD dam, were identified as important to discern the availability of REEs in coal, and the leachability of these REEs into surrounding water bodies. The kinetic and isotherm studies were deemed important as they will likely aid in understanding the adsorbent-adsorbate interaction and diffusion, providing insights into the mechanisms of REE extraction and recovery from AMD.

Materials and Methods

Resin was sourced from CWENGA technologies, South Africa. Lewatit® MonoPlus TP 207 (a weakly acidic, macroporous cation exchange resin with chelating iminodiaceticacid groups designed for the selective extraction of metal cations from weakly acidic to weakly basic solutions), and Lewatit® MonoPlus S 108 H (a strongly acidic, gelular cation exchange resin also with beads of uniform size and based in a styrene-divinylbenzene copolymer), were chosen due to their metal removal and water demineralization applications. Acid mine drainage from a coal mine storage dam in Emalahleni, Mpumalanga was used. Fresh AMD samples were taken from the dam and stored in a temperature-controlled room, while a coal/rock sample was obtained from the area surrounding the AMD dam and analysed directly.

The behavioural parameters of the IX system were tested in the following manners:

1. **AMD REE content:** Samples were analyzed using inductively coupled plasma optical emission spectroscopy (ICP-OES) and inductively coupled plasma mass spectroscopy (ICP-MS) at two external laboratories (University of Johannesburg and De Bruyn Spectroscopic Solutions, South Africa).
2. **Coal tailings metal content:** Coal samples were analyzed for metals content at the University of Johannesburg, using X-ray fluorescence (XRF), X-ray diffraction (XRD) and ICP-MS.
3. **Isotherm Parameters:** The two resins were tested with AMD samples (which were diluted to different concentrations and placed into 900 mL bottles containing 45 mL S108H or 64 mL of TP207). The bottles were agitated

for 3 days at 23°C, at an RPM of 200. The liquid portion in the vessels was filtered and analyzed using ICP-OES and ICP-MS. The data were fitted to four different adsorption models (isotherms). The Freundlich, Langmuir, Temkin, and Dubinin–Radushkevich isotherms were applied to fit the isothermal data.

4. **Batch Kinetics:** 900 mL AMD and 45 mL of S 108H resin, or 800 mL AMD and 64 mL of TP 207 resin, were decanted into plastic bottles. The bottles were agitated on a shaking table for 4 h at 23°C. Liquid samples were collected at different time intervals and filtered for analysis using ICP-OES and ICP-MS. Pseudo-First-order (PFO), Pseudo-Second-order (PSO), Elovich, and Intra-particle (IP) models were used to assess the kinetic data.
5. **Breakthrough capacity and desorption behaviour:**
    a. AMD was passed through the S 108H resin at a rate of 12.7 BV/h. Samples were collected after 28 bed volumes (BV) had passed through the column. Samples were assayed for Fe, Ca, Mg and REEs using ICP-OES and ICP-MS. Iron, Calcium and Magnesium were focused on as these were found in high concentrations in the AMD samples used for this study.
    b. AMD was passed through the TP 207 resin at a rate of 6.6 BV/h. Samples were collected after one bed volume. Samples were assayed for Fe, Ca, Mg and REEs using ICP-OES and ICP-MS.
    c. Loaded S 180H resin was treated with 0.01M of EDTA solution passed through at 6 BV/h. Samples were collected after 0.3 bed volumes and assayed for Fe, Ca, Mg and REEs. A stronger solution of EDTA (0.14M and 0.27M) was tested on a fresh batch of resin.
    d. A similar experiment was run for the TP 207 resin using sulfuric acid instead of EDTA solution; the concentration of sulfuric acid used in the second stage was 2% and in the third stage was 5%. Deionized water was used to rinse the resin in the first section. 10% and 15% sulfuric acid solution were used to increase the desorption efficiency in two new allotments of AMD and resin.

The models which were assessed are discussed in detail in Appendix A.

Discussion

AMD and Coal Tailings REE content

The concentrations of Y, La, Ce, Pr, Nd, Gd and Dy in AMD were 1.97 mg/L, 0.67 mg/L, 6.02 mg/L, 0.28 mg/L, 1.64 mg/L, 0.87 mg/L, and 0.33 mg/L respectively. The same elemental concentrations found in waste coal/rock samples were 7.3 mg/kg, 15 mg/kg, 66 mg/kg, 3.3 mg/kg, 13 mg/kg, 1,9 mg/kg, and 1,4 mg/kg respectively. A further Sm content of 2.29 mg/kg was found in the waste rock. Using current market values for the REEs (IndiaMart, 2022; Institut Seltene Erden, 2022), the potential recovery of REEs per m3 of AMD and per thousand kilograms of waste rock processed (without taking into account cost of treatment or transport) is at least €1 /m3 and €4.34 /1000 kg respectively (Galal, 2023; Statista, 2023). It should be noted that only the data for REEs with a statistical standard deviation of less than 30% among measurements from the same source are presented above. Any REE concentration which was deemed statistically inaccurate was omitted from this study, therefore the potential recovery is assumed to be higher than the results presented in this paper. Once the initial REE content was found, extraction and recovery using IX was then evaluated.

Isotherm Parameters/Equilibrium Models

Behaviour of the less acidic resin (TP207) notably aligned to the Langmuir model for all elements, except for Y and La (please see Appendix A, Table A1 and A2 for model assessment). Both of these elements aligned to the Temkin isotherm model. The results indicated that the Langmuir model could potentially be used for modelling resin adsorption of Fe, Ce, Nd, and Gd in an AMD system, while the Temkin model is best suited for modelling Y and La adsorption on the same resin.

The Langmuir model (for both the weak and strong acidic resins) showed promise in defining the behavior of the adsorption system experiments for the range of REE metals from an AMD solution, with the Temkin model showing potential in governing or defining the TP207's adsorption of Y and La. For both systems, the Temkin modelling showed coefficients of determination higher than that of the Freundlich and the Dubinin–Radushkevich models. It is thus hypothesized that under conditions where the Langmuir isotherm fails, Temkin can be used to model the system in a relatively accurate way. When comparing both resins using the Langmuir Isotherm, the maximal adsorption was seen to be consistently higher using the S 108H.

In the case of the Gd, the adsorption on the S 108 H was over 5 times more than on the TP 207 resin. Interestingly, the Langmuir constant (K), which indicates the extent of interaction between adsorbate and the surface, was seen to be higher in the TP 207 than in the S 108 H resin (although both resins present fairly high values for this constant). This shows that (i) there is a strong interaction between adsorbate and adsorbent for both resins (with REEs in AMD) and (ii) that the ratio of adsorption to desorption rates at this temperature is higher on the TP 207, than on the S 108H resin. Although the Freundlich Isotherm did not display high enough coefficients of determination to be considered in alignment with the data obtained, the intensity of adsorption (n) was consistently over 1 which indicates favourable sorption for both resins.

Batch Kinetics

The data obtained (Appendix A – Table A3 and A4) from the batch kinetic experiments from both resins unequivocally displayed PSO behaviour. The calculated equilibrium adsorption capacity (qe) using the PSO model (138 for Ce on S 108H, and 39 for Ce on TP 207) most closely aligns with the experimental

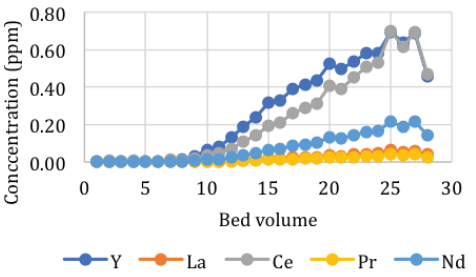


Figure 1 *Breakthrough capacity of MonoPlus S 108 H resin at a rate of 12.7 BV/h (for Fe, Ca, and Mg)*

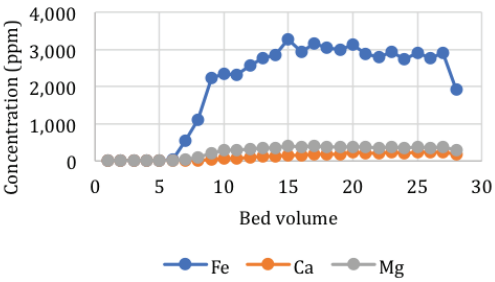


Figure 2 *Breakthrough capacity of MonoPlus S 108 H resin at a rate of 12.7 BV/h (for a range REEs)*

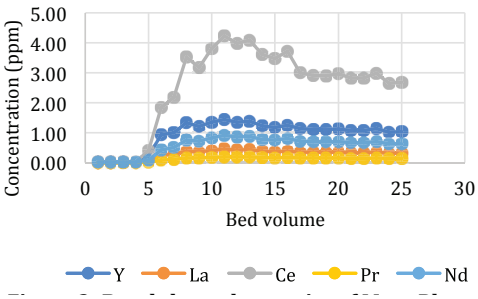


Figure 3 *Breakthrough capacity of MonoPlus TP 207 resin at a rate of 12.7 BV/h (for a range REEs)*

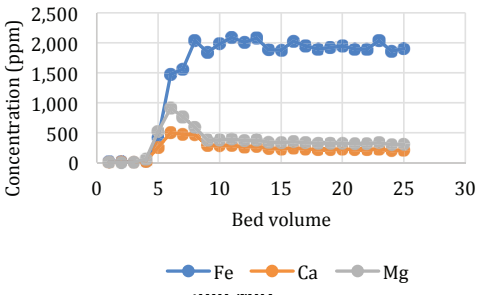


Figure 4 *Breakthrough capacity of MonoPlus TP 207 resin at a rate of 6.6 BV/h (for Fe, Ca, and Mg)*

value (137 and 42,6 respectively)– confirming the applicability of the PSO model. These results likely mean that the rate-limiting step is chemical sorption or chemisorption in both these systems. This can be confirmed using microscopic or spectroscopic methods. This step predicts the behaviour over the entire range of adsorption. The adsorption

Breakthrough

Figure 1 and Figure 2 show a graphical representation of the breakthrough data. Y, Ce, and Nd begin to show breakthrough between 8 and 9 BV, while La and Pr show breakthrough after approximately 11 – 12 BVs. Fe shows breakthrough much sooner than Ca, Mg, and the range of REEs (at a BV of 6), which indicates that this resin is saturated with Fe much sooner than the REEs.

The S 108H resin achieved adsorption of 80% for all REEs with the exception of Th. Conservatively, €0.8 of REEs can practically be removed from 1 m3 of AMD using IX with S 108 H resin. The same method was followed for TP 207 resin; however, the AMD was passed through the column at 6.6 BV/h and samples were collected after one bed volume. Fe, Mg and Ca reached breakthrough on the TP 207 resin at a BV of 4, while the first REEs broke through at a BV of 5 (Figure 3 and Figure 4).

The adsorption of Fe was shown to be much more competitive using the TP 207 (Fe is more likely to be adsorbed by the resin, potentially preventing, or reducing the adsorption of other REEs). As a result, this resin is not practical to use under these conditions. Fe removal prior to IX may improve this function. Breakthrough occurs at lower BV values for all elements using this resin. This is an indication that its maximum adsorption capacity is much lower than that of S 108H. The maximum adsorbent capacity of the TP207 was lower than the S 108H resin, with the maximum adsorption being of Ce at 44.35%.

Desorption

The highest concentration of EDTA used for desorption was a 0,27 M solution. Although there was a link between strength of EDTA solution and the extent desorption, the highest concentration was not deemed effective for elution of the S 108H resin because the average desorption of the range of REEs was 40%. It is known that temperature plays an important role in EDTA reactivity (Çiçek & Keskin, 2015), so conducting this step at a higher temperature of between 50 and 70 °C could improve desorption. However, as this technology aims to generate a profit or revenue stream, use of high temperature or other energy intensive processes are not desirable. The TP 207 desorption system presented more favourable results with an average desorption of 80% (for REEs) using a 15% sulfuric acid solution. Figure 3 shows how the desorption ratio/percent is influenced by the strength of the acid eluant – this is similar for the EDTA solution. The concentration of the eluant can therefore be used as a variable parameter to increase the desorption of the various REEs from the resin.

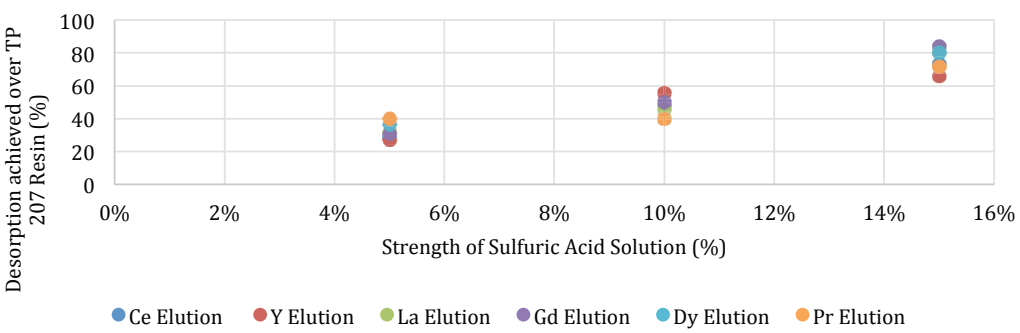


Figure 5 *Relationship between amount of desorption over the TP 207 resin and the strength of the sulfuric acid eluant*

Conclusions

Coal mine AMD contains significant amounts of REEs and could generate substantial revenue if extracted and processed correctly. In countries where AMD is produced in megalitres per day, this could result in either (i) sizeable cost recovery before or after water treatment or (ii) profit generation. Cationic and chelating ion exchange resins can be used effectively to extract REEs from AMD. The cationic resin displays a greater adsorption efficiency for the range of REEs tested, with adsorption of over 80% (up to 95%) of REEs found in AMD, while the chelating resin displayed between 33% and 45% adsorption. The cationic resin showed a greater affinity for adsorption of the REEs – in some cases adsorbing up to 5 times more than the chelating resin.

Adsorption of REEs conforms to the Langmuir isotherm model. Both chelating and cationic resin adsorption (of the range of REEs tested in this study), conform to Langmuir isotherm behaviour, with only the adsorption of Y and La on the chelating resin conforming better to the Temkin isotherm model.

The IX system (both cationic and chelating resins) followed a pseudo-second order kinetic model with regard to adsorption of all REEs tested. The adsorption rate in this type of system is thus dependent on adsorption capacity not on concentration of adsorbate. Desorption of the REEs from the chelating resin was successful using a 1,53 M sulfuric acid solution. Desorption of the REEs from the surface of the cationic resin was deemed unsuccessful using a 027 M solution of EDTA. Elution requires further investigation in this instance.

It was noted that the presence of iron in AMD lowers the adsorption capacity of the resins used in this study. Iron may need to be removed in a pre-treatment step to make extraction of the REEs more efficient and more cost effective. Although further research is required to (i) evaluate the removal of other REEs that could be contained in AMD from different mine sources, (ii) optimise the elution of REEs from the resins, post adsorption (or extraction), and (iii) determine effective methods of iron removal that do not affect (or minimally affects) REE content, these findings provide a successful proof of concept for the application of this technology. Extraction of REEs from AMD using ion exchange technology has the potential to reduce the cost of AMD treatment, generate a profit, and contribute to developing a circular economy in the mining industry.

Acknowledgements

The authors would like to thank the Danida Fellowship Centre for their contributions to the acids to value project.

References

Brewster, E. T., Freguia, S., Edraki, M., Berry, L., & Ledezma, P. (2020). Staged electrochemical treatment guided by modelling allows for targeted recovery of metals and rare earth elements from acid mine drainage. Journal of Environmental Management, 275(August), 111266. https://doi.org/10.1016/j.jenvman.2020.111266

Chen, F., Lv, M., Ye, Y., Miao, S., Tang, X., Liu, Y., Liang, B., Qin, Z., Chen, Y., He, Z., & Wang, Y. (2022). Insights on uranium removal by ion exchange columns: The deactivation mechanisms, and an overlooked biological pathway. Chemical Engineering Journal, 434(December 2021), 134708. https://doi.org/10.1016/j.cej.2022.134708

Çiçek, E., & Keskin, Ö. (2015). The effect of the temperature changes of EDTA and MTAD on the removal of the smear layer: a scanning electron microscopy study. Scanning, May-June 3(3), 193–196. https://doi.org/10.1002/sca.21198

Dahman, Y., Deonanan, K., Dontsos, T., & Iammatteo, A. (2017). Nanopolymers. In Micro and Nano Technologies, Nanotechnology and Functional Materials for Engineers (pp. 121–144). https://doi.org/https://doi.org/10.1016/B978-0-323-51256-5.00006-X

Felipe, E. C. B., Batista, K. A., & Ladeira, A. C. Q. (2021). Recovery of rare earth elements from acid mine drainage by ion exchange. Environmental Technology (United Kingdom), 42(17), 2721–2732. https://doi.org/10.1080/09593330.2020.1713219

Galal, S. (2023). Mining industry revenue in South Africa 2013-2022. Statista. https://www.statista.com/statistics/1342869/south-africa-

mining-revenue/#:~:text=In 2022%2C the total revenue,in the past five years.

Hubicki, Z., Kołodyńska, D., & Ion Exchange Technologies. (1968). Selective Removal of Heavy Metal Ions from Waters and Waste Waters using Ion Exchange Methods. In F. Hellferich (Ed.), Ion Exchange. McGraw-Hill.

IndiaMart. (2022). Gadolinium Metal. Metal Ingots. https://www.indiamart.com/proddetail/gadolinium-metal-8707137812.html

Institut Seltene Erden. (2022). Current Price of Rare Earths. Metal News. https://ise-metal-quotes.com/

Mwewa, B., Tadie, M., Ndlovu, S., Simate, G. S., & Matinde, E. (2022). Recovery of rare earth elements from acid mine drainage: A review of the extraction methods. Journal of Environmental Chemical Engineering, 10(3), 107704. https://doi.org/https://doi.org/10.1016/j.jece.2022.107704.

Sahoo, T. R., & Prelot, B. (2020). Chapter 7 – Adsorption processes for the removal of contaminants from wastewater: the perspective role of nanomaterials and nanotechnology. In B. Bonelli, F. S. Freyria, I. Rossetti, & R. Sethi (Eds.), Nanomaterials for the Detection and Removal of Wastewater Pollutants (pp. 161–222). Elsevier. https://doi.org/https://doi.org/10.1016/B978-0-12-818489-9.00007-4

Simate, G. S., & Ndlovu, S. (2014). Acid mine drainage: Challenges and opportunities. Journal of Environmental Chemical Engineering, 2(3), 1785–1803. https://doi.org/10.1016/j.jece.2014.07.021

Statista. (2023). Average price of selected rare earth oxides from 2015 to 2022. Mining, Metals and Minerals. https://www.statista.com/statistics/617249/price-range-of-selected-rare-earth-oxides/#:~:text=As of the end of,2%2C000 U.S. dollars per kilogram.

Vaziri Hassas, B., Shekarian, Y., & Rezaee, M. (2023). Selective precipitation of rare earth and critical elements from acid mine drainage - Part I: Kinetics and thermodynamics of staged precipitation process. Resources, Conservation and Recycling, 188(August 2022), 106654. https://doi.org/10.1016/j.resconrec.2022.106654

Vecino, X., Reig, M., López, J., Valderrama, C., & Cortina, J. L. (2021). Valorisation options for Zn and Cu recovery from metal influenced acid mine waters through selective precipitation and ion-exchange processes: promotion of on-site/off-site management options. Journal of Environmental Management, 283. https://doi.org/10.1016/j.jenvman.2021.112004

Methodology for the Performance Monitoring of an Unconventional Acidic RO

Jivesh Naidu, Sebastian Franzsen, Johan Espach

Miwatek, Ebene, Mauritius, jiveshn@miwatek.co.za

Abstract

The option to feed ARD directly to a UF and RO system is an attractive treatment technology due to the higher solubility of minerals and the potential to reduce equipment sizes of downstream precipitation systems. The monitoring of such an RO system would require performance normalisation. This paper presents a method to modify conventional performance monitoring equations to develop an acid RO performance monitoring method. Modifications to the performance monitoring equations included calculating TDS / EC ratios specific to ARD using PHREEQC and the PHREEQC.dat database. Further, the osmotic pressure was calculated using a modified version of the Van't Hoff equation for the osmotic pressure of non-ideal solutions. The osmotic pressure coefficient was calculated in PHREEQC using the SIT.dat database.

Data from an acid RO pilot study was used to determine TDS / EC ratios and osmotic pressure coefficients and for the testing of the acid RO method versus vendor-provided performance monitoring methods. TDS / EC conversion factors were found to range from 0.82 to 1.45 and 0.12 to 0.48 for the feed and permeate respectively. It was found that the TDS / EC conversion factor of the feed increased with an increase in EC. The osmotic coefficients were found to be 0.84, 0.97 and 0.80 for feed, permeate and concentrate respectively. Vendor-provided methods compared favourably to the acid RO method in terms of normalised permeate flux plots however differences in the osmotic pressure calculated were observed. The acid RO method provided a more accurate estimate of the osmotic pressure as the method is calibrated to the chemistry of ARD.

Keywords: Acid Rock Drainage, Reverse Osmosis, Performance Monitoring, PHREEQC

Introduction

It is technically feasible to feed acid rock drainage (ARD) directly to ultrafiltration (UF) and reverse osmosis (RO) membrane systems. This unconventional membrane application takes advantage of the higher solubility of the sparingly soluble minerals of iron, aluminium and copper at solution pH values approximately less than 3.5, and is limited by the stability of ferric species and the clean-in-place (CIP) procedures implemented. The application of a RO system to ARD can serve as an economiser to reduce the size of downstream precipitation equipment and pre-concentrate the influent to the precipitation system for improved sulphate reduction. Potential precipitation systems include high-density sludge (HDS) or lime precipitation.

The surface of the RO membranes is subject to fouling or scaling which negatively impacts the performance of the RO system. The performance of an RO system is affected by variables such as feed water, feed pressure, temperature and recovery (Kucera 2015). Determining whether changes in performance are a result of one of these variables or as a result of fouling or scaling requires performance normalisation (Kucera 2015). Performance monitoring is typically conducted by normalising performance to a past operating point to determine how the performance has improved or deteriorated (Boulahfa *et al.* 2019).

Performance monitoring spreadsheets from vendors are readily available using equations and correlations developed for brackish and seawater applications. This paper

presents a method to modify conventional performance monitoring equations for use in the unconventional membrane application. The acid RO performance monitoring method intends to provide accurate and robust normalisation of operational data gathered from an unconventional acid RO application. The method was tested and compared to vendor-provided normalisation methods using data from an acid RO pilot plant.

Methods

Input data into acid RO performance monitoring method

The acid RO performance monitoring method has been developed on the basis that performance monitoring will be required daily with operational data recorded at a frequency of at least 8 times a day, while full-suite analytical data of the feed, permeate and concentrate streams are available at a frequency of at least once a month. The operational parameters required for performance monitoring are the flow rates of the permeate and concentrate streams; feed, concentrate and permeate stream pressures, electrical conductivity (EC) of the feed and permeate streams, and the feed stream temperature.

Test data for acid RO performance monitoring method

Data from a pilot scale acid RO application was used to test the acid RO performance monitoring method. In the pilot plant, the RO pre-treatment consists of a 500 µm prefilter screen, a single UF rack consisting of up to four outside to inside Suez Zeeweed 1500 (ZW1500) UF modules and 2 x 10 µm cartridge guard filters. The RO is a two-stage system consisting of 24 Hydranautics CPA5-LD-4040 elements with sixteen elements in the lead bank and eight elements in the concentrate bank. The UF typically operated at 7.8 m^3/h feed and a volumetric recovery of 92% and the RO was typically operated at 4.5 m^3/h feed with the recovery adjusted between 60% and 70% based on feed chemistry. The feed water quality to the pilot has been summarised in Table 1.

Acid RO performance monitoring method

The methodology used for performance monitoring is: the calculation of feed and permeate total dissolved solids (TDS) from field EC readings using TDS / EC conversion factors, calculation of the osmotic pressure of the feed-concentrate channel and permeate stream, calculation of the net driving pressure

Table 1 *Average feed chemistry for acid RO pilot plant*

Parameter	Unit	Average	Range
pH		2.6	2.0 – 3.4
Temperature	˚C	13.9	11.2 – 20.3
Total dissolved solids	mg/L	3420	1100 – 8928
Electrical conductivity	µS/cm	3635	1696 – 5610
Aluminium as Al	mg/L	49.9	15.4 – 85.5
Calcium as Ca	mg/L	215	87.7 – 389
Chloride as Cl	mg/L	12.4	0.72 – 39.6
Copper as Cu	mg/L	45.0	1.92 – 200
Iron as Fe	mg/L	361	19.0 – 1405
Potassium as K	mg/L	6.78	2.35 – 12.2
Magnesium as Mg	mg/L	30.3	10.7 – 53.7
Manganese as Mn	mg/L	9.47	2.46 – 20.1
Sulphate as SO_4	mg/L	2347	802 - 7125

(NDP), temperature correction factor, and membrane permeability coefficient at 25 ˚C, and the calculation of the normalised permeate flux.

The acid RO performance monitoring sought to find a method to determine the TDS/ EC conversion factors for ARD. The aqueous solubility calculation capabilities of PHREEQC (PHREEQC Version: 3.7.3-15968) with the PHREEQC.dat database were used to calculate the EC and TDS from analytical data of the feed and permeate solutions. Through PHREEQC, the specific conductance of a solution is calculated by summing the products of the specific conductivity and molal concentrations of all the specifies in the solutions (Parkhurst and Appelo 1999). PHREEQC also corrects the molal concentration with an electrochemical activity coefficient that is derived from a combination of Kohlrausch's law and the Debye-Hückel equation (Parkhurst and Appelo 1999). The EC was calculated by adjusting the solution temperature to 25˚C. The calculated EC and TDS determined using PHREEQC were used to determine TDS / EC conversion factors for each data point. Trends of the field measured EC and PHREEQC calculated TDS / EC conversion factors for the feed and permeate streams were generated. These trends were used to determine the conversion factors for each data point and convert the field-measured EC into TDS.

The Van't Hoff equation for the osmotic pressure of non-ideal solutions, shown in Equation 1, was used as a starting point to calculate the osmotic pressure of the feed-concentrate channel and the permeate stream. Using Equation 1 requires the molal concentrations (c) and solute activity coefficients (ϒ) of solutes (i) as inputs. This data is obtained through full-suite analytical data which is available once a month. Performance monitoring is required daily therefore modifications to Equation 1 were required. The modified version of the Van't Hoff equation used for the acid RO method has been shown in Equation 2. In Equation 2, the sum of the product of the activity coefficients and concentrations of the solutes in a stream (j) has been replaced by the EC of the stream divided by the product of the EC / TDS conversion factor and the average molar mass of the stream (M). The solute activity coefficients have been omitted as they have already been accounted for in the EC / TDS ratio obtained from PHREEQC.

$$\pi = \emptyset RT \sum_i \gamma_i c_i \qquad \text{Equation 1}$$

$$\pi_j = \emptyset_j RT \frac{EC_j}{\lambda_j M_j} \qquad \text{Equation 2}$$

The osmotic pressure coefficient (Ø) for the feed, permeate and concentrate streams were calculated from analytical data using PHREEQC with the Pitzer.dat and SIT.dat databases. Trends of the field measured EC and calculated osmotic pressure coefficients for the feed, concentrate and permeate streams were generated. These trends were used to determine the osmotic pressure coefficient. The average molar mass of the feed, concentrate and permeate streams were calculated based on the laboratory data. The average molar mass for the feed, permeate and concentrate streams were found to be 67.2 g/mol, 57.3 g/mol and 68.4 g/mol respectively. The average of the feed and concentrate average molar masses were used for the feed-concentrate average molar mass.

The calculation of EC / TDS conversion factors and osmotic pressure coefficients was completed with the aid of Python. A Python code (Python version: 3.9.7) was developed which imported and sorted analytical data for the feed, permeate and concentrate streams, created a PHREEQC script file for each dataset, ran each dataset through PHREEQC with a loop using the PHREEQC COM module (IPhreeqcCOM Module version 3.7.3-15968) and exported the EC, TDS and osmotic pressure coefficient data to excel for each dataset. The code was run on the PHREEQC.dat, Pitzer.dat and SIT.dat databases and the data was exported as one consolidated dataset.

The NDP is calculated using Equation 3 and requires the calculation of the osmotic pressure of the feed-concentrate channel. Equation 4 is used for the calculation of the feed-concentrate channel mass concentration

where R is the recovery of the system. Equations 2 and 4 are combined (Equation 5) to calculate the osmotic pressure of the feed-concentrate channel.

$$NDP = P_F - 0.5\,(P_F - P_C) - P_P - \pi_{FC} + \pi_P \quad \text{Equation 3}$$

$$C_{FC} = C_F \frac{\ln\left(\frac{1}{1-R}\right)}{R} \quad \text{Equation 4}$$

$$\pi_{FC} = \emptyset_{FC} RT \frac{EC_F}{\lambda_F M_{FC}} \frac{\ln\left(\frac{1}{1-R}\right)}{R} \quad \text{Equation 5}$$

The temperature correction factor was calculated using Equation 6 to correct the operating conditions to a reference temperature of 25 ˚C. The membrane permeability coefficient at 25˚C is calculated using Equation 7, where J_W is the flux of water through the membranes at a point in time (k). The normalised permeate flux ($J_{W,\,norm}$) was calculated using Equation 8 where "ref" is the reference point for normalisation.

$$TCF = e^{3020\left(\frac{1}{298} - \frac{1}{273+T}\right)} \quad \text{Equation 6}$$

$$A_k = \frac{J_{w,k}}{NDP_k \times TCF_k} \quad \text{Equation 7}$$

$$J_{w,norm} = A_k \times NDP_{ref} \times TCF_{ref} \quad \text{Equation 8}$$

Generation of vendor performance monitoring curves

Vendor-provided performance monitoring methods were used to generate normalised flux curves for the operational data generated from the pilot plant. The methods used were LG Chem Normalization from LG Water Solutions, FT Norm from Dow and RO DataXL 8.2 from Hydranautics. The spreadsheets provided calculate the normalised permeate flow rates based on vendor equations and inputs from the users. Normalised permeate flow rates were adjusted to permeate flux by accounting for the surface area of the system. The inputs were broken up into discrete runs with each having a fixed reference point and fed into the vendor spreadsheets. The inputs required were feed temperature, flow rates of the permeate and concentrate streams, pressures of the feed, permeate and concentrate streams and EC of the feed and permeate streams. Single-stage array vendor spreadsheets were used.

Results

Inputs into acid RO performance monitoring method

TDS / EC ratio for feed and permeate streams

Figure 1 shows a plot of the calculated TDS / EC conversion factors for the analytical data using PHREEQC versus field-measured EC readings of the respective data points for the feed stream. A plot of the same data for the permeate stream is shown in Figure 2. The data shows that calculated conversion factors for the feed have a range from 0.82 to 1.45 whilst the permeate factors have a range from 0.12 to 0.48. These factors differ from the values used for the feed and permeate streams in brackish water application which are typically in the range of 0.5 – 0.75.

Second-order polynomials were fitted to the TDS / EC conversion factors versus EC for each of the feed and permeate streams. It was observed that the feed conversion factor increased with an increase in EC. The polynomial fitted for the feed conversion factor was used to estimate the conversion factor for the acid RO method. The polynomial fit would not be ideal for data gathered from a scientific experiment but was found to be suitable for data gathered from a pilot study. No trend was observed for the permeate conversion factors. The average permeate TDS / EC conversion factor of 0.24 was used for the acid RO method.

Osmotic pressure coefficient for feed, concentrate and permeate streams

Figure 3 shows a plot of the calculated osmotic pressure coefficient for the analytical data using PHREEQC with both the Pitzer.dat and SIT.dat databases versus field-measured EC readings of the respective data points for the feed stream. Similar plots for the permeate and concentrate streams are shown in Figures 4 and 5 respectively. The calculated osmotic pressure coefficient for the feed stream has an average value of 0.75 with a range from 0.65 to 0.83 using the Pitzer.dat database and an average value of 0.84 with a range from 0.79 to 0.88 using the SIT.dat database. The

concentrate stream has an average value of 0.68 with a range from 0.59 to 0.79 using the Pitzer.dat database and an average value of 0.80 with a range from 0.76 to 0.86 using the SIT.dat database. The permeate stream has an average value of 0.97 with a range from 0.92 to 0.99 using the Pitzer database.dat and an average value of 0.97 with a range from 0.94 to 0.99 using the SIT.dat database.

Fitting of the second-order polynomials to the data shows no trends or best-fit line is possible for all streams irrespective of the database used. The SIT.dat database reports higher osmotic pressure coefficients when compared to the Pitzer.dat database. The Pitzer.dat database was found to have a limited set of master species and does not include aluminium which is typically elevated for ARD. Due to these limitations in the Pitzer.dat database, the averaged values for the osmotic pressure coefficient calculated using SIT.dat databases were used for the acid RO performance monitoring method.

Comparison between acid RO and vendor-provided performance monitoring methods

Operational data from an acid RO pilot plant has been broken up into discrete runs for the comparison of the acid RO performance monitoring method to the vendor-provided performance monitoring methods. The performance monitoring curves for Run 1 are shown in Figure 6, this includes the normalised permeate flux for the various methods, the normalised flux reference point as well as a line showing when a 10% decline in flux from the reference has occurred. Data

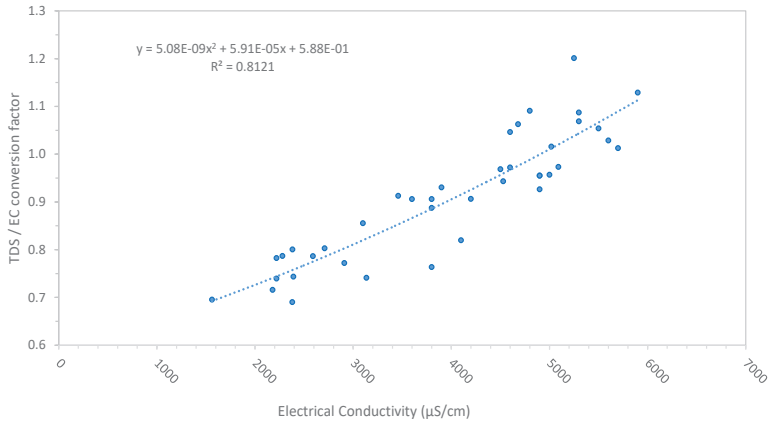


Figure 1 *Plot of TDS / EC conversion factor versus EC for the feed*

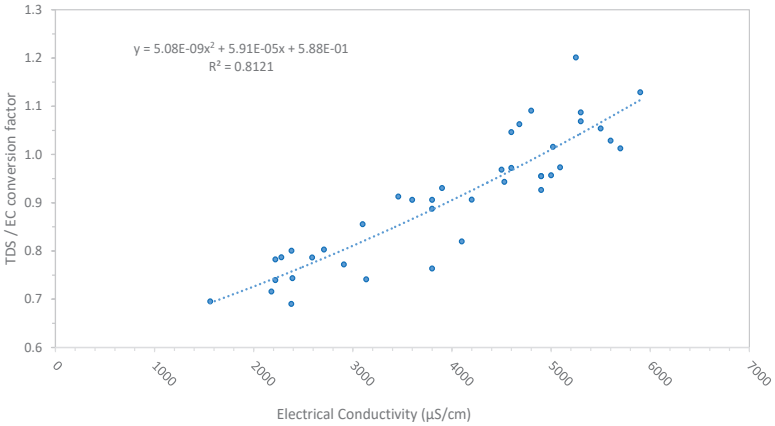


Figure 2 *Plot of TDS / EC conversion factor versus EC for the permeate*

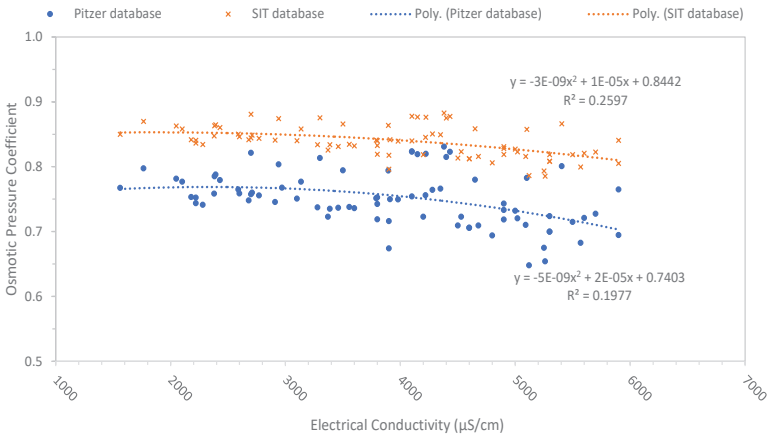


Figure 3 *Plot of osmotic pressure coefficients calculated using the Pitzer and SIT databases versus EC for the feed*

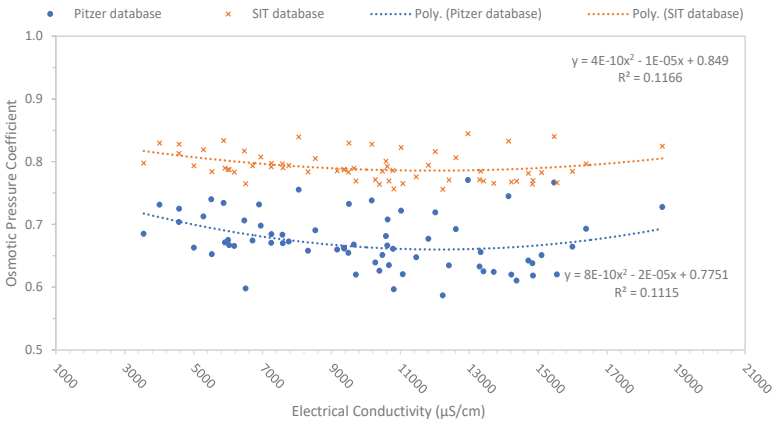


Figure 4 *Plot of osmotic pressure coefficients calculated using the Pitzer and SIT databases versus EC for the concentrate*

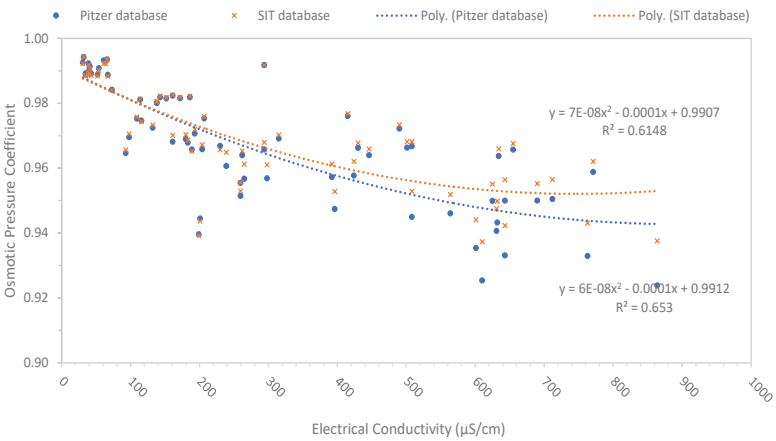


Figure 5 *Plot of osmotic pressure coefficients calculated using the Pitzer and SIT databases versus EC for the permeate*

labels have been included to show CIP points and changes in the recovery of the system. Figure 7 shows the NDP calculated by the various methods for Run 1 data. Similar comparisons of permeate flux and NDP for Run 2 are shown in Figures 8 and 9.

The performance monitoring curves produced for Runs 1 and 2, Figures 6 and 8 respectively, show there is a similarity in the normalised permeate flux calculated by the acid RO method and methods used by LG Water Solutions and Hydranautics. The normalised permeate flux calculated by Dow differs from the values produced through the other methods. Overall, the data further shows that the normalised flux calculated by the acid RO method is lower.

A comparison of the NDP calculated for Runs 1 and 2, Figure 7 and 9 respectively, using the various methods show that the acid RO method calculates a NDP which is higher than vendor-provided methods. NDP values calculated by LG Water Solutions, Hydranautics and Dow are similar. The NDP for all methods is calculated using Equation 3. A difference in the NDP is a result of the feed-concentrate channel osmotic pressure as the permeate osmotic pressure is not high enough to affect the calculations and all other inputs are the same across the methods. The higher NDP from the acid RO method is a result of the modified Van't Hoff equation (Equation 2) calculating a lower feed-concentrate channel osmotic pressure compared to the vendor-provided methods. Vendor-provided methods generally estimate the osmotic pressure using correlations specific to brackish water or seawater. The unsuitability of these correlations to the chemistry of ARD results in a less accurate estimate of the osmotic pressure.

Conclusions

TDS / EC conversion factors and osmotic pressure coefficients were calculated using PHREEQC which were used as inputs into the acid RO performance monitoring method. The data shows that TDS / EC conversion factors for ARD differ from those observed for brackish water. It is possible to predict the feed TDS / EC conversion factor for ARD based on the feed EC. Osmotic pressure coefficients were found to be higher when using the SIT.dat database compared to the Pitzer.dat database. The osmotic pressure coefficient calculated using the SIT.dat database was selected as the input to the acid RO method.

The acid RO method produced normalised permeate flux curves which were similar to those produced by vendor-provided spreadsheets from LG Water Solution and Hydranautics. The normalised permeate flux curves produced by Dow differed from those produced by the other methods. The NDP calculated using the vendor-provided methods was lower compared to the values calculated using the acid RO method. The difference is attributed to the acid RO method calculating a lower feed-concentrate channel osmotic pressure. The acid RO method used a first principles approach which had been calibrated to analytical data to estimate the osmotic pressure. This approach results in a more accurate estimation of the osmotic pressure when compared to correlations used by vendor-provided methods. A potential improvement to the acid RO method is more regular calibrations of the TDS / EC conversion factors and osmotic pressure coefficients as the chemistry of the ARD changes.

References

Boulahfa H, Belhamidi S, Elhannouni F, *et al* (2019) Demineralization of brackish surface water by reverse osmosis: The first experience in Morocco. J Environ Chem Eng 7:102937

Kucera J (2015) Reverse osmosis: industrial processes and applications. John Wiley & Sons

Parkhurst DL, Appelo CAJ (1999) User's guide to PHREEQC (Version 2): A computer program for speciation, batch-reaction, one-dimensional transport, and inverse geochemical calculations

Stream Recovery through Managed Biogeochemical Redox Coupling in Ecologically Engineered Passive Treatment Systems: A Natural Infrastructure Approach

Robert W. Nairn, Nicholas L. Shepherd, Dayton M. Dorman, Justine I. McCann, Robert C. Knox

Center for Restoration of Ecosystems and Watersheds, School of Civil Engineering and Environmental Science, The University of Oklahoma, 202 West Boyd St, Room 334, Norman, OK 73019, nairn@ou.edu

Abstract

Two full-scale mine water passive treatment systems (PTS) were installed in the Tar Creek (Kansas-Oklahoma, USA) watershed of the historic Tri-State Mining District, each including multiple process units designed for specific biogeochemical functions. Both systems produce net alkaline effluents containing metals concentrations meeting in-stream water quality criteria and collectively retain 71000 kg Fe, 3100 kg Zn, 84 kg Pb, 9 kg Cd, and 25 kg As annually. The first order receiving stream demonstrated substantial water quality improvement and ecological recovery, with documented increases in both fish species richness and abundance, as well as the return of other fauna.

Keywords: Nature-based Solutions, Ecosystem Restoration, Water Quality Improvement

Introduction

Ecological engineering, defined by Mitsch and Jorgensen (2004) as "the design of sustainable ecosystems that integrate human society with its natural environment for the benefit of both", has been an established academic discipline since the 1960s (e.g., Odum 1962, 1971). However, in recent years the related terms natural infrastructure and nature-based solutions have become common in both the technical literature and popular press (e.g., Chung *et al* 2021, Cohen-Shacham *et al*. 2016). Although developed on parallel yet separate tracks from these broader areas of inquiry (e.g., Hedin *et al*. 1994, Skousen *et al*. 2017), mine water passive treatment is a representative application of ecological engineering and arguably the ultimate application of natural infrastructure (infrastructure that uses, restores, or emulates natural ecological processes created by nature or human design (Title 23 US Code 2012)) and nature-based solutions (actions to protect, sustainably manage, and restore natural and modified ecosystems that address societal challenges effectively and adaptively, simultaneously benefiting people and nature (IUCN 2023)).

In this study, long-term evaluations of several mine water discharges, two full-scale mine water passive treatment systems (PTS), and a common receiving stream were conducted in the Tar Creek Superfund Site, part of the historic and now derelict Tri-State Lead-Zinc Mining District, USA. Chemical and hydrological characterization of the discharges began in 2004, multi-process unit PTS were installed in 2008 and 2017, and chemical, hydrological, and ecological assessments (e.g., fish community analyses) of the stream have continued since 2004. Individual PTS process units were designed to promote specific biogeochemical mechanisms to address a suite of ecotoxic metals. Multidisciplinary assessments of the PTS and receiving stream provide insight into the success of these ecological engineering technologies.

Methods

The study site includes an unnamed receiving stream (first-order tributary to Tar Creek) and two full scale PTS (Figure 1). The Mayer Ranch (2008) and Southeast Commerce (2017) PTS include ten and four process units, respectively, alternating between promotion

of oxidative (e.g., oxidation and hydrolysis) and reductive (e.g., sulfate reduction) mechanisms. Design, construction, and performance data are summarized in Nairn *et al.* (2010, 2020), Oxenford and Nairn (2010), and Labar and Nairn (2018). Monthly to quarterly water quality, volumetric discharge, and fish community data have been generated since 2004. Water quality efforts include a full suite of physicochemical parameters (pH, dissolved oxygen, specific conductance, oxidation-reduction potential (ORP), total alkalinity, turbidity), anions (SO_4^{2-}, Cl^-, PO_4^{3-}, NO_2^-, NO_3^-) and total and dissolved (<0.45 mm) metals and metalloids (Ag, Al, As, Ba, Ca, Cd, Co, Cr, Cu, Fe, K, Li, Mg, Mn, Na, Ni, Pb, Se, Si, and Zn). University of Oklahoma Center for Restoration of Ecosystems and Watersheds (CREW) standard operating procedures follow US Environmental Protection Agency (USEPA) and US Geological Survey (USGS) methods for all field and laboratory water analyses and include approved quality assurance and quality control practices. Standardized stream fish collections included taking ten seine (3.17 mm mesh, 1.22 m deep, 2.44 m long) hauls per site, including as many microhabitats as possible.

Results

Both PTS have demonstrated effective removal of total and dissolved trace metals. Table 1 summarizes flow-weighted influent and effluent data for selected water quality constituents for Mayer Ranch PTS from November 2008 to December 2022 and for Southeast Commerce PTS from February 2017 to December 2022. Overall changes in total and dissolved Fe, Zn, Cd, and As concentrations are greater than 90% and effective removal of Ni (84-91%) and Pb (62-91%) are also demonstrated. Changes in concentrations of biogeochemically conservative ions (Mg, K, Na, and Cl^-) are less than 5% at Mayer Ranch and less than 18% at Southeast Commerce, indicating promotion of targeted redox-mediated passive treatment

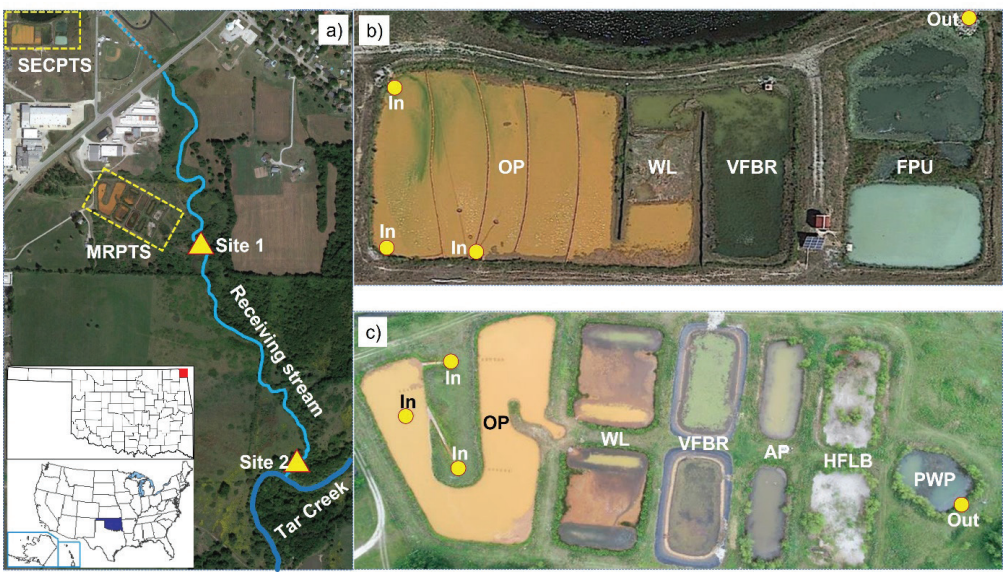


Figure 1 *Study sites showing* ***a)*** *location of two PTS, receiving stream, confluence with Tar Creek, and in-stream sampling locations; inset maps show location of Oklahoma in the US and Ottawa County in Oklahoma;* ***b)*** *Southeast Commerce PTS including inflows and outflow and (from L to R) oxidation pond with baffle curtains (OP), surface flow wetland (WL), vertical flow bioreactor (VFBR) and final polishing unit (FPU);* ***c)*** *Mayer Ranch PTS including inflows and outflow and (from L to R) oxidation pond (OP), parallel trains of surface flow wetlands (WL), vertical flow bioreactors (VFBR), reaeration ponds (AP), horizontal flow limestone beds (HFLB), and a polishing wetland/pond (PWP). Study site image from Google Earth (2021) and PTS images collected by OU CREW small Unoccupied Aerial Vehicle (sUAS).*

mechanisms and limited effects of dilution or evapotranspiration. Nominal volumetric discharge rates were 420 and 600 L/min at Mayer Ranch and Southeast Commerce PTS, respectively.

Figures 2 and 3 demonstrate the role of designed redox manipulations on water quality in these nature-based solutions. Elevated iron concentrations at Mayer Ranch and Southeast Commerce PTS are removed through oxidation, hydrolysis, precipitation, and settling in the OP and WL process units (Oxenford and Nairn 2011); As concentrations are also decreased via sorption to precipitated iron oxyhydroxide solids. Conversely, elevated Zn concentrations, although decreased by sorptive process in oxidative units, are effectively addressed through reductive bio-geochemical means in the VFBR process units (LaBar and Nairn 2018). Other trace metals (Cd, Co, Fe, Ni, and Pb) are retained in the sulfide fraction in VFBR substrates, as

Table 1 *Summarized influent and effluent data for two PTS (median ± standard error (sample size > practical quantitation limit or PQL)). Data for three influent discharges at Mayer Ranch were flow-weighted; at Southeast Commerce, data for one representative influent discharge are presented.*

	Mayer Ranch PTS		Southeast Commerce PTS	
	Influent	**Effluent**	**Influent**	**Effluent**
pH	5.99±0.02(62)	7.06±0.02(61)	5.94±0.02(40)	6.83±0.04(69)
ORP (mV)	-41±13(52)	72±20(53)	-49±24(32)	35.30±15(58)
Alk. (mg/L)	385±3.78(62)	182±5.61(60)	396±2.75(38)	121±5.24(69)
T. Fe (mg/L)	160±2.56(62)	0.33±0.05(61)	140±2.43(38)	1.08±0.14(69)
D. Fe (mg/L)	156±2.58(47)	0.08±0.08(46)	136±3.36(38)	0.21±0.11(68)
T. Zn (mg/L)	6.91±0.14(62)	0.14±0.10(60)	6.54±0.08(38)	0.07±0.13(66)
D. Zn (mg/L)	6.48±0.15(47)	0.05±0.12(47)	6.41±0.08(38)	0.05±0.13(65)
T. Cd (mg/L)	15.16±0.83(61)	1.01±0.15(8)	19.45±0.86(37)	1.08±0.09(16)
D. Cd (mg/L)	15.04±0.98(47)	1.14±0.50(6)	17.67±0.75(37)	1.06±0.41(12)
T. Pb (mg/L)	77.64±10.09(62)	29.63±2.05(18)	279±9.19(38)	24.38±0.71(52)
D. Pb (mg/L)	86.93±12.94(46)	26.29±2.01(19)	254±8.48(38)	24.03±0.70(44)
T. As (mg/L)	61.23±1.62(61)	<PQL(0)	87.22±2.07(37)	<PQL(0)
D. As (mg/L)	64.10±13(45)	<PQL(0)	84.34±28(37)	<PQL(0)
T. Ni (mg/L)	0.81±0.01(62)	0.12±0.03(59)	0.71±0.01(38)	0.07±0.03(67)
D. Ni (mg/L)	0.78±0.01(47)	0.12±0.04(46)	0.70±0.01(38)	0.07±0.03(66)
T. Ca (mg/L)	698±5.69(62)	702±10.76(61)	660±6.10(38)	616±7.14(69)
D. Ca (mg/L)	694±6.56(47)	687±10.62(47)	659±5.74(38)	617±6.80(69)
T. Mg (mg/L)	175±3.05(62)	175±3.62(61)	149±2.37(38)	131±2.07(69)
D. Mg (mg/L)	170±2.44(47)	168±3.00(47)	150±2.45(38)	131±1.94(69)
T. K (mg/L)	24.25±0.26(62)	23.08±0.78(61)	22.13±0.21(38)	20.43±0.39(69)
D. K (mg/L)	23.73±0.30(47)	23.27±1.02(47)	22.33±0.23(38)	20.33±0.39(69)
T. Na (mg/L)	95.29±1.67(62)	95.45±2.09(61)	87.99±1.55(38)	84.11±1.64(69)
D. Na (mg/L)	93.83±1.69(47)	95.71±1.93(47)	90.44±1.62(38)	85.78±1.59(69)
SO_4^{2-} (mg/L)	2193±28(60)	2078±62(59)	2070±52(38)	1822±28(69)
Cl^- (mg/L)	31.65±0.49(35)	32.09±0.72(34)	29.25±0.58(26)	24.05±0.86(27)

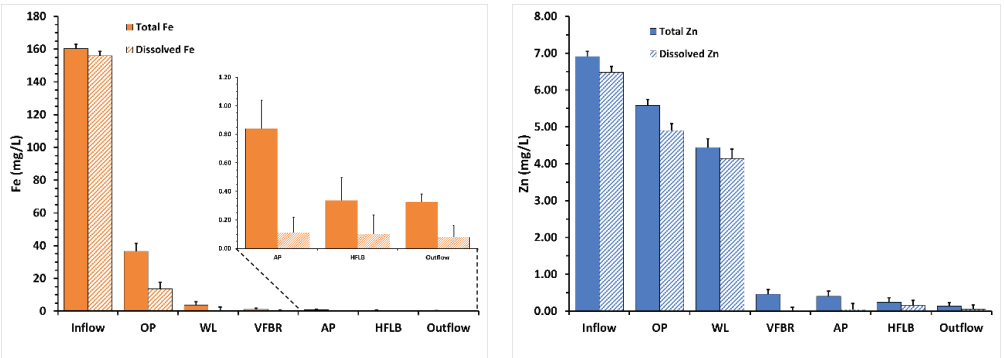


Figure 2 *Changes in iron and zinc concentration with flow through the Mayer Ranch PTS. Iron concentrations decrease to <3 mg/L by oxidative processes in OP and WL units and to <0.5 mg/L in final outflow. Zinc concentrations decrease to <0.5 mg/L by reductive process in the VFBR units and to <0.1 mg/L in the final outflow.*

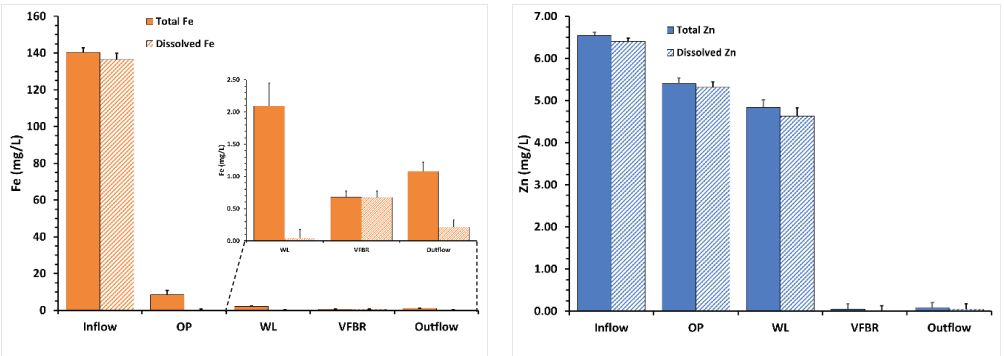


Figure 3 *Changes in iron and zinc concentration with flow through the Southeast Commerce PTS. Total and dissolved iron concentrations decrease to ≈2 and <0.05 mg/L by oxidative processes in OP and WL units. Zinc concentrations decrease to <0.05 mg/L by reductive process in the VFBR units.*

confirmed by acid volatile sulfide/extracted metals, scanning electron microscopy, and x-ray diffraction analyses.

Water quality in the receiving stream was noticeably influenced by biogeochemical changes in PTS effluents resulting from installation of targeted natural infrastructure. The Southeast Commerce PTS effluent enters the receiving stream near its headwaters, while the Mayer Ranch PTS effluent enters approximately 1000 m downstream. Data for two downstream locations are presented in Figure 4. Sites 1 and 2 are approximately 25 and 1000 m, respectively, downstream of the Mayer Ranch PTS effluent confluence with the receiving stream.

Fish communities exhibited demonstrative effects of in-stream water quality improvement. Fish species richness at Sites 1 and 2 increased from 6 to 13 and 7 to 17 species, respectively, after installation of the two PTS as nature-based solutions and is comparable to local unimpacted reference streams. In this small first order tributary, fish assemblages were dominated by small-bodied minnows and centrarchids, including western mosquitofish (*Gambusia affinis*), bluegill sunfish (*Lepomis macrochirus*), green sunfish (*Lepomis cyanellus*), and largemouth bass (*Micropterus salmoides*), although populations of darters, catfish, shiners, shad, suckers, and stonerollers were also noted.

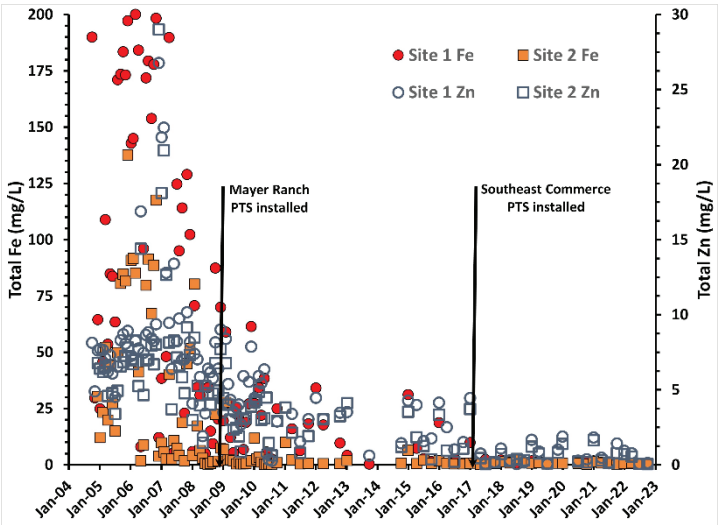


Figure 4 *In-stream total iron and zinc concentrations from October 2004 through December 2022 at two receiving stream locations. Site 1 is approximately 25 m from the Mayer Ranch PTS effluent and 1025 m from the Southeast Commerce PTS effluent. Site 2 is approximately 1000 m from the Mayer Ranch PTS effluent and 2000 m from the Southeast Commerce PTS effluent. The Mayer Ranch and Southeast Commerce PTS began operations in November 2008 and February 2017, respectively. Although dramatically decreased after PTS installation, in-stream concentrations remain slightly elevated due to legacy mining effects including in-stream tailings deposits.*

Since no in-stream habitat was restored, the reestablishment of robust fish communities indicates changes due to water quality improvements. In addition, based on field research activities in this watershed since 1998, robust and active North American beaver (*Castor canadensis*) populations were initially noted in 2013 (after installation the Mayer Ranch PTS in 2008), followed by North American river otter (*Lontra canadensis*) populations in 2022 (after both PTS were operational).

In-stream water quality changes due to mine water passive treatment decreased the magnitude of aquatic ecotoxicity due to trace metals. Toxicity of select trace metals is affected by water hardness. Increased hardness decreases bioavailability and, therefore, resulting ecotoxicity. In-stream hardness-adjusted aquatic life criteria for several metals have been developed by USEPA through the National Recommended Water Quality Criteria process (USEPA 2023). Calculations for the Criterion Maximum Concentration (CMC, representing acute toxicity) and Criterion Continuous Concentration (CCC, representing chronic toxicity) have been empirically derived. The CMC and CCC represent the greatest in-stream concentrations of a toxicant to which organisms can be exposed for a brief period of time (CMC) and for an indefinite period of time (CCC) without causing an adverse effect. For acute toxicity, the equation takes the form of:

$$CMC_{dissolved} = e^{(mA \times [\ln(hardness)] + bA)} \times CF$$

where mA and bA are known metals-specific constants and CF is a freshwater correction factor. The calculation for $CCC_{dissolved}$ takes an identical form where mA and bA are replaced by metals-specific mC, bC, and CF values. Acute and chronic criteria for Cd, Pb, and Zn are hardness dependent. An acute criterion for Fe does not exist and the chronic Fe criterion is constant (1000 mg/L). The PTS dramatically decreased metals concentrations, but calculations of hardness-adjustments aquatic life criteria are

critical for evaluation of acceptable in-stream concentrations.

Examining the acute and chronic criteria for median in-stream metals concentrations demonstrates the effect of the passive treatment on receiving stream ecotoxicity (Table 2). Prior to installation of any nature-based solutions (October 2004 to December 2008, N = 49-51), only the acute criterion for Cd and the acute and chronic criteria for Pb were met at Sites 1 and 2. Zn concentrations were 4 to 5 times the respective criteria, while Fe concentrations exceeded the criterion by 20 to 84 times. After installation of the Mayer Ranch PTS in 2008 but prior to the installation of Southeast Commerce PTS in 2017 (January 2009 to January 2017, N = 37-38), acute and chronic criteria for Cd and Pb were met at both sites, and the Fe criterion was met at Site 2. Zn concentrations were 2 to 3 times the respective criteria, while Fe concentrations at Site 1 exceeded the criterion by 17 times. After installation and operation of both PTS (February 2017 to December 2022, N = 22), acute and chronic criteria for Cd, Pb, Zn and Fe were met at both sites, although in-stream concentrations remain elevated above expected background values due to legacy mining effects, including in-stream tailings deposition.

Conclusions

Water quality impairment due to unabated artesian discharges of trace-metals contaminated mine waters was documented in a first-order tributary to Tar Creek, in the abandoned Tri-State Lead-Zinc Mining District of Ottawa County, Oklahoma, USA, from 2004 to 2008. A natural infrastructure approach, based on design, installation, and operation of specific passive treatment process units promoting targeted redox-specific trace metals retention mechanisms, resulted in improvement in mine water and in-stream water quality and the restoration of in-stream ecological communities. The Mayer Ranch

Table 2 *Median in-stream Cd, Pb, Zn and Fe concentrations compared to hardness-adjusted acute and chronic aquatic life criteria for three periods of time: prior to passive treatment (2004-2008), after installation and operation of the Mayer Ranch PTS (2009-2017), and after installation and operation of both the Mayer Ranch and Southeast Commerce PTS (2017-2022). Bolded values demonstrate that in-stream metals concentrations meet the appropriate aquatic life criteria.*

	Site 1			Site 2		
	In-stream Concentration (mg/L)	Acute criteria (mg/L)	Chronic criteria (mg/L)	In-stream Concentration (mg/L)	Acute criteria (mg/L)	Chronic criteria (mg/L)
2004-2008		*Hardness = 2150 mg/L*			*Hardness = 2155 mg/L*	
Cd	12.41	**31.23**	7.13	8.41	**31.31**	7.14
Pb	38.92	**1395**	**54.37**	28.81	**1399**	**54.53**
Zn	7718	1577	1590	6688	1580	1593
Fe	83674	---	1000	19808		1000
2009-2017		*Hardness = 1994 mg/L*			*Hardness = 2028 mg/L*	
Cd	5.18	**29.01**	**6.71**	2.64	**29.50**	**6.81**
Pb	26.09	**1268**	**49.40**	32.94	**1295**	**50.47**
Zn	3494	1479	1492	2998	1501	1513
Fe	16842	---	1000	713	---	**1000**
2017-2022		*Hardness = 1376 mg/L*			*Hardness = 1500 mg/L*	
Cd	1.04	**20.18**	**4.99**	1.12	**21.96**	**5.35**
Pb	20.67	**790**	**30.80**	21.77	**882**	**34.38**
Zn	418	**1080**	**1089**	335	**1162**	**1172**
Fe	748	---	**1000**	606	---	**1000**

PTS annually retains approximately 36500 kg Fe, 1550 kg Zn, 20 kg Pb, and 3.3 kg Cd, and the Southeast Commerce PTS annually retains approximately 34700 kg Fe, 1575 kg Zn, 64 kg Pb, and 5 kg Cd. The prohibition of historic mass loading of trace metals into the stream resulted in increases in fish community species richness and documented return of aquatic mammals. Nature-based solutions like passive treatment provide effective and low maintenance options promoting recovery of ecosystem services in the receiving stream.

Acknowledgements

The authors thank many previous OU CREW members who contributed to this research and are especially indebted to William J. Matthews and Edie-Marsh-Matthews, who led initial fish community studies, and several private landowners, who provided access and cooperation. Major funding was provided by US Environmental Protection Agency (104(b)(3)X7-97682001), US Geological Survey (04HQAG0131), Oklahoma Department of Environmental Quality and Secretary of Energy and Environment (PO2929019163 and Q015081) and Grand River Dam Authority (100052 and A15-240).

References

Chung MG, Frank KA, Pokhrel Y, Dietz T, and Liu J (2021) Natural infrastructure in sustaining global urban freshwater ecosystem services. Nature Sustainability 4(12): 1068-1075

Cohen-Shacham E, Walters G, Janzen C, and Maginnis S (2016) Nature-based solutions to address global societal challenges. IUCN: Gland, Switzerland, 97:2016-2036.

Hedin RS, Nairn RW, Kleinmann RL (1994) Passive treatment of coal mine drainage. US Department of the Interior, Bureau of Mines IC 9389

International Union for Conservation of Nature (2023) Nature-Based Solutions. https://www.iucn.org/our-work/nature-based-solutions

LaBar JA, Nairn RW (2018) Characterization of trace metal removal products in vertical flow bioreactor substrates at the Mayer Ranch Passive Treatment System in the Tar Creek Superfund Site. Chemosphere 199: 107-113

Mitsch WJ and Jorgensen SE. (2004). Ecological Engineering and Ecosystem Restoration. John Wiley and Sons, Inc., New York, 411 pp.

Nairn RW, LaBar JA, Oxenford LR, Shepherd NL, Holzbauer-Schweitzer BK, Arango JG, Tang Z, Dorman DM, Folz CA, McCann JI, Ingendorf JD, Stanfield HT, Knox RC (2020) Toward Sustainability of Passive Treatment in Legacy Mining Watersheds: Operational Performance and System Maintenance. IMWA, Virtual, 123-128.

Nairn, RW, LaBar JA, Strevett KA, Strosnider WH, Morris D, Neely CA, Garrido A, Santamaria B, Oxenford L, Kauk K, Carter S, Furneaux B (2010) A Large, Multi-Cell, Ecologically Engineered Passive Treatment System for Ferruginous Lead-Zinc Mine Waters. Proc IMWA Sydney, Nova Scotia, Canada, 255-258.

Odum HT (1962) Man in the Ecosystem. In: Proceedings of the Lockwood Conference on the Suburban Forest and Ecology, Bulletin 652, Connecticut Agricultural Station Storrs, CT, p. 57-75

Odum HT (1971) Environment, Power and Society, John Wiley and Sons, Inc., New York, 331 pp.

Oxenford LR, Nairn RW (2010) Progressive iron removal within the initial oxidation cell of a passive treatment system. ASMR, Pittsburgh, Pennsylvania, USA, 767-779

Skousen J, Zipper CE, Rose A, Ziemkiewicz PF, Nairn R, McDonald LM, Kleinmann RL (2017) Review of passive systems for acid mine drainage treatment. Mine Water Environ 36(1): 133-153

Title 23 US Code (2012) https://www.law.cornell.edu/uscode/text/23, 301 pp.

US Environmental Protection Agency (2023) National Recommended Water Quality Criteria https://www.epa.gov/wqc/national-recommended-water-quality-criteria-aquatic-life-criteria-table

How to Determine Financial Guarantees of Water Treatment for Mine Closure: A Summary of Affecting Factors

Emma-Tuulia Nurmesniemi[1], Piia Juholin[1], Päivi Picken[2], Kirsi-Marja Haanpää[1], Anne Vaarasuo[3], Kaisa Vähänen[1]

[1]*FRY Finland Oy, Elektroniikkatie 13, FI-90590, Oulu, Finland, emma-tuulia.nurmesniemi@afry.com, piia.juholin@afry.com, kirsi-marja.haanpaa@afry.com, kaisa.vahanen@afry.com*

[2]*AFRY Finland Oy, Koskikatu 27B, FI-96100 Rovaniemi, Finland, paivi.picken@afry.com*

[3]*AFRY Finland Oy, Puistokatu 2-4 D, FI-40100 Jyväskylä, Finland, anne.vaarasuo@afry.com*

Abstract

Water treatment at mine closure stage can require a considerable amount of money and resources. These costs should be considered already at the planning stage as part of the closure plan. Setting adequate financial guarantees is essential to mitigating the potential environmental impacts of mines, and to ensuring a positive mine legacy. This paper sums up information on factors affecting the determination of financial guarantees of water treatment for mine closure.

Keywords: Mine water, mine closure, mine water treatment, closure plan

Introduction

Financial guarantees to cover closure and post-closure measures are essential for minimizing the long-term environmental impacts of mines. Planning of closure measures is initiated even before mining operations start. The closure plan is updated throughout the life cycle of the mine. The adequacy of the closure measures must be ensured during the closure phase by means of monitoring.

Determination of suitable water treatment technologies at different closure phases considering changes in mine water amount and quality, as well as estimation of treatment period length, is used for estimating the post-closure water treatment costs. The estimated cost is the minimum monetary amount of financial guarantees concerning water treatment at mine closure.

There are many factors affecting the determination of financial guarantees of water treatment for mine closure. This paper provides a comprehensive summary of knowledge of these factors, which include variation in mine water amount and quality during different stages of mine closure and post-closure, suitable water management and treatment technologies during mine closure, and investment and operational costs related to these technologies.

Water Amount and Quality Changes During Mine Closure

Water fraction quantity and quality can vary considerably between mines. In addition, even within the mining area, water fractions of very different quality and quantity can be formed. Operational stage water streams often consist of e.g., mine dewatering water, concentration plant process water which transfers to tailings management facility, and seepage and run-off water from tailings and waste rock deposition areas. The geological characteristics of the pit walls and waste areas, as well as the contact time with water, impacts the formed mine water quality. Chemical reactions such as sulfide minerals oxidation and acid production, as well as carbonate minerals neutralization have an effect on mine water quality. Weathering and fragmenting of rock also influence mine water quality as physical phenomena.

Usually, the amount and quality of water fractions change towards mine closure as mine operations are run down. Process water and tailings production stops at concentration plant and mine dewatering water pumping typically stops and mine is flooded. This leads to mine overflows after mine is filled with water. The amount of seepage is reduced, and the quality improved by covering the waste rock and tailings.

The water fractions that need to be managed and treated in the closure phase are mainly leachate from extractive waste areas. Additionally, there might be need for process water management and treatment in the beginning of mine closure. Overflow from the pit lake, if water is not stratified sufficiently, may also trigger a need for water treatment even decades after termination of mine operations.

Suitable Water Management and Treatment Technologies

During the mine closure phase, suitable techniques for water management and treatment shall be selected on a case-by-case basis, applying best available techniques (BAT) (Garbarino *et al.* 2018). At different stages of closure, the needs of water management and treatment usually change, as the amount and quality of water fractions may vary.

Water quality can be affected by the water management methods. Primarily, the formation of environmentally harmful leachate should be prevented, for example by means of covering structures for waste areas and collecting seepage and run-off from waste areas by means of pumping and drains. Also, clean surface waters should be diverted from waste areas to prevent their contamination.

Water and loading balance modelling is a tool used for water management planning. With water and loading balance model the amounts of mine waters formed, their potential environmental load, need and capacity for water treatment, and the dimensioning of water transfer structures and other water management structures can be assessed.

Only, if preventing of water contamination is not possible nor sufficient from environmental risk management perspective, water should be treated before discharge into the environment. The selection of a suitable water treatment method depends, among other things, on the sensitivity of the receiving water body and the quality and quantity of formed water fractions. Water treatment technologies can be classified as passive that utilise natural water flow along with natural chemical and biological processes, and active that require continuous maintenance, monitoring, and chemicals addition. Also, semi-passive water treatment technologies (Kleinmann *et al.* 2023), such as occasionally adding amendments to enhance otherwise passive treatment processes, are widely used and applicable for post-closure water treatment.

Active mine water treatment technologies such as lime precipitation or coagulation are capable of removing many of the potential pollutants from mine affected water. In the closure phase, active treatment is typically applied, for example, during active closure stage, but also in longer term if required. Passive, or semi-passive, methods are preferred in cases where there is a minor or precautionary need and the emission has already been minimized by primary means, such as covering structures. Passive treatment as polishing treatment for example on wetlands is common, but wetlands' pollutant removal efficiency is limited and affected by temperature. Often after mine closure, water treatment will continue with the technology that was in use during the mine's operational phase as long as necessary, considering the environmental risks and impacts (Garbarino *et al.* 2018).

Water Management Costs

The costs of water management during closure phase consist of e.g. cover structures, pipelines, drains, ponds, pumping stations, and disassembling of existing water management systems. The water management costs are site-specific and depend on many factors (fig. 1).

Cover structures for each waste area need to be designed individually as each waste area has its own unique geochemical, and geotechnical features as well as material balance. Thus, the costs of cover structures can vary a lot. The costs presented below do not include VAT. The estimated unit cost of cover structures varies between 7.3–21.6 €/m2 depending on the cover layer materials, and the thickness of cover layers (Laakso *et al.* 2022). The use of synthetic films or geotextiles as part of the cover structure elevates the costs compared to cover structures built with solely natural materials.

Mine flooding can last for decades. The formation of pit lake can be accelerated by

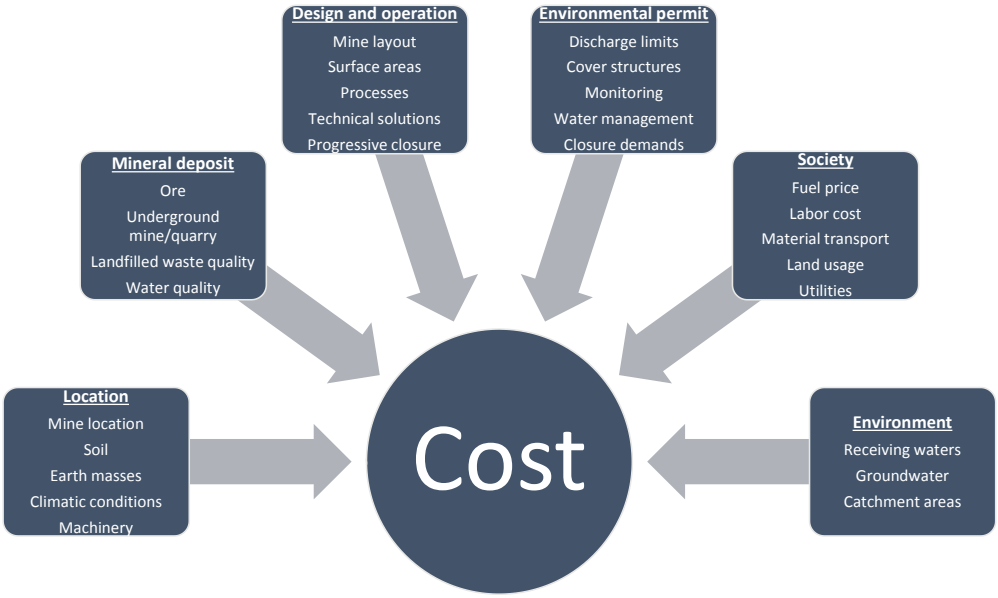


Figure 1 *Factors Affecting the Cost of Closure Measures (from Laakso* et al. *2022).*

directing leachate into open pit mine. At closure stage, the existing water management structures are utilized when possible. However, new pipelines may need to be assembled. The estimated investment unit cost for pipelines varies between 20–500 €/m for pipes, and 70–250 €/m for earth construction works (Laakso *et al.* 2022). In some cases, there might be need for new pumping stations. The estimated investment cost of new pumping station can vary between 10 000–100 000 € (Laakso *et al.* 2022). The water management systems also need maintenance, which results in operational costs.

Water Treatment Costs

The costs of water treatment during the closure phase are affected by, among other things, the chosen water treatment technologies, and the length of the treatment period (fig. 1). Water treatment plants built during the operational phase of the mine can be used during the closure phase, but the use of active treatment plants require maintenance. If the water treatment plant comes to the end of its service life but the quality of environmental discharges is not yet sufficient, it may be necessary to use temporarily, for example, container treatment plants.

In active water treatment, maintenance costs consist of, e.g., equipment maintenance and possible renewal and renovation of buildings. Active water treatment also requires external energy, chemicals, and operating personnel. Because of this, switching from active water treatment to passive methods is preferably done during the closure phase, if the water quality allows.

The costs of passive water treatment methods can include, e.g., earth construction costs, remediation costs, and monitoring costs. As an example, the construction costs of constructed wetlands usually consist of costs derived from excavation works, earth mass movement, insulating structures, and planting of vegetation. However, the operating time of a wetland is limited, and, over time, substances bound to the field can be leached out of it. Because of this, it is possible that the wetland will have to be remediated to prevent leaching. This results in addition of re-construction costs and disposal costs of contaminated soil material.

It is difficult to generalise the costs of water treatment, as the chemical composition of the water, such as pH and concentrations of harmful substances, affect the costs (Sveriges geologiska undersökning 2017).

Table 1 *Indicative Estimates of CAPEX and OPEX of Water Treatment (from Laakso* et al. *2022*

Treatment method	CAPEX	OPEX	Source
Overland-flow wetland	0.14 €/m^2	moderate	AFRY Finland Oy design data 2019
Aerobic wetland	3–30 €/m^2	moderate	Garbarino *et al.* 2018
Anaerobic wetland	20–350 €/m^2	moderate	Garbarino *et al.* 2018
Settling pond	17–90 €/pond-m^3	moderate	AFRY Finland Oy design data 2018-2021
Lime precipitation, field set	930 € per m^3/h design flow	0.02–1.3 €/m^3	AFRY Finland Oy design data 2017-2021
Lime precipitation, plant	5 200-22 000 € per treatment capacity m^3/h	0.02–1.3 €/m^3	Garbarino *et al.* 2018; INAP 2014
Coagulation, plant	3 900 € per m^3/h design flow	Similar cost as lime precipitation	AFRY Finland Oy design data 2019-2021

Table 1 summarizes estimated indicative values of investment and operational costs (CAPEX = Capital expenditure and OPEX = Operational expenditure) of water treatment (VAT excluded).

Estimation of the Length of Water Treatment Period

The length of water treatment period is a key parameter in evaluating financial guarantees of water treatment for mine closure. There are several approaches for the determination of the length of water treatment period. The suitable approach needs to be selected case by case considering the special features of the mine and the available initial information.

The length of the active water treatment period is usually determined with means of modelling. Modelling of mine water quality and quantity should be done as part of the closure planning. For geochemical modelling purposes, representative sampling and laboratory testing of wastes and pit walls are needed. The accuracy level of the emission modelling, as well as the closure plan, will evolve as the mining project progresses. (ICMM 2019) Modelling can also be used after assessment of post-closure emissions to determine the dispersion of mine discharges on the receiving water body. This model will feed to post-closure environmental impact assessment work, which outcome will iteratively feedback to selecting sufficient closure measures. The improved closure methods can be, e.g., modifications of water treatment, improved cover structures for waste areas, or directing leachate into open pit mine.

In some cases, there may be a need for temporal water treatment that is tied to a change in the amount of water rather than change in the water quality. This can be the case, for example, in a slurry deposition tailings area, where water table gradually lowers after the end of production. In the initial phase of drying, the amount of leachate is at its maximum and decreases over time. On certain stage after closure, residual emissions could be on environmentally acceptable level and water treatment could be terminated.

One option for determining the length of the post-closure active water treatment period is to determine the theoretical replacement time of the pore water in the mining waste area. This approach can be well suited, for example, if importance of some factor during production to the mine waste area water quality is overruling the effect of the waste's characteristics. Such factor can be, for example, process water or a factor related to explosives.

The need for water treatment can also be related to the progress of the implementation of closure works, for example, particularly impervious cover structures can be assessed to prevent the interaction of mining waste with its environment to such an extent, that the water treatment can be run down at completion of the cover structures.

Future trends

Progressive mine closure has become more common, especially at waste rock areas (ICMM 2019). Progressive mine closure means that some closure measures are done already during operational period of the mine.

The goal is to reduce the amount of waste formed in mining, which also decreases the amount of waste impacted water and

closure costs. The amount of environmentally harmful leachate generated from waste areas could be reduced already during the production phase by sorting and selective processing of mining waste, and by diversion of unimpacted waters. This would increase costs during operation but could reduce costs at the closure. (Garbarino *et al*., 2018)

On tailings management and management of active water treatment sludges formed on mine sites, dry stacking is gaining favour in comparison to slurry deposition. The advantage of dry stacking is a smaller surface footprint compared to slurry deposition, decreased seepage volumes, and enhanced possibilities for progressive closure. All these factors decrease the post-closure water treatment costs and offer benefits for improved post-closure environmental risk management.

Conclusions

At the early stage of mine closure, the active water treatment technology used during mine operation could be suitable for discharge water treatment. However, the goal is to replace the active treatment with passive or semi-passive, less resource intensive, treatment as soon as the water quality allows it. Passive treatments need also certain amount of maintenance. When the water management measures are at a stage where water quality reaches the set requirements, also passive treatment can be terminated. As part of the closure plan, it is recommended to model mine water quantities, qualities, and environmental discharges until stabilized post-closure stage in order to evaluate the environmental impacts and to select sufficient closure measures related to water management and treatment. The cost estimate of water treatment will then assist on setting sufficient financial guarantees.

This paper describes factors affecting the financial guarantees of water treatment and can help to find a suitable water treatment method, or combination of water treatment methods, in mine closure phase. The information presented on this paper can be used as a reference point in estimation of water treatment costs during closure phase.

Acknowledgements

The findings of this paper are based on the study that was part of the Finnish governmental project Scope Expansion of Financial Guarantees in Mining: Influence on Environmental Protection and Costs. The project was financed by the Finnish Government's analysis, assessment, and research activities and was based on the aim to improve environmental protection in mining by developing provisions on financial guarantees.

References

Garbarino E, Orveillon G, Saveyn, H, Barthe P, Eder P (2018) Best Available Techniques (BAT) Reference Document for the Management of Waste from Extractive Industries in accordance with Directive 2006/21/EC. Publications Office of the European Union, Luxembourg, doi:10.2760/35297.

ICMM (International Council on Mining & Metals) (2019) Integrated mine closure. Good practice Guide, 2nd edition. International Council on Mining & Metals.

INAP (The international network for acid prevention) (2003). Treatment of sulphate in mine effluents. The international network for acid prevention.

Kleinmann R, Sobolewski A, Skousen J (2023) The Evolving Nature of Semi-passive Mine Water Treatment. Mine Water and the Environment 42:170-177.

Laakso T, Picken P, Pölönen I, Vaarasuo A, Anttila E-L, Juholin P, Vähänen K, Nurmesniemi E-T, Haanpää K-M, Kaikkonen I, Tuisku P (2022) Kaivosten jätevakuuden alan laajentamisen ympäristönsuojelullinen vaikuttavuus ja kustannukset. Valtioneuvoston kanslia, Helsinki. ISBN pdf: 978-952-383-185-8.

MEND Report 3.50.1 (2014). Study to identify BATEA for the management and control of effluent quality from mines,

Sveriges Geologiska Undersökning (2017). Utvärdering av efterbehandlad gruvverksamhet. Kartläggning av kostnader för hantering av gruvavfall och för efterbehandling av gruvverksamhet. RR 2017:04, SGUs diarie-nr: 311-888/2016, Naturvårdsverkets diarie-nr: 03195-16.

Wolkersdorfer C. (2022) Mine water treatment – active and passive methods, Springer 2022. ISBN 978-3-662-65770-6. https://doi.org/10.1007/978-3-662-65770-6.

Insights Into Catchment Connectivity Using Water Stable Isotopes To Address Diffuse Mine Pollution In Streams

Barbara Palumbo-Roe[1], Emma Crewdson[1,4], Adam Jarvis[2], Catherine Gandy[2], Vanessa Banks[1], Alex Mulcahy[1], Manny Zarate[1], Carol Arrowsmith[1], Stephen Loft[3], Jasmine Pullen[3], Arabella Moorhouse-Parry[4], Hugh Potter[5]

[1]*British Geological Survey, Nicker Hill, Keyworth, Nottingham, UK, NG12 5GG*

[2]*School of Engineering, Newcastle University, Newcastle upon Tyne, UK, NE1 7RU*

[3]*UK Centre for Ecology & Hydrology, Lancaster Environment Centre, Bailrigg, Lancaster, UK, LA1 4AP*

[4]*The Coal Authority, 200 Lichfield Lane, Mansfield, Nottinghamshire NG18 4RG, United Kingdom*

[5]*Environment Agency, Horizon House, Bristol BS1 5AH, United Kingdom*

Abstract

We used natural water isotope tracers (δ18O, δ2H) in synoptic sampling of boreholes, mine adits and stream water to gain insights into diffuse contaminated groundwater and mine water flow pathways in the Force Crag Mine catchment, Cumbria, UK. Rapid delivery of new water (rain) into both the mine workings and shallow groundwater was seen in the isotope signature. The high degree of spatial and temporal variability of isotope concentrations in the shallow groundwater is evidence of a complex flow system, typical of upland catchments.

Keywords: Isotopes, tracers, groundwater, metal mine, diffuse pollution

Introduction

The role of diffuse groundwater pollution in mine catchments is not well studied. This is in part due to the challenges of monitoring groundwater in mine catchments, often in remote and upland sites with difficult access and the lack of easy means of detecting diffuse subsurface flow paths. Heterogeneity is a key feature of upland catchments and influences catchment water flows, but is difficult to characterise and is often simplified or overlooked. Made ground, inherent of legacy mine sites and altered hydrogeology of the mine workings add to the above complexity. Many metal mine sites are designated as protected areas, because of their natural and cultural importance; hence, undertaking intrusive investigations can present further logistic challenges.

Prediction of the impacts of diffuse groundwater pollution requires an understanding of the pathways through which water moves from a contaminant source to a receptor such as a stream. At the abandoned Force Crag Mine, NW England, monitoring infrastructure has been installed to undertake a study of these diffuse sources, and investigate the hydrological connections between the hillslopes and riparian zones to the stream. The DIFFUSE project applied a combined monitoring approach including stream-centred synoptic sampling and hillslope/riparian-centred geophysical surveys, ground investigation comprising piezometer installation and core sampling and tracer tests. The study confirmed very high zinc concentrations in the shallow groundwaters. Here we present the results of the isotopic investigation conducted to help characterising pathways contributing zinc to the stream. Since water δ18O and δ2H act conservatively as precipitation travels through the subsurface to the stream, water isotopes can be useful tracers in providing insights into hydrological processes. The results also provide initial evidence on the spatial and temporal variability of water isotopes in the upland Coledale catchment, which was previously unknown.

Study site and Methods

Force Crag Mine is situated at the head of Coledale Valley, Cumbria (54.58°N, 3.24°W). Historic mining activities exploited mineral veins hosted in the low-grade metamorphosed siltstone and mudstone bedrock of the Skiddaw Group. Lead was mined from 1839, before zinc and barite associated minerals in the late 1860's, until final abandonment in 1991 (Oswald and Pearson, 1999). The Coledale Valley delineates the upland stream catchment of the Coledale Beck, which flows approximately southwest-northeast into Newlands Beck, a tributary of Bassenthwaite. Superficial deposits of glacial till cover the valley floor, along with a complex heterogenous cover of alluvial deposits comprising clay, gravel and peat, overlain and interbedded with centuries of various grades of mine waste deposits, contributing diffuse pollution.

The site was instrumented with 16 piezometers to intercept shallow groundwater in the riparian zone, hillslope zone and mine waste in three areas A, B and C (Figure 1) to investigate possible connectivity between metal-polluted groundwater and the Beck.

The screened depths of the piezometers were chosen to span above and below the first water strike during drilling. The shallowest piezometer was screened at a depth of 0.2 to 0.6 metre below ground level (mbgl), whilst the deepest was screened at 3.5 to 5.5 mbgl, with most spanning depths of 0.4 to 1.5 mbgl. The most upslope piezometer BH1 has the deepest water level, installed in glacial till. BH2 installed within spoil is dry. Very shallow groundwater levels are encountered at BH7, BH3 and BH6 throughout the year.

We combined synoptic sampling of the surface water, groundwater and mine water inflows, in six sampling rounds, to investigate potential contaminated groundwater and mine water contributions to the Coledale Beck, and how these contributions vary at high and low flow. The sampling locations for the mine water discharges and surface waters, with the hydrochemical data, are reported in a parallel paper in these conference proceedings (Jarvis *et al.* 2023).

Rainfall and stream flow data were obtained from the Coal Authority (Force Crag, GPRS2 Rain Gauge (NC33.22); Force Crag, FC03 Coledale Beck D/S MWTS (NC33.25)- NetDL500). The rainfall amounts in the antecedent 2, 10 days (P2, P10 in mm) to each sampling event and the background streamflow (Q in L/s), a measure of the catchment moisture status, varied as follows: Apr-21 P2: 0, P10: 0, Q: 31; May-21 P2: 0, P10: 81, Q: 163; Jun-21 P2: 0, P10: 33, Q: 36; Aug-21 P2: 0, P10: 1.4, Q: 48; Nov-21- P2: 46, P10: 357, Q: 169; Feb-22 P2: 14, P10: 70, Q: 250.

Groundwater samples were obtained following a low-flow sampling method. To obtain representative samples and maintain constant head, pumping rates of <0.5 L/min were used for at least 15 minutes (to purge 3 well volumes), and until stable field

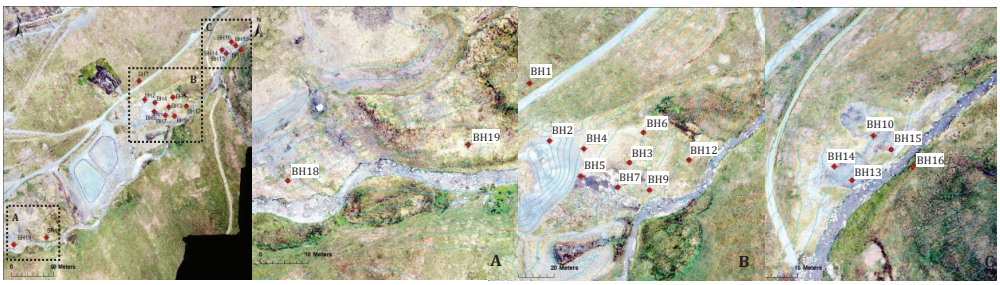


Figure 1 *Location of the piezometers at Force Crag mine.* ***Area A****, downstream of the confluence with the Pudding Beck, upstream of the mine buildings and treatment scheme, comprises of mainly peaty ground which remains wet underfoot even in the driest seasons.* ***Area B****, downstream of the treatment scheme around the 'Tip 3' area, is the most heterogeneous spanning the hillslope zone and riparian zone; ground cover comprises glacial till, mine waste, gravel and peat.* ***Area C****, downstream of the Birkthwaite Beck confluence around the 'Mill 2' area, is mainly covered by coarse mine waste deposits, except for BH16 situated on the southern bank on peaty ground. Aerial photo courtesy of UKCEH (2021).*

parameters were reached in the flow-through cell (pH, temp, oxidation-reduction potential, dissolved oxygen, electrical conductivity). Very low yield in some piezometers precluded pumping, instead samples were collected using 50 ml bailers (except for BH04 where a 1 L bailer was used) and the field parameters measured from a beaker containing the purged water.

The water $\delta^{18}O$ and $\delta^{2}H$ analyses were carried out in the Stable Isotope Facility, BGS, Keyworth. Isotopic ratios ($^{18}O/^{16}O$ and $^{2}H/^{1}H$) are expressed in delta units, $\delta^{18}O$ and $\delta^{2}H$ in ‰ and defined in relation to the standard Vienna Standard Mean Ocean Water 2 (VSMOW2). The analytical precision for the analyses is typically <0.05‰ for $\delta^{18}O$ and ±1.0‰ for $\delta^{2}H$.

Results and Discussion

Water isotope composition for surface water, mine water and groundwater, plotted on a dual $\delta^{18}O$ and $\delta^{2}H$ plot, broadly falls close to the Global Meteoric Water Line (GMWL), with possible near-surface evaporative effects for some boreholes plotting below the GMWL (Figure 2).

Figure 3 shows the spatially and temporally variable δ18O values of Coledale Beck surface water, the mine water discharges and the boreholes, ordered downstream from the mine, during the synoptic sampling events. Some important points are highlighted below: i) The very small spatial δ18O variations in the Coledale Beck from upstream to downstream of Force Crag Mine in each sampling round, with standard deviation (SD) between ±0.04‰ and ±0.1‰ for δ18O, close to the analytical precision. ii) The lack of a contrasting isotopic signature between the stream and the mine water inflows. As such, the water isotope tracer approach is of limited use for identifying the relative contributions of mine water loads to the Coledale Beck in each sampling round. iii) The greater spatial variability of the shallow groundwater isotope concentrations (SD between ±0.3‰ and ±0.6‰ for δ18O) compared to the stream waters, which can be explained by the short flow paths and limited mixing, characteristic of headwater catchments. iv) From the comparison of the six synoptic sampling events, it is noticed that in Nov-21, the wettest sampling event (see P2, P10 values in Methods), the spatial variability of the isotopic composition across the catchment was the lowest (SD ± 0.22‰), which may suggest a greater connectivity of the catchment during large precipitation events, as the various components of runoff tend to converge toward the precipitation signature. This needs to be further explored with longer term monitoring including precipitation samples, but similar catchment rainfall-runoff responses are not unusual (Kendall and Caldwell, 1988).

There is considerably more temporal isotopic variation (with SD ± 0.3‰ to ±0.5‰ for $\delta^{18}O$ and SD ± 2.4‰ to 4.7‰ for $\delta^{2}H$) than spatial variation in the Coledale Beck, as it reflects the contribution of precipitation to streamflow, with fluctuations in the isotope ratios associated with seasonal and event-based factors including provenance, temperature of the air mass and amount of precipitation. The seasonal pattern of precipitation isotope values, with tendency of higher $\delta^{18}O$ and $\delta^{2}H$ /^{18}O- and ^{2}H-enriched

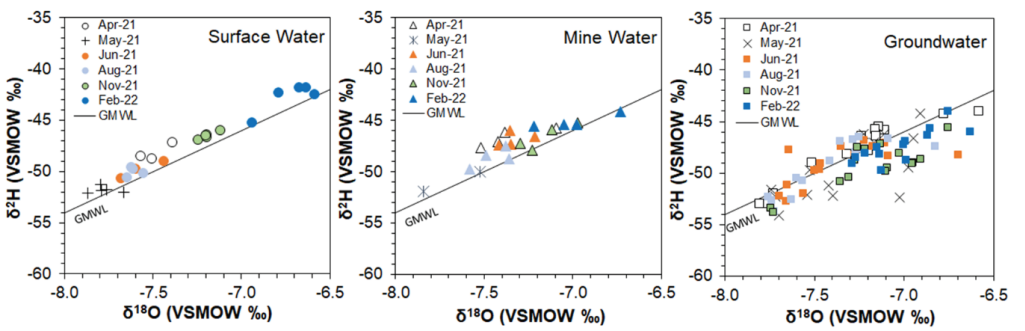


Figure 2 $\delta^{2}H$ versus $\delta^{18}O$ values in surface water, mine water and groundwater in Force Crag mine catchment in the six sampling events from April 2021 to February 2022 against the Global Meteoric Water Line (GMWL)..

values in summer/warmer months and lower $\delta^{18}O$ and $\delta^{2}H$ /^{18}O- and ^{2}H-depleted values in winter/colder months, is, however, not so obvious in our dataset (Figure 2). Nevertheless, day to day variability of rainfall isotope values can be large (Scheliga *et al.* 2018) and can account for the range and differences observed in our low-resolution monitoring. This is the case in the Feb-22 sampling, with the highest $\delta^{18}O$, $\delta^{2}H$ values in Coledale Beck, unexpectedly for a winter precipitation, but confirmed by the ^{18}O- and ^{2}H-enriched values ($\delta^{18}O$ -2.76‰; $\delta^{2}H$ -18.5‰) of the synchronous rain sample collected. Potentially, a similar rainfall composition accounts for the Nov-21 $\delta^{18}O$ in Coledale Beck, relatively higher compared to the April to August samples, although we do not have rain isotope analysis to support that.

The ^{18}O-enriched isotopic signal of the Nov-21 and Feb-22 heavy rainfall events (referred as "new water") was sought in the mine water and groundwater samples as evidence of rapid recharge. Figure 4 illustrates the isotope measurements across the sampling events compared with the Coledale Beck. Low isotopic variability implies an isotopically well-mixed system, where the seasonal isotopic signature of precipitation has been lost due to dispersive mixing/amalgamation of recharge water signatures. This is generally typical of aquifers where intergranular permeability predominates (Darling *et al.* 2003); a pronounced level of isotope damping is also observed in upland catchments, due to high water storage in the organic layers encouraging tracer mixing. On the contrary, larger fluctuations in the isotopic signal indicate a higher fraction of new water entering the system and can be due to preferential flow/shorter residence times/low storage. The analysis of Figure 4 indicates various isotopic responses which took place during the Nov-21 and Feb-22 wet events. Both mine water discharges from Level 1 (sample point FC30) and Level 0 (FC6) show contributions of recent precipitation in the isotopic signature of the Nov-21 samples, to suggest that the mine workings can be quickly recharged by meteoric waters draining through the overlying soils and upslope areas, consistent with Dumpleton

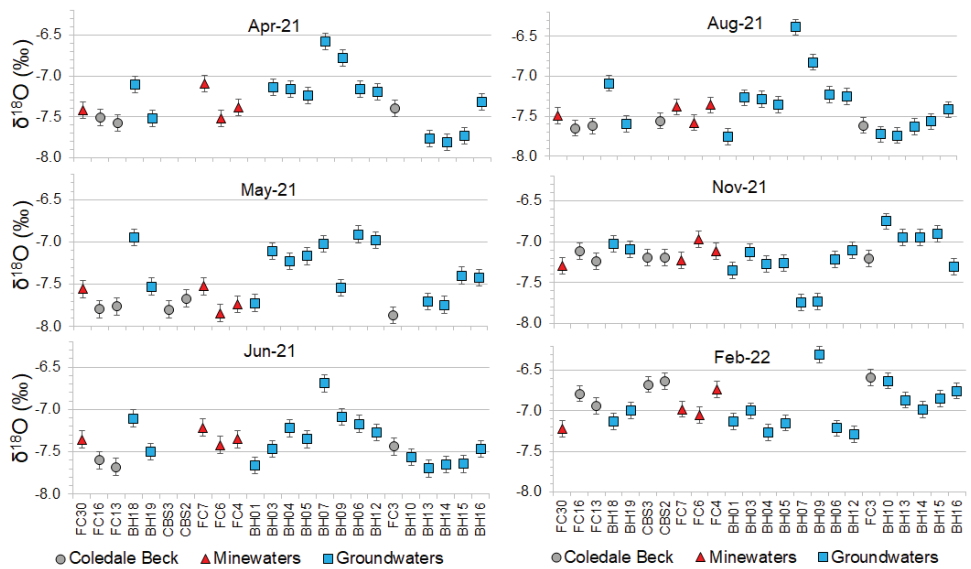


Figure 3 *$\delta^{18}O$ variation across monitoring points (from upstream to downstream the mine) by sampling event. Outside Y-axis range: May-21 BH10 δ18O -8.9‰; Feb-22 BH7 -5‰. Error bar ±0.1‰. Stream water: FC16: u/s mine; FC13: u/s Level 1 overflow A; CBS3: u/s channel C; CBS2: d/s FC8; FC3: d/s mine); mine water (FC30: Level 1; FC7: treatment plant outlet; FC6: Level 0; FC4: Level 0 + Drain B); boreholes from Figure 1.*

et al.'s (1996) hydrogeological assessment of the mine workings. However, there are differences in $\delta^{18}O$, highlighted in Figure 4, between Level 0 and Level 1 in each event. Differences are minimal in the dry sampling events in Apr-21, Jun-21 and Aug-21 and larger in May-21, Nov-21 and Feb-21, corresponding to sampling events with high amount of rainfall in the 10 days prior to sampling. Given the proximity of Level 0 and Level 1, it is likely that the isotopic signature of the rainfall contributing to both discharges (although not confirmed) is the same for any given sampling event; the observed differences may then reflect differences in the recharge (the proportion and travel time of rainfall reaching the mine workings). The water δ18O values of the mine water treatment system, sampled at the outlet (FC7), and of FC4 sampling point, which collects a mixture of culverted Level 0 discharge and crownhole overflow discharge, reflect more the largest variation with a positive δ18O peak of the Feb-22 event; this is instead dampened in Level 1 (FC30) and absent in Level 0 (FC6) samples.

At BH01 on the hillslope near Level 0, $\delta^{18}O$ values show that the monitored borehole is also very responsive to the last two rainfall events, consistent with a recharge area interpreted above.

In the riparian area downslope of Tip 3 (Figure 1, B), very responsive boreholes were identified in BH07 and BH09 (Figure 4), suggesting an active downward recharge and with large $\delta^{18}O$ variation also possibly indicating low storage. BH03, BH05, BH06 and BH12, instead, showed a much more damped response to rainfall events. The water level changes in these latter boreholes, while the isotope values remain relatively stable, suggesting the influx of water other than the new water. In the same area the invariable isotopic concentrations of BH04, a deeper low-yield (screened at 0.5 to 2.5 mbgl) piezometer, drilled at the toe of Tip 3, to intercept any potential mine water plume, are indicative of a lack of direct connection to the surface zone and consistent with a zone of low hydraulic conductivity below Tip 3.

Upstream Tip 3 area, in the riparian area in Figure 1, A, two contrasting isotope temporal variations were observed between BH18 and BH19. Given the borehole proximity, this result highlights the strong influence of local heterogeneity; in particular

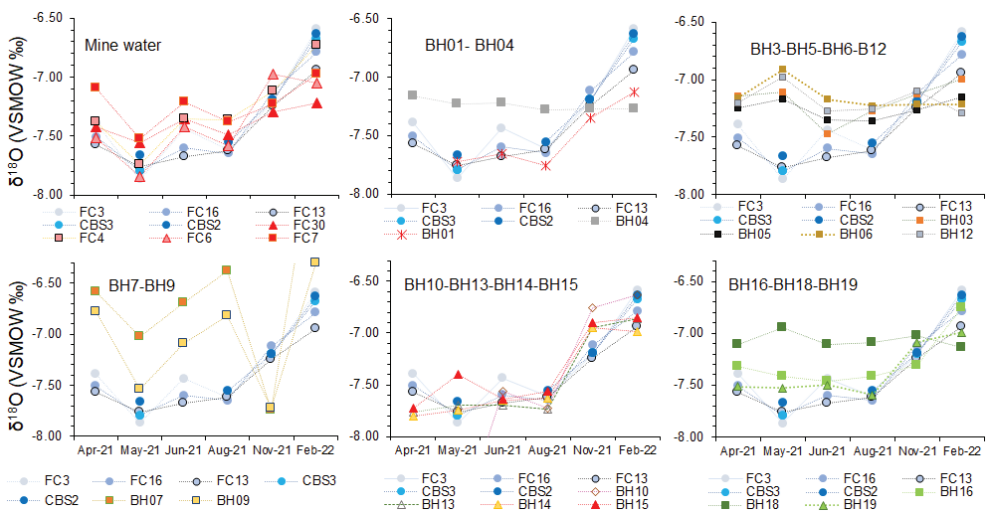


Figure 4 *Temporal variation of $\delta^{18}O$ in the mine waters (FC30: Level 1; FC7: mine water treatment plant; FC6: Level 0; FC4: Level 0+Subsurface Drain B) and all boreholes compared against Coledale Beck (FC16 Coledale Beck u/s the mine; FC13 u/s Level 1 overflow A; CBS2 and CBS3 Coledale Beck receiving point source mine waters; FC3 Coledale Beck d/s the mine). δ18O outside Y-axis: BH7 -5‰ (Feb-22), BH10 -8.9‰ (May-21).*

the upstream BH18 isotope signature shows no signs of new water, while BH19 changes in Nov-21 (with the highest P2), and mimics the Coledale Beck signature in the other sampling rounds.

Another group of boreholes closely mimic the Coledale Beck $\delta^{18}O$ values and patterns. This group includes the riparian BH16 (on the southern river bank opposite to the mine) and all the riparian boreholes at Mill 2 (BH10, BH13, BH14, BH15), although some differences are noted for BH16. This is interpreted as evidence of a common recharge source for these boreholes and the Beck.

High-frequency hydrometric data and low-resolution isotope measurements can complement each other to better understand the hydrologic connections and the areas that contribute to streamflow. Some clues concerning the connectivity between riparian groundwater and the Beck can be found in the hydrographs obtained for some of the boreholes. Figure 5 gives an example of high connectivity between the shallow groundwater and the stream, with the rapid response to rainfall observed in the groundwater heads of BH19, within 3 hours of rainfall events in the wet season and rapid drainage. Both peaks and recession curves of groundwater head and streamflow are coincident with each other, although heads typically rise 3-5 hours before there is a streamflow response in Coledale Beck, and rainfall events of <10mm/day can cause head responses, but do not contribute to streamflow in Coledale Beck.

Conclusions

This study, an assessment of the water isotope signature and spatial and temporal variability in groundwater, collected during synoptic sampling with surface water and mine water, in a UK abandoned mine catchment, has evidenced the high degree of variability of isotope concentrations in the shallow groundwater from various parts of the catchment and the variable relation to stream flow at the time of sampling. This highlights the complexity of various residence times, subsurface storage and mixing processes, as well as the critical dependence on catchment wetness and precipitation intensity. Based on the limited monitoring period and preliminary integration of the isotope data with hydrometric data, we infer connectivity of the groundwater to the stream, and hence a contribution of Zn-contaminated groundwater to the stream, but we expect the groundwater contribution to stream flow to be highly variable in time and space. Given concerns about climate change projections of wetter and warmer winter conditions likely to generate more extreme

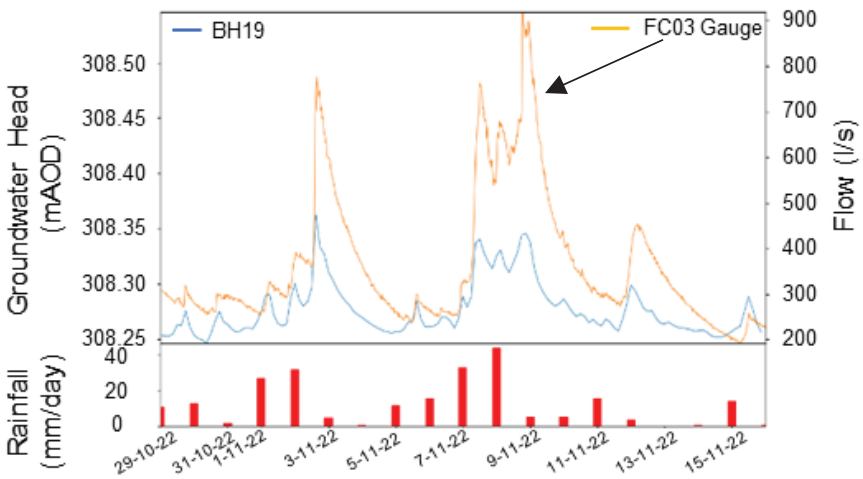


Figure 5 Groundwater heads in metres above ordnance datum (mAOD) in borehole BH19 (blue lines) compared with rainfall (red bars) and streamflow (orange lines) between 29/10/22 to 15/11/22.

flood events, long-term catchment scale monitoring of this type is recommended to provide baseline data to contextualise these extreme events and predict impacts.

Acknowledgements

The research was funded by the UK Coal Authority, (DIFFUSE project CA18/2/1/4), under the umbrella of the Water and Abandoned Metal Mines Programme (WAMM), a partnership between the Environment Agency, the Coal Authority and the UK Department for Environment, Food and Rural Affairs (Defra). We express our gratitude to the National Trust, in particular Mr. John Malley, for site access and background information. The views expressed in this article are those of the authors only, and do not necessarily represent those of any other organisations mentioned herein. BGS authors publish with the permission of the Director of the British Geological Survey (UKRI).

References

Oswald A, Pearson T (1999) Force Crag mine, Cumbria. English Heritage Archaeological Investigation Report Series AI/1/1999, 109 pp.

Darling W G, Bath AH, Talbot JC (2003) The O and H stable isotope composition of freshwaters in the British Isles. 2. Surface waters and groundwater. Hydrology and Earth System Sciences, 7(2), 183-195.

Dumpleton S, Donnelly LJ, Young B (1996) A survey of Force Crag Mine, near Keswick, Cumbria. British Geological Survey Fluid Processes Group Technical Report WE/96/34c, 88 pp.

Jarvis A, Banks V, Crewdson E, Lofts S, Palumbo-Roe B, Pullen J, Gandy (2023) Sources of diffuse zinc and lead contamination in an abandoned mine watershed. IMWA 2023 Conference Proceedings.

Kendall C, Caldwell EA (1998) Fundamentals of isotope geochemistry. In Isotope tracers in catchment hydrology (51-86). Elsevier.

Scheliga B, Tetzlaff D, Nuetzmann G, Soulsby C (2018) Groundwater dynamics at the hillslope–riparian interface in a year with extreme winter rainfall. J Hydrol, 564, 509-528.

Modelling of Coal Pit Lake Quantity and Quality for Mine Closure (Case Study ON2 Area, Lati Mine Operation, Berau Coal)

I K Dwika Paramananda, Abie Badhurahman, Ginting Jalu Kusuma, Sendy Dwiki, Salmawati, Rudy Sayoga Gautama

Department of Mining Engineering, Faculty of Mining and Petroleum Engineering, Bandung Institute of Technology, Indonesia

Abstract

Coal mining in Indonesia can cause long-term environmental impacts including acid mine drainage, which can lead to the formation of acidic pit lakes after mine closure. This study developed a model to predict pit lake quality and quantity based on acid mine drainage management plans, using PhreeqC software and considering land cover changes and mine water treatment. Results showed that managing acid mine drainage with revegetation and treatment could improve water quality and quantity, yet to comply with regulation needs a longer duration. The simple modelling process showed applicability and acted as a key role in predicting the water quality and quantity of pit lakes based on selected acid mine drainage management plans.

Keywords: Pit Lakes, Acid Mine Drainage, Mine Closure, Hydrochemistry, PhreeqC

Introduction

Coal is one of the primary energy commodities in Indonesia, which is mainly mined in surface mining using the open pit method. Open-pit coal method exposes rock layers and potentially poses serious environmental impacts by alteration of the physical, chemical, and biological properties of rock layers including soils. The problems are fundamentally interrelated, requiring strategic reclamation management to produce good post-mining land (Feng *et al*., 2019). On the other hand, the hydrological system changes in terms of water flow paths, quality and quantity of surface runoff will disrupt the overall land ecosystem condition.

Hydrological impact in the form of changing water quality and quantity are imminent in the mining operation stage by the alteration of catchment areas, yet the impact could be extended into post-mining stages as pit lakes formed and exacerbated by the emergence of acid mine drainage (AMD) (Asdak, 2010; Chow, 1988; Setyowati, 2011). These impacts, if not managed properly, could pose negative impacts towards the environment and become a burden for stakeholders. To meet the post-mining success criteria, corrective measurements and mitigation need to be taken, including the reclamation of disturbed areas and the implementation of active and passive treatment to improve water quality. This is to meet the needs of reclamation and post-mining which need to pay attention to fundamental things such as physical stability, chemistry, socio-economic level, land requirements, biodiversity, and culminating in further development. According to the regulation, mine water resulting from the coal mine is expected to meet the following standards: pH 6 – 9; Fe<7 mg/L; Mn<4 mg/L; and TSS/total suspended solid<300 mg/L.

Research related to the formation of pit lakes from the perspective of water quality and quantity in tropical areas/ Indonesia is still scarce and mostly to identify the source of problems and corrective means (Tuheteru, 2021). This research aims to develop a simple yet applicable model of pit lake quality and quantity prediction for the mine closure area, to comply with the regulation of effluent standards from coal mines. In addition, sensitivity analysis was carried out by considering land cover changes and various options for mine water treatments. The modelling is done by mixing surface runoff water quality in the catchment area before and

after land cover changes and improvement and passive treatment implementation in selected locations based on previous research using the software PhreeqC.

Methods

Study area

Lati Mine Operation (LMO) mining area has been in production since 1992 and is located in the northeast mine permit area of Berau Coal. There are two main rivers, namely the Lati River to the east and the Ukud River to the west which flows into the Segah River. Geologically, the Lati site is dominated by sandstone, siltstone, and mudstone with a geological structure of syncline extended North-South of the LMO area.

As shown ON2 post-mining area is located in the northern part of LMO (Fig. 1). In 2022, the ON2 area (based on catchment delineation) covers a total area of 1,316.34 ha divided into naturally vegetated areas (21.72%), revegetation area (35.19%), ex-mining pit (7.50%), and open land/active areas (35.53%). There are three identified mine pits (voids), i.e. Southern ON2, void Northern ON2, and void Eastern ON2. Hydrological tree/water balances of these voids (Fig. 1) denotes that all surface water in this area will be directed to WMP-27 before it reaches the final natural streams (Lati River)

Mine water management plan

The mine water management plan that will be applied to the ON2 post-mining area is described as follow:

1. The ON2 ex-mining pit consists of Southern, Northern, and Eastern ON2. All of the ex-mining pits will be developed into pit lakes.
2. The outlets of the post-mining lakes of Southern ON2 and East Northern ON2 are connected to Northern ON2. The outlet of pit lake Northern ON2 is connected to Sediment Pond WMP 27 before finally being discharged into Lati River.

The management plan is made to centralise the water management plan thus controlling the water quality and quantity into a single

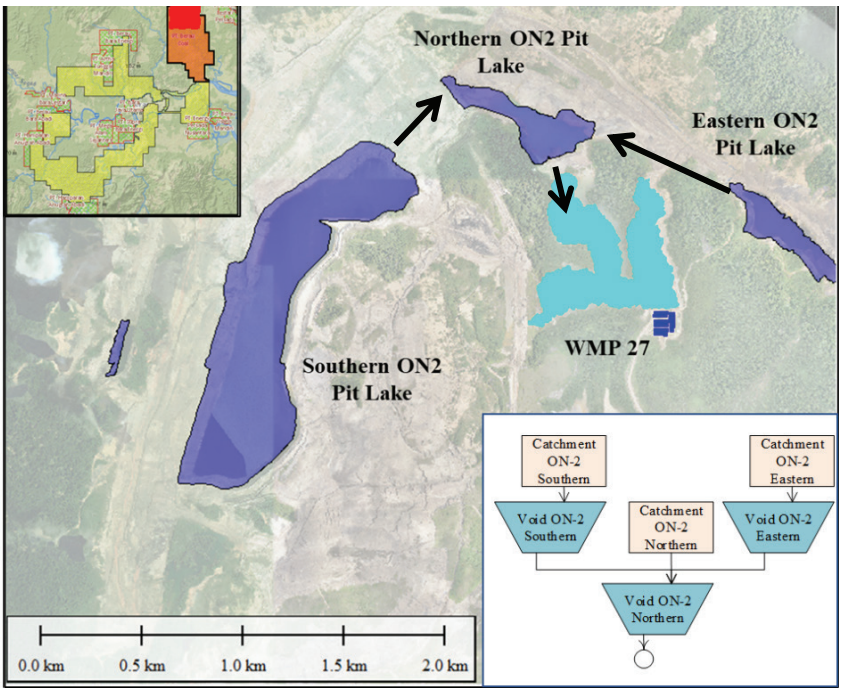


Figure 1 ON2 Post-Mining Area and The Hydrological Tree/Water Balance

outlet point of surface runoff water for the ON2 post-mining area.

To prepare for post-mining conditions in ON2, a model was developed for the revegetation and infrastructure of acid mine drainage. The areas to be revegetated or treated were identified using a 50 ha/year revegetation rate and a 100 ha/year infrastructure construction rate. Open limestone channel infrastructure was modelled based on previous research with adjustments made for ON2's conditions and installed on disturbed areas. Overall land changes will affect the quality and quantity of surface runoff flows into each void.

Water Quality and Quantity Modelling

This study is using water quantity model from land changes using rational equation which differs each year and is assumed to change (Paramananda, et.al., 2022). On the other hand, the calculated water quantity is used as input for mixing processes which determines the ratio of mixing among each water yielded from different land cover/catchments area. The simple modelling process is explained below (Fig. 2).

The model initializes initial void water quality and quantity at t=0. For each increment of time (in this study, the selected time increment is a year), the water quality and quantity of each void will be updated using a mixing process in PhreeqC based on water quality and quantity for each land cover/catchment area, i.e., revegetated area, the disturbed area treated passively using OLC/open limestone channel and direct rainfall into the voids. The process is repeated until t_n=13 or thirteen years from now since the mining will cease in thirteen years. The model is neglecting another hydrological aspect (e.g., no groundwater fluxes, undetermined evaporation process since all other processes have been assumed by selected runoff coefficient) and using simple geochemical processes (instead of other complex models) therefore the model is a simple modelling process. This model is used as a preliminary overview and is expected to be used for a more comprehensive study in terms of predicting the quality and quantity of pit lakes.

Result and Discussion

Water Quantity and Hydrological Characteristics

The quantity of the runoff for each type of land cover is governed mainly by rainfall depth and coefficient of runoff. For the simplification of the model and accounting variability of rainfall, three different yearly rainfall amounts are used, i.e. 1st quartile of 1,690 mm/year, 3rd quartile of 3,647 mm/year, and a yearly average rainfall of 2,831 mm/year. The annual volume of surface

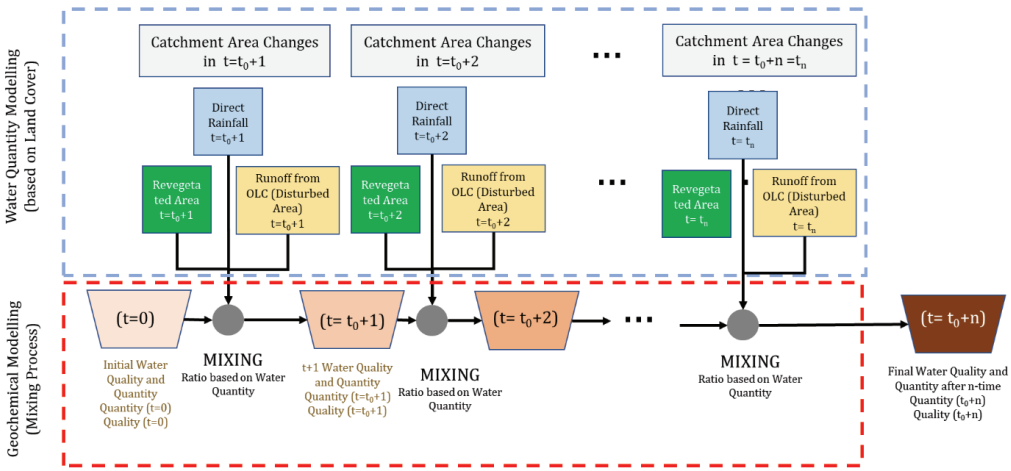


***Figure 2** Description of Mine Water Quality and Quality Modelling*

runoff is calculated using a rational equation (Gautama, 2019; Guo, 2001):

$$V=n.C.P.A$$

n is the unit conversion coefficient; *C* is the runoff coefficient; *P* is the yearly rainfall (L); *A* is the land cover area (L^2). The calculated volume is then to be used as a mixing ratio for geochemical modelling using PhreeqC as explained above-mentioned.

Water Quality Characteristics as Input

The water quality of mine voids is determined by point sampling for each void. Full-suite water quality measurements are carried out in the field (pH, TDS, temperature, EC, ORP) as well as in the laboratory (anions, cations, alkalinity using ICP-MS, Ion Chromatography, AAS and titration. Selected water quality parameters are shown in Table 1.

Based on the physical properties test, the lowest pH was found in the Eastern ON2 post-mining lake with a pH of 2.86. Iron and manganese will be of concern according to applicable regulations. Based on the metal test results presented in Table 1, show a tendency for high Fe values to exceed the quality standard limit of 7 mg/l in all pit lake samples. Meanwhile, Mn is ranging from 2.06 – 6.49 mg/L. All of these data are used as initial conditions (t=0) for void/pit lake water quality.

As described previously, changes in land cover translate into different surface water quality and quality. The following water quality is assumed for the geochemical modelling/ mixing process as presented in Table 2. Water quality data other than assumed water quality from OLC are primary data.

All of these data are used as input alongside water quantity in the mixing process using PhreeqC.

Modelling results

Table 3 presents changes in water quality parameters for post-mining lakes due to modelling the 13 years mixing of surface runoff water quality and post-mining lakes by PhreeqC with improvements in revegetation based on forementioned assumptions and acid mine drainage management.

Table 1 *Voids Water Quality*

Parameter	Unit	Eastern ON2	Southern ON2	Northern ON2
pH		2.86	3.03	3.00
Al	mg/L	4.13	8.40	3.58
Fe	mg/L	13.95	12.23	8.56
Mn	mg/L	3.28	2.06	6.49
SO_4^{2-}	mg/L	357.00	387.00	380.00
Alkalinity as $CaCO_3$	mg/L	0.00	0.00	0.00
Si as SiO_2	mg/L	1.73	3.88	4.89

Table 2 *Other Water Quality Assumed in This Study (Swastika 2013)*

Parameter	Unit	Revegetated Area	Outlet from OLC	Rainfall
pH		4.45	7.06	6.28
Al	mg/L	1.10	0.02	0.01
Fe	mg/L	1.18	0.86	0.01
Mn	mg/L	0.49	1.01	0.01
SO_4^{2-}	mg/L	88	220.00	2.10
Alkalinity as $CaCO_3$	mg/L	102	1.44	8.80
Si as SiO_2	mg/L	0.01	9.70	0.23

Table 3 Pit Lakes Water Quality Modelling Result

Parameter	Unit	Eastern ON2			Southern ON2			Northern ON2		
		1st Quartile	Mean	3rd Quartile	1st Quartile	Mean	3rd Quartile	1st Quartile	Mean	3rd Quartile
pH		5.44	5.55	5.65	3.50	3.71	3.93	4.21	4.65	5.09
Al	mg/L	0.49	0.37	0.24	1.19	0.74	0.30	0.81	0.61	0.40
Fe	mg/L	2.87	2.42	1.97	2.83	2.08	1.32	2.20	1.96	1.71
Mn	mg/L	0.57	0.58	0.58	0.82	0.83	0.85	0.73	0.72	0.71
SO_4^{2-}	mg/L	61.55	62.18	62.82	243.65	250.85	258.05	163.87	152.40	140.93
Alkalinity as $CaCO_3$	mg/L	205.30	212.30	219.30	0.01	0.01	0.01	99.47	117.14	134.80
Si as SiO_2	mg/L	0.70	0.71	0.73	0.37	0.54	0.71	0.37	0.40	0.43

The mixing analysis of surface runoff water and the post-mining lake water was performed annually based on the variations in the surface runoff coefficient and pH. The changes in the volume and pH of surface runoff water that will flow into the post-mining lake under three different annual rainfall conditions are illustrated below (fig. 3), (fig. 4), (fig. 5).

Water quality for Southern ON2 is expected to reach a pH value between 3.50 – 3.93. Water quality for eastern ON2 and Northern ON2 is expected to reach pH values between 5.44 – 5.65 and 4.23 – 5.09, respectively. The differences are due to the larger volume of water in void Southern ON2 related to runoff water produced by its catchment area which produces a slower

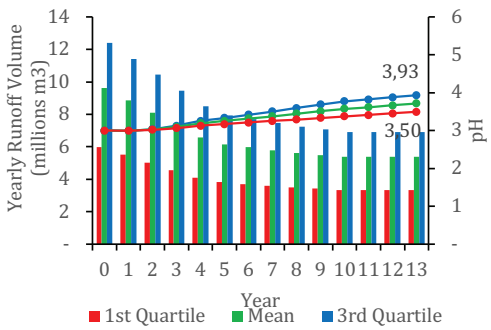


Figure 3 Changes in Runoff Volume and pH of Southern ON2

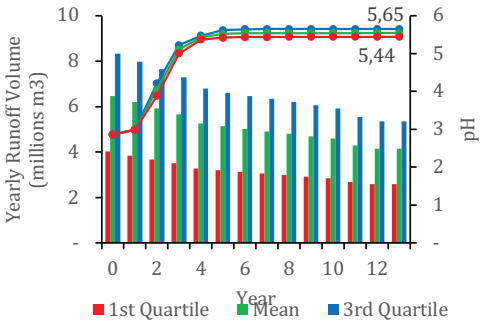


Figure 4 Changes in Runoff Volume and pH of Eastern ON2

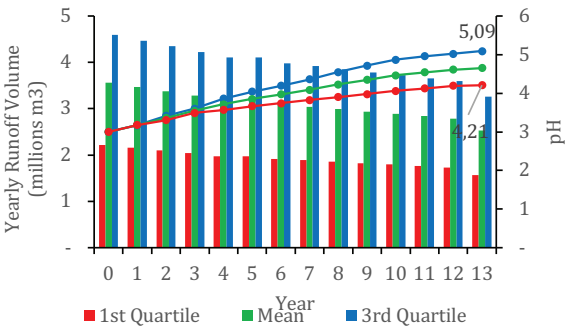


Figure 5 Changes in Runoff Volume and pH of Northern ON2

enhancement of pH value. Notably, the volume ratio of void water of ON2 Eastern to the volume of runoffs produced by its catchment area is lower and therefore elevating the pH condition of void water.

The improvement of the quality of surface water is deemed inadequate in achieving environmental quality standards since all voids are predicted to have pH values less than 6. It is expected to take a considerable amount of time to achieve the desired conditions. Consequently, it is essential to establish an infrastructure to manage final acid mine water as a means of maintaining the quality of water that flows into the Lati River. In addition, the implementation of in situ treatment methods within the pit lake offers the company an opportunity to enhance water quality, resulting in a more favorable outlet. This approach disregards cost considerations, emphasizing the importance of achieving optimal water quality conditions.

Conclusions

Revegetation and integrated treatment infrastructure implementation in the upstream area can effectively manage acid mine drainage and enhance the water quality of post-mining systems. The same outcome is achieved by passive treatment installations such as open limestone channels. Improvement of the quality of surface runoff water in critical rain catchment areas yields a maximum increase of 2.1 points of pH value in the post-mining area. Nevertheless, the pH value achieved in year 13 is still inadequate in achieving environmental quality standards since all voids are predicted to have pH values less than 6. It may take a longer period and the water quality and quantity management options are imperative to achieve the regulated effluent standards

Acknowledgements

The authors would like to thank PT Berau Coal for providing data and assistantships through the ITB-PT Berau Coal Mine Closure Planning Project Scheme.

References

Asdak, Chay (2010) Hidrologi dan Pengelolaan Daerah Aliran Air Sungai: Edisi Revisi Kelima. Yogyakarta: Gadjah Mada University Press Yogyakarta.

Chow, V.T., Maidment, D.R., and Mays, L.W. (1988) Applied Hydrology. New York: McGraw-Hill Book Company.

Cravotta, Charles & Trahan, Mary. (1999). Limestone drains to increase pH and remove dissolved metals from acidic mine drainage. Applied Geochemistry. 581-606. 10.1016/S0883-2927(98)00066-3.

Feng, Y., Wang, J., Bai, Z., Reading, L. (2019) Effects of surface coal mining and land reclamation on soil properties: A review. Earth Sci. Rev. 191, 12–25.

Gautama, R.S. (2019) Sistem Penyaliran Tambang. Bandung: ITB Press.

Guo, J.C. (2001). Rational Hydrograph Method for Small Urban Watersheds. Journal of Hydrologic Engineering, 6, 352-356.

Paramananda, I K Dwika; Gautama, Rudy Sayoga; Kusuma, Ginting Jalu; Dwiki, Sendy; Abfertiawan, M Sonny; Badhurahman, Abie; Gunawan, Firman; Butarbutar, Lionie C (2022) Modelling of Acid Mine Drainage Treatment Development for Mine Closure (Case Study ON2 Area, Lati Mine Operation, Berau Coal), Proceeding of International Symposium of Earth Science and Technology 2022, Kyushu University, Fukuoka, Japan

Setyowati, L.D, Suharini E. (2011) DAS Garang Hulu: Tata Air, Erosi dan Konservasi, Semarang. Widya Karya.

Swastika, A.E. (2013) Evaluasi Sistem Pengolahan Pasif (Open Limestone Channel dan Aerobic Wetland) untuk Penanganan Air Asam Tambang (Studi Kasus PT Berau Coal. Bandung): Institut Teknologi Bandung. Master Thesis.

Tuheteru, E.J. (2021) Pengembangan Model Pembentukan Danau Pascatambang pada Penambangan Batubara di Wilayah Tropis. Bandung: Institut Teknologi Bandung.

Column Adsorption Experiments for the Removal of Arsenic and Fluoride Ions in Mine Drainage using Adsorbents

Seong-Sook Park[1], Kung-Won Choi[2], Chan-Ung Kang[3], Joon-Hak Lee[4], Mi-Sun Park[5], Sun-Joon Kim[6], Ga-Hyeon Lee[7]

[1]*Department of Earth Resources and Environmental Engineering, Hanyang University, Wangsimni-ro 222, Seongdong-gu, Seoul, 04763, Republic of Korea, pss2907@hanyang.ac.kr, ORCID 0000-0001-6934-3704*

[2]*Department of Earth Resources and Environmental Engineering, Hanyang University, Wangsimni-ro 222, Seongdong-gu, Seoul, 04763, Republic of Korea, kung@hanyang.ac.kr*

[3]*Korea Institute of Geoscience and Mineral Resources, Gwahak-ro 124, Yuseong-gu, Daejeon, 34132, Republic of Korea, cukang1001@kigam.re.kr*

[4]*Korea Mine Rehabilitation and Mineral Resources Corporation, Hyeoksin-ro 199, Wonju, Gangwon-do, 26464, Republic of Korea, jun292@komir.or.kr*

[5]*Korea Mine Rehabilitation and Mineral Resources Corporation, Hyeoksin-ro 199, Wonju, Gangwon-do, 26464, Republic of Korea, mspark@komir.or.kr*

[6]*Department of Earth Resources and Environmental Engineering, Hanyang University, Wangsimni-ro 222, Seongdong-gu, Seoul, 04763, Republic of Korea, nnsjkim@hanyang.ac.kr*

[7]*Department of Earth Resources and Environmental Engineering, Hanyang University, Wangsimni-ro 222, Seongdong-gu, Seoul, 04763, Republic of Korea, dlrkgus1122@hanyang.ac.kr*

Abstract

Alum sludge-based adsorbent (ASBA) and granular ferric hydroxide (GFH) were applied in mine drainage and synthetic solutions to investigate the adsorption efficiencies of arsenate (As(V)) and fluoride (F). Whereas the adsorption capacity of ASBA for F decreased rapidly after 513–761 bed volumes (BVs), As(V) could be treated for 930–1,145 BVs. The higher concentration of F than As(V) in the influent may be one of the factors that shortened the breakthrough for F. As(V) for GFH was maintained below 50 μg L^{-1} for 8,212 BVs. These adsorbents could be used to remove As(V) and F under field conditions.

Keywords: Adsorption, arsenate, fluoride, mine drainage, alum sludge-based adsorbent

Introduction

that causes death as well as peripheral neuropathy and skin cancer if the body is exposed to inorganic arsenic for a long time (Jomova et al. 2011). Also, it has been reported that an excessive supply of F in the body results in F deposition, neurological problems, and immune system disorders (Streat et al. 2008; Kim et al. 2013).

In general, the geological features of the area are closely related to the pollutants dissolved in mine drainage. According to Nicolli et al. (2008), F is mainly found in groundwater at high concentrations in granite-rich areas and frequently occurs with arsenic in an alkaline environment. The geology of the Suri (Sujung) abandoned metal mine in the Republic of Korea is a location where biotite granite penetrated at the end of the Cretaceous period along the Ordovician limestone layer in the late Paleozoic era. As(V) and F are present at an average concentration of 79.5 μg L^{-1} and 3.26 mg L^{-1} in alkaline mine water discharged from the waste metal mine, exceeding 50 μg L^{-1} and 3 mg L^{-1} as the maximum contamination level (MCL). Therefore, As(V) and F above a specific concentration flowing out of this abandoned mine area must be removed for the conservation of the aquatic ecosystem and the health of residents living in nearby areas.

The purpose of this study was to investigate the adsorption efficiencies of As(V) and F in abandoned metal mine drainage and synthetic solutions using ASBA produced by wastewater treatment facilities in the Republic of Korea (KOMIR 2021) and

GFH by a cost-saving and easy-to-manage adsorption treatment technique (MIRECO 2017; Kumar et al. 2020). Following X-ray diffraction (XRD), wavelength dispersive X-ray fluorescence (WD-XRF), and extreme high resolution scanning electron microscope (FE-SEM) observations, the crystalline structure and mineralogical composition of ASBA and GFH were examined. Also, laboratory-scale column experiments for 503 days were conducted on ASBA and GFH using mine drainage and synthetic solutions with dissolved As(V) and F.

Materials and methods

Two alum-based adsorbents (ASBA-3 and ASBA-G) of different sizes and shapes and granular ferric hydroxide (GFH) were used in the experiment. ASBA was prepared by the following procedure using sludge obtained from the sedimentation tank of the water treatment facilities: water treatment sludge, water, and dissociation reagents were put into a hydrothermal synthesizer in a certain amount, stirred at 100 rpm under 100 °C control, and the reaction was carried out for 1 d and left for 2 d. Thereafter, the reactant obtained by washing several times with distilled water until the pH of the filtrate became neutral was dried until the moisture content was less than 5 wt.%. An amorphous specimen of 0.2–2.0 mm was selected from the produced dry materials, placed in an electric furnace under air supply conditions, and thermally treated at 500 °C for 1 h to prepare ASBA-G. ASBA-3 was prepared by mixing it properly, injecting it into a mold, shaping it into a sphere, and being thermally treated. GFH purchased and used GEH102 products from GEH Wasserchemie GmbH & Co. KG in Germany. The particle diameter of GFH was 0.2–2.0 mm, and it was sealed to preserve moisture on the surface of the adsorbent and stored in a darkened place.

By using XRD (D8 ADVANCE, Bruker, Germany) and WD-XRF (ZSA PrimusIV, Rigaku, Japan), the mineral properties and constituent elements of the adsorbent samples were examined. Samples were prepared in homogeneous powder using an agate mortar and 100 mesh standards for those analyses. A Brunauer-Emmett-Teller (BET) surface area analyzer (3Flex, Micromeritics, USA) was used to determine the surface area of adsorbents. Also, the pore structure and size distribution of the adsorbent were examined by FE-SEM (Verios G4 UC, FEI, USA). To remove moisture and other impurities present on the adsorbent surface before specific surface area (SSA) measurement, N2 gas was adsorbed and analyzed in an analysis bath of -195.85 °C for 12 h under a nitrogen atmosphere (Badruzaman et al. 2004), and a specimen was observed with a silver paste (Dotite D500) to obtain a high-resolution surface image. The solid addition method (Oladoja and Aliu 2009) was used to determine the point of zero charge (pHPZC) of adsorbent samples.

Laboratory-scale column experiments were performed for 503 days using synthetic solutions containing As(V) and F and mine drainage collected from the waste metal mine Suri (Sujung). Each volume of water was injected through a peristaltic pump at flow rates of 0.28, 0.1665, and 0.0535 mL min^{-1}. Empty bed contact time (EBCT) was set to 88.2 (ASBA-3, ASBA-G, and GFH), 150.9 (ASBA-G2), and 469.7 (ASBA-G3) min, respectively. In the case of ASBA-3, ASBA-G, and GFH, it was treated with mine drainage up to 5,502 BVs, and synthetic solutions spiked with As(V) and F after 5,502 BVs were used because of the difficulties of collecting water samples from this mine site. Also, ASBA-2 and ASBA-3 used synthetic solutions after 2,128 and 683 BVs, respectively. Synthetic solutions simulating mine drainage contaminated with As(V) and F were prepared by diluting a standard solution, in which disodium hydrogen arsenate heptahydrate (Na2HAsO4·7H2O, Sigma-Aldrich, USA) and sodium fluoride (NaF, 99.9%, Sigma-Aldrich, USA) were dissolved at a concentration of 1,000 mg L-1 in deionized water. The prepared standard solution was used after being refrigerated. 0.1 N of hydrochloric acid (HCl, DAEJUNG, Republic of Korea) and sodium hydroxide (NaOH, DAEJUNG, Republic of Korea) were used for pH titration of the experimental solution. They were set up for a bottom-up flow.

Results and discussion

Characteristics of ASBA and GFH

As a result of FE-SEM analysis, ASBA had a bumpy shape, while GFH showed a shape in which small grains were attached to the surface (Figure 1). ASBA was mostly composed of Al_2O_3 (57.32%) and SiO_2 (18.21%), while GFH was most composed of Fe2O3 (89.58%) through WD-XRF analysis (Table 1). GFH and ASBA-G (0.2–2 mm) were granular, and ASBA-3 (3 mm) was spherical. As a result of comparative analysis of the XRD pattern with ICDD's database, ASBA displayed various diffraction peaks, and the main crystal phases were quartz, muscovite, albite, and orthoclase. Iron oxide and akaganeite were detected in GFH as a diffraction pattern close to amorphous (Figure 2). As a result of BET analysis, the SSAs of powdered ASBA-3, ASBA-G, and GFH were 136.34, 126.07, and 257.02 m^2g^{-1}, respectively. According to IUPAC classification, it was classified as IV(a) type adsorption and desorption isotherms, which indicated that mesopores were developed in adsorbents and caused high SSA, porosity, and capillary condensation (Figure 3; Thommes et al. 2015).

As a result of measuring the zero charge point of the adsorbent surface using the solid addition method, ASBA-3 and ASBA-G had pHPZC at value of 5.25 and 5.29, respectively, while GFH had zero charge on the particle surface at a pH of 6.72 (Figure 4). Therefore, ASBA is expected to be negatively charged in a neutral aqueous solution, so it is estimated that the adsorption of As(V) is slightly lower than that of GFH. Meanwhile, GFH has a positive charge on the surface of an acidic or neutral aqueous solution, so it is easy to adsorb As(V) ($H_2AsO_4^-$, $HAsO_4^{2-}$) present in the form of anions.

Table 1 *Major element composition of adsorbents analyzed by WD-XRF.*

Composition (wt.%)	ASBA	GFH
Al_2O_3	57.32	0.69
SiO_2	18.21	0.31
P_2O_5	5.58	0.02
Fe_2O_3	2.94	89.58
MnO	1.26	–
Cr_2O_3	0.01	0.87
CO2	11.53	5.77
Cl	0.05	2.33

As(V) and F treatment efficiencies in laboratory-scale column experiments

To evaluate the adsorption efficiencies of these adsorbents, laboratory-scale column experiments were conducted by changing from mine drainage to synthetic solutions injected into the column at 79.5 μg L^{-1} and 3.26 mg L^{-1} using ASBA and GFH. When mine drainage and synthetic solutions were passed through these adsorbents, breakthrough for As(V) occurred after 1,145 (ASBA-3), 930 (ASBA-G), 949 (ASBA-G2), 1,066 (ASBA-G3), and 8,212 (GFH) BVs granules were packed. As(V) concentration was maintained below 10 μg L^{-1} until GFH reacted with 8,212 BVs (Figure 5). It represented that As(V) had a high affinity for iron compounds, which were the main ingredient in GFH. As the EBCT became shorter, the contact time between As(V) and the adsorption site decreased, indicating that the time to adsorb and remove As(V) below the MCL (50 μg L^{-1}) of discharged water was

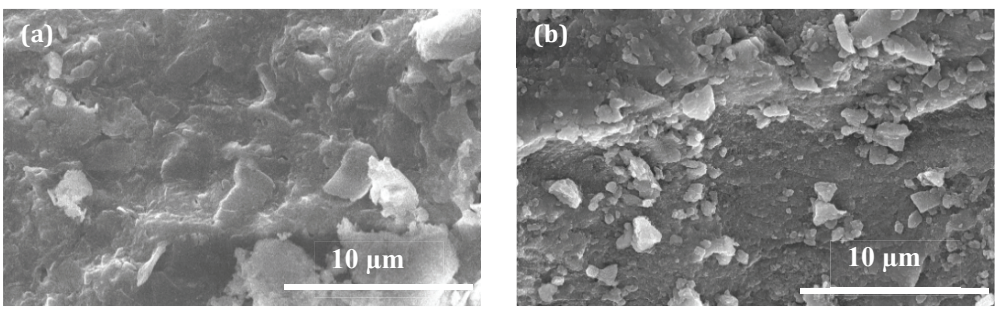


Figure 1 *FE-SEM images of adsorbents (a) ASBA and (b) GFH.*

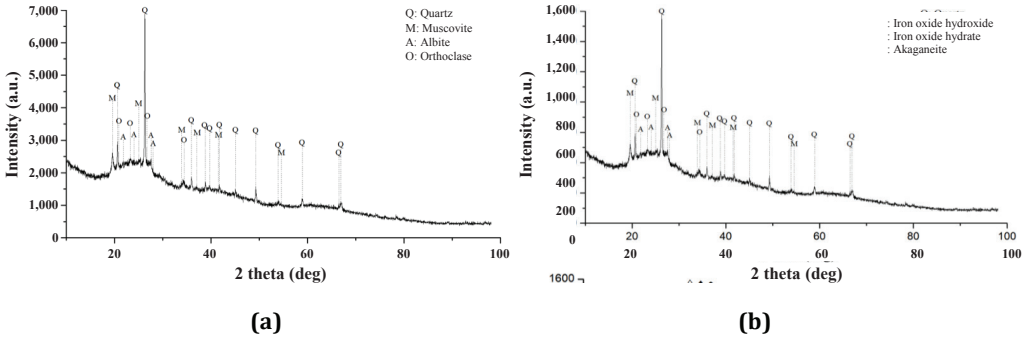


Figure 2 XRD patterns of adsorbents; (a) ASBA and (b) GFH.

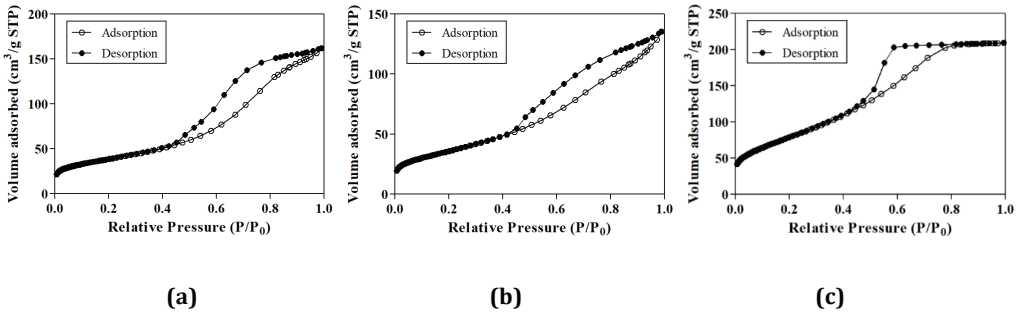


Figure 3 N_2 adsorption-desorption isotherm of adsorbents; (a) ASBA-3, (b) ASBA-G, and (c) GFH.

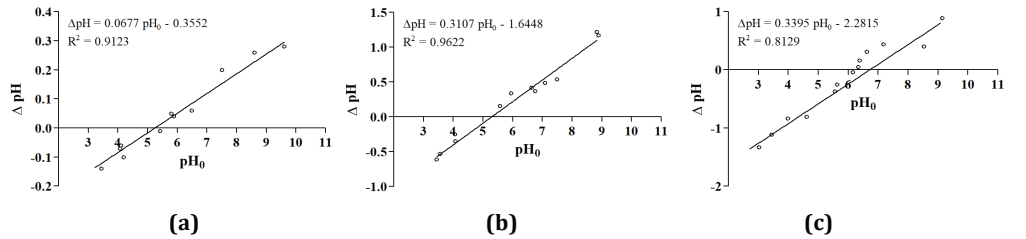


Figure 4 Determination of pHpzc (point of zero charge) of adsorbents; (a) ASBA-3, (b) ASBA-G, and (c) GFH.

insufficient. ASBA-G reached the MCL earlier than ASBA-3. However, ASBA-3 showed a higher As(V) concentration in effluent than ASBA-G, indicating that ASBA-G had a better adsorption capacity than ASBA-3 (Figure 6).

In the case of F in ASBA-G2 and ASBA-G3, the F concentration of effluent increased faster than that of As(V). Thus, breakthrough occurred after 513 (ASBA-G2) and 761 (ASBA-G3) BVs, respectively (Figure 7). In the case of As(V), the breakthrough was reached after treatment with 930 to 1,145 BVs. Meanwhile, the adsorption capacity for F decreased rapidly after treatment with 513 to 761 BVs and the breakthrough then happened. One of the causes that may have reduced the breakthrough time for F was the higher concentration of F than As(V) in the influent, and then F was adsorbed more in ASBA-G2 and ASBA-G3 granules. In addition, because F and hydroxide ions were competitively adsorbed under a pH condition

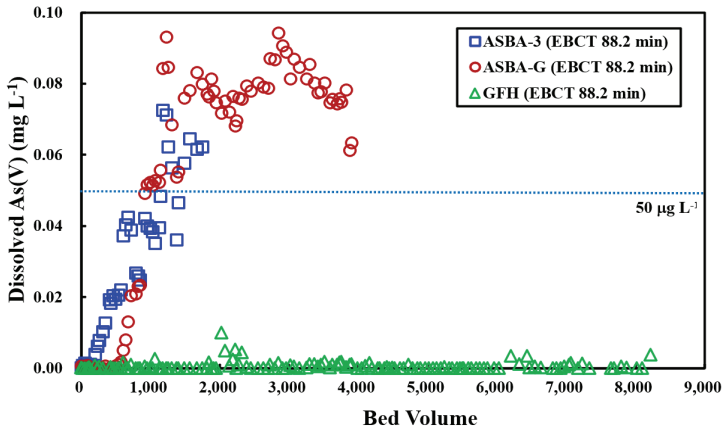


Figure 5 *Changes in As(V) concentration of column effluent at EBCT 88.2 min of adsorbents.*

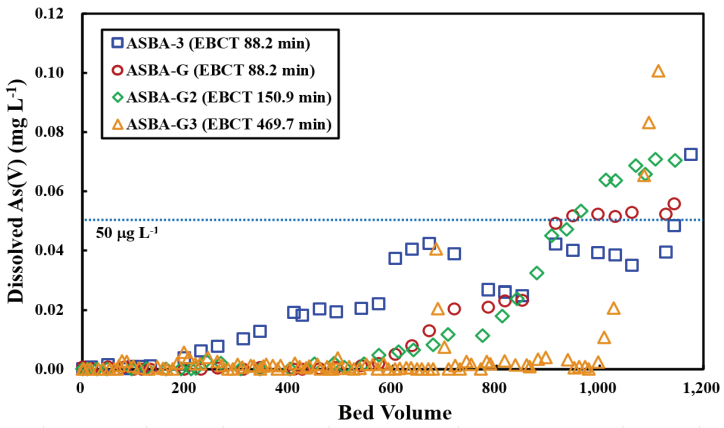


Figure 6 *Changes in As(V) concentration of column effluent according to EBCT of ASBA.*

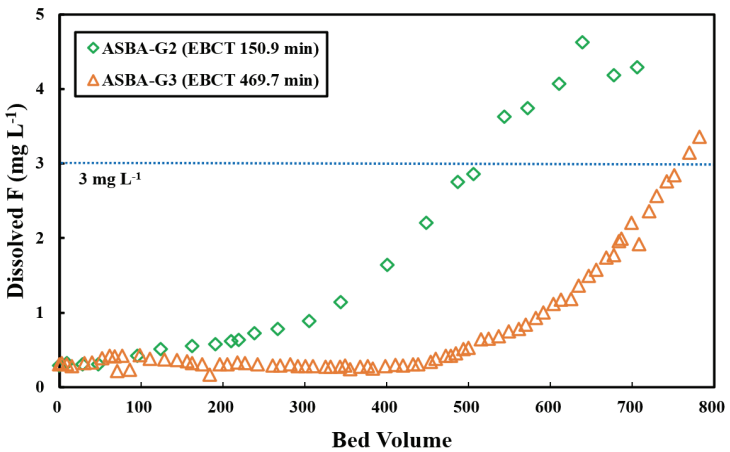


Figure 7 *Changes in F concentration of column effluent according to EBCT of ASBA.*

close to neutral, the adsorption amount of F would have been relatively reduced (Streat et al. 2008). Therefore, ASBA and GFH have the potential to be used under field conditions for the remediation of As(V) and F.

Conclusions

Laboratory-scale column experiments were executed on ASBA and GFH using mine drainage and synthetic solutions for a duration of 503 days. GFH removed As(V) from 79.5 μg L-1 to 10 μg L^{-1} while processing 8,212 BVs. Also, ASBA treated 930–1,145 BVs to eliminate As(V) and 513–761 BVs for the removal of F. Thus, it was found that the length of the EBCT and the breakthrough BV had a proportional relationship. Because the F concentration in the influent was higher than that of As(V), the breakthrough for F was shorter than that of As(V). Therefore, at field sites contaminated with As(V) and F, these adsorbents may contribute to the removal of As(V) and F.

Acknowledgements

This work was supported by R&D Project of the Korea Mine Rehabilitation and Mineral Resources Corporation (KOMIR) in 2020–2021 and 2022–2023, Republic of Korea.

References

Badruzzaman M, Westerhoff P, Knappe DR (2004) Intraparticle diffusion and adsorption of arsenate onto granular ferric hydroxide (GFH). Water Res 38(18):4002–4012. https://doi.org/10.1016/j/watres. 2004.07.007

Jomova K, Jenisova Z, Feszterova M, Baros S, Liska J, Hudecova D, Rhodes CJ, Valko M (2011) Arsenic: toxicity, oxidative stress and human disease. J Appl Toxicol 31(2):95–107. https://doi.org/10.1002/jat.1649

Kim JH, Song YM, Kim SB (2013) Fluoride sorption property of lanthanum hydroxide. J Korean Soc Environ Eng 32(7): 714–721 (in Korean)

KOMIR (2021) Development of site-specific sorption processes to remove heavy metals in low-flow mine drainage. Technology Report 2021-041, Korea Mine Rehabilitation and Mineral Resources Corporation (KOMIR), Republic of Korea (in Korean)

Kumar R, Kang CU, Mohan D, Khan MA, Lee JH, Lee SS, Jeon BH (2020) Waste sludge derived adsorbents for arsenate removal from water. Chemosphere 239:124–832. https://doi.org/10.1016/j.chemosphere.2019.124832

MIRECO (2017) Media evaluation and on-site demonstration to remove arsenic adsorption in mine drainage, Technology Report, Korea Mine Reclamation Corporation (MIRECO), Republic of Korea (in Korean)

Nicolli HB, Tujchneider OC, Paris MDC, Blanco MDC, Barros AJ (2008) Sources and mobility of arsenic in groundwater from centre-north plain of Santa Fe Province, Argentina. In: Proceedings of the 2nd International congress: arsenic in the environment: arsenic from nature to humans, p 21–23

Oladoja NA, Aliu YD (2009) Snail shell as coagulant aid in the alum precipitation of malachite green from aqua system. J Hazard Mater 164(2-3):1496–1502. https://doi.org/10.1016/j.jhazmat.2008.09.114

Streat M, Hellgardt K, Newton NLR (2008) Hydrous ferric oxide as an adsorbent in water treatment: Part 3: Batch and mini-column adsorption of arsenic, phosphorous, fluorine and cadmium ions. Process safety and environmental protection 86(1):21–30. https://doi.org/10.1016/j.psep.2007.10.009

Thommes M, Kaneko K, Neimark AV, Olivier JP, Rodriguez-Reinoso F, Rouquerol J, Sing KS (2015) Physisorption of gases, with special reference to the evaluation of surface area and pore size distribution IUPAC technical report). Pure Appl Chem 87(9–10):1051–1069. https://doi.org/10.1515/pac-2014–1117

The Contribution of Major Historical Orefields to Coastal Trace Metal(loid) Fluxes in North-East England

Alex L. Riley[1], Patrizia Onnis[2], Catherine J. Gandy[3], Chimaobim V. Kanu1, Chinedu V. Umeobika[1], James Cameron[1], Ian T. Burke[4], Karen A. Hudson-Edwards[2], Adam P. Jarvis[3], William M. Mayes[1]

[1]*School of Environmental Sciences, University of Hull, Kingston upon Hull, UK, a.l.riley@hull.ac.uk*

[2]*Environment and Sustainability Institute and Camborne School of Mines, University of Exeter, Penryn, UK*

[3]*School of Engineering, Newcastle University, Newcastle upon Tyne, UK*

[4]*School of Earth and Environment, University of Leeds, Leeds, UK*

Abstract

Mine waters and tailings are key inputs to riverine metal(loid) transport to the coast. However, coastal areas also face local contaminant pressures, e.g. active industries and abandoned landfill sites. Annual riverine metal(loid) flux data were assessed alongside respective fluxes from coastal industries and legacy landfills along the North-East England coastline to quantify relative contaminant contribution. The majority of each contaminant flux (56-97%) entered the sea via riverine transport from inland orefields. However, coastal landfills contributed non-trivial fluxes of some contaminants (<93 t/yr Pb, <38 t/yr Ni, <17 t/yr As), indicating that inland management alone may not sufficiently remediate coastal waters.

Keywords: Coastal Erosion, Legacy Waste, Abandoned Landfill, Contaminant Flux, Source Apportionment, Mining Waste.

Introduction

The environment of the United Kingdom (UK) contains an abundance of mining wastes deposited prior to contemporary waste management practices (Johnston *et al*., 2008). Such 'legacy' mining wastes are distributed predominantly in former orefields, with recent estimates suggesting 52800 ha of mine spoil deposited in the UK (Riley *et al*., 2021). Of particular concern with legacy mine deposits is the potential release of metal(loid) contaminants (e.g. Zn, Pb, As) due to erosion and leaching (e.g. Singer *et al*., 2020), which alongside direct mine water discharges, are known to enter coastal waters via riverine transport (Mayes *et al*., 2013).

In addition to inland deposits, mining wastes are also commonly encountered in coastal areas (covering ≈4500 ha), with coal spoils being the third most prevalent waste type deposited in these regions (Riley *et al*., 2022). Such coastal deposits are also subject to atmospheric weathering and associated contaminant release, but coastal erosion and tidal flooding, which are both predicted to increase in severity and frequency with continued climate change (Toimil *et al*., 2020; Vitousek *et al*., 2017), pose additional risks at these sites (Riley *et al*., 2022). Further to mine-related sources, it is important to consider sources of contamination to the coastal environment that are not mining-related but may release a similar suite of metal(loid)s. Examples of which are legacy metallurgical and industrial waste deposits (covering ≈1000 and ≈3500 ha of coastal land in the UK, respectively; Riley *et al*., 2022) and long sea outfalls from contemporary industrial activity.

Given that multiple sources of potential contaminants enter coastal waters (i.e., transported from inland or originating within the coastal zone itself), it is critical to properly understand the relative importance of each source in order to inform proper environmental management and protect

coastal water quality. Contaminant flux assessments are an effective tool in apportioning the relative contribution of these different sources. Indeed, previous national assessments of contaminant flux from abandoned mines in England and Wales (e.g. Mayes *et al*., 2010; 2013) have been invaluable for understanding the scope of impacts from legacy mine wastes. Therefore, this paper will assess and incorporate the relative diffuse metal(loid) fluxes from coastal mine spoil deposits, in addition to other coastal legacy waste deposits, and contemporary riverine and coastal point sources. This will provide detailed information on contaminant sources at local and regional scales to aid in management decision-making.

Methods

Geographical extent

The coastline of North-East England, between the Rivers Coquet and Tees was used as the geographical extent of this assessment. This coastline was selected as its rivers not only drain the Pb-Zn orefield of the North Pennines and the Great Northern Coalfield, but is also an industrial and populated coastline with a typical distribution of coastal waste deposits (Riley *et al*., 2022). Two flux assessments were performed for the area, the first being an assessment of riverine flux from inland sources and the second an assessment of flux from coastal sources, as detailed below.

Riverine metal(loid) flux

The riverine flux of select metal(loid)s are routinely monitored at the tidal limits of major rivers in the UK by the Environment Agency as part of the OSPAR Commission framework. As such, three years of flux data were retrieved and summarised to calculate the average annual flux of Zn, Cu, Pb, Cd, Cr, Ni, and As at the tidal extents of the Rivers Coquet, Wansbeck, Tyne, Wear, and Tees (ODIMS, 2023). Note that data for the River Blyth were not available for this analysis.

Coastal metal(loid) flux

For the purpose of this research, two sources of potential contamination were considered to represent the coastal sources of metal(loids); the point-source flux from coastally-located active industries, and the diffuse inputs from eroding coastal legacy landfill sites. Point source inputs were also retrieved from the Environment Agency OSPAR data for the aforementioned metal(loid)s of interest. These sites represented 28 individual point inputs within the region of interest, which were a mix of sewage treatment work effluents and industrial outfalls. Flux data were again averaged to calculate average annual flux for each contaminant of interest.

Coastal legacy landfill sites (identified as containing either MSW, coal mine spoil, or iron and steel slag) within 250 m of the coastline were extracted from the spatial databases generated by Riley *et al*. (2020, 2021, 2022), and used to calculate diffuse inputs via two processes: release of contaminated sediments by coastal erosion, and metal(loid) release through leachate formation.

To estimate the annual release of sediments by erosion, 5 m resolution LiDAR raster data (dating from 2019 and 2009) were used to indicate the position of the coastline at each point in time (Digimap, 2023). Within ArcMap 10.8 GIS software, these data were then clipped to the spatial extent of each legacy landfill. Using the surface volume tool (as per Riley *et al*., 2020), the volume of each landfill site was calculated for each time point – the difference between which being an estimate of the volume of material eroded over ten years. This value was divided by 10 to approximate annual material flux in m^3 per year. To convert this to mass, reported bulk density values of 312 and 1,687 kg/m^3 were used for municipal solid waste (MSW) and coal spoil (the two waste types within eroding landfills in this region), respectively (Palanivel and Sulaiman, 2014; Fityus *et al*., 2008). Unpublished data of mean elemental composition (collected from a range of coastal landfill sites around the UK) were then used to estimate the annual flux of specific contaminants via coastal erosion.

To calculate the potential volume of landfill leachate formed, the annual average rainfall (mm converted to m) across the study area (Met Office HadUK-Grid; Hollis *et al*., 2022) was first calculated. This was multiplied by the known area of each landfill (m^2, from Riley *et al*., 2022) to give a theoretical maximum

leachate volume (m^3), and then multiplied by a runoff coefficient of 0.5 to represent the portion of rainfall which typically infiltrates landfill soils (e.g. Zafar and Alappat, 2011). This analysis was repeated for each of the 189 landfill deposits in the study region. Unpublished data of leaching rates of As, Cd, Cr, Cu, Hg, Ni, Pb, and Zn from samples of these wastes under freshwater and seawater conditions (generated using standard method BS EN 12457-2; NBS, 2002) were used in conjunction with the estimated leachate volumes to model leachate composition and the annual load of each metal(loid) released from each legacy landfill site.

Results and Discussion

In addition to the five major rivers entering the North Sea in the study region, a total of 10 industrial point discharges were recorded and 190 legacy landfill sites (within 250 m of the coastline). The total landfill area covered 1,664 ha, of which 1,109 ha consisted of MSW, 449 ha of coal mining spoil, and 106 ha of iron and steel slag. Of the legacy landfill sites, 20 were determined to be eroding, of which 7 contained coal spoil and the remainder MSW.

Modelled annual flux estimates indicated that substantial total loads of trace metal(loids) entered the North Sea in this region from the combination of these sources (Table 1). For the majority of metal(loids), riverine transport was the dominant contributor to the coastal zone, though the physical release of contaminated sediments by coastal erosion was also a high contributor. High fluxes were attributed to coastal coil spoil deposits, the leachates from which contributed far higher loads than leachates from other waste types. Interestingly, the total flux of Pb and Zn, commonly associated with mining wastes, was higher from eroded MSW (<22,108 and <51,347 kg/yr, respectively), though this is likely due to the higher number of eroding MSW deposits in the region.

When considering the relative flux of specific elements, it becomes possible to infer key sources and pathways to coastal waters, and the geographical regions in which higher fluxes were observed. Of particular concern due to its toxicity, it was determined that the majority of As flux to coastal waters originated within the coastal zone (11,495 kg/yr) rather than riverine transport from inland

Table 1 *Modelled annual high/low estimates of metal(loid) flux (kg/yr) from riverine sources, coastal point sources, and coastal legacy waste sites (via leachate formation and erosion)*

Source		As	Cd	Cr	Cu	Ni	Pb	Zn
Riverine Transport	Low	1,702	507	7,458	23,212	6,741	66,324	192,653
	High	5,016	602	7,929	23,214	23,093	66,354	193,164
Coastal Point Sources	Low	42.0	14.0	610	4,289	370	1,892	10,371
	High	121	29	625	4,289	729	1,893	10,374
MSW Leachate	Low	14.3	1.4	17.9	46.6	17.9	3.6	151
	High	14.3	1.6	28.7	50.2	28.7	7.2	215
Coal Spoil Leachate	Low	0.2	0.1	0.1	0.3	0.5	0.1	7.3
	High	3,743	63.5	1,037	2,043	8,031	387	12,971
Iron & Steel Slag Leachate	Low	0.2	0.0	0.2	0.2	0.2	1.7	0.3
	High	0.2	0.0	1.0	3.4	0.7	1.7	15.7
MSW Erosion	Low	205	4.0	694	363	435	533	2,112
	High	2,000	411	2,594	14,720	3,203	22,108	51,347
Coal Spoil Erosion	Low	594	0.0	869	866	495	332	948
	High	5,616	54	3,012	5,562	2,770	2,747	13,799
Total	Low	2,558	527	9,649	28,777	8,060	69,086	206,243
	High	16,511	1,161	15,227	49,882	37,855	93,498	281,886

sources (5,016 kg/yr; Fig. 1). Approximately 31% of this coastal flux (3,640 kg/yr) was via the formation of landfill leachates, which represent a diffuse aqueous source. Geographically, the more dominant fluxes of As were located between the Tyne and Tees, with a typically higher flux from all sources between these rivers. The area between the Wear and Tees was a particular hotspot for As release via coastal erosion (1,446 kg/yr), likely due to the prominence of eroding coal spoil deposits in this region (representing 6 of the 9 eroding landfills on that stretch of coastline).

Contrary to As, the majority of modelled Ni flux was attributed to riverine sources (23,093 kg/yr vs. 11,059 kg/yr), with the River Tyne being the highest single contributor (9,615 kg/yr; Fig. 2). Nevertheless, coastal sources still contributed a non-trivial flux of Ni to the environment (11,059 kg/yr), the majority of which via the formation of aqueous leachates, albeit in a diffuse manner across multiple legacy waste sites. Whilst minor in comparison, a reasonable flux of Ni from contemporary point discharges (<729 kg/yr) was observed (Fig. 2).

The relative flux assessment of Pb (Fig. 3) revealed strikingly different patterns than As or Ni, with the vast majority (85%) of the total flux originating from riverine sources. Coastal Pb flux was dominated by the erosion of contaminated sediments with a relatively low contribution from landfill leachates. Given the low solubility of Pb in solution (Gao and Bradshaw, 1995), it is perhaps unsurprising that modelled leachates contributed little towards Pb flux. However, despite its low solubility, the high flux of Pb from aqueous sources (especially rivers) illustrates the widespread scale of the issue of Pb transport from historical orefields and the potential impacts this may be having in coastal regions.

Conclusions

It is apparent that substantial fluxes of potentially problematic metal(loids) are entering coastal waters along the North-East coast of England, but it is only through relative flux assessments, such as this, where the relative contributions of different sources may be determined. Through consideration of coastal sources of metal(loid) flux, such

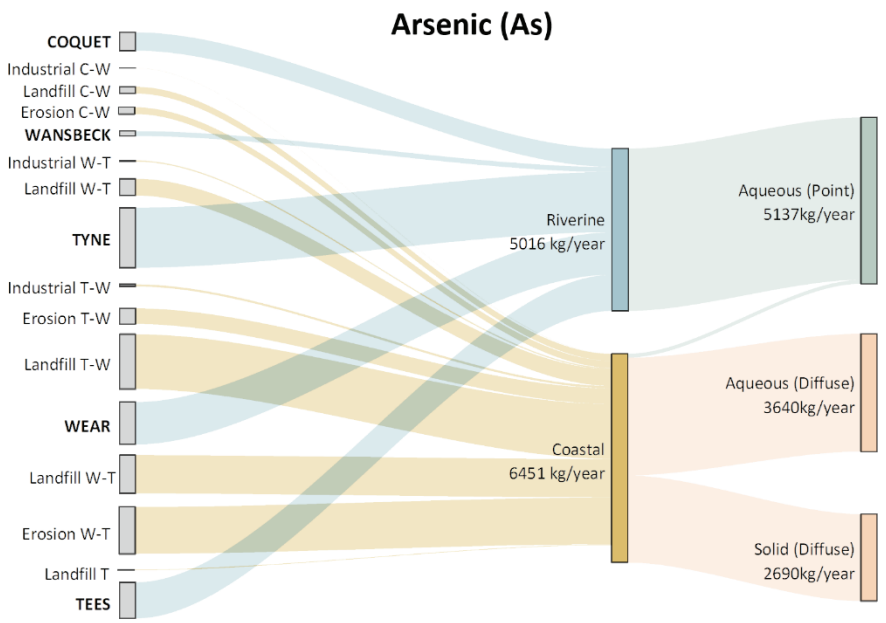


Figure 1 *Relative annual flux of As (kg/yr) from riverine and coastal sources ("industrial" = industrial discharges, "landfill" = landfill leachates, "erosion" = eroded material, suffixes relate to the source position between rivers, e.g. "C-W" = Coquet – Wansbeck). Major rivers are listed from North to South (top to bottom).*

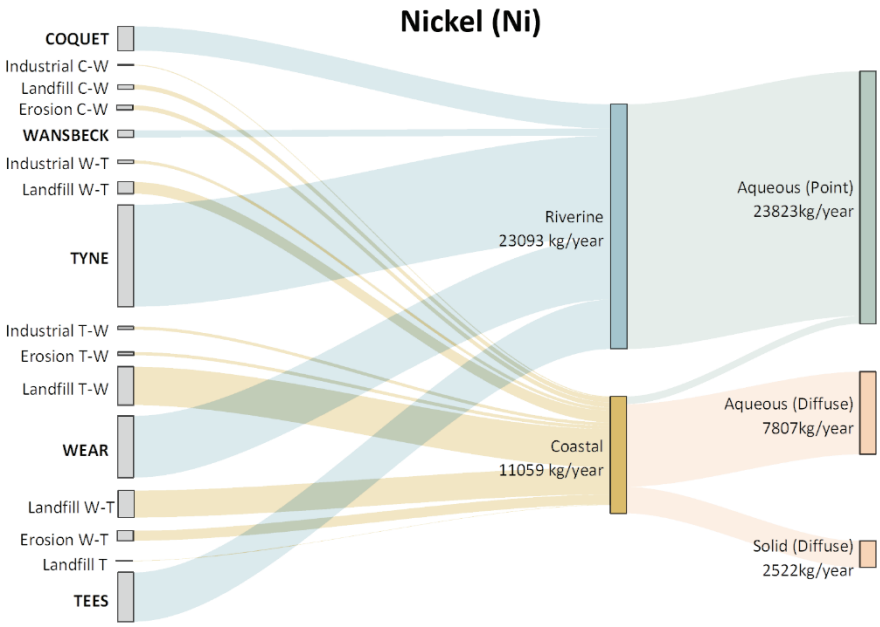


Figure 2 Relative annual flux of Ni (kg/yr) from riverine and coastal sources. Major rivers are listed from North to South (top to bottom).

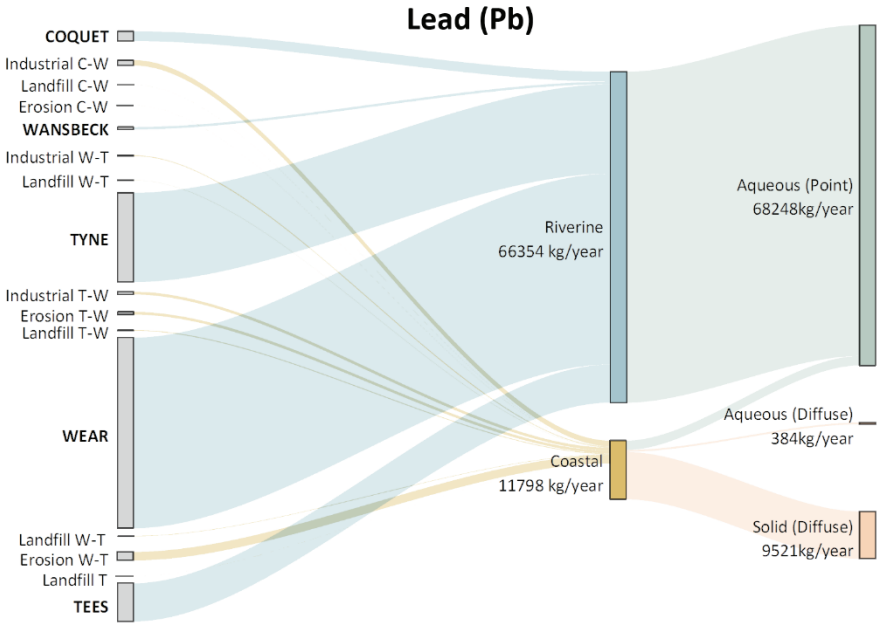


Figure 3 Relative annual flux of Pb (kg/yr) from riverine and coastal sources. Major rivers are listed from North to South (top to bottom).

as contemporary industrial discharges and legacy waste landfills (including mining wastes), alongside traditional riverine flux assessments, it is possible to determine the contribution of mining wastes to coastal fluxes in a holistic manner.

The influence of major historical orefields to coastal metal(loid) fluxes (via riverine transport) varied depending upon the specific metal(loid) in question. For some, e.g. Pb and Ni, it was determined that inland sources were likely the main contributor to coastal fluxes, whereas for As, the contribution of coastal sources was more prominent. Further to this, the source and transportation pathways of contaminants (i.e. point or diffuse, aqueous or solid) were assessed, indicating that while aqueous point sources (e.g. rivers, industrial discharges) are major contributors, diffuse aqueous and solid sources (i.e. landfill leachates and eroded material) should not be overlooked. Findings such as these are critical for ensuring good coastal water quality, as effective management will depend on appropriately addressing the exact sources of specific contaminants. Whilst contemporary point discharges may be easier to control, diffuse contamination from coastal landfills and riverine transport of contaminants from historical orefields may require landscape-scale management, which brings additional challenges.

Acknowledgements

The authors would like to thank the Natural Environment Research Council (NERC), who funded this research under grant numbers NE/T003022/1, NE/T003286/1, and NE/T002824/1 (Legacy wastes in the coastal zone: Environmental risks and management futures).

References

Digimap (2023) Lidar Data Download [online] Available at https://digimap.edina.ac.uk/lidar

Fityus S, Hancock G, Wells T (2008) Geotechnical characteristics of coal mine spoil. Australian Geomechanics 43(3), 13-22.

Gao Y, Bradshaw AD (1995) The containment of toxic wastes: II. Metal movement in leachate and drainage at Parc lead-zinc mine, North Wales. Environ Pollut 90(3), 379-382.

Hollis D, McCarthy M, Kendon M, Legg T (2022) HadUK-Grid Gridded Climate Observations on a 5km grid over the UK, v1.0.3 (1862-2020) [online] Available at https://cata logue.ceda.ac.uk/uuid/aeb4ca481d634ec597831282c3baed32

Johnston D, Potter H, Jones C, Rolley S, Watson I, Pritchard J (2008) Abandoned mines and the water environment. Science Project SC030136-41. Environment Agency, Bristol.

Mayes WM, Potter HAB, Jarvis AP (2010) Inventory of aquatic contaminant flux arising from historical metal mining in England and Wales. Sci Tot Environ 408(17):3576-3583.

Mayes WM, Potter, HAB, Jarvis AP (2013) Riverine Flux of Metals from Historically Mined Orefields in England and Wales. Water Air Soil Poll 224: 1425.

NBS (2002) BS EN 12457-2:2002 Characterisation of waste - Leaching - Compliance test for leaching of granular waste materials and sludges. One stage batch test at a liquid to solid ratio of 10 l/kg for materials with particle size below 4 mm (without or with size reduction), British Standards Institution, London.

ODIMS (2023) OSPAR Data & Information Management System [online] Available at https://odims.ospar.org/en/

Palanivel T, Sulaiman H (2014) Generation and Composition of Municipal Solid Waste (MSW) in Muscat, Sultanate of Oman. APCBEE Procedia 10, 96-102.

Riley AL, MacDonald JM, Burke IT, Renforth P, Jarvis AP, Hudson-Edwards KA, McKie J, Mayes WM (2020) Legacy iron and steel wastes in the UK: Extent, resource potential, and management futures. J Geochem Explor 219:106630.

Riley AL, Onnis P, Jennings E, Crane RA, Hudson-Edwards KA, Comber SDW, Burke IT, Byrne P, Gandy CJ, Jarvis AP, Mayes WM (2021) A GIS-Based Prioritisation of Coastal Legacy Mine Spoil Deposits in England and Wales for Effective Future Management. Proceedings of International Mine Water Association Conference 2021 p 458-464.

Riley AL, Amezaga J, Burke IT, Byrne P, Cooper N, Crane RA, Comber SDW, Gandy CJ, Hudson-Edwards KA, Jennings E, Lewis E, Lofts S, MacDonald JM, Malcolm H, Mayes WM, Onnis P, Olszewska J, Spears B, Jarvis AP (2022)

Incorporating conceptual site models into national-scale environmental risk assessments for legacy waste in the coastal zone. Front Environ Sci 10:1045482

Singer D, Herndon E, Zemanek L, Cole K, Sanda T, Senko J, Perdrial N (2020) Biogeochemical Controls on the Potential for Long-Term Contaminant Leaching from Soils Developing on Historic Coal Mine Spoil. Soil Systems 5(1):1-24.

Toimil A, Camus P, Losada IJ, Le Cozannet G, Nicholls RJ, Idier D, Maspataud A (2020) Climate change-driven coastal erosion modelling in temperate sandy beaches: Methods and uncertainty treatment. Earth-Sci Rev 202:103110.

Vitousek S, Barnard PL, Fletcher CH, Frazer N, Erikson L, Storlazzi CD (2017) Doubling of coastal flooding frequency within decades due to sea-level rise. Sci Rep-UK, 7:1399.

Zafar M, Alappat BJ (2011) Landfill Surface Runoff and Its Effect on Water Quality on River Yamuna. J Environ Sci Heal A 39(2), 375-384.

Field Trials of Dispersed Alkaline Substrate to Passively Treat Highly Polluted Acid Mine Drainage at two Emblematic Abandoned Mines in Wales

Tobias Stefan Roetting[1],*, Iain Hall[2], Gareth Digges La Touche[2], Louise Siddorn[3], Peter Stanley[3]

[1]*WSP UK Ltd, The Mailbox, Level 2, 100 Wharfside Street, Birmingham, B1 1RT, UK, tobias.roetting@wsp.com*

[2]*WSP UK Ltd, 7 Lochside View, Edinburgh Park, Edinburgh, EH12 9DH, UK*

[3]*Natural Resources Wales, Tŷ Cambria, Newport Rd., Cardiff, CF24 0TP, UK, geowyddor@cyfoethnaturiol-cymru.gov.uk*

Abstract

Dispersed alkaline substrate is a passive treatment technology for sites with high metal concentrations and has been trialled successfully at field pilot-scale at two mine discharges. At the abandoned Cwm Rheidol lead-zinc mining complex, a two-step DAS system operated for over one year, removing Fe, Al, Zn, Pb, Cd and other metals. At Parys Mountain, a volcanogenic massive sulphide deposit which was the world's largest copper mine in the 18th century, a three-step DAS system is removing Fe, Cu, Zn, Al, SO_4 and other contaminants. DAS achieved very high metal removal rates for all contaminants of potential concern.

Keywords: ispersed alkaline substrate, passive mine water treatment, remediation, clogging, passivation

Introduction

Acid mine drainage (AMD) is a major cause of water contamination world-wide. Conventional treatment plants can be expensive to build and operate, and application at remote sites may be impractical. Passive treatment systems, which only require naturally available energy sources and infrequent maintenance, may be an economical option to treat these waters. When used to treat water with high metal concentrations or high acidity loads, they are however prone to loss of permeability and reactivity or may require excessively large land areas. Moreover, the passive removal of high concentrations of divalent metals (e.g., Zn, Mn, Cu, Pb, Ni, Cd) poses major challenges.

Methods and Field Sites

Dispersed Alkaline Substrate

Dispersed alkaline substrate (DAS) is an innovative passive treatment technology that can be implemented at sites with high metal concentrations (Roetting *et al.* 2006, 2008a, 2008b, 2008c). DAS consists of a fine-grained alkaline reagent mixed with a coarse matrix. The fine grain size of the alkaline reagent increases the dissolution rate due to the increased specific reactive surface area and therefore reduces armouring, while the coarse matrix provides a large pore space to store precipitates and retard clogging.

Calcite-DAS provides the main source of alkalinity to neutralise the bulk acidity of the mine drainage by buffering the pH between 6 and 8, efficiently removing trivalent metals such as Fe(III) and Al, but not divalent metals. Removal of divalent metals is achieved in an additional DAS reactor containing magnesium oxide or barium carbonate. MgO hydration and dissolution buffers the pH between 9 and 10. In this pH range, most divalent metals display very low solubility and are readily removed. If BaCO3 is used instead of MgO, the system also removes SO4, and the hardness that was added in the calcite-DAS reactor(s).

In the trials reported here, two different types of wood flakes were mixed with the DAS materials. In some of the reactors,

fresher (mainly ash) wood cuttings were used. In other reactors, pine wood shavings were used.

Cwm Rheidol

The Ystumtuen or Cwm Rheidol mining complex is located 15 km east of Aberystwyth, Ceredigion, and includes the mines of Cwm Rheidol, Ystumtuen (early records dating back to 1698), Penrhiw, Bwlchgwyn and Llwynteifi. The five mines are connected underground, enabling the extensive workings to drain to the Afon Rheidol via adits No. 6 and No. 9, which emerge on the steep valley slopes. Both discharges are acidic and contain elevated concentrations of metals including Zn, Pb and Cd. These discharges are subsequently contributing to the Afon Rheidol, failing European Water Framework Directive (WFD) standards for Zn and Cd for 18 km downstream of the mine to its tidal limit. Adit 6 (discharging at a higher elevation) has a higher flow rate but lower concentrations and a higher pH than Adit 9 (discharging at a lower elevation). The main contaminants in the combined discharge (flow-weighted average during the period 2015 – 2019) in the combined discharge are SO4 (216 mg/L), Zn (20.3 mg/L), Fe (17.8 mg/L), Al (5.5 mg/L), Mn (0.95 mg/L), Pb (0.62 mg/L), Ni (0.28 mg/L), Cu (50 µg/L), Cd (40 µg/L), and the combined pH is approximately 4.1. The average composition of Adit 9 water in the same period is SO4 (824 mg/L), Zn (85.5 mg/L), Fe (126 mg/L), Al (29 mg/L), Mn (4 mg/L), Pb (0.01 mg/L), Ni (1.26 mg/L), Cu (100 µg/L), Cd (120 µg/L), with a pH of 3.0.

A total of four different treatment train configurations were tested at Cwm Rheidol (Figure 1):

- Treatment train 1: Calcite DAS + BaCO3 DAS (using fresh ash wood cuttings), fed with combined Adit 6+9 water. This treatment train was operated from December 2020 until October 2022.
- Treatment train 2: Calcite DAS + MgO DAS (using dried pine wood shavings), fed with combined Adit 6 + 9 water.

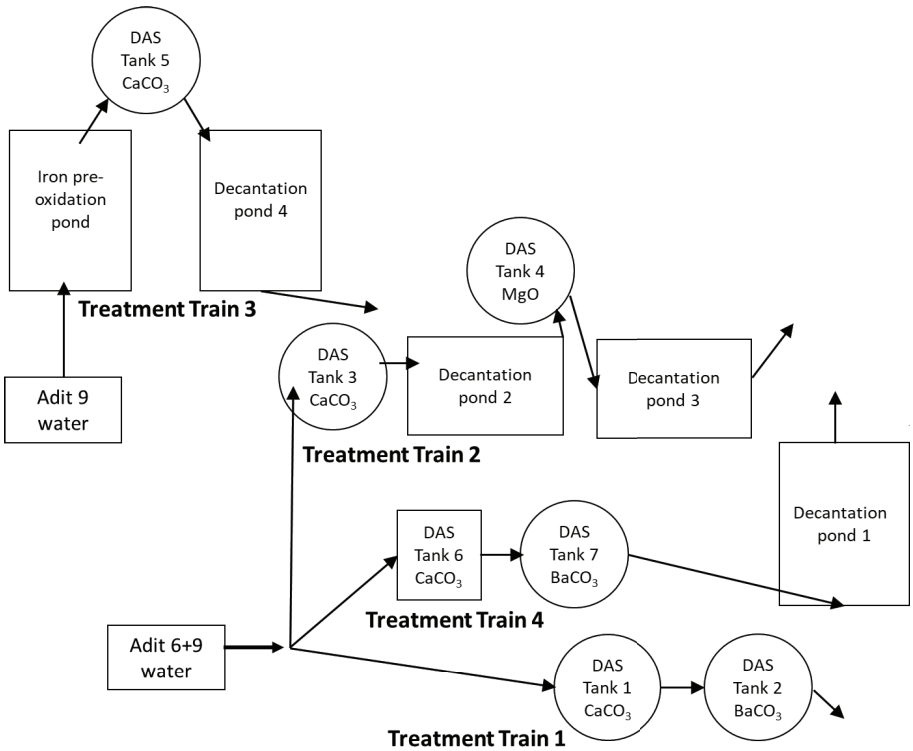


Figure 1 *Schematic site layout of the Cwm Rheidol DAS pilot trial.*

This treatment train was operated from December 2020 until October 2022.

- Treatment train 3: Calcite DAS only (using fresh wood cuttings), with pre-oxidation pond, fed with Adit 9 water only. This treatment train was operated from December 2020 until December 2021.
- Treatment train 4: Calcite DAS + BaCO3 DAS (using dried pine wood shavings), fed with combined Adit 6+9 water. This treatment train was operated from April 2022 until October 2022.

Parys Mountain

Parys Mountain Mine was the world's largest source of copper in the 18th Century. Today the site is a valuable resource for tourism, research and education, but is also one of the biggest single point sources of pollution in Wales, discharging more dissolved metals into the Irish Sea than the River Mersey, despite having less than 0.3% of the flow.

Most of the mine drainage from the site currently discharges from the Dyffryn Adda Adit into the Afon Goch Amlwch. The main contaminants (average during the period 2015 – 2019) in the discharge are SO_4 (2,263 mg/L), Fe (646 mg/L), Zn (78 mg/L), Al (73 mg/L), Cu (42 mg/L), Mn (16 mg/L), As (0.67 mg/L), Co (0.42 mg/L), Ni (160 µg/L), Cd (150 µg/L), Pb (20 µg/L). The average pH is 2.5.

Due to the high Fe concentrations at Parys Mountain, it was necessary to install two $CaCO_3$-DAS tanks in sequence (each followed by an aeration cascade and decantation pond) ahead of an MgO-DAS or $BaCO_3$-DAS tank to completely remove the Fe and Al before the water contacts the third DAS treatment stage. Two treatment trains were installed (Figure 2): Train 1 with MgO as the final treatment step and Train 2 with BaCO3 as the final treatment step. All DAS tanks were filled using fresh wood cuttings.

Contaminant removal efficiency calculations

Relative removal efficiencies r of metals and metalloids are calculated using the following equation:

$$r = \frac{c_{in} - c_{out}}{c_{in}} \times 100\%,$$

where c_{in} is the inflow concentration and cout is the outflow concentration.

Results

Cwm Rheidol

Table 1 displays median inflow and outflow total concentrations in treatment train 1.

In treatment train 1, removal efficiencies of >99% are calculated for Al, Cd, Fe, Pb and Zn. Removal efficiencies are 98.9% for Ni, 97.6% for SO_4, 83.6% for Cu, 78.8% for Cr, and 56.4% for Mn. Alkalinity increases substantially, but also organic carbon, total hardness, Ca, K, Mg, and Sr.

In treatment train 2, removal efficiencies of >99% are observed for Al, Cd, Fe, Mn, Pb, and Ni. Removal efficiencies are 98.1% for Cu, 82.2% for Cr, 63.9% for Sr, 56.4% for Mn, and 15.7% for SO_4. Mg, as expected, increases in its median concentration after the MgO-DAS tank. Organic carbon also increases, but less than in Train 1.

In treatment train 3, removal efficiencies of >99% are observed for Al and Cd. High removal efficiencies are also noted for Cu (98.5%), Cr (95.8%), Pb (83.1%), and Fe

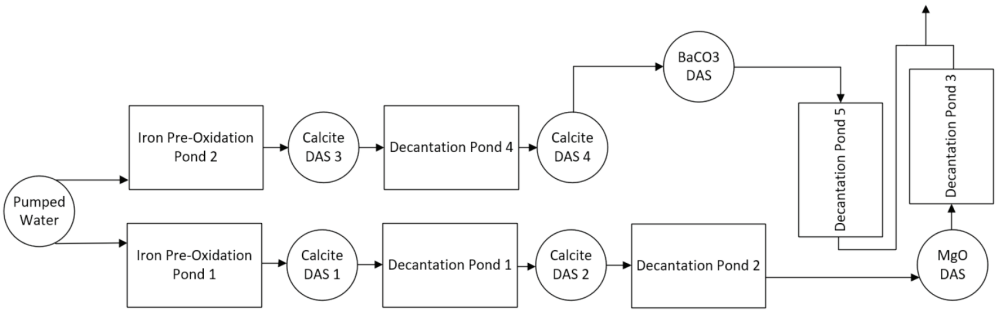


Figure 2 *Schematic site layout of the Parys Mountain DAS pilot trial.*

(77.0%). Removal efficiencies between 3.6% and 27.2% are observed for Li (6.0%), Mg (3.6%), Mg (7.9%), Na (13.5%), Ni (14.7%), SO4 (11.6%), and Zn (27.2%).

In treatment train 4, removal efficiencies of >99% are observed for Al, Fe, and Pb. 98.8% of Cd, 97.0% of Cu, 95.8% of Zn, 90.5% of SO4, 84.5% of Ni, 84.1% of Cr, and 79.4% of Mn are also removed.

In terms of absolute removal, the largest contributions to metal mass load reduction across the treatment trains are achieved for Zn, Fe, Al, Mn, and Pb.

The water flowing out from treatment trains 1 and 3, which used fresh wood cuttings to mix the DAS materials, displayed a dark colour and a strong rotten egg smell, indicative of bacterial sulfate reduction reactions. In trains 2 and 4, which used dried pine wood shavings, the outflow was clear and odourless.

Parys Mountain

Table 2 Table 1 displays median inflow and outflow total concentrations in treatment train 1.

In treatment train 1, removal efficiencies of >99.8% are observed for Al, Cd, Cu, Fe, and Zn. Removal efficiencies are 98.5% for Mn, 96.6% for Cr, 96.2% for Ni, and 89.9% for Pb. Median SO_4 removal is 16.9% in train 1.

In treatment train 2, removal efficiencies of >99.8% are observed for Al, Cd, Cu, Fe, and Zn. Removal efficiencies are 99.0% for Ni, 89.9% for Pb, 87.5% for Mn, 96.7% for Cr, and 92.9% for SO_4. Sr increases substantially across train 2, both in the $CaCO_3$-DAS tanks and the BaCO3-DAS tank.

In terms of absolute removal, the largest contributions to metal mass elimination in both treatment trains are achieved for Fe, Al, Zn and Cu. All four contaminants are removed within the $CaCO_3$-DAS tanks.

Table 1 *Median inflow and outflow water quality of the Cwm Rheidol DAS treatment trains during the trial period (total concentrations unless otherwise stated).*

Parameter	Unit	Adit 6 + 9 mixed	Train 1 out	Train 2 out	Train 4 out	Adit 9	Train 3 out
pH	---	3.48	7.86	9.42	8.17	2.93	6.92
Alkalinity	mg/L	0	310.0	62.5	175.0	0	265.0
Diss. Oxygen	mg/L	10.42	4.61	7.58	n.d.	7.90	6.83
Org. Carbon (Filt.)	mg/L	0.74	59.90	3.38	6.82	0.53	29.10
Redox Pot.	mV	433.8	8.1	29.3	67.3	456.1	8.3
Hardness	mg/L	121.8	394.7	277.6	190.8	346.9	945.9
Al	mg/L	5.69	0.02	0.01	0.03	29.90	0.02
Ba	mg/L	0.01	51.40	0.05	5.23	0.01	0.02
Ca	mg/L	29.3	106.0	30.4	47.7	71.2	298.0
Cd	mg/L	0.0445	0.0001	0.0003	0.0007	0.1295	0.0004
Cr	mg/L	0.0024	0.0005	0.0005	0.0005	0.0120	0.0005
Cu	mg/L	0.0534	0.0087	0.0010	0.0016	0.0971	0.0015
Fe	mg/L	16.70	0.10	0.03	0.04	101.00	23.20
K	mg/L	0.97	1.37	1.00	0.96	0.82	1.28
Li	mg/L	0.10	0.10	0.10	0.10	0.18	0.17
Mg	mg/L	12.8	15.1	46.2	15.6	44.1	42.5
Mn	mg/L	0.98	0.43	0.01	0.25	4.57	4.21
Na	mg/L	10.4	4.6	7.6	8.2	7.9	6.8
Ni	mg/L	0.284	0.003	0.002	0.057	1.33	1.14
Pb	mg/L	0.736	0.005	0.002	0.002	0.012	0.002
SO_4	mg/L	229.0	5.6	207.0	24.6	841.0	743.0
Sr	mg/L	0.07	1.08	0.03	0.46	0.24	0.38
Zn	mg/L	20.70	0.21	0.41	1.07	89.20	64.90

n.d.: not determined

SO4 removal also accounts for an important decrease of total contaminant mass in the $CaCO_3$-DAS tanks of both trains, with substantial additional SO4 removal achieved in the $BaCO_3$-DAS tank, but not in the MgO-DAS tank. The removal of SO_4 and Zn in the $CaCO_3$-DAS tanks was likely due to the reducing conditions that developed in the tanks, promoted by the fresh wood cuttings. The water flowing out from both trains displayed a dark colour and a strong rotten egg smell, indicative of bacterial SO_4 reduction reactions.

Conclusions

All treatment trains at both field trial sites achieved very high metal removal rates during the trial period.

Overall, treatment performance for most metals was similar for the treatment trains, and most metals were almost completely removed within the $CaCO_3$-DAS tank of each train. Only Mn and SO^4 displayed no or low removal in the $CaCO_3$-DAS tanks and required MgO-DAS (for Mn) or $BaCO_3$-DAS (for Mn and SO_4) to improve removal efficiency.

One issue in the trial performance at both sites was unpleasant odour and dark discolouration of the water flowing out of treatment trains that used fresh wood cuttings in the DAS reactors, due to reductive microbiological reactions. These unwanted reactions were prevented by using dried pine wood shavings, which demonstrated excellent results in treatment trains 2 and 4 at Cwm Rheidol. The pine shavings have natural antimicrobial properties and release much less organic carbon.

At Parys Mountain, substantial amounts of Fe were removed in the iron pre-oxidation ponds (on average, about 150 mg/L in each train) and in the decantation pond after the first $CaCO_3$-DAS tank in each train (on average about 150 mg/L in train 1 and about 100 mg/L in train 2). The iron pre-oxidation ponds had however particularly very long residence times (about eight days), which

Table 2 *Median inflow and outflow water quality of the Parys Mountain DAS Treatment Trains (total concentrations unless otherwise stated).*

Parameter	Unit	Inflow	Train 1 Outlet	Train 2 Outlet
pH	---	2.51	9.41	8.13
Alkalinity	mg/L	n.d.	n.d.	n.d.
Dissolved Oxygen	mg/L	2.7	5.1	5.1
Organic Carbon (Filt.)	mg/L	3.15	114.6	55.1
Redox Potential	mV	461.3	84.1	136.8
Hardness	mg/L	601.3	2111.5	931.2
Al	mg/L	69.85	0.013	0.022
Ba	mg/L	0.01	0.40	2.53
Ca	mg/L	75.7	52.3	223.0
Cd	mg/L	0.146	0.00015	0.00033
Cr	mg/L	0.0150	0.0005	0.0005
Cu	mg/L	36.6	0.006	0.012
Fe	mg/L	615.00	0.40	0.26
K	mg/L	1.4	27.3	20.5
Li	mg/L	0.16	0.12	0.18
Mg	mg/L	102.0	641.5	106.0
Mn	mg/L	17.4	0.27	2.2
Na	mg/L	18.6	53.7	30.3
Ni	mg/L	0.151	0.006	0.002
Pb	mg/L	0.020	0.002	0.002
SO_4	mg/L	2040	1695	145
Sr	mg/L	0.13	0.14	2.15
Zn	mg/L	62.65	0.11	0.24

n.d.: not determined

may be prohibitive for a full-scale application. Modifications to the pilot system in 2023 (already commissioned) will test the use of a vertical flow reactor (VFR, e.g., Sapsford and Williams 2008) instead of the iron pre-oxidation pond in train 1, to compare the iron removal performance for a lower treatment plant footprint.

The main differences in treatment performance between trains using MgO-DAS or $BaCO_3$-DAS were as follows:

- Trains with MgO achieved greater removal of Mn and Zn and displayed lower increases in Ba and Sr. The outflowing water had however higher concentrations of SO_4, K, hardness and a more alkaline pH.
- Trains with $BaCO_3$ achieved greater removal of SO4, had lower concentrations of K and hardness, more near-neutral pH values, but higher Ba and Sr concentrations.

The field trials have been successful and demonstrate the ability of the DAS system to be considered for scaling up to full sized treatment plants at both sites.

Acknowledgements

This study is funded by the joint Metal (Non-Coal) Mine Programme of NRW and The Coal Authority sponsored by Welsh Government. We extend our thanks to Dr Nina Menichino, Team Leader, Evidence Portfolio, Programmes and Processes at NRW for supporting this paper.

References

Roetting TS, Cama J, Ayora C, Cortina J-L, DePablo J (2006) Use of Caustic Magnesia to Remove Cadmium, Nickel, and Cobalt from Water in Passive Treatment Systems: Column Experiments. Env Sci Technol 40(20):6438—6443, doi:10.1021/es061092g

Roetting TS *et al.* (2016) Procedimiento para la depuración de aguas contaminadas por metales e instalación correspondiente. (Patent, in Spanish), Huelva University, patent number ES-2534806.

Roetting TS, Thomas RC, Ayora C, Carrera J (2008a) Passive treatment of acid mine drainage with high metal concentrations using Dispersed Alkaline Substrate. J Env Qual, 37(5):1741—1751, doi:10.2134/jeq2007.0517

Roetting TS, Caraballo MA, Serrano JA, Ayora C, Carrera J (2008b) Field application of calcite Dispersed Alkaline Substrate (calcite-DAS) for passive treatment of acid mine drainage. Appl Geochem, 23(6):1660—1674, doi:10.1016/j.apgeochem.2008.02.023

Roetting TS, Ayora C, Carrera J (2008c) Improved passive treatment of high Zn and Mn concentrations using Caustic Magnesia (MgO): Particle size effects. Env Sci Technol, 24(42), 9370—9377, doi:10.1021/es801761a

Sapsford DJ, Williams KP (2009) Sizing criteria for a low footprint passive mine water treatment system. Water Res 43(2): 423—432, doi:10.1016/j.watres.2008.10.043

Wildfire effects on a watercourse affected by acid mine drainage (Odiel River, SW Spain)

Jonatan Romero-Matos*, Carlos R. Cánovas, Francisco Macías, Rafael León, Ricardo Millán-Becerro, José Miguel Nieto

Department of Earth Sciences & Research Center on Natural Resources, Health and the Environment. University of Huelva, Campus "El Carmen", 21071, Huelva, Spain, jonatan.romero@dct.uhu.es

Abstract

Unlike in common hydrological years, when a sharp increase in dissolved concentrations and decrease in pH values is observed after the first autumn rainfalls, a different response is observed during the rainy events recorded afterwards the occurrence of a wildfire. Decreases in most major elements, electrical conductivity (EC) and slight increases in pH were observed. Wildfire-ash flushed during these events may have supplied sufficient alkalinity to attenuate the acidity, neutralizing the dominant efflorescent salts washout effect and the associated increase of AMD-elements concentrations in the river during the first rains of autumn in the Odiel watercourse.

Keywords: Wildfire-ash, Net Acidity, Efflorescent Salts, Washout, Seasonal Variations.

Introduction

The Odiel and Tinto watersheds in the Huelva province (SW Spain), two world case scenarios of highly polluted watercourses by acid mine drainage (AMD), present low pH values and extreme concentrations of dissolved contaminants, mostly metal(oid)s and sulfate, due to the contribution of diverse acidic leachates from historical massive sulfide mining-sites of the Iberian Pyrite Belt (IPB) (Cánovas *et al.* 2021). Their current water quality is of major concern given the limited water resources availability in the study area, located in a Mediterranean semi-arid region, and the severe contamination that the pollutant load carries on to the Ría de Huelva estuary, part of which is a declared protected natural environment, reaching eventually the Atlantic Ocean (Nieto *et al.*, 2013).

Hydrochemical conditions of both basins are strongly dependent on several geochemical processes such as washout of efflorescent soluble salts, the transport of sulfide oxidation products from mine sites, mineral precipitation/dissolution with sorption/desorption processes or dilution by runoff (Cánovas *et al.* 2017). These processes in semi-arid climates are mainly controlled by hydrological seasonal variations. The warm-dry season is characterized by an intense precipitation of evaporitic salts which serve as a temporary storage of metal(loid)s and sulfate. With the beginning of the rainy season, the flushing of these soluble salts (and also sulfide oxidation products), stored along riverbeds and mine sites, releases an extreme load of acidity, thus registering annual maximum concentrations of dissolved elements and drastic pH drops in AMD-affected watercourses. Thereupon, decreases in concentrations are observed due to dilution processes, when no salts remaining in riverbanks are left to be washout, and pH generally increases (Cánovas *et al.* 2008). Additionally, there are other factors that may play a key role in the AMD hydrochemistry (e.g. the settlement of treatment plants, adits sealing and tailings restauration, mine spills and/or factors related to climate change).

Climate models predict a magnification of wildfire events in Mediterranean regions. Wildfires can induce changes in soil physicochemical properties, increases in runoff and erosion rates, and modify inputs of sediments, nutrients and other water constituents (Smith *et al.* 2011). The mineralogy of the wildfire-ash generated in Mediterranean climates is highly alkaline (greatly soluble and reactive in water) with inert amorphous silica (Ulery *et al.* 1993; Pereira *et al.* 2012).

In fact, biomass ash have been used as reagent for acidic leachates treatment (Bogush *et al.* 2020; Millán-Becerro *et al.* 2021). Accordingly, a sampling campaign was undertaken to evaluate the fire consequences in the Odiel River hydrochemistry, after the first rainfalls of autumn. This is believed to be the first time that the direct consequences of a wildfire on an AMD-affected watercourse have been studied.

Methods

A sampling point located in the Odiel River middle basin was selected given its severe affection by the fire. The sampling campaign began after the cease of the wildfire, coinciding with the first rainfall after the dry season. Besides, this location is crucial in the Odiel River because it receives the acidic leachates from the Riotinto Mining District throughout the Agrio Creek, the main pollutant contributor to the Odiel watershed (Galván *et al.* 2016).

Different physicochemical parameters such as pH, electrical conductivity (EC) and redox potential (ORP) were measured in the field with a previously calibrated multi-parameter portable equipment. Water samples were filtered (Millipore 0.22 µm filters) and acidified to pH<1 with suprapur HNO_3 (2%) immediately after sampling, for a total of 22 samples. Major elements were analyzed with ICP-OES, although only Fe, Al, SO_4, K, Ca and Mg concentrations are shown in this study. Net acidity was calculated using

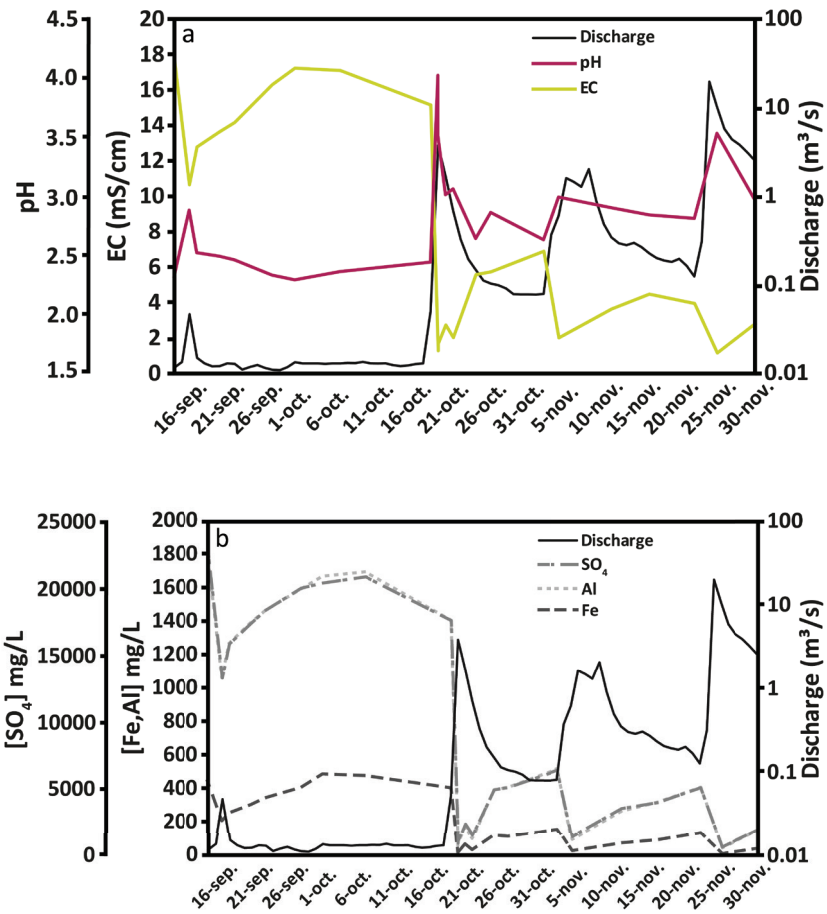


Figure 1 *a. Temporal evolution of main physicochemical parameters and riverflow during the sampling period b. Concentration evolution of dissolved Fe, Al and SO_4 throughout the campaign.*

the modified method of Kirby and Cravotta (2005). Flow data were obtained from the Sotiel Coronada gauging station, located downstream of the sampling point (23 km), and correlated with precipitation data from a pluviometric station located around 7 km from the sampling point.

Results

Contrasting the usual AMD behavior during the previous hydrological years, when a sharp rise in dissolved elements concentrations and lower pH values are observed after the warm-dry period coinciding with the first rainfalls of autunm, a different response was recorded during the post-fire rain events.

All major elements underwent a drastic fall in concentration in the sampling point. Thus, during the first rainy event, the EC saw a substantial drop, caused by a decrease in the concentration of most dissolved elements (Fe: from 443 to 205 mg/L; Al: from 1805 to 1059 mg/L; sulfate: from 22.8 to 13.3 g/L), coinciding with a slight increase in pH (fig. 1), contrary to the expected hydrochemistry changes in these waters during the fall season. Net acidity lessens from an initial value of 12 to 7 g/L of $CaCO_3$ equivalent. It is rather noteworthy since the registered streamflow increment during the first rains may be not sufficient to provoke this response by dilution processes. This could be due to the dissolution of ashes accumulated after the fire. Wildfire-ash flushed during these events possess high alkalinity (Ulery *et al.* 1993; Pereira *et al.* 2012) and may have attenuated the acidity carried by the Odiel River, neutralizing the dominant effect of evaporitic salts washout and causing the precipitation of pollutant elements during the first autumn rains. This neutralization capacity of biomass ash has been widely reported (e.g. Bogush *et al.* 2020). In the following days, a recovery towards the original conditions is observed.

The second rainy event caused a major riverflow rise than the previous one. Hydrochemical conditions showed a further decline in dissolved elements concentrations, reaching a net acidity of 0.36 g/L of $CaCO_3$ eq. and a reduction of more than 90 % for the major elements. EC declined from 15 to 1 mS/cm and pH values increased to 4 (fig. 1). In this event, the washout of salts and probably ash must have been negligible, since most of it would have been dissolved during the first rains, dominating in this case a strong dilution process. Finally, the last two events were controlled by run-off dilution processes.

Discussion

In an effort to determine the influence of ashes dissolution on the water hydrochemistry,

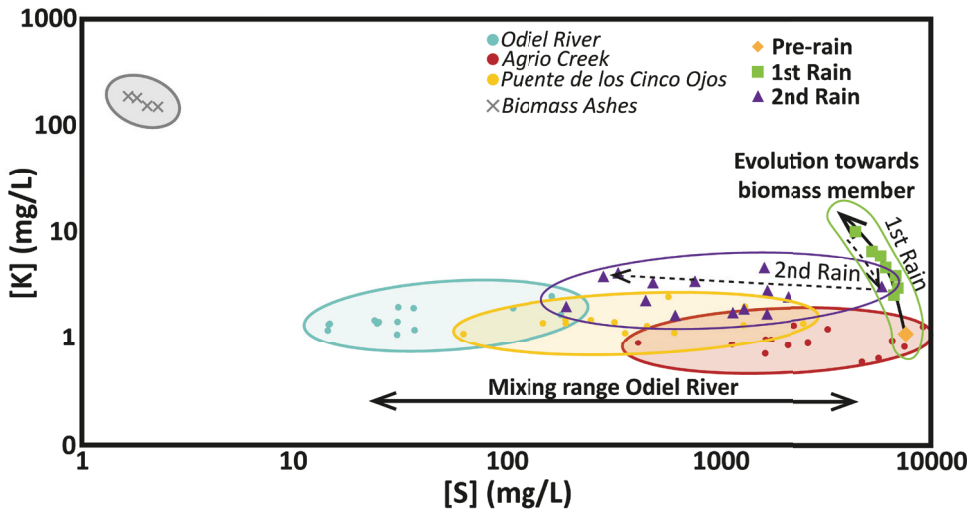


Figure 2 *Potassium and sulfur concentrations in the Odiel River during the study period. Extreme end-members (biomass ash and AMD-affected waters) , are also represented to study their influence on the river hydrochemistry.*

some geochemical tracers were considered. Additionally, Fe/SO_4 and Ca/Mg ratios were calculated to infer the geochemical processes dominating during the sampling period.

Potassium (K) is a main inorganic compound of wildfire-ash forming base mineral phases which are easily soluble in water (Ulery *et al.* 1993; Pereira *et al.* 2012). Given its high content in ash, K was considered as a geochemical tracer, along with S, common in AMD-affected watercourses (fig. 2) but less present in ash. "Pre-rain" samples show the river conditions after the fire but before the beginning of the rains (the Odiel River is homogenized with the Agrio Creek discharge hydrochemistry during the summer); "1st Rain" and "2nd Rain" samples represent the evolution after the first and second rainfall events associated to slight and a great increase in streamflow, respectively.

Geochemical data are available from an annual series of the Odiel River prior to the wildfire (2015-2016), represented by the Odiel before the Agrio River (main discharge of the basin), the Agrio Creek itself, and the Odiel at the Puente de los Cinco Ojos (downstream of the confluence), coinciding with the sampling point of the study. This series shows the conditions of the Odiel during a hydrological year, showing a range of mixtures between the Agrio and the Odiel, resulting in the final mixture of Puente de los Cinco Ojos. On the other hand, biomass ash composition from regional vegetation as an analogous to wildfire-ash is available. A first trend is observed within the first rains towards the biomass ash member (fig. 2). Given the high K content in ash and this initial evolution, opposite to the normal trend towards the usual mixture member during the second rain (and other subsequent rain events recorded), it is suggested that ashes may have been entirely washed out during the first rains after the dry season. However, there is a slight deviation, towards the biomass ash member, which could be interpreted as the remaining influence of ash dissolution on the river hydrochemistry.

Element ratios (fig. 3) suggest an intense precipitation of Fe oxyhydroxysulfates during the study period. The Fe/SO4 ratio decreases during the first rainy event evidencing a precipitation of these mineral phases instead of the common ratio increment, which results from efflorescent salts washout observed after the dry season. In this sense, the soluble Fe-sulfate salts accumulated along riverbeds have high Fe/SO4 ratios (iron concentration is greater than sulfate within evaporitic salts, than in the river waters) so that its flushing may cause a rise in the Fe/SO4 ratio. Thus, the alkalinity provided by the ashes rises the pH and induces the precipitation of Fe mineral phases reducing the Fe/SO4 ratio. In addition, it is expected that other elements co-precipitate and/or absorb with these mineral phases. The progressive increase of the ratio the following days may be due to

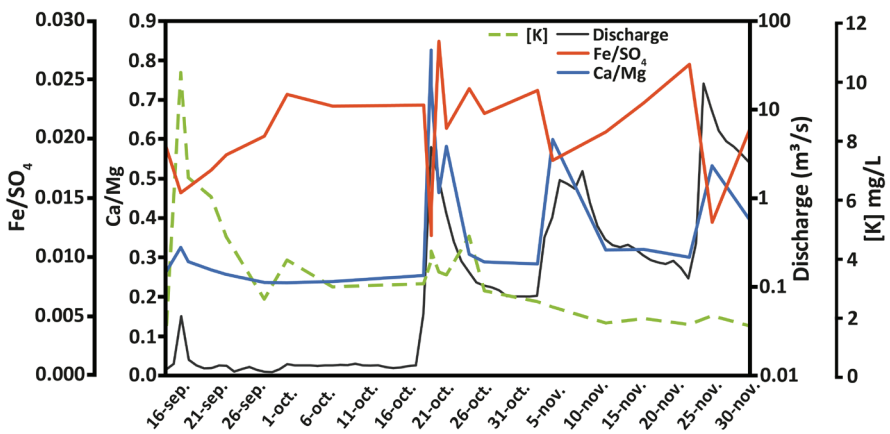


Figure 3 *Fe/SO_4 and Ca/Mg ratios reflecting the geochemical processes ocurring during the sampling period. Potassium concentration is also shown to asses the influence of the ashes.*

transport of sulfide oxidation products from mine sites which may increase again the ratio in the river. During the second rainy event, the ratio drastically decreases as a result of a strong dilution process with due pH increase leading to Fe precipitation (maybe coupled with the dissolution of remaining ashes from the first event). The decrease is followed by an increase that could be interpreted as effective evaporitic salts dissolution into the river water, coinciding with a slight EC increment (fig. 1).

Ca/Mg ratio increases during the two main rain events (fig. 3). Since evaporitic salts are richer in Mg than in Ca, their dissolution into the water would decrease the ratio. Therefore, these rises evidence the existence of Ca inputs, probably by the dissolution of deposited ash, considering that Ca is also a major compound of biomass ashes in Mediterranean climates (Pereira *et al*., 2012). Potassium concentration peaks coincide with the ratios (fig. 3) suggesting a clear ash influence on the river hydrochemistry during the research period. Generally, these ratios support the interpretation of the given neutralization of the evaporitic salts washout process by ash alkalinity.

Conclusions

Wildfire-ash flushing during the first autumn rainfalls may have supplied sufficient alkalinity to attenuate the washout of AMD-evaporitic salts commonly observed in AMD-affected sites of semiarid climates and its implications (major pollution peaks of the year), preventing the usual increase in the Odiel River acidity. However, the acidity neutralization is temporary and punctual, with the river rapidly recovering its original conditions after this quick dissolution and after the arrival of acidic leachates from mine sites. The results of this study shed light on the response of rivers to certain climate change effects, since climate models predict an increase in the number and intensity of wildfires, especially in Mediterranean climates.

References

Bogush AA, Dabu C, Tikhova VD, Kim JK, Campos LC (2020) Biomass ashes for acid mine drainage remediation. Waste Biomass Valorization 11(9):4977-4989.

Cánovas CR, Hubbard CG, Olías M, Nieto JM, Black S, Coleman ML (2008) Hydrochemical variations and contaminant load in the Río Tinto (Spain) during flood events. J Hydrol 350:24–40.

Cánovas CR, Macías F, Olías M, Pérez-López R, Nieto JM (2017) Metal-fluxes characterization at a catchment scale: Study of mixing processes and end-member analysis in the Meca River watershed (SW Spain). J Hydrol 550:590-602.

Cánovas CR, Macías F, Basallote MD, Olías M, Nieto JM, Pérez-López R (2021) Metal(loid) release from sulfide-rich wastes to the environment: the case of the Iberian Pyrite Belt (SW Spain). Curr Opin Environ Sci Health 20:100240.

Galván L, Olías M, Cánovas CR, Sarmiento AM, Nieto JM (2016) Hydrological modeling of a watershed affected by acid mine drainage (Odiel River, SW Spain). Assessment of the pollutant contributing areas. J Hydrol 540:196-206.

Millán-Becerro R, Canovas CR, Pérez-López R, Macías F, Leon R (2021) Combined procedure of metal removal and recovery of technology elements from fertilizer industry effluents. J Geochem Explor 221:106698.

Nieto JM, Sarmiento AM, Canovas CR, Olias M, Ayora C (2013) Acid mine drainage in the Iberian Pyrite Belt: 1. Hydrochemical characteristics and pollutant load of the Tinto and Odiel rivers. Environ Sci Pollut Res 20(11):7509-7519

Pereira P, Úbeda X, Martin DA (2012) Fire severity effects on ash chemical composition and water-extractable elements. Geoderma 191:105–114.

Smith HG, Sheridan GJ, Lane PN, Nyman P, Haydon S (2011) Wildfire effects on water quality in forest catchments: a review with implications for water supply. J Hydrol 396(1-2):170-192.

Ulery AL, Graham RC, Amrhein C (1993) Wood-ash composition and soil pH following intense burning. Soil Sci 156:358–364.

Beyond Piramid: The Coal Authority's Approach to Design of Passive and Semi-Passive Treatment Schemes for Ferruginous Mine Waters in the UK

Christopher J. Satterley, Arabella M L. Moorhouse-Parry

The Coal Authority, 200 Lichfield Lane, Mansfield, Nottinghamshire, NG18 4RG, United Kingdom

Abstract

Since the publication of the Piramid guidelines in 2003, the Coal Authority has brought over 40 passive treatment schemes into operation that treat 72 billion litres per year of ferruginous mine waters. Over this time the organisation's approach to design has followed the recommendations of Piramid, with adaptions based on our operational experience. Key areas of development include the move away from areal removal rates for iron to the use of a combination of operationally derived rate constants and minimum residence times for design of lagoons and reed beds; the use of multiple treatment trains to accommodate high flows; and the treatment of saline and seasonably variable water qualities. The key applications for this work are to inform practitioners managing similar net-alkaline mine waters on the approach adopted by the Coal Authority that can help promote more effective adoption of passive treatment approaches internationally.

Keywords: Treatment design, coal mine water, ferruginous, net-alkaline, passive

Introduction

Since their publication, the guidelines produced by the Piramid Consortium (2003) have become a key resource in the design, construction, operation and maintenance of mine water treatment schemes (MWTS). The guidelines represent a concerted effort to collate the key scientific and technical knowledge on mine water treatment available at the time and have been used successfully in the development of MWTS across the globe.

In the UK, the Coal Authority has responsibility for the management of mine water originating from coal mining activities and currently manages a portfolio of 75 treatment schemes. This operational portfolio includes over 40 passive coal MWTS designed and built following the publication of the Piramid guidelines. These treatment schemes combined treat a total of 72 billion litres per year of ferruginous mine waters, preventing almost 1,000 tonnes of iron and 50 tonnes of manganese from entering UK watercourses each year.

Over the last 20 years the Coal Authority's approach to passive treatment design has been based on the recommendations of Piramid. However in recent years, the approach has been adapted based on our more recent operational experience. This paper will outline how our approach has moved on from the Piramid guidelines based on 20 years of design, construction and operational experience of passive mine water treatment across aeration, settlement and the use of aerobic wetlands (reed beds).

UK Coal Mine Water Chemistry

Coal mining has occurred across large parts of the island of Great Britain peaking in the deep coal mining activities in the late 19th and early to mid-20th centuries, with major coal mining areas across the Central Belt of Scotland, the North and Midlands of England and South Wales. The resultant mine water chemistry from these abandoned mines is variable, but is largely circum-neutral and net alkaline in nature due to the carboniferous limestone geology present in most UK coal mining areas.

UK coal mine waters typically contain appreciable levels of iron (present in ferrous and ferric states) as well as levels of manganese but generally very low levels of ecologically toxic metals such as zinc, cadmium or lead. The levels of anionic species can vary between mining areas with some mine waters being significantly more saline than others with

salinity largely dominated by chloride and sulfate. In a small number of cases, UK coal mine waters can be marginal or net-acidic in nature or show variations in acidity related to the seasonal interaction of water with local geological and mining features.

Table 1 shows some examples mine water chemistries for a range of UK coal mine waters to demonstrate the discussion above. It is noted that mine water flow rates experienced in the UK can also be highly variable, ranging from a few L/s to several hundred L/s.

Passive treatment for net-alkaline circum-neutral ferruginous mine waters

The general approach to treatment of typical UK coal mine waters adopted by the Coal Authority remains in line with that recommended by the Piramid guidelines in that a combination of aeration units, settlement lagoons and aerobic wetlands (reed beds) are used to remove iron from mine waters. Depending on the iron levels and discharge requirements following aeration, either settlement lagoons, aerobic wetlands or a combination of both are used to reduce iron levels to typically 1-3 mg/L prior to discharge to the environment.

Mine water aeration

Aeration of mine waters is achieved through the use of stepped cascades. The Piramid guidelines state that a range of step heights/ numbers and cascade designs were possible including the use of deep plunge pools to aid in aeration. Operational experience on a range of sites constructed since 2003 have enabled the Coal Authority to develop a standard design that allows the construction to be undertaken using concrete units of standard dimensions as per Figure 1.

Standard cascade designs currently utilise five steps, each with a typical drop of 500 – 525 mm and a step length of ≈1000 mm, with a slight fall back towards the upper step to allow a very shallow pool of water to be present. Step widths are a standard 100 mm per 1 L/s of flow in line with Piramid recommendations, with a maximum width of 2.5 m (equivalent to 25 L/s) for a single cascade unit to enable safe access for inspection and maintenance. Where flows greater than 25 L/s require treatment, multiple cascade units arranged in parallel are used (usually within an overall single structure).

Such cascade designs show good aeration performance with dissolved oxygen concentrations of 70-90% saturation achieved. This enables oxidation of between 30 - 50 mg/L of ferrous iron per aeration stage without the need to use large plunge pools. For design purposes, a more conservative maximum of 30 mg/L ferrous iron is used per aeration stage, as recommended by Priamid. However, where site constraints (such as available land area and/or topography) prevent passive re-aeration over subsequent cascades then the use of a chemical oxidation (such as hydrogen peroxide) may be required.

At ferrous iron concentrations between 30–50 mg/L, it is possible that sufficient aeration may be achieved using a single cascade; the Coal Authority has a number of examples where single cascades provide sufficient oxidation of iron at these concentrations (e.g. Great Clifton, Cumbria and Horden, Country Durham). Consequently, where it is not feasible to install secondary cascades at sites when iron concentrations fall within this range, provision is made for the subsequent installation of peroxide dosing equipment if it is found to be necessary, rather than installing equipment in the initial design. A typical standard cascade construction is shown in Figure 2.

Table 1 *Examples of typical coal mine water chemistry and flows (annual averages) in the UK*

Mine water discharge	Total Iron mg/L	Dissolved Iron mg/L	pH	Alkalinity mg/L eq. $CaCO_3$	Chloride mg/L	Flow L/s
Woodside (Derbyshire)	5	3	7.7	808	1216	110
Bullhouse (South Yorkshire)	63	57	5.4	56	72	30
Deerplay (Lancashire)	30	29	7.1	238	8	25
Dawdon (Co. Durham)	54	53	6.7	465	18678	100
Sheephouse Wood (South Yorkshire)	31	22	6.1	119	82	5

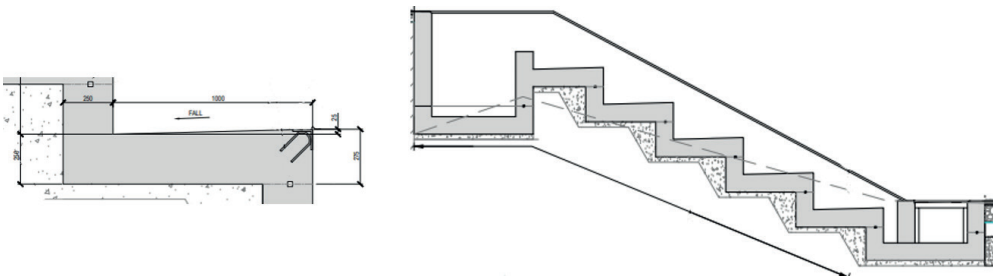


Figure 1 Aeration cascade pre-cast unit standard design cross section (left, all measurements in mm) and typical overall arrangement cross-section including inlet and outlet channels (right)

Settlement Lagoons

For mine waters where iron concentrations are >10 mg/L, settlement lagoons are deployed to allow for the completion of the oxidation and settlement of iron solids prior to further treatment in wetlands. The Coal Authority has followed the recommendations of the Piramid guidelines in terms of typical depth (3m) and side slope ratio (2:1, where ground conditions allow). Settlement lagoons are lined with an impermeable liner to prevent ingress of partially treated mine water into underlying aquifers prior to discharge. Various methodologies for sizing of such lagoons were noted in the Piramid guidelines including the use of a nominal 48 hour residence time, an allowance of 100m^2 of lagoon area per L/s of water and using areal removal rates derived from anaerobic wetlands (e.g. 10 g/m^2/day derived from the work of Hedin *et al.* (1994)). It is acknowledged that these methods lead to a wide range of treatment areas and thus run the risk of under- or over-sizing these lagoons. Initial work by the Coal Authority to derive relationships between iron removal and hydraulic retention time from our operational schemes was also mentioned (Parker 2003). A review of 15–20 years' worth of additional operational data from our 75 operational mine water treatment schemes in the UK has allowed further refinement of that approach, utilising prior research by Tarutis *et al.* (1999) with a first order relationship derived initially for wetland treatment (Eq. 1).



Figure 2 A recent cascade installation (2021) for a maximum flow rate of 80 L/s split into 4 cascades of 2 m individual width to aid in access of inspection and maintenance (Bullhouse, South Yorkshire)

$$\text{Eq. 1} \quad A = \frac{Q}{k_1 \ln(C_{in} - C_{out})}$$

Where A is the treatment area (m^2), Q is the mine water flow (m3/day), C_{in} and C_{out} are inlet and outlet iron concentrations (mg/L) respectively, and k_1 is the first order removal constant (m/day).

For existing schemes where treatment areas, flows and inlet and outlet concentrations are known, it is possible to calculate the removal constants, which can then be used in future designs. These constants are under continuous review but currently a removal constant of 0.8 m/day is used for the design of new settlement lagoons. In order to add some conservatism to a scheme design however, all lagoon treatment areas calculated using this approach are compared to the treatment area required for a minimum hydraulic residence time of 24 hours per lagoon, to prevent under-sizing of lagoons. This approach represents a more narrowly defined potential range of treatment areas than the previous methodologies proposed in the Piramid guidelines and ensures that performance from actual schemes forms the core basis for future designs.

In addition to absolute sizing for treatment performance, a number of other factors need

to be considered to aid in the successful operation and maintenance of treatment schemes. Based on prior experience, the Coal Authority uses a maximum flow rate of 50 L/s for a single treatment train, therefore, for higher flow rates, multiple treatment trains are generally recommended. This is to ensure that individual treatment units can be taken off-line for maintenance activities with minimal impact to overall treatment performance. Furthermore, allowances in settlement lagoon design for sludge accumulation must also be considered. The Coal Authority uses an assumption that sludge accumulates as 3 wt% $Fe(OH)_3$ based on the iron removal rate with a planned de-sludge cycle of five years in normal circumstances.

Another key consideration for the successful operation of lagoons is maintaining an even distribution of flow across the treatment unit. Water inlet channels are designed to maximise the lateral distribution of water across the full width of the lagoons using crenelated weirs to reduce dead zones. Baffles have also been installed at some sites (e.g. at Clough Foot and Deerplay, Lancashire) to improve flow distribution, but the success of these has been limited to date.

The above approach has allowed the Coal Authority to reliably design settlement lagoons to achieve treatment down to 10 mg/L or less on its passive treatment schemes enabling further treatment by aerobic wetlands where required. This approach has been applied to high flow rates such as the Lynemouth MWTS (constructed 2015–2019) in Northumberland that can treat up to 240 L /s of mine water with a typical raw iron concentration between 40–50 mg/L (Figure 3). This scheme features a total of seven rectilinear treatment ponds in three treatment trains with a total treatment area of 28,000m^2 reliably treating water to <10 mg/L total iron ready for discharge into the North Sea.

Polishing – Aerobic wetlands (reed beds)

Where further iron reduction to achieve final discharge concentrations <3 mg/L is required (i.e. where discharge is to occur to an inland watercourse) then passive treatment using aerobic surface flow wetlands (or reed beds) is standard practice for the Coal Authority. In the UK, mine water treatment reed beds are typically planted with common reed (*Phragmites australis*), Bulrush (*Typha latifolia*) or a combination of the two. *Phragmites* has been found to be a generally hardy plant when exposed to a range of mine waters and UK climates. For example, reed bed wetlands have been successfully operated by the Coal Authority treating high chloride mine waters (typically approx. 10,000 mg/L) in a coastal setting (e.g. Horden, County Durham, constructed 2011), in exposed upland areas (elevation 400 m AOD, Deerplay, Lancashire,



Figure 3 *Aerial photograph of the Lynemouth mine water treatment scheme in Northumbria showing a series rectilinear ponds. In the background is the Lynemouth Power Station and in the foreground is a stocking area for dried and bagged iron ochre produced by the scheme for use in anaerobic digestion.*

constructed 2002) and at northerly latitudes (56˚N, Lathallan Mill, Fife, constructed 2004). The latter of these examples is considerably more northerly than the recommended 53˚N as stated in the Piramid guidelines, however this may due to the impacts of the North Atlantic Drift and climate change on the UK climate, as well as the feed of constant temperature mine water throughout the year. For reference the city of Stoke-on-Trent is located at a latitude of 53°N.

The Coal Authority also utilises the Tarutis first order relationship to assess and size reed beds for the treatment of coal mine waters (Eq 1). Performance of reed beds for iron removal has been found to be quite variable with first order rate constant for UK reed beds typically in the range of 0.2–3.0 m/day, equivalent to areal removal rates of between 1–14 g/m^2/day with overall average performance for the Coal Authority's reed beds yielding a removal constant of 1.2 m/day equivalent to an areal removal rate of 3.2 g/m^2/day) meaning that the standard recommended areal removal rate of 10 g/m2/day would tend to undersize a reed bed. With such large variations in performance within the Coal Authority's schemes, final decisions on reed bed areas for a new scheme are made on a risk-based approach, which considers areas derived from the range of observed rate constants alongside site specific factors such as land availability, local climate, elevation, mine water quality and impact of underperformance amongst other factors.

In the Piramid guidelines a number of recommendations were made regarding the design of reed beds to improve their habitat and amenity value as well as performance. These include discouraging the use of liners, using uneven surfaces with spits and islands, avoiding significant concrete structures and softening edges of reed beds. Coal Authority reed beds have impermeable liners to prevent potential contamination of the water table. Lined reed beds have generally performed well in our experience with liner damage being a rare occurrence. The use of uneven surfaces, islands and spits creates challenges in terms of effective maintenance (reed cutting and refurbishment) of reed beds, in addition to the creation of 'dead zones' where water flows are low; inclusion of these features is no longer part of standard Coal Authority designs. The use of rectilinear reed beds with concrete inlet and outlet structures does not appear to have the detrimental impact to amenity and habitat value feared within the Piramid guidelines. The Coal Authority has a number of such reed beds that function well, are used as amenity areas by local communities and have observed biodiversity comparable to natural wetlands (Athorn 2018) with a range of insects, flora, small mammals and birds observed at our sites.

In recent years, reed bed designs have begun to include provision for an unplanted open water zone at the front of primary reed beds where iron concentrations are highest. This helps to prevent reed fouling of inlet structures and allows further precipitation of ochre which can be easily removed during maintenance without disturbing the reed area. It is important to note that for new schemes, such areas must be considered in addition to the calculated reed bed areas.

The above principles have been applied to a range of reed beds for coal mine waters in the UK including at schemes with high flows. A key example is the Blindwells scheme, East Lothian, which is a series of three reed beds (total area 17,415 m^2, design flow rate 450 L/s) typically treating a flow of 300 L/s of mine water with an average iron concentration of 5 mg/L and an average iron removal rate of 90% (Figure 4).

Chemical dosing (semi-passive treatment) & seasonally acidic mine waters

In some cases UK coal mine waters can experience seasonal variations in chemistry changing from net-alkaline in the summer, to net-acidic in the winter. This is understood to be related to higher winter water levels interacting with weathered coal and other mineral workings that are usually not flooded in the summer months. One example of this is at Clough Foot, West Yorkshire where net-alkaline mine waters turn net acidic with increased aluminium levels in winter months. Whilst passive alkalinity provision is possible as outlined in the Piramid guidelines, sizing such units for variable water qualities is

highly challenging, as is the management of such systems with relatively high iron concentrations (e.g. Clough Foot raw total iron concentrations are ≈30 mg/L).

To counter this, the Coal Authority's approach has been to use sodium hydroxide dosing as this not only has a lower land footprint, but is more flexible in providing alkalinity during seasonal water chemistry variations. Dosing rates are determined by calculating the alkalinity demand for iron and aluminium precipitation, as well as including a pH correction to a defined target value (typically pH 7.0–7.5) using data obtained from routine sampling. Based on experience a conservative assumption of 80% chemical efficiency is used to ensure reliable treatment of the mine water is achieved and to account for any chemistry variations between monitoring rounds.

Conclusions

This paper provides a high level discussion of the Coal Authority's current approach to treating ferruginous coal mine waters in the UK. The key applications for this work are to inform mine water practitioners who may be dealing with similar mine waters on the approach adopted by the Coal Authority that can help promote more effective adoption of passive treatment approaches internationally as we look towards updating the Piramid guidelines in the coming years.

Acknowledgements

The authors would like to thank the UK Department for Energy Security and Net Zero for sponsoring the work of the Coal Authority and the colleagues, researchers and consultants who have contributed to the development of and understanding of coal mine water treatment in the UK over the last 20 years.

References

Athorn, M. (2018) Conservation value of constructed reedbeds. PhD thesis, University of Nottingham.

Hedin, R.S., Nairn, R.W. and Kleinmann, R.L.P. (1994a) Passive Treatment of Polluted Coal Mine Drainage. Bureau of Mines Information Circular 9389. United States Department of Interior, Washington DC.

Parker, K. (2003) Mine water management on a national scale - experiences from the Coal Authority. Land Contamination and Reclamation, 11, (2), 181 - 190.

PIRAMID Consortium (2003) Engineering guidelines for the passive remediation of acidic and/or metalliferous mine drainage and similar wastewaters. European Commission 5th Framework RTD Project no. EVK1-CT-1999-000021 "Passive in-situ remediation of acidic mine / industrial drainage" (PIRAMID). University of Newcastle upon Tyne, Newcastle upon Tyne UK.

Tarutis, W.J., Stark, L.R. and Williams, F.M. (1999) Sizing and performance estimation of coal mine drainage wetlands. Ecological Engineering, (12), 353-372.



Figure 4 *Aerial photograph of the Blindwells scheme in East Lothian, showing a cascade and three reed beds in series with a conditioning zone at the front of the primary reed bed (©Vexcel imaging ©2023 Microsoft, Microsoft Bing Maps screen shot reprinted with permission from Microsoft Corporation).*

Life-Cycle Water Balance Modelling as a Tool for Water Management Risk Assessment to Minimise Legacy Effects

Roxane Schmidt[1]

[1]*Jones & Wagener (Pty) Ltd, 59 Bevan Road, Johannesburg, South Africa, roxane@jaws.co.za*

Abstract

This paper presents a cyclic methodology for non-operational water management risk assessment to help minimise legacy effects by using an integrated mine water balance as a characterisation tool. The methodology aims to identify possible legacy effects that a current mining operation might pose; and assess the effect that recommended mitigation measures might have to reduce the identified effects. An example case study is presented using the proposed methodology for a platinum mine in South Africa.

Keywords: Integrated water balance model, water management risk assessment, GoldSim

Introduction

Operational mines have multiple entities that require comprehensive water management to ensure minimal risk of contamination to the environment and continual production capacity throughout the life of the mine. The day-to-day operations do not necessarily consider the closure status of the mine and the subsequent legacy effects those entities might have, if left unrehabilitated during operation, when these entities cease operation, temporarily or permanently. Typically, in water balance modelling a key assumption is that all entities are managed according to the design criteria and for the entity's designed lifespan or the expected Life-of-Mine (LOM). Therefore, the effect of an entity being non-operational at any instance in its lifespan, in relation to the entire mining operation, is typically not considered. An abrupt change in the lifespan and operational scheduling of an entity could potentially have a larger legacy effect than the original lifespan of that entity considering its planned closure date. This paper presents a non operational water management risk assessment methodology to identify and minimise legacy effects. It also presents how an integrated mine water balance can be used as a tool to undertake the assessment.

Water Management Risk Assessment

Water management is a structured approach to managing water across a site that is usually driven by a preferred environmental outcome and a water balance model is a tool developed to assist in achieving this outcome (Punkkinen *et al*., 2016). The principle of mass conservation is critical when constructing a water balance model and should be followed throughout (Department of Water Affairs and Forestry, 2006). A water balance model replicates the flow network across a site and simulates where water is stored and how water is moved. Incorporated into a water balance model is the environmental flow generated by the site in the form of rainfall, runoff, evaporation and infiltration, site-related flows as well as any site-related configurations/ assumptions (Julien *et al*., 2005).

In this study, GoldSim was used as a modelling software to dynamically model an integrated mine water balance and can be used as a tool in water management assessments. As mining conventions and management over the life of a mine continuously change an additional level of complexity in the water balance model is required to account for the operational changes. GoldSim has the capability to model complex site-specific systems that can be continuously updated/

modified. This modelling software uses Monte Carlo simulations to generate a probabilistic set of outcomes (Krogerusk & Pasanen, 2016). This provides a flexible approach to water management of a site (Nalecki & Gowan, 2008).

Quantifying the environmental risk of an entity with regards to its potential legacy effect at any point in its lifespan is an important consideration when modelling the status of the mining operation. Current and potential legacy environmental effect quantification provides the opportunity to identify possible interventions or new technologies to minimise the legacy effect an entity might have on the environment. Financial implications should be considered together with the environmental effects and risks when assessing the possible interventions or new technologies as this could require larger financial investment or risk, making the possible intervention undesirable.

The cyclic methodology for the non-operational water management risk assessment (Figure. 1) uses a multi-criteria approach to assess and rank the potential legacy effects of each entity, in an integrated mine water balance, being non-operational at any instance in its lifespan.

As part of the methodology an integrated mine water balance model is developed. A mine specific list of potential legacy effects is then complied. This list is then used in determining the environmental and financial evaluation criteria of the risk assessment. Each entity in the integrated water balance model is assumed then to be non-operational, e.g., a prolonged halt in production, and evaluated on its potential environmental effects, as well as the probability of occurrence of these

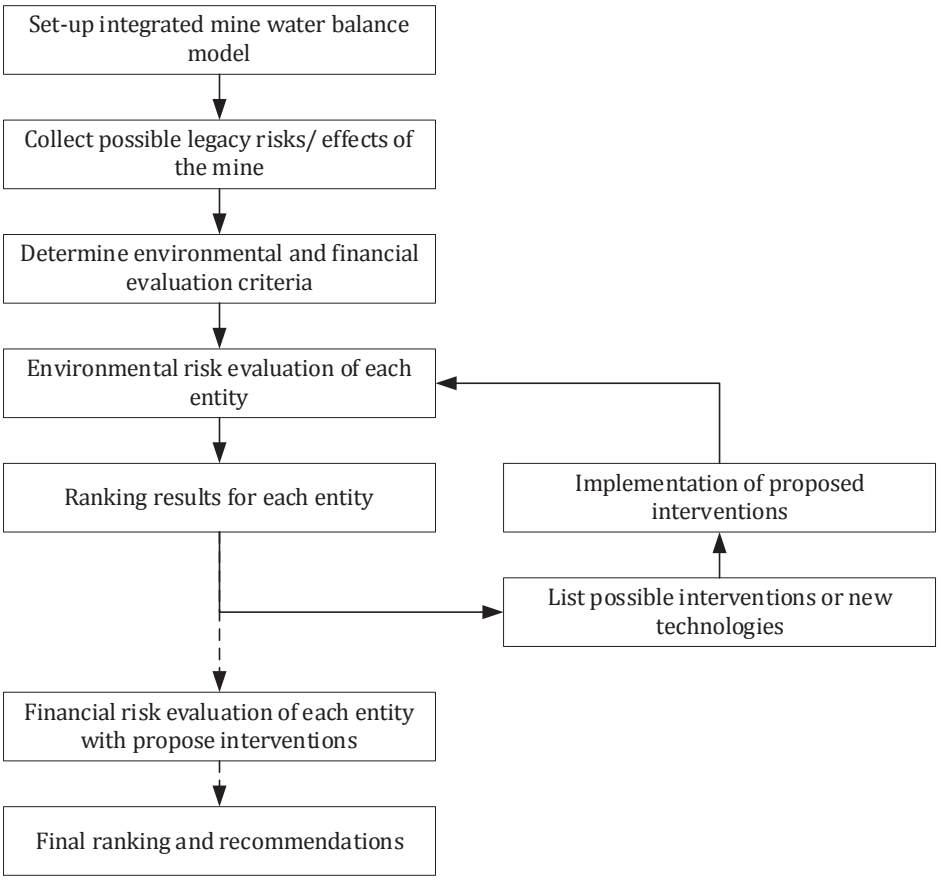


Figure 1 *Schematic of the proposed cyclical methodology for the non-operational water management risk assessment.*

effects. The entities are then ranked according to the evaluation results. A recommended list of proposed interventions is then compiled for each entity. Ranking of temporal urgency for intervention and/or mitigation provides guidance regarding entity prioritisation and potential for implementation of new technologies. The proposed interventions can then be applied in the integrated water balance model and non-operational water management risk assessment. Evaluation can then be repeated assuming the proposed interventions are implemented. The evaluation will indicate if the proposed interventions are expected to decrease the likelihood of legacy effects by comparing the re-evaluated environmental and financial ranking of the proposed interventions to the results of preceding evaluation iterations. This provides a final risk ranking when further iterations show no notable variance. Using the final ranking the most effective proposed interventions can then be recommended with the ranking indicating the recommended temporal priority.

Example Case Study

An integrated mine water balance model in GoldSim for an open cast platinum mine in South Africa is used to demonstrate the proposed cyclic methodology for a non-operational water management risk assessment. This example simplifies the list of mine entities in the assessment to avoid repetition of entities within the integrated mine water balance. The simplified list of entities includes an open pit, pollution control dam (PCD) containing stormwater runoff from a waste rock dump (WRD), PCD containing stormwater runoff from the concentrator plant area, tailings storage facility (TSF) and the TSF return water dam (RWD).

The legacy effects that the mine poses are the contamination of mine affected and surrounding areas; as well as contamination of water resources (surface and groundwater) in the area. In addition, the mine has altered the natural landform of the mining area which has resulted in land disturbances. These legacy effects were considered when compiling the evaluation criteria for the mine. A list of environmental aspects considered at each entity together with the financial aspects of the proposed interventions, with weighted percentages, were compiled (Table. 1). The evaluation criteria for the environmental and financial aspects were then determined (Table. 2).

The integrated mine water balance assumes that production was suspended, and all major operations ceased. It was assumed that the open pit did not pump any water and a pit lake formed. No ore was processed at the concentrator and thus no slurry was deposited on the TSF. The water balance also assumed that the water storage facilities were required to contain all stormwater generated from associated catchments and no additional water was imported to the mine. Using these assumptions, the initial environmental risk evaluation was undertaken, and each entity was ranked according to the lowest environmental score (Table. 3).

Table 1 *Environmental and financial aspects with associated weight percentage.*

Environmental			Financial		
Aspect	Description	Weight (%)	Aspect	Description	Weight (%)
Discharge Risk	Discharge risk to the environment from water storage facilities	30	Capital cost	New required infrastructure and/or upgrades/changes to the current system.	40
Land disturbance	Footprint of dirty catchment areas	10	Operational Cost	Pumping costs and ongoing maintenance	30
Open Pit System	Water quality and quantity in the unused pit/s	20	Permitting	Timing, specialist studies, approval viability	30
Contamination	From water storage facilities through discharge or seepage	40			
Sub-total		100	Sub-total		100

Table 2 Environmental and financial evaluation criteria.

Aspect	Rating			
	1	2	3	4
Environmental				
Discharge Risk	<1:1 year discharge risk	<1:10 year discharge risk	<1:50 year discharge risk	No change to discharge risk
Land disturbance	Major effect to environment	Minimum effect to environment	Effect limited to already affected areas	Reduction in already affected areas
Open Pit System	Seepage from pit to environment and effect to pit water quality	Major effect to pit water quality	Moderate effect to pit water quality	No charge
Contamination	Serious effect & impairment of ecosystem	Moderate effect to environment	Minimum effect to environment	No lasting effects
Financial				
Capital cost	Major upgrades / changes	Moderate upgrades / changes	Minor upgrades / changes	No upgrades/changes
Operational Cost - Pumping distance	>10km	<10km	<5km	<2km
Operational Cost - Maintenance	Major pumping required	Moderate pumping required	Minor pumping required	No additional pumping required
Permitting	Potentially nonviable	Viable, 3–5 years reg. process	Viable, 1–2 years reg. process	Within current Water Use Licence / Environmental Impact Assessment

Table 3 Environmental evaluation and ranking.

Aspect	Entity Rating				
	Open pit	PCD - WRD	PCD - Concentrator Plant	TSF	RWD-TSF
Environmental Score (%)	68	78	53	78	45
Environmental ranking	3	4	2	4	1

The ranking (Table. 3) indicated that the TSF RWD and concentrator PCD should be prioritised as these entities had the highest risk ranking, followed by the TSF, and then lastly the open pit and PCD containing stormwater runoff from a WRD. An intervention for each entity was identified and applied in the water balance. The proposed interventions for the TSF RWD included pumping excess stormwater from the RWD to the open pit, commencing with rehabilitation of the TSF side-slopes and reducing external clean water catchments. For the concentrator PCD proposed interventions included commencing with rehabilitation of the concentrator area to reduce dirty catchments and pumping excess stormwater to the open pit. The care and maintenance and rehabilitation plan for the TSF should commence and concurrent rehabilitation of WRDs should be considered. At the open pit, a pit lake study should be undertaken.

The evaluation for each entity was reiterated with these interventions and an updated risk ranking complied. A final risk ranking was then determined by combining the environmental and financial results (Table. 4). From the final risk ranking it can be inferred that the future mine planning should investigate the implementation of an integrated pumping system to allow all stormwater dams to pump to a central facility or pit where water can be contained and managed. The TSF care and maintenance and rehabilitation plan should continuously be updated throughout the life of the facility when major operational changes occur to ensure its continued validity. A closure

Table 4 Final environmental and financial evaluation and ranking.

Aspect	Entity Rating				
	Open pit	PCD - WRD	PCD - Concentrator Plant	TSF	RWD-TSF
Environmental Score (%)	68	80	70	78	55
Environmental ranking	2	5	3	4	1
Financial Score (%)	75	65	50	58	50
Financial ranking	4	3	1	2	1
Final ranking	4	5	2	3	1

pit lake assessment should be undertaken and anticipated effects on the groundwater sources in the area quantified. Lastly concurrent rehabilitation of WRDs should be considered in the current water management plan of the mine.

This case study demonstrates that the quantified ranking of the rehabilitation schedule could decrease legacy effects in future as proven by the increasing environmental scores of the reiterated assessment when compared to the environmental scores in the initial assessment. This methodology can thus be applied cyclically to assist in the identification of possible interventions or new technologies to minimise legacy effects throughout the life cycle of the mine.

Conclusions

The example case study illustrates how the proposed methodology can be used in practice. Applying this methodology cyclically has been quantifiably proven by this study to assist in the identification and sequential implementation of mitigation measures relating to potential legacy effects from the evaluated entities of the mining operation. This allows for a pro-active approach in identifying possible interventions while compiling the water balance for prevailing site conditions. Documenting these recommendations as part of a water balance project can be used in future mine planning to aid in reducing legacy effects.

Acknowledgements

The author would like to thank Jones & Wagener for the opportunity and Altus Huisamen for his guidance and input.

References

Department of Water Affairs and Forestry, 2006. Best Practice Guideline G2: Water and Salt Balances. South Africa.

Julien, M.R., Gowan, M., Nalecki, P. and Kissiova, M., 2005. Water balance and its integration in mine operation through the use of real-world systems modelling tools. In 2005 Symposium Mines and the Environment, Rouyn-Noranda, Quebec, Canada.

Krogerus, K. and Pasanen, A., 2016. Management of water balance in mining areas–WaterSmart.

Nalecki, P. and Gowan, M., 2008. Mine water management–Dynamic, probabilistic modelling approach. Rapantova, N. & Hrkal, Z, pp.533-536.

Punkkinen, H., Räsänen, L., Mroueh, U.M., Korkealaakso, J., Luoma, S., Kaipainen, T., Backnäs, S., Turunen, K., Hentinen, K., Pasanen, A. and Kauppi, S., 2016. Guidelines for mine water management. VTT Technology, 266, pp.1-157.

Challenges of Water Management at the Uranium Mining Site Schlema-Alberoda of Wismut (Germany)

Andrea Schramm[1], Dr. Jürgen Meyer[2], Thomas Metschies[1], Dr. Ulf Jenk[1]

[1]Wismut GmbH, Jagdschänkenstr. 29, 09117 Chemnitz; 2former Wismut GmbH, Jagdschänkenstr. 29, 09117 Chemnitz

Abstract

In 1991, Uranium mining at Schlema-Alberoda (Saxony) finally ceased. In 45 years of operation the mine produced some 80,000 tons of Uranium. Numerous waste rock dumps deposited in the immediate vicinity of residential area as well as a tailings pond subsequently shaped the townscape of Schlema. Since the end of Uranium mining, a number of remediation measures have been realised above and below ground, which minimise the environmental impact. The article indicates that the remediation measures were able to considerably reduce the pollutant load in the Zwickauer Mulde stream.

Keywords: Uranium mining, water management, sustainable remediation

Introduction

From 1946 through 1990, the SAG/SDAG Wismut Company mined uranium ore in the territories of Saxony and Thuringia of the reunified Germany. By the end of 1990, a total of about 216,000 tonnes of uranium had been produced at a number of sites in the southern part of East Germany (Schramm *et al.* 2013). The mining legacy included 1,500 km of open mine workings, 311 million m³ of waste rock and 160 million m³ of radioactive sludge (tailings) located in densely populated areas.

During the production phase from 1946 to 1990, the Schlema-Alberoda site in Saxony, produced approx. 80,000 tonnes of uranium. Remediation of the Schlema-Alberoda mine is a huge challenge as the underground workings on 60 levels were reaching down to –1,800 m. As a consequence, 21 waste rock dumps (WRD) with a total volume of about 47 million m³ deposited in the immediate vicinity of residential areas as well as a tailings pond subsequently determined the townscape of Schlema.

In 1991, Wismut GmbH, being the successor company to SDAG Wismut and restructured as a federally owned company, started to remediate the legacies left behind. Controlled flooding of the Schlema-Alberoda mine was initiated in 1991 accompanied by the gradual decommissioning of the underground mine dewatering system. The in situ remediation of the majority of the WRDs at the site started in 1992. This was the beginning of a series of remediation measures to avoid danger for the affected population, to reduce emitted pollutant loads and thus to improve the status of surface waters, especially in the Zwickauer Mulde stream.

Initial Situation and environmental impact at the remediation site

The Wismut Act regulating the remediation of Uranium mining in Saxony and Thuringia came into force in December 1991. This set the course for a federally financed remediation of the legacies of Uranium mining above and below ground. First, priority lists and remediation concepts for the Wismut sites were created with the participation of experts from Germany and abroad. Thus, work was initiated with the aim of reducing the risk potential for people and the environment.

At the Schlema-Alberoda site, the remediation concept included the following tasks:

- decommissioning and safekeeping of the mine Schlema-Alberoda in accordance with the rules of the Federal Mining Act and the Radiation protection regulations, while the safekeeping of the mine near the surface had special priority
- controlled flooding of the Schlema-Alberoda mine including an adapted

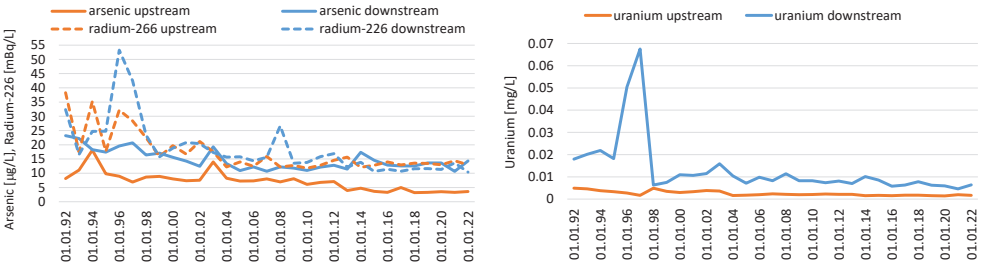


Figure 1 *Uranium, radium-226 and arsenic concentration in the Zwickauer Mulde stream*

monitoring (geomechanics, hydrogeology, radiation protection, mine ventilation, mining damage)
- remediation of WRDs, preferably in-situ, including profiling, covering, planting, hydraulic engineering and road construction
- remediation of the Borbachtal tailings pond by dry in-situ stabilisation and subsequent covering with waste rock material and mineral soil
- water treatment of contaminated mine and seepage water as well as the safe storage of the residues of water treatment
- long-term monitoring (soil, water, air, biosphere).

Due to the geological situation, the release of the accumulated weathering products by the mine flooding and the discharge behaviour at the site, the focus of environmentally relevant emissions is at uranium, radium and arsenic. Figure 1 shows the concentrations of uranium, radium-226 and arsenic at a measuring point before (upstream) and after the Wismut mining area (downstream) in the Zwickauer Mulde stream. The loads can be calculated based on the concentration differences between the two measuring points and using the official flow rates assigned to river gauges. In the case of arsenic, the background concentration of the Zwickauer Mulde stream is already increased by the historical ore mining and ore processing in the Schneeberg mining area (not under responsibility of Wismut GmbH) and is additionally influenced by the mine water and seepage water of Wismut uranium mining.

For the period from 1992 to 1998, before the water treatment plant (WTP) Schlema-Alberoda was put into operation, a mean annual load increment of approx. 9,200 kg uranium, approx. 2,600 MBq radium-226 and approx. 3,800 kg arsenic was calculated as input between the two measuring points using this balancing method. With the effects of the remediation measures described below, it was possible to reduce the mean annual load increment in the period 2016 to 2022 to approx. 1,400 kg uranium and approx. 2,800 kg arsenic. The current analysis result of radium-226 is often below the limit of quantification, particularly at the downstream measuring point. This clearly limits the evaluation using this balance sheet method. Theoretically, no load increase for radium-226 can be detected in the remediation area for the current period. Balance uncertainties are primarily due to measurement error in stream flow measurement.

Chronology of remediation measures

The main surface and underground remediation measures at the Schlema-Alberoda uranium mining site are described below in chronological order.

Mine Flooding and water treatment

The dense network of working levels between the shafts extends up to 1.8 km below valley level and acts as an intensive water drainage. The Schlema-Alberoda mine has a floodable cavity of 36.5 million m³. The mine workings represent a complex system of linear mining cavities that are spatially connected to each other. Between 1991 and 1997, the pumping stations in the Schlema-Alberoda mine, which had been staggered over the depth, were gradually liquidated. The mine cavities were flooded step by step. At the same time

other measures were realised to secure the long-term success of this mine remediation (prevention of surface subsidence by safekeeping of mine cavities, ventilation of open levels). By the end of 2000, the influx of some 32 million m³ had filled approximately 87% of the open mine volume. By reaching the level -120 m level (212 m a.s.l. – above sea level), the dynamic part of the mine flooding at the Schlema-Alberoda site was completed.

In 1999, after detailed planning, the new WTP went into operation. With the commissioning of the WTP, the mine flooding could be continued in a controlled manner. Two years later, the treatment capacity was expanded to a maximum of 1,150 m³/h with a second sub-system. Until 2007, the remaining flooding took place step by step to the-30 m level, where a working and buffer storage of the WTP Schlema-Alberoda will be operated for the long term (0.52 million m³). The mining containment work at a level of up to 300 m a.s.l. was completed in 2007.

Since 2009, the collected seepage water (WRD 371/I) with the highest loads has been treated for the main purpose of separating uranium. A separate ion exchange treatment was set up and put into operation. Although this was operated as intended, various procedural deficiencies occurred. The ion exchange process caused a much higher manual support effort than planned. Therefore an alternative procedure had been discussed with the authorities. After approval the alternative approach, hydrotechnical reconnection work was carried out in 2014 to discharge the seepage water into the underground mine where it was included into the treatment at the WTP. For some less significant seepage streams at the site, a discharge into the mine was also realized in connection with the remediation of the assigned dump objects.

Another remediation measure was the mining expansion of a new connecting adit ("Südumbruch") to the historical Markus Semmler adit in the Oberschlema deformation area to ensure the free drainage of mine water from the neighbouring former Schneeberg ore mine (initial operation autumn 2018). With the implementation of this measure, a probable overloading of the WTP Schlema-Alberoda by the contaminated water from the Schneeberg historical ore mine is excluded in the future.

Since 2008, the mined cavity between 300 and 316 m a.s.l. has been used as an internal mine storage to buffer high inflow rates or reduced capacity due to maintenance at the WTP. This internal storage has been expanded to 287 up to 316 m a.s.l. due to different reasons. These include shaft safekeeping, as well as risk preparedness during the pandemic (staff shortages) and a possible response to shortages of treatment chemical supply. Regarding the supply shortages for treatment chemicals, the discharge of seepage from WRD 371/I was stopped in October 2022 in order to reduce the treatment volume.

The amount of water to be treated annually at WTP Schlema-Alberoda varies between 4.3 and 9.5 million m³. Uranium, radium, arsenic, iron, and manganese have to be removed from the water rising from the Schlema-Alberoda mine site to reach compliance with regulatory standards prior to discharge into the Zwickauer Mulde stream. The water is pumped from the mine and fed to the WTP Schlema-Alberoda for treatment. The plant consists of two nearly identical treatment lines and includes several process stages for the physical-chemical precipitation of the pollutants. It has been technically expanded and optimised several times.

Water treatment residues are immobilised and the resulting crumbly product is then disposed into an engineered storage cell at WRD 371. Treatment of the mine water will have to continue until contaminant levels will be below regulatory standards to allow direct discharge into the receiving stream. Until 2011, the flooding was controlled with the pump system in shaft 208, which tapped the flooding water from the depth range below 500 m. After that, the flooding was controlled via the new pumping system in the investigation cavity UG 212 as near-surface tapping from the -60 m level (270 m a.s.l.). Depending on the development of the concentration of the flooding water, the treatment will have to be continued in the medium to long term until the treatment goals are reached. In Figure 2, the flooding process was illustrated graphically and linked in time

to the development of the concentrations in the flooding water and to the progress of the remediation of the dump objects.

Remediation of WRDs

Beside flooding and water treatment, another important task of Wismut is to remediate numerous WRDs. Remediation by covering of WRDs has to meet several criteria: Cover systems have to safely contain the waste rocks, control direct radiation and emissions, control percolation through the cover and offer good conditions for projected vegetation type (Schramm *et al.* 2013). The design of the two-layer-cover at Schlema-Alberoda site was optimised considering site-specific boundary conditions and remediation objectives. The primary objective of the cover system was not to control the cover percolation rate and thus oxygen ingress but to reduce radon emission. Secondary, the interaction of cover and vegetation shall increase the evapotranspiration as main component of the water balance (Schramm *et al.* 2015).

The largest waste rock dumps in the Schlema-Alberoda mining area were left in place to be rehabilitated in situ (without a base sealing). This involves regrading of the slopes. Finally, they are capped with a one-metre-thick cover consisting of a sealing/storage layer and a humus-rich topsoil to enhance vegetation growth. Comprehensive work was done with regard to the construction of trails and in terms of hydraulic engineering work. As the last step the WRDs were vegetated (initial with grass, later planted with trees). In some cases, concepts for subsequent use have been implemented on the WRDs, such as the construction of a golf course or model airfield.

For preserving and maintaining the remedial performance, maintenance and environmental monitoring will have to be conducted for several years. At the moment, 98% of the WRDs at the Schlema-Alberoda site have been rehabilitated. The WRD 371/I with the depository of the residues from the water treatment is considered to be the last project of the WRD rehabilitation. However, storage of residues from the WTP will remain in operation in the long term.

Load Balancing

The main part of the liquid discharges into the Zwickauer Mulde at the Schlema-Alberoda site comes from the Schlema-Alberoda uranium mine. The focus of contamination is uranium, followed by arsenic and radium-226. Further pollution comes from the WRDs, where long-term weathering processes and leaching by the infiltrating waters result in a contaminant release. The comparison of the loads caused by uranium mining at the beginning of the remediation (1990 – 1999) with those of the last ten years (2013 – 2022) shows a distinct reduction of loads, especially for uranium and radium (Table 1). In the case

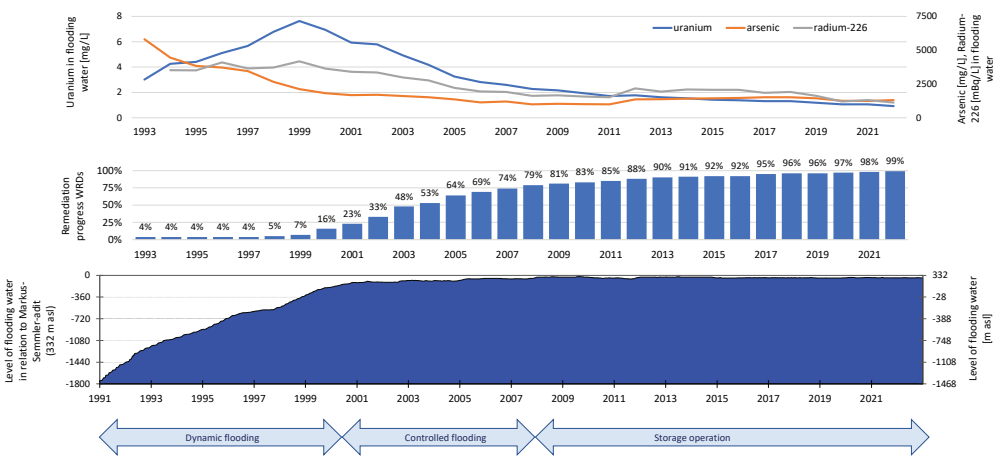


Figure 2 *Chronological classification of the remedial measures: flooding process, development of concentrations in flooding water and progress of dump remediation*

Table 1 Liquid discharges from Wismut remediation objects at the Schlema-Alberoda site

Years	Uranium [kg/year]	Radium-226 [MBq/year]	Arsenic [kg/year]
1990–1999	5120	1460	850
2013–022	1190	180	410

of arsenic, a high level of mobilization in the upstream of the Wismut remediation area is visible. There are a number of diffuse sources that are related to the historical ore mining/processing in the Schneeberg mining area.

The primary loads in the remediation area, which are caused by uranium mining, would be significantly higher (uranium: approx. factor 7, arsenic: approx. factor 15 to 20) without taking into account the water treatment of mine water and the collection and treatment of contaminated seepage water. These data underline the effectiveness of the complex and overlapping rehabilitation measures between 1990 and the present day.

Irrespective of this, the contribution of the mine water of uranium mine Schlema-Alberoda to the total load at the site remains dominant. With regard to the share of loads from dump objects, only uranium is relevant. The highest loads come from WRD 371, from the Borbach valley and from WRD 382 West. Figure 3 shows the load contributions for the period 2014 to 2021 including the load contribution from the Schneeberg mining area. The load balance is based on regular quantity and concentration measurements at the marked measuring points (reliable results).

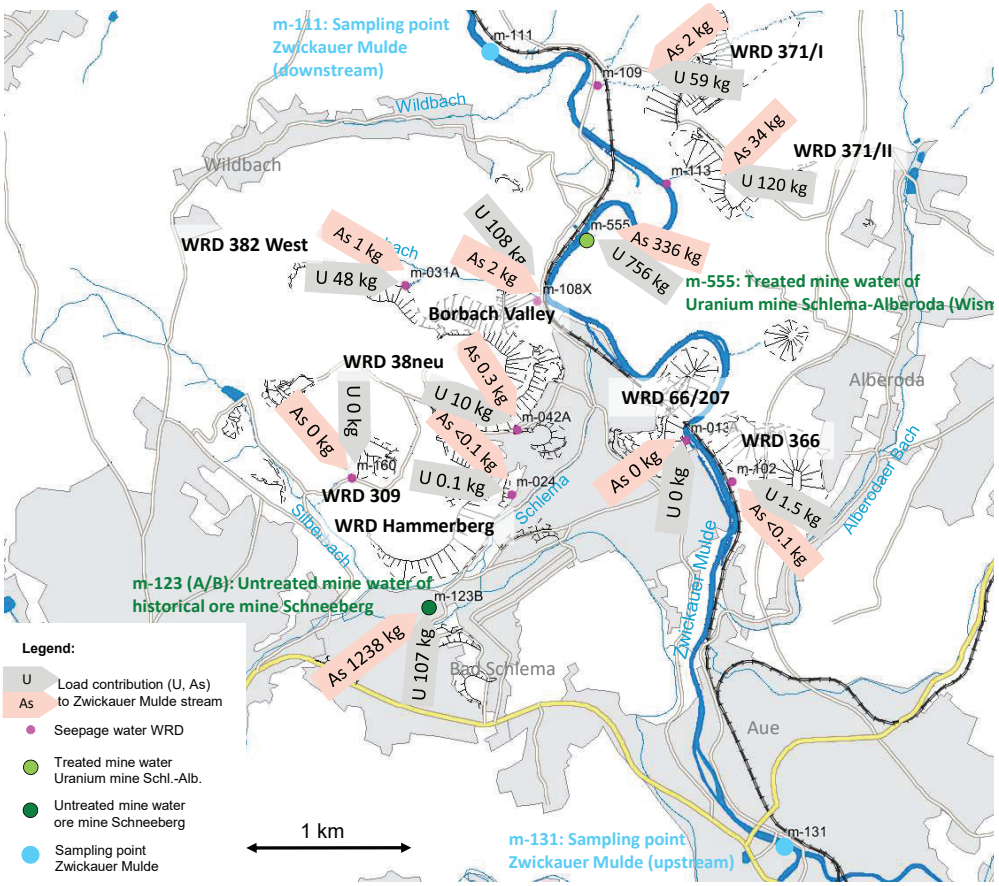


Figure 3 Real uranium and arsenic loads at Schlema-Alberoda site (period 2014–2021)

Conclusions

The target reduction of liquid contaminant loads at the Schlema-Alberoda site caused by uranium mining through the complex remediation measures described above has been successful. The most effective remediation measure is the treatment of contaminated mine water as the largest source of the uranium mining site Schlema-Alberoda. One of the current challenges in water management is the modernisation of the Schlema-Alberoda water treatment plant. The operation of the treatment plant has to be adapted to the changing conditions in the long term, e.g. with regard to the water quantities to be treated, the raw water qualities as well as the requirements on the plant performance (Paul *et al*. 2015). At the same time, immobilisation must be optimised.

The costs of water treatment, which have currently risen to approx. 1.3 €/m³ (mine water inlet, treatment, storage of residues, personnel, analysis), and monitoring costs of approx. 567,000 €/year (analysis, personnel, sampling and maintenance for groundwater and surface water monitoring) must also be taken into account. Both optimisation of procedures/processes and reduction of the scope of analysis are to be reviewed regularly.

A further gradual reduction of load inputs (especially uranium) to Zwickauer Mulde stream, is expected due to the implemented remediation measures. In the medium term, the completion and effect of the dump remediation and the long-term flooding of the mine including the water treatment will have a positive effect. With the targeted remediation of the mining area at Schlema-Alberoda site, Wismut meets the current objectives of the legislator for the gradual and sustainable improvement of water quality in accordance with the European Water Framework Directive.

Acknowledgements

The authors would like to thank everyone who was actively involved in the remediation measures to reduce the environmental impact at the Schlema-Alberoda site through collegial cooperation.

References

Paul M, Meyer J, Jenk U, Kassahun A, Schramm A, Baacke D, Forbrig N, Metschies T (2015) Kernaspekte des langfristigen Wassermanagements an den sächsisch-thüringischen Wismut-Standorten. Proceedings des Internationalen Bergbausymposiums WISSYM 2015, Bad Schlema, Germany, pp. 71-85

Schramm A.; Roscher M. (2013): Two-layer soil covers on selected radioactive waste rock dumps at WISMUT: results of more than 10 years of hydrological monitoring. Proceedings of the Eighth International Conference on Mine Closure, Cornwall, England, pp. 207-220

Schramm A.; Löser R. (2015): Results of long-term investigations of water balance aspects of covered waste rock dumps at the Schlema-Alberoda site. Proceedings des Internationalen Bergbausymposiums WISSYM 2015, Bad Schlema, Germany, pp. 273-282

Cost Effective Method to Depressurise Perched Aquifers to Prevent Slope Failures in Open-Pit Mines, South Africa

Heinrich Schreuder[1], Paul Joël Havemann Lourens[1], Petrus Daniel Vermeulen[1], Rolene Lubbe[1]

[1]*Institute for Groundwater Studies, University of the Free Sate, PO Box 339, Bloemfontein, 9300, South Africa, lourenspjh@ufs.ac.za, vermeulenpd@ufs.ac.za, lubber1@ufs.ac.za*

Abstract

Effective depressurising and/or dewatering of localised perched aquifers at open pit mines is often overlooked. An investigation was initiated to develop a practical and cost-effective solution to depressurise a localised perched aquifer and if successful develop a step-by-step guide for similar scenarios. The depressurisation system was designed and installed based on the conceptual model that was constructed by conducting a detailed survey of seepage zones along the highwall of the open pit mine and reviewing available geological, hydrogeological, and geotechnical data. The investigation concluded that it is possible to develop a practical and cost-effective solution to depressurise localised perched aquifers.

Keywords: Depressurisation, slope failure, perch aquifer, open pit mine

Introduction

The depressurising and/or dewatering of localised perched aquifers at open pit mines is often overlooked. The focus generally remains on lowering the regional groundwater level to below the lowest mining elevation. Perched aquifers within the study area have led to seepage zones directly linked to slope failures within the softer geological layers/units, causing a risk to mine safety and production. A perched aquifer is an aquifer that is isolated from the regional water table and is generally a relatively small body of water with an impermeable base underlain by an unsaturated zone (DWA 2011).

Conventional depressurising systems (such as in-pit horizontal drain holes and sumps) requires large capital expenses. A practical and cost-effective solution was required to abstract and dispose of the groundwater at the source.

Materials and Methods

A desktop study was completed to understand the nature of the highwall failures by reviewing the available hydrogeological-, geotechnical-, and geological conceptual site models in conjunction with pit face mapping. This information was used to design a practical and cost-effective depressurisation system.

A cost-benefit analysis was conducted that compared the capital expenditure between the proposed depressurisation system and conventional slope protection mechanisms at high-risk slope failure areas. The capital expenditure required for rehabilitation if single-and multi-bench failures was also included in the analysis.

The depressurisation system installed, consisted of abstraction, injection, and monitoring boreholes. The pore pressures at the study area were monitored for a period of nine months (baseline data) before the pumps for groundwater abstraction was commissioned. Abstraction took place over a period of 26 months.

Site Description

Topography and Climate

The surface elevation at the mining site ranges between 1210 and 1305 mamsl and slopes towards the south. To the west of the mining area, prominent hills striking north to south, rise above the plains.

Climatic conditions are semi-arid, with an annual rainfall (MAP) that ranges between 300 mm and 500 mm. Rainfall is received in

the summer months and generally in the form of thunderstorms. The average maximum temperature ranges between 17 and 31 and the average minimum temperature ranges between 6 and 21 (South African Weather Service 2019)

Regional Geology

The study area lies geologically within the Paleoproterozoic Transvaal Supergroup, deposited within two distinct fault-controlled basins known as the Transvaal- and the Griqualand West Basins(Alchin and Botha 2006). The basins formed on the rocks of the Archean Kaapvaal craton during the intracratonic extension on the stable Kaapvaal-Limpopo-Zimbabwe block. The Transvaal basin contains a succession of siliciclastic and volcanic rocks, while the Griqualand West basin consists mainly of volcanic rocks and chemical sediments such as the Postmasburg Group (fig.1).

Local Geology

The study area is located within the Griqualand West Basin of the Transvaal Supergroup at the southern tip of a narrow north-south trending belt of iron- and manganese-bearing lithologies within the southern extent of the Maremane Dome and the western edge of the Kaapvaal Craton (fig. 2). The underlying geology of the region was subjected to protracted series of events (Thomas and Basson 2015) such as intensive structural

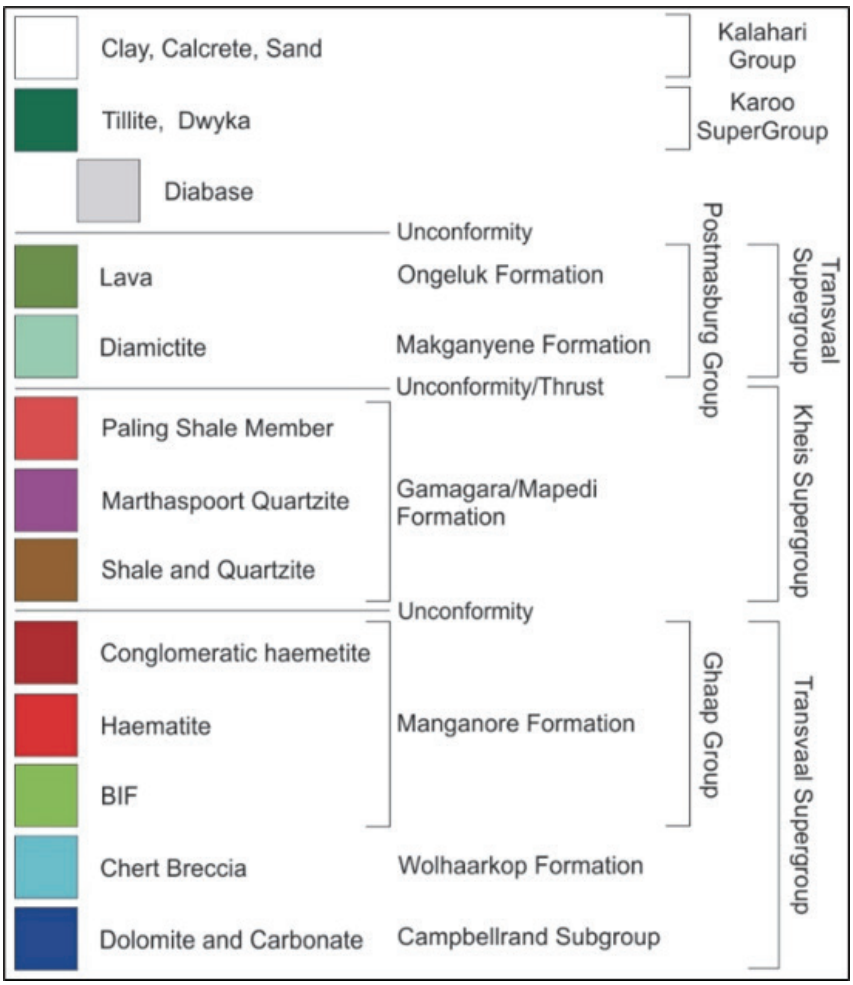


Figure 1 *Simplified lithostratigraphy (Steenekamp 2005)*

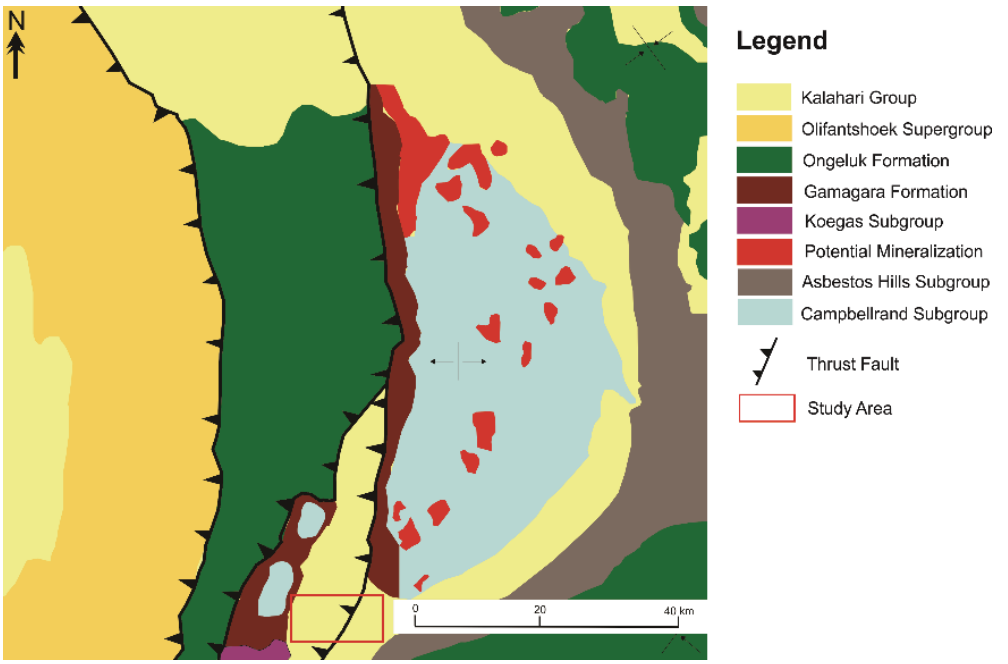


Figure 2 Simplified geology map (modified from Carney and Mienie 2003)

deformation in the form of thrusting, folding, and faulting that led to a series of northwest-southeast (NW-SE) striking fracture zones (Carney and Mienie 2003).

Hydrogeology

Three significant aquifers have been identified in the area (fig. 3) (Viljoen 2006). The first is the upper semiconfined to unconfined primary aquifers that occur in the sand and calcrete underlain by a clay mainly tillite in most cases with yields of less than 2 L/s. The aquifer usually develops on contact between the calcrete and the underlying clay formation of the Kalahari Group. The surrounding communities mainly use this aquifer for potable, and livestock water and the groundwater are on average 0-60 mbgl. This investigation focuses on the perched aquifers within the Kalahari Group, which mainly comprises the calcrete cut off from the fractured rock aquifers below by the tillite that acts as an aquitard.

The second aquifer is associated with fractures, fissures and joints, and other discontinuities within the older Transvaal Supergroup geology, primarily within the banded iron formation, hematite, gabbro, and chert breccia. The yield consistently pumps within the fractured rock aquifers varies from 1 L/s to 40 L/s at an average depth from 60 m to 120 m.

The third and highest yielding aquifer is located within the permeable dolomite. Groundwater is found within an interconnected karst and fractured rock dolomitic aquifer that produces yields from 20 L/s – 60 L/s at depths of between 120 m to 400 m.

The natural groundwater level has been lowered, and the absence of seepage into dry monitoring boreholes indicates that the geology has been dewatered to below 200 mbgl in the vicinity of the mine pit. The groundwater intercepted in the pit is predominantly situated within dolomitic fractures. The water level drawdown from the mine dewatering programme is relatively homogeneous within a two-kilometre radius around the study area. The natural groundwater flow direction is in a north to south direction. The main water-bearing geological structures feeding the fractured rock aquifers were found to be vertical or near-vertical northwest to southeast (NW-SE) faults (fig. 4).

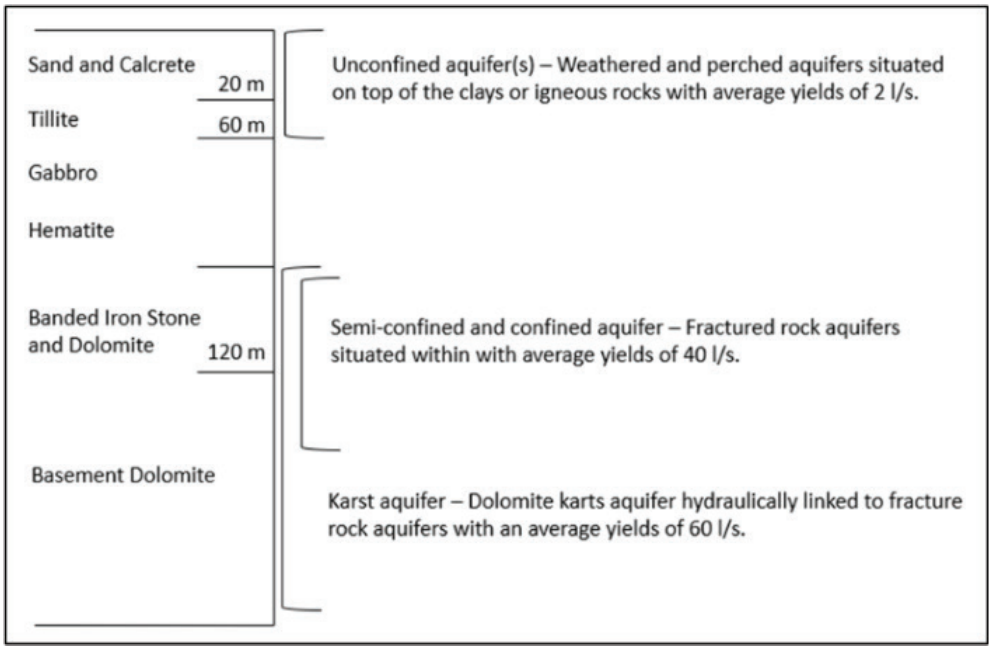


Figure 3 *Aquifers and associated lithological units*

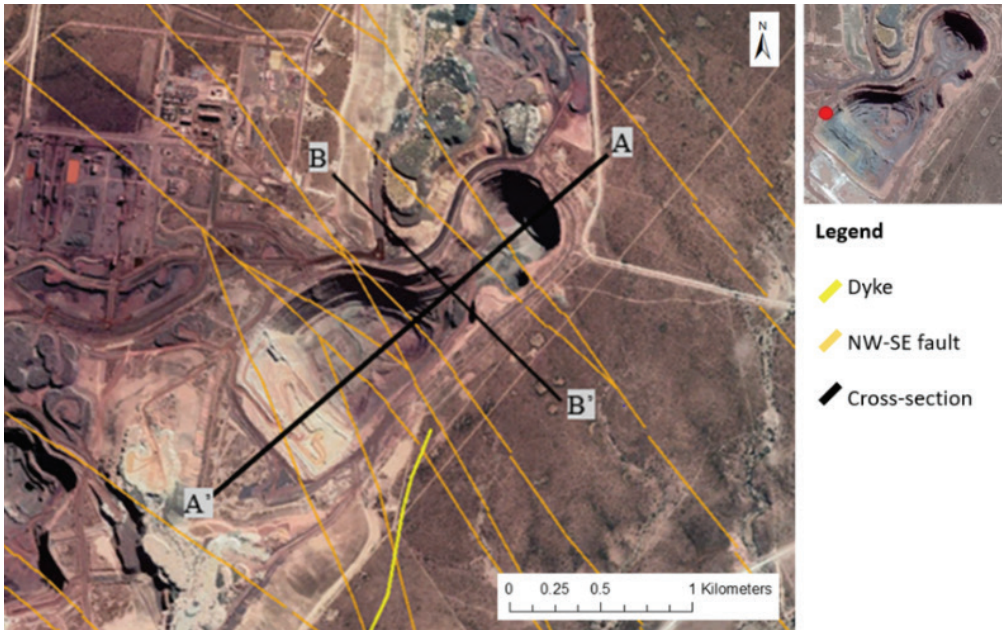


Figure 4 *Major geological structure superimposed on the mining pit*

Results and Discussion

The perched aquifer has been identified as isolated pockets of groundwater situated within the unconfined upper weathered aquifer with two phreatic zones within the Calcrete (Phreatic Level1) and Clay/Tillite (Phreatic Level 2) lithologies on the western side of the mine pit (fig.5). The regional water level within the mining area has been lowered to 250 mbgl. The phreatic zones indicated that the shallow groundwater levels of 8 mbgl in the calcrete and 55 mbgl in the clay/tillite show that the perched aquifer is disconnected from the major fracture rock aquifers and can be identified as perched as per the definition.

Face Mapping

The face-mapping identified six main seepage zones on the third, fourth, and fifth bench (10 m benches) of the western wall of the mining pit (fig. 6). A series of slope-parallel faults also occurs (fig. 6). It was estimated that there was at least 200 kPa driving pressure along the highwall before failure occurred (Beale 2017).

Depressurisation System Design

The depressurisation system was designed based on the seepage zones identified. The system design is illustrated by fig. 7. The basic system is designed to allow for water to be abstracted at the abstraction boreholes and then injected at injection boreholes which targets dolomitic aquifer. The water levels and pore pressures response to abstraction can then be measured with the vibrating wire piezometers (VWP) installed in the monitor ing boreholes.

Cost Benefit Analysis

Based on a high probability of failure for the study area, the financial expenditure was calculated, and three options were considered: i. No mitigatory actions and allow for slope failure repair should a controlled failure take place; ii. install geotechnical controls in the form of catch fence and wire mesh to control rockfall, and iii. Installing a slope depressurisation system to reduce the probability of failure to acceptable levels. The comparison between the different approaches indicates that installing a depressurisation system is more cost-effective than the other approaches (tab. 1).

Depressurisation System Results

The pressure head in both the calcrete and tillite indicated a sharp decline when the depressurisation system was commissioned

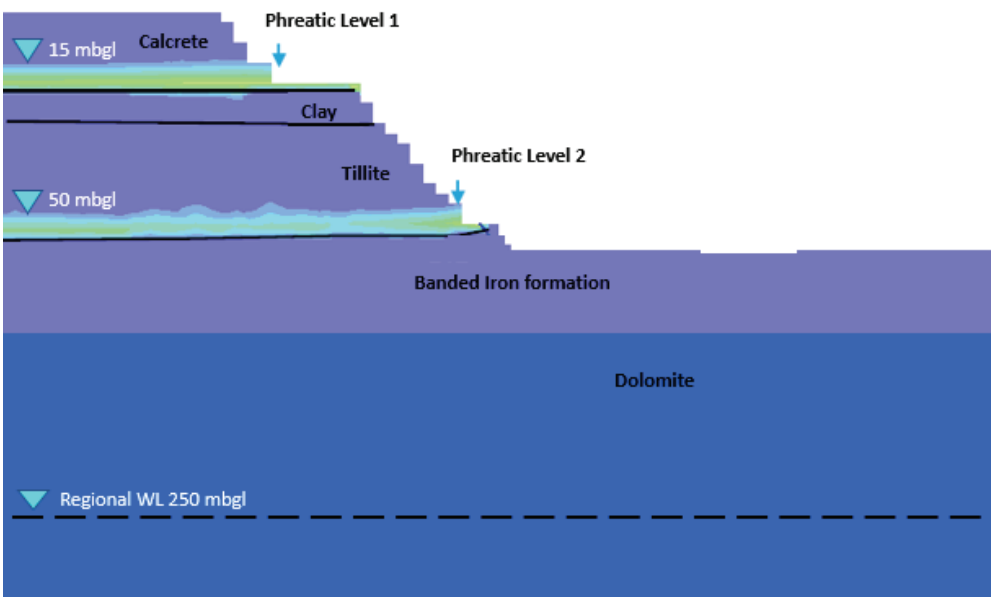


Figure 5 *Perched aquifers phreatic zones*

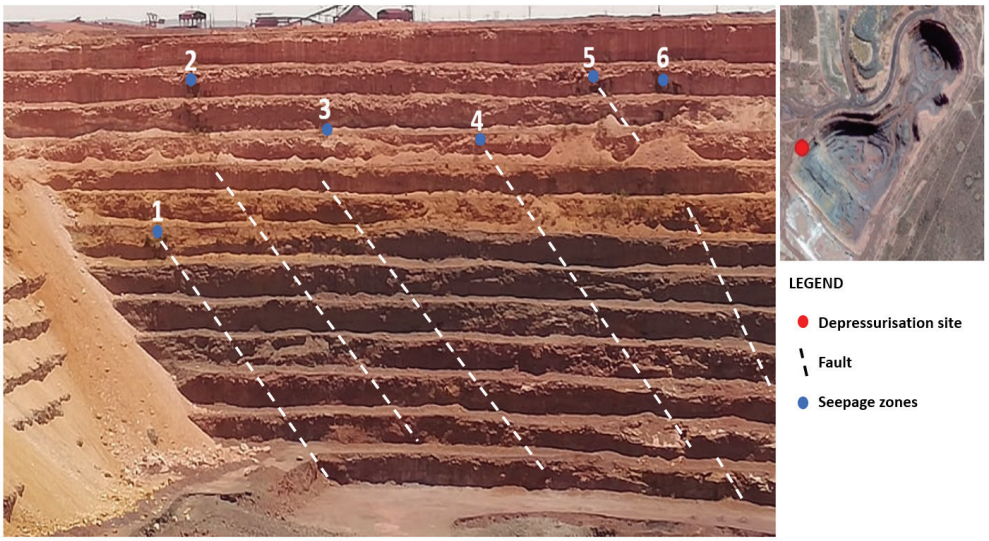


Figure 6 Seepage zones along the western wall

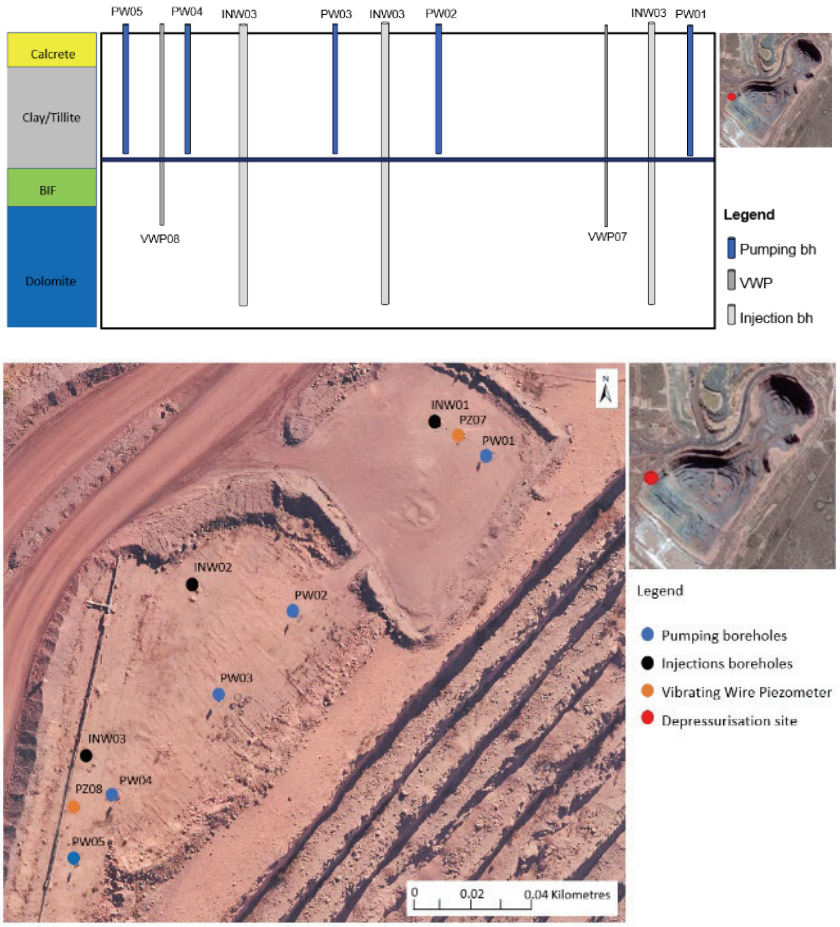


Figure 7 Depressurisation system design

Table 1 Estimated expenditure comparison

Slope Failure Rehabilitation			
Item	Single bench	Double bench	Triple bench
Slope failure repair – material removal	R 2 400 000	R 4 800 000	R 7 200 000
Gross revenue loss – no expit ore	R 12 849 315	R 19 273 972	R 25 698 630
Total	R 15 249 315	R 24 073 972	R 32 898 630
Installing geotechnical controls			
Geotechnical Catch Fence	R 4 000 000	R 4 000 000	R 4 000 000
Geotechnical Wire Mesh	R 560 000	R 1 120 000	R 1 680 000
Radar Deployment and monitoring	R 5 000 000	R 5 000 000	R 5 000 000
Total	R 9 560 000	R 10 120 000	R 10 680 000
Depressurisation System			
Drilling Cost			R 4 788 000
Equipment -Vibrating Wire Piezometers			R 800 000
Equipment - Solar Pumps			R 175 000
Installation			R 250 000
Total			R 6 013 000

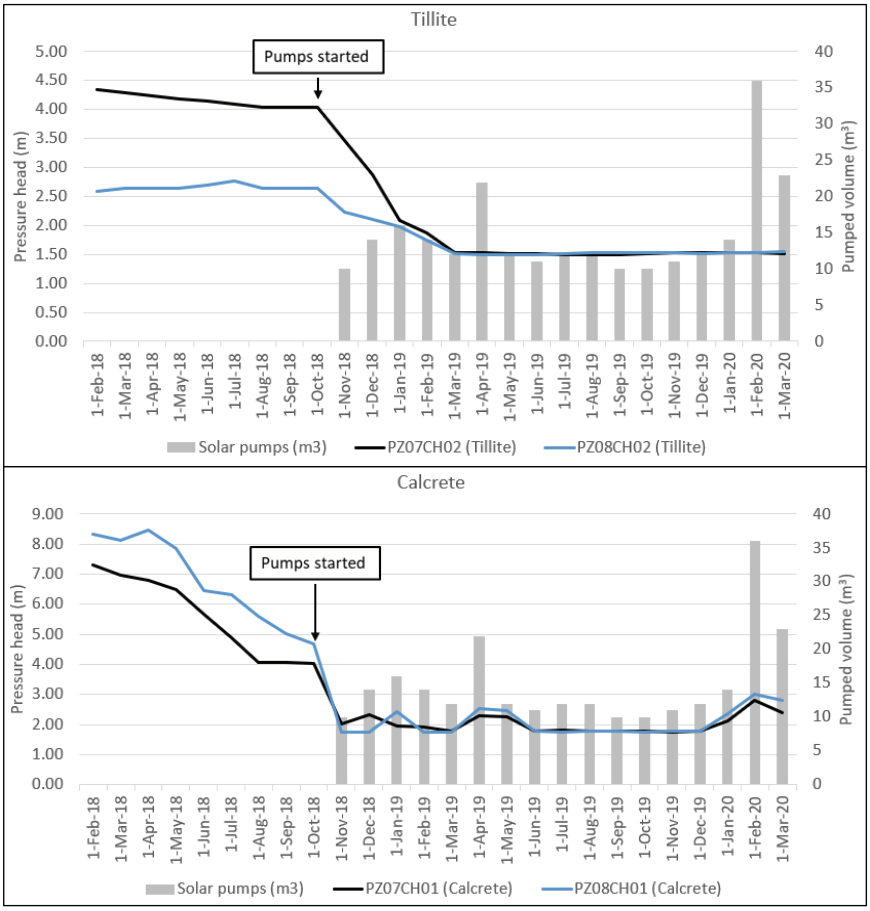


Figure 8 Pressure head change in the calcrete and tillite

(fig. 8). After the initial decline, the pressure head in the calcrete and tillite remained stable, therefore indicating that the pore pressures could be lowered and maintained at acceptable levels. These results prove that the depressurisation system is effective and can reduce the risk of slope failures.

Conclusions

The depressurisation system effectively reduced and maintained the highwall pore pressures to acceptable levels, therefor illustrating that it is possible to develop a practical and cost-effective solution to depressurise localise perched aquifers.

The lessons learned from the investigation were used to develop a step-by-step guide to plan, finance, implement, and monitor a depressurisation system in similar hydrogeological and geotechnical conditions. Hydrogeologists and mining engineers can use these guidelines as a generic plan when planning a depressurisation system.

References

Alchin DJ, Botha WJ (2006) The structural/stratigraphic development of the Sishen South (Welgevonden) iron ore deposit, South Africa, as deduced from ground gravity data modelling. Appl Earth Sci 115:174–186. https://doi.org/10.1179/174327506X138940

Beale G (2017) Leeuwfontein Pit Geotechnical Review Board Report

Carney MD, Mienie PJ (2003) A geological comparison of the Sishen and Sishen South (Welgevonden) iron ore deposits, Northern Cape Province, South Africa. Trans Inst Min Metall Sect B Appl Earth Sci 112:81–88. https://doi.org/10.1179/0371745032501171

DWA (2011) The Groundwater Dictionary, 2nd edn. Department of Water Affairs, Pretoria

South African Weather Service (2019) Climate Data for Weather Sation 0321110, 0320654, and 0320348. Pretoria

Steenekamp G (2005) Sishen South Iron Ore Project. Report on Geohydrological Investigation as part of the EMPR. Clean Stream Groundwater Services. Reference No: SS/GW/01/2005

Thomas S, Basson I (2015) Kapstevel South Mine: Structural Re-interpretation and 3D Modelling in Leapfrog Geo

Viljoen D (2006) Sishen South EIA, Soil Survey of the Farms Kameelhoek, Welgevonden, Olynfontein, Ploegfontein, Leeuwfontein, Klipbankfontein, Kapstevel, and Wolhaarkop. Golder Associates, Pretoria

Multi-Step Passive Treatment Using Limestone, Wood Chips and Concrete Waste Material for Zn and Cd Removal

Yuki Semoto[1], Kengo Horiuchi[1], Takaya Hamai[1], Naoki Ikegami[1], Yusei Masaki[2], Kosuke Takamoto[1], Yutaro Takaya[4,3], Chiharu Tokoro[3,4]

[1]*Metals Environment Management Department, Japan Organization for Metals and Energy Security, Toranomon 2-10-1, Minato-ku, Tokyo, Japan, semoto-yuki@jogmec.go.jp*

[2]*Metals Technology Center, Japan Organization for Metals and Energy Security, Furudate 9-3, Kosaka-kouzan, Kosaka, Akita, Japan*

[3]*Faculty of Science and Engineering, Waseda University, Okubo3-4-1, Shinjuku-ku, Tokyo, Japan*

[4]*Facult of Engineering, The University of Tokyo, Hongo7-3-1, Bunkyo-ku, Tokyo, Japan*

Abstract

Japan Organization for Metals and Energy Security (JOGMEC) has conducted research on passive treatment (PT) methods to reduce costs. This study evaluated the use of concrete waste material (CWM) as a neutralizer for the PT of mine water containing Zn and Cd through a multistep process comprising limestone and CWM reactors. During continuous flow tests, the pH remained above 9 for over 200 days when the CWM reactors contained a 1:2 ratio of CWM to woodchips. The dissolved Zn and Cd were decreased by an average of 98.8% and 98.6% during this period without maintenance.

Keywords: Passive Treatment, Concrete Waste Material, Limestone, Acid Mine Drainage, Abandoned Mine

Introduction

Active treatment of mine water is being conducted in approximately 100 abandoned mines in Japan, incurring considerable annual costs. Japan Organization for Metals and Energy Security (JOGMEC) has conducted research on passive treatment (PT) to reduce costs, though there been few domestic examples of PT of mine water. Generally, a process using sulfate-reducing bacteria is employed to realize PT removal of Zn and Cd (Sato *et al*. 2018, Habe *et al*. 2018). However, this process is difficult to apply at sites with low winter temperatures and low sulfate ion concentrations in the mine water; in such cases, the pH must be increased to remove Zn and Cd. Furthermore, limestone, a commonly used neutralizer in PT, is not expected to sufficiently increase the pH. Therefore, a neutralizer with a high pH that is adaptable to PT is essential to realize the removal of Zn and Cd from mine water. This study accordingly evaluated the use of concrete waste material (CWM), generated during the manufacture of concrete products, as a neutralizer for PT (Takaya *et al*. 2022). As CWM contains calcium hydroxide as a major component, it is expected to have a strong pH-raising effect (Adrian Brown. 2022). Therefore, this study evaluated a novel multistep process using limestone and CWM for PT of mine water containing high concentrations of Zn and Cd.

Methods

Mine water profile of the target mine

The water profile of the target mine considered in this study at the experiment site is listed in Table 1.

Materials

A high-purity limestone crystal neutralizer (20-40 mm) supplied by Ookubo Rozai Co., Ltd. was used as the limestone and PAdeCS (5-20 mm) derived from concrete sludge marketed by Nippon Concrete Industries Co., Ltd. was used as the CWM. This PAdeCS not only has a high alkaline content but is less expensive than limestone. The chemical and mineralogical compositions of the limestone and CWM were determined using X-ray

Table 1 Water profile of the target mine

	pH	Temp.	Zn	Cd	Cu	Pb	Fe	SO_4^{2-}
	(-)	(°C)	(mg L^{-1})	(mg L^{-1})	(mg L^{-1})	(mg L^{-1})	(mg L^{-1})	(mg L^{-1})
Ave.	3.8	10.7	21	0.24	11	0.24	1.8	138
Max.	5.1	13.5	52	0.54	26	4.3	18	300
Min.	3.2	9.1	9.4	0.11	3.6	0.7	0.3	94

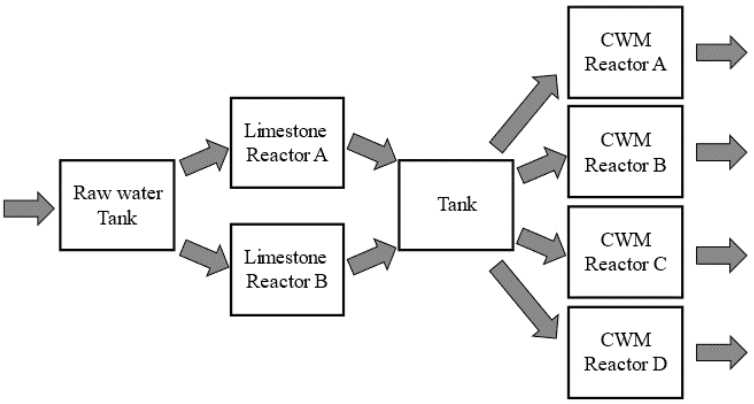


Figure 1 *Flow chart of continuous flow tests*



Figure 2 *Reactors employed in the continuous flow test; limestone reactor (right), CWM reactor (left)*

fluorescence (XRF, ZSX Primus 2, Rigaku, Japan) and X-ray diffraction (XRD, Ultima 4, Rigaku, Japan), shown in Table 2. Finally, woodchips less than 40 mm long, marketed by Mogami Mokushitsu Energy and comprising a mixture of tree species, were also employed in the CWM reactor.

Continuous flow tests

Two vertical downflow limestone reactors (400 mm wide, 300 mm long, and 610 mm deep) and four vertical downflow CWM reactors (543 mm wide, 340 mm long, and 295 mm deep) were installed in series, as

Table 2 *The characterisation of limestone and CWM*

		Limestone	CWM (PAdeCS)
			
Particle Size (mm)		20 - 40	5 - 20
Mineral Components		$CaCO_3$	$CaCO_3$ $Ca(OH)_2$
Elements (mass%)	Ca	70.1	43.5
	Mg	0.39	0.7
	Si	0.18	9.87
	Al	0.02	3.16

Table 3 *The contents and HRTs for the CWM reactors*

	Limestone/CWM/woodchips volume ratio	Limestone Volume (L)	CWM Volume (L)	Woodchips Volume (L)	HRT (h)
CWM reactor A	0/1/0	-	9	-	3 ※4
CWM reactor B	1/1/0	9	9	-	3 ※4
CWM reactor C	0/1/1	-	9	9	3 ※4
CMW reactor D	0/1/2	-	6	12	3

※ After 169 days of water flow, HRT was changed from 3 to 4 hours.

illustrated in the flow chart in Figure 1, in a tunnel at the mine site, as shown in Figure 2. Mine water was introduced at the top of each reactor from the preceding tank using an electric pump. The headspace of each reactor was open, and the CWM reactors were designed to drain from the bottom. Each limestone reactor was filled with a 300 mm thick layer of limestone and the water level was set at 50 mm above the top of this layer. The hydraulic retention time (HRT) in the limestone reactors was set to 2 – 4 h. Each CWM reactor was filled with a 300 mm thick layer comprising different volume ratios of limestone, CWM, and woodchips, and the water level was set at 40 mm above top of this layer. The HRT in the CWM reactors was set to 3–4 h and the contents and HRTs for the four CWM reactors are summarized in Table 3. This reactor configuration has been employed in an ongoing continuous flow test that was begun in June 2022.

Monitoring parameters and analytical methods

Water temperature and pH were monitored at the mine site at all times, and water samples of the effluent from each reactor were regularly collected to determine the concentrations of total Zn, Cd, Cu, Pb, and Fe using inductively coupled plasma optical emission spectrometry (ICP-OES; Agilent 5110 ICP-OES, Agilent Technologies Inc., USA). A membrane filter with a pore size of 0.45 μm was used to filter the suspended metals from the water sample and thereby determine the contents of soluble Zn, Cd, Cu, Pb, and Fe within.

Results and Discussion

The water temperature in each CWM reactor increased during the summer and decreased only slightly during the winter. The effluent from the limestone reactors had a pH of approximately 6. The measured pH changes in each CWM reactor are shown in Figure 3, which indicates that Reactors A, B, and C maintained a stable pH above 9 for approximately 60 d after water began to flow at an HRT of 3 h. This stability was a result of the dissolution of calcium hydroxide, a major component of CWM, providing hydroxide. The effluent from the reactors containing CWM mixed with limestone or woodchips exhibited a higher pH than that from the CWM-only reactor. This indicates that CWM has a strong pH-raising effect and is effective as a neutralizer, and that its effectiveness is enhanced when it is mixed with limestone or woodchips. However, approximately 60 d after water flow began, the pH in these reactors decreased and became unstable. Flushing, in which the water and precipitation in the reactor are drained vigorously out of the reactor by opening a cock installed at the bottom of the reactor, was subsequently performed to prevent the pH from decreasing further, causing the pH to recover for approximately 20 d. However, the pH again became unstable, and the pH recovery effect was reduced following a second flushing. The HRT was subsequently increased from 3 to 4 h, causing the pH of the effluent to stabilize and largely remained above 9 thereafter. In contrast, Reactor D maintained a stable pH above 9 for over 200 d at an HRT of 3 h without maintenance. These results indicate that the effluent from a reactor containing CWM and woodchips will remain stable at a higher pH than that from a reactor containing CWM alone or CWM with limestone, and that a CWM-to-woodchip volume ratio of 1:2 is optimal.

The measured changes in the total concentrations of Zn and Cd in the raw water, limestone reactor effluent, and effluent from each CWM reactor are shown in Figures 4 and 5, respectively. Soluble Zn and Cd in the effluent from all four CWM reactors were removed by an average of over 99.1% and 96.4%, respectively, over the first ≈60 d after water flow began. Furthermore, the correlation between the Cd concentration and pH shown in Fig. 6 shows that soluble Cd concentrations in the effluent from each CWM reactor were less than theoretically predicted at the given pH for removal of Cd as a hydroxide. During treatment, the mine water passed through the limestone reactor and then the CWM reactor, where it was supplied with hydroxide and carbonate, facilitating the removal of Zn and Cd, respectively. However, approximately 60 d after water flow began, as the pH decreased,

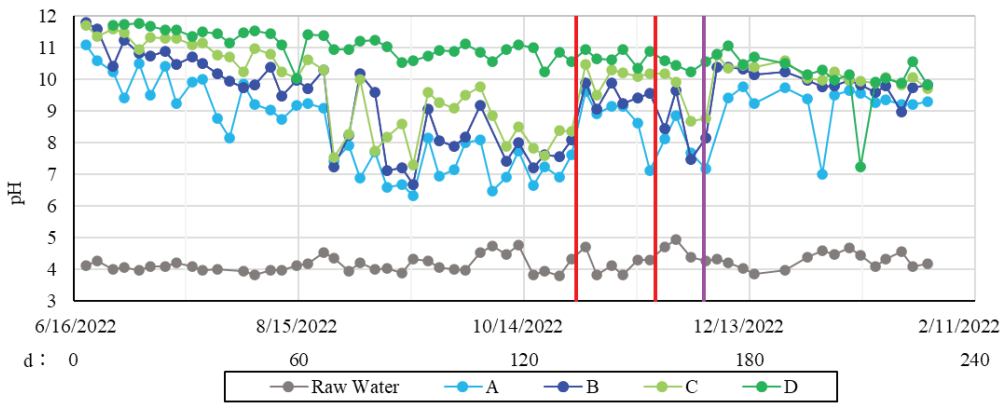


Figure 3 *Changes in CWM reactor pH over time; Flushing in CWM reactor A, B and C (red line), HRT changed 3 h to 4 h in CWM reactor A, B and C (purple line)*

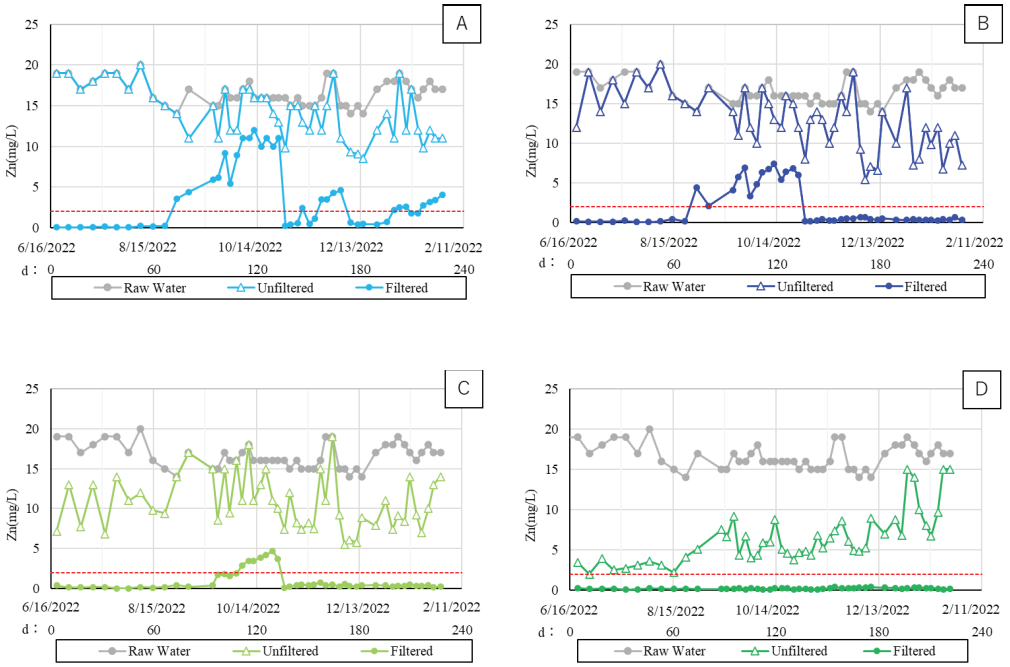


Figure 4 *Zn concentrations in CWM reactor effluent over time (the dashed line indicates the maximum allowed by the domestic discharge standard)*

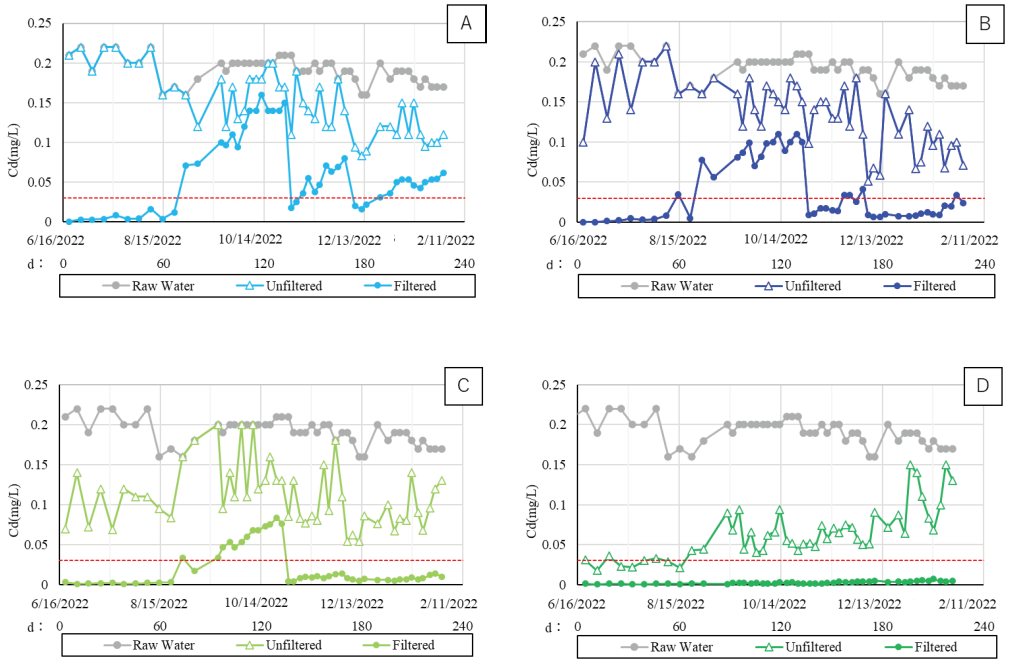


Figure 5 *Cd concentrations in CWM reactor effluent over time (the dashed line indicates the maximum allowed by the domestic discharge standard)*

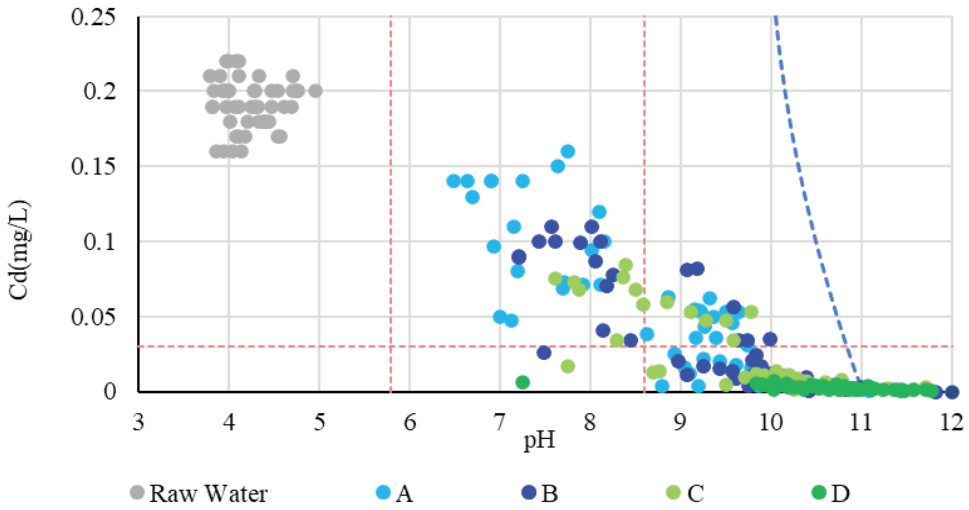


Figure 6 *Correlation between pH and Cd concentration in CWM reactor effluent; the pH and the maximum concentrations allowed by the domestic discharge standard (red dashed lines), Cd concentrations at theoretical pH for removal as hydroxide (Blue dashed line)*

the soluble Zn and Cd concentrations in the effluent from CWM Reactors A, B, and C increased, whereas soluble Zn and Cd in the effluent from CWM Reactor D were decreased uniformly by an average of 98.8% and 98.6% for over 200 d. This confirms that CWM is effective in the PT of mine water containing Zn and Cd, and that a 1:2 volumetric ratio of CWM to woodchips provides optimal treatment. However, the total Zn and Cd in the effluent from the CWM reactors exceeded the domestic discharge standard because they were partially present as suspended particles which were not completely removed by the current process. Therefore, a settling reactor will be placed in series with the CWM reactors in the future.

Conclusions

Continuous flow tests were conducted to treat mine water containing Zn and Cd at a mine site in Japan using a multistep process comprising limestone reactors with an HRT of 2–4 h in series with different CWM reactors with an HRT of 3–4 h. The pH values of the CWM reactor effluents remained above 9 for approximately 60 d for CWM reactors containing CWM only, a 1:1 ratio of limestone to CWM, and 1:1 ratio of CWM to woodchips. The pH remained above 9 for over 200 d for the CWM reactor containing a 1:2 ratio of CWM to woodchips, during which time the soluble Zn and Cd in the effluent were decreased by an average of 98.8% and 98.6% without maintenance. In particular, soluble Cd concentrations were found to be less than the Cd concentrations at theoretical pH for removal as Cd hydroxide. These results can be attributed to the supply of carbonate in the limestone reactor and the increase of the pH in CWM reactor, which removed Zn and Cd as hydroxide as well as carbonate. This result suggests that CWM is applicable as a neutralizer for the PT of mine water containing Zn and Cd, and that a multi-step process comprising limestone and CWM reactors represents a more effective configuration than a CWM-only reactor in terms of the pH requirement and long-term neutralization. Tests will continue to be conducted to remove Zn and Cd suspensions and to clarify of the effects of woodchips and the long-term effectiveness of the proposed PT system.

References

Sato Y, Hamai T, Hori T, Habe H, Kobayashi M and Sakata T (2018) Year-round Performance of a Passive Sulfate-reducing Bioreactor Using Rice Bran as an Organic Carbon Source for Treating Acid Mine Drainage.Mine Water Environ 37 ,586-594

Habe H, Sato Y, Aoyagi T, Inaba T, Hori T, Hamai T, Hayashi K, Kobayashi M, Sakata T and Sato N(2020) Design, application, and microbiome of sulfate-reducing bioreactors for treatment of mining-influenced water. Appl Microbiol Biotechnol 104, 6893–6903.

Takaya Y, Fuchida S, Hamai T, Horiuchi K, Masaki Y, Tokoro C (2022) Prediction of Acid Mine Drainage Treatment by Open Limestone-Alkaline Material Channel and Implications for the Large Scale Implementation of Passive Treatment. Proceedings of The Mining and Materials Processing Institute of Japan. Minato-ku,Tokyo,Japan. 7-9 March 2022 (Online)

Brown, Adrian(2018): Passive Metal Mining and Mine Water Treatment Using Crushed Concrete. – In: Wolkersdorfer, Ch.; Sartz, L.; Weber, A.; Burgess, J. & Tremblay, G.: Mine Water – Risk to Opportunity (Vol II). – p. 1029 – 1036; Pretoria, South Africa (Tshwane University of Technology).

The Development of A Multi Parameter Respirometric Laboratory Testing Method to Estimate Site-Specific Net Carbon Dioxide Flux from Metalliferous Mine Waste

Rosalia Shiimi[1], Rhys Savage[1,3], Steven Pearce[1], Andrew Barnes[2], Mark Roberts[2], Daniel Schoen[1,2], Devin Sapsford[3]

[1]*Mine Environment Management Ltd, Wales, UK rhys.savage@memconsultants.co.uk, rshiimi@memconsultants.co.uk, spearce@memconsultants.co.uk ,*

[2]*Geochemic Ltd, Wales, UK, mroberts@geochemic.co.uk, abarnes@geochemic.co.uk, dschoen@geochemic.co.uk*

[3]*Cardiff University, Wales, UK, sapsforddj@cardiff.ac.uk*

Abstract

The mining industry has a large part to play in the global transition to low carbon technologies, however this will involve continued production of large volumes of tailings and waste rock materials. Recent research has focused on assessing suitable silicate bearing mining wastes as potential feedstocks for large-scale carbon dioxide removal technologies (CDRT). However, reactive sulfide and carbonate minerals within certain mine wastes have also been identified as having the potential to emit CO2, while also influencing discharge water quality. At present no standardised testing methods or monitoring, reporting and verification (MRV) systems exist for the quantitative assessment of sequestering carbon dioxide using mine waste materials or consideration of net CO_2 flux within mine waste storage facilities.

Keywords: Carbon dioxide removal technologies, net CO_2 flux, respirometric measurement system, titration analysis, total inorganic carbon analysis

Introduction

This paper presents the findings from the development of a novel approach to estimate CO_2 flux balance of mining waste materials through the use of standard laboratory equipment as part of a multi parameter respirometric measurement system (RMS). The primary aim of the research is to develop a methodology for estimating the carbon balance (i.e., the balance between CO_2 emissions and CO_2 sequestration) within mining waste facilities during operations and post closure. The novel approach to validating site-specific estimates for generated CO_2 emissions was realised through the utilisation of gas pressure monitoring technology along with a NaOH absorbent media, total carbon analysis and hydrochloric acid (HCl) titrations to provide a multi analysis solution. It is important to note that testing conditions allowed simulation of site parameters meaning the results are site specific.

Methods

Sample Preparation

All testing was undertaken at the Geochemic Ltd laboratory facility located in Wales, UK. Cardiff University and Petrolab UK were also utilised for selective characterisation methods. Testing was undertaken on composites of individual discrete waste rock samples. The composite waste rock used within the study was reduced to <6.3mm size fraction. To emulate field conditions, a 7.5% water content is added to the dry composite waste rock samples.

To assess CO_2 generation and CO_2 consumption in mine wastes, the WTW OxiTop-C and OxiTop-C/B pressure measuring heads, designed to determine aerobic respiration rates according to EN ISO 16072:2011 are used within this study. To differentiate between the different gas vessels used, the O2 consumption vessels will be referred to as "Oxitops" and

CO_2 consumption vessels will be called "Carbitops." The OxiTops utilise Warburg constant (Bryant 1964) volume respirometry method where the O_2 and CO_2 consumption rates are determined through monometric determination of the pressure drop within a sealed container of fixed volume (Barnes *et al.* 2022). Within this study, the method was altered from a standard method by Platen and Wirtz (1999) and the ideal gas law is applied to calculate the moles of O_2 or CO_2 within the sealed vessels containing waste samples.

Oxitop Experiment

A novel method is developed to access CO_2 production by utilising the adjusted Oxitop method and adding a NaOH solution to the vessels to absorb any CO_2 produced during sulfide oxidation and subsequent carbonate dissolution. This absorbent media can be back titrated in order to estimate the total CO_2 emitted by a material over a set time period. This can be cross checked through total inorganic carbon (TIC) analysis. Both analyses were carried out in this study to allow validation of the novel NaOH solution method.

Carbitop Experiment

Previous studies by Savage *et al.* (2019) identified two main stages of carbon dioxide exchanges within the pressure vessels due to the observed sharp initial decrease in pressure. These two stages are assumed to be (1) Initial surface absorption and pore water dissolution and (2) Mineral weathering and subsequent carbonation reactions. Considering these assumptions within this study, waste materials were allowed to equilibrate in a CO2 enriched environment for seven days. This allowed the samples to go through the initial stage of surface absorption and pore water dissolution, reducing the impact on the initial experimental readings. Once sealed and placed in a 25°C incubator after the 7 days equilibration period, it is assumed that the measured change in pressure is predominantly due to mineral carbonation. Upon completion the moles CO2 in the vessel at each time instance were calculated using the ideal gas law.

Results

NaOH Back Titration

The chemical reaction between NaOH and CO_2 resulted in the formation of HCO_3^- which is equivalent to CO_2 absorbed by the NaOH. The moles of HCO_3^- are determined from the moles of HCl added (from pH 8.3 to 2.5) because of the 1:1 mole ratio between the two (i.e., the moles of HCl added from 8.3 to 2.5 is equivalent to the moles of HCO_3^-

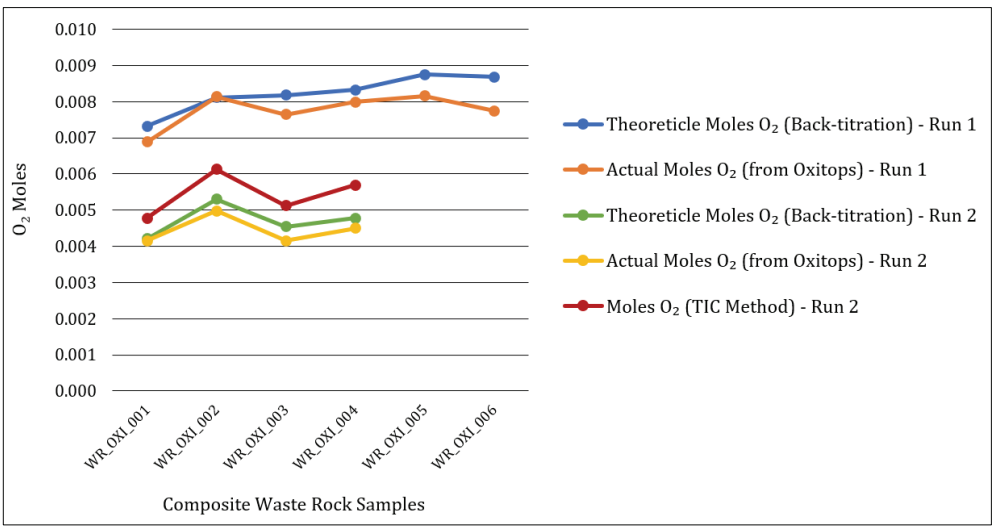


Figure 1 *O_2 moles estimated from back-titration, Oxitops and TIC method during experimental Run 1 and Run 2.*

Table 1 Summary of average calculated CO_2 emissions generated by mining waste samples.

Waste Material	Run 1 (Titration) kg (CO_2)/tonne/year	Run 2 (Titration) kg (CO_2)/tonne/year	Run 2 (TIC Method) kg (CO_2)/tonne/year
Waste Rock	1.95	1.12	1.04

in the solution). Given the stoichiometric relationship between pyrrhotite oxidation and dolomite neutralisation, a key finding from the back titration results show that the stoichiometric moles of O_2 calculated from the titration method compare very well with the O_2 moles estimated from the Oxitops (Figure 1). To validate the calculated CO_2 emission estimated by the titration method, the NaOH solution was analysed for carbon using the total inorganic carbon (TIC) method.

CO2 Production Rates

Back titrations were carried out on NaOH sample solutions from the waste rock Oxitops after both Run 1 and Run 2 of the experimental protocol. TIC analysis validations were carried out after run 2 and therefore were only comparable to Run 2 NaOH back titrations. Table 1 shows the calculated CO_2 emissions for the waste rock sample in Run 1 and Run 2. It can be seen that minimal variation was observed between NaOH back titration values and values measured through direct TIC analysis.

CO_2 Consumption

Carbon dioxide consumption rates of waste materials were estimated by converting changes in vessel pressure to direct consumption rates using the ideal gas law. Figure 2 shows the results obtained in Run 1 and Run 2 for waste rock material. Waste materials held an average CO_2 consumption

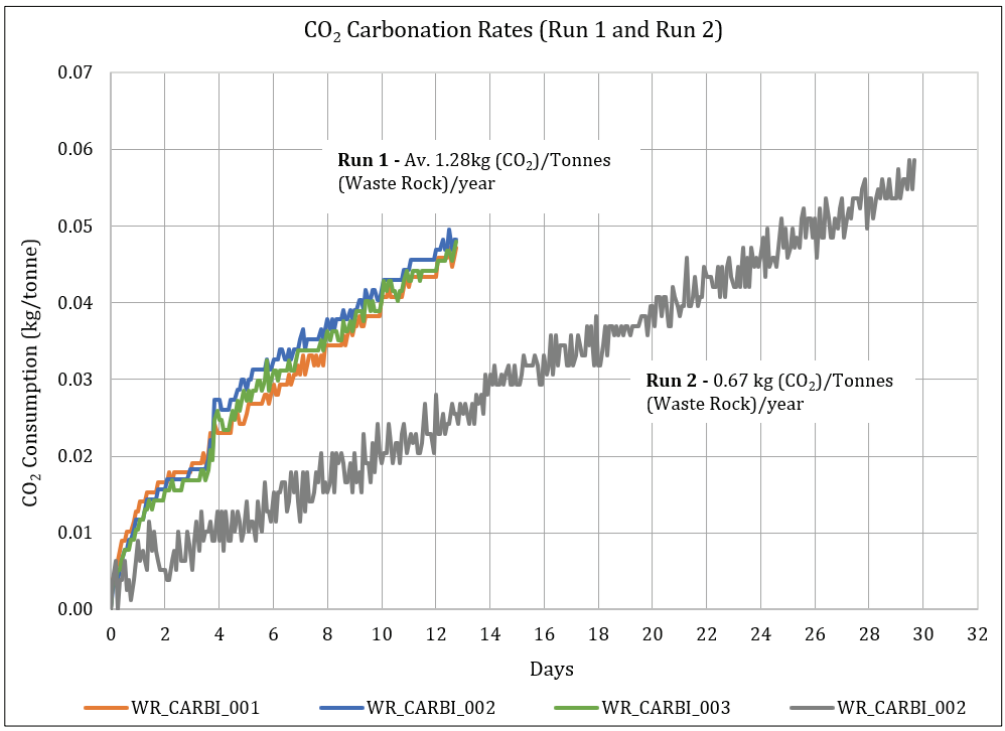


Figure 2 Carbonation rate results measured in waste rock material.

Table 2 Calculated net CO_2 released and sequestered (Carbon balance).

Waste Material	Estimated CO_2 Released (Back Titration	Estimated CO2 Released (TIC method)	Average Estimated CO_2 Production (Oxitops)	Estimated CO_2 Consumption (Carbitops)	Net CO_2 Emitted/ Sequested
			kg (CO_2)/tonne/year		
Waste Rock (Run 1)	1.94	-	1.94	1.28	0.66
Waste Rock (Run 2)	1.12	1.04	1.08	0.67	0.41

rate of 1.28 kg (CO_2)/tonne per year during Run 1, compared to 0.67 kg (CO_2)/tonne per year for waste rock materials during Run 2.

The Carbon Balance

Utilising the Oxitops and Carbitops results, a preliminary estimated balance between CO_2 sequestered and CO_2 emitted by mine waste materials can be estimated. Table 2 shows results of the CO_2 production rates from mine wastes, estimated from the Oxitops using the titration and TIC methods; and the CO_2 consumption rates estimated from the Carbitops. The difference between emitted and sequestered CO_2 will result in a net CO_2 release or net CO_2 consumption. The results of this test work are shown graphically in Figure 3. Based on the preliminary results of this study, the waste rock materials were identified to be potentially net carbon dioxide emitting in the presence of an oxygen rich atmosphere, although further testing is required to validate these preliminary findings.

Key Observations/Discussion

Oxygen Consumption

The pressure evolution of all the waste samples from both test runs indicate that a pressure decrease is common in all the Oxitop experiments. It was important to determine the oxygen consumption rates (OCR) as they give an insight into sulphide oxidation which is directly related to CO_2 production. According to Barnes *et al.* (2022), the weathering signature of mine waste facilities is

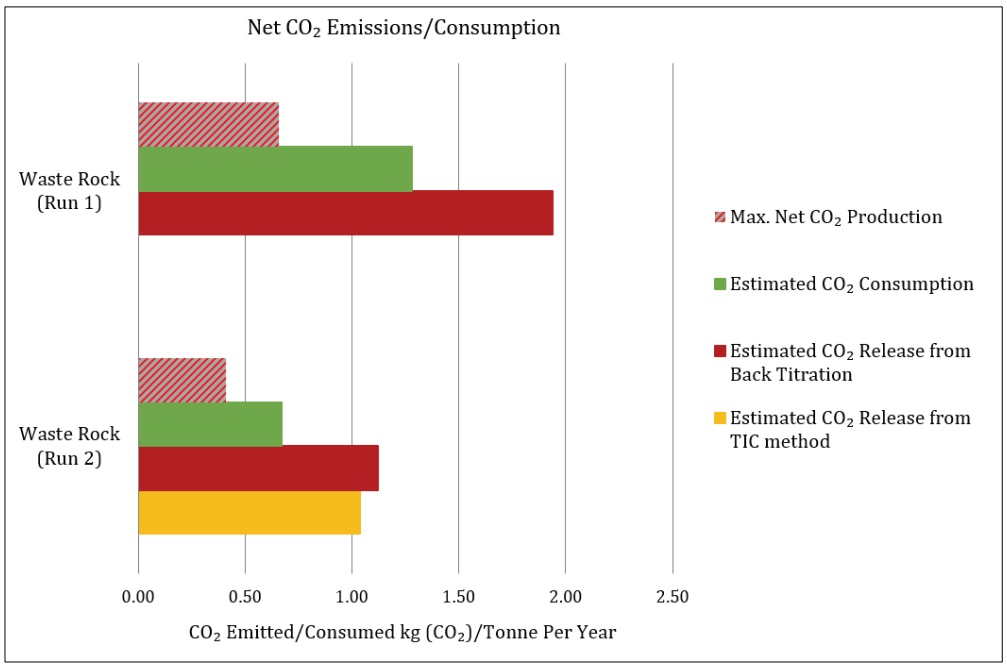


Figure 3 Net carbon emissions/consumption estimated for waste rock materials.

closely linked to the availability, depletion, and transport of oxygen. Key to these processes is the rate at which oxygen is consumed through oxidation of sulfide minerals within mining wastes. Additionally, there are many other aspects of the OCR that are inherent to the waste material, such as sulphide mineral content, type and reactivity, degree of sulphide mineral liberation, particle size distribution and exposed reactive surface area.

CO_2 Production

The pressure reduction within the Oxitops was due to pyrrhotite consuming oxygen. That coupled with the dissolution of dolomite with sulphuric acid results in the production of carbon dioxide (Torres, West and Li, 2014; Ross *et al*., 2018). For this reason, a NaOH solution was added to the Oxitop vessels with the aim to absorb any CO_2 produced due to pyrrhotite oxidation and dolomite neutralisation. NaOH is such a rapid absorber of CO_2 that it far surpasses the rate at which the silicate minerals can absorb CO_2. Effectively, any CO_2 produced by the waste is immediately absorbed by NaOH, therefore completely separating out any CO_2 produced through sulphide oxidation and carbonate dissolution. The validation of the back titrations by analysing for carbon using the total inorganic carbon (TIC) method is novel and shows great promise for furthering the ability to estimate CO_2 emissions via lab-scale experimentation.

A very close correlation is observed between theoretical O_2 moles (calculated from the stoichiometric relationship between pyrrhotite oxidation and dolomite neutralisation) and the O_2 moles measured from Oxitops (estimated moles using the ideal gas law). The interpretation that the number of moles estimated from the Oxitops is approximately equal to the number of moles calculated from the stoichiometric ratio of O_2 and H_2CO_3 (CO_2) during pyrrhotite oxidation and dolomite neutralisation is an important outcome from this study which signifies that CO_2 production rates within a system can be estimated from Oxitops by using the estimated number of O_2 moles due to the change in pressure using the ideal gas law.

CO_2 Consumption

The estimated CO_2 consumption is based on a 100% CO_2 atmosphere, therefore, the calculated CO_2 consumption rates within this study represent idealised carbonation rates in such an atmosphere. More testing at various pCO_2 conditions are required to develop a better understating of the potential carbonation kinetic rates under varied conditions.

Carbon Balance

The CO_2 production rates estimated were between 1.04 and 1.94kg (CO_2) per tonne of waste rock per year. It should be noted that these are maximum estimated rates as they were measured at room temperature and at atmospheric oxygen concentrations. Carbitop experiments revealed idealised carbonation rates between 0.67 and 1.28kg (CO_2) per tonne per year of waste rock. These are maximum estimated carbonation rates, measured in a pure CO_2 atmosphere. The Oxitop and Carbitop experiments allowed the estimation of the net carbon emissions or net carbon sequestration by calculating the difference between maximum CO_2production and maximum CO_2 consumption rates.

In terms of the carbon balance, the data indicates that under atmospheric gas conditions waste rock material may produce more CO_2 due to sulphide oxidation and carbonate dissolution than it can consume with an estimated net CO_2 emission rate between 0.41 and 0.66 and kg (CO_2) per tonne per year. However, the results also indicate that in a gas atmosphere where O_2 availability is reduced (for example in a waste storage facility that has been encapsulated post closure), the waste rock will produce less CO_2, as sulfide oxidation is reduced. Under this gas atmosphere condition, the rate of carbon sequestration will not be impacted by lower O_2 concentrations and will be proportional to pore gas CO_2 concentrations (which are typically elevated where O_2 availability is low). As such in this situation the results indicate that the balance of the system may reverse and become net carbon negative (as CO_2 consumption is higher than production).

Conclusions

To date, no universal, robust, practical and cost/time effective benchtop laboratory method has been developed to determine empirically the potential CO_2 release and uptake (and thus balance) within typical sulfide metalliferous mine wastes (waste rock and tailings). Utilising the back titration method along with the RMS method, this study was able to quantify CO_2 emissions and uptake from samples of waste rock from a metalliferous mine, further the results were able to be validated by the TIC method. From the Oxitop and Carbitop results, this study was able to develop a novel empirical methodology to assess the carbon balance of mine wastes which is likely to become a critical aspect for future mine waste characterisation.

Using the developed carbon balance methodology, the results of the study indicates that emissions of CO_2 are likely higher in the waste rock tested than the uptake of CO_2 in a situation where pore gas is close to atmospheric composition. However, the results indicate that where pore gas conditions become oxygen limited (for example in mine waste that is stored within a facility that has engineered oxygen limiting design such as low permeability cover system), the balance has the potential to become a net neutral. As such the results of the testing produced from the method outlined allows relative and quantitative assessment of the potential carbon balance for mine waste under given scenarios. Therefore, the method provides a very valuable tool for operational and closure mine planning, specifically for the design of waste storage facilities and assessment of opportunities and risks related to CO_2 net emissions from the short-long term storage of mine waste. Future research will look to further assess the net CO_2 flux within tailings, by utilising this study's carbon balance methodology to test tailings material.

Acknowledgements

We would like that acknowledge Cardiff University for the use of their laboratory facilities during this study as part of an MSc course placement. We would also like to thank the external mining operator that funded this experimental work as part of the first authors MSc placement. This operator has chosen to remain anonymous at the time of publication.

References

Barnes, A., Pearce, S., Savage, R., Roberts, M., Brookshaw, D., Rama, M., Kauppila, T., Mueller, S., Hertrijana, J., and Bowell, R. (2022). Application Of the Warburg Constant Volume Respirometer Method For Determination Of Oxygen Consumption Rates Of Mining Waste. International Conference on Acid Rock Drainage 2022, Australia.

Bryant, J.O. (1964). SOME ASPECTS OP GAS TRANSFER IN THE WARBURG RESPIROMETER. MSc Thesis, Rice University.

EN ISO 16072:2002 (2011). Soil quality. Laboratory methods for determination of microbial soil respiration.

Platen, H. and Wirtz, A. (1999). Application report Oxygen consumption and carbon dioxide generation. Matrix: Soils and solids Application report Respiration activity of soils (standard test preparation). Available at: http://www.fh-giessen.de/WEB_TG/uht.htm.

Ross, M.R.V., Nippgen, F., Hassett, B.A., McGlynn, B.L. and Bernhardt, E.S. (2018). Pyrite Oxidation Drives Exceptionally High Weathering Rates and Geologic CO2 Release in Mountaintop-Mined Landscapes. Global Biogeochemical Cycles 32(8), pp. 1182–1194. doi: 10.1029/2017GB005798.

Savage, R.J., Pearce, S., Mueller, S., Barnes, A., Renforth, P. and Sapsford, D. (2019). Methods for assessing acid and metalliferous drainage mitigation and carbon sequestration in mine waste: A case study from Kevitsa mine, Finland. In: Proceedings of the International Conference on Mine Closure. Australian Centre for Geomechanics, pp. 1073–1086. doi: 10.36487/ACG_rep/1915_86_Savage.

Torres, M.A., West, A.J. and Li, G. (2014). Sulphide oxidation and carbonate dissolution as a source of CO2 over geological timescales. Nature 507(7492), pp. 346–349. doi: 10.1038/nature13030.

Assessment of Hydrogeological Hazards in Operational Mines using Objective-Focussed Modelling and Hazard Mapping Tools

Ivan Shubin, Sheila Imrie, Tony Rex

SRK Consulting (UK) Limited, 5th Floor, Churchill House, 17 Churchill Way, Cardiff, CF10 2HH, Wales, UK.

ishubin@srk.co.uk, simrie@srk.co.uk, arex@srk.co.uk

Abstract

The workflow and methods outlined in this paper provide a recommended approach to proactive groundwater-related hazard assessment. Key steps include the undertaking of an initial hazard mapping exercise, the development of a local hazard-focussed groundwater model, and a detailed hazard mapping exercise designed to identify and prioritise hazard types and locations. The outputs inform hazard control measures including effective management decision-making, future monitoring requirements, mine planning and hazard-specific Trigger Action Response Plans. This targeted workflow for hazard management improves outcomes compared with other, less proactive approaches.

Introduction

Sudden underground water inrushes are an example of potentially catastrophic events that can result from lack of hazard awareness and planning, and supporting information and data, during mine operations. The iterative cycle of Monitor -> Model -> Manage that forms the basis of mine site groundwater management is effective but does not deal well with unexpected and unpredicted events that can occur under a variety of circumstances through life of mine. Such events can result in loss of production and, in the worst cases, loss of life and/or loss of the mine (i.e., a catastrophic inflow).

An ongoing awareness of potential hydrogeological hazards combined with clearly defined and structured hazard assessment methodologies and tools enable mines to mitigate these risks.

Water Inrush Hazards

Inrush hazards in mining are associated with a variety of geological and hydrogeological contexts. To understand and mitigate such hazards, the mine design and mine development planning processes must consider the local and semi-regional hydrology and hydrogeology.

In underground potash mining, for example, the predominant threat is from permeable units in the hanging-wall (and to some extent the footwall also) combined with local 'problem zones', for example, geological structures, areas of atypical geology in the mining horizon, thickness of salt above or below the mineral horizon etc. Water hazards are also encountered at shafts (both during sinking and operations) in such settings. Prugger and Prugger (1991), in their overview of water problems in Saskatchewan potash mines, concluded that "*a continuous awareness of the water hazard and the careful consideration of the possibilities of water inflows must be foremost in the mind of all potash miners*". They cite loss of knowledge (when key staff at a mine move on or retire) as a primary issue and they promote an open exchange of information as a key mitigating process.

Water inrush can occur in many other mine settings beyond evaporite deposits. Causes of inrushes can be classified into those associated with the natural geological/hydrogeological system (e.g., intercepting a water-bearing fault) and those associated with the mining process itself (e.g. the hydraulic opening of an area of old,

interconnected workings). Typical scenarios involving unexpected inrush include: a new development encountering water; a raise bore pilot hole intercepting workings with no test work or hydraulic checks prior to breakthrough; mine workings intercepting unsealed boreholes that are open to surface.

Control of ground conditions, including inflow hazards, are typically evaluated and managed through a Ground Control Management Plan (GCMP). The GCMP includes safe design, implementation and verification of ground control measures designed to mitigate the risks associated with the particular mining operation. At some operations a specific Inflow and Inundation Management Plan or equivalent will be established (for example; Perenti, 2020).

Groundwater Hazard Workflow

Here we present workflow techniques and tools to assess risks associated with specific hydrogeological hazards within the context of clear, focussed objectives. This approach has been applied on several projects the authors have been involved with recently and involves the following steps (refer to Figure 1):

- The first step is typically to undertake an initial hazard mapping exercise, whereby we use spatial and statistical software to identify and prioritise hazard types and locations.
- Depending on the data already available this may be followed by focussed test work, installation of instrumentation and data collection.
- The next step comprises development of a local hazard-focussed groundwater model whereby targeted approaches and modelling techniques are applied to meet the objectives of a specific hazard risk assessment.
- Multiple datasets of contributing factors, along with outputs from the local hazard model, form inputs to a more detailed hazard mapping exercise designed to predict where hazard-related risk is greatest. Datasets are given weightings using an analytical hierarchy process and are spatially and statistically analysed using multi-criteria decision analysis.
- The outputs inform management decisions, future monitoring requirements, mine planning and hazard-specific TARPs (Trigger Action Response Plans).

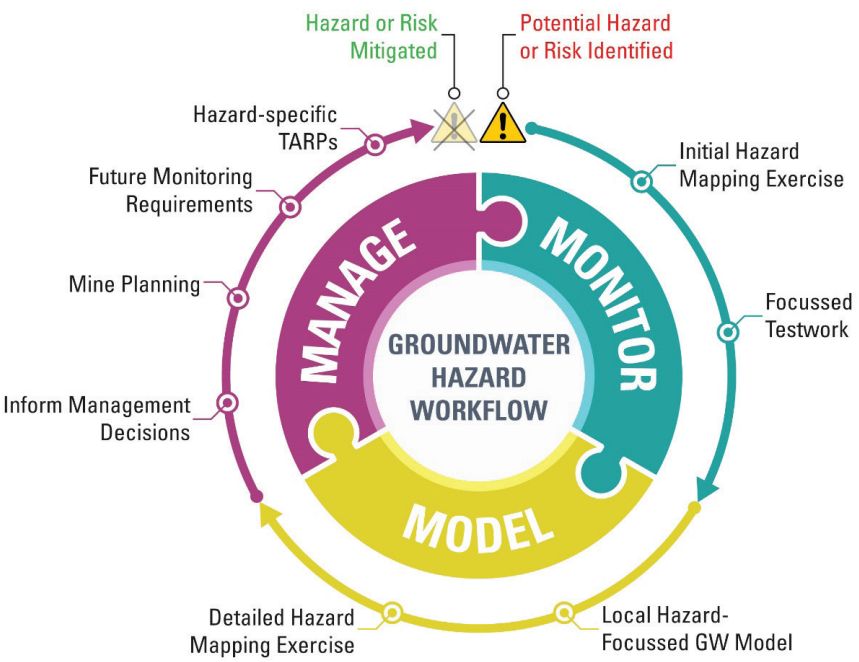


Figure 1 Groundwater Hazard Workflow

The workflow aligns with the Monitor > Model > Manage cycle but involves a single pass of these stages in order to understand and put in place targeted preventative/ mitigating measures.

Identification of Potential Hazard and Risk

The groundwater hazard workflow is triggered by the identification of the potential hazard. This trigger can occur at any of the stage of the routine site Monitor -> Model -> Manage iterative cycle. In an ideal world, the hazard would be identified during the routine site monitoring or modelling stages. However, in the worst case, and possibly most commonly, the inrush event is identified and addressed, through mitigation, during the management stage once the hazard trigger (such as a tunnel or shaft penetrating a permeable aquifer) has already been initiated. Once the potential hazard has been identified and assessed, then our workflow for hazard mitigation is as per the clockwise steps in the outer circle of **Figure 1**. This is similar to the routine Monitor -> Model -> Manage approach, but is completed on a shorter timescale and is non-iterative.

Initial Hazard Mapping Exercise (IHME)

The IHME involves a high-level assessment of the potential hazard and associated risks. The aim is to pre-empt the event and take steps to reduce that worst-case impact. A trigger event to initiating the IHME might comprise; unusual responses in a monitoring programme, an atypically high magnitude/ prolonged rainfall event or period, awareness of a potential change in geology/ ground conditions predicted during mine advancement, or observations of increased seepage at a mine face.

Alternatively, where sudden or catastrophic inflow is a constant risk to the mining operation the initial hazard mapping exercise may be a routine and regular exercise which is constantly being updated with new information from monitoring and other data sources. Here, more targeted spatial and statistic software may be employed to continually re-assess risks through methods such as composite hazard analysis.

Once groundwater hazard workflow is triggered the aim of the IHME is to focus on the potential hazard and collate all relevant information and data. A preliminary conceptual hydrogeological model (CHM) supports this process by focussing on two considerations; firstly, what are the key factors that both characterise the hazard and determine the possible range of events that could result; second, which of these factors and system characteristics are understood and which are not. Increased knowledge and level of certainly equates to reduced risk; the CHM helps identify which factors are constrained (through existing assessment; monitoring etc) and which are poorly constrained. It is the latter where focussed testwork is required.

Focussed Testwork

Many methods can be employed, through targeted testwork beyond the mine's routine monitoring infrastructure, to improve hydrogeological understanding and constrain risks associated with an identified inflow hazard. Geophysics plays a major role in underground potash environments (Funk et al, 2019). Water injection tests are considered a reliable method for determining seepage potential in specific host rock horizons and also for targeted features such as faults, particularly in coal mine settings (Cao et al, 2022). Often the focus is simply on collecting more observational data, such as seepage rates, and sampling /monitoring data such as water chemistry and responses in piezometers.

Local Hazard-Focussed Modelling

At this point in the workflow, there is often a requirement for a more refined CHM based on data from the preceding workflow steps, followed by numerical groundwater modelling of the hazard. If a regional model already exists for the site, it is tempting to assume its direct use for the hazard scenarios, however we have rarely found it to be the best option. Instead, the regional model, if available, should form one of the many inputs to the development of a local Hazard-focussed Groundwater Model (HGM).

Some of our key approaches and modelling techniques, specific to the objectives of a hazard risk assessment, are summarised below:

- *Model domain*. The key advantages of decreasing the HGM model domain are to allow for increased grid discretisation around the area of interest and shorter time steps for evaluation of short-term climatic variability and response to extreme events. These changes will typically decrease scenario run times and improve convergence. The regional model (if available) and analytical data are used to extract appropriate groundwater boundary conditions. Whilst it is relatively standard practice to significantly reduce the total planar area of the model domain by considering the zone of influence (e.g., drawdown), our methodology also includes potential vertical reduction of the model domain, as applicable. This requires a robust understanding of the CHM such that the specific hydrogeological unit(s) of relevance to the hazard are identified, and vertical recharge/discharge interactions be appropriately represented in the specified boundary conditions. An example of a local HGM Domain (horizontally and vertically) and associated boundary conditions is illustrated in **Figure 2**.
- *Discretisation*. Finer discretisation should be considered for the specific inrush hazard. The balance between model discretisation and model scenario run times and convergence is project-specific and occasionally more than one grid discretisation model setup is required to meet the objectives of various predictive scenarios. This potential flexibility should be included in the model design.
- *Parameterisation*. Due to the local scale of the HGM, the traditional 'representative elementary volume' (REV) approach to represent bulk hydraulic properties may not be directly applicable. Spatially variable three-dimensional anisotropy may be used to align with the dips and strikes of formation bedding and/or structures, and modelling of discrete features and fracture zones may also be required. Zones may also have high variability in hydraulic properties over very short distances. The use of discrete hydrostratigraphic zones may need to be replaced with interpolation surfaces and numerical functions.

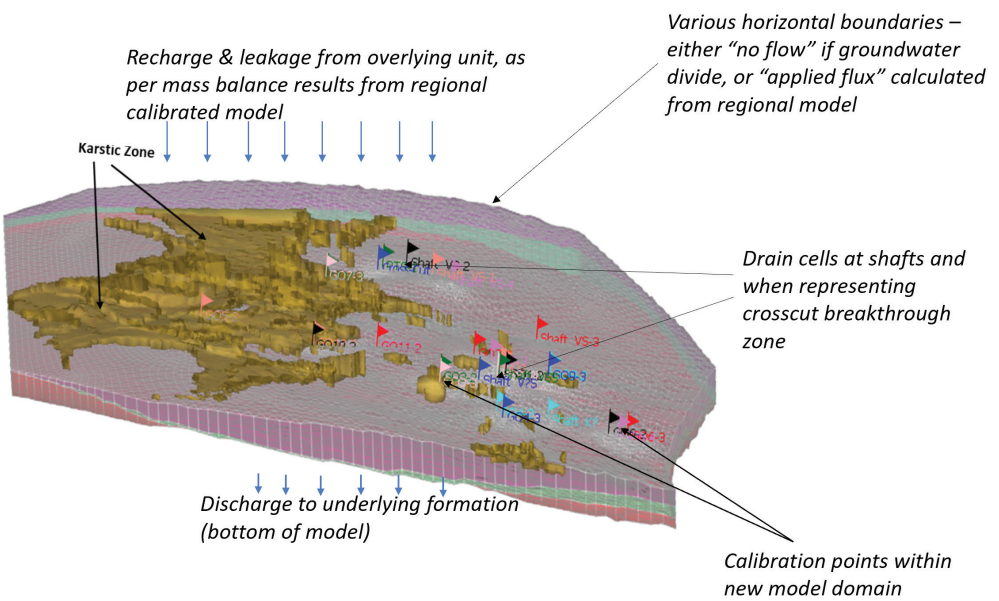


Figure 2 *Example Boundary Conditions for Revised HGM Domain*

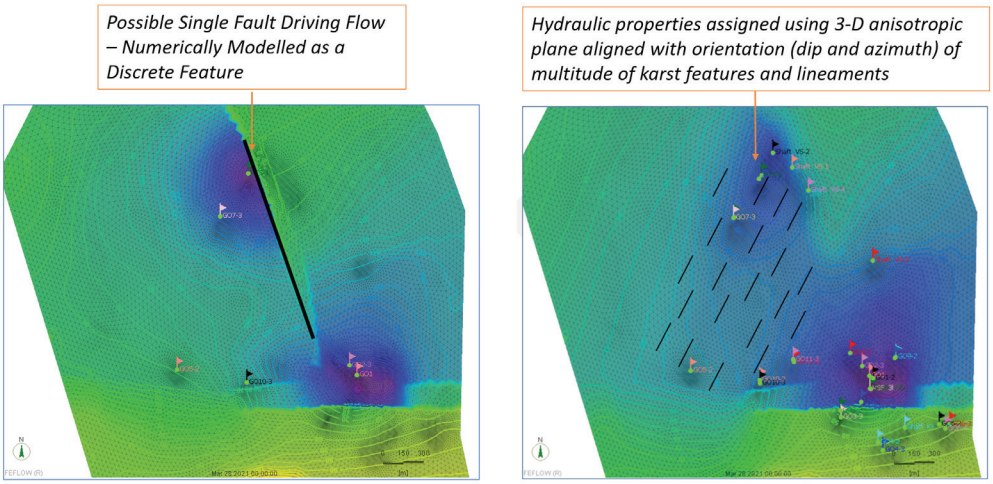


Figure 3 *Example Hydrostratigraphic Zoning Methodologies Tested during Hazard Modelling Scenarios*

Additionally, different methodologies may be required to represent the same area for different scenarios, and flexibility is required in the HGM so as to represent the various conceptual model hypotheses. **Figure 3** illustrates this concept by showing an example of two different zoning methodologies used for test scenarios of inrush responses.

- *Calibration*. Calibration requirements for HGM modelling require careful upfront consideration, including calibration priorities. Inflows and mass balance are often of primary importance. Local head pressures are relevant but may not be easily measurable at the site and thus thorough analysis of the local observation data is required. Calibrating to previous responses to events, such as a breakthrough event, will greatly enhance model confidence. Note that there will not necessarily be a direct correlation between the HGM and regional model parameterisation due to the REV assumptions, as discussed in the previous point, and thus the two models should not be forced to align in this regard.
- *Predictive scenarios*. Model scenarios need to be focussed on the model objectives. Model outputs will form a key input to the detailed hazard mapping and other groundwater management and monitoring advice, as discussed in the following sub-sections.
- *Uncertainty*. Sensitivity and uncertainty are a key aspect of the HGM scenarios. Consideration should be applied to the use of deterministic, stochastic, or a hybrid approach, for the model scenarios. Confidence in the underlying geological model is a critical consideration for any uncertainty analysis given the risks associated with poorly constrained or unknown geological structures.

Detailed Hazard Mapping

Datasets of contributing factors form inputs to a more detailed hazard mapping exercise designed to predict where hazard-related risk is spatially greatest. Spatial values for each contributing factor are informed by a combination of base data (e.g., extent and age of workings) or outputs from the numerical modelling exercise (e.g., permeability distribution). Datasets are given weightings using an analytical hierarchy process and are spatially and statistically analysed using multi-criteria decision analysis. This is typically undertaken on a GIS platform whereby combinations of factors can be analysed spatially (Donglin et al 2012; Wu et al, 2008).

This approach uses several criteria considered to be contributing factors. By way of example, take five contributory factors; i. the distance between a potentially hazardous aquifer (in this case, a dolomitic limestone in the hangingwall) and a mine development,

ii. the distribution of faults, iii. the hydraulic behaviour of each fault (i.e., whether the structure is behaving as a flow barrier or a flow conduit), iv. the permeability/degree of karstification within the aquifer and v. the proximity of the recharge zone to the aquifer. An Analytical Hierarchy Process can be applied and an overall relevance modifier value calculated for each factor. The composite probability of water inrush can then be calculated on a geospatial basis to produce, in a GIS environment, a spatial inundation probability map.

In potash mines and other evaporite environments there are specific criteria associated with, for example, the creep deformation characteristics of evaporite minerals, the strength of overburden strata, the natural 'anomalies' within the evaporite strata and the characteristics of groundwater in the overlying strata. Broad factors for consideration in any mine environment include:

- Natural geological conditions
- Mine design, layout and age of working
- Rock mass response due to mining
- Regulatory criteria
- Backfilling and other mitigation measures
- Monitoring systems, both surface and underground
- Management, expertise and 'expert' knowledge.

Managing the Hazard

The outputs from the monitoring and modelling exercises inform the hazard management process via one or more broad action routes:

- Inform Management Decisions Based on the preceding analysis management can make targeted decisions around future actions and assess the level of urgency required in applying these actions. The key benefit of this workflow approach to hazard analysis is that it is informed and focused. The aim is to reduce uncertainty where possible, but also to expose and highlight areas of lower certainty (and hence heightened risk) to allow targeted action accordingly.
- Mine Planning Changes to mine designs are often required to reduce inflow risks in the light of new hazards. Responses can include measures such as installing more pumping capacity, installing bulkheads, adjusting mine layouts and increasing barrier pillars.
- Future monitoring requirements Ongoing monitoring is intended to avoid an inundation or inrush event by identifying potential problems in advance. The hazard assessment workflow enables augmented monitoring to be established that targets the specific high-risk factors identified and informs the Hazard-Specific TARPs (Triggered Action Response Plans).
- Hazard-Specific TARPs should be reviewed and modified to ensure they reflect the specific outputs from the targeted hazard assessment. New TARPs should be drafted where a specific hazard type has previously not been identified.

The benefit of the workflow approach presented here is that the hazard management strategy is tailored to specifically manage the potential or identified hazard, rather than it being a more general and less targeted, strategy which is commonly the case.

Summary and Conclusions

The workflow and methods outlined in this paper provide a recommended approach to proactive groundwater-related hazard assessment. This approach uses objective-focussed models, tools and methods to inform appropriate action to reduce the likelihood of future potential catastrophic groundwater-related failures at mine sites. The approach is targeted to specific hazards and is structured and comprehensive. As such it has many advantages over more generic approaches, and is particularly effective in managing and mitigating hazards associated with unexpected and unpredicted events.

References

Cao Z, Gu Q, Huang Z, Fu J (2002) Risk assessment of fault water inrush during deep mining. International Journal of Mining Science and Technology, 32: 423–434. https://doi.org/10.1016/j.ijmst.2022.01.005

Donglin D, Wenjie S, Sha X (2012) Water-inrush assessment using a GIS-based Bayesian network for the 12-2 Coal Seam of the Kailuan Donghuantuo Coal Mine in China. Mine Water Environ, 31, 138–146.

Funk, C, Isbister, J, LeBlanc, T, Brehm, R (2019) Mapping How Geophysics is Used to Understand Geohazards in Potash Mines. CSEG Recorder, 44, 07.

Perenti Group (2020) Critical risk standard: control of ground conditions including inrush. https://perentigroup.com/wp-content/uploads/2020/06/Control-of-ground-conditions-including-inrush.pdf

Prugger FF, Prugger AF (1991) Water problems in Saskatchewan potash mining – what can be learned from them? CIM Bulletin, 84 (945) 58 – 66

Wu Q, Xu, H, Pang, W (2008). GIS and ANN coupling model: an innovative approach to evaluate vulnerability of karst water inrush in coalmines of north China. Environ Geol, 54 937–943. DOI 10.1007/s00254-007-0887-3

The Development of a Sample Preparation Technique for the Analysis of Trace Elements in Mine Impacted Waters containing High Levels of Iron

Janet Smith[1,2,3], Ed Hardwick[3,5], Jenny Falconer[5], Craig Sheridan[2,4], Tamlyn Naidu[2,4], Peter Engelund Holm[6], Lizelle Van Dyk[2,3]

[1]*Crundwell Management Solutions Metallurgical Consultancy and Laboratory (Pty) Ltd, Pinelands Office Park, Unit T5, 1 Ardeer Road, Modderfontein, 1609, South Africa*

[2]*Centre in Water Research and Development, University of the Witwatersrand, Johannesburg, Private Bag 3, Wits, 2050, South Africa,*

[3]*School of Chemical and Metallurgical Engineering, University of the Witwatersrand, Johannesburg, Private Bag 3, Wits, 2050, South Africa,*

[4]*School of Geography, Archaeology and Environmental Studies, University of the Witwatersrand, Johannesburg, Private Bag 3, Wits, 2050, South Africa,*

[5]*CwengaTechnologies (Pty) Ltd, 28 Boeing Road East, Dunvegan, 1609, South Africa*

[6]*Department of Plant and Environmental Sciences, University of Copenhagen, Thorvaldsensvej 40, 1187 Frederiksberg C, Denmark*

Abstract

Inductively coupled plasma optical emission spectroscopy (ICP-OES) and mass spectrometry (ICP-MS) are suitable techniques for trace multiple-element analysis but may have difficulty with these analyses when samples comprise complex matrices (due to spectral interference and matrix effects). High iron concentrations (>3 g/L) in acid mine drainage (AMD) necessitate large dilutions to render samples suitable for analysis. In these cases, trace element concentrations (0.2-5 mg/L) are reduced to method detection limits, where the uncertainty of measurement increases and precision decreases.

Selective ion-exchange (IX) resins, weak-based anion, weak-acid cation, chelating resins, and selective silica-based media were explored as an alternate method to precipitation techniques. The polyamine weak-based media, and the functionalised silica-based exchanger showed selective iron loading, thereby reducing concomitant trace metals losses by occlusion or adsorption, and reducing dilution requirements for instrumental analysis. Findings from this study suggest that IX and other adsorbers can potentially be used successfully to reduce interference and increase the accuracy of trace element analysis in AMD.

Keywords: Mine impacted water, ion exchange resin, inductively coupled plasma, iron removal

Introduction

Acid mine drainage (AMD) in South Africa is typically caused by the oxidation of pyrite resulting in an acidic ferrous sulfate solution. Valuable trace elements, such as Rare Earth Elements (REE), may also be present. Recovery of REEs from AMD would achieve a two-fold benefit of creating value from sale of the REEs, and remediation of the water as part of the value recovery process.

Quantification of low trace element concentrations is challenging owing to, the high ionic strength (due to the presence of protons and sulfate), and high iron (Fe) concentrations, which could be present in as much as four orders of magnitude higher than the trace elements of interest. Inductively coupled plasma optical emission spectroscopy (ICP-OES) and inductively coupled plasma mass spectroscopy (ICP-MS), are multi-element techniques suitable

for simultaneous analysis of several elements in samples comprising varied concentration levels. ICP-OES can tolerate higher total dissolved solids (TDS) concentrations and is fast and simple to operate, while ICP-MS has high sensitivity, can achieve lower detection limits, and has a wider dynamic range. ICP-OES suffers spectral overlap, while ICP-MS can be prone to isobaric interferences, is complex to operate, has slower analysis times, and higher set-up and operating costs (Agilent Technologies Inc., 2021). Dilution is required to reduce the complex sample matrix which also decreases the already low trace element concentrations to instrument and method detection limits, where the uncertainty of measurement is increased. ICP-MS is more suitable for analysis of analytes at low concentration, and atomic/isotope mass selection avoids spectral inter-element overlap, making it the preferable technique. If Fe could be removed, less dilution would be required, which would also limit the reduction of trace element concentrations and enable more accurate measurement of trace elements by ICP-OES. Analysis using ICP-OES has the advantage of being a more cost effective and robust method for trace element analysis that can provide fast turn-around to support rapid decision making for optimisation of upgrading testwork conditions.

Removal of Fe by precipitation (using pH adjustment) was considered in previous work, however significant quantities of REEs were co-precipitated using this approach. A pH alteration from 2.3 to 3.4 using lime addition and agitation, resulted in co-precipitation (likely due to occlusion) of multiple REEs ranging between 53 % (scandium) and 99 % (thorium) (Naidu *et al*., 2022).

An alternative method of Fe removal prior to analysis was therefore investigated using several specialised and commercially available ion exchange resins. Given that the aim of this work was to create a laboratory scale method, recovery and reuse of the resin media were not prioritised, and because of this it was possible to test some resins that have been reported to be extremely selective for Fe as to be irreversibly bound (Lee & Nicol, 2007).

Methods

The initial test work consisted of batch contact between the resins and the AMD solution. This is commonly known as an isotherm test. Seven resins were selected, Lewatit CNP80, Lewatit TP272, Lewatit TP308, Lewatit A365, Purolite MTS9570, PhosphonicS POH1, and Lewatit MonoPlus TP260 in both the hydrogen the monosodium forms. A strong acid cation resin Lewatit MonoPlus S108 was tested in previous work and showed a selectivity of REEs over Fe and so was not re-tested (Naidu *et al*., 2022).

Chelating resins with phosphonic groups are known to have a high selectivity for Fe (POH1, MTS9570 and TP260) (Fortin-Lecomte *et al*., 2022). This is also predicted by the hard and soft acids and bases (HSAB) theory. The POH1 is a functionalised silica media and has been recommended as a potential Fe removal sorbent.

Weak-based anion (WBA) resins have tertiary amine groups and can remove acidity and precipitate metal oxides. Polyamine WBA resins such as A365 may also have chelating effects (Amphlett *et al*., 2018; Ogden *et al*., 2017). Strong based anion (SBA) resins have a quaternary amine group that have a positive charge and are known to sorb acids by acid retardation and can also load metal anionic complexes (Yang *et al*., 2007). A solvent impregnated resin, TP272 was also tested.

Adsorption studies were conducted where fixed volume to volume ratios (1:10, 1:20, 1:50 and 1:100) of media to AMD were measured out for each resin tested and contacted for 4 hours at ambient temperature. The pH of the solution was measured after contact. The resin and any resulting precipitate were removed from the solution by gravity filtration, and the filtrates were submitted for ICP-OES and ICP-MS analysis. The resin was photographed under a Celestron 44308 Digital Handheld Pro Microscope at x100 magnification. The precipitates were not analysed as part of this work.

Samples were diluted x10 and x100 and made up to volume in 2 % nitric acid (HNO3) prior to submission to an external laboratory in South Africa, for ICP-MS analysis, where they were analysed using a Spectro, quadrupole mass spectrometer. An original AMD sample was also submitted

to the University of Copenhagen, Denmark, where concentrations of trace elements were determined by inductively coupled plasma mass spectroscopy (ICP-MS) (Agilent Technologies, Agilent 7500C). Polyatomic interferences were removed with an octupole reaction system (ORS) pressurized with He or H2. External calibration was applied, and drift corrected for by periodic recalibration. For all analysis categories repeated analyses of selected samples showed that the analytical uncertainties were acceptable.

ICP-OES analysis was conducted at CM-Solutions MetLab analytical laboratory facilities, using an Agilent 5800 VDV ICP-OES instrument. Measurement conditions were set to axial viewing, which allows the optical system to view the plasma end-on, facilitating increased sensitivity and lower detection limits.

Calibration standards were prepared from a 1000 mg/L Ultraspec multi-element certified reference standard, purchased from De Bruyn Spectroscopic Solutions, and traceable to NIST Standard Reference Materials. Calibration was performed prior to analysis, requiring regression coefficients (R2) of 0.999 for all elements analysed, and averaged results were reported from three replicate readings. Samples were analysed as received, at x10 and x100 dilutions. All dilutions were prepared in 2 % HNO3. ICP-OES analysis was carried out with and without automated addition of a 10 mg/L indium internal standard to account for non-spectral interferences. Internal standards are used to account for physical interferences such as viscosity effects, whereby the emission intensities of the internal standard in the calibration standards and samples are measured and ratioed to the initial emission intensity measured in the sample blank. This enables correction of intensity readings for all elements by this ratio and thereby improving the accuracy and the precision of results.

Results and discussion

ICP-OES and ICP-MS analysis for metal quantification of AMD

Samples from adsorption tests were analysed by both spectroscopic techniques, and results demonstrated effective removal of Fe. Comparison of data between the two methods indicated similar concentrations, with some variances noted for selected analytes. The concentration differences were attributed to spectral interferences encountered on the ICP-OES owing to the complex sample matrix (Gilleland *et al*., 2022; Liu *et al*., 2020; Michaud & Mermet, 1982). An original AMD sample was analysed, prior to IX testwork (Batch 0), and with each sample batch, as a control, and these data showed that concentration variations also occurred between batches for the individual techniques (Table 1).

Table 1 *Comparison of data for the original acid mine drainage sample for elements of interest.*

Instrument	Analyte	Batch 0	Batch 1 #1098	Batch 2 #1110	Batch 3 #1123
ICP-OES/ICP-MS	Analyte	mg/L	mg/L	mg/L	mg/L
ICP-OES	Ce	—*	4.62	3.66	4.42
ICP-MS	Ce	4.86	5.57	4.18	4.53
ICP-OES	Dy	—*	0.13	0.25	0.29
ICP-MS	Dy	0.26	0.33	0.26	0.27
ICP-OES	Fe	3186	3255	2742	2722
ICP-MS	Fe	3445	3062	2952	2593
ICP-OES	La	0.59	0.55	0.46	0.53
ICP-MS	La	0.64/0.61	0.70	0.47	0.57
ICP-OES	Nd	—*	1.11	1.04	1.26
ICP-MS	Nd	1.06	1.34	1.01	1.11
ICP-OES	Pr	—*	0.26	0.23	0.29
ICP-MS	Pr	0.23	0.27	0.21	0.23
ICP-OES	Y	—*	1.79	1.55	1.47
ICP-MS	Y	1.73	1.96	1.60	1.73

*Element/analyte not analysed

Optimisation of the ICP-OES method to achieve better agreement with ICP-MS data can be achieved using the method development tools available as part of Agilent ICP Expert operating software. An IntelliQuant analysis tool enables a semi-quantitative assessment of the relative elemental composition in an unknown sample, by collecting data between the 167 and 785 nm spectral range. Recommended wavelengths, with intensities, and possible interferences are provided by the software, and optimal wavelength selection is guided by selecting wavelengths that are least affected by spectral interferences from analytes identified by IntelliQuant analysis, and that have sufficient intensity to quantify the analyte of interest at the expected concentration level (Gilleland *et al*., 2022; Liu *et al*., 2020; Michaud & Mermet, 1982).

Not all interfering analytes, are mitigated by wavelength selection, and some spectral overlap may still be present. In this instance, several instrument software background correction options are available of which the Fast Automated Curve-fitting technique (FACT), is particularly suited to complex matrices, and uses spectral modelling to "mathematically deconvolute the analyte signal from the raw spectrum" (Agilent Technologies Inc., 2020).

As an example, Batch 1 ICP-MS data reported three times higher dysprosium (Dy) concentrations than ICP-OES. Review of the Dy 364.540 nm wavelength used for ICP-OES analysis indicated several immediate high–intensity, spectral interferences that could have affected this analysis outcome. The Dy 353.171 nm wavelength, was selected as an alternative wavelength, which offered higher intensity, and fewer, lower–intensity interferences. ICP-OES analysis data for batches 2 and 3 reported Dy concentrations that achieved better agreement with the ICP–MS concentrations. The method was subsequently modified to include FACT corrections for spectral interferences from cerium (Ce), manganese (Mn), thorium (Th), and sulfur (S) on dysprosium. Re-analysis of the original AMD sample with FACT correction reported a reduced concentration of 0.28 mg/L for both the x10 and x100 dilutions, compared with the 0.30 and 0.33 mg/L concentrations that would have been reported for these dilutions respectively, and which provided better agreement with ICP-MS data previously reported. Figure 1 shows the Dy analyte peak without and with FACT correction, where the Dy has been separated from the interfering analytes.

Method development is continuing, and

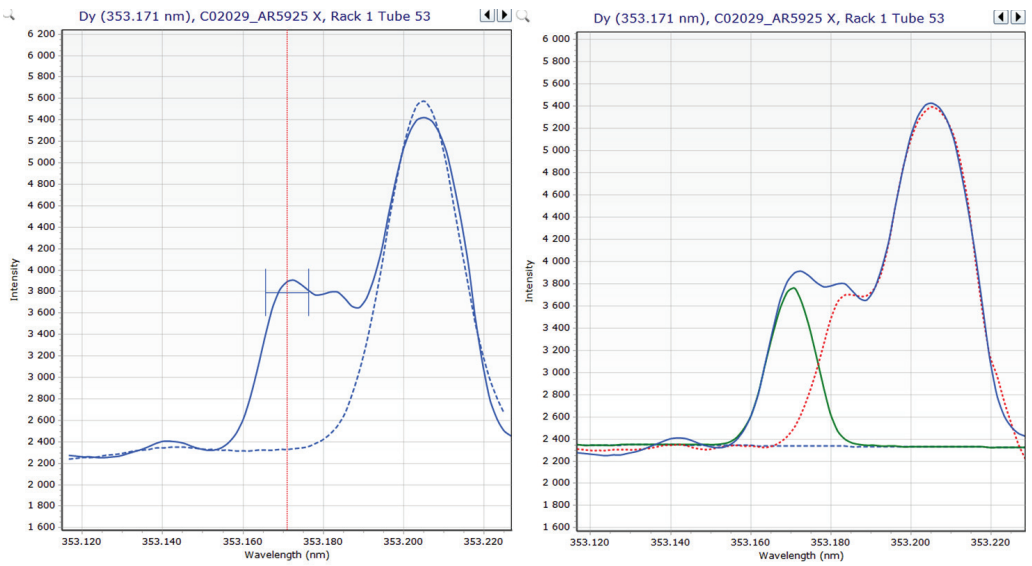


Figure 1 *A screenshot of dysprosium peaks without and with FACT correction*

seeks to quantify the effects of sample dilution, different internal standards, calibration using matrix matched standards, and the use of FACT, and/or other background correction tools, to further improve the method detection limits and reliability.

Ion Exchange Tests

Figure 2 shows the percentage removal of the REEs under investigation during this study, along side the removal of Fe from solution in the 1:20 ratio. The CNP80, TP272 and TP308 caused a loss of 2.7-3.3 % of the REEs analysed during treatment, but the Fe removal was low at 13 % for the TP272 ranging to 38 % Fe removal for the CNP80. Even at the highest solid to liquid ratios these resins did not show sufficient capacity for Fe to be useful for this application as a single step solution. Multiple contacts, or column tests might prove to be effective.

The TP260 performed poorly but has been reported to have a very high susceptibility to poisoning by Fe (III) in the metallurgical field, thus these results are expected (Arroyo-Torralvo *et al.*, 2017). It was interesting to note that in this case the resin did not perform particularly favourably in either the hydrogen or monosodium forms compared to the other resins evaluated. This could be due to kinetic effects, as the rate limiting step is likely to be particle diffusion and reaction between the Fe and the functional group. The MTS9570 was more effective at removing Fe, but also removed more of the REEs. This was unexpected as the dual functional groups should be more selective. The POH1 shows high Fe removal and low REE losses, and therefore shows promise for this application. In cases where the ion exchange caused a pH shift in the solution during contact a precipitation was observed and removed prior to analysis (Table 2). As this work did not include analysis of the solids, no distinction has been made to constituents loaded onto the resin, and those lost due to precipitation caused by the resin treatment. Tests on a larger scale would allow for a precipitate to be analysed to get a complete mass balance.

The A365 resin was able to remove the Fe quantitatively, while partially removing the REEs. This was the only resin able to remove Fe so that it was within an order of magnitude of the REEs. A mechanism proposed is that the resin is causing the Fe to precipitate with a very low level of supersaturation and thereby minimising coprecipitation. This contrasts with the conventional precipitation

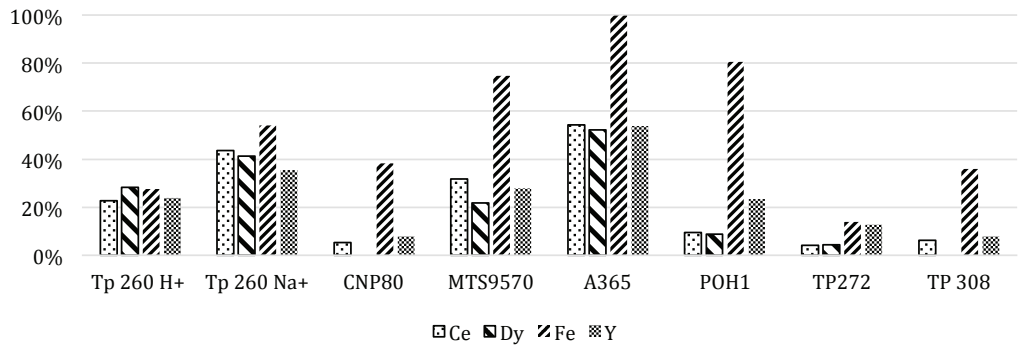


Figure 2 *Percentage ion removal by resin at the 1:20 contact ratio*

Table 2 *Effect of resin on pH of the AMD solution after contact and resulting precipitation.*

Resin	TP260 H+	TP260Na+	CNP80	MTS9570	A365	POH1	TP272	TP308
pH change		1.4	1.2	0.9	7.9	0.9	1.3	1.2
Precipitate	No	Slight		No	Yes	No		

techniques using the addition of a base containing reagent, such as the slag, caustic or lime work previously done (Naidu *et al.*, 2022). In the case of trivalent Fe $K_{sp} = [Fe^{3+}] \times [OH^-]^3 = 2 \times 10^{-39}$, which means that addition of base will result in supersaturation above a pH of 3. Typically, the precipitate is gelatinous, with a large surface area. The ferric oxide hydrate is amphoteric and can act as a cation exchange itself, loading the REEs and other cations onto its surface. Figure 3 shows one of the intermediate forms that the Fe can occur in, in the process of precipitation.

Conclusions

Adsorption test results demonstrated effective removal of Fe. Data comparison indicated similar results for Fe, with some variances noted for selected trace elements. ICP-MS isotope selection avoids inter-element overlap, making it the preferable technique, particularly when high dilutions are required.

Data showed that good agreement could be achieved between ICP-OES and ICP-MS data, and that ICP-OES can be reliably used for the analysis of trace elements, provided that samples are properly characterised to optimise wavelength selection and that the required inter-element interference corrections are applied.

The use of ion exchange and other adsorbers shows promise as an analytical technique to be developed further for the removal of Fe from complex solutions.

Acknowledgements

The authors thank all co-organisers for hosting the IMWA2023 Conference. Richard Stanton for his continuing contributions to the method development, Mandla Radebe for execution of the instrumental method set up, and implementation of the background corrections, Karabo Mothupi, Tshepi Sekatane, Mmushi Mathabathe and Khanyisile Mlangeni for performing the sample analysis. Glenna Thomas from the University of Copenhagen, for conducting a comparative ICP-MS analysis on the original AMD sample. Thanks to Lungile Ndhlovu and Mantsha Mathibela at the Cwenga applications laboratory for completing the resin test work. The authors would like to thank the Danida Fellowship Centre for their contributions to the acids to value project.

References

Agilent Technologies Inc. (2020). Agilent ICP Expert Software: Powerful software with smart tools for ICP-OES. www.agilent.com/chem

Agilent Technologies Inc. (2021). How To Choose the Right Atomic Spectroscopy Technique? November.

Amphlett, J. T. M., Ogden, M. D., Foster, R. I., Syna, N., Soldenhoff, K. H., & Sharrad, C. A. (2018). The effect of contaminants on the application of polyamine functionalised ion exchange resins for uranium extraction from sulfate based mining process waters. Chemical Engineering Journal, 354(July), 633–640. https://doi.org/10.1016/j.cej.2018.07.209

Arroyo-Torralvo, F., Rodríguez-Almansa, A., Ruiz, I., González, I., Ríos, G., Fernández-Pereira, C., & Vilches-Arenas, L. F. (2017). Optimizing operating conditions in an ion-exchange column treatment applied to the removal of Sb and Bi impurities from an electrolyte of a copper electro-refining plant. Hydrometallurgy, 171(June), 285–297. https://doi.org/10.1016/j.hydromet.2017.06.009

Fortin-Lecomte, C., Tran, L. H., Rioux, G., Coudert, L., & Blais, J. F. (2022). Recovery of indium from acidic leach solutions of spent LCD panels using ion exchange. Hydrometallurgy, 210(March). https://doi.org/10.1016/j.hydromet.2022.105845

Gilleland, G., Drvodelic, N., Hasty, E., Harris, M., CEM Corporation, & Agilent Technologies Inc. (2022). Analysis of Rare Earth Elements in Base Metal Ores by ICP-OES: Overcoming complex spectral interferences using an Agilent 5800 VDV ICP-OES. www.agilent.com/chem/5800icp-oeS

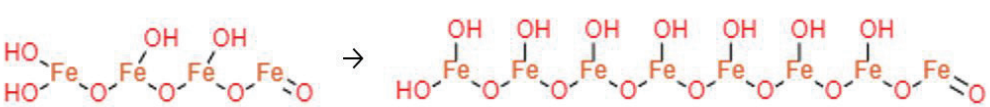


***Figure 3** Depiction of Trivalent Fe (Kolthoff* et al.*, 1969)*

Lee, M.-S., & Nicol, M. (2007). Removal of iron from cobalt sulfate solutions by ion exchange with Diphonix resin and enhancement of iron elution with titanium(III). Hydrometallurgy, 86(1), 6–12. https://doi.org/10.1016/j.hydromet.2006.10.002

Liu, Y., Xue, D., Li, W., Li, C., & Wan, B. (2020). A simple method for the precise determination of multi-elements in pyrite and magnetite by ICP-MS and ICP-OES with matrix removal. Microchemical Journal, 158(May), 105221. https://doi.org/10.1016/j.microc.2020.105221

Michaud, E., & Mermet, J. M. (1982). Iron spectrum in the 200-300 nm range emitted by an inductively coupled argon plasma. Spectrochimica Acta, 37B(2), 145–164. https://doi.org/0584-8547/82/020145-20503.00/0

Naidu, T. S., Moyo, N., Falconer, J., Hardwick, E., Smith, J., & Sheridan, C. (2022). Environmentally and economically sustainable water treatment system for post-mining waste Testwork Report. In Internal Testwork Report (Issue October). https://doi.org/10.2307/j.ctv2xqngb9.6

Ogden, M. D., Moon, E. M., Wilson, A., & Pepper, S. E. (2017). Application of chelating weak base resin Dowex M4195 to the recovery of uranium from mixed sulfate/chloride media. Chemical Engineering Journal, 317, 80–89. https://doi.org/10.1016/j.cej.2017.02.041

Yang, S.-T., Huang, H., Tay, A., Qin, W., Guzman, L. De, & Nicolas, E. C. S. (2007). Extractive Fermentation for the Production of Carboxylic Acids,. In Bioprocessing for Value-Added Products from Renewable Resources (pp. 421–446). Elsevier. https://doi.org/https://doi.org/10.1016/B978-044452114-9/50017-7.

Preventative methods to avoid Blow-out at Cwm Rheidol Adit 9, Ystumtuen Mine Sett

Peter Terry[1], John Leyland[1], David Mason[1], Heilyn Williams[2], Liz Jones[2], Richard Carline[1], Peter Stanley[2]

[1]*The Coal Authority, 200 Lichfield Lane, Mansfield, NG18 4RG, UK, peterterry@coal.gov.uk, johnleyland@coal.gov.uk, davidmason@coal.gov.uk and richardcarline@coal.gov.uk*

[2]*Natural Resources Wales, Tŷ Cambria, Newport Rd., Cardiff, CF24 0TP, UK, geowyddor@cyfoethnaturiol-cymru.gov.uk*

Abstract

An adit roof collapse 15 m within Adit No.9 of Cwm Rheidol mine was observed triggering a requirement for detailed blow-out assessment, revealing 2,112 m3 of trapped mine water. Intervention works since included replacing deteriorated stream linings, flow gauging of river reaches and extending the blow-out lagoon. A new blow-out channel constructed from Adit No.9 to the lagoon was overlaying two new pipes conveying mine water to the original riverside filter beds. Detailed design of adit dewatering requiring an offline tunnel to be excavated through mine spoil and bedrock, entering the adit 40 m behind the portal, providing a permanent drainage solution.

Keywords: Blow-out, assessment, remediation, intervention, tunnelling

Introduction

Ystumtuen is situated 15 km east of Aberystwyth, Ceredigion. The lead-zinc mine complex comprises Ystumtuen, Penrhiw, Bwlchgwyn and Llwynteifi mines on the mountain plateau and Cwm Rheidol in the valley. The mines exploited the Castell Lode within mudstones and sandstones of the Llandovery Series of the Silurian. The mineralisation is of quartz cemented breccias hosting galena, sphalerite, marcasite and pyrite. Marcasite is more abundant in the west of the lode.

The Cwm Rheidol Adit No.6 and Adit No.9 are key features relevant to this project. The shallower Adit No.6 was driven in 1822 through bedrock at 170 m above Ordnance Datum (aOD) with ore initially processed close to the portal. Spoil and gangue were tipped down the steep valley side. The deep drainage Adit No.9 was driven in 1901 at 110 m aOD through 30 m of mine spoil. Both adits continue to discharge low pH, metal mine water.

Natural Resources Wales (NRW) captured both adit discharges in 2009, conveying mine water by pipe to limestone filter beds that discharge via cascade to the Afon Rheidol. The filter beds, installed in the 1960's were initially successful in removing lead and zinc but having become ineffective in the 1970's are now dilapidated.

Adit No.9 has a known history of blow-out or outburst. In October 1969, during enabling works for exploration drilling an outburst caused the Afon Rheidol to turn red down to Cardigan Bay (Jones et al. 1975). In 1992, a shale dam had formed from a roof collapse within Adit No.9 holding back an estimated 2,273m^3 of acidic mine water. Subsequent intervention works in March 1993 required draw down of mine water to a lagoon, in order to replace adit roof lagging and install of 6 m of 225 mm diameter drainage pipe to competent ground (Mason 2011). When the mine water levels were reduced during these works, it was found that the legs of the support arches had rotted away. In November 1993, a ground collapse at Nant Bwlchgwyn occurred resulting in the stream flowing to workings and contributing to flow from Adit No.6, the increased flow across mine spoil resulted in mass movement that smothered Adit No.9 below. The surface water inflow was mitigated

through the installation of a halfpipe in the stream bed (Plate 1) spanning the collapse. Basic restoration around Adit No.9 was also carried out with mine water in the Adit No.9 tunnel kept elevated to prevent access. In 2008, the mine water levels in Adit No.9 were drained down to reduce risk of outburst and in 2009 rigid corrugated plastic pipes were installed at the adit portals to convey mine water from Adits No.6 and No.9 to the now failing filter beds. During maintenance (rodding) of the Adit No.9 drainage pipe in March 2016 a rumbling noise was heard and a sudden discharge occurred. The released water was directed toward the former lagoon area to dissipate.

Analysis of flow and chemistry data for both discharges since 2010 showed little variation in chemistry, excepting a period from January to May 2012 when Pb increased at Adit No.9 (Coal Authority 2017). Adit No.6 has had flows measured volumetrically typically in the range 3 to 12 Ls-1 dependent on seasonality but has shown occasional large spikes of 20 to 30 Ls^{-1}, indicative of direct surface water inflows. Adit No.9 has generally been consistently at or below 1 Ls^{-1} except for the period following the sudden outrush in March 2016.

NRW and the Coal Authority are partners in the joint Metal (Non-Coal) Mine Programme (MMP) and when undertaking feasibility in 2019 observed a roof collapse 15 m inbye of the Adit No.9 portal. This observation triggered a detailed Blow-out Assessment which identified an estimated 2,112 m^3 of trapped mine water.

The Blow-out Assessment identified a need for repairs and upgrades to previous surface water inflow measures and to assess other potential losses to workings on the mountain plateau. The assessment also identified a need to re-establish and upgrade blow-out mitigation engineering below Adit No.9. Including the immediate provision of a channel and attenuation lagoon to manage water in the event of a blow-out and to allow work on the adit blockage. It also recommended installation of permanent flow gauging stations for Adits No.6 and No.9, maintenance of the mine water pipelines to the filter beds and monitoring of mine water levels within the mine system (Coal Authority 2019).

Limiting Surface Water Inflow

Surface water inflow to the mine system has long been a problem. The three upper stream catchments Upper Afon Tuen to the west, Nant-yr-Oerfa in the north, that enters Nant Bwlchgwyn in the east joining the Lower Afon Tuen downstream of Ystumtuen with an area of approximately 200 ha. They cross the worked lodes and in Nant Bwlchgwyn a 6m by 900mm section of corrugated steel Armco half pipe was laid over a collapse in the stream bed in 1994. Flow gauging of Nant Bwlchgwyn using an impeller flow meter on a gravelly river bed during January 2004 identified a loss of 2 Ls^{-1} coinciding with a shallow depression in a stream channel. The depression appeared to represent a crown hole on an open stope, upstream of the Llwyn Teifi reservoir (NGR 2741102909055). A further loss of 4 Ls^{-1} was identified across the temporary stream

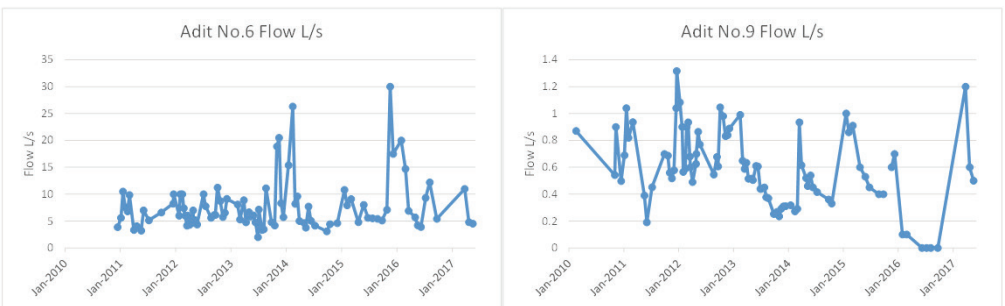


Figure 1 *Mine Water Flows at Adits 6 and 9 from 2010 to 2017 (Coal Authority 2017)*

bed (SRK 2004). Whilst there is uncertainty regarding flow observations and data, an estimated total 7 Ls^{-1} is lost to ground along the Nant Bwlchgwyn stream section. Rhodamine tracer testing in 2003 confirmed hydraulic connectivity between the collapsed shaft and Adit No.6. The estimated stream loss from Nant Bwlchgwyn would account for approximately half the flow discharging at Adit No.6. In 2007 a stream diversion was completed to prevent flow into the crown hole.

Further flow assessment was undertaken in June 2019 by Coal Authority and NRW. Flow in the Upper Afon Tuen reaches, Nant Bwlchgwyn and Adit No.6 was gauged using salt dilution methods. The fieldwork followed a period of rainfall when flows were greater than anticipated making gauging challenging. Flow measurements were as follows: Afon Tuen 145–282 Ls^{-1}, Nant Bwlchgwyn 17–31 Ls^{-1} and Adit No.6, 7 Ls 1. The results confirmed downstream increases in water volume with stream bed losses small, as such it was recommended that the exercise be repeated.

The condition of the steel halfpipe 1994 intervention (Plate 1)) had deteriorated over time with visible holes and opening lapped joints (Plate 2). Following removal and scanning the stone filled opening beneath, a replacement plastic half pipe with mortared headwalls was installed in September 2020 (Plate 3 and 4). Repeat flow gauging (Coal Authority 2021) during low flows indicated no losses on the Afon Tuen and no visible losses around the new half pipe though flows were too low to perform accurate flow gauging on Nant Bwlchgwyn.

A discharge into workings continues at Lee's Shaft above Nant Bwlchgwyn and downgradient of a 6 ha catchment with shallow and redundant reservoir that retains shallow pools, the reservoir area is now mostly vegetated in Juncus on boggy ground. The South lode runs parallel to and in front of the former embankment and has been worked to near surface and to surface in part. Lee's Shaft is at the eastern end of the embankment tucked into the hillside and the stream from the former reservoir crosses the lode northward toward Nant Bwlchgwyn that flows to the west.

The collapse around Lee's Shaft was large in 2018, but by September 2020 a further collapse into the stope of approximately 4 m occurred. The failure was likely related to water migration at the base of the weathered zone, with visible seepages seen at rockhead flowing to the void following the collapse. Six piezometers were installed, four on the embankment and two north of Lee's Shaft in clusters of two, which confirmed variable groundwater levels. Geophysical methods to identify preferential seepages along the embankment are being considered to appreciate if an intervention such as cut off



Plate 1 *Nant Bwlchgwyn 1994 halfpipe (Mason 2011)*

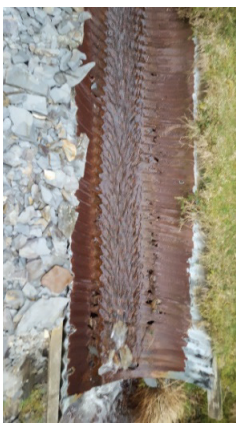


Plate 2 *Nant Bwlchgwyn 1994 halfpipe (NRW 2018)*



Plate 3 *Nant Bwlchgwyn replacement halfpipe (NRW 2020)*



Plate 4 *Nant Bwlchgwyn replacement 6m x 900mm halfpipe (NRW 2020)*

wall sections on the up gradient embankment have merit.

Cwm Rheidol Adit No.9 Interventions

During a feasibility site walkover in February 2019 with Cambrian Mines Trust members and eminent mineralogist John Mason to record important mine heritage and features a roof collapse 15 m inbye of the portal was noted. The photographs available from reconstruction (Mason 2011) identify the steel arches on timber blocks. Using these and more recent photographs one can conject 0.5 m of ochre in the Adit No.9 portal. It is also evident that the steel arches have deformed over time.

To understand mine working connectivity, old mine plans, conceptual sections (Lord 2018) and previous reports on intervention work (Mason 2011) were reviewed. It became evident that prior to 1993 a collapse in workings on Level 6 inbye of Penrhiw had enabled water to build up and flow to Level 9 via a connecting level and winze. The removal of this blockage and introduction of twin corrugated plastic pipes enabled mine water to discharge again via Adit No.6. It is reported that a collapse or a wall obscured by ochre close to the boundary between Ystumtuen and Penrhiw on the Great Lode in Level 6 is considered a barrier restricting or preventing water from passing from Level 6 to Level 9.

The deteriorating condition of Adit No.9 necessitated further surveys in order to develop interventions. Surveying the adit, the roof collapse and the surroundings has included visual CCTV, thermal imagery, topographic survey, geospatial laser scanning, gas monitoring and UAV drone inspections. The challenging conditions in the adit required the use of a push rodded floated craft to deploy robotic sewer CCTV camera with LED lighting and a GeoSLAM REVO mobile mapping laser scanner to access the adit from portal to blockage. Three survey control points were marked out around the adit portal and georeferenced using a Leica GPS RTK SmartNet GNSS receiver to OSGB 36 National Grid. Three spheres were placed over the survey control points and a laser scan survey of the spheres, adit entrance and adit surroundings carried out, using the GeoSLAM REVO mobile mapping laser scanner. The data from all laser scans were composited to generate a 3D representation of the surface and outer portion of the adit including the overlying collapse feature (fig. 2).

Later visits using roped access above the adit allowed laser scanning of the collapse feature, this data being added to the 3D model (fig. 2). The collapse feature was also installed with a telemetered pressure transducer to monitor and record water levels in the adit level inbye of the near surface blockages. This data has been used in conjunction with recorded mine plans, photographs and reports to estimate that 2,112m3 of mine water is trapped.

The Project has undertaken three ground investigations, with five boreholes and seven trials pits in the attenuation pond and Adit No.9 area in the first phase. A second investigated the original lagoon embankment crest by means of four window sampler holes. The third comprised eleven rotary boreholes, seven machine excavated trial pits and three hand dug pits in the attenuation lagoon and associated construction compound areas.

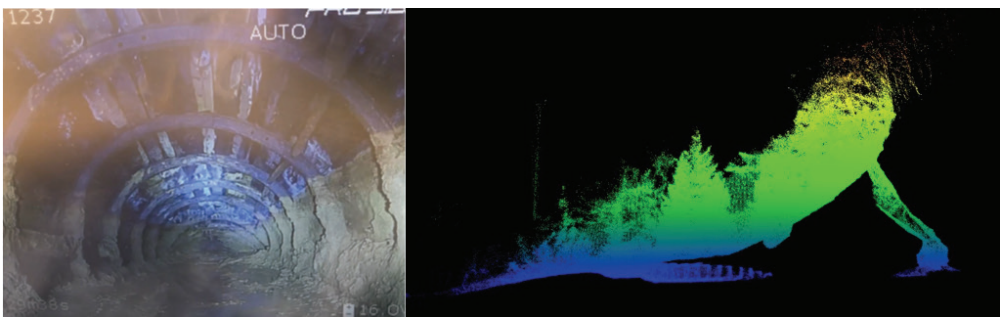


Figure 2 *Adit No.9 roof & combined laser scanned imagery (Geoterra 2019)*

The rotary boreholes were progressed to a maximum depth of 10 m. Investigations were completed with heritage and habitat watching briefs to enable access and micro siting. The evidence gained fed the Coal Authority's detailed design of Phase 1: the blow-out channel from Adit No.9, crossing the two new mine water discharge pipes; the manifold with trench box flow measurement stations for both Adit No.6 and Adit No.9 discharges and the attenuation lagoon capacity and freeboard expansion. Soil and core material sampling data was used to prepare a Materials Management Plan using the CL:AIRE definition of waste, code of practice. These Phase 1 works were delivered by Walters and completed in 2022. The potential blow-out risk is mitigated by a constructed concrete canvas lined bund at the adit portal and a flow control chamber that directs blow-out water to pipework and the lined channel. The water level in Adit No.9 is continuously monitored with alarms to alert of changed water level conditions.

The Phase 2 design aims to bypass the blockages in Adit No.9 by way of a 40 m long 1.5m diameter offset tunnel which will be progressed by means of pipe jacking. The tunnel is designed to enter the adit level behind support arches and props as recorded during original intervention work (Mason 2022). This work will entail the requirement to temporarily open the mine under the Mines Regulations 2014 with a designated Mine Owner, Mine Operator and Mine Manager (Competent Person). The new tunnel will include 160 mm diameter pipework with shut off valves to provide permanent blow-out resistant drainage, connected to existing mine water pipework. The original Adit No.9 portal and collapsed roof will be stabilised with cementitious grout or equivalent and with walling in local stone as recognition of the original feature.

Planning

The Cwm Rheidol Phases 1 and 2 works, and the Nant Bwlchgwyn halfpipe replacement, were carried out using permitted development rights NRW possess under the provisions of Part 15 Class A(b) of the Town and Country Planning (General Permitted Development) Order 1995. This enables development in, on or under any watercourse and required in connection with the improvement, maintenance or repair of that watercourse or those works. The Project was screened against the Environmental Impact Assessment (Land Drainage Improvement Works)(Amendment Regulations) 2017/585 to ascertain whether a statutory Environmental Impact Assessment (EIA) was required and an Environmental Statement needed production. Whilst the screening concluded a statutory EIA was not required, an Environmental Action Plan (EAP) was developed in accordance with NRW good practice and to ensure potential environmental risks of the Project were appropriately managed and mitigated.

An Ordinary Watercourse Consent under Section 23 of the Land Drainage Act 1991 was granted. A Water Framework Directive Preliminary Assessment and a Habitat Regulations Assessment was also completed by the Coal Authority. The Habitat Regulations Assessment concluded that the works would have no direct impact on the nearby internationally designated Rheidol Woods and Gorge Special Area of Conservation (SAC) and the downstream West Wales marine SAC and North Cardigan Bay Special Protected Area (SPA).

Habitat, Heritage & Landscape Constraints & Opportunities

The industrial archaeology and lower plant species provide rich heritage and habitat at the metal mine sites. In developing the EAP it was necessary to gather pertinent evidence and in relation to habitat, previous studies identified compartments and species at Ystumtuen, Penrhiw, Bwlchgwyn and Llwynteifi plus Cwm Rheidol (Simkin 2015). The lichens at Nant Bwlchgwyn include seven metallophytes, one with a conservation status of near-threatened, and four that are nationally scarce. Cwm Rheidol is undisturbed by livestock and hosts areas of mature calaminarian communities rich in lichens and bryophytes. Eighteen bryophytes and 71 lichens and lichenicolous fungi were recorded as well as a large population of the vascular plant *Silene uniflora* around the crusher house buildings. The lichenous species include twelve metallophytes, one with

a conservation status of near-threatened, two nationally rare and nine that are nationally scarce. The sites are identified as Regionally Important Geological Sites (RIGS) in Special Landscape Area (SLA-11), Rheidol Valley with promoted footpaths, cycle paths and Vale of Rheidol narrow gauge railway (LFS 2019). No bats were identified to be roosting or commuting in the immediate environs of Adit No.9 and a bridleway through the lagoon area has been temporarily diverted. Lagoon works presented opportunities to improve metallophyte succession by removing invasive scrub and creation of new substrate for lichen and bryophyte colonisation established by translocation.

Cwm Rheidol mine site is located within the designated Upland Ceredigion Landscape of Historical interest. The Historic Environment Record, National Monument Record and site archaeological appraisal visit (HRSWales 2019) identified that only a few significant historic features of importance remained including Penlefel Cottage and Magazine Hut by Adit No.6, crushing house walls, a former leat and yellow ochre spoil heaps. A recommendation included a need to be aware of buried heritage features and archaeology. Accordingly watching briefs for both archaeology and habitat were required for access with plant machinery, and during position selection for intrusive excavations. During these activities recording of features and translocation of rare Calaminarian grassland species was undertaken.

Conclusions

The site work is essential to reduce the risk of mine water blow-out should hydrostatic pressure exceed the resistive forces of the near surface blockage. The offset tunnelling provides a controlled means of gaining level entry rather than working in the original adit. Completion of the blow-out works will enable the MMP to focus on the metal mine water treatment scheme required to negate the polluting impact of the adit and diffuse discharges. The need to gather evidence prior to and during works is essential in delivering sustainable sympathetic solutions and necessitates careful multi-disciplinary coordination across partners, organisations and stakeholders.

Acknowledgements

This study is funded by the joint Metal (Non-Coal) Mine Programme of NRW and The Coal Authority sponsored by Welsh Government. We extend our thanks to Dr Nina Menichino, Team Leader, Evidence Portfolio, Programmes and Processes at NRW for supporting this paper.

Acknowledgements

This study is funded by the joint Metal (Non-Coal) Mine Programme of NRW and The Coal Authority sponsored by Welsh Government. We extend our thanks to Dr Nina Menichino, Team Leader, Evidence Portfolio, Programmes and Processes at NRW for supporting this paper.

References

Jones, A.N. and Howells, W.R. 1975. The partial recovery of the metal polluted river Rheidol. In: Chadwick, M.J. and Goodman, G.T. (eds).The Ecology of Resource Degradation and Renewal, pp. 443–445. Blackwell, London.

Mason J. (2011) Diary of an eco-nazi part two: the hands-on approach (geologywales.co.uk) last accessed 23/03/2023

Lord I. (2018) Rich Mountains of Lead – The metal mining industry of Cwm Rheidol and Ystumtuen.

Coal Authority (2017) Hydrogeological assessment of risk of blowout at Cwm Rheidol Adit No. 9 – Phase 1.

SRK (2004) Cwmrheidol Site Investigation Tender Reference 12642. Report 2 Recommended Design and Management for Remediation of the Mining Complex.

Coal Authority (2019) Cwm Rheidol – Ystumtuen Flow Gauging.

Coal Authority (2021) Cwm Rheidol – Ystumtuen Flow Gauging.

Coal Authority (2019) Cwm Rheidol Blow-Out Potential and Mitigation (BOP2 Report).

Geoterra (2019) Subsurface Laser Scan & CCTV Surveys Old Mine Drainage Adit No 9 Cwm Rheidol, Aberystwyth, Ceredigion Mid Wales, SY23 3NB

Mason J. (2022) No. 9 Adit, Cwmrheidol. Notes from the day-book kept during its dewatering in March 1993 with additional discussion, suggestions and images.

Simkin (2015) A Survey of Calaminarian Grassland in Mid Wales. Evidence Report No. 061.

Lingard Farrow Styles (2019) Preliminary Landscape Appraisal, Cwm Rheidol Mine, Ceredigion.

HRSWales (2019) Cwm Rheidol Lead Mine, Ystumtuen, Ceredigion. Cultural Heritage & Archaeological Feasibility Study.

Rainfall Induced Transient Pressure Wave Mechanisms in Tailings Dams

Charné Theron[1,2], Simon A. Lorentz[3]

[1]*Department of Spatial Planning, Rijks University of Groningen (RUG), Netherlands, c.theron@rug.nl ORCID 0000-0002- 2900-5513*

[2]*Department of Natural Sciences, University of the Western Cape, South Africa*

[3]*SRK Consulting, South Africa, ORCID 0000-0003- 3058-6789*

Abstract

The failure of tailings dams are most frequently attributed to liquefaction, erosion and overtopping. The purpose of this study is to investigate alternative physical/hydrological processes resulting from high rainfall intensities causing slope instability. In particular, the advancing wetting front may cause transient air pressure waves to rapidly increase the phreatic surface and change pore water suction status. Some research has been conducted on this phenomenon in natural hillslopes but have not been considered in the case of tailings dams. In order to quantify these physical processes, specific experiments have been conducted. Laboratory work included a large leak-proof column filled up to 2.65 m with silica fines material with similar hydraulic characteristics as platinum tailings at *in-situ* dry bulk density. The column was instrumented with seven data ports, each consisting of a time domain reflectometry probe to measure volumetric water content, a mini tensiometer to sense pore water pressure and a pore air pressure probe. The experimental setup allowed for the application of artificial rainfall at different intensities and controlled boundary conditions, during automatic logging of the hydraulic state variables. Recorded observations showed that after the application of water to the soil surface, pore air pressure ahead of the wetting front increased rapidly, causing air pressure wave propagation to mobilise pre-event water and reduce pore water suction. This led to the conclusion that high intensity rainfall events are likely to contribute to the generation of transient pressure waves in tailings porous medium, thereby inducing the rapid transmission of pressure head to a potential failure plane, where changes to effective stress may contribute to slope instability.

Keywords: Pore Air Propagation, Groundwater Mobilisation

Introduction

Previous research studies, conducted on natural hillslopes, found that high rainfall intensity events lead to excessive infiltration while rainfall frequency impacts on antecedent moisture conditions and the generation of pre-event water (Guo *et al.* 2008) (Rahardjo *et al.* 2001). Both these event characteristics (intensity and frequency) could contribute to tension saturated or near saturated conditions and have an impact on physical and hydrological processes that regulate the structural integrity of engineered slopes and earth embankments. According to Rahardjo *et al.* (2004) surface infiltration during and after a rainfall event cause slope instability by increasing pore water pressure, which leads to a decrease in the shear strength of residual soils. Zang *et al.* (2019) argue that water infiltrating the soil profile, combined with pre-event water contained in the capillary cringe, provides ideal conditions for the rapid mobilisation of groundwater and eventual slope failure. The contribution of pre-event water to stormflow could be attributed to a range of hydrological processes, including transmissivity feedback, non-Darcian pressure waves, and preferential flows. Cloke *et al.* (2006) argue that the fine nature of tailings media allows for a greater propensity for capillary fringe rise, thereby reducing the probability of Darcian flux

occurring. This paper builds on research previously presented by Waswa and Lorentz (2015) that found transient pressure waves in natural hillslopes to be responsible for the rapid release and mobilisation of previously antecedent moisture through the mechanisms of Groundwater Ridging (GWR) and the Lisse Effect (LE).

Mechanisms contributing to the rapid mobilisation of groundwater

Several studies describe GWR as the rapid response and disproportionate rise in the water table after a rainfall event in shallow groundwater systems (Zang *et al*. 2019; Meyboom 1967). According to Zang *et al*. (2019) GWR ridging only occurs if the capillary fringe extends from the water table to the natural ground surface. Gillham (1984) argues that the 'capillary fringe effect' causes a transient influence on the position of the water table and that the magnitude of rapid water table response is enhanced by fine-grained geologic materials. Under such conditions, the near-saturated porous medium in the capillary zone provides a continuous pore water phase that is entirely dominated by tension. The addition of a small amount of water relieves this tension, thereby releasing pre-event water to combine with the phreatic surface, resulting in a magnitude of GWR much greater than the amount of surface infiltration. This argument is supported by Cloke *et al*. (2006) who state that even a small amount of infiltrated water can rapidly convert the negative capillary pressure head in the capillary fringe to a positive pressure head, thereby changing the water table gradient and forcing pre-event water out. In contrast, the energy hypothesis was proposed by Waswa and Lorentz (2015), finding that the intensity of a rainfall event provides additional energy required to convert water in the unsaturated zone to water below the phreatic surface. Similar to previous studies, Waswa and Lorentz (2015) found that the extension of the capillary fringe is necessary to enable GWR by providing contact between the kinetic-energy-carrying intense raindrops and the potential-energy-deficient pore water. They further postulated that the only difference between the capillary fringe and phreatic zone would therefore be the energy content (Waswa and Lorentz 2016).

A number of earlier studies have recognised the exaggerated response of the water table after surface recharge and infiltration (Meyboom 1967). Guo *et al*. (2008) described this occurrence as the LE and found it to develop after the build-up of air pressure between the wetting front and the phreatic surface. Zang (2019) describes the process of conversion as being due to the increasing pore air pressure that increases pore water pressure below the advancing wetting front, converting negative pore water pressure to positive pore water pressure. During a rainfall event, surface infiltration produces a downward moving wetting front, forming a restriction to the outflow of air (Meyboom 1967) (Guo *et al*., 2008). Weeks (2005) explains that the encroaching wetting front causes rapid pressure transmission to the top of the capillary fringe and continues to build up until entrapped air pressure is higher than the pressure head of the infiltration profile. According to Cloke *et al*. (2005) this increase in pore air pressure is accompanied by the induction of transient pressure waves. The corresponding increase in pore water pressure creates a continuous water phase in the capillary fringe, which allows for the rapid transmission of antecedent water. Even though some air will escape, the temporary rise in saturated zone pressure may be enough to induce slope instabilities. The LE, similar to GWR, is particularly dependent on the intensity of a rainfall event. High rainfall intensity events often lead to infiltration that fills the entire soil pore space but it is also possible that rainfall intensity during a critical event may exceed the infiltration capacity of surface soil, resulting in ponding (Fredlund and Stianson 2011). Simulation results compiled by Guo *et al*. (2008) indicate an increase in ponding depths to contribute to a substantial rise in the water level of the observation well. Meyboom (1967) states that ponding would inhibit the escape of air from the soil which contributes to higher compression values in the unsaturated zone, thereby intensifying the magnitude of the LE. It is therefore recognised that high intensity rainfall events, would be more prone to

generating conditions required for both GWR and the LE to occur.

Methods

The experimental design involved infiltration experiments under controlled boundary conditions while monitoring the physical response of hydraulic state variables to simulated rainfall events. Laboratory work included a large 2.85 m high leak-proof column (600 mm ID) filled up to 2.65 m with tailings replica at *in-situ* dry bulk density. Similar to the procedure described by Waswa (2013), the PVC pipe was packed in 300 mm layers and administered the same number of blows after each deposit to ensure uniform bulk density. The complex nature of physical and hydrological processes in the vadose zone required sensing devices and automated data acquisition techniques to accurately determine hydraulic properties of a homogeneous tailings medium and simulate the generation of transient pressure waves. For this reason, the PVC column was instrumented with seven data ports, spaced vertically down the column. Each port was comprised of three custom made instruments including a time domain reflectometry (TDR) to measure volumetric water content, a 1 bar mini tensiometer (MT) to measure soil pore water pressure and a pore air pressure probe (PAPP). Ports were installed at 500, 600, 700, 800, 1100, 1400 and 1700 mm from the bottom of the pipe while automatic logging of the hydraulic state variables ensured accurate uninterrupted data of phreatic surface dynamics, the soil moisture profile and pore water/air pressure responses. Schematic details of the column apparatus and test setup (Figure 1) follow a similar design as the soil columns used by Waswa (2013) and Salas-García *et al.* (2017). The PAPP was connected

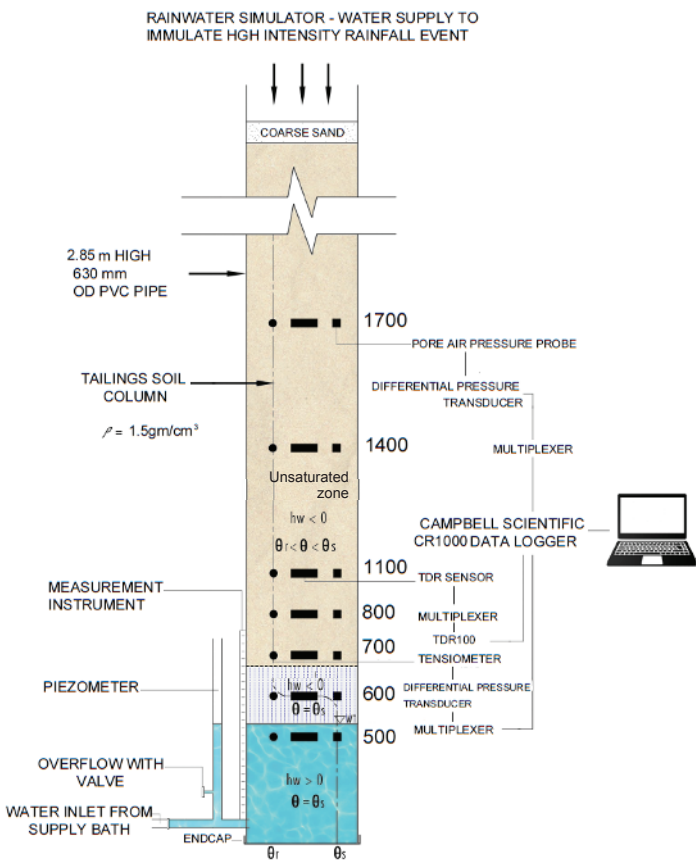


Figure 1 *Schematic diagram of the column test apparatus and setup. θr = residual soil water content, θs = saturated soil water content.*

to the 0.1 differential pressure sensor which was connected to the CR1000 data logger. The TDR probes were connected to the CR1000 data logger via the SDMX50 Multiplexer and Campbell Scientific TDR100 wave generator. The 1 bar pressure transducer connected the MTs to a data logger in order to obtain measurements. These sensors are connected to the CR1000 data logger via the multiplexer. After setup, the installation was allowed to settle. De-aired water was introduced from the bottom of the soil column, from the supply bath through an inlet valve positioned 200 mm from the base of the column, to prevent the capture of pore air and eliminate a disproportionate water table response (Waswa and Lorentz, 2016). Water was allowed to come to equilibrium, establishing a stable pre-simulation piezometric water level, positioned just below the lowest port at 450 mm from the base.

All sensors were monitored, by downloading data and plotting graphically, to ensure stability over at least four hours preceding the application of water at the surface boundary. Proceeding with the experiment, the coarse-grained topsoil surface was subjected to the artificial application of rainfall at three different ponding depths (event 3 not discussed), simulating surface recharge. These infiltration tests were conducted to investigate the effects of different boundary conditions and the advancement of the wetting front. The volume of each application was based on the depths of design rainfall events of particular return periods (1:200, 1:100 and 1:50 years) and calculated based on the inside area of the soil column. See Table 1. Design storms were obtained from station-specific data relevant to the area under study and applied in volumes calculated on the column's surface area. After each application the hydrostatic condition of the entire soil column was monitored by automated readings at 20 second intervals. This enabled the analysis of hydraulic properties and identification of transient profiles during the redistribution phase.

Laboratory results and experimental data analysis

After application of simulated rainfall events, there were several instant responses observed as soon as water was ponded onto the soil surface. Event 1 also showed some delayed responses. It should also be mentioned that in some instances it was impossible to define an accurate phreatic surface. Waswa (2013) owes this to the fact that the zero-pressure line may rise above the capillary fringe. It is also suggested that the particular fine nature of the soil medium allows for an undefined water table and extended capillary zone. The most significant responses will be discussed below.

Before application, the piezometric water level was measured manually with the use of the piezometer, which indicated

Table 1 *Description of incremental addition of water to tall soil column. Rainfall depths based on station specific data (Smithers and Schulze, 2002)*

Event	Return period	Rainfall depth	Volume	Addition of water to tall soil column
1	1:200 year	84.1 mm/h	24 L/h	9 L/30 min, 14 L/15 min & 1 L/15 min
2	1:100 year	74.9 mm/h	21.2 L/h	8 L/15 min & 13.2 L/45 min

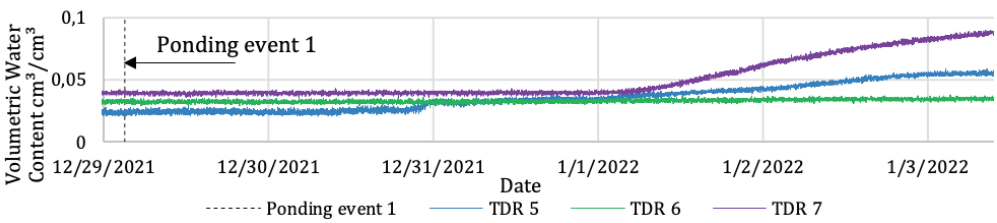


Figure 2 *Volumetric Water Content after event 1*

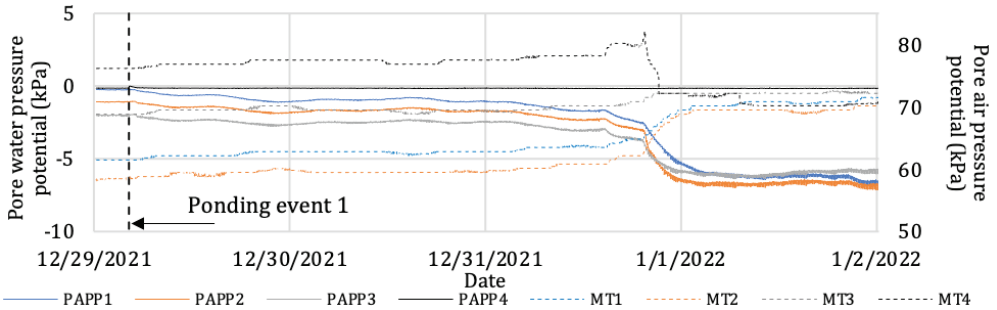


Figure 3 *Pore pressure response after the surface application of ponding event 1*

the location of the water level directly on Port 1. It is presumed that Port 2 was in the capillary fringe and since Ports 3 and 4 indicated unsaturated conditions, they were most likely located above the capillary fringe, together with the three shallow TDRs. Figure 2 illustrates the advancing wetting front that reached shallow TDRs (0.95 m below surface) after 50 hours.

The response in pore air pressure in the vicinity of the water table, to the advancing wetting front is shown in Figure 3. Compressed pore air pressure also brought about corresponding responses of pressure potential in the region of the capillary fringe. These results suggest that the magnitude of groundwater level responses is directly related to the magnitude of compressed pore air pressure. Waswa (2013) observed a similar simultaneous response in tensiometric pore water pressure at different soil depths, after a rainfall event of 67.8 mm, that also consisted of a high peak 1-minute intensity of 228 mm/h. There was found to be a clear relationship between the total change in pressure potential, in the vicinity of the water table, and the amount of compressed pore air pressure, imposed on the capillary fringe, after an extended time. Similar to Torres *et al.* (1998), Waswa (2013) assumed this to be the result of compressed pore air ahead of the wetting front. The proportional and corresponding change between pore air pressure and pore water pressure is therefore suggested to signal the presence of a pressure wave.

According to Koseki *et al.* (2010) a reduction in pore air pressure could be caused by the expansion of dense soil, possibly indicating mobilization along a failure plane. These conclusions were drawn while investigating the generation of negative pore air pressure in the filling of retaining walls during the simulation of earthquakes. However, even though soil saturation and an increase in porewater pressure reduces slope stability, it has been found that even a small reduction in pore-air pressure can significantly increase the factor of safety in slopes (Ba-Te, 2005, as cited in Fredlund *et al.,* 2012). Based on the principle of effective stress, it is suggested that the change in volumetric water content at the deep probes (not shown) is caused by the swelling or consolidation of soil due to the change in pore pressure above the air entry value. The small magnitude of the volumetric water content is attributed to the low compressibility of the soil matrix. It is therefore recognised that recorded changes in water content and pore water pressure are likely brought about by the rapid (downward) propagation of pore air pressure induced by rainfall.

After application of ponding event 2, volumetric water content at the three shallow probes immediately recorded changes, while the four deep probes increased shortly after (although at far less magnitude). This is shown in Figure 4. These results are similar to the infiltration tests conducted by Salas-Garcia *et al. (*2017) whereby a sharp increase in water content at the top of the column, eight minutes after ponding, decreased shortly after ponded infiltration stopped. Comparable to the present study, water content measured by the deep instruments increased and decreased at a delayed time and at a slower rate as compared with those for the upper section. Similarly, Waswa (2013) observed

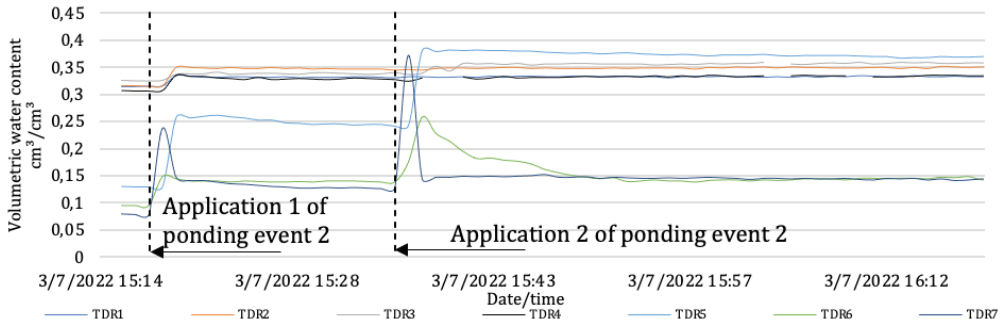


Figure 4 VWC after the surface application of ponding event 2

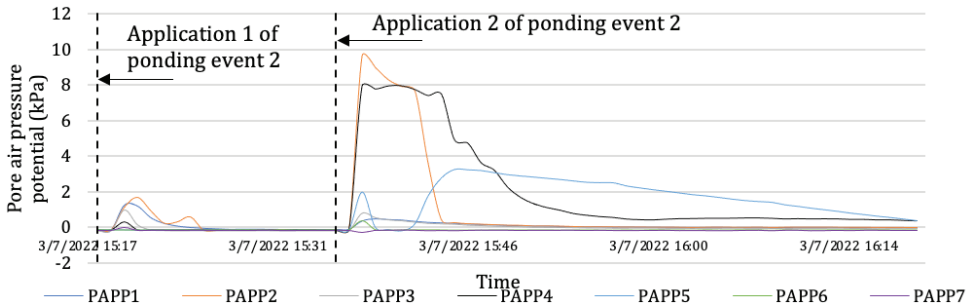


Figure 5 Instant response in pressure potential proportional (ponding event 2)

volumetric water content at the shallowest sensor to respond after 44 minutes from the start of the experiment, before arrival of the wetting front.

Ponding resulted in an instant response in pore air pressure potential. The magnitude of increase between application 1 and 2, shown in Figure 5, illustrates its sensitivity to ponding depth, which in turn is determined by rainfall intensity.

Discussion and Conclusions

Most pore air pressure sensors, tensiometric pore water pressure sensors, and water content sensors responded as soon as or shortly after water was applied to the soil surface. The significant response of deep MTs indicates that pore air pressure ahead of the wetting front caused the propagation of pressure waves that mobilised pre-event water and reduced pore water suction. These observations indicate that tensiometric pore water pressure responded to the compressed pore air pressure, before the arrival of the wetting front and supports salient literature on the hydrologic response of saturated soil confirming the unique relationship between pressure head and water content (Bear, 1972). It was also established that the rise of the phreatic surface is regulated by time-dependent flux boundary conditions and that the magnitude of water table response is regulated by the magnitude of compressed pore air pressure which in turn is determined by the intensity of a rainfall event. These pressure diffusion mechanisms cause an exacerbated increase in water content, independent of infiltration. It is therefore suggested that transient pressure wave mechanisms that are generated by high intensity rainfall events, originate in the unsaturated zone of tailings porous medium, thereby contributing to slope instability through changes in effective stress.

References

Ba-Te, B. (2005). Flow of air-phase in soils and its application in emergent stabilization of soil slopes. M.Phil thesis, Department of Civil Engineering, Hong Kong University of Science and Technology.

Bear, J. (1972). Dynamics of Fluids in Porous Materials. New York: Elsevier (reprinted by Dover Publications, 1988).

Cloke HL, Anderson MG, McDonnell JJ, Renaud JP (2006) Using numerical modelling to evaluate the capillary fringe groundwater ridging hypothesis of streamflow generation. J. Hydrol. 316(1–4):141–162

Fredlund DG, Rahardjo H, Fredlund MD (2012) Unsaturated soil mechanics in engineering practice. John Wiley & Sons Inc

Fredlund DG, Stianson J (2011) Quantification of moisture flux boundary conditions from climatic datasets. Proc., nSAT 2011 Symposium on Unsaturated Soils. Pirenopolis, Brazil, September 19 – 21, 2011

Gillham RW (1984) The capillary fringe and its effect on water-table response. J. Hydrol. 67(1–4):307–324

Guo H, Jiao JJ, Weeks EP (2008) Rain-induced subsurface airflow and Lisse effect. Water Resources Research, 44(7):1–9

Koseki, J., Kimhor, H., Nakajima, S., Mulmi, S., Watanabe, K., & Tateyama, M. (2010). Negative pore air pressure generation in backfill of retaining walls during earthquakes and its effect on seismic earth pressure. Soils and Foundations, 50(5), 747–755.

Meyboom P (1967) Groundwater studies in the Assiniboine river drainage basin: Hydroloic Characteristics of Phreatophytic vegetation in the south-central Saskatchewan. Geol. Surv. Can. Bull, 139

Rahardjo, H., Li, X. W., Toll, D. G., & Leong, E. C. (2001). The effect of antecedent rainfall on slope stability. Geotechnical and Geological Engineering, 19(3–4), 371–399. https://doi.org/10.1023/A:1013129725263

Rahardjo, H., Choon, L. E., & Tami, D. (2004). Capillary Barrier for Slope Stabilisation. Geotechnics, 17(January), 70–72.

Salas-García, J., Garfias, J., Martel, R., & Bibiano-Cruz, L. (2017). A Low-Cost Automated Test Column to Estimate Soil Hydraulic Characteristics in Unsaturated Porous Media. Geofluids, 2017, 1–13. https://doi.org/doi.org/10.1155/2017/6942736

Smithers, J. C., & Schulze, R. E. (2002). Design Rainfall and Flood Estimation in South Africa. December, 1–180.

Torres, R. D., Montgomery, W. E., Anderson, S. P., & Loague, K. (1998). Unsaturated zone processes and the hydrologic response of a steep, unchanneled catchment. Water Resource Res., 34(8), 1865–1879.

Waswa, G. W. (2013). Transient pressure waves in hillslopes. Doctor of Philosophy. Department of Civil Engineering. University of Kwa-Zulu Natal.

Waswa GW, Lorentz SA (2015) Energy considerations in groundwater-ridging mechanism of streamflow generation. Hydrological Processes Journal, 29:4932–4946

Waswa GW, Lorentz SA (2016) Transmission of pressure head through the zone of tension saturation in the Lisse effect phenomenon. Hydrological Sciences Journal, 61(10):1770–1777

Weeks, E.P. (2005). The Lisse effect revisited. Ground Water, 40(6), 652–656. https://doi.org/10.1111/j.1745-6584.2002.tb02552.x

Zang YG, Sun DM, Feng P, Semprich S (2019) Numerical analysis of Groundwater Ridging processes considering water-air flow in a hillslope. Groundwater, 56(4): 5

Pre-mining Waste Rock Sampling – A Case Study in Sample Selection

[1]Kgaugelo Thobejane, [1]Levi Ochieng, [1]Kopano Mokoena

[1]*Digby Wells Environmental, Turnberry Office Park, 48 Grosvenor Road, Bryanston, 2197, South Africa, kgaugelo.thobejane@digbywells.com*

[2]*Barrick Gold Corporation*

Abstract

This paper presents a systematic or targeted approach used in a case study for selecting waste rock samples for Environmental Impact Assessment (EIA) study. The sample selection process involved reviewing the geochemical characterisation report from a previous EIA report, examining the diamond drill hole database, and assessing sulfide assays. By comparing the sampling data from the previous report with the drill hole data, common factors were identified. Thereafter, classic statistical methods, such as calculating averages, medians, and percentiles for sulfur assays, were used to identify sampling gaps in the study area.

Although time intensive, the systematic sampling approach, coupled with comprehensive data analysis techniques, facilitated a detailed understanding of the environmental geochemistry associated with waste rock materials.

Keywords: Sample Selection, Representativity, Sampling Program

Introduction

Digby Wells Environmental was assigned the task of conducting an Environmental Impact Assessment (EIA) for a prospective greenfield opencast mine. This paper specifically focuses on the sampling program of the EIA, with a specific emphasis on the environmental geochemistry component related to potential waste rock materials.

The geochemical exploration phase entails a rigorous drilling program that plays a crucial role in identifying undiscovered mineral deposits. This program involves the sampling of the drill core, which provides valuable information about the extent of mineral sources (Zuo, Wang, Xiong, & Wang, 2021). The drill core covers a significant portion of the exploration area and encompasses the various rock types that will be excavated during the project. This offers insights into the potential waste rock materials that might be deposited in a waste rock dump facility. The exploration phase generates a comprehensive database that includes the location of exploration holes, grade assessments, and visual observations of geological conditions such as discrete geological units, mineralization, alterations, and weathering/leaching. These data is very valuable for selecting waste rock samples before the operational phase of mining.

Approach

During the sample selection process, a three-step approach was employed, which involved (1) reviewing the existing information, (2) identifying the common factors between the reviewed information, and (3) addressing any gaps in the previous sampling efforts. It was crucial to ensure that an adequate number of samples were taken to effectively capture the variability and central tendencies of the target parameters, including measures such as average, median, and percentiles (5th, 50th, and 95th). The approach aimed to provide a comprehensive and representative characterization of the waste rock material at reduced costs.

Description of the databases

A previous geochemical study collected a total of 369 waste rock samples. The samples were collected from sections of the drill core or rejected drill chips from Reverse Circulation

(RC) drilling. The sample descriptions included lithologies, sulphur assays and drill core logs.

To supplement the previous work, a Diamond Drilled Hole (DDH) database was provided by the client, which contained 6685.37 core intervals from 84 exploration holes (*Table 1*). The core intervals considered in this study were from exploration holes drilled after the EIA process. The objective of our study was to select approximately 50 samples from the DDH database by identifying gaps in the previous sampling programme. The information available in the DDH database included exploration hole ID, depths, lithologies and lithology codes, alteration characteristics, chalcopyrite-pyrite ratios, estimated copper percentage, and visual representations of estimated sulphide and total sulfur percentages.

A common factor identified between the previous study database and the DDH database was total sulfur. The previous report provided laboratory results for total sulfur, while the DDH database represented total sulfur visually. To facilitate comparisons and identify any gaps, the total sulfur data from the previous report, referred to as the Acid-Base Accounting (ABA) database, was merged with the DDH database.

Total Sulfur (ABA and Visual Analysis)

Total sulfur was identified as the common factor across all the reviewed available information, and classic statistics and exploratory data analysis techniques (Hawkes & Webb, 1962; Tukey, 1977) were employed to establish clear relationships within the data. These techniques included calculations for minimum, mean, mode, median, maximum, range, standard deviation, median absolute deviation, coefficient of variation, quartiles, quantiles, percentiles, skewness, kurtosis, and graphical displays such as histograms and cumulative frequency distributions. These analyses aimed to uncover the underlying structure of the data and mitigate the impact of outliers on the results (Kiirzl, 1988; Reimann, 2005).

Figure 1 illustrates the relative distribution of drill core intervals based on lithologies. The dominant lithologies in the pit were identified as VIN SCC (Volcanic Intermediate-Coarse Porphyritic – Oxidized), VIN MIX (Volcanic Intermediate-Coarse Porphyritic – Mixed), and VFL MIX (Volcanic Fine Laminated – Mixed). The previous report analyzed a total of 65, 21, and 10 samples from these lithologies, respectively, and indicated that 80% of these waste rocks have the potential for acid generation. Additionally, VIN MIX and VIN SCC were found to be the most problematic materials in terms of leachate quality.

To identify gaps within the database, various plots and statistical analyses were conducted. The box and whisker plot were employed to display the distribution of total sulfur across different lithologies and exploration holes. The box represents the interquartile range (25th to 75th percentile), with the line indicating the median (50th percentile). The whiskers extend to the maximum and minimum values recorded. Figure 1 presents the box and whisker plot for the distribution of total sulfur (both ABA and visual representation) relative to exploration holes and lithologies. Statistical analysis utilized a total of 2200 visual total sulfur analysis results from the DDH database to supplement the 369 samples from the ABA database already analyzed. A comparison between the two databases revealed that the ABA total sulfur ranged from 0.3% to 8.4% (as shown in Table 2), with 95% of the ABA analyzed samples exhibiting sulfur concentrations above 1.0%. The mean and

Table 1 *Distribution of drill core intervals for Pit*

	ABA database	DDH Database	Total
Count (n)	369	5035	5404
Lithologies	59	47	
Number of Exploration Holes	65	84	149
Intervals Total of Core (meters)		6685.37	6685.37

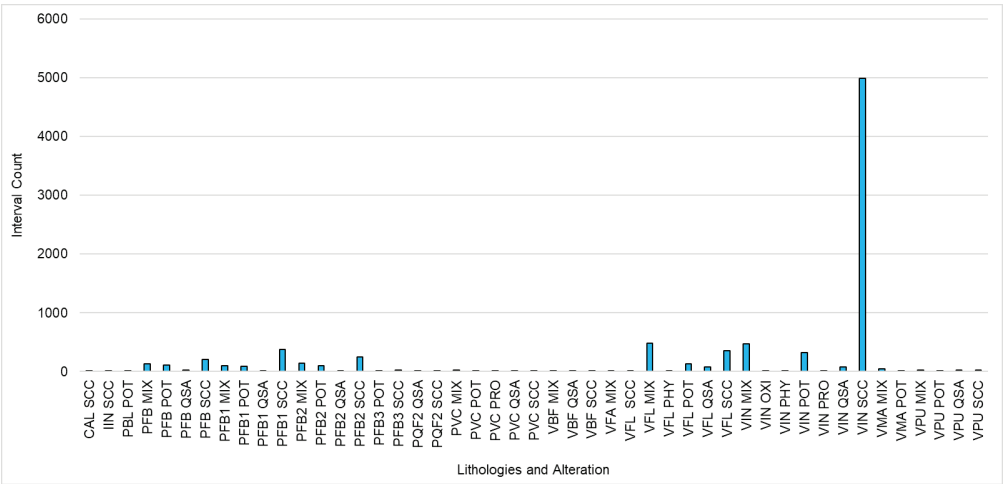


Figure 1 *Stratigraphic distribution of drill core intervals*

Table 2 *Statistical Analysis Interpretation for Pit*

Statistical Analysis	ABA TS	DDH TS	Statistical Analysis	ABA TS	DDH TS
Mean	4.02	3.84	Skewness	0.27	0.83
Standard Error	0.30	0.02	Range	8.1	6.32
Median	4.00	3.64	Minimum	0.3	1.06
Mode	2.30	3.18	Maximum	8.4	7.38
Standard Deviation	1.90	1.09	Sum	157	8442
Sample Variance	3.60	1.20	Count	39	2200
Kurtosis	-0.39	1.48	Confidence Level (95.0%)	0.61	0.05

median total sulfur values were 4.0%, and the 95th percentile was 0.61%. The similarity between the median and mean values suggests that the database is symmetric.

Within the DDH dataset, the total sulfur ranged from 1.2% to 7.4%, with all visual assessment data indicating total sulfur concentrations above 1.0%. The mean total sulfur was calculated as 3.8%, the median was 3.6%, and the 95th percentile was 0.05%. The slightly lower median compared to the mean suggests a right-skewed distribution, indicating a non-symmetric database.

Through the analysis of cumulative percentage plots in Figure 4, several gaps in the total sulfur data were identified. These gaps fell within the ranges of 0.9-2.2%, 3.3-4.9%, and 6-7%, indicating the need for further analysis within these ranges. Another gap was observed in the exploration holes located in a specific area, where only visual total sulfur analysis had been conducted. In contrast, other regions lacked any total sulfur analysis in their exploration holes. Consequently, this identified gap became the focus for sample selection within those specific exploration holes.

The second step involved identifying gaps in total sulfur data relative to different lithologies identified during core logging (Figure 3). It was noted that VIN lithology was the dominant lithology type, and 65 samples had already been analyzed for this category. Therefore, no additional samples were needed for this lithology type. Instead, additional samples were selected from minor lithologies to supplement the ABA database or to analyze lithologies that had not been previously analyzed.

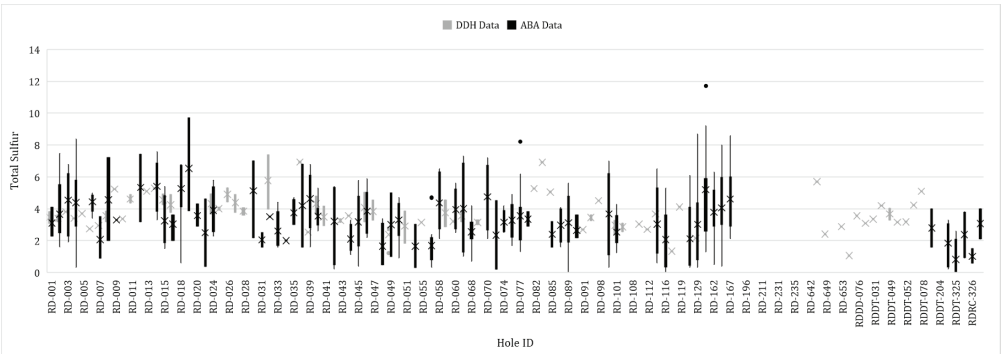


Figure 2 *Exploration holes relative to total sulfur*

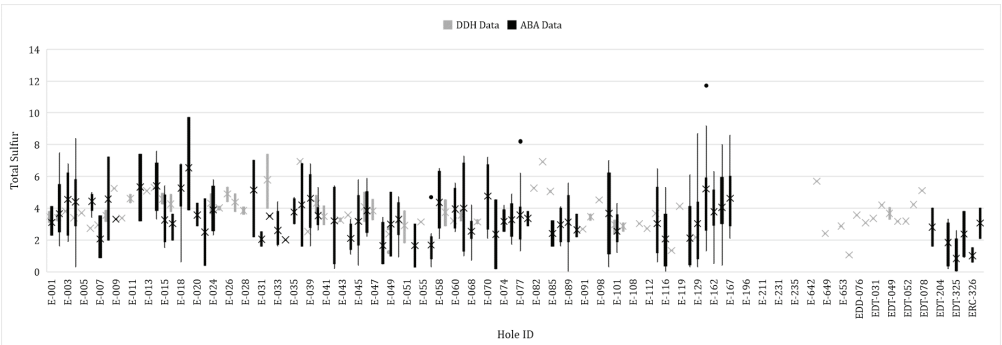


Figure 3 *Pit Lithologies Relative to total sulfur*

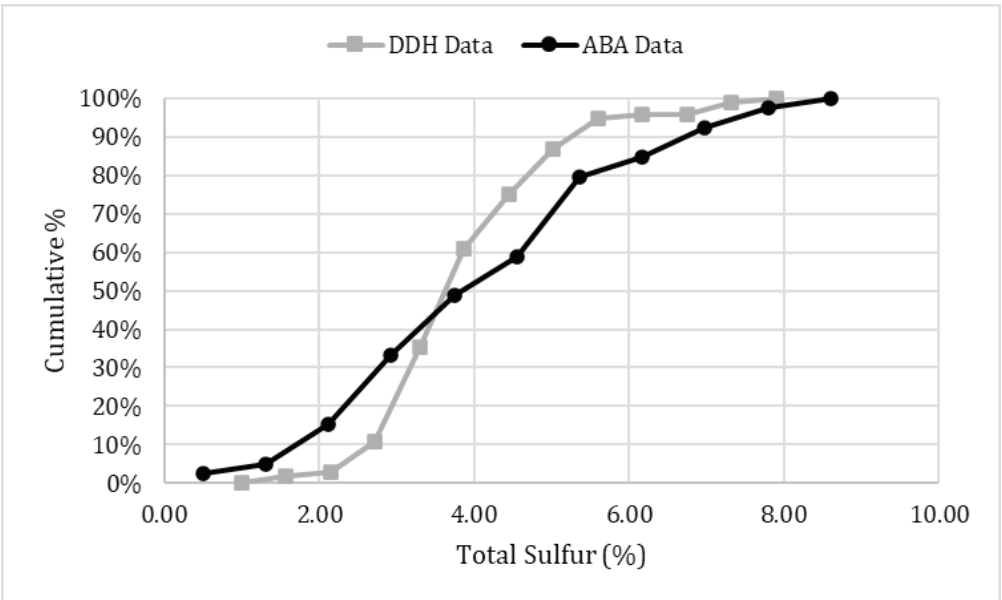


Figure 4 *Cumulative frequency plot for ABA and DDH database*

Pit Wall Samples and Spatial Representativity

Another important gap identified was the absence of pit wall samples in the previous EIA. To address this gap, pit wall sample selection was conducted using Leapfrog software, with access provided by the geologist. The objective was to understand the chemistry of these rocks, as they have the potential to influence the quality of the pit lake water. Leapfrog software was utilized to create a 3-dimensional model of the resource, incorporating all available exploration holes. Based on depth and lithologies, samples were selected from the pit wall and Figure 5 indicates only the exploration holes where pit samples were selected.

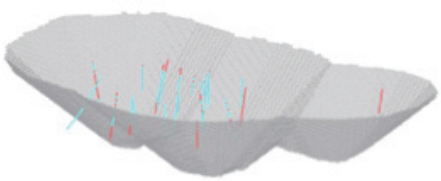


Figure 5 *Leapfrog pit wall sample selection*

To visualize the distribution of the selected samples and ensure comprehensive coverage, a scatter plot was generated. This plot depicted exploration hole IDs on the x-axis and depth on the y-axis, providing a visual representation of the sample distribution across different depths. The scatter plot allowed for a comprehensive assessment of the selected samples, ensuring that they not only addressed the identified gaps in total sulfur and lithologies but also covered various depths (as shown in Figure 6).

Assessment of the Sampling Approach

A targeted or systematic geochemical sampling approach was adopted in this case study. The approach allowed for the collection of samples from specific locations of interest. This targeted sampling helped focus efforts on the gap areas to avoid unnecessary duplication of samples. By utilizing the systematic approach, the sampling was optimized to cover a large area efficiently while minimizing costs. This approach helped allocate resources effectively and reduce unnecessary sampling efforts in areas less likely to yield valuable results. The approach ensured that representative samples were collected, leading to accurate and reliable data.

On the other hand, depending on the complexity of the project, this systematic approach can be time-consuming. Review of previous information and data, interrogation of the data, extensive consultation with site geologist, and integration with Leapfrog block modelling all require significant time and resources. This factor should be considered in project scheduling and budgeting.

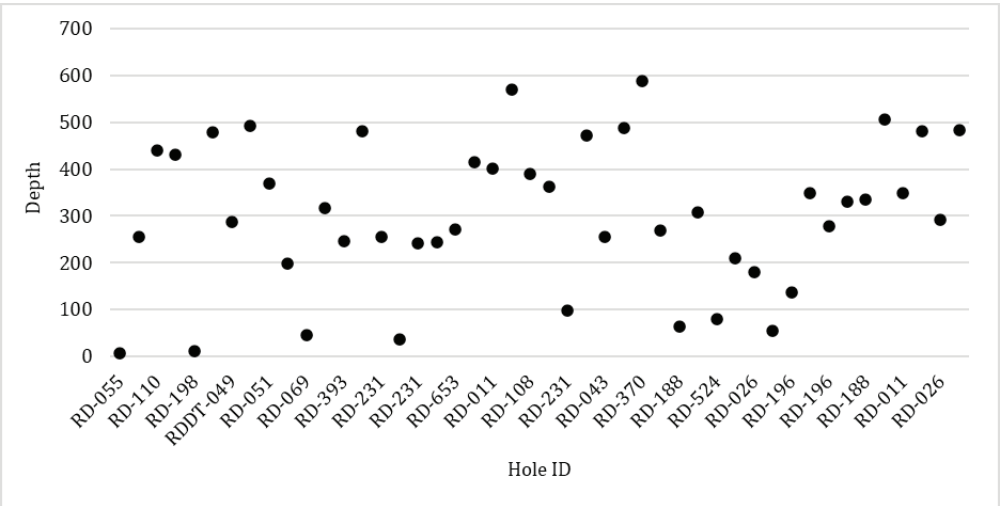


Figure 6 *Spatial representativity relative to depth if the Pit*

Conclusion

The targeted sampling approach adopted in this study allowed for focused efforts on specific areas of interest, minimizing unnecessary sampling. By optimizing the sampling process, it efficiently allocated resources and reduced costs. Additionally, the approach ensured representative samples were collected, leading to accurate data and reliable interpretations. This systematic sampling approach, coupled with comprehensive data analysis techniques, facilitated a detailed understanding of the environmental geochemistry associated with waste rock materials. If the time intensive limitation is considered in project scheduling and budgeting, then the approach is excellent for geochemical sampling program for environmental assessments.

Acknowledgements

I would like to thank my fellow collaborators for ensuring a successful geochemical sampling program and particularly Dr Levi Ochieng' who has consistently pushed me to be better. Thank you to Digby Wells Environmental for providing us with an opportunity to be able to share this case study.

References

Hannigan , R. (2007). What goes around comes around: Today's environment. *Developments in Environmental Science*, 1-8.

Hawkes, H., & Webb, J. (1962). *Geochemistry in Mineral Exploration*. New York: Harper and Row.

Kiirzl, M. (1988). Exploratory data analysis: recent advances for the interpretation of geochemical data. *Journal of Geochemical Exploration, 30*, 309-322.

Reimann, C. (2005). Sub-continental-scale geochemical mapping: sampling, quality control and data analysis issues. *Geochem. Explor. Environ. Anal., 5,* 311–323.

Turkey, J. (1977). *Exploratory Data Analysis*. Reading, MS: Addison-Wesley.

U.S. Environmental Protection Agency. (1994). *Technical Document Acid Mine Drainage Prediction*. Washington DC.

Zuo, R., Wang, J., Xiong, Y., & Wang, Z. (2021). The processing methods of geochemical exploration data: past, present, and future. *Applied Geochemistry*, 132, 1-9.

Evaluation of Leakage Potential from Tailing Dam of Sungun Copper Mine Using Hydrogeological Findings and Numerical Modelling

Abdorreza Vaezihir[1]; Younes Jowdat[1]; Nader Mazaheri[2]; Somayeh Aghili[1]

[1]*Department of Earth Sciences, University of Tabriz, Iran;*

[2]*Environment Office, Sungun copper mine, Iran;*

Abstract

This research predicted the hydraulic behaviour of the Sungun copper mine tailings dam (NW Iran) in the reservoir's final height and introduced the best sealing to prevent downstream leakage. 14 locations upstream and downstream and several boreholes in dam abutments were sampled. PLAXIS numerical modelling predicted the dam's hydraulic behaviour and sealing procedures for various leakage scenarios. For each abutment of the dam, simulation scenarios have been considered, including simulation in the current and final height of the tailings. Suspended injection curtain and full injection curtain in two different positions were studied, as well. Results showed no pollution leakage at the current level of tailings. The PLAXIS model also predicts a reservoir tailings leakage at the final height. Then, the rise in hydraulic head would induce pollution discharge in the downstream areas. With the assumption that the concentration of elements in the effluent from the tailings dam would remain constant, 41 kg per year of heavy elements will flow the downstream waters. It was determined that a full injection curtain with a height of 200 meter, a width of 3 meters and a permeability of 10-8 m/s, near the dam axis had the least amount of leakage (0.13 L/s) in the final level (125 meter) of the left abutment. Then, the PLAXIS model was utilized for the right abutment, which, in the current level, allows leakage (0.06 L/s) and also in the final level (0.18 L/s); thus, the implementation of the injection curtain in the right abutment is not advised.

Keywords: Dam Leakage, Pollution Leakage, PLAXIS Model, Tailings Dam

Introduction

Tailings are waste materials produced during the separation of ores, and have the lowest content of desired components (Hu *et al.* 2021). They consist mainly of insignificant amounts of minerals (metallic and rock forming), process chemicals and water which can be categorized as slurry, paste, filtered or cake, based on the availability of water and solids in it (Munanku *et al.* 2023). Tailings dams are large man-made high-level "debris flow" hazard sources formed by the long-term cycle of hydraulic filling and consolidation. In most cases, they are highly vulnerable due to hydrogeological, geomorphological, and artificial disturbance (Clarkson and Williams 2021). There is also an unavoidable impact on soil and the ecological environment due to storing tailings over long periods (Guimarães *et al.* 2022; Uugwanga and Kgabi 2020). Geotechnical investigations of rock mass permeability coefficient, special applications in groundwater-related issues, such as the quantity of water leakage and estimation of rock mass potential of injection, are on the agenda. Sungun Copper Mine's tailings dam contains semi-solid sediments from Sungun copper mine's concentration process. This is a kind of high-faced dams with a clay core and also the least expensive and simplest type of tailings dams, which must have sufficient strength and unconstrained height. The dam will reach 186 meters, up from 145 meters in 2020. Semi-solid sediments and wastewater will fill the tailings dam reservoir to 270 million cubic meters. A dam leak or

failure could harm the environment and local inhabitants. This research predicts the hydraulic behaviour of the tailings dam in the final reservoir height and introduces the best sealing to prevent downstream leakage. PLAXIS numerical modelling is used to design dam components and predict the dam's abutments and body's behaviour before construction. It also predicted the dam's hydraulic behaviour and appropriate sealing procedures for various scenarios of leakage.

Study area

Sungun Copper Mine's tailings dam is located southeast of the mine, upstream of the Zarnekab watershed in northern Iran. The Sungun porphyry deposit, located in East Azerbaijan province, 105 km northeast of Tabriz, Northwest Iran, on the international metallurgical belt known as Alp Himalaya, possesses about one billion tons of sulphide copper ore (Aghili *et al*. 2018; Nasrabadi *et al*. 2009).

Materials and Methods

Hydrochemistry: The sampling was done in the October of 2019, and the samples were immediately transferred to the laboratory of Tabriz University. The standard sampling procedure was carried out from the downstream side of the potential pollution source (such as a seepage or tailing dam). Surface water samples were taken along the stream beginning at the toe of the dam. Sampling from the tailings dam and the seepage dam was also done in order to establish a more precise correlation between the quality of surface and groundwater and the water contained behind these dams. Water samples were also gathered from nearby springs to examine the quality of the groundwater and any potential implications the tailings dam could have on it. In total, 14 samples were collected, comprising 2 boreholes, 2 tailings dam and seepage dam locations, 5 surface water locations, and 5 groundwater locations. Besides, one borehole in the riverbed and two boreholes in the tailings dam abutments were dug due to a number of factors, such as a more thorough examination of the quality of groundwater to determine whether the tailings dam has any impact on it. Besides, the concentration of heavy elements such as Cu, Fe, Pb and Mn were examined using an atomic absorption machine (Jene_vairo06 analytical model).

Numerical modelling: In this study, a numerical model was employed to predict hydraulic behavior and determine the most effective sealing procedure. The PLAXIS model is capable of modeling and simulating deformation, stability, and analysis of soil

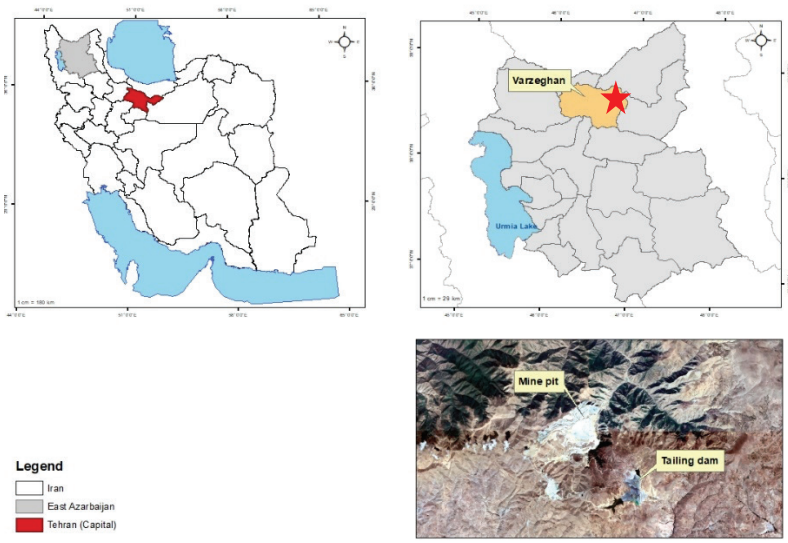


Figure 1 *Location of the study area*

structures using 6- and 15-node triangular elements based on the finite element method. In this model, it is also possible to calculate the flow of water in the dam's abutment, and if there is a pressure difference between the two environments, taking into account all the boundary conditions of the entry and exit of water from one environment into the other, the free surface can be determined. It calculates and draws the current and equipotential lines in the environment using the free surface of the resulting current. For the numerical analysis of contaminant discharge, input information for the PLAXIS model was acquired using data from boreholes drilled during the research and also data from boreholes drilled during the study phase of dam construction. Notably, after conducting the Lugeon test inside the boreholes, permeability data was obtained.

Results and discussion

The majority of the stations were neutral in terms of pH and have a pH above 7 (Fig. 1). Only the station connected to the tailings dam (ST-A-TD) has an extremely low pH because the tailings dam's pH was decreased by the chemicals introduced during the concentration stage. Although a large variation in EC between the tailings dam station (St-A-TD) and other stations was anticipated, the difference between that station and the seepage dam station (ST-A-SD) suggested that the spring waters have been mixed (Fig. 2). On the other hand, the station ST-A-S000, which is located inside the village of Aghababa Sang, displayed anthropogenic impacts such as human and animal waste in this station. Due to the high value of EC in the pollution source (tailings dam and seepage dam), it may be used as a natural tracer to detect the leakage, however the likelihood of leakage is minimal due to the substantial difference in its value in the downstream stations.

Anomalies in the concentrations of Fe at various stations suggested that they come from the ground (local igneous rocks), as some stations upstream of the dam had concentrations of Fe that were even greater than those in the reservoir sample (Fig. 3).

Pb was present in the highest concentration at the tailings dam station, but its low concentration at other sample sites that were around the source of the pollution suggested that there is no leakage of pollutants

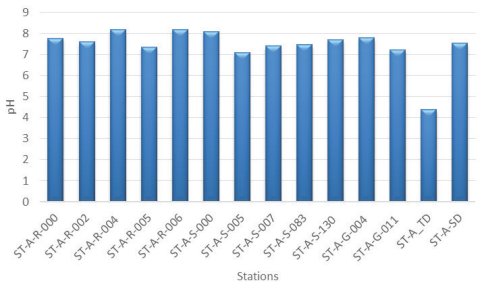


Figure 2 pH in sampling stations

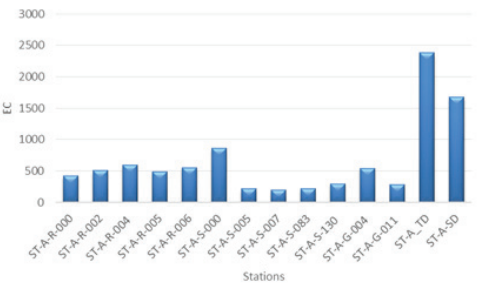


Figure 3 EC in sampling stations

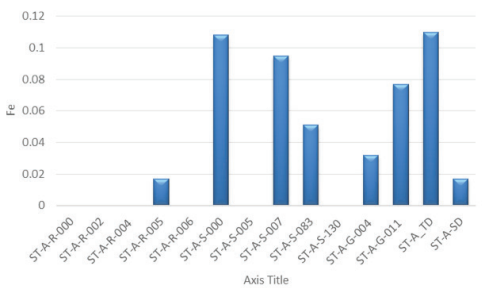


Figure 4 Concentration of Fe in sampling stations

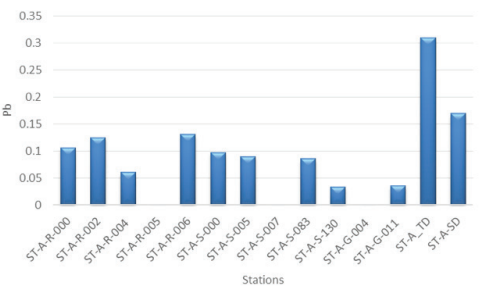


Figure 5 Concentration of Pb in sampling stations

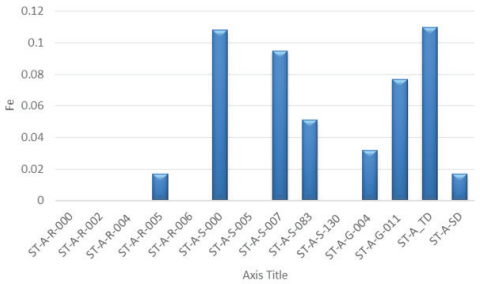


Figure 6 Concentration of Cu in sampling stations

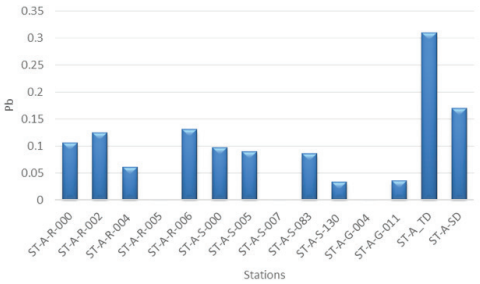


Figure 7 Concentration of Mn in sampling stations

at the present time (Fig. 4). As anticipated, due to the processing of various sulphide ores, particularly copper ores, the concentration of Cu was highest in the tailings dam reservoir, whereas the very low concentration of this element at other stations indicated that the reservoir was devoid of water (Fig. 5). In fact, Cu concentration changes in comparison to the seepage dam indicated blending with spring water and natural attenuation. Mn concentration was high in the tailings dam reservoir and seepage dam, and its concentration can increase as the level of the dam storage rises, followed by an increase in the concentration of other elements, causing numerous environmental problems (Fig 6). Similar to Pb, Mn can be utilized as a natural tracer to examine leakage at higher concentrations.

Development of PLAXIS model for the abutments

To create the model, first the geometry of the model was defined based on its scale for the both abutments, then based on the results of Lugeon test and its changes at various depths based on the permeability, 17 layers for the left abutments and 15 layers for the right abutments was outlined on the geometry of the model. Then parameters such as horizontal permeability (Kx), vertical permeability (Ky), saturated weight (Ψsat), unsaturated weight (Ψunsat), adhesion (C), internal friction angle (Φ), Poisson's ratio, modulus of elasticity (Young Modulo) and shear modulus (G) were examined and entered to the model. The permeability was estimated at $2 * 10^{-5}$ (m/day) by analyzing the excavations conducted within coring process. In order to grid the model in the left abutment, the number of elements was 679 and their average size was 13.11 meters in an arrangement with triangular cells, which finally created 5611 nodes and 8148 stress points in the grid. In the right abutment, the number of model elements was 877, the number of nodes was 7203, the number of stress points was 10524, and the average distance between elements was 12.15 meters. For each abutment of the dam, simulation scenarios have been considered, including simulation in the current and final height of the tailings. Various scenarios including suspended injection curtain and full injection curtain in two different positions were studied, as well.

Development of PLAXIS model for left abutment

The first scenario is a simulation of the reservoir's current water level, which is approximately 95 meters above the bottom of the valley. In addition, to improve the precision of the calculations, the iterative procedure is manually defined for the model, and the acceptable error tolerance was set at 0.001. The second scenario of the simulation is related to the time when the water level behind the dam is at its highest level after the completion of the tailings dam promotion. In this scenario, the final water level will be 125 meters (Fig. 8). Considering the leakage rate of the left abutment at the final level (171 m^3/day) means that 62415 cubic meters of pollutants will enter the surface and ground waters downstream every year. The leakage amount of the elements with the concentrations in the summer of 2019 has

been calculated according to the leakage rate at the final level in this abutment. Finally, it was determined that the tailings dam will release 41 kg of heavy elements per year into the waters downstream. With the assumption that the concentration of elements in the effluent of the tailings dam will remain at the current level, and taking into account the irreversible environmental effects of heavy elements and other toxic elements, sealing techniques are required to prevent pollutant leakage. This injection curtain was suspended in the model with a width of 3 meters and a permeability of 10^{-8} m/S.

Suspended/full injection curtain in the final level (position A)

In order to prevent pollutant leakage in the final level, the application of the injection curtain in the left abutment was investigated. The depth of the suspended injection curtain and full injection curtain are 136 and 200, respectively. The total discharge and extreme velocity in these scenarios are shown in Figure 9. According to the results, the performance of the full injection curtain is more effective than the suspended injection curtain. According to the nature of the materials stored behind the dam, the amount of discharge per year if this plan is implemented is 4,259,550 liters (0.13 L/S), which reduces the risk of contamination of the downstream areas even less than the previous scenario. Therefore, another scenario was investigated in order to reduce as much as possible the amount of pollutant leakage in the left abutment and also the best place to implement the injection curtain.

Suspended/full injection curtain in the final level (position B)

The injection curtain was applied in the vicinity of the valley (location of leakage) where the hydraulic head difference is high, with a depth of 110 m and 140 m for the suspended injection curtain and full injection curtain, respectively (Fig. 10). The extreme velocity ($90.82*10^{-3}$ meters per day) and the total discharge (45.5 m3/d) in suspended injection curtain scenario showed a relatively large change compared to the scenario of the suspended injection curtain in position A, and this indicates a lower efficiency. The injection curtain suspended in position A was aimed at reducing the amount of pollutant leakage, so the use of the full injection curtain in this position was investigated in the next scenario. In full injection curtain scenario, the amount of discharge does not show a significant reduction compared to the scenario of the suspended injection curtain at this point, and in comparison with the full injection curtain applied in position A (adjacent to the dam axis), it shows a much lower efficiency, so that the leakage flow has increased by 27% (40 m^3/d). With the current discharge rate, the input amount of heavy elements in the final level and taking into account the full injection curtain in the left abutment in position B, a total of 9.68 kg per year will be released from the dam (Tab. 2). Therefore, with the water level reaching its maximum, it is felt necessary to implement sealing techniques to prevent any pollution from leaking downstream.

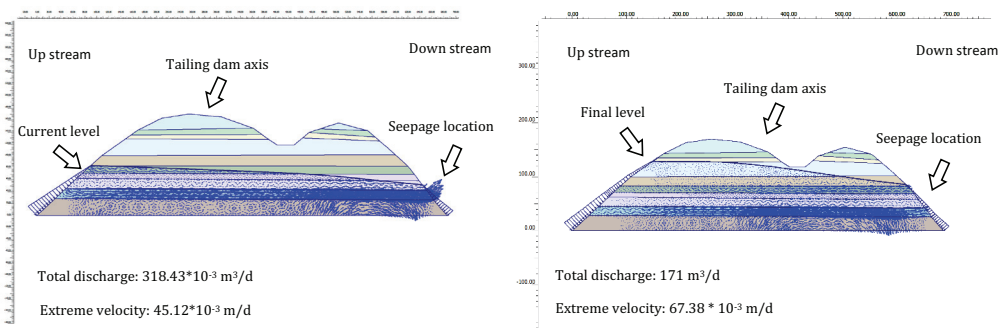


Figure 8 *Development of PLAXIS model for the left abutment in the first and second scenarios.*

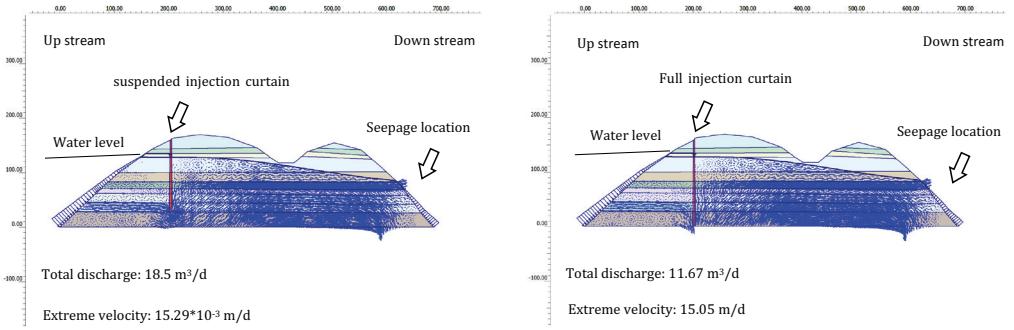


Figure 9 *Suspended/ full injection curtain in the final level (position A)*

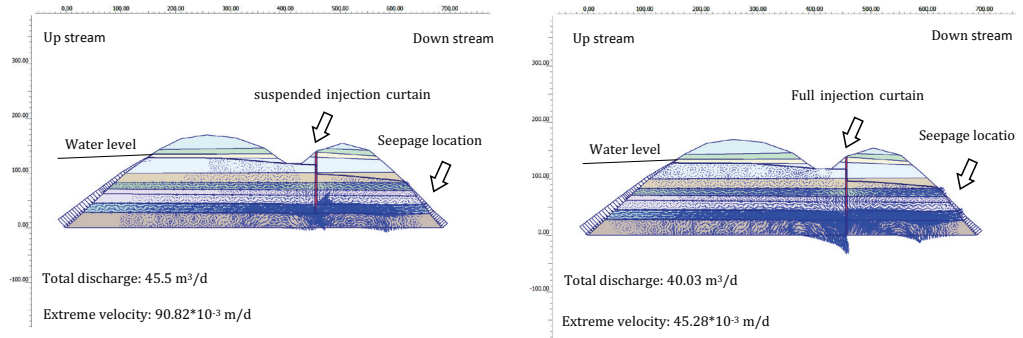


Figure 10 *Suspended/ full injection curtain in the final level (position B)*

Table 1 *Total discharge and the amount of heavy elements leakage (per year)*

Scenarios	Suspended injection curtain (position A)	Suspended injection curtain (position B)	Full injection curtain (position A)	Full injection curtain (position B)
(m^3/d) Total discharge	18.5	45.5	11.67	40.03
Heavy elements leakage (per year)	4.44	10.77	2.8	9.6

Development of PLAXIS model for right abutment

Unlike the left abutment, which is not covered with mineral waste, in this abutment, the waste itself prevents the penetration of more and more pollutants and acts as a waterproof layer. The total discharge in this case is 5300 L/d (0.06 L/S), which will be 1934 m^3 per year, that is much less compared to the discharge of the left abutment. In fact, mineral tailings in the right abutment acts as the injection curtain in the left abutment, and it has greatly reduced the amount of leakage and decrease it down to almost zero. The second scenario was run for the maximum level of tailings and water in order to simulate the behavior of the tailings dam and to estimate the amount of possible discharge. In this scenario, the total discharge was not significantly different from the current level due to the increase in tailings level, and only the velocity has increased, which is the possible reason for the increase in hydraulic head as a result of raising the reservoir level. The discharge rate will be 15.5 m^3/d (0.18 liters per second). Therefore, it is not necessary to implement sealing procedures such as injection curtains.

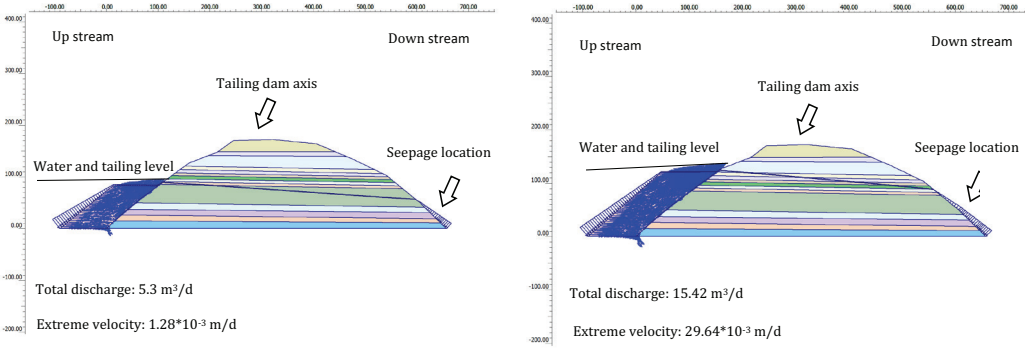


Figure 11 *Development of PLAXIS model for the right abutment in the first and second scenarios.*

Conclusion

There was no pollutant leakage at the current level of tailings or its concentration is not detectable due to natural attenuation. Alternatively, based on the results of the PLAXIS model a leak can be probable in the final height of the tailings in the reservoir. Then, the rise in hydraulic head would induce pollution leakage in the downstream areas, which will enhance its environmental and social warning due to the existence of dam storage and agricultural fields. With the assumption that the concentration of elements in the effluent from the tailings dam would remain constant, 41 kg per year of heavy elements will flow the downstream waters. It was determined that a full injection curtain with a height of 200 meter, a width of 3 meters and a permeability of 10^{-8} m/s, near the dam axis had the least amount of leakage (0.13 L/s) in the final level of the left abutment. PLAXIS model implementation for the right abutment, showed that due to low leakage amount of 0.06 L/s in the current level and 0.18 L/s in the final level, utilizing the injection curtain in the right abutment is not advised.

References

Aghili S, Vaezihir A, Hosseinzadeh M (2018) Distribution and modeling of heavy metal pollution in the sediment and water mediums of Pakhir River, at the downstream of Sungun mine tailing dump, Iran. Environmental earth sciences 77:1-13

Clarkson L, Williams D (2021) An overview of conventional tailings dam geotechnical failure mechanisms. Mining, Metallurgy & Exploration 38(3):1305-1328

Guimarães RN, Moreira VR, Cruz JRA, Saliba APM, Amaral MCS (2022) History of tailings dam failure: Impacts on access to safe water and influence on the legislative framework. Science of The Total Environment 852:158536. https://doi.org/https://doi.org/10.1016/j.scitotenv.2022.158536

Hu W, Xin CL, Li Y, Zheng YS, van Asch TWJ, McSaveney M (2021) Instrumented flume tests on the failure and fluidization of tailings dams induced by rainfall infiltration. Engineering Geology 294:106401. https://doi.org/https://doi.org/10.1016/j.enggeo.2021.106401

Munanku T, Banda K, Nyimbili PH, Mhlongo SE, Masinja J (2023) Development of a multi-criteria decision analysis tool for the assessment of the potential pollution risk of tailings dumps to the environment – An approach validated using selected Zambian Mine tailings. Journal of African Earth Sciences 200:104880. https://doi.org/https://doi.org/10.1016/j.jafrearsci.2023.104880

Nasrabadi T, Nabi Bidhendi G, Karbassi A, Hoveidi H, Nasrabadi I, Pezeshk H, Rashidinejad F (2009) Influence of Sungun copper mine on groundwater quality, NW Iran. Environmental Geology 58:693-700

Uugwanga MN, Kgabi NA (2020) Assessment of metals pollution in sediments and tailings of Klein Aub and Oamites mine sites, Namibia. Environmental Advances 2:100006. https://doi.org/https://doi.org/10.1016/j.envadv.2020.100006

Treatment Of A Mine Water Containing Arsenic And Thiocyanates: Four Years Results On A Pilot Plant Scale

Stéphane Vaxelaire, Fabienne Battaglia-Brunet

BRGM: 3 avenue Claude Guillemin, 45060 Orléans, France, s.vaxelaire@brgm.fr

Abstract

About 8 million metric tons storage of cyanidation tailings from a former French gold mine produces a 6.5 m3/h mine drainage that contains between 11 mg/L and 15 mg/L of As and around 1 g/L of SCN– and is currently treated with a lime process. The existing treatment plant produces large amounts of sludge reflecting the large amounts of sulfate present in water and calcium from the lime. The aim of the present study is to validate at pilot scale a semi-passive mine water treatment process that would produce a lower amount of sludge and improve treatment efficiency with target discharge level below 100 µg/L of arsenic. After a review and lab-scale experiments (Vaxelaire 2019) for arsenic and thiocyanates removal, the process tested in the pilot is the adsorption of arsenic on ferrihydrite precipitate combined with the biodegradation of SCN–.

Introduction

The lime treatment of arsenic waters is a precipitation process and has commonly been used in metallurgical production units (Riveros 2001). Arsenic (V) co-precipitates to give calcium arsenate according to:

$$6Ca(OH)_{2(s)} + 4H_3AsO_{4(aq)} \rightarrow 2Ca_3(AsO_4)_{2(s)} + 12H_2O$$

This process generates large amounts of contaminated sludge, potentially able to release arsenic with time, thus it is not efficient at long term.

In the lime process, arsenic is trapped as calcium arsenate. Process efficiency reaches 90% on average, the outlet concentration being between 0.5 and 1 mg/L of arsenic when objective is generally 0.1 mg/L in discharge waters. However, calcium arsenate is an unstable product that reacts with atmospheric CO2 to form soluble arsenic and calcite (Riveros 2001). In addition, the current process does not remove thiocyanate from the effluent. Instability of calcium arsenate, the large quantities of sludge produced and high operating cost of lime process led the post-mining department (DPSM) of BRGM (the French geological survey, in charge of the site since 2009) to look for a more efficient process.

In order to develop a new treatment process after a bibliographic review, lab experiments were first performed (Vaxelaire 2019) in batch conditions for assessing different treatments options that gave the following preliminary findings:

- sulfate reduction is difficult to implement due to water pH between 7.5 and 8, and its buffering capacity, because arsenic sulfide solubility is elevated at high pH;
- adsorption on iron hydroxide sludge is effective and allows sufficient removal of arsenic to meet a discharge threshold of about 50 or 100 µg/L, but it requires large quantities of iron hydroxide sludge that will be converted in As-polluted waste;
- treatment by adding an iron sulfate solution seems to be the most promising.

Subsequently, continuous lab experiment were implemented in columns filled with pozzolana for both thiocyanate bio-oxidation and arsenic adsorption on freshly precipitated iron oxides onto pozzolana, and finally this column was replaced by a settling tank for Fe II oxidation, arsenic adsorption and co-precipitation with iron.

Main results obtained in lab experiments are:

- for thiocyanate biodegradation: a degradation rate of 4.5 ± 1 mg/L/h was observed repeatedly in batch experiments and a 2.5 mg/L/h degradation rate was observed in continuous experiments in columns filled with pozzolana. Higher rate (81 mg/L/h) was obtained by Dictor (1997) over the course of a 6-months

optimization experiment with the same type of mine effluent. The short duration of our experiments could explain the observed low degradation rate. The lack of biofilm development is suspected to be the major factor limiting the degradation rate.

- For arsenic adsorption on iron hydroxide, batch experiments have shown that iron (II) was more efficient than iron (III). Continuous lab experiments in column filled with pozzolana shown that 98% of arsenic removal can be achieved, reaching a discharge concentration below 100 µg/L. This result was obtained by adding a concentrated ferrous sulfate solution to the contaminated water flow in order to have an iron concentration of 20 mg/L corresponding to a molar ratio iron-arsenic of 4.4. In order to improve the process and to optimize operational cost, a simpler process was tested. It consists of mixing iron and contaminated water in a tube before injecting it in a longitudinal settling tank. An arsenic removal rate of 70% has been obtained in settler tank with a discharged concentration of 300 µg/L dissolved arsenic.

Finally, these experiments led to the definition and scaling of the treatment process retained for the pilot experiments. This process consists of a first stage of biodegradation of thiocyanates in aerated pozzolana filter and a second step of treatment of arsenic by addition of ferrous sulfate, composed of a mixer/settling tank followed by a pozzolana filter to remove the particles remaining in suspension at the outlet of the settling tank.

Pilot plant description

Figure 1 shows the process diagram of the on-site pilot plant. The pilot is fed with a representative mixture of water collected from tailings storage, 70% water from the "penstocks" bottom drain and 30% water from "top drains". These waters are pumped and mixed in a tank which allows to feed the pilot by gravity. The treatment of the water in the pilot plant is then carried out in four steps. The first step is the degradation of the thiocyanates by bio-oxidation using three aerated pozzolana filters in series of one cubic meter each, i.e. a total filter volume of about 3 m3 with a working volume of 1.9 m3 evaluated by measuring residence times. A second treatment step allows the arsenic to be removed by adding iron and adsorbing the arsenic on the formed iron oxi-hydroxide precipitate. This second treatment step is made up of a settling tank with a volume of 3 m3, i.e. an initial theoretical residence time of 30 h. This volume should also allow the produced sludge to be stored for the duration of experiments with the pilot. A concentrated solution of FeSO4 is injected at the entrance to the settling tank. At the outlet of the settling tank, a third step is achieved by a 1 m^3 pozzolana filter which should stop fine particles that have not settled. A 6 m2 pond

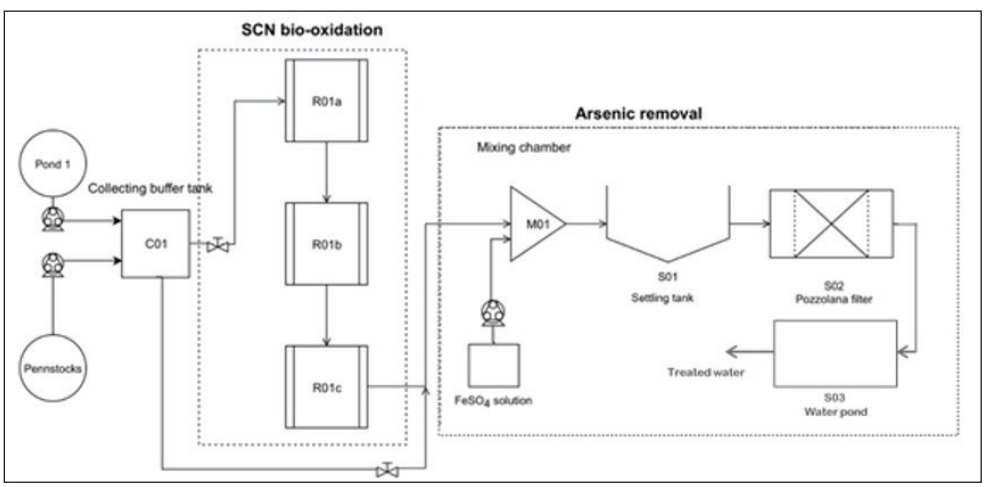


Figure 1 Process flow diagram of on-site pilot experiment.

for a "finishing" treatment as final step (figure 2b) has been added in 2021.

Operating conditions and monitoring program of on-site pilot

The pilot was operated and monitored on site during four years, between 2019 and 2022. Table 1 shows average operating conditions during the years of monitoring. The pilot plant has treated a 0.08 ± 0.03 m^3/h flow of contaminated drainage water. The pilot plant was scaled for treating a contaminated water inflow of 0.1 m3/h, but due to the clogging of the pumps by iron precipitates, it was difficult to maintain flow at 0.1 m^3/h. Table 2 shows average composition of inflow-contaminated water. Inflow arsenic concentrations were between 11 and 15 mg/L and thiocyanates concentrations were between 0.87 and 1.1 g/L. Arsenic concentrations were also under estimated at the pilot design step due to an increase of arsenic concentrations in mine drainage. In order to reach an arsenic discharge concentration below 100 µg/L, the flow of concentrated $FeSO_4$ solution have thus been adapted to obtain a molar rate iron-arsenic around 4.4 as determined in lab experiments.

The monitoring of the pilot was carried out at a weekly frequency during the first 3 years of monitoring and a bi-monthly frequency in 2022, at four points and then 5 points (after the addition of the pond) at the inlet and outlet of the different treatment steps. The physicochemical parameters (pH, ORP, conductivity, temperature and dissolved oxygen) and the substances presented in Table 2 were monitored. The monitoring of thiocyanates, ammonia and NTK allows to make a balance on nitrogen. Determination of arsenic species (Arsenic III and Arsenic V) was also carried out at the different sampling points in 2019 by separation on ion exchange resin (Ficklin 1983, Montiel 1996, Edwards 1998). These results are partially exploitable because of the uncertainties of the results, mainly because it was not possible to make balance on arsenic: [total arsenic] ≠ [arsenic III] + [arsenic V]. However, from these analyses, it was possible to determine that 70% of the arsenic in the pilot inlet water was in the form of arsenic (III).

On-site pilot plant results and discussion

Table 3 shows the average results obtained for each year of experiment and figures 3 and 4 show the results of the monitoring obtained in the year 2021. The hatched areas in figure 4 represent the periods during which the pilot was not supplied with iron sulfate.

Thiocyanate bio oxidation:

The average results (table 3 and figure 3) show a thiocyanate biodegradation rate between 13 and 20%. Thiocyanate degradation kinetics observed from the pilot plant are increasing from year to year between 7 to 12 mg/h/L, over 2020 to 2022. These kinetics are also higher than those observed during the laboratory experiments, ranging from 2.5 to 4.5 mg/h/L.



Figure 2 *Pictures of on-site pilot (a: pozzolana bio-filter and iron oxi-hydroxide settling tank, b: finishing pond).*

Table 1 Operating conditions.

Parameter	Unit	2019	2020	2021	2022
Water flow	L/h	86	86.9 ± 13.9	82.4 ± 20	86 ± 35
SCN flow	g/h	–	78 ± 25	94 ± 34	98 ± 55
Dissolved As flow	g/h	0.93 ± 0.07	1.1 ± 0.2	0.95 ± 0.31	1.3 ± 0.6
Fe^{2+} flow	g/h	2.6	3.6 ± 0.4	3.2 ± 0.3	4.2 ± 1
Molar ratio Fe/As	–	3.32 ± 0.46	4.31 ± 0.83	4.9 ± 1.8	5.4 ± 2.6

These results confirm the assumptions made during the design of the pilot (Jally 2019) invoking the slow development of the biofilm. However, the degradation kinetics observed in the biofilters remain lower than the one observed by Dictor (1997) of 81 mg/L/h. It could be explored to stimulate the biological activity that allows the degradation of thiocyanates either:

- by providing nutrients in particular phosphates, however the latter are competitors of arsenic and adsorb on iron hydroxides and can cause a release of arsenic (Senn 2018).
- or by using another support than pozzolana such as activated carbon favoring the development of a more important biofilm (Dictor 1997).

Arsenic adsorption on iron oxi-hydroxide:

The average results show a dissolved arsenic removal rate of 99.5% from 2020 to 2022. The rate is only 96% in 2019 but in this experiment the iron / arsenic molar ratio was only 3.32 and oxidation of the iron sulfate solution was observed during the experiment. The dissolved arsenic concentration in the discharge is less than 100 µg/L. A concentration of 20 µg/L has been reached in 2022 with an iron/arsenic molar ratio of 5.4. These yields for dissolved arsenic are comparable with the highest obtained in the laboratory experiments which was 98%. The iron / arsenic molar ratios and yields obtained are comparable to that obtained by Halder (2018) who showed that it was possible to remove 99.9% of As V in the form of arsenical ferrihydrite with an iron / arsenic molar ratio between 3 and 6.

The total arsenic removal rate is about 70% over the 4 years of testing. In addition, Figure 4 shows peaks in total arsenic concentration, which correspond to the release of iron oxi-hydroxide particles in suspension. The addition of a pond (end of 2021) to the pilot plant has improved the total arsenic removal, the efficiency at the outlet of the pond being 83 ± 11% with a discharge concentration of 2.6 ± 2.0 mg/L during the year 2022.

The experiments also show that it is more difficult to remove total arsenic, which is associated with iron hydroxide particles suspended in the water, than dissolved arsenic. Our results, with a yield of 70% removal of total arsenic, was comparable to the yield observed at the settling tank outlet during laboratory experiments. A pond treatment system allows the removal of these suspended particles with a surface removal rate (Ra) of 5.9 ± 3.0 g/m2/d.

Moreover, the treatment by addition of ferrous iron (II) appears to be efficient despite the presence of thiocyanates in solution. Finally, it was observed during the experiments that the oxidation of iron (II) into iron (III) of the concentrated iron sulfate solution could reduce the performance of the treatment. One of the possible explanations for the better efficiency of ferrous iron (II) can originate from the fact that the oxidation of iron (II) into iron (III) is coupled with an oxidation of arsenic (III) to arsenic (V) by Fenton effect (Ding 2018). The arsenic (V) then precipitates as arsenical ferrihydrite.

Conclusion

This study was conducted in order to develop and build an optimized mine water treatment plant that will replace the current lime treatment plant. The goal is to develop a more efficient (reduced amount of sludge) and cost effective process. In order to achieve this goal, after lab scale experiments, on-site pilot plant experiments were conducted and key data for the treatment of a mine water containing arsenic and thiocyanate were

Table 2 Average composition of inflow contaminated water.

Substance	Unit	2019	2020	2021	2022
SO_4^{2-}	mg/L	5725 ± 171	5840 ± 230	5910 ± 630	6120 ± 1000
Na^+	mg/L	2900 ± 476	2240 ± 420	2200 ± 510	2140 ± 370
SCN^-	mg/L	1126 ± 67	868 ± 245	1120 ± 260	940 ± 310
HCO_3^-	mg/L	190 ± 8	221 ± 28	199 ± 20	190 ± 38
Cl^-	mg/L	170 ± 8	764 ± 222	174 ± 25	260 ± 250
K^+	mg/L	77.2 ± 1.5	120 ± 17	79 ± 10	87 ± 19
NH_4^+	mg/L	61 ± 57	0.10 ± 0.02	48 ± 20	60 ± 22
NTK	mg N/L	317 ± 21	252 ± 74	302 ± 55	250 ± 54
As_{tot}	mg/L	11.4 ± 2.0	13.3 ± 1.8	14.0 ± 4.3	14,9 ± 3,7
As_{dis}	mg/L	12.3 ± 1.9	12.9 ± 1.5	12.0 ± 1.4	13,5 ± 3,4
Mn_{tot}	mg/L	0.91 ± 0.08	0.75 ± 0.13	0.93 ± 0.20	1,02 ± 0,23
Mn_{dis}	mg/L	0.98 ± 0.16	0.52 ± 0.10	0.83 ± 0.20	0,96 ± 0,22
Fe_{tot}	mg/L	0.44 ± 0.18	0.40 ± 0.14	1.0 ± 1.1	0,57 ± 0,39
Fe_{dis}	mg/L	0.16 ± 0.03	0.08 ± 0.02	0.17 ± 0.21	0,14 ± 0,04

Table 3 Average results by year.

Parameter	Unit	2019	2020	2021	2022
SCN treatment ratio	%	–	20 ± 13	13.4 ± 6.0	17.8 ± 7.4
SCN degradation rate	mg/h/L	–	7.0 ± 4.0	9.6 ± 3.9	12 ± 11
Asdis treatment ratio	%	96 ± 6	99.5 ± 0.5	99.6 ± 0.8	99.9 ± 0.1
Asdis discharge concentration	µg/L	205 ± 400	62 ± 64	50 ± 97	20 ± 12
Astot treatment ratio	%	70 ± 12	76 ± 19	67 ± 34	71 ± 16
Astot discharge concentration	mg/L	3.45 ± 1.6	3.2 ± 2.5	4.3 ± 4.6	4.6 ± 2.9

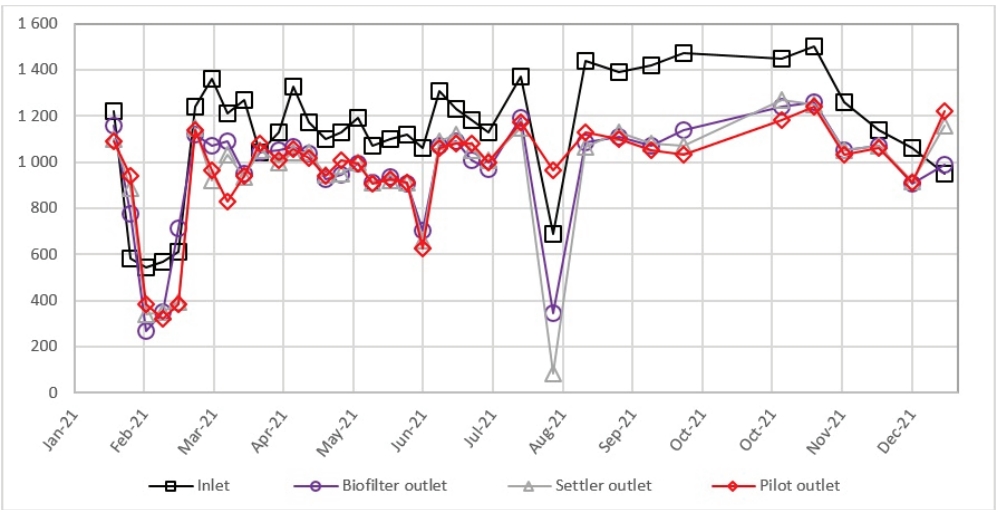


***Figure 3** Evolution of thiocyanate concentration in the pilot during year 2021.*

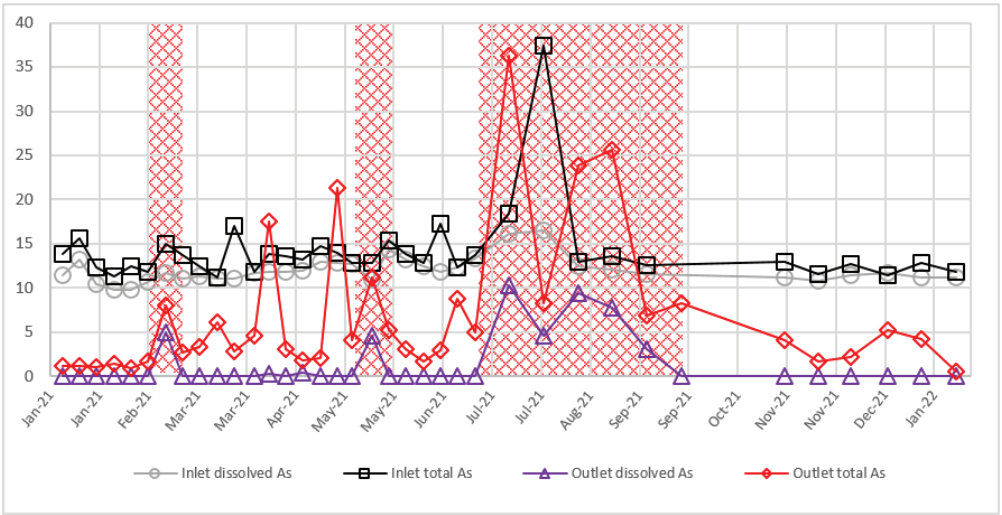


Figure 4 *Evolution of arsenic concentration at the inlet and outlet of the pilot during the experiments in 2021.*

validated. The experiments showed that it is possible to reduce dissolved arsenic to meet a discharge level lower than 100 µg/L without having to remove thiocyanate in a first step. If thiocyanate should be treated to meet a discharge level, the experiments carried out on the pilot plant have validated that it is possible to decrease thiocyanate concentration by biodegradation. In order to scale up to a treatment plant, these experiments must be completed with a technical and economic analysis to evaluate the benefits of implementing this treatment compared to the current lime treatment.

References

Riveros P, Dutrizac J and Spencer P (2001). Arsenic Disposal Practices in the Metallurgical Industry

Dictor MC, Battaglia-Brunet F, Morin D, Bories A and Clarens M (1997) Biological treatment of gold ore cyanidation wastewater in fixed bed reactors. Environmental Pollution 97 (3) pp. 287–294. doi.org/10.1016/S0269-7491(97)00077-8

Ding W, Xu J, Chen T, Liu C, Li J, Wu F. (2018). Co-oxidation of As(III) and Fe(II) by oxygen through complexation between As(III) and Fe(II)/Fe(III) species. Water Research, Volume 143, 2018, pp. 599-607, ISSN 0043-1354, https://doi.org/10.1016/j.watres.2018.06.072.

Edwards M, Patel S, Chen H, Frey M, Eaton A.D, Antweiler R, Taylor H.E. (1998) Considerations in As analysis and speciation. Journal AWWA. Vol 90 issue 3. pp. 103-113, March 1998. https://doi.org/10.1002/j.1551-8833.1998.tb08402.x

Ficklin, W. H. (1983). Separation of arsenic (III) and arsenic (V) in ground waters by ion-exchange. Talanta, Volume 30, Issue 5, 1983, pp. 371-373, ISSN 0039-9140, https://doi.org/10.1016/0039-9140(83)80084-8.

Halder D, Lin J, Essilfie-Dughan J, Das S, Robertson J, Hendry M. J. (2018). Implications of the iron(II/III)-arsenic ratio on the precipitation of iron-arsenic minerals from pH 2.5 to 10.5. Applied Geochemistry, Volume 98, 2018, pp. 367-376, ISSN 0883-2927, https://doi.org/10.1016/j.apgeochem.2018.10.012.

Jally B. (2018). Développement d'un procédé de traitement semi-passif pour une eau de mine arséniée – Internship report. INP ENSIACET.

Montiel A, Weté B. (1996). Elimination de l'arsenic dans les eaux destinées à la consommation humaine. Colloque spécialisé AIDE ; « Micropolluants d'origine naturelle – arsenic et autres composés. Vienne.

Senn A. C, Hug S. J, Kaegi R, Hering J. G, Voegelin A. (2018). Arsenate co-precipitation with Fe (II) oxidation products and retention or release during precipitate aging. Water Research, Volume 131, 2018, pp. 334-345, ISSN 0043-1354, https://doi.org/10.1016/j.watres.2017.12.038.

Vaxelaire S, Jally B, Battaglia-Brunet F, Jacob J (2019). The Development Of A Treatment Process For The Mine Water Containing Arsenic And Thiocyanate From Lab Scale To Pilot Plant Scale. Proceedings of the IMWA 2019 Conference.

Pit Lake Runstedt as "Reactor" for Remediation – on the Way to better Energy Efficiency

Anne Weber[1], Stefan Bruns[2], Petra Wolf[3]

[1]*Lausitzer und Mitteldeutsche Bergbau-Verwaltungsgesellschaft mbH, Walter-Köhn-Straße 2, 04356 Leipzig, Leipzig, Germany, anne.weber@lmbv.de, ORCID 0000-0003-2582-5327*

[2]*Polyplan-Kreikenbaum Gruppe GmbH, Überseetor 14, 28217 Bremen, Germany, bruns@polyplan-kreikenbaum.eu*

[3]*FCB Fachbüro für Consulting und Bodenmechanik GmbH Espenhain, Verwaltungsring 10, 04571 Rötha, Espenhain, Germany, petra.wolf@bodenmechanik.de*

Abstract

Pit lakes with subaquatic dumps are rare and each of them provides a specific challenge. Between 1969 and 1995, 24 million m³ of waste were dumped at the Großkayna lignite mine, mostly ash from the nearby lignite power plant and waste from fertilizer production. An intensively discussed remediation concept included flooding the pit and using the resulting Lake Runstedt as an active part of the remediation of the – then subaqueous – landfill. Target contaminant is ammonium.

Since 2002, a deep-water aeration system (Tibean) promotes microbial nitrification during the summer stagnation period. Authorities require a minimum hypolimnetic oxygen concentration of 4 mg/L and, since 2013, a fixed switch-on time for aeration on June 1. However, aeration at high oxygen saturation, typical of early summer, is physically ineffective. In the interests of energy-efficiency, demand-driven operation times are aimed.

Hydrodynamic modelling based on monitoring data was applied as a tool for adjusting aeration times. Initial results provide information on the inertia of the hypolimnion response to aeration in terms of hydrodynamic and reactive transport. This was used to determine the hypolimnion oxygen concentration at which aeration should commence to not fail regulations. Concepts for future approaches towards even further reduction of aeration are derived.

Keywords: Subaqueous landfill, hydrodynamic modeling, ammonium, lignite mining

Previous development and motivation

Until the 1980s, lignite was the backbone of energy and material supply in the former East Germany. At that time, vast open-cast mines and accompanying industry shaped the landscape with environmental concerns being of minor importance. In this course, the pit of the Großkayna lignite mine – situated 30 km west of Leipzig – was used for disposal of waste. Between 1969 and 1995, some 24 million m³ were dumped, mostly ash from the nearby lignite power plant, but also waste from fertilizer production in the close by famous "Leuna Werke". After German reunification in 1990, East German industry and lignite mining ceased widely. The original plan to completely fill the remaining pit was abandoned and environmental concerns became more prominent.

Since 1994, the Lausitz and Central German Mining Administration Company (LMBV) manages the common burden of rehabilitating the former East German lignite mining areas. Under a special contract, LMBV is also responsible for remediation of the Großkayna mine site, posing unique challenges due to its industrial landfill.

Together with consulting and research institutions LMBV developed a **remediation concept** for the Großkayna landfill. This concept (CUI 2000) involved flooding the pit and utilizing the resulting **Lake Runstedt** as a compartment for active remediation of the – then subaqueous – landfill. Swift flooding in 2001 and 2002 was necessary to guarantee geotechnical stability of an overburden dam towards an adjacent pit, which now inhabits the largest artificial lake in Germany (Geiseltalsee). Lake Runstedt (fig. 1) developed to a monomictic lake with about 6 km shoreline and up to 33 m depth. Additional parts of the remediation concept include:

- maintaining circumferential groundwater inflow to Lake Runstedt to avoid spreading of contaminated landfill pore water into surrounding aquifers,
- understanding ammonium as target contaminant due to its high mass fraction and mobility in landfill pore water,
- hypolimnetic aeration to enhance natural nitrification of ammonium,
- supporting natural reed belts for denitrification.



Figure 1 *Pit Lake Runstedt with Pit Lake Geiseltalsee in background and the narrow overburden dam separating them (image: LMBV, 2019).*

In their Planning Resolution (RP Halle 2001) authorities require a minimum hypolimnetic oxygen concentration of 4 mg/L for the Runstedt pit lake. Reasons for this are a) to prevent nutrient re-dissolution from the sediment and ensure living conditions for aquatic organisms and b) no harmful outgassing of ammonium and hydrogen sulfide to be feared.

To comply with this limit, since 2002, a **deep-water aeration system** with three separate units promotes microbial nitrification within the hypolimnion during the summer stagnation (fig. 2). This process relies on initiating circulation in the hypolimnion and enriching oxygen concentration there. It is accompanied by a sophisticated **monitoring** of groundwater, limnic and pelagic lake water, lake sediment and soil gas to monitor remediation.

Along with monitoring, **modeling** enhances conceptual understanding of relevant processes at the site. Large-scale groundwater modeling was applied, predicting several centuries duration of ammonium release from the landfill to lake water (IHU 2012). Furthermore, hydrodynamic modeling was applied to design the deep-water aeration system (POLYPLAN 2003).

Since 2013, authorities order annually **fixed operation times for aeration**, with the first aerator starting on June 1 and a second August 1. However, aeration at high oxygen saturation – typical of early summer – is physically ineffective.



Figure 2 *Deep water aeration system, top: on shore during renovation in 2017 (image: Christian Bedeschinski), bottom: in operation in 2019 (image: Peter Radke).*

Current work

Since 2013 the permitted 4 mg O2/L was complied with. Volume averaged hypolimnetic oxygen concentrations together with aeration times are shown in fig. 3 for the years 2020 to 2022. After almost a decade of fixed aeration times, LMBV is aiming for **demand-based operation**. The motivation bases on the official Planning Resolution (RP Halle 2001) itself, which mandates a review to reduce aeration. Moreover, principles of energy-efficiency require demand-driven operation times. Economic pressure also increases due to rising energy prices. This is supported by declining ammonium fluxes from landfill pore water, observed much earlier than predicted by previous modeling.

As a first step away from fixed aeration times, **hydrodynamic modelling** should identify key figures for aerator-initiated flow in the hypolimnion. It is known that turning on the aerators does not immediately increase the oxygen concentration in the hypolimnion:

1. Flow through the hypolimnion must first be stimulated (hydraulic inertia).
2. So much oxygen must first be made available through the aerators to compensate for the loss through consumptive processes (reaction inertia). Here, oxygen is not only consumed due to microbial nitrification of ammonium from the landfill, but primarily by the decomposition of organic matter from the lake's internal biomass production.

Understanding times to compensate for these inertias, the next step was to derive oxygen concentrations at which aeration should start to ensure the 4 mg/L requirement.

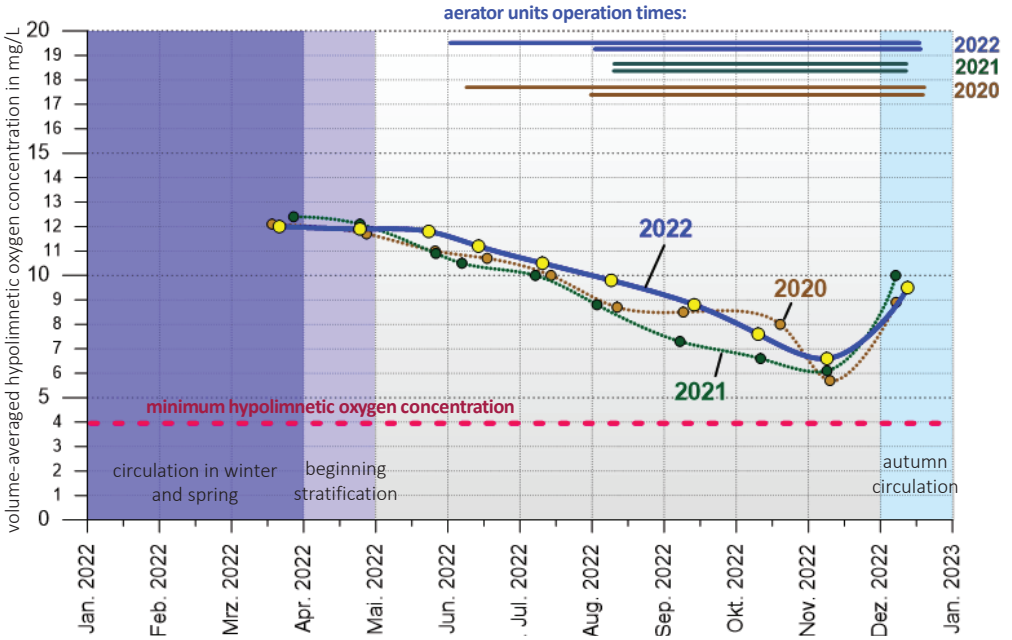


Figure 3 Volume averaged oxygen concentrations in the hypolimnion from profile measurements.

Hydrodynamic flow and transport models were set up in MIKE 3 (version 2019, DHI 2000) and in @SEA (scenario S2 see below, Bruns and Schubert 2023, Schubert 1994) to solve this task. The @SEA model is specified by:

- @SEA: 2.5D transient flow depending on density ratios, external buoyancy, and currents,
- a grid with 11235 elements and 2809 nodes representing morphometry of the lake's hypolimnion (from 12 m below surface),
- implementation of the three deep-water aerators with: 1220 m^3/h volume flow, oxygen enrichment by 8.8 mg/L, withdrawal at 30 m and discharge at 19.4 m and 17.4 m depth (discharge of aerator 1 was prolonged by 2 m in 2017),
- starting conditions from measurements July 2021,
- simulated time: 30 days.

Two scenarios were implemented:

1. S1 using 0 mg O_2/L as starting concentration to determine the time until 95 % of the hypolimnion ground was caught by flow initiated from the aerators (**hydraulic inertia**).
2. S2 using depth-dependent O_2 distribution and consumption from depth profile measurements in July and August 2021 to determine the time until the trend of decreasing oxygen concentration can be reversed by aeration from 1, 2 or 3 aerators (**reaction inertia**).

In 2021, on-demand aeration was tested, with aeration starting on August 5. It was therefore possible to use data from the two previous measurements, which represent the undisturbed (not aerated) system. Depth-dependent oxygen consumption was calculated from the depth-specific difference in oxygen concentration between these two measurements.

Fig. 4 shows a vertical cross section of oxygen concentration in S2 after 30 days. Starting from oxygen concentrations spanning from 12 mg/L down to 2.5 mg/L directly above ground, it can be concluded that three aerators cause sufficient mixing within the hypolimnion to avoid anaerobic zones.

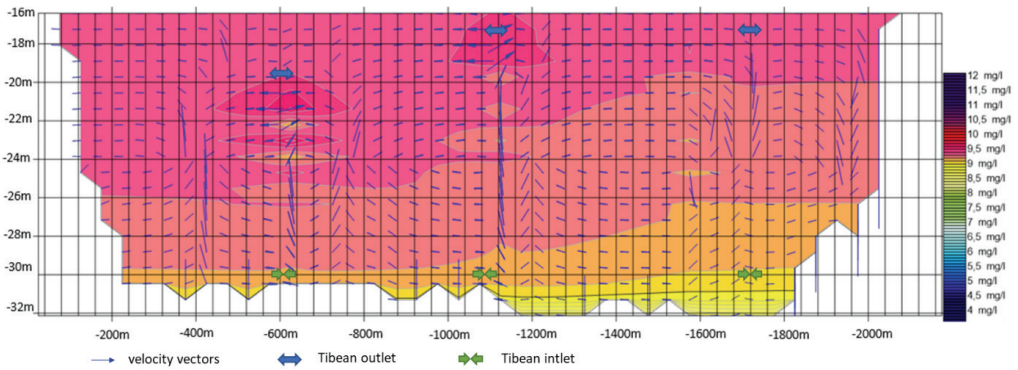


Figure 4 Modeled oxygen concentration and flow vectors. Vertical cross section with position of the three aeration units for scenario S2 after 30 days.

Results from hydrodynamic modeling can be summarized:

- After two weeks of operation, the aerators initiate flow in the hypolimnion.
- After 18 days, 80% (1 unit in operation) resp. 95% (3 units in operation) of the hypolimnion is reached by the initiated flow.
- No "dead water zones" develop.
- Above the lake bottom, after about 15 days, a reversal of the trend of decreasing O_2 concentration is modeled.
- Volume averaged O_2 concentration in hypolimnion 1 month after start of aeration show:
  - 1 aerator: decrease by 1.2 mg/L,
  - 2 aerators: decrease by 0.7 mg/L,
  - 3 aerators: increase by 0.3 mg/L.
- Considering depth-dependent oxygen consumption rates and the oxygen in the hypolimnion as a depot, the hypolimnion in July 2021 contained sufficient oxygen for about 4.5 more months (August to mid-December).

With these results concentration criteria were derived for a demand driven operation and proposed for the authorities. Accordingly, the first aerator should be switched on when the volume-averaged oxygen concentration in the hypolimnion falls below 9 mg/L, the second at less than 7 mg/L. As an additional criterion, the concentration of oxygen in the 5 m lamella above ground was assigned limit values. Furthermore, the monitoring interval (depth profiles) should be increased from every four to every two weeks to secure a quick reaction in case of rapid drop of O2 concentration (as e.g., in Oct/Nov 2020, see fig. 3).

Perspectives

The **overall methodology** towards energy efficient aeration bases on several approaches:

- increase system understanding by stepwise reduction of aeration and monitoring,
- applying models as a tool to quantify and predict relevant processes (hydrodynamic modelling of the lake and groundwater transport modeling),
- coordination with authorities on approvable procedures (changes in planning permissions).

Long-term goal of LMBV is a stepwise reduction of aeration and ceasing aeration as soon as it is warranted. Already now, monitoring data show decreasing ammonium fluxes from the landfill and hypolimnetic oxygen demand is dominated by internal biomass production.

In a first step LMBV aims to move away from fixed operation times towards **concentration criterion-based operation times** as described above. If agreement is reached with the authorities on demand-based operation times, the hydrodynamic model should be extended. It could then be used as a tool for predicting and controlling the seasonal state of the lake and for predicting on-demand activation times for aeration to meet the regulatory minimum of 4 mg/L oxygen in the hypolimnion. In addition, monitoring will be expanded to include

a chlorophyll probe to estimate seasonal biomass production. This is important as the hypolimnetic oxygen demand is dominated by biomass decomposition, while ammonium fluxes from the subaqueous landfill are decreasing.

As understanding of the system increases, the regulatory limit of 4 mg/L oxygen as the minimum average concentration in the hypolimnion should also be questioned. The goal should be to avoid anaerobic conditions in an aboveground zone to prevent remobilization of contaminants from the landfill. As shown in current modeling, the **hypolimnion can be understood as a depot of oxygen** available during stagnation. Applying this approach, aerators would be used to induce hypolimnetic circulation that delivers oxygen vertically from the upper layers to the lower layers and to the critical zone above ground. Updated monitoring concepts and modeling should be tools to predict oxygen demand for the current season. With this hypolimnetic depot approach, a demand-driven supply could be implemented. However, the future approach depends on agreements with the relevant authorities.

Conclusions

With its former use as a landfill, the Runstedt pit lake is rather unique among the dozens of lignite pit lakes in eastern Germany. Its history shows that the environmental sins of the past will be costly for decades to come, in this case the aeration of lake water to oxidize ammonium from the subaqueous landfill. In this context, an efficient use of resources is particularly important. This in turn requires a deep understanding of the processes, supported by monitoring and modeling.

Moreover, the case is an example for competing interests regarding various nature conservation issues, here water quality versus energy consumption. It should be avoided that efforts for one protected good lead to compromising other protected goods more strongly. But guidelines for comparing potential hazards, especially those with effects farther in the future are lacking in everyday remediation practice.

Acknowledgements

We are especially grateful to Dr. Martin Schultze (Helmholtz Centre for Environmental Research, Magdeburg, Germany) for providing valuable thoughts and complementary perspectives to this work as well as Aseya Khatun (Polyplan) for her commitment to modeling. Mine reclamation is always the work of many people and decades. Therefore, many colleagues from LMBV, partners from research and consulting institutions and authorities contributed to what is presented here.

References

Bruns S, Schubert R (2023) Programmdokumentation @SEA P3 (internal documentation, in German)

Schubert R (1994) Ein Softwaresystem zur parallelen interaktiven Strömungssimulation und visualisierung. PhD, Institut für Strömungsmechanik, Universität Hannover (in German)

CUI (2000) Fortgeschriebenes Sanierungsrahmenkonzept für das Tagebaurestloch Großkayna. CUI GmbH, Halle/Saale (internal report, in German)

DHI (2000) MIKE 3: Environmental Hydraulics. DHI Software User Guide, Documentation and Reference Manual

IHU (2012) Hydrogeologisches Großraummodell Geiseltal – Präzisierung 2011. IHU GmbH, Nordhausen, 23th November 2012 (internal report, in German)

POLYPLAN (2003) Monitoring und Sanierungskonzept Tagebaurestloches Großkayna Jahrgang 2002/2003. POLYPLAN GmbH, Bremen, 30th June 2003 (internal report, in German)

RP Halle (2001) Planfeststellungsbeschluss für die Flutung des Tagebaurestloches Großkayna – Herstellung Runstedter See, im Landkreis Merseburg – Querfurt, auf dem Gebiet der Gemeinden Frankleben und Großkayna. Regierungspräsidium Halle, 19.04.2001 (in German)

Schultze M, Boehrer B, Friese K, Koschorreck M, Stasik S, Wendt-Pothoff (2011) Disposal of waste materials at the bottom of pit lakes. In: Fourie AB, Tibbett M, Beersing A (Eds), Mine Closure 2011, Australian Centre for Geomechanics, Perth, p 555—564

Modelling the Behaviour of Ferric and Ferrous Iron in a Goldmine Tailings Environment, Free State – South Africa

Megan Welman-Purchase[1], Robert Hansen[2]

[1]*Geology Department, University of the Free State, 205 Nelson Mandela drive, Bloemfontein, 9300, South Africa, purchasemd@ufs.ac.za*

[2]*Centre for Mineral Biogeochemistry (CMBG), University of the Free State, 205 Nelson Mandela drive, Bloemfontein, 9300, South Africa*

Abstract

Cyanide has a high affinity for gold and other metals (including iron) attributing to its usage in the goldmine extraction process. After the extraction process, waste material is disposed of onto tailings facilities, where cyanide has previously been found. This study delves into the modelling of the behaviour of iron in a tailings system and the effect that cyanide and iron-cyanide compounds/complexes have on this. Results of this study revealed that jarosite and goethite/ferrihydrite affect the formation of Prussian blue but requires Fe^{2+} in the system to form.

Keywords: Cyanide, ferric/ferrous iron, prussian blue, goethite/ferrihydrite, jarosite

Introduction

Cyanide, that is still widely used worldwide in the gold extraction process, has a high affinity for metals (such as iron and gold) (Bakatula and Tutu 2016, Wang and Forssberg 1990, Zagury *et al.* 2004). A portion of this cyanide is believed to be expelled of onto tailings dams, where iron and aluminium are among the most copious metal cations existing in acid mine drainage (AMD) (Sánchez-España *et al.* 2005).

Iron in this environment, originates from the oxidation of pyrite, according to the equation 1 (Williamson and Rimstidt 1994). In environments where the pH is less than 3, the Fe2+ product from equation 1, is further oxidised to Fe3+ in equation 2 (Stumm and Lee 1961, Jones *et al.* 2014). Above pH 3, iron- hydroxide minerals form. As the concentration of Fe3+ increases, the oxidation of pyrite is further enhanced according to the equation 3 (Williamson and Rimstidt 1994). Contrarily, if the pH of the system is greater than 3, hydroxide minerals form (equation 4) (Jones *et al.* 2014):

$$FeS_2(s) + \frac{7}{2}O_2 + H_2O(l) \leftrightarrow Fe^{2+} + 2SO_4^{2-} + 2H^+ \quad (1)$$

$$Fe^{2+} + \frac{1}{4}O_2 + H^+ \leftrightarrow Fe^{3+} + \frac{1}{2}H_2O + e^- \quad (2)$$

$$FeS_2 + 14Fe^{3+} + 8H_2O = 15Fe^{2+} + 2SO_4^{2-} + 16H^+ \quad (3)$$

$$4Fe^{2+} + 10H_2O + O_2 = 4Fe(OH)_3(s) + 8H^+ \quad (4)$$

Ferrous iron (Fe^{2+}) is more soluble than ferric iron (Fe^{3+}), remaining in solution at a pH <8, whereas Fe^{3+}, seen in the reaction 4, precipitates as a variety of ocherous minerals (pH >3) (Sánchez-España 2007). The distribution of the precipitation of iron species is thus pH dependent. In the environment discussed in this study, not only iron is present but also SO_4^{2-} ions, which strongly affects the complexation of iron (Sánchez-España *et al.* 2005). Thus, the ocherous minerals include jarosite ($KFe_3(SO_4)_2(OH)_6$ - forms at a pH of ~ 2), schwertmannite ($Fe_8O_8(OH)_6.nH_2O$ - forms at a pH of ~ 2.5-4) and ferrihydrite ($Fe(OH)_3$ - forms at a pH of > 5). According to Villacís-Garcia *et al.* (2015), goethite forms from an increase in temperature and aging of ferrihydrite.

These matters have been studied, whereas this research focuses on iron and the mineralization of iron-cyanide compounds/complexes and the effect that ocherous minerals mineralization in the goldmine tailings dams have on the formation of iron-cyanide compounds. Specifically on Prussian blue – $Fe_4[Fe(CN)_6]_3$ and Turnbull's blue – $Fe_3[Fe(CN)_6]_2$ (Ghosh *et al.* 1999) and possible compounds associated with them.

Geological setting

A large percentage of South Africa's gold is extracted from the Witwatersrand supergroup, which has generated approximately a third of the world's gold to date (Tucker *et al.* 2016). This supergroup comprises successions of sedimentary deposits within the Witwatersrand basin which extends from the north of Johannesburg to south of Welkom (Tucker *et al.* 2016). The goldfields of the Witwatersrand supergroups are the Evander, East Rand, Central Rand, West Rand, South Deep, Western Areas, Carletonville, Far West Rand and Free State Rand goldfields (Frimmel *et al.* 2005). This study involves samples from a tailings dam outside of Welkom in the Free State goldfields.

Post gold extraction, the waste material is discarded of on tailings dams, consisting gangue minerals (such as quartz, mica, plagioclase), as well as possible contaminants used in the extraction process (such as cyanide, metals). According to Hansen (2018), the tailings dams display the zones in Figure 1, which are believed to be onion-like, not horizontal. The outer zone is the oxidation zone, adjacent to the transition zone and the core is the reducing zone.

Methods

9 samples were collected from a tailings dam close to Welkom in the Free State goldfields, South Africa. 3 samples were extracted at different depths from 3 different positions on the tailings dams. Samples 1.1 – 2.3 were collected from the top surface of the tailings dam and 3.1 – 3.3 from the side slope. The samples were milled in a carbon steel ring and puck mill, followed by the determination of the loss on ignition (LOI) by weighing sample loss after heating a portion of the sample to 950 °C. A fusion disc and pressed pellet (Na_2O only) were produced for each sample to analyse major elements using a Rigaku, Primus IV (4kW generator) X-ray Fluorescence (XRF). Total cyanide of sample 2.1 was determined by X-Lab earth laboratories in Johannesburg. Modelling was completed with PHREEQC, a United States Geological Survey project developed by Parkhurst and Appelo (2013). Parameters used for the modelling were taken from Sánchez-España (2007), where the solution contains 0.1 M of SO_4^{2-} and 0.02 M of Fe^{3+} as a function of pH. In addition to this, the concentration of cyanide found in the tailings sample 2.1 was also added to the solution to model the effects that it may have on the precipitation of other ocherous minerals. Sensitivity analysis was also completed, altering the Fe^{3+}, cyanide and oxygen concentrations.

Results

Samples from the tailings dam are fine grained and vary from pale to more orange in colour. This is an indication of the iron present in the samples. A blue staining was found in the sample 2.1, seen in Figure 2, believed to be an iron-cyanide compound. This total sample contained 10 $mg.L^{-1}$ total cyanide.

The XRF results are displayed in Table 1, where the tailings consist mostly of SiO2 (85.66 – 88.62 wt%) followed by Al2O3 (5.82 – 8.43 wt%). For this study the Fe2O3 composition is important, with an average of 2.25 wt%.

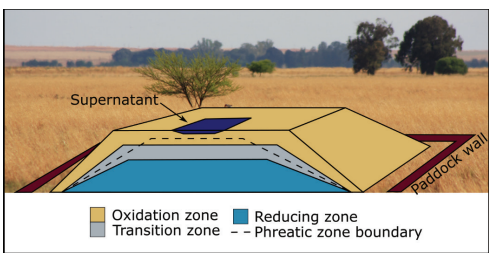


Figure 1 *A simplified diagram displaying the geochemical structure of a tailings dam, modified after Hansen (2018).*



Figure 2 *Blue staining found on the tailings dam in Welkom, South Africa. This is believed to be an Fe-CN compound and is ~3 cm in length.*

Table 1 XRF results of the 9 samples from a tailings dam in the Free State goldfields.

XRF major elements (wt%)	1.1	1.2	1.3	2.1	2.2	2.3	3.1	3.2	3.3
SiO_2	87.18	87.41	88.62	86.93	86.38	85.66	85.94	85.66	87.46
TiO_2	0.25	0.28	0.28	0.31	0.35	0.35	0.27	0.26	0.27
Al_2O_3	5.82	6.52	6.39	7.17	7.88	8.43	6.38	6.30	6.40
Fe_2O_3	2.69	1.69	2.27	2.09	2.48	2.54	2.21	2.14	2.15
MgO	1.26	0.40	0.49	0.56	0.41	0.44	0.46	0.44	0.45
MnO	0.02	0.02	0.02	0.04	0.03	0.03	0.02	0.02	0.02
CaO	0.68	0.41	0.41	0.31	0.69	0.43	0.52	0.50	0.51
Na_2O	0.28	0.43	0.34	0.54	0.49	0.45	0.31	0.31	0.37
K_2O	0.31	0.48	0.52	0.55	0.46	0.52	0.44	0.44	0.43
P_2O_5	0.03	0.02	0.03	0.03	0.03	0.03	0.03	0.02	0.03
LOI	2.01	2.28	2.42	2.53	2.73	2.91	2.44	2.35	2.43
Total	100.53	99.94	101.80	101.05	101.92	101.78	99.02	98.43	100.51

At pH values between 0 and 3, SO_4 compounds form, which correlates with the literature as the conditions where jarosite forms. Above a pH of 3, hydroxide complexes form, where above a pH of 6, ferrihydrite forms. Between a pH of 8 and 14 all compounds decrease to <0.01% and 99.99% of the Fe^{3+} in the modelling produces $Fe(OH)_4^-$. Included in Figure 4 is the concentrations of cyanide compounds. This graph reveals that initially HCN is produced, which is consumed as soon as Prussian blue precipitates. At a pH of >4, Turnbull's blue precipitates, consuming a small portion of the production of Prussian blue.

Increasing the Fe^{3+} concentration results in the higher concentrations of the same compounds, exclusive of the concentration of the iron-cyanide compounds. Contrarily, increasing the cyanide concentration in solution, results in the majority of the formation of Prussian blue. In addition to this, a model was run in a reducing environment, in order to mimic the core of the tailings dam. The only compounds that formed are Turnbull's blue and Fe2+ ions. No ocherous minerals form.

Discussion

The iron-cyanide compounds have previously been found by other authors in tailings samples, namely Bakatula and Tutu (2016) (South Africa – Central Rand goldfields) and Jambor *et al.* (2009) (Balmer lake in Canada - gold mining discharge). These compete for the iron in the system, with minerals such as ferrihydrite and jarosite. All of the

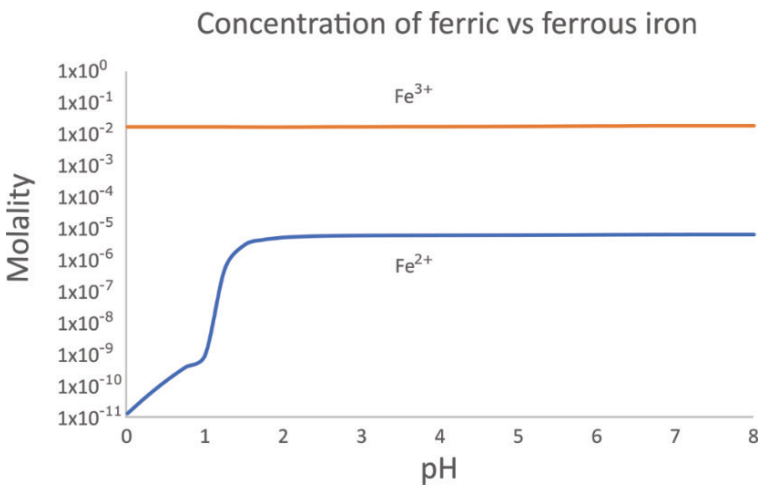


Figure 3 Modelling results of the oxidation states of iron in solution.

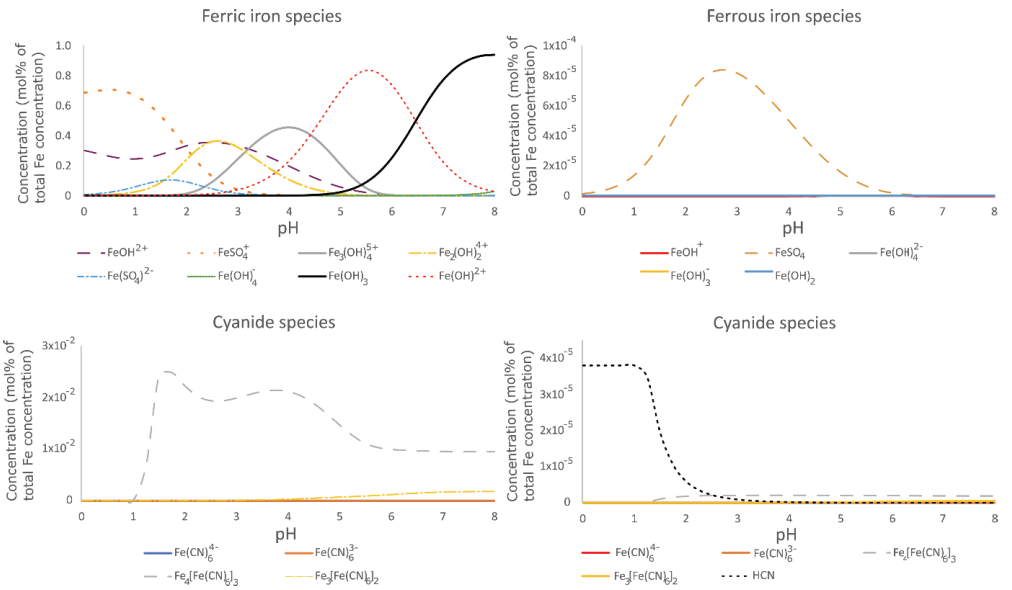


Figure 4 *Speciation results of the PHREEQC modelling. 0.02 M ferrous iron, 0.1 M of SO_4^{2-} and 10 mg.L^{-1} were added to the model in order to compare them to the results in Sánchez-España (2007). Owing to the large discrepancies in the concentration, the results were displayed in separate diagrams.*

above-mentioned minerals, including iron-cyanide compounds, require an Fe^{3+} source, additionally Prussian and Turnbull's blue require an Fe^{2+} source. Modelling revealed that the production of jarosite, ferrihydrite and other iron-hydroxide minerals are dependent on the pH and only form in an oxidizing environment. Goethite forms with an increase in temperature or from aging. Comparing these results to the study by Sánchez-España (2007) is displayed in Figure 5, where the largest difference is a shift of all peaks. This may be due to the addition of cyanide or that an additional compound is present in the modelling. Yet further studies will need to be completed to confirm this.

Prussian blue precipitation is dependent on the presence of both Fe^{2+} and Fe^{3+}, and on the redox conditions. The modelling revealed that Prussian blue is the dominant iron-cyanide compound that forms in an oxidizing environment but Turnbull's blue coprecipitates with Prussian blue above a pH of 4. As these compound precipitate, so the concentration of HCN diminishes to 0.04% of the cyanide compounds. In a reducing environment only Turnbull's blue precipitates. Kyle (1997) proposed that producing iron-cyanide compounds could assist in cyanide remediation. Iron-cyanide complexes are CN_{SAD} (strong acid dissociable cyanide compounds) (Zagury *et al.*, 2004), and thus are stable. If these compounds are stable, precipitate spontaneously and prevent

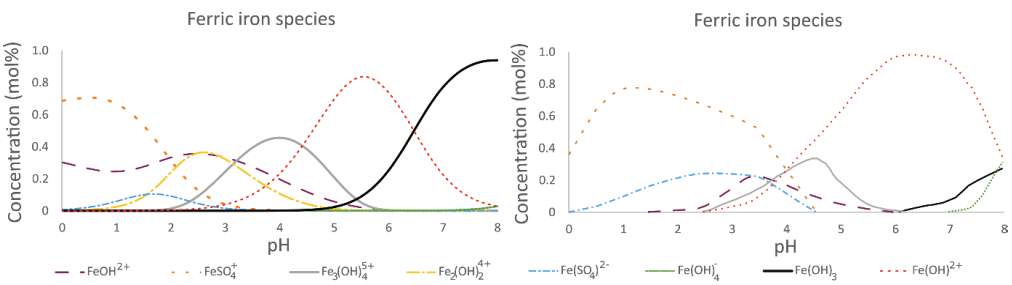


Figure 5 *Comparison between the results of this study (left) and the results of Sánchez-España (2007) (right). The results of this study are shifted to the left.*

the production of HCN, then they may be a good candidate for remediation.

Conclusions

This study was initiated to understand the behaviour of the different oxidation states of iron, their precipitates and the effect that the addition of cyanide to the system may have using PHREEQC modelling. In order to mimic gold mine tailings environments. It was determined that the precipitation of jarosite, ferrihydrite and other hydroxide minerals, which has been studied previously, is dependent on pH in an oxidizing environment. Fe3+ was added to the solution, yet a small portion converts to Fe^{2+}, this allows for Prussian blue to form, when the Fe^{2+} concentration decreases as $FeSO_4$, $Fe_2OH_2^{4+}$ and $FeOH^{2+}$ form and at a pH higher than 4, Turnbull's blue and $Fe(OH)_3$ form. Prussian blue also results in the consumption of the cyanide in the system and thus prevents the production of HCN (to less than 0.04%). This study concluded that the precipitation of Prussian blue is affected by the presence of jarosite and goethite/ferrihydrite but requires Fe^{2+} in the system to form.

Acknowledgements

The authors would like to thank Iphakade and the CMBG for financial support.

References

Bakatula EN and Tutu H (2016) Characterization and speciation modelling of cyanide in effluent from an active slime dam. S Afr J Chem 69:140-147

Frimmel HE, Groves DI, Kirk J, Ruiz J, Chelsey J and Minter WEL (2005) The Formation and Preservation of the Witwatersrand Goldfields, the World's Largest Gold Province. Econ Geol 100th Anniversary Volume 769–797

Ghosh RS, Dzombak DA, Luthy RG and Smith JR (1999) In situ treatment of cyanide-contaminated groundwater by iron cyanide precipitation. Water Environ Research 71(6):1272-1228

Hansen RN (2018) Inter-comparison geochemical modelling approaches and implications for environmental risk assessments: A Witwatersrand gold tailings source term characterisation study. Applied Geochem, Elsevier 95:71-84

Jambor JL, Martin AJ and Gerits (2009) The post-depositional accumulation of metal-rich cyanide phases in submerged tailings deposits. Applied Geochem 24:2256-2265

Jones AM, Griffin PJ, Collins RN and Waite TD (2014) Ferrous iron oxidation under acidic conditions – the effect of ferric oxide surfaces. Geochim. Cosmochim. Acta 145, 1–12

Kyle JH (1997) Stability of metal-cyanide and hydroxide complexes. World Gold '97 Conference, 163-169.

Parkhurst DL and Appelo CAJ (2013) Description of Input Examples for PHREEQC Version 3 – a Computer Program for Speciation, Batch-reaction, One-dimensional Transport, and Inverse Geochemical Calculations. book 6, chapter A43. US Geological Survey Techniques and Methods, pp. 497, Available only at http://pubs.usgs.goc/tm/06/a43/.

Sánchez-España J (2007) The Behavior of Iron and Aluminum in Acid Mine Drainage: Speciation, Mineralogy, and Environmental Significance. Thermodynamics, Solubility and Environmental Issues, Chapter 7

Sánchez-España J, López Pamo E, Santofimia E, Aduvire O, Reyes J and Barettino D (2005) Acid mine drainage in the Iberian Pyrite Belt (Odiel river watershed, Huelva, SW Spain): Geochemistry, mineralogy and environmental implications. Applied Geochem 20(7):1320-1356

Stumm W and Lee GF (1961) Oxygenation of ferrous iron. Ind. Eng. Chem. 53:143–146

Tucker RF, Viljoen RP and Viljoen MJ (2016) A Review of the Witwatersrand Basin -The World's Greatest Goldfield. IUGS, Journal of International Geosciences, Episodes 39(2):105-133

Villacís-Garcia M, Ugalde-Arzate M, Vaca-Escobar K, Villalobos M, Zanella R and Martínez-Villegas (2015) Laboratory synthesis of goethite and ferrihydrite of controlled particle sizes. Geológica Mexicana 67(3):433-446

Wang X and Forssberg KSE (1990) The chemistry of cyanide-metal complexes in relation to hydrometallurgical processes of precious metals. Mineral Processing and Extractive Metallurgy Review 6:81-125

Williamson MA and Rimstidt JD (1994) The kinetics and electrochemical rate-determining step of aqueous pyrite oxidation. Geochimica Cosmochimica Acta 58:5443–5454

Zagury GJ, Oudjehani K and Deschênes L (2004) Characterization and availability of cyanide in solid mine tailings from gold extraction plants. Science of the total environ 320:211-224

Sensitivity analysis of factors influencing mine water rebound in underground coal mines by the Design of Experiment approach

Sebastian Westermann[1], Dmytro V. Rudakov[2], Christian Melchers[1]

[1]*Technische Hochschule Georg Agricola University, Research Center of Post-Mining, Herner Str. 45, Bochum, Germany, sebastian.westermann@thga.de, christian.melchers@thga.de*

[2]*Dnipro University of Technology, D. Yavornytskoho Ave, 19, Dnipro 49005, rudakov.d.v@nmu.one*

Abstract

This study presents the joint application of an analytical groundwater flow model and Design of Experiment to examine the relevance of different factors including residual cavity volume, rock conductivity, scale of area hydraulically affected by mine water, and infiltration rate. For the first time, Design of Experiment were applied to post-mining water management. These results allowed evaluation of both the relevance of individual factors (single effect) and their interaction (interdependence) relating to the conditions of the mine flooded. The case studies included the collieries Ibbenbüren, Königsborn and Westfalen that differ in their geological structure.

Keywords: Mine water rebound, analytical modelling, sensitivity analysis, flood-influencing factor

Introduction

Hard-coal mining in Europe is in decline and mines in many European regions have been closed over the past decades (Melchers *et al*. 2019). During the operational stage of coalmining, water abstraction from underground workings is required to ensure safe mining conditions. At mine closure, abstraction is often terminated or may be reduced that leads to mine water rebound in the underground workings.

Prediction of mine water rebound is complicated due to variable rock properties, the different geological structural and hydrogeological settings of a mine, complex underground mine geometry, and lack of data and information. Access into closed and abandoned underground mine workings is difficult or impossible so data cannot be readily collected without extensive and expensive investigations. The complexity of the mining geometry and the hydrogeological rock qualities specific for each location result in the fact that mine water rebounds behave differently at each site. This variability, in conjunction with the frequently occurring lack of knowledge on the parameter distribution, complicates any prediction of a mine water rebound.

Depending on the objective and size of the area investigated, different model approaches can be applied to calculate the flows of both groundwater and mine water (Younger & Adams 1999). For more than two decades, mostly numerical models (Paul *et al*. 1998) have been applied in mine water management, however, their development and testing require detailed knowledge of natural and anthropogenic properties distributed in space at the deposit. Numerical modelling of previous mine flooding cases has often incorrectly estimated the rates of rising water level; mine water rebound has taken another time than predicted (e.g. Ibbenbüren colliery [Westfeld]; Goerke-Mallet 2000). The inaccurate forecast disregarding model parameter relevance was often the reason why no respective measures were taken timely when closing the mine. The deviation in the flooding duration is often due to insufficient information about the input data required by the model.

Analytical modelling

RThis study applies a model of transient radial groundwater flow to the shaft in order to calculate the mine water level and the inflow rate; this model has been developed based on analytical methods of groundwater

dynamics and water balance relationships. One shaft is assumed for similarity with the pattern of radial free surface groundwater flow governed by Dupuit-Thiem formula. Compared to numerical models of a more complex structure such as MODFLOW, FEFLOW, Spring, Boxmodel, the developed analytical model requires less extensive knowledge of how the hydrogeological and mining parameters are spatially distributed. Moreover, the analytical approach allows for a purposeful variation of selected factors (either single or combined) whose impact on the mine water rebound can be evaluated in a clear manner.

The analytical model simplifies natural conditions by dividing the deposit into horizontal layers and calculates minimum, maximum, and expected estimates of factors, such as the residual volume of underground workings created by mining (fig. 1), for each of the layers. The model parameters are assumed to be constant within each geological layer. This simplified model structure is applicable to underground workings which are hydraulically isolated from adjacent mines, although additional flows from other mines or aquifers can be included in the water balance equation within a more complicated model.

Design of Experiments

One standardised method for the systematic design and statistical evaluation of test series is the Design of Experiments method, originally introduced by Sir Ronald Aylmer Fisher in 1935 as the Design of Experiments (Fisher 1935). Contrary to the trial-and-error approach or the OFAT method in which only one factor is varied, the Design of Experiments method allows for investigating the interdependent influences on a system by varying several factors at the same time within a fixed range of values (Goh 2013). Since the 1980s, this method has increasingly been used in research, development, and industry; however, it has not been widely applied in post mining hydrogeology.

The application and evaluation of the Design of Experiments method can be facilitated by using specific statistics software (for example, Design Expert [STATCON GmbH], Stavex [AICOS Technologies AG]). For this investigation, we used the software MODDE Pro (version 12.1) of Sartorius Stedim Data Analytics AB (Sweden) (Eriksson *et al.* 2008).

Case studies

The DoE approach in combination with the analytical model was applied to the

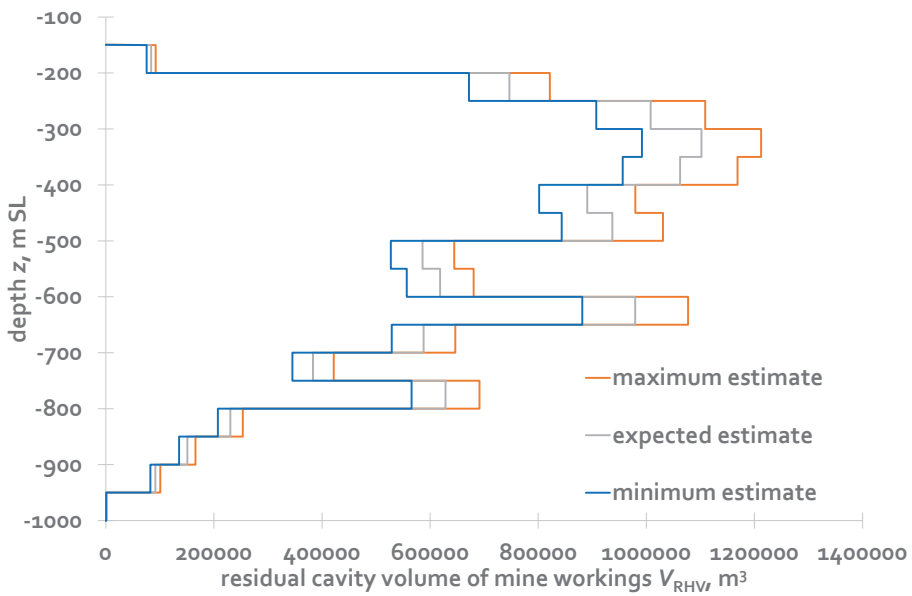


Figure 1 *Estimated residual volumes of underground workings for each layer (Königsborn colliery).*

Ibbenbüren (closed in 1979), Königsborn (Unna; closed in 1981; water abstraction was stopped in 1996) and Westfalen (Ahlen; closed in 2000) collieries of the North-Rhine Westphalia coalfield in Germany. These mines have been closed a considerable time ago and mine water drainage had been terminated. Thus, the mine water rebound has already advanced a lot and has been monitored by measurements and documented. Underground workings have no hydraulic connection to adjacent mines. The main differences between the collieries selected are the thickness of their overburdens which consist of clay marl rocks of low hydraulic conductivity (Emscher formation, Upper Cretaceous) and lime marl rocks of a higher hydraulic conductivity (Cenomanium and Turonium, Upper Cretaceous). Ibbenbüren colliery shows no overburden, whereas the overburden thickness of the other two collieries range between 300 m (Königsborn colliery) and 800 m (Westfalen colliery).

Modelling results

The model yields a data series that show how the mine water level and the flow rate of both groundwater and mine water are evolving in time. At all three collieries investigated, only little differences between the data series of the measurements and calculations were found (tab. 1) for the basic variant interpreted as the variant that generates the minimal deviation from the actual measured curve. As the example, the mine water rebound with minor deviations during the period of measurements is shown for the basic variant evaluated for the Königsborn colliery (fig. 2).

This investigation analyses the impact of a four-factor variation on the development

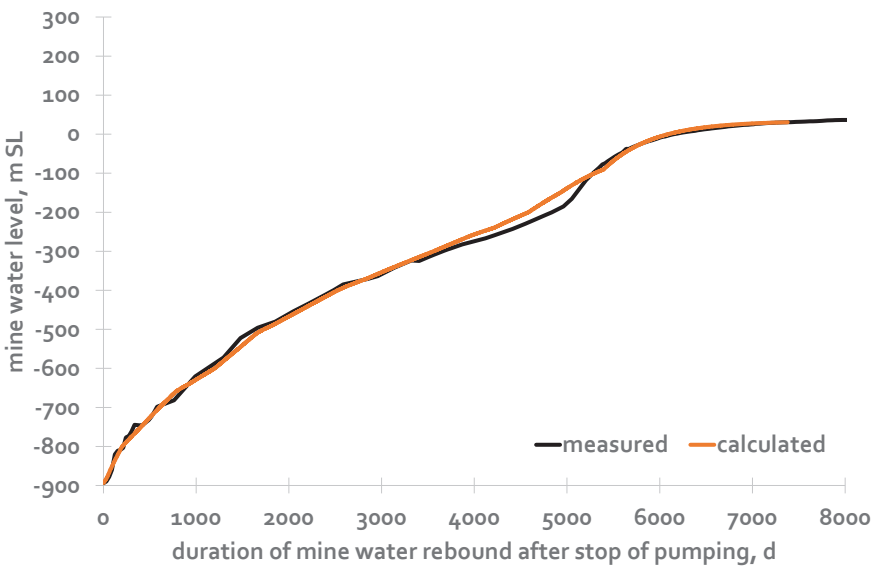


Figure 2 *Comparison of measured curve (black) and optimal variant (orange) with minimum deviation for the Königsborn colliery.*

Table 1 *Mean square deviations between the data series of the measured and calculated (base variant) temporal development of the mine water (pressure) area and inflow rate.*

	Ibbenbüren colliery %	Königsborn colliery %	Westfalen colliery %
mine water level	2.1	1.2	1.0
initial inflow rate	0.8	0.1	0.1

of the mine water rebound in each of the collieries. These four factors comprise:

- residual cavity volume created by mining
- distance to the outer limit of the depression cone
- hydraulic conductivity of the rock
- infiltration (recharge) rate

The factors were varied within the predefined value ranges by the relative expected value *X*E (0.9 *X*E < *X*E < 1.1 *X*E). These result in the set of curves (fig. 3). From a mathematical viewpoint, the sensitivity is quantified by the mean deviation between the data series calculated for the basic variant and that of the respective model curve.

The data series of the mine water level are based on individual measurements (weekly to monthly sounding measurements in shafts over a multiyear period); however, the data series of the inflow rate include only a measurement made before the mine water rebound began, whereas the inflow rate at the end of the mine water rebound is only estimated. Thus, there are no further considerations regarding the inflow rate. Nevertheless, the available data series enable making important conclusions on the flooding process in the underground workings.

Results of Design of Experiments and Interpretation

The functional interdependence of one or more factors (independent variables) and a target value (dependent variable) is described using a non-linear, multiple description model. The regression coefficients – calculated by the statistics software – enable the quantification of not only any individual factor but also of the square and interdependent terms on a process. The results were interpreted according to the following rule: the greater the regression coefficient, the higher the impact. These coefficients are also referred to as sensitivity coefficients.

The sensitivity coefficients determined are always site-specific; however, their results can be generalised and transferred to natural conditions, thus, making them site-independent. To do that, the sensitivity coefficients will be compared to the specific hydrogeological features of the deposit. The proportion of overburden thickness to total

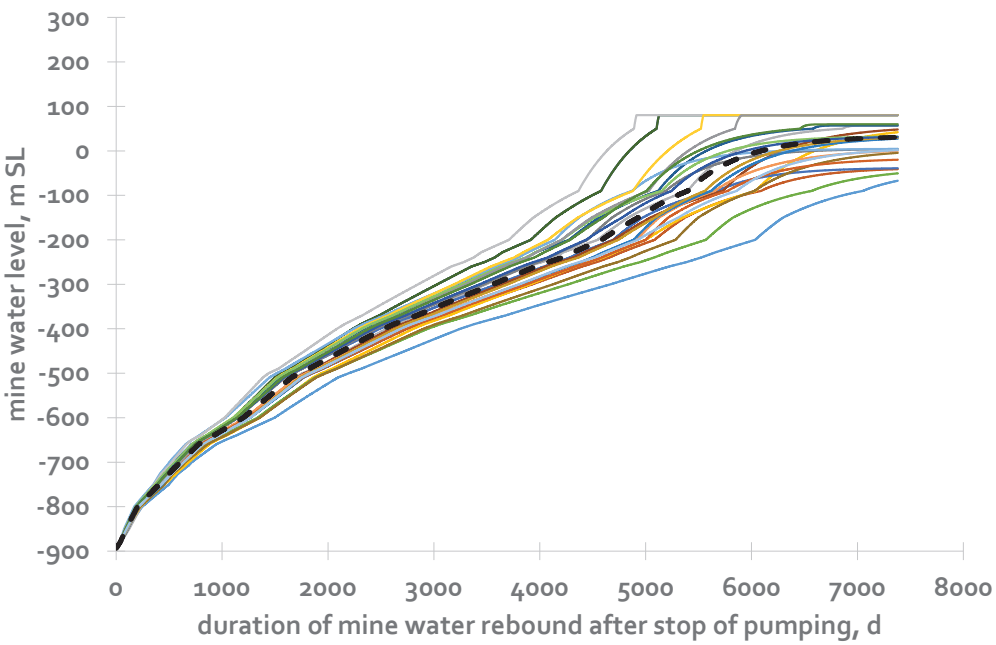


Figure 3 *Set of mine water rebound curves resulting from the variation of factors (optimal variant: black dotted) shown by the example of Königsborn colliery.*

depth considers, for example, the impact of the overburden on the mine water rebound (fig. 4). Deposits without overburden, such as Ibbenbüren Colliery, are characterised by low proportions (close to 0), in contrast, deposits with thick overburden layers demonstrate higher proportions tending to 1.

This chart helps to recognise the trends for the factors in relation to the overburden thickness. The influence of the factor "infiltration rate" on the mine water level steadily decreases with an increasing overburden thickness. At the same time, the factor "hydraulic conductivity" becomes more significant with increasing overburden thickness. This trend emphasizes the increasing importance of the hydraulic rock conductivity for deposits where the overburden is flowed through as part of the mine water rebound once the open mine workings have been flooded.

Conclusion

The combination of an analytical modelling approach with the Design of Experiment method enables a systematic investigation of the key factors of flooding the mines. In conjunction with the Design of Experiment method, the influence of these factors including their linear, square and interdependent terms on the mine water rebound process is quantified within sensitivity analysis. This classification and the subsequent prioritisation of factors contribute to optimising the monitoring measures at all stages of the mining life cycle by focusing the investigation on the system-relevant factors. Factors which are less system-relevant can be assessed cost-efficiently and without a larger time investment using experiential values and analogous comparisons.

References

Eriksson, L, Johannson, E, Kettaneh-Wold, N, Wikström, C, Wold, S (2008) Design of Experiments. Principles and Applications. 3rd edition, 459 p.; Umea (Umetrics Academy).

Fisher, RA (1935): The Design of Experiments. XI+252 p., 5 figures, 40 tables; Edinburgh (Oliver & Boyd).

Goerke-Mallet, P. (2000): Untersuchungen zu raumbedeutsamen Entwicklungen im

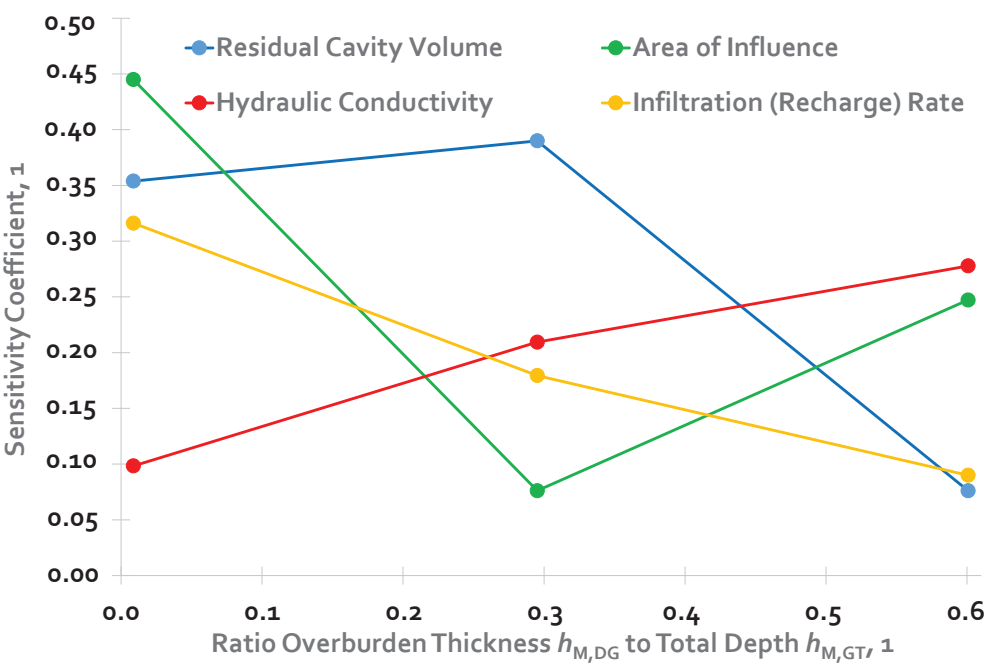


Figure 4 Effectiveness depending on the proportion between overburden thickness and total depth of underground mine workings.

Steinkohlenrevier Ibbenbüren unter besonderer Berücksichtigung der Wechselwirkungen von Bergbau und Hydrologie. – Dissertation, RWTH Aachen: 226 p.; Aachen (Mainz).

Goh, T.N. (2013): Management of parametric response in Design of Experiments. - Quality and Reliability Engineering International, 30 (8): 1191–1195, 1 figure.

Melchers, C, Westermann, S, Reker, B (2019) Evaluation of mine water rebound processes in the German coalfields of Ruhr, Saar, Ibbenbüren, and the adjacent European countries. Berichte zum Nachbergbau, 1, 129 p., 60 figures, 5 tables; Bochum (Selbstverlag des Deutschen Bergbau-Museums).

Paul, M, Sänger, H.-J, Snagowski, S, Märten, H, Eckart, M (1998) Flutungsprognose am Standort Ronneburg. Ergebnisse eines integrierten Modellansatzes. Uranium Mining and Hydrogeology, 2: 130–139, 5 figures; Freiberg.

Rudakov, D, Westermann, S (2021) Analytical modelling of mine water rebound: Three case studies in closed hard-coal mines in Germany. Mining of Mineral Deposits, 15(3): 22–30.

Westermann, S (2020) Modellbasierte Sensitivitätsanalyse systembestimmender Faktoren eines Grubenwasseranstiegs in Untertagebergwerken mittels statistischer Versuchsplanung. Berichte zum Nachbergbau, 2: 220 p., 50 figures, 45 tables; Clausthal-Zellerfeld (Papierflieger).

Younger, PL, Adams, R (1999) Predicting mine water rebound. Research & Development Technical Report W179, 109 p.; Bristol (Environment Agency).

The Colourful Lakes in Wieściszowice, Sudetes Mountains, Poland – An example of Chemical Variation in Abandoned Pyrite Mine Pit Lakes

Christian Wolkersdorfer[1], Magdalena Worsa-Kozak[2], Krzysztof Chudy[2]

[1]*Tshwane University of Technology (TUT), South Africa, Christian@Wolkersdorfer.info*

[2]*Wrocław University of Science and Technology, Poland, Magdalena.Worsa-Kozak@pwr.edu.pl, Krzysztof.Chudy@pwr.edu.pl*

Extended Abstract

Abandoned flooded mines, especially pit lakes, are places where various geochemical processes affecting water quality and the environment can be studied (Chudy *et al.* 2021). Understanding the water chemistry and processes in post-mining lakes is crucial, especially for those that became popular tourist and recreational attractions. Details about the complexity of post-mining lakes have been given by various researchers in four comprehensive monographs over the last two decades, providing an overview of former metal, lignite and hard coal open-cast mines affected by acid mine drainage. Abandoned open pit mines, which eventually form pit lakes, are common wherever easily accessible, shallow mineral deposits are found. The best-explored open pit lakes are in Germany, Australia, Spain, Portugal, the USA, Canada, and Poland. Yet, the Colourful Lakes (Fig. 1), one of the most popular touristic sites in southwest Poland, are a stimulating site for hydrogeological and isotopic investigations because of their differences from the Iberian pyrite belt pit lakes. While the former are relatively small with acid to circumneutral pH-values, the latter are much larger with commonly low pH-values and a high acidity. This study aims to understand temporal and spatial changes in the chemistry (major and trace elements) and stable isotope composition of shallow pit lakes, exemplified by the Wieściszowice Colourful Lakes. None of the previous studies on the Colourful Lakes have investigated the possible lake stratification and the chemical mechanisms occurring in different seasons. Therefore, this study fills the knowledge gap of long abandoned (almost 100 years) shallow and unremediated metal mining lakes.

The Colourful Lakes near the village of Wieściszowice, Poland, refer to four abandoned mining lakes, commonly called Yellow, Purple, Blue, and Green Lakes, created after mining and sulfuric acid production ceased in 1925. This area was shaped by historic surface and underground mining of mineral resources from the late 18th to the early 20th century. Nowadays, the higher parts of the Wielka Kopa hill (Blue Lake location) are covered with pine-spruce forests, while deciduous trees dominate the lower parts (Purple and Yellow Lakes locations) with a high proportion of birch. Only after intense rainfall the Green Lake appears, and as it was dry at the time of sampling, it was not investigated during this study. The Blue Lake



Figure 1 *Images showing three of the Colourful lakes near Wieściszowice, Poland. From left to right: Blue, Purple, and Yellow Lakes (from Chudy* et al. *2021).*

is 150 m long, 30–50 m wide, and 7–8 m deep, while the Purple Lake has dimensions of about 430 × 110 m, a very variable shoreline, and depth mainly dependent on rainfall. About 20 years ago, the Yellow Lake formed between the mined dumps, disappearing in dry years with low rainfall. Geological research has been carried out in Wieściszowice, with the first scientific activities mainly related to mineral exploitation dating back to the 18th century, when pyrite deposits were discovered. Subsequent geological research was related to the attempt to resume sulfide mining after the World Wars, but exploitation was eventually abandoned.

Blue Lake, Purple Lake, and Yellow Lake are located around mine tailings and are characterised by different chemical compositions, pH values and electrical conductivities (Table 1, Fig. 2). In addition to chemical analysis, the lake's water chemistry results were analysed using hierarchical cluster and principal component analysis. As shown, each lake falls into its own cluster, indicating that the individual chemistry of the three lakes was statistically significantly different and could be discussed individually. Of all the lakes, the Blue Lake was found to have the highest pH, the lowest TDS and the lowest concentration of trace elements. Purple and Yellow Lakes were found to be in the Fe-buffer range and had higher electrical conductivities attributed to the influence of pyrite weathering and efflorescent minerals from the waste rock. Finally, the results highlight that, in addition to rainfall, the Blue Lake is fed by the intermittent Rdzawy Potok stream. In contrast, the Purple and Yellow Lakes are predominantly fed by groundwater.

The isotopic composition of the lakes was investigated to determine the sulfate source in the water. Results from the Blue Lake show seasonal variations in sulfate concentrations and $\delta^{34}S(SO_4^{2-})$ and $\delta^{18}O(SO_4^{2-})$, with the

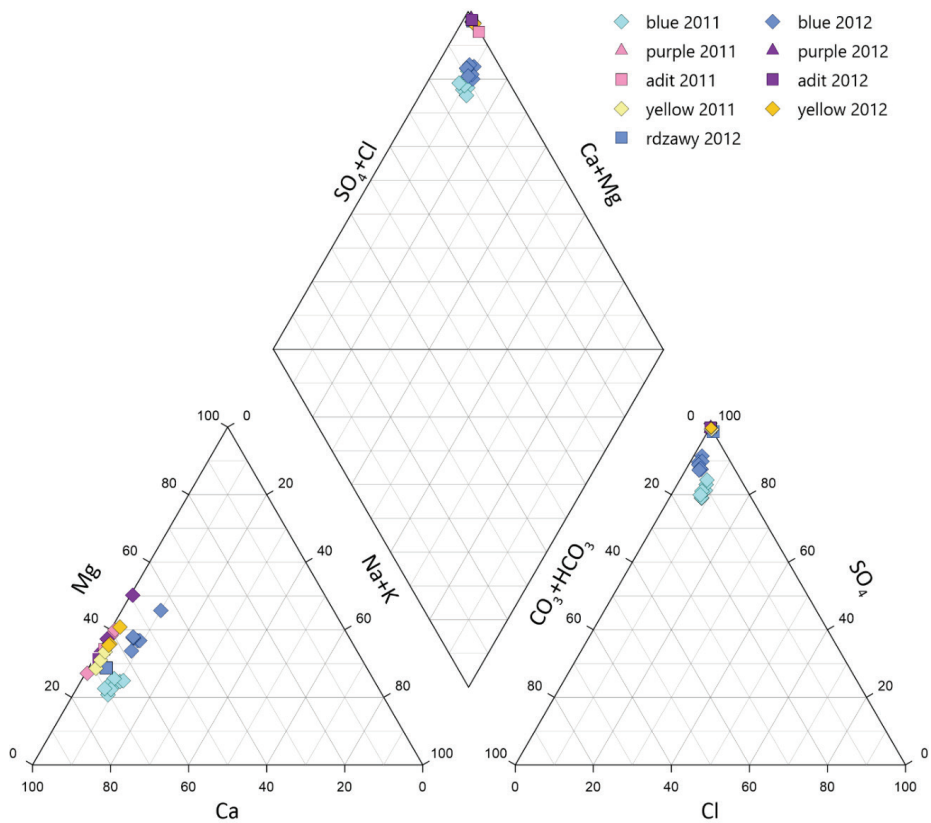


Figure 2 *Piper diagram of the Wieściszowice Colorful Lakes water samples (from Chudy* et al. *2021).*

Table 1 *Summarized results of the chemical and physicochemical parameters of the two sampling campaigns in the Colourful Lakes. TDS: total dissolved solids, EC: electrical conductivity, b.d.l.: below detection limit, –: not analyzed, IB error: PHREEQC ion balance error (from Chudy* et al. *2021).*

	Blue Lake, *n* = 15				Purple Lake, *n* = 6				Yellow Lake, *n* = 6			
	min.	max.	x̄	σ	min.	max.	x̄	σ	min.	max.	x̄	σ
T, °C	11.2	20.4	16.7	2.7	15.7	22.3	18.3	2.7	13.7	19.4	16.4	2.5
pH, –	4.85	5.74	5.14	0.24	2.37	2.88	2.62	0.26	2.25	2.90	2.61	0.31
Eh, mV	479	532	503	20	659	785	717	47	732	792	759	23
pE, –	8.48	9.42	8.91	0.37	11.65	13.88	12.68	0.84	12.94	14.02	13.45	0.41
EC, µS/cm	160	188	180	7	2470	3950	3130	648	1540	1956	1678	161
TDS, mg/L	80	144	114	22	2500	4776	3313	839	1236	1624	1360	141
Cl-, mg/L	1.54	5.13	3.51	1.55	0.64	2.57	1.43	0.79	1.35	4.54	2.64	1.28
HCO3-, mg/L	7.93	14.03	10.82	2.02	–	–	–	–	–	–	–	–
SO42-, mg/L	62.9	88.8	74.1	6.9	1268	3108	1930	650.1	618.8	837.6	716.1	86.1
NO3-, mg/L	0.05	4.21	1.10	1.19	7.68	20.79	13.68	4.46	4.14	8.97	5.90	2.05
PO43-, mg/L	b.d.l.	0.30	0.08	0.10	0.01	0.45	0.13	0.17	0.01	0.11	0.06	0.05
NH4+, mg/L	b.d.l.	0.41	0.13	0.15	0.08	1.09	0.54	0.42	b.d.l.	1.31	0.57	0.59
Na+, mg/L	2.29	3.61	2.98	0.41	2.73	4.77	3.53	0.81	3.24	4.14	3.60	0.37
K+, mg/L	0.07	0.25	0.14	0.06	0.04	0.16	0.11	0.05	0.15	0.40	0.26	0.11
Mg2+, mg/L	4.18	6.98	5.66	1.10	67.9	138.2	103.5	29.7	32.62	38.50	35.24	2.12
Ca2+, mg/L	11.32	25.99	19.80	4.11	179.9	619.5	303.7	161.7	86.25	137.74	112.28	19.88
Mn2+, mg/L	0.12	0.21	0.17	0.03	1.62	3.31	2.43	0.71	0.39	0.68	0.48	0.11
Fetot, mg/L	0.06	0.21	0.13	0.06	25.38	109.34	68.82	38.19	12.16	71.74	39.76	29.12
SiO2, mg/L	31.92	36.41	34.82	1.46	86.38	154.73	119.89	26.62	33.27	73.12	54.04	14.59
Al, mg/L	0.40	5.49	2.15	1.73	34.66	84.28	57.42	20.98	10.17	22.80	15.07	4.88
Ag, µg/L	0.01	2.80	0.69	1.09	0.04	2.19	0.55	0.85	0.06	4.60	1.76	2.08
As, µg/L	b.d.l.	2.13	1.10	0.73	37.03	84.83	68.76	20.52	1.61	11.50	7.86	3.81
Ba, µg/L	2.70	10.53	7.15	2.81	6.05	8.77	7.37	1.11	b.d.l.	7.77	4.02	3.28
Cd, µg/L	0.02	0.26	0.14	0.10	0.39	3.81	2.12	1.52	0.13	1.52	0.84	0.46
Co, µg/L	26.17	39.05	33.68	3.48	115.2	1072.0	518.9	384.0	345.7	420.8	370.7	27.4
Cr, µg/L	b.d.l.	0.67	0.20	0.23	49.33	125.04	89.44	32.49	19.80	27.77	23.47	2.79
Cu, µg/L	2.26	3.72	2.96	0.42	24.45	471.35	202.40	194.01	6.97	49.04	27.43	21.15
Mo, µg/L	b.d.l.	2.70	0.68	0.96	b.d.l.	b.d.l.	b.d.l.	b.d.l.	b.d.l.	5.13	1.49	2.46
Ni, µg/L	1.82	35.25	11.39	11.25	47.27	327.11	182.60	116.75	26.54	159.37	65.84	53.31
Pb, µg/L	b.d.l.	13.08	4.99	4.79	b.d.l.	4.81	2.09	2.07	b.d.l.	7.89	3.40	3.58
Sn, µg/L	b.d.l.	0.03	0.01	0.01	b.d.l.	0.04	0.02	0.02	b.d.l.	0.06	0.02	0.03
Sr, µg/L	2.56	3.82	3.13	0.47	30.09	44.03	37.45	5.41	16.98	21.99	19.94	1.77
Ti, µg/L	b.d.l.	12.83	4.00	4.81	b.d.l.	19.34	9.50	9.67	11.70	20.82	17.20	4.84
Zn, µg/L	7.47	29.10	11.99	7.13	80.84	839.10	356.19	290.38	22.70	159.80	65.46	52.41
IB error, %	-13.01	3.05	-2.59	4.08	-17.04	7.24	-5.47	10.5	-15.06	25.05	4.79	18.18

main source of sulfate being surface runoff containing sulfate and oxidised organic sulfur (Fig. 3). There was no evidence of sulfate from direct oxidation of pyrite, which would have negative $\delta^{34}S(SO_4^{2-})$ values ranging from about –4.5‰ to about –3.5‰. Consequently, the sulfate in the lake is thought to be derived from leaching of efflorescent salts in the adjacent tailings surrounding this water body. In contrast, the Purple Lake has high sulfate concentrations, with both sulfate concentrations and $\delta^{34}S(SO_4^{2-})$ and $\delta^{18}O(SO_4^{2-})$ showing seasonal variations. As the correlations between sulfate concentrations, $\delta^{34}S(SO_4^{2-})$ and $\delta^{18}O(SO_4^{2-})$, are statistically significant, a common source can be expected. Furthermore, the study found that the sulfate source is related to anthropogenic activities, such as the mining and ore processing. The isotopic composition of oxygen and hydrogen results in the lakes show small variations in September 2011. Greater variations were found in June 2012, but there was no relationship between depth and $\delta^{2}H(H_2O)$ or $\delta^{18}O(H_2O)$, indicating good mixing processes.

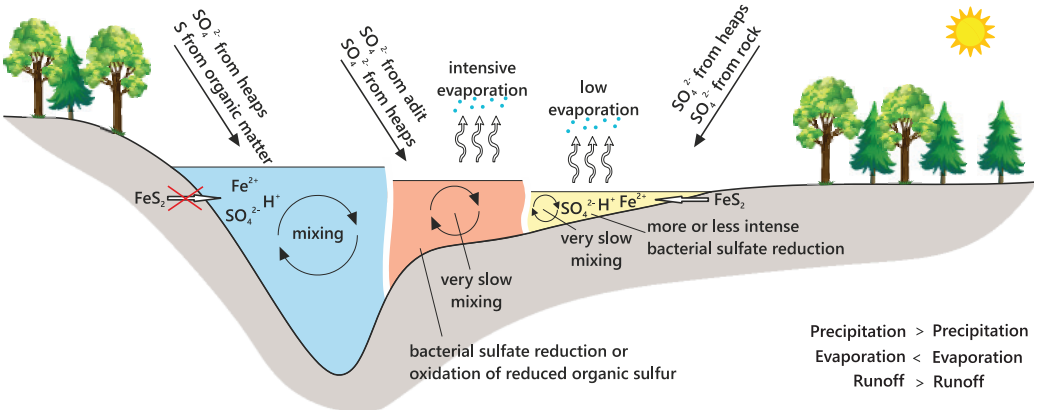


Figure 3 *Graphical abstract that shows the processes that take place around the Colourful Lakes (from Chudy* et al. *2021).*

Based on the PHREEQC results, the dominant phases controlling the chemistry of the in Blue Lake were identified as $Al(OH)_3(a)$, barite and $Fe(OH)_3(a)$, while in the Purple and Yellow Lakes the dominant phases were anhydrite, gypsum and chalcedony (though rather amorphous SiO_2 would be expected). Distinctively, the distribution of species and saturation indices in the three lakes showed a pattern that differentiated them. While the Blue Lake showed a slight stratification with a tendency to lower saturation indices with increasing depth, indicating possible evaporation, the Yellow and Purple Lakes were buffered, indicating precipitation and mixing reactions. PHREEQC speciation results showed that SO_4^{2+} dominated all three lakes and inflows, followed by Ca^{2+}, with the inflow to Blue Lake having the same species distribution as the Blue Lake itself. Predominance diagrams (Eh-pH) supported the results of the chemical thermodynamic PHREEQC calculations and were used to understand the dominant species and potential reactions in the system.

This study investigated the processes controlling the chemical composition of shallow post-mining lakes, namely the Blue, Purple, and Yellow Lakes, in the Wieściszowice region of southwestern Poland. As the results show, each of the three lakes should be separately considered since there is a noticeable difference in their chemical composition due to different natural and anthropogenic factors affecting their geochemical conditions. While the general processes of inflowing water flowing through weathered mining residues and leaching efflorescent salts from pyrite and rock weathering are similar around all three lakes, the differences result from diverse factors affecting each lake. Blue Lake, for example, is mainly recharged by the Rdzawy Potok River throughout the year and periodically by precipitation. On the other hand, Purple Lake most of the year is fed by the Neues-Glück-adit, which drains the eastern part of the hills, and the rainfall. The study shows that evaporation is a major contributor to the chemical composition of Purple Lake, resulting in a slow flow towards the bottom where a twofold increase in mineralisation and SO_4^{2-} is recorded with very high Fetot concentrations. Furthermore, this study also included the first-time isotopic sampling of the lakes in determining the spatiotemporal variability of water chemistry and isotopic composition. In the overall context, this study highlights the importance of considering the natural and anthropogenic factors that influence the geochemical conditions of any lake to understand its chemical composition fully.

Acknowledgments

The authors thank Agnieszka Wójcik, Wojciech Drzewicki, Dominika Konsencjusz, Danuta Szyszka, Michał Rysiukiewicz and Piotr Szumilas for sample and data analysis and their help in the field during the sampling campaigns. Roswitha Reinhold, Sonja

Reinhold, Dirk Metzig and Johannes Rösner from the "Arbeitskreis Landeshut" provided historical data and publications about Rohnau.

Remarks

This text is an extended abstract of a paper written by the authors using tables and figures used therein. Details can be found in the below mentioned publication.

References

Chudy K, Worsa-Kozak M, Wójcik A, Wolkersdorfer C, Drzewicki W, Konsencjusz D, Szyszka D (2021) Chemical Variations in Mine Water of Abandoned Pyrite Mines Exemplified by the Colorful Lakes in Wieściszowice, Sudetes Mountains, Poland. J Hydro Regional Stud. https://doi.org/10.1016/j.ejrh.2021.100974

Abandoned mines as a source of heat and cold for quarter solutions

Timm Wunderlich[1], Lukas Oppelt[1], Tom Ebel[1], Thomas Grab[1], Tobias Fieback[1]

[1]*TU Bergakademie Freiberg, Chair for Technical Thermodynamics, Gustav-Zeuner-Straße 7, 09599 Freiberg, Germany*

Abstract

The communities bordering the former coal mining area of Lugau/Oelsnitz in south-west Saxony (Germany) were shaped by active mining for over 100 years. Structural change requires activities for aftercare, especially considering the possible leakage of mine water (if no countermeasures are taken) in 2032. In this context, the paper shows the investigation of using the mine water to be discharged as a thermal energy source. For the town of Gersdorf, 11 different residential buildings were simulated in MATLAB Simulink. The solutions were examined in terms of technical, economic, and ecological factors in relation to a local district heating network.

Keywords: Mine water, heat pump, district heating network, simulation, MATLAB

Introduction

In the Lugau/Oelsnitz, located in the south-west of the state of Saxony, area, a sedimentary package was formed during the Upper Carboniferous period approximately 305 million years ago, resulting in a thickness of up 200 m in the mining area hosting 12 economically viable coal seams. The first coal mining in this area began in 1831 and was subsequently expanded from 1844. The communities surrounding the former coalfield of Lugau/Oelsnitz have been shaped by active mining. Thus, making it one of the first hard coal mining areas in Germany during of the Industrial Revolution. Figure 1 shows the study area of about 70 km² – including of the municipalities of Oelsnitz (Erzgeb.), Gersdorf, Hohndorf and Lugau/Erzgeb., which are between the cities of Chemnitz and Zwickau and home to around 24,000 inhabitants. This suburban area developed around the mining sites and their surrounding vicinities became economic, cultural, and social centres of the area. [1]

During the 1950, at the peak of mining activities, coal mining operations extended for a total distance of approximately 140 km below the ground. The heading ways were located on 6 levels at different depths. The roadways on these levels can be considered hydraulic roadways. The lower-lying western minefield is separated from the higher-lying eastern minefield by the Pluto shaft fault. However, a connection between the two pit fields exists via the -146 m and the +25 m levels, due to the rising flood level indicating that the flooding level is balanced in the pit. The two pit fields are hydraulically connected via these levels. [2]

The excavation and extraction of coal and non-coal materials such as dead rocks, caused the land above these areas to sink. The mining-induced deformations at the surface, led to segregation processes in Oelsnitz of up to 17.34 meters. [3] Between 1859 and 1971, approximately 142 million tons of usable coal were extracted in the Lugau/Oelsnitz district [4]. As coal mining and dewatering discontinued approx. 150 million m³cavity began to flood. Due to subsidence and the sinking of the land, it is estimated that around 47 million m³ of free drifts and shafts are still present in the mining area, corresponding to 32 % of the raw mining volume. All other spaces are assumed to be filled with downfall of rocks. [1]

Since the closure of the mining activities in 1971, uncontrolled flooding has been occurring, with the flooding volume being determined by groundwater recharge. This average amount of flooding is expected to be 30 m³/h in 2032 and it´s estimated to be even

higher due to the current deep inflows. This volume flow quantifies the annual average and is subject to seasonal fluctuations [5].

Due to the lack of monitoring and intervention measures in place, there was no data available on the current flooding level until the beginning of the millennium. Therefore, there was no possibility of actively influencing the flooding process. [1] However, in 2003, the State of Saxony established a mine water monitoring station (MWMS) in Oelsnitz (633 m below ground level) to monitor the flooding level and to check the water quality of the mine water. A second MWMS was set up in Gersdorf in 2014, which is located 674 m below ground level and focuses on data collection of the flooding level. [6]

In the southwest of the district is the community of Gersdorf which has the lowest valley elevation (+320 m meters above standard zero). If no preventive measures are taken, the mine water level is expected to rise and surface by 2032 due to subsidence. Near this area in the community are the former "Kaisergrubenschächt", which have been secured by mining as shown in Figure 1.

To prevent uncontrolled flooding due to escape of mine water, preventive measures must be taken, e. g. pumping out the inflowing mine water through a borehole.

Methods

Measures for aftercare are required for the regional structural change, especially due to the potential leakage of mine water from 2032. However, the municipalities in the area of interest, like most municipalities in Germany, still face challenges to implement renewable heating and cooling in the building sector. Some mine waters have temperatures above 20 °C which offers opportunities for combining technical and energy measures (renewable heating and cooling). The utilisation of mine water to produce energy has been discussed in detail by Grab *et al.* [7] and Oppelt *et al.* [8]. In addition, it is worth exploring the combination of necessary aftercare measures, e. g. pumping out the mine water, rehabilitating galleries, and renewable energy supply, particularly through energy supply networks such as heating and cooling grids to facilitate a climate-neutral energy local heating in the communities affected by structural change.

Two scenarios for a grid-connected supply are possible.

- supply with a cold network and corresponding heat pumps in the buildings
- supply using one or more large heat pumps directly to the buildings,

To calculate the potential, the mine water needs to be cooled down to a minimum

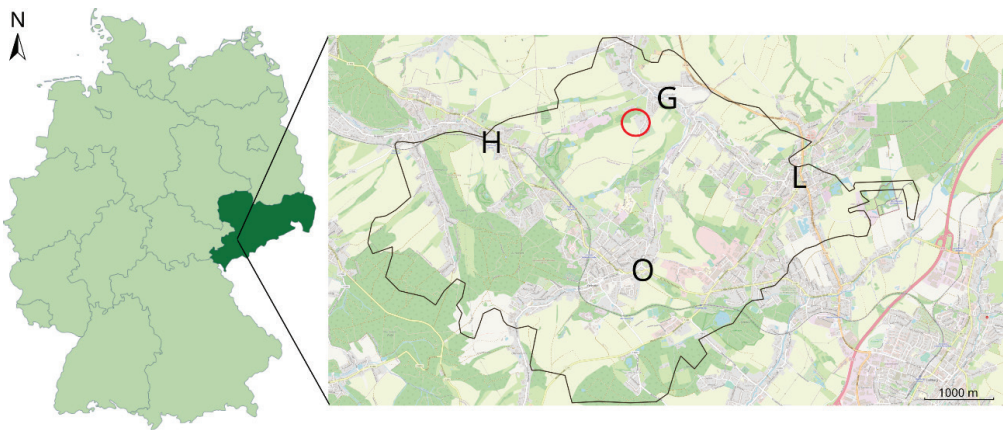


Figure 1 *Black outlines the location of the mining area, the surrounding municipalities H-Hohndorf, O-Oelsnitz, L-Lugau, G-Gersdorf and the location of former "Kaisergrubenschächte" and object of investigation in Gersdorf marked in red*

temperature. This extracts the heat from the water so that it can be utilised for a specific process later.

A maximum of 5°C (outward temperature) is set as the maximum possible cooling of the mine water. The mine water temperatures are set at 25 °C (655 m depth) resulting in an effective usable temperature range of 20 K. The calculation is made with 5 K, based on existing power plants. More data are shown in the following table 1. [5]

The heat potential of the mine water is given by the formula (1):

$$Q = V \times \rho \times cp \times \Delta T \quad (1)$$

Where rho is the density, cp the specific heat and ΔT the change in temperature. Table 1 provided all the other necessary data.

This potential represents the heat source compared to the above-ground consumers in the network (heat sink). With a constant source temperature of about 25 °C throughout the year, the house in the heat network can achieve a high annual coefficient of performance when using heat pumps in combination. [10]

Various terms are used for networks that operate with low temperatures. Along with the term "cold local heating network", terms such as energy networks or heat networks 5.0 are also in use. The main characteristic of these heat networks is that the network temperature with values between 5-40 °C (mostly 10-25°C) is insufficient for directly heating a building. Therefore, decentralised HPs must be installed in the building´s, which raise the heat from the network to the inlet temperature of the building energy system. Moreover, heat transfer stations in the buildings can facilitate the operation of the HP, allowing the same district network to meet the heating and cooling needs of the connected users (bidirectional supply). These networks can be used to meet cooling demand, such as by supplying chilled water for cooling purposes (i.e., free cooling) or to feed decentralized chillers with very high efficiency. In addition, the integration of renewable energy sources into these networks is facilitated. [11]

The Kaisergrubenschacht quarter in Gersdorf is situated on the formerly restricted area of the Kaisergrubenschacht I and II, covering an area of approx. 9.000 m². The district is planned to include 11 households and the mine water plant, resulting in a division of 12 plots. As the single houses are scheduled to be built after 2030, the legal framework for the construction adheres to the passive house standard.

Since the development plan has not been finalised, no specific statements can be made regarding the layer of the lots and/or apartment composition. Therefore, three types of houses and two different roof shapes were selected within the framework of the project. Representing possible composition of the district; Furthermore, some residential units will have a basement representing the possible composition of the district. To make recommendations for optimal development, various buildings were simulated using MATLAB Simulink. Figure 2 shows the resulting building placement, two semi-detached houses are built in the northern part of the area, while bungalows are located in the southern due to the resulting shadows because of their height.

To represent a diverse occupant structure, various typical households were examined in

Table 1 *Parameters and calculated heat potentials of the mine water*

	Diameter	Value	Source
Conveying rate: at 300 m above sea level	m^3/h	32.5	[5]
Heat exchanger efficiency:		0,5	[9]
Transmittable heat output:	kW	94.67	
Transmittable energy quantity (8760 h/a)	MWh	829.3	

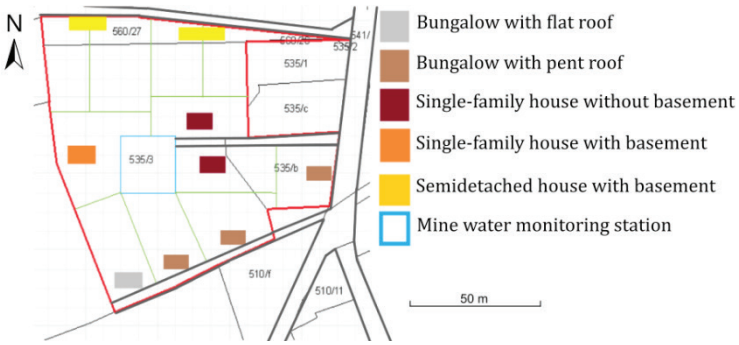


Figure 2 Building distribution ***and designation on the site under consideration***

detail. Various simulations were carried out for two to four-person households, each of which performs different activities.

Simulation settings

The simulations were carried out using the Simulink program and is an add-on to the MATLAB software. Additionally, the CARNOT Toolbox was employed, which is an application for Simulink developed by the University of Applied Sciences Aachen [12]. The toolbox provides ready-made blocks for designing technical systems such as thermodynamics, hydraulic, electrical, and chemical systems, and can be further customised by adjusting the specific parameters. The CARNOT blocks have been used to integrate fixed framework parameters and create interdependencies. The resulting models simulate the thermodynamic and hydraulic processes of the buildings [12].

Since no concrete building projects are planned, a modular approach was used to develop the models, allowing for easy adjustment of the model parameters and structure of relationships between the blocks. The parameters of the model can be easily adjusted and the structure of the individual relationships between the blocks can be changed. This allows for flexibility to adapt the models to future construction planning specifications with minimal effort. In addition, several input factors or framework conditions were incorporated into the model to obtain an authentic and realistic picture of the neighbourhood. The weather data used in the simulations originate from the German Weather Service data set for the Gersdorf site was used, which includes temperature, radiation values, wind direction and speed, relative humidity, cloud cover, and barometric data [13].

In the simulation, the building model comprises individual rooms, which are thermodynamically connected to the rest of the building and the outdoor environment through air exchange and wall surfaces allowing for heat transport within and from outside the building to be considered. Furthermore, different roof types, as well as the connection between the basement-ground floor and the ground floor, were considered in the simulation. Another important component in the simulation of the energy demand is the use of individual load profiles. Individual load profiles were used to represent the internal loads of the house in seconds, with the "LoadprofileGenerator" [14], [15] developed by N. PFLUGRADT which enables the creation of individual load profiles for different consumer scenarios. This allows extremely accurate simulations of the building components, including small electrical appliances.

The heat network purchase corresponds to the environmental energy required by the heat pumps, which in the neighbourhood concept is obtained from a local heating network that utilises mine water. However, if there´s a centralised heat supply, large heat pumps must be used to meet the heating and cooling requirements of the building.

In the respective scenarios, the annual heat grid demand is 41.035 kWh, which must

be fulfilled by using mine water. Assuming a maximum mine water capacity of 95 kW and a continuous operation of 8760 h per year, the energy quantity that can be transferred is 829.309 kWh. Thus, MWMS II provides more energy per year than is consumed by the simulated neighbourhood. If the performance values of the decentralised grid are calculated using an average performance factor of 4.475 (the average of all annual performance factors of the neighbourhood buildings), the energy consumption of the MWMS II is much higher than that of the simulated quarter. A maximum capacity of 57 kW (27 kW heating/cooling and 30 kW domestic hot water), The heating network is allocated 44.3 kW of a maximum capacity of 57 kW (27 kW heating/cooling and 30 kW domestic hot water). Therefore, the power transfer at the heat exchanger of the MWMS II is the limiting factor for decentralised supply.

In the centralised example, the overall cost of the system is approx. 137,200 €, which includes the circulation pumps, heat exchangers, heat pumps, intermediate circuit, and other components. In contrast, the decentralised system cost does not include the expenses for heat pumps and intermediate circuits, which cost approx. 23,300 €.

The results for the central local heating network are listed in table 2 below.

Heat network supply

The average district heating costs are currently around 90 €/MWh [16]. Thus, the cost of the mine water system is noticeably less expensive than that of district heating. However, since grid pump electricity is not accounted for due to missing parameters, this computation is incomplete. As a result, the heating cost of the mine water system in the selected configuration is expected to be comparable to that of district heating. Nonetheless, through optimisation of the buildings and the selection of specially configured heat pumps, the heating cost can be significantly reduced.

Based on the calculated energy demand for the centralised and decentralised supply, the primary energy factor (PEF) of the buildings and systems can be estimated. neighbourhood considered in this study has a grid supply of 24,000 kWh, resulting in a total primary energy demand of 43,500 kWh per year. Considering the total energy reference area of the neighbourhood of 1,500 m², the average primary energy demand is calculated to be 28.7 kWh/m² per year. This value is significantly lower than the passive house requirements of 120 kWh/m² per year. In the case of the centralised supply option, the electricity consumption amounts to 19,700 kWh resulting in a primary energy demand of 23,600 kWh per year.

To supply the new quarter with power, it is estimated that a ring main of 250 m and a supply of 110 m will be required. The installation costs for decentralised local heating network amount to 99,500 €, whereas for a centralised local heating network amount to 196,300 €. It should be noted, that due to the passive house standard, a total output must be assumed, and thus only very small output diameters with a nominal diameter of DN 20 are sufficient to supply the buildings.

For the ecological assessment, a CO2 emission factor of 0.537 [t_{CO2}/MWh] was calculated based on current German grid electricity, among other factors.

Conclusions

It was shown how an after-use concept for the Gersdorf mining site in Saxony could look in the future. The concept includes the use of pumped mine water for the local heat supply of 11 surrounding houses, which consist of different building and household

Table 2 *Heat price for central district heating supply (calculated with German prices [16])*

Energy demand Heating [kWh]	Energy demand Cooling [kWh]	Energy demand TWW [kWh]	Electricity demand MineW. system [€/MWh]	Heat price [€/MWh]
20,133.5	41,882.1	31,093.3	19,565	80.92

types in passive house standards. The potential of the mine water to be pumped out was calculated, evaluated, and transferred into a demo case. Various simulations were carried out with different building and roof types and the option with or without a basement. As a further important component in the simulation of the energy demand, different load profiles of groups of people were included in the consideration. The supply of the buildings was investigated and calculated utilizing two variants of supply using centralised and decentralised network variants. The total costs of the centralised system would amount to approx. 353,650 €. This resulted in a heating price of 80.92 €/MWh and a CO_2 emission factor of 0.537 [t_{CO2}/MWh] for the centralised supply variant. The transmission capacity and energy supply of the mine water are completely sufficient for the district under consideration. The neighbourhood would have a very low primary energy demand and a very good CO_2 balance if the electrical energy for the heat pumps came from solar electricity from the roofs of the buildings under consideration. Finally, a significant improvement in the single-family house cooling demand can be achieved, if the buildings are cooled regeneratively in summer using the system.

Acknowledgements

The authors thank all co-participants involved in the project. Especially the mayors of the municipalities of Gersdorf, Hohndorf, Lugau and Oelsnitz as well as the students Marcus Fröhlich and Undine Fleischmann.

References

[1] M. Felix and H.-J. Berger, "Steinkohlebergbau und Bergbaufolgen im Steinkohlerevier Lugau/ Oelsnitz – Geoprofil 14," Landesamt für Umwelt, Landwirtschaft und Geologie, Dresden, 2010.

[2] M. Felix, S. Görne and H.-J. e. a. Berger, "Zur geothermischen Nutzbarkeit des Grubenwassers im Steinkohlenrevier Lugau/Oelsnitz," 2007.

[3] H. Neuber, "Zustand des unter Tage Bauwerke im Revier Lugau/ Oelsnitz," 2022.

[4] BEYER, C. u. a. (1974): Bergschadenskundliche Analyse „Lugau-Oelsnitz". – Unveröff., VEB Baugrund Berlin, Produktionsbereich Zwickau & VEB Steinkohlenwerk Oelsnitz, Zwickau, Archiv Oberbergamt; Freiberg

[5] M. Eckart, J. Kowarik and P. e. a. Rüterkamp, "Potenzialstudie – Entnahme von aufsteigendem Grubenwasser aus Solequellen des ehemaligen Steinkohlenreviers Lugau-Oelsnitz und Betrachtungen ökologisch nachhaltiger Verwendungsmöglichkeiten im Falle einer Förderung," DMT-Leipzig, Leipzig, Oktober 2014.

[6] M. Hübschmann and C. Jahns, "Aktuelle Aktivitäten des geologischen Diensts in der Steinkohleregion Zwickau-Oelsnitz. FLOEZ – Future for Lugau-Oelsnitz-Zwickau," Oelsnitz/ Erzgebirge, 2018.

[7] Grab, T., Storch, T., Groß, U.: Energetische Nutzung von Grubenwasser aus gefluteten Bergwerken, Erschienen in: Bauer, M., Freeden, W., Jacobi, H., Neu, T. (Hrsg.): Handbuch Oberflächennahe Geothermie, Kapitel 17, Springer Spektrum, 2018, ISBN: 978-3-662-50306-5, DOI: 10.1007/978-3-662-50307-2_17

[8] L. Oppelt, T. Grab, S. Pose, T. Storch, T. Fieback: Mine water geothermal energy as a regenerative energy source – status quo and results from five years of monitoring, Oil Gas EUROPEAN MAGAZINE, 47. Edition, 1/2021, S 15-19, März 2021, DOI: 10.19225/2103054

[9] L. Oppelt, T. Grab, T. Wunderlich, T. Storch, T. Fieback: Mine Water Geothermal Energy – Abandoned Mines As A Green Energy Source, CLIMA 2022-Proceedings, Rotterdam, 2022, DOI: 10.34641/clima.2022.55

[10] T. Y. N. Reiners. „Auslegung kalter Wärmenetze zur regenerativen Quartiersversorgung am Beispiel der Nutzung von Grubenwasserwärme im Wohnquartier Wasserstadt Aden". Diss.

[11] M. Pellegrini and A. Bianchini, "The Innovative Concept of Cold District Heating Networks: A Literature Review," Energies 11, p. 236, 2018.

[12] Fachhochschule Aachen. CARNOT Toolbox. url: https://www.fh-aachen.de/forschung/solar-institut-juelich/carnot.

[13] Deutscher Wetterdienst. Testreferenzjahre (TRY). url: https://www.dwd.de/DE/leistungen/testreferenzjahre/testreferenzjahre.html.

[14] Noah. D. Pflugradt. LoadprofileGenerator. url: www.loadprofilegenerator.de., 08.09.2022

[15] Noah.D. Pflugradt. „Modellierung von Wasser -und Energieverbräuchen in Haushalten"., 08.09.2022

[16] co2online gemeinnützige Beratungsgesellschaft mbH, „Fernwärme: Technik, Nutzung, Kosten und Alternativen", https://www.co2online.de/modernisieren-und-bauen/heizung/fernwaerme/#:~:text=Die%20durchschnittlichen%20Fernw%C3%A4rme%2DKosten%20pro,entsprechend%2094%20Euro%20je%20MWh.,12.04.2023

Long-term Mine Water Management of Abandoned Coal Mines in the United Kingdom: Almost 30 Years of Process, Experience, and Lessons Learned

Lee M Wyatt, John Leyland, Ian A Watson

Coal Authority, 200 Lichfield Lane, Mansfield, NG18 4RG, leewyatt@coal.gov.uk

Abstract

During the closure of the UKs coal mines little consideration was given to mine water risks and management. Since, 1994, the Coal Authority have gained experience and learnt valuable lessons through the efforts made to manage mine water problems and risks. Throughout the history of mine water management in the UK there has been a progression in the process adopted to identify and assess risks and manage long-term legacies of mine water and abandoned mines. Lessons learned and forward looking outlook are essential for long-term mine water.

Keywords: Mine Water, Management, Long-term, Abandoned Mine

Introduction

The UK has a long history of coal mining, with activity in many areas dating back several centuries. The age, depth, and type of mining can vary within an individual mine or mining area. The process of mining creates voids, which, capture, store and transmit water. Excess water in workings presents a challenge for mining and continues to do so post abandonment. Within the UK (and other parts of the world) management of water in mines has been a key part of mining successfully and safely. At present the Coal Authority treat approximately 120 billion litres of mine water per annum (3800 L/s, average of 50 L/s per site). A simplified development history of mine water management in mines and mining areas, based on Younger, 2004 follows:

1. Use of buckets to bail out from shallow workings
2. Under-drainage by adits from mine workings to a valley low point
3. Pumping of water from the mines to surface (or to drainage adits)
4. Installation of barriers to stop or restrict excessive flows of water; or divert water to unflooded abandoned mine workings

During post nationalisation "modern mining" in the UK, various efforts were made to standardise mine water operational management practices with typical approaches outlined below.

Where a colliery (underground coal mine) comprises a simple isolated mining system (well-connected workings, no other nearby collieries or historical workings) – water pumped at a single location or discharged via gravity drainage adits to surface.

In more complex situations where a number of formerly independent collieries were operating water management may have been amalgamated with centralisation of pumping effort. In order for this to function, deliberate connections were made between previously unconnected working sets. Engineered connections may have served multiple purposes such as safety (improved access and egress), transport of coal as well as water management. In addition, investigation and management of "old" (abandoned workings for which records may have been poor and/or unavailable at the time) was undertaken, to understand mining risks (collapse, gas, inrush). These investigation boreholes and connections were in some cases used to drain water from historical workings to manage risk. In some cases connections were made unintentionally or as side effect of mining operations (direct connection or fracture connection). As well as augmenting connections in some cases, the opposite was done, with stoppings and dams constructed

to prevent flows of water between and around mine workings.

Following the privatisation of mining and the associated tranche of mine closures, the Coal Authority was formed in 1994 to manage the legacy and liabilities of nationalised coal mining in the UK. Privatised mines continued to operate around the UK during the late 90s and the early 2000s. Since then, the majority of underground coal mining has ceased, the last major colliery to close was Kellingley in 2015. The original remit of the Coal Authority was related to the management of ongoing subsidence claims and British Coal property interests. Later changes to legislation meant the Coal Authority were given powers to manage and treat mine water – although the Coal Authority do not have any statutory liability for any mine water discharges. The Coal Authority work in partnership with government funded environmental regulators to manage mine water pollution.

Due to the nature of the mines, mine systems and uncertainties about hydraulic connectivity between mine workings (and mines), there are several broad categories of mine water management currently present in the UK:

1. Recovered – mine water is controlled by discharges either to groundwater or the surface. Typically all recharge will discharge, though mining connections, and storage within the mine workings may result in water level variability. In some instances the flow rates of gravity discharges will vary, and under certain conditions may dry completely.
2. Recovered / pumping for treatment – mine water recovered to surface and caused pollution of receiving watercourse. Pumping is undertaken to stop mine water discharge(s), the water is treated to remove iron before being discharged to appropriate surface watercourse
3. Continuation of historical pumping (from before formation of the Coal Authority in 1994) – mine water is pumped to prevent uncontrolled pollution across a wide area and multiple possible surface discharge locations. Mine water can be treated or untreated before discharge to appropriate surface waterbody
4. Resumption of pumping following mine closures – mine water pumping was originally ceased at a mine or in a mine area, the mine workings were allowed to flood (often monitored). Mine water pumping was restarted by the Coal Authority to prevent pollution to surface water and drinking water aquifers
5. Ongoing mine water recovery – mine water pumping ceased and there is ongoing monitoring or assessment of a mine system to confirm if or when mine water management may be needed in the future
6. Unknown mine water status – some mine water systems are considered to have no or minimal risks to the environment, and thus have not been monitored. There are some areas where it is uncertain if mine water is recovered or recovery is ongoing

Coal Authority coal mine water management: progression

In 1994, when the Coal Authority was formed, they were a total of 28 pumping stations abstracting mine water. These pumping stations were predominantly ones operated by mining companies to allow the continued extraction of coal (underground not surface).

Through the 1990's there was a reduction in the number of pumping stations (tab. 1 and fig. 1), this was due to changes in mining operations and centralisation of pumping operations. Throughout the 2000's operational mining decreased, and some pumping stations were transferred to the Coal Authority. During the same time period, proactive management of rising mine water areas (to prevent pollution) by the Coal Authority began. In addition to new mine water management sites, cessation of some pumping stations led to new engineered gravity discharges being implemented. Engineered gravity discharges were a result of a need for cost saving, and actions being taken from assessments of mine water management in parts of the UK. Throughout the 2010's the remaining operational mines ceased pumping, and the Coal Authority added a few additional sites to continue to manage rising mine water.

Table 1 Types of Coal Authority mine water management (1994 to 2023).

Year	Pumped (untreated discharge)	Pumped (treated discharge)	Coal Authority engineered gravity discharge	Sites ceased pumping since previous date	Pumped by underground mine operator
1994	10	1	1	0	17
2004	5	15	2	6	8
2014	3	20	3	8	1
2023	4	21	4	1	0

Note that some operator pumping sites transferred to the Coal Authority for pumping, either a continuation, or at a later date

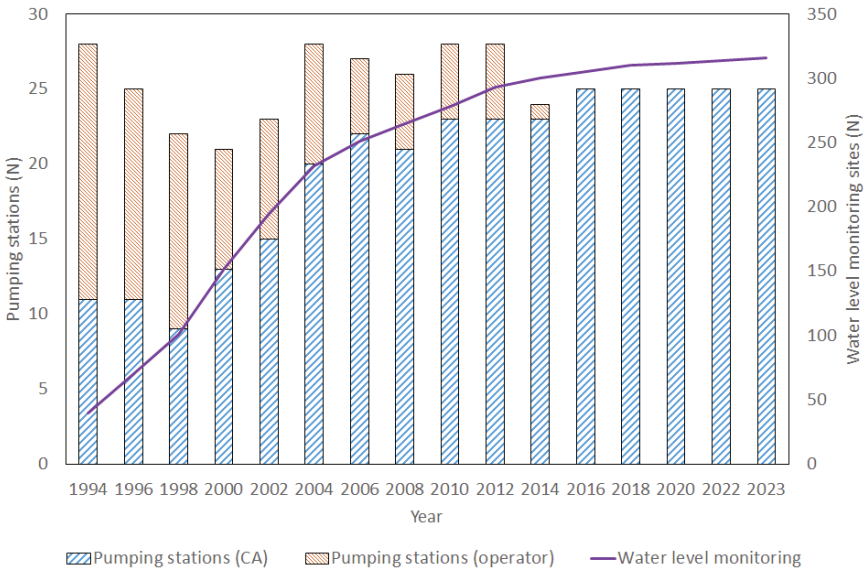


Figure 1 Graph of coal mine water pumping stations in the UK 1994 to 2023. (note there are 548 water level monitoring points across 316 water level sites)

Methodology of progressing mine water management in the UK

In terms of coal mine water management, the Coal Authority work alongside environmental regulators to prevent new pollution, and where feasible to remediate existing pollution. The ethos of the Coal Authority is to promote efficient and sustainable methods for mine water management.

Since 1994, the main aspects that the Coal Authority have adapted to coal mine water management are:

1. Reduce pumping where feasible, yet manage the risks associated with mine water
2. Cease pumping where feasible, and manage the risks associated with mine water
3. Set appropriate pumping control bands to allow for flexibility, whilst managing risks associated with mine water
4. Plan for future mine water management needs and new sites
5. Plan for future changes to existing mine water management strategy
6. Identify possible benefits from mine water management
7. Adapt to changes and requirements for mine water management
8. Evaluate existing mine water management systems

Throughout the early stages of the Coal Authority and mine water management in the 1990s, the main focus was continued pumping at existing sites; followed by strategic reduction in the numbers of pumping stations and centralisation of pumping at fewer locations within each mine water block. Typically this approach was achieved through evaluation of the most appropriate site, based on aspects such as existing pumping infrastructure and site locations for controlling mine water across the area. Much of the early progress in the 1990s was made based on studies done by British Coal (nationalised mining operator until 1994) or other similar bodies, and through pumping and recovery testing (fairly short-term) across different sites.

In the 1990s very little pumped mine water was treated, at best treatment was partial, using settlement ponds. Throughout the later 1990s and into the 2000s, it was recognised that pumped mine water, should be treated where feasible. In 1994, they were a total of 28 coal mine water pumping stations, with only one of them being partially treated. Currently, in 2023 there are 25 coal mine water pumping stations and 21 of them are treated, primarily by passive means. Since 1994, pumping had ceased at some sites, and there have been an extra 3 engineered gravity discharges locations (fig. 2), of which one of those is treated. The ones where treatment is not undertaken have been assessed and are thought to not be beneficial for treatment on the basis they cause very little pollution, and / or are within loading based discharge consents.

Continuing in to the 2000s, regional-scale mine water studies were undertaken to identify the risks of rising mine water to the surrounding environment, including likely timescales and scale of potential risk. Where required, additional studies focussed on areas specifically at risk, and areas where mine water management and treatment could be undertaken. At that time, limited assessment of cost-benefit or long-term sustainability was undertaken.

In certain instances, water level control bands were determined before pumping was started, the bands were based on conservative estimates of mine water gradients. The Coal Authority continues to take a conservative approach to estimated mine water recovery predictions, though the accuracy of predictions is constantly improving as the long-term monitoring dataset grows and the understanding of system behaviours develops.

Through the early parts of the 2010s, the Coal Authority mine water management approach was based on mine water studies undertaken in the 1990s/2000s. Despite limited resources in the Coal Authority the interpretation of monitoring data to inform on the performance of mine water management activities and to plan future interventions was done in-house. To add further challenge to the mine water management approach around



Figure 2 *Photographs of Page Bank, former pumping station left, and gravity discharge right*

this time, much of the operational and early Coal Authority mine water management experience was being lost to retirement.

During the 2010s and 2020s the Coal Authority developed the following process / steps for mine water management.

At existing pumping stations

Determine mine water control bands based type of mine system, mine water gradients between the pumping station and risk area, and long-term monitoring data from a network of water level monitoring sites. The Coal Authority currently use the following control band levels for pumping stations:

a. Overflow / discharge Level: Water level at the pumping station must be kept below this level. Likely or known decant point from the mine workings to the surface or aquifer
b. High Level: Water level at the pumping station needs to be kept below this level. Used as a buffer between this and the Decant level, a pumping station should not go above this level. Buffer based on observed or estimated values for recovery time during pump outages / no pumping
c. Control Level: Water level at the pumping station should be kept to, this allows a for pump maintenance and some flexibility for scheme maintenance and planned pump down-time
d. Too Low Level: The water level should be kept above this level, and ideally it should not go too far below it. This is used to maximise pump efficiency for the chosen pump

Pumping control levels are reviewed on a regular basis to confirm if the control levels are correct, or if they need amending.

Coalfield strategy documents are undertaken and / or reviewed to confirm if the mine water management system for a coalfield, or mine water block is correct, or if it can be improved. A coalfield strategy document can also look at future needs within the block.

Regular liaison and working partnerships with regulator and other key stakeholders confirm if the mine water level management is appropriate, and if any changes are needed.

At future areas requiring pumping (rising mine water areas)

Undertake a coalfield strategy study to review any existing data and reports. The coalfield strategy document will highlight expected timescales of any rising mine water, along with a high-level review of associated potential risks. The coalfield strategy will also help to identify a strategy for future mine water management, and also some future requirements such as pumping tests. The document will also highlight key stakeholders that may be involved or included as a project progresses, typically these will include regulator and water companies, and other internal departments at the Coal Authority.

An enhanced coalfield strategy is used to build upon a coalfield strategy, where it is required. Such a study will also review mining information to determine an initial conceptual model, or improve any existing model. The study will also help to determine appropriate location(s) for mine water management along with gaps in understanding, and where future monitoring can be focussed.

Due to previous experience and lessons learned about predicting mine water flow rates and mine water quality (Wyatt *et al* 2013), the Coal Authority will look to obtain this data from pumping tests. The pumping tests undertaken by the Coal Authority can be variable, and in some instances a site can have multiple parts. To help in the assessment of a site for pumping and along with assessment of mine water risks, the Coal Authority would undertake a selection of the following:

1. Electrical conductivity-temperature profiling, along with grab samples from shafts and boreholes are considered to be representative of potential mine water risks. These may be undertaken at regular intervals throughout the life of a project, and may also be used to continually assess mine water management (Wyatt *et al*, 2021)
2. Purge-test. A short duration pumping test, used to remove the water column within a borehole or shaft, and to obtain water quality data from a purged system In an ideal situation, the purge should be done

until a constant electrical conductivity, although given the nature of the mine system, this may not be achieved in a reasonable time frame.

3. Short-term pumping test: Typically 3 to 6 months long though sometimes shorter. These are used as an initial test to confirm whether further work is needed ahead of future tests. Typically used to establish scale of treatment required during a future longer duration pumping test. In some instances partial treatment may be required. The short-term pumping test is usually at a lower abstraction rate than full scale testing. Often half the estimated full test abstraction requirement is sufficient.
4. Long-term pumping test: Typically these are more than 6 months and may be several years duration. Such a test may require partial or full treatment of the mine water prior to discharge. A long-term pumping test will help improve refine assessments made from shorter-term pumping tests. A long-term pumping test is often required to confirm if a mine system can be fully controlled by the site and for a full range of likely flow rates and water quality.
5. Assessment of any water treatment requirements for pumping tests – based on conservative estimates of water quality and receiving water-courses for dilution and impacts. Done working with the regulators to progress a feasible and viable solution.

Throughout different stages of the process for future mine water management, the Coal Authority will have regular liaison with the regulator and other key stakeholders. These are to confirm things like mine water treatment requirements, appropriate time scales for a pumping test, and other potential benefits of a pumping test.

Conclusions and discussions

Throughout the past 30 years, the Coal Authority have made changes to the way mine water management is undertaken. Improvements have been made in to how water is managed, and the efficiency of mine water management. Improvements have also been made in respect to requirements and desire to treat mine water where applicable and to cause minimal pollution from mine water management. It should be recognised that future changes to current mine water management strategies are likely to occur.

Future issues, challenges, and benefits to mine water management are already being researched and investigated, and include possibilities of improved mine heat schemes (not to duplicate pumping mine water); groundwater flooding; inland saline mine water concerns; better utilising the mine water (such as grey water and for irrigation).

Within a complex mine system, where there are unknowns about the mine system and mine water data, there are ongoing issues, which current mine water management strategies cannot prevent. Primarily, such instances would be issues such as sudden releases of mine water to the environment, or future changes to underground mine water flow paths.

References

Wyatt LM, Moorhouse AML, Kershaw S, Iwanskyj B (2013) Mine water: management post-closure and lessons learned, risk from poor closure management and mine water management. In Tibbett M, Fourie AB, Digby C (eds) (2013) Mine closure 2013: Proceeding of the eighth international seminar on mine closure, Australian Centre for Geomechanics, Cornwall pp279-292, doi: 10.36487/ACG_rep/1352_23/Wyatt

Wyatt LM, Cropper J, Watson IA (2021) Spatial and temporal changes of Physico-chemisty aspects of mine water, due to post-closure water management. In Stanley *et al* (eds) (2021) Mine water management for future generations, International mine water association virtual conference, 2021.

Younger PL (2004) 'Making water': the hydrogeological adventures of Britain's early mining engineers. In Mather JD (ed) (2004). 200 Years of British Hydrogeology. Geological Society of London, Special Publications 225, pp121-157, doi: 10.1144/GSL.SP2004.225.01.09

Pumping borehole for saline mine water in Whitburn, North East England: Problems and novel resolution

Lee M Wyatt, John Leyland, Ian A Watson

Coal Authority, 200 Lichfield Lane, Mansfield, NG18 4RG, leewyatt@coal.gov.uk

Abstract

Pumping of saline mine water at Whitburn is required to prevent pollution of a drinking water aquifer. Initially pumping was from a monitoring borehole drilled in 2010, however, due to its construction it started to fail and needed replacing. During construction of a new replacement abstraction borehole, several problems were experienced, some related to the geology encountered, though the main issue was poor connectivity to the target mine workings. Project constraints prevented a full re-siting of the borehole. Therefore, options to achieve the required connectivity to workings and thereby performance, from the drilled borehole were explored and implemented.

Keywords: Saline, pumping, borehole, problems, water-jetting

Introduction

Whitburn lies within the Westoe-Wearmouth mine water block, which includes several connected collieries and workings within at least 16 coal seams. The mine water block includes workings that are onshore (approximately 93 km2) and offshore (approximately 85km2). The Permian drinking water aquifer overlies approximately 63% of the mine water blocks onshore extent, and Permian strata overlies all of its offshore extent. Following the cessation of mining and pumping in 1993 the workings flooded.

To improve the understanding of rising mine water in the block, a monitoring borehole was drilled at the former Whitburn Colliery site. The data from which would inform assessment of mine water management requirement and options. A pumping test at Westoe Shaft in 2011, established a likely future pumping need of between 10 and 20L/s, with highly saline mine water (up to 96000µS/cm at 25°C). Following the identification of this need it was determined that the Whitburn monitoring borehole was sufficient for pumping, which started in 2015.

Whitburn first borehole (BH1)

The borehole at Whitburn was constructed in 2010 and targeted an underground roadway (125 m from the No.2 shaft) in the Yard (regional index G) Seam (fig. 1). The borehole was originally designed to be a monitoring borehole, rather than specifically for abstraction. A summary of key construction details for BH1 is as follows (all depth are metres below surface):

a) Final internal diameter of 201mm to 147m, and 140mm to 183m
b) Deviation of 7m to the west, at the full depth of 190m
c) Solid steel casing (324mm ID) from surface to 18m, outer annulus grouted from base to surface
d) Solid steel casing (lining) (201mm ID) from surface to 149m, outer annulus grouted from base to 17m
e) Solid steel (water well) (140mm ID) casing from 147m to 183m (there is a reduction in internal diameter in the borehole), outer annulus grouted from base to 147m
f) Open hole from 183m to 190m. Gravel packs or well screen are not typically included for Coal Authority pumping borehole – these are to underground roadways, and well screens typically become clogged
g) Mine water level at time of construction was 111m
h) Base of quarry backfill at 16 m, and base of Permian (limestone aquifer) at 107m

Due to issues relating to borehole construction (material, diameter and deviation), and

its use for pumping (pump install, pump material) the borehole started to develop issues. Interactions between the casing and pump, compounded by the saline water and dissimilar metals present caused the pump-to-riser connection to corrode and fail. The pump dropped down the borehole and therefore required recovery and replacement. In addition, the innermost set of casing had started to deteriorate. The causes of damage are likely to have included, removal and install of pump and associated infrastructure, and galvanic corrosion between the mild steel casing and dissimilar metals in the pump. The failing borehole exhibited reduced yield and repeated pump outages. Attempts to remedy yield issues were made, but had limited success. Based on ongoing issue with pumping and the stability of the borehole itself, it was decided to replace the borehole with one purpose-built for pumping.

Whitburn replacement borehole (BH2) specification

The replacement borehole needed to take in to account issues experienced with BH1. The replacement borehole needed to meet to the following key specifications:

a) Minimum final internal diameter of 305mm to allow pump install without damaging the borehole, and also to provide a yield of up to 30L/s
b) Verticality with a maximum deviation of 1 m from vertical at the base of the borehole, to allow improved pump install, and intersect the underground target
c) Expected depth of 194m to a roadway in the Yard Seam at Whitburn
d) Innermost casing to withstand the highly saline mine water present within the borehole (tab. 1)
e) Casing and grout at different horizons to prevent any interaction between the mine water and surrounding environment, including the Permian drinking water aquifer
f) Design life of at least 20 years
g) Restricted locations in the current site compound, due to site head works and underground target locations (fig. 1)

In addition to the drilling specifications for the Project, there were other concerns relating to control of mine water at Whitburn and the mine water block. Whitburn has a pumping water level control band based on risks to the overlying Permian aquifer. Across much of the mine water block, the groundwater and mine water levels are unknown, whilst available measurements show continuing rise of the mine water. To manage the risk of pollution to the overlying Permian aquifer, the control band at Whitburn is based on the highest known water level in the block (Boldon) and the lowest Permian water level (one of the drinking water abstraction wells), with a 10 m conservative protection buffer allowing for uncertainties.

Prior to construction of Whitburn BH2, a liaison group was set up between the Coal Authority, the Environment Agency (regulator) and Northumbria Water Limited (municipal drinking water supplier). The group worked together to propose a temporary revised control band, to allow some mine water rise during construction of the new borehole. At the same time as the planned mine water drilling works, one of the Permian groundwater supply wells was scheduled for maintenance. This aided the relaxation of the mine water pumping control band. With the revised pumping control band, the drilling works could be undertaken

Table 1 *Summary of pumped mine water laboratory chemistry at Whitburn BH1, mean values 2015 to 2022*

	Electrical conductivity (µS/cm at 25°C)	Chloride (mg/L)	Sulphate (mg/L)	Total Iron (mg/L)	Alkalinity (mg/L as $CaCO_3$)
Mean	85417	31297	3237	95.4	300
Minimum	32700	19700	2790	67.2	131
Maximum	102000	52800	3850	156	416

Note: based *on 221 samples, taken by the Coal Authority operational contractors*

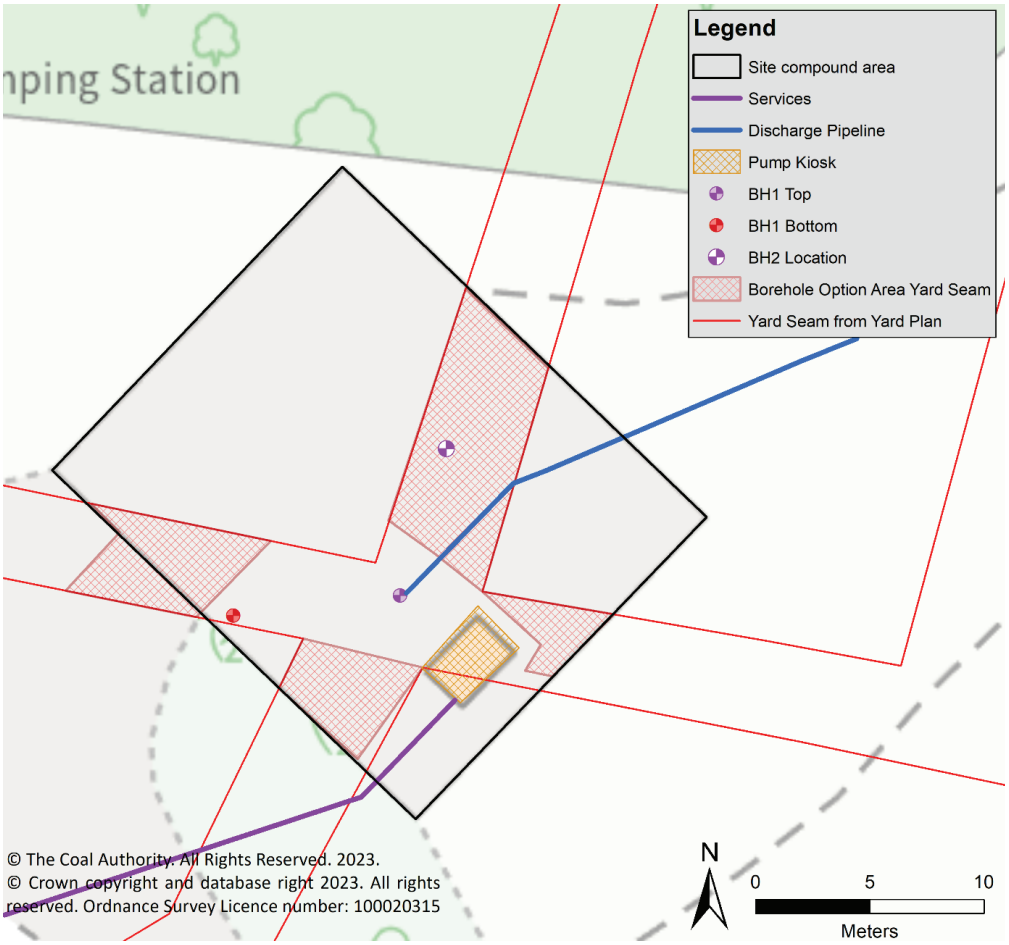


Figure 1 Whitburn site compound with expected underground mine workings in the Yard Seam

with abstraction from BH1 (which is in close proximity to BH2) temporarily halted. BH1 was retained on standby throughout the works such that pumping could quickly be started if required.

Whitburn BH2 construction – summary of problems

The drilling works were planned to start in June 2021 and finish in November 2021, however, due to problems with drilling, the works were completed in December 2021. The main issues effecting drilling works were:

1) Quarry backfill material to a depth of 26m, approximately 10m deeper than expected, based on BH1 (7m away) drilling records. Difference between expected and actual depth of quarry backfill is considered to be due to BH2 being on lower bench than BH1.
2) Casing not installed through full extent of quarry backfill resulting in flush loss and additional grouting requirement.
3) Highly fractured Permian limestone resulted in losses of water and poor flush returns, delays due to additional grouting and water needs.

Although these points delayed the project, unexpected geology is not unusual during drilling works, and can often be mitigated against and / or resolved during drilling works.

Whitburn BH2 – the big problem

In the Coal Measures strata, drilling progressed well and as expected. However, the borehole did not intercept the target underground roadway, instead solid intact coal was encountered. The borehole was progressed to 197m, approximately 4m below

the base of the coal seam (at 190 to 193m). No loss of flush was observed, during drilling of the coal or surrounding strata, flush loss is typical when drilling into mine workings and fractured strata.

Without a connection to the mine workings, there is essentially no yield of mine water, and the borehole will not be useful for pumping mine water. Standard borehole development works, and air-lifting were undertaken in an attempt to create a connection to the mine workings. A falling-head test in BH2, showed a yield of <0.01L/s, compared to the desired minimum yield of 30L/s.

The failure to intercept workings prompted a review of the original target location and depth. Was the borehole in the correct place? Did the borehole go to the correct depth? The target area of the mine was worked in the 1940s with the abandonment plan dated to the 1960s. The plan is considered unlikely to have significant errors. Confidence in referencing to surface is considered high given the target location 125m east along a roadway from mine shafts with known surface locations. The geological information and drilling observations were reviewed with chippings and later geophysical surveys confirming coal present and intact between 190 and 193 m. The geophysical survey also confirmed the bottom of the borehole had deviated by <0.25m and therefore should have contacted the underground roadway (width of 2 to 4m). The information review concluded that the mine plan and roadway position must be incorrect though the source and specifics of the error remain unknown. As a result, it was not known if the recorded roadway would lie to the east or west of the drilled borehole. Further review of Yard Seam workings shown on other seam plans, indicated it to be probable that the borehole was to the west of the roadway, and likely within 1 m.

Whitburn BH2 – initial options

Given the spatial limits of the borehole compound, the presence of the two existing boreholes (and associated infrastructure) and the limited targets in underground workings, a further borehole in the site compound was not feasible. Therefore, should an alternative borehole location be considered it would need a new site area and pumping infrastructure, this would likely result in a significant delay to the replacement of the failing BH1.

Options had to be devised and considered that could be effective and be delivered within a short time scale. Collaboration between the Coal Authority and existing and potential partners generated four initial options for appraisal in January 2022 (tab. 2)

Following initial assessment of options, plans of actions and more detailed assessments of risks were developed for: a combination of water-jetting with or without controlled explosives. In March 2022, the assessment of the options selected the use of water jetting without explosives. The use of explosives within the borehole was considered too great a risk to the plastic casing.

Whitburn BH2 – the final solution

Throughout April and May a method was developed to undertake the works safely and successfully. In the meantime, options for resuming temporary pumping from BH1, and options for a third borehole were being

Table 2 *Summary of pumped mine water chemistry at Whitburn BH1*

Option	Description	Positives	Negatives
Managed explosives	Attempt to control the direction / area of blast to create fractures	Create fractures in multiple directions over a wide area	Innermost plastic casing could fail
Uncontrolled explosives	Uncontrolled blast to create fractures	Create fractures in all directions	Innermost plastic casing could fail
Widening the base of the borehole	Use a narrow drill bit to scour out the base of the borehole	Multiple directions over a large area	Unlikely to have a wide penetration area
Directional pressurised water-jetting	Direct pressurised water to create a slice into the coal	Considered likely to cut the required penetration thickness Unlikely to damage the borehole and casing	Limited direction and depth

progressed. The final method needed satisfy the following requirements:

a) allow resumed pumping from BH1 to prevent rising mine water and aquifer pollution
b) protect BH1 during the water-jetting works – at the time BH1 was the only available borehole to pump from
c) prevent collapse of BH2
d) control any solids in the water during the works, and treat the water produced during the works to meet our discharge consents
e) demonstrate that the required yield improvements in BH2 had been achieved.

A sequential plan to meet all the criteria above, as follows was developed:

1) Clean out the borehole of debris and confirm the pre-works borehole yield
2) Fix the water jetting tool to the drill rods, the drill rods were also used to track the orientation of the water-jetting tool
3) Water jet at the target depth in the likely direction of the roadway. Pressurised water at 2000 to 3000 bar injected laterally from the base of the drill string. Nozzle moved steadily upwards to slice the coal seam, forming a vertical slot in the coal seam wall of BH2.
4) Clean out any debris from the water-jetting and perform yield tests and assess the results
5) Repeat the water-jetting at the same depth and orientation to improve any pathway
6) Clean out any debris from the water-jetting and perform yield tests and assess the results
7) Make BH2 operational for pumping, as per the pre-determined pumping plan to mitigate risks of the borehole and not breach discharge consents

Results

After each set of water-jetting and air-lifting, a falling-head test was undertaken. The first test was undertaken on the 14th June 2022 and showed a yield of >5 L/s with a well loss of 0.2 m, the flow rate was limited during the test. The second falling-head test showed a yield of >30 L/s with a 5 m well loss. For comparison the original borehole BH1 abstracted approximately to 10 to 15 L/s with a well loss of approximately 2 m.

Based on the post jetting tests, it was estimated that the works created a slot in the coal seam, approximately 120 to 150 mm wide and 300 mm high, in the east side of the borehole. The slot dimensions are considered to be similar to the open-hole section in the roadway of the original BH1.

The dimensions of the slot may increase with time, due to ongoing pumping and scouring of the flow pathway between the pump and mine workings.

The water-jetting has been successful and increased the yield of the borehole from <0.01 L/s to >30L/s, this is likely because the jetting created a pathway through the coal to the roadway. Acoustic images and geophysical surveys were taken post water-jetting, the data shows possible fracturing and / or collapses that appeared following the water-jetting works. The precise extent and dimensions of the fractures etc. are unknown. It is also uncertain if the pathway is direct result of the water-jetting, or a secondary result from collapse above the water-jetting zone. Collapses of the borehole between the roadway and base of casing would likely deposit material in the sump at the bottom of the borehole (approximately 8m below the roadway) and at the time of the works, the borehole was seen as effectively not fit for purpose of pumping mine water.

Acknowledgements

The authors would like to acknowledge and thank all those involved in the Whitburn borehole project, and specifically those at the Coal Authority, Integrated Water Services, AECOM, GStow, European Geophysical Services, RGL Services.

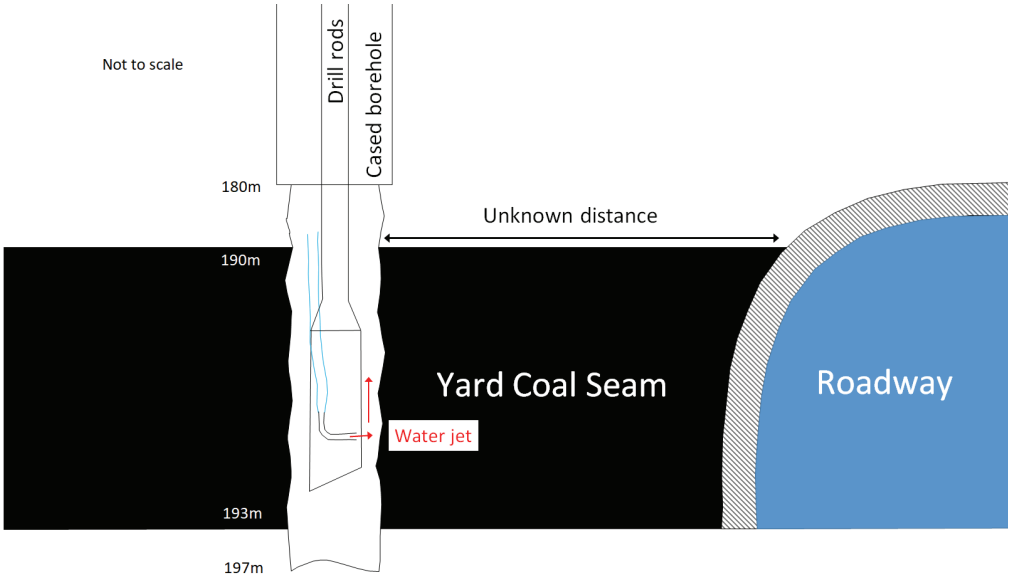


Figure 2 Conceptual diagram of water-jetting



Figure 3 Water jet test at surface (left), and borehole CCTV image post-water jetting (right). Photograph from Integrated Water Services and European Geophysical Services

ESG & Mine Water: A Procedural Approach to Support Setting Water Savings Targets in the Mining Sector

Grace Yungwirth[1], Trevor Coleman[2], William Jay Norwood[3], Priyal Dama-Fakir[2], Mark Bruton[1], Niyaz Ali[1], Givarn Singh[1]

[1]*WSP UK Ltd, Chancery Lane, NG12 5BL, UK, grace.yungwirth@wsp.com, mark.bruton@wsp.com, niyaz.ali@wsp.com, givarn.singh@wsp.com*

[2]*WSP SA Pty, Building 1, Maxwell Office Park, Magwa Crescent West, Waterfall City, Midrand, 1685 P.O. Box 6001, Halfway House, 1685, South Africa trevor.coleman@wsp.com, priyal.dama-fakir@wsp.com*

[3]*WSP USA Ltd, 1575 Treat Boulevard, Suite 201, Walnut Creek CA 94598 USA, jay.norwood@wsp.com*

Abstract

Mining companies are challenged to reduce water consumption as part of their Environmental, Social, and Governance (ESG) commitments. A process was developed to engage mine site stakeholders and multi-disciplinary industry practice leaders to assess the best potential options for integrated water savings and improvement of water recycling and reuse efficiency. This paper outlines this procedure to identify and prioritise water use solutions so that investment can be focused based on cost per megalitre saved or other appropriate criteria. A compiled list of water savings technologies is presented including a description of general considerations for applying them to such a study.

Keywords: Sustainability, ESG, mine water use, water efficiency, mining hydrogeology and hydrology practises, water saving targets

Introduction

Mining companies are facing increasing competition for limited water resources and therefore increased challenges to reduce water consumption and to improve their water use metrics as part of their Water Stewardship and Environmental, Social, and Governance (ESG) commitments (ICMM, 2022). Although traditional efforts to overcome these challenges have focused on interrogating the site water balance and site water management plan, it is recognized that solutions to this complex challenge are likely to be found from a more holistic and multidisciplinary review of the site and its environment.

A water savings project focused on a global portfolio of mine sites with priority in water scarce regions was undertaken by WSP for a confidential mining client. As part of the project, a process was developed to bring together mine site stakeholders, WSP's global industry practice leaders and a large global team of WSP's mine water professionals to assess the potential options for water savings and improvement of water recycling and reuse efficiency across their portfolio of mining and mineral processing sites. At the start of the assessment all the operations had water balances and a global Power Business Intelligence (Power BI) data base containing all water accounting data, which was curated by consultant partner ERM (2022). The study considered technologies currently available or in development and across a multitude of disciplines. Conceptual level engineering, water balance modelling, and significant workshopping along with the presentation of the results in a visual database were tools used as part of the study process to rationalize options in terms of costs per water savings (cost per megalitre saved) and determine the best potential options per site or portfolio.

While the outcomes of the water savings study were site specific and unique to the client's diverse portfolio (copper, base metals, diamonds, platinum), a similar process can be applied to other mining client portfolios or individual sites. In addition to very site-specific solutions, the project also allowed the identification of a list of water savings technologies applicable for use at mine sites or mineral processing sites that are currently available to those in the industry. A compiled list of these water savings

technologies including description of general considerations for applying them to such a study is presented.

Approach

WSP worked together with the client to produce a workflow procedure that would allow the project to evaluate all potential water savings and efficiency opportunities, to develop engineering and modelling supported investment decisions, to document the evaluation and selection process, and allow acceptance of the proposed solutions by the site and company stakeholders at both mining and mineral processing sites. The procedure was developed over the course of the project and included the following steps:

1. Identification of priority sites/portfolio.
2. Benchmarking exercise for water use and water recycle-reuse efficiency.
3. Data review and engagement with site stakeholders.
4. Interrogation of site water balance and water management plan.
5. Long Listing exercise of potentially applicable technology options.
6. Short Listing exercise and ranking.
7. Development of concept level engineering.
8. Evaluation of potential water savings using modelling.
9. Cost estimation and evaluation of results based on cost per ML saved.
10. Presentation of results in a graphical Power BI project to support investment decisions.

This process is represented graphically as Figure 1 with each step discussed further in the following sections.

Identification of Priority Sites/ Portfolio

The sites within the portfolio were chosen based the current most challenging water use and efficiency performance amongst sites located in water stressed regions. This allowed the study to focus on sites where gains were likely to have the greatest positive impact on the local stakeholders as well as the greatest impact on the company's water use metrics.

Benchmarking Exercise for Water Use and Water Recycle-Reuse Efficiency

Using publicly available data, a benchmarking exercise was undertaken to develop an

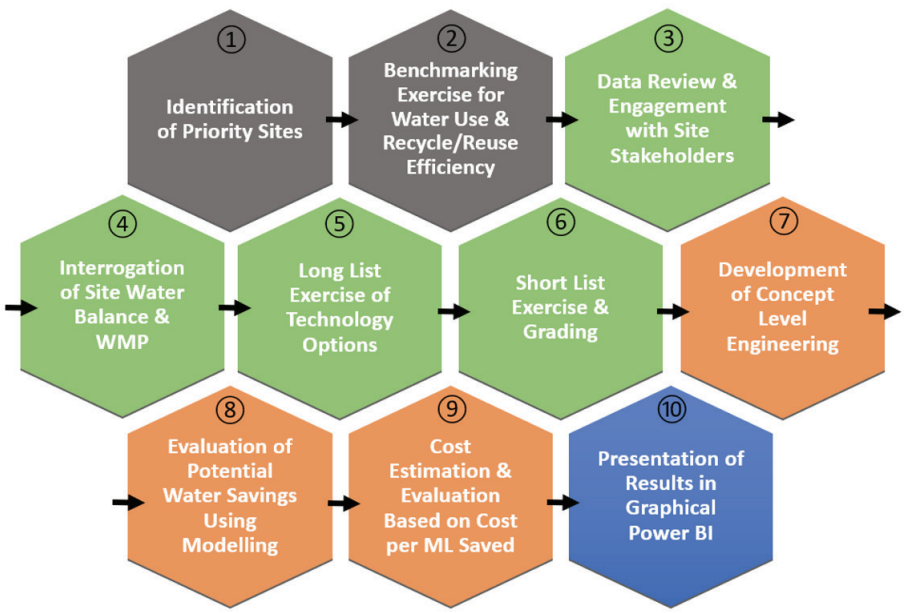


Figure 1 *Workflow Procedure (steps organised as: grey = sites/portfolio selection, green = option development, orange = assessment of prioritised options, blue = presentation of results).*

understanding of water use metrics at similar mines and mineral processing facilities (comparing factors as described in the list below). Sustainability reporting was the primary source of information in this exercise. In practise data were difficult to obtain to the appropriate level of detail to allow useful numbers to be produced for comparison. Understanding was applied to estimate parameters from some of the public information available. Benchmarking data from mineral processing sites were the most challenging to obtain.

Benchmarking comparison metrics included the following:

- Operation type – Open-pit mine, underground mine, mineral processing facility, or a combination of these;
- Climate – Arid, Equatorial, Warm Temperate;
- Region – Delineated by Continent;
- Commodity – Primary commodity produced; and
- Type of Tailings Storage Facility – conventional, thickened, filtered, mixed (if known).

Once developed, this information was presented in a graphical power BI database allowing comparison of the client's portfolio of sites against other similar operations globally. This assessment was then used to further prioritise the focus of the study within the selected portfolio.

Data Review and Engagement with Site Stakeholders

Data review was progressed through provision of a detailed Request for Information (RFI) with information collected primarily through targeted engagements with site stakeholders including but not limited to professionals responsible for water management, processing, tailings management, mine planning, permitting, new project development, and community engagement at the sites. Site visits were undertaken to clarify and refine data collection where possible. Integral to the review was development of an understanding of stakeholder concerns, site constraints, future projects and previous studies.

Data review focused on both existing operation and future planning including:

- Existing water management systems, water balance and site reticulation reports and supporting data sets, water balances, and climate data including predictive water balances if available;
- Previous water savings studies, status of extent of evaluation and implementation of identified options (For example: Concept, Prefeasibility, Feasibility);
- Current and projected ore production and tailings production;
- Process circuit/water circuit information, processes, water quality and water treatment information (if relevant);
- Metrics and definitions for the site;
- Major projects planned at the site; and
- Any relevant change in water balance or inflow predictions that can affect water consumption demand or discharge and reason for water balance change. For example, permit requirements, mine plan, tailings deposition methodology changes required to facilitate permitting renewal.

Interrogation of the Site Water Balance and Water Management Plan

The site water balance for each site was reviewed so that all current metrics were understood and a baseline of water metrics was set as a comparison point from which the outcomes of the study would be measured. The occurrence of unusually dry or wet years was considered and avoided in the selection of the baseline water metrics.

The predictive water balance was also interrogated alongside the site water management plan to understand the anticipated effects of planned major projects, expected climate change, and any planned increase or decrease in production in relation to the baseline metrics. A summary of the key aspects of the existing site water balance along with key challenges of the site water management plan was presented to the site stakeholders in engagement workshops.

Long Listing Exercise of Potentially Applicable Technology Options

Interactive sessions were held with site stakeholders to present the results of the data review and a summary of the existing site water management completed in the previous

step of the process. These sessions were used to produce an opportunities Long List focused on water savings and water recycling reuse efficiency options potentially applicable at each site. Sessions were integrated and attended by stakeholders of different technical backgrounds.

The format was run as a brainstorming session and considered technologies currently available or in development and across a multitude of disciplines. The purpose of the session was to develop a full and complete list of potential opportunities and any key information as to the applicability of these opportunities at the site.

The Long list opportunities development was progressed to capture the complete list of potential options/technologies with may be applicable at the site considering previous efforts/studies by the site and technical expert review of application of the technology to the site.

Short List Development and Ranking

The Long list of opportunities developed in the previous task was then progressed through a short listing and ranking exercise. This included a high-level feasibility assessment of each option based on agreed screening criteria to prioritise the opportunities based on suitability to site requirements and high-level implementation metrics as agreed with the mine site and the mining company's corporate goals.

The short list development and ranking exercise was progressed as follows:

- Develop high level screening criteria to be applied to the Long List (e.g., percentage change/general assessment of effectiveness, community needs, alignment with corporate targets etc) and progress initial screening of options.
- High level evaluation including high level costs if possible.
- Internal workshop with technical leads to assess options, refine list, and revised metrics with focus on priorities set out in the screening criteria.
- Workshops with stakeholders to present results of assessment and agree on the Short List.

Agreement of the final short list by all site stakeholders was a key aspect of the success of the project. The short list was refined to include the top priority options per site, which were progressed to the next stage of evaluation.

Development of Concept Level Engineering

Concept level engineering was progressed on the top priority opportunities identified in the Short List grading session. Engineering was progressed to the extent required to (1) support the evaluation of the potential water savings (timeline, footprint, energy use, throughput, etc.); and, (2) to allow concept level cost estimation. Where available information was insufficient to allow progression to full concept level engineering, experience and benchmarking were used to estimate relevant engineering parameters and costs.

Evaluation of Potential Savings Using Modelling

Output from the concept level engineering was used to inform the forward-looking predictive modelling of the site water balance designed to evaluate the potential for water savings in relation to the baseline metrics. While individual runs were progressed for some options, it was recognised that water savings options are most often interconnected and are not best evaluated individually.

The true prediction of potential water savings is more accurately evaluated by running the predictive water balance as a site focused collection of the most likely water savings opportunities implemented on a realistic schedule given that the combined savings are unlikely to be the same as the additive savings realised from model runs assessing individual options. Where possible it was helpful to collect model outputs on a yearly timestep so that the timeline of potential savings could be evaluated.

Cost Estimation and Evaluation of Results Based on Cost per ML Saved

The concept level engineering was used to develop concept level CAPEX and OPEX estimates for the proposed water savings opportunity. Net Present Value/Cost (NPV/NPC) was calculated over an annualization

period of 20 years or the life of mine (LOM) whatever is shorter. In some cases, opportunities included a revenue stream, which was also factored into the calculation.

The cost estimates were combined with the results of the predictive water balance modelling to produce a basic cost per ML saved over 20 years (or LOM) for each of the water savings opportunities or package of water savings opportunities. Where it was not possible to estimate OPEX, CAPEX only was used in the calculation of cost per ML saved and this was indicated.

Presentation of Results in a Graphical Power BI Project to Support Investment Decisions

Results of the study were presented in a graphical power BI project, which was designed to be fully integrated to allow for evaluation of options individually or as a combination of portfolio metrics. The output was used to compare the opportunities on a cost per ML saved basis and against other metrics relevant to the company (e.g. water stewardship). This output was used by the client to set their medium-term targets and to focus immediate investment. The Power BI project was set up to allow for it to be updated with new data as the options are implemented to support the next wave of investment decisions and realistic operational target setting.

Water Savings Technologies

As part of the process undertaken in the project described above, technologies were identified that could allow for improvements in water saving or efficiency at mining and mineral processing sites. A compiled list of some of these water savings technologies including description of general considerations for applying them to such a study are included in the list below. This is not an exhaustive list however presents a selection of the technologies available which may be broadly applicable at many sites:

1. **Evaporative Covers:** There are three different types, floating photovoltaics, floating covers, solid covers. The covers are well understood however overall cost effectiveness and efficiency depends on site specific factors such as the site's weather condition.
2. **Dust Suppression Additives:** Technology is well understood however overall cost effectiveness and reliability should be verified at the site.
3. **Treated Sewage Effluent Reuse:** Reuse of treated sewage effluent from the mine or from the surrounding community in the mine water circuit replacing the need for higher quality water. The water will likely require additional treatment prior to reuse.
4. **Water Reuse Assessment:** Requires detailed water quality information from all the reticulation points and understanding of reuse tolerances to assess suitability of water streams for reuse with no or minimal treatment. Lack of data is a significant hurdle in applying this solution.
5. **Underground Mud Management:** Settling underground to avoid surface settling ponds and associated pumping and evaporation losses. Suitable underground space is required and recovered water can be reused underground. Underground water temperatures would also need to be considered.
6. **Filtered Tailings:** Requires site specific laboratory testing to determine how much water can be recovered by filtering. Costs are high and the solution is difficult to implement in areas of high rainfall.
7. **Operational Tailings Management:** Reduce amount of water sent to tailings facility by increasing tailings density. Costs and savings are highly dependent on technology selected and site-specific laboratory testing.
8. **Underground Storage of Tailings:** To limit evaporation from the tailings by limited exposure to climate. Requires identification of underground mine voids which could be used for storage.
9. **Gland Seal Water Replacement:** Conversion to pumps using mechanical seals eliminating the need for high quality gland seal water. Commercial success to date in mining are limited however widely adopted in other industries.

10. **Electrocoagulation:** Treatment technology to reduce the volume of makeup water in mineral processing cooling towers. Emerging technology likely requires a pilot programme to confirm savings and costs.
11. **Waterless Scrubbers:** Alternate scrubbing technologies in mineral processing facilities could reduce or eliminate the use of water to remove particulate material and gasses prior to release. Requires a site-specific sampling programme to assess and would be implemented at high CAPEX and OPEX cost.
12. **Waterless Cooling:** Waterless cooling at mineral processing sites such as mechanical refrigeration could eliminate the need for cooling water in smelters. Design and approach will be impacted by seasonal variations in climate and temperature. This is a high cost and high energy solution.

Evaluation of the potential effect on water metrics versus costs of these technology options is site specific for most of these options and must be progressed through concept level engineering, cost estimation, and predictive water balance modelling as described above to properly evaluate.

Conclusions

Mining and mineral processing companies need to be proactively evaluating their water use, efficiency, and stewardship programs to meet ESG commitments at their sites and across their portfolio. Regardless of a site's current water position, it is reasonable to assume that competition for water will increase, and proactive management of water related investments through a defensible program is needed to protect social license and ability to operate.

The procedure outlined in this paper has been tested and shown to provide a comprehensive evaluation of opportunities to improve water use and recycling/reuse efficiency water metrics on mining and mineral processing sites. Benchmarking of water metrics based on publicly available information is challenging however can be used to further focus the project. The appropriateness of opportunities, potential savings and costs are highly site specific and must be evaluated on a per site basis. Evaluation of the top ranked Short List opportunities through concept level engineering, cost estimation, and predictive water balance modelling allows for comparison of the opportunities on a cost per ML saved basis. Water balance modelling is best advanced considering a combination of opportunities at one site given the integrated nature of water metrics. A list of water savings technologies potentially applicable at mining and mineral processing sites has been presented. Presentation of the study results in a graphical Power BI project supports evaluation of the results by multiple metrics and across a portfolio which allows for targeted focus of investment decisions by mining companies.

Key success factors of the process were the close collaboration between the mining company technical water team, the consultants, and engagement of all relevant site stakeholders as well as multi-disciplinary industry leading professionals to allow for the development of a comprehensive opportunities Long List and for agreement and buy-in of the ranked Short List. Appropriate selection of a baseline against which improvement metrics can be compared is also a critical step in the study. This paper presents a robust process by which a defensible water savings, water efficiency, and/or water stewardship program can be developed. This type of focused investment and informed target setting has the potential to speed the mining industry's progression to achievement of ESG goals.

References

ICMM. (2022) International Council on Mining and Metals, Mining with Principles - Mining Principles: Performance Expectations. London United Kingdom: Self Published. Available at: https://www.icmm.com/website/publications/pdfs/mining-principles/mining-principles.pdf?cb=10319 (Accessed April 2023)

ERM. (2022) Power BI Project - Target Setting Water Data All Sites. Bristol United Kingdom: Self Published. Restricted access at: https://app.powerbi.com (Accessed July 2022).



Author Index

A

Abfertiawan, Muhammad Sonny 1, 159
Aghili, Somayeh 510
Aiglsperger, Thomas 148
Alakangas, Lena 148
Ali, Niyaz 564
Alvarez, Ignacio 6
Annandale, John George 13
Anttila, Eeva-Leena 270
Apeiranthitis, Nikolaos 19
Arrowsmith, Carol 402

B

Bäckström, Mattias 25
Badhurahman, Abie 294, 409
Bamforth, Selina 31, 77
Banks, Vanessa 38, 257, 402
Barnes, Andrew 129, 135, 471
Basallote, M Dolores 45
Battaglia-Brunet, Fabienne 51, 303, 517
Beale, Geoff 63
Bellin, James 57, 237
Bennett, Adam 237, 315
Bernasconi, Rachele 320
Blanchard, Ryan 220
Blanchette, Melanie 320
Blumenstein, O 287
Boddaert, Florent 63
Bovim, Alastair 69
Bowell, Rob 77, 122
Brabham, Peter 77
Breckenridge, Larry 83
Brown, Martin 6, 178
Bruce, Edward 38
Bruns, Stefan 523
Bruton, Mark 564
Burke, Ian T 421
Burton, Rob 89
Byfield, Rebecca 108

C

Cameron, James 421
Cánovas, Carlos R. 45, 434
Carline, Richard 108, 491
Carow, Albert 365
Choi, Kung-Won 415
Chudy, Krzysztof 540
Clode, Karen 96
Clulow, Alistair 315
Cochrane, James 102
Cojoianu, Theodor 333
Coleman, Trevor 564
Cooke, Dave 108,
Courtney, Ronan 215
Cox, Melanie 122
Cox, Michael 326
Cox, Nick 31
Craxford, Stuart 102
Crewdson, Emma 257, 402

D

Dama-Fakir, Priyal 564
Dashwood, Benjamin 38
Deane, Karabo 13
Declercq, Julien 57
Dent, Julia 129, 135
Digges La Touche, Gareth 428
Djali, Febriwiadi 1, 159
Dorman, Dayton M 142, 390
du Plessis, Heinrich Meiring 13
Du, YanHui 309
Durce, Delphine 196
Dure, Frederic 51, 250
Dwiki, Sendy 294, 409
Dzimbanhete, Vimbainashe L 148

E

Ebel, Tom 154, 545
Ebeling, Patrick 237
El-Idrysy, Houcyne 166, 227
Engevin, Jérémy 250
Espach, Johan 383

F

Falconer, Jenny 376, 484
Farahnaz, Ibtisani 159
Fieback, Tobias 154, 545
Finlay, Alexander 19
Francoeur, Nicolas 243
Franzsen, Sebastian 383
Freeman, Neil 96

__G

Gandy, Catherine J 38, 257, 402, 421
Gatellier, Gaëlle 51
Gautama, Rudy Sayoga 294, 409
Genc, Mihriban 63
Gerardo, Amaya 45
Gersten, Ben 129
Golian, Saeed 166
Gomes, Patricia 172
Grab, Thomas 154, 545
Greenwell, H. Chris 19
Griffiths, Ruth 122
Guerin, Valérie 250
Gunawan, Firman 1, 159
Gurieff, Nicholas B. 96
Gutierrez, Manuel 178

__H

Haanpää, Kirsi-Marja 270, 397
Hagihara, Kana 344
Hall, Iain 428
Hällström, Lina 185
Hamai, Takaya 344, 464
Handajani, Marisa 1, 159
Hansen, Robert 529
Harding, William 227
Hardwick, Ed 376, 484
Harvey, Todd 83
Hasan, Faiz 1
Heaney, Paul Clive 191
Hegg, Frej 148
Heuer, Sarah Nicole 13
Hietaharju, Eila 276
Holm, Peter Engelund 484
Holopainen, Joonas 203
Horiuchi, Kengo 344, 464
Hubbard, Paul 208
Hudson-Edwards, Karen A 421
Hudson, Ashlene 215
Hudson, Emily 89, 116
van Hullebusch, Eric D. 303
Hughes, Andrew 220
Hurban, Gary 227
Huron, Justine 51, 250

__I

Ikegami, Naoki 464
Im, Dae-Gyu 233, 281, 299
Imrie, Sheila 237, 315, 477

__J

Jackson, Scott 243
Jacob, Jérôme 51, 250
Jarvis, Adam P 257, 402, 421
Jasnowski-Peters, Henning 263
Jenk, Ulf 450
Jessop, Mike 220
Jones, Liz 108, 116, 491
Jowdat, Younes 510
Juholin, Piia 270, 397

__K

Kamiya, Taro 344
Kang, Bu-Sung 299
Kang, Chan-Ung 415
Kanu, Chimaobim V 421
Karlsson, Teemu Eemeli 276
Karlsson, Torbjörn 148
Kauppila, Tommi 276
Kim, Duk-Min 233, 281, 299
Kim, Sun-Joon 415
Kirillov, Nikolai 227
Kirkham, Matthew 38
Knott, Richard 102
Knox, Robert C. 390
Kofoed, Val O. 220
Kotte Hewa, Dileesha Jayahansani 196
Kunze, Katja 287
Kusuma, Ginting Jalu 294, 409
Kwon, Hye-Lim 233, 299

__L

Lafont, Charlotte 303
Lassin, Arnault 250
Laurila, Tea 2 70
Lee, Ga-Hyeon 415
Lee, Joon-Hak 233, 281, 415
Lehto, Vesa-Pekka 203
León, Rafael 434
Leyland, John 491, 552, 558
Liu, WeiTao 309
Loft, Stephen 257, 402
Longstaff, Tim 38
Lorentz, Simon Anthony 315, 497
Lourens, Paul Joël Havemann 456
Lubbe, Rolene 456
Lund, Mark 320
Lynch, Sarah F L 326

__M

Macías, Francisco 434
Maest, Ann 333
Maira, Castellanos 45
Malam, Claudia 135
Mansell, Lindsey 108
Marsden, James 129

Martin, Alan James 338
Masaki, Yusei 344, 464
Mason, David 108, 116, 491
Mayes, William M 421
Mazaheri, Nader 510
McCann, Justine I. 390
Melchers, Christian 263, 534
Merrick, Eddie 19
Metschies, Thomas 450
Meyer, Jürgen 450
Millán-Becerro, Ricardo 434
Millsteed, Barry D 365
Mokoena, Kopano 504
Momeyer, Steve 243
Moorhouse-Parry, Arabella Mary Louise 38, 351, 358, 402, 439
Moreau, Ulysse 250
Morton, Kym Lesley 69, 365
Moyo, Nkosilomusa 376
Msitsini, Moses 365
Mueller, Seth 135
Mugova, Elke 371
Mulcahy, Alex 402
Murnane, John G 215

__N

Naidu, Jivesh 383
Naidu, Tamlyn Sasha 376, 484
Nairn, Robert W 142, 390
Nedumpallile-Vasu, Nikhil 38
Nieto, José Miguel 45, 434
Nissinen, Tuomo Juhani 203
Norwood, William Jay 564
Nurmesniemi, Emma-Tuulia 397

__O

Ochieng', Levi 504
Onnis, Patrizia 421
Oppelt, Lukas 154, 545

__P

Paalumäki, Ville-Pekka 276
Palmer, Mike 208
Palumbo-Roe, Barbara 38, 257, 402
Paramananda, I K Dwika 409
Park, Mi-Sun 233, 281, 299, 415
Park, Seong-Sook 415
Paulsson, Oscar 148
Pearce, Steven 129, 135, 471
Pearson, Callum 57
Peinerud, Elsa 148
Picken, Päivi 270, 397
Potter, Hugh A.B 31, 38, 402
Pullen, Jasmine 257, 402

__R

Rafael, Pérez-López 45
Rex, Tony 477
Riikonen, Joakim 203
Riley, Alex L 421
Roberts, Mark Thomas 129, 135, 471
Roetting, Tobias Stefan 428
Romero Matos, Jonatan 434
Rudakov, Dmitrij 534
Ruthman, Rahardian 63

__S

Salah, Sonia 196
Salmawati, Salmawati 294, 409
Salvador, Silvano 338
Samuel, Toddy 63
Sapsford, Devin 471
Sartz, Lotta 25
Sato, Naoki 344
Satterley, Christopher J. 326, 351, 358, 439
Savage, Rhys John 129, 471
Schmidt, Roxane 445
Schoen, Daniel 471
Schramm, Andrea 450
Schreuder, Heinrich 456
Schultz, Ryan 129
Semoto, Yuki 344, 464
Shepherd, Nicholas L. 390
Sheridan, Craig 376, 484
Shiimi, Rosalia Tuwilika 471
Shubin, Ivan 477
Siddorn, Louise 428
Singh, Givarn 564
Smith, Janet 376, 484
Smithson, Stephen A. 358
Smolders, Erik 196
Sousa, Mafalda 172
Stambuk, Desana 166
Stanley, Peter Clive 102, 108, 116, 129, 428, 491
Stewart, Michael 57
Stockwell, Justin 243
Storey, Michael V. 96
Syafila, Mindriany 1, 159

__T

Tait, David John Knowlan 122
Takamoto, Kosuke 344, 464
Takaya, Yutaro 464
Tanner, Phillip Dale 13

Terry, Peter 491
Theron, Charné 497
Thobejane, Kgaugelo 504
Tiihonen, Tommi 203
Tokoro, Chiharu 464
Tolvanen, Hanna 203

__U

Umeobika, Chinedu V 421

__V

Vaarasuo, Anne 397
Vaezihir, Abdorreza 510
Vähänen, Kaisa 397
Valente, Teresa Maria 172
van der Walt, Gideon 13
van Dyk, Lizelle 376,
van Heerden, Wayne L 365
Vaxelaire, Stéphane 303, 517
Vermeulen, Petrus Daniel 456

__W

Walton, Jack 77
Warnes, Louis 326
Washio, Tsubasa 344
Watson, Ian Andrew 552, 558
Weber, Anne 523
Welman Purchase, Megan Dayl 529
Westermann, Sebastian 534
Williams, Heilyn 102, 108, 491
Williams, Tom 102, 129
Wolf, Petra 523
Wolkersdorfer, Christian 371, 540
Worsa-Kozak, Magdalena 540
Wunderlich, Timm 154, 545
Wyatt, Lee Malcolm 552, 558
Wylie, Richard 116

__Y

Yang, ChunHui 309
Yun, Seong-Taek 233
Yungwirth, Grace 564

__Z

Zarate, Manny 402

Keyword Index

3D

3D modeling 220

A

Abandoned Landfill 421
abandoned mine 257, 464, 552
Acid Mine Drainage 159, 250, 276, 294, 376, 409, 464, 540
Acid Rock Drainage 383
adaptive management 13
adsorption 415, 51
agglomeration 83
aggregate accumulation 309
aging 142
alkaline leachates 215
alkalinization 196
alteration 294
alum sludge-based adsorbent 415
alunite 294
AMD remediation 196
AMD see Acid Mine Drainage ammonium 523
analogue model 371
analytical modelling 534
arsenate 415
Arsenic 51, 517
assessment 491
Autocatalytic oxidation 233

B

baffle 281
batch experiments 45
bauxite residue leachate 215
beryllium 185
bioremediation 338
Block-cave 63
blow-out 491
borehole 558
boundaries 365

C

calaminarian habitat 108
Carbon Dioxide Removal Technologies 471
carbon emission reduction 237
catchment-scale 57
CFD-DEM 309
circular economy 376, 96
classification 294
climate change 166, 191, 227
climate response 38
clogging 250, 428
closure plan 397
CO_2 degassing 129
coal mine drainage 77, 439
coal 243
Coastal Erosion 421
cold climate 270
colloids 172
column experiments 45
compartments 365
Concrete Waste Material 464
constructed wetlands 215
Contaminant Flux 421
Contaminant transport 135
cover structure 276
Critical raw materials 185
Crowdsourcing innovation 96
Cyanide 529

D

dam leakage 510
DAS see Dispersed Alkaline Substrate
data transparency 333
Depressurisation 178, 456
design 89
dewatering 178, 237, 365
diffuse pollution 38, 257, 402
Dispersed Alkaline Substrate 250, 428
Dissolved metals 203
district heating network 545
drainage 116
drawdown 63
dynamic water grouting 309

E

ecosystem restoration 390
Efflorescent Salts 434
Energy efficiency 154
environmental assessment 108
Environmental Protection 122
epithermal deposits 294
erosion 116, 38

ESG 191, 227, 564
ethanol 344
evaporation pond 227
evaporation 51

__F

failure 69
faults 365
ferric/ferrous iron 517, 529
ferruginous 439
first flush 371
flood-influencing factor 534
flow configuration 281
flow data 89
fluoride 415
fracture 63

__G

Geochemistry 540
geophysics 208, 220
geotechnics 38
Geothermal energy 154
geothermal lithium 208
Geotourism 540
Global International Standard for Tailings Management (GISTM) 69
goethite/ferrihydrite 529
gold 83
GoldSim 445, 57
groundwater flow simulation 83
groundwater mobilisation 497
groundwater 220, 402

__H

hard coal 263
Heap leaching 83
heat exchanger 299
Heat pumps 545, 154
heritage 108
High density sludge 326
hydrochemistry 409
hydrodynamic modeling 523
hydrogeology 477
hydrothermal energy 299

__I

IHS 287
inductively coupled plasma 484
Infiltration 315
inflows 365
innovation 31
inrushes 477
Integrated water balance model 445
intervention 102, 108, 116, 491
ion exchange resin 135, 376, 484
iron hydroxide sludge 287
Iron oxides 142
iron removal 484
iron 303, 77
irrigation water quality guidelines 13
isotopes 402

__J

jarosite 529

__K

Kazakhstan 166
Kd 135

__L

landscape 108
Laser Ablation ICP-MS 196
leaching 25
lead 129, 257
Legacy Waste 421
lignite mining 523
Limestone 464
Limnology 320
longevity 215
long-term 552
lysimeter 276

__M

management 552
manganese 303, 351, 77
mass transfer 25
MATLAB 545
meromixis 338
Metal mine waters 31
metal mine 402
metal/load removal 45
metals extraction 19
Metals 159
mine certification 333
mine closure 276, 397, 409
mine drainage 129, 415
mine releases 333
Mine waste 135
Mine water irrigation 13
Mine Water Management 227
mine water rebound 534
mine water treatment 281, 326, 397
mine water use 564
mine water 1, 148, 154, 263, 299, 358, 397, 545, 552

mineralogy 142
mining hydrogeology and hydrology practises 564
mining influenced water 96, 484
Mining Waste 421
mining 122, 166, 25, 89
mixing 320
Mn oxides 233
mobility 148
moisture content 237
Monitoring 69

__N

Natural attenuation 540
Nature-based solutions 390
Nautilus Pond™ 102
Net Acidity 434
Net CO_2 Flux 471
net-alkaline 351, 439
neutral mine drainage 185, 303
nitrate 243
numerical modelling 6, 237, 309, 477

__O

On-site analysis methods 203
Open Pit Mine 456
operational data 351
operational experience 358
operations 89
oxidation 77

__P

packer testing 208
Passive Treatment 19, 196, 172, 233, 250, 344, 351, 358, 428, 439, 464
Perch Aquifer 456
Performance Monitoring 383
Phragmites sp. 172
PHREEQC 383, 409
Pilot plant 31, 517
pit lakes 409
pit seepage 6
PitMod 338
pollution leakage 510
pollution registry 333
Pore air propagation 497
pore structure 309
Predictive Simulations 178
Pressures 69
problems 558
Prussian blue 529
Pumping test 326
pumping 558

__Q

quarry 237

__R

rain events 320
Rare earth elements (REEs) 376
recipient 148
redox 338
REE scavenging mechanisms 196
reed beds 358
Regulations 122
release 25
remediation 102, 19, 428, 491
removal efficiency 303
representativity 504
research and development 96
resilience 191
Respirometric Measurement System 471
Reverse Osmosis 383
rice bran 344
risk assessment 477
Risk management 263
Risk 69
Ruhr District 263
run-off 1, 116

__S

saline 558
Sample selection 504
Särkiniemi 276
Seasonal Variations 434
secondary minerals 185
sediments 159, 25
seepage 51
seismic 220
sensitivity analysis 534
settling pond 281
simulation 545
Slag reactor 233
Slope Failure 456
slope stability 477
socio-economic 299
soil 287
sorption 135, 142
Source Apportionment 421
sources 148
spoil characterisation 38
SSPs scenarios 166
Stable isotopes 540
stratification 371
Structural mapping 365
subaqueous landfill 523

substrate reactor 281
sulfate-reducing bacteria 344
Surface Renewal 315
surface water management 102, 116
Sustainability 19, 142 191, 287, 564
Sustainable Remediation 450
synoptic monitoring 257

__T

tailings dams 69, 510
Tailings Water Modelling 315
Temporary treatment system 326
thermal stratification 320
Thiocyanate 517
Total Inorganic Carbon Analysis 471
Toxicity 172
trace elements 25
tracer test 371
tracers 263, 402
Treatment design 439
treatment 31
tungsten 185
tunnelling 491

__U

U.K. screening criteria 333
uncertainty analysis 89, 178
underground 63
unsaturated flow 83
Uranium Mining 450
uranium 148

__V

vegetative evolution 172

__W

Washout 434
waste recycling 45
Waste rock water balance 243
Water analysis 203
water efficiency 564
water magement 270
water management risk assessment 445
Water Management 166, 450
water quality improvement 390
water quality modelling 243
Water Quality 122
Water resources 227
water risk 57
water saving targets 564
water stewardship 57
water treatment 129, 270
water 19, 191
water-jetting 558
wetland 303
Wildfire-ash 434

__X

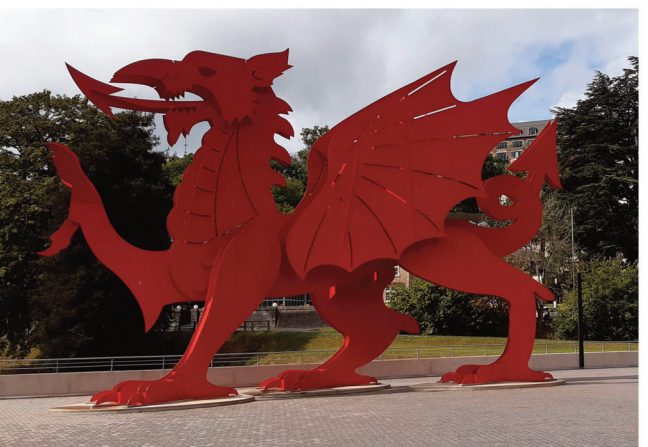
xanthate 270

__Z

zinc 129, 257, 344







The Welsh minerals sector once supplied coal, slate and metals globally. Whilst there remains limited exploitation of reserves, we retain numerous collieries, open cast mines and quarries plus over 1300 abandoned metal mines that negatively affect over 700 km of river reaches.

Wales has introduced innovative legislation on the Well-being of Future Generations that Nikhil Seth as Head of Sustainable Development, United Nations said:

> **"We hope that what Wales is doing today the world will do tomorrow. Action, more than words, is the hope for our current and future generations."**

As public bodies here, must now work together to improve our environment to deliver multiple benefits to protect the long term, we wish to share our ambitions with you.

For a small country, we like to aim high and punch above our weight. In our Non-Coal Mines Programme, we have been trialling new techniques and wish to share them with you.

We really hope that you will like this in-person IMWA conference and that we will be able to provide a warm Welsh welcome to as many of you as possible over the course of the week.

Hwyl fawr, Best wishes and Glückauf!

Peter Stanley

ISBN 978-3-9825293-1-8